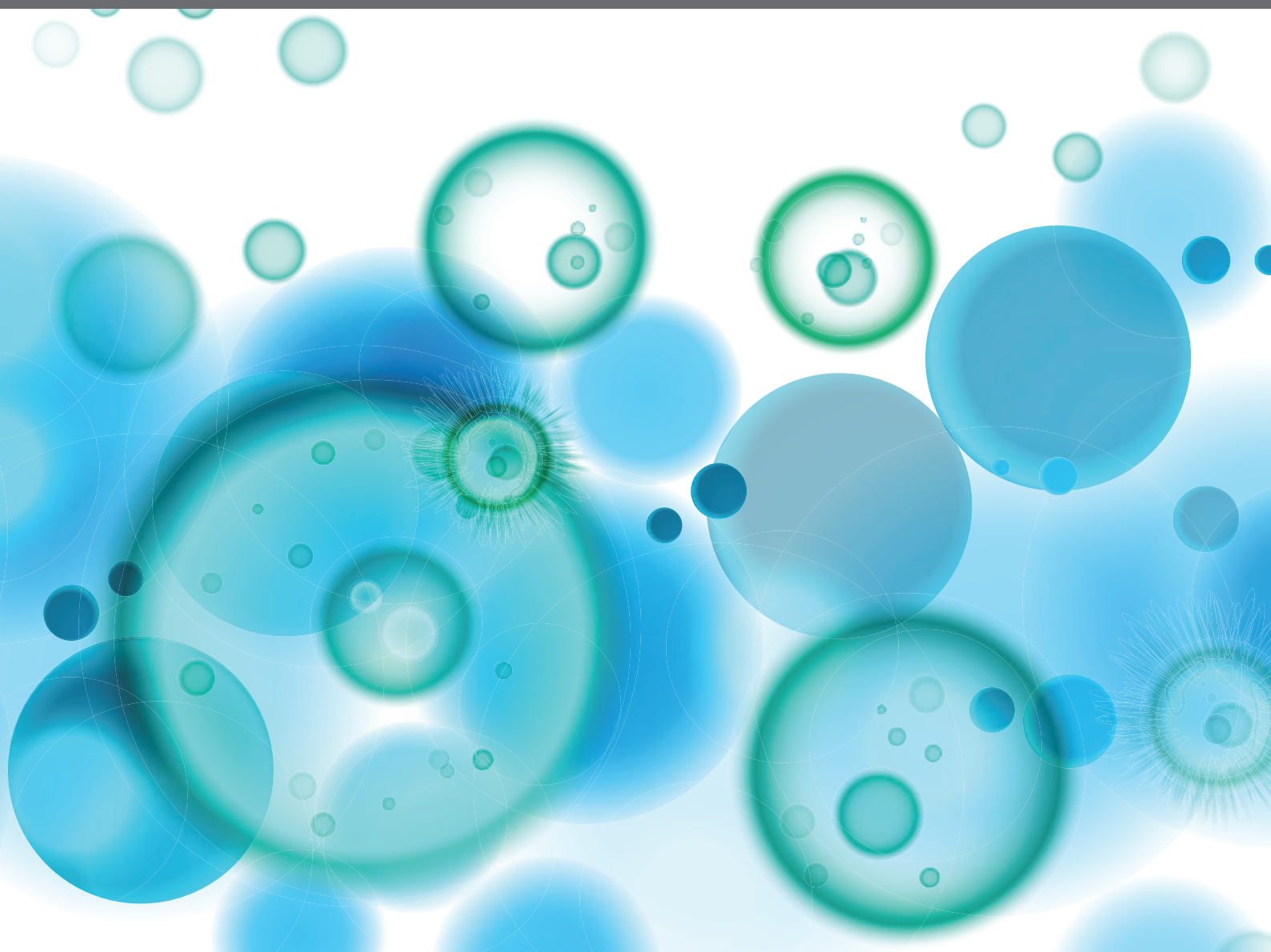


# IMMUNOLOGICAL BIOMARKERS FOR TUBERCULOSIS

EDITED BY: Christof Geldmacher, Hazel Marguerite Dockrell,  
Novel N. Chegou and Adam Penn-Nicholson

PUBLISHED IN: Frontiers in Immunology and Frontiers in Microbiology





# frontiers

## Frontiers eBook Copyright Statement

The copyright in the text of individual articles in this eBook is the property of their respective authors or their respective institutions or funders. The copyright in graphics and images within each article may be subject to copyright of other parties. In both cases this is subject to a license granted to Frontiers.

The compilation of articles constituting this eBook is the property of Frontiers.

Each article within this eBook, and the eBook itself, are published under the most recent version of the Creative Commons CC-BY licence.

The version current at the date of publication of this eBook is CC-BY 4.0. If the CC-BY licence is updated, the licence granted by Frontiers is automatically updated to the new version.

When exercising any right under the CC-BY licence, Frontiers must be attributed as the original publisher of the article or eBook, as applicable.

Authors have the responsibility of ensuring that any graphics or other materials which are the property of others may be included in the CC-BY licence, but this should be checked before relying on the CC-BY licence to reproduce those materials. Any copyright notices relating to those materials must be complied with.

Copyright and source acknowledgement notices may not be removed and must be displayed in any copy, derivative work or partial copy which includes the elements in question.

All copyright, and all rights therein, are protected by national and international copyright laws. The above represents a summary only. For further information please read Frontiers' Conditions for Website Use and Copyright Statement, and the applicable CC-BY licence.

ISSN 1664-8714

ISBN 978-2-88974-186-1

DOI 10.3389/978-2-88974-186-1

## About Frontiers

Frontiers is more than just an open-access publisher of scholarly articles: it is a pioneering approach to the world of academia, radically improving the way scholarly research is managed. The grand vision of Frontiers is a world where all people have an equal opportunity to seek, share and generate knowledge. Frontiers provides immediate and permanent online open access to all its publications, but this alone is not enough to realize our grand goals.

## Frontiers Journal Series

The Frontiers Journal Series is a multi-tier and interdisciplinary set of open-access, online journals, promising a paradigm shift from the current review, selection and dissemination processes in academic publishing. All Frontiers journals are driven by researchers for researchers; therefore, they constitute a service to the scholarly community. At the same time, the Frontiers Journal Series operates on a revolutionary invention, the tiered publishing system, initially addressing specific communities of scholars, and gradually climbing up to broader public understanding, thus serving the interests of the lay society, too.

## Dedication to Quality

Each Frontiers article is a landmark of the highest quality, thanks to genuinely collaborative interactions between authors and review editors, who include some of the world's best academicians. Research must be certified by peers before entering a stream of knowledge that may eventually reach the public - and shape society; therefore, Frontiers only applies the most rigorous and unbiased reviews.

Frontiers revolutionizes research publishing by freely delivering the most outstanding research, evaluated with no bias from both the academic and social point of view. By applying the most advanced information technologies, Frontiers is catapulting scholarly publishing into a new generation.

## What are Frontiers Research Topics?

Frontiers Research Topics are very popular trademarks of the Frontiers Journals Series: they are collections of at least ten articles, all centered on a particular subject. With their unique mix of varied contributions from Original Research to Review Articles, Frontiers Research Topics unify the most influential researchers, the latest key findings and historical advances in a hot research area! Find out more on how to host your own Frontiers Research Topic or contribute to one as an author by contacting the Frontiers Editorial Office: [frontiersin.org/about/contact](https://frontiersin.org/about/contact)



# IMMUNOLOGICAL BIOMARKERS FOR TUBERCULOSIS

Topic Editors:

**Christof Geldmacher**, LMU Munich University Hospital, Germany

**Hazel Marguerite Dockrell**, University of London, United Kingdom

**Novel N. Chegou**, Stellenbosch University, South Africa

**Adam Penn-Nicholson**, Foundation for Innovative New Diagnostics, Switzerland

**Citation:** Geldmacher, C., Dockrell, H. M., Chegou, N. N., Penn-Nicholson, A., eds. (2022). Immunological Biomarkers for Tuberculosis. Lausanne: Frontiers Media SA. doi: 10.3389/978-2-88974-186-1

# Table of Contents

- 07** ***Impact of Persistent Anemia on Systemic Inflammation and Tuberculosis Outcomes in Persons Living With HIV***  
Fernanda O. Demitto, Mariana Araújo-Pereira, Carolina A. Schmaltz, Flávia M. Sant'Anna, Maria B. Arriaga, Bruno B. Andrade and Valeria C. Rolla
- 20** ***GPR183 Regulates Interferons, Autophagy, and Bacterial Growth During Mycobacterium tuberculosis Infection and Is Associated With TB Disease Severity***  
Stacey Bartlett, Adrian Tandhyka Gemiarto, Minh Dao Ngo, Haresh Sajiir, Semira Hailu, Roma Sinha, Cheng Xiang Foo, Léanie Kleynhans, Happy Tshivhula, Tariq Webber, Helle Bielefeldt-Ohmann, Nicholas P. West, Andriette M. Hiemstra, Candice E. MacDonald, Liv von Voss Christensen, Larry S. Schlesinger, Gerhard Walzl, Mette Marie Rosenkilde, Thomas Mandrup-Poulsen and Katharina Ronacher
- 31** ***Increased Frequency of Memory CD4+ T-Cell Responses in Individuals With Previously Treated Extrapulmonary Tuberculosis***  
Beatriz Barreto-Duarte, Timothy R. Sterling, Christina T. Fiske, Alexandre Almeida, Cynthia H. Nochowicz, Rita M. Smith, Louise Barnett, Christian Warren, Amondrea Blackman, Jose Roberto Lapa e Silva, Bruno B. Andrade and Spyros A. Kalams
- 40** ***Systemic Inflammation in Pregnant Women With Latent Tuberculosis Infection***  
Shilpa Naik, Mallika Alexander, Pavan Kumar, Vandana Kulkarni, Prasad Deshpande, Su Yadana, Cheng-Shiun Leu, Mariana Araújo-Pereira, Bruno B. Andrade, Ramesh Bhosale, Subash Babu, Amita Gupta, Jyoti S. Mathad and Rupak Shivakoti
- 49** ***Relevance of QuantiFERON-TB Gold Plus and Heparin-Binding Hemagglutinin Interferon- $\gamma$  Release Assays for Monitoring of Pulmonary Tuberculosis Clearance: A Multicentered Study***  
Carole Chedid, Eka Kokhraidze, Nestani Tukvadze, Sayera Banu, Mohammad Khaja Mafij Uddin, Samanta Biswas, Graciela Russomando, Chyntia Carolina Díaz Acosta, Rossana Arenas, Paulo PR. Ranaivomanana, Crisca Razafimahatratra, Perlinot Herindrainy, Julio Rakotonirina, Antso Hasina Rahehinandrasana, Niaina Rakotosamimanana, Monzer Hamze, Mohamad Bachar Ismail, Rim Bayaa, Jean-Luc Berland, Flavio De Maio, Giovanni Delogu, Hubert Endtz, Florence Ader, Delia Goletti and Jonathan Hoffmann on Behalf of the HINTT Working Group Within the GABRIEL Network
- 60** ***Host Blood RNA Transcript and Protein Signatures for Sputum-Independent Diagnostics of Tuberculosis in Adults***  
Dhanasekaran Sivakumaran, Christian Ritz, John Espen Gjøen, Mario Vaz, Sumithra Selvam, Tom H. M. Ottenhoff, Timothy Mark Doherty, Synne Jenum and Harleen M. S. Grewal
- 70** ***B-Cells and Antibodies as Contributors to Effector Immune Responses in Tuberculosis***  
Willemijn F. Rijnink, Tom H.M. Ottenhoff and Simone A. Joosten

- 89** ***A Two-Gene Signature for Tuberculosis Diagnosis in Persons With Advanced HIV***  
Vandana Kulkarni, Artur T. L. Queiroz, Shashi Sangle, Anju Kagal, Sonali Salvi, Amita Gupta, Jerrold Ellner, Dileep Kadam, Valeria C. Rolla, Bruno B. Andrade, Padmini Salgame and Vidya Mave
- 99** ***A Plasma 5-Marker Host Biosignature Identifies Tuberculosis in High and Low Endemic Countries***  
Bih H. Chendi, Candice I. Snyders, Kristian Tonby, Synne Jenum, Martin Kidd, Gerhard Walzl, Novel N. Chegou and Anne M. Dyrhol-Riise on Behalf of the ScreenTB Consortium
- 112** ***Evaluation of Host Serum Protein Biomarkers of Tuberculosis in sub-Saharan Africa***  
Thomas C. Morris, Clive J. Hoggart, Novel N. Chegou, Martin Kidd, Tolu Oni, Rene Goliath, Katalin A. Wilkinson, Hazel M. Dockrell, Lifted Sichali, Louis Banda, Amelia C. Crampin, Neil French, Gerhard Walzl, Michael Levin, Robert J. Wilkinson and Melissa S. Hamilton for the ILULU Consortium
- 124** ***Validation and Optimization of Host Immunological Bio-Signatures for a Point-of-Care Test for TB Disease***  
Hygon Mutavhatsindi, Gian D. van der Spuy, Stephanus T. Malherbe, Jayne S. Sutherland, Annemieke Geluk, Harriet Mayanja-Kizza, Amelia C. Crampin, Desta Kassa, Rawleigh Howe, Adane Mihret, Jacob A. Sheehama, Emmanuel Nepolo, Gunar Günther, Hazel M. Dockrell, Paul L. A. M. Corstjens, Kim Stanley, Gerhard Walzl, Novel N. Chegou and the AE-TBC ScreenTB Consortia
- 138** ***Identification of Reduced Host Transcriptomic Signatures for Tuberculosis Disease and Digital PCR-Based Validation and Quantification***  
Harriet D. Gliddon, Myrsini Kaforou, Mary Alikian, Dominic Habgood-Coote, Chenxi Zhou, Tolu Oni, Suzanne T. Anderson, Andrew J. Brent, Amelia C. Crampin, Brian Eley, Robert Heyderman, Florian Kern, Paul R. Langford, Tom H. M. Ottenhoff, Martin L. Hibberd, Neil French, Victoria J. Wright, Hazel M. Dockrell, Lachlan J. Coin, Robert J. Wilkinson and Michael Levin on Behalf of the ILULU Consortium
- 151** ***Cell-Mediated Immunological Biomarkers and Their Diagnostic Application in Livestock and Wildlife Infected With Mycobacterium bovis***  
Katrin Smith, Léanie Kleynhans, Robin M. Warren, Wynand J. Goosen and Michele A. Miller
- 168** ***Local Pulmonary Immunological Biomarkers in Tuberculosis***  
Hazel Morrison and Helen McShane
- 176** ***Male Sex Bias in Immune Biomarkers for Tuberculosis***  
Graham H. Bothamley
- 191** ***Validation of Differentially Expressed Immune Biomarkers in Latent and Active Tuberculosis by Real-Time PCR***  
Prem Perumal, Mohamed Bilal Abdullatif, Harriet N. Garland, Isobella Honeyborne, Marc Lipman, Timothy D. McHugh, Jo Southern, Ronan Breen, George Santis, Kalaiarasan Ellappan, Saka Vinod Kumar, Harish Belgode, Ibrahim Abubakar, Sanjeev Sinha, Seshadri S. Vasan, Noyal Joseph and Karen E. Kempsey

- 210 Functional and Activation Profiles of Mucosal-Associated Invariant T Cells in Patients With Tuberculosis and HIV in a High Endemic Setting**  
Avuyonke Balfour, Charlotte Schutz, Rene Goliath, Katalin A. Wilkinson, Sumaya Sayed, Bianca Sossen, Jean-Paul Kanyik, Amy Ward, Rhandzu Ndzhukule, Anele Gela, David M. Lewinsohn, Deborah A. Lewinsohn, Graeme Meintjes and Muki Shey
- 223 Plasma Biomarkers of Risk of Tuberculosis Recurrence in HIV Co-Infected Patients From South Africa**  
Kimesha Pillay, Lara Lewis, Santhuri Rambaran, Nonhlanhla Yende-Zuma, Derseree Archary, Santhanalakshmi Gengiah, Dhineshree Govender, Razia Hassan-Moosa, Natasha Samsunder, Salim S. Abdool Karim, Lyle R. McKinnon, Nesri Padayatchi, Kogieleum Naidoo and Aida Sivro
- 232 Effect of Inflammatory Cytokines/Chemokines on Pulmonary Tuberculosis Culture Conversion and Disease Severity in HIV-Infected and -Uninfected Individuals From South Africa**  
Santhuri Rambaran, Kogieleum Naidoo, Lara Lewis, Razia Hassan-Moosa, Dhineshree Govender, Natasha Samsunder, Thomas J. Scriba, Nesri Padayatchi and Aida Sivro
- 242 Lymphocyte Non-Specific Function Detection Facilitating the Stratification of Mycobacterium tuberculosis Infection**  
Ying Luo, Ying Xue, Yimin Cai, Qun Lin, Guoxing Tang, Huijuan Song, Wei Liu, Liyan Mao, Xu Yuan, Yu Zhou, Weiyong Liu, Shiji Wu, Ziyong Sun and Feng Wang
- 256 Development of ESAT-6 Based Immunosensor for the Detection of Mycobacterium tuberculosis**  
Rishabh Anand Omar, Nishith Verma and Pankaj Kumar Arora
- 268 The Frequency and Effect of Granulocytic Myeloid-Derived Suppressor Cells on Mycobacterial Survival in Patients With Tuberculosis: A Preliminary Report**  
Malika Davids, Anil Pooran, Liezel Smith, Michele Tomasicchio and Keertan Dheda
- 275 Tuberculosis Risk Stratification of Psoriatic Patients Before Anti-TNF- $\alpha$  Treatment**  
Farida Benhadou, Violette Dirix, Fanny Domont, Fabienne Willaert, Anne Van Praet, Camille Loch, Françoise Mascart and Véronique Corbière
- 285 Integrative Multi-Omics Reveals Serum Markers of Tuberculosis in Advanced HIV**  
Sonya Krishnan, Artur T. L. Queiroz, Amita Gupta, Nikhil Gupte, Gregory P. Bisson, Johnstone Kumwenda, Kogieleum Naidoo, Lerato Mohapi, Vidya Mave, Rosie Mngqibisa, Javier R. Lama, Mina C. Hosseinipour, Bruno B. Andrade and Petros C. Karakousis on Behalf of the ACTG A5274 REMEMBER NWCS 414 Study Team
- 295 A 2-Dose AERAS-402 Regimen Boosts CD8<sup>+</sup> Polyfunctionality in HIV-Negative, BCG-Vaccinated Recipients**  
Dhanasekaran Sivakumaran, Gretta Blatner, Rasmus Bakken, David Hokey, Christian Ritz, Synne Jenum and Harleen M. S. Grewal



- 310** *The Evaluation and Validation of Blood-Derived Novel Biomarkers for Precise and Rapid Diagnosis of Tuberculosis in Areas With High-TB Burden*  
Zhen Gong, Yinzong Gu, Kunlong Xiong, Jinxia Niu, Ruijuan Zheng, Bo Su, Lin Fan and Jianping Xie
- 321** *Monocyte and Macrophage miRNA: Potent Biomarker and Target for Host-Directed Therapy for Tuberculosis*  
Pavithra Sampath, Krisna Moorthi Periyasamy, Uma Devi Ranganathan and Ramalingam Bethunaickan
- 332** *Lymphocyte-Related Immunological Indicators for Stratifying Mycobacterium tuberculosis Infection*  
Ying Luo, Ying Xue, Guoxing Tang, Yimin Cai, Xu Yuan, Qun Lin, Huijuan Song, Wei Liu, Liyan Mao, Yu Zhou, Zhongju Chen, Yaowu Zhu, Weiyong Liu, Shiji Wu, Feng Wang and Ziyong Sun
- 346** *Pre-Treatment Neutrophil Count as a Predictor of Antituberculosis Therapy Outcomes: A Multicenter Prospective Cohort Study*  
Anna Cristina C. Carvalho, Gustavo Amorim, Mayla G. M. Melo, Ana Karla A. Silveira, Pedro H. L. Vargas, Adriana S. R. Moreira, Michael S. Rocha, Alexandra B. Souza, María B. Arriaga, Mariana Araújo-Pereira, Marina C. Figueiredo, Betina Durovni, José R. Lapa-e-Silva, Solange Cavalcante, Valeria C. Rolla, Timothy R. Sterling, Marcelo Cordeiro-Santos, Bruno B. Andrade, Elisangela C. Silva, Afrânio L. Kritski and the RePORT Brazil Consortium
- 357** *Antibody Subclass and Glycosylation Shift Following Effective TB Treatment*  
Patricia S. Grace, Sepideh Dolatshahi, Lenette L. Lu, Adam Cain, Fabrizio Palmieri, Linda Petrone, Sarah M. Fortune, Tom H. M. Ottenhoff, Douglas A. Lauffenburger, Delia Goletti, Simone A. Joosten and Galit Alter



# Impact of Persistent Anemia on Systemic Inflammation and Tuberculosis Outcomes in Persons Living With HIV

Fernanda O. Demitto<sup>1†</sup>, Mariana Araújo-Pereira<sup>2,3,4†</sup>, Carolina A. Schmaltz<sup>5</sup>, Flávia M. Sant'Anna<sup>5</sup>, Maria B. Arriaga<sup>2,3,4</sup>, Bruno B. Andrade<sup>2,3,4,6,7,8,9\*†</sup> and Valeria C. Rolla<sup>1,5†</sup>

<sup>1</sup> Programa de Pós-Graduação em Pesquisa Clínica em Doenças Infecciosas, Instituto Nacional de Infectologia Evandro Chagas, Fundação Oswaldo Cruz, Rio de Janeiro, Brazil, <sup>2</sup> Instituto Gonçalo Moniz, Fundação Oswaldo Cruz, Salvador, Brazil, <sup>3</sup> Faculdade de Medicina, Universidade Federal da Bahia, Salvador, Brazil, <sup>4</sup> Multinational Organization Network Sponsoring Translational and Epidemiological Research (MONSTER) Initiative, Salvador, Brazil, <sup>5</sup> Laboratório de Pesquisa Clínica em Micobacterioses (LAPCLIN-TB), Instituto Nacional de Infectologia Evandro Chagas, Fundação Oswaldo Cruz, Rio de Janeiro, Brazil, <sup>6</sup> Escola Bahiana de Medicina e Saúde Pública (EBMSP), Salvador, Brazil, <sup>7</sup> Universidade Salvador (UNIFACS), Laureate International Universities, Salvador, Brazil, <sup>8</sup> Wellcome Centre for Infectious Diseases Research in Africa, Institute of Infectious Disease and Molecular Medicine, University of Cape Town, Cape Town, South Africa, <sup>9</sup> Division of Infectious Diseases, Department of Medicine, Vanderbilt University School of Medicine, Nashville, TN, United States

## OPEN ACCESS

### Edited by:

Novel N. Chegou,  
Stellenbosch University, South Africa

### Reviewed by:

Won Fen Wong,  
University of Malaya, Malaysia  
Isobella Honeyborne,  
University College London,  
United Kingdom

### \*Correspondence:

Bruno B. Andrade  
bruno.andrade@fiocruz.br

<sup>†</sup> These authors have contributed  
equally to this work

### Specialty section:

This article was submitted to  
Microbial Immunology,  
a section of the journal  
Frontiers in Immunology

**Received:** 28 July 2020

**Accepted:** 04 September 2020

**Published:** 24 September 2020

### Citation:

Demitto FO, Araújo-Pereira M, Schmaltz CA, Sant'Anna FM, Arriaga MB, Andrade BB and Rolla VC (2020) Impact of Persistent Anemia on Systemic Inflammation and Tuberculosis Outcomes in Persons Living With HIV. *Front. Immunol.* 11:588405. doi: 10.3389/fimmu.2020.588405

Tuberculosis (TB) is associated with systemic inflammation and anemia, which are aggravated in persons living with HIV (PLWH). Here, we characterized the dynamics of hemoglobin levels in PLWH coinfecting with TB undergoing antitubercular therapy (ATT). We also examined the relationships between anemia and systemic inflammatory disturbance as well as the association between persistent anemia and unfavorable clinical outcomes. Data on several blood biochemical parameters and on blood cell counts were retrospectively analyzed in a cohort of 256 TB/HIV patients from Brazil during 180 days of ATT. Multidimensional statistical analyses were employed to profile systemic inflammation of patients stratified by anemia status (hemoglobin levels <12 g/dL for female and <13.5 g/dL for male individuals) prior to treatment and to perform prediction of unfavorable outcomes, such as treatment failure, loss to follow up and death. We found that 101 (63.63%) of patients with anemia at pre-ATT persisted with such condition until day 180. Such individuals exhibited heightened degree of inflammatory perturbation (DIP), which in turn was inversely correlated with hemoglobin levels. Recovery from anemia was associated with increased pre-ATT albumin levels whereas persistent anemia was related to higher total protein levels in serum. Multivariable regression analysis revealed that lower baseline hemoglobin levels was the major determinant of the unfavorable outcomes. Our findings demonstrate that persistent anemia in PLWH during the course of ATT is closely related with chronic inflammatory perturbation. Early intervention to promote recovery from anemia may improve ATT outcomes.

**Keywords:** HIV, tuberculosis, anemia, inflammation, treatment outcome

## INTRODUCTION

Tuberculosis (TB) remains as a leading cause of death from infection by a single pathogen and also among people living with human immunodeficiency virus (HIV) (1). Persons living with HIV (PLWH) exhibit up to 19 times higher risk of developing active TB (2). In addition, TB is one of the most common opportunistic infections in PLWH. In fact, a total of 1.5 million people died from TB in 2018, including 251,000 PLWH (1). Understanding the determinants of clinical outcomes of PLWH coinfecting with TB is critical to improve patient care.

Anemia is also a global public health problem and is diagnosed based on concentration of hemoglobin (Hb), specifically when it falls below established cut-off values; 12.0 g/dL for women and 13.5 g/dL for men (3). Low concentrations of Hb are a frequent complication of both TB and HIV infections, and its occurrence is associated with increased morbidity and mortality (4). Several causes of anemia are described, including iron deficiency and chronic inflammation (5–7). Prevalence of anemia in TB patients is reported to range between 32 and 96% (8), whereas in PLWH, this estimate varies from 1.3 to 95% (4). The extreme discrepancies in frequency of anemia associated with either TB and/or HIV infections published by several studies are thought to be influenced by factors that include study design, geographic location as well as clinical and epidemiological characteristics of patients.

Many studies have associated anemia with poor prognosis and increased mortality after TB diagnosis (6, 7, 9). In patients with TB, anemia has been attributed to be caused by chronic inflammation (10). It has also been shown that anemia is related to accelerated HIV/AIDS disease progression in PLWH (11). This latter study concluded that Hb levels is a robust biomarker to predict death independent of CD4<sup>+</sup> T-cell count and HIV viral load values (11). More recently, a prospective investigation of antiretroviral therapy (HAART)-naïve PLWH reported that concurrent anemia and systemic inflammation were associated with higher risk of HAART failure (12). A potential explanation for the association between anemia and poor outcomes in HIV/AIDS and/or TB is that low Hb concentrations reflect more advanced disease staging. It is still to be defined the relationship between anemia and systemic inflammation in the context of antitubercular treatment (ATT) in PLWH and whether recovery from anemia during ATT in PLWH is related to improved prognosis.

In a study from Brazil, we have recently described that risk factors for mortality were distinct between HAART-naïve and HAART-experienced PLWH patients coinfecting with TB. Indeed, in HAART-naïve patients, but not in those who were already undertaking antiretrovirals, the odds of death were substantially higher in patients who developed immune reconstitution inflammatory syndrome (IRIS) during the study follow up (13). This finding suggests that inflammation during the course of ATT in PLWH is related to unfavorable outcomes. In the present study, we expanded our analyses to investigate the relationship between the presence and severity of anemia and the cellular and biochemical profile of systemic inflammation in PLWH and TB in Brazil. We also tested whether low

levels of Hb measured at pre-ATT could be used to predict unfavorable outcomes.

## MATERIALS AND METHODS

### Ethics Statement

The study was approved by the Institutional Review Board of the Instituto Nacional de Infectologia Evandro Chagas (INI) (CAAE: 71191417.8.0000.5262). Written informed consent was obtained from all participants, and all clinical investigations were conducted according to the principles expressed in the Declaration of Helsinki.

### Population and Design

A prospective cohort has been followed at the Clinical Research Laboratory on Mycobacteria (LAPCLIN-TB) of the INI Evandro Chagas, Fundação Oswaldo Cruz, Rio de Janeiro, Brazil, since 2000. The present study is a retrospective assessment performed between 2008 and 2016, with data obtained from this cohort. Data were collected from electronic medical records based on standardized information of a defined template used in each patient's visit for the whole cohort. PLWH 18 years and older, with clinical signs and symptoms of TB were included. The diagnosis of TB was made when *Mycobacterium tuberculosis* (Mtb) detection was positive in any sample collected (acid fast bacilli smear, Gene Xpert or culture from clinical specimens). In cases without bacteriological confirmation, the diagnosis was established by suggestive imaging analysis, histopathological examination, together with clinical and epidemiological findings consistent with TB. For those who had a negative culture, a positive therapeutic test with TB drugs was considered, after excluding other opportunistic diseases for differential diagnosis. Patients that initiated TB treatment and were diagnosed later with non-tuberculous mycobacteria as well as those who showed rifampicin and isoniazid resistance (multidrug resistance) were excluded. Patients with bone, mammary, renal or ocular TB were excluded, since these clinical forms can have very subtle, asymptomatic presentations, making it difficult to be compared to the other forms.

### Definitions

Anemia was defined according to World Health Organization (WHO) guideline criteria: Hb value < 13.5 g/dL for men and <12 g/dL for women.

Tuberculosis was classified as pleuropulmonary (when restricted to the lungs and/or pleura), extra-pulmonary (when just one extra-pulmonary site was identified) or disseminated (involving spleen, liver, bone marrow, or at least 2 non-contiguous sites).

Discharge due to cure, with or without etiologic confirmation of the diagnosis of TB, was considered a favorable outcome. Patients were defined as cured through clinical and/or radiologic improvement. Unfavorable outcome was defined as death, loss to follow up and treatment failure following the WHO guidelines. The cause of death was determined after thorough review of

relevant clinical, microbiological and pathological data of each deceased patient.

## Antiretroviral and Antitubercular Therapies

Highly active antiretroviral therapy was offered according to contemporary Brazilian National Guidelines that were periodically updated (14). The first line ATT regimen was the combination of rifampicin, isoniazid and pyrazinamide during the two initial months, followed by rifampicin and isoniazid for 4 months, except when the continuation phase needed to be extended to 7 months such as in cases with central nervous system TB. From July 2009 on, ethambutol was added to the intensive phase regimen following a new recommendation of the National TB program of the Brazilian Ministry of Health (15). TB treatment scheme was adjusted in cases of severe adverse reactions, drug resistance and HAART regimens that precluded the use of rifampicin.

## Follow Up Visits

Visits included in this study were done at baseline, 60 and 180 days after TB therapy initiation. HAART were initiated after TB treatment according to decision from each physician and following the Brazilian TB treatment Guidelines (14). Information collected at the baseline visit included socio demographic data as well as previous TB and HAART, clinical presentation of TB, comorbidities like diabetes, hypertension, hepatitis (B and C), opportunistic diseases as well as CD4<sup>+</sup> T-cell count and HIV VL among other variables. At baseline and in the follow up timepoints, patients underwent blood tests according to the INI's clinical laboratory routine, with complete blood count and biochemical tests (creatinine, urea, total and direct bilirubin, albumin, alkaline phosphatase, uric acid, AST, GGT, ALT and total proteins).

Some patients ( $n = 06$ ) who abandoned TB treatment (ATT loss to follow up) had recorded data on Complete Blood Count (CBC) and biochemical assessments in blood after the date of the outcome established by the present study (non-compliance), because those patients had been following up at INI by other specialties outside the TB outpatient clinic.

## Statistical Data Analysis

Three timepoints were considered: baseline, day 60 (D60) and day 180 (D180) of ATT. To perform baseline analysis, were used data from 256 patients. Due to lack of data in the subsequent timepoints (6.6% were missing data at D60 and 25.4% at D180), only 191 (74.6%) patients with complete laboratory data at all timepoints were considered for longitudinal analysis. Descriptive statistics was used to present data, use the median values with interquartile ranges (IQR) as measures of central tendency and dispersion, respectively, for continuous variables. Categorical variables were described using frequency (no.) and proportions (%). The Pearson chi-square test was used to compare categorical variables between study groups. The Mann-Whitney  $U$  test (for two

unmatched groups), the Wilcoxon matched pairs test (for two matched groups), the Kruskal-Wallis test (for more than 2 unmatched groups) or the Jonckheere-Terpstra permutation and asymptotic test (for time series) were used to compare continuous variables. The Spearman rank test was used to assess correlations between indicated markers, conditions and timepoints. A multivariable logistic regression analysis model was used to identify independent determinants of persistent anemia and unfavorable treatment outcomes. The results were presented in the form of adjusted odds ratio (aOR) and 95% confidence intervals (CI).

The degree of inflammatory perturbation (DIP) is based molecular degree of perturbation (MDP) (16), an adaptation of the molecular distance to health previously described (17). In the present study, instead of using gene expression values, we inputted biochemical markers concentrations, HIV viral load and blood cells counts. Thus, herein, the average level and standard deviation of a baseline reference group (non-anemic at baseline) were calculated for each biomarker. The DIP score of each individual biomarker was defined by z-score normalization, where the differences in concentration levels from the average of the biomarker in reference group was divided by the reference standard deviation. The DIP score represents the differences by number of standard deviations from the control group.

Hierarchical cluster analysis (Ward's method) using values of z-score normalized data was employed to depict the overall expression profile of indicated markers in the study subgroups. In this analysis, the dendrograms represent the Euclidean distance (inferring degree of similarity).

All analyses were pre-specified. Differences with  $p$ -values below 0.05 after adjustment for multiple comparisons (Holm-Bonferroni) were considered statistically significant. The statistical analyses were performed using mdp (version 1.8.0), rstatix (version 0.4.0), stats (version 3.6.2), and caret (version. 6.0.86) R packages.

## RESULTS

### Characteristics of the Study Participants

During the period from 2008 to 2016, 273 patients were screened, but 17 were excluded from all the analyses because of lack of data at baseline. Thus, the initial analysis included 256 patients, out of whom 219 (85.6%) were anemic and 37 (14.4%) were not anemic at baseline. The vast majority of study participants were male (71%), and the median age was 37 years old (IQR: 31–46). Individuals with anemia at baseline were similar to non-anemic participants with regard to, age, sex, overall frequency of comorbidities and life-habits (Table 1). Anemic patients more frequently self-reported weight loss (>10% of body weight) before initiating treatment and displayed lower CD4<sup>+</sup> T-cell counts and higher HIV viral loads than those non-anemic at the study baseline (Table 1). Frequency of HAART use before TB diagnosis was higher in non-anemic study participants (65% in non-anemic vs. 43% in anemic,  $p = 0.021$ ; Table 1).



**TABLE 1 |** Characteristics of the study population.

Characteristic	All (n = 256)	Anemic at baseline (n = 219)	Non-anemic at baseline (n = 37)	p-value
Age (years), median (IQR)	37 (31–46)	37 (30.7–46)	37 (33–46)	0.504
Sex, no. (% male)	182 (71)	157 (71.7)	25 (67.6)	0.996
Weight loss (>10%), no. (%)	190 (74.2)	174 (79.5)	16 (43.2)	<0.01
Smoking, no. (%)	131 (51.2)	114 (52)	17 (45.9)	0.948
Use of illicit drugs, no. (%)	74 (28.9)	60 (27.3)	14 (37.8)	0.185
Alcohol abuse <sup>1</sup> , no. (%)	88 (34.3)	80 (36.5)	8 (21.6)	0.133
Baseline CD4 count (cells/mm <sup>3</sup> ), median (IQR)	170.5 (52–321.2)	153 (42.5–304.5)	294 (158–560)	<0.01
Baseline Viral Load log10 (copies/mL), median (IQR) (n = 165)	4.3 (1.69–0.5.23)	4.41 (2.5–5.31)	1.79 (1.69–4.22)	<0.01
D180 CD4 count (cells/mm <sup>3</sup> ), median (IQR)	292.5 (165–432)	258 (157.5–403)	423 (266–603.5)	0.018
D180 Detectable Viral Load log10 (copies/mL), median (IQR) (n = 76)	3.21 (1.80–4.67)	3.17 (1.79–4.68)	3.42 (2.03–4.03)	0.766
D180 Undetectable VL, no. (%)	133 (52)	105 (65.2)	25 (38.5)	0.320
Days until outcome <sup>2</sup> , median (IQR)	189 (178.7–259.7)	189 (180–265)	189 (168–247.5)	0.564
Viral Hepatitis (B and/or C), no. (%)	25 (9.7)	21 (9.48)	4 (10.8)	0.945
Hypertension, no. (%)	21 (8.2)	16 (7.3)	5 (13.5)	0.270
Diabetes, no. (%)	32 (12.5)	28 (12.7)	4 (10.8)	0.946
Previous tuberculosis (%)	64 (25)	52 (23.7)	12 (32.4)	0.355
Complete TB treatment previous, no. (% of previous TB)	44 (68.8)	35 (67.3)	9 (75)	0.742
HAART use before TB, no. (%)	118 (46)	94 (42.9)	24 (64.8)	0.021
HAART during TB treatment, no. (%)	235 (91.7)	202 (92.3)	33 (89.2)	0.763
IRIS upon HAART initiation, no. (%)	12 (4.68)	12 (5.47)	0 (0)	–

To define anemia according to baseline (D0) hemoglobin, the cut-off point of 12 g/dL for women and 13.5 g/dL for men was used. Data are shown as median and interquartile (IQR) range or frequency (percentage). Data were compared between the clinical groups using the Mann–Whitney U test (continuous variables) or the Pearson's  $\chi^2$  test (for data on frequency). Complete data at baseline: 256 patients; Complete data at day 60: 239 (93.4%) patients; Complete data at day 180: 191 (74.6%) patients. <sup>1</sup>The physicians also collected information about current use of illicit drugs and alcohol (Y/N to each) during the baseline interview. Potential problematic alcohol use was assessed with the CAGE questionnaire, with scores of 2 or greater indicating clinically significant alcohol problems. <sup>2</sup>Outcomes: Favorable (cure) and Unfavorable (failure, loss follow-up or death). IQR, Interquartile Range; IRIS, Immune reconstitution Inflammatory Syndrome; TB, Tuberculosis; HAART, Highly Active Antiretroviral Therapy.

To perform the longitudinal analysis, 82 of these patients were excluded because due to lack of data at some time point of the TB treatment (as described in “Materials and Methods”). Thus, 191 patients were further considered, out of whom 161 (84.3%) were anemic and 30 (15.7%) were not anemic at baseline. The median TB treatment period was 189 days for both groups. At day 180 of treatment, CD4<sup>+</sup> T-cell counts increased in both study groups, but values in the group of participants who were anemic at the study baseline persisted substantially lower than those measured in non-anemic patients ( $p = 0.018$ ; **Table 1**). Nevertheless, both frequency of individuals with undetectable HIV viral loads and median values with detectable viral loads were indistinguishable between study participants stratified based on anemia at baseline. There was no difference in the type of antitubercular treatment regimen between the study groups.

## Presence of Anemia Is Associated With Specific Cellular and Biochemical Profiles in Peripheral Blood of PWH Coinfected With TB

The overall differences in cell counts and values of biochemical parameters measured at pre-ATT for anemic and non-anemic

TB patients are described in **Supplementary Table 1**. As expected, erythrocyte counts, and values of hematocrit and hemoglobin were lower in anemic compared to non-anemic study participants. In addition, anemic patients exhibited lower counts of several leukocytes including lymphocytes and eosinophils at the study baseline (**Supplementary Table 1**). Additional analyses of the CBC parameters using hierarchical clustering of z-score normalized data and computation of fold change were performed to evaluate the dynamicity of the values over time in each group (**Figure 1A**). We observed a distinct profile between the groups, with three clusters defined in the heatmap, where the latter cluster (hemoglobin, hematocrit and erythrocyte) was the most consistent in both groups, with few changes mainly in the group of patients without anemia before treatment (baseline). Furthermore, it was possible to observe that, in the anemic participants, there was a significant difference in all parameters over time, mainly when comparing the baseline with the end of TB treatment (D180).

In regard to biochemical parameters, statistically significant differences were found in levels of ALT, AST and GGT, which were all higher in anemic patients at baseline, whereas the levels of albumin were lower

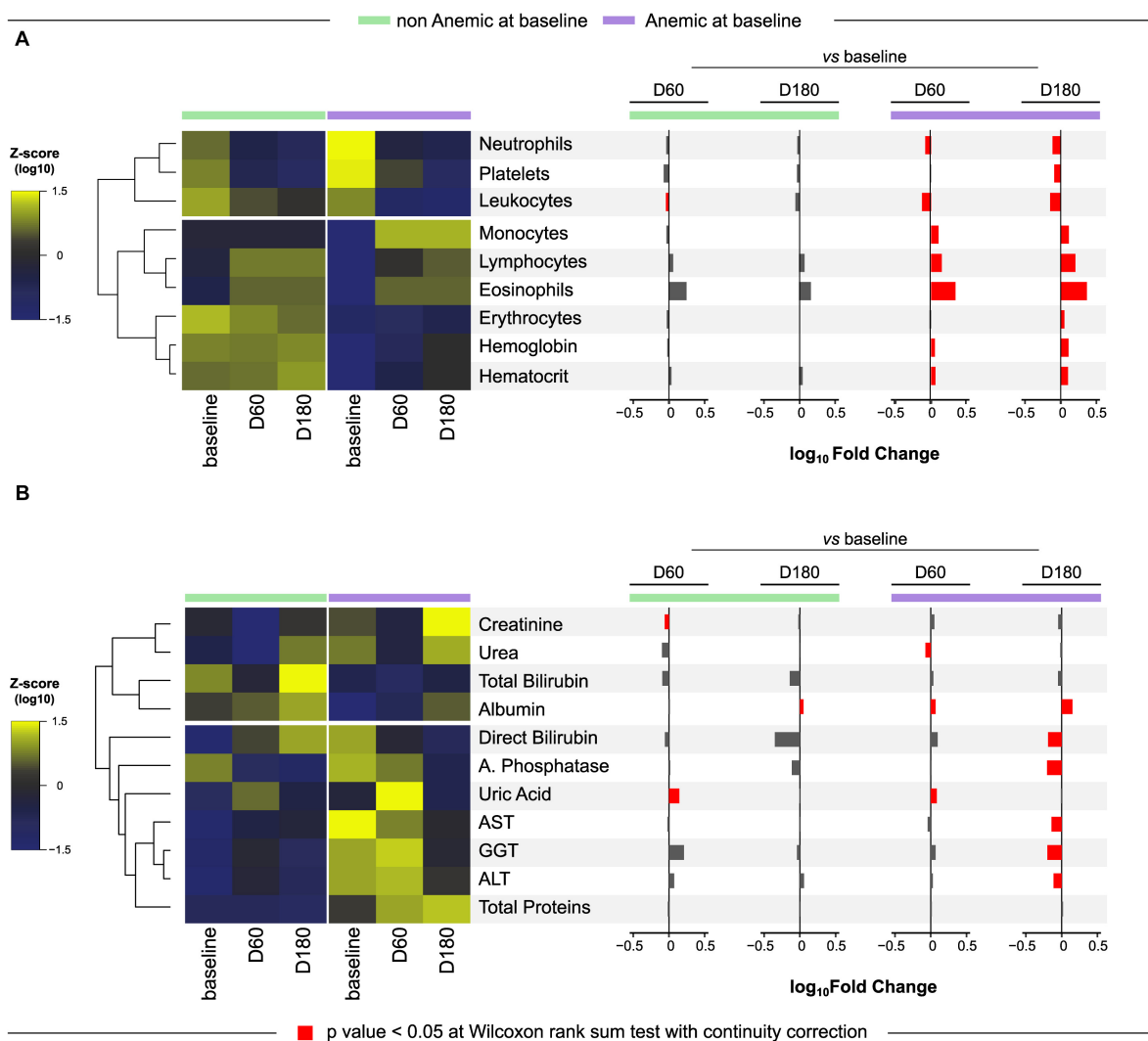


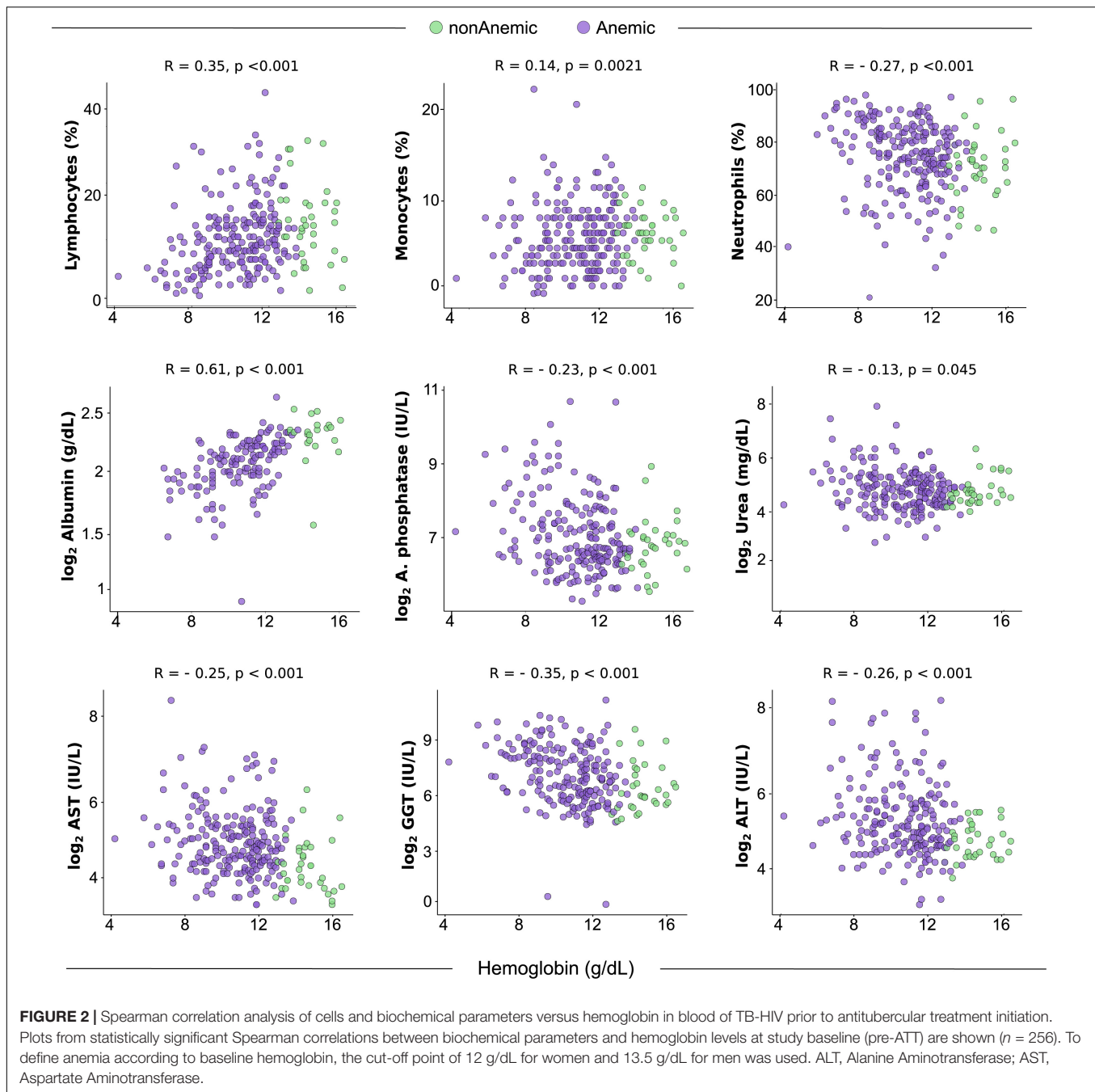
**FIGURE 1 |** Differential change in biomarkers of anemic and non-anemic patients. A Heatmap was designed to depict the overall pattern of complete blood counts (CBC) **(A)** and biochemical markers **(B)** at all timepoints in anemic and non-anemic at different study timepoints of anti-tubercular treatment. A two-way hierarchical cluster analysis (Ward's method) was performed. Dendrograms represent Euclidean distance. Expression scale represents Z-score normalization from the median at each timepoint and group. To define anemia according to baseline hemoglobin, the cut-off point of 12 g/dL for women and 13.5 g/dL for men was used. A  $\log_{10}$  of fold-change was calculated and statistical analyses were performed using the Mann-Whitney  $U$  adjusted test. Significant differences ( $p < 0.05$ ) between anemic and non-anemic patients for each time point are highlighted in red bars. Data are from 191 patients who had complete information on cell counts and biochemical measurements at all study timepoints.

(Supplementary Table 1 and Figure 1B). Additional hierarchical cluster and fold change analysis performed with biochemical parameters revealed a distinct profile between the groups (Figure 1B). Again, small changes over time in the group without anemia at baseline were observed, with increased levels of uric acid and decreased levels of creatinine at D60 and with increase in albumin levels at D180, comparing with baseline. In the group that presented anemia at baseline, the differences in levels of biomarkers were more pronounced. We found that, at D60, a decrease in urea levels and increase in uric acid and albumin levels were detected compared to baseline. At D180, there were significantly higher values

of albumin and lower values of direct bilirubin, alkaline phosphatase, AST, GGT and ALT, than those measured at the study baseline.

### Correlation Between Cells and Biochemical Parameters With Hemoglobin

The results presented above indicate that anemia is associated with a distinct profile of cell counts and biochemical parameters in peripheral blood of patients with HIV-TB coinfection prior to initiation of ATT. We next examined the correlations between Hb levels and cell counts or



values of the biochemical parameters (Figure 2). We observed that gradual increases in Hb values were related with decreases in percentage of neutrophils ( $r = -0.27$ ;  $p < 0.001$ ) and levels of ALT ( $r = -0.26$ ;  $p < 0.001$ ), AST ( $r = -0.25$ ;  $p < 0.001$ ), GGT ( $r = -0.35$ ;  $p < 0.001$ ), Alkaline Phosphatase ( $r = -0.23$ ;  $p < 0.001$ ), and Urea ( $r = -0.13$ ;  $p = 0.045$ ). Furthermore, frequency of lymphocytes ( $r = 0.35$ ;  $p < 0.001$ ) and monocytes ( $r = 0.14$ ;  $p = 0.021$ ), as well as levels of albumin ( $r = 0.61$ ;  $p < 0.001$ ) were increased proportionally to elevations in Hb levels (Figure 2). These findings reinforce the idea that degree of anemia is associated

with changes in cellular and biochemical disturbances in peripheral blood.

## Dynamic Change of Hemoglobin Levels Upon Initiation of Anti-TB Treatment

In order to better understand the impact of ATT commencement in the anemia, we prospectively investigated Hb levels at different time points of therapy (Figure 3). This approach revealed a differential dynamic of changes in Hb levels depending on the anemia status at the study baseline (Figure 3A). Indeed, a gradual

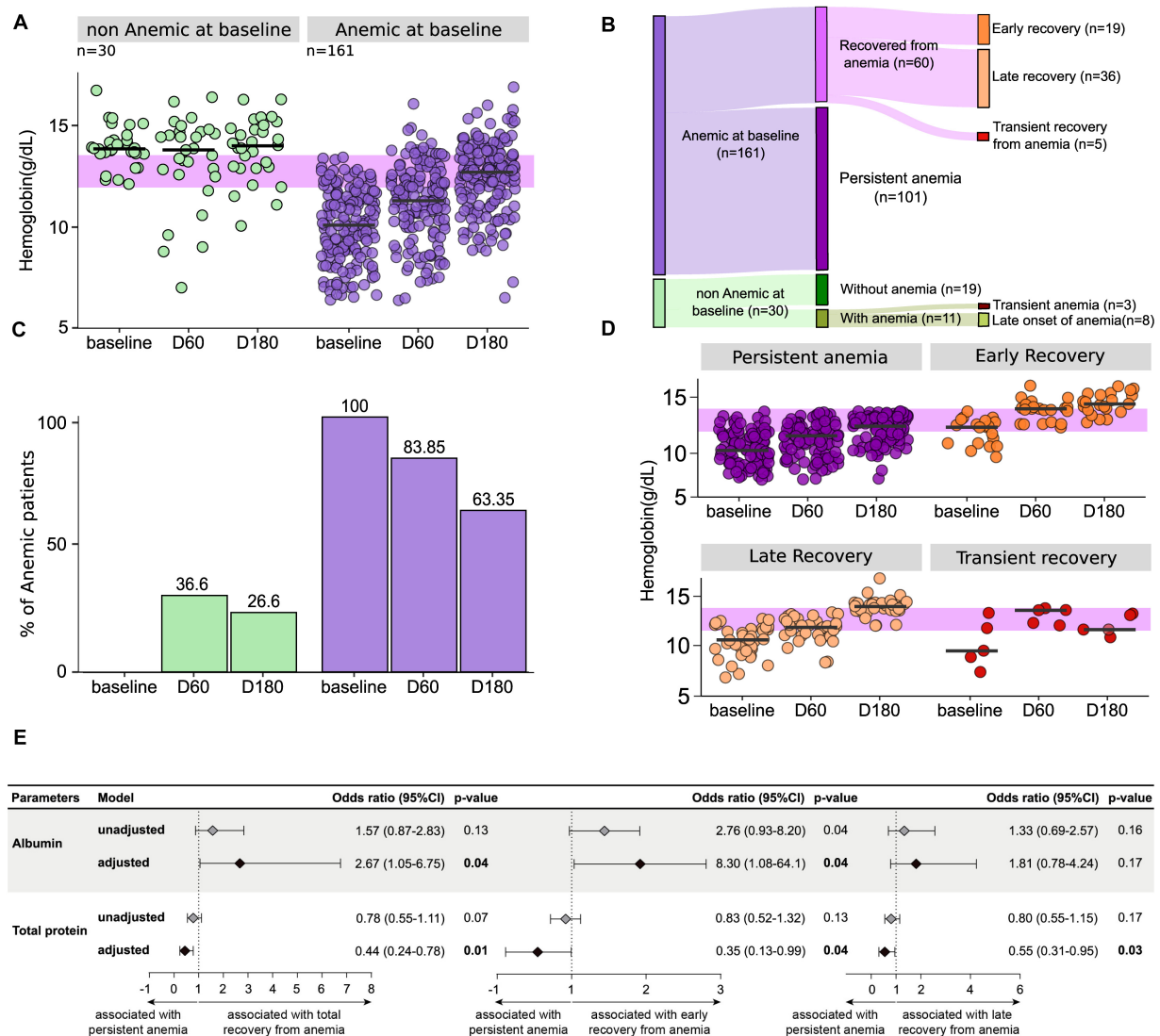


**FIGURE 3 |** The majority of the anemic patients at baseline persist with low levels of hemoglobin after initiation of anti-tubercular treatment. To define anemia according to baseline hemoglobin, the cut-off point of 12 g/dL for women and 13.5 g/dL for men was used. **(A)** Hemoglobin levels at different time points of antitubercular therapy in the longitudinal population ( $n = 191$ ) as well as in the groups of patients with or without anemia at baseline of treatment are shown. Anemic group presented statistically significant difference with  $p < 0.001$  between baseline and timepoints after 2 months (D60 and D180) using Wilcoxon rank sum test with corrections. On Jonckheere-Terpstra permutation test, where an increase in one variable results in an increase or decrease in another variable, both groups presented  $p = 0.001$  to “increase” hypothesis, with number of permutation equal to 1000. Using Jonckheere-Terpstra asymptotic test,  $p$ -value of non-anemic group was 0.851 and  $p$ -value of anemic group was  $< 2.2 \times 10^{-16}$ . Green dots represent non-anemic TB patients at baseline and purple dots represent anemic TB patients at baseline. **(B)** To define a patient as recovered from anemia, were considered normal levels (above the cut-off) of hemoglobin in any time point after D0. Chi-square test comparing D0 and D180 in both groups returned  $p < 0.00001$ . Green bars represent non-anemic TB patients at baseline and purple bars represent anemic TB patients at baseline. **(C)** Of the 161 patients who had anemia before starting treatment, 37.3% ( $n = 60$ ) increased the values to normal hemoglobin levels at some time point. Of these, 95% were completely recovered ( $n = 55$ ), so that 35% ( $n = 19$ ) were recovered early (D60), and 60% ( $n = 36$ ) were recovered late (D180). Finally, 5% ( $n = 5$ ) of the patients who were anemic at study baseline presented a transient recovery (recovered at day 60 but were once again anemic at D180). 36.6% ( $n = 11$ ) of the 30 patients without anemia at baseline developed anemia in D60, but three of them recovered normal hemoglobin values at D180. **(D)** Hemoglobin levels at different time points of antitubercular therapy in the population of anemic patients at baseline, divided according to the time of recovery. Using Jonckheere-Terpstra asymptotic test and Wilcoxon rank sum test with corrections, only the transient recovery group (that showed higher levels of hemoglobin at time 60 but had anemia at 180) did not exhibit a significant  $p$ -value between the timepoints. **(E)** Logistic binomial regression model was used to test independent associations between biochemical and clinical parameters and total recovery from anemia status at baseline, early recovery (recovery from anemia in  $\leq 60$  days from baseline) or late recovery (recovery from anemia in  $> 60$  days from baseline). The condition persistent anemia (anemia from baseline to day 180) was used as reference to test associations. Only parameters which remained with  $p \leq 0.2$  in univariate analysis (**Supplementary Table 2** for details) model were inputted in the adjusted model. (95%CI, 95% confidence interval). Associations reported in **(E)** are for increases in 1 unit in plasma concentrations of the indicated markers. Data are from 191 patients who had complete information on cell counts and biochemical measurements at all study timepoints.



increase in Hb levels over time on treatment was observed in the group of anemic participants (linear trend  $p$ -value:  $<0.001$ ), whereas such levels did not substantially change in those who were not anemic at baseline. Curiously, 11 (36.6%) patients who were non-anemic at baseline developed anemia at day 60, from whom 8 (26.6% of the non-anemic group) were also anemic at day 180 of ATT (**Figure 3B**). Among the initially anemic patients, 83.85% were still anemic at day 60 and 63.35% persisted with anemia at day 180 of therapy (**Figure 3B**). A Sankey diagram was used to illustrate the dynamic change of anemia status over time on ATT (**Figure 3C**).

Hence, we observed that the vast majority of the participants who were anemic at the study baseline persisted with anemia until at least day 180 of therapy, whereas 19 (11.8%) individuals recovered from anemia at day 60 (early recovery), 36 (22.36%) recovered only by day 180 (late recovery), and 5 (3.1%) recovered at day 60 but were once again anemic at day 180 (transient recovery). The characteristics of these subpopulations are shown in the **Supplementary Table 2**. The dynamicity of hemoglobin levels in the different subgroups of anemic patients identified in the Sankey diagram is described in **Figure 3D**. Among the patients who had anemia at the baseline, with the exception of the transient recovery group, all exhibited a significant increase in hemoglobin levels over time of ATT ( $p$ -values  $< 0.05$ ) (**Figure 3D**).

## Persistent Anemia Is Associated With Augmented Degree of Inflammatory Perturbation

Given that the majority of anemic patients persisted with anemia during the time of ATT regardless of the gradual increase in hemoglobin levels, we tested whether such condition was related to a chronic and unresolved inflammatory disturbance. To do so, we employed a mathematical maneuver named Molecular Degree of Perturbation (MDP), which has been used by our group and others to estimate the overall degree of inflammation and/or immune activation (18–20). In the present study, we included cells (from CBC), viral load, CD4 counts and biochemical parameters (creatinine, urea, total and direct bilirubin, albumin, alkaline phosphatase, uric acid, AST, GGT, ALT and total proteins) to create a score henceforth named Degree of Inflammatory Perturbation (DIP) (**Figure 4A**). We found that in general, anemia was associated with increased DIP values measured at both baseline (**Figure 4B**) and at day 180 of ATT (**Figure 4C**), with the highest levels being detected in the group of persistent anemia. Strikingly, the DIP score values exhibited strong inverse correlations with hemoglobin levels both at baseline ( $r = -0.74$ ;  $p < 0.001$ ) and at day 180 ( $r = -0.61$ ;  $p < 0.001$ ), highlighting that the degree of anemia and activation of inflammation are concurrent processes.

Additional analyses demonstrated that, as expected, patients who had an early recovery from anemia exhibited significantly higher baseline values for erythrocytes, Hb, hematocrit, neutrophils (**Supplementary Figure 1**) and albumin (**Supplementary Figure 2**) than those who did not recover. Patients who had a late recovery displayed significantly higher

baseline values of Hb and hematocrit compared to those who persisted anemic (**Supplementary Figures 1, 2**). The prospective comparisons have also identified discrepancies in cell counts and concentrations of biochemical parameters between the subgroups of patients based on recovery from anemia, which are summarized in **Supplementary Figures 1, 2**.

The findings described above led us to hypothesize that the distinct profile of cell counts, and levels of biochemical parameters, measured at pre-ATT, is associated with persistent anemia. Thus, a stepwise binary multivariate logistic regression analysis was performed to test if biochemical parameters measured at pre-ATT (baseline) are able to predict recovery from anemia. Results demonstrated that increases in concentrations of albumin were directly associated with recovery from anemia (aOR: 2.67, 95% CI: 1.05–6.75,  $p = 0.04$ ) whereas increases in total proteins were directly associated with persistent anemia (aOR: 0.44, 95% CI: 0.24–0.78,  $p = 0.01$ ) (**Figure 3E**). Similar trends in associations were observed when the major group of participants who recovered from anemia were further stratified in early and late recovery.

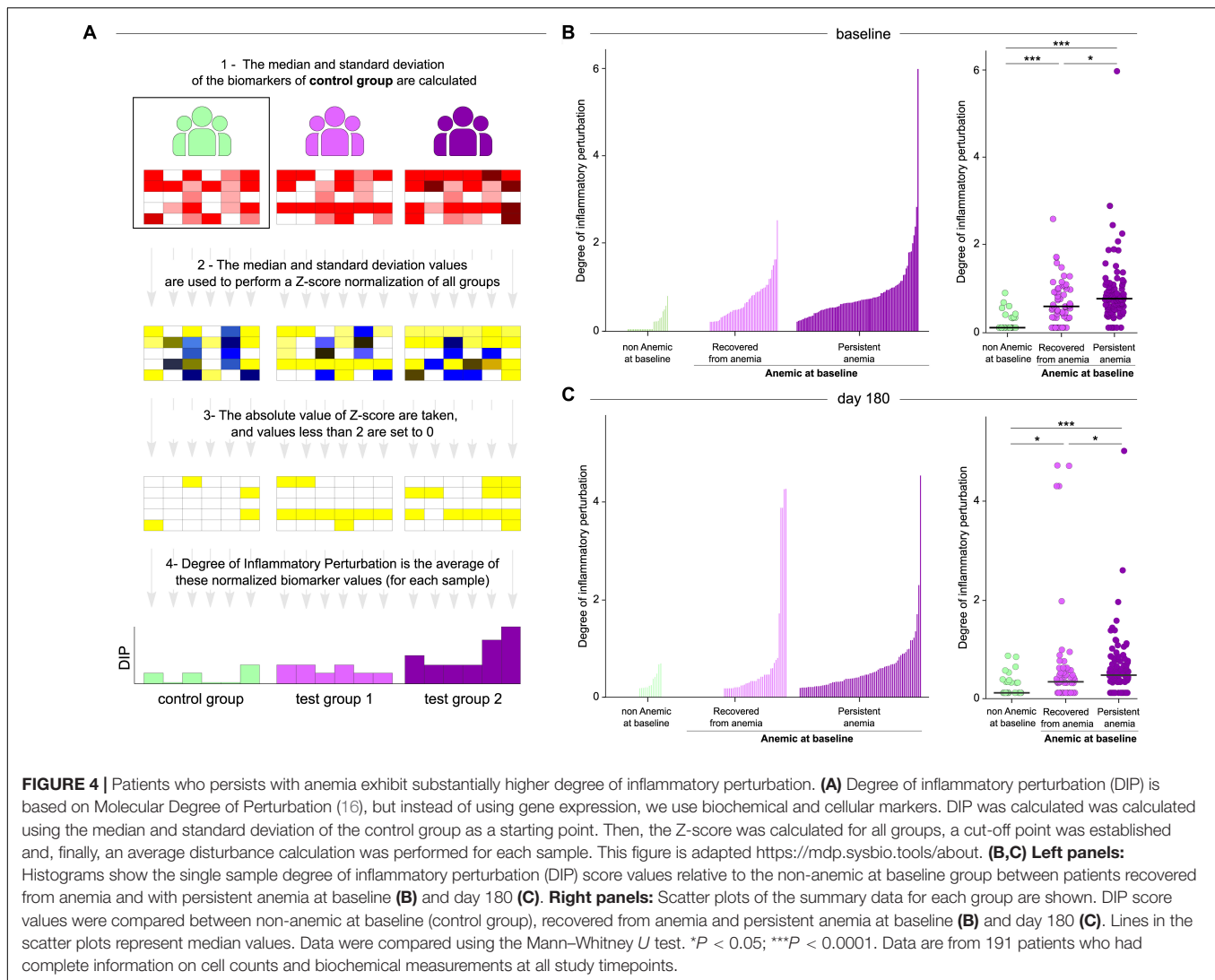
## Lower Concentrations of Hemoglobin at Pre-ATT Are Associated With Increased Risk of Unfavorable Treatment Outcome

In the longitudinal study cohort, 18 patients (9.4%) developed unfavorable outcomes (death attributed to TB:  $n = 3$ ; death attributed to HIV:  $n = 2$ ; ATT failure:  $n = 1$ ; ATT loss to follow up abandonment:  $n = 12$ ). The majority of the cases of unfavorable outcomes was composed by individuals who experienced persistent anemia (14 out of 18 participants, 77.8%) (**Figure 5A**). In fact, the median values of Hb levels gradually increased upon initiation of ATT in patients who were successfully treated (linear trend  $p < 0.001$ ) but did substantially change in those who has unfavorable outcomes (**Figure 5B**). A hierarchical cluster analysis inputting average values of CBC (**Figure 5C**) and biochemical parameters (**Figure 5D**) demonstrated that there were differential trends in values between the study timepoints and the subgroups of favorable vs. unfavorable outcomes.

At study baseline, individuals who further developed unfavorable outcomes exhibited lower levels of Hb ( $p = 0.052$ ), albumin ( $p = 0.035$ ), uric acid ( $p = 0.001$ ), urea ( $p = 0.006$ ), and creatinine ( $p = 0.008$ ) than those who were further successfully treated (**Supplementary Table 3**). A binomial logistic regression analysis was performed to test independent associations between the parameters analyzed and treatment outcome (**Figure 5E**). We found that increases in hemoglobin at pre-ATT were protective against unfavorable outcomes (aOR: 0.80, 95% CI: 0.64–0.99,  $p = 0.04$ ) independent of the other factors (**Figure 5E**). These results highlight the importance of Hb as a prognostic marker in PLWH coinfecting with TB.

## DISCUSSION

Anemia is a common complication associated with both TB and HIV, and it has been reported to occur in between 16 and 94% of TB patients (21–24); whereas in PLWH the prevalence ranges



from 39 to 71% (25–27). These observations were validated by the present study, which was focused on TB-HIV coinfection, and reported that 84.3% of the study participants were anemic at pre-ATT. In addition, our findings demonstrated that anemic patients exhibit higher inflammatory perturbation in the peripheral blood, which is sustained over the course of ATT in those who persisted with low Hb levels. Such condition is shown here to be closely associated with unfavorable outcomes. Early intervention focused on recovery from anemia could be a strategy to optimize the clinical management of PLWH with TB during ATT treatment.

In our cohort, anemic patients more frequently exhibited weight loss, lower CD4<sup>+</sup> T-cell counts and higher HIV viral loads than those who were not anemic. These observations reinforce the idea that anemia infers more advanced stage of disease progression. Our results are in agreement with other previously published findings which demonstrated that lower body mass index (27–29), higher HIV viral loads (28), and lower CD4<sup>+</sup> T-cell counts are all associated with higher prevalence of anemia (25, 26). As previously reported by us in a different

cohort of TB patients, most of the anemia cases are attributed to chronic inflammation rather than to iron deficiency (10). A recent systematic review demonstrated that anemia is related to an increased risk of all-cause mortality and incident TB among PLWH, regardless of the anemia type (30). The magnitude of such effect is thought to be proportional to severity of anemia. Finally, iron supplementation in such cases is still a matter of debate, with inconsistent results reported by clinical trials. The probable determinants of anemia in the context of HIV/AIDS and TB are likely multifactorial and involve several factors including nutritional status (31), chronic inflammation and antibody-mediated erythrophagocytosis (32). Our results demonstrated that anemic patients also exhibit lower counts of other cell types, suggesting that a global effect on the bone marrow may be occurring. Additional mechanistic studies as well as large randomized clinical trials testing different approaches to reduce anemia are necessary to improve our knowledge regarding the molecular targets and to help delineate the best therapeutic schemes.

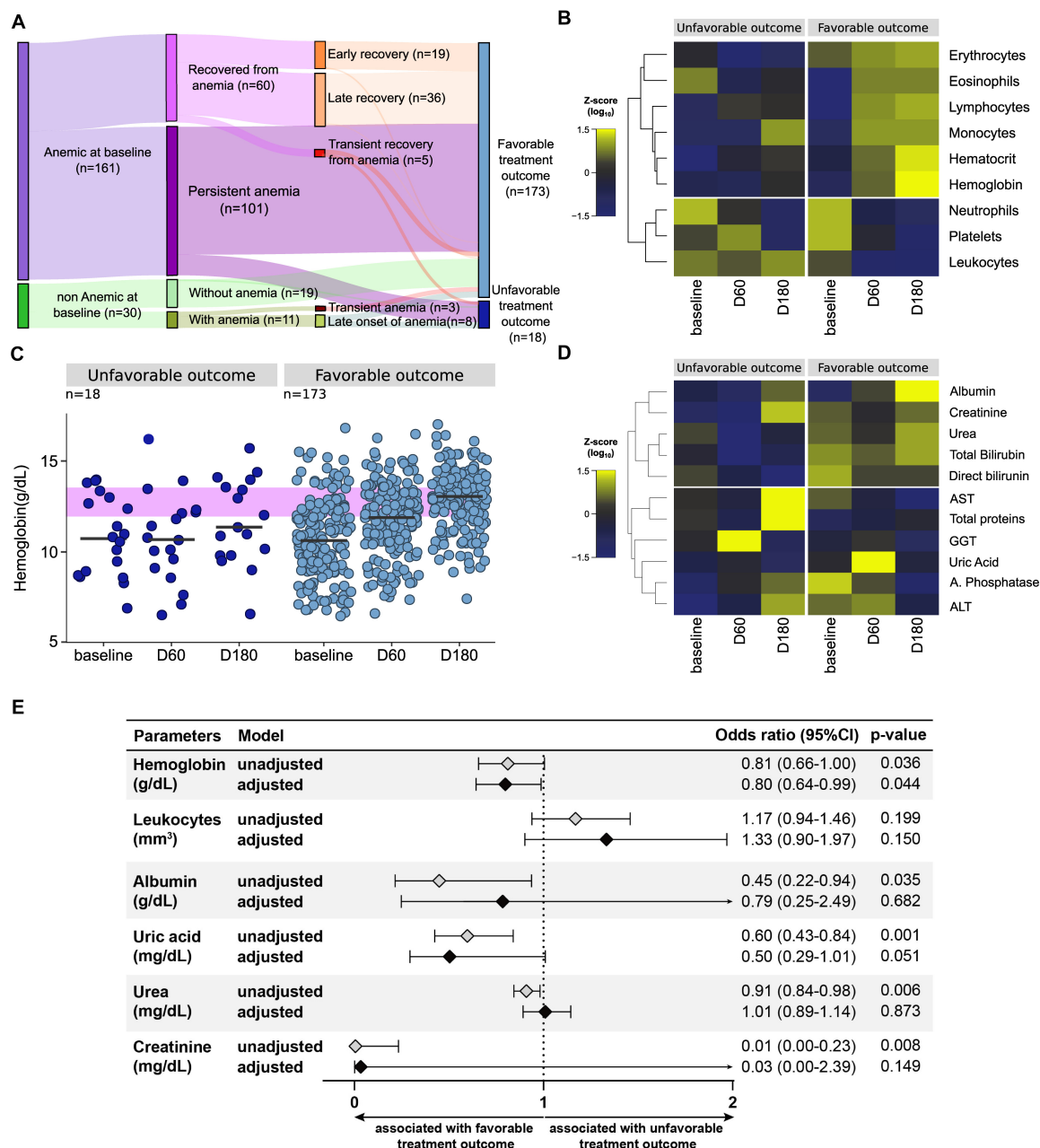


**FIGURE 5 |** Unfavorable outcome occurs mainly in patients with anemia. **(A)** Among all 191 patients who had complete laboratory data from all the study timepoints, only 18 had unfavorable treatment outcomes (death, failure or loss to follow up), whereas 173 were successfully treated (cure). **(B)** 14 of the 18 patients had anemia at baseline and 14 also had anemia at the end of the treatment. **(C,D)** A Heatmap was designed to depict the overall pattern of cells and biochemical markers at all timepoints in favorable and unfavorable outcome of anti-tubercular treatment. A two-way hierarchical cluster analysis (Ward's method) was performed. Dendrograms represent Euclidean distance. Expression scale represents Z-score normalization from the median at each timepoint and group. It is possible to observe that patients who had an unfavorable outcome have a profile opposite to that of patients with a favorable outcome. In **(C)** we can identify that patients with a favorable outcome had an increase in most of the blood count parameters over time, and also a decrease in neutrophils, platelets and leukocytes, returning to normal levels of these components. In patients with an unfavorable outcome, the parameters remain more similar to the baseline, with the exception of neutrophils and platelets, which also decrease. In **(D)** the biochemical markers of both groups do not seem to change much over time, but they visibly present different profiles when comparing favorable and unfavorable. Patients with a favorable outcome have higher levels of albumin, creatinine, urea and bilirubin throughout the treatment. **(E)** Logistic binomial regression model to significant biochemical parameters was used to test independent associations between biochemical and clinical parameters at baseline and treatment outcome after 180 days. The treatment outcome unfavorable (failure, death or loss to follow up) was used as reference to test associations. Only parameters which remained with  $p \leq 0.2$  in univariate analysis model were inputted in the adjusted model. (95%CI, 95% confidence interval). Associations reported in **(E)** are for increases in 1 unit in plasma concentrations of indicated markers.

With regard to the biochemical parameters, our results indicate that low Hb levels accompanied higher values of ALT, AST and GGT, and lower concentrations of albumin. Such findings are similar to those previously published by our group in another cohort of TB patients and reinforce the idea that anemia is related to a distinct biochemical profile and linked to inflammation (10). In our study, the prevalence of hepatitis B or C in anemic patients (9.48%) was very similar to non-anemic patients (10.8%), suggesting that although this comorbidity is present, it is probably not the main factor driving the differences in the levels of liver transaminases. At the end of ATT, none of these biochemical markers demonstrated association with the clinical outcomes. Moreover, out of the 25 patients who had viral hepatitis, 20 (80%) had a favorable outcome, highlighting the low influence of this coinfection on the effectiveness of the treatment.

The results reported here demonstrated that among the study participants with anemia at the baseline, the vast majority persisted with low Hb levels until day 180 of ATT. In addition, within the group of patients who recovered from anemia under the course of ATT, most exhibited a late recovery, occurring between day 60 and day 180 of therapy. Other investigations have reported that anemia frequently has a benign course in TB patients without HIV coinfection, with complete recovery in 64.5% of patients undertaking ATT (5). The discrepancies between the findings presented here and this previous study can be likely explained but the fact that our cohort was composed by PLWH, which may have an additional detrimental effect on inflammation and its related anemia compared to the setting of TB in the absence of HIV. In our study, patients who recovered from anemia presented with relatively higher values of Hb and hematocrit at baseline compared to those who persisted anemic. Individuals who had early recovery from anemia also exhibited higher neutrophil counts and albumin levels. The multivariable logistic regression analysis performed here revealed that albumin was independently associated with recovery from anemia. This observation again reinforces the strong association of albumin levels with recovery from anemia. These findings suggest that the degree of anemia is associated with changes in concentrations of cells and biochemical markers and that more severe anemia before ATT indicates higher odds of persistent anemia for up to 6 months on therapy.

To describe the overall biochemical and cellular disturbances related to anemia in the study population, we used an adaption of the molecular degree of perturbation (18) to estimate the degree of inflammatory perturbation in PLWH and with TB according to anemia status. Our findings indicate that there are important discrepancies in the DIP values between patients with persistent anemia compared to those who recovered during ATT. Individuals who persisted with anemia in the course of ATT exhibited higher DIP values already at pre-ATT, and such profile was sustained at day 180 of therapy. These findings argue that persistent anemia directly associates with increased disturbances in the biochemical and cellular profiles, which were sustained over the course of ATT. The inverse correlations between DIP values and Hb levels both at pre-ATT and at day 180 indicate that the degree of inflammatory perturbation is proportional to the severity of anemia. Whether anemia sets the

stage for persistent inflammation or is just a hallmark of chronic, unfettered, dysregulation of inflammatory responses warrants further investigation. This association between low Hb levels and risk of inflammatory disturbance has been described in PLWH who experience IRIS (33, 34) and also in patients with HIV/TB coinfection (35).

Another important contribution of our study was to test whether lower concentrations of Hb at pre-ATT could be used to predict risk of unfavorable outcomes. We found that the majority of patients who had unfavorable outcomes experienced persistent anemia during the course of ATT. A previous study described that anemia is associated with a 2–3 times increase in the risk of death, recurrence of TB or ATT failure in PLWH/TB (7). Corroborating with these findings, the results from a logistic regression analysis presented here demonstrated that increases in Hb concentrations at pre-ATT play a protective role against unfavorable outcomes independent of other confounding factors.

Our study has some limitations, such as relatively small number of non-anemic participants and of unfavorable outcomes, although the latter is within the expected range in the outpatient clinic from our institution. The small sample size favors a potential bias, as well as the fact that we do not have data on these same patients prior to TB and/or HIV infection, so that we cannot determine whether the anemia was pre-existing or in fact is a consequence of the co-infection. The study population also included few IRIS cases, which precluded additional exploratory analyses. Regardless of such limitations, our study adds to the current knowledge in the field by demonstrating the relevance of persistent anemia in driving inflammatory disturbances related to worse prognosis of PLWH coinfecting with TB. The fact that most patients with an unfavorable outcome persisted with anemia and with a high degree of inflammatory perturbation suggests that early intervention focused on recovery from anemia could be a strategy to optimize the clinical management of PLWH with TB during ATT treatment.

## DATA AVAILABILITY STATEMENT

The raw data supporting the conclusions of this article will be made available by the authors, without undue reservation.

## ETHICS STATEMENT

The studies involving human participants were reviewed and approved by the Institutional Review Board of the Instituto Nacional de Infectologia Evandro Chagas (INI). The patients/participants provided their written informed consent to participate in this study.

## AUTHOR CONTRIBUTIONS

FD, CS, FS'A, and VR contributed to conception and design of the study. FD also collected the data and organized the database. MA-P and MA performed the statistical analysis



and data visualization. FD, MA-P, and BA wrote the first draft of the manuscript. VR and BA supervised the project execution. All authors contributed to the article and approved the submitted version.

## FUNDING

This study was supported in part by the Intramural Research Program of FIOCRUZ. The work of BA was supported by grants from NIH (U01AI115940 and U01AI069923). BA is a senior scientist from the Conselho Nacional de Desenvolvimento Científico e Tecnológico (CNPq), Brazil. MA-P received a fellowship from Coordenação de Aperfeiçoamento de Pessoal de Nível Superior (Finance code: 001). MA received a research

fellowship from the Fundação de Amparo à Pesquisa do Estado da Bahia (FAPESB), Brazil.

## ACKNOWLEDGMENTS

We thank the study participants and the clinical staff.

## SUPPLEMENTARY MATERIAL

The Supplementary Material for this article can be found online at: <https://www.frontiersin.org/articles/10.3389/fimmu.2020.588405/full#supplementary-material>

## REFERENCES

- World Health Organization *WHO Guidelines on Tuberculosis Infection Prevention and Control: 2019 Update*. (2019). Available online at: <http://www.ncbi.nlm.nih.gov/books/NBK539297/> (accessed July 27, 2020).
- World Health Organization *Fact Sheet Tuberculosis (TB)*. (2020). Available online at: <https://www.who.int/news-room/fact-sheets/detail/tuberculosis> (accessed July 27, 2020).
- World Health Organization *Nutritional Anaemias: Tools for Effective Prevention and Control*. Geneva: World Health Organization (2017).
- Belperio PS, Rhew DC. Prevalence and outcomes of anemia in individuals with human immunodeficiency virus: a systematic review of the literature. *Am J Med*. (2004) 116(Suppl. 7A):27S–43S. doi: 10.1016/j.amjmed.2003.12.010
- Lee SW, Kang YA, Yoon YS, Um S-W, Lee SM, Yoo C-G, et al. The Prevalence and Evolution of Anemia Associated with Tuberculosis. *J Korean Med Sci*. (2006) 21:1028. doi: 10.3346/jkms.2006.21.6.1028
- Sahiratmadja E, Wieringa FT, van Crevel R, de Visser AW, Adnan I, Alisjahbana B, et al. Iron deficiency and NRAMP1 polymorphisms (INT4, D543N and 3'UTR) do not contribute to severity of anaemia in tuberculosis in the Indonesian population. *Br J Nutr*. (2007) 98:684–90. doi: 10.1017/S0007114507742691
- Isanaka S, Mugusi F, Urassa W, Willett WC, Bosch RJ, Villamor E, et al. Iron deficiency and anemia predict mortality in patients with tuberculosis. *J Nutr*. (2012) 142:350–7. doi: 10.3945/jn.111.144287
- Barzegari S, Afshari M, Movahednia M, Moosazadeh M. Prevalence of anemia among patients with tuberculosis: a systematic review and meta-analysis. *Indian J Tuberc*. (2019) 66:299–307. doi: 10.1016/j.ijtb.2019.04.002
- Nagu TJ, Spiegelman D, Hertzmark E, Aboud S, Makani J, Matee MI, et al. Anemia at the initiation of tuberculosis therapy is associated with delayed sputum conversion among pulmonary tuberculosis patients in Dar-es-Salaam, Tanzania. *PLoS One*. (2014) 9:e91229. doi: 10.1371/journal.pone.0091229
- Gil-Santana L, Cruz LAB, Arriaga MB, Miranda PFC, Fukutani KE, Silveira-Mattos PS, et al. Tuberculosis-associated anemia is linked to a distinct inflammatory profile that persists after initiation of antitubercular therapy. *Sci Rep*. (2019) 9:1381. doi: 10.1038/s41598-018-37860-5
- Mocroft A, Kirk O, Barton SE, Dietrich M, Proenca R, Colebunders R, et al. Anaemia is an independent predictive marker for clinical prognosis in HIV-infected patients from across Europe. EuroSIDA study group. *AIDS Lond Engl*. (1999) 13:943–50. doi: 10.1097/00002030-199905280-00010
- Shivakoti R, Yang W-T, Gupte N, Berendes S, Rosa AL, Cardoso SW, et al. Concurrent anemia and elevated C-reactive protein predicts HIV clinical treatment failure, including tuberculosis, after antiretroviral therapy initiation. *Clin Infect Dis*. (2015) 61:102–10. doi: 10.1093/cid/civ265
- Demitto FO, Schmaltz CAS, Sant'Anna FM, Arriaga MB, Andrade BB, Rolla VC. Predictors of early mortality and effectiveness of antiretroviral therapy in TB-HIV patients from Brazil. *PLoS One*. (2019) 14:e0217014.
- BRASIL *Guia de Tratamento: Recomendações para Terapia Anti-retroviral em Adultos e Adolescentes Infectados pelo HIV:2008*. Brasília: Ministério da Saúde (2008).
- Brasil *Nota técnica Sobre as Mudanças no Tratamento da Tuberculose no Brasil Para Adultos e Adolescentes*. Brasília: Ministério da Saúde (2010).
- Lever M, Russo P, Nakaya H. *Mdp*. (2018). Available online at: <https://bioconductor.org/packages/mdp> (accessed April 2, 2020).
- Pankla R, Buddhisa S, Berry M, Blankenship DM, Bancroft GJ, Banchereau J, et al. Genomic transcriptional profiling identifies a candidate blood biomarker signature for the diagnosis of septicemic melioidosis. *Genome Biol*. (2009) 10:R127. doi: 10.1186/gb-2009-10-11-r127
- Prada-Medina CA, Fukutani KE, Pavan Kumar N, Gil-Santana L, Babu S, Lichtenstein F, et al. Systems immunology of diabetes-tuberculosis comorbidity reveals signatures of disease complications. *Sci Rep*. (2017) 7:1999. doi: 10.1038/s41598-017-01767-4
- Oliveira-de-Souza D, Vinhaes CL, Arriaga MB, Kumar NP, Cubillos-Angulo JM, Shi R, et al. Molecular degree of perturbation of plasma inflammatory markers associated with tuberculosis reveals distinct disease profiles between Indian and Chinese populations. *Sci Rep*. (2019) 9:8002. doi: 10.1038/s41598-019-44513-8
- Oliveira-de-Souza D, Vinhaes CL, Arriaga MB, Kumar NP, Queiroz ATL, Fukutani KE, et al. Aging increases the systemic molecular degree of inflammatory perturbation in patients with tuberculosis. *Sci Rep*. (2020) 10:11358. doi: 10.1038/s41598-020-68255-0
- Roberts PD, Hoffbrand AV, Mollin DL. Iron and folate metabolism in tuberculosis. *Br Med J*. (1966) 2:198–202. doi: 10.1136/bmj.2.5507.198
- Cameron SJ, Horne NW. The effect of tuberculosis and its treatment on erythropoiesis and folate activity. *Tubercle*. (1971) 52:37–48. doi: 10.1016/0041-3879(71)90029-8
- Baynes RD, Flax H, Bothwell TH, Bezwoda WR, Atkinson P, Mendelow B. Red blood cell distribution width in the anemia secondary to tuberculosis. *Am J Clin Pathol*. (1986) 85:226–9. doi: 10.1093/ajcp/85.2.226
- Olaniyi JA, Aken'Ova YA. Haematological profile of patients with pulmonary tuberculosis in Ibadan, Nigeria. *Afr J Med Med Sci*. (2003) 32:239–42.
- Meidani M, Rezaei F, Maracy MR, Avijgan M, Tayeri K. Prevalence, severity, and related factors of anemia in HIV/AIDS patients. *J Res Med Sci Off J Isfahan Univ Med Sci*. (2012) 17:138–42.
- Shen Y, Wang Z, Lu H, Wang J, Chen J, Liu L, et al. Prevalence of anemia among adults with newly diagnosed HIV/AIDS in China. *PLoS One*. (2013) 8:e73807. doi: 10.1371/journal.pone.0073807
- Mijiti P, Yuexin Z, Min L, Wubuli M, Kejun P, Upur H. Prevalence and predictors of anaemia in patients with HIV infection at the initiation of combined antiretroviral therapy in Xinjiang, China. *Int J STD AIDS*. (2015) 26:156–64. doi: 10.1177/0956462414531935
- Dai G, Xiao J, Gao G, Chong X, Wang F, Liang H, et al. Anemia in combined antiretroviral treatment-naïve HIV-infected patients in China: a retrospective study of prevalence, risk factors, and mortality. *Biosci Trends*. (2016) 9.

29. Mukherjee A, Kaeley N, Dhar M, Kumar S, Bhushan B. Prevalence, characteristics, and predictors of tuberculosis associated anemia. *J Fam Med Prim Care*. (2019) 8:2445–9. doi: 10.4103/jfmpc.jfmpc\_311\_19
30. Abioye AI, Andersen CT, Sudfeld CR, Fawzi WW. Anemia, iron status, and HIV: a systematic review of the evidence. *Adv. Nutr. Bethesda Md.* (2020). doi: 10.1093/advances/nmaa037
31. Feleke BE, Feleke TE, Biadlegne F. Nutritional status of tuberculosis patients, a comparative cross-sectional study. *BMC Pulm Med*. (2019) 19:182. doi: 10.1186/s12890-019-0953-0
32. Dai Y, Cai Y, Wang X, Zhu J, Liu X, Liu H, et al. Autoantibody-mediated erythrophagocytosis increases tuberculosis susceptibility in HIV patients. *mBio*. (2020) 11:e03246-19. doi: 10.1128/mBio.03246-19
33. Thambuchetty N, Mehta K, Arumugam K, Shekarappa UG, Idiculla J, Shet A. The epidemiology of IRIS in Southern India: an observational cohort study. *J Int Assoc Provid AIDS Care*. (2017) 16:475–80. doi: 10.1177/2325957417702485
34. Sereti I, Sheikh V, Shaffer D, Phanuphak N, Gabriel E, Wang J, et al. Prospective international study of incidence and predictors of immune reconstitution inflammatory syndrome and death in people living With human immunodeficiency virus and severe lymphopenia. *Clin Infect Dis Off Publ Infect Dis Soc Am*. (2020) 71:652–60. doi: 10.1093/cid/ciz877
35. Narendran G, Andrade BB, Porter BO, Chandrasekhar C, Venkatesan P, Menon PA, et al. Paradoxical tuberculosis immune reconstitution inflammatory syndrome (TB-IRIS) in HIV patients with culture confirmed pulmonary tuberculosis in India and the potential role of IL-6 in prediction. *PLoS One*. (2013) 8:e63541. doi: 10.1371/journal.pone.0063541

**Conflict of Interest:** The authors declare that the research was conducted in the absence of any commercial or financial relationships that could be construed as a potential conflict of interest.

Copyright © 2020 Demitto, Araújo-Pereira, Schmaltz, Sant'Anna, Arriaga, Andrade and Rolla. This is an open-access article distributed under the terms of the Creative Commons Attribution License (CC BY). The use, distribution or reproduction in other forums is permitted, provided the original author(s) and the copyright owner(s) are credited and that the original publication in this journal is cited, in accordance with accepted academic practice. No use, distribution or reproduction is permitted which does not comply with these terms.



OPEN ACCESS

**Edited by:**

Adam Penn-Nicholson,  
Foundation for Innovative New  
Diagnostics, Switzerland

**Reviewed by:**

Frank Verreck,  
Biomedical Primate Research Centre  
(BPRC), Netherlands  
Andreas Kupz,  
James Cook University, Australia

**\*Correspondence:**

Katharina Ronacher  
katharina.ronacher@mater.uq.edu.au

<sup>†</sup>These authors have contributed  
equally to this work

**Specialty section:**

This article was submitted to  
Microbial Immunology,  
a section of the journal  
Frontiers in Immunology

**Received:** 01 September 2020

**Accepted:** 14 October 2020

**Published:** 06 November 2020

**Citation:**

Bartlett S, Gemiarto AT, Ngo MD,  
Sajir H, Hailu S, Sinha R, Foo CX,  
Kleynhans L, Tshivhula H, Webber T,  
Bielefeldt-Ohmann H, West NP,  
Hiemstra AM, MacDonald CE,  
Christensen LvV, Schlesinger LS,  
Walz G, Rosenkilde MM,  
Mandrup-Poulsen T and Ronacher K  
(2020) GPR183 Regulates Interferons,  
Autophagy, and Bacterial Growth  
During *Mycobacterium tuberculosis*  
Infection and Is Associated With TB  
Disease Severity.  
Front. Immunol. 11:601534.  
doi: 10.3389/fimmu.2020.601534

# GPR183 Regulates Interferons, Autophagy, and Bacterial Growth During *Mycobacterium tuberculosis* Infection and Is Associated With TB Disease Severity

Stacey Bartlett<sup>1†</sup>, Adrian Tandhyka Gemiarto<sup>1†</sup>, Minh Dao Ngo<sup>1</sup>, Haresh Sajir<sup>1</sup>, Semira Hailu<sup>1</sup>, Roma Sinha<sup>1</sup>, Cheng Xiang Foo<sup>1</sup>, Léanie Kleynhans<sup>2</sup>, Happy Tshivhula<sup>2</sup>, Tariq Webber<sup>2</sup>, Helle Bielefeldt-Ohmann<sup>3,4</sup>, Nicholas P. West<sup>3,4</sup>, Andriette M. Hiemstra<sup>2</sup>, Candice E. MacDonald<sup>2</sup>, Liv von Voss Christensen<sup>5</sup>, Larry S. Schlesinger<sup>6</sup>, Gerhard Walz<sup>2</sup>, Mette Marie Rosenkilde<sup>5</sup>, Thomas Mandrup-Poulsen<sup>5</sup> and Katharina Ronacher<sup>1,2,4\*</sup>

<sup>1</sup> Translational Research Institute–Mater Research Institute, The University of Queensland, Brisbane, QLD, Australia,

<sup>2</sup> DSI-NRF Centre of Excellence for Biomedical Tuberculosis Research, South African Medical Research Council Centre for Tuberculosis Research, Division of Molecular Biology and Human Genetics, Faculty of Medicine and Health Sciences, Stellenbosch University, Cape Town, South Africa, <sup>3</sup> School of Chemistry and Molecular Biosciences, The University of Queensland, St Lucia, QLD, Australia, <sup>4</sup> Australian Infectious Diseases Research Centre, The University of Queensland, Brisbane, QLD, Australia, <sup>5</sup> Department of Biomedical Sciences, University of Copenhagen, Copenhagen, Denmark,

<sup>6</sup> Host-Pathogens Interactions Program, Texas Biomedical Research Institute, San Antonio, TX, United States

Oxidized cholesterol have emerged as important signaling molecules of immune function, but little is known about the role of these oxysterols during mycobacterial infections. We found that expression of the oxysterol-receptor GPR183 was reduced in blood from patients with tuberculosis (TB) and type 2 diabetes (T2D) compared to TB patients without T2D and was associated with TB disease severity on chest x-ray. GPR183 activation by 7 $\alpha$ ,25-dihydroxycholesterol (7 $\alpha$ ,25-OHC) reduced growth of *Mycobacterium tuberculosis* (Mtb) and *Mycobacterium bovis* BCG in primary human monocytes, an effect abrogated by the GPR183 antagonist GSK682753. Growth inhibition was associated with reduced IFN- $\beta$  and IL-10 expression and enhanced autophagy. Mice lacking GPR183 had significantly increased lung Mtb burden and dysregulated IFNs during early infection. Together, our data demonstrate that GPR183 is an important regulator of intracellular mycobacterial growth and interferons during mycobacterial infection.

**Keywords:** *Mycobacterium tuberculosis*, diabetes, oxysterols, 7 $\alpha$ ,25-dihydroxycholesterol, GPR183, EBI2, host-direct therapies, autophagy

## INTRODUCTION

Patients with tuberculosis and type 2 diabetes (TB–T2D) comorbidity have increased bacterial burden and more severe disease, characterized by higher sputum smear grading scores and greater lung involvement on chest x-ray compared to TB patients without T2D (1, 2). TB–T2D patients are also more likely to fail TB therapy and to relapse (3). The reason for the increased disease severity has largely been attributed to hyperglycemia-mediated immune dysfunction, but hyperglycemia alone does not fully explain these observations (3, 4). We recently showed that independent of hyperglycemia, cholesterol concentrations in T2D patients vary greatly across different ethnicities (5). However, how cholesterol and its metabolites contribute to *Mycobacterium tuberculosis* (Mtb) infection outcomes remains to be elucidated.

To gain novel insights into the underlying immunological mechanisms of increased susceptibility of T2D patients to TB and to identify novel targets for host-directed therapy (HDT), we performed whole blood transcriptomic screens on TB patients with and without T2D and identified differential regulation of the transcript for oxidized cholesterol-sensing G protein-coupled receptor (GPCR), GPR183. Also known as Epstein Barr virus-induced gene 2 (EBI2), GPR183 is primarily expressed on cells of the innate and adaptive immune system (6–8). Several oxysterols can bind to GPR183 with  $7\alpha,25$ -hydroxycholesterol ( $7\alpha,25$ -OHC) being the most potent endogenous agonist (6, 9, 10). GPR183 has been studied mainly in the context of viral infections (11), immune cells (6, 7, 9, 12–18), and astrocytes (19, 20); it facilitates the chemotactic distribution of lymphocytes, dendritic cells and macrophages to secondary lymphoid organs (12, 15, 16, 21, 22). Little is known about the biological role of GPR183 in the context of bacterial infections, including TB. We show here that GPR183 is a key regulator of intracellular bacterial growth and type-I IFN production during mycobacterial infection and reduced GPR183 expression is associated with increased TB disease severity.

## METHODS

### Study Participants

TB patients and their close contacts were recruited at TB clinics outside Cape Town (South Africa). TB diagnosis was made based on positive GeneXpert MTB/RIF (Cepheid; California, USA) and/or positive MGIT culture (BD BACTED MGIT 960 system, BD, New Jersey, USA) and abnormal chest x-ray. Chest x-rays were scored, based on Ralphy score (23), by two clinicians independently. Participants with LTBI were close contacts of TB patients who tested positive on QuantiFERON-TB Gold in tube assay (Qiagen, Hilden, Germany). All study participants were screened for T2D based on HbA1c  $\geq 6.5\%$  and random plasma glucose  $\geq 200$  mg/dl or a previous history of T2D. Further details are available in the **Supplementary Materials**.

### RNA Extractions and Nanostring Analysis

Total RNA was extracted from cell pellets collected in QuantiFERON-TB gold assay tubes without antigen using the Ribopure Ambion RNA isolation kit (Life Technologies,

California, USA) and eluted RNA treated with DNase for 30 min. Samples with a concentration of  $\geq 20$  ng/ $\mu$ l and a 260/280 and 260/230 ratio of  $\geq 1.7$  were analyzed at NanoString Technologies in Seattle, Washington, USA. Differential expression of 594 genes, including 15 housekeeping genes, was performed using the nCounter GX Human Immunology kit V2. NanoString RCC data files were imported into the nSolver 3 software (nSolver Analysis software, v3.0), and gene expression was normalized to housekeeping genes.

### Cell Culture

Peripheral blood mononuclear cells (PBMCs) were obtained from healthy donor blood by Ficoll-Paque (GE Healthcare, Illinois, USA) gradient centrifugation and monocytes (MNs) isolated using the Pan Monocyte Isolation kit (Miltenyi Biotec, Bergisch Gladbach, Germany), with  $>95\%$  purity assessed by flow cytometry. MNs were plated onto Poly-D-lysine coated tissue culture plates ( $1.3 \times 10^5$  cells/well) and rested overnight at  $37^\circ\text{C}/5\%\text{CO}_2$  in RPMI-1640 medium supplemented with 10% heat-inactivated human AB serum (Sigma Aldrich, Missouri, USA), 2 mM L-glutamine and 1 mM sodium pyruvate before infection. THP-1 cells (ATCC #TIB-202) were differentiated with 25 ng/ml PMA for 48 h and rested for 24 h prior to infection.

### In Vitro Mtb ( $H_{37}R_v$ )/*M. bovis* (BCG) Infection

Mtb  $H_{37}R_v$  or *M. bovis* BCG single cell suspensions were added at a multiplicity of infection (MOI) of 1 or 10 with/without 100 nM  $7\alpha,25$ -dihydroxycholesterol (Sigma Aldrich) and with/without 10  $\mu$ M GSK682753 (Focus Bioscience, Queensland, Australia), followed by 2 h incubation at  $37^\circ\text{C}/5\%\text{CO}_2$  to allow for phagocytosis. Non-phagocytosed bacilli were removed by washing each well twice in warm RPMI-1640 containing 25 mM HEPES (Thermo Fisher Scientific). Infected cells were incubated ( $37^\circ\text{C}/5\%\text{CO}_2$ ) in medium with/without GPR183 agonist and/or antagonist and CFUs determined after 48 h.

To quantify bacterial growth over time, CFUs at 48 h were normalized to uptake at 2 h. Percentages of mycobacterial growth were determined relative to untreated cells. For RNA extraction, MNs were lysed by adding 500  $\mu$ l of TRIzol reagent. Further details are provided in the supplementary information.

### Western Blotting

THP-1 cells were infected with BCG with/without 100 nM  $7\alpha,25$ -OHC and with/without 10  $\mu$ M GSK682753 and lysed at 6 or 24 h post infection (p.i.) in ice-cold RIPA buffer (150 mM sodium chloride, 1.0% Triton X-100, 0.5% sodium deoxycholate, 0.1% SDS, 50 mM Tris, pH 8.0; Thermo Fisher Scientific), supplemented with complete Protease Inhibitor Cocktail (Sigma Aldrich) (120  $\mu$ l RIPA/1  $\times 10^6$  Cells). Protein concentrations were determined using Pierce BCA Protein Assay Kit (Thermo Fisher Scientific) as per manufacturer's protocol. 10  $\mu$ g of protein per sample was loaded on Novex<sup>TM</sup> 10–20% Tris-Glycine protein gels (Thermo Fisher Scientific) and transferred onto iBlot2 Transfer Stacks PVDF membrane (Thermo Fisher Scientific). Membranes were blocked with Odyssey Blocking buffer (Millennium Science, Victoria,



Australia) for 2 h, probed with rabbit anti-human LC3B (1:1,000, Sigma L7543) and rabbit anti-human GAPDH (1:2,500, Abcam 9485) overnight, followed by detection with goat anti-rabbit IgG DyLight 800 (1:20,000; Thermo Fisher Scientific). Bands were visualized using the Odyssey CLx system (LI-COR Biosciences, Nebraska, USA) and analyzed with Image Studio Lite V5.2 (LI-COR Biosciences).

## Immunofluorescence

Differentiated THP-1 cells were seeded onto a poly-D-lysine coated, 96-well glass-bottom black tissue culture plate ( $4.5 \times 10^4$  cells/well) and kept in RPMI-1640 medium minus phenol red (Thermo Fisher Scientific) supplemented with 10% heat-inactivated FBS at  $37^\circ\text{C}/5\% \text{CO}_2$ . Cells were infected with BCG at a MOI of 10, with/without 100 nM  $7\alpha,25\text{-OHC}$ , with/without 10  $\mu\text{M}$  GSK682753 for 2 h, washed and incubated for a further 4 h with agonists and antagonists. Cells were then fixed with 4% paraformaldehyde in PBS for 15 min, permeabilized with 0.05% saponin (Sigma Aldrich) for 20 min and blocked with 1% BSA, 0.05% saponin (Sigma Aldrich) for 1 h. Cells were immunolabeled with rabbit anti-human LC3B (ThermoFisher L10382; 1:1,000), 0.05% saponin at room temperature for 1 h followed by Alexa Fluor<sup>TM</sup> 647 goat anti-rabbit IgG (ThermoFisher A21245; 1:1,000), 0.05% saponin at room temperature for 1 h followed by nuclear staining with Hoechst 33342 (Thermo Fisher Scientific 62249; 1:2,000) for 15 min. Cells were washed, and confocal microscopy was performed using the Olympus FV3000,  $60\times$  magnification. Images obtained were analyzed with the ImageJ software (24).

## Murine GPR183 KO vs WT Model

Equal numbers of male and female C57BL/6 WT and Gpr183<sup>tm1Lex</sup> (age 18–20 weeks, 10 mice per group/timepoint) were aerosol infected with 300 CFU Mtb H<sub>37</sub>R<sub>v</sub> using an inhalation exposure system (Glascol). At 2- and 5-weeks post infection, lungs and blood were collected for RNA and CFU determination. Formalin-fixed lung lobes were sectioned and examined microscopically and scored by a veterinary pathologist. Further details are available in the supplementary information.

## Statistical Analysis

Statistical analysis was performed using GraphPad Prism v.7.0.3 (GraphPad Software). *T*-test and Wilcoxon's test were used to analyze Nanostring data. Mann–Whitney *U* test and *t*-test were used to analyze *in vitro* infection, qPCR, and ELISA data. Data are presented as means  $\pm$  SEM. Statistically significant differences between two groups are indicated in the figures as follows ns,  $P > 0.05$ ; \*,  $P < 0.05$ ; \*\*,  $P < 0.01$ ; \*\*\*,  $P < 0.001$ ; \*\*\*\*,  $P < 0.0001$ .

## Ethics Statement

The human studies were approved by the Institutional Review Board of Stellenbosch University (N13/05/064 and N13/05/064A) and all study participants signed pre-approved informed consent documents prior to enrolment into the studies. All animal studies were approved by the Animal Ethics Committee of the University of Queensland (MRI-UQ/596/18) and conducted in accordance with the *Australian Code for the Care and Use of Animals for Scientific Purposes*.

## RESULTS

### Blood GPR183 mRNA Expression Is Reduced in Patients With TB–T2D Compared to TB Patients Without T2D

Blood was obtained from the study participants with latent TB infection (LTBI,  $n = 11$ ), latent TB infection with T2D (LTBI + T2D,  $n = 14$ ), active pulmonary TB disease (TB,  $n = 9$ ), and active pulmonary TB disease with T2D (TB + T2D,  $n = 7$ ). Total RNA was extracted and NanoString analyses performed. Among genes differentially expressed between TB and TB + T2D we identified a single GPCR, GPR183. We focused on GPR183 as GPCRs are *bona fide* drug targets due to their importance in human pathophysiology and their pharmacological tractability.

GPR183 expression was significantly down-regulated at diagnosis ( $p = 0.03$ , *t*-test) in blood from TB + T2D patients compared to TB patients without T2D (**Figure 1A**). The reduced GPR183 expression was not driven by diabetes *per se*, as there

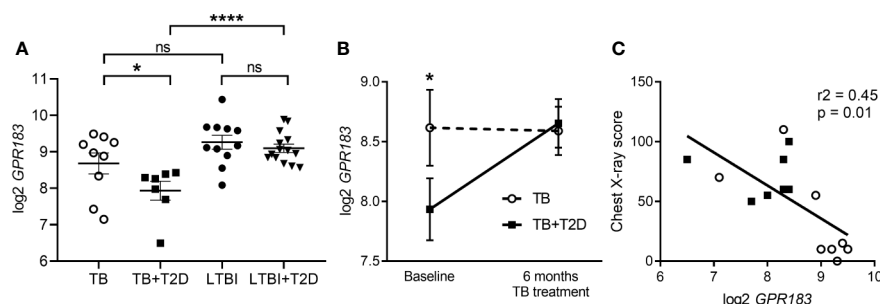


**FIGURE 1** | GPR183 mRNA expression in patients with active and latent TB infection with or without T2D. Total RNA was isolated from whole blood incubated overnight in QuantiFERON-TB Gold. GPR183 mRNA expression was determined and normalized to reference genes using the NanoString technology. GPR183 expression in whole blood of (A) TB ( $n = 9$ ) and TB + T2D ( $n = 7$ ) patients, LTBI ( $n = 11$ ) and LTBI + T2D ( $n = 14$ ) patients, Wilcoxon test. (B) TB ( $n = 9$ ) and TB + T2D ( $n = 7$ ) patients at baseline and 6 month's treatment, *t*-test. (C) Correlation between GPR183 expression and chest x-ray score, TB + T2D patients ( $n = 7$ ) filled squares, TB patients ( $n = 8$ ) open circles. Data are presented as means  $\pm$  SEM; not significance (ns)  $P > 0.05$ ; \* $P \leq 0.05$ ; \*\*\*\* $P \leq 0.0001$ .



were no differences in GPR183 expression between LTBI and LTBI + T2D (**Figure 1A**). After 6 months, at the end of successful TB treatment, we saw GPR183 expression significantly increased ( $p = 0.0156$ ) in TB + T2D patients to a level comparable to the TB patients without T2D (**Figure 1B**). Therefore, we speculated that blood GPR183 expression is associated with extent of TB disease, which is frequently more severe in T2D patients. We indeed determined an inverse correlation between GPR183 mRNA expression in the blood and TB disease severity on chest x-ray (**Figure 1C**).

In order to identify which cell type is associated with decreased expression of GPR183 in the blood, we performed flow cytometry analysis for GPR183 expression on PBMCs from TB patients with and without T2D. We investigated GPR183 expression on CD4+ and CD8+ T-cells, B cells, dendritic cells, NK cells and monocytes. We found that the only cell type with a significant reduction in GPR183 positivity in TB + T2D vs. TB, both in terms of frequency and median fluorescent intensity, was the non-classical monocyte population (**Supplementary Figures 1A, B**). The frequencies of GPR183 + non-classical monocytes from LTBI and LTBI + T2D were not significantly different (**Supplementary Figure 1C**). We therefore next investigated whether GPR183 plays a role in the innate immune response during Mtb infection.

### Oxysterol-Induced Activation of GPR183 Reduces Intracellular Mycobacterial Growth

We investigated whether *in vitro* activation of GPR183 with its endogenous agonist impacts the immune response to mycobacteria in primary human MNs. MNs from 15 healthy donors were infected with BCG ( $n = 7$ ) or Mtb H<sub>37</sub>R<sub>v</sub> ( $n = 8$ ) (**Figure 2**) at a MOI of one in the presence or absence of the GPR183 agonist 7 $\alpha$ ,25-OHC and/or the antagonist GSK682753. Activation of GPR183 by 7 $\alpha$ ,25-OHC significantly increased the uptake of BCG and Mtb H<sub>37</sub>R<sub>v</sub> (**Figure 2A**) at 2 h p.i. This increase in phagocytosis was abolished by the simultaneous addition of the GPR183 antagonist GSK682753, confirming that increased mycobacterial uptake was the result of GPR183 activation. Interestingly, we observed ~50% reduction in the growth of BCG and Mtb H<sub>37</sub>R<sub>v</sub> (**Figure 2B**) by 48h p.i. in 7 $\alpha$ ,25-OHC treated cells, and again, this effect was abrogated by GSK682753. The addition of 7 $\alpha$ ,25-OHC and/or GSK682753 had no detrimental effect on the viability of human THP-1 cells (**Supplementary Figure 2A**). There was also no effect of 7 $\alpha$ ,25-OHC and GSK682753 on BCG growth in liquid culture (**Supplementary Figure 2B**), thus confirming that the significant mycobacterial growth inhibition in MN cultures was attributable to the immune modulatory activity of 7 $\alpha$ ,25-OHC *via* GPR183. Independently, we observed that H<sub>37</sub>R<sub>v</sub> down-regulates GPR183 in primary MNs (**Supplementary Figure 3**).

To confirm the role of GPR183 in phagocytosis and growth inhibition, we next performed GPR183 siRNA knockdown experiments. Differentiated THP-1 cells were transfected with 20 nM of GPR183-targeting siRNA (siGPR183) or negative control siRNA (siControl). We observed ~80% reduction of GPR183 mRNA level and ~50% reduction of protein expression

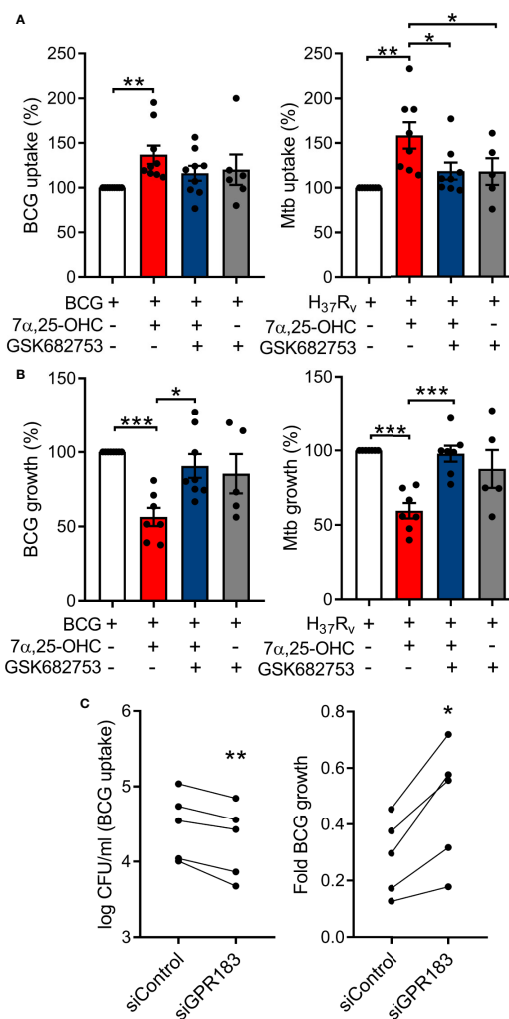


**FIGURE 2 |** Oxysterol-induced activation of GPR183 in primary MNs significantly inhibits intracellular mycobacterial growth, while GPR183 knockdown increases intracellular mycobacterial growth. Primary MNs from eight donors (**A**) and seven donors (**B**) were infected with BCG or Mtb H<sub>37</sub>R<sub>v</sub> (MOI 1),  $\pm$  7 $\alpha$ ,25-OHC (100 nM),  $\pm$  GSK682753 (10  $\mu$ M). Uptake of (**A**) BCG and Mtb H<sub>37</sub>R<sub>v</sub> was determined at 2h p.i. Growth of (**B**) BCG and Mtb H<sub>37</sub>R<sub>v</sub> was determined at 48h post-infection. Percent of mycobacterial growth was calculated as the fold change of CFU at 48h compared to CFU at 2h, normalized to non-treated cells. PMA-differentiated THP-1 cells were transfected with 20 nM of either negative control siRNA or GPR183 siRNA for 48h before infection with BCG (MOI 1). (**C**) Mycobacterial uptake was determined at 2h and intracellular mycobacterial growth was determined at 48h p.i. (normalized to uptake). Data are presented as means  $\pm$  SEM; \* $P \leq 0.05$ ; \*\* $P \leq 0.01$ ; \*\*\* $P \leq 0.001$ ; paired t-test.

in cells transfected with siGPR183 when compared to siControl-transfected cells (**Supplementary Figures 4A, B**) at 48 h. Forty-eight hours after transfection the cells were infected with BCG at a MOI of one. We observed a marked decrease in BCG uptake in cells transfected with siGPR183 ( $p = 0.0048$ ) compared to siControl-transfected cells and a significant increase in intracellular mycobacterial growth over time ( $p = 0.0113$ , **Figure 2C**).

## GPR183 Is a Negative Regulator of the Type I Interferon Pathway in Human MNs

In genome wide association studies GPR183 has been implicated as a negative regulator of the IRF7 driven inflammatory network (25). Therefore, we focused subsequent experiments on type-I IFN regulation. To determine whether GPR183, a constitutively active GPCR (26), has a direct effect on IRFs and *IFNB1* expression, we performed knockdown experiments in primary MNs. GPR183 knockdown (Supplementary Figure 4C) up-regulated *IFNB1* (2.7–5.5 fold;  $P = 0.0115$ ) as well as *IRF1*, *IRF3*, *IRF5*, and *IRF7*, although the latter did not reach statistical significance (Figure 3A).

*IRF1*, *IRF5*, and *IRF7* transcripts were similarly up-regulated in whole blood from TB + T2D patients compared to TB patients (Figure 3B), consistent with the downregulation of *GPR183* mRNA expression (Figure 1). *IRF3* expression was not significantly different between TB and TB + T2D patients (data not shown).

## GPR183 Activation Induces a Cytokine Profile Favoring Mtb Control

Next, we investigated whether the reduced intracellular mycobacterial growth observed in primary MNs treated with 7 $\alpha$ ,25-OHC was associated with a change in MN secreted cytokines. Gene expression of *IFNB1*, *TNF*, and *IL-10* was measured 24 h following infection with Mtb H<sub>37</sub>R<sub>V</sub> at MOI of one (Figure 4A). The concentrations of the corresponding cytokines were measured in cell culture supernatant by ELISA (Figure 4B). Mtb infection significantly up-regulated the expression of *IFNB1* ( $P = 0.0068$ ), *TNF* ( $P = 0.0001$ ), *IL-10* ( $P < 0.0001$ ) (Figure 4A), and *IL-1B* (Supplementary Figure 5A). 7 $\alpha$ ,25-OHC significantly down-regulated Mtb-induced *IFNB1* expression ( $P = 0.0017$ ), while it did not affect *TNF*, *IL-10* or *IL-1B* expression. At the protein level, the concentrations of IFN- $\beta$  and IL-10, but not TNF- $\alpha$  ( $P < 0.0001$  and  $P = 0.0090$ , respectively, Figure 4B) nor IL-1 $\beta$  (Supplementary Figure 5B)

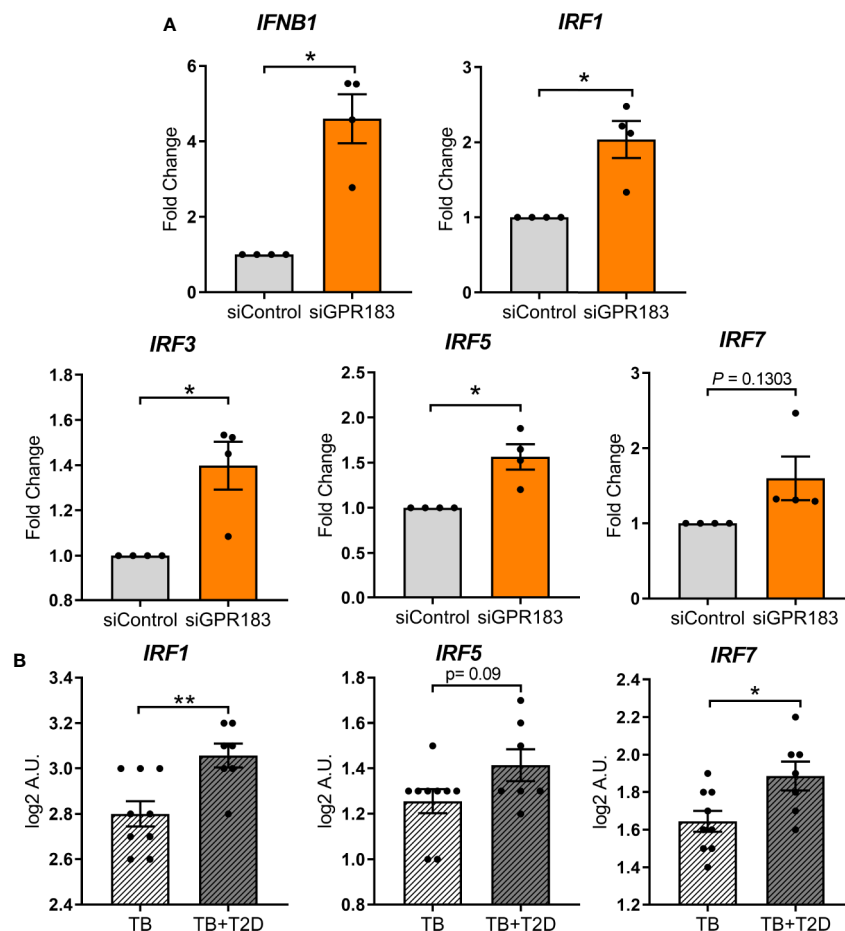


**FIGURE 3 |** GPR183 knockdown increases expression of transcription factors regulating type I interferon responses. **(A)** Total RNA was isolated from primary MNs following 48 h incubation with 20 nM GPR183 siRNA (or negative control siRNA). Gene expression of *IFNB1*, *IRF1*, *IRF3*, *IRF5*, *IRF7* was measured by qRT-PCR using RPS13 as reference gene. Data are normalized to cells transfected with negative control siRNA. **(B)** NanoString analyses of RNA isolated from TB and TB + T2D cohort showed similar increase in type I IFN associated genes *IRF1*, *IRF5*, *IRF7*. Data are presented as fold changes  $\pm$  SEM; \* $P \leq 0.05$ ; \*\* $P \leq 0.01$ ; paired *t*-test.

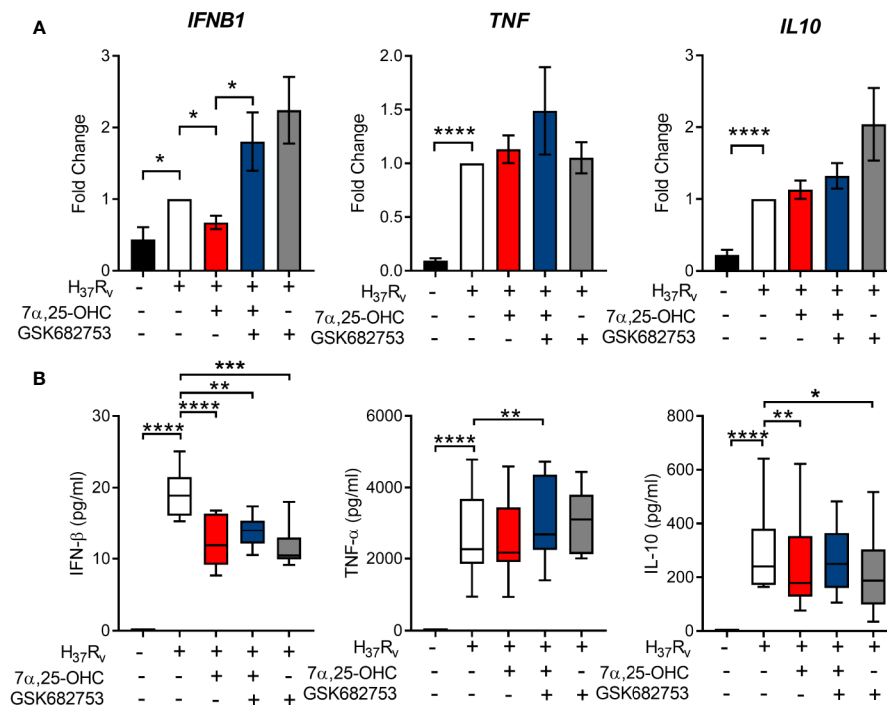


**FIGURE 4 |** Activation of GPR183 leads to cytokine production favoring Mtb control. Primary MN from healthy donors ( $n = 8$ ) were infected for 2 h with Mtb H37Rv (MOI 10:1), 7α,25-OHC (100 nM), and/or GSK682753 (10 μM). Cells were washed and left with drugs for a further 22 h. Changes in the expression of (A) IFNB1, TNF, and IL10 were measured by qPCR and normalized to untreated infected cells. Concentrations of (B) IFN-β, TNF-α, and IL-10 in the culture supernatant were measured by ELISA. Data are presented as mean fold change ± SEM or min to max for box plots; \* $P \leq 0.05$ ; \*\* $P \leq 0.01$ ; \*\*\* $P \leq 0.001$ ; \*\*\*\* $P \leq 0.0001$ ; paired t-test.

were significantly lower in the culture supernatant of 7α,25-OHC-treated Mtb-infected primary MNs compared to untreated infected cells.

## The Oxysterol 7α,25-OHC Induces Autophagy

We aimed to identify whether 7α,25-OHC impacts the production of reactive oxygen species (ROS) and the autophagy pathway. ROS production in BCG-infected primary MNs was not affected by 7α,25-OHC (Supplementary Figure 6); however, we observed an increase in accumulation of the autophagosome marker LC3B-II in BCG-infected THP-1 cells treated with 7α,25-OHC ( $P = 0.0119$ , Figure 5A). We next performed the experiments in the absence and presence of the lysosomal inhibitor chloroquine in order to determine autophagic flux. Autophagic flux in BCG-infected cells was significantly increased with 7α,25-OHC treatment ( $P = 0.0069$ , Figure 5B). The simultaneous addition of the GPR183 antagonist GSK682753 with 7α,25-OHC, decreased the levels of LC3B-II and autophagic flux; however, this did not reach statistical significance.

We next confirmed the induction of autophagy *via* microscopy. The number of LC3B-II puncta per cell increased in 7α,25-OHC stimulated BCG-infected THP-1 cells compared to the untreated BCG-infected cells ( $P = 0.0358$ , Figure 5C). The

7α,25-OHC effect could be reduced by antagonist GSK682753 ( $P = 0.0196$ ).

## GPR183 KO Mice Have Higher Bacterial Burden During the Early Stage of Infection

To confirm the effect of the GPR183 receptor *in vivo*, we infected WT and GPR183 KO mice with aerosolized Mtb. At 2 weeks p.i., GPR183 KO mice showed significantly increased mycobacterial burden in the lungs compared to WT mice ( $P = 0.0084$ , Figure 6A), while the bacterial burden was comparable at 5 weeks p.i. (Supplementary Figure 7). GPR183 KO mice also had higher lung pathology scores although this did not reach significance (Figure 6B). GPR183 KO mice had significantly increased *Ifnb1* expression in the lungs ( $P = 0.0256$ ; Figure 6C), along with increased *Irf3* ( $P = 0.0159$ ); however, *Irf5* (Supplementary Figure 8) and *Irf7* (Figure 6C) remained unchanged. *Irf7* transcription was increased in the blood from GPR183 KO compared to WT mice ( $P = 0.0513$ ; Figure 6D), but *Ifnb1*, *Irf3* and *Irf5* expression was not different (Figure 6D, Supplementary Figure 6). At the RNA level *Tnf*, *Ifng*, and *Il1b* were not significantly different between GPR183 KO and WT mice (Figure 7A). Unexpectedly, at the protein level, the concentrations of IFN-β ( $P = 0.0232$ ) and IFN-γ ( $P = 0.0232$ ) were significantly lower in GPR183 KO mice lung, while TNF-α ( $P = 0.7394$ ) and IL-1β ( $P = 0.0753$ ) were not statistically different (Figure 7B).

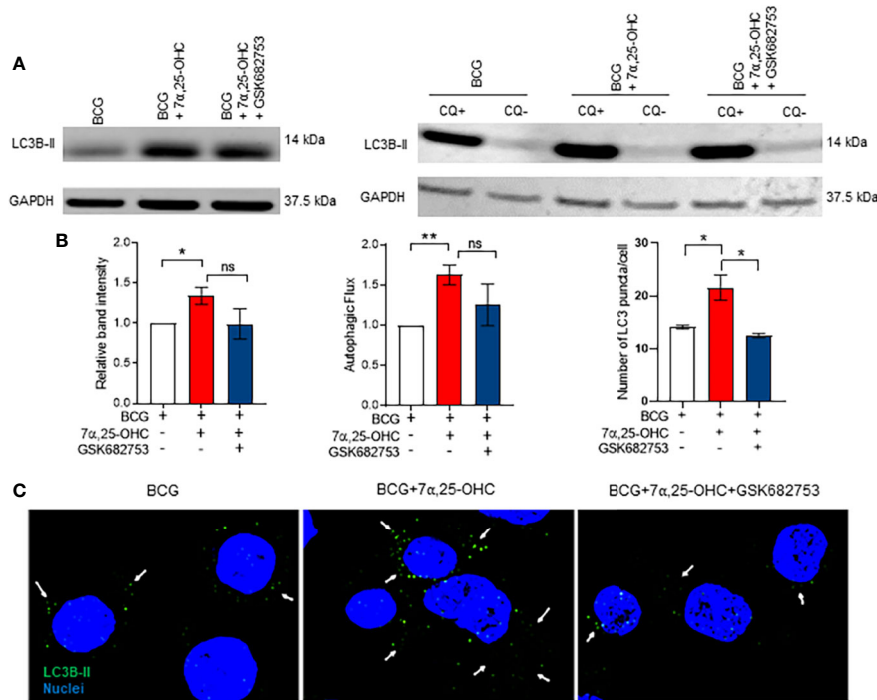


**FIGURE 5 |** Treatment with 7α,25-OHC induces autophagy. PMA-differentiated THP-1 cells were infected/uninfected and co-incubated with ±7α,25-OHC, ±GSK682753, for 2 h. Extracellular BCG was removed, and cells were incubated for a further 4 h or 22 h in RPMI medium containing drugs. **(A)** Cells were lysed at 6 h or 24 h (Flux) p.i. **(B)** The band intensity was then normalized to the reference protein, GAPDH and further normalized to the BCG. Autophagic flux was obtained by subtracting chloroquine positive values with chloroquine negative values. **(C)** Cells were visualized using the Olympus FV 3000 confocal microscope. At least 30 cells were counted for every condition. Data are presented as ± SEM; ns,  $P > 0.05$ ; \* $P \leq 0.05$ ; \*\* $P \leq 0.01$ ; unpaired  $t$ -test.

## DISCUSSION

Historically oxidized cholesterol, so called oxysterols, were considered by-products that increase polarity of cholesterol to facilitate its elimination. However, they have recently emerged as important lipid mediators that control a range of physiological processes including metabolism, immunity, and steroid hormone synthesis (27).

Our findings define a novel role for GPR183 in regulating the host immune response during Mtb infection (summarized in **Figure 8**). We initially identified GPR183 through a blood transcriptomic screen in TB and TB + T2D patients and found an inverse correlation between GPR183 expression and TB disease severity on chest x-ray. Although we demonstrate that the decrease in blood GPR183 in TB + T2D patients is likely due, in part, to a decreased frequency of non-classical monocytes expressing GPR183, we cannot rule out that reduced GPR183 expression in whole blood is partially attributable to neutrophils and eosinophils as preferential loss of neutrophils and eosinophils occurs upon PBMC isolation. In our study the TB patients with T2D had more severe TB compared to those without T2D; therefore we cannot ascertain whether lower GPR183 expression is linked to TB + T2D comorbidity or TB disease severity.

We demonstrate that activation of GPR183 by 7α,25-OHC in primary human MNs during Mtb infection results in significantly

better control of intracellular Mtb growth. This is in contrast to a recently published study showing increased Mtb growth with 7α,25-OHC when added post-infection in murine RAW264.7 cells (28). The discrepancies between the studies could also be attributed to the different cell types and infection dose, which was 25 times higher in the aforementioned study. Consistent with the findings of Tang et al. (28) in murine cells we show that mycobacterial infection down-regulates GPR183 in human MNs, which may be an immune-evasion strategy specific to mycobacteria since LPS, a constituent of Gram-negative bacteria, upregulates GPR183 (15). Whether the observed increase in phagocytosis in the presence of 7α,25-OHC is a non-specific effect driven by internalization of agonist bound GPR183 and non-specific uptake of bacteria or an increase in pattern recognition receptors remains to be elucidated.

We further demonstrate that GPR183 activation by 7α,25-OHC reduces IFN-β expression and secretion in Mtb-infected primary MNs and targeted GPR183 knockdown significantly upregulating *IRF1* and *IFNB1*. Similarly, gene expression of *IRF1*, *IRF5*, and *IRF7* is up-regulated in TB + T2D patients compared to TB patients and corresponds with down-regulation of *GPR183*, thereby demonstrating that GPR183 expression is associated with IFN regulatory factors during human TB, and GPR183 is a negative regulator of type I IFNs in Mtb-infected human MNs.

There is mounting evidence that the production of type-I IFNs is detrimental during Mtb infection (29, 30). Up-regulation

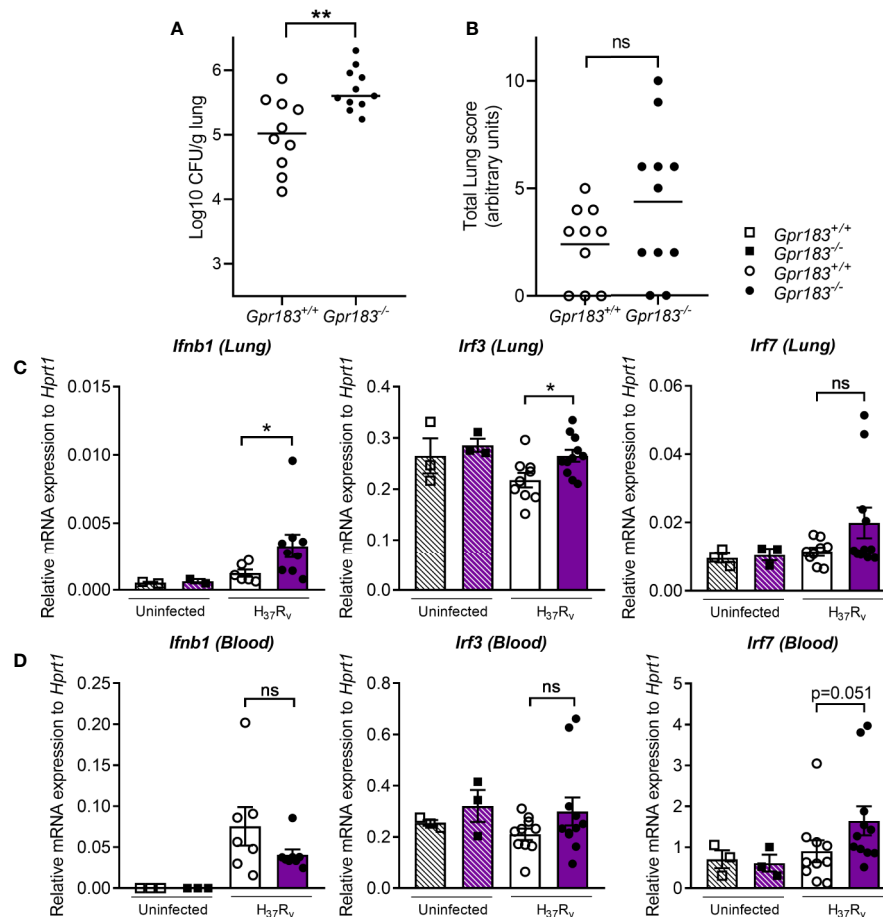


**FIGURE 6 |** GPR183KO mice have higher lung CFU, corresponding with increased expression of transcription factors regulating type I interferon responses. Mice were infected with 300 CFU of aerosol Mtb H<sub>37</sub>R<sub>v</sub>. **(A)** Bacterial lung burden 2 weeks p.i. **(B)** Total histology lung score. RNA was isolated from Mtb-infected lung and blood samples 2 weeks p.i. **(C)** Gene expression of *Ifnb1*, *Irf3*, and *Irf7* in the lungs, **(D)** *Ifnb1*, *Irf3*, and *Irf7* in the blood, was measured by qRT-PCR using *Hprt1* as reference gene. Data are presented as  $\pm$  SEM; ns,  $P > 0.05$ ; \* $P \leq 0.05$ ; \*\* $P \leq 0.01$ .

of type-I IFN blood transcript signatures occurs in TB disease and correlates with disease severity (31). In macrophages, Mtb induces up-regulation of *IFNB1* expression as early as 4 h p.i. to limit IL-1 $\beta$  production, a critical mediator in the host defense against Mtb (32). Although 7 $\alpha$ ,25-OHC significantly reduced *IFNB1* mRNA, we did not observe an increase in *IL1B* mRNA, suggesting that the GPR183-mediated regulation of type-I IFN does not influence *IL1B* expression. In addition to GPR183 mediated reduction in IFN- $\beta$ , we observed a decrease in IL-10 in Mtb-infected primary MNs treated with 7 $\alpha$ ,25-OHC. IL-10 production is induced by type-I IFN signaling (33, 34) and promotes Mtb growth (35) by reducing the bioavailability of TNF- $\alpha$  through the release of soluble TNF receptors and preventing the maturation of Mtb-containing phagosomes (35–38). Collectively, we show that GPR183 is a negative regulator of type-I IFNs in primary MNs, and agonist induced activation of GPR183 reduces Mtb-induced IFN- $\beta$  production, while leaving expression of cytokines important for Mtb control unchanged.

Further confirming the role of GPR183, GPR183 KO mice infected with Mtb had significantly higher bacterial burden in the lung compared to WT mice 2 weeks p.i. (prior to initiation of the adaptive immune response to Mtb) with this effect disappearing at 5 weeks p.i., when T cell responses against Mtb are fully established. Our results thus strengthen the contention that GPR183 plays an important role in the innate immune control of Mtb irrespective of hyperglycemia. We confirmed the importance GPR183 in regulating type-I interferons during Mtb infection *in vivo*. GPR183 KO mice infected with Mtb had significantly increased lung *Ifnb1* and *Irf3* mRNA. Unexpectedly, IFN- $\beta$  and IFN- $\gamma$  secretions were both significantly downregulated in the lung. These differences between mRNA and protein levels may be due to kinetic parameters of transcription *versus* translation or mRNA stability *versus* protein consumption.

Furthermore, we demonstrate that the GPR183 agonist 7 $\alpha$ ,25-OHC promotes autophagy in macrophages infected with mycobacteria. Autophagy is a cellular process facilitating the elimination of intracellular pathogens including Mtb (39).



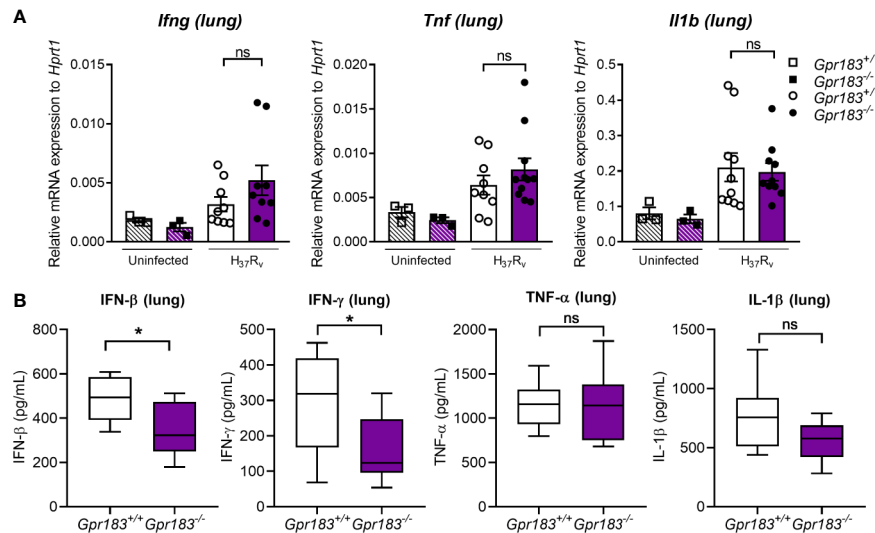


**FIGURE 7** | Pro-inflammatory cytokine expression at 2 weeks p.i. of Mtb H<sub>37</sub>R<sub>v</sub>-infected mice. Mice were infected with 300 CFU of aerosol Mtb H<sub>37</sub>R<sub>v</sub>. **(A)** Gene expression of *Ifng*, *Il1b*, and *Tnf* in the lungs. **(B)** Concentrations of IFN-β, IFN-γ, IL-1β and TNF-α in the culture supernatant were measured by ELISA. Data are presented as ± SEM; ns,  $P > 0.05$ ; \* $P \leq 0.01$ .

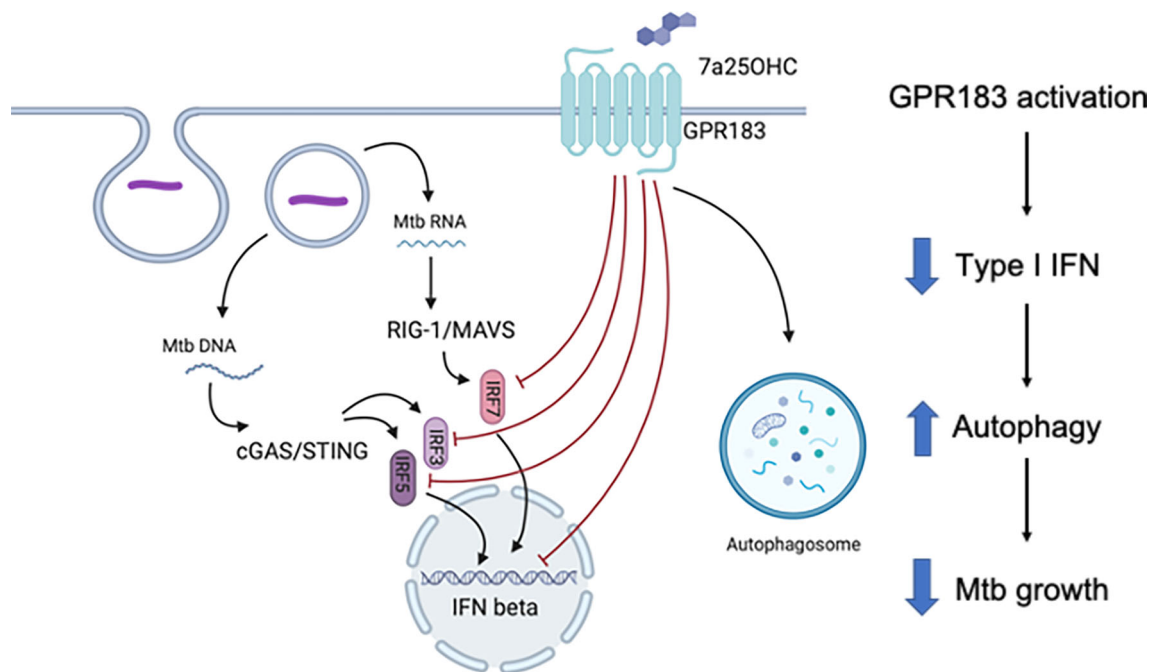


**FIGURE 8** | Schematic summary of the role of GPR183 in Mtb-infected human monocytes.

Antimicrobial autophagy was shown to be inhibited by *Mycobacterium leprae* through upregulation of IFN-β and autocrine IFNAR activation which in turn increased expression of the autophagy blocker OASL (2'-5'-oligoadenylate synthetase like) (40). Whether there is a link between the 7α,25-OHC-induced reduction of IFN-β

production and the increase in autophagy remains to be investigated in future studies.

Several autophagy promoting re-purposed drugs including metformin are currently being assessed as HDTs for TB (41). We propose that GPR183 is a potential target for TB HDT, warranting the development of specific, metabolically stable small-molecule

agonists for this receptor to ultimately improve TB treatment outcomes in TB patients with and without T2D co-morbidity.

## DATA AVAILABILITY STATEMENT

The raw data supporting the conclusions of this article will be made available by the authors, without undue reservation.

## ETHICS STATEMENT

The human studies were approved by the Institutional Review Board of Stellenbosch University (N13/05/064 and N13/05/064A), and all study participants signed pre-approved informed consent documents prior to enrolment into the studies. The patients/participants provided their written informed consent to participate in this study. All animal studies were approved by the Animal Ethics Committee of the University of Queensland (MRI-UQ/596/18) and conducted in accordance with the Australian Code for the Care and Use of Animals for Scientific Purposes.

## AUTHOR CONTRIBUTIONS

AG, SB, and KR wrote the manuscript. AG, SB, RS, SH, HS, MN, CF, LK, HT, TW, HB-O, AH, CM, LV, and NW carried out the experiments. AG, SB, MN, HS, RS, and SH analyzed the data. TM-P, MR, LS, GW, and KR interpreted the data and developed the theoretical framework. KR conceived the original idea. All authors contributed to the article and approved the submitted version.

## REFERENCES

- Magee MJ, Kempker RR, Kipiani M, Gandhi NR, Darchia L, Tukvadze N, et al. Diabetes mellitus is associated with cavities, smear grade, and multidrug-resistant tuberculosis in Georgia. *Int J Tuberculosis Lung Dis* (2015) 19 (6):685–92. doi: 10.5588/ijtld.14.0811
- Dong Z, Shi J, Dorhoi A, Zhang J, Soodeen-Laloo AK, Tan W, et al. Hemostasis and Lipoprotein Indices Signify Exacerbated Lung Injury in TB With Diabetes Comorbidity. *Chest* (2018) 153(5):1187–200. doi: 10.1016/j.chest.2017.11.029
- Critchley JA, Restrepo BII, Ronacher K, Kapur A, Bremer AA, Schlesinger LS, et al. Defining a Research Agenda to Address the Converging Epidemics of Tuberculosis and Diabetes: Part 1: Epidemiology and Clinical Management. *Chest* (2017) 152(1):165–73. doi: 10.1016/j.chest.2017.04.155
- Ronacher K, van Crevel R, Critchley JA, Bremer AA, Schlesinger LS, Kapur A, et al. Defining a Research Agenda to Address the Converging Epidemics of Tuberculosis and Diabetes: Part 2: Underlying Biologic Mechanisms. *Chest* (2017) 152(1):174–80. doi: 10.1016/j.chest.2017.02.032
- Restrepo BII, Kleynhans L, Salinas AB, Abdelbary B, Tshivhula H, Aguilon-Duran GP, et al. Diabetes screen during tuberculosis contact investigations highlights opportunity for new diabetes diagnosis and reveals metabolic differences between ethnic groups. *Tuberculosis (Edinb)* (2018) 113:10–8. doi: 10.1016/j.tube.2018.08.007
- Hannedouche S, Zhang J, Yi T, Shen W, Nguyen D, Pereira JP, et al. Oxysterols direct immune cell migration via EBI2. *Nature* (2011) 475 (7357):524–7. doi: 10.1038/nature10280
- Gessier F, Preuss I, Yin H, Rosenkilde MM, Laurent S, Endres R, et al. Identification and characterization of small molecule modulators of the Epstein-Barr virus-induced gene 2 (EBI2) receptor. *J Med Chem* (2014) 57 (8):3358–68. doi: 10.1021/jm4019355
- Rosenkilde MM, Benned-Jensen T, Andersen H, Holst PJ, Kledal TN, Luttichau HR, et al. Molecular pharmacological phenotyping of EBI2. An orphan seven-transmembrane receptor with constitutive activity. *J Biol Chem* (2006) 281(19):13199–208. doi: 10.1074/jbc.M602245200
- Liu C, Yang XV, Wu J, Kuei C, Mani NS, Zhang L, et al. Oxysterols direct B-cell migration through EBI2. *Nature* (2011) 475(7357):519–23. doi: 10.1038/nature10226
- Benned-Jensen T, Norn C, Laurent S, Madsen CM, Larsen HM, Arfelt KN, et al. Molecular characterization of oxysterol binding to the Epstein-Barr virus-induced gene 2 (GPR183). *J Biol Chem* (2012) 287(42):35470–83. doi: 10.1074/jbc.M112.387894
- Daugvilaite V, Arfelt KN, Benned-Jensen T, Sailer AW, Rosenkilde MM. Oxysterol-EBI2 signaling in immune regulation and viral infection. *Eur J Immunol* (2014) 44(7):1904–12. doi: 10.1002/eji.201444493
- Pereira JP, Kelly LM, Xu Y, Cyster JG. EBI2 mediates B cell segregation between the outer and centre follicle. *Nature* (2009) 460(7259):1122–6. doi: 10.1038/nature08226
- Gatto D, Paus D, Basten A, Mackay CR, Brink R. Guidance of B cells by the orphan G protein-coupled receptor EBI2 shapes humoral immune responses. *Immunity* (2009) 31(2):259–69. doi: 10.1016/j.immuni.2009.06.016

## FUNDING

This study was supported by the National Institutes of Health (NIH), National Institute of Allergy and Infectious Diseases (NIAID) and the South African Medical Research Council under the US-South African Program for Collaborative Biomedical Research (grant number: R01AI116039) to KR and by the TANDEM Grant of the EUFP7 (European Union's Seventh Framework Program) under Grant Agreement NO. 305279 to GW for study participant recruitment, by the Novo Nordisk Foundation to MR and TM-P. All other laboratory-based research activities were supported by grants from the Australian Infectious Diseases Research Center, The Australian Respiratory Council and the Mater Foundation to KR. The Translational Research Institute is supported by a grant from the Australian Government.

## ACKNOWLEDGMENTS

We thank the clinical research team at Stellenbosch University for assistance with identification and recruitment of study participants as well as coordination of clinical and administrative activities. We thank Matthew Sweet for critical review of the manuscript. Illustrations were created with Biorender.com. This manuscript has been released as a pre-print at bioRxiv (42).

## SUPPLEMENTARY MATERIAL

The Supplementary Material for this article can be found online at: <https://www.frontiersin.org/articles/10.3389/fimmu.2020.601534/full#supplementary-material>

14. Chalmin F, Rochemont V, Lippens C, Clottu A, Sailer AW, Merkler D, et al. Oxysterols regulate encephalitogenic CD4(+) T cell trafficking during central nervous system autoimmunity. *J Autoimmun* (2015) 56:45–55. doi: 10.1016/j.jaut.2014.10.001
15. Preuss I, Ludwig MG, Baumgarten B, Bassilana F, Gessier F, Seuwen K, et al. Transcriptional regulation and functional characterization of the oxysterol/EBI2 system in primary human macrophages. *Biochem Biophys Res Commun* (2014) 446(3):663–8. doi: 10.1016/j.bbrc.2014.01.069
16. Gatto D, Wood K, Caminschi I, Murphy-Durland D, Schofield P, Christ D, et al. The chemotactic receptor EBI2 regulates the homeostasis, localization and immunological function of splenic dendritic cells. *Nat Immunol* (2013) 14(5):446–53. doi: 10.1038/ni.2555
17. Chiang EY, Johnston RJ, Grogan JL. EBI2 is a negative regulator of type I interferons in plasmacytoid and myeloid dendritic cells. *PLoS One* (2013) 8(12):e83457. doi: 10.1371/journal.pone.0083457
18. Emgard J, Kammoun H, Garcia-Cassani B, Chesne J, Parigi SM, Jacob JM, et al. Oxysterol Sensing through the Receptor GPR183 Promotes the Lymphoid-Tissue-Inducing Function of Innate Lymphoid Cells and Colonic Inflammation. *Immunity* (2018) 48(1):120–32. doi: 10.1016/j.immuni.2017.11.020
19. Rutkowska A, Preuss I, Gessier F, Sailer AW, Dev KK. EBI2 regulates intracellular signaling and migration in human astrocyte. *Glia* (2015) 63(2):341–51. doi: 10.1002/glia.22757
20. Rutkowska A, Shimshek DR, Sailer AW, Dev KK. EBI2 regulates pro-inflammatory signalling and cytokine release in astrocytes. *Neuropharmacology* (2018) 133:121–8. doi: 10.1016/j.neuropharm.2018.01.029
21. Li J, Lu E, Yi T, Cyster JG. EBI2 augments Tfh cell fate by promoting interaction with IL-2-quenching dendritic cells. *Nature* (2016) 533(7601):110–4. doi: 10.1038/nature17947
22. Suan D, Nguyen A, Moran I, Bourne K, Hermes JR, Arshi M, et al. T follicular helper cells have distinct modes of migration and molecular signatures in naive and memory immune responses. *Immunity* (2015) 42(4):704–18. doi: 10.1016/j.immuni.2015.03.002
23. Ralph AP, Ardian M, Wiguna A, Maguire GP, Becker NG, Drogumuller G, et al. A simple, valid, numerical score for grading chest x-ray severity in adult smear-positive pulmonary tuberculosis. *Thorax* (2010) 65(10):863–9. doi: 10.1136/thx.2010.136242
24. Rueden CT, Schindelin J, Hiner MC, DeZonia BE, Walter AE, Arena ET, et al. ImageJ: ImageJ for the next generation of scientific image data. *BMC Bioinf* (2017) 18(1):529. doi: 10.1186/s12859-017-1934-z
25. Benned-Jensen T, Smethurst C, Holst PJ, Page KR, Sauls H, Sivertsen B, et al. Ligand modulation of the Epstein-Barr virus-induced seven-transmembrane receptor EBI2: identification of a potent and efficacious inverse agonist. *J Biol Chem* (2011) 286(33):29292–302. doi: 10.1074/jbc.M110.196345
26. Benned-Jensen T, Rosenkilde MM. Structural motifs of importance for the constitutive activity of the orphan 7TM receptor EBI2: analysis of receptor activation in the absence of an agonist. *Mol Pharmacol* (2008) 74(4):1008–21. doi: 10.1124/mol.108.049676
27. Mutemberezi V, Guillemot-Legrès O, Muccioli GG. Oxysterols: From cholesterol metabolites to key mediators. *Prog Lipid Res* (2016) 64:152–69. doi: 10.1016/j.plipres.2016.09.002
28. Tang J, Shi YN, Zhan L, Qin C. Downregulation of GPR183 on infection restricts the early infection and intracellular replication of mycobacterium tuberculosis in macrophage. *Microbial Pathogenesis* (2020) 145:104234. doi: 10.1016/j.micpath.2020.104234
29. Donovan ML, Schultz TE, Duke TJ, Blumenthal A. Type I Interferons in the Pathogenesis of Tuberculosis: Molecular Drivers and Immunological Consequences. *Front Immunol* (2017) 8:1633:1633. doi: 10.3389/fimmu.2017.01633
30. Moreira-Teixeira L, Mayer-Barber K, Sher A, O'Garra A. Type I interferons in tuberculosis: Foe and occasionally friend. *J Exp Med* (2018) 215(5):1273–85. doi: 10.1084/jem.20180325
31. Berry MP, Graham CM, McNab FW, Xu Z, Bloch SA, Oni T, et al. An interferon-inducible neutrophil-driven blood transcriptional signature in human tuberculosis. *Nature* (2010) 466(7309):973–7. doi: 10.1038/nature09247
32. Novikov A, Cardone M, Thompson R, Shenderov K, Kirschman KD, Mayer-Barber KD, et al. Mycobacterium tuberculosis triggers host type I IFN signaling to regulate IL-1 $\beta$  production in human macrophages. *J Immunol* (2011) 187(5):2540–7. doi: 10.4049/jimmunol.1100926
33. McNab F, Mayer-Barber K, Sher A, Wack A, O'Garra A. Type I interferons in infectious disease. *Nat Rev Immunol* (2015) 15(2):87–103. doi: 10.1038/nri3787
34. Mayer-Barber KD, Andrade BB, Barber DL, Hieny S, Feng CG, Caspar P, et al. Innate and adaptive interferons suppress IL-1 $\alpha$  and IL-1 $\beta$  production by distinct pulmonary myeloid subsets during Mycobacterium tuberculosis infection. *Immunity* (2011) 35(6):1023–34. doi: 10.1016/j.immuni.2011.12.002
35. Beamer GL, Flaherty DK, Assogba BD, Stromberg P, Gonzalez-Juarrero M, de Waal Malefyt R, et al. Interleukin-10 promotes Mycobacterium tuberculosis disease progression in CBA/J mice. *J Immunol* (2008) 181(8):5545–50. doi: 10.4049/jimmunol.181.8.5545
36. Hart PH, Hunt EK, Bonder CS, Watson CJ, Finlay-Jones JJ. Regulation of surface and soluble TNF receptor expression on human monocytes and synovial fluid macrophages by IL-4 and IL-10. *J Immunol* (1996) 157(8):3672–80.
37. O'Leary S, O'Sullivan MP, Keane J. IL-10 blocks phagosome maturation in mycobacterium tuberculosis-infected human macrophages. *Am J Respir Cell Mol Biol* (2011) 45(1):172–80. doi: 10.1165/rcmb.2010-0319OC
38. Armstrong L, Jordan N, Millar A. Interleukin 10 (IL-10) regulation of tumour necrosis factor  $\alpha$  (TNF- $\alpha$ ) from human alveolar macrophages and peripheral blood monocytes. *Thorax* (1996) 51(2):143–9. doi: 10.1136/thx.51.2.143
39. Chandra P, Kumar D. Selective autophagy gets more selective: Uncoupling of autophagy flux and xenophagy flux in Mycobacterium tuberculosis-infected macrophages. *Autophagy* (2016) 12(3):608–9. doi: 10.1080/15548627.2016.1139263
40. Toledo Pinto TG, Batista-Silva LR, Medeiros RCA, Lara FA, Moraes MO. Type I Interferons, Autophagy and Host Metabolism in Leprosy. *Front Immunol* (2018) 9:806:806. doi: 10.3389/fimmu.2018.00806
41. Cerni S, Shafer D, To K, Venketaraman V. Investigating the Role of Everolimus in mTOR Inhibition and Autophagy Promotion as a Potential Host-Directed Therapeutic Target in Mycobacterium tuberculosis Infection. *J Clin Med* (2019) 8(2):232. doi: 10.3390/jcm8020232
42. Bartlett S, Gemiarto AT, Ngo MD, Saijiir H, Hailu S, Sinha R, et al. GPR183 regulates interferons and bacterial growth during Mycobacterium tuberculosis infection: interaction with type 2 diabetes and TB disease severity. *bioRxiv* (2020). doi: 10.1101/2020.07.15.203398

**Conflict of Interest:** MMR is a co-founder of Antag Therapeutics and of Synklino.

The remaining authors declare that the research was conducted in the absence of any commercial or financial relationships that could be construed as a potential conflict of interest.

Copyright © 2020 Bartlett, Gemiarto, Ngo, Saijiir, Hailu, Sinha, Foo, Kleynhans, Tshivhula, Webber, Bielefeldt-Ohmann, West, Hiemstra, MacDonald, Christensen, Schlesinger, Walz, Rosenkilde, Mandrup-Poulsen and Ronacher. This is an open-access article distributed under the terms of the Creative Commons Attribution License (CC BY). The use, distribution or reproduction in other forums is permitted, provided the original author(s) and the copyright owner(s) are credited and that the original publication in this journal is cited, in accordance with accepted academic practice. No use, distribution or reproduction is permitted which does not comply with these terms.



# Increased Frequency of Memory CD4+ T-Cell Responses in Individuals With Previously Treated Extrapulmonary Tuberculosis

## OPEN ACCESS

### Edited by:

Adam Penn-Nicholson,  
Foundation for Innovative New  
Diagnostics, Switzerland

### Reviewed by:

Jiezuan Yang,  
Zhejiang University, China  
Xu Wang,  
First Affiliated Hospital of Jilin  
University, China

### \*Correspondence:

Bruno B. Andrade  
bruno.andrade@fiocruz.br

<sup>†</sup>These authors share first authorship

<sup>‡</sup>These authors share last authorship

### Specialty section:

This article was submitted to  
Microbial Immunology,  
a section of the journal  
Frontiers in Immunology

**Received:** 12 September 2020

**Accepted:** 13 November 2020

**Published:** 17 December 2020

### Citation:

Barreto-Duarte B, Sterling TR,  
Fiske CT, Almeida A, Nochowicz CH,  
Smith RM, Barnett L, Warren C,  
Blackman A, Lapa e Silva JR,  
Andrade BB and Kalams SA (2020)  
Increased Frequency of Memory  
CD4+ T-Cell Responses in Individuals  
With Previously Treated  
Extrapulmonary Tuberculosis.  
Front. Immunol. 11:605338.  
doi: 10.3389/fimmu.2020.605338

Beatriz Barreto-Duarte<sup>1,2,3,4†</sup>, Timothy R. Sterling<sup>5,6†</sup>, Christina T. Fiske<sup>5,6</sup>,  
Alexandre Almeida<sup>4</sup>, Cynthia H. Nochowicz<sup>5,6</sup>, Rita M. Smith<sup>5,6</sup>, Louise Barnett<sup>5,6</sup>,  
Christian Warren<sup>5,6</sup>, Amndrea Blackman<sup>5,6</sup>, Jose Roberto Lapa e Silva<sup>4</sup>,  
Bruno B. Andrade<sup>1,2,3,4,7,8,9\*‡</sup> and Spyros A. Kalams<sup>5,6‡</sup>

<sup>1</sup> Instituto Gonçalo Moniz, Fundação Oswaldo Cruz, Salvador, Brazil, <sup>2</sup> Multinational Organization Network Sponsoring Translational and Epidemiological Research (MONSTER) Initiative, Salvador, Brazil, <sup>3</sup> Universidade Salvador (UNIFACS), Laureate Universities, Salvador, Brazil, <sup>4</sup> Faculdade de Medicina, Universidade Federal do Rio de Janeiro, Rio de Janeiro, Brazil, <sup>5</sup> Division of Infectious Diseases, Department of Medicine, Vanderbilt University Medical Center, Nashville, TN, United States, <sup>6</sup> Vanderbilt Tuberculosis Center, Vanderbilt University Medical Center, Nashville, TN, United States, <sup>7</sup> Faculdade de Medicina, Universidade Federal da Bahia, Salvador, Brazil, <sup>8</sup> Curso de Medicina, Centro Universitário Faculdades de Tecnologia e Ciências (UnifTC), Salvador, Brazil, <sup>9</sup> Curso de Medicina, Escola Bahiana de Medicina e Saúde Pública, Salvador, Brazil

Extrapulmonary TB (EPTB) occurs with increased frequency in persons with underlying immunodeficiency. Even after recovery from acute illness, differences in immune phenotype and activation persist. Studies defining characteristics of immune responses after recovery from extrapulmonary TB may provide insights into factors that increase TB risk. We performed two case-control studies (in the United States and Brazil) among HIV-seronegative adults with previous EPTB (n = 9; 25), previous pulmonary TB (n = 7; 25), latent *M. tuberculosis* (Mtb) infection (n = 11; 25), and uninfected TB contacts (n = 10; 25). We assessed the frequency of dual CD4+ interferon- $\gamma$  and tumor necrosis factor- $\alpha$  responses after stimulation with overlapping Mtb peptides from ESAT-6 or CFP-10, or gamma-irradiated Mtb H37Rv, proliferative responses to Mtb antigens, T-regulatory cell (Treg) frequency and phenotype. In both study populations, individuals with prior EPTB had the highest frequency of intracellular cytokine-producing cells in response to Mtb antigens ( $p < 0.05$ ;  $p < .0001$ ). Persons with prior EPTB in Brazil had the highest levels of CD4 proliferation to Mtb antigens ( $p < 0.0001$ ), and the highest expression of CD39 on Tregs ( $p < 0.0001$ ). Individuals with treated EPTB maintained high frequencies of Mtb-specific memory responses and active Treg cells, suggesting that susceptibility to EPTB occurs despite the ability to develop and maintain enhanced adaptive immune responses.

**Keywords:** tuberculosis, extrapulmonary tuberculosis, memory T-cell responses, cytokine, CD4+ T cell



## INTRODUCTION

The global burden of tuberculosis (TB) is enormous, with an estimated one-quarter of the world's population (approximately 2 billion people) infected with *M. tuberculosis* (Mtb) and 10 million new cases of TB each year (1). According to the World Health Organization, Mtb is among the leading causes of death due to an infection, causing approximately 1.4 million deaths in 2019 (2).

The immune response to Mtb involves monocytes, macrophages and T-lymphocytes that produce cytokines such as IFN- $\gamma$ , TNF- $\alpha$ , IL-12, and CXCL8 (IL-8) (3, 4). Over 80% of tuberculosis (TB) disease in low TB incidence settings is due to reactivation of latent Mtb infection (5) yet only 5–10% of persons with latent TB infection (LTBI) progress to TB disease (6–8). The transition from LTBI to active disease could be due to a breakdown in host immune surveillance, a change in the mycobacteria from a dormant to an active state, or a combination of both. There is likely a spectrum of disease activity that includes incipient and sub-clinical disease, in addition to latent/quiescent and active (symptomatic) TB (9). Discovery of factors that predispose to active disease will help identify individuals with LTBI at increased risk for progression to TB so that effective preventive measures can be initiated. Conversely, such information may also help identify protective immune responses that could be induced by TB vaccines.

Extrapulmonary TB (EPTB) is commonly associated with underlying immune defects. Persons with HIV (PWH) are at increased risk of EPTB and this risk increases as the CD4+ T-lymphocyte count declines (10). Young children also have an increased incidence of EPTB, specifically TB meningitis, presumably due to immature immune responses (11). We have previously noted reduced peripheral blood mononuclear cell (PBMC) cytokine production and CD4+ T-lymphocytes in HIV-seronegative adults with previous EPTB compared to persons with previous pulmonary TB or LTBI (12). We also found that persons with previous EPTB had increased T-regulatory (Treg) cell frequency and CD4+ lymphocyte activation, indicating possible immune dysregulation (13).

Active TB disease is associated with increased generalized immune activation, and infiltration of activated T-cells and Tregs at the site of disease (14–19). A sub-population of Tregs (defined as CD4+CD25<sup>high</sup>FOXP3+) expresses CD39, a surface ectonucleotidase which metabolizes pro-inflammatory extracellular ATP (20). These “active Tregs” exhibit robust and stable suppression of immune function (21). Individuals with active TB have higher frequencies of Treg-expressing CD39 after *in vitro* stimulation with Mtb antigens, and depletion of these cells enhances cytokine secretion in response to Mtb antigens (22, 23). These observations have led to a model whereby secretion of immunomodulatory cytokines such as IL-10 by Tregs impairs Mtb-specific CD4+ and CD8+ T-cell activation and proliferation (24). Studies of Treg frequency during Mtb infection have been limited to individuals with active disease. While it is plausible that expansion of these cells may limit immune responses, and potentially play a role in TB pathogenesis, it is unknown whether high frequencies of Tregs

at the time of initial Mtb infection predisposes individuals to develop active TB disease.

The goal of this study was to determine whether features of immune responses could differentiate individuals with LTBI from those with prior treated TB disease. We compared the frequencies of cytokine-producing T-cells and proliferation responses of T-cells stimulated with Mtb peptides (ESAT-6 and CFP10) and gamma-irradiated Mtb in persons with previous extrapulmonary or pulmonary TB disease, LTBI and uninfected individuals who had been exposed to TB. We also measured surface expression of CD39 on Tregs as a possible marker of regulatory function. Two case-control studies were performed—one in the United States and one in Brazil. The correlates of protection from active disease are unknown, but analysis of immune parameters among persons who have recovered from acute illness could provide clues into factors that increase TB risk.

## METHODS

### Design of the Case-Control Studies

For both case-control studies, cases were defined as persons with previously treated extrapulmonary TB. There were three sets of controls: 1) persons with previously treated pulmonary TB, 2) persons with LTBI (defined as a tuberculin skin test (TST) >5 mm induration or positive interferon gamma release assay (IGRA); regardless of whether they had previously been treated), and 3) persons who had been exposed to culture-positive pulmonary TB but were not infected (i.e., TST <5 mm induration or negative IGRA). Persons with both pulmonary and extrapulmonary TB were considered extrapulmonary for the purposes of analysis, given the presence of disseminated disease. Inclusion criteria consisted of: age  $\geq 18$  years at time of diagnosis of TB disease or infection; HIV-seronegative; culture-confirmed disease and either near completion (within one month) or after completion of therapy (for extrapulmonary TB cases and pulmonary TB controls). We did not require persons to complete therapy for LTBI to be enrolled because such persons are asymptomatic and latent Mtb infection is unlikely to alter systemic cytokine production, unlike active TB disease. Only contacts of culture-positive pulmonary TB cases were included as controls—both those with and without evidence of Mtb infection. Contacts of culture-positive pulmonary TB cases were tested for LTBI at the beginning of the contact investigation and 8–12 weeks later if the initial test was negative (25). Exclusion criteria consisted of: serum creatinine >2 mg/dL; use of corticosteroids or other immunosuppressive agents at the time of diagnosis or study entry; malignancy; and diabetes mellitus. HIV-positive persons were excluded because of the known increased risk of extrapulmonary TB associated with HIV/AIDS (10, 26, 27). Pleural TB has exaggerated (not diminished) local cell-mediated immune responses (28) Although it is unclear whether this affects the systemic immune response, we excluded persons with previous pleural TB because they may exhibit a unique immunopathogenesis compared with the other forms of extrapulmonary (disseminated) TB.



In the U.S. study population, all cases and controls were enrolled from Tennessee. Extrapulmonary TB cases and pulmonary TB controls were identified by review of the Tennessee Department of Health TB registry. Ongoing contact investigations at local and regional TB clinics were reviewed to identify patients in the remaining control groups. Demographic and clinical characteristics were collected from the patient or the Tennessee TB registry.

### United States Study: Sample Preparation

Peripheral blood mononuclear cells (PBMC) were isolated under sterile conditions by Ficoll-Paque (GE Healthcare Bio-Science) density gradient centrifugation and cryopreserved in 90% of fetal bovine serum (FBS) (GemCell-Gemini Bioproducts) and 10% DMSO (Dimethyl sulfoxide) (29). Blood samples were submitted to a commercial laboratory for HIV serology and complete blood counts.

### In Vitro Stimulation of PBMC for Intracellular Cytokine Staining

Peripheral blood mononuclear cells (PBMCs) from each subject were thawed, and cultured at  $10 \times 10^6$  cells/ml in 48-well plates ( $2 \times 10^6$  cells/well) in R10 medium (RPMI 1640 containing 10% heat inactivated FCS, 2 mM L-glutamine, 50 µg/ml penicillin, 50 µg/ml streptomycin, and 10mM Hepes) and co-stimulated with anti-CD28 (1µg/ml, BD Biosciences) and anti-CD49d (1µg/ml, BD). Cells were stimulated with overlapping *M. tuberculosis* peptides from the ESAT-6 or CFP-10 proteins (BEI Resources) (2 µg/ml), or gamma-irradiated h37RV (10 µg/ml) (BEI Resources). As a negative control, PBMCs were incubated with media alone and as a positive control with Staphylococcal Enterotoxin B (SEB) (1 µg/ml, Sigma). One hour after stimulation, brefeldin was added; after overnight incubation, PBMCs were recovered, washed, and stained with the appropriate antibodies. Cytometry was performed (BD LSRFortessa) at the Vanderbilt University Medical Center Flow Cytometry Shared Resource and analyzed using FlowJo v10.0.8 (Tree Star).

### Flow Cytometry Antibody Panels

Antibodies for intracellular cytokine staining included: anti-CD3-AF700, CD4-PcPCy5.5, CD8-PECF594, IFNγ-FITC, CD14-V500, CD19-V500, TNFα-APC, CD38-PECy7, HLA-DR-BV605 (BD Biosciences); PD-1-PE, IL-2-BV421 (BioLegend); Live-Dead-AquaViD (LifeTechnologies).

The T regulatory cell/activation panel included: anti-CD3-AF700, CD25-PE, HLA-DR-FITC (BD); CD4-PETxR, CD8-APC AF750, Live-Dead-AquaViD (LifeTechnologies); CD39-PECy7, FOXP3-APC (eBioscience); CD127- PE Cy5.5 (Beckman Coulter); CD38- BV421 (BioLegend).

### Cell Proliferation Assay

PBMC were thawed, washed with PBS, and labeled with CellTrace Violet (Life Technologies) at a final concentration of 5 µM. Cells ( $2 \times 10^6$  cells per condition) were incubated with Media, SEB 1 µg/ml, gamma-irradiated h37rv (10 µg/ml), ESAT-6 peptide pool (2 µg/ml per peptide), CFP-10 peptide pool (2 µg/ml per peptide). IL-2 at a final concentration of 1 U/ml was added at day 3. On day 6 cells were washed, and stained with anti

-CD3, -CD4, -CD8, -CD14/CD19 (dump channel), and the % of CellTrace Violet low cells was measured.

### The Brazilian Case-Control Study

In the Brazilian study population, cryopreserved PBMC samples and corresponding clinical and epidemiological data were obtained from participants enrolled in a translational study performed at the Instituto Brasileiro para Investigação da Tuberculose (IBIT) and at the Hospital Especializado Octavio Mangabeira (HEOM), Salvador, Bahia, northeast Brazil, between December 2015 and January 2018 (30). All persons with extrapulmonary TB had lymphatic disease.

The parent study was focused on characterization of inflammatory markers in different clinical forms of TB and recruited 1,792 individuals with presumptive TB at the referral primary care clinics. Participants underwent clinical assessments and chest x-ray examination. In addition, acid-fast bacilli (AFB) screening in sputum smears (by microscopy) and sputum cultures (Lowenstein-Jensen solid cultures) was performed in all patients. The patients with active TB were treated following the Brazilian National Guidelines (31). The parent study collected 10 ml of venous blood in sodium heparin tubes for isolation of PBMCs from a subset of participants who consented to blood collection. Blood collection occurred prior to initiation of anti-TB therapy (baseline), at month 2 and month 6 of treatment, and at month 18 after enrollment. Cells were cryopreserved in liquid nitrogen at the biorepository of the Laboratory of Inflammation and Biomarkers, Fundação Oswaldo Cruz, Salvador, Brazil.

The parent study also included participants who were asymptomatic contacts of pulmonary TB index cases. All TB contacts were actively screened for TB through clinical, radiologic, and microbiologic investigation (32). At the time of study enrollment, individuals not living with HIV who tested positive for QuantiFERON TB Gold-in-Tube (QFT) enzyme-linked immunosorbent assay (Qiagen) and also exhibited a positive tuberculin skin test (TST) result ( $> 5$  mm) were considered to have latent TB infection (LTBI), and individuals who were QFT-negative and had negative TST result ( $< 5$  mm) were considered uninfected controls (30).

The present investigation was a sub-study focused on characterization of T-cell responses at month 18 after enrollment (approximately 1 year after patients achieved microbiologic cure) in patients with drug-sensitive PTB or EPTB. We selected individuals with confirmed pulmonary or extrapulmonary TB, matching by age ( $\pm 5$  years) and sex, as well as for controls with or without LTBI. Samples from TB patients  $>18$  years old, HIV-negative, and no treatment failure, abandonment or relapse were included in the study. The exclusion criteria were the same used for the sub-study performed in USA.

### Flow Cytometry in the Brazilian Study

Cryopreserved PBMCs were thawed and resuspended in 1640 Roswell Park Memorial Institute medium supplemented with 10% fetal bovine serum at  $10^6$  cells per well in 96-well plates and rested for 2 h at 37°C in 5% CO<sub>2</sub>. Cells were washed and resuspended in complete media with Brefeldin-A (Biolegend, San Diego, CA) and

Monensin (Biolegend, San Diego, CA) to block cytokine secretion and stimulated with ESAT-6 and CFP-10 peptide pools (10 µg/ml) or irradiated H37Rv strain of *M. tuberculosis* (MOI: 5) (all from BEI Resources) overnight at 37°C in 5% CO<sub>2</sub>. Cells were then stained for cell surface markers with the following panel of antibodies: CD3 (clone OKT3), CD4 (clone RPA-T4), CD8 (clone OKT8), CD127 (clone eBioRDR5), CD25 (clone PC61.5), CD39 (clone eBioA1), and PD1 (clone J43), all from ThermoFisher. Cells were then fixed and permeabilized using the Foxp3 Fixation and Permeabilization Buffer (eBioscience). Intracellular staining was performed to detect IFN-γ (clone 4S.B3), TNF-α (clone Mab11), and all from ThermoFisher. In parallel experiments, we performed cell proliferation assay using the CellTrace Violet Cell Proliferation Kit (ThermoFisher) following the manufacturer's protocol. Acquisition of stained cells was performed using a BD LSRFortessa cell analyzer (BD Bioscience, San Jose, CA) and analyzed using FlowJo software (BD Bioscience, San Jose, CA).

## Statistical Analysis

In the U.S. study population, a convenience sample of available specimens from a previous study was used (33). In the Brazil study population, sample size was determined based on power of 80% (alpha error, 5%) to detect differences in median frequencies of T-cell subsets >2.5% between EPTB cases and TST negative controls, based on a previous study from our group (30).

Categorical variables were compared using the Pearson's chi-square test. Distributions of continuous variables were compared using the rank-sum and Kruskal-Wallis tests with Dunn's multiple comparisons *ad hoc* test. The chi-square test for trend was used to evaluate the fraction of responders across groups. Two-sided p values of <0.05 were considered statistically significant. Statistical analyses were performed using Graphpad Prism 8.0 (GraphPad Software, San Diego, CA).

## RESULTS

In the U.S. study population, there were 10 controls without LTBI, 11 controls with LTBI, 7 pulmonary TB controls, and 9 extrapulmonary TB cases. In the Brazilian study population, there were 25 participants in each of the four patient groups. The clinical and demographic characteristics of the study populations are in **Tables 1** and **2**. In both study populations, cases and controls were similar according to age, sex, tobacco use, and alcohol use. In the U.S. study population, participants with LTBI were more likely to be of black race, and persons with extrapulmonary TB were more likely to be born outside of the United States. Both extrapulmonary TB cases and pulmonary TB controls were evaluated a median of at least one year after TB treatment completion.

## Individuals With Prior Extrapulmonary TB Had the Highest Level of Intracellular Cytokine Responses to *M. tuberculosis* Antigens

We evaluated cytokine responses to overlapping peptides from the ESAT-6 and CFP-10 proteins as well as whole lysate of

**TABLE 1 |** Clinical and demographic characteristics of the study population in the United States (Tennessee).

Characteristic	No LTBI	LTBI	Prior PTB	Prior EPTB	P-value
N	10	11	7	9	
Age (years), median (IQR)	49 (30,52)	51 (39,57)	50 (38,66)	39 (36,45)	0.66
Male sex, no. (%)	6 (60)	6 (55)	6 (86)	5 (56)	0.55
Hispanic ethnicity, no. (%)	0 (0)	1 (9)	1 (14)	2 (22)	0.49
Black race, no. (%)	3 (30)	7 (64)	0 (0)	2 (22)	0.02
Foreign born, no. (%)	1 (10)	2 (18)	1 (14)	6 (67)	0.03
Tobacco use <sup>1</sup> , no. (%)	2 (20)	3 (27)	5 (71)	2 (22)	0.13
Alcohol use <sup>2</sup> , no. (%)	4 (40)	2 (18)	2 (29)	1 (11)	0.54
Years from treatment completion to blood draw (years), median (IQR)	N/A	N/A	1.2 (0.60,2.80)	1.7 (0.94, 4.0)	0.34

LTBI, latent tuberculosis infection, based on a positive tuberculin skin test; PTB, pulmonary tuberculosis;

EPTB, extrapulmonary tuberculosis.

Data are shown as median and interquartile (IQR) range or frequency (percentage). Data were compared between the clinical groups.

Using the Kruskal-Wallis test (continuous variables) or the Pearson's  $\chi^2$  test (for data on frequency).

<sup>1</sup>More than 10 cigarettes/day;

<sup>2</sup>Four or more drinks/week;

N/A Not applicable.

**TABLE 2 |** Clinical and demographic characteristics of the study population in Brazil (Bahia).

Characteristic	No LTBI	LTBI	Prior PTB	Prior EPTB	P-value
N	25	25	25	25	
Age (years), median (IQR)	24 (20–31)	26 (20–33)	28 (19–31)	26 (21–28)	> 0.99
Male sex, no. (%)	13 (52)	12 (48)	13 (52)	14 (56)	0.96
Non-white race, no. (%)	22 (88)	20 (80)	24 (96)	23 (92)	0.31
Illicit drug use <sup>1</sup> no. (%)	2 (8)	3 (12)	4 (16)	3 (12)	0.86
Smoking <sup>2</sup> no. (%)	1 (4)	3 (12)	7 (28)	3 (12)	0.10
Alcohol abuse <sup>3</sup> no. (%)	5 (20)	7 (28)	10 (40)	14 (56)	0.08
Acid-fast bacilli smear grade no. (%)					0.58
0	25 (100)	25 (100)	0 (0)	0 (0)	
1+/scanty	0 (0)	0 (0)	1 (4)	3 (12)	
2+	0 (0)	0 (0)	14 (56)	13 (52)	
≥3+	0 (0)	0 (0)	10 (40)	9 (36)	

LTBI, latent tuberculosis infection, based on a positive tuberculin skin test; PTB, pulmonary tuberculosis; EPTB, extrapulmonary tuberculosis.

Data are shown as median and interquartile (IQR) range or frequency (percentage). Data were compared between the clinical groups using the Kruskal-Wallis test (continuous variables) or the Pearson's  $\chi^2$  test (for data on frequency).

*Mycobacterium tuberculosis* from either sputum or extrapulmonary site; all extrapulmonary disease was lymphatic.

The frequency of individuals with different values of acid-fast bacilli smear grade at the time of diagnosis was compared between PTB and EPTB groups (the groups of individuals without and with LTBI, as well as persons with negative smears, were excluded from this analysis).

Smear grade was from sputum samples for PTB patients or lymph node aspirates for EPTB. All individuals tested negative for HIV infection.

<sup>1</sup>Illicit drugs: cannabis, cocaine, or crack;

<sup>2</sup>Past or current cigarette smoking;

<sup>3</sup>Two or more points on the CAGE questionnaire.

inactivated (gamma-irradiated) *Mtb* (gRV) (**Figure 1**). In the U.S. study population in response to the CFP10 peptide pool, the median frequency of interferon (IFN)- $\gamma$  and TNF- $\alpha$  producing cells tended to be highest among those with prior EPTB ( $P = >0.05$ ; Kruskal-Wallis) (**Figure 1A**). Compared to controls without LTBI, persons with prior EPTB had the highest magnitude response ( $P = 0.02$ ; Dunn's posttest). In the Brazilian study population in response to CFP10 and ESAT6, persons with prior EPTB had the highest IFN- $\gamma$  and TNF- $\alpha$  producing cells ( $P < 0.001$ ; Kruskal-Wallis) (**Figure 1B**). Similar trends of higher responses in persons with prior EPTB was observed in response to inactivated *Mtb* organisms, in both study populations (**Figures 1C, D**).

## Individuals With Prior Extrapulmonary TB Had High Levels of CD4+ Proliferation in Response to *M. tuberculosis* Antigens

In Brazil, persons with prior EPTB had the highest levels of CD4 proliferation to *M. tuberculosis* antigens ( $P < 0.0001$ ) (**Figure 2**). Although not seen to the same extent in the U.S. population,

among persons with prior EPTB there were 3 outliers with high levels of CD4 proliferation.

## T Regulatory Cell Frequency Phenotype Among Individuals

We measured both Treg cell frequency and expression of the CD39 marker on Treg and non-Treg CD4+ T cells in these individuals (**Figure 3**). In the U.S. population we found no significant differences in Treg frequencies across groups ( $p > 0.05$ ; Kruskal-Wallis; **Figure 3A**). While the individuals with the highest expression of CD39 were in the EPTB group, the median expression was not statistically significant across groups (**Figure 3C**). We also measured PD-1 expression and saw no trend across groups (data not shown).

In the Brazil study population, Treg CD39 expression was the lowest in the LTBI group, and highest in the EPTB group overall ( $p < 0.0001$ ; Kruskal-Wallis; **Figure 3D**). Indeed, Treg CD39 expression among persons with LTBI was lower than that in the no LTBI ( $p = 0.0003$ ); PTB ( $p = 0.0001$ ) and EPTB groups ( $p = 0.0001$ ) after adjustment for multiple comparisons. Although

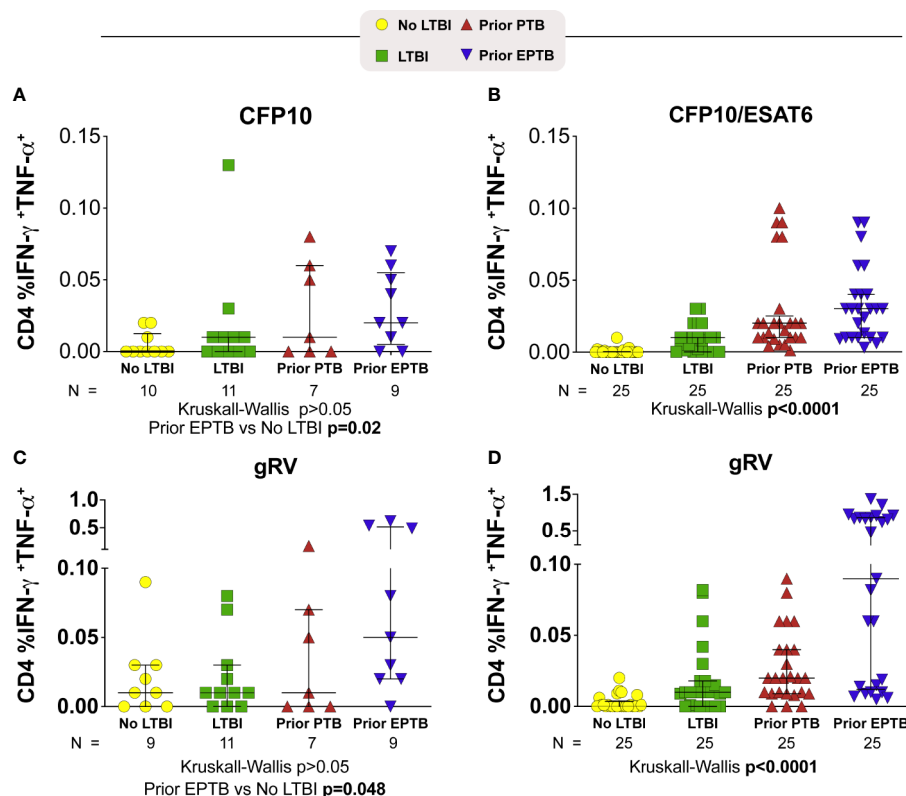


**FIGURE 1** | CD4+ T-cell intracellular cytokine responses to *M. tuberculosis* antigens. Scatter plots depicting the expression of intracellular cytokine by CD4+ T-lymphocytes from TB patients with PTB or EPTB presentation and controls (TST+ and TST-). Frequencies of IFN- $\gamma$ +TNF- $\alpha$ +CD4+ T cells from whole blood obtained and compared according to the stimulation. (**A, B**) Frequencies of IFN- $\gamma$ +TNF- $\alpha$ +CD4+ T cells responses to stimulation with a pool of CFP-10 peptides (A; U.S. study population) or CFP-10 and ESAT-6 (B; Brazilian study population). (**C, D**) Frequencies of IFN- $\gamma$ +TNF- $\alpha$ +CD4+ T cells responses after incubation of PBMC with gRV (C; U.S. study population) (D; Brazilian study population). Background has been subtracted out. Lines represent median values and interquartile ranges (IQR). The differences in median values (and IQR) between groups were compared using the Kruskal-Wallis test with Dunn's multiple comparisons post-test. TB, tuberculosis; PTB, pulmonary tuberculosis; EPTB, extrapulmonary tuberculosis; TST, tuberculin skin test.

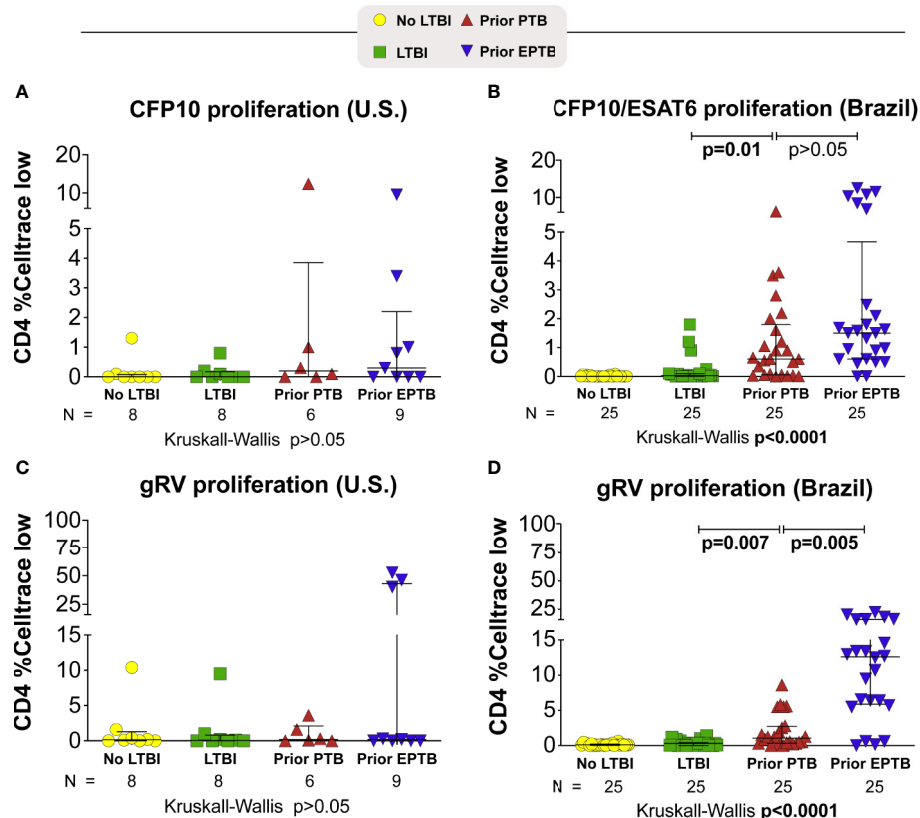


**FIGURE 2** | Proliferative responses to *M. tuberculosis* antigens. Briefly, PBMC were incubated with *M. tuberculosis* antigens for 6 days. Proliferating cells were identified as Celltrace violet low. **(A, B)** Celltrace low expression in CD4+ T-cells stimulated with CFP-10 pool or CFP-10 pool and ESAT-6 **(A)** U.S. study population. **(B)** Brazilian study population. **(C, D)** Celltrace low expression in CD4+ T-cells stimulated with gRV. Lines represent median values and interquartile ranges (IQR). The differences in median values (and IQR) between groups were compared using the Kruskal-Wallis test with Dunn's multiple comparisons post-test. TB, tuberculosis; PTB, pulmonary tuberculosis; EPTB, extrapulmonary tuberculosis; TST, tuberculin skin test; CFP, Culture filtrate protein; ESAT, early secretory antigen of tuberculosis; gRV,  $\gamma$ -irradiated *M. tuberculosis*.

PTB had lower than EPTB Treg CD39 expression, this was not statistically significant ( $p > 0.05$ ).

## DISCUSSION

We sought to determine whether functional differences in immune responses were present among individuals after successful treatment of pulmonary or extrapulmonary TB. Most studies describing immune function in the setting of differing manifestations of TB have compared individuals with active disease to individuals with LTBI (34, 35). Chronic infection is associated with changes in immune function due to chronic activation and subsequent immune exhaustion (23). In a prior study, we found that even several months to years after clearance of TB disease, individuals with prior extrapulmonary TB had persistently elevated immune activation and increased frequencies of circulating Treg cells (13). Here, we extended this analysis to evaluate the frequencies of Mtb-reactive T cells and

perform a more detailed phenotypic analysis of circulating Treg cells.

We found levels of Mtb-reactive responses to be highest in persons with previous EPTB. This finding was consistent in both the U.S. and Brazilian study populations. These cells were polyfunctional, as they were able to secrete IFN- $\gamma$  and TNF- $\alpha$ . Our findings contrast with Scriba et. al, who found lower frequencies of Mtb-reactive cells in individuals with self-reported previously treated TB disease (36). This may be because we included a group with confirmed prior extrapulmonary TB, while in the other study the location of TB disease was not specified. Future studies to evaluate the immune factors associated with control of *M. tuberculosis* infection should specifically study the extent of active disease.

In our prior work, we found increased levels of immune activation and Treg frequency in individuals with prior extrapulmonary TB. In this smaller North American cohort, we found a similar trend toward higher frequencies of Treg cells in individuals with prior EPTB. CD39 expression is associated



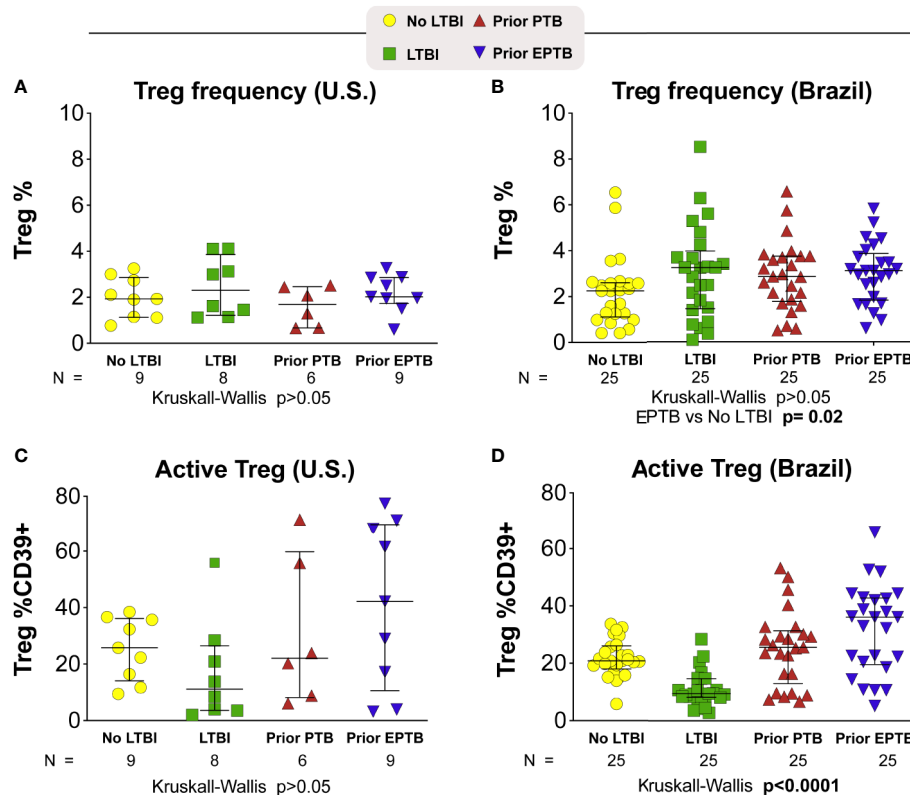


**FIGURE 3** | T-regulatory cell frequency and phenotype. Scatter plots depicting the Treg frequency (A) in U.S. study population (B) in Brazilian study population. Frequency of Treg CD39+ (C) in U.S. study population (D) in Brazilian study population. Lines represent median values and interquartile ranges (IQR). The differences in median values (and IQR) between groups were compared using the Kruskal-Wallis test with Dunn's multiple comparisons post-test. TB, tuberculosis; PTB, pulmonary tuberculosis; EPTB, extrapulmonary tuberculosis; TST, tuberculin skin test; CFP, Culture filtrate protein; ESAT, early secretory antigen of tuberculosis; gRV,  $\gamma$ -irradiated *M. tuberculosis*.

with active T regulatory cells and has been shown to be elevated during active TB disease (23). In the U.S. cohort we found no difference in median CD39 expression across the four study groups, but individuals with prior EPTB had the highest level of CD39 expression on Treg cells. In the larger Brazilian cohort, we found the same pattern, but demonstrated differences among groups with a high level of statistical significance. This suggests that a high frequency of circulating active Tregs is an immunological feature of individuals with successfully treated TB.

One hypothesis to explain increased susceptibility to EPTB would be some degree of immune deficiency. Individuals with HIV infection have a higher incidence of active TB disease, and a higher incidence of extrapulmonary disease (37), suggesting that a lack of pathogen-specific CD4+ T-cell responses may lead to more severe disease manifestations. Scriba et al. recently published data suggesting lower overall frequencies of Mtb-reactive T-cell responses in individuals with previously treated TB compared to individuals with LTBI, and these differing responses were dependent on the epitopes recognized (36). The cytokine profile of responding cells may be important for immune control. Arleham et al. found that individuals with a higher proportion of Mtb-

reactive CD4+ T-cells with a TH1/TH17 cytokine profile were less likely to progress to active disease (38), and this population of cells appears to be preferentially depleted in the setting of HIV infection (39). However, the population of TH1/TH17 cells is still a small proportion of Mtb-reactive cells in these individuals, so it remains to be determined whether these cells are specifically responsible for immune control of LTBI.

The biggest limitation of our study was the small sample size. However, demonstration of similar results in two independent study populations decreased this concern. We measured systemic immune responses since they are likely to be a critical determinant of the extent and severity of disease. We measured immune responses specific to Mtb and did not assess responses to other microbial pathogens. However, immune responses to Mtb are likely most pertinent in TB pathogenesis. In addition, Th17 cells were not evaluated. Studies delineating immune cell sub-types could provide more insights into the pathogenesis of extrapulmonary TB. This could also provide insights into possible links between chronic inflammation and other immune-mediated diseases.

Despite our partial understanding of risk factors associated with progression from LTBI to active TB disease, it is unclear



which immune responses are responsible for continued control of LTBI in the majority of infected individuals. Here we demonstrated that individuals with treated EPTB maintain higher frequencies of Mtb-reactive CD4<sup>+</sup> memory T-cells compared with individuals with prior pulmonary disease or LTBI. These cells are “polyfunctional” with regard to their ability to generate IFN- $\gamma$  and TNF- $\alpha$  in response to Mtb antigens. Consistent with our prior work, we found trends toward these individuals having higher frequencies of Tregs (13) as well higher Treg expression of CD39. It remains to be determined whether higher frequencies of Tregs or Treg CD39 expression was a feature of these individuals prior to active TB disease, and therefore increased their risk of developing EPTB. A goal of future longitudinal studies will be to identify individuals with LTBI prior to the development of active TB disease to determine whether there are immune signatures predictive of continued control of LTBI or that identify individuals at risk for disseminated disease.

## DATA AVAILABILITY STATEMENT

The raw data supporting the conclusions of this article will be made available by the authors, without undue reservation.

## ETHICS STATEMENT

In the U.S. study, all participants provided written informed consent. The study was approved by the institutional review boards of Vanderbilt University Medical Center, Nashville Davidson Metro Public Health Department, and the Tennessee Department of Health. The study in Brazil was approved by the Maternidade Clímério de Oliveira Ethics Committee, Federal University of Bahia. The patients/participants provided their written informed consent to participate in this study.

## REFERENCES

- Houben RMGJ, Dodd PJ. The Global Burden of Latent Tuberculosis Infection: A Re-estimation Using Mathematical Modelling. *PLoS Med* (2016) 13(10):e1002152. doi: 10.1371/journal.pmed.1002152
- World Health Organization. *WHO guidelines on tuberculosis infection prevention and control: 2019 update*. World Health Organization (2019). Available at: <http://www.ncbi.nlm.nih.gov/books/NBK539297/>.
- Flynn JL, Chan J. Immunology of Tuberculosis. *Annu Rev Immunol* (2001) 19(1):93–129. doi: 10.1146/annurev.immunol.19.1.93
- Flynn JL, Chan J. Tuberculosis: Latency and Reactivation. *Infect Immun* (2001) 69(7):4195–201. doi: 10.1128/IAI.69.7.4195-4201.2001
- Shea KM, Kammerer JS, Winston CA, Navin TR, Horsburgh CR. Estimated rate of reactivation of latent tuberculosis infection in the United States, overall and by population subgroup. *Am J Epidemiol* (2014) 179(2):216–25. doi: 10.1093/aje/kwt246
- Sutherland I. Recent studies in the epidemiology of tuberculosis, based on the risk of being infected with tubercle bacilli. *Adv Tuberc Res* (1976) 19:1–63.
- Kritski AL, Marques MJ, Rabahi MF, Vieira MA, Werneck-Barroso E, Carvalho CE, et al. Transmission of tuberculosis to close contacts of

## AUTHOR CONTRIBUTIONS

BB-D, TS, CF, AA, CN, RS, LB, CW, AB, JL, BA, and SK contributed to conception and design of the study. SK, BB-D, BA, and TS performed the data curation. BB-D, TS, CF, CN, LB, CW, and AB processed and analyzed the data. KS and BA worked on data visualization. BB-D, TS, SK, and BA wrote the first draft of the manuscript. All authors contributed to the article and approved the submitted version.

## FUNDING

The study was supported by grants from the National Institutes of Health, NIAID 1R21AI127129-01 (SK); NIH U01 AI069923 (CCASAnet and RePORT-Brazil: LB, AB, JL, BA, TS), NIAID 1 P30AI110527-03 Tennessee Center for AIDS Research (TNCfAR) (CN, CW, SK, TS); Brazilian Research Council/CNPq 469607/2014-9 (AA, JL), K23AI091692 (CF). The work from BA was supported by the Intramural Research Program of Fundação Oswaldo Cruz. BA and JL are senior scientists from CNPq. The work from LB was supported by the National Institutes of Health (U01 AI069923). BB-D received a research fellowship from the Coordenação de Aperfeiçoamento de Pessoal de Nível Superior (CAPES).

## ACKNOWLEDGMENTS

The authors thank the study participants.

## SUPPLEMENTARY MATERIAL

The Supplementary Material for this article can be found online at: <https://www.frontiersin.org/articles/10.3389/fimmu.2020.605338/full#supplementary-material>

- patients with multidrug-resistant tuberculosis. *Am J Respir Crit Care Med* (1996) 153(1):331–5. doi: 10.1164/ajrccm.153.1.8542139
- Reichler MR, Khan A, Sterling TR, Zhao H, Moran J, McAuley J, et al. Risk and Timing of Tuberculosis Among Close Contacts of Persons with Infectious Tuberculosis. *J Infect Dis* (2018) 14218(6):1000–8. doi: 10.1093/infdis/jiy265
- Scriba TJ, Coussens AK, Fletcher HA. *Human Immunology of Tuberculosis. Microbiology Spectrum*, Vol. 5. Microbiology Spectrum (American Society for microbiology press) (2017). Available at: <http://www.asmscience.org/content/journal/microbiolspec/10.1128/microbiolspec.TB2-0016-2016>.
- Jones BE, Young SM, Antoniskis D, Davidson PT, Kramer F, Barnes PF. Relationship of the manifestations of tuberculosis to CD4 cell counts in patients with human immunodeficiency virus infection. *Am Rev Respir Dis* (1993) 148(5):1292–7. doi: 10.1164/ajrccm/148.5.1292
- Lewinsohn DA, Gennaro ML, Scholvinck L, Lewinsohn DM. Tuberculosis immunology in children: diagnostic and therapeutic challenges and opportunities. *Int J Tuberc Lung Dis* (2004) 8(5):658–74.
- Antas P, Ding L, Hackman J, Reeveshammock L, Shintani A, Schiffer J, et al. Decreased CD4<sup>+</sup> lymphocytes and innate immune responses in adults with previous extrapulmonary tuberculosis. *J Allergy Clin Immunol* (2006) 117(4):916–23. doi: 10.1016/j.jaci.2006.01.042

13. de Almeida AS, Fiske CT, Sterling TR, Kalams SA. Increased Frequency of Regulatory T Cells and T Lymphocyte Activation in Persons with Previously Treated Extrapulmonary Tuberculosis. *Clin Vaccine Immunol* (2012) 19 (1):45–52. doi: 10.1128/CVI.05263-11
14. Guyot-Revol V, Innes JA, Hackforth S, Hinks T, Lalvani A. Regulatory T cells are expanded in blood and disease sites in patients with tuberculosis. *Am J Respir Crit Care Med* (2006) 173(7):803–10. doi: 10.1164/rccm.200508-1294OC
15. Ribeiro-Rodrigues R, Resende Co T, Rojas R, Toossi Z, Dietze R, Boom WH, et al. A role for CD4+CD25+ T cells in regulation of the immune response during human tuberculosis. *Clin Exp Immunol* (2006) 144(1):25–34. doi: 10.1111/j.1365-2249.2006.03027.x
16. Rahman S, Gudetta B, Fink J, Granath A, Ashenafi S, Aseffa A, et al. Compartmentalization of immune responses in human tuberculosis: few CD8+ effector T cells but elevated levels of FoxP3+ regulatory T cells in the granulomatous lesions. *Am J Pathol* (2009) 174(6):2211–24. doi: 10.2353/ajpath.2009.080941
17. Marin ND, Paris SC, Vélez VM, Rojas CA, Rojas M, García LF. Regulatory T cell frequency and modulation of IFN- $\gamma$  and IL-17 in active and latent tuberculosis. *Tuberculosis (Edinb)* (2010) 90(4):252–61. doi: 10.1016/j.tube.2010.05.003
18. Pang H, Yu Q, Guo B, Jiang Y, Wan L, Li J, et al. Frequency of Regulatory T-Cells in the Peripheral Blood of Patients with Pulmonary Tuberculosis from Shanxi Province, China. *PLoS One* (2013) 8(6):e65496. doi: 10.1371/journal.pone.0065496
19. Sahmoudi K, Abbassi H, Bouklata N, El Alami MN, Sadak A, Burant C, et al. Immune activation and regulatory T cells in Mycobacterium tuberculosis infected lymph nodes. *BMC Immunol* (2018) 19(1):33. doi: 10.1186/s12865-018-0266-8
20. Borsellino G, Kleinewietfeld M, Di Mitri D, Sternjak A, Diamantini A, Giammetto R, et al. Expression of ectonucleotidase CD39 by Foxp3+ Treg cells: hydrolysis of extracellular ATP and immune suppression. *Blood* (2007) 110(4):1225–32. doi: 10.1182/blood-2006-12-064527
21. Gu J, Ni X, Pan X, Lu H, Lu Y, Zhao J, et al. Human CD39hi regulatory T cells present stronger stability and function under inflammatory conditions. *Cell Mol Immunol* (2017) Jun14(6):521–8. doi: 10.1038/cmi.2016.30
22. Chiacchio T, Casetti R, Butera O, Vanini V, Carrara S, Girardi E, et al. Characterization of regulatory T cells identified as CD4(+)CD25(high)CD39 (+) in patients with active tuberculosis. *Clin Exp Immunol* (2009) 156(3):463–70. doi: 10.1111/j.1365-2249.2009.03908.x
23. Kim K, Perera R, Tan DBA, Fernandez S, Seddiki N, Waring J, et al. Circulating mycobacterial-reactive CD4+ T cells with an immunosuppressive phenotype are higher in active tuberculosis than latent tuberculosis infection. *Tuberculosis (Edinb)* (2014) 94(5):494–501. doi: 10.1016/j.tube.2014.07.002
24. Jasenosky LD, Scriba TJ, Hanekom WA, Goldfeld AE. T cells and adaptive immunity to Mycobacterium tuberculosis in humans. *Immunol Rev* (2015) 264(1):74–87. doi: 10.1111/imr.12274
25. Centers for Disease Control and Prevention (CDC). *National Tuberculosis Controllers, Centers for Disease Control and Prevention. Guidelines for the investigation of contacts of persons with infectious tuberculosis*. Centers for Disease Control and Prevention (CDC) (2005). Available at: <https://www.cdc.gov/mmwr/pdf/rr/rr5415.pdf>.
26. Shafer RW, Edlin BR. Tuberculosis in patients infected with human immunodeficiency virus: perspective on the past decade. *Clin Infect Dis* (1996) 22(4):683–704. doi: 10.1093/clinids/22.4.683
27. Sodhi A, Gong J, Silva C, Qian D, Barnes PF. Clinical correlates of interferon gamma production in patients with tuberculosis. *Clin Infect Dis* (1997) 25 (3):617–20. doi: 10.1086/513769
28. Barnes PF, Lu S, Abrams JS, Wang E, Yamamura M, Modlin RL. Cytokine production at the site of disease in human tuberculosis. *Infect Immun* (1993) 61(8):3482–9. doi: 10.1128/IAI.61.8.3482-3489.1993
29. Barcelo H, Faul J, Crimmins E, Thyagarajan B. A Practical Cryopreservation and Staining Protocol for Immunophenotyping in Population Studies. *Curr Protoc Cytom* (2018) 84(1):e35. doi: 10.1002/cpcy.35
30. Silveira-Mattos PS, Barreto-Duarte B, Vasconcelos B, Fukutani KF, Vinhaes CL, Oliveira-De-Souza D, et al. Differential Expression of Activation Markers by Mycobacterium tuberculosis-specific CD4+ T Cell Distinguishes Extrapulmonary From Pulmonary Tuberculosis and Latent Infection. *Clin Infect Dis* (2020) 71(8):1905–11. doi: 10.1093/cid/ciz1070
31. BRASIL. Manual de Recomendações para o Controle da Tuberculose no Brasil. (2019) 2a):366.
32. Araújo NCN, Cruz CMS, Arriaga MB, Cubillos-Angulo JM, Rocha MS, Silveira-Mattos PS, et al. Determinants of losses in the latent tuberculosis cascade of care in Brazil: A retrospective cohort study. *Int J Infect Dis* (2020) 93:277–83. doi: 10.1016/j.ijid.2020.02.015
33. Fiske CT, Blackman A, Maruri F, Rebeiro PF, Huaman M, Kator J, et al. Increased vitamin D receptor expression from macrophages after stimulation with M. tuberculosis among persons who have recovered from extrapulmonary tuberculosis. *BMC Infect Dis* (2019) 19:366. doi: 10.1186/s12879-019-3958-7
34. Rozot V, Vigano S, Mazza-Stalder J, Idrizi E, Day CL, Perreau M, et al. Mycobacterium tuberculosis-specific CD8+ T cells are functionally and phenotypically different between latent infection and active disease. *Eur J Immunol* (2013) 43(6):1568–77. doi: 10.1002/eji.201243262
35. Adekambi T, Ibegbu CC, Cagle S, Kalokhe AS, Wang YF, Hu Y, et al. Biomarkers on patient T cells diagnose active tuberculosis and monitor treatment response. *J Clin Invest* (2015) 125(5):1827–38. doi: 10.1172/JCI77990
36. Scriba TJ, Penn-Nicholson A, Shankar S, Hraha T, Thompson EG, Sterling D, et al. Sequential inflammatory processes define human progression from M. tuberculosis infection to tuberculosis disease. *PLoS Pathog* (2017) 13(11):e1006687. doi: 10.1371/journal.ppat.1006687
37. Shivakoti R, Sharma D, Mamoon G, Pham K. Association of HIV infection with extrapulmonary tuberculosis: a systematic review. *Infection* (2017) 45 (1):11–21. doi: 10.1007/s15010-016-0960-5
38. Arlehamn CL, Seumois G, Gerasimova A, Huang C, Fu Z, Yue X, et al. Transcriptional profile of tuberculosis antigen-specific T cells reveals novel multifunctional features. *J Immunol* (2014) 193(6):2931–40. doi: 10.4049/jimmunol.1401151
39. Murray LW, Satti I, Meyerowitz J, Jones M, Willberg CB, Ussher JE, et al. HIV infection impairs Th1 and Th17 Mycobacterium tuberculosis-specific T cell responses. *J Infect Dis* (2018) 217(11):1782–92. doi: 10.1093/infdis/jiy052

**Conflict of Interest:** The authors declare that the research was conducted in the absence of any commercial or financial relationships that could be construed as a potential conflict of interest.

The handling editor declared a past co-authorship with the authors BA and TS.

Copyright © 2020 Barreto-Duarte, Sterling, Fiske, Almeida, Nochowicz, Smith, Barnett, Warren, Blackman, Lapa e Silva, Andrade and Kalams. This is an open-access article distributed under the terms of the Creative Commons Attribution License (CC BY). The use, distribution or reproduction in other forums is permitted, provided the original author(s) and the copyright owner(s) are credited and that the original publication in this journal is cited, in accordance with accepted academic practice. No use, distribution or reproduction is permitted which does not comply with these terms.



# Systemic Inflammation in Pregnant Women With Latent Tuberculosis Infection

Shilpa Naik<sup>1,2</sup>, Mallika Alexander<sup>1</sup>, Pavan Kumar<sup>3</sup>, Vandana Kulkarni<sup>1</sup>, Prasad Deshpande<sup>1</sup>, Su Yadana<sup>4</sup>, Cheng-Shiun Leu<sup>5</sup>, Mariana Araújo-Pereira<sup>6,7,8</sup>, Bruno B. Andrade<sup>6,7,8,9,10,11</sup>, Ramesh Bhosale<sup>1,2</sup>, Subash Babu<sup>3</sup>, Amita Gupta<sup>1,12</sup>, Jyoti S. Mathad<sup>13</sup> and Rupak Shivakoti<sup>4\*</sup>

<sup>1</sup> Byramjee-Jeejeebhoy Government Medical College-Johns Hopkins University Clinical Research Site, Pune, India, <sup>2</sup> Department of Obstetrics and Gynecology, Byramjee Jeejeebhoy Government Medical College, Pune, India, <sup>3</sup> International Center for Excellence in Research, National Institutes of Health, National Institute for Research in Tuberculosis, Chennai, India, <sup>4</sup> Department of Epidemiology, Columbia University Mailman School of Public Health, New York, NY, United States, <sup>5</sup> Department of Biostatistics, Columbia University Mailman School of Public Health, New York, NY, United States, <sup>6</sup> Instituto Goncalo Moniz, Fundação Oswaldo Cruz, Salvador, Brazil, <sup>7</sup> Multinational Organization Network Sponsoring Translational and Epidemiological Research, Fundação José Silveira, New York, NY, Brazil, <sup>8</sup> Faculdade de Medicina, Universidade Federal da Bahia, Salvador, Brazil, <sup>9</sup> Curso de Medicina, Faculdade de Tecnologia e Ciências, Salvador, Brazil, <sup>10</sup> Escola de Medicina, Universidade Salvador (UNIFACS), Laureate International Universities, Salvador, Brazil, <sup>11</sup> Curso de Medicina, Escola Bahiana de Medicina e Saúde Pública (EBMSP), Salvador, Brazil, <sup>12</sup> Department of Medicine, Johns Hopkins University School of Medicine, Baltimore, MD, United States, <sup>13</sup> Department of Medicine, Weill Cornell Medical College, New York, NY, United States

## OPEN ACCESS

### Edited by:

Christof Geldmacher,  
University of Munich, Germany

### Reviewed by:

Patrice Mawa,  
Medical Research Council, Uganda  
Gerhard Walzl,  
Stellenbosch University, South Africa

### \*Correspondence:

Rupak Shivakoti  
rs3895@cumc.columbia.edu

### Specialty section:

This article was submitted to  
Microbial Immunology,  
a section of the journal  
Frontiers in Immunology

Received: 26 July 2020

Accepted: 09 December 2020

Published: 27 January 2021

### Citation:

Naik S, Alexander M, Kumar P, Kulkarni V, Deshpande P, Yadana S, Leu C-S, Araújo-Pereira M, Andrade BB, Bhosale R, Babu S, Gupta A, Mathad JS and Shivakoti R (2021) Systemic Inflammation in Pregnant Women With Latent Tuberculosis Infection. *Front. Immunol.* 11:587617. doi: 10.3389/fimmu.2020.587617

**Background:** Recent studies in adults have characterized differences in systemic inflammation between adults with and without latent tuberculosis infection (LTBI+ vs. LTBI-). Potential differences in systemic inflammation by LTBI status has not been assessed in pregnant women.

**Methods:** We conducted a cohort study of 155 LTBI+ and 65 LTBI- pregnant women, stratified by HIV status, attending an antenatal clinic in Pune, India. LTBI status was assessed by interferon gamma release assay. Plasma was used to measure systemic inflammation markers using immunoassays: IFN $\beta$ , CRP, AGP, I-FABP, IFN $\gamma$ , IL-1 $\beta$ , soluble CD14 (sCD14), sCD163, TNF, IL-6, IL-17a and IL-13. Linear regression models were fit to test the association of LTBI status with each inflammation marker. We also conducted an exploratory analysis using logistic regression to test the association of inflammatory markers with TB progression.

**Results:** Study population was a median age of 23 (Interquartile range: 21–27), 28% undernourished (mid-upper arm circumference (MUAC) <23 cm), 12% were vegetarian, 10% with gestational diabetes and 32% with HIV. In multivariable models, LTBI+ women had significantly lower levels of third trimester AGP, IL1 $\beta$ , sCD163, IL-6 and IL-17a. Interestingly, in exploratory analysis, LTBI+ TB progressors had significantly higher levels of IL1 $\beta$ , IL-6 and IL-13 in multivariable models compared to LTBI+ non-progressors.

**Conclusions:** Our data shows a distinct systemic immune profile in LTBI+ pregnant women compared to LTBI- women. Data from our exploratory analysis suggest that LTBI+ TB progressors do not have this immune profile, suggesting negative association of this

profile with TB progression. If other studies confirm these differences by LTBI status and show a causal relationship with TB progression, this immune profile could identify subsets of LTBI+ pregnant women at high risk for TB progression and who can be targeted for preventative therapy.

**Keywords:** latent tuberculosis infection, tuberculosis disease, inflammation, pregnancy, cytokines, LTBI, TB

## INTRODUCTION

Active tuberculosis (TB) disease elicits host responses characterized by an immune profile that is clearly distinct from healthy individuals (1, 2). As the causative agent *Mycobacterium tuberculosis* (*Mtb*) is actively replicating during TB disease, it causes constant antigen stimulation from the bacterium that shapes the immune response. In contrast, with latent TB infection (LTBI), *Mtb* is not actively replicating in the host and antigen stimulation with *Mtb* antigens is required to generate *Mtb*-specific immune responses (1). While differences in immunity with *Mtb* antigen stimulation has been extensively studied for active disease or LTBI compared to healthy individuals (1–5), there are limited studies characterizing differences by LTBI status in circulating inflammatory markers, in the absence of antigen stimulation (6–8). This information could potentially explain why an increased risk of certain adverse outcomes (e.g. acute myocardial infarction) has been observed among LTBI+ individuals, or help identify immune profiles associated with TB progression (9, 10).

One hypothesis on levels of inflammation by LTBI status is that there is no difference in circulating inflammatory markers between LTBI+ and LTBI– individuals. *Mtb* infection is mainly quiescent during LTBI and can remain in this form for a long time without harm to most individuals (11, 12). However, recent data from studies in adults suggest that there might be differences in systemic inflammation by LTBI status (6–8, 13). For example, a study of Indian adults observed that after adjusting for potential confounders, LTBI+ individuals had significantly higher levels of circulating pro-inflammatory mediators IL-6 and MCP-1 but lower levels of C-reactive protein (CRP), another pro-inflammatory marker, compared to LTBI– individuals (6).

While studies have started to assess potential differences in systemic inflammation by LTBI status in non-pregnant adults (6–8, 13), there is no data on pregnant women. Pregnant women have a distinct immune profile compared to adults, and there are temporal changes in immunity during pregnancy (14). It is not currently known whether there is a difference in systemic inflammation between LTBI+ and LTBI– pregnant women, and how this might change by trimester of pregnancy. Furthermore, LTBI+ women have a higher risk of *Mtb* progression during pregnancy and *post-partum*, but the reasons are not clear (15–17). The immune profile during pregnancy, including the systemic inflammatory milieu, may inform on potential changes to immunity that increase susceptibility to TB disease during pregnancy. In order to address this research gap in our understanding of systemic immunity in LTBI+ pregnant women, we compared the levels

of systemic inflammatory markers, at the second and third trimesters, by LTBI status in a cohort of pregnant women from Pune, India and explored the association of these immune markers with TB progression during pregnancy and post-partum.

## METHODS

### Study Design and Population

A cohort study of pregnant women was conducted at Byramjee Jeejeebhoy Government Medical College (BJGMC) in Pune, India from 2016 to 2019. Adult pregnant women, aged 18–40 years and between 13 and 34 weeks of gestation (confirmed by early pregnancy ultrasound), receiving antenatal care at BJGMC were enrolled for this study. Pregnant women with active TB at entry were excluded. We enrolled four cohorts of pregnant women based on their latent tuberculosis infection (LTBI) and HIV status: 1) LTBI+HIV+ (N = 35), 2) LTBI+HIV– (N = 130), 3) LTBI–HIV+ (N = 44) and 4) LTBI–HIV– (N = 25). The sample size for this cohort was based on the primary objective of the cohort study which was to compare the concentrations of Th1 cytokines after MTB-specific antigen stimulation by stage of pregnancy. LTBI status was determined using Interferon Gamma Release Assay (IGRA Quantiferon TB-Gold) according to manufacturer's instructions. Sampling within each cohort was based on convenience sampling of those that met eligibility criteria.

### Ethics Statement

All clinical investigations were conducted according to the principles expressed in the Declaration of Helsinki. Written informed consent was obtained from all participants. This study was approved by the institutional review boards and ethics committees at BJGMC, Johns Hopkins University, Weill Cornell and Columbia University. We followed guidelines for human experimentation from the US Department of Health and Human Services.

### Data Collection and Laboratory Procedures

Sociodemographic information and clinical data were collected from pregnant women at the enrollment visit (13–34 weeks of gestation), at the third trimester visit (for those enrolled in the second trimester), at delivery and approximately every 3 months *post-partum*. At each follow-up visit, women were administered a World Health Organization (WHO) TB symptom screening questionnaire. Women with a positive WHO symptom screen, unintentional weight loss since last visit or with clinical findings



on examination were further investigated with sputum GeneXpert, acid-fast bacilli test, chest X-ray and abdominal ultrasound. Culture in Lowenstein Jensen (LJ) media and liquid Mycobacteria Growth Indicator Tube (MGIT) were performed for further confirmation in those with positive findings.

Relevant to this analysis, blood was also collected at each visit in heparin tubes and plasma samples were stored in  $-80^{\circ}\text{C}$  until further use. We conducted single-plex immunoassays on second and third trimester plasma samples according to the manufacturer's (R&D Systems, Minneapolis, MN) directions for soluble CD163 (sCD163), soluble CD14 (sCD14), intestinal fatty acid-binding protein (I-FABP), C-reactive protein (CRP), alpha 1-acid glycoprotein (AGP) and interferon- $\beta$  (IFN $\beta$ ). The sensitivity of the assays were as follows: 0.613 ng/ml for sCD163, 125 pg/ml for sCD14, 6.21 pg/ml for I-FABP, 0.02 ng/ml for CRP, 0.54 ng/ml for AGP, and 50 pg/ml for IFN $\beta$ . Multiplex immunoassays (Luminex assays from R&D systems) measuring IFN $\gamma$ , Interleukin (IL)-1 $\beta$ , IL-6, IL-13, IL-17A and TNF were also performed on these samples. The sensitivity of the assays were as follows: 0.40 pg/ml for IFN $\gamma$ , 0.80 pg/ml for IL-1 $\beta$ , 1.7 pg/ml for IL-6, 36.6 pg/ml for IL-13, 1.8 pg/ml for IL-17A, and 1.2 pg/ml for TNF. These markers were chosen based on their importance to TB, HIV and pregnancy outcomes. For Single-plex immunoassays, SpectraMax plate readers were used with SofMax Pro 6 software. Luminex xMAP technology MAGPIX platform was used for multiplex immunoassays with xPONENT software.

## Statistical Analysis

We combined the LTBI+ cohorts (HIV+ and HIV-) and LTBI- cohorts (HIV+ and HIV-) to study the relationship of LTBI status with second or third trimester inflammatory markers among 220 women with available inflammatory data. Differences in study population characteristics by LTBI status were determined using Fisher's exact test for categorical variables and Wilcoxon rank-sum test for continuous variables. A p-value less than 0.05 was considered statistically significant and a p-value of less than 0.004 (0.05/12) was considered statistically significant after Bonferroni correction for multiple comparisons. We also compared median levels of each inflammatory marker, during the second and third trimester, between LTBI+ and LTBI- pregnant women using the Wilcoxon rank-sum test. Inflammatory markers were log<sub>2</sub>-transformed for the data to approximate normality.

We conducted univariable and multivariable linear regression to determine the change in log<sub>2</sub> concentrations of each inflammatory marker (outcome variable) by change in LTBI status (exposure variable), with separate cross-sectional analyses for markers measured in second trimester or third trimester. Multivariable models adjusted for age, mid-upper arm circumference (MUAC), HIV status, vegetarian diet and gestational diabetes status. We also tested models that further adjusted for smoking, education or preeclampsia. MUAC at the time of plasma sample collection (i.e. second or third trimester) was used in multivariable models as it is a more reliable indicator of nutritional status during pregnancy compared to body mass

index. Sub-set analysis was performed using Wilcoxon rank-sum test to determine whether similar relationships between LTBI status and inflammatory markers were observed for only HIV-negative populations.

We also conducted an exploratory analysis, using univariable and multivariable logistic regression analyses, to determine whether third trimester inflammation levels (exposure variable) was associated with TB progression during pregnancy or postpartum (outcome variable). Progressors were defined as those who prospectively developed active TB after sample collection in third trimester and within study follow-up of one-year *postpartum*. We used STATA software version 15.0 for the data analysis.

## RESULTS

### Study Population Characteristics

Our study population of pregnant Indian women (N = 220) had a median age of 23 years (interquartile range (IQR): 21–27) (**Table 1**). Only 25% had an education of less than secondary education, and 34% had an income below India's poverty line (monthly income <10,255 Indian rupees). Around 28% of the women had a mid-upper arm circumference (MUAC) less than 23 cm [an indicator of undernutrition in pregnancy (18)] and 7% had an MUAC >30.5 cm, indicative of overweight (**Table 1**). Most of the women (88%) did not smoke, and 12% were vegetarians. Ten percent had gestational diabetes, and 11% had preeclampsia. As this cohort was stratified by HIV status, 32% of the pregnant women were HIV+ (all on antiretroviral therapy). Study population characteristics did not differ by LTBI status except for lower proportion of HIV (p-value <0.001) in LTBI+ women; as mentioned above, this was due to the stratified design of the study. LTBI+ women also had a lower proportion of gestational diabetes (p = 0.08) and less post-high school education (p = 0.09), but these differences were not statistically significant (**Table 1**).

### Levels of Inflammatory Markers by LTBI Status

We compared the median log<sub>2</sub>-transformed levels of third trimester inflammatory markers by LTBI status using Wilcoxon-rank sum tests (**Figure 1**). IL-1 $\beta$  (3.64 vs. 2.25 pg/ml; p = 0.0002), TNF (1.76 vs. 1.54 pg/ml; p = 0.004), IL-6 (4.08 vs. 1.25 pg/ml; p < 0.0001) and IL-17a (2.48 vs. 2.16 pg/ml; p = 0.0001) were significantly higher in LTBI- women compared to LTBI+ women (**Figure 1**). IFN $\gamma$  production upon *Mtb* antigen stimulation is used to define LTBI positivity; of note, IFN $\gamma$  was lower (3.63 vs. 3.73 pg/ml; p = 0.15) in plasma (i.e. unstimulated samples) of LTBI- women compared to LTBI+ women, but this association was not statistically significant (**Figure 1**). Similar results were also observed when using log<sub>2</sub> concentrations of markers measured in plasma samples from the second trimester (**Supplementary Figure 1**). LTBI- women had significantly higher levels of second trimester AGP, I-FABP, IL-1 $\beta$ , TNF, IL-6, and IL-17a compared to LTBI+ women (**Supplementary**



**TABLE 1** | Characteristics of the study population (N = 220).

	Overall (N = 220)	LTBI+ (N = 155)	LTBI- (N = 65)	P-value
Age median (IQR)	23 (21–27)	23 (21–27)	24 (21–27)	0.51
Monthly Income				0.54
Rs. 10,255	75 (34)	51 (33)	24 (38)	
Rs. 10,255	143 (66)	103 (67)	40 (62)	
Education				0.09
None to primary	54 (25)	40 (26)	14 (22)	
Middle school to high school	139 (63)	101 (65)	38 (58)	
Post-high school	27 (12)	14 (9)	13 (20)	
Mid-upper arm circumference				0.37
<23 cm	62 (28)	48 (31)	14 (21)	
23–30.5 cm	143 (65)	97 (63)	46 (71)	
>30.5 cm	15 (7)	10 (6)	5 (8)	
Smoking status				0.50
Yes	26 (12)	20 (13)	6 (9)	
No	194 (88)	135 (87)	59 (91)	
Preeclampsia				0.99
Yes	25 (11)	18 (12)	7 (11)	
No	195 (89)	137 (88)	58 (89)	
Gestational Diabetes status				0.08
Yes	21 (10)	11 (7)	10 (16)	
No	195 (90)	141 (93)	54 (84)	
HIV				<0.001
Yes	70 (32)	31 (20)	39 (60)	
No	150 (68)	124 (80)	26 (40)	

Data are presented as number (%) of subjects unless otherwise stated. P-values were calculated using Fisher's exact test for categorical variables and Wilcoxon rank-sum for continuous variables to determine the difference between LTBI+ and LTBI- pregnant women.

**Figure 1**). LTBI- women also had lower levels of IFN $\gamma$  compared to LTBI+ women, although this was not statistically significant (p = 0.08) (**Supplementary Figure 1**).

## Association of LTBI Status With Inflammation

Next, we assessed the relationship of third trimester inflammation with LTBI status using univariable and multivariable linear regression models. LTBI+ women had significantly lower levels of I-FABP (mean log<sub>2</sub> change: -0.41, 95% confidence intervals (CI): -0.78 to -0.04; p = 0.03), IL1 $\beta$  (mean log<sub>2</sub> change: -1.03, 95% CI: -1.53 to -0.54; p < 0.001), IL-6 (mean log<sub>2</sub> change: -1.36, 95%

CI: -1.93 to -0.80; p < 0.001), and IL-17a (mean log<sub>2</sub> change: -0.34, 95% CI: -0.50 to -0.17; p < 0.001) compared to LTBI- women in univariable models (**Figure 2**). AGP (mean log<sub>2</sub> change: -0.20, 95% CI: -0.42 to 0.02; p < 0.08) and sCD163 (mean log<sub>2</sub> change: -0.18, 95% CI: -0.39 to 0.03; p < 0.10) was also lower in LTBI+ women but this relationship was not statistically significant (**Figure 2**).

After adjusting for age, third trimester MUAC, HIV status, vegetarian diet, and gestational diabetes in multivariable models, levels of IL-1 $\beta$  (mean log<sub>2</sub> change: -1.15, 95% CI: -1.70 to -0.60; p < 0.001), IL-6 (mean log<sub>2</sub> change: -1.22, 95% CI: -1.87 to -0.58; p < 0.001) and IL-17a (mean log<sub>2</sub> change: -0.39, 95% CI: -0.57 to -0.21; p < 0.001), but not I-FABP (mean log<sub>2</sub> change:

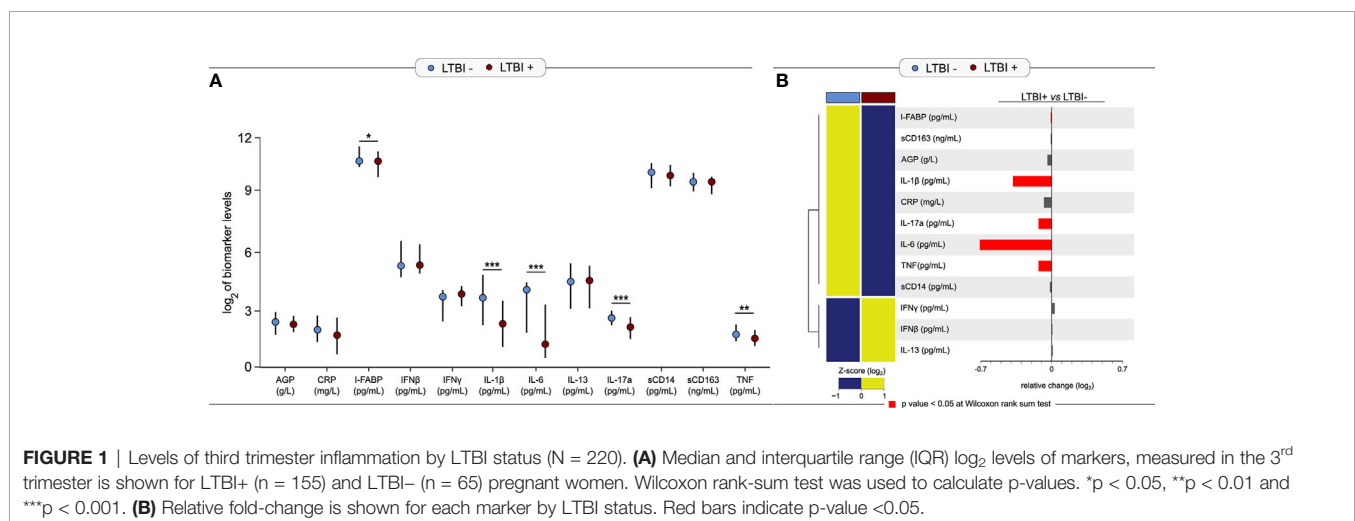


**FIGURE 1** | Levels of third trimester inflammation by LTBI status (N = 220). **(A)** Median and interquartile range (IQR) log<sub>2</sub> levels of markers, measured in the 3<sup>rd</sup> trimester is shown for LTBI+ (n = 155) and LTBI- (n = 65) pregnant women. Wilcoxon rank-sum test was used to calculate p-values. \*p < 0.05, \*\*p < 0.01 and \*\*\*p < 0.001. **(B)** Relative fold-change is shown for each marker by LTBI status. Red bars indicate p-value < 0.05.

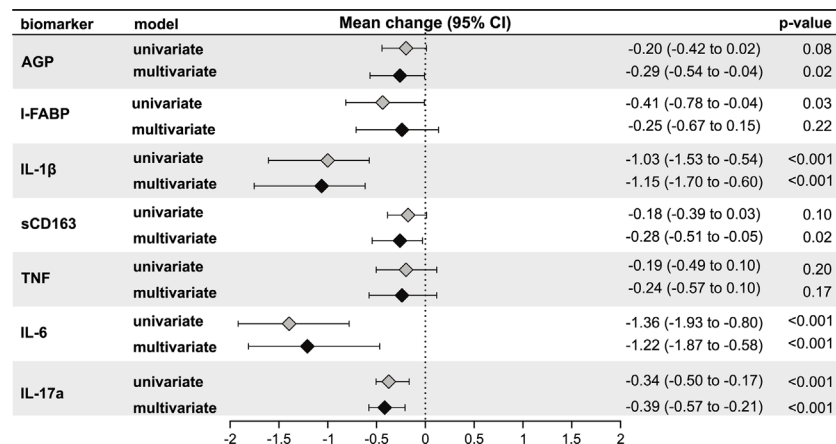


**FIGURE 2** | Association of LTBI status with third trimester inflammation (N = 220). Using linear regression, the mean change in  $\log_2$  concentrations of each inflammation marker and 95% confidence intervals (95% CI) among LTBI+ individuals compared to LTBI- individuals are shown in the forest plot. Inflammation markers were measured in samples collected at the third trimester of pregnancy. Multivariate models adjusted for age, mid-upper arm circumference, HIV status, diet and gestational diabetes status. Only immune markers with a p-value <0.2 in the univariate model are shown.

-0.25, 95% CI: -0.67 to 0.15;  $p = 0.22$ ), remained significantly lower in LTBI+ women compared to LTBI- women (**Figure 2**). In addition, AGP was also significantly lower in LTBI+ women (mean  $\log_2$  change: -0.29, 95% CI: -0.54 to -0.04;  $p = 0.02$ ) (**Figure 2**). After Bonferroni correction to adjust for multiple comparisons, third trimester IL1 $\beta$ , IL-6 and IL-17a were significantly lower in LTBI+ women in multivariable models.

Further adjusting for smoking, education or preeclampsia in multivariable models did not change the direction or significance of the results. Finally, we also conducted sensitivity analysis to show

that when we limited the analysis only to HIV- subjects, the levels of these inflammatory markers were still lower in LTBI+ pregnant women compared to LTBI- women (**Supplementary Figure 2**), suggesting that HIV was not driving the observed relationships.

Results using second trimester inflammatory markers instead of third trimester showed similar associations with LTBI status (**Figure 3**). In univariable models, LTBI+ pregnant women had significantly lower levels of AGP, I-FABP, IL1 $\beta$ , TNF, IL-6 and IL-17a compared to LTBI- pregnant women (**Figure 3**). In multivariable models, we observed similar results observed in

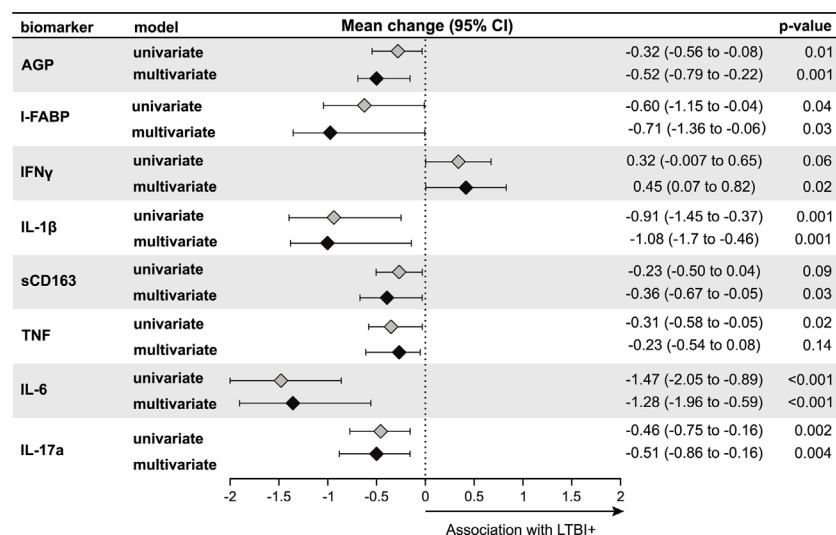


**FIGURE 3** | Association of LTBI status with second trimester inflammation (N = 187). Using linear regression, the mean change in  $\log_2$  concentrations of each inflammation marker and 95% confidence intervals (95% CI) among LTBI+ individuals compared to LTBI- individuals are shown in the forest plot. Inflammation markers were measured in samples collected at the second trimester of pregnancy. Multivariate models adjusted for age, mid-upper arm circumference, HIV status, diet and gestational diabetes status. Only immune markers with a p-value <0.2 in the univariate model are shown.

univariable models with significantly lower levels of the AGP, I-FABP, IL-1 $\beta$ , IL-6, and IL-17a, but not TNF in LTBI+ compared to LTBI- women (**Figure 3**). In addition, sCD163 levels were significantly lower and IFN $\gamma$  was significantly higher in LTBI+ women compared to LTBI- women (**Figure 3**). After Bonferroni correction to adjust for multiple comparisons, second trimester AGP, IL1 $\beta$ , IL-6 and IL-17a were significantly lower in LTBI+ women in multivariable models.

## Inflammatory Markers During Pregnancy and Progression of TB

We also conducted an exploratory analysis to test whether the systemic immune profile observed in LTBI+ pregnant women was associated with progression to active TB during pregnancy or post-partum. In our study, there were nine women, all LTBI+ at study baseline, who progressed to active TB either during the third trimester of pregnancy ( $n = 1$ ) or *post-partum* (*i.e.* within one year of delivery) ( $n = 8$ ). Given that all of the progressors were LTBI+ women, we present data comparing progressors and non-progressors only among LTBI+ women. Interestingly, levels of these markers in LTBI+ progressors, while higher than non-progressor LTBI+ pregnant women, were similar to LTBI- women (data not shown), suggesting that lower levels of these markers might be protective against TB progression in LTBI+ pregnant women. There was a significantly increased odds of progression per log<sub>2</sub> increase in third trimester plasma levels of IL-1 $\beta$  (adjusted odds ratio (aOR): 1.64, 95% CI: 1.05–2.57), IL-6 (aOR: 1.58, 95% CI: 1.05–2.39), and IL-13 (aOR: 2.43, 95% CI: 1.12–5.27) after adjusting for age, MUAC and HIV status (**Figure 4**). There was also an increased odds for IL-17a (aOR: 5.49, 95% CI: 0.84–35.97), but this association was not statistically significant (**Figure 4**). Similar results were observed when we limited the analysis only to post-partum progressors (data not shown).

## DISCUSSION

In our study of LTBI+ and LTBI- pregnant women from India, LTBI+ women had lower levels of various pro-inflammatory cytokines such as IL-1 $\beta$ , IL-6 and IL-17a compared to LTBI- women. In contrast, the levels of IFN $\gamma$  were higher (significant in second trimester) in LTBI+ women. While increased levels of IFN $\gamma$  might be related to the use of this cytokine to define IGRA-based LTBI (19), the results with the other cytokines were surprising. These findings suggest that LTBI in pregnancy is characterized by a distinct immune profile with higher levels of IFN $\gamma$  but lower levels of other immune markers with known roles in TB disease. Interestingly, LTBI+ women who progressed to active TB during pregnancy and *post-partum* did not have this profile in our exploratory analysis, suggesting the distinct immune profile in LTBI+ pregnant women might have a protective role against TB progression. Future larger studies will need to confirm these findings and determine whether these markers play a causal role and could be used to identify LTBI+ pregnant women at increased risk for TB progression and a target for preventative therapy.

LTBI+ pregnant women had significantly increased levels of IFN $\gamma$  in the second trimester compared to LTBI- women. While the association was not statistically significant, the IFN $\gamma$  levels were also higher for LTBI+ women in the third trimester. In our study, we used the IGRA test, which is dependent on IFN $\gamma$  production (19), to define LTBI status; thus it might be expected IFN $\gamma$  is higher in LTBI+ women. On the other hand, it should be noted that we measured IFN $\gamma$  in plasma samples, and it is not obvious that IFN $\gamma$  levels in circulation should also be higher for LTBI+ individuals. Our results here do indicate that higher levels of IFN $\gamma$  are observed in circulation for LTBI+ pregnant women even without *Mtb* antigen stimulation. Similar results for IFN $\gamma$  have also been observed from plasma samples of non-pregnant LTBI+ adults (13, 20). While the reasons are not clear, it is

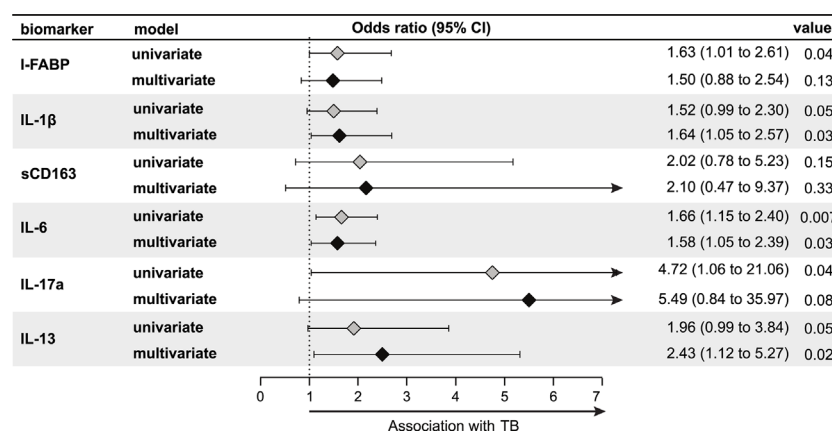


**FIGURE 4** | Association of third trimester inflammation markers with TB progression ( $N = 155$ ; nine progressors). Using logistic regression, the odds ratio and 95% confidence intervals (95% CI) of TB progression per log<sub>2</sub> increase in each inflammation marker among LTBI+ pregnant women are shown in the forest plot. Progressors were defined as those who developed TB either during the third trimester of pregnancy ( $n = 1$ ) or up to one year *post-partum* ( $n = 8$ ). Inflammation markers were measured in samples collected at the third trimester of pregnancy. Multivariable models adjusted for age, mid-upper arm circumference and HIV status. Only immune markers With a p-value <0.2 in the univariate model are shown.

possible that despite being a latent infection, there could be periodic activity of some component (e.g. mRNA, protein) or low-level replication of *Mtb* that induces IFN $\gamma$  production (13). Furthermore, LTBI is thought to be a spectrum of host–pathogen interactions, with ongoing replication and metabolic activity in certain subsets while quiescence in other *Mtb* subsets (9, 21).

Our data showed lower levels of immune markers, especially IL-1 $\beta$ , IL-6, IL-17a and AGP, in both trimesters, in LTBI+ women compared to LTBI– women. Higher levels of IFN $\gamma$  can partly explain the lower levels of these other markers, as studies of *Mtb* have shown that IFN $\gamma$  can have counteractive roles with IL-1 $\beta$ , IL-6 and IL-17a in certain instances (22–24). Pregnancy-specific changes in immune profile could also in part help explain these observations (14). For example, during pregnancy there is an increase in neutrophil levels (25, 26), which have been linked to lower levels of IL-6 and IL-17 in *Mtb* infection (1, 27).

Interestingly, in our exploratory analyses, LTBI+ TB progressors had a profile more similar to LTBI– women, with higher levels of IL-1 $\beta$ , IL-6, IL-13 and IL17a and generally lower levels of IFN $\gamma$  compared to LTBI+ non-progressors. These inflammatory markers have been recognized for their complex role in TB disease where while a deficiency is linked to reduced control of *Mtb* infection, excessive levels can result in tissue damage and immunopathology (1, 28–33) as well as progression to active TB disease in non-pregnant adults (34). Given the small number of progressors in this study, these findings will need to be confirmed in other studies with a larger sample size. If these findings are confirmed, this profile could be used to identify subsets of LTBI+ pregnant women (*i.e.* those without this profile) at an increased risk of TB progression and would further support the idea of LTBI as a spectrum where subgroups of LTBI+ are protected from progression while others are not (9, 10). In addition, future studies would also need to determine whether this relationship of the systemic immune profile with TB progression is causal as it could partly explain the increased risk of *Mtb* progression during pregnancy and *post-partum* (15–17).

Our study has some limitations. We did not have data on inflammation markers from pregnant women during the first trimester or non-pregnant women. This data would be informative to understand whether the relationship of these markers with LTBI status was also similar in early pregnancy compared to later pregnancy, or in pregnant women compared to non-pregnant women. Regardless, our study did have longitudinal data on inflammatory markers in the second and third trimesters of pregnancy and showed consistent results with LTBI status in both trimesters that was robust to adjustments for multiple comparisons. Another limitation of this study is that we only assessed soluble markers of inflammation. The next steps for this study is to better understand the cellular sources of these differences by assessing potential differences in immune cell phenotype and function by LTBI status. The sample size for the analysis of TB progression was limited; while we were able to detect significant differences in multiple markers, this was an exploratory analysis that will need to be confirmed in larger studies. Future large studies should also address whether the changes in inflammatory markers due to LTBI status impacts the risk of birth and infant health outcomes.

In summary, we characterize the systemic immune profile in LTBI+ pregnant women showing higher levels of IFN $\gamma$  but lower levels of other immune markers compared to LTBI– pregnant women. These findings describe a circulating cytokine and immune milieu indicating a distinct immune profile in LTBI+ women. Exploratory analysis suggests that this profile is negatively associated with TB progression. Future studies should confirm these findings in diverse settings in order to test the potential causal role along with the utility of this profile to identify women at high risk for TB progression and who may benefit from preventative therapy.

## DATA AVAILABILITY STATEMENT

The raw data supporting the conclusions of this article will be made available by the authors, without undue reservation.

## ETHICS STATEMENT

The studies involving human participants were reviewed and approved by Johns Hopkins University; Columbia University; Weill Cornell Medicine; BJ Medical College. The patients/participants provided their written informed consent to participate in this study.

## AUTHOR CONTRIBUTIONS

SN contributed to study design, implementation and interpretation. MA contributed to study design and interpretation and led the data collection. PK and SB conducted the laboratory assessments and contributed to interpretation of findings. VK and PD contributed to laboratory data collection and writing of this manuscript. SY and C-SL contributed to data analysis. MA-P and BA created the statistical scripts used to plot the analyses and graphs, and helped with the interpretation of findings. RB, AG, and JSM led the parent study and also contributed to the design, implementation and interpretation of this study. RS led the conceptual design, analysis and wrote the primary version of the manuscript. All authors contributed to the article and approved the submitted version.

## FUNDING

This work was supported primarily by the United States National Institutes of Health, NIH, Bethesda, MD, USA (R00HD089753 to RS and R01HD081929 to AG). JSM received support from NIAID (K23AI129854). Additional support for this work was the NIH-funded Johns Hopkins Baltimore-Washington-India Clinical Trials Unit for NIAID Networks (U01AI069465 to AG). BA is a senior investigator from the Conselho Nacional de Desenvolvimento Científico e Tecnológico (CNPq), Brazil. MA-P received a research fellowship from the Coordenação de Aperfeiçoamento de Pessoal de Nível Superior (CAPES; finance code 001). The content is solely the responsibility of the authors and does not necessarily represent the official views of the NIH.



## ACKNOWLEDGMENTS

The authors thank the study participants for their time and contributions as well as the study staff who meticulously collected detailed data.

## REFERENCES

- O'Garra A, Redford PS, McNab FW, Bloom CI, Wilkinson RJ, Berry MP. The immune response in tuberculosis. *Annu Rev Immunol* (2013) 31:475–527. doi: 10.1146/annurev-immunol-032712-095939
- Cliff JM, Kaufmann SH, McShane H, van Helden P, O'Garra A. The human immune response to tuberculosis and its treatment: a view from the blood. *Immunol Rev* (2015) 264(1):88–102. doi: 10.1111/imr.12269
- Mack U, Migliori GB, Sester M, Rieder HL, Ehlers S, Goletti D, et al. LTBI: latent tuberculosis infection or lasting immune responses to M. tuberculosis? A TBNET consensus statement. *Eur Respir J* (2009) 33(5):956–73. doi: 10.1183/09031936.00120908
- de Martino M, Lodi L, Galli L, Chiappini E. Immune Response to Mycobacterium tuberculosis: A Narrative Review. *Front Pediatr* (2019) 7:350. doi: 10.3389/fped.2019.00350
- Tufariello JM, Chan J, Flynn JL. Latent tuberculosis: mechanisms of host and bacillus that contribute to persistent infection. *Lancet Infect Dis* (2003) 3(9):578–90. doi: 10.1016/S1473-3099(03)00741-2
- LaVergne S, Umlauf A, McCutchan A, Heaton R, Benson C, Kumarasamy N, et al. Impact of Latent Tuberculosis Infection on Neurocognitive Functioning and Inflammation in HIV-Infected and Uninfected South Indians. *J Acquir Immune Defic Syndr* (2020) 84(4):430–6. doi: 10.1097/QAI.0000000000002368
- Jensen AV, Jensen L, Faurholt-Jepsen D, Aabye MG, Praygod G, Kidola J, et al. The prevalence of latent Mycobacterium tuberculosis infection based on an interferon-gamma release assay: a cross-sectional survey among urban adults in Mwanza, Tanzania. *PLoS One* (2013) 8(5):e64008. doi: 10.1371/journal.pone.0064008
- Cowan J, Pandey S, Filion LG, Angel JB, Kumar A, Cameron DW. Comparison of interferon-gamma-, interleukin (IL)-17- and IL-22-expressing CD4 T cells, IL-22-expressing granulocytes and proinflammatory cytokines during latent and active tuberculosis infection. *Clin Exp Immunol* (2012) 167(2):317–29. doi: 10.1111/j.1365-2249.2011.04520.x
- Huaman MA, Ticona E, Miranda G, Kryscio RJ, Mugruza R, Aranda E, et al. The Relationship Between Latent Tuberculosis Infection and Acute Myocardial Infarction. *Clin Infect Dis* (2018) 66(6):886–92. doi: 10.1093/cid/cix910
- Andrews JR, Noubary F, Walensky RP, Cerda R, Losina E, Horsburgh CR. Risk of progression to active tuberculosis following reinfection with Mycobacterium tuberculosis. *Clin Infect Dis* (2012) 54(6):784–91. doi: 10.1093/cid/cir951
- Comstock GW, Livesay VT, Woolpert SF. The prognosis of a positive tuberculin reaction in childhood and adolescence. *Am J Epidemiol* (1974) 99(2):131–8. doi: 10.1093/oxfordjournals.aje.a121593
- Vynnycky E, Fine PE. Lifetime risks, incubation period, and serial interval of tuberculosis. *Am J Epidemiol* (2000) 152(3):247–63. doi: 10.1093/aje/152.3.247
- Huaman MA, Deepe GS Jr., Fichtenbaum CJ. Elevated Circulating Concentrations of Interferon-Gamma in Latent Tuberculosis Infection. *Pathog Immun* (2016) 1(2):291–303. doi: 10.20411/pai.v1i2.149
- Mor G, Cardenas I. The immune system in pregnancy: a unique complexity. *Am J Reprod Immunol* (2010) 63(6):425–33. doi: 10.1111/j.1600-0897.2010.00836.x
- Jonsson J, Kuhlmann-Berenzon S, Berggren I, Bruchfeld J. Increased risk of active tuberculosis during pregnancy and postpartum: a register-based cohort study in Sweden. *Eur Respir J* (2020) 55(3):1901886. doi: 10.1183/13993003.01886-2019
- Mathad JS, Gupta A. Tuberculosis in pregnant and postpartum women: epidemiology, management, and research gaps. *Clin Infect Dis* (2012) 55(11):1532–49. doi: 10.1093/cid/cis732
- Zenner D, Kruijsaar ME, Andrews N, Abubakar I. Risk of tuberculosis in pregnancy: a national, primary care-based cohort and self-controlled case series study. *Am J Respir Crit Care Med* (2012) 185(7):779–84. doi: 10.1164/rccm.201106-1083OC
- Ververs MT, Antierens A, Sackl A, Staderini N, Captier V. Which anthropometric indicators identify a pregnant woman as acutely malnourished and predict adverse birth outcomes in the humanitarian context? *PLoS Curr* (2013) 5. doi: 10.1371/currents.dis.54a8b618c1bc031ea140e3f2934599c8
- Pai M, Riley LW, Colford JM Jr. Interferon-gamma assays in the immunodiagnosis of tuberculosis: a systematic review. *Lancet Infect Dis* (2004) 4(12):761–76. doi: 10.1016/S1473-3099(04)01206-X
- Huaman MA, Henson D, Rondan PL, Ticona E, Miranda G, Kryscio RJ, et al. Latent tuberculosis infection is associated with increased unstimulated levels of interferon-gamma in Lima, Peru. *PLoS One* (2018) 13(9):e0202191. doi: 10.1371/journal.pone.0202191
- Barry CE, Boshoff HI, Dartois V, Dick T, Ehrt S, Flynn J, et al. The spectrum of latent tuberculosis: rethinking the biology and intervention strategies. *Nat Rev Microbiol* (2009) 7(12):845–55. doi: 10.1038/nrmicro2236
- Eigenbrod T, Bode KA, Dalpke AH. Early inhibition of IL-1beta expression by IFN-gamma is mediated by impaired binding of NF-kappaB to the IL-1beta promoter but is independent of nitric oxide. *J Immunol* (2013) 190(12):6533–41. doi: 10.4049/jimmunol.1300324
- Nandi B, Behar SM. Regulation of neutrophils by interferon-gamma limits lung inflammation during tuberculosis infection. *J Exp Med* (2011) 208(11):2251–62. doi: 10.1084/jem.20110919
- Dutta RK, Kathania M, Raje M, Majumdar S. IL-6 inhibits IFN-gamma induced autophagy in Mycobacterium tuberculosis H37Rv infected macrophages. *Int J Biochem Cell Biol* (2012) 44(6):942–54. doi: 10.1016/j.biocel.2012.02.021
- Luppi P, Haluszczak C, Trucco M, Deloia JA. Normal pregnancy is associated with peripheral leukocyte activation. *Am J Reprod Immunol* (2002) 47(2):72–81. doi: 10.1034/j.1600-0897.2002.10041.x
- Sacks GP, Studena K, Sargent K, Redman CW. Normal pregnancy and preeclampsia both produce inflammatory changes in peripheral blood leukocytes akin to those of sepsis. *Am J Obstet Gynecol* (1998) 179(1):80–6. doi: 10.1016/S0002-9378(98)70254-6
- Zhang X, Majlessi L, Deriaud E, Leclerc C, Lo-Man R. Coactivation of Syk kinase and MyD88 adaptor protein pathways by bacteria promotes regulatory properties of neutrophils. *Immunity* (2009) 31(5):761–71. doi: 10.1016/j.immuni.2009.09.016
- Zhang G, Zhou B, Li S, Yue J, Yang H, Wen Y, et al. Allele-specific induction of IL-1beta expression by C/EBPbeta and PU.1 contributes to increased tuberculosis susceptibility. *PLoS Pathog* (2014) 10(10):e1004426. doi: 10.1371/journal.ppat.1004426
- Shen H, Chen ZW. The crucial roles of Th17-related cytokines/signal pathways in M. tuberculosis infection. *Cell Mol Immunol* (2018) 15(3):216–25. doi: 10.1038/cmi.2017.128
- Martinez AN, Mehra S, Kaushal D. Role of interleukin 6 in innate immunity to Mycobacterium tuberculosis infection. *J Infect Dis* (2013) 207(8):1253–61. doi: 10.1093/infdis/jit037
- Barber DL, Andrade BB, McBerry C, Sereti I, Sher A. Role of IL-6 in Mycobacterium avium-associated immune reconstitution inflammatory syndrome. *J Immunol* (2014) 192(2):676–82. doi: 10.4049/jimmunol.1301004
- Tadokera R, Meintjes G, Skolimowska KH, Wilkinson KA, Matthews K, Seldon R, et al. Hypercytokinaemia accompanies HIV-tuberculosis immune reconstitution inflammatory syndrome. *Eur Respir J* (2011) 37(5):1248–59. doi: 10.1183/09031936.00091010
- Martinez Cordero E, Gonzalez MM, Aguilar LD, Orozco EH, Hernandez Pando R. Alpha-1-acid glycoprotein, its local production and immunopathological participation in experimental pulmonary tuberculosis. *Tuberculosis (Edinb)* (2008) 88(3):203–11. doi: 10.1016/j.tube.2007.10.004
- Manabe YC, Andrade BB, Gupta N, Leong S, Kintali M, Matoga M, et al. A Parsimonious Host Inflammatory Biomarker Signature Predicts Incident TB

## SUPPLEMENTARY MATERIAL

The Supplementary Material for this article can be found online at: <https://www.frontiersin.org/articles/10.3389/fimmu.2020.587617/full#supplementary-material>



and Mortality in Advanced HIV. *Clin Infect Dis* (2019) 71(10):2645–54. doi: 10.1093/cid/ciz1147

**Conflict of Interest:** The authors declare that the research was conducted in the absence of any commercial or financial relationships that could be construed as a potential conflict of interest.

The reviewer GW declared a past co-authorship with one of the authors BA to the handling editor.

Copyright © 2021 Naik, Alexander, Kumar, Kulkarni, Deshpande, Yadana, Leu, Araújo-Pereira, Andrade, Bhosale, Babu, Gupta, Mathad and Shivakoti. This is an open-access article distributed under the terms of the Creative Commons Attribution License (CC BY). The use, distribution or reproduction in other forums is permitted, provided the original author(s) and the copyright owner(s) are credited and that the original publication in this journal is cited, in accordance with accepted academic practice. No use, distribution or reproduction is permitted which does not comply with these terms.



# Relevance of QuantiFERON-TB Gold Plus and Heparin-Binding Hemagglutinin Interferon- $\gamma$ Release Assays for Monitoring of Pulmonary Tuberculosis Clearance: A Multicentered Study

## OPEN ACCESS

### Edited by:

Adam Penn-Nicholson,  
Foundation for Innovative New  
Diagnostics, Switzerland

### Reviewed by:

Edward A. Graviss,  
Houston Methodist Research  
Institute, United States  
Björn Corleis,  
Friedrich-Loeffler-Institute, Germany

### \*Correspondence:

Carole Chedid  
carole.chedid@fondation-merieux.org

<sup>†</sup>These authors share senior  
authorship

### Specialty section:

This article was submitted to  
Microbial Immunology,  
a section of the journal  
Frontiers in Immunology

**Received:** 12 October 2020

**Accepted:** 03 December 2020

**Published:** 02 February 2021

### Citation:

Chedid C, Kokhraidze E, Tukvadze N,  
Banu S, Uddin MKM, Biswas S,  
Russomando G, Acosta CCD,  
Arenas R, Ranaivomanana PPR,  
Razafimahatratra C, Herindrainy P,  
Rakotonirina J, Raherinandrasana AH,  
Rakotosamimanana N, Hamze M,  
Ismail MB, Bayaa R, Berland J-L,  
De Maio F, Delogu G, Endtz H, Ader F,  
Goletti D and Hoffmann J (2021)  
Relevance of QuantiFERON-TB Gold  
Plus and Heparin-Binding  
Hemagglutinin Interferon- $\gamma$  Release  
Assays for Monitoring of Pulmonary  
Tuberculosis Clearance: A  
Multicentered Study.  
Front. Immunol. 11:616450.  
doi: 10.3389/fimmu.2020.616450

Carole Chedid<sup>1,2\*</sup>, Eka Kokhraidze<sup>3</sup>, Nestani Tukvadze<sup>3</sup>, Sayera Banu<sup>4</sup>,  
Mohammad Khaja Mafij Uddin<sup>4</sup>, Samanta Biswas<sup>4</sup>, Graciela Russomando<sup>5</sup>,  
Chyntia Carolina Díaz Acosta<sup>5</sup>, Rossana Arenas<sup>6</sup>, Paulo PR. Ranaivomanana<sup>7</sup>,  
Crisca Razafimahatratra<sup>7</sup>, Perlinot Herindrainy<sup>7</sup>, Julio Rakotonirina<sup>8</sup>,  
Antso Hasina Raherinandrasana<sup>8</sup>, Niaina Rakotosamimanana<sup>7</sup>, Monzer Hamze<sup>9</sup>,  
Mohamad Bachar Ismail<sup>9</sup>, Rim Bayaa<sup>9</sup>, Jean-Luc Berland<sup>1</sup>, Flavio De Maio<sup>10,11</sup>,  
Giovanni Delogu<sup>10</sup>, Hubert Endtz<sup>12</sup>, Florence Ader<sup>13</sup>, Delia Goletti<sup>14†</sup>  
and Jonathan Hoffmann<sup>1†</sup> on behalf of the HINTT working group within the  
GABRIEL network

<sup>1</sup> Laboratoire des Pathogènes Emergents, Fondation Mérieux, Centre International de Recherche en Infectiologie, INSERM U1111, Lyon, France, <sup>2</sup> Département de Biologie, Ecole Normale Supérieure de Lyon, Lyon, France, <sup>3</sup> National Center for Tuberculosis and Lung Diseases (NCTBLD), Tbilisi, Georgia, <sup>4</sup> International Centre for Diarrhoeal Disease Research, Bangladesh (icddr), Dhaka, Bangladesh, <sup>5</sup> Instituto de Investigaciones en Ciencias de la Salud, National University of Asunción, Asunción, Paraguay, <sup>6</sup> Hospital General de San Lorenzo, MSPyBS, Asunción, Paraguay, <sup>7</sup> Institut Pasteur de Madagascar, Antananarivo, Madagascar, <sup>8</sup> Centre Hospitalier Universitaire de Soins et Santé Publique Analakely (CHUSSPA), Antananarivo, Madagascar, <sup>9</sup> Laboratoire Microbiologie, Santé et Environnement (LMSE), Doctoral School of Sciences and Technology, Faculty of Public Health, Lebanese University, Tripoli, Lebanon, <sup>10</sup> Dipartimento di Scienze di Laboratorio e Infettivologiche, Fondazione Policlinico Universitario "A. Gemelli", IRCCS, Rome, Italy, <sup>11</sup> Dipartimento di Scienze biotecnologiche di base, cliniche intensivologiche e perioperatorie – Sezione di Microbiologia, Università Cattolica del Sacro Cuore, Rome, Italy, <sup>12</sup> Fondation Mérieux, Lyon, France, <sup>13</sup> Service des Maladies Infectieuses et Tropicales, Hospices Civils de Lyon, Lyon, France, <sup>14</sup> Translational Research Unit, Department of Epidemiology and Preclinical Research, "L. Spallanzani" National Institute for Infectious Diseases (INMI), IRCCS, Rome, Italy

**Background:** Tuberculosis (TB) is a leading infectious cause of death. To improve treatment efficacy, quicker monitoring methods are needed. The objective of this study was to monitor the response to a heparin-binding hemagglutinin (HBHA) interferon- $\gamma$  (IFN- $\gamma$ ) release assay (IGRA) and QuantiFERON-TB Gold Plus (QFT-P) and to analyze plasma IFN- $\gamma$  levels according to sputum culture conversion and immune cell counts during treatment.

**Methods:** This multicentered cohort study was based in Bangladesh, Georgia, Lebanon, Madagascar, and Paraguay. Adult, non-immunocompromised patients with culture-confirmed pulmonary TB were included. Patients were followed up at baseline (T0), after two months of treatment (T1), and at the end of therapy (T2). Clinical data and blood samples were collected at each timepoint. Whole blood samples were stimulated with QFT-P antigens or recombinant methylated *Mycobacterium tuberculosis* HBHA

(produced in *Mycobacterium smegmatis*; rmsHBHA). Plasma IFN- $\gamma$  levels were then assessed by ELISA.

**Findings:** Between December 2017 and September 2020, 132 participants completed treatment, including 28 (21.2%) drug-resistant patients. rmsHBHA IFN- $\gamma$  increased significantly throughout treatment (0.086 IU/ml at T0 vs. 1.03 IU/ml at T2,  $p < 0.001$ ) while QFT-P IFN- $\gamma$  remained constant (TB1: 0.53 IU/ml at T0 vs. 0.63 IU/ml at T2,  $p = 0.13$ ). Patients with low lymphocyte percentages (<14%) or high neutrophil percentages (>79%) at baseline had significantly lower IFN- $\gamma$  responses to QFT-P and rmsHBHA at T0 and T1. In a small group of slow converters (patients with positive cultures at T1;  $n = 16$ ), we observed a consistent clinical pattern at baseline (high neutrophil percentages, low lymphocyte percentages and BMI, low TB1, TB2, and MIT IFN- $\gamma$  responses) and low rmsHBHA IFN- $\gamma$  at T1 and T2. However, the accuracy of the QFT-P and rmsHBHA IGRAs compared to culture throughout treatment was low (40 and 65% respectively). Combining both tests improved their sensitivity and accuracy (70–80%) but not their specificity (<30%).

**Conclusion:** We showed that QFT-P and rmsHBHA IFN- $\gamma$  responses were associated with rates of sputum culture conversion. Our results support a growing body of evidence suggesting that rmsHBHA IFN- $\gamma$  discriminates between the different stages of TB, from active disease to controlled infection. However, further work is needed to confirm the specificity of QFT-P and rmsHBHA IGRAs for treatment monitoring.

**Keywords:** tuberculosis, immunomonitoring, interferon-gamma release assays, heparin-binding haemagglutinin adhesin, QuantiFERON, treatment monitoring, inflammatory markers

## INTRODUCTION

Tuberculosis (TB) is one of the leading causes of death by infectious disease in the world, causing 1.5 million deaths in 2019 (1). The treatment of pulmonary TB requires antibiotic multitherapies that last at least six months (2, 3) and can have toxic side effects. Consequently, treatment adherence is not optimal, especially in primary care settings (4, 5). Currently, anti-TB treatment monitoring relies on *Mycobacterium tuberculosis* (*M. tuberculosis*) detection by sputum smear microscopy and culture when possible (6). Sputum culture is the gold standard, but it is slow and requires high biosafety laboratory environments (7), while smear microscopy is highly sample- and operator-dependent and has poor sensitivity (8, 9). There is a clinical need for quicker anti-TB treatment monitoring tests adapted to primary care settings (10), that require accessible samples (blood, urine, feces) and limited laboratory equipment (11).

QuantiFERON-TB Plus (QFT-P; Qiagen) is an ELISA-based IFN- $\gamma$  release assay (IGRA) that tests for exposure to *M. tuberculosis*. While it is useful for the triage of suspected TB patients, it cannot discriminate between active and latent TB (12) and has shown little clinical relevance for TB treatment monitoring so far (10). Previous works highlighted a general decrease in IFN- $\gamma$  levels across TB treatment (13–18), and a study on QuantiFERON Gold In-Tube highlighted the presence of downregulated non-TB specific IFN- $\gamma$  responses (Mitogen tube) were associated with poor treatment outcomes (19). However, persistently high quantitative results as well as heterogeneous

QFT-P conversion rates make the test unlikely to be adapted for individual treatment monitoring (20–22).

Recently, the use of QFT-P in combination with the detection of IFN- $\gamma$  responses to recombinant *Mycobacterium smegmatis* heparin-binding hemagglutinin (hereafter called “rmsHBHA IGRA”) as an additional stimulation antigen has shown promise to stratify TB cases by stage of infection and progression to disease (23–27), and to monitor TB treatment outcomes (28). In particular, negative or low levels of IFN- $\gamma$  production in response to rmsHBHA stimulation have been associated with active TB disease as opposed to latent infection. However, this assay has been explored only in studies in non-TB endemic settings, or with no drug-resistant TB patients.

The primary objective of this prospective multicentered cohort study was to monitor the plasma IFN- $\gamma$  response to rmsHBHA and QFT-P antigens during anti-TB treatment. Moreover, recent data collected in the same cohort highlighted an association between baseline circulating white blood cells (WBC) and TB treatment outcome (29); hence, a secondary objective was to describe rmsHBHA and QFT-P IFN- $\gamma$  values in subsets of patients stratified according to demographics, immune cell counts, and culture conversion during treatment. For that purpose, we conducted a cohort study in five countries with low- or middle income status and high- or middle TB incidence rates (30) (Bangladesh, Georgia, Lebanon, Madagascar, and Paraguay), focusing on adult, HIV-uninfected, culture confirmed drug-susceptible or drug-resistant pulmonary TB patients.

## MATERIALS AND METHODS

### Study Design and Sample Population

This descriptive study was nested within a multicenter prospective cohort study assessing the prognostic value of blood-based immunological markers for TB treatment monitoring. The study was based in five institutions from the Mérieux Foundation GABRIEL network (31), with the approval of national TB programs and the following ethical committees: the international center for diarrheal diseases and research, Bangladesh (icddr,b) in Dhaka, Bangladesh; the National Center for Tuberculosis and Lung Diseases (NTCLD) in Tbilisi, Georgia; the *Laboratoire Microbiologie, Santé et Environnement (LMSE, Université Libanaise)*, in Tripoli, Lebanon; the *Institut Pasteur de Madagascar* in Antananarivo, Madagascar; and the *Instituto de Investigaciones en Ciencias de la Salud (Universidad Nacional de Asunción; IICS-UNA)* in Asunción, Paraguay. All recruited patients provided written informed consent and standard biosecurity and institutional safety procedures were followed in all study sites.

### Cohort Recruitment, TB Diagnosis, and Patient Follow-Up

The sample size was evaluated to detect a difference in rmsHBHA IFN- $\gamma$  between baseline and end of treatment, with the following assumptions: we aimed for a level of significance of 95% and a power of 80%, assuming a minimum average expected difference of 1.6 IU/ml in rmsHBHA IFN- $\gamma$  levels throughout treatment based on reported estimates (32), with an expected standard deviation of 3 IU/ml at each repeated measurement. We calculated (33) that a sample size of 117 was required to reach significance. As this study was nested in a cohort study with a sample size of 200, we aimed to enroll more patients to account for missing data. Patients were recruited if diagnosed with microbiologically confirmed pulmonary TB (positive culture and/or sputum smear and/or GeneXpert). Patients with HIV or diabetes mellitus and children under 15 years were excluded. In downstream analyses, patients under immunocompromising treatment, patients with negative cultures at inclusion, and patients who were lost-to-follow-up were excluded. Detailed procedures for microbiological diagnosis, drug sensitivity testing, and therapeutic regimen composition were described previously (29).

Patients were followed up: at inclusion (T0), after two months of treatment (T1), at the end of therapy [T2; 6 months for drug-susceptible (DS-TB) patients, nine to 24 months for drug-resistant (DR-TB) patients]. Data were presented for all patients followed up until T2 at least. Patients were on Directly Observed Treatment (DOT) and received treatment according to standard protocols (2, 3, 34). In this study, culture conversion at T1 was used to define three patient subsets: fast converters (definitive culture conversion between T0 and T1), slow converters (definitive culture conversion between T1 and T2), and patients with poor treatment outcome (positive culture results at T2: treatment failure; or positive culture at T3: relapse).

### On-Site Whole Blood Collection and Cell Count

At every follow-up visit, 10 ml of whole blood were drawn: 4 ml was used for other downstream analyses, 1 ml was collected in

EDTA tubes and used to measure whole blood cell counts by standardized automated systems available in the study sites as listed previously (29), and 5 ml was used for *in vitro* blood stimulation. For the QFT-P assay, 1 ml of whole blood was seeded directly into each of four QuantiFERON-TB Gold Plus (QFT-P, Qiagen) tubes as per the manufacturer's instructions. The NIL tube contained no antigens and was used as a negative control. The TB1 and TB2 QFT-P tubes are coated with commercial *M. tuberculosis*-specific antigenic peptide pools. TB1 tubes contain two mycobacterial peptides, ESAT-6 (>15aa) and CFP-10 (8–13aa), which elicit specific immune responses from CD4+ T lymphocytes (35). TB2 tubes contain an additional commercial peptide pool designed to induce CD8+ T lymphocyte stimulation. MIT tubes are coated with commercial phytohemagglutinin-like bacterial antigens and were used as a positive control (35). For the rmsHBHA assay, 1 ml of blood was seeded into a NIL tube which was complemented with rmsHBHA (provided by the Delogu laboratory, UNICATT, Rome, Italy (23)), at a final concentration of 5  $\mu$ g/ml. Within 2 h of blood collection, samples were placed at 37°C in a 5% CO<sub>2</sub> atmosphere and incubated for 24 h. After incubation, plasmas were separated from the cell fraction by decantation, and stored at –80°C until further use.

### Interferon- $\gamma$ Release Assay

IFN- $\gamma$  secretion was quantified using the QFT-P ELISA kit (Qiagen) according to the manufacturer's instructions. Briefly, plasma samples were thawed at room temperature, and 50  $\mu$ l of plasma was tested. Optical density results were compared to log-normalized values from freshly reconstituted IFN- $\gamma$  kit standards. To account for potential immunomodulation phenomena unrelated with TB treatment, baseline IFN- $\gamma$  level values (NIL tubes) were subtracted from antigen-stimulated IFN- $\gamma$  values (MIT, TB1, TB2, rmsHBHA). According to the kit's sensitivity range, the maximum for IFN- $\gamma$  level values was set at 10 IU/ml and negative values were rescaled to 0.

### Assay Comparability Between Study Sites

To optimize comparability, a sample handling and processing protocol common to all study sites was developed, and on-site trainings were performed to standardize experimental processes such as instrument settings and timings. A tracking sheet was developed and used to follow sample shipment and standardize storage conditions in all sites. As the models of measurement instruments used in the different sites could not be homogenized, instrument readings were tested with QuantiFERON Control Panel (Qiagen) prior to launching the project. Finally, internal controls were added to each ELISA run to control for experimental variation and verify storage quality. Briefly, whole blood from a healthy donor was collected and stimulated with QFT-P antigens following the same protocol as described previously. Plasma was then separated and aliquoted and added to each ELISA run.

### Clinical Data Collection and Statistical Analysis

Standardized clinical report and data collection forms were implemented to ensure dataset homogeneity as described previously (29). Data were entered into the CASTOR database

system (Version 1.4, Netherlands) (36), and cleaned and analyzed in R (version 3.6.2). Discrete variables were analyzed using Fisher's Exact test with Bonferroni's *post-hoc* test (37). Normal, continuous variables were analyzed with Student's *t*-test. Non-normal, continuous variables were analyzed with the Mann–Whitney test, or the Kruskal–Wallis rank sum test with Dunn's Kruskal–Wallis Multiple Comparisons *post-hoc* test (38). Repeated measures of non-independent continuous variables were analyzed using the Friedman rank sum test, with the Wilcoxon–Nemenyi–McDonald–Thompson *post-hoc* test (39). As the HBHA IGRA was not commercialized and QFT-P was designed to screen latent rather than active TB patients, we used Receiver Operating Curve (ROC) analyses to identify optimal IFN- $\gamma$  thresholds adapted for this cohort, discriminating culture positive from culture negative patients. The overall QFT-P test was considered positive if either TB1 or TB2 was above their respective thresholds. ROC analyses and logistic regression were performed as described previously (29). In particular, multivariate logistic regression analyses were adjusted with the combination of variables that minimized the Akaike Information Criterion (AIC) for most tested predictors, while including important adjustment variables (age, sex, drug sensitivity, country).

## RESULTS

### Sociodemographic, Clinical, and Microbiological Characteristics of the Cohorts

Between December 2017 and September 2020, 199 eligible patients with culture confirmed active pulmonary TB were

recruited in Dhaka (Bangladesh), Tbilisi (Georgia), Tripoli and Akkar (Lebanon), Antananarivo (Madagascar), and Asunción (Paraguay). As of September 2020, 132 of them were followed at least until the end of treatment and had available IGRA data (**Figure 1**). Among these patients, 21.2% (28/132) were diagnosed with DR-TB. The sociodemographic characteristics of DS-TB and DR-TB patients were similar at inclusion (**Table 1**). Sociodemographic characteristics were compared between study sites, and significant differences were observed concerning age, BMI at inclusion, and BCG vaccination rates (**Supplementary Table 1**). All enrolled patients were sputum culture positive at inclusion. Most patients were also positive for sputum smear microscopy (sensitivity: 78.0%, 103/132) and/or GeneXpert (98.4%, 125/132). Three (3.9%) cases of treatment failure and one (0.7%) case of relapse were recorded (**Table 1**).

### Dynamics of Interferon- $\gamma$ Levels During Treatment and Influence of Sociodemographic Factors

Plasma IFN- $\gamma$  levels in response to TB1, TB2, or HBHA stimulations were measured during anti-TB treatment (**Figure 2**). The median IFN- $\gamma$  response to TB1 and TB2 remained constant over time, while the median response to rmsHBHA increased significantly (**Figure 2A**). Individual IFN- $\gamma$  levels were heterogeneous in all three stimulation conditions (**Figure 2B**). To account for individual variations, rmsHBHA/TB1 and rmsHBHA/TB2 IFN- $\gamma$  ratios were evaluated, and a significant increase in both ratios was still observed overall (**Supplementary Figures 1A–C**). We also measured the TB2–TB1 IFN- $\gamma$  response, as a proxy for the QFT-P CD8<sup>+</sup> T-cell response (**Supplementary Figure 1D**). No significant difference was detected over time.

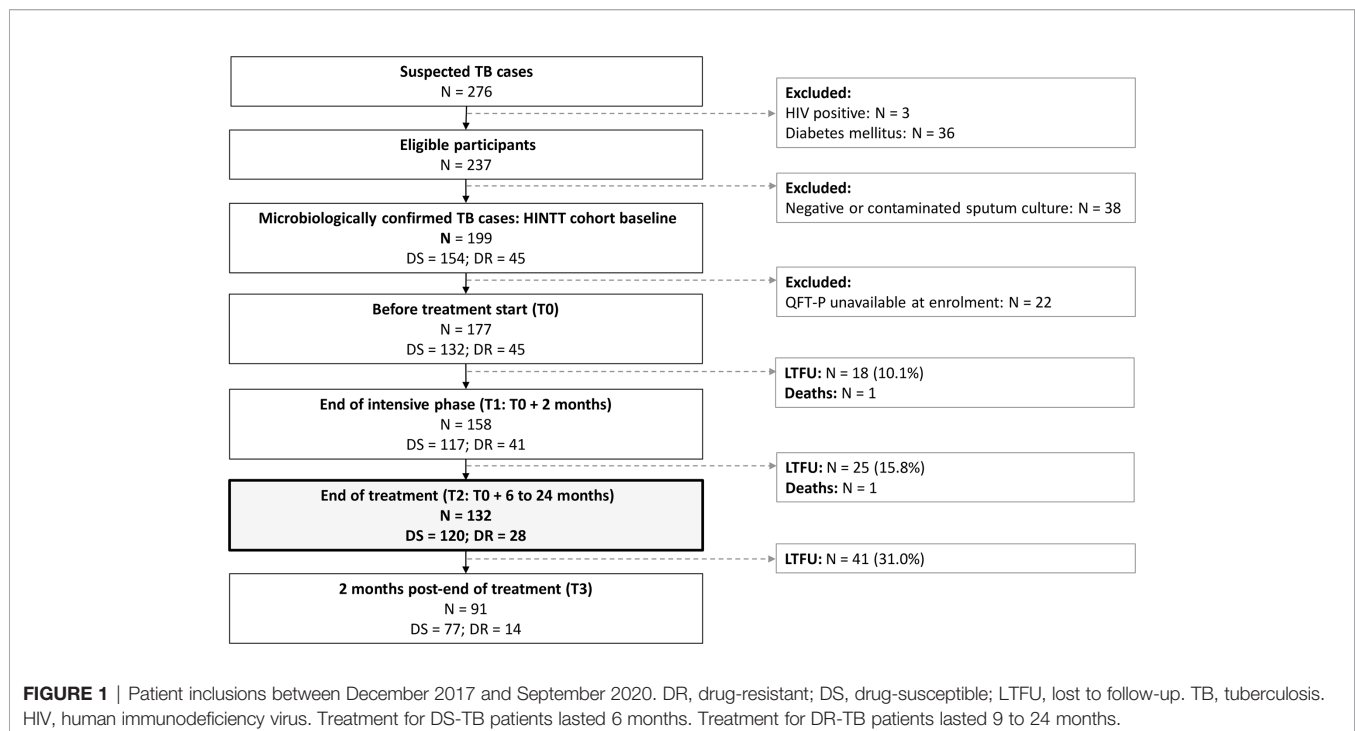




**TABLE 1 |** Sociodemographic and clinical characteristics of drug-susceptible and drug-resistant patients at inclusion.

N	ALL 132	DS-TB 104	DR-TB 28	p
<b>Patient demographics</b>				
Age (years)	27 (21–36.2)	27 (21–37.2)	27.5 (19.7–33.2)	0.41
Sex (male)	62.9% (83/132)	64.4% (67/104)	57.1% (16/28)	0.51
Treatment outcome				
Cured and completed	95.5% (126/132)	94.2% (98/104)	100% (28/28)	0.34
Completed	1.5% (2/132)	1.9% (2/104)	0	-
Failure	2.3% (3/132)	2.9% (3/104)	0	-
Relapse	0.8% (1/132)	1% (1/104)	0	-
Country of origin				
Bangladesh	28.8% (38/132)	20.2% (21/104)	60.7% (17/28)	>0.001
Georgia	23.5% (31/132)	20.2% (21/104)	35.7% (10/28)	0.13
Lebanon	5.3% (7/132)	6.7% (7/104)	0	0.34
Madagascar	27.3% (36/132)	34.6% (36/104)	0	>0.001
Paraguay	15.2% (20/132)	18.3% (19/104)	3.6% (1/28)	0.073
BMI at inclusion	18.7 (16.9–21.3)	18.83 (16.9–21.4)	18.7 (17.5–21.0)	0.79
WBC absolute count at inclusion (cells/mm <sup>3</sup> )	9745 (7365–12032)	9695 (7350–12055)	10150 (7725–11850)	0.65
Neutrophils at inclusion (% of WBC)	75 (68–79.1)	75 (68.3–79)	78 (66.7–80.2)	0.34
Lymphocytes at inclusion (% of WBC)	18 (14–25)	18 (14–25)	17 (13.7–24.5)	0.52
Monocytes at inclusion (% of WBC)	4.4 (2–7)	5 (2–8.0)	4 (3–5.2)	0.42
Number of household contacts	4 (3–6)	4 (3–6)	4 (3.75–6.2)	0.86
BCG vaccination	86.2% (94/109)	86.4% (76/88)	85.7% (18/21)	1
<b>Risk factors and comorbidities</b>				
Smoking	46.2% (61/132)	46.2% (48/104)	46.4% (13/28)	1
Alcohol abuse	22% (29/132)	24% (25/104)	14.3% (4/28)	0.57
Injectable drug use	3.8% (5/131)	2.9% (3/104)	7.4% (2/27)	0.27
Jail detention history	8.5% (11/130)	9.8% (10/102)	3.6% (1/28)	0.57
Chronic HCV infection	1.6% (2/129)	2% (2/101)	0	0.75
Other disease <sup>1</sup>	6.2% (7/113)	7.8% (7/90)	0	0.34
<b>History of TB</b>				
Prior exposure to active TB patients	29% (38/131)	29.1% (30/103)	28.6% (8/28)	0.23
Documented previous TB episode	15.1% (20/132)	11.5% (12/104)	28.5% (8/28)	0.048
<b>Previous TB outcome</b>				
Cured and completed	61.1% (11/18)	61.5% (8/13)	60% (3/5)	1
Treatment completed	11.1% (2/18)	7.7% (1/13)	20% (1/5)	0.49
Outcome not evaluated or unknown	16.7% (3/18)	15.4% (2/13)	20% (1/5)	1
Treatment failure	11.1% (2/18)	15.4% (2/13)	0	-

Data are given as % (N) or median (interquartile range). DS-TB, drug-susceptible tuberculosis; DR-TB, drug-resistant tuberculosis; BMI, body mass index; WBC, white blood cells; 1: asthma, hypertension, inflammation. P-values are given for DS-TB vs. DR-TB.

No patients had HIV, non-TB chronic pulmonary diseases, renal diseases, solid tumors, chronic HBV infection, were pregnant, or under immunosuppressive therapies (corticosteroids, calcineurin inhibitors, biologics).

The impact of sociodemographic parameters on IFN- $\gamma$  levels was assessed but no significant association was detected (data not shown).

Overall, QFT-P positivity rates remained constant during treatment (T0 vs. T2: 52 vs. 55%,  $p = 0.71$ ), whereas rmsHBHA positivity rates increased significantly (T0 vs. T2: 31 vs. 67%,  $p < 0.001$  (Table 2). We also calculated the slopes of rmsHBHA and QFT-P IFN- $\gamma$  variations during treatment (Table 2). An increased INF- $\gamma$  response to TB1, TB2, and rmsHBHA was observed in 55.3% (73/132), 56.8% (75/132), and 77.3% (102/132) of patients respectively.

IFN- $\gamma$  levels over time were then stratified per study site (Figures 2C–E). Similar trends were observed in all cohorts for TB1 and TB2 IFN- $\gamma$  levels, except in the Madagascar site in which an increase in TB1 IFN- $\gamma$  was recorded between T0 and T2. Variation in IFN- $\gamma$  levels produced by rmsHBHA-stimulated samples was different between study sites: similar in increase and order of magnitude in the Bangladesh and Georgia cohorts on the one hand, as well as in Paraguay and Lebanon on the other

hand; however, no increase was observed in the Madagascar cohort, as well as lower IFN- $\gamma$  values (Supplementary Table 2). Mitogen IFN- $\gamma$  levels were also significantly lower in the Madagascar cohort than in the Georgia cohort at all timepoints (Supplementary Table 2).

### Effect of Neutrophil and Lymphocyte Percentages on Interferon- $\gamma$ Release Assay Interferon- $\gamma$ Response During Treatment

We analyzed the distribution of neutrophil percentages, and stratified IFN- $\gamma$  results according to three groups: low neutrophils (less than the first quartile), intermediate neutrophils (between first and third quartiles), and high neutrophils (Figure 3A; threshold values are available in Supplementary Table 3). Similar analyses were performed with lymphocyte percentages (Figure 3C). We also evaluated the proportion of QFT-P and rmsHBHA positivity at each timepoint, stratified by neutrophil (Figure 3B) and

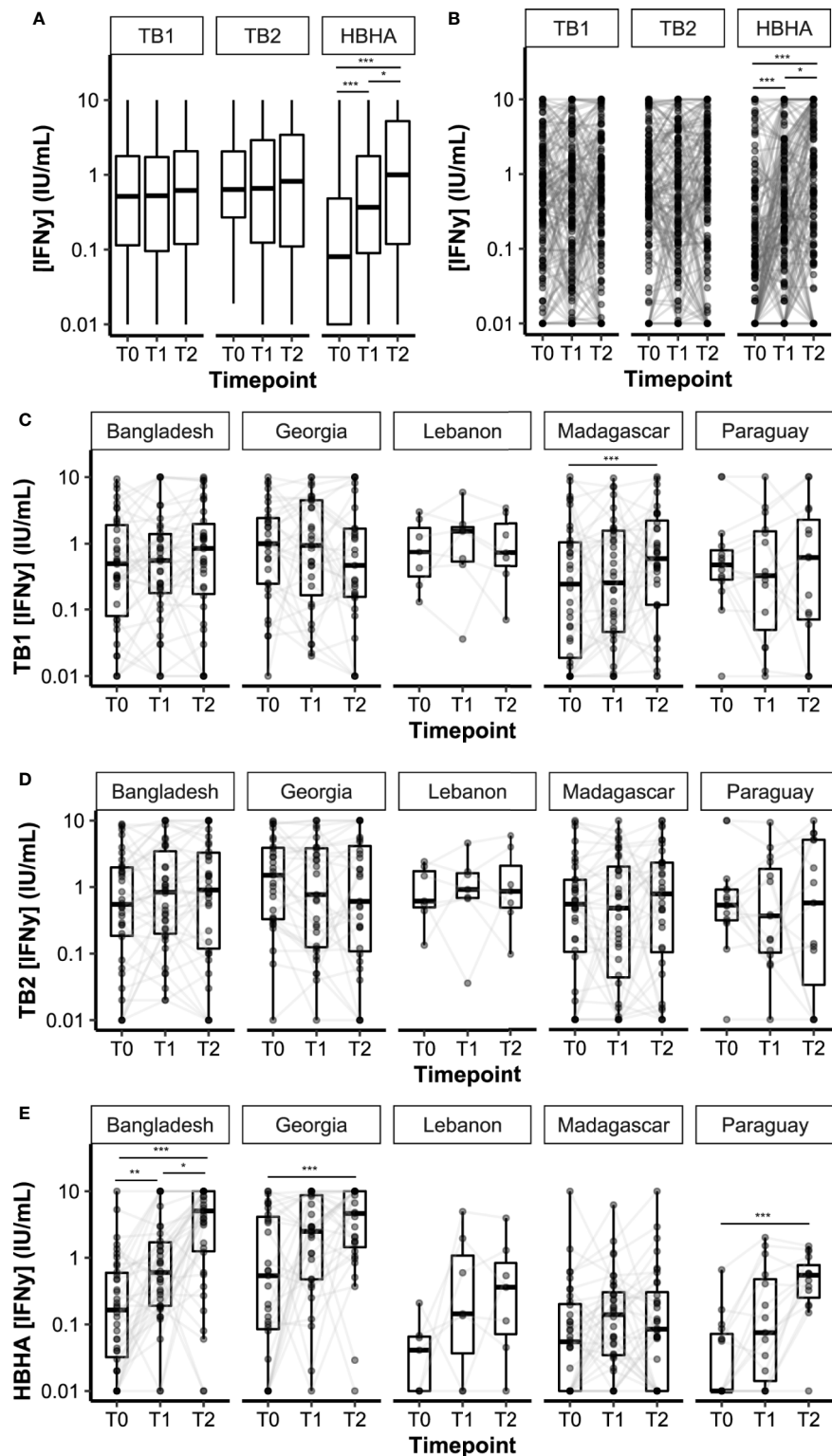


**FIGURE 2 |** Dynamics of plasma IFN- $\gamma$  response to QFT-P and HBHA stimulations over the course of TB therapy. Data are given as median + interquartile range. Each black dot represents one patient at one timepoint. Grey lines connect data points from the same patient. **(A)** Median IFN- $\gamma$  responses in the complete cohort (n = 132 per timepoint). **(B)** Individual IFN- $\gamma$  responses in the complete cohort. **(C–E)** Stratification per study site. Bangladesh (n = 38), Georgia (n = 31), Lebanon (n = 7), Madagascar (n = 36), Paraguay (n = 20). T0: baseline. T1: baseline + 2 months. T2: end of treatment. Data were compared using Friedman's Exact Test with the Wilcoxon–Nemenyi–McDonald–Thompson *post-hoc*, or the Mann–Whitney U test **(B)**. \*p < 0.05; \*\*p < 0.01; \*\*\*p < 0.001.

**TABLE 2** | Qualitative evolution of QFT-P and HBHA IFN- $\gamma$  levels during treatment.

Positivity rate at each timepoint	HBHA	TB1 only	TB2 only	QFT-P (TB1 and/or TB2)
T0	31.1% (41/132)	4.5% (6/132)	34.8% (46/132)	52.3% (69/132)
T1	56.1% (74/132)	2.3% (3/132)	42.4% (56/132)	50.8% (67/132)
T2	67.4% (89/132)	2.3% (3/132)	43.9% (58/132)	55.3% (73/132)
<b>Trend between T0 and T1</b>				
Increase	66.7% (88/132)	56.1% (74/132)	47.7% (63/132)	–
Decrease	24.2% (32/132)	41.7% (55/132)	47.7% (63/132)	–
Constant	9.1% (12/132)	2.3% (3/132)	4.5% (6/132)	–
<b>Trend between T0 and T2</b>				
Increase	77.3% (102/132)	55.3% (73/132)	56.8% (75/132)	–
Decrease	15.2% (20/132)	40.9% (54/132)	41.7% (55/132)	–
Constant	7.6% (10/132)	3.8% (5/132)	1.5% (2/132)	–

Data are given as % (N). T0, baseline; T2, end of treatment; QFT-P, QuantiFERON-TB Gold Plus; Constant, no difference in IFN- $\gamma$  levels between T0 and T2, regardless of variations during treatment. Positivity was set at 0.75 IU/ml for QFT-P and at 0.22 IU/ml for HBHA based on ROC analyses.

lymphocyte percentages (**Figure 3D**). As HBHA stimulation was not performed using a commercial kit, Receiver Operating Curve (ROC) analyses were performed to identify the optimal rmsHBHA IFN- $\gamma$  threshold value differentiating culture-positive patients from culture-negative patients at any timepoint. The resulting Area Under the Curve (AUC) was maximized for an IFN- $\gamma$  cutoff value of 0.24 IU/ml (AUC 0.725, 95% CI 0.674–0.777). Overall, neutrophil and lymphocyte percentages directly impacted IFN- $\gamma$  responsiveness to TB-specific antigens: QFT-P and rmsHBHA IFN- $\gamma$  levels and positivity rates were significantly higher in patients with low neutrophil (**Figures 3A, B**) or with high lymphocyte proportions (**Figures 3C, D**). This statistically significant trend was also observed when comparing the

subgroup of patients with both low neutrophil and high lymphocyte percentages to the rest of the cohort (data not shown).

### Effect of the Culture Conversion Status at 2 Months on the Interferon- $\gamma$ Release Assay Interferon- $\gamma$ Response Throughout Treatment

Overall, 112 patients had available culture data at T0, T1, and T2. Most patients were fast converters (definitive culture conversion between T0 and T1; 82.1%, 92/112) or slow converters (definitive culture conversion between T1 and T2; 14.2%, 16/112). Poor treatment outcomes were recorded in four patients (treatment failure, 2.7%, 3/112; relapse, 0.9%, 1/112; data not shown).

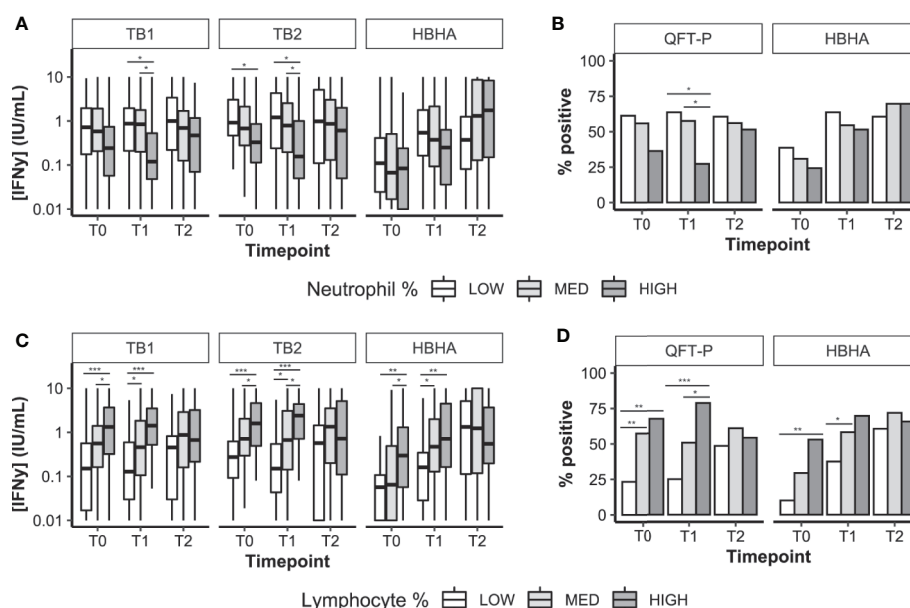


**FIGURE 3** | Plasma IFN- $\gamma$  response to TB-specific QFT-P antigens or HBHA stimulation in patients stratified by WBC counts over the course of TB therapy. **(A, C)** Quantitative IFN- $\gamma$  response. Data are given as median + interquartile range and were compared using Kruskal–Wallis' test with Dunn's *post-hoc* when necessary. **(B, D)** Data were given as a percentage of each group and were compared using Fisher's Exact Test with Bonferroni's correction when necessary. Positivity was set at 0.75 IU/ml for QFT-P TB1, 0.71 IU/ml for QFT-P TB2 (the overall QFT-P result was positive if TB1 and/or TB2 were positive) and at 0.22 IU/ml for HBHA, based on ROC analyses. Low, medium, and high WBC or lymphocyte groups were defined as follows: low: <1<sup>st</sup> quartile; medium: 1<sup>st</sup>–3<sup>rd</sup> quartiles; high: >3<sup>rd</sup> quartile. WBC, white blood cells; T0, baseline; T1, baseline + 2 months; T2, end of treatment; \**p* < 0.05; \*\**p* < 0.01; \*\*\**p* < 0.001.

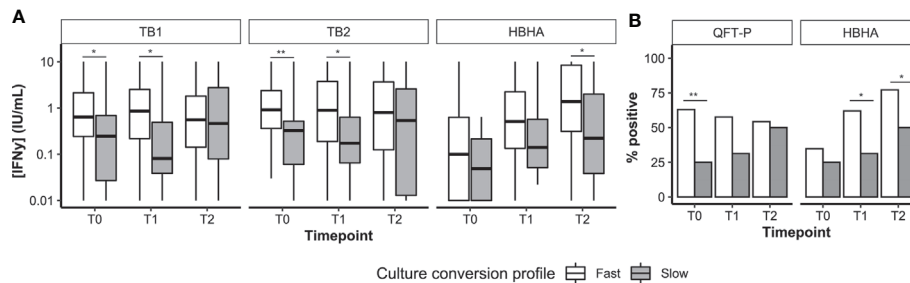


**FIGURE 4 |** Culture conversion profiles and plasma IFN- $\gamma$  dynamics. Plasma IFN- $\gamma$  levels (**A**, represented as medians + interquartile range) and IGRA positivity rates (**B**). T0, enrolment; T1, T0 + 2months; T2, end of treatment; Fast, conversion between T0 and T1 ( $n = 92$ ). Slow, conversion between T1 and T2 ( $n = 16$ ). \* $p < 0.05$ ; \*\* $p < 0.01$  (Mann-Whitney U Test or Fisher's Exact Test).

Among successfully cured patients ( $n = 108$ ), median IFN- $\gamma$  levels (**Figure 4A**) as well as QFT-P and rmsHBHA IGRA positivity rates (**Figure 4B**) were stratified according to the culture conversion profiles. In slow converters, TB1 and TB2 IFN- $\gamma$  levels at T0 and T1 and rmsHBHA IFN- $\gamma$  levels at T2 were significantly lower than in fast converters. Similarly, QFT-P positivity rates at T1 and rmsHBHA positivity rates at T1 and T2 were significantly lower in slow converters.

Then, we calculated the sensitivity, specificity, and accuracy of the QFT-P and rmsHBHA IGRAs for TB treatment monitoring at T1 and T2, using culture as a reference standard (**Supplementary Table 4**). At T1 and T2 respectively, the accuracy of the QFT-P IGRA was of 44 and 46%, and the accuracy of TB2-TB1 was of 52 and 55%. For the rmsHBHA IGRA, we evaluated the test performances of negative rmsHBHA results (*i.e.* rmsHBHA IFN- $\gamma \leq 0.22$  IU/ml), since lower rmsHBHA IFN- $\gamma$  values were observed before treatment. The accuracy of the rmsHBHA IGRA was of 64 and 65% at T1 and T2, respectively. Finally, we generated a score which was positive when the QFT-P result was positive and the rmsHBHA result was negative. The sensitivity of this combined score was of 86% at T1 and 82% at T2, and its accuracy reached 77% at T1 and 81% at T2, but its specificity remained inferior to 30% at both timepoints. Similar results were observed with a score combining rmsHBHA and TB2-TB1.

## Association Between White Blood Cell Counts, Culture Conversion, and Interferon- $\gamma$ Release Assay Interferon- $\gamma$ Response During Treatment

We compared the immune cell counts (**Supplementary Table 5**) and the baseline sociodemographic characteristics (**Supplementary Table 6**) of patients according to their culture conversion profiles. No difference was detected between slow and fast converters for immune cell counts, but at T0 and T1, patients with treatment failure or relapse had significantly higher neutrophil percentages (at T0, median 84%, interquartile range (IQR) 81.5–86.5; at T1, 79%, IQR 75–81.75), and lower lymphocyte percentages (at T0, 12.5%, IQR 9.2–15.2; at T1, 15.5%, IQR 11–21.2) than successfully treated patients. The BMI at inclusion was significantly lower in slow than in fast converters, and slower conversion rates were observed in the Madagascar cohort.

Then, logistic regression analyses were performed to identify associations between slow culture conversion and immune cell counts or IGRA results (**Table 3**). In univariate analyses, significant associations were detected between slow conversion and MIT IFN- $\gamma$  at T0 (odds ratio (OR) 0.78,  $p = 0.001$ ) and T1 (OR 0.84,  $p = 0.021$ ), with QFT-P IGRA positivity at T0 (OR 0.19,  $p = 0.008$ ), and with rmsHBHA IGRA positivity at T1 (OR 0.24,  $p = 0.015$ ) and T2 (OR 0.29,  $p = 0.029$ ). The BMI at inclusion was also associated (OR 0.791,  $p = 0.025$ ).

In multivariate analyses, significant associations were maintained for MIT IFN- $\gamma$  at T0 (adjusted OR 0.65,  $p = 0.009$ ), QFT-P IGRA positivity at T0 (aOR 0.045,  $p = 0.013$ ), and HBHA IGRA positivity at T1 (aOR 0.076,  $p = 0.045$ ). No significant association was found otherwise (**Supplementary Table 7**). Adjusting the models with neutrophil and monocyte proportions at baseline yielded similar results, but with higher AIC values (**Supplementary Table 8**).

Overall, we observed a slow converter profile including consistent clinical patterns at baseline (low BMI, high neutrophil percentages, low lymphocyte percentages, low TB1 and TB2 IFN- $\gamma$  responses), as well as a downregulated rmsHBHA response at the end of treatment.

## DISCUSSION

In this multicentered prospective study, we assessed the value of QFT-P or rmsHBHA-based IGRAs for pulmonary TB sputum culture conversion monitoring in five cohorts (Bangladesh, Georgia, Lebanon, Madagascar, and Paraguay). We recruited 132 HIV-uninfected culture confirmed pulmonary TB patients, including 28 DR-TB cases. To our knowledge, this is the first time that QFT-P and HBHA IGRAs are prospectively evaluated for treatment monitoring in DS-TB and DR-TB cohorts from high-TB incidence countries.

Consistently with previous works (20, 21), we found that individual monitoring of TB1 and TB2 IFN- $\gamma$  levels during treatment showed little relevancy; we observed important inter-patient heterogeneity, and no significant changes in median values over time. On the contrary, median rmsHBHA

**TABLE 3 |** Associations between time to culture conversion, IFN- $\gamma$  response, and selected clinical parameters.

Parameter	Timepoint	Descriptive analysis (n = 108)			Univariate analysis		Multivariate analysis <sup>1</sup>			
		Slow responders (n = 16; reference)	Fast responders (n = 92)	P	OR (95%CI)	p	aOR (95%CI)	p	C	AIC
MIT IFN- $\gamma$ (IU/ml)	T0	4.9 (1.8–10)	10 (9.82–10)	0.0028	0.78 (0.67–0.91)	0.001	0.65 (0.44–0.86)	0.009	0.75	57.5
	T1	8.3 (3.9–10)	10 (9.93–10)	0.0039	0.84 (0.72–0.98)	0.021	0.77 (0.56–1.01)	0.076	0.68	63.9
	T2	9.4 (4.8–10)	10 (9.94–10)	0.023	0.88 (0.76–1.04)	0.11	0.78 (0.57–1.05)	0.10	0.66	64.7
Positive QFT-P IGRA	T0	25% (4/16)	63% (58/92)	0.006	0.19 (0.051–0.61)	0.008	0.045 (0.002–0.35)	0.013	0.77	57.6
	T1	31.2% (5/16)	56.5% (52/92)	0.10	0.33 (0.099–0.99)	0.059	0.39 (0.064–1.97)	0.27	0.64	66.2
	T2	50% (8/16)	53.3% (49/92)	0.98	0.88 (0.29–2.57)	0.81	3.27 (0.59–24.1)	0.20	0.65	65.7
Positive HBHA IGRA	T0	25% (4/16)	35.9% (33/92)	0.57	0.62 (0.16–1.96)	0.44	0.39 (0.075–1.71)	0.24	0.64	66.7
	T1	31.2% (5/16)	65.2% (60/92)	0.013	0.24 (0.071–0.73)	0.015	0.076 (0.003–0.67)	0.045	0.74	61.9
	T2	50% (8/16)	77.2% (71/92)	0.033	0.29 (0.097–0.89)	0.029	0.79 (0.17–4.13)	0.77	0.61	67.1
Lymphocyte % of WBC	T0	17.5 (12.8–19.5)	19.0 (15–26)	0.099	0.93 (0.84–1.00)	0.086	0.94 (0.83–1.05)	0.33	0.64	66.4
	T1	23.0 (16.2–28.0)	25.0 (20.7–31)	0.099	0.93 (0.86–0.99)	0.052	0.92 (0.83–0.99)	0.078	0.68	63.3
	T2	29.5 (23.5–36.2)	30.0 (25.9–36)	0.93	1.01 (0.95–1.06)	0.76	1.01 (0.94–1.08)	0.89	0.62	67.5
Body mass index	T0	17.0 (16.3–18.6)	19.7 (17.4–21.5)	0.0088	0.79 (0.63–0.93)	0.025	0.78 (0.56–1.02)	0.098	0.65	65.5

T0, inclusion. T1, T0 + 2 months. T2, end of treatment. OR, odds ratio; aOR, adjusted odds ratio; CI, confidence interval; WBC, white blood cells; C, model C statistic; AIC, Akaike Information Criterion. Only parameters with significant association to the outcome were shown; other tested parameters are available in **Supplementary Table 7**. Slow culture conversion was defined as a persistently positive culture result at T1 followed by a culture conversion at T2. For MIT IFN- $\gamma$ , associations were calculated for each unit increase. For lymphocyte proportions, associations were calculated for each increase of 5%. <sup>1</sup>models were adjusted for age, sex, country of origin, drug resistance strain, body mass index at inclusion, and BCG vaccination rate.

IFN- $\gamma$  levels increased significantly throughout treatment, and an increase was observed in most patients. This is consistent with studies associating high rmsHBHA IFN- $\gamma$  levels to latency and controlled infection (23, 25–27), as well as in children (28) and in adults (32) receiving anti-TB treatment. The differences observed between the QFT-P and rmsHBHA IFN- $\gamma$  responses during treatment can be explained by distinct antigen compositions. TB1 and TB2 are peptide pools obtained from secreted antigens, whereas rmsHBHA is a native protein found in mycobacterial cell walls *in vivo*; hence, antigen processing and presentation may differ. Bacterial pathogenesis mechanisms (40) as well as the bactericidal effect of anti-TB treatment could also affect the release of QFT-P and HBHA antigens. In addition, mycobacterial immune escape mechanisms involving HBHA (41, 42) could explain the downregulated *in vitro* IFN- $\gamma$  responses to rmsHBHA during active disease.

Characterization of the association between QFT-P, rmsHBHA IFN- $\gamma$ , and mycobacterial clearance has led us to identify two subsets of conversion rates. In particular, slower culture conversion was associated with QFT-P negativity at T0, consistently with a prior study linking negative or indeterminate QFT-P results with poor treatment outcomes (43), and with HBHA IGRA negativity at T1. More generally, both a general immunosuppression with low non-specific IFN- $\gamma$  (44), and low *M. tuberculosis*-specific IFN- $\gamma$  (45) have been demonstrated during active TB. Thus, an anergic early T-cell-driven response might be involved in slower mycobacterial clearance (43). At the other end of the spectrum, lower levels of IFN- $\gamma$  in slow converters at T2 suggest a link between magnitude of the rmsHBHA-mediated response and mycobacterial clearance.

Our data indicate that rmsHBHA and/or QFT-P IFN- $\gamma$  had low specificity and accuracy compared to the gold standard culture conversion. Because of the small cohort size, this result must be interpreted with caution; but if confirmed, it could suggest that the increase in rmsHBHA IFN- $\gamma$  might be

representative of general immune recovery during treatment rather than a specific response to *M. tuberculosis*. Here, this hypothesis is supported by the fact that a low IFN- $\gamma$  response to non-TB specific stimulation (Mitogen tubes) at T0 was also significantly associated with slow culture conversion in multivariate analysis. In addition, immune cross-reactions with HBHA homologs present in environmental mycobacteria have been previously reported (23).

Finally, our study had several limitations. The sample size was relatively small, and patients were included in diverse geographical areas and had different antibiotic regimens. As a consequence, malnutrition levels, untested co-infections (besides HIV and virus B and C hepatitis), different genetic and epigenetic backgrounds, or potential differences in bacterial loads during sputum collection could not be controlled. We were intrigued by differences in IFN- $\gamma$  response to HBHA in the different study sites, which could be linked to ethnic-specific influences over *M. tuberculosis* responses (46). Although adjustment with sociodemographic factors and optimism corrections with a method adapted to small sample sizes (47) were performed, our results need to be confirmed in larger cohorts.

In conclusion, this study described the associations between mycobacterial clearance and immune responses to QFT-P and rmsHBHA IGRAs throughout anti-TB treatment. Lower QFT-P and rmsHBHA IFN- $\gamma$  levels were associated with slower mycobacterial clearance. Our results support a growing body of evidence suggesting that rmsHBHA IFN- $\gamma$  discriminates between the different stages of TB. However, the specificity of both IGRAs was insufficient for treatment monitoring. Further research is needed to clarify how the rmsHBHA response is regulated at the cellular level during treatment, and whether there is any specific interaction with mycobacterial clearance. In particular, evaluating how long rmsHBHA IFN- $\gamma$  values remain stable after treatment would help assess whether it could be a relevant biomarker for relapse prediction.



## DATA AVAILABILITY STATEMENT

The raw data supporting the conclusions of this article will be made available by the authors, without undue reservation.

## ETHICS STATEMENT

The studies involving human participants were reviewed and approved by: in Bangladesh, the Research Review Committee and the Ethical Review Committee of icddr, b; in Georgia, the Institutional Review Board of the NTCLD (IORG0009467); in Lebanon, the Institutional Review Board of NINI hospital (IRB-F-01); In Madagascar, the Ministry of Public Health and the Ethical Committee for Biomedical Research (reference number: n°099-MSANP/CERBM); in Paraguay, the Research Ethics Committee and the Scientific Committee of the IICS-UNA (IRB number: IRB00011984; Federalwide Assurance number: FWA00029097). The patients/participants provided their written informed consent to participate in this study.

## AUTHOR CONTRIBUTIONS

JH is the principal investigator and initiated the project together with DG, NT, SBa, GR, NR, and MH. Data were collected by EK, MU, SBi, CA, PR, CR, PH, JR, AR, and RB. CC performed all the analyses and wrote the manuscript. All authors contributed to the article and approved the submitted version.

## REFERENCES

1. World Health Organization Geneva. *Global tuberculosis report 2020*. Geneva: World Health Organization (2020).
2. World Health Organization Geneva. *Guidelines for treatment of drug-susceptible tuberculosis and patient care* Vol. vol. 1. Geneva: World Health Organization (2017).
3. World Health Organization Geneva. *WHO consolidated guidelines on drug-resistant tuberculosis treatment*. Geneva: World Health Organization (2019).
4. Woimo TT, Yimer WK, Bati T, Gesesew HA. The prevalence and factors associated for anti-tuberculosis treatment non-adherence among pulmonary tuberculosis patients in public health care facilities in South Ethiopia: a cross-sectional study. *BMC Public Health* (2017) 17:1–10. doi: 10.1186/s12889-017-4188-9
5. Munro SA, Lewin SA, Smith HJ, Engel ME, Fretheim A, Volmink J. Patient Adherence to Tuberculosis Treatment: A Systematic Review of Qualitative Research. *PLoS Med* (2007) 4(7):e238. doi: 10.1371/journal.pmed.0040238
6. World Health Organization Geneva. *Global Tuberculosis Report 2018*. Geneva: World Health Organization (2018).
7. Horne DJ, Royce SE, Gooze L, Narita M, Hopewell PC, Nahid P, et al. Sputum monitoring during tuberculosis treatment for predicting outcome: systematic review and meta-analysis. *Lancet Infect Dis* (2010) 10:387–94. doi: 10.1016/S1473-3099(10)70071-2
8. Parrish NM, Carroll KC. Role of the clinical mycobacteriology laboratory in diagnosis and management of tuberculosis in low-prevalence settings. *J Clin Microbiol* (2011) 49:772–6. doi: 10.1128/JCM.02451-10
9. World Health Organization. *Early detection of Tuberculosis: an overview of approaches, guidelines and tool*. World Health Organization (2011).
10. Goletti D, Arlehamn CSL, Scriba TJ, Anthony R, Cirillo DM, Alonzi T, et al. Can we predict tuberculosis cure? Current tools available. *Eur Respir J* (2018) 52:1801089. doi: 10.1183/13993003.01089-2018

## FUNDING

This work was supported by Fondation Mérieux, Fondation Christophe et Rodolphe Mérieux, and Fondation AnBer, and the grant ANR-18-CE17-0020. A minor part of the study was supported by the Italian Ministry of Health “Ricerca Corrente, Linea 4.”

## ACKNOWLEDGMENTS

We would like to thank all the patients participating in our study, as well as the local healthcare staff in each clinical site. In particular, we are very grateful to Leticia Rojas and Laura Franco, from the Molecular Biology Department at the Instituto de Investigaciones en Ciencias de la Salud (Asunción, Paraguay) for their valuable help with patient data collection. Finally, we would like to dedicate this work to the memory of María Maldonado, from the Hospital General de San Lorenzo (Asunción, Paraguay). We are beyond grateful to her for her dedication during the recruitment and follow-up process of the patients in this study, as well as for her unflinching involvement in the fight against tuberculosis in Paraguay.

## SUPPLEMENTARY MATERIAL

The Supplementary Material for this article can be found online at: <https://www.frontiersin.org/articles/10.3389/fimmu.2020.616450/full#supplementary-material>

11. MacLean E, Broger T, Yerlikaya S, Fernandez-Carballo BL, Pai M, Denkiner CMA. A systematic review of biomarkers to detect active tuberculosis. *Nat Microbiol* (2019) 4(5):748–58. doi: 10.1038/s41564-019-0380-2
12. Goletti D, Lee MR, Wang JY, Walter N, Ottenhoff THM. Update on tuberculosis biomarkers: From correlates of risk, to correlates of active disease and of cure from disease. *Respirology* (2018) 23:455–66. doi: 10.1111/resp.13272
13. Liang L, Shi R, Liu X, Yuan X, Zheng S, Zhang G, et al. Interferon-gamma response to the treatment of active pulmonary and extra-pulmonary tuberculosis. *Int J Tuberc Lung Dis* (2017) 21:1145–9. doi: 10.5588/ijtld.16.0880
14. Chang P, Wang PH, Chen KT. Use of the QuantiFERON-TB Gold In-Tube Test in the Diagnosis and Monitoring of Treatment Efficacy in Active Pulmonary Tuberculosis. *Int J Environ Res Public Health* (2017) 14(3):236. doi: 10.20944/preprints201701.0035.v1
15. Petruccioli E, Chiacchio T, Vanini V, Cuzzi G, Codecasa LR, Ferrarese M, et al. Effect of therapy on Quantiferon-Plus response in patients with active and latent tuberculosis infection. *Sci Rep* (2018) 8(1):1–11. doi: 10.1038/s41598-018-33825-w
16. Kamada A, Amishima M. QuantiFERON-TB Gold Plus as a potential tuberculosis treatment monitoring tool. *Eur Respir J* (2017) 49:10–2. doi: 10.1183/13993003.01976-2016
17. Goletti D, Carrara S, Mayanja-Kizza H, Baseke J, Mugerwa MA, Girardi E, et al. Response to M. tuberculosis selected RD1 peptides in Ugandan HIV-infected patients with smear positive pulmonary tuberculosis: A pilot study. *BMC Infect Dis* (2008) 8(1):1–13. doi: 10.1186/1471-2334-8-11
18. Kabeer BSA, Raja A, Raman B, Thangaraj S, Lepointier M, Ippolito G, et al. IP-10 response to RD1 antigens might be a useful biomarker for monitoring tuberculosis therapy. *BMC Infect Dis* (2011) 11(1):135. doi: 10.1186/1471-2334-11-135
19. Feng JY, Pan SW, Huang SF, Chen YY, Lin YY, Su WJ. Depressed Gamma Interferon Responses and Treatment Outcomes in Tuberculosis Patients:

- a Prospective Cohort Study. *J Clin Microbiol* (2018) 56(10):e00664–18. doi: 10.1128/JCM.00664-18
20. Denkinger CM, Pai M, Patel M, Menzies D. Gamma Interferon Release Assay for Monitoring of Treatment Response for Active Tuberculosis : an Explosion in the Spaghetti Factory. *J Clin Microbiol* (2013) 51:607–10. doi: 10.1128/JCM.02278-12
  21. Bartalesi F, Spinicci M, Mencarini J, Veloci S, Mantella A, Bartoloni A. The role of QuantiFERON-TB Gold in-Tube in the diagnosis and treatment monitoring of active tuberculosis The role of QuantiFERON-TB Gold in-Tube in the diagnosis and treatment monitoring of active tuberculosis. *Infect Dis (Auckl)* (2017) 49(6):474–7. doi: 10.1080/23744235.2017.1279747
  22. Clifford V, He Y, Zufferey C, Connell T, Curtis N. Interferon gamma release assays for monitoring the response to treatment for tuberculosis : A systematic review. *Tuberculosis* (2015) 95:639–50. doi: 10.1016/j.tube.2015.07.002
  23. Delogu G, Chiacchio T, Vanini V, Butera O, Cuzzi G, Bua A, et al. Methylated HBHA produced in *M. smegmatis* discriminates between active and non-active tuberculosis disease among RD1-responders. *PLoS One* (2011) 6(3):e18315. doi: 10.1371/journal.pone.0018315
  24. Loch C, Hougardy JM, Rouanet C, Place S, Mascart F. Heparin-binding hemagglutinin, from an extrapulmonary dissemination factor to a powerful diagnostic and protective antigen against tuberculosis. *Tuberculosis* (2006) 86:303–9. doi: 10.1016/j.tube.2006.01.016
  25. Hougardy JM, Schepers K, Place S, Drowart A, Lechevin V, Verscheure V, et al. Heparin-binding-hemagglutinin-induced IFN- $\gamma$  release as a diagnostic tool for latent tuberculosis. *PLoS One* (2007) 2(10):e926. doi: 10.1371/journal.pone.0000926
  26. Corbière V, et al. Risk stratification of latent tuberculosis defined by combined interferon gamma release assays. *PLoS One* (2012) 7. doi: 10.1371/journal.pone.0043285
  27. Tang J, Huang Y, Jiang S, Huang F, Ma T, Qi Y, et al. QuantiFERON-TB Gold Plus combined with HBHA-Induced IFN- $\gamma$  release assay improves the accuracy of identifying tuberculosis disease status. *Tuberculosis* (2020) 124:101966. doi: 10.1016/j.tube.2020.101966
  28. Sali M, Buonsenso D, D'Alfonso P, De Maio F, Ceccarelli M, Battah B, et al. Combined use of QuantiFERON and HBHA-based IGRA supports tuberculosis diagnosis and therapy management in children. *J Infect* (2018) 77(6):526–33. doi: 10.1016/j.jinf.2018.09.011
  29. Chedid C, Kokhraidze E, Tukvadze N, Banu S, Uddin MKM, Biswas S, et al. Association of baseline white blood cell counts with tuberculosis treatment outcome: a prospective multicentered cohort study. *Int J Infect Dis* (2020) 100:199–206. doi: 10.1016/j.ijid.2020.09.017
  30. World Health Organization Geneva. *Global Tuberculosis Report 2019*. Geneva: World Health Organization (2019).
  31. Komurian-Pradel F, Grundmann N, Siqueira MM, Chou M, Diallo S, Mbacham W, et al. Enhancing research capacities in infectious diseases: The GABRIEL network, a joint approach to major local health issues in developing countries. *Clin Epidemiol Glob Heal* (2013) 1(1):40–3. doi: 10.1016/j.cegh.2012.11.002
  32. Wen HL, Li CL, Li G, Lu YH, Li HC, Li T, et al. Involvement of methylated HBHA expressed from *Mycobacterium smegmatis* in an IFN- $\gamma$  release assay to aid discrimination between latent infection and active tuberculosis in BCG-vaccinated populations. *Eur J Clin Microbiol Infect Dis* (2017) 36(8):1415–23. doi: 10.1007/s10096-017-2948-1
  33. Guo Y, Logan HL, Glueck DH, Muller KE. Selecting a sample size for studies with repeated measures. *BMC Med Res Methodol* (2013) 13(1):100. doi: 10.1186/1471-2288-13-100
  34. Aung KJM, Van Deun A, Declercq E, Sarker MR, Das PK, Hossain MA, et al. Successful '9-month Bangladesh regimen' for multidrug-resistant tuberculosis among over 500 consecutive patients. *Int J Tuberc Lung Dis* (2014) 18(10):1180–7. doi: 10.5588/ijtld.14.0100
  35. Qiagen. QuantiFERON®-TB Gold Plus (QFT®-Plus) Package Insert. (2013) 96:1101062.
  36. Castor EDC. Castor Electronic Data Capture [online]. (2019). Available at: <https://castoredc.com>.
  37. Kim H-Y. Statistical notes for clinical researchers: Chi-squared test and Fisher's exact test. *Restor Dent Endod* (2017) 42:152. doi: 10.5395/rde.2017.42.2.152
  38. Dunn OJ. Multiple Comparisons Using Rank Sums. *Technometrics* (1964) 6:241–52. doi: 10.1080/00401706.1964.10490181
  39. Pedro HDSP, Nardi SMT, Pereira MIF, Oliveira RS, Suffys PN, Gomes HM, et al. Clinical and epidemiological profiles of individuals with drug-resistant tuberculosis. *Mem Inst Oswaldo Cruz* (2015) 110(2):235–48. doi: 10.1590/0074-02760140316
  40. Delogu G, et al. The hbhA gene of *Mycobacterium tuberculosis* is specifically upregulated in the lungs but not in the spleens of aerogenically infected mice. *Infect Immun* (2006) 74:3006–11. doi: 10.1128/IAI.74.5.3006-3011.2006
  41. Zheng Q, et al. Heparin-binding hemagglutinin of *Mycobacterium tuberculosis* is an inhibitor of autophagy. *Front Cell Infect Microbiol* (2017) 7:1–11. doi: 10.3389/fcimb.2017.00033
  42. Hougardy JM, et al. Regulatory T cells depress immune responses to protective antigens in active tuberculosis. *Am J Respir Crit Care Med* (2007) 176:409–16. doi: 10.1164/rccm.200701-084OC
  43. Auld SC, Lee SH, Click ES, Miramontes R, Day CL, Gandhi NR, et al. IFN- $\gamma$  release assay result is associated with disease site and death in active tuberculosis. *Ann Am Thorac Soc* (2016) 13(12):2151–8. doi: 10.1513/AnnalsATS.201606-482OC
  44. Roberts T, Beyers N, Aguirre A, Walz G. Immunosuppression during Active Tuberculosis Is Characterized by Decreased Interferon- $\gamma$  Production and CD25 Expression with Elevated Forkhead Box P3 , Transforming Growth Factor - b , and Interleukin-4 mRNA Levels. *J Infect Dis* (2007) 195(6):870–8. doi: 10.1086/511277
  45. Goletti D, Butera O, Bizzoni F, Casetti R, Girardi E, Poccia F. Region of Difference 1 Antigen-Specific CD4 + Memory T Cells Correlate with a Favorable Outcome of Tuberculosis. *J Infect Dis* (2006) 194(7):984–92. doi: 10.1086/507427
  46. Jasenosky LD, Scriba TJ, Hanekom WA, Goldfeld AE. T cells and adaptive immunity to *Mycobacterium tuberculosis* in humans. *Immunol Rev* (2015) 264:74–87. doi: 10.1111/imr.12274
  47. Smith GCS, Seaman SR, Wood AM, Royston P, White IR. Correcting for optimistic prediction in small data sets. *Am J Epidemiol* (2014) 180:318–24. doi: 10.1093/aje/kwu140

**Conflict of Interest:** MH, MI, and RB had logistic support from the National TB program in Lebanon. DG reports personal fees from Quidel, Qiagen, Janssen, BioMérieux, and Celgene, outside the submitted work. All authors have submitted the ICMJE Form for Disclosure of Potential.

Copyright © 2021 Chedid, Kokhraidze, Tukvadze, Banu, Uddin, Biswas, Russomando, Acosta, Arenas, Ranaivomanana, Razafimahatratra, Herindrainy, Rakotonirina, Raheerinandrasana, Rakotosamimanana, Hamze, Ismail, Bayaa, Berland, De Maio, Delogu, Endtz, Ader, Goletti and Hoffmann. This is an open-access article distributed under the terms of the Creative Commons Attribution License (CC BY). The use, distribution or reproduction in other forums is permitted, provided the original author(s) and the copyright owner(s) are credited and that the original publication in this journal is cited, in accordance with accepted academic practice. No use, distribution or reproduction is permitted which does not comply with these terms.



# Host Blood RNA Transcript and Protein Signatures for Sputum-Independent Diagnostics of Tuberculosis in Adults

Dhanasekaran Sivakumaran<sup>1,2</sup>, Christian Ritz<sup>1,3</sup>, John Espen Gjølén<sup>4</sup>, Mario Vaz<sup>5</sup>, Sumithra Selvam<sup>6</sup>, Tom H. M. Ottenhoff<sup>7</sup>, Timothy Mark Doherty<sup>8</sup>, Synne Jenum<sup>9</sup> and Harleen M. S. Grewal<sup>1,2\*</sup>

<sup>1</sup> Department of Clinical Science, Faculty of Medicine, University of Bergen, Bergen, Norway, <sup>2</sup> Department of Microbiology, Haukeland University Hospital, University of Bergen, Bergen, Norway, <sup>3</sup> Department of Nutrition, Exercise and Sports, University of Copenhagen, Copenhagen, Denmark, <sup>4</sup> Department of Paediatrics, Haukeland University Hospital, Bergen, Norway, <sup>5</sup> Department of Physiology, St. John's Medical College and Division of Health and Humanities, St. John's Research Institute, Bangalore, India, <sup>6</sup> Division of Infectious Diseases, St. John's Research Institute, Bangalore, India, <sup>7</sup> Department of Infectious Diseases, Leiden University Medical Center, Leiden, Netherlands, <sup>8</sup> GlaxoSmithKline Vaccines, Wavre, Belgium, <sup>9</sup> Department of Infectious Diseases, Oslo University Hospital, Oslo, Norway

## OPEN ACCESS

### Edited by:

Novel N. Chegou,  
Stellenbosch University, South Africa

### Reviewed by:

Wenhong Zhang,  
Huashan Hospital, China  
Fatoumatta Darboe,  
Medical Research Council The  
Gambia Unit (MRC), Gambia

### \*Correspondence:

Harleen M. S. Grewal  
Harleen.Grewal@uib.no

### Specialty section:

This article was submitted to  
Microbial Immunology,  
a section of the journal  
Frontiers in Immunology

**Received:** 04 November 2020

**Accepted:** 21 December 2020

**Published:** 04 February 2021

### Citation:

Sivakumaran D, Ritz C, Gjølén JE, Vaz M, Selvam S, Ottenhoff THM, Doherty TM, Jenum S and Grewal HMS (2021) Host Blood RNA Transcript and Protein Signatures for Sputum-Independent Diagnostics of Tuberculosis in Adults. *Front. Immunol.* 11:626049. doi: 10.3389/fimmu.2020.626049

To achieve the ambitious targets for tuberculosis (TB) prevention, care, and control stated by the End TB Strategy, new health care strategies, diagnostic tools are warranted. Host-derived biosignatures are explored for their TB diagnostic potential in accordance with the WHO target product profiles (TPPs) for point-of-care (POC) testing. We aimed to identify sputum-independent TB diagnostic signatures in newly diagnosed adult pulmonary-TB (PTB) patients recruited in the context of a prospective household contact cohort study conducted in Andhra Pradesh, India. Whole-blood mRNA samples from 158 subjects (PTB,  $n = 109$ ; age-matched household controls,  $n = 49$ ) were examined by dual-color Reverse-Transcriptase Multiplex Ligation-dependent Probe-Amplification (dcRT-MLPA) for the expression of 198 pre-defined genes and a Mesoscale discovery assay for the concentration of 18 cytokines/chemokines in TB-antigen stimulated QuantiFERON supernatants. To identify signatures, we applied a two-step approach; in the first step, univariate filtering was used to identify and shortlist potentially predictive biomarkers; this step may be seen as removing redundant biomarkers. In the second step, a logistic regression approach was used such that group membership (PTB vs. household controls) became the binary response in a Lasso regression model. We identified an 11-gene signature that distinguished PTB from household controls with AUCs of  $\geq 0.98$  (95% CIs: 0.94–1.00), and a 4-protein signature (IFN $\gamma$ , GM-CSF, IL7 and IL15) that differentiated PTB from household controls with AUCs of  $\geq 0.87$  (95% CIs: 0.75–1.00), in our discovery cohort. Subsequently, we evaluated the performance of the 11-gene signature in two external validation data sets viz, an independent cohort at the Glenfield Hospital, University Hospitals of Leicester NHS Trust, Leicester, UK (GSE107994 data set), and the Catalysis treatment response cohort (GSE89403 data set) from South Africa. The 11-gene signature validated and distinguished PTB from healthy and asymptomatic

*M. tuberculosis* infected household controls in the GSE107994 data set, with an AUC of 0.95 (95% CI: 0.91–0.98) and 0.94 (95% CI: 0.89–0.98). More interestingly in the GSE89403 data set, the 11-gene signature distinguished PTB from household controls and patients with other lung diseases with an AUC of 0.93 (95% CI: 0.87–0.99) and 0.73 (95% CI: 0.56–0.89). These criteria meet the WHO TTP benchmarks for a non-sputum-based triage test for TB diagnosis. We suggest that further validation is required before clinical implementation of the 11-gene signature we have identified markers will be possible.

**Keywords:** transcript signature, protein signature, tuberculosis, adult, non-sputum

## INTRODUCTION

Tuberculosis (TB) is one of the top 10 causes of death worldwide and the single infectious pathogen responsible for the most deaths—even after the emergence of the covid-19 pandemic. In 2018, a total of 1.5 million lives were lost to TB (1), and the goals of the End TB Strategy; to achieve a 90% reduction in TB incidence and a 95% reduction in TB mortality by 2035, are challenging (2). Much of the mortality attributed to TB occur in low-resource settings, so effective diagnostic tests applicable in these settings are essential to meet these goals. The WHO has defined the performance and operational characteristics of tests applicable for primary care or at the point-of-care (POC) in its high-priority target product profiles (TPPs) (3). To meet the TPPs, a rapid biomarker-based test would ideally be i) instrument-free or feasible with limited instrumentation and ii) based on easily accessible samples such as blood, urine, or breath (4).

In recent years, efforts have been made to identify which of the diagnostic needs should be of highest priority for biomarker-based assays balancing efficiency, affordability, and access in high-endemic limited resource settings (3, 5). The top priority is a rapid biomarker-based, non-sputum POC test i) to detect TB disease and guide immediate initiation of TB treatment, thus avoiding loss of cases from diagnostic delay (3, 5), and ii) for triage, ruling out TB disease with high sensitivity, allowing targeted referral to more expensive and accurate confirmatory tests (6). Ideally, such POC tests would perform satisfactorily with pulmonary and extrapulmonary disease in both children and adults regardless of HIV coinfection (7). In recent years, there have been exciting developments, including sputum-based and non-sputum-based TB diagnostics. However, the Lipoarabinomannan (LAM) test, which detects *M. tuberculosis* (*Mtb*) complex LAM in urine, is hitherto the only non-sputum test endorsed by WHO.

Over the past few years, the search for host biomarker(s) or biosignatures has gained increased attention in attempts to develop companion diagnostic platforms (8–20). Although expensive and resource-demanding, genome-wide analyses of transcriptomes offer unbiased identification of genes and immunologic pathways relevant for the understanding of TB pathogenesis, and risk of progression to disease (21–23). In the search for a unifying signature, a landmark study by Sweeney et al. (24) using data from publicly available human genome repositories, identified a 3-gene signature (3-gene TB score)

derived from three discovery datasets of adults, that separated subjects with TB from healthy controls, *Mtb* infection, and other diseases in validation datasets of children and adults. However, the mean diagnostic accuracy obtained in the validation sets did not meet initial WHO criteria for a diagnostic POC test. Subsequently, Warsinke HC et al. (25) evaluated the performance of the 3-gene TB score in three different TB cohorts (25–27) and found that outcomes approached the WHO TTP benchmarks for a non-sputum-based triage test, with a high negative predictive value. Further, a very recent study evaluated 27 eligible identified signatures in a systematic meta-review, from which four signatures (Sweeney3, Kaforou25, Roe3, and BATF2) fulfilled the WHO minimum diagnostic accuracy parameters required for a TB triage test (28).

Genome-wide analysis of transcriptomes has been applied as a first step in identifying markers with potential for subsequent refinement as POC tests (12). To simplify the search for transcriptional signatures with diagnostic relevance in TB, we applied a user-friendly and inexpensive technique; the dual-color-Reverse-Transcriptase-Multiplex-Ligation-dependent-Probe-Amplification (dc-RT MLPA). In addition, a Mesoscale discovery assay was applied for protein analysis. The present study aimed to: i) Identify transcriptional and proteomic signatures with the ability to distinguish pulmonary TB (PTB) from household controls. ii) Validate the identified transcriptional signature in an independent cohort from the UK (17) comprising adult TB patients and healthy household contacts with/without *Mtb* infection as well as in the South African *Catalysis Treatment Response Cohort* (CTRC) (27) comprising adult TB patients, subjects with other lung diseases, and healthy controls. iii) Investigate the performance of the signature in adult TB patients identified in the present study in a recently-described pediatric population (11). iv) Compare the diagnostic abilities of the previously identified 10-gene signature (11) for pediatric PTB in the present adult study population.

## MATERIALS AND METHODS

### Ethical Consideration

Ethical approval for this study was obtained from the Institutional Ethical Review Board (IERB) of St. John's Medical College, Bangalore (IERB/1/527/08). The material transfer agreement between St. John's Medical College, Bangalore, and



the University of Bergen, Norway was obtained from the Department of Biotechnology, Government of India (No.BT/Med.II/Adv (SS)/Misc./02/2012). Ethical approval was also obtained (Ref no: 2018/1614 D) from the Regional Committee for Medical and Health Research Ethics, Western Norway.

## Study Population

A prospective cohort study of adult PTB index cases and their household contacts were conducted in Palamaner and Kuppam Taluks, Chittoor district, Andhra Pradesh, India (3.200°N, 72.7500°E, altitude 683 m) between September 2010 and April 2012. In total, 176 index cases were identified at the microscopy centres of the Revised National Tuberculosis Control Program (RNTCP) (Government of India). Of these, 164 were recruited following written informed consent, and 150 had confirmed TB (presence of *Mtb* in sputum smear and/or culture) with/without abnormal chest X-rays. All were treated with standard anti-TB treatment (ATT) and followed until the end of the 6-month ATT course. Household contacts of the 176 index cases were asked to participate and 525 household contacts recruited following written informed consent were followed for one year. For all children parents/guardians gave their written informed consent to participation. For participants >7 years, an additional written assent was obtained.

## Clinical Assessments and Sampling

*Baseline Assessments of PTB Index Cases and Household Contacts:* Medical History (including BCG vaccination status, history of TB exposure, prior TB/TB treatment and habitual risk factors), demographic, anthropometric, and clinical data were recorded. At baseline, a tuberculin skin test (TST) was performed by a trained nurse (2 TU/0.1 ml of tuberculin; Span Diagnostics, Surat, India) and read after 48–72 h; an induration  $\geq 10$  mm was defined as positive. Three independent radiologists interpreted the chest X-ray (anteroposterior view) at baseline. Agreement by at least two radiologists was required for a conclusion of findings suggestive of TB. Although not a pre-requisite for participation, HIV testing was performed in consenting subjects following pre-test counseling.

## External Validation Cohort

Gene expression data from the Singhania A et al; GSE107994 (an independent cohort of PTB and close contacts of household at the Glenfield Hospital, University Hospitals of Leicester NHS Trust, Leicester from UK) (17) and Thompson EG et al; GSE89403 (CTRC from South Africa) (27) data sets were used for external validation. The normalized log 2 data were back-transformed and multiplied by 100, to match the expression level with the dcRT-MLPA assay).

Gene expression data from our previous pediatric TB cohort (11) was used for validation. In addition, the 10-gene signature originally identified in the pediatric cohort (which consists of TB cases and asymptomatic TB-exposed household controls) was evaluated in the present adult PTB study cohort.

For the external validation, no proteomic data from TB-antigen (ag) stimulated QuantiFERON (QFT) supernatants were available for the proteomic signature evaluation.

## Sample Collection, RNA Extraction, and Selection of Transcriptional Biomarkers

Peripheral whole blood (approx. 2.5 ml) was drawn into PAXgene blood RNA tubes (PreAnalytiX, Hombrechtikon, Switzerland) and stored at  $-80^{\circ}\text{C}$  until RNA extraction (PAXgene Blood RNA kit; PreAnalytiX, Hilden, Germany). Total RNA concentration and purity were measured using a Nanodrop spectrophotometer (Thermoscientific, Wilmington, DE, USA) and ranged between 0.4–13.2  $\mu\text{g}$  (average  $3.8 \pm 1.65 \mu\text{g}$ ).

A total of 198 genes (including 4 housekeeping genes), distributed in 3 panels were assessed, based primarily on their posited or confirmed roles in TB immunology; the first 48-gene set (identified by the partners in the Bill and Melinda Gates Foundation Grand Challenge project #6 consortium) has been described in our previous studies (10, 13). The second 92-gene set included genes known to be involved in general inflammation and myeloid cell activation, and genes involved in the adaptive immune system, comprising Th1/Th2-responses, regulatory T-cell markers, and B-cell associated genes. The third 58-gene set included type 1-interferon-inducible genes (21) known to be up-regulated in adult TB and genes associated with prediction of TB risk in South African neonates (29). In total, thirty genes were present in more than one panel. For the 30 repeated genes that were present in more than one panel, geometric mean expression was used as done in our previous studies (11, 30). In total, there were 145 unique genes were analyzed and presented in the **Supplementary Table 1** (11, 30).

## Dual-Color-Reverse-Transcriptase-Multiplex-Ligation-Dependent-Probe-Amplification (dcRT-MLPA)

For each target sequence, a specific RT primer was designed, located immediately downstream of the left- and right-hand half-probe target sequence. A total of 125 ng RNA was used for reverse transcription, applying MMLV reverse transcriptase (Promega, Madison, WI, USA), followed by hybridization of left- and right-hand half-probes to the cDNA at  $60^{\circ}\text{C}$  overnight. The remaining steps were performed as described elsewhere (13, 31). All 158 samples were run in two (96-well) plates for each of the gene panels. The PCR fragments were analyzed on a 3730-capillary sequencer in Gene scan mode (Life Technologies, Carlsbad, CA, USA), using GeneMapper version 5.0 (Life Technologies, Carlsbad, California, USA). Primers and probes were obtained from the Department of Infectious Diseases, Leiden Medical University, the Netherlands. GAPDH was used for normalization.

## Multiplex Cytokine/Chemokine Assays

Biomarkers at the proteomic level were analyzed in peripheral whole blood stimulated with a mixture of *Mtb*-specific antigens (e.g., QFT supernatants): Early Secretory Antigenic Target-6 (ESAT-6), Culture Filtrate Protein-10 (CFP-10) and TB antigen 7.7. A pilot study was conducted on 12 randomly selected baseline samples from TB Cures ( $n = 4$ ), Treatment Failures ( $n = 4$ ) and household controls ( $n = 4$ ) using the V-plex



human pro-inflammatory, cytokine, and chemokine panels from Meso Scale Discovery (MSD, Rockville, Maryland, USA) according to the manufacturer's instructions. Six of ten biomarkers from each panel [pro-inflammatory panel (IL1 $\beta$ , IL10, IL4, IL12p70, IFN $\gamma$ , and TNF $\alpha$ ), cytokine panel (GM-CSF, IL15, IL17A, IL5, IL7, and VEGF), and chemokine panel (Eotaxin3, IL8, IP10, MCP1, MDC, and MIP1 $\beta$ )] were analyzed. The analysis of biomarkers at the proteomic level has been described elsewhere (30).

## Data Analysis

Patient characteristics were summarized using mean and minimum/maximum or count and percentage, as appropriate. TB disease and household controls were compared using the Mann-Whitney test, Pearson's chi-square test with Yates Continuity Correction, or Fisher's exact test, as appropriate.

Both PTB cases ( $n = 48$ ) and age-matched household controls irrespective of *Mtb* infection status ( $n = 49$ ) were randomly divided into a training set (2/3), and a test set (1/3). Signatures were identified by means of a two-step approach previously used for biosignature identification (11). In short, the approach consisted of 1) univariate feature selection analysis using logistic regression, selecting markers by applying stringent  $p$ -value ( $p < 0.01$ ), and LASSO regression analysis based on the markers identified in step 1. The resulting LASSO model fits provided estimated coefficients (not reported in the present study, see Sivakumaran et al. (30) for an example). The model fits also enabled prediction of the probability of being a PTB for each participant. A predicted probability of  $>0.5$  resulted in classification as a PTB case and  $<0.5$  resulted in classification as a control. This model-based classification was compared to the actual "true" classification of participants and the number of correctly classified participants could be identified. Specifically, the predictive abilities of the signatures (to classify participants correctly) in both training and test set were summarized by means of receiver operator characteristic (ROC) curves, specifically sensitivity, specificity, and area under the curve

(AUC). Analyses were carried out using R (R Core Team) (32) through the graphical user interface RStudio ([www.rstudio.com](http://www.rstudio.com)).

## RESULTS

### Baseline Clinical Characteristics of the PTB Index Cases

Blood samples at baseline were obtained from 109 of the 150 participants with confirmed TB, but only 48 were collected before ATT initiation and thus selected for further biomarker analysis. The remaining PTB ( $n = 61$ ) cases were stratified based on timepoint for sample collection after ATT initiation ( $\leq 72$  or  $>72$  h) and analyzed separately (Figure 1). In the training set, the mean age was 43.9 years in PTB cases (range: 19–70) and 35.7 years in household controls (range: 18–80), and in the test set, 46.5 years in PTB cases (range: 19–69) and 38.2 years (range: 19.5–65) for household controls. In the training set, males constituted 90.6% (29/32) of PTB cases, and 31.3% (10/32) of household controls ( $p < 0.001$ ); in the test set, males constituted 75.0% (16/17) of PTB cases and 23.5% (4/17) of household controls ( $p < 0.01$ ; Table 1). Further baseline characteristics are shown in Table 1.

The mean age of the UK cohort was 40.3 (range: 20–75), 39.6 (range: 16–72), and 35.2 (range: 16–79) years for PTB, healthy *Mtb* infected household contacts, and contacts, respectively. Males constituted 67.9%, 57.1%, and 60% of each cohort. For PTB cases in the CTCR cohort the mean age was 33 years (range: 17–66) and males constituted 65.0%.

### Identification of an 11-Gene Signature

The mean expression of unique 145 transcriptional biomarkers (in arbitrary units) are shown in Supplementary Table 1. We identified an 11-gene signature, comprising *CASP8*, *CD3E*, *CD8A*, *CD14*, *GBP5*, *GNLY*, *NLRP2*, *NOD2*, *TAGAP*, *TLR5*, and *TNF* (Table 2A) able to distinguish PTB cases from

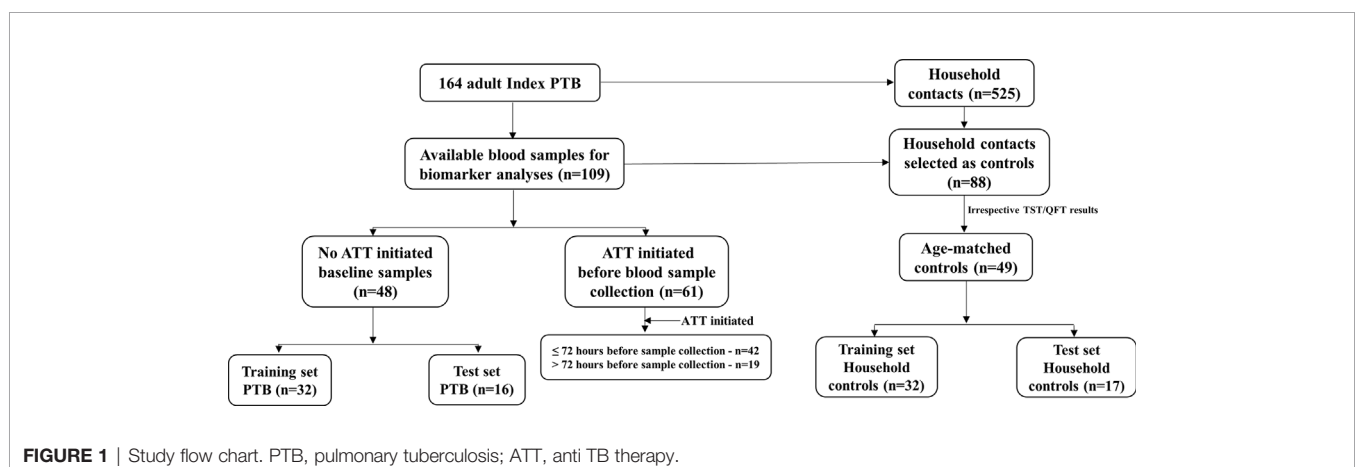


**TABLE 1 |** Baseline characteristics of discovery data sets.

Clinical Characteristics	Training set		p-value	Test set		p-value
	TB disease (n = 32)	Household controls (n = 32)		TB disease (n = 16)	Household controls (n = 17)	
Demographics						
Age in years (mean)	43.9	35.7	0.012	46.5	38.2	0.1
Range	19–70	18–80		19–69	19.5–65	
Gender (Male)	29	10	<0.001	12	4	0.003
Mycobacterial exposure						
Known BCG vaccination	12	15	0.6	8	11	0.65
Unknown	4	5		2	1	
Tuberculin skin test						
Positive (≥10 mm)	26	17	0.02	11	9	0.5
Median (mm)	16.8	14.2		15.5	15.3	
QuantIFERON Gold in tube						
Positive (≥0,35 IU/ml)	24	19	0.14	12	8	0.09
Indeterminate	1	1		0	0	
Median (IU/ml)	3.05	2.78		5.07	8.2	
Symptoms						
Cough >2 weeks	29	0	<0.001	16	0	<0.001
Fever >1 week	25	1	<0.001	13	0	<0.001
Weight loss	22	0	<0.001	11	0	<0.001
Findings						
Abnormal Chest X-ray	31	0	<0.001	16	0	<0.001
BMI < 18.5 (under weight)	23	10	0.001	10	11	0.89

The significant *p*-values are in bold.

**TABLE 2A |** Expression and regression coefficients for each biomarker of the identified 11-gene signature.

TB disease expression	Genes	Regression co-efficient
Increased	CD14	6.24E-05
	GBP5	4.92E-05
	NOD2	5.12E-04
	TLR5	4.22E-04
Decreased	CASP8	-1.41E-04
	CD3E	-2.65E-04
	CD8A	-1.83E-04
	GNLY	-2.16E-06
	NLRP2	-2.31E-04
	TAGAP	-2.59E-04
	TNF	-2.15E-03

**TABLE 2B |** Expression and regression coefficients for each biomarker of the identified 4-protein signature.

TB disease expression	Proteins	Regression co-efficient
Increased	IL7	2.07E+00
	IL15	7.87E-02
Decreased	IFN $\gamma$	-1.10E-06
	GMCSF	-7.65E-03

household controls with an AUC of 0.99 and 0.98 in the training and test sets, respectively (**Table 3A**).

Subsequently, we tested the performance of this 11-gene signature in PTB index cases  $\leq 72$  h and  $>72$  h after ATT initiation as prior work suggested that in some cases gene

expression can change significantly within first week of treatment (33). In this case, the results showed that  $\leq 72$  h after ATT-initiation, the TB cases had a similar, or marginally lower AUC (0.97, 95% CI, 0.94–1.00) compared to the  $>72$  h ATT-initiated TB cases (AUC = 0.99; 95% CI, 0.99–1.00).

## Evaluation of the Identified 11-Gene Signature in Other Data Sets

### Study 1: Singhanian A et al.; GSE107994

#### Adult Data Set

The performance of the 11-gene signature was then evaluated in the GSE107994 data set (UK cohort as validation set 1 and 2), which provided an AUC of 0.95 (95% CI: 0.91–1.00) correctly classifying 41 of 53 PTB (sensitivity 77.4%, 95% CI, 63.5–87.3), and 46 of 50 healthy *Mtb*-uninfected household contacts (specificity 92.0%, 95% CI, 79.9–97.4). Similarly, the 11-gene signature differentiated PTB from *Mtb*-infected household contacts with an AUC of 0.94 (95% CI: 0.89–0.98), with a specificity of 89.8% (95% CI, 77.0–96.2; **Table 3A** and **Figure 2**).

### Study 2: Thompson EG et al.; GSE89403

#### Adult Data Set

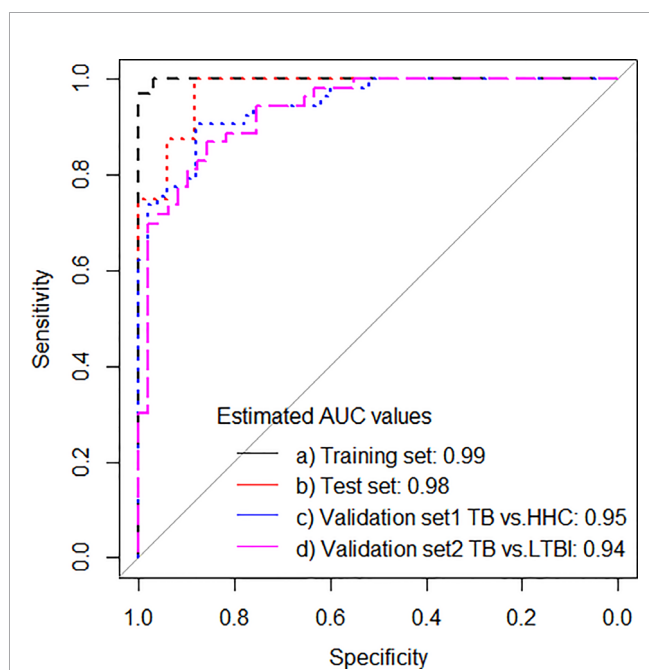
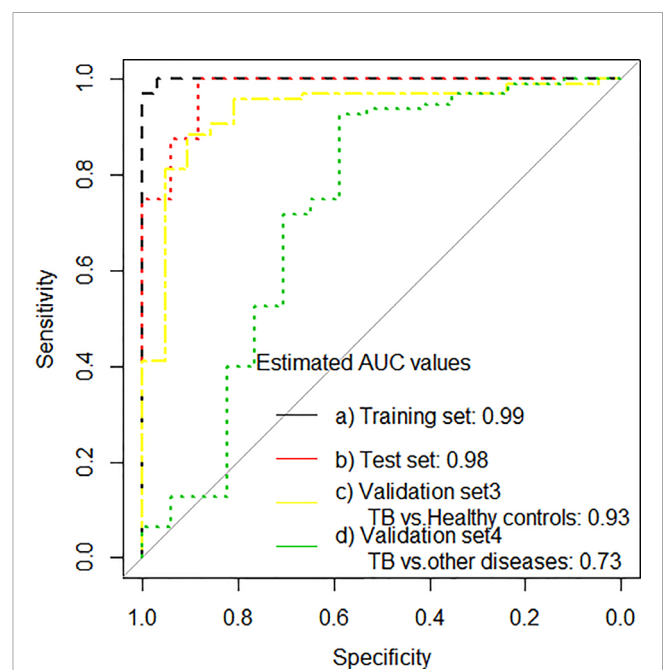
The performance of the 11-gene signature was also evaluated in the GSE89403 data set (South African CTRC as validation set 3 and 4), where it gave an AUC of 0.93 (95% CI: 0.87–0.99) correctly classifying 50 of 95 PTB cases (sensitivity 52.6%, 95% CI, 42.2–62.8), and 20 of 21 healthy controls (specificity 95.2%, 95% CI, 75.1–99.7). Interestingly, given the real-life diagnostic challenges faced in differentiating TB patients from other symptomatic patients, the 11-gene signature differentiated PTB from other lung diseases with an AUC of 0.73 (95% CI: 0.56–0.89), with a specificity of 82.4% (95% CI, 55.8–95.3; **Table 3A** and **Figure 3**).

**TABLE 3A** | Identification and performance of 11-gene signature.

Data sets	Sensitivity (95% CI)	Specificity (95% CI)	AUC (95% CI)	Accuracy in %
<b>PTB vs. Household controls</b>				
Training set	93.8 (77.8–98.9)	100.0 (86.7–100.0)	0.99 (0.99–1.00)	96.9
Test set	100 (75.9–100.0)	88.2 (62.3–97.9)	0.98 (0.94–1.00)	93.9
<b>PTB vs. Household controls</b>				
Validation set 1	77.4 (63.5–87.3)	92.0 (79.9–97.4)	0.95 (0.91–0.99)	84.5
<b>PTB vs. <i>Mtb</i> infected</b>				
Validation set 2	77.4 (63.5–87.3)	89.8 (77.0–96.2)	0.94 (0.89–0.98)	83.3
<b>PTB vs. Healthy controls</b>				
Validation set 3	52.6 (42.2–62.8)	95.2 (75.1–99.7)	0.93 (0.87–0.99)	60.3
<b>PTB vs. Other lung diseases</b>				
Validation set 4	52.6 (42.2–62.8)	82.4 (55.8–95.3)	0.73 (0.56–0.89)	57.1
<b>PTB vs. Household/asymptomatic controls</b>				
Validation set 5	36.2 (23.1–51.5)	94.4 (80.0–99.0)	0.69 (0.57–0.80)	61.4

**TABLE 3B** | Identification of 4-protein signature.

<b>PTB vs. Household controls</b>				
Training set	87.5 (70.1–95.9)	90.6 (73.8–97.5)	0.96 (0.92–1.00)	89.1
Test set	68.8 (41.5–87.9)	94.1 (69.2–99.7)	0.87 (0.75–0.99)	81.8

**FIGURE 2** | ROC curves for signature that distinguishes PTB from household controls in the training set, test set, whereas in validation set 1 (ATB vs. healthy recent contacts) and validation set 2 (ATB vs. LTBI).**FIGURE 3** | ROC curves for signature that distinguishes PTB from household controls in the training set, test set and in validation set 3 (PTB from healthy controls) and validation set 4 (PTB from other lung diseases).

### Study 3: JE GjØen et al.; Pediatric Data Set

Finally, the performance of the 11-gene signature was evaluated in a pediatric data set collected previously by our group (validation set 5), presented an AUC of 0.69 (95% 0.57–

0.80), which correctly classified 17 of 47 PTB (sensitivity 36.2%, 95% CI, 23.1–51.5), and 34 of 36 household controls (specificity 94.4%, 95% CI, 80.0–99.0; **Table 3A** and **Figure 4A**).

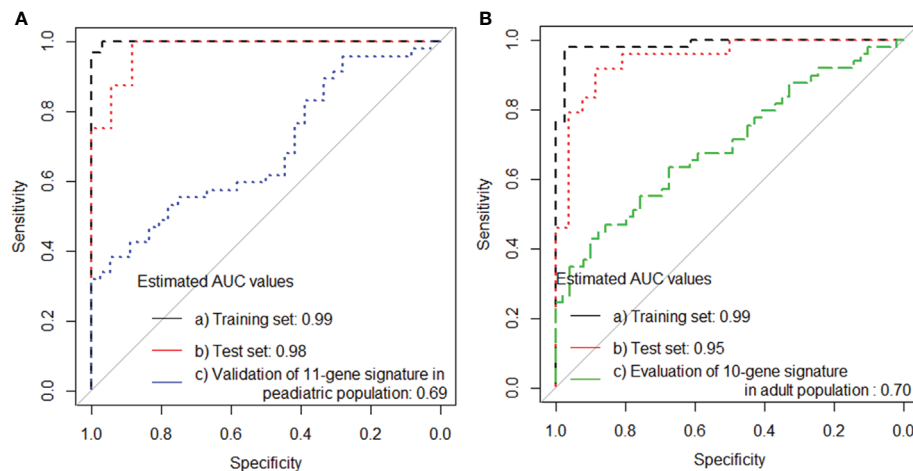


**FIGURE 4** | ROC curves for signature that distinguishes PTB from household controls **(A)** the training set, test set, validation of adult 11-gene signature in the pediatric population and **(B)** the training set, test set, validation of pediatric 10-gene signature in the adult population.

## Evaluation of Our Pediatric 10-Gene Signature in the Adult TB Population in the Present Study

As the 11-gene signature identified in adults performed poorly in children, we asked if our previously identified diagnostic 10-gene pediatric signature would perform better in our adult PTB cases, but the AUC of 0.70 (95% CI, 0.60–0.80) obtained was similar to validation set 5 (**Figure 4B**).

## Identification of Proteomic Signature

The median concentration (pg/ml) of the 18 protein biomarkers measured are shown in **Supplementary Table 2**. We applied Lasso regression analysis directly on data from the 18 protein biomarkers tested, and identified a 4-protein signature, comprising IFN $\gamma$ , GMCSF, IL7, and IL15 (**Table 2B**) that differentiated PTB from healthy household controls with an AUC of 0.96 (95% CI, 0.92–1.00) in the training set, correctly classifying 28 of 32 PTB cases (sensitivity 87.5%, 95% CI, 70.1–95.9), and 29 of 32 household controls (specificity 90.6%, 95% CI, 73.8–97.5). In the test set, the identified signature generated an AUC of 0.87 (95% CI, 0.75–0.99), correctly classifying 11 of 16 PTB cases (sensitivity 68.8%, 95% CI, 41.5–87.9), and 16 of 17 household controls (specificity 94.1%, 95% CI, 69.2–99.7; **Table 3B** and **Figure 5**).

Similarly, we tested the performance of the 4-protein signature in the ATT-initiated participants vs. household controls. PTB cases initiated on ATT  $\leq 72$  prior to sampling had a slightly higher AUC value (0.89, 95% CI, 0.81–0.97) compared to PTB cases initiated on ATT  $> 72$  h prior to sampling (AUC = 0.88; 95% CI, 0.75–0.99).

## DISCUSSION

An ideal diagnostic biomarker or multiple marker biosignature for TB could be either pathogen- or host-derived and should be

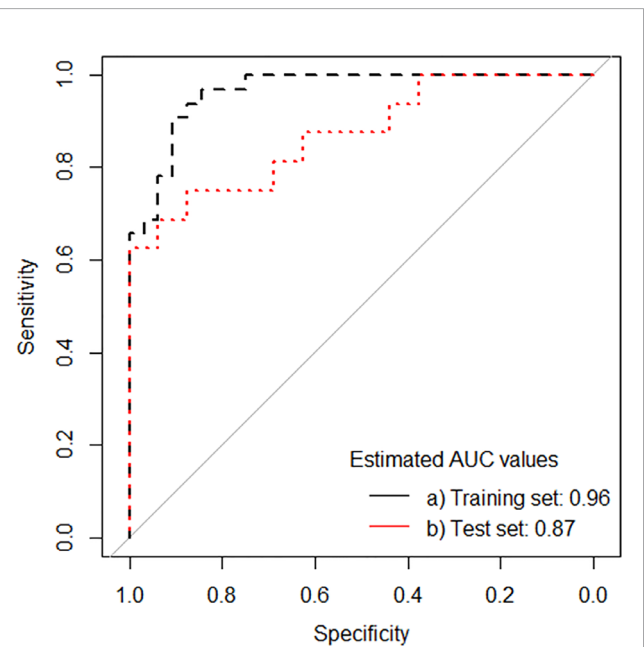


**FIGURE 5** | ROC curves for protein signature that distinguishes PTB from household controls in the training set and test set.

specific to the underlying disease process (4, 34). Several transcriptional signatures based on testing in different ethnic populations have been proposed for this purpose by numerous research groups (14, 17, 21, 24, 35, 36). However, limited overlap in genes differentially expressed between PTB and household controls have been found when comparing these signatures. A recent meta-analysis identified eight signatures with an equivalent performance that showed moderate to high correlation for diagnosing incipient TB. Overlapping constituent genes only partially accounted for correlation between signatures,

suggesting that they reflect different dimensions of the typical host response to infection with *Mtb*, and strongly supported the identification of IFN and TNF signaling pathways as statistically enriched upstream regulators of the genes across the eight signatures (37). Several attempts have been made to reduce the large number of genes identified by these studies as potentially relevant into smaller candidate signatures that could form the basis of a potential clinical diagnostic. However, there is still no agreement as to which genes to include in an optimal diagnostic signature.

In this study, we report that our 11-gene whole blood transcriptomic signature gave promising diagnostic performance across diverse populations (India, UK, South Africa) from both low-endemic and high-endemic countries, based on a capacity to distinguish PTB from household controls with an AUC  $\geq$  0.93. However, the 11-gene signature was less successful in efficiently discriminating TB disease from other lung diseases. The evaluation of this 11-gene signature in the UK-derived cohort indicated reasonable diagnostic accuracy ( $> 80.0$ , **Table 3**) for the identification of PTB. However, in the CTRC cohort, the performance of the 11-gene signature was lower. Aiming for a POC triage test to ascertain targeted referral of symptomatic subjects in the field, this shortcoming in accuracy can to some extent be overcome by clinical algorithms that include reassessment and referral of subjects with lack of improvement from assumed intercurrent infections (with or without antibiotics dependent on clinical presentation). The reasons for discrepancy between the two cohorts are likely multifactorial reflecting differences in ethnicity, sample size, mean age (in years) and lack of other lung disease controls in our cohort. The transcriptional signature identified in the present study meets WHO TTP minimal requirement for a screening test, but further evaluation will be required before clinical implementation is possible.

Warsinske HC, et al. (25) have analyzed the performance of the 3-gene TB score (*GBP5*, *DUSP3*, and *KLF2*) in three different TB cohorts. i) *South African adolescent cohort of TB progressors (age in years, 12–18)*: those who progressed from latent *Mtb* infection to PTB compared with non-progressors (26), ii) *Brazil Active Screening Study Cohort (age in years, 18–80)*: all positive sputum culture for *Mtb* compared with controls that were sputum culture-negative (25), iii) *South African CTR Cohort (age in years, 17–66)*: comprises culture-positive patients with PTB, healthy controls, and patients with other lung diseases (pneumonia or asthma). PTB patients all received standard treatment following diagnosis (27). Across all three cohorts, at a TB disease prevalence of 4%, the 3-gene TB score identified TB patients with a 90% sensitivity, a specificity of 70%, and a negative predictive value of 99.3% (25). Notably, the *GBP5* gene was also up-regulated and is included in our pediatric 10-gene and adult 11-gene signatures. Besides, *GBP5* was also reported previously by Esterhuysen MM (38) and Zak DE (26) et al. These findings suggest that *GBP5* could be a potential component in a unified biomarker signature for TB.

Previous studies have identified different transcript signatures for distinguishing TB from latent TB and other diseases in Malawian and South African pediatric (35) and adult (14)

cohorts, which could highlight the differences in pathogenesis of adult versus pediatric TB. This is consistent with the findings from the present study where the adult biosignature's poor performance in the pediatric cohort and vice versa suggests that it may be challenging to find a universally-applicable POC triage test for TB. This is despite the fact that the differentially expressed genes (whether down or up-regulated) showed the same trend in both pediatric and adult populations. Despite decades of research, significant investment, and numerous reports on new biomarker candidates, few biomarkers have been independently validated for both clinical trials and routine clinical use, and translated into new diagnostic tests (39, 40). This problem is not unique to TB; it is true for biomarker research in general that very few of the identified biomarkers have advanced to approved diagnostic tests in clinical use.

Interestingly, 3 genes do overlap (*GBP5*, *NOD2*, and *CD3E*) between the pediatric 10-gene signature and the adult 11-gene signature. Of these, two genes were up-regulated (*GBP5* and *NOD2*) and one gene down-regulated (*CD3E*) in PTB disease compared to household controls. Notably, both signatures were identified in an Indian population recruited from the same area when applying the same dcRT-MLPA method. This method is sensitive, and has high-throughput, but gives limited transcriptional data compared to RNA sequencing. This may explain some of the lack of overlap with transcript signatures identified in other studies, as not all genes of interest reported in other studies were included in our pre-defined gene panels.

In recent years, there have been more studies attempted to identify protein signature for TB disease in adults (9, 18, 41, 42) and children (43). A recent study hypothesized that a blood protein-based host response signature for active PTB could discriminate it from other TB-like disease (OTD) in adult patients with persistent cough and provide the foundation for a community-based triage test for PTB. The study identified a host blood protein signature consisting of IL-6, IL-8, IL-18, and VEGF, that discriminated active PTB from OTD with an AUC of 0.80, corresponding to a sensitivity of 80% and a specificity of 65% (41). The present study also identified a 4-protein signature (IFN $\gamma$ , GM-CSF, IL15, and IL7) in TB-ag stimulated QFT supernatants that distinguishes PTB patients from their household controls with AUCs  $\geq$  0.87, providing proof of concept for a protein-based approach.

The present study has some limitations: i) No formal sample size calculation was carried out since the maximum sample size was defined by the availability of samples for biomarker analysis, a factor exacerbated by the need to divide the samples into training and test sets. To some extent, however, this limitation was offset by the use of multiple validation cohorts, as described; ii) Lack of validation in extra-pulmonary TB cases—a population in which non-sputum based diagnostics are strongly needed; iii) Inability to cross-validate the identified proteomic signature due to the lack of comparable samples from other cohorts. Although host-response-based diagnostics are believed to be less dependent on bacterial load, an obvious advantage for TB diagnosis, it is unclear if these tools can be further optimized



to meet the WHO target for a universally applicable POC test. With the increasing number of blood-based signatures for TB diagnosis being proposed, it is crucial to pool data across cohorts' diverse in geographic, genetic, demographic and endemic characteristics in order to diminish time and costs for POC test evaluation with regard to the WHO TPP, and subsequent validation prior to translation to clinical practice.

## DATA AVAILABILITY STATEMENT

The raw data supporting the conclusions of this article will be made available by the authors, without undue reservation.

## ETHICS STATEMENT

Ethical approval for this study was obtained from the Institutional Ethical Review Board (IERB) of St. John's Medical College, Bangalore (IERB/1/527/08). The material transfer agreement between St. John's Medical College, Bangalore, and the University of Bergen, Norway was obtained from the Department of Biotechnology, Government of India (no. BT/Med.II/Adv (SS)/Misc./02/2012). Ethical approval was also obtained (ref no: 2018/1614 D) from the Regional Committee for Medical and Health Research Ethics, Western Norway. Written informed consent to participate in this study was provided by the participants' legal guardian/next of kin.

## AUTHOR CONTRIBUTIONS

DS, JG, SJ, MV, TMD, CR, and HMSG conceptualized and designed the biomarker study. SS and MV coordinated patient recruitment and follow-up. DS wrote the manuscript with contribution from MV, CR, JG, SJ, TMD, and HMSG. DS performed all laboratory experiments. DS performed the data analysis and generated Tables and Figures. CR supervised the statistical analysis, wrote the section on statistical analysis, and reviewed the manuscript. TO contributed to the study design and analysis and reviewed the manuscript. HMSG had primary responsibility for the final content of the manuscript. All authors contributed to the article and approved the submitted version.

## REFERENCES

1. WHO. *Global Tuberculosis Report 2019* (2019). Available at: [https://www.who.int/tb/publications/global\\_report/en](https://www.who.int/tb/publications/global_report/en) (Accessed Nov 3 2020).
2. WHO. *The End TB Strategy, Global strategy and targets for tuberculosis prevention, care and control after 2015* (2014). Available at: [https://www.who.int/tb/post\\_2015\\_tb\\_presentation.pdf](https://www.who.int/tb/post_2015_tb_presentation.pdf) (Accessed Nov 3 2020).
3. Kik SV, Denkinger CM, Casenghi M, Vadnais C, Pai M. Tuberculosis diagnostics: which target product profiles should be prioritised? *Eur Respir J* (2014) 44(2):537–40. doi: 10.1183/09031936.00027714
4. MacLean E, Broger T, Yerlikaya S, Fernandez-Carballo BL, Pai M, Denkinger CM. Author Correction: A systematic review of biomarkers to detect active tuberculosis. *Nat Microbiol* (2019) 4(5):899. doi: 10.1038/s41564-019-0452-3
5. WHO. *High-priority target product profiles for new tuberculosis diagnostics: report of a consensus meeting* (2014). Geneva, Switzerland. Available at:

## FUNDING

Research Council of Norway Global Health and Vaccination Research (GLOBVAC) projects: RCN 179342, 192534, and 248042, the University of Bergen (Norway); EDCTP2 program supported by the European Union; the St. John's Research Institute, Bangalore. We also acknowledge EC FP7 ADITEC (grant agreement no. 280873); EC HORIZON2020 TBVAC2020 (grant agreement no. 643381) [the text represents the authors' views and does not necessarily represent a position of the Commission who will not be liable for the use made of such information].

## ACKNOWLEDGMENTS

We thank Drs Rajini Macaden, Nelson Jesuraj, Anto Jesuraj Udaykumar, and Vandana A at St. John's Research Institute, Bangalore; Aud Eliassen at the sequencing laboratory at Haukeland University Hospital, Bergen, Norway. We thank Dr. Marielle C. Haks at the Dept. of Infectious Diseases, Leiden Medical University, Leiden, The Netherlands for providing the dcRT-MLPA probes and primers (Reverse transcription gene target specific primers, right hand and left-hand half MLPA probes, FAM labeled MLPA primers, HEX labeled MAPH primers). We thank Aeras (a non-profit organization), USA for their contributions to establishing the TB vaccine trial site at Palamaner Taluk, Chittoor district, Andhra Pradesh, India; Meso Scale Discovery (MSD), USA for the loan of the instrument and for the technical support and advice provided by Tynde Sandor (MSD) and Gail Calvert (MSD). Further, we would like to gratefully acknowledge the work of Prof. Anne O'Garra group (UK cohort biomarker study) and Prof. Daniel E. Zak group (South African CTR cohort).

## SUPPLEMENTARY MATERIAL

The Supplementary Material for this article can be found online at: <https://www.frontiersin.org/articles/10.3389/fimmu.2020.626049/full#supplementary-material>

[https://apps.who.int/iris/bitstream/handle/10665/135617/WHO\\_HTM\\_TB\\_2014.18\\_eng.pdf](https://apps.who.int/iris/bitstream/handle/10665/135617/WHO_HTM_TB_2014.18_eng.pdf) (Accessed Nov 3 2020).

6. Yerlikaya S, Broger T, MacLean E, Pai M, Denkinger CM. A tuberculosis biomarker database: the key to novel TB diagnostics. *Int J Infect Dis* (2017) 56:253–7. doi: 10.1016/j.ijid.2017.01.025
7. Drain PK, Heichman KA, Wilson D. A new point-of-care test to diagnose tuberculosis. *Lancet Infect Dis* (2019) 19(8):794–6. doi: 10.1016/S1473-3099(19)30053-2
8. Bloom CI, Graham CM, Berry MP, Rozakeas F, Redford PS, Wang Y, et al. Transcriptional blood signatures distinguish pulmonary tuberculosis, pulmonary sarcoidosis, pneumonias and lung cancers. *PLoS One* (2013) 8(8):e70630. doi: 10.1371/journal.pone.0070630
9. Chegou NN, Sutherland JS, Malherbe S, Crampin AC, Corstjens PL, Geluk A, et al. Diagnostic performance of a seven-marker serum protein biosignature for the diagnosis of active TB disease in African primary healthcare clinic

- attendees with signs and symptoms suggestive of TB. *Thorax* (2016) 71 (9):785–94. doi: 10.1136/thoraxjnl-2015-207999
10. Dhanasekaran S, Jenum S, Stavrum R, Ritz C, Faurholt-Jepsen D, Kenneth J, et al. Identification of biomarkers for Mycobacterium tuberculosis infection and disease in BCG-vaccinated young children in Southern India. *Genes Immun* (2013) 14(6):356–64. doi: 10.1038/gene.2013.26
  11. Gjoen JE, Jenum S, Sivakumaran D, Mukherjee A, Macaden R, Kabra SK, et al. Novel transcriptional signatures for sputum-independent diagnostics of tuberculosis in children. *Sci Rep* (2017) 7(1):5839. doi: 10.1038/s41598-017-05057-x
  12. Jenum S, Dhanasekaran S, Lodha R, Mukherjee A, Kumar Saini D, Singh S, et al. Approaching a diagnostic point-of-care test for pediatric tuberculosis through evaluation of immune biomarkers across the clinical disease spectrum. *Sci Rep* (2016) 6:18520. doi: 10.1038/srep18520
  13. Joosten SA, Goeman JJ, Sutherland JS, Opmeer L, de Boer KG, Jacobsen M, et al. Identification of biomarkers for tuberculosis disease using a novel dual-color RT-MLPA assay. *Genes Immun* (2012) 13(1):71–82. doi: 10.1038/gene.2011.64
  14. Kaforou M, Wright VJ, Oni T, French N, Anderson ST, Bangani N, et al. Detection of tuberculosis in HIV-infected and -uninfected African adults using whole blood RNA expression signatures: a case-control study. *PloS Med* (2013) 10(10):e1001538. doi: 10.1371/journal.pmed.1001538
  15. Lau SK, Lee KC, Curreem SO, Chow WN, To KK, Hung IF, et al. Metabolomic Profiling of Plasma from Patients with Tuberculosis by Use of Untargeted Mass Spectrometry Reveals Novel Biomarkers for Diagnosis. *J Clin Microbiol* (2015) 53(12):3750–9. doi: 10.1128/JCM.01568-15
  16. Maertzdorf J, Repsilber D, Parida SK, Stanley K, Roberts T, Black G, et al. Human gene expression profiles of susceptibility and resistance in tuberculosis. *Genes Immun* (2011) 12(1):15–22. doi: 10.1038/gene.2010.51
  17. Singhania A, Verma R, Graham CM, Lee J, Tran T, Richardson M, et al. A modular transcriptional signature identifies phenotypic heterogeneity of human tuberculosis infection. *Nat Commun* (2018) 9(1):2308. doi: 10.1038/s41467-018-04579-w
  18. De Groote MA, Sterling DG, Hraha T, Russell TM, Green LS, Wall K, et al. Discovery and Validation of a Six-Marker Serum Protein Signature for the Diagnosis of Active Pulmonary Tuberculosis. *J Clin Microbiol* (2017) 55 (10):3057–71. doi: 10.1128/JCM.00467-17
  19. Cho Y, Park Y, Sim B, Kim J, Lee H, Cho SN, et al. Identification of serum biomarkers for active pulmonary tuberculosis using a targeted metabolomics approach. *Sci Rep* (2020) 10(1):3825. doi: 10.1038/s41598-020-60669-0
  20. Manyelo CM, Solomons RS, Snyders CI, Mutavhatsindi H, Manngo PM, Stanley K, et al. Potential of Host Serum Protein Biomarkers in the Diagnosis of Tuberculous Meningitis in Children. *Front Pediatr* (2019) 7:376. doi: 10.3389/fped.2019.00376
  21. Berry MP, Graham CM, McNab FW, Xu Z, Bloch SA, Oni T, et al. An interferon-inducible neutrophil-driven blood transcriptional signature in human tuberculosis. *Nature* (2010) 466(7309):973–7. doi: 10.1038/nature09247
  22. Joosten SA, Fletcher HA, Ottenhoff TH. A helicopter perspective on TB biomarkers: pathway and process based analysis of gene expression data provides new insight into TB pathogenesis. *PloS One* (2013) 8(9):e73230. doi: 10.1371/journal.pone.0073230
  23. Ottenhoff TH, Dass RH, Yang N, Zhang MM, Wong HE, Sahiratmadja E, et al. Genome-wide expression profiling identifies type 1 interferon response pathways in active tuberculosis. *PloS One* (2012) 7(9):e45839. doi: 10.1371/journal.pone.0045839
  24. Sweeney TE, Braviak L, Tato CM, Khatri P. Genome-wide expression for diagnosis of pulmonary tuberculosis: a multicohort analysis. *Lancet Respir Med* (2016) 4(3):213–24. doi: 10.1016/S2213-2600(16)00048-5
  25. Warsinske HC, Rao AM, Moreira FMF, Santos PCP, Liu AB, Scott M, et al. Assessment of Validity of a Blood-Based 3-Gene Signature Score for Progression and Diagnosis of Tuberculosis, Disease Severity, and Treatment Response. *JAMA Netw Open* (2018) 1(6):e183779. doi: 10.1001/jamanetworkopen.2018.3779
  26. Zak DE, Penn-Nicholson A, Scriba TJ, Thompson E, Suliman S, Amon LM, et al. A blood RNA signature for tuberculosis disease risk: a prospective cohort study. *Lancet* (2016) 387(10035):2312–22. doi: 10.1016/S0140-6736(15)01316-1
  27. Thompson EG, Du Y, Malherbe ST, Shankar S, Braun J, Valvo J, et al. Host blood RNA signatures predict the outcome of tuberculosis treatment. *Tuberculosis (Edinb)* (2017) 107:48–58. doi: 10.1016/j.tube.2017.08.004
  28. Turner CT, Gupta RK, Tsaliki E, Roe JK, Mondal P, Nyawo GR, et al. Blood transcriptional biomarkers for active pulmonary tuberculosis in a high-burden setting: a prospective, observational, diagnostic accuracy study. *Lancet Respir Med* (2020) 8(4):407–19. doi: 10.1016/S2213-2600(19)30469-2
  29. Fletcher HA, Filali-Mouhim A, Nemes E, Hawkrige A, Keyser A, Njikan S, et al. Human newborn bacille Calmette-Guerin vaccination and risk of tuberculosis disease: a case-control study. *BMC Med* (2016) 14:76. doi: 10.1186/s12916-016-0617-3
  30. Sivakumaran D, Jenum S, Vaz M, Selvam S, Ottenhoff THM, Haks MC, et al. Combining host-derived biomarkers with patient characteristics improves signature performance in predicting tuberculosis treatment outcomes. *Commun Biol* (2020) 3(1):359. doi: 10.1038/s42003-020-1087-x
  31. Haks MC, Goeman JJ, Magis-Escarra C, Ottenhoff TH. Focused human gene expression profiling using dual-color reverse transcriptase multiplex ligation-dependent probe amplification. *Vaccine* (2015) 33(40):5282–8. doi: 10.1016/j.vaccine.2015.04.054
  32. R Core Team. *A Language and Environment for Statistical Computing (R Foundation for Statistical Computing)* (2019). Vienna, Austria. Available at: <https://www.r-project.org> (Accessed Nov 3, 2020).
  33. Cliff JM, Lee JS, Constantinou N, Cho JE, Clark TG, Ronacher K, et al. Distinct phases of blood gene expression pattern through tuberculosis treatment reflect modulation of the humoral immune response. *J Infect Dis* (2013) 207(1):18–29. doi: 10.1093/infdis/jis499
  34. Wallis RS, Kim P, Cole S, Hanna D, Andrade BB, Maeurer M, et al. Tuberculosis biomarkers discovery: developments, needs, and challenges. *Lancet Infect Dis* (2013) 13(4):362–72. doi: 10.1016/S1473-3099(13)70034-3
  35. Anderson ST, Kaforou M, Brent AJ, Wright VJ, Banwell CM, Chagaluka G, et al. Diagnosis of childhood tuberculosis and host RNA expression in Africa. *N Engl J Med* (2014) 370(18):1712–23. doi: 10.1056/NEJMoa1303657
  36. Singhania A, Wilkinson RJ, Rodrigue M, Haldar P, O'Garra A. The value of transcriptomics in advancing knowledge of the immune response and diagnosis in tuberculosis. *Nat Immunol* (2018) 19(11):1159–68. doi: 10.1038/s41590-018-0225-9
  37. Gupta RK, Turner CT, Venturini C, Esmail H, Rangaka MX, Copas A, et al. Concise whole blood transcriptional signatures for incipient tuberculosis: a systematic review and patient-level pooled meta-analysis. *Lancet Respir Med* (2020) 8(4):395–406. doi: 10.1016/S2213-2600(19)30282-6
  38. Esterhuysen MM, Weiner J3rd, Caron E, Loxton AG, Iannaccone M, Wagman C, et al. Epigenetics and Proteomics Join Transcriptomics in the Quest for Tuberculosis Biomarkers. *mBio* (2015) 6(5):e01187–15. doi: 10.1128/mBio.01187-15
  39. Goletti D, Petruccioli E, Joosten SA, Ottenhoff TH. Tuberculosis Biomarkers: From Diagnosis to Protection. *Infect Dis Rep* (2016) 8(2):6568. doi: 10.4081/idr.2016.6568
  40. Gardiner JL, Karp CL. Transformative tools for tackling tuberculosis. *J Exp Med* (2015) 212(11):1759–69. doi: 10.1084/jem.20151468
  41. Ahmad R, Xie L, Pyle M, Suarez MF, Broger T, Steinberg D, et al. A rapid triage test for active pulmonary tuberculosis in adult patients with persistent cough. *Sci Transl Med* (2019) 11(516):1–14. doi: 10.1126/scitranslmed.aaw8287
  42. Yang Q, Chen Q, Zhang M, Cai Y, Yang F, Zhang J, et al. Identification of eight-protein biosignature for diagnosis of tuberculosis. *Thorax* (2020) 75 (7):576–83. doi: 10.1136/thoraxjnl-2018-213021
  43. Togun T, Hoggart CJ, Agbla SC, Gomez MP, Egere U, Sillah AK, et al. A three-marker protein biosignature distinguishes tuberculosis from other respiratory diseases in Gambian children. *EBioMedicine* (2020) 58:102909. doi: 10.1016/j.ebiom.2020.102909

**Conflict of Interest:** TMD is an employee of and holds shares in the GSK group of companies but participated in the current work as an independent investigator.

The remaining authors declare that the research was conducted in the absence of any commercial or financial relationships that could be construed as a potential conflict of interest.

Copyright © 2021 Sivakumaran, Ritz, Gjoen, Vaz, Selvam, Ottenhoff, Doherty, Jenum and Grewal. This is an open-access article distributed under the terms of the Creative Commons Attribution License (CC BY). The use, distribution or reproduction in other forums is permitted, provided the original author(s) and the copyright owner(s) are credited and that the original publication in this journal is cited, in accordance with accepted academic practice. No use, distribution or reproduction is permitted which does not comply with these terms.



# B-Cells and Antibodies as Contributors to Effector Immune Responses in Tuberculosis

Willemijn F. Rijnink, Tom H.M. Ottenhoff and Simone A. Joosten\*

Department of Infectious Diseases, Leiden University Medical Center, Leiden, Netherlands

## OPEN ACCESS

### Edited by:

Christof Geldmacher,  
University of Munich, Germany

### Reviewed by:

Stephen Cose,  
University of London, United Kingdom  
Sunil Joshi,  
University of Miami, United States

### \*Correspondence:

Simone A. Joosten  
s.a.joosten@LUMC.nl

### Specialty section:

This article was submitted to  
Microbial Immunology,  
a section of the journal  
Frontiers in Immunology

**Received:** 10 December 2020

**Accepted:** 29 January 2021

**Published:** 18 February 2021

### Citation:

Rijnink WF, Ottenhoff THM and  
Joosten SA (2021) B-Cells and  
Antibodies as Contributors to Effector  
Immune Responses in Tuberculosis.  
Front. Immunol. 12:640168.  
doi: 10.3389/fimmu.2021.640168

Tuberculosis (TB), caused by *Mycobacterium tuberculosis* (Mtb), is still a major threat to mankind, urgently requiring improved vaccination and therapeutic strategies to reduce TB-disease burden. Most present vaccination strategies mainly aim to induce cell-mediated immunity (CMI), yet a series of independent studies has shown that B-cells and antibodies (Abs) may contribute significantly to reduce the mycobacterial burden. Although early studies using B-cell knock out animals did not support a major role for B-cells, more recent studies have provided new evidence that B-cells and Abs can contribute significantly to host defense against Mtb. B-cells and Abs exist in many different functional subsets, each equipped with unique functional properties. In this review, we will summarize current evidence on the contribution of B-cells and Abs to immunity toward Mtb, their potential utility as biomarkers, and their functional contribution to Mtb control.

**Keywords:** *Mycobacterium tuberculosis*, tuberculosis, humoral immunity, B-cells, antibodies, biomarker

## INTRODUCTION

Tuberculosis (TB), caused by *Mycobacterium tuberculosis* (Mtb), remains a significant health threat to mankind and is undoubtedly the most successful disease caused by a single infectious agent ever (1). TB killed ~1.5 million individuals in 2018 alone, and a total of around 1,000,000,000 people over the last 200 years (2, 3). In fact, approximately one-fourth to one-third of the world's population is infected with Mtb, giving rise to an estimated 10 million new cases annually (2). Mtb-infection leads to a spectrum of infectious states ranging from various levels of asymptomatic states, collectively referred to as latent tuberculosis infection (LTBI) and to a spectrum of active tuberculosis diseases (ATB), ranging from local to pulmonary to disseminating ATB (4, 5). About 5–10% of individuals with LTBI will progress to ATB during their lifetime; the remainder is able to contain the infection lifelong unless immunosuppressed, such as by coinfecting viruses [e.g., human immunodeficiency virus (HIV)] or iatrogenically (1, 6–8). These data highlight the high level of adaptation of Mtb to infect, and survive in the human host (7).

TB control is hampered by the lack of an effective vaccine: the efficacy of the only available vaccine, *Mycobacterium bovis* Bacillus Calmette-Guérin (BCG), ranges from 0 to 80% (9). A much better understanding of the (protective) immune response to Mtb, the mechanisms by which Mtb manipulates the host response and the identification of robust correlates of protection are all urgently needed to combat this deadly infection.

Large scale, unbiased approaches using advanced -omics technologies analyzing blood samples have been performed over the last decade and identified biomarkers associated with the different disease stages of TB, i.e., which could differentiate LTBI from ATB. In addition, biomarkers for the

risk of progression from LTBI toward ATB were uncovered in several large prospective studies (8, 10–15). A frequently appearing transcriptional biomarker which was often a component of signatures able to distinguish ATB from LTBI was *FCGR1A*, a gene encoding the activating high-affinity crystallizable fragment (Fc) gamma receptor I (FcγRI; CD64) (15–22). Fc-Receptors (FcRs) potentially can engage antibodies (Abs) that have opsonized Mtb, and thereby impact mycobacterial survival. Furthermore, in many transcriptomic studies also components of the complement pathway were identified, predominantly transcript-markers from the classical pathway, that were differentially expressed in the blood of ATB compared to LTBI: in particular Complement component 1qB (*C1QB*) and *C1QC* were higher expressed, and in support of this, serum C1q-protein was found to be a diagnostic biomarker for ATB (18, 20, 23–25). More recently, it was reported that the combined measurement of serum C1q and whole blood type-1 interferon (IFN) signature might help improving the diagnosis of ATB (26). Together, these studies hint to the potential influence of humoral immune components in TB, including innate and possibly also adaptive humoral immunity. Indeed, in support of this initial data, B-cells and Abs were later proposed to correlate with protective immunity against TB (4, 6, 27–31). This review will explore the role and possible utility of B-cells and Abs as biomarkers of immune protection against Mtb.

As a facultative intracellular bacterium that resides primarily in lung alveolar macrophages, the vast majority of TB research efforts has traditionally focused on understanding cell-mediated immunity (CMI) [reviewed in Cooper (32), Lin and Flynn (33), Ottenhoff (34), North and Jung (35)]. By contrast, the role of B-cell- and antibody-mediated immunity (AMI) in TB has remained understudied for decades. This was due to the historical dogma, established in the early twentieth century, that postulated that host defense against intracellular pathogens is mediated by

CMI, whereas the response to extracellular pathogens is mediated by Abs produced from B-cells (4, 7, 36–39). B-cells, however, do not only produce Abs, they are also competent antigen (Ag)-presenting cells (APCs), and produce a wide range of cytokines. All of these B-cell properties can influence the function of a broad range of other immune cells, including T-cells, macrophages, neutrophils and dendritic cells in their response to pathogens (7, 37). AMI combats extracellular pathogens via various mechanisms, such as viral and toxin neutralization (e.g., neutralizing extracellular microorganisms or their products), opsonization (e.g., facilitating bacterial phagocytic uptake by, and recruitment of neutrophils) and complement activation, which can further enhance opsonization and bacterial lysis, but also phagocytosis through complement receptors (40, 41). The effector mechanisms used by specific Abs to remove pathogens is dependent on a variety of features, which include Ag specificity, Ab isotype and subclass, as well as post-translational modifications, like glycosylation (42) (Figure 1).

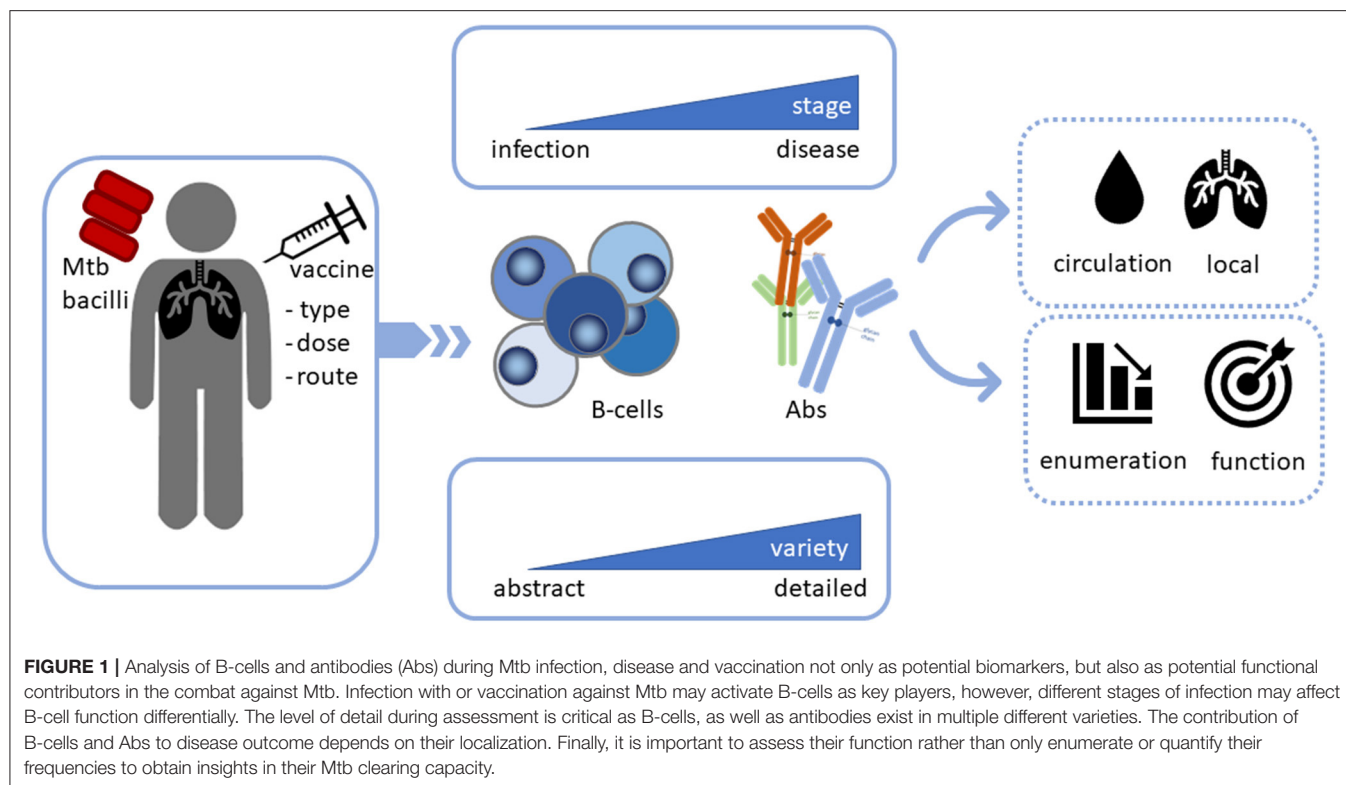
As Mtb is an intracellular pathogen, Mtb-specific Abs were classically considered to be unable to gain access to phagosomal Mtb bacilli (43). However, several experimental studies in recent decades have shown that B-cells/AMI can contribute to protective immunity, or at least considerably influence host defense, against pathogens with a preferred intracellular niche, such as *Chlamydia trachomatis* (44, 45), *Salmonellae* (46–48), *Ehrlichia chaffeensis* (49), *Leishmania major* (50), *Leishmania amazonensis* (51), *Leishmania panamensis* (52), *Cryptococcus neoformans* (53, 54), *Coxiella burnetii* (55), *Trypanosoma cruzi* (56), *Francisella tularensis* (57), and *Plasmodium chabaudi* (58). Similarly, proof that B-cells and certain Abs can modulate TB disease is gradually accumulating as discussed in this review and previously elsewhere (7, 29–31, 37, 59–64). The evidence for a contribution of B-cells and antibodies to Mtb clearances varies greatly, which variability may be partly the result of genetic or environmental differences in study populations, which are in particular present in the diverse populations studied in the context of TB, which supports the need of more global assessment of effector responses, including humoral responses. Moreover, although studies in experimental animals have been highly informative, the immune system, including the B-cell compartment, differs amongst species and cannot be completely extrapolated to human infectious diseases. Therefore, a more comprehensive unbiased approach to investigate the functional involvement of cellular immunity, B-cells and humoral immunity, their relative importance, as well as their interconnections in protective immunity against Mtb could enhance our understanding of host defense in Mtb and ultimately might translate into the development of more efficacious therapeutic and preventive tools.

## THE ROLE OF B-CELLS IN HOST-DEFENSE AGAINST MTB

The contribution of B-cells and Abs to immunity against Mtb has been investigated for over 100 years, but results have been inconsistent and sometimes even contradictory (64, 65). A

**Abbreviations:** Ab, antibodies; Acr, α-crystallin; ADCC, antibody-dependent cell-mediated cytotoxicity; ADCP, antibody-dependent cellular phagocytosis; Ag, antigen; AM, arabinomannan; AMI, antibody-mediated immunity; AP, activator protein; APC, antigen-presenting cell; ATB, active tuberculosis disease; BAL, bronchoalveolar lavage; BCF, B-cell follicle; BCG, Bacillus Calmette-Guérin; Breg, regulatory B-cell; C1q, Complement component 1q; Ca<sup>2+</sup>, calcium; CFP-10, 10 kDa culture filtrate protein; CMI, cell-mediated immunity; CVID, common variable immunodeficiency; CXCL, CXC chemokine ligand; CXCR, CXC chemokine receptor; ESAT-6, early secreted Ag of 6 kDa; Fab, Ag-binding fragment; FASL, Fas ligand; Fc, crystallizable fragment; FcγRI, Fc gamma receptor I; FcR, Fc receptor; GC, germinal center; HBHA, heparin-binding hemagglutinin adhesin; HIV, human immunodeficiency virus; iBAL, inducible bronchus-associated lymphoid tissue; IFN, interferon; Ig, immunoglobulin; IGRA, IFN-γ release assay; iNOS, inducible nitric oxide synthase; IRF, interferon regulatory factor; IVIg, intravenous immunoglobulin; LAM, lipoarabinomannan; LAMP-1, lysosomal-associated membrane protein 1; LTBI, latent tuberculosis infection; mAb, monoclonal antibody; ManLAM, mannose-capped lipoarabinomannan; Mtb, *Mycobacterium tuberculosis*; MVA85A, Ankara virus modified to express Ag85A; NF-κB, nuclear factor kappa-light-chain-enhancer of activated B-cells; NHP, non-human primate; NK, natural killer; pIgR, polymeric immunoglobulin receptor; PIM, phosphatidyl-myo-inositol mannoside; PPD, protein purified derivative; PS, polysaccharide; QFN, QuantiFERON-TB Gold In-Tube test; QFT, QuantiFERON-TB Gold; SCID, severe combined immunodeficient; sIgA, secretory IgA; TB, tuberculosis; Th, T helper; TLR, Toll-like receptor; TNF, tumor necrosis factor; TRIM21, FcR tripartite motif-containing protein 21; TST, tuberculin skin test; WT, wild type; XLA, X-linked agammaglobulinemia.





plethora of human and animal studies has suggested though that B-cells and Abs contribute to resolution of TB (Figure 1).

In the past two decades, several studies have reanalyzed the role -protective, neutral or detrimental- of B-cells in TB, using various experimental murine TB-models, including B-cell deficient mice. Some of the results were not in full agreement or even contradictory, with reports showing reduced immunity, delayed dissemination, or even marginal or no detectable effects following genetic deletion (66–73). Both short-term (72) and long-term (70, 71) aerosol infections using virulent Mtb-strain H37Rv (72), Erdman strains (70) or clinical isolate CDC 1551 (71) [with inocula of ~50–100 (70, 71) or 100–1,000 (72) viable bacilli per lung], showed no detectable differences in lung bacterial loads in wild type (WT) vs. B-cell deficient mice. Conversely, studies administering a higher intravenous (73) or intrabronchial (69) dose of Mtb,  $10^6$  Mtb H37Rv (73) or four to eight colony forming units of Mtb Erdman (69), respectively, reported an augmented susceptibility to infection, as measured by tissue bacterial burden, in B-cell deficient compared to control mice. Adoptive transfer of B-cells reversed the increased lung immunopathology in B-cell knock-out mice, demonstrating a contribution of B-cells to the control of Mtb (69). In concordance, a high-dose aerosol infection murine TB-model reported exuberated pulmonary pathology with enhanced pulmonal neutrophil recruitment in B-cell deficient mice (67). This study additionally showed that subcutaneous BCG-vaccination elicited an impaired Th1 response in the absence of B-cells. In another vaccination study, adoptive B-cell transfer did not augment anti-TB protection in B-cell knockout mice, but protection required the presence of T-cells (66). However,

here the human adenovirus-based vaccine was a powerful T-cell activator that might have acted independently of B-cells.

Extending beyond mouse models, in a CD20<sup>+</sup> B-cell depleted acute Mtb-infected cynomolgus macaque model, analysis of individual lesions revealed that some, but not all, lesions contained an increased mycobacterial burden and lower levels of inflammation compared to non-depleted animals (74). Thus, despite studies reporting a detrimental or neutral effect of B-cells on anti-TB immunity, there is also increasing evidence for B-cells in promoting optimal protection against Mtb. The contradictory data from studies in B-cell deficient mice may have resulted from differences in the dose and route of delivery, the phase of infection, the mycobacterial strain and the mice strains used (67–72) as was also previously discussed (7).

## THE ROLE OF Abs IN THE HOST DEFENSE AGAINST MTB

### Passive Transfer Studies

A major breakthrough in the immunology and treatment of infectious diseases was the discovery of serum therapy in the mid-1890s (65, 75). A comprehensive account of these early and later studies (from 1880 until mid-1990s) and their limitations was reviewed by Glatman-Freedman and Casadevall (65). Three passive polyclonal immunoglobulin (Ig)G or serum transfer studies provided support for the protective nature of immune serum against Mtb (76–78). Serum therapy with polyclonal Abs against Mtb effectively protected against disease reactivation in Mtb-infected severe combined immunodeficient (SCID) mice after partial treatment with anti-tuberculous drugs (77). In



addition, human high-dose intravenous immunoglobulin (IVIg) administration to Mtb-infected C57BL/6, but not nude mice, induced a substantial decline in mycobacterial numbers in the lungs and spleen (78). Sera from some LTBI or highly exposed, but uninfected, healthcare-workers contained protective Abs as shown by serum transfer into mice challenged with aerosol Mtb (76). Thus, in spite of the mixed results obtained in the early passive transfer studies, newer reports underscore the protective capacity of some, but not all, sera and Abs against Mtb. These results call for detailed characterization of the precise properties of polyclonal Ab responses capable of reducing mycobacterial burden.

## Monoclonal Antibody Therapeutic Studies

The development of the hybridoma technology in 1975 provided a tool to overcome the limitations of passive serum transfer with polyclonal Abs, through the production of monoclonal antibodies (mAbs). At the end of the 1990s, one of the first studies that generated mAbs against Mtb evaluated the capacity of three mAbs to influence the course of infection in mice that mainly displayed progressive TB disease (79). Only one mouse mAb, an IgG3 mAb (clone 9d8) specific for the mycobacterial capsular polysaccharide arabinomannan (AM), was able to prolong survival after Mtb challenge via improved tuberculous granulomatous containment of the pathogen (80). Since this pioneering study, several independent studies exploiting mAbs, including different isotypes, IgA (81–88), IgG1 (89), IgG2b (90), and IgG3 (91), against diverse mycobacterial Ags, such as  $\alpha$ -crystallin (Acr) (81, 83–88), MPB83 (90), lipoarabinomannan (LAM) (89), and heparin-binding hemagglutinin adhesin (HBHA) (91), have additionally reported protective potential. Efficacy was evaluated by prolonged survival time (89, 90), reduced dissemination (91), diminished tissue pathology (83, 85, 87, 90) and decreased mycobacterial burden as assessed through colony-forming units (82–89). The antibody-isotype is critical for effector function as switching the constant region of the IgA monoclonal 2E9 to Acr abrogated the protective efficacy (81). Interestingly, adoptive transfer of IgA combined with IFN- $\gamma$  had a strong effect on the bacterial load in a multi-drug resistant Mtb model in mice. Further passive transfer studies of mAbs preferably side-by-side, and including a BCG-immunized control group for referencing, are required to compare and validate the effects of Ab-mediated protection against the tubercle bacillus. Moreover, the development of human or humanized mAbs toward key Mtb epitopes might further define protective humoral responses with significant preventive and/or therapeutic potential.

## Human Observational Studies

In addition to passive transfer and mAb therapeutic studies, insights were also obtained from human observational studies. A meta-analytic study in China showed that patients with X-linked agammaglobulinemia (XLA), a deficiency that results in the absence of B-cells and serum Igs, did not have an elevated risk to developing ATB (92). Likewise, patients with common variable immunodeficiency (CVID) did not have increased susceptibility to TB (93). However, these observations could be confounded

by IVIg therapy given to most patients (92, 93). Moreover, an argument often used to argue against a significant role of Abs in the control of Mtb is that humans treated with Rituximab, a B-cell depleting anti-CD20 mAb, did not have an increased risk of reactivating TB (94, 95). Counter arguments, however, include that Rituximab has a limited depleting effect on CD20-negative Ab secreting plasma cells and is also not able to modify pre-existing Ab levels, thus not excluding that the absence of increased susceptibility seen in these patients might be the result of remaining Abs (94, 95). Moreover, Rituximab is mostly used in developed countries where TB-incidence and thus the risk of acquiring Mtb-infection is very low. In addition, patients about to start this treatment are routinely screened for LTBI and will first receive preventive antibiotic treatment before initiating anti-CD20 therapy. Hence, the argumentation that Rituximab does not induce an elevated risk on acquiring TB is not convincing.

While the first two studies described above (92, 93) provide an observational analysis in populations characterized by the absence of Abs, other studies have investigated the potential protective roles for Abs in Mtb containment more directly. Costello et al. reported that children from the United Kingdom and Southeast Asia with disseminated ATB disease had lower LAM-specific IgG serum-titers in comparison to individuals with localized ATB lesions (96). In agreement, the decrease in LAM IgG-titers from placentally transferred maternal IgGs until increased production of infant IgGs correlated with the peak incidence of disseminated ATB (96–98). Similarly, the absence of Abs binding to the mycobacterial 38 kDa Ag correlated with disseminated TB in children and TB-meningitis in adults (99). In addition, other serological studies have also found lower Ab serum-titers in both children and adults with extrapulmonary, active and/or disseminated TB (100–105). These human observational findings implicate that some Abs specific for particular Ags could contribute to Mtb control although causality cannot be established.

## THE MECHANISTIC ROLE OF B-CELLS IN TB

Intriguingly, B-cells and Abs are not only detected in the circulation, but are also hallmarks of TB-associated granulomas, the highly organized structures formed in the lung to contain the bacilli. In particular, B-cells in the tuberculous lung have the ability to form aggregates that display features of germinal centers (GCs), bona fide organizational marks of secondary lymphoid tissues.

## B-Cell Organization in Ectopic Germinal Center-Like Structures in Tuberculous Granuloma in the Lung

### Structural Organization of Granulomas in Tuberculous Lungs

B-cells are components of the granulomatous lesions in the lungs of Mtb-infected mice (69, 106–111), non-human primates (NHPs) (112), and ATB patients (106, 110, 113, 114). A classical TB-granuloma contains a central region, which usually

comprises Mtb-infected macrophages and can be infiltrated with neutrophils; can develop into necrotic with caseous cellular debris, or alternatively form mineralized lesions (7). Surrounding this necrotic center is a layer of foamy and epithelioid macrophages interspersed with Langhans giant-cells, which in turn is surrounded by an outer layer of lymphocytes scattered with macrophages (115, 116). At the periphery, B-cells form highly organized structures resembling B-cell follicles of secondary lymphoid organs, which are called tertiary lymphoid organs, ectopic lymphoid follicles or, if formed in the lung, inducible bronchus-associated lymphoid tissue (iBALT) (61, 117). These lesional B-cell aggregates are the predominant site of immune proliferation in the lungs of pulmonary ATB patients (114). Furthermore, immunohistochemical and flow cytometric characterization demonstrated the presence of peanut agglutinin and GL7 (two GC markers) expressing B-cells, CD68<sup>+</sup> macrophages, central CD21<sup>+</sup> follicular dendritic cells, CXCR5 (CXC chemokine receptor 5)<sup>+</sup> inducible co-stimulator<sup>+</sup> CD3<sup>+</sup> T-cells (e.g., classical T follicular helper cell) and tissue expression of CXCL13 (CXC-chemokine-ligand-13) in these TB-ectopic aggregates (69, 106). Together, this indicates that B-cell follicles (BCFs) in the proximity of TB-granulomas are ectopic GCs at the cellular, molecular and structural level (117, 118) and are therefore, presumably, the product of lymphoid neogenesis, a highly complex process that occurs during chronic inflammation where GC-like structures are formed ectopically in non-lymphoid tissues [reviewed in Pitzalis et al. (118), Aloisi and Pujol-Borrell (119)].

### Role of Ectopic B-Cell Follicles in Granulomas During Mtb-Infection

The impact of ectopic BCFs on the course of Mtb-infection is unclear (115, 117). Kondratieva et al. reported that an abolished lung granulomatous architecture had no effect on severity of Mtb-infection in mice (120). Likewise, Slight et al. claimed that BCF-formation does not control tubercle bacillary growth, but that formation of these follicles is merely a result of correct CXCR5<sup>+</sup>CD4<sup>+</sup> T-cell localization within the lung-parenchyma (106). On the other hand, Maglione et al. have shown that B-cell deficient mice, lacking BCFs in the lungs, have abnormal granulomatous responses correlating with augmented pulmonary pathology and suboptimal bacterial control (69). Moreover, during Mtb-infection CXCR5<sup>+</sup>CD4<sup>+</sup> T-cells accumulated within BCFs and locally produced proinflammatory cytokines required for effective macrophage activation and optimal bacterial control (106). Yet, in disordered BCFs associated with irregular CXCR5<sup>+</sup>CD4<sup>+</sup> T-cell localization there was no protection against Mtb indicating a protective rather than deleterious role of organized BCFs (106, 110). In agreement, lung BCF formation in ATB-patients correlated with containment of lung Mtb-infection (121). In a murine TB-model, the presence of ectopic B-cell aggregates was associated with granuloma formation and prevention of Mtb dissemination (108). Mtb and host-specific triggers that engender protective vs. pathological outcomes for BCFs are just starting to be elucidated, but probably include Ag type, type and duration of the response induced, as well

as the type of Ig-subclasses involved (117, 122). Likely Mtb factors are directly guiding the organization of the granulomas and their associated BCFs (115). Collectively, this suggests a potentially protective role for ectopic pulmonary B-cell follicles during Mtb-infection.

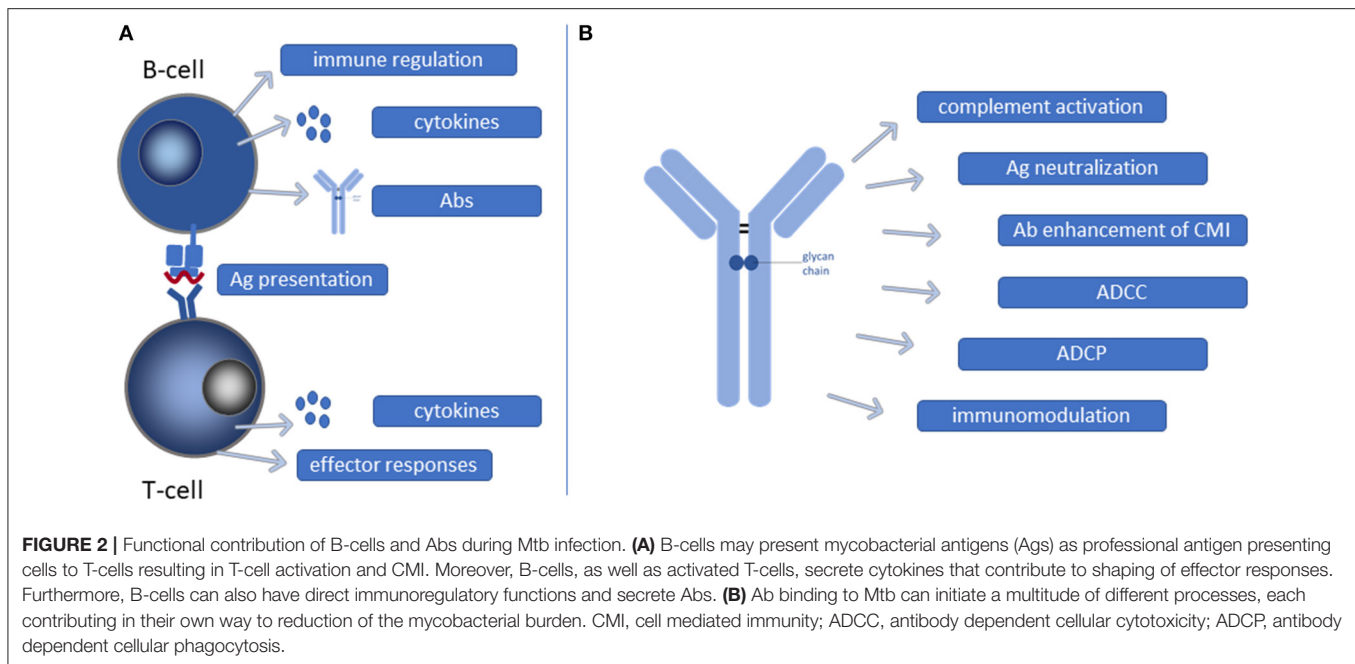
### B-Cell Phenotypes and Frequencies During Mtb-Infection

The functional role of B-cells has mostly been investigated by assessing total B-cells, however, B-cells exist in multiple flavors, each with unique properties and contributions to the host immune response. Detailed assessment of these different roles may provide an additional level of depth in the understanding of B-cell function during TB (**Figure 2A**).

Enumeration of B-cells during clinical TB has yielded contradictory results (116, 123–127). Significantly decreased B-cell frequencies were detected in the peripheral blood of ATB (116, 123–125) or LTBI (124) individuals compared to healthy controls. Others reported unaltered (124, 127), or even increased (126) B-cell frequencies in the blood of ATB. These conflicting data are likely the result from differences between study designs and groups of patients enrolled, varying by age, gender, ethnicity, form and severity of TB disease (61).

### B-Cell Subsets During Mtb-Infection

Only few studies have assessed B-cell subset frequencies and relative changes during Mtb-infection (60, 116, 128–133). Patients with ATB and LTBI had, in comparison to healthy controls, elevated circulating populations of atypical (CD21<sup>−</sup>CD27<sup>−</sup> or IgD<sup>−</sup>CD27<sup>−</sup>) and activated (IgD<sup>−</sup>CD27<sup>+</sup>) B-cells, whilst the population of naïve (IgD<sup>+</sup>CD27<sup>−</sup>) B-cells was reduced in both patient groups (116). Atypical B-cells were not only increased in frequency, but were also functionally impaired with reduced proliferation, cytokine and Ab production. Upon successful antibiotic treatment, B-cell numbers and function were restored (116, 134). These frequency differences were confirmed in another study involving patients with ATB, other lung diseases, and following ATB-treatment (129). The circulating proportion of non-class switched marginal zone (CD19<sup>+</sup>IgM<sup>+</sup>CD27<sup>+</sup>CD23<sup>−</sup>) and class-switched mature (CD19<sup>+</sup>IgM<sup>−</sup>) B-cells was significantly lower in ATB-patients compared to other lung diseases, suggesting that Mtb-infection suppresses and/or exhausts B-cell effector functions, comparable to what has been observed in HIV-positive people (135). In contrast, memory B-cells (CD19<sup>+</sup>IgM<sup>−/+</sup>CD27<sup>++</sup>), plasmablasts (CD19<sup>+</sup>IgM<sup>−/+</sup>CD138<sup>+</sup>CD27<sup>+</sup>), memory-plasmablasts (CD19<sup>+</sup>IgM<sup>−</sup>CD138<sup>+</sup>CD27<sup>++</sup>) and circulating marginal zone (CD19<sup>+</sup>CD27<sup>+</sup>CD23<sup>−</sup>) B-cells were significantly increased at diagnosis compared to post-treatment, suggesting their potential utility as TB-treatment response biomarkers (129). A study comparing multi-drug resistant-TB patients with healthy controls revealed decreased rates of non-class switched memory (IgD<sup>+</sup>CD27<sup>+</sup>) B-cells and circulating plasma cells (CD19<sup>dim</sup>IgD<sup>−</sup>CD38<sup>+++</sup>CD27<sup>++</sup>), with increased numbers of circulating type-1 transitional (IgD<sup>+</sup>CD38<sup>++</sup>), CD69<sup>+</sup> and Toll-like receptor 9 (TLR9)<sup>+</sup> B-cells in the peripheral blood of multi-drug resistant-TB patients (131). Another study reported



increased frequencies of marginal zone ( $CD19^+CD21^+CD23^-$ ) B-cells in QuantiFERON-TB Gold In-Tube test (QFN) positive compared to QFN-negative individuals (136).

Studies characterizing and enumerating B-cell phenotypes during TB not only analyzed the presence of various B-cell subpopulations in peripheral blood, but also in the lungs and pleural cavity. Approximately 85% of B-cells present in both unaffected and Mtb-infected mouse lungs expressed surface markers typical of follicular B-cells or B2-cells (e.g.  $CD19^+B220^{high(hi)}IgM^{low(lo)}IgD^{hi}$  with the phenotype  $CD21/35^+CD11b^-CD1d^-CD5^-CD43^-$ ), whilst 15% exhibited a surface expression that is characteristic of antibody producing B1-cells (e.g.  $CD19^+B220^{lo}IgM^{hi}IgD^{lo}CD23^-CD5^-/CD5^-$ ) (128). In the lungs, the B1/B2 ratio was comparable between infected and uninfected mice. In the pleural cavity, however, progression of TB was associated with an elevated proportion of the B2-population (from 25 to 60%) (128).

Another important B-cell subset are regulatory B-cells (Bregs), which balance immune activation following inflammatory responses during infection. An increased frequency of  $CD19^+CD1d^+CD5^+$  Bregs in the circulation of ATB-patients coincided with increased inhibition of T-helper (Th) 17 responses and interleukin-22 (IL-22) generation, while Th1 responses remained unchanged (132, 137). The fact that this Breg-subpopulation was also present in healthy donors, but with decreased suppressive activity, suggests that  $CD19^+CD1d^+CD5^+$  Bregs have activity regulated in response to infection (137). Furthermore, patients with cavitory TB, a severe clinical manifestation of ATB, had increased numbers of  $CD19^+CD1d^+CD5^+$  Bregs in the peripheral blood in comparison to ATB-patients without cavitation (132). Thus,  $CD19^+CD1d^+CD5^+$  Bregs might dampen protective anti-Mtb effector responses, and indeed Mtb Ag-specific IL-22

responses during ATB-treatment were related to reduced  $CD19^+CD1d^+CD5^+$  Breg numbers (132).

Another type of Bregs includes a rare subset, called killer B-cells ( $CD19^+CD5^+IgM^+$ ), which are characterized by Fas-ligand (FASL, CD178) expression (138). Reduced levels of FASL transcript, a diminished incidence of FASL expressing B-cells and a lower level of soluble FASL were detected in the bronchoalveolar lavage (BAL) fluid of ATB-patients at diagnosis compared to the end of successful anti-TB treatment (139). The expression of FASLG and IL5RA was lower in ATB-patients compared to healthy controls, but upon anti-TB treatment, levels were completely restored (140). The frequency of FASL expressing B-cells was lower in whole blood from ATB-patients compared to healthy controls (138). FASL expressing B-cells were present during both ATB and LTBI, but the frequency of this Breg-subset was higher in LTBI and was even further elevated after B-cell re-stimulation with BCG (138). Thus, killer B-cells may contribute to protective immunity during Mtb-infection. Further work is required to decipher the exact role of killer B-cells during Mtb-infection.

Overall, these data implicate that the relative frequencies and function of B-cell subsets are affected during Mtb-infection, “protective” B-cell subsets are decreased in numbers, whilst potentially pathological B-cell subpopulations are increased during ATB-disease. Importantly, patients cured from ATB-disease have normalized B-cell numbers, with normal phenotype distributions and functional properties, indicating restoration of the responses.

## B-Cell Modulation of Effector Cells During Mtb-Infection

B-cells are players in the formation of effective immune responses since B-cells are not only potent APCs, but also represent

powerful producers of a wide range of cytokines and Abs (7, 37). All of these B-cell features can influence the function of a broad range of immune cells, such as T-cells, macrophages, neutrophils and dendritic cells.

## B-Cells Guiding T-Cell Responses

### *B-Cell Antigen-Presenting Capacity as Modulator of T-Cell Immunity*

The ability of B-cells to function as APCs may contribute to the orchestration of Mtb specific CD4<sup>+</sup> T-cell immunity (60). Surprisingly, Ag presentation by B-cells during Mtb-infection has hardly been assessed (128, 141). In B-cell deficient mice, it was demonstrated that correct programming and induction of effector cells specific for Mtb Ags necessitated presentation of these particular Ags to CD4<sup>+</sup> T-cells by B-cells (141). Moreover, aerosol challenge of genetically Mtb-susceptible I/St mice slightly increased the level of major histocompatibility complex-class II molecules on the surface of lung B-cells during Mtb-infection, and their efficacy to present Mtb Ags to CD4<sup>+</sup> T-cells was comparable to that of their splenic counterparts (128). Importantly, the APC-function of B-cells during Mtb-infection appears to become progressively more relevant at lower Ag load, but likely superfluous at higher Ag loads (142, 143). The Ag-presenting potential of B-cells was also shown to increase vaccine-effectiveness (including TB-vaccines), and to strongly boost BCG primed immunity (144–146).

### *B-Cells and Their Cytokines as Powerful T-Cell Rheostats*

B-cells isolated from lungs of Mtb-infected mice produced and released a wide range of cytokines (7, 37). In a cynomolgus macaque (*Macaca fascicularis*) model a role for granulomatous B-cells in producing IL-6 and IL-17 was discovered, and to a lower degree IL-10 and IFN- $\gamma$ , during the acute phase of Mtb-infection (74). B-cell depletion, however, only resulted in diminished secretion of IL-6, but not IL-17 (74), suggesting functional cellular interactions for B-cells in lesions. In agreement with the ability of B-cells to produce IL-6, Linge et al. demonstrated that lung B-cells in I/St mice can secrete high to moderate levels of proinflammatory IL-6 and IL-11 when challenged with Mtb-strain H37Rv (128). Atypical B-cells with reduced production of intracellular IL-6 were isolated from the blood of both ATB and LTBI patients (116). Taken the diverse stages of TB disease into consideration, du Plessis et al. attempted to map the B-cell derived cytokine profile during LTBI (147). B-cells could produce both pro- and anti-inflammatory cytokines when stimulated with Mtb (or TLR agonists), including IL-1 $\beta$ , IL-10, IL-17, IL-21 and tumor necrosis factor-alpha (TNF- $\alpha$ ) (147).

B-cells produce and release specific cytokines upon activation, and thereby a.o. shape (T-cell) immune responses against Mtb. Specifically, IL-1 $\beta$  and IL-6 have been reported to play a critical role in establishing and sustaining Th17-responses to Mtb (148–150). In addition, IL-6 directs differentiation of Th1-cells from naïve T-cells (151). Although the function of IL-11 in anti-Mtb immunity remains to be elucidated, in multiple sclerosis this cytokine is a potent stimulator of Th17 responses (152, 153). Moreover, IL-21 has been shown to play a critical role in T-cell immune responses against

Mtb by enhancing CD8<sup>+</sup> T-cell priming, increasing T-cell accumulation in the lungs and potentially by inhibiting T-cell exhaustion (148). Similarly, TNF- $\alpha$  has been shown to enhance T-cell responses through augmenting Ag-presentation and cross-priming (154). Furthermore, both TNF- $\alpha$  and IL-17 can regulate chemokine-expression and thereby modulate the recruitment and maintenance of immune cells, including T-cells, at the site of infection (155–157). In contrast, IL-10 can dampen Mtb-specific Th1 responses through inhibition of TNF- $\alpha$  and the Th1-polarizing cytokine IL-12 and human leukocyte antigen-class II expression, thereby limiting Ag-presentation, cross-priming and migration of Th1-cells toward the lungs (158–161). Collectively, these data point to an important role for B-cell produced cytokines in the generation and regulation of CMI to TB.

## THE MECHANISTIC ROLE OF Abs IN TB

Besides their antigen presentation capacity and their ability to skew T-cell responses through cytokine secretion, B-cells are best known for their capacity to secrete Abs. Like B-cells, Abs exist in multiple isotypes and subclasses, each with distinctive functional properties, which are further diversified by post-translational modifications, representing an enormous functional potential for Abs in effector immunity toward Mtb (**Figure 2B**). TB disease, but not Mtb infection itself, may significantly alter the functional properties, including the avidity, of Abs against heterologous (162), reflecting modification of humoral responses by Mtb likely by altering B-cell function. In this chapter, we will focus on the Mtb specific responses.

### **Abs as Potential Biomarkers for Protective Immunity Against Mtb**

“Natural immunity” against Mtb has recently been studied in various human “resistor” or “early clearers” cohorts, amongst which were health care workers (76), household TB contacts (163–165) and gold miners (166). These studies consistently identified that ~5–15% of the tested individuals in a TB-endemic region are resistant to acquire latent Mtb-infection as determined by tuberculin skin test (TST) or QuantiferonTB Gold (QFT) conversion (167). Genome-wide linkage analysis in a panel of South African families living in a hyperendemic area demonstrated that the locus called *TST1* was associated with TST reactivity (168). A deep sequencing study showed preferential rearrangement of V<sub>H</sub>3-23-D3-3-J<sub>H</sub>4 fragments in IgA molecules in TST-negative nurses with long-term exposure to Mtb compared to their TST-positive colleagues (169). Moreover, healthy nurses in a TB ward had a strong Ab-response specific toward the TB69 epitope of the 14-kDa Ag, possibly linked to resistance to acquiring Mtb-infection (170). Individuals with persistent negative TSTs, despite years of exposure to ATB patients, had elevated anti-Mtb IgG levels, and their serum was able to block proliferation of peripheral blood mononuclear cells in response to protein purified derivative (PPD) (171). In concordance, highly exposed, but TST-negative, Colombian individuals displayed high anti-PPD Abs titers, which inhibited autologous T-cell proliferation after PPD stimulation (172).



Abs specific for CFP-10 and ESAT-6 in QFT supernatants independently separated LTBI from ATB (173). More recently, Lu et al. reported that highly exposed, but TST- and IFN- $\gamma$  release assay (IGRA)-negative, Ugandan individuals harbored Mtb-specific IgM and IgG, while diminished CD4-mediated IFN- $\gamma$  responses directed toward Mtb early secreted Ag of 6 kDa (ESAT-6), 10 kDa culture filtrate protein (CFP-10), Ag85A and Ag85B were found (163). Taken together, these studies implicate that humoral immunity is detectable in frequently exposed individuals with persistently negative skin testing or QFN evaluation, which represent read-outs of effector T-cell responses. In such settings, Abs may be considered biomarkers of protective immunity.

## Ab Effector Functions Against Mtb

Although Abs may be interesting biomarkers of Mtb-infection or resistance to disease progression, they may also contribute functionally to reduce bacterial loads. However, when considering a role in prevention of infection Abs need to localize to sites where the pathogen enters the host to inhibit, or contribute to early clearance of, infection. In addition, Abs need to trigger the right effector responses, therefore functional assessment rather than mere quantification is critical to evaluate the contribution of Abs to the immune response. Typically, Abs are located in both the upper and lower respiratory tract, where IgA dominates in the upper airways and IgG in the lower airways. It has been shown that human infection with Mtb resulted in mycobacterial specific IgA and IgG in BAL fluid (174, 175). Abs can bind Mtb-specific Ags at the site of disease (30, 60), such as the tuberculous granuloma where plasma cells have been demonstrated to secrete Abs (112), which could potentially interact with extracellular Mtb and/or free Mtb Ags present in the granuloma itself, or in the pleural fluid (112, 176, 177). In addition, Mtb is extracellular during its reinfection phase and during expectoration. Thus, in spite of being a facultative intracellular pathogen, Mtb is possibly susceptible to numerous mechanisms of AMI (6, 178). These comprise, but are not limited to, mycobacterial neutralization (82, 91, 179), antibody-dependent cellular phagocytosis (ADCP) (180, 181), complement activation (182–184), antibody-dependent cell-mediated cytotoxicity (ADCC) (185), Mtb-Ab immune complex sensing by intracellular FcR tripartite motif-containing protein 21 (TRIM21) (186, 187), stimulation of CMI (43, 188, 189) and modulation of the strength and nature of the inflammatory response during Mtb-infection (6, 31, 36, 69, 185, 190–193).

## Ab-Dependent Opsono-Phagocytosis of Mtb

One of the most important Ab effector functions against Mtb is opsono-phagocytosis, also called ADCP (63). ADCP is mediated by mononuclear phagocytes and granulocytes upon engaging FcRs or, following complement opsonization, complement receptors (42). Mtb inhibits phagosome-lysosome fusion to evade exposure to the antimicrobial lysosomal content (194–197). However, Ab-mediated phagocytosis of opsonized mycobacteria can overcome this inhibition by triggering phagolysosomal fusion (197). Similarly, more recent studies have found increased phagosome maturation in the presence of opsonizing

Abs and showed decreased mycobacterial viability upon phagolysosomal fusion (180, 181, 189, 198). Opsonizing Abs restricted Mtb growth in macrophages by significantly increasing the microbicidal potency through increased lysosomal-associated membrane protein 1 (LAMP-1; a phagosome maturation marker) and inducible nitric oxide synthase (iNOS) phagosomal localization and enhanced phagosome acidification, as well as by increased levels of the proinflammatory cytokines IFN- $\gamma$  and IL-6 (194). Another study described that IgG-coated BCG induced increased microbicidal activity by alveolar macrophages associated with an elevated oxidative burst in phagosomes (199). Mtb opsonized with LAM-specific Abs bound Fc $\gamma$ Rs on macrophages and stimulated mycobacterial killing, which was associated with increased calcium ( $\text{Ca}^{2+}$ ) concentrations that promoted phagosome maturation (196). Uptake of Mtb mannose-capped LAM (ManLAM) beads into human alveolar macrophages via mannose receptors initiated a specific phagocytic pathway that limited phagosomal fusion, whereas phagocytosis of anti-LAM mAb coated beads through Fc $\gamma$ Rs did not inhibit the fusogenic property of phagosomes (200). In agreement with these results, uptake of phosphatidyl-myo-inositol mannoside (PIMs)-coated beads into macrophages via engagement of mannose receptors resulted in restricted phagolysosomal fusion (201). Thus, Mtb cell entry via mannose-, complement- and probably other phagocytic receptors allows intracellular survival and replication of bacilli by limiting phagosome maturation while on the other hand, increased phagolysosomal fusion is observed after phagocytosis of Ab-opsonized mycobacteria via FcR signaling (198). Indeed, Chen et al. have demonstrated that increased Mtb phagocytosis and the subsequent increased phagolysosomal fusion observed in THP-1 cells infected with Mtb opsonized with sera containing high anti-AM IgG titers derived from asymptomatic volunteers, was Fc $\gamma$ R mediated (180). Furthermore, a significant decline in Mtb phagocytosis by human anti-Mtb Abs was observed when blocking Fc $\gamma$ RI (CD64), which was even more prominent when Fc $\gamma$ RII (CD32) was blocked. In contrast to (180), Lu et al. found that enhanced functionality of polyclonal LTBI IgG was correlated with selective Fc $\gamma$ RIII (CD16) binding, which was associated with increased phagosome maturation and elevated macrophage killing of intracellular tubercle bacilli (185). Intriguingly, CD16 positive, non-classical monocytes were strongly associated with reduced mycobacterial outgrowth upon recent Mtb exposure (202). The discrepancies between studies can likely be attributed to differences in Abs related to the stage of TB disease, and differences in assays and phagocytosing cells (203, 204), as THP-1 cells do not express Fc $\gamma$ RIII (CD16), whilst monocyte-derived macrophages do (205, 206). In summary, Ab opsonization of Mtb and subsequent FcR signaling can target Mtb to the degradative lysosomal pathway, which is directly antimicrobial even though it may not be capable to induce complete elimination (194).

## Ab-Mediated Classical Complement Activation in TB Disease

An additional mechanism by which AMI could influence the host response against Mtb is through Ab-mediated complement engagement and deposition (182–184). As discussed



previously, transcripts of different complement genes were strongly increased during active TB-disease, which were considered important biomarker candidates (18, 20, 23–26). In addition, increased concentrations of circulating immune complexes were detected in serum of patients with subclinical and clinical ATB (24), however, the antigen in these complexes remains unknown. In Indian TB patients anti-LAM IgG2, but not IgM, was associated with classical pathway complement activation (184). Likewise, human IgG, and to a lesser degree IgM, was shown to increase complement deposition on BCG via classical pathway activation (183). Moreover, human anti-Mtb IgG augmented complement activation resulting in enhanced phagocytosis of Mtb by macrophages (182). Thus, complement activation by anti-Mtb Abs seems possible, but has been investigated to a very limited extent, nonetheless, it may significantly contribute to Mtb phagocytosis.

### Ab-Mediated Cellular Cytotoxicity in TB Disease

ADCC might represent another classical mechanism that could possibly help controlling Mtb. IgG-mediated ADCC might stimulate killing of Mtb and could play a vital role in the early containment of Mtb upon their re-entry into the extracellular space. Indeed, PPD specific IgG from both LTBI and ATB-patients increased natural killer (NK) cell-mediated ADCC (185). IgG derived from LTBI patients revealed a preferential interaction with the activating FcγRIIIa (CD16a) associated with an increased on-rate in comparison to IgG isolated from ATB patients (185). This enhanced FcγRIIIa (CD16a) binding profile correlated with increased NK cell activation, elevated ADCC and enhanced Mtb control. These findings suggest a protective role for ADCC in host defense against Mtb.

### Intracellular Sensing of Mtb-Ab Immune Complexes by TRIM21

Going beyond Ag-Ab immune complex recognition by classical FcRs, Ab binding to Mtb might also be detected intracellularly via the ubiquitously expressed cytosolic Ab FcR called TRIM21. Interestingly, the TRIM21 pathway was identified as important pathway in TB when interconnectivity of multiple biomarkers was analyzed in unbiased transcriptomic studies, suggesting TRIM21 may not only be a biomarker of TB-disease, but also functionally involved in reducing the bacterial load (8). Ab-coated pathogen binding to TRIM21 has been demonstrated to result in the activation of signaling pathways, including nuclear factor kappa-light-chain-enhancer of activated B-cells (NF-κB), activator protein (AP)-1 and the IFN-regulatory factor (IRF) family, and stimulate the production of proinflammatory cytokines via K63-linked ubiquitination (186, 187). Hence, TRIM21 triggering elicits an anti-pathogenic state and can provide protective immunity against non-enveloped viruses and intracellular bacteria, such as adenoviruses, *Salmonella enterica* and *Toxoplasma gondii* (186, 187, 207, 208). Importantly, a requirement for TRIM21-mediated signaling and neutralization includes relocation of Abs from the extracellular space toward the cytosol, where Abs are normally not found (186, 187). In the case of Mtb, the bacillus is able to disrupt the phagosomal membrane, which allows Mtb together with bound Abs to enter the cytosol

(209). Thus, the cytosolic localization of both Mtb specific Abs and TRIM21 in combination with the circumstantial evidence described above might open up attractive new roles for Abs in the battle against Mtb.

## The Role of Abs in Mucosal Immunity Against TB

The cumulative work presented above clearly indicates the pleiotropic effect of Abs in the immune response to Mtb, in which the particular Ab effector function utilized is dependent on Ag specificity, Ab isotype and subclass (28, 42, 59, 210). The pulmonary compartment represents the predominant route of Mtb-infection, and the distribution of Ig isotypes in the mucosal lining includes predominantly secretory IgA (sIgA), lower amounts of soluble IgM, and even lower soluble IgG. Belay et al. have demonstrated that exposed healthy controls have a significantly increased anti-HBHA IgA titer in comparison to untreated TB-patients and their QFN-negative household contacts at baseline, suggesting that anti-HBHA IgA could function as a biomarker for immune control of Mtb (211). Mucosal BCG-vaccination by bronchial instillation in rhesus macaques induced pulmonary IgA (measured in BAL fluid), which correlated with protection against low-dose TB-challenge (212). Interestingly, another strongly protective regimen, intravenous BCG-vaccination, also induced increased levels of pulmonary IgA in NHPs (213). Thus, local IgA may represent a correlate of protection, and may functionally contribute to control of mycobacteria.

For functional assessment, polyclonal human sIgA purified from colostrum from healthy volunteers was found to be reactive to both BCG and Mtb Ags (214). Prophylactic intratracheal incubation or pre-incubation of tubercle bacilli with human sIgA resulted in reduced Mtb viability, which was associated with reduced lung tissue damage, as indicated by better granuloma organization and smaller pneumonic areas in the lungs of Mtb-infected mice. Likewise, when IgA deficient (IgA<sup>-/-</sup>) and WT littermate mice were intranasally inoculated with the mycobacterium surface phosphate-binding protein PstS-1 (215), IgA<sup>-/-</sup> mice were still capable of generating PstS-1 specific IgM and IgG, but revealed an increased susceptibility to BCG infection in comparison to WT mice: this was indicated by elevated mycobacterial loads in the lungs at 4 weeks post-infection, and decreased production of IFN-γ and TNF-α. Similarly, mice lacking the polymeric immunoglobulin receptor (pIgR) that enables IgA transcytosis, inoculated with PstS-1 Ags, developed decreased PstS-1 specific IgA titers in their saliva (216). These mice additionally showed increased susceptibility to intranasal BCG, which again correlated with an impaired Th1-response, as manifested by diminished IFN-γ and TNF-α levels in the lungs, and with delayed and reduced mycobacterial-induced immune responses during early infection. These studies collectively indicate that sIgA participates in protection against Mtb-infection and this effect is mediated via modulation of the inflammatory response at the mucosal level and/or by immune exclusion, a process that refers to the capability of sIgA to prevent

pathogens and Ags from acquiring entry to the epithelium (217, 218).

Given the importance of mucosal IgA in host defense against Mtb (219), significant prophylactic and therapeutic improvement could be achieved when eliciting a mucosal immune response at the port of Mtb entry in addition to a systematic immune response. Passive immunization with mAbs has opened avenues for potential protective roles of mucosal IgA and the ability to explore different routes of delivery and their subsequent effects. In fact, in a mouse model of mycobacterial lung infection, intranasal immunization of mice with an IgA mAb (TBA61) directed against Mtb Acr1, induced a transient reduction in bacterial counts in the lungs following aerosol or intranasal challenge (88). This protective effect was improved and prolonged (3–4 weeks) when the Ab was co-administered with mouse recombinant IFN- $\gamma$  alone (87) or in combination with IL-4 neutralization (86) and was demonstrated to be both isotype and epitope specific (88). This finding is in agreement with the observation that intratracheal mAb TBA61 pre-treatment resulted in decreased mycobacterial loads in mouse lungs, which was correlated with milder histopathology following Mtb-challenge (85). More recently, it has been shown that in human Fc $\alpha$ R (CD89) transgenic mice, intranasal administration of a human IgA1 mAb specific for Acr1 combined with recombinant mouse IFN- $\gamma$  significantly reduced bacterial load after intranasal Mtb-infection. Thus, the observed protective effect of IgA in this setting was Fc $\alpha$ R (CD89) dependent (81, 83). Collectively, IgA mAb can influence the intracellular fate of Mtb via potentiation of mycobactericidal functions of infected macrophages and by modulation of the inflammatory response (87, 219–221).

Together, the work described above highlights the importance of mucosal immunity in host defense against Mtb. Although local IgA production correlated with protection induced by intravenous or mucosal BCG vaccination, its functional capacity to control mycobacteria remains to be demonstrated.

## Glycosylation Patterns as Modulators of Ab Functionality in TB

Modification of Abs, like glycosylation, influences the function of Abs (222). These glycans modify the Ab Fc region structure, and addition or removal of glycan-molecules modifies Ab FcR engagement and Ab functionality (222, 223). Specifically, recent new data obtained from several viral and bacterial diseases implicate that infection, and the associated inflammatory state of the individual, alters Ab glycosylation and hence functionality (224, 225).

Given the dynamic nature of glycan alterations that is impacted by the inflammatory milieu (226), Ab glycosylation changes could also occur during the course of TB disease. Using systems serology, Lu et al. showed that the LTBI Ab glycome of total and PPD-specific IgG had accumulated digalactosylated (G2) glycans with an increased level of sialylation, but less core fucosylation in comparison to ATB IgG (185). This finding resonates with the observation that individuals with ATB displayed a marked elevation of agalactosylated (G0) and asialylated IgG glycans (227–229). Although the absence

of galactose is considered to be correlated with increased inflammatory activity in general (223, 226), agalactosylated (G0) IgG could trigger the lectin complement pathway (230). The presence of sialic acid has been correlated with an anti-inflammatory state in rheumatoid arthritis patients (231), and this could reflect diminished inflammation in LTBI compared to ATB patients. Increased Fc $\gamma$ RIIIa (CD16a) engagement by polyclonal IgG from LTBI individuals led to increased Mtb-specific ADCC and killing of tubercle bacilli in infected primary human monocyte-derived macrophages in comparison to purified IgG derived from ATB-patients (185). Interestingly, NK-cell frequencies and CD16 function were associated with LTBI (124). Together, these data highlight that the discrete Ab glycosylation patterns observed in LTBI persons might correlate with increased Mtb control.

Removal of polysaccharides from purified IgG decreased the level of ADCC, showing that Ab glycosylation is essential for anti-Mtb activity (185). Glycosylation profiles differed for divergent Mtb reactive Ab populations (e.g., recognizing PPD and Ag85A), suggesting possible differential modulation of glycosylation across IgGs against different Mtb-specific Ags (232). Furthermore, parallel profiling of whole IgG and Ag-binding fragment (Fab) and Fc region-specific IgG glycosylation, showed that the main alterations in Ab glycan moieties across divergent TB-disease states (185) were located in the Fc-region. Stringent multivariate analysis further demonstrated that Fc-region glycosylation can distinguish between LTBI and ATB disease states (232). Digalactosylated (G2) glycan structures and the discrete structure G1S1F (characterized by one galactose, one sialic acid, and one fucose) located on the IgG-Fc region discriminated LTBI from ATB individuals, and likewise distinguished successfully treated ATB individuals from ATB patients (Grace et al., under review). In addition, Mtb-specific IgG4 titers were identified as a novel biomarker for TB disease, in which IgG4 levels were increased during ATB compared to LTBI and individuals that had successfully completed TB-treatment. IgG4-depletion increased Ab effector function, suggesting regulation of the overall humoral response. In addition, LTBI individuals could be distinguished from successfully treated ATB patients by lower Mtb-specific IgM and IgG1 levels and decreased opsonophagocytic function (Grace et al., under review). Mtb resisters (characterized as highly Mtb exposed individuals that persistently tested negative in both TST and IGRA), similar to health care worker cohorts described above, revealed distinct PPD-specific IgG Fc-glycosylation patterns compared to individuals with LTBI, in which their IgG showed accumulated monogalactosylated (G1) glycans with an increased level of fucosylation and bisecting GlcNAc, but less core sialylation (163). These selectively enriched glycan structures were associated with increased NK cell IFN- $\gamma$  release facilitated by augmented Fc $\gamma$ RIIIa (CD16a) engagement leading to better *in vitro* Mtb control (124, 185). Collectively, Mtb-specific Fc-glycosylation may serve as biomarker to differentiate between ATB and LTBI.

Based on the wide variety of Ab effector functions available, AMI can significantly contribute to protection against Mtb at different stages of infection. Moreover, B-cells and Abs,

specifically mucosal IgA, might also be useful biomarkers for vaccine induced protective immunity against Mtb. However, the majority of studies only include quantification of Ab levels, while not taking into account functional assessment of Mtb-specific Abs. Hence, more functional read-outs are needed for B-cells and Abs to evaluate them as correlates of protection and to gain a deeper understanding of the quality of humoral immunity during different stages of Mtb-infection (Figures 1, 2).

## B-CELLS AND Abs AS TARGETS FOR VACCINATION

The majority of designed novel TB-vaccines has concentrated on the induction of CMI (64, 233). Some vaccines, including BCG, induce memory as reflected by the detection of PPD specific memory B-cells (234). However, several recent vaccine studies in mice, NHPs and humans have shown significant induction of Abs against Mtb as well, which might contribute to the vaccine efficacy observed.

Prados-Rosales et al. (235–240) conducted a study with a TB-vaccine that selectively elicits AMI against the tubercle bacillus (241). More specifically, two polysaccharide (PS)-conjugate vaccines were created, by linking the capsular PS AM to either Ag85b or to *Bacillus anthracis* protective Ag. Both PS-conjugate vaccines substantially diminished lung inflammation and mycobacterial dissemination to the spleen in mice challenged with virulent Mtb. More importantly, passive transfer of immune serum derived from AM-immunized mice offered protection, as assessed by decreased mycobacterial loads in both the lungs and spleen when delivered before aerosol Mtb-infection of naïve mice (241). Corroborating these data, mice immunized with a PS-conjugate vaccine of Ag85b and AM generated high AM-specific IgG levels and showed protection against Mtb, reflected by both prolonged survival and diminished lung pathology (239). More recently, booster vaccination with a whole cell inactivated vaccine (heat-killed MTBVAC) increased protection against Mtb after intranasal vaccination of BCG-primed mice in comparison to subcutaneous BCG only (235). This improved protection correlated with induction of PPD-specific Abs in the BAL fluid that opsonized Mtb. These data were supported by similar data obtained in NHPs (235).

In other NHP studies, vaccine-induced local Ab responses correlated with protection against Mtb-infection and disease (212). BCG vaccination was delivered to rhesus macaques either via the standard intradermal route or via endobronchial instillation, a mucosal route of immunization, which resulted in strong protection against subsequent repeated low-dose infection with Mtb, as measured by reduced lung bacillary loads and diminished histopathology. Interestingly, mucosally vaccinated rhesus macaques had high levels of Ag-specific IgA locally in the BAL fluid. Similarly, intravenous administration of BCG in rhesus macaques induced protection against TB and superior Mtb-specific IgG, IgA and IgM responses in BAL fluid and plasma in comparison to intradermal BCG vaccination (213). Together, these studies describe an association between (local) humoral immune responses and protection against Mtb after

BCG immunization, putting humoral immunity forward as a potential correlate of protection.

In humans, several TB-vaccine trials showed correlations between specific Abs and vaccine efficacy against Mtb-infection and/or disease. In a large-scale phase 2b efficacy trial in BCG vaccinated South African infants, utilizing the recombinant vaccinia Ankara virus modified to express Ag85A (MVA85A) (242), the presence of Ag-specific IgG titers correlated with a reduced risk of developing TB disease (101). Furthermore, protection was achieved using a subunit vaccine in the M72/ASO1E vaccine trial (243). This clinical phase 2b trial demonstrated that the incidence of ATB disease was significantly reduced in Mtb-infected adults vaccinated with M72/ASO1E relative to placebo. Besides robust activation of T-cells, the vaccine also elicited a strong Ag-specific IgG response that persisted up to at least 36 months post immunization (244, 245). Thus, collectively, the data obtained from mouse, NHP and human vaccination studies support the possibility that AMI might contribute to the protective effects of certain TB-vaccines.

## Preventive and Therapeutic TB-Vaccine Design

An ideal anti-TB-vaccine would protect against both Mtb-infection in exposed individuals and the establishment of disease in already Mtb-infected persons. There is a desperate need for the development of more effective TB-vaccines for children, adolescents and adults. To that end, the emerging appreciation of the role of B-cells and Abs in combatting Mtb (6, 7, 30, 31, 37) in combination with the existence of naturally arising human Abs that are probably functionally protective against Mtb-infection (76), points toward an exciting and promising new path to explore.

BCG as neonatal vaccination against TB has not only reduced the incidence of severe forms of TB in children, but has also reduced all-cause childhood mortality as a result of heterologous protection against non-related pathogens (246–249). BCG vaccinated children had increased levels of Abs in their serum indicating enhanced activation of cell-mediated responses, in particular of humoral immune components (246–249). Although most studies focused on heterologous protection in young children, more recently, it was suggested that also vulnerable elderly could benefit from BCG vaccination to protect against unrelated pathogens (250, 251). BCG did not only enhance responses against natural infections, but also increased the magnitude of humoral responses induced by vaccines against non-related pathogens (246). The mechanism behind these heterologous protective effects is called trained innate immunity and reflects an increased state of responsiveness of mostly innate immune cells due to epigenetic alterations and metabolic rewiring independent of Ag (252). However, it is unknown if similar processes may also alter the response-readiness state of Ag specific adaptive immune players, in particular because the reprogramming occurs in the hematopoietic stem and progenitor compartment (253). Nevertheless, training of innate players by live vaccines, most prominently BCG, will have significant effects on the magnitude of both innate and adaptive responses,

including humoral immunity, which will significantly contribute to vaccine induced protection. Novel live vaccines may have a similar training capacity, in particular BCG variants or live attenuated Mtb strains, and thereby might enhance humoral responses, however for other vaccine formulations this remains to be investigated. Prime-boost regimens, including those with a BCG prime, may be superior in activating B-cells partly by enhanced, trained status of key players. A more detailed analysis of these effects for each of the novel vaccine candidates is strongly encouraged.

For the development of a TB-vaccine that elicits not only cellular, but also functional humoral responses, it is of importance to take the route of delivery into consideration (254). Pre-exposure vaccines that aim at preventing infection with Mtb may need to induce IgA production locally in the lungs (255), whereas post-exposure vaccines that aim to either modify or prevent clinical disease in already Mtb-infected individuals most likely will need to trigger a systemic response including IgG (180).

## DISCUSSION

*Mycobacterium tuberculosis* remains a challenging and threatening pathogen, affecting many people globally. Ample epidemiological studies indicate that progression of disease is strongly associated with the immunological competency of the host, and therefore, a more in-depth understanding of the effector anti-TB immune responses is pivotal for the design of next-generation preventive and therapeutic approaches in the fight against this pathogen. The complementary effect of immune components other than classical Th1/Th17 cellular responses, such as Abs, should be considered. Abs and B-cells on their own may not be sufficient to combat Mtb, however there is accumulating evidence that they can complement and enhance CMI. Clinical vaccine evaluation studies should incorporate not only the quantitative assessment of these responses, but also their functional capacity to reduce Mtb burden to assess their future value as correlates of protection and as mediators of protection (Figure 1).

The majority of Ab studies largely concentrated on their utility as diagnostic tools, with little to no attention for dissection of Abs at the isotype and subclass level in relation to TB pathogenesis and resolution (256). However, both Ab isotype, subclass and post-translation modifications might alter functional properties toward Mtb (180). Such differences are most likely a result of structural, antigenic and functional divergences in the Fab and Fc region of Ab isotypes (257). Hence, a more comprehensive insight through detailed immunoprofiling of Mtb-specific Ab responses during disease progression and resolution is essential, not only for TB diagnosis, but also potentially for therapeutic monitoring, and the identification of correlates of protection and markers of disease.

As B-cells and Abs significantly add to the repertoire of effector responses against TB, these two immune components could represent interesting targets for vaccination. However, due to highly heterogenous Ab responses during natural TB infection and disease (258), it might be required to employ strategic vaccine design and specific delivery routes to effectively induce

protective rather than enhancing Abs. Mucosal vaccination routes may be more likely to induce protective Mtb specific IgA, however, possibly also other protective vaccines may induce similar mucosal responses, but they have not yet been rigorously assessed. Live vaccines or selected adjuvants may skew strong Ab responses and influence Ab isotype and/or Fc glycosylation profiles (259, 260). Adjuvants characterized by low inflammatory and reactogenic profiles that could be safely administered through the mucosal route may be promising candidates (261).

While the discovery of BCG and antibiotics has been ground-breaking in the prevention and treatment of ATB, major knowledge gaps remain regarding better prevention and treatment of Mtb in both children and adults. Novel host-directed therapeutic and vaccine development efforts will need to go beyond harnessing and improving only cellular immune responses, and should likely also engage the broad range of B-cell and Ab effector functions. As a next step, new tools that probe specificity, affinity, isotype, subclass, function and glycosylation of Abs should be developed. All accumulated evidence so far warrants detailed monitoring of B-cells and Abs in future vaccine efficacy studies, not only as correlates of protection, but also as potential contributors to protection. Since Abs are highly diverse, and this diversity relates to their functional tenures, it is important to not only assess their levels and titers, but also to dissect their functional contribution to mycobacterial inhibition and killing. Even though B-cells and Abs may not be fully sufficient on their own, they clearly can contribute to the total effector response and thereby provide novel and important targets for future studies and interventions against Mtb and other intracellular pathogens.

## AUTHOR CONTRIBUTIONS

WR, TO, and SJ drafted the original manuscript outline, composed the initial draft and corrected the manuscript to its final version. All authors contributed to the article and approved the submitted version.

## FUNDING

Work in the laboratory of the contributors would not have been possible without external funding. Therefore, we acknowledge EC HORIZON2020 SMA-TB (Grant No. 847762), The Netherlands Organization for Scientific Research (NWO-TOP Grant No. 91214038), the National Institute of Allergy And Infectious Diseases of the National Institutes of Health under Award Number R21AI127133 and R01AI141315 for support of our work. The content is solely the responsibility of the authors and does not necessarily represent the official views of the National Institutes of Health or any funder.

## ACKNOWLEDGMENTS

We would like to acknowledge Dr. Edward Knol, Utrecht University, Utrecht, The Netherlands for valuable advice during writing of this manuscript.



## REFERENCES

- Cardona P. The progress of therapeutic vaccination with regard to tuberculosis. *Front Microbiol.* (2016) 7:1536. doi: 10.3389/fmicb.2016.01536
- World Health Organization. *Global Tuberculosis Report 2019*. Geneva. (2019). Available online at: <https://apps.who.int/iris/bitstream/handle/10665/329368/9789241565714-eng.pdf?ua=1> (accessed December 1, 2020).
- Paulson T. Epidemiology: a mortal foe. *Nature.* (2013) 502:S2–3. doi: 10.1038/502S2a
- Kawahara JY, Irvine EB, Alter G. A case for antibodies as mechanistic correlates of immunity in tuberculosis. *Front Immunol.* (2019) 10:996. doi: 10.3389/fimmu.2019.00996
- de Martino M, Lodi L, Galli L, Chiappini E. Immune response to *Mycobacterium tuberculosis*: a narrative review. *Front Pediatr.* (2019) 7:350. doi: 10.3389/fped.2019.00350
- Achkar JM, Casadevall A. Antibody-mediated immunity against tuberculosis: implications for vaccine development. *Cell Host Microbe.* (2013) 13:250–62. doi: 10.1016/j.chom.2013.02.009
- Kozakiewicz L, Phuah J, Flynn J, Chan J. The role of B cells and humoral immunity in *Mycobacterium tuberculosis* infection. *Adv Exp Med Biol.* (2013) 783:225–50. doi: 10.1007/978-1-4614-6111-1\_12
- Joosten SA, Fletcher HA, Ottenhoff TH. A helicopter perspective on TB biomarkers: pathway and process based analysis of gene expression data provides new insight into TB pathogenesis. *PLoS ONE.* (2013) 8:73230. doi: 10.1371/journal.pone.0073230
- Fine PE. Variation in protection by BCG: implications of and for heterologous immunity. *Lancet.* (1995) 346:1339–45. doi: 10.1016/S0140-6736(95)92348-9
- Zak DE, Penn-Nicholson A, Scriba TJ, Thompson E, Suliman S, Amon LM, et al. A blood RNA signature for tuberculosis disease risk: a prospective cohort study. *Lancet.* (2016) 387:2312–22. doi: 10.1016/S0140-6736(15)01316-1
- Petrucchioli A, Scriba TJ, Petrone L, Hatherill M, Cirillo DM, Joosten SA, et al. Correlates of tuberculosis risk: predictive biomarkers for progression to active tuberculosis. *Eur Respir J.* (2016) 48:1751–63. doi: 10.1183/13993003.01012-2016
- Anderson ST, Kaforou M, Brent AJ, Wright VJ, Banwell CM, Chagaluka G, et al. Diagnosis of childhood tuberculosis and host RNA expression in Africa. *N Engl J Med.* (2014) 370:1712–23. doi: 10.1056/NEJMoal303657
- Kaforou M, Wright VJ, Oni T, French N, Anderson ST, Bangani N, et al. Detection of tuberculosis in HIV-infected and uninfected African adults using whole blood RNA expression signatures: a case-control study. *PLoS Med.* (2013) 10:e1001538. doi: 10.1371/journal.pmed.1001538
- Ottenhoff TH, Dass RH, Yang N, Zhang MM, Wong HE, Sahiratmadja E, et al. Genome-wide expression profiling identifies type 1 interferon response pathways in active tuberculosis. *PLoS ONE.* (2012) 7:e45839. doi: 10.1371/journal.pone.0045839
- Berry MP, Graham CM, McNab FW, Xu Z, Bloch SA, Oni T, et al. An interferon-inducible neutrophil-driven blood transcriptional signature in human tuberculosis. *Nature.* (2010) 466:973–7. doi: 10.1038/nature09247
- Corrêa RdS, Rodrigues LS, Pereira LHL, Nogueira OC, Leung J, Sousa MdS, et al. Neutrophil CD64 expression levels in IGRA-positive individuals distinguish latent tuberculosis from active disease. *Mem Inst Oswaldo Cruz.* (2019) 114:e180579. doi: 10.1590/0074-02760180579
- Sutherland J, Loxton A, Haks M, Kassa D, Ambrose L, Lee J, et al. Differential gene expression of activating Fcγ receptor classifies active tuberculosis regardless of human immunodeficiency virus status or ethnicity. *Clin Microbiol Infect.* (2014) 20:O230–8. doi: 10.1111/1469-0691.12383
- Cliff JM, Lee J, Constantinou N, Cho J, Clark TG, Ronacher K, et al. Distinct phases of blood gene expression pattern through tuberculosis treatment reflect modulation of the humoral immune response. *J Infect Dis.* (2013) 207:18–29. doi: 10.1093/infdis/jis499
- Joosten S, Goeman J, Sutherland J, Opmeer L, De Boer K, Jacobsen M, et al. Identification of biomarkers for tuberculosis disease using a novel dual-color RT–MLPA assay. *Genes Immun.* (2012) 13:71–82. doi: 10.1038/gene.2011.64
- Maertzdorf J, Repsilber D, Parida SK, Stanley K, Roberts T, Black G, et al. Human gene expression profiles of susceptibility and resistance in tuberculosis. *Genes Immun.* (2011) 12:15–22. doi: 10.1038/gene.2010.51
- Maertzdorf J, Ota M, Repsilber D, Mollenkopf HJ, Weiner J, Hill PC, et al. Functional correlations of pathogenesis-driven gene expression signatures in tuberculosis. *PLoS ONE.* (2011) 6:e26938. doi: 10.1371/journal.pone.0026938
- Jacobsen M, Repsilber D, Gutschmidt A, Neher A, Feldmann K, Mollenkopf HJ, et al. Candidate biomarkers for discrimination between infection and disease caused by *Mycobacterium tuberculosis*. *J Mol Med (Berl).* (2007) 85:613–21. doi: 10.1007/s00109-007-0157-6
- Lubbers R, Sutherland JS, Goletti D, De Paus RA, Van Moersel CH, Veltkamp M, et al. Complement component C1q as serum biomarker to detect active tuberculosis. *Front Immunol.* (2018) 9:2427. doi: 10.3389/fimmu.2018.02427
- Esmail H, Lai RP, Lesosky M, Wilkinson KA, Graham CM, Horswell S, et al. Complement pathway gene activation and rising circulating immune complexes characterize early disease in HIV-associated tuberculosis. *Proc Natl Acad Sci USA.* (2018) 115:E964–73. doi: 10.1073/pnas.1711853115
- Cai Y, Yang Q, Tang Y, Zhang M, Liu H, Zhang G, et al. Increased complement C1q level marks active disease in human tuberculosis. *PLoS ONE.* (2014) 9:e92340. doi: 10.1371/journal.pone.0092340
- Schrijver B, Dijkstra DJ, Borggreven NV, La Distia Nora R, Huijser E, Versnel MA, et al. Inverse correlation between serum complement component C1q levels and whole blood type-1 interferon signature in active tuberculosis and QuantIFERON-positive uveitis: implications for diagnosis. *Clin Transl Immunol.* (2020) 9:e1196. doi: 10.1002/cti2.1196
- Correia-Neves M, Fröberg G, Korshun L, Viegas S, Vaz P, Ramanlal N, et al. Biomarkers for tuberculosis: the case for lipoarabinomannan. *ERJ Open Res.* (2019) 5:00115–2018. doi: 10.1183/23120541.00115-2018
- Steigler P, Verrall AJ, Kirman JR. Beyond memory T cells: mechanisms of protective immunity to tuberculosis infection. *Immunol Cell Biol.* (2019) 97:647–55. doi: 10.1111/imcb.12278
- Achkar JM, Prados-Rosales R. Updates on antibody functions in *Mycobacterium tuberculosis* infection and their relevance for developing a vaccine against tuberculosis. *Curr Opin Immunol.* (2018) 53:30–7. doi: 10.1016/j.coi.2018.04.004
- Jacobs AJ, Mongkolsapaya J, Sreaton GR, McShane H, Wilkinson RJ. Antibodies and tuberculosis. *Tuberculosis.* (2016) 101:102–13. doi: 10.1016/j.tube.2016.08.001
- Achkar JM, Chan J, Casadevall A. B cells and antibodies in the defense against *Mycobacterium tuberculosis* infection. *Immunol Rev.* (2015) 264:167–81. doi: 10.1111/imr.12276
- Cooper AM. Cell-mediated immune responses in tuberculosis. *Annu Rev Immunol.* (2009) 27:393–422. doi: 10.1146/annurev.immunol.021908.132703
- Lin PL, Flynn JL. CD8 T cells and *Mycobacterium tuberculosis* infection. *Semin Immunopathol.* (2015) 37:239–49. doi: 10.1007/s00281-015-0490-8
- Ottenhoff T. The knowns and unknowns of the immunopathogenesis of tuberculosis. *Int J Tuberc Lung Dis.* (2012) 16:1424–32. doi: 10.5588/ijtld.12.0479
- North RJ, Jung Y. Immunity to tuberculosis. *Annu Rev Immunol.* (2004) 22:599–623. doi: 10.1146/annurev.immunol.22.012703.104635
- Casadevall A. Antibody-based vaccine strategies against intracellular pathogens. *Curr Opin Immunol.* (2018) 53:74–80. doi: 10.1016/j.coi.2018.04.011
- Chan J, Mehta S, Bharrhan S, Chen Y, Achkar JM, Casadevall A, et al. The role of B cells and humoral immunity in *Mycobacterium tuberculosis* infection. *Semin Immunol.* (2014) 26:588–600. doi: 10.1016/j.smim.2014.10.005
- Acosta A, Lopez Y, Nor NM, Pando RH, Alvarez N, Sarmiento ME, et al. The role of antibodies in the defense against tuberculosis. *Tuberculosis.* (2013) 86:191–7. doi: 10.5772/53950
- Casadevall A. Antibody-mediated immunity against intracellular pathogens: two-dimensional thinking comes full circle. *Infect Immun.* (2003) 71:4225–4228. doi: 10.1128/IAI.71.8.4225-4228.2003
- Janeway CA, Capra JD, Travers P, Walport M. *Immunobiology: The Immune System in Health and Disease*. New York, NY: Garland Science. (1999). p. 884.
- Moore BB, Moore TA, Toews GB. Role of T- and B-lymphocytes in pulmonary host defences. *Eur Respir J.* (2001) 18:846–56. doi: 10.1183/09031936.01.00229001
- Lu LL, Suscovich TJ, Fortune SM, Alter G. Beyond binding: antibody effector functions in infectious diseases. *Nat Rev Immunol.* (2018) 18:46–61. doi: 10.1038/nri.2017.106

43. Li H, Javid B. Antibodies and tuberculosis: finally coming of age? *Nat Rev Immunol.* (2018) 18:591–6. doi: 10.1038/s41577-018-0028-0
44. Yang X, Brunham RC. Gene knockout B cell-deficient mice demonstrate that B cells play an important role in the initiation of T cell responses to Chlamydia trachomatis (mouse pneumonitis) lung infection. *J Immunol.* (1998) 161:1439–46.
45. Su H, Feilzer K, Caldwell HD, Morrison RP. Chlamydia trachomatis genital tract infection of antibody-deficient gene knockout mice. *Infect Immun.* (1997) 65:1993–9. doi: 10.1128/IAI.65.6.1993-1999.1997
46. Nanton MR, Way SS, Shlomchik MJ, McSorley SJ. Cutting edge: B cells are essential for protective immunity against Salmonella independent of antibody secretion. *J Immunol.* (2012) 189:5503–5507. doi: 10.4049/jimmunol.1201413
47. Lin FYC, Ho VA, Khiem HB, Trach DD, Bay PV, Thanh TC, et al. The efficacy of a Salmonella typhi Vi conjugate vaccine in two-to-five-year-old children. *N Engl J Med.* (2001) 344:1263–9. doi: 10.1056/NEJM200104263441701
48. Mastroeni P, Simmons C, Fowler R, Hormaeche CE, Dougan G. Igh-6(-/-) (B-cell-deficient) mice fail to mount solid acquired resistance to oral challenge with virulent Salmonella enterica serovar typhimurium and show impaired Th1 T-cell responses to Salmonella antigens. *Infect Immun.* (2000) 68:46–53. doi: 10.1128/IAI.68.1.46-53.2000
49. Li JS, Winslow GM. Survival, replication, and antibody susceptibility of Ehrlichia chaffeensis outside of host cells. *Infect Immun.* (2003) 71:4229–37. doi: 10.1128/IAI.71.8.4229-4237.2003
50. Woelbing F, Kostka SL, Moelle K, Belkaid Y, Sunderkoetter C, Verbeek S, et al. Uptake of Leishmania major by dendritic cells is mediated by Fcγ receptors and facilitates acquisition of protective immunity. *J Exp Med.* (2006) 203:177–88. doi: 10.1084/jem.20052288
51. Gibson-Corley KN, Boggiatto PM, Bockenstedt MM, Petersen CA, Waldschmidt TJ, Jones DE. Promotion of a functional B cell germinal center response after Leishmania species co-infection is associated with lesion resolution. *Am J Pathol.* (2012) 180:2009–17. doi: 10.1016/j.ajpath.2012.01.012
52. Rodriguez-Pinto D, Saravia NG, McMahon-Pratt D. CD4 T cell activation by B cells in human Leishmania (Viannia) infection. *BMC Infect Dis.* (2014) 14:108. doi: 10.1186/1471-2334-14-108
53. Casadevall A, Pirofski L. Insights into mechanisms of antibody-mediated immunity from studies with Cryptococcus neoformans. *Curr Mol Med.* (2005) 5:421–33. doi: 10.2174/1566524054022567
54. Szymczak WA, Davis MJ, Lundy SK, Dufaud C, Olszewski M, Pirofski LA. X-linked immunodeficient mice exhibit enhanced susceptibility to Cryptococcus neoformans infection. *mBio.* (2013) 4:e00265–13. doi: 10.1128/mBio.00265-13
55. Zhang G, Peng Y, Schoenlaub L, Elliott A, Mitchell W, Zhang Y. Formalin-inactivated Coxiella burnetii phase I vaccine-induced protection depends on B cells to produce protective IgM and IgG. *Infect Immun.* (2013) 81:2112–22. doi: 10.1128/IAI.00297-13
56. Bermejo DA, Jackson SW, Gorosito-Serran M, Acosta-Rodriguez EV, Amezcua-Vesely MC, Sather BD, et al. Trypanosoma cruzi trans-sialidase initiates a program independent of the transcription factors RORγ and Ahr that leads to IL-17 production by activated B cells. *Nat Immunol.* (2013) 14:514–22. doi: 10.1038/ni.2569
57. Culkin SJ, Rhinehart-Jones T, Elkins KL. A novel role for B cells in early protective immunity to an intracellular pathogen, Francisella tularensis strain LVS. *J Immunol.* (1997) 158:3277–84.
58. Langhorne J, Cross C, Seixas E, Li C, von der Weid T. A role for B cells in the development of T cell helper function in a malaria infection in mice. *Proc Natl Acad Sci USA.* (1998) 95:1730–4. doi: 10.1073/pnas.95.4.1730
59. Tran AC, Kim M, Reljic R. Emerging themes for the role of antibodies in tuberculosis. *Immune Netw.* (2019) 19:e24. doi: 10.4110/in.2019.19.e24
60. Loxton AG. B cells and their regulatory functions during tuberculosis: latency and active disease. *Mol Immunol.* (2019) 111:145–51. doi: 10.1016/j.molimm.2019.04.012
61. Dyatlov AV, Apt AS, Linge IA. B lymphocytes in anti-mycobacterial immune responses: pathogenesis or protection? *Tuberculosis.* (2019) 114:1–8. doi: 10.1016/j.tube.2018.10.011
62. Rao M, Valentini D, Poiret T, Dodoo E, Parida S, Zumla A, et al. B in TB: B cells as mediators of clinically relevant immune responses in tuberculosis. *Clin Infect Dis.* (2015) 61:S225–34. doi: 10.1093/cid/civ614
63. Abebe F, Bjune G. The protective role of antibody responses during Mycobacterium tuberculosis infection. *Clin Exp Immunol.* (2009) 157:235–43. doi: 10.1111/j.1365-2249.2009.03967.x
64. Glatman-Freedman A. The role of antibody-mediated immunity in defense against Mycobacterium tuberculosis: advances toward a novel vaccine strategy. *Tuberculosis.* (2006) 86:191–7. doi: 10.1016/j.tube.2006.01.008
65. Glatman-Freedman A, Casadevall A. Serum therapy for tuberculosis revisited: reappraisal of the role of antibody-mediated immunity against Mycobacterium tuberculosis. *Clin Microbiol Rev.* (1998) 11:514–32. doi: 10.1128/CMR.11.3.514
66. Khera AK, Afkhami S, Lai R, Jeyanthan M, Zganiacz A, Mandur T, et al. Role of B Cells in Mucosal Vaccine-Induced Protective CD8+ T Cell Immunity against Pulmonary Tuberculosis. *J Immunol.* (2015) 195:2900–7. doi: 10.4049/jimmunol.1500981
67. Kozakiewicz L, Chen Y, Xu J, Wang Y, Dunussi-Joannopoulos K, Ou Q, et al. B cells regulate neutrophilia during Mycobacterium tuberculosis infection and BCG vaccination by modulating the interleukin-17 response. *PLoS Pathog.* (2013) 9:e1003472. doi: 10.1371/journal.ppat.1003472
68. Torrado E, Fountain JJ, Robinson RT, Martino CA, Pearl JE, Rangel-Moreno J, et al. Differential and site specific impact of B cells in the protective immune response to Mycobacterium tuberculosis in the mouse. *PLoS ONE.* (2013) 8:e61681. doi: 10.1371/journal.pone.0061681
69. Maglione PJ, Xu J, Chan J. B cells moderate inflammatory progression and enhance bacterial containment upon pulmonary challenge with Mycobacterium tuberculosis. *J Immunol.* (2007) 178:7222–34. doi: 10.4049/jimmunol.178.11.7222
70. Turner J, Frank A, Brooks J, Gonzalez-Juarrero M, Orme I. The progression of chronic tuberculosis in the mouse does not require the participation of B lymphocytes or interleukin-4. *Exp Gerontol.* (2001) 36:537–45. doi: 10.1016/S0531-5565(00)00257-6
71. Bosio CM, Gardner D, Elkins KL. Infection of B cell-deficient mice with CDC 1551, a clinical isolate of Mycobacterium tuberculosis: delay in dissemination and development of lung pathology. *J Immunol.* (2000) 164:6417–25. doi: 10.4049/jimmunol.164.12.6417
72. Johnson C, Cooper A, Frank A, Bonorino C, Wysoki L, Orme I. Mycobacterium tuberculosis aerogenic rechallenge infections in B cell-deficient mice. *Tuber Lung Dis.* (1997) 78:257–61. doi: 10.1016/S0962-8479(97)90006-X
73. Vordermeier H, Venkataprasad N, Harris D, Ivanyi J. Increase of tuberculous infection in the organs of B cell-deficient mice. *Clin Exp Immunol.* (1996) 106:312–6. doi: 10.1046/j.1365-2249.1996.d01-845.x
74. Phuah J, Wong EA, Gideon HP, Maiello P, Coleman MT, Hendricks MR, et al. Effects of B cell depletion on early Mycobacterium tuberculosis infection in cynomolgus macaques. *Infect Immun.* (2016) 84:1301–11. doi: 10.1128/IAI.00083-16
75. Casadevall A, Scharff MD. Return to the past: the case for antibody-based therapies in infectious diseases. *Clin Infect Dis.* (1995) 21:150–61. doi: 10.1093/clinids/21.1.150
76. Li H, Wang XX, Wang B, Fu L, Liu G, Lu Y, et al. Latently and uninfected healthcare workers exposed to TB make protective antibodies against Mycobacterium tuberculosis. *Proc Natl Acad Sci USA.* (2017) 114:5023–8. doi: 10.1073/pnas.1611776114
77. Guirado E, Amat I, Gil O, Díaz J, Arcos V, Caceres N, et al. Passive serum therapy with polyclonal antibodies against Mycobacterium tuberculosis protects against post-chemotherapy relapse of tuberculosis infection in SCID mice. *Microb Infect.* (2006) 8:1252–9. doi: 10.1016/j.micinf.2005.12.004
78. Roy E, Stavropoulos E, Brennan J, Coade S, Grigorieva E, Walker B, et al. Therapeutic efficacy of high-dose intravenous immunoglobulin in Mycobacterium tuberculosis infection in mice. *Infect Immun.* (2005) 73:6101–9. doi: 10.1128/IAI.73.9.6101-6109.2005
79. Glatman-Freedman A, Martin JM, Riska PF, Bloom BR, Casadevall A. Monoclonal antibodies to surface antigens of Mycobacterium tuberculosis and their use in a modified enzyme-linked immunosorbent spot assay for detection of mycobacteria. *J Clin Microbiol.* (1996) 34:2795–802. doi: 10.1128/JCM.34.11.2795-2802.1996
80. Teitelbaum R, Glatman-Freedman A, Chen B, Robbins JB, Unanue E, Casadevall A, et al. A mAb recognizing a surface antigen of Mycobacterium

- tuberculosis enhances host survival. *Proc Natl Acad Sci USA*. (1998) 95:15688–93. doi: 10.1073/pnas.95.26.15688
81. Tran AC, Diogo GR, Paul MJ, Copland A, Hart P, Mehta N, et al. Mucosal therapy of multi-drug resistant tuberculosis with IgA and interferon- $\gamma$ . *Front Immunol*. (2020) 11:582833. doi: 10.3389/fimmu.2020.582833
  82. Zimmermann N, Thormann V, Hu B, Köhler A, Imai-Matsushima A, Loch C, et al. Human isotype-dependent inhibitory antibody responses against *Mycobacterium tuberculosis*. *EMBO Mol Med*. (2016) 8:1325–39. doi: 10.15252/emmm.201606330
  83. Balu S, Reljic R, Lewis MJ, Pleass RJ, McIntosh R, van Kooten C, et al. A novel human IgA monoclonal antibody protects against tuberculosis. *J Immunol*. (2011) 186:3113–9. doi: 10.4049/jimmunol.1003189
  84. Buccheri S, Reljic R, Caccamo N, Meraviglia S, Ivanyi J, Salerno A, et al. Prevention of the post-chemotherapy relapse of tuberculosis infection by combined immunotherapy. *Tuberculosis*. (2009) 89:91–4. doi: 10.1016/j.tube.2008.09.001
  85. López Y, Yero D, Falero-Diaz G, Olivares N, Sarmiento ME, Sifontes S, et al. Induction of a protective response with an IgA monoclonal antibody against *Mycobacterium tuberculosis* 16 kDa protein in a model of progressive pulmonary infection. *Int J Med Microbiol*. (2009) 299:447–52. doi: 10.1016/j.ijmm.2008.10.007
  86. Buccheri S, Reljic R, Caccamo N, Ivanyi J, Singh M, Salerno A, et al. IL-4 depletion enhances host resistance and passive IgA protection against tuberculosis infection in BALB/c mice. *Eur J Immunol*. (2007) 37:729–37. doi: 10.1002/eji.200636764
  87. Reljic R, Clark S, Williams A, Falero-Diaz G, Singh M, Challacombe S, et al. Intranasal IFN $\gamma$  extends passive IgA antibody protection of mice against *Mycobacterium tuberculosis* lung infection. *Clin Exp Immunol*. (2006) 143:467–73. doi: 10.1111/j.1365-2249.2006.03012.x
  88. Williams A, Reljic R, Naylor I, Clark SO, Falero-Diaz G, Singh M, et al. Passive protection with immunoglobulin A antibodies against tuberculosis early infection of the lungs. *Immunology*. (2004) 111:328–33. doi: 10.1111/j.1365-2567.2004.01809.x
  89. Hamasur B, Haile M, Pawlowski A, Schröder U, Källénus G, Svenson S. A mycobacterial lipoarabinomannan specific monoclonal antibody and its F(ab')<sub>2</sub> fragment prolong survival of mice infected with *Mycobacterium tuberculosis*. *Clin Exp Immunol*. (2004) 138:30–8. doi: 10.1111/j.1365-2249.2004.02593.x
  90. Chambers MA, Gavier-Widen D, Glyn Hewinson R. Antibody bound to the surface antigen MPB83 of *Mycobacterium bovis* enhances survival against high dose and low dose challenge. *FEMS Immunol Med Microbiol*. (2004) 41:93–100. doi: 10.1016/j.femsim.2004.01.004
  91. Pethe K, Alonso S, Biet F, Delogu G, Brennan MJ, Loch C, et al. The heparin-binding haemagglutinin of *M. tuberculosis* is required for extrapulmonary dissemination. *Nature*. (2001) 412:190–4. doi: 10.1038/35084083
  92. Chen XF, Wang WF, Zhang YD, Zhao W, Wu J, Chen TX. Clinical characteristics and genetic profiles of 174 patients with X-linked agammaglobulinemia: report from Shanghai, China (2000–2015). *Medicine*. (2016) 95:e4544. doi: 10.1097/MD.0000000000004544
  93. Dogru D, Kiper N, Özçelik U, Yalçın E, Tezcan I. Tuberculosis in children with congenital immunodeficiency syndromes. *Tuberk Toraks*. (2010) 58:59–63.
  94. Alkadi A, Alduaiji N, Alrehaily A. Risk of tuberculosis reactivation with rituximab therapy. *Int J Health Sci*. (2017) 11:41–4.
  95. Kimby E. Tolerability and safety of rituximab (MabThera). *Cancer Treat Rev*. (2005) 31:456–473. doi: 10.1016/j.ctrv.2005.05.007
  96. de L. Costello A, Kumar A, Narayan V, Akbar M, Ahmed S, Abou-Zeid C, et al. Does antibody to mycobacterial antigens, including lipoarabinomannan, limit dissemination in childhood tuberculosis? *Trans R Soc Trop Med Hyg*. (1992) 86:686–92. doi: 10.1016/0035-9203(92)90192-F
  97. Donald PR, Marais BJ, FABarry, Clifton E, 3rd, Barry CE, 3rd. Age and the epidemiology and pathogenesis of tuberculosis. *Lancet*. (2010) 375:1852–4. doi: 10.1016/S0140-6736(10)60580-6
  98. Fairchok MP, Rouse JH, Morris SL. Age-dependent humoral responses of children to mycobacterial antigens. *Clin Diagn Lab Immunol*. (1995) 2:443–7. doi: 10.1128/CDLI.2.4.443-447.1995
  99. Bothamley G, Udani P, Rudd R, Festenstein F, Ivanyi J. Humoral response to defined epitopes of tubercle bacilli in adult pulmonary and child tuberculosis. *Eur J Clin Microbiol Infect Dis*. (1988) 7:639–45. doi: 10.1007/BF01964242
  100. Logan E, Luabeya AKK, Mulenga H, Mrdjen D, Ontong C, Cunningham AF, et al. Elevated IgG responses in infants are associated with reduced prevalence of *Mycobacterium tuberculosis* infection. *Front Immunol*. (2018) 9:1529. doi: 10.3389/fimmu.2018.01529
  101. Fletcher HA, Snowden MA, Landry B, Rida W, Satti I, Harris SA, et al. T-cell activation is an immune correlate of risk in BCG vaccinated infants. *Nat Commun*. (2016) 7:11290. doi: 10.1038/ncomms11290
  102. Ziegenbalg A, Prados-Rosales R, Jenny-Avital ER, Kim RS, Casadevall A, Achkar JM. Immunogenicity of mycobacterial vesicles in humans: identification of a new tuberculosis antibody biomarker. *Tuberculosis*. (2013) 93:448–55. doi: 10.1016/j.tube.2013.03.001
  103. Gupta S, Bhatia R, Datta K. Serological diagnosis of childhood tuberculosis by estimation of mycobacterial antigen 60-specific immunoglobulins in the serum. *Tuber Lung Dis*. (1997) 78:21–7. doi: 10.1016/S0962-8479(97)90012-5
  104. Bothamley GH. Serological diagnosis of tuberculosis. *Eur Respir J Suppl*. (1995) 20:676s–88s.
  105. Sada D E, Ferguson LE, Daniel TM. An ELISA for the serodiagnosis of tuberculosis using a 30,000-Da native antigen of *Mycobacterium tuberculosis*. *J Infect Dis*. (1990) 162:928–31. doi: 10.1093/infdis/162.4.928
  106. Slight SR, Rangel-Moreno J, Gopal R, Lin Y, Fallert Junecko BA, Mehra S, et al. CXCR5(+) T helper cells mediate protective immunity against tuberculosis. *J Clin Invest*. (2013) 123:712–26. doi: 10.1172/JCI65728
  107. Kondratieva E, Logunova N, Majorov K, Averbakh M, Apt A. Host genetics in granuloma formation: human-like lung pathology in mice with reciprocal genetic susceptibility to *M. tuberculosis* and *M. avium*. *PLoS ONE*. (2010) 5:e10515. doi: 10.1371/journal.pone.0010515
  108. Khader SA, Rangel-Moreno J, Fountain JJ, Martino CA, Reiley WW, Pearl JE, et al. In a murine tuberculosis model, the absence of homeostatic chemokines delays granuloma formation and protective immunity. *J Immunol*. (2009) 183:8004–14. doi: 10.4049/jimmunol.0901937
  109. Kahnert A, Höpken UE, Stein M, Banderhann S, Lipp M, Kaufmann SH. *Mycobacterium tuberculosis* triggers formation of lymphoid structure in murine lungs. *J Infect Dis*. (2007) 195:46–54. doi: 10.1086/508894
  110. Ulrichs T, Kosmiadi GA, Jörg S, Pradl L, Titukhina M, Mishenko V, et al. Differential organization of the local immune response in patients with active cavitary tuberculosis or with nonprogressive tuberculoma. *J Infect Dis*. (2005) 192:89–97. doi: 10.1086/430621
  111. Gonzalez-Juarrero M, Turner OC, Turner J, Marietta P, Brooks JV, Orme IM. Temporal and spatial arrangement of lymphocytes within lung granulomas induced by aerosol infection with *Mycobacterium tuberculosis*. *Infect Immun*. (2001) 69:1722–8. doi: 10.1128/IAI.69.3.1722-1728.2001
  112. Phuah JY, Mattila JT, Lin PL, Flynn JL. Activated B cells in the granulomas of nonhuman primates infected with *Mycobacterium tuberculosis*. *Am J Pathol*. (2012) 181:508–14. doi: 10.1016/j.ajpath.2012.05.009
  113. Tsai MC, Chakravarty S, Zhu G, Xu J, Tanaka K, Koch C, et al. Characterization of the tuberculous granuloma in murine and human lungs: cellular composition and relative tissue oxygen tension. *Cell Microbiol*. (2006) 8:218–32. doi: 10.1111/j.1462-5822.2005.00612.x
  114. Ulrichs T, Kosmiadi GA, Trusov V, Jörg S, Pradl L, Titukhina M, et al. Human tuberculous granulomas induce peripheral lymphoid follicle-like structures to orchestrate local host defence in the lung. *J Pathol*. (2004) 204:217–28. doi: 10.1002/path.1628
  115. Choreño-Parra JA, Bobba S, Rangel-Moreno J, Ahmed M, Mehra S, Rosa B, et al. *Mycobacterium tuberculosis* HN878 infection induces human-Like B-cell follicles in mice. *J Infect Dis*. (2020) 221:1636–46. doi: 10.1093/infdis/jiz663
  116. Joosten SA, van Meijgaarden KE, Del Nonno F, Baiocchi A, Petrone L, Vanini V, et al. Patients with tuberculosis have a dysfunctional circulating B-cell compartment, which normalizes following successful treatment. *PLoS Pathog*. (2016) 12:e1005687. doi: 10.1371/journal.ppat.1005687
  117. Marin ND, Dunlap MD, Kaushal D, Khader SA. Friend or foe: the protective and pathological roles of inducible bronchus-associated lymphoid tissue in pulmonary diseases. *J Immunol*. (2019) 202:2519–26. doi: 10.4049/jimmunol.1801135



118. Pitzalis C, Jones GW, Bombardieri M, Jones SA. Ectopic lymphoid-like structures in infection, cancer and autoimmunity. *Nat Rev Immunol.* (2014) 14:447–62. doi: 10.1038/nri3700
119. Aloisi F, Pujol-Borrell R. Lymphoid neogenesis in chronic inflammatory diseases. *Nat Rev Immunol.* (2006) 6:205–17. doi: 10.1038/nri1786
120. Kondratieva T, Linge I, Kondratieva E, Dyatlov A, Drutskaya M, Zvartsev R, et al. Formation of compact aggregates of B-lymphocytes in lung tissue during mycobacterial infection in mice depends on TNF production by these cells and is not an element of the host's immunological protection. *Biochemistry.* (2014) 79:1358–62. doi: 10.1134/S0006297914120098
121. Zhang M, Wang Z, Graner MW, Yang L, Liao M, Yang Q, et al. B cell infiltration is associated with the increased IL-17 and IL-22 expression in the lungs of patients with tuberculosis. *Cell Immunol.* (2011) 270:217–23. doi: 10.1016/j.cellimm.2011.05.009
122. Dunlap MD, Prince OA, Rangel-Moreno J, Thomas KA, Scordo JM, Torrelles JB, et al. Formation of lung inducible bronchus associated lymphoid tissue is regulated by *Mycobacterium tuberculosis* expressed determinants. *Front Immunol.* (2020) 11:1325. doi: 10.3389/fimmu.2020.01325
123. Corominas M, Cardona V, Gonzalez L, Cayla J, Rufi G, Mestre M, et al. B-lymphocytes and co-stimulatory molecules in *Mycobacterium tuberculosis* infection. *Int J Tuberc Lung Dis.* (2004) 8:98–105.
124. Chowdhury RR, Vallania F, Yang Q, Angel CJL, Darboe F, Penn-Nicholson A, et al. A multi-cohort study of the immune factors associated with *M. tuberculosis* infection outcomes. *Nature.* (2018) 560:644–8. doi: 10.1038/s41586-018-0439-x
125. Hernandez J, Velazquez C, Valenzuela O, Robles-Zepeda R, Ruiz-Bustos E, Navarro M, et al. Low number of peripheral blood B lymphocytes in patients with pulmonary tuberculosis. *Immunol Invest.* (2010) 39:197–205. doi: 10.3109/08820130903586346
126. Wu Y, Zhang S, Peng W, Li K, Li K, Jiang J, et al. Changes in lymphocyte subsets in the peripheral blood of patients with active pulmonary tuberculosis. *J Int Med Res.* (2009) 37:1742–9. doi: 10.1177/147323000903700610
127. Barcelos W, Martins-Filho OA, Guimarães, Tânia Mara Pinto Dabés, Oliveira MHP, Spíndola-de-Miranda S, Carvalho BN, et al. Peripheral blood mononuclear cells immunophenotyping in pulmonary tuberculosis patients before and after treatment. *Microbiol Immunol.* (2006) 50:597–605. doi: 10.1111/j.1348-0421.2006.tb03834.x
128. Linge I, Dyatlov A, Kondratieva E, Avdienko V, Apt A, Kondratieva T. B-lymphocytes forming follicle-like structures in the lung tissue of tuberculosis-infected mice: dynamics, phenotypes and functional activity. *Tuberculosis.* (2017) 102:16–23. doi: 10.1016/j.tube.2016.11.005
129. Du Plessis WJ, Keyser A, Walzl G, Loxton AG. Phenotypic analysis of peripheral B cell populations during *Mycobacterium tuberculosis* infection and disease. *J Inflamm.* (2016) 13:23. doi: 10.1186/s12950-016-0133-4
130. Lundy SK, Klinker MW, Fox DA. Killer B lymphocytes and their fas ligand positive exosomes as inducers of immune tolerance. *Front Immunol.* (2015) 6:122. doi: 10.3389/fimmu.2015.00122
131. Abreu MT, Carvalheiro H, Rodrigues-Sousa T, Domingos A, Segorbe-Luis A, Rodrigues-Santos P, et al. Alterations in the peripheral blood B cell subpopulations of multidrug-resistant tuberculosis patients. *Clin Exp Med.* (2014) 14:423–9. doi: 10.1007/s10238-013-0258-1
132. Zhang M, Zeng G, Yang Q, Zhang J, Zhu X, Chen Q, et al. Anti-tuberculosis treatment enhances the production of IL-22 through reducing the frequencies of regulatory B cell. *Tuberculosis (Edinb).* (2014) 94:238–44. doi: 10.1016/j.tube.2013.12.003
133. Lundy SK. Killer B lymphocytes: the evidence and the potential. *Inflamm Res.* (2009) 58:345–57. doi: 10.1007/s00011-009-0014-x
134. Lyashchenko KP, Vordermeier HM, Waters WR. Memory B cells and tuberculosis. *Vet Immunol Immunopathol.* (2020) 221:110016. doi: 10.1016/j.vetimm.2020.110016
135. Moir S, Ho J, Malaspina A, Wang W, DiPoto AC, O'Shea MA, et al. Evidence for HIV-associated B cell exhaustion in a dysfunctional memory B cell compartment in HIV-infected viremic individuals. *J Exp Med.* (2008) 205:1797–805. doi: 10.1084/jem.20072683
136. Moore DK, Leisching GR, Snyders CI, Gutschmidt A, Van Rensburg IC, Loxton AG, et al. Immunoglobulin profile and B-cell frequencies are altered with changes in the cellular micro-environment independent of the stimulation conditions. *BioRxiv.* (2019). doi: 10.1101/818153
137. Zhang M, Zheng X, Zhang J, Zhu Y, Zhu X, Liu H, et al. CD19 CD1d CD5 B cell frequencies are increased in patients with tuberculosis and suppress Th17 responses. *Cell Immunol.* (2012) 274:89–97. doi: 10.1016/j.cellimm.2012.01.007
138. van Rensburg IC, Loxton AG. Killer (FASL regulatory) B cells are present during latent TB and are induced by BCG stimulation in participants with and without latent tuberculosis. *Tuberculosis.* (2018) 108:114–7. doi: 10.1016/j.tube.2017.11.010
139. van Rensburg IC, Kleynhans L, Keyser A, Walzl G, Loxton AG. B-cells with a FasL expressing regulatory phenotype are induced following successful anti-tuberculosis treatment. *Immunity Inflamm Dis.* (2017) 5:57–67. doi: 10.1002/iid3.140
140. van Rensburg IC, Wagman C, Stanley K, Beltran C, Ronacher K, Walzl G, et al. Successful TB treatment induces B-cells expressing FASL and IL5RA mRNA. *Oncotarget.* (2017) 8:2037–43. doi: 10.18632/oncotarget.12184
141. Dubois Cauwelaert N, Baldwin SL, Orr MT, Desbien AL, Gage E, Hofmeyer KA, et al. Antigen presentation by B cells guides programming of memory CD4 T-cell responses to a TLR4-agonist containing vaccine in mice. *Eur J Immunol.* (2016) 46:2719–29. doi: 10.1002/eji.201646399
142. Lund FE, Randall TD. Effector and regulatory B cells: modulators of CD4 T cell immunity. *Nat Rev Immunol.* (2010) 10:236–47. doi: 10.1038/nri2729
143. Bouaziz JD, Yanaba K, Venturi GM, Wang Y, Tisch RM, Poe JC, et al. Therapeutic B cell depletion impairs adaptive and autoreactive CD4+ T cell activation in mice. *Proc Natl Acad Sci USA.* (2007) 104:20878–83. doi: 10.1073/pnas.0709205105
144. Andersen CS, Dietrich J, Agger EM, Lycke NY, Lovgren K, Andersen P. The combined CTA1-DD/ISCOMs vector is an effective intranasal adjuvant for boosting prior *Mycobacterium bovis* BCG immunity to *Mycobacterium tuberculosis*. *Infect Immun.* (2007) 75:408–16. doi: 10.1128/IAI.01290-06
145. Helgeby A, Robson NC, Donachie AM, Beackock-Sharp H, Lovgren K, Schon K, et al. The combined CTA1-DD/ISCOM adjuvant vector promotes priming of mucosal and systemic immunity to incorporated antigens by specific targeting of B cells. *J Immunol.* (2006) 176:3697–706. doi: 10.4049/jimmunol.176.6.3697
146. Hon H, Oran A, Brocker T, Jacob J. B lymphocytes participate in cross-presentation of antigen following gene gun vaccination. *J Immunol.* (2005) 174:5233–242. doi: 10.4049/jimmunol.174.9.5233
147. du Plessis WJ, Kleynhans L, du Plessis N, Stanley K, Malherbe ST, Maasdorp E, et al. The functional response of B cells to antigenic stimulation: a preliminary report of latent tuberculosis. *PLoS One.* (2016) 11:e0152710. doi: 10.1371/journal.pone.0152710
148. Shen H, Chen ZW. The crucial roles of Th17-related cytokines/signal pathways in *M. tuberculosis* infection. *Cell Molecular Immunol.* (2018) 15:216–225. doi: 10.1038/cmi.2017.128
149. Stephen-Victor E, Sharma VK, Das M, Karnam A, Saha C, Lecerf M, et al. IL-1β, but not programmed death-1 and programmed death ligand pathway, is critical for the human Th17 response to *Mycobacterium tuberculosis*. *Front Immunol.* (2016) 7:465. doi: 10.3389/fimmu.2016.00465
150. da Silva MV, Tiburcio MGS, Machado JR, Silva DAA, Rodrigues DBR, Rodrigues V, et al. Complexity and controversies over the cytokine profiles of T helper cell subpopulations in tuberculosis. *J Immunol Res.* (2015) 2015:639107. doi: 10.1155/2015/639107
151. Leal IS, Smedegard B, Andersen P, Appelberg R. Interleukin-6 and interleukin-12 participate in induction of a type 1 protective T-cell response during vaccination with a tuberculosis subunit vaccine. *Infect Immun.* (1999) 67:5747–54. doi: 10.1128/IAI.67.11.5747-5754.1999
152. Zhang X, Kiapour N, Kapoor S, Khan T, Thamilarasam M, Tao Y, et al. IL-11 Induces encephalitogenic Th17 cells in multiple sclerosis and experimental autoimmune encephalomyelitis. *J Immunol.* (2019) 203:1142–50. doi: 10.4049/jimmunol.1900311
153. Zhang X, Tao Y, Chopra M, Dujmovic-Basuroski I, Jin J, Tang Y, et al. IL-11 Induces Th17 cell responses in patients with early relapsing-remitting multiple sclerosis. *J Immunol.* (2015) 194:5139–49. doi: 10.4049/jimmunol.1401680
154. Olsen A, Chen Y, Ji Q, Zhu G, De Silva AD, Vilcheze C, et al. Targeting *Mycobacterium tuberculosis* tumor necrosis factor alpha-downregulating



- genes for the development of antituberculous vaccines. *mBio*. (2016) 7:e01023–15. doi: 10.1128/mBio.01023-15
155. Cavalcanti YVN, Brelaz MCA, Neves, Juliana Kelle de Andrade Lemoine, Ferraz JC, Pereira VRA. Role of TNF- $\alpha$ , IFN- $\gamma$ , and IL-10 in the development of pulmonary tuberculosis. *Pulmonary Med.* (2012) 2012:745483. doi: 10.1155/2012/745483
  156. Lin PL, Plessner HL, Voitenok NN, Flynn JL. Tumor necrosis factor and tuberculosis. *J Invest Dermatol Symp Proc.* (2007) 12:22–5. doi: 10.1038/sj.jidsymp.5650027
  157. Flynn JL, Chan J. What's good for the host is good for the bug. *Trends Microbiol.* (2005) 13:98–102. doi: 10.1016/j.tim.2005.01.005
  158. Moreira-Teixeira L, Redford PS, Stavropoulos E, Ghilardi N, Maynard CL, Weaver CT, et al. T cell-derived IL-10 impairs host resistance to *Mycobacterium tuberculosis* infection. *J Immunol.* (2017) 199:613–23. doi: 10.4049/jimmunol.1601340
  159. Abdalla AE, Lambert N, Duan X, Xie J. Interleukin-10 family and tuberculosis: an old story renewed. *Int J Biol Sci.* (2016) 12:710–17. doi: 10.7150/ijbs.13881
  160. Redford P, Murray P, O'garra A. The role of IL-10 in immune regulation during *M. tuberculosis* infection. *Mucosal Immunol.* (2011) 4:261–70. doi: 10.1038/mi.2011.7
  161. Higgins DM, Sanchez-Campillo J, Rosas-Taraco AG, Lee EJ, Orme IM, Gonzalez-Juarrero M. Lack of IL-10 alters inflammatory and immune responses during pulmonary *Mycobacterium tuberculosis* infection. *Tuberculosis.* (2009) 89:149–57. doi: 10.1016/j.tube.2009.01.001
  162. Kimuda SG, Andia-Biraro I, Sebina I, Egesa M, Nalwoga A, Smith SG, et al. *Mycobacterium tuberculosis* infection is associated with increased B cell responses to unrelated pathogens. *Sci Rep.* (2020) 10:14324. doi: 10.1038/s41598-020-71044-4
  163. Lu LL, Smith MT, Krystle K, Luedemann C, Suscovich TJ, Grace PS, et al. IFN- $\gamma$ -independent immune markers of *Mycobacterium tuberculosis* exposure. *Nat Med.* (2019) 25:977–87. doi: 10.1038/s41591-019-0441-3
  164. Mave V, Chandrasekaran P, Chavan A, Shivakumar, Shri Vijay Bala Yogendra, Danasekaran K, Paradkar M, et al. Infection free “resisters” among household contacts of adult pulmonary tuberculosis. *PLoS ONE.* (2019) 14:e0218034. doi: 10.1371/journal.pone.0218034
  165. Seshadri C, Sedaghat N, Campo M, Peterson G, Wells RD, Olson GS, et al. Transcriptional networks are associated with resistance to *Mycobacterium tuberculosis* infection. *PLoS ONE.* (2017) 12:e0175844. doi: 10.1371/journal.pone.0175844
  166. Hanifa Y, Grant A, Lewis J, Corbett E, Fielding K, Churchyard G. Prevalence of latent tuberculosis infection among gold miners in South Africa. *Int J Tuberc Lung Dis.* (2009) 13:39–46.
  167. Kaipilyawar V, Salgame P. Infection resisters: targets of new research for uncovering natural protective immunity against *Mycobacterium tuberculosis*. *F1000Research.* (2019) 8:F1000 Faculty Rev-1698. doi: 10.12688/f1000research.19805.1
  168. Cobat A, Gallant CJ, Simkin L, Black GF, Stanley K, Hughes J, et al. Two loci control tuberculin skin test reactivity in an area hyperendemic for tuberculosis. *J Exp Med.* (2009) 206:2583–91. doi: 10.1084/jem.20090892
  169. Chin ST, Ignatius J, Suraiya S, Tye GJ, Sarmiento ME, Acosta A, et al. Comparative study of IgA VH 3 gene usage in healthy TST- and TST population exposed to tuberculosis: deep sequencing analysis. *Immunology.* (2015) 144:302–11. doi: 10.1111/imm.12372
  170. Bothamley GH, Beck JS, Potts RC, Grange JM, Kardjito T, Ivanyi J. Specificity of antibodies and tuberculin response after occupational exposure to tuberculosis. *J Infect Dis.* (1992) 166:182–6. doi: 10.1093/infdis/166.1.182
  171. Encinales L, Zuñiga J, Granados-Montiel J, Yunis M, Granados J, Almeciga I, et al. Humoral immunity in tuberculin skin test anergy and its role in high-risk persons exposed to active tuberculosis. *Mol Immunol.* (2010) 47:1066–73. doi: 10.1016/j.molimm.2009.11.005
  172. Feris EJ, Encinales L, Awad C, Stern JN, Tabansky I, Jiménez-Alvarez L, et al. High levels of anti-tuberculin (IgG) antibodies correlate with the blocking of T-cell proliferation in individuals with high exposure to *Mycobacterium tuberculosis*. *Int J Infect Dis.* (2016) 43:21–4. doi: 10.1016/j.ijid.2015.12.004
  173. Kimuda SG, Andia-Biraro I, Egesa M, Bagaya BS, Raynes JG, Levin J, et al. Use of QuantiFERON®-TB Gold in-tube culture supernatants for measurement of antibody responses. *PLoS ONE.* (2017) 12:e0188396. doi: 10.1371/journal.pone.0188396
  174. Raja A, Baughman RP, Daniel TM. The detection by immunoassay of antibody to mycobacterial antigens and mycobacterial antigens in bronchoalveolar lavage fluid from patients with tuberculosis and control subjects. *Chest.* (1988) 94:133–7. doi: 10.1378/chest.94.1.133
  175. Demkow U, Białas-Chromiec B, Filewska M, Sobiecka M, Kuś J, Szturmowicz M, et al. Humoral immune response against mycobacterial antigens in bronchoalveolar fluid from tuberculosis patients. *J Physiol Pharmacol.* (2005) 56(Suppl. 4):79–84.
  176. Feng L, Li L, Liu Y, Qiao D, Li Q, Fu X, et al. B lymphocytes that migrate to tuberculous pleural fluid via the SDF-1/CXCR4 axis actively respond to antigens specific for *Mycobacterium tuberculosis*. *Eur J Immunol.* (2011) 41:3261–9. doi: 10.1002/eji.201141625
  177. Grosset J. *Mycobacterium tuberculosis* in the extracellular compartment: an underestimated adversary. *Antimicrob Agents Chemother.* (2003) 47:833–6. doi: 10.1128/AAC.47.3.833-836.2003
  178. Achkar JM, Chan J, Casadevall A. Role of B cells and antibodies in acquired immunity against *Mycobacterium tuberculosis*. *Cold Spring Harb Perspect Med.* (2014) 5:a018432. doi: 10.1101/cshperspect.a018432
  179. Schlesinger LS, Hull SR, Kaufman TM. Binding of the terminal mannose units of liparabinomannan from a virulent strain of *Mycobacterium tuberculosis* to human macrophages. *The J Immunol.* (1994) 152:4070–9.
  180. Chen T, Blanc C, Liu Y, Ishida E, Singer S, Xu J, et al. Capsular glycan recognition provides antibody-mediated immunity against tuberculosis. *J Clin Invest.* (2020) 130:1808–22. doi: 10.1172/JCI128459
  181. Chen T, Blanc C, Eder AZ, Prados-Rosales R, Souza ACO, Kim RS, et al. Association of human antibodies to arabinomannan with enhanced mycobacterial opsonophagocytosis and intracellular growth reduction. *J Infect Dis.* (2016) 214:300–10. doi: 10.1093/infdis/jiw141
  182. Manivannan S, Rao VN, Ramanathan V. Role of complement activation and antibody in the interaction between *Mycobacterium tuberculosis* and human macrophages. *Indian J Exp Biol.* (2012) 50:542–50.
  183. Carroll MV, Lack N, Sim E, Krarup A, Sim RB. Multiple routes of complement activation by *Mycobacterium bovis* BCG. *Mol Immunol.* (2009) 46:3367–78. doi: 10.1016/j.molimm.2009.07.015
  184. Hetland G, Wiker HG, Høgåsen K, Hamasur B, Svenson SB, Harboe M. Involvement of antilipoarabinomannan antibodies in classical complement activation in tuberculosis. *Clin Diagn Lab Immunol.* (1998) 5:211–8. doi: 10.1128/CDLI.5.2.211-218.1998
  185. Lu LL, Chung AW, Rosebrock TR, Ghebremichael M, Yu WH, Grace PS, et al. A functional role for antibodies in tuberculosis. *Cell.* (2016) 167:433–43.e14. doi: 10.1016/j.cell.2016.08.072
  186. McEwan WA, Tam JC, Watkinson RE, Bidgood SR, Mallery DL, James LC. Intracellular antibody-bound pathogens stimulate immune signaling via the Fc receptor TRIM21. *Nat Immunol.* (2013) 14:327–36. doi: 10.1038/ni.2548
  187. Geijtenbeek TB, Gringhuis SI. An inside job for antibodies: tagging pathogens for intracellular sensing. *Nat Immunol.* (2013) 14:309–11. doi: 10.1038/ni.2574
  188. Maglione PJ, Xu J, Casadevall A, Chan J. Fc gamma receptors regulate immune activation and susceptibility during *Mycobacterium tuberculosis* infection. *J Immunol.* (2008) 180:3329–38. doi: 10.4049/jimmunol.180.5.3329
  189. de Valliere S, Abate G, Blazevic A, Heuertz RM, Hoft DF. Enhancement of innate and cell-mediated immunity by antimycobacterial antibodies. *Infect Immun.* (2005) 73:6711–20. doi: 10.1128/IAI.73.10.6711-6720.2005
  190. Casadevall A, Pirofski L. A new synthesis for antibody-mediated immunity. *Nat Immunol.* (2012) 13:21–8. doi: 10.1038/ni.2184
  191. Clynes R. Protective mechanisms of IVIG. *Curr Opin Immunol.* (2007) 19:646–51. doi: 10.1016/j.coi.2007.09.004
  192. Casadevall A, Pirofski L. A reappraisal of humoral immunity based on mechanisms of antibody-mediated protection against intracellular pathogens. *Adv Immunol.* (2006) 91:1–44. doi: 10.1016/S0065-2776(06)91001-3
  193. Casadevall A, Pirofski L. The damage-response framework of microbial pathogenesis. *Nat Rev Microbiol.* (2003) 1:17–24. doi: 10.1038/nrmicro732
  194. Kumar SK, Singh P, Sinha S. Naturally produced opsonizing antibodies restrict the survival of *Mycobacterium tuberculosis* in human

- macrophages by augmenting phagosome maturation. *Open Biol.* (2015) 5:150171. doi: 10.1098/rsob.150171
195. Fratti RA, Chua J, Vergne I, Deretic V. *Mycobacterium tuberculosis* glycosylated phosphatidylinositol causes phagosome maturation arrest. *Proc Natl Acad Sci USA.* (2003) 100:5437–42. doi: 10.1073/pnas.0737613100
  196. Malik ZA, Denning GM, Kusner DJ. Inhibition of Ca(2+) signaling by *Mycobacterium tuberculosis* is associated with reduced phagosome-lysosome fusion and increased survival within human macrophages. *J Exp Med.* (2000) 191:287–302. doi: 10.1084/jem.191.2.287
  197. Armstrong JA, Hart PD. Phagosome-lysosome interactions in cultured macrophages infected with virulent tubercle bacilli. Reversal of the usual nonfusion pattern and observations on bacterial survival. *J Exp Med.* (1975) 142:1–16. doi: 10.1084/jem.142.1.1
  198. Joller N, Weber SS, Muller AJ, Sporri R, Selchow P, Sander P, et al. Antibodies protect against intracellular bacteria by Fc receptor-mediated lysosomal targeting. *Proc Natl Acad Sci USA.* (2010) 107:20441–6. doi: 10.1073/pnas.1013827107
  199. Suga M, Tanaka F, Muranaka H, Nishikawa H, Ando M. Effect of antibacterial antibody on bactericidal activities of superoxide and lysosomal enzyme from alveolar macrophages in rabbits. *Respirology.* (1996) 1:127–32. doi: 10.1111/j.1440-1843.1996.tb00021.x
  200. Kang PB, Azad AK, Torrelles JB, Kaufman TM, Beharka A, Tibesar E, et al. The human macrophage mannose receptor directs *Mycobacterium tuberculosis* liparabinomannan-mediated phagosome biogenesis. *J Exp Med.* (2005) 202:987–99. doi: 10.1084/jem.20051239
  201. Torrelles JB, Azad AK, Schlesinger LS. Fine discrimination in the recognition of individual species of phosphatidyl-myo-inositol mannosides from *Mycobacterium tuberculosis* by C-type lectin pattern recognition receptors. *J Immunol.* (2006) 177:1805–16. doi: 10.4049/jimmunol.177.3.1805
  202. Joosten SA, van Meijgaarden KE, Arend SM, Prins C, Oftung F, Korsvold GE, et al. Mycobacterial growth inhibition is associated with trained innate immunity. *J Clin Invest.* (2018) 128:1837–51. doi: 10.1172/JCI97508
  203. Forrester MA, Wassall HJ, Hall LS, Cao H, Wilson HM, Barker RN, et al. Similarities and differences in surface receptor expression by THP-1 monocytes and differentiated macrophages polarized using seven different conditioning regimens. *Cell Immunol.* (2018) 332:58–76. doi: 10.1016/j.cellimm.2018.07.008
  204. Fleit HB, Kobasiuk CD. The human monocyte-like cell line THP-1 expresses FcγRI and FcγRII. *J Leukoc Biol.* (1991) 49:556–65. doi: 10.1002/jlb.49.6.556
  205. Kedzierska K, Ellery P, Mak J, Lewin SR, Crowe SM, Jaworowski A. HIV-1 down-modulates gamma signaling chain of Fc gamma R in human macrophages: a possible mechanism for inhibition of phagocytosis. *J Immunol.* (2002) 168:2895–903. doi: 10.4049/jimmunol.168.6.2895
  206. Daëron M. Fc receptor biology. *Annu Rev Immunol.* (1997) 15:203–34. doi: 10.1146/annurev.immunol.15.1.203
  207. Foltz C, Napolitano A, Khan R, Clough B, Hirst EM, Frickel E. TRIM21 is critical for survival of *Toxoplasma gondii* infection and localises to GBP-positive parasite vacuoles. *Sci Rep.* (2017) 7:5209. doi: 10.1038/s41598-017-05487-7
  208. Rakebrandt N, Lentes S, Neumann H, James LC, Neumann-Staubitz P. Antibody- and TRIM21-dependent intracellular restriction of *Salmonella enterica*. *Path Dis.* (2014) 72:131–7. doi: 10.1111/2049-632X.12192
  209. Bussi C, Gutierrez MG. *Mycobacterium tuberculosis* infection of host cells in space and time. *FEMS Microbiol Rev.* (2019) 43:341–61. doi: 10.1093/femsre/fuz006
  210. McLean MR, Lu L, Kent SJ, Chung AW. An inflammatory story: antibodies in *Mycobacterium tuberculosis* co-morbidities. *Front Immunol.* (2019) 10:2846. doi: 10.3389/fimmu.2019.02846
  211. Belay M, Legesse M, Mihret A, Ottenhoff TH, Franken KL, Bjune G, et al. IFN-γ and IgA against non-methylated heparin-binding hemagglutinin as markers of protective immunity and latent tuberculosis: results of a longitudinal study from an endemic setting. *J Infect.* (2016) 72:189–200. doi: 10.1016/j.jinf.2015.09.040
  212. Dijkman K, Sombroek CC, Vervenne RA, Hofman SO, Boot C, Remarque EJ, et al. Prevention of tuberculosis infection and disease by local BCG in repeatedly exposed rhesus macaques. *Nat Med.* (2019) 25:255–62. doi: 10.1038/s41591-018-0319-9
  213. Darrah PA, Zeppa JJ, Maiello P, Hackney JA, Wadsworth MH, Hughes TK, et al. Prevention of tuberculosis in macaques after intravenous BCG immunization. *Nature.* (2020) 577:95–102. doi: 10.1038/s41586-019-1817-8
  214. Alvarez N, Otero O, Camacho F, Borrero R, Tirado Y, Puig A, et al. Passive administration of purified secretory IgA from human colostrum induces protection against *Mycobacterium tuberculosis* in a murine model of progressive pulmonary infection. *BMC Immunol.* (2013) 14(Suppl. 1):S3. doi: 10.1186/1471-2172-14-S1-S3
  215. Rodríguez A, Tjärnlund A, Ivanji J, Singh M, García I, Williams A, et al. Role of IgA in the defense against respiratory infections: IgA deficient mice exhibited increased susceptibility to intranasal infection with *Mycobacterium bovis* BCG. *Vaccine.* (2005) 23:2565–72. doi: 10.1016/j.vaccine.2004.11.032
  216. Tjärnlund A, Rodríguez A, Cardona P, Guirado E, Ivanyi J, Singh M, et al. Polymeric IgR knockout mice are more susceptible to mycobacterial infections in the respiratory tract than wild-type mice. *Int Immunol.* (2006) 18:807–16. doi: 10.1093/intimm/dx1017
  217. Mantis NJ, Rol N, Corthésy B. Secretory IgA's complex roles in immunity and mucosal homeostasis in the gut. *Mucosal Immunol.* (2011) 4:603–11. doi: 10.1038/mi.2011.41
  218. Corthésy B. Secretory immunoglobulin A: well beyond immune exclusion at mucosal surfaces. *Immunopharmacol Immunotoxicol.* (2009) 31:174–9. doi: 10.1080/08923970802438441
  219. Reljic R, Williams A, Ivanyi J. Mucosal immunotherapy of tuberculosis: is there a value in passive IgA? *Tuberculosis.* (2006) 86:179–90. doi: 10.1016/j.tube.2006.01.011
  220. Reljic R, Ivanyi J. A case for passive immunoprophylaxis against tuberculosis. *Lancet Infect Dis.* (2006) 6:813–18. doi: 10.1016/S1473-3099(06)70658-2
  221. Reljic R, Crawford C, Challacombe S, Ivanyi J. Mouse IgA inhibits cell growth by stimulating tumor necrosis factor-α production and apoptosis of macrophage cell lines. *Int Immunol.* (2004) 16:607–14. doi: 10.1093/intimm/dxh070
  222. Jennewein MF, Alter G. The immunoregulatory roles of antibody glycosylation. *Trends Immunol.* (2017) 38:358–72. doi: 10.1016/j.it.2017.02.004
  223. Irvine EB, Alter G. Understanding the role of antibody glycosylation through the lens of severe viral and bacterial diseases. *Glycobiology.* (2020) 30:241–53. doi: 10.1093/glycob/cwaa018
  224. Vadrevu SK, Trbojevic-Akmagic I, Kossenkov AV, Colomb F, Giron LB, Anzurez A, et al. Frontline science: plasma and immunoglobulin G galactosylation associate with HIV persistence during antiretroviral therapy. *J Leukoc Biol.* (2018) 104:461–71. doi: 10.1002/JLB.3HI1217-500R
  225. Moore JS, Wu X, Kulhavy R, Tomana M, Novak J, Moldoveanu Z, et al. Increased levels of galactose-deficient IgG in sera of HIV-1-infected individuals. *AIDS.* (2005) 19:381–9. doi: 10.1097/01.aids.0000161767.21405.68
  226. Alter G, Ottenhoff TH, Joosten SA. Antibody glycosylation in inflammation, disease and vaccination. *Semin Immunol.* (2018) 39:102–10. doi: 10.1016/j.smim.2018.05.003
  227. Pilkington C, Yeung E, Isenberg D, Lefvert A, Rook G. Agalactosyl IgG and antibody specificity in rheumatoid arthritis, tuberculosis, systemic lupus erythematosus and myasthenia gravis. *Autoimmunity.* (1995) 22:107–11. doi: 10.3109/08916939508995306
  228. Parekh R, Isenberg D, Rook G, Roitt I, Dwek R, Rademacher T. A comparative analysis of disease-associated changes in the galactosylation of serum IgG. *J Autoimmun.* (1989) 2:101–14. doi: 10.1016/0896-8411(89)90148-0
  229. Rademacher TW, Parekh RB, Dwek RA, Isenberg D, Rook G, Axford JS, et al. The role of IgG glycoforms in the pathogenesis of rheumatoid arthritis. *Springer Sem Immunopath.* (1988) 10:231–49. doi: 10.1007/BF01857227
  230. Malhotra R, Wormald MR, Rudd PM, Fischer PB, Dwek RA, Sim RB. Glycosylation changes of IgG associated with rheumatoid arthritis can activate complement via the mannose-binding protein. *Nat Med.* (1995) 1:237–43. doi: 10.1038/nm0395-237
  231. Seeling M, Brückner C, Nimmerjahn F. Differential antibody glycosylation in autoimmunity: sweet biomarker or modulator of disease activity? *Nat Rev Rheumatol.* (2017) 13:621–30. doi: 10.1038/nrrheum.2017.146

232. Lu LL, Das J, Grace PS, Fortune SM, Restrepo BI, Alter G. Antibody Fc glycosylation discriminates between latent and active tuberculosis. *J Infect Dis.* (2020) 222:2093–102. doi: 10.1093/infdis/jiz643
233. Ottenhoff TH, Kaufmann SH. Vaccines against tuberculosis: where are we and where do we need to go? *PLoS Pathog.* (2012) 8:e1002607. doi: 10.1371/journal.ppat.1002607
234. Sebina I, Cliff JM, Smith SG, Nogaro S, Webb EL, Riley EM, et al. Long-lived memory B-cell responses following BCG vaccination. *PLoS ONE.* (2012) 7:e51381. doi: 10.1371/journal.pone.0051381
235. Aguilo N, Uranga S, Mata E, Tarancon R, Gómez AB, Marinova D, et al. Respiratory immunization with a whole cell inactivated vaccine induces functional mucosal immunoglobulins against tuberculosis in mice and non-human primates. *Front Microbiol.* (2020) 11:1339. doi: 10.3389/fmicb.2020.01339
236. Shin HJ, Franco LH, Nair VR, Collins AC, Shiloh MU. A baculovirus-conjugated mimotope vaccine targeting *Mycobacterium tuberculosis* lipoarabinomannan. *PLoS ONE.* (2017) 12:e0185945. doi: 10.1371/journal.pone.0185945
237. Wang L, Feng S, An L, Gu G, Guo Z. Synthetic and immunological studies of mycobacterial lipoarabinomannan oligosaccharides and their protein conjugates. *J Org Chem.* (2015) 80:10060–75. doi: 10.1021/acs.joc.5b01686
238. Glatman-Freedman A, Casadevall A, Dai Z, Jacobs WR Jr, Li A, Morris SL, et al. Antigenic evidence of prevalence and diversity of *Mycobacterium tuberculosis* arabinomannan. *J Clin Microbiol.* (2004) 42:3225–31. doi: 10.1128/JCM.42.7.3225-3231.2004
239. Hamasur B, Haile M, Pawlowski A, Schröder U, Williams A, Hatch G, et al. *Mycobacterium tuberculosis* arabinomannan-protein conjugates protect against tuberculosis. *Vaccine.* (2003) 21:4081–93. doi: 10.1016/S0264-410X(03)00274-3
240. Hamasur B, Källenius G, Svenson SB. Synthesis and immunologic characterisation of *Mycobacterium tuberculosis* lipoarabinomannan specific oligosaccharide-protein conjugates. *Vaccine.* (1999) 17:2853–61. doi: 10.1016/S0264-410X(99)00124-3
241. Prados-Rosales R, Carreño L, Cheng T, Blanc C, Weinrick B, Malek A, et al. Enhanced control of *Mycobacterium tuberculosis* extrapulmonary dissemination in mice by an arabinomannan-protein conjugate vaccine. *PLoS pathogens.* (2017) 13:e1006250. doi: 10.1371/journal.ppat.1006250
242. Tameris MD, Hatherill M, Landry BS, Scriba TJ, Snowden MA, Lockhart S, et al. Safety and efficacy of MVA85A, a new tuberculosis vaccine, in infants previously vaccinated with BCG: a randomised, placebo-controlled phase 2b trial. *Lancet.* (2013) 381:1021–8. doi: 10.1016/S0140-6736(13)60177-4
243. Van Der Meeren O, Hatherill M, Nduba V, Wilkinson RJ, Muyoyeta M, Van Brakel E, et al. Phase 2b controlled trial of M72/AS01E vaccine to prevent tuberculosis. *N Engl J Med.* (2018) 379:1621–34. doi: 10.1056/NEJMoa1803484
244. Penn-Nicholson A, Geldenhuys H, Burny W, van der Most R, Day CL, Jongert E, et al. Safety and immunogenicity of candidate vaccine M72/AS01E in adolescents in a TB endemic setting. *Vaccine.* (2015) 33:4025–34. doi: 10.1016/j.vaccine.2015.05.088
245. Tait DR, Hatherill M, Van Der Meeren O, Ginsberg AM, Van Brakel E, Salaun B, et al. Final analysis of a trial of M72/AS01E vaccine to prevent tuberculosis. *N Engl J Med.* (2019) 381:2429–39. doi: 10.1056/NEJMoa1909953
246. Zimmermann P, Donath S, Perrett KP, Messina NL, Ritz N, Netea MG, et al. The influence of neonatal bacille calmette-guerin (BCG) immunisation on heterologous vaccine responses in infants. *Vaccine.* (2019) 37:3735–44. doi: 10.1016/j.vaccine.2019.03.016
247. de Bree, L Charlotte J, Koeken VA, Joosten LA, Aaby P, Benn CS, van Crevel R, et al. Non-specific effects of vaccines: current evidence and potential implications. *Semin Immunol.* (2018). 39:35–43. doi: 10.1016/j.smim.2018.06.002
248. Jensen KJ, Larsen N, Biering-Sørensen S, Andersen A, Eriksen HB, Monteiro I, et al. Heterologous immunological effects of early BCG vaccination in low-birth-weight infants in Guinea-Bissau: a randomized-controlled trial. *J Infect Dis.* (2015) 211:956–67. doi: 10.1093/infdis/jiu508
249. Kleinnijenhuis J, van Crevel R, Netea MG. Trained immunity: consequences for the heterologous effects of BCG vaccination. *Trans R Soc Trop Med Hyg.* (2015) 109:29–35. doi: 10.1093/trstmh/tru168
250. Giamarellos-Bourboulis EJ, Tsilika M, Moorlag S, Antonakos N, Kotsaki A, Domínguez-Andrés J, et al. Activate: randomized clinical trial of BCG vaccination against infection in the elderly. *Cell.* (2020) 183:315–23e9. doi: 10.1016/j.cell.2020.08.051
251. Bulut O, Kilic G, Domínguez-Andrés J, Netea MG. Overcoming immune dysfunction in the elderly: trained immunity as a novel approach. *Int Immunol.* (2020) 32:741–53. doi: 10.1093/intimm/daa052
252. Divangahi M, Aaby P, Khader SA, Barreiro LB, Bekkering S, Chavakis T, et al. Trained immunity, tolerance, priming and differentiation: distinct immunological processes. *Nat Immunol.* (2021) 22:2–6. doi: 10.1038/s41590-020-00845-6
253. Cirovic B, de Bree, L Charlotte J, Groh L, Blok BA, Chan J, van der Velden, Walter JFM, et al. BCG vaccination in humans elicits trained immunity via the hematopoietic progenitor compartment. *Cell Host Microbe.* (2020) 28:322–34. e5. doi: 10.1016/j.chom.2020.05.014
254. Boyack PN. Inducing Mucosal IgA: a challenge for vaccine adjuvants and delivery systems. *J Immunol.* (2017) 199:9–16. doi: 10.4049/jimmunol.1601775
255. Kaufmann SH. Envisioning future strategies for vaccination against tuberculosis. *Nat Rev Immunol.* (2006) 6:699–704. doi: 10.1038/nri1920
256. Hussain R, Dawood G, Abrar N, Toossi Z, Minai A, Dojki M, et al. Selective increases in antibody isotypes and immunoglobulin G subclass responses to secreted antigens in tuberculosis patients and healthy household contacts of the patients. *Clin Diagn Lab Immunol.* (1995) 2:726–32. doi: 10.1128/CDLI.2.6.726-732.1995
257. Abebe F, Belay M, Legesse M, KLMC F, Ottenhoff TH. IgA and IgG against *Mycobacterium tuberculosis* Rv2031 discriminate between pulmonary tuberculosis patients, *Mycobacterium tuberculosis*-infected and non-infected individuals. *PLoS ONE.* (2018) 13:e0190989. doi: 10.1371/journal.pone.0190989
258. Kunnath-Velayudhan S, Salamon H, Wang HY, Davidow AL, Molina DM, Huynh VT, et al. Dynamic antibody responses to the *Mycobacterium tuberculosis* proteome. *Proc Natl Acad Sci USA.* (2010) 107:14703–8. doi: 10.1073/pnas.1009080107
259. Mahan AE, Jennewein MF, Suscovich T, Dionne K, Tedesco J, Chung AW, et al. Antigen-specific antibody glycosylation is regulated via vaccination. *PLoS pathogens.* (2016) 12:e1005456. doi: 10.1371/journal.ppat.1005456
260. Karagouni E, Hadjipetrou-Kourounakis L. Regulation of isotype immunoglobulin production by adjuvants in vivo. *Scand J Immunol.* (1990) 31:745–54. doi: 10.1111/j.1365-3083.1990.tb02826.x
261. Stewart E, Triccas JA, Petrovsky N. Adjuvant strategies for more effective tuberculosis vaccine immunity. *Microorganisms.* (2019) 7:255. doi: 10.3390/microorganisms7080255

**Conflict of Interest:** The authors declare that the research was conducted in the absence of any commercial or financial relationships that could be construed as a potential conflict of interest.

Copyright © 2021 Rijnink, Ottenhoff and Joosten. This is an open-access article distributed under the terms of the Creative Commons Attribution License (CC BY). The use, distribution or reproduction in other forums is permitted, provided the original author(s) and the copyright owner(s) are credited and that the original publication in this journal is cited, in accordance with accepted academic practice. No use, distribution or reproduction is permitted which does not comply with these terms.



# A Two-Gene Signature for Tuberculosis Diagnosis in Persons With Advanced HIV

Vandana Kulkarni<sup>1†</sup>, Artur T. L. Queiroz<sup>2,3\*†</sup>, Shashi Sangle<sup>1</sup>, Anju Kagal<sup>1</sup>, Sonali Salvi<sup>1</sup>, Amita Gupta<sup>4</sup>, Jerrold Ellner<sup>5</sup>, Dileep Kadam<sup>1</sup>, Valeria C. Rolla<sup>6</sup>, Bruno B. Andrade<sup>2,3†</sup>, Padmini Salgame<sup>5†</sup> and Vidya Mave<sup>1,4\*†</sup>

<sup>1</sup> Byramjee-Jeejeebhoy Government Medical College-Johns Hopkins University Clinical Research Site (BJGMC-JHU CRS), Pune, India, <sup>2</sup> Instituto Gonçalo Moniz, Fundação Oswaldo Cruz, Salvador, Brazil, <sup>3</sup> Multinational Organization Network Sponsoring Translational and Epidemiological Research (MONSTER) Initiative, Salvador, Brazil, <sup>4</sup> Johns Hopkins University School of Medicine, Baltimore, MD, United States, <sup>5</sup> Rutgers- New Jersey Medical School, Center for Emerging Pathogens, Newark, NJ, United States, <sup>6</sup> Instituto Nacional de Infectologia Evandro Chagas, Fundação Oswaldo Cruz, Rio de Janeiro, Brazil

## OPEN ACCESS

### Edited by:

Novel N. Chegou,  
Stellenbosch University, South Africa

### Reviewed by:

Marielle C. Haks,  
Leiden University Medical  
Center, Netherlands  
Jiezuan Yang,  
Zhejiang University, China

### \*Correspondence:

Vidya Mave  
vidyamave@gmail.com  
Artur T. L. Queiroz  
artur.queiroz@fiocruz.br

<sup>†</sup>These authors have contributed  
equally to this work

### Specialty section:

This article was submitted to  
Microbial Immunology,  
a section of the journal  
Frontiers in Immunology

**Received:** 19 November 2020

**Accepted:** 03 February 2021

**Published:** 22 February 2021

### Citation:

Kulkarni V, Queiroz ATL, Sangle S, Kagal A, Salvi S, Gupta A, Ellner J, Kadam D, Rolla VC, Andrade BB, Salgame P and Mave V (2021) A Two-Gene Signature for Tuberculosis Diagnosis in Persons With Advanced HIV. *Front. Immunol.* 12:631165. doi: 10.3389/fimmu.2021.631165

**Background:** Transcriptomic signatures for tuberculosis (TB) have been proposed and represent a promising diagnostic tool. Data remain limited in persons with advanced HIV.

**Methods:** We enrolled 30 patients with advanced HIV (CD4 < 100 cells/mm<sup>3</sup>) in India; 16 with active TB and 14 without. Whole-blood RNA sequencing was performed; these data were merged with a publicly available dataset from Uganda ( $n = 33$ ; 18 with TB and 15 without). Transcriptomic profiling and machine learning algorithms identified an optimal gene signature for TB classification. Receiver operating characteristic analysis was used to assess performance.

**Results:** Among 565 differentially expressed genes identified for TB, 40 were shared across India and Uganda cohorts. Common upregulated pathways reflect Toll-like receptor cascades and neutrophil degranulation. The machine-learning decision-tree algorithm selected gene expression values from *RAB20* and *INS3* as most informative for TB classification. The signature accurately classified TB in discovery cohorts (India AUC 0.95 and Uganda AUC 1.0;  $p < 0.001$ ); accuracy was fair in external validation cohorts.

**Conclusions:** Expression values of *RAB20* and *INS3* genes in peripheral blood compose a biosignature that accurately classified TB status among patients with advanced HIV in two geographically distinct cohorts. The functional analysis suggests pathways previously reported in TB pathogenesis.

**Keywords:** HIV, tuberculosis, transcriptomics, diagnosis, gene signature

## INTRODUCTION

Tremendous advances in tuberculosis diagnosis have been made based on nucleic acid amplification of bacteria in the sputum, such as Xpert MTB/RIF sputum smear and culture, which provides results in 2 h (1–5). However, sputum-based diagnostics remain problematic in the context of HIV infection. Sputum smear is often negative for TB bacilli, and the sensitivity of Xpert



MTB/RIF is only 67% (6–8). Persons living with advanced HIV ( $CD4 < 100$  cells/mm<sup>3</sup>) are at particularly high risk for TB and are likely to have smear-negative pulmonary or extrapulmonary TB, underscoring the need for non-sputum-based TB diagnostics to support TB control efforts (9–15).

Blood-based transcriptomic signatures, including several parsimonious gene signatures, have been proposed to diagnose and differentiate TB from other respiratory diseases (ORD) and are in various stages of validation (14, 16, 17). However, the majority of studies do not include persons living with advanced HIV. A recent case-control study from Uganda found that transcript levels of *FcGRI1A* and *BATF2* and plasma protein levels of interferon gamma (IFN- $\gamma$ ) and CXCL10 were individually accurate classifiers of active TB in the context of advanced HIV (18). However, geographic differences may exist and could impact performance when transcriptomic profiles developed in one population are applied to other geographically distinct populations.

To address the potential influence of geography and the reduced number of TB gene expression signatures addressing persons living with HIV (PLWH), we established a discovery cohort comprising the publicly available RNA sequencing (RNA-seq) dataset from the aforementioned Uganda case-control study ( $n = 33$ ) (18) and RNA-seq data from our prospective case-control study in India among persons with advanced HIV with or without active TB ( $n = 30$ ). Using transcriptomic profiling and a machine-learning approach, we aimed to develop and validate a gene signature to fairly classify TB status among persons with advanced HIV from geographically distinct sites.

## METHODS

### Discovery Cohorts

#### India Cohort

Between January 2018 and June 2019, we enrolled 30 consecutive adults attending the antiretroviral treatment (ART) clinic at Byramjee Jeejeebhoy Government Medical College (BJGMC) and Sassoon General Hospitals (SGH), which provides HIV care to residents of Pune, India, and the surrounding area. Eligibility criteria were ART-naïve and ART-experienced adults ( $>18$  years) with advanced HIV, defined as  $CD4 < 100$  cells/mm<sup>3</sup>, with or without newly diagnosed active TB. Exclusion criteria were previous history of TB or anti-tuberculosis treatment (ATT) before enrolment. All potential participants underwent TB symptom screen and GeneXpert MTB/RIF, sputum smear and culture. Cases (TB-HIV), defined as any positive microbiologic TB investigations or ATT initiation based on high clinical suspicion (active TB), were enrolled up to  $n = 15$ ; controls (HIV-only), defined as no evidence of active TB, were enrolled up to  $n = 15$ . Medical, demographic, socio-economic characteristics, and chest radiograph were obtained at enrolment, and blood samples were collected at baseline for HIV quantitative RNA and CD4+

T-cell count. Individual participant consent as well as BJGMC ethics committee and Johns Hopkins University institutional review committee approvals were obtained.

#### Uganda Cohort

A published case-control study conducted among 33 adults with advanced HIV ( $CD4$  count  $<100$  cells/mm<sup>3</sup>) in Uganda. The study population comprised 18 cases with active TB (TB-HIV; 16 with smear-positive or microbiologically-confirmed TB and 2 undergoing ATT) and 15 controls (HIV-only) with no clinical symptoms of TB. All participants underwent whole-blood RNA sequencing (RNA-seq) and plasma cytokine/chemokine analysis (18).

### Whole Blood Sample Processing and RNA Sequencing

At enrolment, whole blood (5 mL) was collected from all 30 India participants in two PAXgene Blood RNA tubes (Qiagen, catalog #762165) and directly frozen at  $-80^{\circ}\text{C}$ . RNA was extracted using the PAXgene Blood RNA kit (Qiagen, catalog #762174) and quantified using Qubit RNA assay HS (Invitrogen, Cat #Q32852). RNA purity was checked using QIAxpress, and RNA integrity was assessed on TapeStation using RNA HS ScreenTapes (Agilent, Cat #5067-5579). NEB Ultra II Directional RNA-Seq Library Prep kit protocol was used to prepare libraries for total RNA sequencing. Prepared libraries were quantified using Qubit High Sensitivity Assay (Invitrogen, Cat #Q32852), pooled and diluted to final optimal loading concentration before cluster amplification on Illumina flow cell. Once the cluster generation was completed, the cluster flow cell was loaded on Illumina HiSeqX instrument to generate 150bp paired-end reads.

### Gene Expression Analysis

Raw RNA-seq data from the India cohort were retrieved from Illumina HiSeqX in fastq formatted files and processed using the protocol for paired-end reads in the quality check and mapping step; raw RNA-seq data from the Uganda cohort were downloaded from the NCBI SRA database using sra-tools (<https://ncbi.github.io/sra-tools/fastq-dump.html>) and processed using the single-end protocol in the quality check and mapping step. Low quality bases were removed from all samples, and adapters were trimmed using Trimmomatic V0.32 (19). A total of 5 samples failed in the quality check process from India Cohort and were removed from analysis. A total of 58 samples from both sites were used in downstream analysis. After the quality check, sequences were aligned to the human transcriptome (GRCh38 version 100), comprising mRNA and ncRNA, using Salmon v1.2.0 (20). After the mapping step, the Salmon output was converted to count tables using the tximport R package (21). Count gene expression matrix was examined using the DESeq2 R package (22) to identify differentially expressed genes (DEG) for cases. Changes in gene expression with false discovery rate (FDR)-adjusted  $p$ -value  $<0.05$  and  $\log_2$ fold-change  $\pm 1.4$  were considered significant. Candidate DEGs were visualized using volcano plots and Venn diagrams using the VennDiagram R package and scanned with the REACTOME pathway database (23) using the compareCluster

**Abbreviations:** ART, antiretroviral therapy; ATT, anti-tuberculosis treatment; AUC, area under the curve; DEG, differentially expressed genes; HIV, human immunodeficiency virus; TB, tuberculosis; PLWH, people living with HIV; PCA, principal component analysis.

R package (24). The entire gene expression data set from India cohort is available at the GEO database (Accession number GSE162164, <https://www.ncbi.nlm.nih.gov/geo/query/acc.cgi?acc=GSE162164>).

## Machine Learning Approach

Following variance-stabilizing transformation and batch effect correction [sva package (25)], gene expression measurements were used to perform a machine learning approach. Using the rpart R package (26), a decision-tree algorithm with leave-one-out cross-validation was applied to identify the minimal variable set (gene set) exhibiting higher classification power to describe cases. The resulting genes were retrieved from each dataset. Sample clustering and classification were assessed using Heatmaps and the Principal component analysis (PCA) plot and applied to the variance-stabilizing transformed gene expression values from each cohort.

## Signature Performance Analysis

We conducted a performance comparison using 36 previously published gene expression signatures for TB diagnosis, progression and treatment provided by the TBSignatureProfiler package (<https://github.com/compbio/TBSignatureProfiler>). In addition, we have included Risk6 signature cohort for comparison (27) (**Supplementary Table 1**). We applied a general linear model to gene expression values from each signature gene. The outcomes were binarized to measure the sensitivity and specificity of classification, allowing us to measure each group rate and plot area under the curve (AUC) values to identify the best classifier.

## Validation of the Gene Signature

To validate the gene signature, we applied the gene expression model to gene expression data, which was log 2 normalized, from three independent and publicly available patient cohorts (28–30). The first study developed and validated transcriptomic signatures to distinguish TB from latent TB infection (LTBI) using a case-control design among African adults with and without HIV (28); validation was performed by comparing TB-HIV (with and without culture-confirmed TB) vs. HIV-only. The second study identified and validated transcriptomic signatures to distinguish active TB from other respiratory diseases as well as LTBI among large pediatric cohorts from South Africa, Malawi and Kenya (29); the comparison for validation was TB-HIV vs. HIV and other respiratory diseases.

## Statistical Analysis

All analyses were pre-specified. Clinical data were compared among cases and controls using the Mann-Whitney *U* test (continuous variables) or Pearson's chi-square test (categorical variables). Correlations between gene expression and clinical variables were tested using Spearman's rank correlation coefficient. Receiver Operator Characteristics (ROC) were used to assess the accuracy of a gene signature to distinguish between comparison groups specified in the India/Uganda datasets and each validation dataset (*in-silico* validation cohorts). We measured the z-scores with the scales function. Analyses were

**TABLE 1 |** Baseline characteristics among cases (TB-HIV) and controls (HIV-only) enrolled in the India cohort (*n* = 30).

Characteristic	HIV-only ( <i>n</i> = 14)	TB-HIV ( <i>n</i> = 16)	<i>p</i> -value
<b>Sex</b>			
Female, <i>n</i> (%)	4 (29%)	3 (18%)	0.68
Male, <i>n</i> (%)	10 (71%)	13 (82%)	
Median age, <i>y</i> (IQR)	41 (31–52)	45 (38–52)	0.42
<b>Smoker, <i>n</i> (%)</b>			
Never	10 (71%)	11 (69%)	>0.95
Former	0	1 (6%)	
Current	4 (29%)	4 (25%)	
Body mass index, kg/m <sup>2</sup>	20.0 (16.8–21.4)	17.6 (16.4–19.9)	0.23
Median HIV viral load, log <sub>10</sub> copies/mL	4.92 (4.24–5.77)	5.50 (4.97–5.87)	0.32
Median CD4 count, cells/mm <sup>3</sup> (IQR)	53 (32–75)	48 (31–65)	0.60
Median CD8 count, cells/mm <sup>3</sup> (IQR)	645 (320–861)	430 (244–589)	0.13
Median CD3 count, cells/mm <sup>3</sup> (IQR)	739.5 (407–1,043)	491 (290–679.5)	0.15

BMI, body mass index; HIV, human immunodeficiency virus; TB, tuberculosis.

performed using the base package from R 4.0.2. Differences with *p*-values <0.05 were considered statistically significant.

## RESULTS

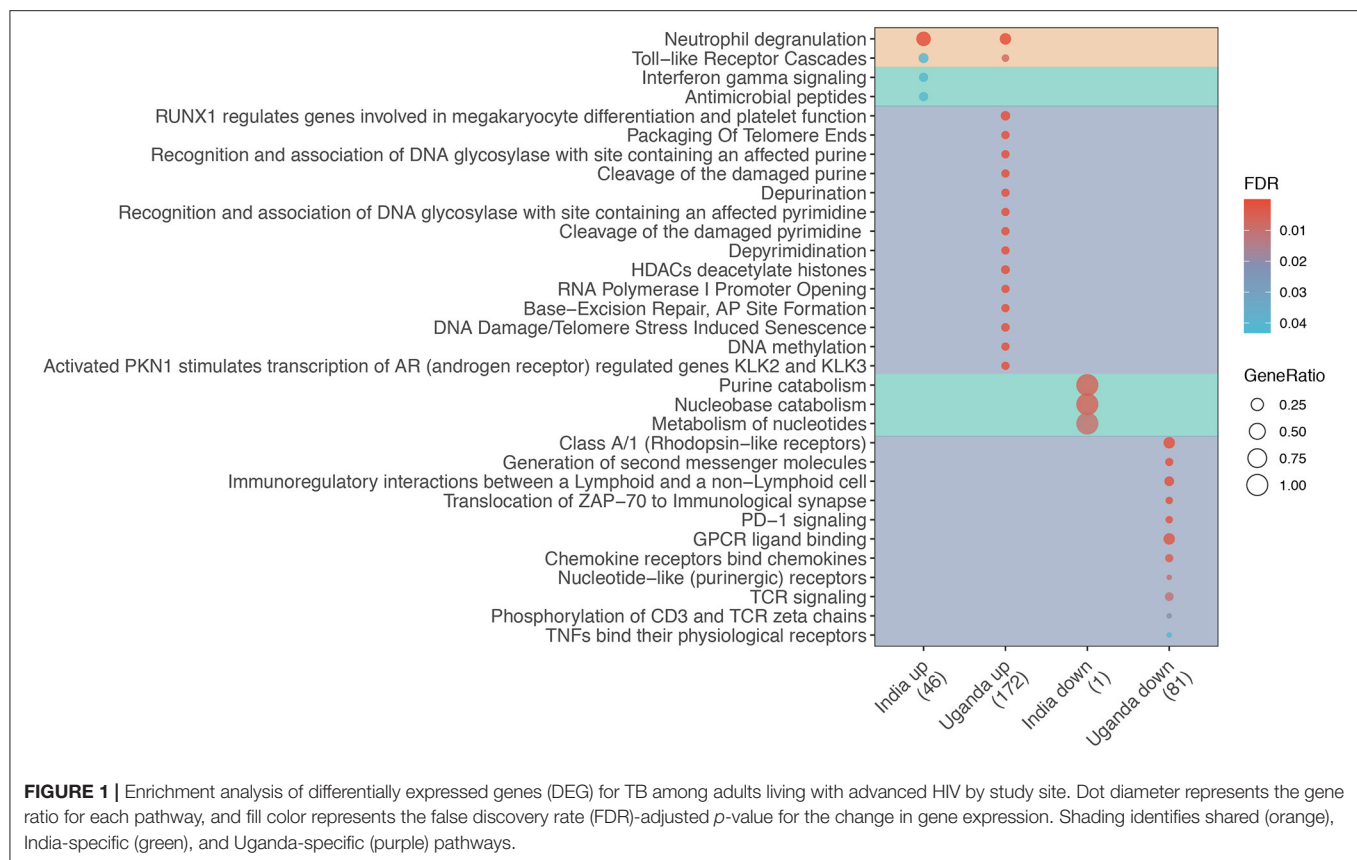
### Description of Discovery Cohorts

Cases (*n* = 16) and controls (*n* = 14) from the India cohort (*n* = 30) did not significantly differ among baseline characteristics, including sex (82% male vs. 71% male), median age (45 vs. 41 years), median CD4 count (45 vs. 53 cells/mm<sup>3</sup>) and median HIV viral load (5.50 vs. 4.92 log copies/mL) (**Table 1**). The Uganda cohort (*n* = 33) was 62% female, median age was 32 years and median CD4 count was 50 cells/mm<sup>3</sup> with no significant differences between cases (*n* = 18) and controls (*n* = 15) (18).

### Gene Expression Analysis

A total of 565 DEGs were identified for cases (active TB) among the discovery cohorts. Of these, the majority (488 DEGs) were specific to the Uganda cohort, including 265 upregulated and 223 downregulated genes; 37 were specific to the India cohort, including 32 upregulated and 5 downregulated genes; and 40 were shared by both cohorts (**Supplementary Figure 1, Supplementary Table 2**). Cluster analysis revealed that DEGs identified at each site were able to distinguish samples from cases and controls, but with some misclassifications (**Supplementary Figure 2**).

The majority of shared DEGs were upregulated (38 upregulated vs. 2 downregulated). The enrichment analysis shown in **Figure 1** reveals that only two pathways were enriched in both discovery cohorts, namely Toll-like receptor cascades and Neutrophil degranulation. Among Uganda-specific DEGs, upregulated pathways predominantly reflect



DNA repair and regulation, and downregulated pathways reflect immune cell response regulation. In contrast, India-specific upregulated pathways reflect IFN- $\gamma$  signaling and antimicrobial peptide response while downregulated pathways reflect nucleotide metabolism.

## Machine Learning

Gene expression values from DEGs were used to perform machine learning. The decision tree identified *INSL3* and *RAB20* (Decision-tree genes) as the optimal gene set to classify tuberculosis status among patients from both sites (**Figure 2A**). Dot plots show that threshold gene expression values for *INSL3* and *RAB20* fairly classified samples from both study sites, correctly classifying 100% of Uganda samples and returning only 3 classification errors in the India cohort (**Figures 2B,C**). Receiver operator characteristic (ROC) analysis indicates accurate TB classification among samples from India [AUC 0.95 (0.87–1.00)] and Uganda (AUC 1.00) (**Figure 2D**). Compared to DEGs and 36 proposed TB gene expression signatures, the Decision-tree genes best classified TB status among samples from both cohorts (**Figures 2E,F**). Although the Maertzdorf\_4, Roe\_3 and Suliman\_4 signatures and Decision-tree genes performed comparably in the India cohort, the Maertzdorf and Suliman signatures comprises 4 genes and Roe signature comprises 3 genes, and was not as accurate in the Uganda cohort where the Rajan\_HIV\_5 and Decision-tree signatures performed best. Reviewing potential associations between Decision-tree genes

and previously proposed TB signatures revealed that *RAB20* is included in the Bankley\_380 (383 genes) and Barry\_393 (290 genes) signatures (**Supplementary Figure 3A**), yet the Decision-tree genes had superior performance in both cohorts.

## Correlation of Clinical Variables With Decision-Tree Gene Expression

Among the India cohort, CD8+ and CD3+ cell counts were significantly lower in cases than controls (**Supplementary Figures 3B–D**). Comparing Decision-tree gene expression to clinical variables, Spearman correlation values indicate a significant negative correlation between *INSL3* expression and both CD8+ and CD3+ cell counts. No cluster was associated with clinical variables (Smoke, Cough, Cavitation, Death, Viral load, CD4, Age or BMI) (**Figure 3**).

## Validation of the Decision-Tree Signature

We performed ROC analysis to determine the sensitivity of the 2-gene signature to distinguish active TB among three validation cohorts. As shown in **Figure 4**, the Decision-tree signature performed best among South African cohorts with AUC ranging between 0.683 and 0.748; performance was lower among Malawi cohorts with AUC ranging between 0.615 and 0.623 (**Figures 4A,B**). The 2-gene signature demonstrated high accuracy to predict active TB with an AUC of 0.945 for distinguishing culture-confirmed TB from culture-negative TB (**Figure 4C**).

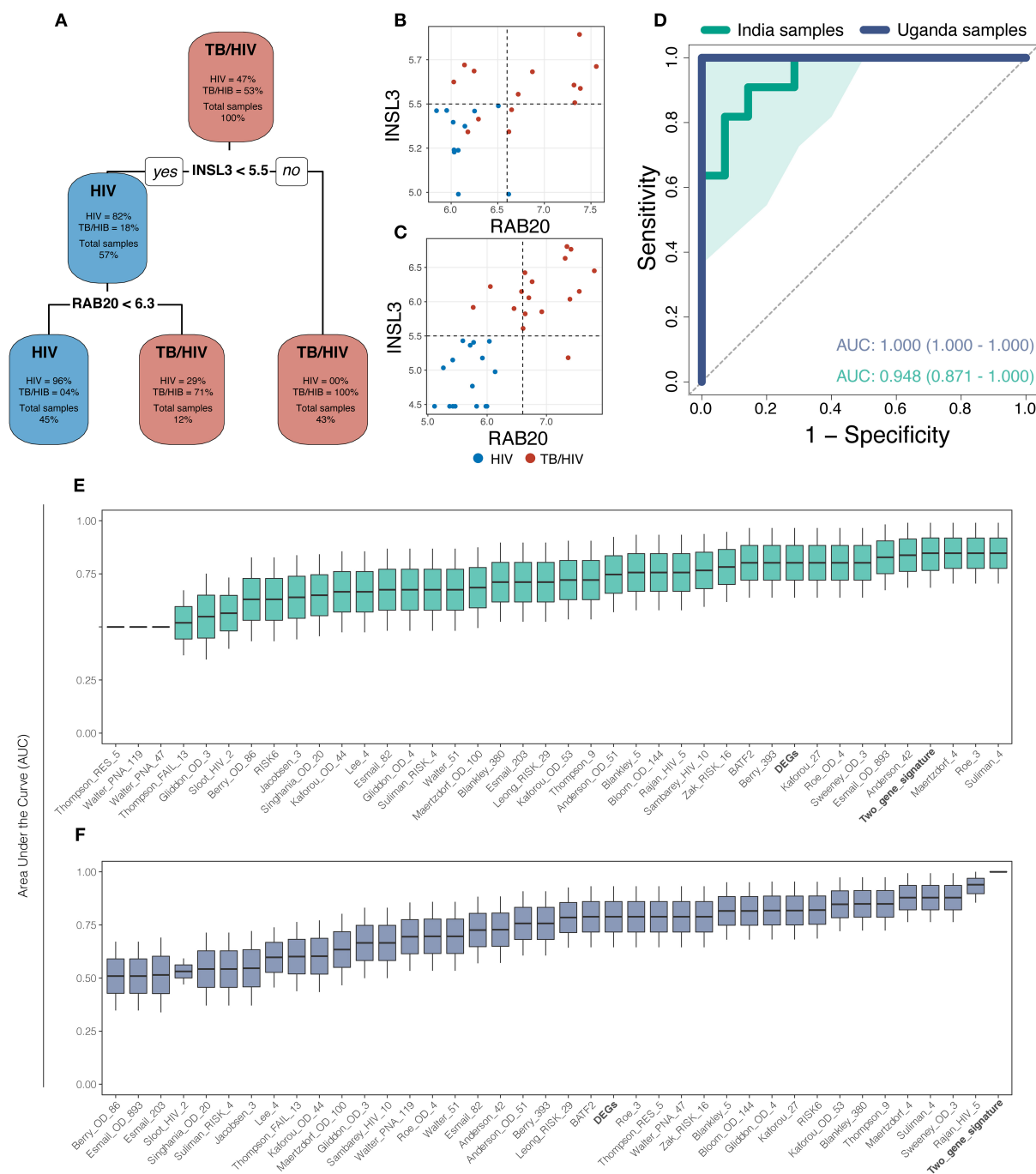
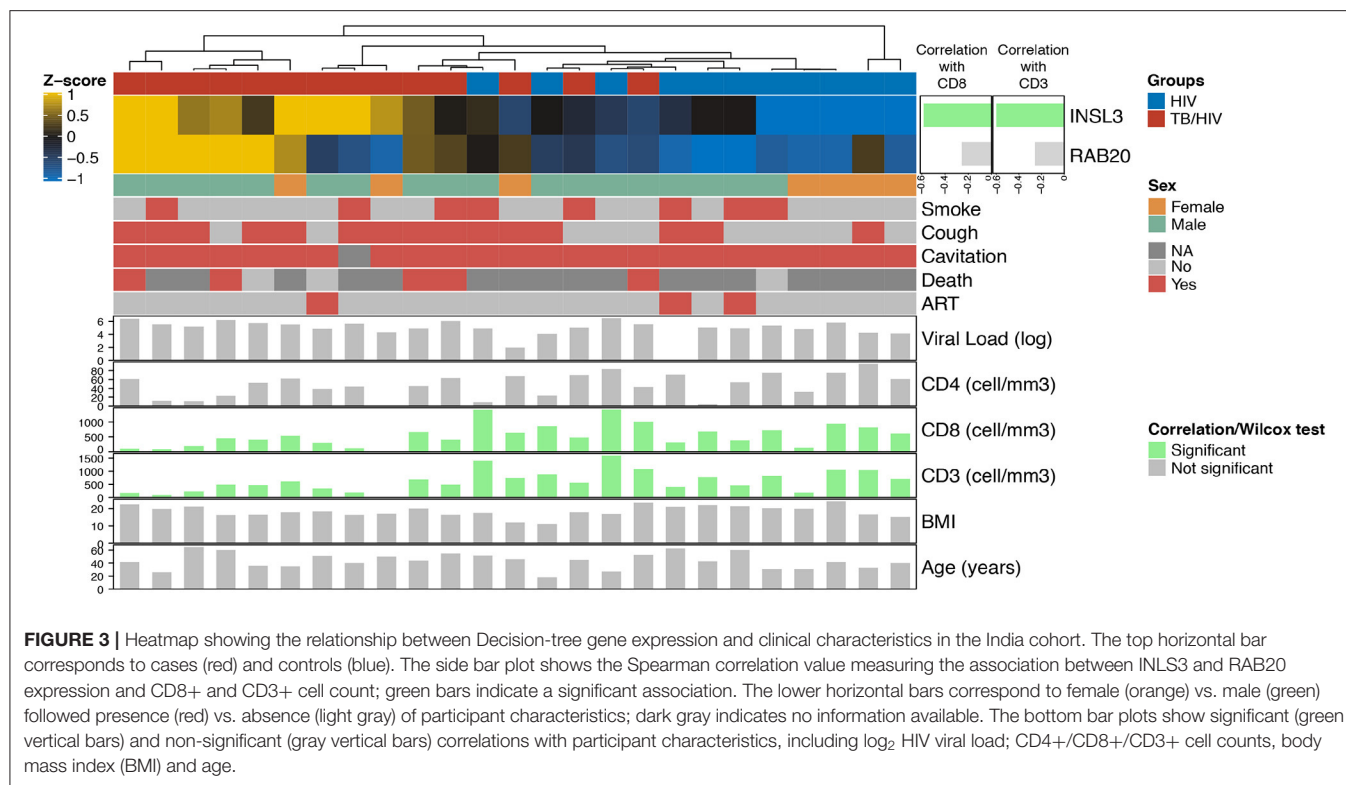


**FIGURE 2 |** The machine learning approach identified a 2-gene signature (INSL3 and RAB20) that best classified tuberculosis status across study sites. **(A)** The decision-tree algorithm selected INSL3 and RAB20 genes to classify tuberculosis status among the discovery cohorts. **(B,C)** Dot plots show that Decision-tree genes correctly classify TB status for most samples from the India cohort **(B)** and for 100% of samples from the Uganda cohort **(C)**; vertical and horizontal dotted lines represent decision thresholds for RAB20 and INSL3 genes, respectively. **(D)** Receiver operating characteristic (ROC) curve analysis shows strong TB classification performance of Decision-tree genes among samples from India (green line) and Uganda (purple line) with area under the curve (AUC) of 0.948 and 1.00, respectively; shaded area represents standard deviation. Boxplots show the AUC, measured by general linear modeling, for Decision-tree genes (Bold), differentially expressed genes (Bold), and publicly available TB gene expression signatures identifying the Decision-tree genes as the best TB classifier across India **(E)** and Uganda **(F)** cohorts.





## DISCUSSION

Transcriptomic signatures for TB diagnosis have been previously identified using various approaches, including differentially expressed genes, pathway analysis and subsetting genes associated to symptomatology (15, 16, 31). Although the blood transcriptomic profiling can improve diagnosis and understanding of TB infection, population-specific gene expression could interfere with performance across different regions (32). This study identified a 2-gene parsimonious signature that accurately classified active TB among people with advanced HIV infection in two geographically distinct cohorts. More importantly, the signature fared well to distinguish active TB from latent tuberculosis infection (LTBI) as well as other respiratory diseases when applied to other African datasets. Finally, the signature performed best among those with culture-confirmed TB and is likely an indicator of mycobacterial replication, suggesting the potential to extrapolate its use for TB treatment monitoring.

The prediction of TB diagnosis in PLWH improved when Indian and Ugandan datasets were combined. The two genes generated by the machine learning algorithm (*RAB20* and *INSL3*) were able to accurately distinguish active TB from non-TB. *RAB20*, a member of the RAS Oncogene Family, is involved in the maturation and acidification of phagosomes. More specifically, *RAB20* regulates the endosomal membrane, thus playing an important role in phagosome integrity and control of *Mycobacterium tuberculosis* (*Mtb*) replication in infected

macrophages (33). This mechanism is also regulated by IFN- $\gamma$ , assisting with *Mtb* infection control in macrophages (34). In contrast, *INSL3* is part of an insulin-like hormone superfamily and is associated with human testicular cell tumors (35), but has not been previously associated with TB infection or disease. Notably, the strong negative correlation observed between *INSL3* expression and CD8+/CD3+ cell count ( $\rho = -0.6$ ) suggests a significant role in immune cell regulation among PLWH with active TB from India. The influence of *INSL3* on CD8+ and CD3+ cells could be associated with its regulation of *TIMP2* (36), a member of the NF-KappaB Family Pathway.

Although the 2-gene signature performed well in both discovery cohorts, we observed considerable geographic differences in gene expression between India and Uganda. Specifically, samples from Africa presented more DEGs (528 genes) than India (77 genes), and only 40 common DEGs were identified across the sites. A multitude of factors alter the immune response and may explain the observed differences, including ethnic population, dietary, environmental and seasonal differences (37, 38). Variable performance of TB signatures in Indian and African discovery cohorts provides additional evidence of population-specific gene expression. The performance of TB signatures varied with lower AUC observed among India samples compared to Uganda. Even signatures proposed among PLWH, such as Esmail\_82, Esmail\_203, Esmail\_893 (31), Kaforou\_27, Kaforou\_OD\_44, Kaforou\_OD\_53 (28), Sambarey\_HIV\_10 (39), and Rajan\_HIV\_5 (40), demonstrated differential performance

among Indian and Ugandan cohorts. The total number of genes varies widely across signatures, ranging from 5 to 893 genes, and could explain the differential performance (AUC) in classifying TB status among PLWH, but also suggests a possible population bias in each signature that could interfere with its use in other geographic locations.

The differential gene expressions observed between Indian and Ugandan cohorts was not unexpected. Despite the differences, however, the discovery cohorts shared 40 differentially expressed genes for TB, and two important pathways were found to be upregulated in both cohorts (18). The Toll-like receptor cascade pathway has been previously associated with TB and HIV, indicating the role of *Mtb* in the regulation of HIV replication (41). The neutrophil degranulation pathway has also been associated with TB, but the exact role of neutrophils remains ambiguous with potential to be associated with *Mtb* clearance as well as increased disease severity and mortality (42). Overall, these pathways suggest that TB disease may influence peripheral blood mononuclear cell expression in PLWH.

The performance of the novel 2-gene signature is heterogeneous in the external validation data sets, but the 2-gene signature has fair overall accuracy to distinguish TB. Accuracy ranged from 0.683 to 0.748 in the African cohort comprising children and adults, and inferior performance was observed in the Malawi cohort with AUC values ranging from 0.615 to 0.623. The difference in performance suggests that population-associated gene expression interferes with TB classification in PLWH. Despite the unsatisfactory performance of the 2-gene signature in these data, some aspects should be accounted. In this dataset, the control group was composed of PLWH and other respiratory diseases. The control group composition and population bias may have contributed to reduced AUC values. Interestingly, TB classification accuracy was high for patients with culture-confirmed TB in the Kenya cohort (AUC 0.954) while reduced performance was observed among patients without culture-confirmed TB (AUC 0.627). This finding suggests an association of the two-gene signature with bacterial load and that longitudinal change in expression of this gene signature could also be used to monitor bacillary load in response to treatment.

Gene signatures derived from multiple cohorts were validated using a targeted approach, reverse transcriptase multiplex ligation-dependent probe amplification (RT-MLPA) in a multisite study that comprised cohorts with and without HIV. The analysis revealed FCGR1A [high-affinity IgG Fc receptor 1 (CD64)] as a consistent single-gene classifier of active TB disease, in the presence and absence of HIV (43). FcGR1A was also reported to function as a consistent single gene classifier of active TB even in advanced HIV in the Uganda cohort included in this study (18). In an Ethiopian cohort, five genes (CD8A, TIMP2, CCL22, FCGR1A, and TNFRSF1A), were shown to segregate active TB from non-active TB in HIV patients (44). In another study, also in an Ethiopian cohort of HIV co-infected TB patients, 7 genes (FCGR1A, RAB24, TLR1, TLR4, MMP9, NLRC4, and IL1B) accurately discriminated between active tuberculosis disease and latent

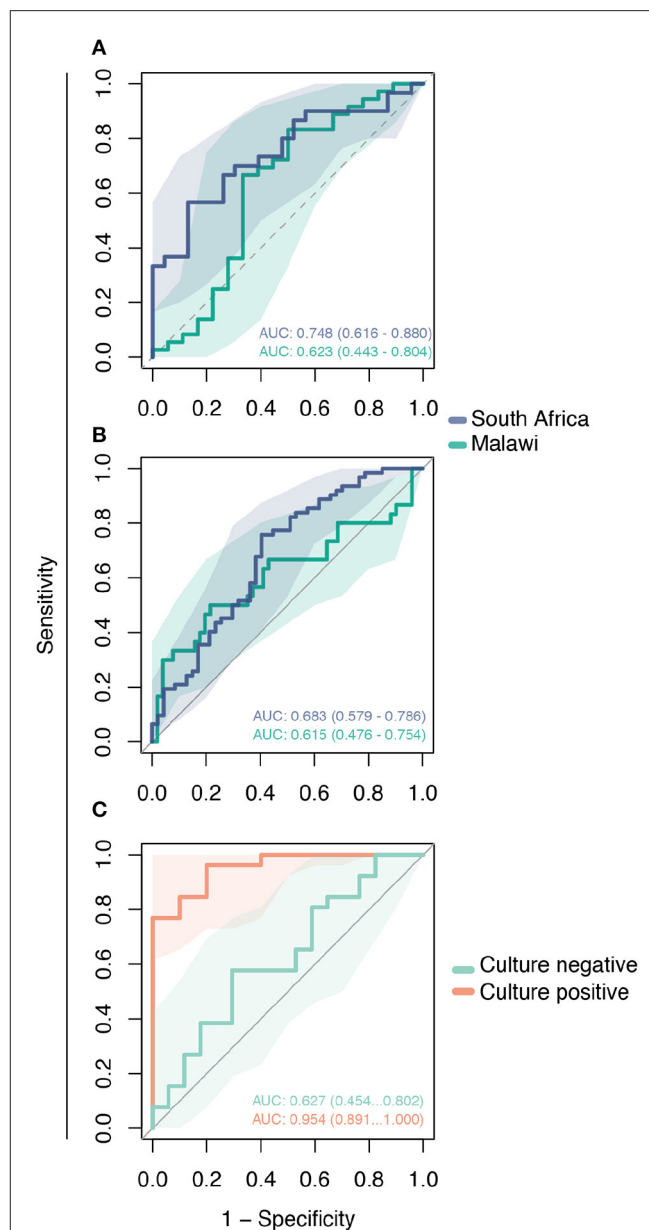


**FIGURE 4 |** Validation of the Decision-tree gene signature using publicly available microarray datasets. Receiving operating characteristic curve analysis evaluating the performance of the 2-gene signature to distinguish comparison groups in the: **(A)** GSE39940 dataset—children living with HIV from South Africa and Malawi coinfected with TB or other respiratory diseases (ORD) (HIV-TB vs. HIV-ORD); **(B)** GSE37250 dataset—adults living with HIV from South Africa and Malawi coinfected with TB or ORD (HIV-TB vs. HIV-ORD); and **(C)** GSE39939 dataset from Kenya—patients with HIV-TB co-infection with and without culture-confirmed TB (culture-positive vs. culture-negative).

infection (45). RISK6 is a prognostic signature derived from baseline blood samples in a SA adolescent cohort of progressors and non-progressors (27). The signature is an aggregate of nine transcript pairs that was derived by separately linking each of three transcripts upregulated in progressors (GBP2,

FCGR1B, and SERPING1), to three transcripts downregulated in progressors (TUBGCP6, TRMT2A, and SDR39U1), relative to non-progressors. RISK6 also performed well in diagnosing active TB in HIV-uninfected and HIV-infected persons (27). Of note, none of the studies included cohorts from India. Additional head-to-head comparative studies in larger cohorts are needed to determine whether the 2-gene signature reported here works across ethnicities and comorbidities, including HIV. Furthermore, whether the same gene signatures will perform well in segregating TB from HIV with differing CD4 counts and differing peripheral inflammation also needs to be determined.

Despite yielding interesting results, our study has some limitations. First, the sampling size is not ideal, with 25 samples from India and 33 from Uganda, and has resulted in more variability observed in the study. Second, the metadata from all validation datasets do not have the CD4 count value for each patient, but the overall cohort data report much higher CD4 value than our cohort. This may have contributed to reduction in performance of our signature. For clinical application, more studies are required to standardize a gene expression-based protocol. Furthermore, RNA seq-based signatures need to be further developed for use in clinical practice to distinguish PLWH with TB from those with LTBI or other respiratory diseases.

In conclusion, despite populational-specific differential gene expression, the *RAB20* and *INS3* genes outperformed all previously proposed TB signatures to accurately distinguish TB from non-TB among multiple cohorts from different geographical regions. This parsimonious 2-gene signature also performed well among those with culture-positive TB, indicating its potential use for TB treatment monitoring. Our study provides evidence supporting a promising, novel and non-sputum-based biomarker for TB diagnosis, especially for those with advanced HIV infection in whom TB diagnosis is often difficult with sputum-based diagnostics. Future studies are needed to confirm our findings.

## DATA AVAILABILITY STATEMENT

The datasets presented in this study can be found in online repositories. The names of the repository and accession number can be found here: GEO database (Accession number GSE162164, <https://www.ncbi.nlm.nih.gov/geo/query/acc.cgi?acc=GSE162164>).

## ETHICS STATEMENT

The studies involving human participants were reviewed and approved by (1) Byramjee Jeejeebhoy Government Medical College Clinical Trials Unit. (2) INI-FIOCRUZ, Brazil; FMT, Brazil. (3) Johns Hopkins University School of Medicine, USA. (4) Boston Medical Campus (BUMC), USA. (5) Rutgers New Jersey Medical School IRB, USA. The patients/participants provided their written informed consent to participate in this study.

## AUTHOR CONTRIBUTIONS

VM, DK, VR, PS, and JE contributed to study design. VK, AQ, and BA contributed toward data acquisition. PS, AQ, and BA contributed equally toward data interpretation. VK, SSan, AK, SSa, DK, and VM were responsible for patient recruitment, sample collection, storage, and analysis of clinical data. VK, AQ, VM, PS, and BA contributed equally to writing the manuscript. All authors read and approved the final manuscript.

## FUNDING

The research work was primarily supported by CRDF Global (Award number DAA3-17-63158-1/Country: India). Research data in this manuscript were collected, in part, as part of the Regional Prospective Observational Research for Tuberculosis (RePORT) India Consortium. This work was funded in whole or in part by federal funds from the Government of India Department of Biotechnology (DBT); the Indian Council of Medical Research (ICMR); the National Institutes of Health National Institute of Allergy and Infectious Diseases Office of AIDS Research; CRDF Global; the National Institutes of Health Baltimore-Washington-India Clinical Trials Unit for National Institute of Allergy and Infectious Diseases Networks (UM1AI069465 to VM and AG); and the National Institutes of Health (R01AI1097494 to VM and AG). The work of BBA was supported by the Intramural Research Program of the Oswaldo Cruz Foundation, and the National Council for Scientific and Technological Development (senior CNPq fellowship—tier 1D), Brazil. The contents of this publication are solely the responsibility of the authors and do not represent the official views of the DBT, ICMR, National Institutes of Health, or CRDF Global. Any mention of trade names, commercial projects, or organizations does not imply endorsement by any of the sponsoring organizations. The content of this paper is solely the responsibility of the authors and does not represent the official views of the funders.

## ACKNOWLEDGMENTS

We would like to thank the study participants, ART center nurses, study counselor, and laboratory staff for their efforts in enrollment, sample processing, storage and shipment.

## SUPPLEMENTARY MATERIAL

The Supplementary Material for this article can be found online at: <https://www.frontiersin.org/articles/10.3389/fimmu.2021.631165/full#supplementary-material>

**Supplementary Figure S1 | (A,B)** Volcano plots showing differentially expressed genes (DEG) for TB using whole-blood samples from India **(A)** and Uganda **(B)** cohorts. Red indicates DEGs, defined as change in gene expression with  $\log_2$  Fold Change  $\pm 1.4$  and FDR  $< 0.05$ ; green indicates change in gene expression with  $\log_2$  Fold Change  $\pm 1.4$ ; blue indicates change in gene expression with FDR  $< 0.05$ ; and gray indicates no significant change in gene expression. **(C)** The Venn diagram shows the number of site-specific and shared DEGs. **(D)** The Bar plot shows the  $\log_2$  Fold Change of the 40 DEGs shared across study sites.

**Supplementary Figure S2** | Heatmap of the differentially expressed genes (DEG) for TB identified in the India (A) and Uganda (B) cohorts.

**Supplementary Figure S3** | The dot plot demonstrates the presence of Decision-tree genes (INSL3 and RAB20) in previously proposed TB gene expression signatures (A). Boxplots show the associations of CD3 (B), CD8 (B), and CD4 (C) cell counts and HIV viral load (D) with TB-HIV co-infection status in the India cohort. Clinical variables were compared among cases (TB-HIV) and controls (HIV-only) using the Wilcoxon test. Only CD3 and CD8 cell counts were significantly associated with TB status.

**Supplementary Table 1** | Systematic literature review but restricted to the signatures present in TBSignatureProfiler package, plus the RISK6 used as reference. Signature names represent the first author's name of the corresponding publication, suffixed with number of constituent genes that are present in the RNAseq dataset. Table includes number of genes, method, population, HIV status and treatment, geographical region, and participant condition. TB, tuberculosis; LTBI, latent tuberculosis infection; HHC, household contacts; SARC, sarcoidosis.

**Supplementary Table 2** | File with the differentially expressed genes (DEG) list from India, Uganda cohort, and the common genes. The log2 Fold Change, log2 Fold Change SE, p-value, and FDR are also provided for each gene.

## REFERENCES

1. Kebede A, Beyene D, Yenew B, Diriba G, Mehamd Z, Alemu A, et al. Monitoring quality indicators for the Xpert MTB/RIF molecular assay in Ethiopia. *PLoS ONE*. (2019) 14:e0225205. doi: 10.1371/journal.pone.0225205
2. Lawn SD, Nicol MP. Xpert® MTB/RIF assay: development, evaluation and implementation of a new rapid molecular diagnostic for tuberculosis and rifampicin resistance. *Future Microbiol.* (2011) 6:1067–82. doi: 10.2217/fmb.11.84
3. Vittor AY, Garland JM, Gilman RH. Molecular diagnosis of TB in the HIV positive population. *Ann. Glob. Health.* (2015) 80:476. doi: 10.1016/j.aogh.2015.01.001
4. Yusuf NW. Rapid diagnosis of tuberculosis using Xpert MTB/RIF assay—report from a third world country. *Pak. J. Med. Sci.* 31:105–10. doi: 10.12669/pjms.311.6970
5. Agizew T, Chihota V, Nyirenda S, Tedla Z, Auld AF, Mathebula U, et al. Tuberculosis treatment outcomes among people living with HIV diagnosed using Xpert MTB/RIF versus sputum-smear microscopy in Botswana: a stepped-wedge cluster randomised trial. *BMC Infect. Dis.* (2019) 19:1058. doi: 10.1186/s12879-019-4697-5
6. Akanbi MO, Achenbach C, Taiwo B, Idoko J, Ani A, Isa Y, et al. Evaluation of gene Xpert for routine diagnosis of HIV-associated tuberculosis in Nigeria: a prospective cohort study. *BMC Pulm. Med.* (2017) 17:87. doi: 10.1186/s12890-017-0430-6
7. Sedky M, Wakil IA, Rashed M, Salama A. The role of genexpert in diagnosis of sputum-negative pulmonary tuberculosis. *Egypt. J. Chest Dis. Tuberc.* (2018) 67:419–26. doi: 10.4103/ejcd.ejcdt\_57\_18
8. Steingart KR, Schiller I, Horne DJ, Pai M, Boehme CC, Dendukuri, N. Xpert® MTB/RIF assay for pulmonary tuberculosis and rifampicin resistance in adults. *Cochrane Database Syst. Rev.* (2014) 2014:CD009593. doi: 10.1002/14651858.CD009593.pub3
9. Blankley S, Graham CM, Turner J, Berry MPR, Bloom CI, et al. The transcriptional signature of active tuberculosis reflects symptom status in extra-pulmonary and pulmonary tuberculosis. *PLoS ONE*. (2016) 11:e0162220. doi: 10.1371/journal.pone.0162220
10. Burel JG, Babor M, Pomaznoy M, Lindestam Arlehamn CS, Khan N, Sette A. Host transcriptomics as a tool to identify diagnostic and mechanistic immune signatures of tuberculosis. *Front. Immunol.* (2019) 10:221. doi: 10.3389/fimmu.2019.00221
11. Darboe F, Mbandi SK, Naidoo K, Yende-Zuma N, Lewis L, Thompson EG, et al. Detection of tuberculosis recurrence, diagnosis and treatment response by a blood transcriptomic risk signature in HIV-infected persons on antiretroviral therapy. *Front. Microbiol.* (2019) 10:1441. doi: 10.3389/fmicb.2019.01441
12. Mulenga H, Bunyasi EW, Mbandi SK, Mendelsohn SC, Kagana B, Penn-Nicholson A, et al. Performance of host blood transcriptomic signatures for diagnosing and predicting progression to tuberculosis disease in HIV-negative adults and adolescents: a systematic review protocol. *BMJ Open*. (2019) 9:e026612. doi: 10.1136/bmjopen-2018-026612
13. Turner CT, Gupta RK, Tsaliki E, Roe JK, Mondal P, Nyawo GR, et al. Blood transcriptional biomarkers for active pulmonary tuberculosis in a high-burden setting: a prospective, observational, diagnostic accuracy study. *Lancet Respir. Med.* (2020) 8:407–19. doi: 10.1016/S2213-2600(19)30469-2
14. Zak DE, Penn-Nicholson A, Scriba TJ, Thompson E, Suliman S, Amon LM, et al. A blood RNA signature for tuberculosis disease risk: a prospective cohort study. *Lancet*. (2016) 387:2312–22. doi: 10.1016/S0140-6736(15)01316-1
15. Sweeney TE, Braviak L, Tato CM, Khatri, P. Genome-wide expression for diagnosis of pulmonary tuberculosis: a multicohort analysis. *Lancet Respir. Med.* (2016) 4:213–24. doi: 10.1016/S2213-2600(16)00048-5
16. Singhania A, Wilkinson RJ, Rodrigue M, Haldar P, O'Garra, A. The value of transcriptomics in advancing knowledge of the immune response and diagnosis in tuberculosis. *Nat. Immunol.* (2018) 19:1159–68. doi: 10.1038/s41590-018-0225-9
17. Warsinske H, Vashisht R, Khatri, P. Host-response-based gene signatures for tuberculosis diagnosis: a systematic comparison of 16 signatures. *PLoS Med.* (2019) 16:e1002786. doi: 10.1371/journal.pmed.1002786
18. Verma S, Du P, Nakanjako D, Hermans S, Briggs J, Nakiyingi L, et al. Tuberculosis in advanced HIV infection is associated with increased expression of IFN $\gamma$  and its downstream targets. *BMC Infect. Dis.* (2018) 18:220. doi: 10.1186/s12879-018-3127-4
19. Bolger AM, Lohse M, Usadel B. Trimmomatic: a flexible trimmer for illumina sequence data. *Bioinformatics*. (2014) 30:2114–20. doi: 10.1093/bioinformatics/btu170
20. Patro R, Duggel G, Love MI, Irizarry RA, Kingsford C. Salmon provides fast and bias-aware quantification of transcript expression. *Nat. Methods*. (2017) 14:417–9. doi: 10.1038/nmeth.4197
21. Soneson C, Love MI, Robinson MD. Differential analyses for RNA-seq: transcript-level estimates improve gene-level inferences. *F1000Res*. (2015) 4:1521. doi: 10.12688/f1000research.7563.1
22. Love MI, Huber W, Anders S. Moderated estimation of fold change and dispersion for RNA-seq data with DESeq2. *Genome Biol.* (2014) 15:550. doi: 10.1186/s13059-014-0550-8
23. Yu G, He Q-Y. ReactomePA: an R/Bioconductor package for reactome pathway analysis and visualization. *Mol. Biosyst.* (2016) 12:477–9. doi: 10.1039/C5MB00663E
24. Yu G, Wang L-G, Han Y, He Q-Y. clusterProfiler: an R package for comparing biological themes among gene clusters. *OMICS*. (2012) 16:284–7. doi: 10.1089/omi.2011.0118
25. Leek JT, Johnson WE, Parker HS, Fertig EJ, Jaffe AE, Zhang Y, et al. sva: Surrogate Variable Analysis. R package version 3.38.0 (2020).
26. Therneau T, Atkinson B, Ripley B. rpart: Recursive Partitioning and Regression Trees. R package version 4.1-102015 (2019).
27. Penn-Nicholson A, Mbandi SK, Thompson E, Mendelsohn SC, Suliman S, Chegou NN, et al. RISK6, a 6-gene transcriptomic signature of TB disease risk, diagnosis and treatment response. *Sci. Rep.* (2020) 10:8629. doi: 10.1038/s41598-020-65043-8
28. Kaforou M, Wright VJ, Oni T, French N, Anderson ST, Bangani N, et al. Detection of tuberculosis in HIV-infected and -uninfected african adults using whole blood RNA expression signatures: a case-control study. *PLoS Med.* (2013) 10:e1001538. doi: 10.1371/journal.pmed.1001538
29. Anderson ST, Kaforou M, Brent AJ, Wright VJ, Banwell CM, Chagaluka G, et al. Diagnosis of childhood tuberculosis and host RNA expression in Africa. *N. Engl. J. Med.* (2014) 370:1712–23. doi: 10.1056/NEJMoa1303657
30. Marais S, Lai RPJ, Wilkinson KA, Meintjes G, O'Garra A, Wilkinson RJ. Inflammasome activation underlying central nervous system deterioration in HIV-associated tuberculosis. *J. Infect. Dis.* (2017) 215:677–86. doi: 10.1093/infdis/jiw561



31. Esmail H, Lai RP, Lesosky M, Wilkinson KA, Graham CM, Horswell S, et al. Complement pathway gene activation and rising circulating immune complexes characterize early disease in HIV-associated tuberculosis. *Proc. Natl. Acad. Sci. U.S.A.* (2018) 115:E964. doi: 10.1073/pnas.1711853115
32. Wang L, Rishishwar L, Mariño-Ramírez L, Jordan IK. Human population-specific gene expression and transcriptional network modification with polymorphic transposable elements. *Nucl. Acids Res.* 45:2318–28. doi: 10.1093/nar/gkw1286
33. Schnettger L, Rodgers A, Repnik U, Lai RP, Pei G, Verdoes M, et al. A Rab20-dependent membrane trafficking pathway controls m. tuberculosis replication by regulating phagosome spaciousness and integrity. *Cell Host Microbe.* (2016) 21:619–28.e5. doi: 10.1016/j.chom.2017.04.004
34. Das R, Koo M-S, Kim BH, Jacob ST, Subbian S, Yao J, et al. Macrophage migration inhibitory factor (MIF) is a critical mediator of the innate immune response to *Mycobacterium tuberculosis*. *Proc. Natl. Acad. Sci. U.S.A.* (2013) 110:E2997–3006. doi: 10.1073/pnas.1301128110
35. Rossato M, Tavolini IM, Calcagno A, Gardiman M, Dal Moro F, Artibani, W. The novel hormone INSL3 is expressed in human testicular Leydig cell tumors: a clinical and immunohistochemical study. *Plagiarism.* (2011) 29:33–7. doi: 10.1016/j.urolonc.2008.10.015
36. Hampel U, Klonisch T, Sel S, Schulze U, Paulsen FP. Insulin-like factor 3 promotes wound healing at the ocular surface. *Endocrinology.* (2013) 154:2034–45. doi: 10.1210/en.2012-2201
37. Ross SA, Davis CD. The emerging role of microRNAs and nutrition in modulating health and disease. *Annu. Rev. Nutr.* (2014) 34:305–36. doi: 10.1146/annurev-nutr-071813-105729
38. Ter Horst R, Jaeger M, Smeekens SP, Oosting M, Swertz MA, Li Y, et al. Host and environmental factors influencing individual human cytokine responses. *Cell.* (2016) 167:1111–24.e13. doi: 10.1016/j.cell.2016.10.018
39. Sambarey A, Devaprasad A, Mohan A, Ahmed A, Nayak S, Swaminathan S, et al. Unbiased identification of blood-based biomarkers for pulmonary tuberculosis by modeling and mining molecular interaction networks. *EBioMedicine.* (2017) 15:112–26. doi: 10.1016/j.ebiom.2016.12.009
40. Rajan JV, Semitala FC, Mehta T, Seielstad M, Montalvo L, Andama A, et al. A novel, 5-transcript, whole-blood gene-expression signature for tuberculosis screening among people living with human immunodeficiency virus. *Clin. Infect. Dis.* (2019) 69:77–83. doi: 10.1093/cid/ciy835
41. Ranjbar S, Jasenosky LD, Chow N, Goldfeld AE. Regulation of Mycobacterium tuberculosis-dependent HIV-1 transcription reveals a new role for NFAT5 in the toll-like receptor pathway. *PLoS Pathogens.* (2012) 8:e1002620. doi: 10.1371/journal.ppat.1002620
42. Kroon EE, Coussens AK, Kinnear C, Orlova M, Möller M, Seeger A, et al. Neutrophils: innate effectors of TB resistance? *Front. Immunol.* (2018) 9:2637. doi: 10.3389/fimmu.2018.02637
43. Sutherland JS, Loxton AG, Haks MC, Kassa D, Ambrose L, Lee JS, et al. Differential gene expression of activating Fcγ receptor classifies active tuberculosis regardless of human immunodeficiency virus status or ethnicity. *Clin. Microbiol. Infect.* (2014) 20:O230–8. doi: 10.1111/1469-0691.12383
44. Kassa D, Ran L, Jager W, van den Broek T, Jacobi R, Mekonen M, et al. Discriminative expression of whole blood genes in HIV patients with latent and active TB in Ethiopia. *Tuberculosis.* (2016) 100:25–31. doi: 10.1016/j.tube.2016.06.003
45. Gebremicael G, Kassa D, Quinten E, Alemayehu Y, Gebreegziavier A, Belay Y, et al. Host gene expression kinetics during treatment of tuberculosis in HIV-coinfected individuals is independent of highly active antiretroviral therapy. *J. Infect Dis.* (2018) 218:1833–46. doi: 10.1093/infdis/jiy404

**Conflict of Interest:** The authors declare that the research was conducted in the absence of any commercial or financial relationships that could be construed as a potential conflict of interest.

Copyright © 2021 Kulkarni, Queiroz, Sangle, Kagal, Salvi, Gupta, Ellner, Kadam, Rolla, Andrade, Salgame and Mave. This is an open-access article distributed under the terms of the Creative Commons Attribution License (CC BY). The use, distribution or reproduction in other forums is permitted, provided the original author(s) and the copyright owner(s) are credited and that the original publication in this journal is cited, in accordance with accepted academic practice. No use, distribution or reproduction is permitted which does not comply with these terms.



# A Plasma 5-Marker Host Biosignature Identifies Tuberculosis in High and Low Endemic Countries

Bih H. Chendi<sup>1,2</sup>, Candice I. Snyders<sup>2</sup>, Kristian Tonby<sup>1,3</sup>, Synne Jennum<sup>3</sup>, Martin Kidd<sup>4</sup>, Gerhard Walzl<sup>2</sup>, Novel N. Chegou<sup>2†</sup> and Anne M. Dyrhol-Riise<sup>1,3\*†</sup> on behalf of the ScreenTB Consortium

<sup>1</sup> Institute of Clinical Medicine, Faculty of Medicine, University of Oslo, Oslo, Norway, <sup>2</sup> Division of Molecular Biology and Human Genetics, Department of Science and Technology-National Research Foundation (DST-NRF) Centre of Excellence for Biomedical Tuberculosis Research, Faculty of Medicine and Health Sciences, South African Medical Research Council Centre for Tuberculosis Research, Stellenbosch University, Cape Town, South Africa, <sup>3</sup> Department of Infectious Diseases, Oslo University Hospital, Oslo, Norway, <sup>4</sup> Department of Statistics and Actuarial Sciences, Centre for Statistical Consultation, Stellenbosch University, Cape Town, South Africa

## OPEN ACCESS

### Edited by:

Paul Laszlo Bollyky,  
Stanford University, United States

### Reviewed by:

Yean Kong Yong,  
Xiamen University, Malaysia  
Roberta Olmo Pinheiro,  
Oswaldo Cruz Foundation, Brazil

### \*Correspondence:

Anne M. Dyrhol-Riise  
a.m.d.riise@medisin.uio.no

†These authors have contributed  
equally to this work

### Specialty section:

This article was submitted to  
Microbial Immunology,  
a section of the journal  
Frontiers in Immunology

**Received:** 21 September 2020

**Accepted:** 03 February 2021

**Published:** 24 February 2021

### Citation:

Chendi BH, Snyders CI, Tonby K,  
Jennum S, Kidd M, Walzl G,  
Chegou NN and Dyrhol-Riise AM  
(2021) A Plasma 5-Marker  
Host Biosignature Identifies  
Tuberculosis in High and Low  
Endemic Countries.  
Front. Immunol. 12:608846.  
doi: 10.3389/fimmu.2021.608846

**Background:** Several host inflammatory markers have been proposed as biomarkers for diagnosis and treatment response in Tuberculosis (TB), but few studies compare their utility in different demographic, ethnic, and TB endemic settings.

**Methods:** Fifty-four host biomarkers were evaluated in plasma samples obtained from presumed TB cases recruited at the Oslo University Hospital in Norway, and a health center in Cape Town, South Africa. Based on clinical and laboratory assessments, participants were classified as having TB or other respiratory diseases (ORD). The concentrations of biomarkers were analyzed using the Luminex multiplex platform.

**Results:** Out of 185 study participants from both study sites, 107 (58%) had TB, and 78 (42%) ORD. Multiple host markers showed diagnostic potential in both the Norwegian and South African cohorts, with I-309 as the most accurate single marker irrespective of geographical setting. Although study site-specific biosignatures had high accuracy for TB, a site-independent 5-marker biosignature (G-CSF, C3b/iC3b, procalcitonin, IP-10, PDGF-BB) was identified diagnosing TB with a sensitivity of 72.7% (95% CI, 49.8–82.3) and specificity of 90.5% (95% CI, 69.6–98.8) irrespective of geographical site.

**Conclusion:** A 5-marker host plasma biosignature has diagnostic potential for TB disease irrespective of TB setting and should be further explored in larger cohorts.

**Keywords:** tuberculosis, biomarkers, diagnosis, treatment response, endemic settings, biosignatures

## INTRODUCTION

An estimated 10 million people were reported to have tuberculosis (TB) and nearly 1.5 million died of the disease in 2018 (1). New tools for TB diagnosis and monitoring of treatment responses are needed, particularly in resource-constrained settings (2). The limitations of sputum smear microscopy and sputum culture are widely published (2–5). Culture conversion after 2 months of TB treatment is mostly used when monitoring treatment response in clinical trials but has limited utility in individual patients (5, 6). Also, smear microscopy and the Xpert MTB/RIF tests are not

suitable for TB treatment monitoring purposes as they cannot discriminate between dead and live bacteria (6–8). Thus, there has been an intensified search for suitable host immune biomarkers for TB diagnostics and monitoring treatment response.

Several studies that made use of specimens collected in Africa or other high TB burden settings have identified promising biomarkers in serum or plasma (9–11), *M.tb* antigen-stimulated blood (12–14), and other bodily fluids including saliva and urine (5, 15–17). Other studies conducted in high income/low endemic settings aiming to differentiate active TB from latent TB infection (LTBI) irrespective of HIV status, and for evaluating TB treatment (18–21) led to the identification of interferon-gamma inducible protein (IP)-10 as a candidate biomarker for TB diagnosis. Still, despite the numerous promising biomarkers identified so far only interferon-gamma (IFN- $\gamma$ ) release assays (IGRA) currently exist in clinical practice, but IGRAs do not distinguish active TB from LTBI (22) and are not useful in high burden settings (23). As highlighted in a recent report, host biomarker-based studies are often poorly designed and promising biomarkers are mostly evaluated at single-sites, without independent validation cohorts (24). Therefore, new studies evaluating promising biomarkers in multiple independent cohorts including participants recruited in both low and high endemic settings are needed (4, 25–27).

In the current study, we evaluated the potential utility of previously published plasma-derived biomarkers for TB diagnosis and monitoring of treatment response in adults with suspected active TB from low endemic (Norway) and high endemic (South Africa) settings.

## METHODOLOGY

### Study Participants

Participants were recruited through longitudinal observational cohort studies at the Department of Infectious Diseases, Oslo University Hospital (OUH), Norway (*Prognostic Immunological markers in Tuberculosis*) from 2012 to 2019, and the Fisantekraal Clinic, a peripheral level health care center in the outskirts of Cape Town, South Africa; a field site for a larger biomarker study (*ScreenTB* project) from 2016 to 2019 (Figure 1).

Briefly, Norwegian study participants were patients admitted for medical evaluation on suspicion of having active TB. Adults with active TB and consenting to participate were recruited into the observational cohort. Medical history including comorbidities and HIV co-infection were registered at inclusion. Clinical examination and chest X-rays were performed, and if indicated, supplemented with further radiological and/or histological investigations. TB diagnosis was based on either positive *Mtb* culture/ PCR or clinical diagnosis based on symptoms, radiological findings, and histology consistent with TB where anti-TB-therapy was started. Active TB patients were further categorized into pulmonary TB (PTB), extrapulmonary TB (EPTB) or combined (PTB + EPTB). TB patients were followed up with new visits at week 2, month 2, and month 6 after initiation of TB treatment. All patients were clinically cured at the end of treatment. Participants grouped as other respiratory

diseases (ORD) were recruited from patients with symptoms of lower respiratory infections admitted to OUH in the same period.

South African study participants self-presented at the clinic with symptoms requiring investigation for active PTB and were recruited prior to the diagnosis of TB or ORD. TB was confirmed or ruled out using a combination of clinical, laboratory, and radiological findings as described in previous reports (9, 10). All individuals classified as ORD had suggestive TB symptoms, but with negative microbiological *M.tb* diagnostics and were never initiated on TB treatment by the national TB control program.

### Sample Collection

For both the Norwegian and South African study participants, whole blood was collected by venepuncture into EDTA (Norway) or heparinized (South Africa) BD vacutainer tubes (BD Biosciences, Franklin Lakes, NJ, USA). After centrifugation (at 2,000 rpm for 10 min), plasma was harvested, aliquoted, and frozen at  $-80^{\circ}\text{C}$  until use. Induced sputum samples and/or biopsies were obtained for acid-fast staining and culture by BACTEC 960 MGIT liquid culture media (BD Biosciences) or Lovenstein Jensen solid media. Positive MGIT cultures were examined for acid-fast bacilli using the Ziehl-Neelsen technique (to check for contamination).

### Ethical Considerations

The Norwegian participants were included in the ongoing cohort “*Prognostic Immunological markers in tuberculosis*” at the Department of Infectious Diseases, OUS, Norway (approved by Regional Ethics Committee, REK 2016/2123). Biological samples were stored in the biobank “*Research Biobank Infectious Diseases*” (REK nr.6.2008.173). South African participants enrolled into the *ScreenTB* study was approved by the Health Research Ethics Committee of the University of Stellenbosch (N16/05/070). All participants gave written informed consent before study inclusion. All methods were performed in accordance with the relevant guidelines and regulations.

### Multiplex Immunoassay

The 54 candidate TB diagnostic host markers were selected after literature searches (9, 10, 24, 28, 29) and evaluated in plasma specimens from all participants using the Luminex multiplex immunoassay platform. These markers are listed in Table 1. Samples were randomly assigned for testing on different assay plates, with the laboratory staff blinded to the clinical classification of study participants. All samples including the laboratory internal quality controls were diluted according to the recommendations of the manufacturers before analysis. The levels of the different biomarkers in the quality control reagents were within the expected ranges. Assays were performed on the Bio-Plex platform (Bio-Plex 200 and/or Magpix; Bio-Rad Laboratories, Hercules, USA) with the Bio-Plex Manager Software (version 6.1) used for bead acquisition and analysis of median fluorescent intensity, in an ISO15189:2007 accredited laboratory.

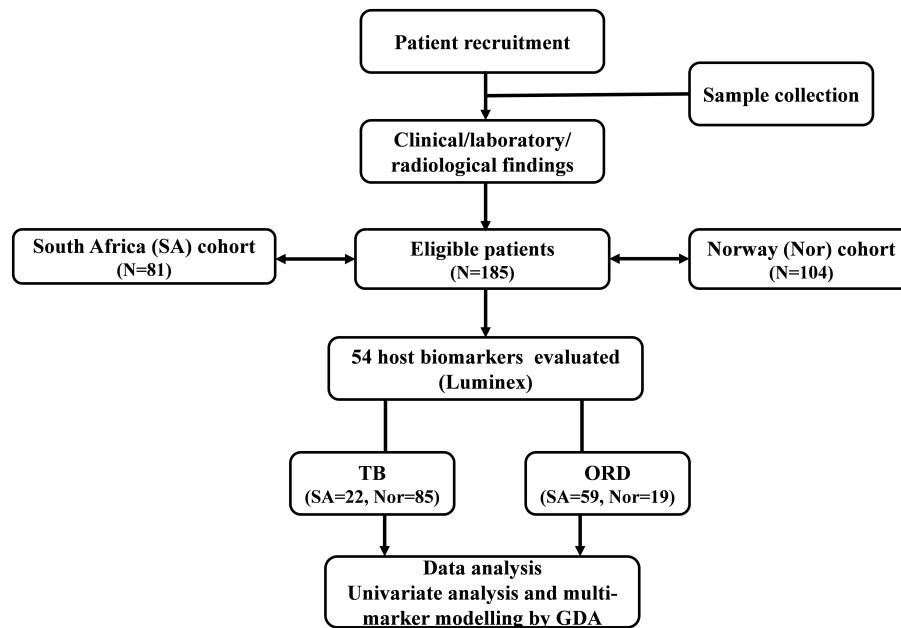


**FIGURE 1 |** STARD diagram showing the study design and classification of study participants. TB, Tuberculosis cases; ORD, Individuals presenting with symptoms and investigated for pulmonary TB but in whom TB disease was ruled out; ROC, Receiver operator characteristics; GDA, General discriminant analysis.

## Statistical Analysis

Box-cox transformation and winsorization were performed in preparation for statistical analysis for analytes requiring transformation. Differences in the concentrations of host markers between the different groups were analyzed using the non-parametric Mann-Whitney U test. Mixed-effects linear models using the *lmer* package in the R were used to carry out univariate analyses for repeated measures (Baseline, Week 2, Month 2, and Month 6). The diagnostic abilities of host markers were assessed by receiver operator characteristics (ROC) curve analysis. Optimal cut-off values and associated sensitivity and specificity were determined based on the Youden's Index. The predictive abilities of combinations of host markers were investigated using general discriminant analysis (GDA). Depending on the size of the observations, data were randomly split into a training (70%) and test set (30%) whereby, models built on the training set were validated on the test set, otherwise, by leave-one-out cross-validation (that is, after each data point is removed, a model is built on the rest of the data and a prediction is made at that point and later tested on all the data). The best subset based on the Wilks lambda method was used in selecting analytes for the different biosignatures.  $P \leq 0.05$  were considered significant for differences between groups. The data were analyzed using Statistica (TIBCO Software Inc., CA, USA), Graphpad Prism version 8 (Graphpad Software Inc., CA, USA), and R programming language.

## RESULTS

### Study Participants

Of a total of 185 included participants from both Norway and SA, 107 (57.8%) were diagnosed with TB and 78 (42.2%) with

ORD. Among the Norwegian TB cases, 23 (68%)/21 (62%), and 13 (33%)/9 (23%) were confirmed TB (culture and/or PCR) in the PTB and EPTB cases, respectively. All 22 South African TB cases had PTB; 21 (95%) and 14 (64%) of whom were culture and smear-positive, respectively. The mean age of all TB cases was  $36.8 \pm 13.3$  years, 9 (5%) were HIV infected and 69 (64%) were males. Participants with ORD had a mean age of  $47.1 \pm 14.6$  years and 31 (40%) were males. An overview of the clinical and demographic characteristics of TB cases and ORD in the respective countries is shown in **Table 2**.

Plasma concentrations of I-309, MMP-1, MPO, PDGF-BB, RANTES, CRP, and Pentraxin3 show potential as TB diagnostic candidates irrespective of the study cohort.

### Norwegian Cohort

The baseline concentrations of 15 of the 54 analytes investigated had significantly different levels in all TB patients ( $n = 85$ ) compared to ORD patients ( $n = 19$ ) ( $0.0465 < P < 0.0001$ ) (**Supplementary Table 1**). There were significantly higher levels of I-309, MDC, VEGFR3, MMP-1, PDGF-BB, and RANTES in the TB patients compared to ORD, whereas the levels of CCL18, VCAM-1, GDF-15, MPO, pentraxin3, ferritin, myoglobin, CRP, and procalcitonin were significantly lower. The area under the ROC curve (AUC) was  $\geq 0.70$  for 10 of these markers namely, I-309, GDF-15, VEGFR3, MPO, MMP-1, Pentraxin3, PDGF-BB, RANTES, Ferritin, and CRP, whereas Myoglobin and Procalcitonin diagnosed TB with  $AUC \geq 0.80$  (**Supplementary Figure 1**). When only the individuals with pulmonary TB were compared to those with ORD, significant differences were observed for SAA, CRP, VEGFR3, RANTES, Pentraxin3, Ferritin, CCL18, MPO, GDF-15, MMP-1, PDGF-BB, Procalcitonin, MDC, Myoglobin, and VCAM-1. The diagnostic



**TABLE 1 |** Host markers evaluated in this study.

Abbreviation	Full name
<b>Reagent kits purchased from Merck Millipore, Billerica, Massachusetts, USA</b>	
CRP	C-reactive protein
SAA	Serum amyloid A
SAP	Serum amyloid P component
ApoA1	Apolipoprotein A1
C1q	Complement component 1q
C3b/iC3b	Complement component 3b
CC3	Complement component 3
CC4	Complement component 4
CFB	Complement factor B
CFH	Complement factor H
<b>Reagent kits purchased from R&amp;D Systems, Minneapolis, Minnesota, USA</b>	
Anti-thrombin III	Anti-thrombin III
ADAMTS13	A disintegrin and metalloproteinase with a thrombospondin type 1 motif, member 13
TGF- $\alpha$	Transforming growth factor alpha
IFN- $\gamma$	Interferon gamma
IP-10	Interferon gamma
TNF- $\alpha$ , TNF- $\beta$	IFN- $\gamma$ -inducible protein
Ferritin	Tumor necrosis factor-(alpha), beta
Myoglobin	Ferritin
PCT	Myoglobin
Pentraxin 3	Procalcitonin
CCL1/I-309	Pentraxin 3
MIG/CXCL9	Chemokine (C-C motif) ligand 1
VEGF	Monokine induced by gamma interferon
VEGFR3	Vascular endothelial growth factor
GDF-15	Vascular endothelial growth factor receptor 3
NCAM	Growth/differentiation factor 15
TNFR1	Neural cell adhesion molecule
RANTES	Tumor necrosis factor receptor 2
PDGF-BB	Regulated on activation, normal T cell expressed and secreted
MCP-1	Platelet derived growth factor BB
MDC	Monocyte chemoattractant protein 1
G-CSF	Macrophage derived chemokine
ICAM-1	Granulocyte colony stimulating factor
VCAM-1	Intercellular adhesion molecule 1
sCD40L	Vascular cell adhesion protein 1
MPO	Soluble CD40 ligand
MMP-(1, 2, 9)	Myeloperoxidase
CCL18	Matrix metalloproteinase
MIP-1 $\alpha$ , MIP-1 $\beta$	Chemokine (C-C motif) ligand 18
IL-(22, 1 $\beta$ , 12(p40), 12(p70), 2, 8, 13)	Macrophage inflammatory protein 1 (alpha), (beta)
IL-1Ra	Interleukin
IL-4Ra	Interleukin-1 receptor antagonist
IL-2Ra	Interleukin-4 receptor alpha
IL-6Ra	Interleukin-2 receptor alpha
	Interleukin-6 receptor alpha

accuracies of these markers as ascertained by ROC curve analysis showed potential, with AUC ranging from 0.69 to 0.89 (Supplementary Table 2).

### South African Cohort

The median baseline concentrations of 25 markers were significantly higher in TB patients than ORD patients namely; C3b/iC3b, IL-4Ra, C1q, procalcitonin, CFB, CCL18, GDF-15,

**TABLE 2 |** Demographic and clinical characteristics of study participants.

Characteristics	TB		ORD	
	Norway	South Africa	Norway	South Africa
Participants (N)	85	22	19	59
Age, mean $\pm$ SD	36.7 $\pm$ 13.9	37.2 $\pm$ 11.2	60.6 $\pm$ 12.1	41.9 $\pm$ 13.8
Males, n (%)	55 (65)	14 (64)	7 (37)	24 (41)
HIV pos, n (%)	8 (9)	1 (5)	0 (0)	0 (0)
<b>Type of TB, n (%)</b>				
PTB	34 (40)	22 (100)	NA	NA
EPTB	39 (46)	/		
PTB + EPTB	12 (14)	/		
<b>Ethnicity, n (%)</b>				
Caucasian	27 (32)	/	18 (95)	/
Asian	22 (26)	/	1 (5)	/
African	34 (40)	/	/	2 (3)
Colored (SA)	/	22 (100)	/	57 (97)

Other Respiratory Diseases (ORD) in the Norwegian cohort consisted of lower respiratory infections, mostly confirmed as bacterial pneumonia by chest X-ray and routine blood cultures. As described in (12), the South African ORD group consisted of individuals with a range of other diagnoses including acute exacerbations of chronic obstructive pulmonary disease or asthma, upper and lower respiratory tract infections including viral and bacterial infections. Attempts to identify these organisms by bacterial or viral cultures were not made. TB, tuberculosis; ORD, other respiratory diseases; PTB, Pulmonary TB; EPTB, Extrapulmonary TB; SD, standard deviation; pos, positive.

VCAM-1, TNF- $\alpha$ , ferritin, MPO, SAA, CRP, IL-2Ra, IFN- $\gamma$ , IP-10, PDGF-BB, VEGF, pentraxin3, MMP-1, RANTES, TNFR1, MIG, sCD40L, and I-309 (Supplementary Table 3). After ROC curve analysis, 13 of these biomarkers (MPO, SAA, CRP, IL-2Ra, IFN- $\gamma$ , IP-10, PDGF-BB, VEGF, pentraxin3, MMP-1, RANTES, TNFR1, MIG discriminated between the TB and ORD groups with AUC  $\geq$  0.70 and sCD40L and I-309 were the most promising, with AUC  $\geq$  0.80 (Supplementary Figure 2).

### Norwegian and South African Cohorts Combined

When data from all study participants were analyzed irrespective of the study site, the median concentrations of 21 of the 54 analytes were significantly different between the TB patients and those with ORD. The levels of SAA, VEGFR3, TNF- $\alpha$ , IL-2Ra, C1q, IL-12p70, MIG, TNFR1, C3b/iC3b, CC3, IP-10, I-309 were significantly higher in TB patients whereas, GDF-15, myoglobin, MMP-2, anti-thrombin III, IL-1Ra, MMP-9, and G-CSF levels were significantly higher in the ORD group (Supplementary Table 4). After ROC curve analysis, the AUC was  $\geq$  0.70 for CC3, IP-10, and I-309 (Supplementary Figure 3). When further univariate analysis was carried out in study participants from both cohorts excluding those with EPTB, the concentrations of C1q, CC3, C3b/iC3b, MIG, IL-12p70, TNFR1, VEGFR3, I-309, MIP-1a, IP-10, and G-CSF showed significant differences between the pulmonary TB and ORD groups (Supplementary Table 5).

Baseline concentrations of I-309, MPO, MMP-1, PDGF-BB, RANTES, CRP, and pentraxin3 thus showed diagnostic potential (AUC  $\geq$  0.70) both in the Norwegian and South African cohorts. However, irrespective of the study site, I-309 was the most useful single marker that discriminated between TB and

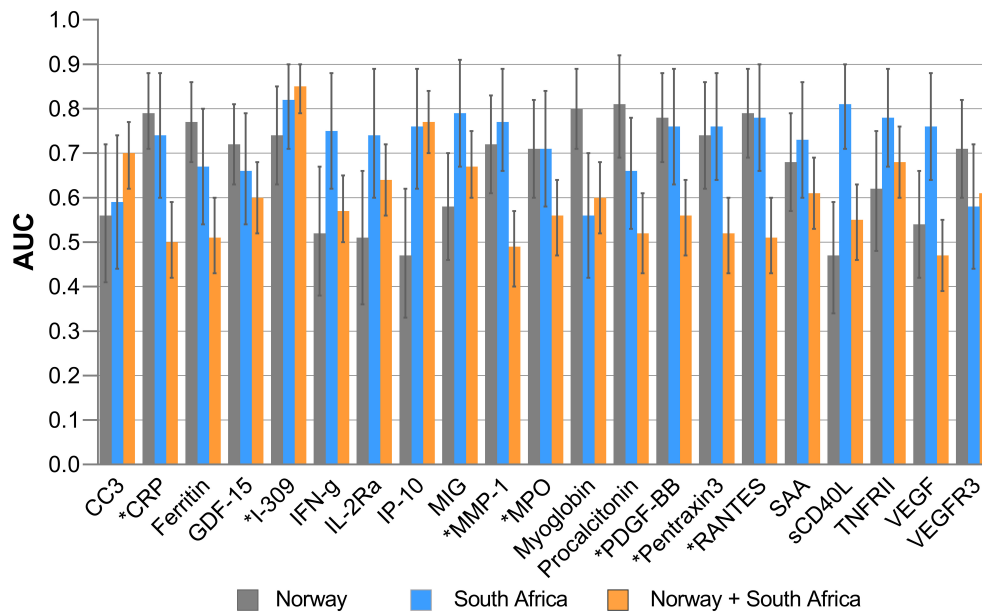


**FIGURE 2 |** Areas under the receiver operator characteristics (ROC) curves of significant biomarkers. AUC for individual analytes with significant differences in Norway and South Africa and their performance when all study participants from both settings were merged. Error bars represent 95% confidence interval of AUC. \*Highlights markers with promising diagnostic accuracy in both Norwegian and South African cohorts.

ORD (Figure 2). CCL18, CRP, GDF-15, ferritin, Procalcitonin, Pentraxin3, MPO, and VCAM-1 were highly expressed in patients with ORD from the Norwegian cohort in contrast to the South African cohort where these markers were higher in TB patients (Supplementary Figures 1, 2).

## Evaluation of Diagnostic Biosignatures in Tuberculosis

### Norwegian Cohort

We evaluated biosignatures in all Norwegian TB patients encompassing EPTB patients followed by analyses when only PTB was included and thereafter, assessed their performance on the South African cohort. When data obtained from the TB patients were analyzed by general discriminant analysis (GDA), optimal diagnosis of TB was achieved with a combination of four analytes. The most optimal biosignature was made up of 4-markers (I-309, procalcitonin, CRP, and PDGF-BB) which identified TB cases with an AUC of 0.98 (Figure 3A). After leave-one-out cross validation, the sensitivity of the 4-marker biosignature was 91.8% (95% CI, 83.8–96.8%) and specificity 89.5% (95% CI, 66.9–98.7%). The positive and negative predictive values (PPV and NPV) were 97.5% (95% CI, 91.3–99.3%) and 70.8% (54–83.4%), respectively. The frequency of markers in the top 20 most accurate 4-marker GDA models for the diagnosis of TB is shown in Figure 3B.

When the 4-marker biosignature was applied to South African study participants, with the latter being used as a validation cohort, this biosignature diagnosed TB with reduced sensitivity to 68.2% (95%CI, 45.1–86.1) and specificity of 91.5% (95% CI, 81.3–97.2) (Table 3). Moreover, when the signature was

optimized to meet the minimal requirements of the World Health Organization (WHO) target product profile for a triage test for use in a high TB setting (sensitivity >90% and specificity >70%), the specificity obtained was 76% for the targeted sensitivity of 90%.

When the analysis was performed only in study participants with PTB against ORD, optimal prediction of TB disease was achieved with the 5-marker signature made up of a combination of C1q, procalcitonin, CRP, PDGF-BB, and Ferritin. This 5-marker signature diagnosed TB with an accuracy of 100%, with sensitivity and specificity of 100% obtained after leave-one-out cross validation. The performance of the signature was reduced when applied to the South African cohort, with a sensitivity of 63.6% (95% CI, 40.7–82.8) and specificity 57.6% (95% CI, 44.1–70.4) (Table 3).

### South African Cohort

When data obtained from the South African participants were similarly fitted into GDA models, optimal prediction of TB was achieved with a combination of three markers. The most accurate 3-marker signature; MMP-9, IP-10 and sCD40L diagnosed TB with an AUC of 0.90 (95% CI, 0.83–0.97) (Figure 3C). After leave-one-out cross validation, the sensitivity of the biosignature was 68.2% and specificity was 88.1% (95% CI, 77.1–95.1%), with the PPV and NPV being 68.2% (95% CI, 50.3–82%) and 88.1% (95% CI, 80–93.2%), respectively (Table 3). When applied to the Norwegian cohort, the optimal 3 marker biosignature ascertained TB with reduced sensitivity and specificity of 48.2% (95% CI, 37.3–59.3) and 36.8% (95% CI, 16.3–61.6) respectively (Table 3). In the Norwegian study participants with PTB, an even reduced

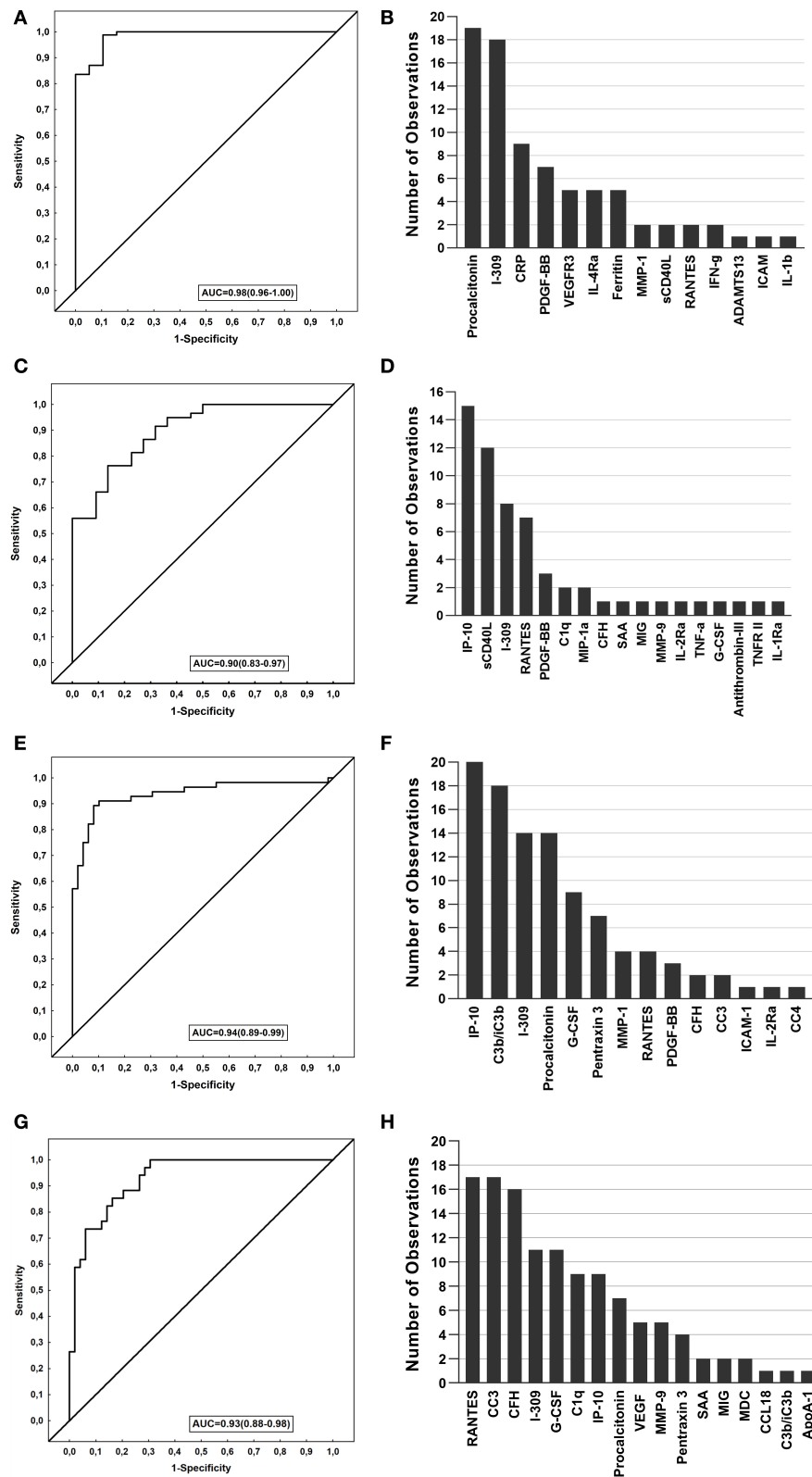


**FIGURE 3 |** Performance of biosignatures in the diagnosis of TB disease. The Receiver operator characteristics (ROC) curves showing the accuracies of the biosignatures generated. The bar graphs show the number of times each analyte was included in the top 20 general discriminant analysis (GDA) models for

(Continued)

**FIGURE 3 |** diagnosing TB. **(A)** ROC curve of the most accurate 4-marker biosignature (I-309, procalcitonin, CRP, PDGF-BB) which diagnosed TB in the Norwegian cohort. **(B)** Frequency of analytes in the top 20 GDA models that classified TB cases from ORD in Norwegian patients. **(C)** ROC curve of the most accurate 3-marker biosignature (MMP-9, IP-10 and sCD40L) which diagnosed TB in the South African cohort. **(D)** Frequency of analytes in the top 20 GDA model that classified the TB cases from ORD in South African patients. **(E)** ROC curve of the most accurate 5-marker biosignature (G-CSF, C3b/iC3b, procalcitonin, IP-10, and PDGF-BB) in diagnosing TB in all study participants from both cohorts. **(F)** Frequency of analytes in the top 20 GDA model that classified the TB cases from ORD in all study participants from both cohorts. **(G)** ROC curve of the most accurate 6-marker biosignature (RANTES, G-CSF, C1q, CC3, CFH, IP-10) in diagnosing pulmonary TB in all study participants from both cohorts. **(H)** Frequency of analytes in the top 20 GDA models that classified pulmonary TB from ORD in all study participants from both cohorts.

sensitivity of 29.4% (95% CI, 15.1–47.5) and specificity of 31.6% (95% CI, 12.6–56.6) was observed. Albeit the reduced diagnostic accuracy of the signature when applied to Norwegian study patients, the model ascertained TB with a specificity of 68% when optimizing for a higher sensitivity at  $\geq 90\%$ , and a sensitivity of 86% at a specificity  $\geq 70\%$ . The frequency of markers in the top 20 most accurate 3-marker GDA models for diagnosing TB is shown in **Figure 3D**.

### Norwegian and South African Cohorts Combined

To identify the potentially most useful biosignature for diagnosing TB irrespective of the study cohort, participants from the two study sites were combined and randomly assigned into a training (70%) and test (30%) sets. A 5-marker signature comprising of G-CSF, C3b/iC3b, procalcitonin, IP-10 and PDGF-BB that was identified in the training sample set performed in the test set with a sensitivity of 72.7% (95% CI, 49.8–82.3%), specificity of 90.5% (95% CI, 69.6–98.8%), PPV of 88.9% (95% CI, 67.2–96.8%) and NPV of 76% (95% CI, 61.2–86.4%). The signature obtained a specificity of 78% when the target for sensitivity was set at 90%, therefore meeting the WHO TPP criteria for a triage TB test (**Table 3**). The most frequent markers in the top 20 most accurate 5-marker GDA models for discriminating between TB and ORD when participants were combined are shown in **Figure 3F**. When the patients with EPTB were excluded prior to analysis of the merged data (Norway and South-Africa), the most optimal TB diagnostic biosignature was comprised of six markers (RANTES, G-CSF, C1q, CC3, CFH, IP-10), and ascertained TB with an AUC of 0.93 (**Table 3** and **Figures 3G,H**).

### Performance of Previously Identified African Signatures in the Norwegian Cohort

Finally, we evaluated the performance of previously reported host serum (CRP, SAA, IFN- $\gamma$ , IP-10, CFH, ApoA-1, transthyretin) (9) and plasma (CRP, SAP, NCAM, ferritin, I-309/CCL-1, GDF-15) (10) biosignatures in the Norwegian cohort (**Table 4**). As transthyretin was not available for evaluation in this study, we assessed the performance of combinations between the other six markers from the Chegou et al. signature. Generally, these biosignatures performed well with good diagnostic accuracies (AUC 0.84 to 0.94) despite reduced sensitivity and specificity. The serum biosignature by Chegou et al. (9) identified TB disease with a sensitivity of 67.5% (95% CI, 56.3–77.4) and specificity of 64.7% (95% CI, 38.3–85.8) while the plasma biosignature by Jacobs et al. (10) obtained a sensitivity of 78.9% (95% CI,

69–86.8) and specificity of 89.5% (95% CI, 66.9–98.7). Similar diagnostic performance was obtained for these signatures when analyses were performed on the Norway and South Africa cohorts combined.

### Changes in the Concentrations of Biomarkers During Treatment

To evaluate whether any of the biomarkers have the potential to be used for TB treatment monitoring, longitudinally collected plasma was analyzed in the Norwegian cohort. Out of the 85 TB cases 57 (67%), 62 (73%), and 49 (58%) provided specimens at week 2, months 2, and 6, respectively. The concentrations of 19 markers changed significantly in the course of TB treatment. There was a general decrease in the concentrations of CRP, ferritin, I-309, IFN- $\gamma$ , IP-10, IL-1 $\alpha$ , IL-2 $\alpha$ , IL-4 $\alpha$ , MDC, MMP-1, pentraxin3, procalcitonin, TNF- $\alpha$ , and SAA from baseline to month 6, whereas ADAMTS13, MMP-2, MCP-1, ApoA-1, and NCAM-1 levels significantly increased in the course of treatment (**Figure 4**). Significant changes were already observed for IFN- $\gamma$ , MMP-2, and SAA already at week 2 of treatment while levels of ADAMTS13, ApoA-1, CRP, ferritin, I-309, IL-1 $\alpha$ , IL-4 $\alpha$ , IP-10, MCP-1, MDC, MMP-1, NCAM-1, pentraxin3, procalcitonin and TNF- $\alpha$  became significantly changed first from month 2. The change in the concentrations of MIG, CCL18, TNFR1, IL-2, IL-12p70, and G-CSF only became significant at the end of treatment (month 6) compared to baseline levels. Finally, CFB, sCD40L, ICAM-1, IL-8, and VCAM-1 showed a decreasing trend during treatment with no overall significant changes (**Supplementary Table 6**).

### DISCUSSION

We present data on the performance of plasma host biosignatures in patients from two different TB endemic settings to assess the usefulness of already identified promising biomarkers. An optimal 5-marker biosignature (G-CSF, C3b/iC3b, Procalcitonin, IP-10, PDGF-BB) was identified which diagnosed TB if no pre-conditions were set, with a sensitivity of 72.7% and specificity of 90.5% irrespective of geographical site. When optimized with sensitivity set at  $>90\%$  (the minimum threshold set in the WHO TPPs for a triage TB test), the specificity of this 5-marker biosignature was 78%. When the specificity was fixed at  $>70\%$ , the sensitivity of the biosignature was 93%. The performance of this biosignature therefore met the minimum requirements for a triage TB test in the current study. When evaluated as potential biomarkers for monitoring TB treatment response, the concentrations of 19 markers changed with treatment, thereby



**TABLE 3 |** Accuracy of the biosignatures identified in the present study in the diagnosis of active TB.

Biosignature	AUC (95% CI)	Accuracy in training set		Accuracy in test set or after leave-one-out cross-validation				Performance according to WHO TPP	
		Sens (95%CI)	Spec (95%CI)	Sens (95%CI)	Spec (95%CI)	PPV (95%CI)	NPV (95%CI)	Sens (at Spec ≥70%)	Spec (at Sens ≥90%)
4-marker biosignature (I-309, procalcitonin, CRP, PDGF-BB) identified in the Norwegian cohort									
	0.98 (0.96–1.00)	92.9% (85.3–97.4)	89.5% (66.9–98.7)	91.8% (83.8–96.6)	89.5% (66.9–98.7)	97.5% (91.3–99.3)	70.8% (54–83.4)	100	89
Performance of the 4-marker biosignature in the South African cohort									
	0.90 (0.82–0.98)	68.2% (45.1–86.1)	93.2% (83.5–98.1)	68.2% (45.1–86.1)	91.5% (81.3–97.2)	75% (55.3–87.9)	88.5% (80.6–93.5)	91	76
5- marker biosignature (C1q, procalcitonin, CRP, PDGF-BB, Ferritin) identified in Pulmonary TB from the Norwegian cohort									
	1.00 (1.00–1.00)	100% (89.9–100)	100% (79.4–100)	100% (89.9–100)	100% (79.4–100)	100%	100%	100	100
Performance of the 5-marker biosignature in the South African cohort									
	0.76 (0.65–0.88)	77.3% (54.6–92.2)	57.6% (44.1–70.4)	63.6% (40.7–82.8)	57.6% (44.1–70.4)	35.9 (26.6–46.4)	80.9 (70.1–88.5)	59	44
3-marker biosignature (MMP-9, IP-10, sCD40L) identified in the South African cohort									
	0.90 (0.83–0.97)	68.2% (45.1–86.1)	88.1% (77.1–95.1)	68.2% (45.1–86.1)	88.1% (77.1–95.1)	68.2% (50.3–82)	88.1% (80–93.2)	86	68
Performance of the 3-marker biosignature in the Norwegian cohort									
	0.58 (0.44–0.72)	49.4% (38.4–60.5)	57.9% (33.5–79.7)	48.2% (37.3–59.3)	36.8% (16.3–61.6)	77.4% (69.4–83.7)	13.7% (7.9–22.9)	38	16
Performance of the 3-marker biosignature in Pulmonary TB from the Norwegian cohort									
	0.50 (0.34–0.66)	38.2% (22.2–56.4)	68.4% (43.4–87.4)	29.4% (15.1–47.5)	31.6% (12.6–56.6)	43.5% (29.6–58.5)	20% (11.1–33.4)	47	0
5-marker biosignature (G-CSF, C3b/iC3b, procalcitonin, IP-10, PDGF-BB) identified in the Norwegian and South African cohorts combined									
	0.94 (0.89–0.99)	84.2% (72.1–92.5)	91.8% (80.4–97.7)	72.7% (49.8–82.3)	90.5% (69.6–98.8)	88.9% (67.2–96.8)	76% (61.2–86.4)	93	78
6-marker biosignature (RANTES, G-CSF, C1q, CC3, CFH, IP-10) identified in Pulmonary TB from the Norwegian and South African cohorts combined									
	0.93 (0.88–0.98)	82.4% (65.5–93.2)	83.7% (70.3–92.7)	66.7% (38.4–88.2)	81% (58.1–94.6)	71.4% (49.1–86.6)	77.3% (61.7–87.6)	91.2	73.5

Biosignatures generated from data obtained in the Norwegian cohort (pulmonary TB + extrapulmonary TB), South African cohort (pulmonary TB) and when the cohorts (Norway and SA) were combined are shown. The Leave-one-out cross-validation method was applied to the Norwegian cohort (N = 104) and South African cohort (N = 81), whereas the training and test set method was used when both cohorts were combined (N = 185) to determine the predictive accuracy of biosignatures. The performance of biosignatures were also evaluated against the minimum sensitivity and specificity values of the minimum WHO target product profile (TPP) for a triage test. AUC, Area under the ROC curve; Sens, sensitivity; Spec, specificity; PPV, Positive Predictive Value; NPV, Negative Predictive Value; CI, Confidence Interval.

showing that they may be potential candidates for monitoring therapy responses.

The development of a rapid and simple non-sputum based immunodiagnostic tool will be ideal for the fight against TB in both high and low TB burden settings, most especially, in resource-limited settings. Validation of promising diagnostic host biomarkers for translation into novel point-of-care tests in multiple sites is thus of utmost importance. In our findings, I-309 (CCL1) was the most accurate single marker with diagnostic potential irrespective of the geographical site. I-309 is an inflammatory mediator, a member of the CC chemokine family, which stimulates the migration of human monocytes and whose expression is induced by Mtb and Toll-Like-Receptor (TLR) ligands expressed on macrophages (30). CCL18, CRP, GDF-15, ferritin, procalcitonin, pentraxin3, MPO, and VCAM-1 showed different response patterns in the different cohorts. They were highly expressed in patients with ORD in the Norwegian cohort and high among TB patients in the South African cohort. This

could be a result of the differences in clinical settings in the two geographical sites. Whereas, in South Africa where the risk of TB is high, it is low in Norway for a patient admitted to the hospital with respiratory symptoms. Norwegian ORD patients were clinically diagnosed with lower respiratory infections, predominately bacterial pneumonia implying the presence of systemic inflammatory markers such as CRP, procalcitonin, and pentraxin3. The South-African ORD cohort was somewhat younger and more diverse with a range of respiratory tract infections which were not further investigated as previously reported by Chegou et al. (12). Furthermore, the differences between the highly expressed markers in study participants might be due to differences in geographical settings and ethnicity. Most of the patients in the Norwegian cohort were immigrants from different African and Asian countries as comparable to the South African cohort which was made up of mostly South African colored citizens. Some previous works showed that the inflammatory profile identified in TB was associated with

**TABLE 4 |** Performance of previously identified African signatures in the diagnosis of TB disease in the Norwegian cohort and the combined Norwegian and South African cohort.

Biosignature	AUC (95% CI)	Sens (95%CI)	Spec (95%CI)	Sens (95%CI)	Spec (95%CI)	PPV (95%CI)	NPV (95%CI)
Accuracy in training set				Accuracy in test set or after leave-one-out cross-validation			
NORWEGIAN COHORT							
*Chegou et al. (9) (CRP, SAA, IFN-γ, IP-10, CFH, ApoA-1)	0.84 (0.75–0.93)	69.9% (58.8–79.5)	88.2% (63.6–98.5)	67.5% (56.3–77.4)	64.7% (38.3–85.8)	90.3% (82.8–94.8)	30% (20.3–39.4)
Jacobs et al. (10) (CRP, SAP, NCAM-1, Ferritin, I-309, GDF-15)	0.94 (0.90–0.99)	81.2% (71.2–88.8)	94.7% (74–99.9)	78.8% (68.6–86.9)	89.5% (66.9–98.7)	97.1% (89.9–99.2)	48.6% (37.9–59.4)
NORWEGIAN AND SOUTH AFRICAN COHORTS COMBINED							
Training set (n = 105; n = 56 TB, n = 49 ORD)				Test set (n = 43; n = 22 TB, n = 21 ORD)			
*Chegou et al. (9) (CRP, SAA, IFN-γ, IP-10, CFH, ApoA-1)	0.85 (0.77–0.92)	75% (61.6–85.6)	77.6% (63.4–88.2)	63.6% (40.7–82.8)	80.9% (58.1–94.5)	77.8% (57.8–89.9)	68% (54.1–79.3)
Jacobs et al. (10) (CRP, SAP, NCAM-1, Ferritin, I-309, GDF-15)	0.87 (0.80–0.94)	75% (61.6–85.6)	85.7% (72.8–94.1)	63.6% (40.7–82.8)	76.2% (52.8–91.7)	73.7% (55–86.5)	66.7% (52.3–78.5)

Previously published biosignatures; a serum biosignature (9), and a plasma biosignature (10), were evaluated in the Norwegian cohort and in Norwegian and South African cohorts combined.

\*One of the key biomarkers in the 7-marker serum biosignature (transthyretin) was unavailable, hence data shown is for performance of the remaining 6 analytes in the signature.

AUC, Area under the ROC curve; Sens, sensitivity; Spec, specificity; PPV, Positive predictive value; NPV, Negative predictive value; CI, Confidence Interval.

ethnic variation in host genotype, (26, 31). Nevertheless, baseline concentrations of I-309, MMP-1, MPO, PDGF-BB, RANTES, CRP, pentraxin3 showed diagnostic potential for TB both in Norway, a low TB endemic setting, and in South Africa, a high TB burden area.

As observed in previous biomarker reports, the combination of different single markers performed better in diagnosing TB than individual markers. A 4-marker biosignature (I-309, CCL-1, procalcitonin, CRP, PDGF-BB) performed best in the Norwegian cohort, whereas a 3-marker biosignature (MMP-9, IP-10, sCD40L) was the most optimal in the South African cohort. When participants from both cohorts were combined, the 5-marker biosignature (G-CSF, C3b/iC3b, procalcitonin, IP-10, PDGF-BB) offered the best accuracy.

The WHO target profile (TPP) for a point-of-care non-sputum-based triage test capable of detecting people suspected of having TB recommends a diagnostic tool with a sensitivity > 90% and a specificity > 70% (32). After optimizing the signatures identified in this study with these threshold values pre-specified, the specificities of the Norwegian 4-marker and the joint 5-marker signature fell within the accepted range (specificity > 70%) for sensitivity > 90%. Thus, the diagnostic accuracy of these biosignatures identified in the present study meets the minimum WHO target product profiles for a triage test when benchmarked against these criteria. A test based on these signatures has the potential to be used as a good rule-out test for TB disease whilst awaiting further systematic screening in TB suspects most especially in high TB burden areas with limited resources. Bodily, further investigation is required on

the performance of these biomarkers and signatures, including evaluation of the influence of HIV infection.

In defiance of different biosignatures identified in the present study, the Norwegian 4-marker signature showed potential as a rule-out test even when it was applied to South African participants after optimizing for higher sensitivity. Conjointly, the optimal 5-marker biosignature obtained when all sites were combined showed promise regardless of the different populations present in the joint cohort with heterogeneity in immune responses (pulmonary and EPTB TB patients combined). These findings were in contrast to the performance of the 3-marker signature identified in the South African cohort when assessed on the Norwegian cohort. We also observed a reduced sensitivity and specificity of previously published Africa-wide-derived 6-marker plasma and 7-marker serum signature (albeit, reduced to six markers because of the unavailability of one of the key biomarkers; transthyretin) in the Norwegian and combined cohorts. Although the reasons for the reduced performances is uncertain, there is a chance that biosignatures derived from studies designed differently, especially different levels of the health care settings may not validate in the respective cohorts. South Africa, a high burden area was represented by self-reporting individuals presenting with symptoms at a primary health care setting in contrast to hospitalized patients recruited in Norway, a high income and low TB burden setting. Other factors which might have influenced the differences observed in the current study could include differences in the types of both TB cases and individuals with ORD that were recruited at the different study sites, as well as the extent of disease in the

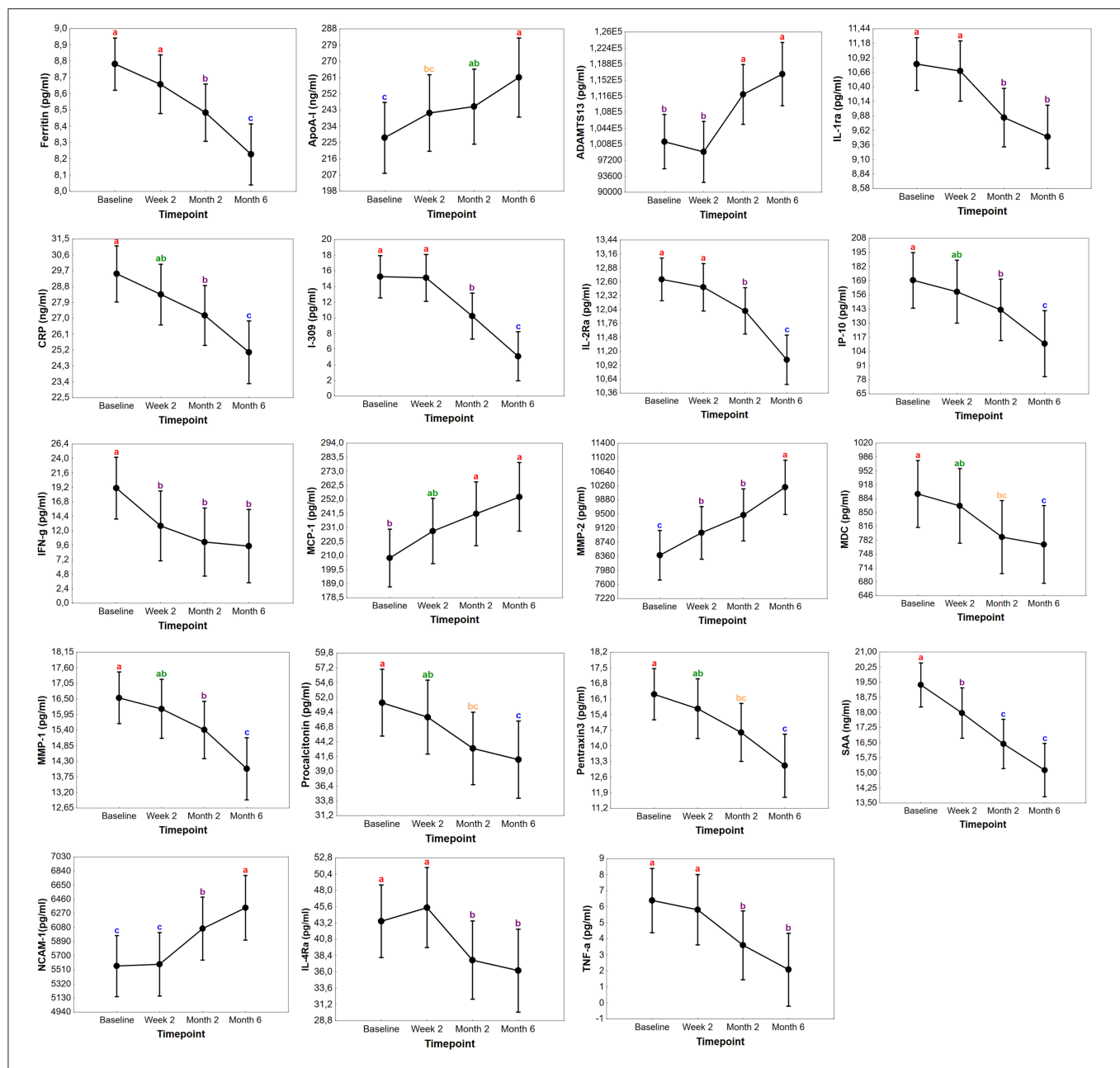


**FIGURE 4 |** Changes in the concentrations of biomarkers in TB patients during treatment in Norway. Concentrations of plasma markers in samples of Norwegian TB patients with significant differences before the start of TB treatment (baseline), at week 2, month 2, and month 6. Data points in each graph represent the mean and the error bars indicate the 95% confidence intervals. The concentrations of ADAMTS13, MMP-2, NCAM-1, MCP-1, ferritin, I-309, IFN- $\gamma$ , IL-1Ra, IL-2Ra, pentraxin3, procalcitonin, IP-10, MMP-1, TNF- $\alpha$ , IL-4Ra, MDC are expressed as pg/ml while ApoA-1, SAA, and CRP as ng/ml. The letters a-c indicates statistical significance where values with the same letter are not significantly different from each other.

patients, which was beyond the scope of the current study. In the Norwegian cohort, there were both PTB and EPTB cases as compared to the South African cohort that consisted only of definite PTB cases. Nonetheless, when the analysis was performed only on the PTB cases compared to the ORD group in the Norwegian cohort, an optimal signature of 5-markers (C1q, procalcitonin, CRP, PDGF-BB, ferritin) performed excellently with a sensitivity and specificity of 100%. The accuracy and

performance of this signature were reduced when applied on the South African cohort while the identified South African 3-marker biosignature performed poorly in the new Norwegian data set (PTB vs. ORD). Although there might be differences in the immune response associated with PTB and EPTB, similar markers showing significant differences between TB and ORD were observed regardless of whether the EPTB patients were included or excluded during data analysis. That is, the markers

that showed potential individually in discriminating between TB and ORD (C1q, CC3, C3b/iC3b, MIG, IL-12p70, TNFR1I, VEGFR3, I-309, MIP-1a, IP-10, G-CSF in PTB vs. ORD) when Norwegian and South African study participants were combined were the same markers that showed potential when EPTB patients were excluded. That notwithstanding, a different 6-marker biosignature showed the most promise when only the PTB patients were compared to individuals with ORD (Norway and South Africa combined). Previous work by Fortún et al. highlighted no differences in biomarker concentrations between PTB and EPTB patients (33), whilst Ranaivomanana et al. reported differences in only TNF- $\alpha$  and VEGF after macrophage stimulation (34). Furthermore, blood transcriptional signatures reflecting immune response in PTB and EPTB patients were similar across sites of disease with varying degrees of responses correlating to the presence or absence of symptoms in another study (35). It is thus unclear whether geographical setting and patient recruitment strategy are the only contributing factors to the variation seen in the expression of biomarkers across sites. Still, all the promising biomarkers from the current study, are well-known proteins that have been widely investigated in TB, using different sample types (10, 24, 28). These markers in unison with frequently occurring markers in the top 20 GDA models may be considered strong candidate biomarkers for further investigations in multi-centre studies and point-of-care TB test development.

The concentration of several biomarkers changed significantly during TB treatment when evaluated in the Norwegian cohort. These markers could thus be useful as potential markers for monitoring TB treatment. The changes in concentrations after treatment initiation could be reflective of host immune function restoration due to a reduction in bacterial load. Our observation of increasing levels of ApoA-1, MMP-2 and MCP-1 is in agreement with previous reports (10, 36, 37). Amongst markers with a significant decrease during treatment were acute phase proteins (CRP, SAA, pentraxin3, procalcitonin and ferritin) as well as the pro-inflammatory markers IP-10, IFN- $\gamma$ , TNF- $\alpha$ , and MMP-1 which are in accordance with several other works reporting their potential in evaluating TB treatment and as markers of disease severity and bacterial burden (10, 36, 38–42). Withal, host biomarkers have also shown potential in predicting month 2 culture status and poor TB treatment outcomes (relapse and failure), but assessment of the predictive accuracy of the biomarkers for different treatment outcomes was outside the scope of this study.

A particular strength of this study is the inclusion of study participants from different settings, which allowed us to test the robustness of previously published biomarkers in the diagnosis of TB in patients recruited using different protocols across different geographical settings. Investigations were carried out in a data set with a lot of heterogeneity between the study cohorts in terms of the ORD group and type of TB cases. Our study provides evidence that some of the biomarkers investigated may be strong, robust candidates for a globally relevant test. We also evaluated the usefulness of the biomarkers as tools for monitoring TB treatment responses in clinically responded patients at that time point, although we could not evaluate treatment outcome due to the small size of month 2 culture positive samples. Additionally,

we were unable to assess the influence of HIV infection on the performance of the biomarkers due to the low proportion (5%) of the HIV infected study participants. We acknowledge that the proportion of HIV positive study participants particularly in the South African cohort was not representative of what is estimated for Sub-Saharan African countries. This bias was introduced by the random selection of study participants from our biobank, with the clinical information of participants only known during data analysis. That notwithstanding, previous work carried out in South Africa showed that the identified biosignatures performed well irrespective of HIV infection (9, 10, 13). However, well-designed studies in which the performance of the signatures is assessed in HIV positive patients that are stratified according to CD4 cell counts and viral loads are required. As the cohorts used in the present study were recruited using different strategies (hospitalized patients recruited in a low TB endemic setting vs. self-reported patients presenting with symptoms requiring investigation for TB at a high burden setting), not using the same protocols for recruitment of study participants may be seen as a limitation. The lack of sample size calculations prior to the start of the study is a limitation. However, the number of study participants employed in the study is similar to the numbers used in other previous biomarker-based work. Further multi-center confirmatory studies including people recruited in both high and low TB endemic settings are thus required. It may be necessary to standardize the study protocols so that bias due to different study designs does not affect study findings. However, it is important that such future studies enroll participants that are relevant to the different clinical settings, so that findings are clinically relevant. The biomarkers that performed well in the study may be considered as strong candidates for future evaluation and consideration for globally relevant point-of-care tests.

In conclusion, among 54 potential TB biomarkers evaluated in this study, we identified strong individual candidate biomarkers and a 5-marker plasma protein biosignature (G-CSF, C3b/iC3b, procalcitonin, IP-10, PDGF-BB) which showed potential in diagnosing TB regardless of the endemic setting. The concentrations of some of the markers also changed significantly during TB treatment, suggesting their potential utility as biomarkers for monitoring response to TB treatment. Our data highlights the importance of validating host immunological biomarkers in different geographical and ethnic settings, in the global search for non-sputum-based biomarkers for point-of-care diagnosis of active TB.

## DATA AVAILABILITY STATEMENT

The raw data supporting the conclusions of this article will be made available by the authors, without undue reservation.

## ETHICS STATEMENT

The studies involving human participants were reviewed and approved by Regional Ethics Committee REK 2016/2123) at the Department of Infectious Diseases, OUS, Research Biobank Infectious Disease (REK nr.6.2008.173), and the Health Research Ethics Committee of the University of Stellenbosch



(N16/05/070). The patients/participants provided their written informed consent to participate in this study.

## AUTHOR CONTRIBUTIONS

NC and AD-R had the idea for and designed the study. NC, GW, and AD-R set up the clinical cohorts at the respective hospitals. KT, SJ, AD-R, GW, and NC included patients and collected data. CS and BC performed the multiplex analyses. BC and MK did the statistical analyses. BC, NC, and AD-R interpreted the data and drafted the paper. All authors critically reviewed the manuscript for important intellectual content and gave final approval for the version to be published. All authors agree to be accountable for all aspects of the work in ensuring that questions related to the accuracy or integrity of any part of the work are appropriately investigated and resolved.

## FUNDING

The ScreenTB Consortium was funded by the EDCTP with grant number DRIA2014-311. The project received funding from *The Gilead Sciences Nordic Fellowship Program 2018*. The funders had no role in study design, data collection, and analysis, decision to publish, or preparation of the manuscript.

## ACKNOWLEDGMENTS

We are grateful to all participants for contributing to this study and to all the staff at the Oslo University Hospital,

especially Linda Gail Skeie, Sarah Nur and Mette Sannes, and the Stellenbosch University Immunology research groups for including patients.

## THE SCREENTB CONSORTIUM

Stellenbosch University, South Africa: Gerhard Walzl, Novel N. Chegou, Petri Ahlers, Stephanus T. Malherbe, Gian van der Spuy, Ilana van Rensburg, Hygon Mutavhatsindi, Portia Manngo, Kim Stanley, Andriette Hiemstra, Shirley McAnda. Medical Research Council Gambia at LSHTM: Jayne Sutherland, Joseph Mendy, Awa Gindeh, Georgetta Mbayo, Ebrima Trawally, Olumuyiwa Owolabi Makerere University, Uganda: Harriet Mayanja-Kizza, Mary Nsereko, Anna-Rita Namuganga, Saudah Nambiru Kizito. Armauer Hansen Research Institute, Addis Ababa, Ethiopia: Adane Mihret, Sosina Ayalew, Rawleigh Howe, Azab Tarekegne, Bamlak Tessema. University of Namibia, Namibia: Emmanuel Nepolo, Joseph Sheehama, Gunar Gunther, Azaria Diergaardt, Uapa Pazvakavambwa. London School of Hygiene and Tropical Medicine, UK: Hazel Dockrell. Leiden University Medical Centre, Netherlands: Tom Ottenhoff, Elisa Tjon Kon Fat, Shannon Herdigein, Paul Corstjens, Annemieke Geluk.

## SUPPLEMENTARY MATERIAL

The Supplementary Material for this article can be found online at: <https://www.frontiersin.org/articles/10.3389/fimmu.2021.608846/full#supplementary-material>

## REFERENCES

- World Health Organization. *WHO Global Tuberculosis Report 2019* (2020).
- Amicosante M, D'Ambrosio L, Munoz M, Mello FCQ, Tebruegge M, Chegou NN, et al. Current use and acceptability of novel diagnostic tests for active tuberculosis: a worldwide survey. *J Bras Pneumol.* (2017) 43:380–92. doi: 10.1590/s1806-37562017000000219
- Chegou NN, Hoek KG, Kriel M, Warren RM, Victor TC, Walzl G. Tuberculosis assays: past, present and future. *Exp Rev Anti Infect Ther.* (2011) 9:457–69. doi: 10.1586/eri.11.23
- Goletti D, Lee M-R, Wang J-Y, Walter N, Ottenhoff THM. Update on tuberculosis biomarkers: from correlates of risk, to correlates of active disease and of cure from disease. *Respirology.* (2018) 23:455–66. doi: 10.1111/resp.13272
- Goletti D, Petruccioli E, Joosten SA, Ottenhoff THM. Tuberculosis biomarkers: From diagnosis to protection. *Infect Dis Rep.* (2016) 8:24–32. doi: 10.4081/idr.2016.6568
- Walzl G, Ronacher K, Hanekom W, Scriba TJ, Zumla A. Immunological biomarkers of tuberculosis. *Nat Rev Immunol.* (2011) 11:343–54. doi: 10.1038/nri2960
- Horne DJ, Royce SE, Gooze L, Narita M, Hopewell PC, Nahid P, et al. Sputum monitoring during tuberculosis treatment for predicting outcome: systematic review and meta-analysis. *Lancet Infect Dis.* (2010) 10:387–94. doi: 10.1016/S1473-3099(10)70071-2
- Miotto P, Bigoni S, Migliori GB, Matteelli A, Cirillo DM. Early tuberculosis treatment monitoring by Xpert® MTB/RIF. *Eur Respir J.* (2012) 39:1269–71. doi: 10.1183/09031936.00124711
- Chegou NN, Sutherland JS, Malherbe S, Crampin AC, Corstjens PLAM, Geluk A, et al. Diagnostic performance of a seven-marker serum protein biosignature for the diagnosis of active TB disease in African primary healthcare clinic attendees with signs and symptoms suggestive of TB. *Thorax.* (2016) 71:785–94. doi: 10.1136/thoraxjnl-2015-207999
- Jacobs R, Malherbe S, Loxton AG, Stanley K, van der Spuy G, Walzl G, et al. Identification of novel host biomarkers in plasma as candidates for the immunodiagnosis of tuberculosis disease and monitoring of tuberculosis treatment response. *Oncotarget.* (2016) 7:57581–92. doi: 10.18632/oncotarget.11420
- Mihret A, Bekele Y, Bobosha K, Kidd M, Aseffa A, Howe R, et al. Plasma cytokines and chemokines differentiate between active disease and non-active tuberculosis infection. *J Infect.* (2013) 66:357–65. doi: 10.1016/j.jinf.2012.11.005
- Chegou NN, Black GF, Kidd M, van Helden PD, Walzl G. Host markers in Quantiferon supernatants differentiate active TB from latent TB infection: preliminary report. *BMC Pulm Med.* (2009) 9:21 doi: 10.1186/1471-2466-9-21
- Chegou NN, Sutherland JS, Namuganga AR, Corstjens PLAM, Geluk A, Gebremichael G, et al. Africa-wide evaluation of host biomarkers in QuantiFERON supernatants for the diagnosis of pulmonary tuberculosis. *Sci Rep.* (2018) 8:2675. doi: 10.1038/s41598-018-20855-7
- Awoniyi DO, Teuchert A, Sutherland JS, Mayanja-Kizza H, Howe R, Mihret A, et al. Evaluation of cytokine responses against novel Mtb antigens as diagnostic markers for TB disease. *J Infect.* (2016) 73:219–30. doi: 10.1016/j.jinf.2016.04.036
- Jacobs R, Tshela E, Malherbe S, Kriel M, Loxton AG, Stanley K, et al. Host biomarkers detected in saliva show promise as markers for the diagnosis of pulmonary tuberculosis disease and monitoring of the response to tuberculosis treatment. *Cytokine.* (2016) 81:50–6. doi: 10.1016/j.cyt.2016.02.004

16. Phalane KG, Kriel M, Loxton AG, Menezes A, Stanley K, Van Der Spuy GD, et al. Differential expression of host biomarkers in saliva and serum samples from individuals with suspected pulmonary tuberculosis. *Mediators Inflamm.* (2013) 2013:981984. doi: 10.1155/2013/981984
17. Namuganga AR, Chegou NN, Mubiri P, Walzl G, Mayanja-Kizza H. Suitability of saliva for tuberculosis diagnosis: comparing with serum. *BMC Infect Dis.* (2017) 17:1–11. doi: 10.1186/s12879-017-2687-z
18. Ruhwald M, Dominguez J, Latorre I, Losi M, Richeldi L, Pasticci MB, et al. A multicentre evaluation of the accuracy and performance of IP-10 for the diagnosis of infection with *M. tuberculosis*. *Tuberculosis.* (2011) 91:260–7. doi: 10.1016/j.tube.2011.01.001
19. Vanini V, Petruccioli E, Gioia C, Cuzzi G, Orchi N, Rianda A, et al. IP-10 is an additional marker for tuberculosis (TB) detection in HIV-infected persons in a low-TB endemic country. *J Infect.* (2012) 65:49–59. doi: 10.1016/j.jinf.2012.03.017
20. Wergeland I, Pullar N, Assmus J, Ueland T, Tonby K, Feruglio S, et al. IP-10 differentiates between active and latent tuberculosis irrespective of HIV status and declines during therapy. *J Infect.* (2015) 70:381–91. doi: 10.1016/j.jinf.2014.12.019
21. Wergeland I, Assmus J, Dyrhol-Riise AM. Cytokine patterns in tuberculosis infection; IL-1ra, IL-2 and IP-10 differentiate borderline QuantiFERON-TB samples from uninfected controls. van Zyl-Smit R, editor. *PLoS ONE.* (2016) 11:e0163848. doi: 10.1371/journal.pone.0163848
22. Pai M, Denkinger CM, Kik SV, Rangaka MX, Zwerling A, Oxlade O, et al. Gamma interferon release assays for detection of *Mycobacterium tuberculosis* infection. *Clin Microbiol Rev.* (2014) 27:3–20. doi: 10.1128/CMR.00034-13
23. WHO. *Use of Tuberculosis Release Assays (IGRAs) in Low and Middle-Income Countries.* World Heal Organ Policy Statement (2011). p. 1–70.
24. MacLean E, Broger T, Yerlikaya S, Fernandez-Carballo BL, Pai M, Denkinger CM. A systematic review of biomarkers to detect active tuberculosis. *Nat Microbiol.* (2019) 4:748–58. doi: 10.1038/s41564-019-0380-2
25. Sackett DL, Haynes RB. The architecture of diagnostic research. *BMJ.* (2002) 324:539–41. doi: 10.1136/bmj.324.7336.539
26. Colli A, Fraquelli M, Casazza G, Conte D, Nikolova D, Duca P, et al. The architecture of diagnostic research: from bench to bedside-research guidelines using liver stiffness as an example. *Hepatology.* (2014) 60:408–18. doi: 10.1002/hep.26948
27. Leeftang MMG, Allerberger F. How to: evaluate a diagnostic test. *Clin Microbiol Infect.* (2019) 25:54–9. doi: 10.1016/j.cmi.2018.06.011
28. Wang S, Li Y, Shen Y, Wu J, Gao Y, Zhang S, et al. Screening and identification of a six-cytokine biosignature for detecting TB infection and discriminating active from latent TB. *J Transl Med.* (2018) 16:206. doi: 10.1186/s12967-018-1572-x
29. Zhao Y, Yang X, Zhang X, Yu Q, Zhao P, Wang J, et al. IP-10 and RANTES as biomarkers for pulmonary tuberculosis diagnosis and monitoring. *Tuberculosis.* (2018) 111:45–53. doi: 10.1016/j.tube.2018.05.004
30. Zhao Y, Bu H, Hong K, Yin H, Zou YL, Geng SJ, et al. Genetic polymorphisms of CCL1 rs2072069 G/A and TLR2 rs3804099 T/C in pulmonary or meningeal tuberculosis patients. *Int J Clin Exp Pathol.* (2015) 8:12608–20.
31. Coussens AK, Wilkinson RJ, Nikolayevskyy V, Elkington PT, Hanifa Y, Islam K, et al. Ethnic Variation in inflammatory profile in tuberculosis. *PLoS Pathog.* (2013) 9:e1003468. doi: 10.1371/journal.ppat.1003468
32. WHO. High-priority target product profiles for new tuberculosis diagnostics: report of a consensus meeting. *WHO Meet Rep.* (2014) 1–98.
33. Fortún J, Martín-Dávila P, Gómez-Mampaso E, Vallejo A, Cuartero C, González-García A, et al. Extra-pulmonary tuberculosis: a biomarker analysis. *Infection.* (2014) 42:649–54. doi: 10.1007/s15010-014-0602-8
34. Ranaivomanana P, Raberahona M, Rabarioelina S, Borella Y, Machado A, Randria MJDD, et al. Cytokine biomarkers associated with human extra-pulmonary tuberculosis clinical strains and symptoms. *Front Microbiol.* (2018) 9:275. doi: 10.3389/fmicb.2018.00275
35. Blankley S, Graham CM, Turner J, Berry MPR, Bloom CI, Xu Z, et al. The transcriptional signature of active tuberculosis reflects symptom status in extra-pulmonary and pulmonary tuberculosis. *PLoS ONE.* (2016) 11:e0162220. doi: 10.1371/journal.pone.0162220
36. Sigal GB, Segal MR, Mathew A, Jarlsberg L, Wang M, Barbero S, et al. Biomarkers of tuberculosis severity and treatment effect: a directed screen of 70 host markers in a randomized clinical trial. *EBioMed.* (2017) 25:112–21. doi: 10.1016/j.ebiom.2017.10.018
37. Djoba Siawaya JF, Beyers N, Van Helden P, Walzl G. Differential cytokine secretion and early treatment response in patients with pulmonary tuberculosis. *Clin Exp Immunol.* (2009) 156:69–77. doi: 10.1111/j.1365-2249.2009.03875.x
38. Rockwood N, du Bruyn E, Morris T, Wilkinson RJ. Assessment of treatment response in tuberculosis. *Exp Rev Respir Med.* (2016) 10:643–54. doi: 10.1586/17476348.2016.1166960
39. Trajcevska M, Sandevski A, Simonovska L. Acute phase reaction in pulmonary tuberculosis during treatment. *Eur Respir J.* (2015) 46(suppl 59):PA4529. doi: 10.1183/13993003.congress-2015.PA4529
40. Kumar NP, Moideen K, Banurekha VV, Nair D, Babu S. Plasma proinflammatory cytokines are markers of disease severity and bacterial burden in pulmonary tuberculosis. *Open Forum Infect Dis.* (2019) 6:ofz257. doi: 10.1093/ofid/ofz257
41. Hoel IM, Jørstad MD, Marijani M, Ruhwald M, Mustafa T, Dyrhol-Riise AM. IP-10 dried blood spots assay monitoring treatment efficacy in extrapulmonary tuberculosis in a low-resource setting. *Sci Rep.* (2019) 9:3871. doi: 10.1038/s41598-019-40458-0
42. Tonby K, Ruhwald M, Kvale D, Dyrhol-Riise AM. IP-10 measured by dry plasma spots as biomarker for therapy responses in mycobacterium tuberculosis infection. *Sci Rep.* (2015) 5:9223. doi: 10.1038/srep09223

**Conflict of Interest:** The authors declare that the research was conducted in the absence of any commercial or financial relationships that could be construed as a potential conflict of interest.

Copyright © 2021 Chendi, Snyders, Tonby, Jenum, Kidd, Walzl, Chegou and Dyrhol-Riise. This is an open-access article distributed under the terms of the Creative Commons Attribution License (CC BY). The use, distribution or reproduction in other forums is permitted, provided the original author(s) and the copyright owner(s) are credited and that the original publication in this journal is cited, in accordance with accepted academic practice. No use, distribution or reproduction is permitted which does not comply with these terms.



# Evaluation of Host Serum Protein Biomarkers of Tuberculosis in sub-Saharan Africa

Thomas C. Morris<sup>1\*</sup>, Clive J. Hoggart<sup>1,2</sup>, Novel N. Chegou<sup>3</sup>, Martin Kidd<sup>4</sup>, Tolu Oni<sup>5,6</sup>, Rene Goliath<sup>5</sup>, Katalin A. Wilkinson<sup>5,7</sup>, Hazel M. Dockrell<sup>8</sup>, Lifted Sichali<sup>9</sup>, Louis Banda<sup>9</sup>, Amelia C. Crampin<sup>9,10,11</sup>, Neil French<sup>12</sup>, Gerhard Walzl<sup>3</sup>, Michael Levin<sup>1</sup>, Robert J. Wilkinson<sup>1,5,7</sup> and Melissa S. Hamilton<sup>1\*</sup> for the ILULU Consortium

<sup>1</sup> Department of Infectious Disease, Faculty of Medicine, Imperial College London, London, United Kingdom, <sup>2</sup> Department of Genetics and Genomic Sciences, Icahn School of Medicine at Mount Sinai, New York, NY, United States, <sup>3</sup> DST-NRF Centre of Excellence for Biomedical Tuberculosis Research, South African Medical Research Council Centre for Tuberculosis Research, Division of Molecular Biology and Human Genetics, Department of Biomedical Sciences, Faculty of Medicine and Health Sciences, Stellenbosch University, Cape Town, South Africa, <sup>4</sup> Centre for Statistical Consultation, Stellenbosch University, Cape Town, South Africa, <sup>5</sup> Department of Medicine, Wellcome Centre for Infectious Diseases Research in Africa, Institute of Infectious Disease and Molecular Medicine, University of Cape Town, Cape Town, South Africa, <sup>6</sup> MRC Epidemiology Unit, University of Cambridge, Cambridge, United Kingdom, <sup>7</sup> The Francis Crick Institute, London, United Kingdom, <sup>8</sup> Department of Infection Biology, Faculty of Infectious and Tropical Diseases, London School of Hygiene & Tropical Medicine, London, United Kingdom, <sup>9</sup> Malawi Epidemiology and Intervention Research Unit, Karonga Prevention Study, Lilongwe, Malawi, <sup>10</sup> Department of Infectious Disease Epidemiology, Faculty of Epidemiology and Population Health, London School of Hygiene & Tropical Medicine, London, United Kingdom, <sup>11</sup> Institute of Health and Wellbeing, University of Glasgow, Glasgow, United Kingdom, <sup>12</sup> Department of Clinical Infection, Microbiology and Immunology, Institute of Infection and Global Health, University of Liverpool, Liverpool, United Kingdom

## OPEN ACCESS

### Edited by:

Buka Samten,  
University of Texas at Tyler,  
United States

### Reviewed by:

Zissis Chronos,  
Pennsylvania State University,  
United States  
Roberta Olmo Pinheiro,  
Oswaldo Cruz Foundation, Brazil  
Edward Chan,  
Rocky Mountain Regional VA Medical  
Center, United States

### \*Correspondence:

Thomas C. Morris  
thomasmorris@doctors.org.uk  
Melissa S. Hamilton  
s.hamilton@imperial.ac.uk

### Specialty section:

This article was submitted to  
Microbial Immunology,  
a section of the journal  
Frontiers in Immunology

**Received:** 08 December 2020

**Accepted:** 27 January 2021

**Published:** 25 February 2021

### Citation:

Morris TC, Hoggart CJ, Chegou NN, Kidd M, Oni T, Goliath R, Wilkinson KA, Dockrell HM, Sichali L, Banda L, Crampin AC, French N, Walzl G, Levin M, Wilkinson RJ and Hamilton MS (2021) Evaluation of Host Serum Protein Biomarkers of Tuberculosis in sub-Saharan Africa. *Front. Immunol.* 12:639174. doi: 10.3389/fimmu.2021.639174

Accurate and affordable point-of-care diagnostics for tuberculosis (TB) are needed. Host serum protein signatures have been derived for use in primary care settings, however validation of these in secondary care settings is lacking. We evaluated serum protein biomarkers discovered in primary care cohorts from Africa reapplied to patients from secondary care. In this nested case-control study, concentrations of 22 proteins were quantified in sera from 292 patients from Malawi and South Africa who presented predominantly to secondary care. Recruitment was based upon intention of local clinicians to test for TB. The case definition for TB was culture positivity for *Mycobacterium tuberculosis*; and for other diseases (OD) a confirmed alternative diagnosis. Equal numbers of TB and OD patients were selected. Within each group, there were equal numbers with and without HIV and from each site. Patients were split into training and test sets for biosignature discovery. A nine-protein signature to distinguish TB from OD was discovered comprising fibrinogen, alpha-2-macroglobulin, CRP, MMP-9, transthyretin, complement factor H, IFN-gamma, IP-10, and TNF-alpha. This signature had an area under the receiver operating characteristic curve in the training set of 90% (95% CI 86–95%), and, after adjusting the cut-off for increased sensitivity, a sensitivity and specificity in the test set of 92% (95% CI 80–98%) and 71% (95% CI 56–84%), respectively. The best single biomarker was complement factor H [area under the receiver operating characteristic curve 70% (95% CI 64–76%)]. Biosignatures consisting of host serum proteins may function as point-of-care screening tests for TB in African hospitals. Complement factor H is identified as a new biomarker for such signatures.

**Keywords:** serum, protein, biomarker, tuberculosis, diagnosis, HIV, Africa

## INTRODUCTION

Tuberculosis (TB) remains a leading cause of death from any infection worldwide. The number of people accessing treatment is increasing each year, but in 2019 there were still an estimated 10 million cases and 1.4 million deaths (1). The region with the highest incidence and fatality rate is Africa, where the prevalence of HIV co-infection in some areas exceeds 50% (1).

The potential for rapid diagnosis of TB in African hospitals has been enhanced by the roll-out of the GeneXpert MTB/RIF test (Xpert, Cepheid, Sunnyvale, California, USA). Xpert is a sputum-based PCR assay with high sensitivity and specificity (2), but has several practical limitations. These include high cost, need for annual overseas calibration, laboratory containment facilities, and continuous electricity. In addition, as a laboratory-based assay, Xpert is not a true point-of-care (POC) test that can deliver a result within a single consultation.

An alternative to pathogen detection is quantification of host-derived biomarkers, such as serum proteins. Serum proteins are generally of higher abundance than pathogen products, are amenable to existing POC technologies such as lateral flow immunoassay (LFA), and have been shown to discriminate between different infections when combined as biosignatures (3–6). In 2016, a cohort study was published by the African European TB Consortium (AE-TBC) in which a seven-protein signature was reported that distinguished pulmonary TB from other respiratory diseases with an area under the receiver operating characteristic (ROC) curve of 91% (7). The study was conducted in primary care clinics across five countries in Africa. Participants presenting with symptoms requiring investigation for TB were recruited. The seven proteins were selected from a shortlist of 22 that had been discovered in pilot studies.

An accurate, cheap, user-friendly POC test for TB for use in secondary care hospital settings in sub-Saharan Africa would also be highly desirable. We therefore retested the signature and all 22 biomarkers from the AE-TBC study in cohorts from a case-control study that recruited adults presenting with features of TB to hospitals in Cape Town, South Africa, and Karonga, Malawi, and a TB clinic in Cape Town (the “ILULU-TB study”) (8). Equal numbers of patients were recruited with and without HIV to both TB and other diseases (OD) groups (8). Recruitment of TB patients at all sites was on the basis of culture positivity. All OD patients were recruited from hospitals. We therefore considered this cohort to be reflective of patients presenting to secondary care. We hypothesised that the seven-protein signature from the AE-TBC study, or a new signature derived from the same 22 proteins, would distinguish TB from OD in patients from the ILULU-TB study, regardless of HIV status, with a similar degree of accuracy as in the AE-TBC study.

## METHODS

### ILULU-TB Patient Recruitment and Biobank Sampling

Between 2007 and 2010, 674 adults were recruited to the ILULU-TB study from Cape Town, South Africa, and Karonga District, Malawi. These sites have differing prevalences of ODs such

as parasitic infection and differing environmental exposures (urban vs. rural). Details of recruitment have been described previously (8). Briefly, patients in the TB and OD groups were recruited consecutively and based on intention of the local clinician to test for TB. The criterion for inclusion in the TB group was at least one positive culture (sputum or tissue) for *Mycobacterium tuberculosis* (Mtb), which is the WHO gold standard (1). Laboratory identification of Mtb was confirmed by polymerase chain reaction (PCR). All of the TB patients that were enrolled had pulmonary TB. OD patients had an established alternative diagnosis, negative cultures for Mtb and an observed improvement of symptoms after follow-up without TB treatment. In Cape Town, TB patients were recruited from either an outpatient clinic (Khayelitsha site B) or hospital sites (Groote Schuur and GF Jooste), whereas OD patients were all recruited from the hospital sites. In Karonga, both TB and OD patients were recruited from Karonga District Hospital. As healthy controls, adults with latent TB infection (LTBI) were also recruited. LTBI status was defined by positive tuberculin skin tests and in-house interferon-gamma release assays in the absence of TB symptoms (9). Sera were collected from all participants at recruitment and stored at  $-80^{\circ}\text{C}$ . All groups had HIV-1 status ascertained.

For the present study, sera from 438 individuals were selected from the ILULU-TB biobank using random number generation (Microsoft Excel 2013). Equal numbers were selected for each of the TB, OD, and LTBI groups. Within each group, equal numbers were selected with and without HIV, and from each of the two sites (Table 1). The primary aim was to distinguish TB from OD, regardless of HIV status or site. The selection process with regard to the TB and OD patients is illustrated in Figure 1. No sera from the AE-TBC study were re-analysed as part of this study.

### Immunoassays

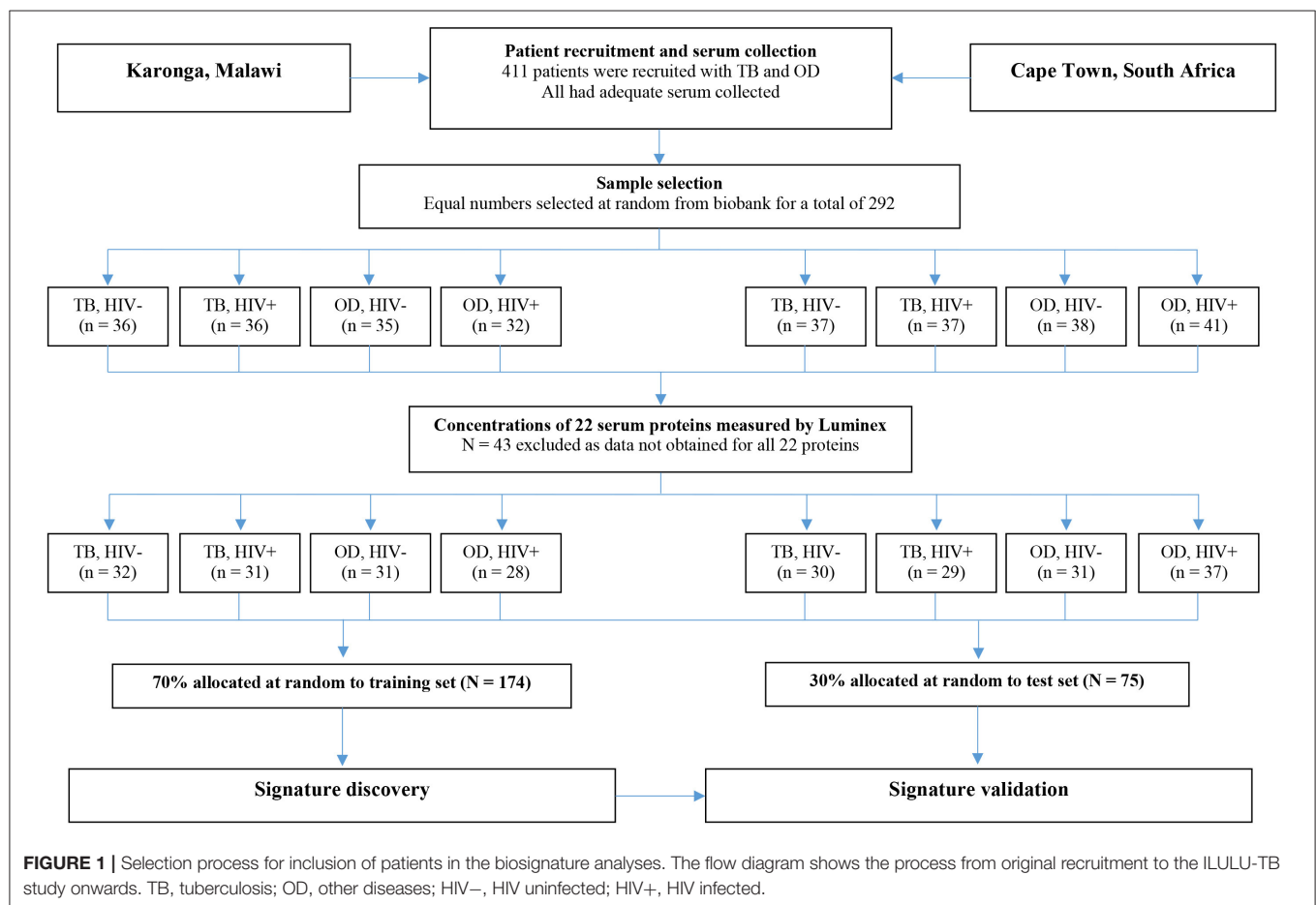
Luminex assays were used as per the AE-TBC study for quantification of interleukin-1 receptor antagonist (IL-1RA), transforming growth factor alpha (TGF-alpha), interferon gamma (IFN-gamma), IFN-gamma-inducible protein 10 (IP-10), tumour necrosis factor alpha (TNF-alpha), IFN-alpha-2, vascular endothelial growth factor (VEGF), matrix metalloproteinase-2 (MMP-2), MMP-9, apolipoprotein A-I (apo-AI), apo-CIII, transthyretin, complement factor H (complement FH) (Merck Millipore, Billerica, Massachusetts, USA); and C-reactive protein (CRP), serum amyloid A (SAA), serum amyloid P (SAP), fibrinogen, ferritin, tissue plasminogen activator (tPA), procalcitonin (PCT), haptoglobin, and alpha-2-macroglobulin (alpha-2-M) (Bio-Rad Laboratories, Hercules, California, USA) (7). Patients were randomised across the series of assays. Sera were diluted as per manufacturers' instructions, except for MMP-2 and -9 which were diluted 1 in 100, and apo-AI, apo-CIII, transthyretin and complement FH which were diluted 1 in 30,000 following optimisation. Assays were performed in single wells with three patients run in duplicate on each plate to estimate intra-assay variability. Quality controls were run on each plate. Plates were read on Bio-Plex 200 instruments at Imperial College London with Bio-Plex Manager v6.1 software (Bio-Rad). Intra-assay variability, calculated



**TABLE 1** | Demographic and clinical features for the 438 participants randomly selected from the ILULU-TB cohort for this study.

	TB, HIV-		TB, HIV+		LTBI, HIV-		LTBI, HIV+		OD, HIV-		OD, HIV+	
	CPT	Karonga	CPT	Karonga	CPT	Karonga	CPT	Karonga	CPT	Karonga	CPT	Karonga
Number	37	36	37	36	40	33	37	36	38	35	41	32
Age (IQR)	32.5 (26.5–41.9)	36 (25.5–53.4)	33.8 (29–37.9)	33.2 (28–39.7)	20.7 (19.3–23.4)	39 (32.4–51.4)	31.2 (27.9–35.1)	44.5 (35.5–49)	41.2 (29.2–51)	43.2 (27.5–53.6)	33.6 (28.6–36.7)	33.3 (29.4–41.2)
Male (n (%))	25 (69.4)	19 (52.8)	16 (43.2)	19 (52.8)	16 (40)	15 (45.5)	10 (27)	9 (25)	17 (44.7)	11 (31.4)	16 (40)	11 (34.4)
CD4+count (IQR)	n/a	n/a	170 (69–293)	168 (45–276) <sup>a</sup>	n/a	n/a	345 (231–523)	312 (246–421)	n/a	n/a	183 (95–272)	182 (107–229)
On ART (n (%))	n/a	n/a	2 (5.4)	8 (22.2)	n/a	n/a	1 (2.7)	0 (0)	n/a	n/a	18 (45)	12 (37.5)
BMI (IQR)	20.4 (18.4–23.6) <sup>b</sup>	18.4 (16.6–19.3)	20.9 (18.6–23.4)	18.8 (18–20.8)	23.6 (21.5–28.7)	22.7 (20.6–23.7)	24.3 (20.9–27.9)	21.6 (18.7–23.7)	22.4 (20.1–23.8) <sup>c</sup>	20.8 (19.6–23)	21.2 (19.8–23.9) <sup>d</sup>	19.6 (18.1–21.5)

These are shown by study site for each of the six clinical groups: active TB (TB), healthy controls with latent TB (LTBI), and unwell patients with other diseases (OD) who initially had TB in their differential diagnosis. The definition of a TB case was culture positivity for *Mycobacterium tuberculosis* (Mtb). The definition of an OD case was a confirmed other diagnosis plus exclusion of TB. HIV+, HIV infected; HIV-, HIV uninfected; CPT, Cape Town; IQR, interquartile range; ART, antiretroviral therapy; BMI, body mass index; n/a, not applicable. Numbers of missing values were <5 except where indicated by letters a–d (a = 6, b = 5, c = 19, d = 20).



as the mean of the coefficients of variance for each analyte individually across all plates, was <12% for all proteins. Results for quality controls fell within expected ranges. If results

were below the lower limit of detection, they were assigned a value of zero. If above the upper limit, they were retested at a higher dilution.

## Statistical Analyses

For analyses of individual proteins, all patients with results for that protein were included. Protein concentrations were compared between the TB group and each of the OD and LTBI groups in turn using one-sided Mann-Whitney *U*-tests. The performance of each of the 22 proteins to distinguish TB from each of OD and healthy LTBI in turn by their serum concentration, regardless of HIV status or site, was assessed by the area under the respective ROC curve (ROC AUC). Analyses were performed using GraphPad Prism v7 (GraphPad Software, La Jolla, California, USA).

For the biosignature analyses, as shown in **Figure 1**, only those patients (i.e., TB and OD) for whom data was gathered for all 22 proteins were included ( $n = 249$ ). This was because a finite number of kits were purchased at the outset, hence if serum from any patient had to be re-tested because a protein concentration was too high, the total number of patients with results for that protein was reduced. Healthy LTBI controls were omitted from these analyses. Patients were classified as TB if the model predicted the probability of TB was  $>0.5$  ( $p > 0.5$ ).

To retest the seven-protein signature from the AE-TBC study, data on the entire AE-TBC cohort were used for discovery ( $n = 701$ ) and on this sample of the ILULU-TB cohort for validation ( $n = 249$ ). The same method was used as for the AE-TBC signature [Generalised Discriminant Analyses (GDA)] using Statistica (Statsoft, Ohio, USA) (7).

For discovery of the optimal new signature, data on the ILULU-TB cohort alone was used. For consistency with the AE-TBC study, patients were randomly allocated to training and test sets at a ratio of 70:30, regardless of HIV status or study site. The same signature discovery methods were also used, namely GDA and Random Forest analyses of log-transformed values. In addition, we also performed variable selection using the Parallel Regularised Regression Model Search method (PReMS) on decile-normalised values using “R” v3.2.2 (R Foundation for Statistical Computing, Vienna, Austria). This is a logistic regression-based method designed to minimise the number of biomarkers selected (10). For each method, the same allocation of patients to training and test sets was used. Assuming the AE-TBC signature had the same accuracy in our data, we had 95% power to show a sensitivity of  $>90\%$  and specificity of  $>66.5\%$  with these new signatures.

For a screening test, albeit for community settings, the WHO recommend a minimum sensitivity of 90% (11). No criteria for a rule-in test are specified. After obtaining the best new signature from each method, we therefore re-tested them after adjusting the cut-off for diagnosis to increase each of the sensitivity and specificity in turn to 90%. This was to assess the performance of each signature as either a rule-out or rule-in test for TB. There were no indeterminate test results.

## Ethics Statement

Ethical approval for this study was covered by the approvals for the ILULU-TB study: the Human Research Ethics Committee of the University of Cape Town, South Africa (HREC012/2007), the National Health Sciences Research Committee, Malawi

**TABLE 2 |** Major clinical diagnoses in the Other Diseases groups of the sample of the ILULU-TB cohort that was selected for this study.

	HIV uninfected		HIV infected		Total (% of OD group)
	Karonga	Cape Town	Karonga	Cape Town	
Pneumonia/ Bronchitis/PCP	12 (33%)	6 (16%)	15 (47%)	15 (38%)	48 (33%)
Malignancy or neoplasia other than KS*	3 (8%)	13 (35%)	1 (3%)	2 (5%)	19 (13%)
Genitourinary	6 (17%)	4 (11%)	2 (6%)	1 (3%)	13 (9%)
Meningitis (bacterial/viral/ unspecified)	4 (11%)	0 (0%)	4 (13%)	2 (5%)	10 (7%)
Gastroenteritis/ Hepatitis	0 (0%)	2 (5%)	0 (0%)	6 (15%)	8 (6%)
Kaposi's Sarcoma	0 (0%)	0 (0%)	1 (3%)	6 (15%)	7 (5%)
Pyelonephritis	0 (0%)	7 (19%)	0 (0%)	0 (0%)	7 (5%)
Cryptococcal meningitis	0 (0%)	0 (0%)	2 (6%)	3 (8%)	5 (3%)
Pleural effusion/empyema (non-TB)	0 (0%)	1 (3%)	0 (0%)	4 (10%)	5 (3%)
Bacteraemia (source not identified)	1 (3%)	0 (0%)	4 (13%)	0 (0%)	5 (3%)
Other**	5 (14%)	0 (0%)	0 (0%)	0 (0%)	5 (3%)
Hepatobiliary disease	0 (0%)	4 (11%)	0 (0%)	0 (0%)	4 (3%)
Peritonitis	3 (8%)	0 (0%)	1 (3%)	0 (0%)	4 (3%)
Malaria	1 (3%)	0 (0%)	1 (3%)	0 (0%)	2 (1%)
IBD	0 (0%)	0 (0%)	0 (0%)	1 (3%)	1 (1%)
Pyomyositis	1 (3%)	0 (0%)	0 (0%)	0 (0%)	1 (1%)
Persistent generalised lymphadenopathy	0 (0%)	0 (0%)	1 (3%)	0 (0%)	1 (1%)
<b>TOTAL</b>	<b>36</b>	<b>37</b>	<b>32</b>	<b>40</b>	<b>145</b>

Data are stratified by HIV status and site. \*Lung cancer ( $n = 7$ ), lymphoma ( $n = 3$ ), dermatological tumour ( $n = 2$ ), unspecified ( $n = 2$ ), mesothelioma ( $n = 1$ ), hepatocellular carcinoma ( $n = 1$ ), metastatic adenocarcinoma ( $n = 1$ ), benign salivary gland tumour ( $n = 1$ ). \*\*Epilepsy ( $n = 3$ ), headache ( $n = 1$ ), pain unspecified ( $n = 1$ ). One patient had no diagnosis listed, hence data is shown for 145 patients.

(NHSRC/447), and the Ethics Committee of the London School of Hygiene and Tropical Medicine (5212).

## RESULTS

Demographic and clinical features of individuals selected for this study are shown in **Table 1**. The range of diagnoses that comprised the OD group is shown in **Table 2**. Medians and interquartile ranges of proteins in each group are shown in **Supplementary Table 1**.

## Performance of Biomarkers Individually

The best performing protein was complement factor H (FH). As shown in **Table 3**, this had a ROC AUC of 70% (95% confidence interval (CI): 64–76%). This performance was preserved across

**TABLE 3 |** Diagnostic accuracy of protein biomarkers individually.

Protein	Number tested from ILULU-TB cohort	ROC AUC in ILULU-TB study (%)	ROC AUC in AE-TBC study (%)
Complement FH	292	70 (64–76)	58 (53–62)
IP-10	282	66 (60–73)	82 (79–86)
IFN-gamma	284	66 (60–72)	80 (76–84)
SAA	263	65 (58–71)	83 (80–86)
VEGF	278	64 (57–71)	70 (65–74)
Haptoglobin	263	64 (58–71)	62 (57–66)
SAP	267	64 (57–71)	58 (53–63)
Transthyretin	292	61 (55–68)	78 (74–82)
Apo-CIII	292	58 (51–64)	65 (61–70)
Ferritin	263	57 (50–64)	78 (75–82)
tPA	263	57 (50–64)	72 (68–76)
Alpha-2-M	267	57 (50–64)	54 (49–58)
Fibrinogen	263	56 (49–63)	73 (69–77)
TGF-alpha	284	55 (49–62)	73 (69–77)
TNF-alpha	284	53 (46–59)	69 (65–74)
MMP-9	292	53 (47–60)	59 (53–64)
Apo-AI	292	52 (45–59)	69 (65–73)
Procalcitonin	263	52 (45–59)	68 (63–72)
IFN-alpha-2	284	52 (45–58)	67 (62–71)
MMP-2	292	52 (45–58)	54 (49–59)
CRP	267	51 (43–58)	84 (81–87)
IL-1RA	283	51 (44–58)	63 (58–68)

Areas under the receiver operating characteristic curve (ROC AUCs) for the performance of each protein in distinguishing TB ( $n = 146$ ) from OD ( $n = 146$ ) are shown, regardless of HIV status or site. Proteins are listed in descending order of performance in the ILULU-TB cohort with the numbers of patients for which results were obtained for that protein. ROC AUCs are shown as percentages. Results from the AE-TBC study are shown to the right for comparison (6). Bracketed values indicate 95% confidence intervals.

the sites (70% in Cape Town, 71% in Karonga) and HIV status (71% in HIV uninfected, 69% in HIV infected). ROC curves for these subdivisions are shown in **Supplementary Figure 1**. In addition, as shown in **Figure 2**, in comparison with the healthy LTBI control group, concentrations were higher in the TB group but trended toward being lower in the OD group ( $p = 0.072$ ). This contrasted with the other 21 proteins, in which concentrations in the TB and OD groups differed from those in the LTBI group in the same direction.

The concentrations of the top four individual biomarkers in each group are shown in **Figure 2**, and a display of all individual ROC AUCs is shown in **Table 3**. In comparison with the AE-TBC study, four proteins performed better in the ILULU-TB cohort (complement FH, SAP, haptoglobin, and alpha-2-M). The remaining 18 showed inferior performance, and the protein with the largest drop in performance was CRP, which was the best performing biomarker in the AE-TBC study and part of the seven-protein signature. Individual ROC AUCs in order of their difference compared to the AE-TBC study are shown in **Supplementary Figure 2**.

The performance of each protein was then stratified by HIV status. 16 proteins performed better in HIV uninfected

patients: complement FH, IP-10, SAA, VEGF, haptoglobin, SAP, transthyretin, apo-CIII, ferritin, alpha-2-M, TGF-alpha, TNF-alpha, MMP-9, apo-AI, PCT, and CRP. Five proteins performed better in HIV co-infected patients: IFN-gamma, fibrinogen, IFN-alpha-2, MMP-2, and IL-1RA. Confidence intervals overlapped for every protein, however (**Figure 3**).

Finally, while the main aim was to assess performance of proteins to distinguish TB from OD, we also examined their performance to distinguish TB from LTBI. The protein with the highest ROC AUC for this purpose was CRP (92%, **Supplementary Table 2**).

## Performance of the AE-TBC Signature in the ILULU-TB Cohort

For the biosignature analyses, 122 TB patients and 127 OD patients for whom results were available for all 22 proteins were included. There was an equal distribution of patients across the clinical groups, sites, and HIV status (**Figure 1**).

The performance of the seven-protein signature from the AE-TBC study in the ILULU-TB cohort is shown in **Table 4**. With the cut-off for defining a positive test at the default setting ( $p > 0.5$ ), the sensitivity was greater than in the AE-TBC study [98% (95% CI: 94–100%)], but specificity was markedly reduced [12% (7–19%)]. On comparison of biomarker concentrations between studies, there were significant differences in some proteins, especially apo-AI (**Supplementary Figure 3**). To understand this, we compared concentrations of apo-AI in our healthy LTBI controls with published normal concentrations. Concentrations in our LTBI group were 4-fold lower than those published (medians 324 vs. 1,180 ug/ml) (12). Concentrations of apo-CIII, however, which was part of the same multiplexed panel, matched those published (medians 114 vs. 114 ug/ml) (13). In addition, concentrations of apo-AI in the AE-TBC TB cohort were higher than published normal concentrations (2,000 vs. 1,180 ug/ml), even though apo-AI concentrations decrease in TB (7).

## Performance of New Signatures Derived in the ILULU-TB Cohort

The numbers of patients in each subgroup of the ILULU-TB cohort that were randomised to each of the train and test sets are shown in **Table 5**. The same patients were used for this set of analyses as for the re-test of the AE-TBC signature ( $n = 249$ : 122 TB and 127 OD). The results of the best new signatures from each of the GDA, Random Forests and PReMS methods are shown in **Tables 6–8**. Results are shown with the cut-off at the default setting, and after increasing each of sensitivity and specificity in turn to 90%. Positive and negative predictive values (PPV and NPV) are also shown in each case, based on the equal sizes of the TB and OD groups in this study.

The GDA method yielded a five-protein signature comprising complement factor H, IP-10, CRP, SAA, and transthyretin. The ROC AUC in the training set was 84% (**Table 6**). Sensitivities and specificities in the test set were 81% and 63% initially, 79% and 41% after increasing sensitivity, and 58% and 89% after increasing specificity.

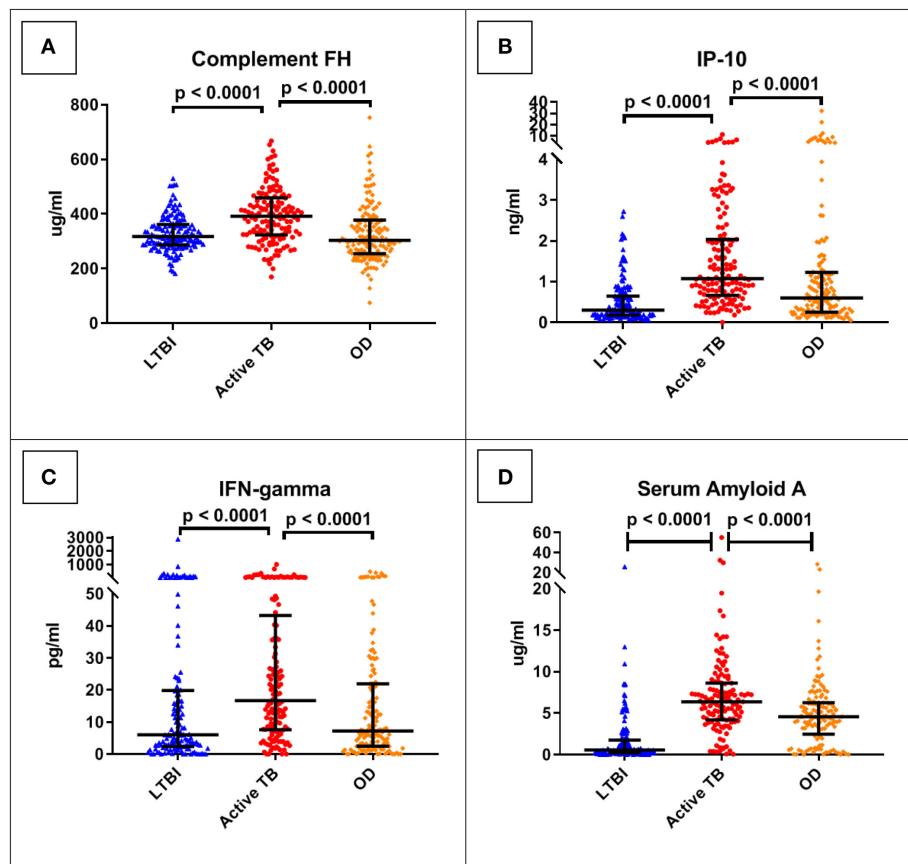


**FIGURE 2 |** Serum concentrations of the top four protein biomarkers (panels **A–D**) by clinical group. Scatter-dot plots show results for each patient in the ILULU-TB cohort, regardless of HIV status or site. *P*-values are 1-sided and derived from Mann-Whitney tests. Error bars represent medians and interquartile ranges. IP-10, IFN-gamma-inducible protein 10; IFN-gamma, interferon-gamma.

The results of the Random Forests analyses, using all 22 proteins, are shown in **Table 7**. Sensitivities and specificities in the test set were 73% and 71% initially, 92% and 58% after increasing sensitivity, and 95% and 43% after increasing specificity.

The PReMS method yielded a nine-protein signature comprising fibrinogen, alpha-2-M, CRP, MMP-9, transthyretin, complement FH, IFN-gamma, IP-10, and TNF-alpha. As shown in **Table 8**, this had a ROC AUC of 90% in the training set and 84% in the test set. Sensitivities and specificities in the test set were 86% and 74% initially, 92% and 71% after increasing sensitivity, and 75% and 81% after increasing specificity. At the cut-off for increased sensitivity, PPV and NPV in the test set were 75% and 90%, respectively. The performance in each of the HIV uninfected and co-infected halves of the test set in terms of ROC AUC was 84% for HIV uninfected patients (95% CI: 72–97%) and 86% for co-infected patients (95% CI: 71–100%), regardless of site. The ROC AUC at each of the two sites was 94% at Cape Town (95% CI: 86–100%) and 78% at Karonga (95% CI: 63–93%), regardless of HIV status. The difference between the ROC AUCs at the two sites was not significant by DeLong's test, however ( $p = 0.069$ ) (14).

## DISCUSSION

In the field of host serum proteomics-based TB diagnostics, this study stands out for several reasons. Firstly, it was conducted in Africa, where the burden of TB is highest, and included equal numbers of patients with and without HIV. This is important because the host response to TB may vary by ethnicity (15, 16), and is also distinct in the setting of HIV co-infection. Differences in concentrations of serum proteins between TB patients with and without HIV co-infection have not been extensively studied, although concentrations of neopterin and beta-2-microglobulin have both been found to be significantly higher in TB patients with HIV than without (17). This may reflect a state of “immune activation” in HIV-associated TB, which is well-recognised (18–20). Fundamentally, however, the pathogenesis of TB in HIV co-infection differs significantly, with impaired granuloma formation, less pulmonary cavitation and more dissemination (21–23). With the prevalence of HIV amongst patients presenting with active TB as high as 50% in some areas of Africa, and the TB case fatality rate in HIV co-infection being approximately twice that of HIV uninfected individuals (1), it is essential that any biosignature for use in such settings be derived from a



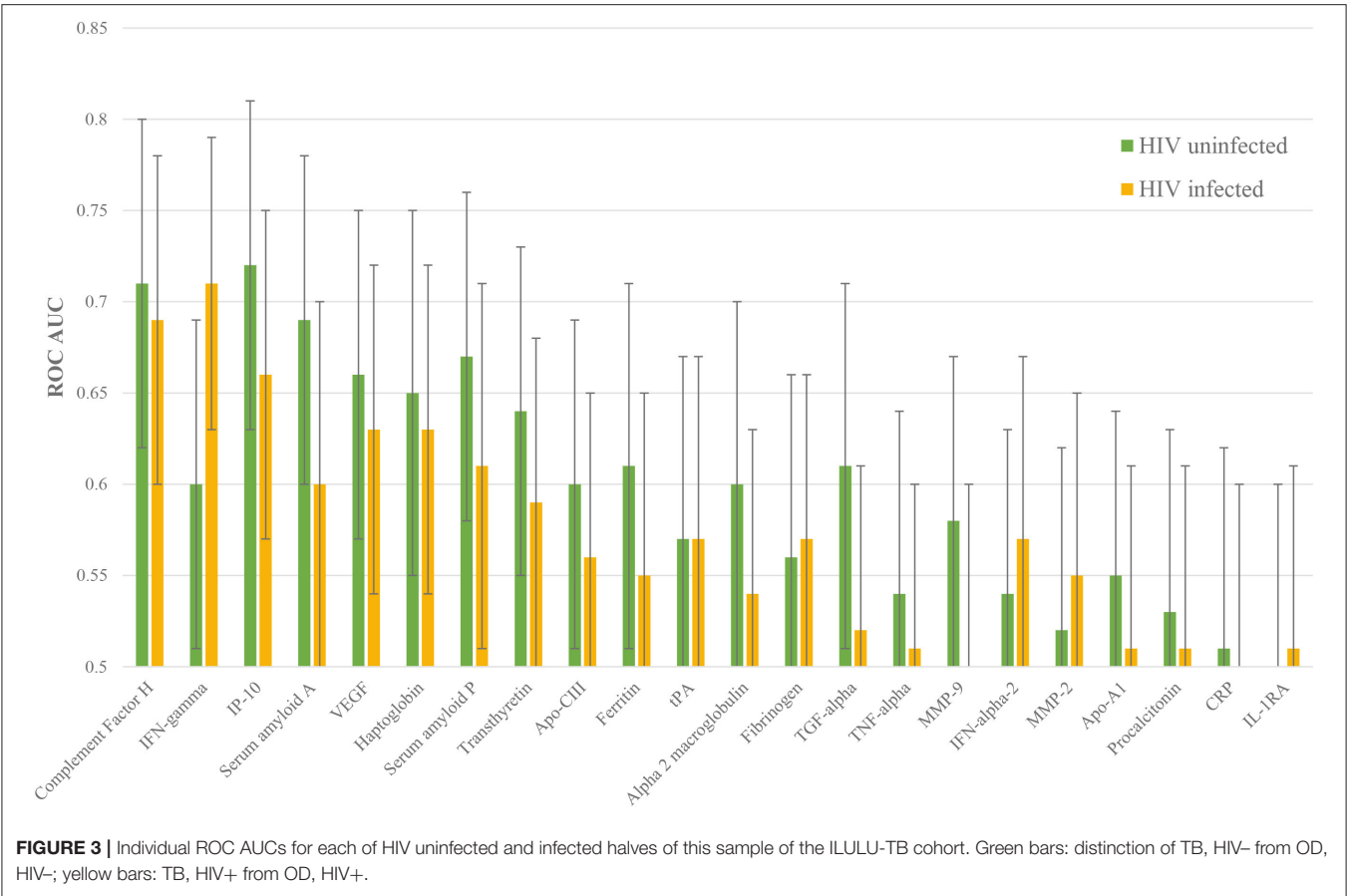


**TABLE 4 |** Performance of the seven-protein signature from the AE-TBC study in the ILULU-TB cohort.

	AE-TBC cohort (discovery set)	ILULU-TB cohort (validation set)
ROC AUC	91 (89–93)	
Sensitivity	85 (80–90)	98 (94–100)
Specificity	85 (81–88)	12 (7–19)
PPV	71 (65–76)	52 (45–58)
NPV	93 (90–95)	88 (64–99)

For this analysis, the entire AE-TBC cohort was used as the discovery set ( $n = 701$ ), and the whole sample of the ILULU-TB cohort as the validation set ( $n = 249$ ). Results are shown with the threshold for defining a case of TB at the default setting ( $p > 0.5$ ). All results are given as percentages. PPV, positive predictive value. NPV, negative predictive value. Bracketed values represent 95% confidence intervals.

representative population. The range of other diseases to be distinguished from TB is also strongly associated with both geographical location and HIV prevalence. Previous studies have derived promising serum protein signatures using techniques including mass spectrometry, but these were either not set in Africa or did not include or amalgamate sufficient numbers of HIV co-infected patients in both TB and OD (or control) groups (24–29). The two sites in Cape Town and Karonga were also

**TABLE 5 |** Numbers of patients in the ILULU-TB cohort allocated to train and test sets, for novel biosignature discovery.

Site	Clinical group	Train (70%)	Test (30%)	TOTAL
Karonga	TB, HIV-	29	3	32
	TB, HIV+	14	17	31
	OD, HIV-	11	20	31
	OD, HIV+	24	4	28
Cape Town	TB, HIV-	21	9	30
	TB, HIV+	21	8	29
	OD, HIV-	27	4	31
	OD, HIV+	27	10	37
TOTAL		174	75	249

Numbers in each of the clinical subgroups and at each study site are shown. Patients were allocated to train or test set at random. Only those patients with results for all 22 proteins were included.

selected in this study to represent the spread of epidemiological settings in Africa. Cape Town was selected to represent urban sites, and also had a low prevalence of malaria. Karonga was selected as a rural site, and had a high prevalence of malaria and other parasitic infections. The second major strength of this study was that patients were prospectively recruited from a point of

**TABLE 6 |** Performance of a new five-protein signature derived from Generalised Discriminant Analyses (GDA).

	Training set	Test set
ROC AUC	84 (78–90)	
Sensitivity	82 (73–90)	81 (65–92)
Specificity	74 (64–83)	63 (46–78)
PPV	75 (65–84)	68 (52–81)
NPV	81 (71–89)	77 (59–90)
<b>After adjustment of cut-off for increased sensitivity</b>		
Sensitivity	89 (80–94)	79 (63–90)
Specificity	48 (37–59)	41 (25–58)
PPV	64 (55–73)	58 (43–71)
NPV	80 (67–90)	65 (43–84)
<b>After adjustment of cut-off for increased specificity</b>		
Sensitivity	61 (50–71)	58 (41–74)
Specificity	91 (82–96)	89 (75–97)
PPV	87 (76–94)	85 (65–96)
NPV	69 (59–77)	67 (52–80)

This analysis was performed using data on the ILULU-TB cohort only ( $n = 249$ ). Patients were randomly assigned to training and test sets at a ratio of 70:30. The signature comprised Complement FH, IP-10, CRP, SAA, and Transthyretin. Results are shown both before and after adjusting the probability threshold in the training set for diagnosing TB to increase each of sensitivity and specificity in turn to 90%.

differential diagnosis. An early study by Agranoff et al. included African sera, but the OD group comprised a selection of diseases whose clinical features “can overlap with” those of TB (26). This is less rigorous, since a population which is more homogenous clinically (such as ours) is likely to be more homogenous in their serum proteomes, and therefore a more challenging one from which to derive markers of host response that are TB-specific. Thirdly, our signatures were tested using immunocapture. Whilst not arising from an untargeted proteomic approach, this ensured that any such signatures were more easily translatable to lateral flow immunoassay. To our knowledge, none of the relevant mass spectrometry-based studies published in the literature performed full technical validation by immunocapture (24–28). Fourthly, the patients recruited to this study were largely hospital attendees, which is also a population currently under-represented in the literature. Two studies recruited hospital patients from sites including in Africa, but either did not include HIV co-infected patients in the discovery cohort, or had a low number of HIV infected patients in the OD group (25, 26). Several recent studies have employed immunocapture to discover new signatures including in patients from Africa, but recruitment was limited to primary care settings (29–33). Patients presenting to hospitals are likely to be more unwell than those presenting to primary care settings, and therefore to have a greater degree of disturbance to their serum proteome. The TB patients in Cape Town were recruited from a clinic, however all were culture positive as per the study design, and therefore likely to have had more advanced disease than cohorts that included clinical diagnoses. Severity of TB is known to affect the concentrations of serum proteins, including CRP, procalcitonin, and serum amyloid A, hence the

**TABLE 7 |** Performance of a new 22-protein signature derived from Random Forests analyses.

	Training set	Test set
Sensitivity	72 (61–81)	73 (56–86)
Specificity	80 (70–88)	71 (54–85)
PPV	77 (66–86)	71 (54–85)
NPV	75 (65–83)	73 (56–86)
<b>After adjustment of cut-off for increased sensitivity</b>		
Sensitivity	82 (73–90)	92 (78–98)
Specificity	64 (53–74)	58 (41–74)
PPV	69 (59–77)	68 (53–80)
NPV	79 (68–88)	88 (69–97)
<b>After adjustment of cut-off for increased specificity</b>		
Sensitivity	65 (54–75)	43 (27–61)
Specificity	89 (80–94)	95 (82–99)
PPV	85 (74–92)	89 (65–99)
NPV	72 (63–81)	63 (49–76)

This analysis was performed using data on the ILULU-TB cohort only ( $n = 249$ ). The same patients with the same allocations to training and test sets were used as for the GDA analyses (Table 4).

**TABLE 8 |** Performance of a nine-protein signature derived from Parallel Regularised Regression Model Search.

	Training set	Test set
ROC AUC	90 (86–95)	84 (73–94)
Sensitivity	83 (75–90)	86 (73–95)
Specificity	82 (73–89)	74 (58–86)
PPV	84 (75–91)	85 (70–94)
NPV	82 (73–89)	76 (62–87)
<b>After adjustment of cut-off for increased sensitivity</b>		
Sensitivity	90 (83–95)	92 (80–98)
Specificity	71 (61–80)	71 (56–84)
PPV	75 (66–82)	75 (62–86)
NPV	89 (80–95)	90 (76–97)
<b>After adjustment of cut-off for increased specificity</b>		
Sensitivity	73 (63–82)	75 (60–87)
Specificity	90 (82–95)	81 (67–91)
PPV	87 (78–94)	80 (65–91)
NPV	78 (69–85)	77 (63–88)

This analysis was performed using data on the ILULU-TB cohort only ( $n = 249$ ). The same patients and allocations were used as for the GDA and Random Forests analyses (Tables 4, 5). This signature comprised fibrinogen, alpha-2-M, CRP, MMP-9, transthyretin, complement FH, IFN-gamma, IP-10, and TNF-alpha.

importance of evaluating biomarker performance at this different level of the healthcare system (34, 35). Other strengths of the study design were that diagnoses were confirmed in all patients, and that healthy controls with LTBI infection were included for reference.

The design of this study was also well-suited to re-testing the biomarkers from the AE-TBC study. The countries in which

recruitment took place were a subset of the countries in the AE-TBC study (Malawi and South Africa); the assays were performed using the same Luminex kits and analyser; and the same statistical methods were applied to the data, by the same statistician (7). To complement the signature discovery process, an additional method (PReMS) was also used.

Limitations included the fact that even though the recruitment process was open to extrapulmonary TB (EPTB) cases, no cases of culture positive TB without pulmonary involvement were included. In addition, none of the OD cases were documented as having non-tuberculous mycobacterial disease (NTM), which may more closely resemble TB in terms of host response (36). Secondly, this study was limited to the 22 proteins that had been selected by the AE-TBC based on previous performance in primary care settings. This was a strength in that the biomarkers had been through prior selection to diagnose the disease of interest (TB), but a weakness since they had not all previously been selected from presentations to secondary care. A third weakness was that, in terms of the comparison of biomarker performance between the ILULU-TB and AE-TBC studies, the study designs were different: ILULU-TB was case-control, with group sizes held equal, whereas AE-TBC was a cohort study. The group sizes in the latter therefore reflected local epidemiology, including with regards to HIV prevalence. Another difference was that our OD group comprised both pulmonary and non-pulmonary diseases, whereas AE-TBC focussed on lung diseases only. A final limitation was that our study did not include an external cohort in which to validate any new signatures.

Overall, the performance of the proteins individually was less good in the ILULU-TB cohort, except for complement FH, SAP, haptoglobin, and alpha-2-M. The results for complement FH were particularly promising in that diagnostic performance was sustained across site and HIV status. In addition, the fact that concentrations of complement FH in the TB and OD groups moved in a different direction from each other relative to the healthy controls implies that rising concentrations of complement FH may be TB-specific. Complement FH did distinguish TB from OD (or “no-PTB”) in the AE-TBC study, with higher concentrations in the TB group, but this difference was more pronounced in the ILULU-TB cohort. A possible reason for that might be that transcription of complement FH *in vitro* is driven by IFN-gamma (37, 38), which in turn has a central role in the host response in TB (39, 40). In keeping with this, IFN-gamma serum concentrations were higher in our TB group than OD group (**Figure 2C**). As discussed above, the TB cases in the ILULU-TB study were likely more advanced than those in the AE-TBC study, which may have driven serum FH concentrations up higher. An additional possibility is that FH concentrations were lower in our OD group, again due to more severe illnesses. Complement FH concentrations in serum/plasma have not been extensively studied in other infections, but are known to decrease in inflammatory conditions such as lupus nephritis and myaesthesia gravis as a result of excessive complement consumption (41, 42). Enhanced complement activation and consumption has also been shown to occur in HIV-infected patients with sepsis (43), and this may have been relevant for a proportion of our OD cohort.

By contrast, the particularly poor performance of CRP in this study is interesting, since this was the best-performing biomarker individually in the AE-TBC study, with concentrations being higher in the TB group. Whilst concentrations trended toward being higher in the TB group in the ILULU-TB study, this difference was not statistically significant, and CRP did not function as a standalone biomarker. This was likely reflective, again, of the more severely ill state of the OD patients in the ILULU-TB cohort, rather than any reduction of levels in our TB cohort. This is supported by CRP being the top individual biomarker to distinguish TB from LTBI in our cohort, and also by previous observations that CRP performs significantly less well in hospital than in community settings (44, 45).

The application of the 7-protein signature from the AE-TBC study directly to the data from the ILULU-TB study was hampered by the fact that concentrations of some of the proteins differed significantly between the two studies. Data accuracy and precision within each of the two studies was good, which suggests that the commonly observed phenomenon of lot-lot variation between multiplexed kits was the main contributor (46). It is possible that the marked decrease in concentrations of apo-AI in our study represent over-correction of calibration by the manufacturer of previously high concentrations, such as were reported in the AE-TBC study.

The newly derived 5-protein GDA signature had a moderately high ROC AUC in the training set of 84% (78–90%). In the test set, however, sensitivity and specificity were less promising. The five proteins were a subset of the seven that comprised the AE-TBC signature, however, which validates them as being among the best biomarkers for TB diagnosis. The Random Forests method produced performances in the test set that were slightly greater, but this was with all 22 proteins included in the model, which is less feasible for translation to a POC test.

The best performing test emerged from the PReMS method in the form of a nine-protein signature comprising fibrinogen, alpha-2-M, CRP, MMP-9, transthyretin, complement factor H, IFN-gamma, IP-10, and TNF-alpha. The highest combined results came from optimising the sensitivity, which yielded 92% sensitivity and 71% specificity in the test set. This was comparable with the performance of the seven-protein signature in the AE-TBC study. It also exceeded the WHO minimum requirements for a “triage test” for TB, which is notable, even though that particular target was designed with community settings in mind (11). The potential benefit of a screening test in hospital settings is clear, since it would decrease the number of sputum-based investigations that would be needed, including by GeneXpert, as well as unnecessary courses of TB treatment. The performance of the signature was unaffected by HIV status, which is promising for use in African settings, and also contrasts with the performance of sputum smear microscopy, which is significantly less sensitive in HIV co-infected patients (47).

This study focussed on culture positive TB, in order to derive a signature based on confirmed cases. Future validation studies, however, should include culture negative pulmonary TB cases, as well as EPTB, and OD groups including NTM disease. In addition, translation to POC will depend on the availability of

LFA platforms for measuring multiple proteins. LFAs have been shown to be feasible for use in sub-Saharan African settings and accurate across four orders of magnitude, without the need for a cold chain for distribution or storage (6). Multiplexing technology is also emerging for LFAs, with multiple proteins either being detected in series, along one strip (48, 49), or in parallel, with multiple strips contained within one handheld device (50).

In summary, we retested the performance of 22 host serum protein biomarkers of TB that had originally been selected from primary care studies in Africa in a large sample from a well-characterised cohort recruited largely from hospitals. The top-performing single biomarker was complement factor H, which is a novel marker of TB in this setting. A nine-protein biosignature was discovered which showed promise for use as a POC screening test in hospital settings, and performed equally well in individuals co-infected with HIV. Translation to this will depend on validation in independent cohorts and on development of accurate POC platforms.

## DATA AVAILABILITY STATEMENT

The raw data supporting the conclusions of this article will be made available by the authors, without undue reservation.

## ETHICS STATEMENT

The studies involving human participants were reviewed and ethical approval for this study was covered by the approvals for the ILULU-TB study: the Human Research Ethics Committee of the University of Cape Town, South Africa (HREC012/2007), the National Health Sciences Research Committee, Malawi (NHSRC/447), and the Ethics Committee of the London School of Hygiene and Tropical Medicine (5212). The patients/participants provided their written informed consent to participate in this study.

## AUTHOR CONTRIBUTIONS

HD, ML, RW, and MH: conceived and designed the experiments. TM: performed the experiments. TM, CH, and MK: analysed the data. TM, CH, NC, MK, NF, GW, ML, RW, and MH: provided input into data interpretation. TM, CH, NC, RW, and MH: contributed to writing the first version of the manuscript. NC, TO, KW, HD, AC, NF, RW, and MH: contributed to revisions of the manuscript. TO, RG, LS, LB, ML, and RW: enrolled patients used in this study. TO, RG, KW, LS, and AC: data collection on patients used in this study. All authors contributed to the article and approved the submitted version.

## FUNDING

This study was funded by the James Maxwell Grant Proffit Fellowship 2016-17 (Royal College of Physicians, London) to TM. RW was funded by Wellcome (104803 and 203135); The Francis Crick Institute which is funded by UKRI-MRC

(FC0010218), CRUK (FC0010218) and Wellcome (FC0010218); National Institutes of Health (AI115940); Foundation for National Institutes of Health (WILK116PTB); and EDCTP2 (SRIA2015-1065). The authors also wish to acknowledge the funding source of the ILULU-TB project which was EU Action for Diseases of Poverty program grant (Sante/2006/105-061).

## ACKNOWLEDGMENTS

The authors wish to thank all members of the ILULU Consortium: *Institute of Infectious Diseases and Molecular Medicine, University of Cape Town* Nonzwakazi Bangani, Lizl Bashe, Melina Carr, Hannah P. Gideon, RG, Yekiwe Hlombe, Vanessa January, Bekekile Kwaza, Suzaan Marais, Marc Mendelson, TO, Fadheela Patel, Ronnett Seldon, Relebohile Tsekela, KW, RW, Kathryn Wood; *London School of Hygiene & Tropical Medicine/Karonga Prevention Study* Lyn Ambrose, AC, HD, NF, Lumbani Munthali, Bagrey Ngwira, Amos Phiri, Femia Zgambo; *Red Cross War Memorial Children's Hospital, University of Cape Town* Margaret Cooper, Brian Eley, Mabel Gcuwa, Spasina King, Glynis Kossew, Karen McCabe, Wonita Petersen, Sandra Pienaar, Vashini Pillay; *Liverpool School of Tropical Medicine/Malawi-Liverpool-Wellcome Trust Clinical Research Programme, University of Malawi College of Medicine* Benjamin Allubha, George Chagaluka, Angeziwa Chunga, Janet Dube, Robert S. Heyderman, Annie Joabe, Martha Kalembe, Anne Kerr, Monica Matola, Rachel Mlotha, Agnes Mwale, David Mzinza; *Brighton and Sussex Medical School, University of Sussex* Suzanne T. Anderson, Gillian Baker, Claire M. Banwell, Terry Bishop, Natalie Chaplin, Julian Golland, Florian Kern, Susan Poore, Jayne Wellington; *Imperial College London* Andrew J. Brent, Lachlan J. Coin, Hariklia Eleftherohorinou, Shea Hamilton, Myrsini Kaforou, Paul R. Langford, ML, Stephanie Menikou, Victoria J. Wright.

The authors also wish to acknowledge all members of the AE-TBC: *Stellenbosch University, South Africa*: GW, NC, Magdalena Kriel, Gian van der Spuy, Andre G Loxton, Kim Stanley, Stephanus Malherbe, Belinda Kriel, Leigh A Kotzé, Dolapo O Awoniyi, Elizna Maasdorp. *MRC Unit, The Gambia*: Jayne S Sutherland, Olumuyiwa Owolabi, Abdou Sillah, Joseph Mendy, Awa Gindeh, Simon Donkor, Toyin Togun, Martin Ota. *Karonga Prevention Study, Malawi*: AC, Felanji Simukonda, Alemayehu Amberbir, Femia Chilongo, Rein Houben. *Ethiopian Health and Nutrition Research Institute, Ethiopia*: Desta Kassa, Atsbeha Gebrezgabher, Getnet Mesfin, Yohannes Belay, Gebremedhin Gebremichael, Yodit Alemayehu. *University of Namibia, Namibia*: Marieta van der Vyver, Faustina N Amutenya, Josefina N Nelongo, Lidia Monye, Jacob A Sheehama, Scholastica Ipinge. *Makerere University, Uganda*: Harriet Mayanja-Kizza, Ann Ritah Namuganga, Grace Muzanyne, Mary Nsereko, Pierre Peters. *Armauer Hansen Research Institute, Ethiopia*: Rawleigh Howe, Adane Mihret, Yonas Bekele, Bamlak Tessema, Lawrence Yamuah. *Leiden University Medical Centre, The Netherlands*: Tom HM Ottenhoff, Annemieke Geluk, Kees LMC Franken, Paul LAM Corstjens, Elisa M Tjon Kon Fat, Claudia J de Dood, Jolien J van der Ploeg-van Schip. *Statens*



Serum Institut, Copenhagen, Denmark: Ida Rosenkrands, Claus Aagaard. Max Planck Institute for Infection Biology, Berlin, Germany: Stefan HE Kaufmann, Maria M. Esterhuyse. London School of Hygiene and Tropical Medicine, London, UK: Jacqueline M Cliff, Hazel M Dockrell.

## REFERENCES

- World Health Organization. *Global Tuberculosis Report*. Geneva: WHO Press (2020).
- Steingart KR, Schiller I, Horne DJ, Pai M, Boehme CC, Dendukuri N, et al. Xpert® MTB/RIF assay for pulmonary tuberculosis and rifampicin resistance in adults. *Cochrane Database Syst Rev*. (2014) 1:CD009593. doi: 10.1002/14651858.CD009593.pub3
- Papadopoulos MC, Abel PM, Agranoff D, Stich A, Tarelli E, Bell AB, et al. A novel and accurate diagnostic test for human African trypanosomiasis. *Lancet*. (2004) 363:1358–63. doi: 10.1016/S0140-6736(04)16046-7
- van Houten CB, de Groot JAH, Klein A, Srugo I, Chistyakov I, de Waal W, et al. A host-protein based assay to differentiate between bacterial and viral infections in preschool children (OPPORTUNITY): a double-blind, multicentre, validation study. *Lancet Infect Dis*. (2017) 17:431–40. doi: 10.1016/S1473-3099(16)30519-9
- Srugo I, Klein A, Stein M, Golan-Shany O, Kerem N, Chistyakov I, et al. Validation of a novel assay to distinguish bacterial and viral infections. *Pediatrics*. (2017) 140:e20163453. doi: 10.1542/peds.2016-3453
- Corstjens PL, Tjon Kon Fat EM, de Dood CJ, van der Ploeg-van Schip JJ, Franken KLMC, Chegou NN, et al. Multi-center evaluation of a user-friendly lateral flow assay to determine IP-10 and CCL4 levels in blood of TB and non-TB cases in Africa. *Clin Biochem*. (2016) 49:22–31. doi: 10.1016/j.clinbiochem.2015.08.013
- Chegou NN, Sutherland JS, Malherbe S, Crampin AC, Corstjens PLAM, Geluk A, et al. Diagnostic performance of a seven-marker serum protein biosignature for the diagnosis of active TB disease in African primary healthcare clinic attendees with signs and symptoms suggestive of TB. *Thorax*. (2016) 71:785–94. doi: 10.1136/thoraxjnl-2015-207999
- Kaforou M, Wright VJ, Oni T, French N, Anderson ST, Bangani N, et al. Detection of tuberculosis in HIV-infected and -uninfected African adults using whole blood RNA expression signatures: a case-control study. *PLoS Med*. (2013) 10:e1001538. doi: 10.1371/journal.pmed.1001538
- Schölvinc E, Wilkinson KA, Whelan AO, Martineau AR, Levin M, Wilkinson RJ. Gamma interferon-based immunodiagnosis of tuberculosis: comparison between whole-blood and enzyme-linked immunospot methods. *J Clin Microbiol*. (2004) 42:829–31. doi: 10.1128/JCM.42.2.829-831.2004
- Hoggart CJ. PReMS: Parallel Regularised Regression Model Search for sparse biosignature discovery. *bioRxiv [Preprint]*. (2018) 355479. doi: 10.1101/355479
- World Health Organization. *High priority target product profiles for new tuberculosis diagnostics: report of a consensus meeting*. (2014). Geneva: World Health Organization.
- McQueen MJ, Hawken S, Wang X, Ounpuu S, Sniderman A, Probstfield J, et al. Lipids, lipoproteins, and apolipoproteins as risk markers of myocardial infarction in 52 countries (the INTERHEART study): a case-control study. *Lancet*. (2008) 372:224–33. doi: 10.1016/S0140-6736(08)61076-4
- Aroner SA, Yang M, Li J, Furtado JD, Sacks FM, Tjønneland A, et al. Apolipoprotein C-III and high-density lipoprotein subspecies defined by apolipoprotein C-III in relation to diabetes risk. *Am J Epidemiol*. (2017) 186:736–44. doi: 10.1093/aje/kwx143
- DeLong ER, DeLong DM, Clarke-Pearson DL. Comparing the areas under two or more correlated receiver operating characteristic curves: a nonparametric approach. *Biometrics*. (1988) 44:837–45. doi: 10.2307/2531595
- Coussens AK, Wilkinson RJ, Nikolayevskiy V, Elkington PT, Hanifa Y, Islam K, et al. Ethnic variation in inflammatory profile in tuberculosis. *PLoS Pathog*. (2013) 9:e1003468. doi: 10.1371/journal.ppat.1003468
- Oliveira-de-Souza D, Vinhaes CL, Arriaga MB, Kumar NP, Cubillos-Angulo JM, Shi R, et al. Molecular degree of perturbation of plasma inflammatory markers associated with tuberculosis reveals distinct disease profiles between Indian and Chinese populations. *Sci Rep*. (2019) 9:8002. doi: 10.1038/s41598-019-44513-8
- Skogmar S, Schön T, Balcha TT, Sturegård E, Jansson M, Björkman P. Plasma levels of neopterin and C-Reactive Protein (CRP) in Tuberculosis (TB) with and without HIV coinfection in relation to CD4 cell count. *PLoS ONE*. (2015) 10:e0144292. doi: 10.1371/journal.pone.0144292
- Vanham G, Edmonds K, Qing L, Hom D, Toossi Z, Jones B, et al. Generalized immune activation in pulmonary tuberculosis: co-activation with HIV infection. *Clin Exp Immunol*. (1996) 103:30–4. doi: 10.1046/j.1365-2249.1996.907600.x
- Toossi Z, Funderburg NT, Sirdeshmuk S, Whalen CC, Nanteza MW, Johnson DE, et al. Systemic immune activation and microbial translocation in dual HIV/tuberculosis-infected subjects. *J Infect Dis*. (2013) 207:1841–9. doi: 10.1093/infdis/jit092
- Meng Q, Sayin I, Canaday DH, Mayanja-Kizza H, Baseke J, Toossi Z. Immune activation at sites of HIV/TB Co-infection contributes to the pathogenesis of HIV-1 disease. *PLoS ONE*. (2016) 11:e0166954. doi: 10.1371/journal.pone.0166954
- Gilks CF, Brindle RJ, Otieno LS, Bhatt SM, Newnham RS, Simani PM, et al. Extrapulmonary and disseminated tuberculosis in HIV-1-seropositive patients presenting to the acute medical services in Nairobi. *AIDS*. (1990) 4:981–5. doi: 10.1097/00002030-199010000-00006
- Lawn SD, Evans AJ, Sedgwick PM, Acheampong JW. Pulmonary tuberculosis: radiological features in west Africans coinfecting with HIV. *Br J Radiol*. (1999) 72:339–4. doi: 10.1259/bjr.72.856.10474493
- Walker NE, Clark SO, Oni T, Andreu N, Tezera L, Singh S, et al. Doxycycline and HIV infection suppress tuberculosis-induced matrix metalloproteinases. *Am J Respir Crit Care Med*. (2012) 185:989–97. doi: 10.1164/rccm.201110-1769OC
- Sandhu G, Battaglia F, Ely BK, Athanasakis D, Montoya R, Valencia T, et al. Discriminating active from latent tuberculosis in patients presenting to community clinics. *PLoS ONE*. (2012) 7:e38080. doi: 10.1371/journal.pone.0038080
- Achkar JM, Cortes L, Croteau P, Yanofsky C, Mentinova M, Rajotte I, et al. Host protein biomarkers identify active tuberculosis in HIV uninfected and co-infected individuals. *EBioMedicine*. (2015) 2:1160–8. doi: 10.1016/j.ebiom.2015.07.039
- Agranoff D, Fernandez-Reyes D, Papadopoulos MC, Rojas SA, Herbst M, Loosemore A, et al. Identification of diagnostic markers for tuberculosis by proteomic fingerprinting of serum. *Lancet*. (2006) 368:1012–21. doi: 10.1016/S0140-6736(06)69342-2
- Xu D, Li Y, Li X, Wei LL, Pan Z, Jiang TT, et al. Serum protein S100A9, SOD3, and MMP9 as new diagnostic biomarkers for pulmonary tuberculosis by iTRAQ-coupled two-dimensional LC-MS/MS. *Proteomics*. (2015) 15:58–67. doi: 10.1002/pmic.201400366
- Liu J, Jiang T, Wei L, Yang X, Wang C, Zhang X, et al. The discovery and identification of a candidate proteomic biomarker of active tuberculosis. *BMC Infect Dis*. (2013) 13:506. doi: 10.1186/1471-2334-13-506
- Ahmad R, Xie L, Pyle M, Suarez MF, Broger T, Steinberg D, et al. A rapid triage test for active pulmonary tuberculosis in adult patients with persistent cough. *Sci Transl Med*. (2019) 11:eaaw8287. doi: 10.1126/scitranslmed.aaw8287
- De Groote MA, Sterling DG, Hraha T, Russell TM, Green LS, Wall K, et al. Discovery and validation of a six-marker serum protein signature for the diagnosis of active pulmonary tuberculosis. *J Clin Microbiol*. (2017) 55:3057–71. doi: 10.1128/JCM.00467-17
- Chegou NN, Sutherland JS, Namuganga AR, Corstjens PL, Geluk A, Gebremichael G, et al. Africa-wide evaluation of host biomarkers in

## SUPPLEMENTARY MATERIAL

The Supplementary Material for this article can be found online at: <https://www.frontiersin.org/articles/10.3389/fimmu.2021.639174/full#supplementary-material>

- QuantiFERON supernatants for the diagnosis of pulmonary tuberculosis. *Sci Rep.* (2018) 8:2675. doi: 10.1038/s41598-018-20855-7
32. Manngo PM, Gutschmidt A, Snyders CI, Mutavhatsindi H, Manyelo CM, Makhoba NS, et al. Prospective evaluation of host biomarkers other than interferon gamma in QuantiFERON Plus supernatants as candidates for the diagnosis of tuberculosis in symptomatic individuals. *J Infect.* (2019) 79:228–35. doi: 10.1016/j.jinf.2019.07.007
  33. Jacobs R, Malherbe S, Loxton AG, Stanley K, van der Spuy G, Walzl G, et al. Identification of novel host biomarkers in plasma as candidates for the immunodiagnosis of tuberculosis disease and monitoring of tuberculosis treatment response. *Oncotarget.* (2016) 7:57581–92. doi: 10.18632/oncotarget.11420
  34. Sigal GB, Segal MR, Mathew A, Jarlsberg L, Wang M, Barbero S, et al. Biomarkers of tuberculosis severity and treatment effect: a directed screen of 70 host markers in a randomized clinical trial. *EBioMedicine.* (2017) 25:112–21. doi: 10.1016/j.ebiom.2017.10.018
  35. Liu Q, Chen X, Hu C, Zhang R, Yue J, Wu G, et al. Serum protein profiling of smear-positive and smear-negative pulmonary tuberculosis using SELDI-TOF mass spectrometry. *Lung.* (2010) 188:15–23. doi: 10.1007/s00408-009-9199-6
  36. Teklu T, Wondale B, Taye B, Hailemariam M, Bekele S, Tamirat M, et al. Differences in plasma proteomes for active tuberculosis, latent tuberculosis and non-tuberculous mycobacterial lung disease patients with and without ESAT-6/CFP10 stimulation. *Proteome Sci.* (2020) 18:10. doi: 10.1186/s12953-020-00165-5
  37. Brooimans RA, van der Ark AA, Buurman WA, van Es LA, Daha MR. Differential regulation of complement factor H and C3 production in human umbilical vein endothelial cells by IFN-gamma and IL-1. *J Immunol.* (1990) 144:3835–40.
  38. van den Dobbelaars ME, Verhasselt V, Kaashoek JG, Timmerman JJ, Schroeijers WE, Verweij CL, et al. Regulation of C3 and factor H synthesis of human glomerular mesangial cells by IL-1 and interferon-gamma. *Clin Exp Immunol.* (1994) 95:173–80. doi: 10.1111/j.1365-2249.1994.tb06033.x
  39. Cooper AM, Dalton DK, Stewart TA, Griffin JP, Russell DG, Orme IM. Disseminated tuberculosis in interferon gamma gene-disrupted mice. *J Exp Med.* (1993) 178:2243–7. doi: 10.1084/jem.178.6.2243
  40. Chackerian A, Perera T, Behar S. Gamma interferon-producing CD4+ T lymphocytes in the lung correlate with resistance to infection with *Mycobacterium tuberculosis*. *Infect Immun.* (2001) 69:2666–74. doi: 10.1128/IAI.69.4.2666-2674.2001
  41. Wang FM, Yu F, Tan Y, Song D, Zhao MH. Serum complement factor H is associated with clinical and pathological activities of patients with lupus nephritis. *Rheumatology.* (2012) 51:2269–77. doi: 10.1093/rheumatology/kes218
  42. Romi F, Kristoffersen EK, Aarli JA, Gilhus NE. The role of complement in myasthenia gravis: serological evidence of complement consumption *in vivo*. *J Neuroimmunol.* (2005) 158:191–4. doi: 10.1016/j.jneuroim.2004.08.002
  43. Huson MA, Wouters D, van Mierlo G, Grobusch MP, Zeerleder SS, van der Poll T. HIV coinfection enhances complement activation during sepsis. *J Infect Dis.* (2015) 212:474–83. doi: 10.1093/infdis/jiv074
  44. Santos VS, Goletti D, Kontogianni K, Adams ER, Molina-Moya B, Dominguez J, et al. Acute phase proteins and IP-10 as triage tests for the diagnosis of tuberculosis: systematic review and meta-analysis. *Clin Microbiol Infect.* (2019) 25:169–77. doi: 10.1016/j.cmi.2018.07.017
  45. Yoon C, Semitala FC, Atuhumuza E, Katende J, Mwebe S, Asege L, et al. Point-of-care C-reactive protein-based tuberculosis screening for people living with HIV: a diagnostic accuracy study. *Lancet Infect Dis.* (2017) 17:1285–92. doi: 10.1016/S1473-3099(17)30488-7
  46. Butterfield LH, Potter DM, Kirkwood JM. Multiplex serum biomarker assessments: technical and biostatistical issues. *J Transl Med.* (2011) 9:173. doi: 10.1186/1479-5876-9-173
  47. Boehme CC, Nicol MP, Nabetta P, Michael JS, Gotuzzo E, Tahirli R, et al. Feasibility, diagnostic accuracy, and effectiveness of decentralised use of the Xpert MTB/RIF test for diagnosis of tuberculosis and multidrug resistance: a multicentre implementation study. *Lancet.* (2011) 377:1495–505. doi: 10.1016/S0140-6736(11)60438-8
  48. Bartosh AV, Sotnikov DV, Hendrickson OD, Zherdev AV, Dzantiev BB. Design of multiplex lateral flow tests: a case study for simultaneous detection of three antibiotics. *Biosensors.* (2020) 10:17. doi: 10.3390/bios10030017
  49. van Hooij A, van den Eeden S, Richardus R, Tjon Kon Fat E, Wilson L, Franken KLMC, et al. Application of new host biomarker profiles in quantitative point-of-care tests facilitates leprosy diagnosis in the field. *EBioMedicine.* (2019) 47:301–8. doi: 10.1016/j.ebiom.2019.08.009
  50. Zhao Y, Wang H, Zhang P, Sun C, Wang X, Wang X, et al. Rapid multiplex detection of 10 foodborne pathogens with an up-converting phosphor technology-based 10-channel lateral flow assay. *Sci Rep.* (2016) 6:21342. doi: 10.1038/srep21342

**Conflict of Interest:** The authors declare that the research was conducted in the absence of any commercial or financial relationships that could be construed as a potential conflict of interest.

Copyright © 2021 Morris, Hoggart, Chegou, Kidd, Oni, Goliath, Wilkinson, Dockrell, Sichali, Banda, Crampin, French, Walzl, Levin, Wilkinson and Hamilton. This is an open-access article distributed under the terms of the Creative Commons Attribution License (CC BY). The use, distribution or reproduction in other forums is permitted, provided the original author(s) and the copyright owner(s) are credited and that the original publication in this journal is cited, in accordance with accepted academic practice. No use, distribution or reproduction is permitted which does not comply with these terms.



OPEN ACCESS

# Validation and Optimization of Host Immunological Bio-Signatures for a Point-of-Care Test for TB Disease

**Edited by:**

Mario Alberto Flores-Valdez,  
CONACYT Centro de Investigación y  
Asistencia en Tecnología y Diseño del  
Estado de Jalisco (CIATEJ), Mexico

**Reviewed by:**

Claudia Denking,  
Heidelberg University Hospital,  
Germany  
Luis Cuevas,  
Liverpool School of Tropical Medicine,  
United Kingdom  
John Davis,  
Yale University, United States

**\*Correspondence:**

Gian D. van der Spuy  
gvds@sun.ac.za

<sup>†</sup>These authors share first authorship

<sup>‡</sup>These authors have contributed  
equally to this work

**Specialty section:**

This article was submitted to  
Microbial Immunology,  
a section of the journal  
Frontiers in Immunology

**Received:** 18 September 2020

**Accepted:** 18 January 2021

**Published:** 26 February 2021

**Citation:**

Mutavhatsindi H, van der Spuy GD,  
Malherbe ST, Sutherland JS, Geluk A,  
Mayanja-Kizza H, Crampin AC,  
Kassa D, Howe R, Mihret A,  
Sheehama JA, Nepolo E, Günther G,  
Dockrell HM, Corstjens PLAM,  
Stanley K, Walzl G, Chegou NN and  
the AE-TBC ScreenTB Consortia  
(2021) Validation and Optimization of  
Host Immunological Bio-Signatures for  
a Point-of-Care Test for TB Disease.  
*Front. Immunol.* 12:607827.  
doi: 10.3389/fimmu.2021.607827

Hygon Mutavhatsindi<sup>1†</sup>, Gian D. van der Spuy<sup>1\*†</sup>, Stephanus T. Malherbe<sup>1</sup>,  
Jayne S. Sutherland<sup>2</sup>, Annemieke Geluk<sup>3</sup>, Harriet Mayanja-Kizza<sup>4</sup>, Amelia C. Crampin<sup>5</sup>,  
Desta Kassa<sup>6</sup>, Rawleigh Howe<sup>7</sup>, Adane Mihret<sup>7</sup>, Jacob A. Sheehama<sup>8</sup>,  
Emmanuel Nepolo<sup>8</sup>, Gunar Günther<sup>8</sup>, Hazel M. Dockrell<sup>9</sup>, Paul L. A. M. Corstjens<sup>10</sup>,  
Kim Stanley<sup>1</sup>, Gerhard Walzl<sup>1‡</sup>, Novel N. Chegou<sup>1‡</sup> and the AE-TBC ScreenTB Consortia

<sup>1</sup> Department of Science and Innovation - National Research Foundation (DSI-NRF) Centre of Excellence for Biomedical  
Tuberculosis Research, South African Medical Research Council Centre for Tuberculosis Research, Division of Molecular  
Biology and Human Genetics, Faculty of Medicine and Health Sciences, Stellenbosch University, Cape Town, South Africa,

<sup>2</sup> TB Research Group, Medical Research Council Gambia at London School of Hygiene and Tropical Medicine (LSHTM),  
Banjul, Gambia, <sup>3</sup> Department of Infectious Diseases, Leiden University Medical Centre, Leiden, Netherlands, <sup>4</sup> Department of  
Internal Medicine and Immunology, School of Medicine, Makerere University, Kampala, Uganda, <sup>5</sup> Karonga Prevention Study,  
London School of Hygiene and Tropical Medicine, Karonga, Malawi, <sup>6</sup> Infectious and Non-Infectious Diseases Research  
Directorate, Ethiopian Health and Nutrition Research Institute, Addis Ababa, Ethiopia, <sup>7</sup> Department of Immunology, Armauer  
Hansen Research Institute, Addis Ababa, Ethiopia, <sup>8</sup> Department of Biochemistry & Microbiology, School of Medicine,  
University of Namibia, Windhoek, Namibia, <sup>9</sup> Department of Infection Biology, Faculty of Infectious and Tropical Diseases,  
London School of Hygiene and Tropical Medicine, London, United Kingdom, <sup>10</sup> Department of Molecular Cell Biology, Leiden  
University Medical Centre, Leiden, Netherlands

The development of a non-sputum-based, point-of-care diagnostic test for tuberculosis (TB) is a priority in the global effort to combat this disease, particularly in resource-constrained settings. Previous studies have identified host biomarker signatures which showed potential, but there is a need to validate and refine these for development as a test. We recruited 1,403 adults presenting with symptoms suggestive of pulmonary TB at primary healthcare clinics in six countries from West, East and Southern Africa. Of the study cohort, 326 were diagnosed with TB and 787 with other respiratory diseases, from whom we randomly selected 1005 participants. Using Luminex<sup>®</sup> technology, we measured the levels of 20 host biomarkers in serum samples which we used to evaluate the diagnostic accuracy of previously identified and novel bio-signatures. Our previously identified seven-marker bio-signature did not perform well (sensitivity: 89%, specificity: 60%). We also identified an optimal, two-marker bio-signature with a sensitivity of 94% and specificity of 69% in patients with no history of previous TB. This signature performed slightly better than C-reactive protein (CRP) alone. The cut-off value for a positive diagnosis differed for human immuno-deficiency virus (HIV)-positive and -negative individuals. Notably, we also found that no signature was able to diagnose TB adequately in patients with a prior history of the disease. We have identified a two-marker, pan-African bio-signature which is more robust than CRP alone and meets the World Health

Organization (WHO) target product profile requirements for a triage test in both HIV-negative and HIV-positive individuals. This signature could be incorporated into a point-of-care device, greatly reducing the necessity for expensive confirmatory diagnostics and potentially reducing the number of cases currently lost to follow-up. It might also potentially be useful with individuals unable to provide sputum or with paucibacillary disease. We suggest that the performance of TB diagnostic signatures can be improved by incorporating the HIV-status of the patient. We further suggest that only patients who have never had TB be subjected to a triage test and that those with a history of previous TB be evaluated using more direct diagnostic techniques.

**Keywords:** bio-signature, diagnostic, validation, blood, biomarkers, point of care, *M. tuberculosis* (*M. tb*)

## INTRODUCTION

Tuberculosis (TB) remains a major global health burden with the World Health Organization (WHO) reporting 10.4 million new TB cases and 1.6 million TB-related deaths worldwide in 2018. TB is also the leading cause of death for people infected with the human immunodeficiency viruses (HIV) (1). The lack of rapid, accurate, point-of-care diagnostic tests poses a serious challenge to control efforts (2). The Ziehl Nielsen sputum smear test is often the only affordable diagnostic tool available in resource constrained environments, even though its limitations, notably its low sensitivity, are well publicized (3, 4). *Mycobacterium tuberculosis* (*M.tb*) culture, the reference test, is not widely available in these settings. It also has several drawbacks which include a long turnaround time, high costs, and significant rate of contamination (3). The GeneXpert® MTB/RIF sputum test (Cepheid, USA), one of the major advances in TB diagnosis, produces results within 2 h and is coupled with the detection of rifampicin resistance. The GeneXpert® test is widely available in developed countries but limitations, including relatively high operating costs and infrastructural requirements hinder its use in resource-constrained settings (5, 6). It also has significantly reduced sensitivity in paucibacillary disease although this has been somewhat remedied by the newer Xpert Ultra® (7). A common and very important limitation of the above-mentioned diagnostic tests is that they are all sputum-based which renders them unsuitable for use in individuals who have difficulty in providing good quality sputum. This is particularly true of children, who typically develop paucibacillary disease (8), and also of individuals with extra-pulmonary TB or who are HIV-positive. There is, therefore, an urgent need for alternative diagnostic tests that are suitable for use in all patient types, especially in resource-poor settings (9).

Transcriptome-based diagnostic markers have attracted a good deal of interest as an alternative to current tests. They are particularly attractive as detection technologies are well established and require minimal adaptation, irrespective of the target markers. While this approach shows some promise and has the advantage of being relatively easy to implement, as a result of small sample numbers or inappropriate controls, most studies to date have failed to yield a performance which meets the requirements of the WHO for a viable diagnostic (10).

Immunodiagnostics have received considerable attention as an alternative for the detection of TB disease in recent years (11, 12). They are particularly promising as they could be developed into point-of-care tests, which would be easily accessible to resource limited settings. Such tests would also be useful in cases where a sputum-based diagnosis (GeneXpert®, smear microscopy or culture) is difficult or not available (13). The emergence of interferon gamma release assays (IGRAs) was a prominent advancement in the development of immunodiagnostic tools for *M.tb*. Commercially available IGRAs rely on the reaction of the immune system to antigens encoded within the region of difference 1 (RD1) of the *M.tb* genome, namely early secreted antigenic target 6 (ESAT-6) and culture filtrate protein 10 (CFP-10) (14). These assays are useful in diagnosis of infection with *M.tb*, however, they are of limited value in high TB-endemic areas as they cannot discriminate between active TB and latent *M.tb* infection. Attempts have been made to identify antigens that may be useful in the diagnosis of active TB (15–17). However, the requirement for overnight culture precludes the use of these assays as point-of-care tests.

Host immunological markers detected in *ex vivo* samples have shown potential for the diagnosis of TB disease (13, 18–21). These markers may be incorporated into a field-friendly, point-of-care test based on finger-prick blood and lateral flow technology. One such test, currently under development, relies on a seven-marker host bio-signature identified in serum (20). However, tests based on large signatures such as this are expensive, complex to design and manufacture and rely on the continued production of numerous components by suppliers. It would, therefore, be of benefit to devise a small, reliable bio-signature implementable in a test device that would be cost-effective and relatively simple to produce. One such signature that has been previously identified in a high-TB incidence setting in HIV-positive participants is C-reactive protein (CRP) (22). It appears to be one of the more promising markers and consequently worth validating in this study in a broader context.

An important characteristic of TB, which complicates its diagnosis, is its frequent association with HIV infection (23). Any diagnostic test that is to be useful should be capable of detecting TB in both HIV-positive and -negative patients. Immunological responses of patients to *M.tb* may differ, dependent on their genetic profiles as well as the bacterial



strain with which they are infected (24). It is, therefore, important that a diagnostic test be sufficiently robust as to yield valid results irrespective of host-genetic background and prevalent *M.tb* strains.

This study investigated the potential of several previously identified, serum protein host markers to detect pulmonary TB in patients presenting at primary healthcare clinics, in seven sites across six African countries, with symptoms indicating possible TB (20). We further aimed to investigate the diagnostic potential of modified bio-signatures identified by us and combinations of other markers from the literature (20, 21). The study comprised a large cohort of HIV-negative and HIV-positive participants from different regions of the African continent in order to ensure that any bio-signature identified would be widely applicable in a point-of-care test for TB disease.

## METHODS

### Study Participants

We prospectively recruited 1,403 adults (18 years or older) (**Figure 1**), presenting with symptoms suggestive of pulmonary TB disease at primary healthcare clinics at seven field sites in six African countries as previously described (20). Both HIV-positive and -negative participants were included. Participants in this study were recruited as part of the EDCTP-funded African-European Tuberculosis Consortium (AE-TBC) which included Stellenbosch University (SUN), South Africa; Makerere University, Uganda (UCRC); Medical Research Council Unit, The Gambia at the London School of Hygiene and Tropical Medicine (MRCG); Karonga Prevention Study (KPS), Malawi; University of Namibia (UNAM), Namibia; Ethiopian Health and

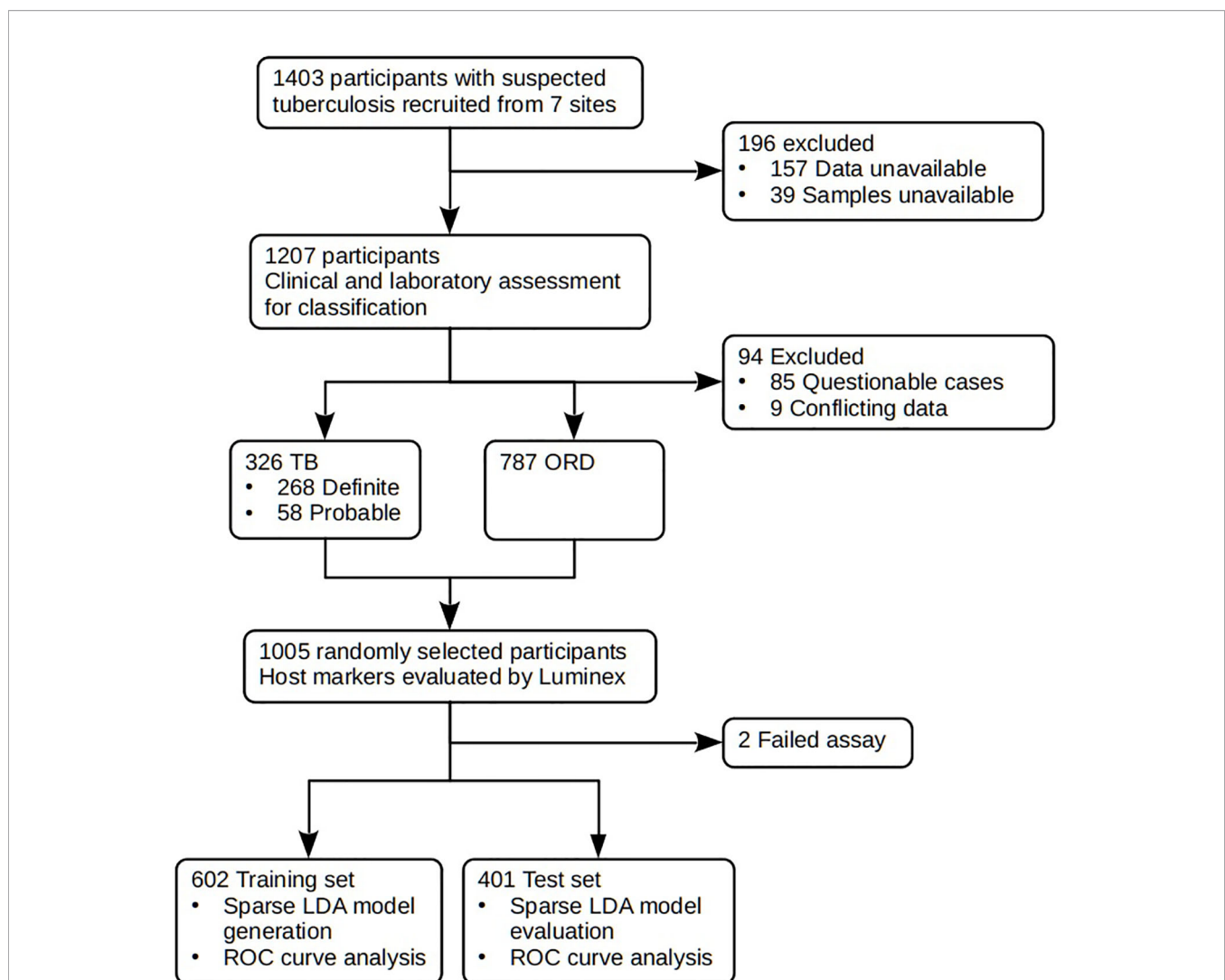


**FIGURE 1** | STARD diagram showing the study design and classification of study participants. TB, pulmonary TB; ORD, individuals presenting with symptoms and investigated for pulmonary TB but in whom TB disease was ruled out; ROC, receiver operator characteristic. STARD, Standards for Reporting of Diagnostic Accuracy.

Nutrition Research Institute (EHNRI), Ethiopia and The Armauer Hansen Research Institute (AHRI), Ethiopia.

Criteria for inclusion in the study were a cough persisting for more than 2 weeks together with any one of the following: fever, recent weight-loss, night-sweats, hemoptysis, chest-pain, or anorexia. Participants were included in the study if they were 18 years or older, willing to give written informed consent, including for HIV testing using a rapid test (Abbott, Germany), and sample storage. Exclusion criteria for the study included severe anemia (hemoglobin <10g/l), pregnancy, other known chronic diseases such as diabetes mellitus, current anti-TB treatment, anti-TB treatment in the last 3 months, use of quinolone or aminoglycoside antibiotics in the past 2 months, or residency in the study area for less than 3 months. Study participants were recruited between November 2010 and November 2012.

Approval for the study was granted by the Human Research Ethics Committee of Stellenbosch University (N10/08/274) as well as the ethics committees of the respective partner institutions.

## Classification of Study Participants

Prior to the commencement of recruitment, harmonized case definitions were established to be used for the classification of study participants at all study sites. Using a combination of clinical, radiological, and laboratory findings, participants were classified as either definite TB cases, probable TB cases, or other respiratory disease (ORD) as previously described (20). The ORD cases were participants diagnosed as having a range of other respiratory conditions including upper and lower respiratory tract bacterial or viral infections (although no attempt was made to identify organisms by culture), and acute exacerbations of chronic obstructive pulmonary disease or asthma. In assessing the diagnostic accuracy of the markers investigated in the present study, all the definite and probable TB cases were classified as “TB,” and then compared to the ORD cases (Figure 1). Participants who could not be diagnosed with an acceptable degree of certainty due to insufficient or contradictory clinical evidence (Table 2) were excluded from the analysis.

## Reading of Chest X-Rays

Each chest X-ray was reviewed by research medical officers at each site, who decided whether the quality was adequate for classification and then classified it as either normal, abnormal and suggestive of active TB, or abnormal and not suggestive of active TB. Repeat X-rays were compared to baseline X-rays and classified as wither resolved, improved, unchanged, or deteriorated. Lesion types were also documented for abnormal X-rays. The central study clinician reviewed X-rays of all participants whose main study classification (definite TB, probable Tb, No TB) was dependent on the chest X-ray findings. Cases in which the central study clinician's opinion differed from that of the research medical officer were discussed with the study PI.

## Sample Collection and Microbiological Diagnostic Tests

Harmonized protocols were used for collection and processing of samples across all study sites. Briefly, blood samples were

collected at first contact with the patient in 4ml plain BD Vacutainer serum tubes (BD Biosciences) and transported within 3 h at ambient temperature to the laboratory. Tubes were then centrifuged at 2,500 rpm for 10 min, after which serum was harvested, aliquoted into bar-coded cryotubes, and frozen at  $-80^{\circ}\text{C}$  until use. Sputum samples were collected from all participants and cultured using either the *Mycobacteria* growth indicator tube (MGIT) method (BD Biosciences) or Lowenstein-Jensen media, depending on facilities available at the study site. Specimens demonstrating growth of micro-organisms were examined for acid-fast bacilli using the Ziehl-Neelsen method followed by either Capilia TB testing (TAUNS, Numazu, Japan) or polymerase chain reaction (PCR) to confirm the isolation of organisms of the *M.tb* complex before being designated as positive cultures.

## Luminex® Multiplex Immunoassay

Using Luminex® technology, we measured the levels of 20 host biomarkers using antibodies supplied by Merck Millipore, Billerica, Massachusetts, USA and R&D Systems, Minneapolis, Minnesota, USA (Table 1). All samples were evaluated undiluted or diluted according to the manufacturers recommendations. Samples were randomized to assay plates with the experimenter blinded to sample data. All assays were performed and read in a central laboratory (SUN) on the Bio-Plex platform (Bio-Rad), with the Bio-Plex Manager Software (ver. 6.1) used for bead acquisition and analysis.

## Data Management and Statistical Analysis

All participant and laboratory data were captured using a central REDCap database hosted at SUN (25). Participant and sample management was done using a multi-site study management REDCap plugin application developed at SUN.

**TABLE 1 |** Host markers evaluated in this study nomenclature.

Abbreviation	Full Name
<i>Merck Millipore, Billerica, Massachusetts, USA</i>	
CRP	C-reactive protein
SAA	Serum amyloid A
SAP	Serum amyloid P component
FIBR	Fibrinogen
NCAM	Neural cell adhesion molecule
ApoA1	Apolipoprotein A1
Apo-CIII	Apolipoprotein C-III
CFH	Complement factor H
<i>R&amp;D Systems, Minneapolis, Minnesota, USA</i>	
TGF- $\alpha$	Transforming growth factor alpha
IFN- $\gamma$	Interferon gamma
IP-10	IFN- $\gamma$ -inducible protein
TNF- $\alpha$	Tumour necrosis factor alpha
Serpin C	Serpin C
Ferritin	Ferritin
CCL14/HCC-1	Chemokine (C-C motif) ligand 14
CCL1/I-309	Chemokine (C-C motif) ligand 1
MIG/CXCL9	Monokine induced by gamma interferon
VEGF-A	Vascular endothelial growth factor A
BDNF	Brain-derived neurotrophic factor
GDF15	Growth/differentiation factor 15

**TABLE 2 |** Classification definitions used to identify study participants groups.

Classification	Definition
Definite TB	Sputum culture-positive for MTB. OR2 positive smears and symptoms responding to TB treatment. OR1 positive smear plus CXR suggestive of PTB
Probable TB	1 positive smear and symptoms responding to TB treatment. ORCXR evidence and symptoms responding to TB treatment.
ORD	Negative cultures, negative smears, negative CXR and treatment never initiated by healthcare providers

CXR, chest X-ray; MTB, *Mycobacterium tuberculosis*; ORD, other respiratory disease; TB, pulmonary TB. (Reproduced from Chegou et al., *Thorax* 2016) (20).

All statistical analysis was done using R (ver. 3.6.1) [R Core Team (2019). R: A language and environment for statistical computing. R Foundation for Statistical Computing, Vienna, Austria. URL <https://www.R-project.org/>] working in the RStudio (ver. 1.2.5019) environment (RStudio Team (2019), RStudio: Integrated Development for R. RStudio, Inc., Boston, MA URL <http://www.rstudio.com/>) running on Kubuntu Linux 19.04. Unless otherwise stated, graphs were produced using the ggplot2 package (ver. 3.2.1). Parallel processing was facilitated by the doParallel package.

Missing values for SAA fluorescence data were imputed for 42 records using the missForest package using sex, age, HIV status, TB status, and all analytes as predictors.

Due to the presence of a few extreme fluorescence values for some of the analytes, the fluorescence data were subjected to winsorization whereby values greater than 10 median absolute deviations from the median were proportionally shrunk toward the median absolute deviation as calculated with the exclusion of the outliers.

Data were randomly divided into a training set (60%) and a test set (40%). Representivity of each study site in the training set ranged from 55 to 66% of the site's data.

Sparse Linear Discriminant Analysis (sparseLDA) models were trained using the Caret package (ver. 6.0-84) with predictor variables normalized using the YeoJohnson transformation, centered and scaled. Smote resampling was used to balance the proportions of TB and non-TB cases. Models were optimized for maximum sensitivity at a minimum specificity of 0.7 using a customized version of Caret's twoClassSummary function.

A model based on a previously published combination of 7 markers was trained using 32-times repeated, 10-fold cross-validation to select the optimal number of terms and the value for the regularization parameter, lambda. The model allowed interactions between the predictors.

An optimal model was developed by first selecting a set of markers by training a model using 32-times repeated, 10-fold cross-validation without interactions. These markers were then used to generate a new model, which allowed interactions between the predictors, using cross-validation to select the optimal number of terms and value for the regularization term, lambda, which reduces the risk of overfitting.

A model, weighted to compensate for the lower prevalence of HIV-positive cases in the dataset, was generated similarly, but

with the addition of a weights vector to the caret::train function. HIV-positive cases were assigned a weight inversely proportional to the number of HIV-positive cases and likewise for HIV-negative cases.

Receiver-operator characteristic (ROC) curves were produced using the pROC package. The 95% confidence intervals for sensitivity were generated by bootstrap resampling (R=10,000). Optimal cut-off values were selected as the highest sensitivity such that specificity remained above 70% where possible. Area under the curve (AUC) values were compared using the bootstrap method.

## RESULTS

### Clinical and Demographic Characteristics of Study Participants

In the current study we recruited a total of 1,403 participants (**Figure 1**). Of these, 196 participants were excluded due to the unavailability of data or samples. Using pre-established case definitions (**Table 2**), 268 (22.2%) of the remaining 1,207 study participants were classified as definite pulmonary TB cases and 58 (4.8%) as probable TB cases, together representing the active TB group (326 participants; 27.0%). 787 (65.2%) were classified as ORD cases. Ninety-four (7.8%) participants could not be reliably classified due to incomplete data or loss to follow-up and were excluded from the study. 1,005 of the remaining participants were randomly selected for further analysis. Demographic and clinical details of the participants are given in **Table 3**.

### Performance of Individual Serum Biomarkers in the Diagnosis of TB Disease

Using the training data-set, 17 of the 20 serum markers investigated in the study showed significant differences ( $p < 0.0025$  corrected for multiple testing) between the TB and ORD cases, irrespective of HIV infection status or country of sample origin. Those that did not were IFN- $\gamma$ , ApoA-1, and Serpin C1. When we investigated the ability of the markers to diagnose TB disease using ROC curve analysis, the areas under the ROC curve (AUC) were between 0.70 to 0.86 for 12 out of the 20 investigated analytes, namely; ApoCIII, BNDF, I-309, CRP, IP-10, MIG, ferritin, fibrinogen, IFN- $\gamma$ , SAA, SAP, and TNF- $\alpha$  (**Figures 2 and 3**).

### Performance of Serum Multi-Analyte Models in the Diagnosis of TB Disease Performance of the Optimal Bio-Signature

In order to identify the best performing marker combination, we generated a model using the sparseLDA algorithm with no constraint on marker number. This identified a two-marker, optimal bio-signature. The selected markers were: I-309 and CRP. We constructed a sparseLDA model from these markers, including interactions between terms, which yielded a sensitivity of 93% and a specificity of 68% on the test set. The area under the ROC curve (AUC) for this model was 0.90 (**Table 4**) (26).

**TABLE 3 |** Clinical and demographic characteristics of analyzed study participants from the seven study sites.

Study site	AHRI	EHNRI	KPS	MRCG	SUN	UCRC	UNAM	Total
<b>Participants</b>	149	185	109	188	156	170	46	1003
<b>Age in years, mean <math>\pm</math> SD</b>	33.4 $\pm$ 11.6	35.1 $\pm$ 14.7	39.7 $\pm$ 13.8	35.4 $\pm$ 12.6	37.5 $\pm$ 11.5	32.6 $\pm$ 9.9	35.6 $\pm$ 11.0	35.4 $\pm$ 12.5
<b>Males, n (%)</b>	75 (50.3)	76 (41.1)	56 (51.3)	109 (58.0)	64 (41.0)	87 (51.2)	27 (58.7)	494 (49.3)
<b>Previous TB, n (%)</b>	20 (13.4)	19 (10.2)	9 (8.3)	14 (7.4)	65 (41.7)	4 (2.4)	11 (23.9)	142 (14.2)
<b>HIV pos TB pos, n (%)</b>	6 (10.7)	13 (24.1)	12 (60.0)	8 (15.1)	4 (16.0)	7 (11.3)	15 (58.3)	71 (25.5)
<b>HIV pos TB neg, n (%)</b>	5 (4.1)	16 (12.0)	49 (55.7)	9 (6.7)	24 (18.3)	21 (19.4)	5 (50.0)	129 (17.8)
<b>Definite TB, n (%)</b>	28 (18.8)	53 (28.6)	17 (15.6)	44 (23.4)	21 (13.5)	58 (34.1)	31 (67.4)	252 (25.1)
<b>Probable TB, n (%)</b>	0 (0)	0 (0)	3 (2.8)	9 (4.8)	4 (2.6)	4 (2.4)	5 (10.9)	25 (2.5)
<b>Total TB, n (%)</b>	28 (18.8)	53 (28.6)	20 (18.3)	53 (28.2)	25 (16.0)	62 (36.5)	36 (78.3)	277 (27.6)
<b>ORD, n (%)</b>	121 (81.2)	132 (71.4)	89 (81.7)	135 (71.8)	131 (84.0)	108 (63.5)	10 (21.7)	726 (72.4)
<b>ORD QFTpos/tested, (%)</b>	ND	ND	29/86 (33.7)	40/129 (31.0)	86/127 (67.7)	59/104 (56.7)	7/10 (70.0)	224/456 (49.1)

TotalTB, sum of definite and probable TB cases; ORD QFT, quantiferon results for ORD participants.

While training the model, we noted that the optimal cut-off for HIV-positive participants was different to that for HIV-negatives. In order to maximize the performance of the model, it was therefore necessary to choose separate cut-off values for these two groups. The model then yielded sensitivities and specificities of 91 and 73% for HIV-negative cases and 87 and 64% for HIV-positive cases respectively (**Table 4; Figure 4**). Attempting to improve the model's performance on HIV-positive cases by weighting their contribution to the model by the inverse of their proportion during training did not produce any noticeable effect.

### Performance of the Best Bio-Signature Without CRP

To determine the degree of dependence on CRP, we repeated the optimal model construction, excluding CRP from the available set of markers. In this scenario, the algorithm selected I-309, NCAM and SAA. The performance of this signature was marginally inferior to, that of the optimal signature in both HIV-negative and HIV-positive individuals (**Table 4, Figure S3**). Weighting the data to increase the contribution of HIV-positive cases did not significantly improve the performance of the model on this group.

### Performance of the Previously Identified Seven-Marker Bio-Signature

We previously identified a seven-marker bio-signature comprising: ApoA-1, CFH, CRP, IFN- $\gamma$ , IP-10, SAA, and transthyretin (20). This had a sensitivity and specificity of 93.8 and 73.3% respectively when the model was applied to a test set. The data for that study was generated from an early-recruitment subset of the samples used in the current study, from five of the seven field-sites. We investigated the diagnostic potential of the seven-marker serum bio-signature, with transthyretin removed, as antibodies for this marker were no longer available for Luminex<sup>®</sup>. To do this, we used a 60% training set which was a super-set of samples from the participants common to this and the original study. Model performance was evaluated on a test set comprising the remainder of the samples in the current study. These had not been part of the original study. This signature did not perform well. The sensitivity and specificity in HIV-negative individuals was 88 and 61% respectively and in HIV-positive individuals, 80 and 57% (**Table 4; Figure 5**).

### Performance of CRP

We built a model to validate the previously identified single diagnostic marker, CRP (22). We found a sensitivity of 89% and specificity of 75% in HIV-negative participants and 90 and 67% respectively when tested against HIV-positive participants (**Table 4; Figure 6**).

### Performance with Respect to History of Previous TB

We investigated the performance of the optimal model separately on participants with a history of previous TB and those without. We found that the bio-signature performed well for participants with no history of previous TB. For HIV-positive participants, we achieved a sensitivity of 95% and a specificity of 64% and for HIV-negatives, a sensitivity of 93% and specificity of 76% (**Table 4; Figure 7**). For participants with a previous episode of TB, however, the bio-signature was far less informative. In this case, for HIV-positive participants, we measured a sensitivity of 70% and a specificity of 73%, while for HIV-negatives, the values were 82 and 68% respectively (**Table 4; Figure 8**). The optimal bio-signature therefore met the requirements of the WHO TPP for a triage test in patients without a history of previous TB, although the specificity for HIV-positive patients was slightly lower than desired (26).

### Comparison of Model Performance

In comparing the AUCs of the ROC curves of the various models, we found that the optimal signature significantly outperformed CRP on its own ( $p=0.032$ , stratified bootstrap). This was also the case when we compared the sensitivities of these two models at a specificity of 0.7 ( $p=0.032$ , stratified bootstrap). There were no significant pairwise differences between any of the other models.

## DISCUSSION

The development of a better diagnostic tool for TB is an important goal in the fight against this disease. To this end, we investigated the ability of 20 previously identified host serum protein biomarkers to diagnose TB disease in individuals presenting with symptoms suggestive of TB disease at peripheral healthcare clinics in six African countries. Twelve of



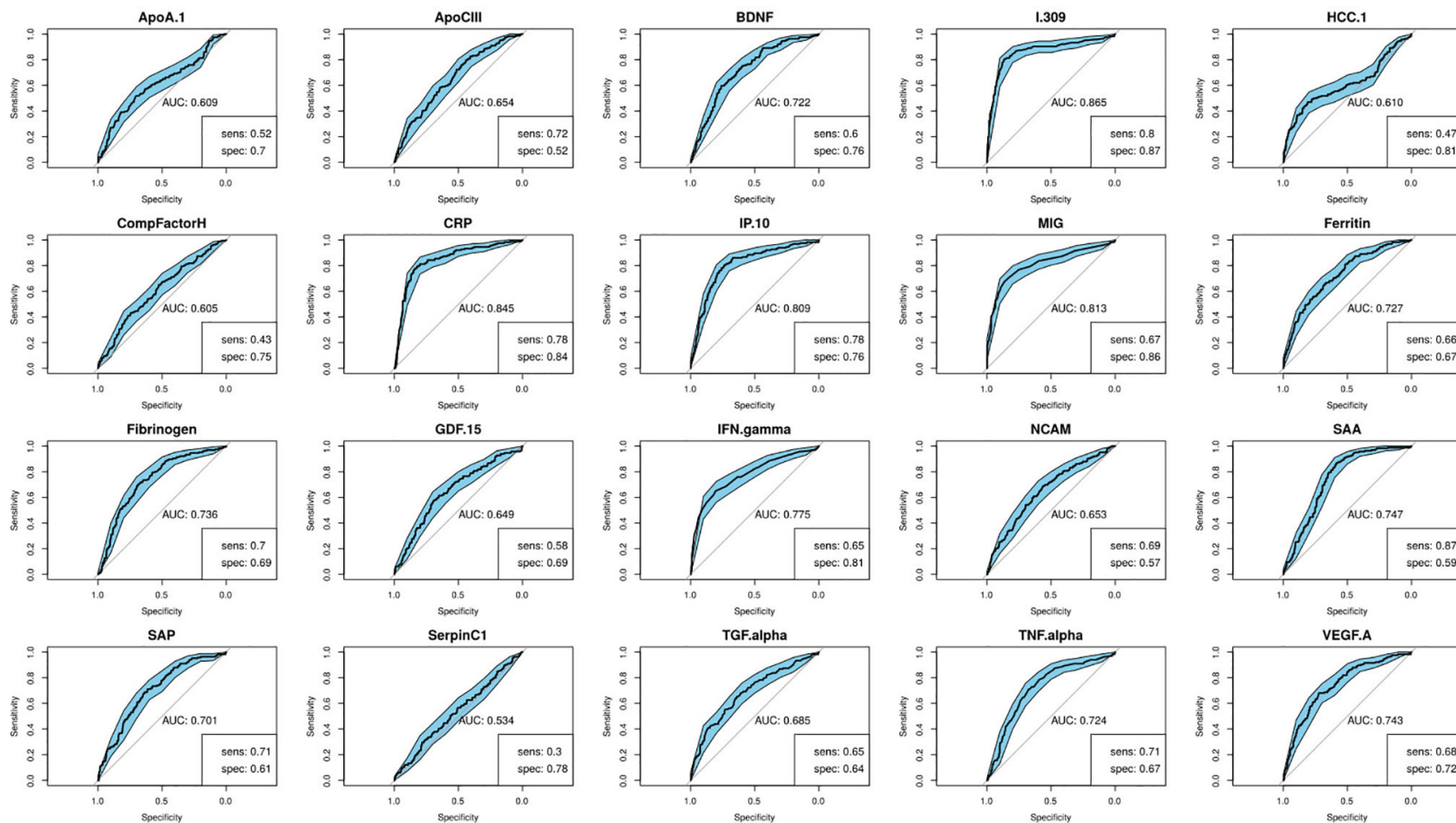


**FIGURE 2 |** Receiver-operator characteristic (ROC) curves of the diagnostic performance of the individual biomarkers in the training set. Sensitivity and specificity are given for the maximized Youden's J statistic cut-off point.

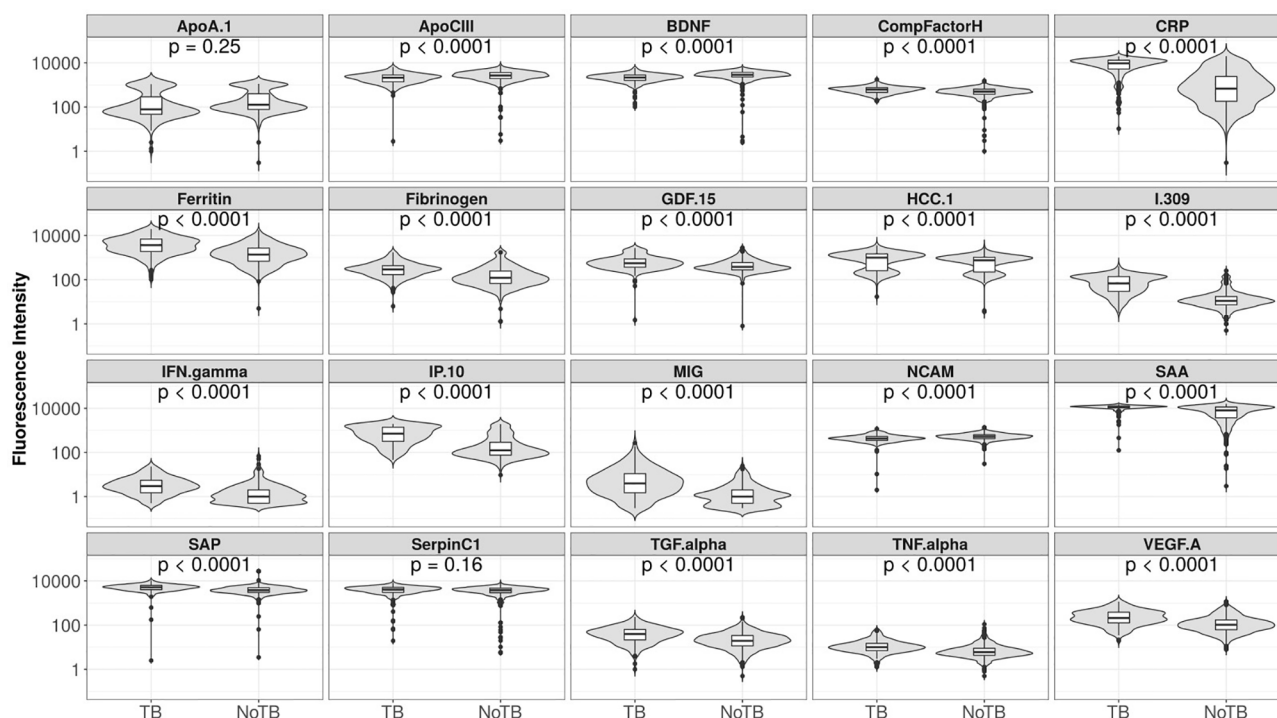


**FIGURE 3** | Fluorescent intensities on a log scale of biomarkers detected in the serum samples of participants with tuberculosis (TB) and those with other respiratory disease (ORD), for all 20 markers analyzed. Unadjusted permutation test p-values for the difference between the means of the groups are given for each biomarker (105 permutations).

**TABLE 4** | Performance of the predictive models.

Signature	N	AUC (95% CI)	Sensitivity (95% CI)	Specificity (95% CI)
<b>CRP</b>	401	0.85 (0.81-0.88)	0.85 (0.81-0.88)	0.74 (0.54-0.84)
HIV pos	85	0.79 (0.70-0.87)	0.83 (0.56-0.93)	0.72 (0.39-0.83)
HIV neg	316	0.86 (0.81-0.90)	0.86 (0.79-0.92)	0.70 (0.54-0.85)
<b>6-marker</b>	350	0.85 (0.80-0.90)	0.89 (0.81-0.96)	0.60 (0.34-0.82)
HIV pos	41	0.80 (0.65-0.92)	0.80 (0.65-0.95)	0.57 (0.14-0.95)
HIV neg	309	0.85 (0.79-0.91)	0.88 (0.80-0.96)	0.61 (0.29-0.85)
<b>Optimal</b>	401	0.90 (0.86-0.94)	0.93 (0.87-0.97)	0.68 (0.36-0.82)
HIV pos	85	0.89 (0.80-0.95)	0.87 (0.73-1.00)	0.64 (0.47-0.89)
HIV neg	316	0.90 (0.86-0.94)	0.91 (0.84-0.98)	0.73 (0.40-0.89)
<b>No Previous TB</b>	338	0.92 (0.88-0.95)	0.94 (0.89-0.99)	0.69 (0.36-0.87)
HIV pos	64	0.92 (0.84-0.97)	0.95 (0.85-1.00)	0.64 (0.50-0.89)
HIV neg	274	0.92 (0.87-0.96)	0.93 (0.86-0.99)	0.74 (0.43-0.92)
<b>Previous TB</b>	63	0.83 (0.70-0.93)	0.81 (0.67-1.00)	0.60 (0.29-0.93)
HIV pos	21	0.84 (0.62-0.97)	0.70 (0.40-1.00)	0.73 (0.27-1.00)
HIV neg	42	0.79 (0.60-0.95)	0.82 (0.45-1.00)	0.68 (0.13-0.97)
<b>Optimal Excluding CRP</b>	401	0.89 (0.85-0.94)	0.92 (0.86-0.97)	0.70 (0.47-0.84)
HIV pos	85	0.88 (0.79-0.94)	0.93 (0.77-1.00)	0.56 (0.40-0.84)
HIV neg	316	0.89 (0.84-0.93)	0.89 (0.81-0.96)	0.77 (0.52-0.92)

Signatures: Six-marker (ApoA-1, CFH, CRP, IFN- $\gamma$ , IP-10, SAA), optimal (I-306 and CRP), optimal excluding CRP (I-309, NCAM and SAA). N=test-set samples.

the 20 investigated biomarkers showed promise in this study for diagnosing TB disease as their ROC curves when distinguishing between the TB and ORD groups had AUCs greater than 0.7.

Although many biomarkers obtained from various body-fluids show promise individually for diagnosing TB, single markers tend

to be less robust than combination bio-signatures due to their non-specificity and tendency to be affected by other factors such as HIV-infection (20). This was the case when we attempted to validate the previously identified biomarker, CRP, which was less effective at diagnosing TB than the optimal two-marker model.

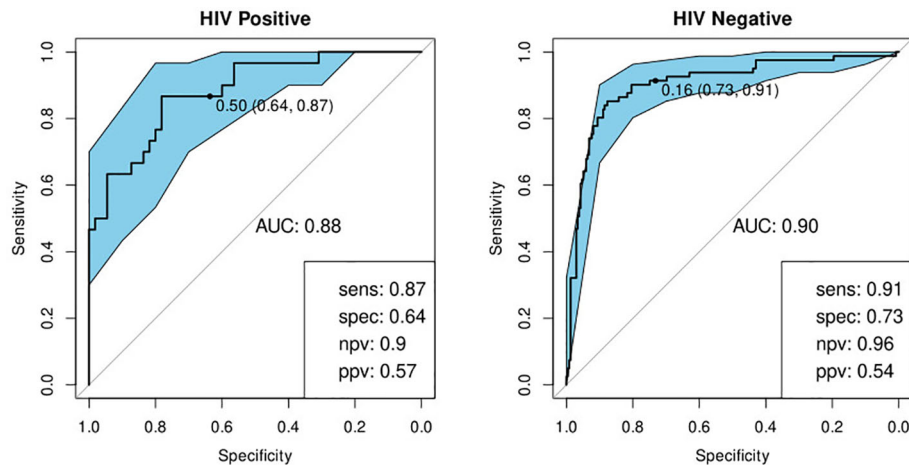


**FIGURE 4** | Receiver-operator characteristic (ROC) curve for the optimal bio-signature (CRP and I-309) for HIV-positive (N=85) and HIV-negative (N=316) individuals. The optimal sensitivity and specificity are shown on the bottom right corner together with the negative and positive predictive values.

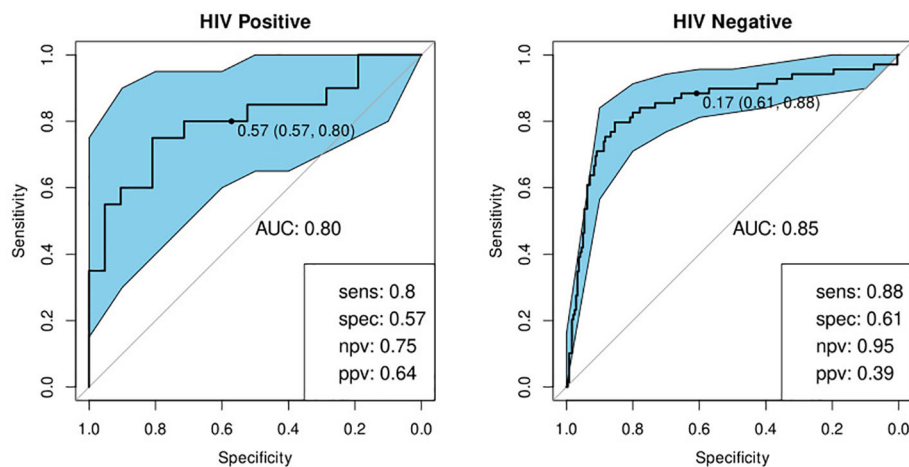


**FIGURE 5** | Receiver-operator characteristic (ROC) curve for the modified seven marker bio-signature originating from Chegou and colleagues, excluding transthyretin, for HIV-positive (n=41) and HIV-negative (n=309) individuals (20). The optimal sensitivity and specificity bottom right together with the negative and positive predictive values.

We identified an optimal diagnostic bio-signature, irrespective of African country of origin, comprising two markers: the chemoattractant, I.309 and CRP. This signature meets the WHO minimum requirements for a triage test, which is a sensitivity of 90% and specificity of 70%, in HIV-negative patients and in HIV-positive patients with no previous history of TB (26). Given the frequent co-morbidity of TB and HIV infection and the difficulties this creates for diagnosing TB, it is encouraging that our diagnostic bio-signature is successful regardless of HIV infection status, albeit with wider confidence intervals in the case of HIV positive participants. It should be noted, however, that I.309 is present in blood at far lower

concentrations than CRP which poses a technological challenge for measurement in a point-of-care device.

The poor performance that we observed for our bio-signature in participants with a history of previous TB has not, as far as we are aware, been previously reported and raises the question as to whether any surrogate biomarker for TB disease can perform well in patients in this category. It is worth noting that this is a limitation shared by the Xpert Ultra<sup>®</sup> technology (27). The number of patients falling into this group in the test set was small (n=63) which may explain the lack of significant difference in the performance of the model between this and the first-time TB group. However, it is also possible that this group had an

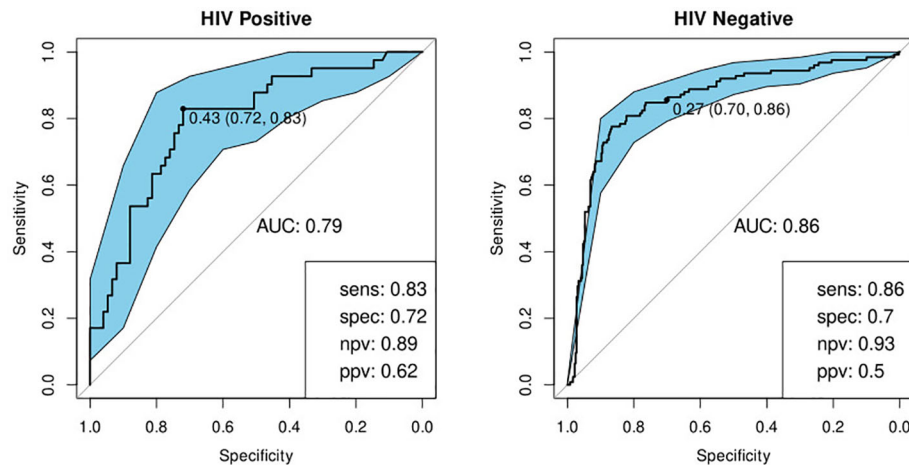


**FIGURE 6** | Receiver-operator characteristic (ROC) curve for CRP only for HIV-positive (N=85) and HIV-negative (N=316) individuals. The optimal sensitivity and specificity are shown on the bottom right corner together with the negative and positive predictive values.

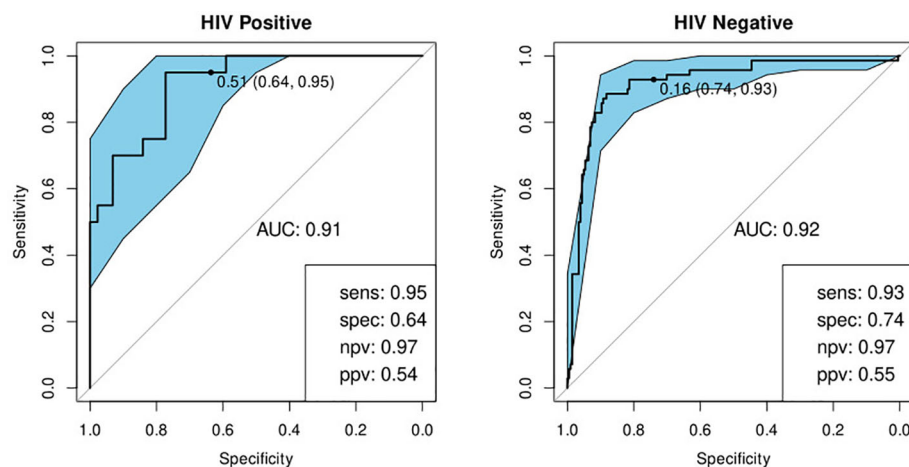


**FIGURE 7** | Receiver-operator characteristic (ROC) curves of the performance of the optimal bio-signature (CRP and I-309) for HIV-positive (n=64) and HIV-negative (n=274) individuals with no previous history of TB. The optimal sensitivity and specificity are shown on the bottom right corner of each ROC curve together with the negative and positive predictive values.

inherently greater variability in marker levels leading to the very wide observed confidence intervals. Considering that most candidate markers for active TB are related to inflammation and that previous TB episodes often cause chronic lung damage, in turn leading to chronic inflammation, it is not entirely unexpected that the performance of these markers could be influenced by previous TB episodes. These preliminary findings will need to be confirmed by further studies. Since it has been established that a prior episode of TB tends to increase the risk of a repeat episode, it could be argued that such patients, on presenting with suspected TB, should bypass the triage test and be referred for confirmatory testing (28). It would be interesting to know whether the time elapsed since the previous episode affects the predictive power of the test.

However, this will need to be examined in a follow-up investigation as this data was not available in the present study.

Yoon et al. previously reported on a CRP-based point-of-care screening test for TB (89% sensitivity and 72% specificity with a pre-determined threshold of 10mg/L) in antiretroviral therapy-naïve, HIV-infected individuals with low CD4-cell counts from Uganda (22). We found CRP to be a common factor in, and indeed, the most important component of all our bio-signatures. When we excluded this marker from use by the modeling algorithm, we observed a slight, but non-significant, decrease in discriminatory power of the resultant model as has been previously reported (29). While raised levels of CRP are by no means specific to TB, this marker does appear to be the strongest differentiator between this and other lung diseases. An advantage



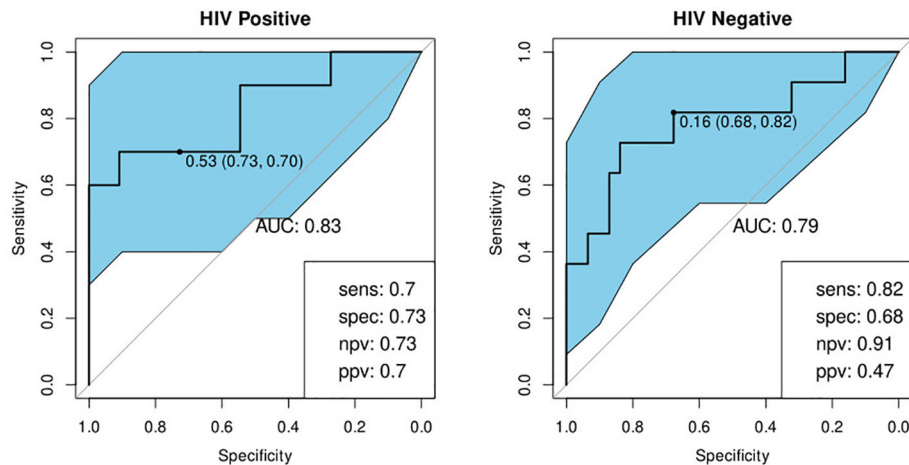


**FIGURE 8** | Receiver-operator characteristic (ROC) curves of the performance of the optimal bio-signature (CRP and I-309) for HIV-positive ( $n=21$ ) and HIV-negative ( $n=42$ ) individuals with a history of previous TB. The optimal sensitivity and specificity are shown on the bottom right corner of each ROC curve together with the negative and positive predictive values.

of CRP as a biomarker is its applicability, regardless of HIV infection status, due to its lack of dependence on the presence of CD4 cells (29). This feature, however, is not unique to CRP as other biomarkers such as IP-10, SAA, and ferritin are also produced in the context of HIV infection and may, therefore, be suitable substitutes (30, 31). It seems clear, however, that any serum protein-based bio-signature is likely to require the inclusion of CRP, but that additional markers may aid in boosting its performance above the WHO's TPP threshold.

Ideally, a point-of-care test would be capable of analyzing a raw, unprocessed sample such as finger-prick blood. Given that the current results are based on serum analyzed using a highly sophisticated laboratory instrument, it is likely that any point-of-care test based on the same analytes would demonstrate different characteristics, resulting in a possible loss of performance in translation to the final product. However, the significant degree of correlation between many immunological biomarkers means that it would be quite possible to substitute a marker which did not perform as desired in the end-product device with an alternative. It should also be noted that the performance of our bio-signatures exceeded the minimum criteria by a considerable degree in three of the sites which suggests that there may be some margin for loss of performance without dropping below these values.

Our attempt to validate our previously reported, seven-marker bio-signature was not successful. This failure may partially be explained by the necessary exclusion of transthyretin, which was an important component of the original signature, but was not available on the Luminex® platform. Nevertheless, this result highlights the importance of subjecting promising results to validation on independent datasets.

A major strength of this study is the diversity of the study sites, including participants from East, West, and Southern Africa. We were able to demonstrate that our bio-signatures

performed well in sites from all three African regions, although performance in three sites (KPS, UNAM, and EHNRI) was less than optimal. This is particularly pertinent as Africa accounts for 16 of the 30 countries with a high burden of TB and is also subject to resource limitations, making a point-of-care test highly beneficial in this context (1). Site-specific performance of the optimal model is presented in the supplemental data (**Figure S2**).

The under-performance of the bio-signatures in certain sites is a source of some concern. In the case of UNAM, participant numbers were approximately half that of the other sites with the result that there were only 19 participants from this site in the test set. In addition, due to overly rigorous screening at this site, only 22% of participants fell into the ORD group. In addition, UNAM and KPS had much higher proportions of HIV-positive participants than the other sites which may have negatively impacted their results. It should also be noted that these three sites experienced a number of logistical difficulties such as remote location, unreliable power supply, and less experienced staff which may have impacted on the quality of the samples and data.

The pan-African performance of our bio-signature is very encouraging, however, it remains to be seen whether this success translates to other settings where differing conditions or population genetics may have a negative impact. It also remains for the bio-signature identified in this study to be validated using finger-prick blood and technology appropriate to a point-of-care test. Further studies addressing these questions are in progress.

Being blood-based, rather than requiring the production of sputum, our bio-signature may also prove to be useful in children, who typically develop paucibacillary disease, as well as in individuals presenting with extra-pulmonary TB. Performance in these cohorts should be addressed once the signature has been validated in field-tests in adult pulmonary TB patients.

A potential source of error in this study, and others of this nature, stems from the existence of a subgroup of participants

whose diagnosis is uncertain. A rule-out test, such as the one proposed here, ought to classify these as TB so that they would be subject to further investigation. Unfortunately, this cannot be verified as these participants were excluded from this study. This is a point which should be addressed in a field-trial of the diagnostic test.

We suggest that the results presented here constitute strong evidence that the development of a TB triage diagnostic test based on a small number of immunological biomarkers is feasible. Such a tool would be of substantial benefit, particularly in under-resourced setting, which tend to have the highest burden of disease, by reducing the number of unnecessary referrals for expensive, confirmatory diagnostics such as GeneXpert®. As a result of its rapid turn-around time, it would also have the benefit of reducing the number of TB cases currently lost to follow-up which, in turn, would decrease the infection pressure in the affected communities.

## SCREENTB CONSORTIUM

**Stellenbosch University, South Africa:** Gerhard Walzl, Novel N. Chegou, Petri Ahlers, Stephanus T. Malherbe, Gian D van der Spuy, Ilana van Rensburg, Hygon Mutavhatsindi, Portia Manngo, Kim Stanley, Candice I Snyders, Andriette Hiemstra, Shirley McAnda, Marika Flinn, Bronwyn Smith

**Medical Research Council Gambia at LSHTM:** Jayne S Sutherland, Joseph Mendy, Awa Gindeh, Georgetta Mbayo, Ebrima Trawally, Olumuyiwa Owolabi

**Makerere University, Uganda:** Harriet Mayanja-Kizza, Mary Nsereko, Anna-Ritah Namuganga, Saudah Nambiru Kizito

**Armauer Hansen Research Institute, Addis Ababa, Ethiopia:** Adane Mihret, Sosina Ayalew, Rawleigh Howe, Azab Tarekegne, Bamlak Tessema

**University of Namibia, Namibia:** Emmanuel Nepolo, Joseph Sheehama, Gunar Gunther, Azaria Diergaardt, Uapa Pazvakavambwa  
London School of Hygiene and Tropical Medicine, United Kingdom: Hazel Dockrell

**Leiden University Medical Centre, Netherlands:** Tom Ottenhoff, Elisa Tjon Kon Fat, Shannon Herdigein, Paul Corstjens, Annemieke Geluk, Anouk van Hooij

## DATA AVAILABILITY STATEMENT

The raw data supporting the conclusions of this article will be made available by the authors, without undue reservation.

## ETHICS STATEMENT

The studies involving human participants were reviewed and approved by Health Research Ethics Committee, Stellenbosch University. The patients/participants provided their written informed consent to participate in this study.

## AE-TB CONSORTIUM

**Stellenbosch University, South Africa:** Gerhard Walzl, Novel N. Chegou, Magdalena Kriel, Gian D van der Spuy, Andre G Loxton, Kim Stanley, Stephanus Malherbe, Belinda Kriel, Leigh A Kotzé, Dolapo O Awoniyi, Elizna Maasdorp

**Medical Research Council Gambia at LSHTM:** Jayne S Sutherland, Olumuyiwa Owolabi, Abdou Sillah, Joseph Mendy, Awa Gindeh, Simon Donkor, Toyin Togun, Martin Ota

**Karonga Prevention Study, Malawi:** Amelia C Crampin, Felanji Simukonda, Alemayehu Amberbir, Femia Chilongo, Rein Houben

**Ethiopian Health and Nutrition Research Institute, Ethiopia:** Desta Kassa, Atsbeha Gebrezgabher, Getnet Mesfin, Yohannes Belay, Gebremedhin Gebremichael, Yodit Alemayehu.

**University of Namibia, Namibia:** Marieta van der Vyver, Faustina N Amutenya, Josefina N Nelongo, Lidia Monye, Jacob A Sheehama, Scholastica Iipinge

**Makerere University, Uganda:** Harriet Mayanja-Kizza, Ann Ritah Namuganga, Grace Muzanye, Mary Nsereko, Pierre Peters

**Armauer Hansen Research Institute, Ethiopia:** Rawleigh Howe, Adane Mihret, Yonas Bekele, Bamlak Tessema, Lawrence Yamuah

**Leiden University Medical Centre, Netherlands:** Tom HM Ottenhoff, Annemieke Geluk, Kees LMC Franken, Paul LAM Corstjens, Elisa M Tjon Kon Fat, Claudia J de Dood, Jolien J van der Ploeg-van Schip

Statens Serum Institut, Copenhagen, Denmark: Ida Rosenkrands, Claus Aagaard.

Max Planck Institute for Infection Biology, Berlin, Germany: Stefan HE Kaufmann, Maria M. Esterhuysen

London School of Hygiene and Tropical Medicine, London, United Kingdom: Jacqueline M Cliff, Hazel M Dockrell

## AUTHOR CONTRIBUTIONS

HM and GS co-wrote the first draft of the manuscript. GS analyzed the data and wrote the final draft of the manuscript. HM performed the Luminex analysis. SM, JSS, HM-K, AC, DK, RH, AM, JAS, and EN oversaw local data and sample collection. GW, NC, JSS, AG, HM-K, AC, DK, RH, JAS, EN, GG, HD, and PC were responsible for the study design. SM was responsible for the participant clinical classification. GS, SM, AG, and NC interpreted the results. GS and KS managed the central data collection. HM, SM, JSS, AG, HM-K, GG, HD, PC, GW, and NC critically revised the manuscript. All authors contributed to the article and approved the submitted version.

## FUNDING

This study is part of the EDCTP2 program supported by the European Union (grant numbers IP\_2009\_32040-AE-TBC, DRIA2014-311-ScreenTB, SRIA2015-1065-PredictTB). (URL: <https://www.edctp.org/>) These grants were awarded to GW.

The funders had no role in study design, data collection and analysis, decision to publish, or preparation of the manuscript. HM was funded by the South African Medical Research council through its Division of Research Capacity Development under the Internship Scholarship Program.

## REFERENCES

- World Health Organization. *Global tuberculosis report 2018* (2018). WHO. Available at: <http://www.who.int/iris/handle/10665/274453> (Accessed April 11, 2019).
- McNerney R, Maeurer M, Abubakar I, Marais B, McHugh TD, Ford N, et al. Tuberculosis diagnostics and biomarkers: needs, challenges, recent advances, and opportunities. *J Infect Dis* (2012) 205(Suppl 2):S147–58. doi: 10.1093/infdis/jir860
- Chegou NN, Hoek KGP, Kriel M, Warren RM, Victor TC, Walzl G. Tuberculosis assays: past, present and future. *Expert Rev Anti Infect Ther* (2011) 9:457–69. doi: 10.1586/eri.11.23
- Desikan P. Sputum smear microscopy in tuberculosis: is it still relevant? *Indian J Med Res* (2013) 137:442–4.
- Trébucq A, Enarson DA, Chiang CY, Van Deun A, Harries AD, Boillot F, et al. Xpert® MTB/RIF for national tuberculosis programmes in low-income countries: when, where and how? *Int J Tuberc Lung Dis Off J Int Union Tuberc Lung Dis* (2011) 15:1567–72. doi: 10.5588/ijtld.11.0392
- Miotto P, Bigoni S, Migliori GB, Matteelli A, Cirillo DM. Early tuberculosis treatment monitoring by Xpert(R) MTB/RIF. *Eur Respir J* (2012) 39:1269–71. doi: 10.1183/09031936.00124711
- Steingart KR, Schiller I, Horne DJ, Pai M, Boehme CC, Dendukuri N. Xpert® MTB/RIF assay for pulmonary tuberculosis and rifampicin resistance in adults. *Cochrane Database Syst Rev* (2014) 1:CD009593. doi: 10.1002/14651858.CD009593.pub3
- Marais BJ, Pai M. New approaches and emerging technologies in the diagnosis of childhood tuberculosis. *Paediatr Respir Rev* (2007) 8:124–33. doi: 10.1016/j.prrv.2007.04.002
- Corstjens PLAM, Tjon Kon Fat EM, de Dood CJ, van der Ploeg-van Schip JJ, Franken KLMC, Chegou NN, et al. Multi-center evaluation of a user-friendly lateral flow assay to determine IP-10 and CCL4 levels in blood of TB and non-TB cases in Africa. *Clin Biochem* (2016) 49:22–31. doi: 10.1016/j.clinbiochem.2015.08.013
- MacLean E, Broger T, Yerlikaya S, Fernandez-Carballo BL, Pai M, Denkiner CM. A systematic review of biomarkers to detect active tuberculosis. *Nat Microbiol* (2019) 4:748–58. doi: 10.1038/s41564-019-0380-2
- Nyendak MR, Lewinsohn DA, Lewinsohn DM. New diagnostic methods for tuberculosis. *Curr Opin Infect Dis* (2009) 22:174–82. doi: 10.1097/QCO.0b013e3283262fe9
- Goyal B, Kumar K, Gupta D, Agarwal R, Latawa R, Sheikh JA, et al. Utility of B-cell epitopes based peptides of RD1 and RD2 antigens for immunodiagnosis of pulmonary tuberculosis. *Diagn Microbiol Infect Dis* (2014) 78:391–7. doi: 10.1016/j.diagmicrobio.2013.12.018
- Jacobs R, Malherbe S, Loxton AG, Stanley K, van der Spuy G, Walzl G, et al. Identification of novel host biomarkers in plasma as candidates for the immunodiagnosis of tuberculosis disease and monitoring of tuberculosis treatment response. *Oncotarget* (2016) 7:57581–92. doi: 10.18632/oncotarget.11420
- Adams S, Ehrlich R, Baatjes R, Dendukuri N, Wang Z, Dheda K. Predictors of discordant latent tuberculosis infection test results amongst South African health care workers. *BMC Infect Dis* (2019) 19:131. doi: 10.1186/s12879-019-3745-5
- Chegou NN, Black GF, Loxton AG, Stanley K, Essone PN, Klein MR, et al. Potential of novel Mycobacterium tuberculosis infection phase-dependent antigens in the diagnosis of TB disease in a high burden setting. *BMC Infect Dis* (2012) 12:10. doi: 10.1186/1471-2334-12-10
- Essone PN, Chegou NN, Loxton AG, Stanley K, Kriel M, van der Spuy G, et al. Host cytokine responses induced after overnight stimulation with novel M. tuberculosis infection phase-dependent antigens show promise as diagnostic candidates for TB disease. *PloS One* (2014) 9:e102584. doi: 10.1371/journal.pone.0102584
- Goletti D, Vincenti D, Carrara S, Butera O, Bizzoni F, Bernardini G, et al. Selected RD1 peptides for active tuberculosis diagnosis: comparison of a gamma interferon whole-blood enzyme-linked immunosorbent assay and an enzyme-linked immunospot assay. *Clin Diagn Lab Immunol* (2005) 12:1311–6. doi: 10.1128/CDLI.12.11.1311-1316.2005
- Jacobs R, Maasdorp E, Malherbe S, Loxton AG, Stanley K, van der Spuy G, et al. Diagnostic Potential of Novel Salivary Host Biomarkers as Candidates for the Immunological Diagnosis of Tuberculosis Disease and Monitoring of Tuberculosis Treatment Response. *PloS One* (2016) 11:e0160546. doi: 10.1371/journal.pone.0160546
- Chegou NN, Detjen AK, Thiarl L, Walters E, Mandalakas AM, Hesselning AC, et al. Utility of host markers detected in Quantiferon supernatants for the diagnosis of tuberculosis in children in a high-burden setting. *PloS One* (2013) 8:e64226. doi: 10.1371/journal.pone.0064226
- Chegou NN, Sutherland JS, Malherbe S, Crampin AC, Corstjens PLAM, Geluk A, et al. Diagnostic performance of a seven-marker serum protein biosignature for the diagnosis of active TB disease in African primary healthcare clinic attendees with signs and symptoms suggestive of TB. *Thorax* (2016) 71:785–94. doi: 10.1136/thoraxjnl-2015-207999
- Phalane KG, Kriel M, Loxton AG, Menezes A, Stanley K, van der Spuy GD, et al. Differential expression of host biomarkers in saliva and serum samples from individuals with suspected pulmonary tuberculosis. *Mediators Inflammation* (2013) 2013:981984. doi: 10.1155/2013/981984
- Yoon C, Semitala FC, Atuhumuza E, Katende J, Mwebi S, Asege L, et al. Point-of-care C-reactive protein-based tuberculosis screening for people living with HIV: a diagnostic accuracy study. *Lancet Infect Dis* (2017) 17:1285–92. doi: 10.1016/S1473-3099(17)30488-7
- Wasserman S, Meintjes G. The diagnosis, management and prevention of HIV-associated tuberculosis. *South Afr Med J Suid Afr Tydskr Vir Geneeskde* (2014) 104:886–93. doi: 10.7196/SAMJ.9090
- Mbugi EV, Katala BZ, Streicher EM, Keyyu JD, Kendall SL, Dockrell HM, et al. Mapping of Mycobacterium tuberculosis Complex Genetic Diversity Profiles in Tanzania and Other African Countries. *PloS One* (2016) 11:e0154571. doi: 10.1371/journal.pone.0154571
- Harris PA, Taylor R, Thielke R, Payne J, Gonzalez N, Conde JG. Research electronic data capture (REDCap)—a metadata-driven methodology and workflow process for providing translational research informatics support. *J BioMed Inform* (2009) 42:377–81. doi: 10.1016/j.jbi.2008.08.010
- World Health Organization. *High priority target product profiles for new tuberculosis diagnostics: report of a consensus meeting* (2014). WHO. Available at: <http://www.who.int/iris/handle/10665/135617> (Accessed April 16, 2019).
- Theron G, Venter R, Calligaro G, Smith L, Limberis J, Meldau R, et al. Xpert MTB/RIF Results in Patients With Previous Tuberculosis: Can We Distinguish True From False Positive Results? *Clin Infect Dis Off Publ Infect Dis Soc Am* (2016) 62:995–1001. doi: 10.1093/cid/civ1223
- Verver S, Warren RM, Beyers N, Richardson M, van der Spuy GD, Borgdorff MW, et al. Rate of reinfection tuberculosis after successful treatment is higher than rate of new tuberculosis. *Am J Respir Crit Care Med* (2005) 171:1430–5. doi: 10.1164/rccm.200409-1200OC
- Geluk A, Corstjens P. CRP: tell-tale biomarker or common denominator? *Lancet Infect Dis* (2017) 17:1225–7. doi: 10.1016/S1473-3099(17)30472-3
- Aabye MG, Ruhwald M, Praygod G, Jeremiah K, Faurholt-Jepsen M, Faurholt-Jepsen D, et al. Potential of interferon- $\gamma$ -inducible protein 10 in improving tuberculosis diagnosis in HIV-infected patients. *Eur Respir J* (2010) 36:1488–90. doi: 10.1183/09031936.00039010
- Ruhwald M, Dominguez J, Latorre I, Losi M, Richeldi L, Pasticcini MB, et al. A multicentre evaluation of the accuracy and performance of IP-10 for the diagnosis of infection with M. tuberculosis. *Tuberc Edinb Scotl* (2011) 91:260–7. doi: 10.1016/j.tube.2011.01.001

## SUPPLEMENTARY MATERIAL

The Supplementary Material for this article can be found online at: <https://www.frontiersin.org/articles/10.3389/fimmu.2021.607827/full#supplementary-material>

**Conflict of Interest:** The authors declare that the research was conducted in the absence of any commercial or financial relationships that could be construed as a potential conflict of interest.

Copyright © 2021 Mutavhatsindi, van der Spuy, Malherbe, Sutherland, Geluk, Mayanja-Kizza, Crampin, Kassa, Howe, Mihret, Sheehama, Nepolo, Günther, Dockrell,

Corstjens, Stanley, Walzl, Chegou and the AE-TBC ScreenTB Consortia. This is an open-access article distributed under the terms of the Creative Commons Attribution License (CC BY). The use, distribution or reproduction in other forums is permitted, provided the original author(s) and the copyright owner(s) are credited and that the original publication in this journal is cited, in accordance with accepted academic practice. No use, distribution or reproduction is permitted which does not comply with these terms.





# Identification of Reduced Host Transcriptomic Signatures for Tuberculosis Disease and Digital PCR-Based Validation and Quantification

## OPEN ACCESS

### Edited by:

Malcolm Scott Duthie,  
HDT Biotech Corporation,  
United States

### Reviewed by:

Simon C. Mendelsohn,  
South African Tuberculosis Vaccine  
Initiative SATVI, South Africa  
Jiezuan Yang,  
Zhejiang University, China

### \*Correspondence:

Myrsini Kaforou  
m.kaforou@imperial.ac.uk

†These authors have contributed  
equally to this work

### Specialty section:

This article was submitted to  
Microbial Immunology,  
a section of the journal  
Frontiers in Immunology

**Received:** 02 December 2020

**Accepted:** 03 February 2021

**Published:** 02 March 2021

### Citation:

Gliddon HD, Kaforou M, Alikian M,  
Habgood-Coote D, Zhou C, Oni T,  
Anderson ST, Brent AJ, Crampin AC,  
Eley B, Heyderman R, Kern F,  
Langford PR, Ottenhoff THM,  
Hibberd ML, French N, Wright VJ,  
Dockrell HM, Coin LJ, Wilkinson RJ  
and Levin M (2021) Identification of  
Reduced Host Transcriptomic  
Signatures for Tuberculosis Disease  
and Digital PCR-Based Validation and  
Quantification.  
Front. Immunol. 12:637164.  
doi: 10.3389/fimmu.2021.637164

Harriet D. Gliddon<sup>1,2†</sup>, Myrsini Kaforou<sup>1\*†</sup>, Mary Alikian<sup>3,4</sup>, Dominic Habgood-Coote<sup>1</sup>,  
Chenxi Zhou<sup>5</sup>, Tolu Oni<sup>6</sup>, Suzanne T. Anderson<sup>7,8</sup>, Andrew J. Brent<sup>9,10</sup>,  
Amelia C. Crampin<sup>11,12,13</sup>, Brian Eley<sup>14,15</sup>, Robert Heyderman<sup>16</sup>, Florian Kern<sup>17,18</sup>,  
Paul R. Langford<sup>1</sup>, Tom H. M. Ottenhoff<sup>19</sup>, Martin L. Hibberd<sup>20</sup>, Neil French<sup>21,22</sup>,  
Victoria J. Wright<sup>1</sup>, Hazel M. Dockrell<sup>23</sup>, Lachlan J. Coin<sup>5</sup>, Robert J. Wilkinson<sup>24,25,26</sup> and  
Michael Levin<sup>1</sup> on behalf of the ILULU Consortium

<sup>1</sup> Section of Paediatrics, Department of Infectious Disease, Faculty of Medicine, Imperial College London, London, United Kingdom, <sup>2</sup> National Public Health Speciality Training Programme, South West, United Kingdom, <sup>3</sup> Imperial Molecular Pathology, Imperial Healthcare Trust, Hammersmith Hospital, London, United Kingdom, <sup>4</sup> Centre for Haematology, Faculty of Medicine, Imperial College London, London, United Kingdom, <sup>5</sup> Institute for Molecular Bioscience, University of Queensland, Brisbane, QLD, Australia, <sup>6</sup> School of Public Health and Family Medicine, Faculty of Health Sciences, University of Cape Town, Cape Town, South Africa, <sup>7</sup> Brighton and Sussex Medical School, Brighton, United Kingdom, <sup>8</sup> Brighton and Malawi Liverpool Wellcome Trust Unit, Blantyre, Malawi, <sup>9</sup> Nuffield Department of Medicine, University of Oxford, Oxford, United Kingdom, <sup>10</sup> Oxford University Hospitals National Health Service (NHS) Foundation Trust, Oxford, United Kingdom, <sup>11</sup> Malawi Epidemiology and Intervention Research Unit, Chilumba, Malawi, <sup>12</sup> London School of Hygiene & Tropical Medicine, London, United Kingdom, <sup>13</sup> Karonga Prevention Study, Chilumba, Malawi, <sup>14</sup> Paediatric Infectious Diseases Unit, Red Cross War Memorial Children's Hospital, Cape Town, South Africa, <sup>15</sup> Department of Paediatrics and Child Health, University of Cape Town, Cape Town, South Africa, <sup>16</sup> Division of Infection and Immunity, Faculty of Medical Sciences, University College London, London, United Kingdom, <sup>17</sup> Brighton and Sussex Medical School, University of Sussex, Brighton, United Kingdom, <sup>18</sup> Brighton and Sussex University Hospitals National Health Service (NHS) Trust, Brighton, United Kingdom, <sup>19</sup> Department of Infectious Diseases, Leiden University Medical Center, Leiden, Netherlands, <sup>20</sup> Faculty of Infectious and Tropical Diseases, London School of Hygiene and Tropical Medicine, London, United Kingdom, <sup>21</sup> Tropical and Infectious Disease Unit, Royal Liverpool and Broadgreen University Hospitals National Health Service (NHS) Trust, Liverpool, United Kingdom, <sup>22</sup> Centre for Global Vaccine Research, Institute of Infection & Global Health, University of Liverpool, Liverpool, United Kingdom, <sup>23</sup> Department of Immunology and Infection, and Tuberculosis (TB) Centre, London School of Hygiene and Tropical Medicine, London, United Kingdom, <sup>24</sup> The Francis Crick Institute, London, United Kingdom, <sup>25</sup> Department of Medicine, Imperial College London, London, United Kingdom, <sup>26</sup> Wellcome Centre for Infectious Diseases Research in Africa, Institute of Infectious Diseases and Molecular Medicine, University of Cape Town, Cape Town, South Africa

Recently, host whole blood gene expression signatures have been identified for diagnosis of tuberculosis (TB). Absolute quantification of the concentrations of signature transcripts in blood have not been reported, but would facilitate diagnostic test development. To identify minimal transcript signatures, we applied a transcript selection procedure to microarray data from African adults comprising 536 patients with TB, other diseases (OD) and latent TB (LTBI), divided into training and test sets. Signatures were further investigated using reverse transcriptase (RT)—digital PCR (dPCR). A four-transcript signature (*GBP6*, *TMCC1*, *PRDM1*, and *ARG1*) measured using RT-dPCR distinguished TB patients from those with OD (area under the curve (AUC) 93.8% (CI<sub>95%</sub> 82.2–100%).

A three-transcript signature (*FCGR1A*, *ZNF296*, and *C1QB*) differentiated TB from LTBI (AUC 97.3%,  $CI_{95\%}$ : 93.3–100%), regardless of HIV. These signatures have been validated across platforms and across samples offering strong, quantitative support for their use as diagnostic biomarkers for TB.

**Keywords:** tuberculosis, transcriptomics, dPCR, gene expression, signatures, biomarkers

## INTRODUCTION

Despite over a century's research effort to identify new diagnostic tools we still lack diagnostic tests for tuberculosis (TB) that are sensitive, affordable and robust. The majority of TB diagnostics are based on identifying the pathogen in sputum, by microscopy, culture or PCR. However, current methods fail to identify the pathogen in a significant proportion of cases, either due to inadequacies in sputum collection, paucibacillary disease, HIV infection or in patients with extrapulmonary forms (1). As a result the World Health Organization (WHO) estimates that approximately three in every ten TB cases go unreported or undiagnosed (2). Given the problems associated with using sputum as a clinical sample, the WHO and the Foundation for Innovative New Diagnostics published a target product profile (TPP) for a non-sputum biomarker test in 2014 (3). This specified the seven proposed key characteristics of a rapid biomarker-based non-sputum-based test for detecting TB including minimal and optimal sensitivity and specificity of such a test and also discussed sample accessibility, time to result, maintenance and cost.

Recent years have seen a rise in the emergence of host-response-based infectious disease diagnostics. These detect evidence of a host immune response to an infection, which is advantageous when there are very low numbers of the pathogen in the body or when pathogens colonize inaccessible sites. A number of disease specific "omic" signatures have been identified, facilitated by advances in technology to analyse the genome, transcriptome, epigenome, lipidome, metabolome, and proteome in a high-throughput and quantitative manner (4). As well as improving our understanding of the pathogenesis of a range of infectious diseases, these signatures have the potential to be used as diagnostic biomarkers.

Gene expression studies have significantly enhanced our knowledge of the roles of various components of the immune system in TB disease (5–7). A number of gene expression signatures have been published that can distinguish TB from healthy controls (HCs) and correlate with disease progression (8–10). These could serve as important indicators of disease progression from latent TB infection (LTBI) to TB, and therefore guide antibiotic selection (11).

The most clinically important need is for biomarkers to distinguish TB from the range of other conditions with similar clinical presentation. TB shares symptoms and clinical signs with many other diseases (OD), including a wide range of infectious, inflammatory and malignant conditions, such as pneumonia or other HIV-associated opportunistic infections. Distinguishing between TB and OD is particularly important in patients living

with HIV, because extrapulmonary TB is more common in these patients (12, 13) such that most sputum-based tests are poorly sensitive, and HIV-associated malignancies or opportunistic infections can have similar clinical presentations. However, the majority of TB gene expression studies published to date have compared TB cohorts to HCs, LTBI or patients with OD, mostly in the absence of HIV infection.

A previous study Kafroui et al. (14) addressed these issues by studying patients with symptoms suggestive of TB in Malawi and South Africa (including both HIV-infected and uninfected persons) and classifying them as TB, LTBI or OD. Blood gene expression signatures were identified using genome-wide microarrays that distinguished TB from OD and LTBI (14). A 44-transcript signature was found to distinguish TB from OD with sensitivity of 93% ( $CI_{95\%}$  83–100) and specificity of 88% ( $CI_{95\%}$  74–97). A 27-transcript signature distinguished TB from LTBI with sensitivity of 95% ( $CI_{95\%}$  87–100) and specificity of 90% ( $CI_{95\%}$  80–97). These signatures showed only slightly reduced accuracy in HIV-coinfected individuals (14).

Further reduction in the number of transcripts comprising these gene expression signatures makes their use as diagnostic markers more feasible for clinical translation, particularly at the point-of-care and in resource-limited settings (15). This has been the subject of significant research effort and a number of bioinformatics approaches have been employed. Sweeney et al. identified a three-gene signature for TB, comprised of *GBP5*, *DUSP3*, and *KLF2* in a meta-analysis of publicly available gene expression microarray data (16). Maertzdorf et al. used random forest models and confidence interval decision trees to identify a four-transcript signature comprising *GBP1*, *IFITM3*, *P2RY14*, and *ID3*, that distinguished between TB and HC, regardless of HIV infection status (17). Other recent studies identified minimal gene expression signatures in populations from high-endemic countries that predict progression from latent infection to active TB disease with accuracy, excluding cases with HIV co-infection (18, 19).

Quantification of individual TB gene expression signature transcripts would be useful to determine the limits of detection required for diagnostic tests based on these signatures. The established method of choice for performing absolute quantification of nucleic acids is quantitative PCR (qPCR), where amplicon generation is measured in real time and related back to the starting concentration of template. While RNA-seq has emerged as a powerful technique for investigating RNA species within a given sample, it can only provide *relative* quantification of RNA species (20). In recent years, digital PCR (dPCR) has emerged as a promising alternative to qPCR. dPCR is a

useful method for quickly and efficiently providing absolute quantification of individual mRNA species and has been shown to be more reproducible and less prone to inhibition than qPCR (21, 22). The high precision offered by dPCR makes it ideally suited to the detection of rare point mutations and the accurate detection of low microbial loads, among other applications (23–25).

We hypothesized that we could further reduce the number of transcripts comprising the previously reported signatures distinguishing TB from OD and LTBI Kaforou et al. (14) using feature selection algorithms applied to microarray data, and that reverse transcription-dPCR (RT-dPCR) could be used to quantify the concentrations of individual gene transcripts in purified RNA from whole blood. We postulated that this cross-sample, cross-platform (microarray and RT-dPCR), cross-population study will aid the advance of the TB transcriptomics field toward developing and establishing the use of host transcriptomics for TB diagnosis.

## MATERIALS AND METHODS

### Ethics Statement

The study was approved by the Human Research Ethics Committee of the University of Cape Town, South Africa (HREC012/2007), the National Health Sciences Research Committee, Malawi (NHSRC/447), and the Ethics Committee of the London School of Hygiene and Tropical Medicine (5212). Written information was provided by trained local health workers in local languages and all patients provided written consent.

### Derivation of Reduced Signatures Using Microarray Data

The patient cohorts recruited in South Africa and Malawi for the original prospective cohort microarray study were fully described previously, including the diagnostic procedures and patient assignment as TB, OD or LTBI (14). In addition, the whole-blood genome-wide expression measured in this cohort was reported (14), and made publicly available at NCBI's Gene Expression Omnibus, accessible through GEO Series accession number GSE37250. The microarray data was pre-processed as described in (14). Data from the processed and normalized expression set were split randomly into training and test set (80–20 split). FS-PLS (26, 27) was employed in order to generate smaller gene expression signatures. FS-PLS is an iterative forward selection algorithm which at each step selects the most strongly associated variable after projecting the data matrix into a space orthogonal to all the variables previously selected. It combines the dimensionality reduction strength of PLS and the model simplicity and interpretability of FS regression. The classificatory performance of the signatures was evaluated in the test set using the disease risk score method (DRS), as in (14). The derived signatures were further validated in two publicly available gene expression studies (5, 28) (**Supplementary Material**). The FS-PLS code is available for download and use (27).

### Power Calculations for RT-dPCR Study Size

For the retrospective RT-dPCR study, as the discrimination using the DRS had a binary outcome and followed a binomial distribution, in order to achieve a statistic significance level of 0.05, and assuming the dPCR sensitivity to be at least 75% for patient classification, we used 40 samples for each comparison (TB vs. OD and TB vs. LTBI) to assess the performance of each signature, with equal numbers of samples for each group ( $n_{TB} = 20$ ,  $n_{OD} = 20$ ,  $n_{LTBI} = 20$ ) (**Supplementary Tables 1, 2**). Samples were chosen at random from a microarray test patient cohort for TB vs. OD, stratified for HIV status and country of origin, which had not been used to derive the signature. An additional 10 LTBI HIV-infected and 10 LTBI HIV-uninfected samples from the test microarray cohort were analyzed.

### Patient Characteristics for RNA Samples Used in the RT-dPCR

Patient recruitment was conducted in two highly contrasting study sites in Cape Town, South Africa and Karonga District, Northern Malawi. Patients were classified as having active TB disease only upon culture confirmation. Patients were deemed to have OD if they presented with symptoms that might suggest the possibility of TB disease, but for whom an alternative diagnosis was found and TB treatment was not administered. These patients were followed up 26 weeks post diagnosis to confirm they remained TB-free. Healthy LTBI controls were classified according to the results of interferon-gamma release assay (IGRA) and tuberculin skin test (TST) investigations (14).

### RNA Purification From Whole Blood and Storage

2.5 ml whole blood was collected at the time of recruitment (before or within 24 h of commencing TB treatment in suspected patients) in PAXgene blood RNA tubes (PreAnalytiX), frozen within 3 h of collection, and later extracted using PAXgene blood RNA kits (PreAnalytiX). RNA was shipped frozen and stored at  $-80^{\circ}\text{C}$ .

### Assessment of RNA Purity and Integrity

Before proceeding with reverse transcription, the RNA quality of the samples was assessed using an Agilent 2100 Bioanalyzer (Agilent Technologies, Santa Clara, CA, USA).

### Reverse Transcription of Purified RNA From Whole Blood

RNA concentration was measured using a NanoDrop 2000c (Thermo Scientific) and 500 ng was used for the reverse transcription reaction in a total volume of 10  $\mu\text{L}$  nuclease-free  $\text{H}_2\text{O}$ . RT was performed in one batch using the High-Capacity cDNA RT Kit (Applied Biosystems) according to the manufacturer's instructions. The cycle was  $25^{\circ}\text{C}$  for 10 min,  $37^{\circ}\text{C}$  for 120 min,  $85^{\circ}\text{C}$  for 5 min, followed by a hold at  $4^{\circ}\text{C}$ . cDNA samples were stored at  $-20^{\circ}\text{C}$  for fewer than 6 months before use.

## dPCR Using the QuantStudio™ Platform

Up to 5  $\mu\text{L}$  of RT product was added to 7.5  $\mu\text{L}$  QuantStudio 3D Digital PCR Master Mix (Thermo Fisher Scientific), 0.75  $\mu\text{L}$  of TaqMan Assay (20X) (Thermo Fisher Scientific) (see **Supplementary Table 3**) and the volume made up to 15  $\mu\text{L}$  using nuclease-free  $\text{H}_2\text{O}$  (**Supplementary Figure 3**). All TaqMan Assays were inventoried and none were custom-made. At least one no template control was used for each TaqMan assay on each PCR run. The reaction mix was applied to each QuantStudio 3D Digital PCR 20K Chip (Applied Biosystems) according to the manufacturer's instructions. The dPCR was run on a GeneAmp PCR System 9700 (Applied Biosystems) with a cycle of 10 min at  $96^\circ\text{C}$ , followed by 39 cycles of  $60^\circ\text{C}$  for 60 s and  $98^\circ\text{C}$  for 30 s, followed by 2 min at  $60^\circ\text{C}$  before holding at  $10^\circ\text{C}$ . Chips were read, and absolute quantification (copies per  $\mu\text{L}$ ) determined using the QuantStudio 3D Digital PCR Instrument (Thermo Fisher Scientific).

## Data Analysis RT-dPCR

Data was exported and analyzed using QuantStudio 3D AnalysisSuite Cloud Software Version 3.0.3 (Thermo Fisher Scientific). The quantification algorithm selected was Poisson. The software assesses whether the data on a chip is reliable based upon loading, signal, and noise characteristics and displays quality indicators for each chip. Any chip that gave a precision value of  $>10\%$  was deemed to have failed and was repeated. Similarly, if the negative and positive wells did not separate into distinct populations, the sample and probe combination was repeated. This failure to separate into two populations could be caused by the chips leaking, evaporation or a loading issue of the sample onto the chip. This methodology is further explained in the supporting information (**Supplementary Figure 1**) and all dilutions, FAM call thresholds and lambda values are given in

**Supplementary Table 4**, in accordance with the MIQE guidelines (21). The output given by the QuantStudio software is in copies/ $\mu\text{L}$ . This value was then corrected according to the dilution of cDNA used for the dPCR in order to determine the absolute concentration of a given transcript in purified RNA samples (**Supplementary Figure 3**). RT-dPCR derived copies per  $\mu\text{L}$  values are reported. The DRS method was used to classify patients on the basis of  $\log_2$  (copies per  $\mu\text{L}$ ).

## Statistical Analysis

The datasets were analyzed in "R" Language and Environment for Statistical Computing version 3.4.1 (29, 30). In order to evaluate the performance of the DRS as a binary classifier, the area under the curve (AUC) for a receiver operating characteristic (ROC) curve was calculated, as well as the sensitivity and specificity using pROC (29). The calculation of the confidence intervals (CI) for the AUC was based on the DeLong method (31), an asymptotically exact method to evaluate the uncertainty of an AUC, except for the one case that  $\text{AUC} = 100\%$ , where we used a smoothed ROC followed by DeLong for the calculation of the lower 95% bound. For each data set we report the point estimate for sensitivity as the closest value  $>90\%$  (as specified in the WHO TPP) and the corresponding specificity.

## RESULTS

### Discovery and Validation of Small Signatures From Microarray Data Using FS-PLS and DRS

In order to derive reduced gene expression signatures with diagnostic potential, the variable selection method, FS-PLS, was applied to the previously published microarray data (80% training set) ( $n = 293$  for TB vs. OD,  $n = 285$  for TB vs. LTBI

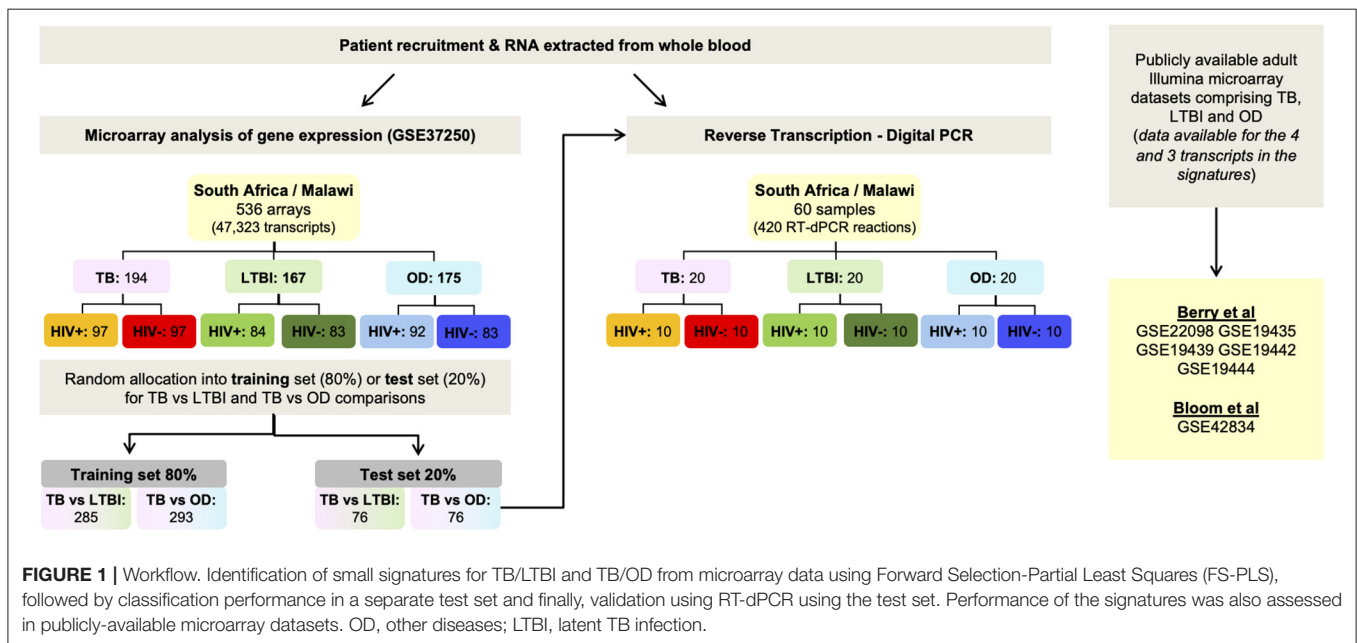




**TABLE 1 |** Forward Selection-Partial Least Squares (FS-PLS) signatures for (A) TB/LTBI and (B) TB/OD.

Gene symbol and name*	Illumina Probe ID	Direction of regulation*
<b>A</b>		
<i>GBP6</i> Guanylate Binding Protein Family Member 6	ILMN_1756953	Up
<i>TMCC1</i> Transmembrane and Coiled-Coil Domain Family 1	ILMN_1677963	Down
<i>PRDM1</i> PRV/SET Domain 1	ILMN_2294784	Up
<i>ARG1</i> Arginase 1	ILMN_1812281	Down
*In patients with TB compared to OD.		
Gene symbol and name*	Illumina Probe ID	Direction of regulation*
<b>B</b>		
<i>FCGR1A</i> Fc Fragment of IgG Receptor 1a	ILMN_2176063	Up
<i>ZNF296</i> Zinc Finger Protein 296	ILMN_1693242	Down
<i>C1QB</i> Complement C1q B Chain	ILMN_1796409	Up

\*In patients with TB compared to LTBI.

These were taken forward for further characterization and validation using dPCR, and subsequently development as diagnostic biomarkers for TB. Gene names are according to HUGO Gene Nomenclature Committee. LTBI, Latent TB infection; OD, other diseases.

including HIV co-infected cases), tested in the test set ( $n = 76$  TB vs. OD and TB vs. LTBI including HIV co-infected cases), and further validated in two other publicly available studies (Figure 1) (5, 28). Using the FSPLS method we identified a signature comprising four transcripts for TB/OD in the training set and a signature comprising three transcripts for TB/LTBI; the signatures are detailed in Tables 1A,B, respectively. The TB/OD FS-PLS signature using the DRS had an AUC of 93.9% CI<sub>95%</sub> (88.4–99.4%) in the 20% test set, which had not been used for discovery (Figure 2), sensitivity of 90.5 CI<sub>95%</sub> (77.4–97.3) and specificity of 82.4% CI<sub>95%</sub> (65.5–93.2), with confidence intervals overlapping with the previously identified the 44-transcript elastic net signature for TB/OD (14). The TB/LTBI FS-PLS signature using the DRS had an AUC of 95.4% (CI<sub>95%</sub> 91.2–99.6%) in the 20% test set, which had not been used for discovery, sensitivity of 91.9 CI<sub>95%</sub> (78.1–98.3) and specificity of 84.6% CI<sub>95%</sub> (69.5–94.1), with confidence intervals overlapping with the previously reported 27-transcript elastic net signature (14) (Figure 2, Supplementary Table 5).

## Validation of the FS-PLS TB/OD and TB/LTBI Signatures in External Datasets

In order to further validate the performance of the DRS based on the TB/OD four transcript and TB/LTBI three transcript signature, we employed the whole blood expression datasets

of Berry et al. (5) and Bloom et al. (28) (GEO: GSE19491, GSE42834) as validation cohorts. The cohorts comprised HIV-uninfected individuals; TB, LTBI, and OD including pneumonia, lung cancer, Still's disease, adult and pediatric Systemic Lupus Erythematosus (ASLE, PSLE), *Staphylococcus*, and *Streptococcus* (Table 2). The TB/OD four transcript signature distinguished TB from all other diseases with an AUC ranging from 88 to 98%, with the exception of sarcoidosis. The TB/LTBI three transcript signature had an AUC of over 91% in the datasets tested.

## Clinical Characteristics of Cohorts Used in RT-dPCR Analysis

The clinical characteristics of each disease cohort used for RT-dPCR analysis with the TB/LTBI signature genes and the TB/OD signature genes are shown in Tables 3A,B, respectively. The mean age, body mass index (BMI) and TST induration are shown. The clinical diagnoses of the OD cohort are listed in Supplementary Table 2. The range of diagnoses among this cohort is representative of the variety of conditions that have similar clinical presentations to TB.

## Absolute Quantification by RT-dPCR of Genes Comprising the Four-Transcript FS-PLS Signature for TB/OD (Cross-Platform, Cross-Sample Validation)

Figure 3A shows the concentration (in copies per  $\mu\text{L}$ ) of each of the transcripts comprising the FS-PLS signature for TB/OD in purified RNA from whole blood, as determined by RT-dPCR. *GBP6* transcript levels are higher in TB patients, compared to those with OD. The opposite case is observed for the *ARG1* transcript, which is more abundant in patients with OD compared to TB. For *TMCC1* and *PRDM1*, there is more overlap between concentration values of TB and OD patients. All four of these genes were identified in the 44 gene expression signature for TB/OD, and although *GBP6* is induced by the interferon (IFN) cytokine family, its levels were significantly higher in active TB cases when compared to confirmed viral and bacterial infections the GSE73464 (32) and GSE39941 (33) datasets (Supplementary Figure 2). The original concentration (in copies per  $\mu\text{L}$ ) for the samples stratified by HIV status is shown in Supplementary Figure 4.

## Absolute Quantification by RT-dPCR of Genes Comprising the Three-Transcript FS-PLS Signature for TB/LTBI

The concentrations (in copies per  $\mu\text{L}$ ) of each of the transcripts comprising the FS-PLS signature for TB/LTBI in purified RNA from whole blood, as determined by RT-dPCR, are shown in Figure 3B. The genes *FCGR1A* and *C1QB* are more abundant in patients with TB compared to LTBI, whereas *ZNF296* is downregulated. All three genes were identified in the original 27 TB/LTBI signature (14). Supplementary Figure 4 shows the concentration (in copies per  $\mu\text{L}$ ) for the samples stratified by HIV status.

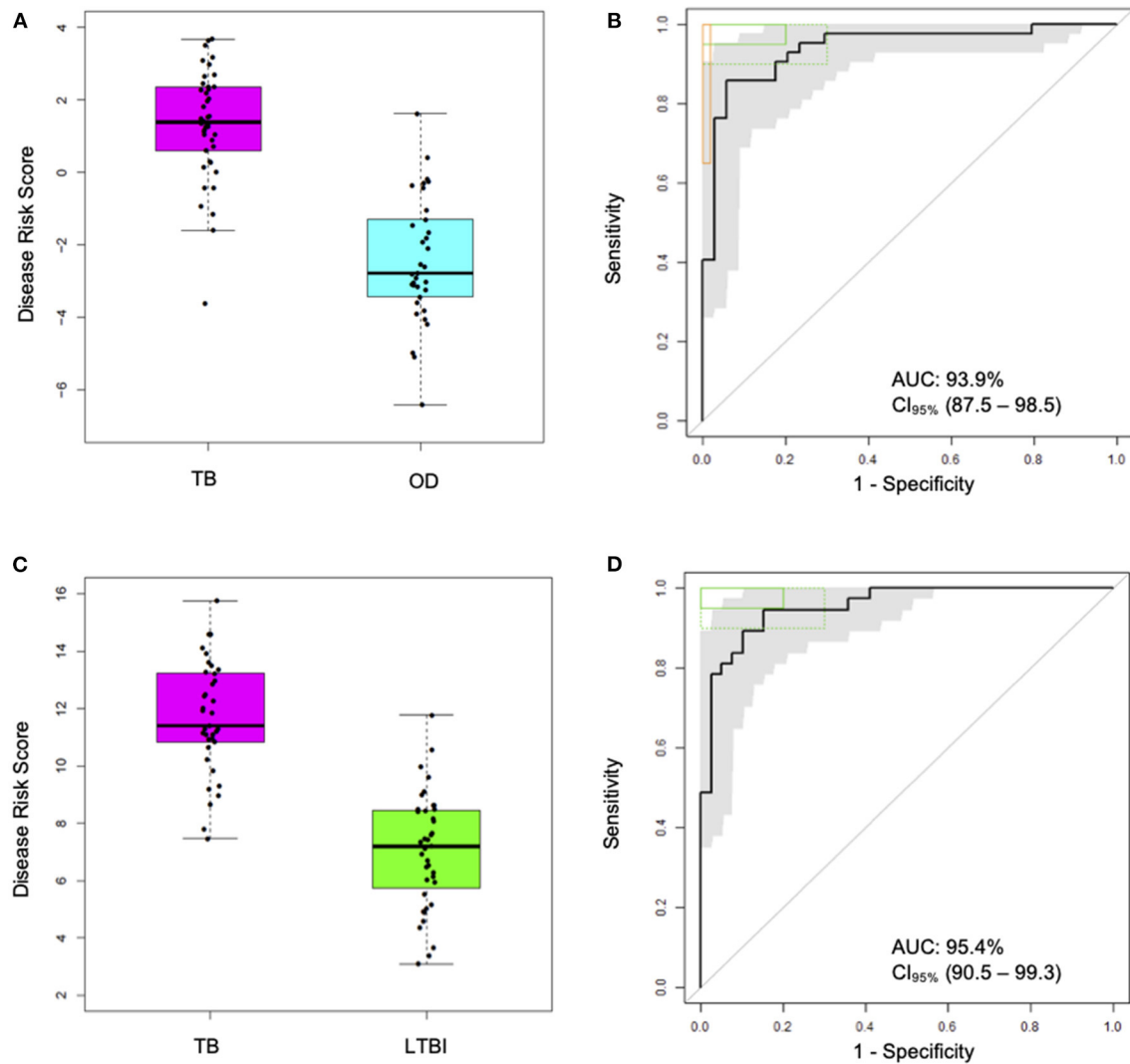


**FIGURE 2 |** Classification performance of the FS-PLS-derived four-transcript signatures for TB/OD and three-transcript for TB/LTBI using microarray gene expression data (only test dataset shown). **(A)** Box plots of DRS and **(B)** receiver operating characteristic (ROC) curve based on the TB/OD FS-PLS signature applied to the combined HIV  $\pm$  TB and OD SA/Malawi cohorts (TB DRS vs. OD DRS Mann–Whitney  $p = 1.33 \times 10^{-13}$ ). **(C)** Box plots of DRS and **(D)** ROC curve based on the TB/LTBI FS-PLS signature applied to the combined HIV  $\pm$  TB and LTBI SA/Malawi cohorts (TB DRS vs. LTBI DRS Mann–Whitney  $p = 4.92 \times 10^{-15}$ ). Gray shaded areas represent the 95% CIs of the ROC curve sensitivities, plotted at 0.5% specificity intervals. ROC curves **(B,D)** have been benchmarked against target criteria for a tuberculosis triage test (green boxes): Minimum criteria (90% sensitivity, 70% specificity) are indicated by the dashed green boxes and optimum criteria (95% sensitivity, 80% specificity) are indicated by the green solid boxes. The TB vs. OD ROC curve **(B)** has been benchmarked against the minimum criteria for a confirmatory test (65% sensitivity, 98% specificity) which are indicated by the orange box. AUC, area under the curve; OD, other diseases; LTBI, latent TB infection.

## Correlation of the Microarray Intensity Values and the RT-dPCR Concentration Values

The expression profiles of the seven genes comprising the two signatures described above were compared between the two platforms, at individual sample level. High correlations were observed between the gene expression profiles generated by the two platforms for most of the genes (Figure 4). However, differences in expression profiles were also apparent between the two platforms, with a number of samples/genes exhibiting relatively higher expression values in either platform. Pearson correlation and  $p$ -values for all the genes can be

found in **Supplementary Table 6**. The Illumina microarray probes and the RT-dPCR TaqMan assays are provided in **Supplementary Table 3**.

## Performance of the Four-Transcript FS-PLS Signature for TB/OD Using RT-dPCR Analysis Disease Classification in HIV-Infected and HIV-Uninfected Individuals

The performance of the FS-PLS signature for TB/OD was evaluated by applying the DRS to the concentration values that

**TABLE 2 |** Performance of FS-PLS signatures in classifying TB and other diseases (OD), or TB and latent TB infection (LTBI), in other publicly available microarray datasets.

Comparison	Cohort	N	AUC (95% CI)
TB vs. OD	Berry (Overall)	213	92.8 (87.6–97.9)
TB vs. OD	Berry (Still's disease)	85	94.7 (88.9–100)
(non-pulmonary)	Berry (adult systemic lupus erythematosus; ASLE)	82	94.6 (89.0–100)
	Berry (pediatric systemic lupus erythematosus; PSLE)	136	91.9 (86.0–97.8)
	Berry ( <i>Staphylococcus</i> )	94	88.3 (79.6–96.9)
TB vs. OD	Berry ( <i>Streptococcus</i> )	66	98.3 (95.2–100)
	Bloom (Lung cancer)	51	94.6 (87.2–100)
	Bloom (Pneumonia)	49	90.4 (75.0–100)
	Bloom (Sarcoidosis)	96	63.4 (54.6–74.0)
TB vs. LTBI	Berry (South Africa)	51	98.9 (96.8–100)
	Berry (UK training + test)	72	90.6 (83.2–98.1)

**TABLE 3 |** Clinical characteristics of patients used for the RT-dPCR analysis of the (A) TB/OD signature and (B) the TB/LTBI signature.

Group	TB HIV+	TB HIV–	OD HIV+	OD HIV–
<b>A</b>				
Number	10	10	10	10
Age (years) mean (range)	32.3 (26.3–48.0)	31.9 (18.1–60.7)	34.3 (24.9–53.1)	41.1 (19.1–68.1)
Sex (male, %)	50	50	20	30
BMI (kg/m <sup>2</sup> ) mean (range)	19.5 (16.8–22.9)	19.4 (15.3–24.2) <sup>a</sup>	24.3 (18.0–39.3)	22.1 (17.2–33.0) <sup>b</sup>
CD4 count (mm <sup>3</sup> ) mean (range)	222.5 (29.2–646.0)	NA	252.8 (19.3–838.0)	NA
Anti-retroviral therapy (%)	0	NA	50	NA

<sup>a</sup>One missing value; <sup>b</sup>Three missing values.

Group	TB HIV+	TB HIV–	LTBI HIV+	LTBI HIV–
<b>B</b>				
Number	10	10	10	10
Age (years) mean (range)	32.6 (24.2–47.5)	39.7 (290.0–59.8)	36.7 (22.5–53.2) <sup>a</sup>	31.9 (18.9–59.2)
Sex (male, %)	60	50	20	40
BMI (kg/m <sup>2</sup> ) mean (range)	20.3 (16.8–25.1)	20.4 (14.3–29.4)	21.6 (16.5–25.8) <sup>a</sup>	21.9 (17.7–29.4)
CD4 count (mm <sup>3</sup> ) mean (range)	226.0 (29.2–345.0)	NA	466.1 (227.0–958.0) <sup>b</sup>	NA
Anti-retroviral therapy (%)	0	NA	0	NA
TST induration (mm) mean (range)	ND	ND	22.9 (4.0–50.0) <sup>a</sup>	16.6 (10.0–21.0)

<sup>a</sup>One missing value; <sup>b</sup>Two missing values.

BMI, body mass index; NA, not applicable; ND, not done; TST, tuberculin skin test; LTBI, Latent TB infection; OD, other diseases.

were derived from the RT-dPCR data. **Figures 5A–D** shows the cross-platform (from microarray to RT-dPCR) and cross-sample (from the training set to the test set) performance of the four gene signature DRS in TB vs. OD. In the combined SA/Malawi HIV-infected and -uninfected cohort, the signature had an AUC of 93.8% (CI<sub>95%</sub>: 82.2–100), a sensitivity of 95.0% (CI<sub>95%</sub>: 85.0–100), and a specificity of 85.0% (CI<sub>95%</sub>: 75.0–100) (**Figures 5A,B, Supplementary Table 6**). The mean accuracy of classification varied with HIV status, although there was extensive overlap in the 95% confidence intervals. The four gene TB/OD signature had an AUC of 91.0% (CI<sub>95%</sub>: 73.3–100%) among the HIV-uninfected individuals, and an AUC of 93.0% (CI<sub>95%</sub>: 82.4–100%) for the HIV-infected cohort (**Figures 5C,D**).

## Performance of the Four-Transcript FS-PLS Signature for TB/LTBI Using dPCR Analysis

The performance of the FS-PLS signature for TB/LTBI was evaluated by applying the DRS to the absolute log<sub>2</sub> transformed concentration values that were derived from the RT-dPCR data. **Figures 5E–H** show the cross-platform and cross-sample performance of the three gene signature DRS in TB vs. LTBI. In the combined SA/Malawi HIV-infected and uninfected cohort the signature had an AUC of 97.3% (CI<sub>95%</sub>: 93.3–100%), sensitivity of 95.0% (CI<sub>95%</sub>: 85.0–100), and specificity of 85.0% (CI<sub>95%</sub>: 75.0–100) (**Figures 5E,F**).

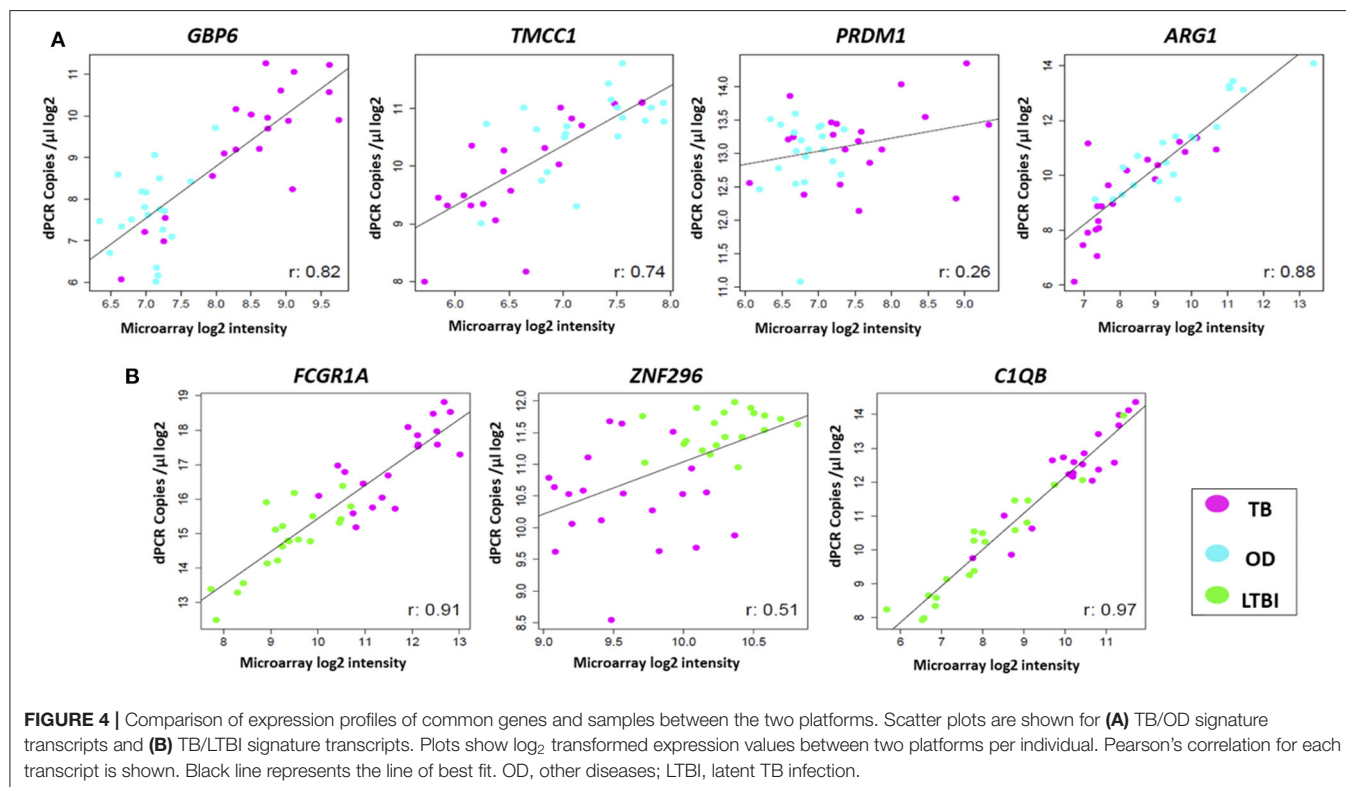
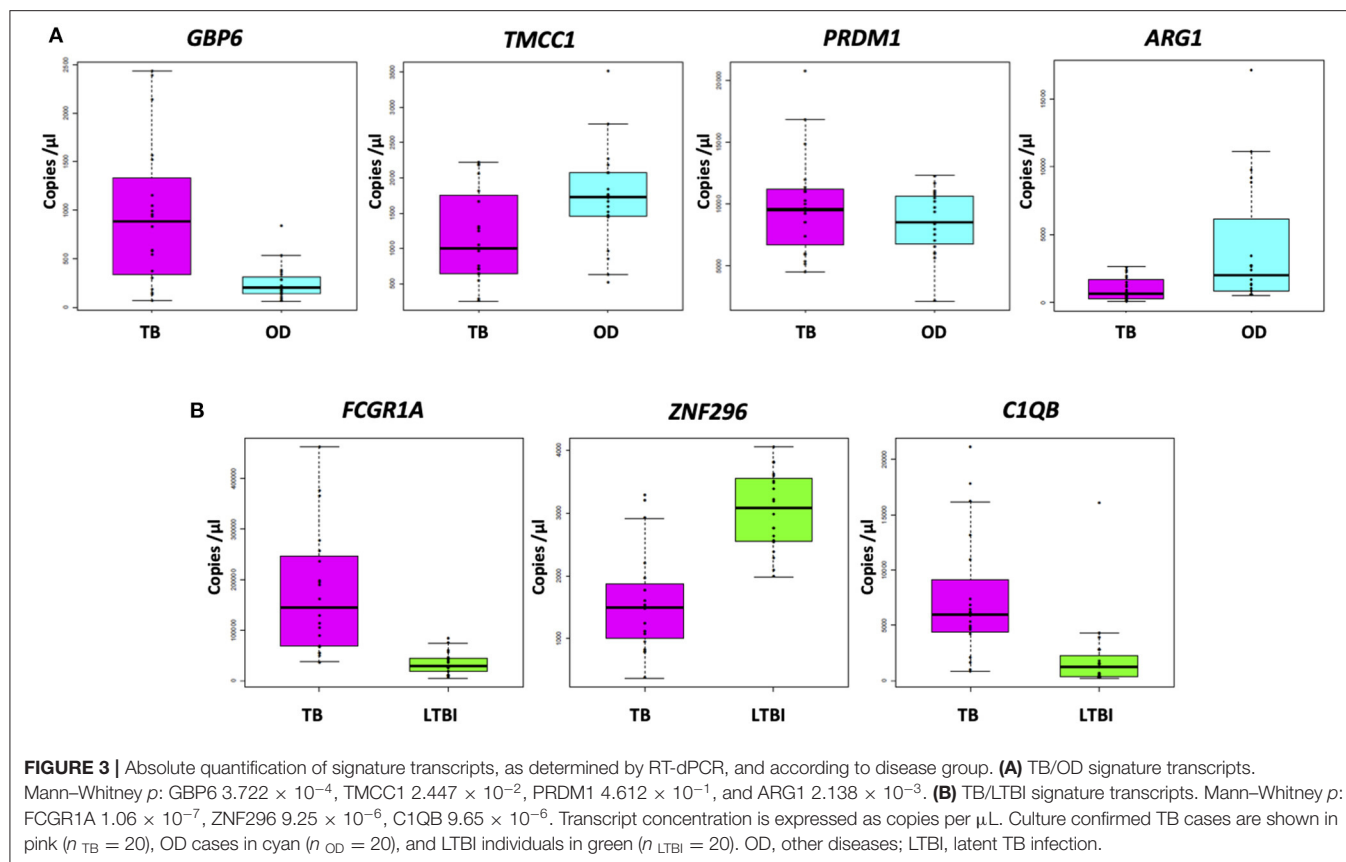
As observed previously, the mean accuracy of classification varied with HIV status, although again, there was extensive overlap in the 95% confidence intervals. The four gene TB/LTBI signature had an AUC of 100% (CI<sub>95%</sub>: 94.2–100%) among the HIV-uninfected individuals and an AUC of 94.0% (CI<sub>95%</sub>: 84.1–100%) among HIV-infected cohort (**Figures 5G,H, Supplementary Table 6**).

## Contribution of Individual Genes to Disease Classification

Finally, we examined the contribution of each gene to the AUC for the classification of the TB/OD and TB/LTBI patients in the microarray and RT-dPCR datasets in a stepwise manner. By definition, in the FS-PLS algorithm, each gene needs to significantly increase the AUC to be included in the signature in the training set (**Supplementary Figure 5**). The sequential addition of all genes is increasing the AUC in the microarray test and RT-dPCR for the TB/OD comparison, while the inclusion of C1QB in the TB/LTBI signature is not increasing the AUC in the microarray test and RT-dPCR sets, in contrast to the microarray training dataset. As the confidence intervals are largely overlapping, further work is needed to explore the potential of further minimizing the TB/LTBI signature.

## DISCUSSION

In this study, we report a four-gene signature discriminating TB from OD (TB/OD) and a three-gene signature discriminating TB from LTBI (TB/LTBI). These signatures were identified by applying an advanced methodology, FS-PLS, furthering previous





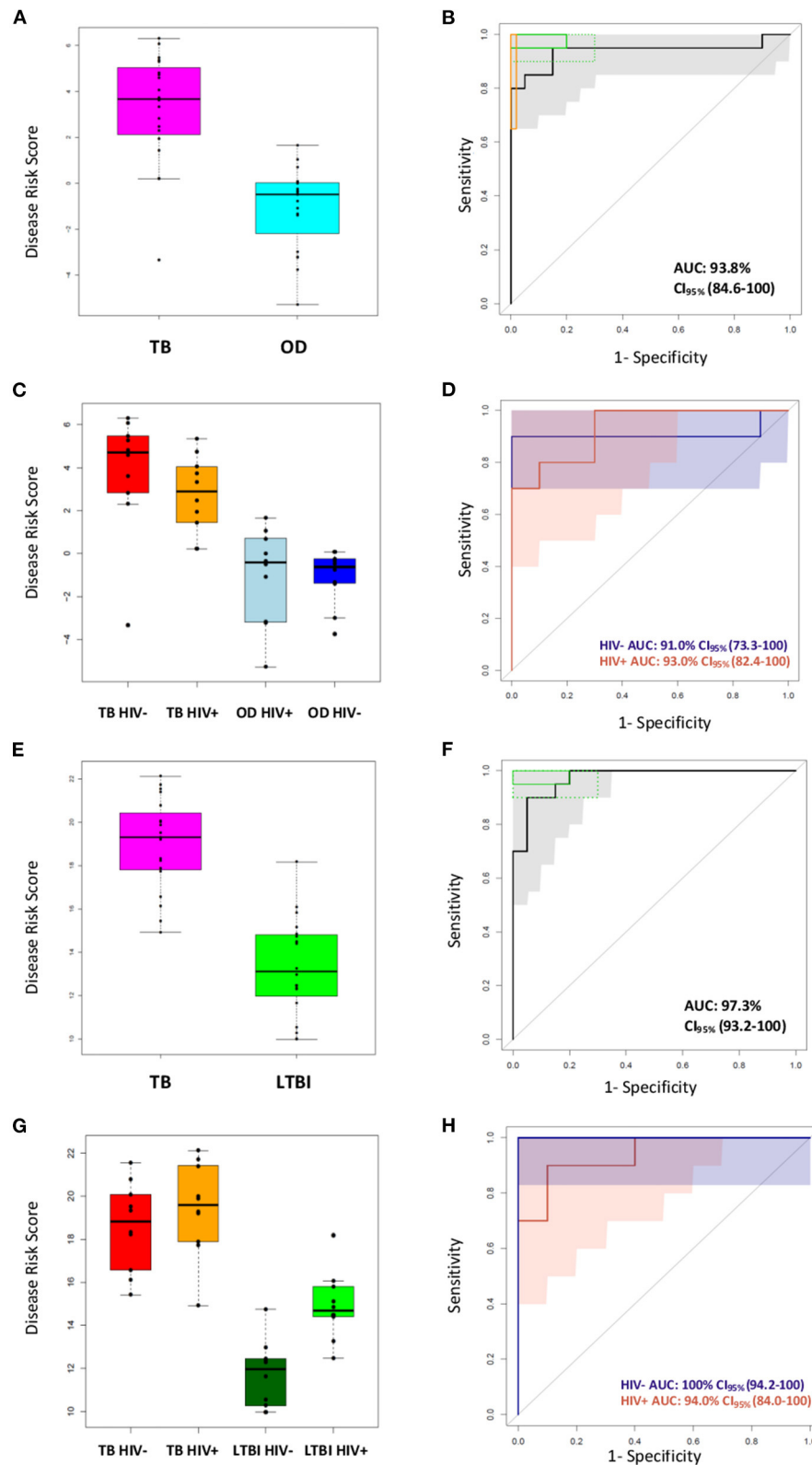


**FIGURE 5 |** Classification of the SA/Malawi cohorts using the DRS based on the FS-PLS signature RT-dPCR results. **(A)** Box plots of disease risk score (DRS) (TB vs. OD DRS  $p = 1.34 \times 10^{-7}$ ) and **(B)** Receiver operating characteristic (ROC) curve based on the TB/OD FS-PLS signature applied to the combined TB and OD cohorts ( $n_{TB} = 20$ ,  $n_{OD} = 20$ ). Gray shaded areas represent the 95% CIs of the ROC curve sensitivities, plotted at 0.5% specificity intervals. The ROC curve has been (Continued)

**FIGURE 5 |** benchmarked against target criteria for a tuberculosis triage test: Minimum criteria (90% sensitivity, 70% specificity) are indicated by the dashed green boxes and optimum criteria (95% sensitivity, 80% specificity) are indicated by the green solid boxes; and the minimum criteria for a confirmatory test (65% sensitivity, 98% specificity) which are indicated by the orange box. **(C)** Box plots of DRS (TB vs. OD DRS HIV uninfected  $p = 1.05 \times 10^{-3}$ , HIV infected  $p = 4.871 \times 10^{-4}$ ), and **(D)** ROC curve for TB/OD signature, according to HIV infection status (red line is HIV infected; blue line is HIV uninfected) ( $n_{TBHIV-} = 10$ ,  $n_{TBHIV+} = 10$ ,  $n_{ODHIV-} = 10$ ,  $n_{ODHIV+} = 10$ ). Blue and orange shaded areas represent the 95% CIs of the ROC curve sensitivities, plotted at 0.5% specificity intervals. **(E)** Box plots of DRS (TB vs. LTBI DRS  $p = 2.83 \times 10^{-9}$ ) and **(F)** ROC curve based on the TB/LTBI FS-PLS signature applied to the combined TB and LTBI cohorts ( $n_{TB} = 20$ ,  $n_{LTBI} = 20$ ). Gray shaded areas represent the 95% CIs of the ROC curve sensitivities, plotted at 0.5% specificity intervals. The ROC curve has been benchmarked against target criteria for a tuberculosis triage test: Minimum criteria (90% sensitivity, 70% specificity) are indicated by the dashed green boxes and optimum criteria (95% sensitivity, 80% specificity) are indicated by the green solid boxes. **(G)** Box plots of DRS (TB vs. LTBI DRS HIV uninfected  $p = 1.083 \times 10^{-5}$ , HIV infected  $p$ -value  $3.248 \times 10^{-4}$ , and **(H)** ROC curve for TB/LTBI signature, according to HIV infection status (red line is HIV infected; blue line is HIV uninfected) ( $n_{TBHIV-} = 10$ ,  $n_{TBHIV+} = 10$ ,  $n_{LTBIHIV-} = 10$ ,  $n_{LTBIHIV+} = 10$ ). 95% confidence intervals are shown in brackets. The orange shaded area represents the 95% CIs of the ROC curve sensitivities, plotted at 0.5% specificity intervals. The blue shaded area for the perfect classifier represents the 95% CI for sensitivity. All  $p$ -values reported are Mann-Whitney  $p$ -values. AUC, area under the curve; OD, other diseases; LTBI, latent TB infection.

work in TB transcriptomics (14, 17). The performance of the two novel transcriptomic signatures, for TB/OD and TB/LTBI was assessed in the 20% test set and publicly available cohorts. The two signatures were subsequently validated using RT-dPCR and samples from the test cohort, confirming their accuracy of patient classification. We also report estimates for the abundance of each of the individual transcripts in the signatures in purified RNA from whole blood. A weighted regression model was not used in this work, reducing the risk of overfitting and providing more flexibility for application transfer in different detection platforms. This work provides compelling evidence of the robustness and reproducibility of the FS-PLS signatures and the DRS in classifying patients with TB, OD, and LTBI and the results presented here support the excellent discriminatory power of both the small gene number TB/OD and TB/LTBI FS-PLS signatures. The point estimates of sensitivity and specificity for our FS-PLS-derived signature, expressed as DRS and measured by both microarray and RT-dPCR, were benchmarked against the WHO TPP recommendations (3). For the microarray test dataset, both the TB/OD and TB/LTBI signatures' point estimates were within the WHO TPP minimum recommendations for a triage test. For the RT-dPCR, the TB/OD signature's point estimates met the WHO TPP requirements of a confirmatory/diagnostic test for TB, and both the TB/OD and TB/LTBI signatures' point estimates overlapped with the requirements of a triage test. While the findings support the discriminatory performance of both signatures, the relatively small sample size and wide confidence intervals of the point estimates should be considered when interpreting these results.

To our knowledge, this study is the first example of the use of RT-dPCR for absolute quantification of transcriptomic signatures in infectious diseases, as anticipated by review articles (34). Previous studies showed that RT-dPCR has a high accuracy for assessing absolute quantification of RNA and did not show significant inter-assay agreement (22). However, it should be noted that the efficiency of reverse transcriptase enzymes can be extremely variable and future investigations will be needed to provide further information on absolute abundances of individual RNA transcripts in purified RNA from whole blood. Nevertheless, the concentration values reported in this study provide novel insights that could be of significant use to the diagnostics development research community, providing information regarding the required limits of detection and dynamic range for assays designed to detect

signature transcripts. Although high correlation was observed between the gene/sample measurements for the two platforms for most of the genes, the differences reported highlight that a larger number of highly correlated candidate biomarker genes and different target regions within the genes themselves need to be screened with technology reflective of the point-of-care platforms intended to be used in order to ensure maximum diagnostic potential.

Clinical applications of dPCR exploit its ability to perform absolute quantification of nucleic acids without the need for rigorous calibration or standardization between laboratories. This advantage is a result of the design of dPCR assays, which involve large numbers of reaction partitions, and the Poisson statistics that are used to calculate initial concentrations of nucleic acids (21). RT-dPCR and dPCR have been used to determine copy numbers for a range of pathogens, including the hepatitis B virus, HIV, *Mycobacterium tuberculosis*, *Helicobacter pylori*, and *Plasmodium* spp. (23). While dPCR is more technologically advanced than qPCR, offering absolute rather than relative quantification, the implementation of dPCR in clinical laboratories has been impeded by its relatively low throughput, higher complexity and cost. However, as new instrumentation for dPCR becomes more widely available and simpler to use, it is highly likely that it will play a key role in diagnostic laboratories in the near future (23).

Out of the four transcripts in the TB/OD transcript signature *GBP6* and *PRDM1* are upregulated, and *TMCC1* and *ARG1* are downregulated, in patients with TB compared to OD. Genes in the guanylate-binding protein gene cluster (such as *GBP2*, *GBP5*, and *GBP6*) appear in numerous TB gene signatures (10). These are induced by the interferon (IFN) cytokine family (35) and have been shown to be important for cell-autonomous defense against intracellular pathogens (36). *PRDM1* encodes a DNA-binding protein that acts as a transcriptional repressor of various genes, including IFN- $\beta$  (37) by binding specifically to the PRDI (positive regulatory domain I element). *PRDM1* has also been shown to regulate the differentiation of B cells into plasma cells that produce antibodies, as well as myeloid cells, such as macrophages and monocytes (38). Little is known about the function of *TMCC1* in TB pathogenesis, but expression of *ARG1* is induced by toll-like receptor signaling in macrophages (39). The gene product, ARG1, plays an important role in the production of nitric oxide (NO), used to kill intracellular pathogens, when nitric oxide synthase-2 (NOS2) is unable to metabolize arginine in

hypoxic environments, such as the granuloma (40). ARG1 is able to produce NO in the absence of oxygen and is therefore critical for the control of intracellular TB (41).

The three gene signature for TB/LTBI reported here consists of two genes that are upregulated (*FCGR1A* and *C1QB*) and one gene that is downregulated (*ZNF296*) in TB compared to LTBI. *FCGR1A* appears in a number of other gene expression signatures for TB (10), and was the most discriminatory gene in a three-gene signature for TB/LTBI (6). Fc receptors (FcR) play an important role in regulating the immune system and are expressed by a number of innate immune effector cells, particularly monocytes, macrophages, dendritic cells, basophils and mast cells (42). It has been shown that the monocytic THP-1 cell line upregulates surface expression of Fcγ-RI in response to IFN-γ (43). *C1QB* encodes a component of the complement 1 (C1Q) complex, part of the complement immune system. Expression of genes encoding components of C1Q have been shown to correlate with the progression of active TB compared to HC and LTBI cohorts (44) and a recent study showed that, in four independent cohorts, components of the C1Q complex are elevated in patients with active TB compared to those with LTBI (45). *ZNF296* encodes a member of the C2H2 zinc-finger protein family, which contain DNA binding motifs often found in transcription factors. A microarray study identified this gene as upregulated in response to viral infection (46). The TB/LTBI signature presented here was evaluated by Gupta et al. (8) for the purposes of predicting progression from LTBI to active TB disease. Out of a total of 17 candidate signatures identified, eight accurately predicted incipient TB among people at risk of disease over a two-year time period with AUCs ranging from 70% (CI<sub>95%</sub>: 64–76%) to 77% (CI<sub>95%</sub>: 71–82%). Our TB/LTBI signature ranked second in terms of point estimate for AUC, with overlapping 95% confidence intervals with the other top-ranking signatures. Significantly lower AUCs were found for the remaining nine signatures.

This study has certain limitations. Although a case-control validation study is an important step in the biomarker discovery pipeline, it has certain limitations in extrapolating how the findings would transfer in a real-world clinical setting. A prospective cohort study design where positive and negative predictive values of a test would be the next step to evaluate the signatures' potential and applicability. This study is further limited by the small sample size used for the RT-dPCR evaluation, which is reflected in the relatively wide 95% confidence intervals reported for the classification measure.

It is widely accepted that TB diagnosis using transcriptomic signatures offers a number of clear advantages over various sputum-based techniques. However, there are a number of technical challenges of detecting mRNA from whole blood, including sample processing to extract mRNA transcripts that is generally intracellular and inherently less stable than DNA, and that can vary in concentrations by multiple orders of magnitude between samples.

The gene expression signatures for TB/LTBI and TB/OD reported in this study represent extremely promising biomarkers for TB, particularly since they can be measured in whole blood and comprise few analytes. A number of technologies exist that

might facilitate their translation into a test, which could include the use of nanomaterials, to quantify mRNA transcripts without an amplification step (47). A whole blood-based diagnostic test for TB would transform the diagnostic pipeline and enable earlier treatment commencement for patients that would otherwise be missed, and thus prevent onward transmission of the disease, contributing toward paving the way for the end of the TB epidemic by 2030, Goal 3.3 of the Sustainable Development Goals, as set out by the United Nations (48).

## DATA AVAILABILITY STATEMENT

The datasets presented in this study can be found in online repositories. The names of the repository/repositories and accession number(s) can be found at: [www.ncbi.nlm.nih.gov/geo/](http://www.ncbi.nlm.nih.gov/geo/), GSE37250.

## ETHICS STATEMENT

The studies involving human participants were reviewed and approved by Human Research Ethics Committee of the University of Cape Town, South Africa (HREC012/2007) The National Health Sciences Research Committee, Malawi (NHSRC/447) The Ethics Committee of the London School of Hygiene and Tropical Medicine (5212). The patients/participants provided their written informed consent to participate in this study.

## AUTHOR CONTRIBUTIONS

HG, MK, NF, HD, LC, RW, and ML: data curation. HG, MK, DH-C, CZ, and LC: formal analysis (application of statistical, mathematical, computational, or other formal techniques to analyze or synthesize study data) and validation (verification, whether as a part of the activity or separate, of the overall replication/reproducibility of results/experiments and other research outputs). MK, VW, SA, AC, BE, FK, PL, THMO, MH, NF, HD, LC, RW, and ML: funding acquisition. HG and MK: investigation (conducting a research and investigation process, specifically performing the experiments, or data/evidence collection). HG, MK, MA, CZ, and LC: methodology. HG, MK, VW, RW, and ML: project administration. HG, MK, MA, AC, FK, PL, THMO, MH, NF, HD, LC, RW, and ML: resources (provision of study materials, reagents, materials, patients, laboratory samples, animals, instrumentation, computing resources, etc.). MK, DH-C, CZ, and LC: software programming, software development, designing computer programs, implementation of the computer code and supporting algorithms, testing of existing code components. MK, MH, NF, HD, LC, RW, and ML: supervision. HG and MK: visualization (preparation, creation and/or presentation of the published work, specifically visualization/data presentation). HG, MK, and ML: writing—original draft preparation. All authors: conceptualization of study, writing—review and editing. All authors contributed to the article and approved the submitted version.

## FUNDING

This study was funded by an EU Action for Diseases of Poverty program grant (Sante/2006/105-061) and made use of infrastructure and staff at the Wellcome Trust-supported programs in Karonga and University of Cape Town and the Imperial College Center for Clinical Tropical Medicine. The Karonga Prevention Study is supported by the Wellcome Trust, UK (079828/079827). RW and AB were supported by the Wellcome Trust, UK (104803 and 203135). RW is also supported by the Francis Crick Institute which receives its core funding from Cancer Research UK (FC00110218), the UK

Medical Research Council (FC00110218), and The Wellcome Trust (FC00110218). The funders had no role in study design, data collection and analysis, decision to publish, or preparation of the manuscript. ML and MK receive support from the Imperial College BRC. MK also acknowledges support from the Wellcome Trust (Sir Henry Wellcome Fellowship grant 206508/Z/17/Z).

## SUPPLEMENTARY MATERIAL

The Supplementary Material for this article can be found online at: <https://www.frontiersin.org/articles/10.3389/fimmu.2021.637164/full#supplementary-material>

## REFERENCES

- Zar HJ, Tannenbaum E, Apolles P, Roux P, Hanslo D, Hussey G. Sputum induction for the diagnosis of pulmonary tuberculosis in infants and young children in an urban setting in South Africa. *Arch Dis Child.* (2000) 82:305–8. doi: 10.1136/adc.82.4.305
- WHO. *Global Tuberculosis Report 2020*. Geneva: World Health Organisation (2020).
- WHO. *High-Priority Target Product Profiles for New Tuberculosis Diagnostics: Report of a Consensus Meeting*. Geneva: World Health Organisation (2014).
- Hasin Y, Seldin M, Lusis A. Multi-omics approaches to disease. *Genome Biol.* (2017) 18:83. doi: 10.1186/s13059-017-1215-1
- Berry MP, Graham CM, McNab FW, Xu Z, Bloch SA, Oni T, et al. An interferon-inducible neutrophil-driven blood transcriptional signature in human tuberculosis. *Nature.* (2010) 466:973–7. doi: 10.1038/nature09247
- Maertzdorf J, Ota M, Repsilber D, Mollenkopf HJ, Weiner J, Hill PC, et al. Functional correlations of pathogenesis-driven gene expression signatures in tuberculosis. *PLoS ONE.* (2011) 6:e26938. doi: 10.1371/journal.pone.0026938
- Jacobsen M, Repsilber D, Gutschmidt A, Neher A, Feldmann K, Mollenkopf HJ, et al. Candidate biomarkers for discrimination between infection and disease caused by *Mycobacterium tuberculosis*. *J Mol Med-Imm.* (2007) 85:613–21. doi: 10.1007/s00109-007-0157-6
- Gupta RK, Turner CT, Venturini C, Esmail H, Rangaka MX, Copas A, et al. Concise whole blood transcriptional signatures for incipient tuberculosis: a systematic review and patient-level pooled meta-analysis. *Lancet Respir Med.* (2020) 8:395–406. doi: 10.1016/S2213-2600(19)30282-6
- Turner CT, Gupta RK, Tsaliki E, Roe JK, Mondal P, Nyawo GR, et al. Blood transcriptional biomarkers for active pulmonary tuberculosis in a high-burden setting: a prospective, observational, diagnostic accuracy study. *Lancet Respir Med.* (2020) 8:407–19. doi: 10.1016/S2213-2600(19)30469-2
- Mulenga H, Zauchenberger CZ, Bunyasi EW, Mbandi SK, Mendelsohn SC, Kagana B, et al. Performance of diagnostic and predictive host blood transcriptomic signatures for Tuberculosis disease: a systematic review and meta-analysis. *PLoS ONE.* (2020) 15:e0237574. doi: 10.1371/journal.pone.0237574
- Deffur A, Wilkinson RJ, Coussens AK. Tricks to translating TB transcriptomics. *Ann Transl Med.* (2015) 3(Suppl. 1):S43. doi: 10.3978/j.issn.2305-5839.2015.04.12
- Yang Z, Kong Y, Wilson F, Foxman B, Fowler AH, Marrs CF, et al. Identification of risk factors for extrapulmonary tuberculosis. *Clin Infect Dis.* (2004) 38:199–205. doi: 10.1086/380644
- Chamie G, Luetkemeyer A, Walusimbi-Nanteza M, Okwera A, Whalen CC, Mugerwa RD, et al. Significant variation in presentation of pulmonary tuberculosis across a high resolution of CD4 strata. *Int J Tuberc Lung Dis.* (2010) 14:1295–302.
- Kaforou M, Wright VJ, Oni T, French N, Anderson ST, Bangani N, et al. Detection of tuberculosis in HIV-infected and -uninfected African adults using whole blood RNA expression signatures: a case-control study. *PLoS MED.* (2013) 10:e1001538. doi: 10.1371/journal.pmed.1001538
- Gliddon HD, Herberg JA, Levin M, Kaforou M. Genome-wide host RNA signatures of infectious diseases: discovery and clinical translation. *Immunology.* (2018) 153:171–8. doi: 10.1111/imm.12841
- Sweeney TE, Braviak L, Tato CM, Khatri P. Genome-wide expression for diagnosis of pulmonary tuberculosis: a multicohort analysis. *Lancet Respir Med.* (2016) 4:213–24. doi: 10.1016/S2213-2600(16)00048-5
- Maertzdorf J, McEwen G, Weiner J, Tian S, Lader E, Schriek U, et al. Concise gene signature for point-of-care classification of tuberculosis. *EMBO Mol Med.* (2016) 8:86–95. doi: 10.15252/emmm.201505790
- Zak DE, Penn-Nicholson A, Scriba TJ, Thompson E, Suliman S, Amon LM, et al. A blood RNA signature for tuberculosis disease risk: a prospective cohort study. *Lancet.* (2016) 387:2312–22. doi: 10.1016/S0140-6736(15)01316-1
- Suliman S, Thompson E, Sutherland J, Weiner Rd J, Ota MOC, Shankar S, et al. Four-gene Pan-African blood signature predicts progression to tuberculosis. *Am J Respir Crit Care Med.* (2018). doi: 10.1164/rccm.201711-2340OC
- Lowe R, Shirley N, Bleackley M, Dolan S, Shafee T. Transcriptomics technologies. *PLoS Comput Biol.* (2017) 13:e1005457. doi: 10.1371/journal.pcbi.1005457
- Huggett JF, Foy CA, Benes V, Emslie K, Garson JA, Haynes R, et al. The digital MIQE guidelines: minimum information for publication of quantitative digital PCR experiments. *Clin Chem.* (2013) 59:892–902. doi: 10.1373/clinchem.2013.206375
- Sanders R, Mason DJ, Foy CA, Huggett JF. Evaluation of digital PCR for absolute RNA quantification. *PLoS ONE.* (2013) 8:e75296. doi: 10.1371/journal.pone.0075296
- Kuypers J, Jerome KR. Applications of digital PCR for clinical microbiology. *J Clin Microbiol.* (2017) 55:1621–8. doi: 10.1128/JCM.00211-17
- Alikian M, Ellery P, Forbes M, Gerrard G, Kasperaviciute D, Sosinsky A, et al. Next-generation sequencing-assisted DNA-based digital PCR for a personalized approach to the detection and quantification of residual disease in chronic myeloid leukemia patients. *J Mol Diagn.* (2016) 18:176–89. doi: 10.1016/j.jmoldx.2015.09.005
- Alikian M, Whale AS, Akiki S, Piechocki K, Torrado C, Myint T, et al. RT-qPCR and RT-Digital PCR: a comparison of different platforms for the evaluation of residual disease in chronic myeloid leukemia. *Clin Chem.* (2017) 63:525–31. doi: 10.1373/clinchem.2016.262824
- Herberg JA, Kaforou M, Wright VJ, Shailes H, Eleftherohorinou H, Hoggart CJ, et al. Diagnostic test accuracy of a 2-transcript host RNA signature for discriminating bacterial vs. viral infection in febrile children. *JAMA.* (2016) 316:835–45. doi: 10.1001/jama.2016.11236
- Coin LJ. *Lachlancoin/fspls: Minimal TB Biomarkers (Version 0.5.1)*. Zenodo (2018).
- Bloom CI, Graham CM, Berry MP, Wilkinson KA, Oni T, Rozakeas F, et al. Detectable changes in the blood transcriptome are present after two weeks of antituberculosis therapy. *PLoS ONE.* (2012) 7:e46191. doi: 10.1371/journal.pone.0046191
- Robin X, Turck N, Hainard A, Tiberti N, Lisacek F, Sanchez JC, et al. pROC: an open-source package for R and S+ to analyze and compare ROC curves. *BMC Bioinformatics.* (2011) 12:77. doi: 10.1186/1471-2105-12-77



30. Team RC. R: A Language and Environment for Statistical Computing. R Foundation for Statistical Computing, Vienna (2016).
31. DeLong ER, DeLong DM, Clarke-Pearson DL. Comparing the areas under two or more correlated receiver operating characteristic curves: a nonparametric approach. *Biometrics*. (1988) 44:837–45. doi: 10.2307/2531595
32. Wright VJ, Herberg JA, Kaforou M, Shimizu C, Eleftherohorinou H, Shailes H, et al. Diagnosis of Kawasaki disease using a minimal whole-blood gene expression signature. *JAMA Pediatr*. (2018) 172:e182293. doi: 10.1001/jamapediatrics.2018.2293
33. Anderson ST, Kaforou M, Brent AJ, Wright VJ, Banwell CM, Chagaluka G, et al. Diagnosis of childhood tuberculosis and host RNA expression in Africa. *N Engl J Med*. (2014) 370:1712–23. doi: 10.1056/NEJMoa1303657
34. Casamassimi A, Federico A, Rienzo M, Esposito S, Ciccociola A. Transcriptome profiling in human diseases: new advances and perspectives. *Int J Mol Sci*. (2017) 18:1652. doi: 10.3390/ijms18081652
35. Olszewski MA, Gray J, Vestal DJ. In silico genomic analysis of the human and murine guanylate-binding protein (GBP) gene clusters. *J Interferon Cytokine Res*. (2006) 26:328–52. doi: 10.1089/jir.2006.26.328
36. Kim BH, Shenoy AR, Kumar P, Bradfield CJ, MacMicking JD. IFN-inducible GTPases in host cell defense. *Cell Host Microbe*. (2012) 12:432–44. doi: 10.1016/j.chom.2012.09.007
37. Kuo TC, Calame KL. B lymphocyte-induced maturation protein (Blimp)-1, IFN regulatory factor (IRF)-1, and IRF-2 can bind to the same regulatory sites. *J Immunol*. (2004) 173:5556–63. doi: 10.4049/jimmunol.173.9.5556
38. Sciammas R, Davis MM. Modular nature of blimp-1 in the regulation of gene expression during B cell maturation. *J Immunol*. (2004) 172:5427–40. doi: 10.4049/jimmunol.172.9.5427
39. El Kasmi KC, Qualls JE, Pesce JT, Smith AM, Thompson RW, Henaio-Tamayo M, et al. Toll-like receptor-induced arginase 1 in macrophages thwarts effective immunity against intracellular pathogens. *Nat Immunol*. (2008) 9:1399–406. doi: 10.1038/ni.1671
40. Duque-Correa MA, Kuhl AA, Rodriguez PC, Zedler U, Schommer-Leitner S, Rao M, et al. Macrophage arginase-1 controls bacterial growth and pathology in hypoxic tuberculosis granulomas. *Proc Natl Acad Sci USA*. (2014) 111:E4024–E32. doi: 10.1073/pnas.1408839111
41. Pessanha AP, Martins RAP, Mattos-Guaraldi AL, Vianna A, Moreira LO. Arginase-1 expression in granulomas of tuberculosis patients. *Fems Immunol Med Mic*. (2012) 66:265–8. doi: 10.1111/j.1574-695X.2012.01012.x
42. Nimmerjahn F, Ravetch JV. Fc gamma receptors as regulators of immune responses. *Nat Rev Immunol*. (2008) 8:34–47. doi: 10.1038/nri2206
43. Kincaid EZ, Ernst JD. *Mycobacterium tuberculosis* exerts gene-selective inhibition of transcriptional responses to IFN-gamma without inhibiting STAT1 function. *J Immunol*. (2003) 171:2042–9. doi: 10.4049/jimmunol.171.4.2042
44. Cai Y, Yang QT, Tang YQ, Zhang MX, Liu HY, Zhang GL, et al. Increased complement C1q level marks active disease in human tuberculosis. *PLoS ONE*. (2014) 9:e92340. doi: 10.1371/journal.pone.0092340
45. Lubbers R, Sutherland JS, Goletti D, de Paus RA, van Moersel CHM, Veltkamp M, et al. complement component C1q as serum biomarker to detect active tuberculosis. *Front Immunol*. (2018) 9:2427. doi: 10.3389/fimmu.2018.02427
46. Terasaka Y, Miyazaki D, Yakura K, Haruki T, Inoue Y. Induction of IL-6 in transcriptional networks in corneal epithelial cells after herpes simplex virus type 1 infection. *Invest Ophthalmol Vis Sci*. (2010) 51:2441–9. doi: 10.1167/iovs.09-4624
47. Gliddon HD, Howes PD, Kaforou M, Levin M, Stevens MM. A nucleic acid strand displacement system for the multiplexed detection of tuberculosis-specific mRNA using quantum dots. *Nanoscale*. (2016) 8:10087–95. doi: 10.1039/C6NR00484A
48. United Nations General Assembly. *Transforming Our World: The 2030 Agenda for Sustainable Development. Draft resolution referred to the United Nations summit for the adoption of the post-2015 development agenda by the General Assembly at its sixty-ninth session*. New York, NY: United Nations General Assembly. (2015).

**Conflict of Interest:** The authors declare that the research was conducted in the absence of any commercial or financial relationships that could be construed as a potential conflict of interest.

Copyright © 2021 Gliddon, Kaforou, Alkian, Habgood-Coote, Zhou, Oni, Anderson, Brent, Crampin, Eley, Heyderman, Kern, Langford, Ottenhoff, Hibberd, French, Wright, Dockrell, Coin, Wilkinson and Levin. This is an open-access article distributed under the terms of the Creative Commons Attribution License (CC BY). The use, distribution or reproduction in other forums is permitted, provided the original author(s) and the copyright owner(s) are credited and that the original publication in this journal is cited, in accordance with accepted academic practice. No use, distribution or reproduction is permitted which does not comply with these terms.



# Cell-Mediated Immunological Biomarkers and Their Diagnostic Application in Livestock and Wildlife Infected With *Mycobacterium bovis*

Katrin Smith, Léanie Kleynhans, Robin M. Warren, Wynand J. Goosen and Michele A. Miller\*

Division of Molecular Biology and Human Genetics, Department of Science and Innovation-National Research Foundation Centre of Excellence for Biomedical Tuberculosis Research, Faculty of Medicine and Health Sciences, South African Medical Research Council Centre for Tuberculosis Research, Stellenbosch University, Cape Town, South Africa

## OPEN ACCESS

### Edited by:

Adam Penn-Nicholson,  
Foundation for Innovative New  
Diagnostics, Switzerland

### Reviewed by:

Marisa Mariel Fernandez,  
Institute of Studies on Humoral  
Immunity (IDEHU), Argentina  
Felix Ngosa Toka,  
Ross University School of Veterinary  
Medicine, Saint Kitts and Nevis

### \*Correspondence:

Michele A. Miller  
miller@sun.ac.za

### Specialty section:

This article was submitted to  
Microbial Immunology,  
a section of the journal  
Frontiers in Immunology

**Received:** 09 December 2020

**Accepted:** 08 February 2021

**Published:** 04 March 2021

### Citation:

Smith K, Kleynhans L, Warren RM,  
Goosen WJ and Miller MA (2021)  
Cell-Mediated Immunological  
Biomarkers and Their Diagnostic  
Application in Livestock and Wildlife  
Infected With *Mycobacterium bovis*.  
Front. Immunol. 12:639605.  
doi: 10.3389/fimmu.2021.639605

*Mycobacterium bovis* has the largest host range of the *Mycobacterium tuberculosis* complex and infects domestic animal species, wildlife, and humans. The presence of global wildlife maintenance hosts complicates bovine tuberculosis (bTB) control efforts and further threatens livestock and wildlife-related industries. Thus, it is imperative that early and accurate detection of *M. bovis* in all affected animal species is achieved. Further, an improved understanding of the complex species-specific host immune responses to *M. bovis* could enable the development of diagnostic tests that not only identify infected animals but distinguish between infection and active disease. The primary bTB screening standard worldwide remains the tuberculin skin test (TST) that presents several test performance and logistical limitations. Hence additional tests are used, most commonly an interferon-gamma (IFN- $\gamma$ ) release assay (IGRA) that, similar to the TST, measures a cell-mediated immune (CMI) response to *M. bovis*. There are various cytokines and chemokines, in addition to IFN- $\gamma$ , involved in the CMI component of host adaptive immunity. Due to the dominance of CMI-based responses to mycobacterial infection, cytokine and chemokine biomarkers have become a focus for diagnostic tests in livestock and wildlife. Therefore, this review describes the current understanding of host immune responses to *M. bovis* as it pertains to the development of diagnostic tools using CMI-based biomarkers in both gene expression and protein release assays, and their limitations. Although the study of CMI biomarkers has advanced fundamental understanding of the complex host-*M. bovis* interplay and bTB progression, resulting in development of several promising diagnostic assays, most of this research remains limited to cattle. Considering differences in host susceptibility, transmission and immune responses, and the wide variety of *M. bovis*-affected animal species, knowledge gaps continue to pose some of the biggest challenges to the improvement of *M. bovis* and bTB diagnosis.

**Keywords:** cell-mediated, cytokines, immunological biomarkers, livestock, *Mycobacterium bovis*, wildlife

## INTRODUCTION

*Mycobacterium bovis* infection and the resulting disease, commonly referred to as bovine tuberculosis (bTB), affects a broad range of species including humans, domestic animals, and wildlife (1, 2). Although *M. bovis*, as the name suggests, mainly affects bovids including cattle (*Bos taurus*), bison (*Bison bison*), African and Asian buffaloes (*Syncerus caffer* and *Bubalus bubalis*), it has been isolated from numerous other mammals, compromising animal and human health worldwide with reports of this species on all continents except Antarctica (3–5). Infection of wildlife further impacts livestock health due to the development of maintenance and spillover hosts within wildlife populations, including badgers (*Meles meles*) in the United Kingdom (UK), African buffaloes in southern Africa, and farmed and wild cervids in the United States (US) (6–8). In the UK and Ireland, *M. bovis* in badgers complicates bTB control efforts and similarly in the US, New Zealand, and Spain where deer, possum, and wild boar, respectively, are also recognized *M. bovis* reservoirs (4, 9). In the Americas, there are 15 wild species reported as infected with *M. bovis* (10). In South Africa, bTB is endemic in two major national parks, namely Kruger National and Hluhluwe-iMfolozi Parks (7). Moreover, *M. bovis* has been identified in more than 21 wildlife species in private and public sectors (11, 12).

In addition to the control challenges posed by infected wildlife species, bTB negatively affects wildlife-related industries, resulting in consequences for conservation, tourism, and game sales. Infection and disease in livestock and wildlife may lead to decreased productivity, trade restrictions, impacts on food security and zoonotic transmission, resulting in significant economic losses (5, 12). Bovine tuberculosis costs the global cattle industry alone 3 billion US dollars annually (13). In addition, ~5 million deer are farmed worldwide and bTB is the primary health threat across multiple species in this growing economic venture (14, 15). Despite effective bTB control measures in the US, states such as Michigan have endemic bTB in white-tailed deer (*Odocoileus virginianus*) populations that negatively affects the hunting and wildlife industry, in addition to the regular spillback affecting cattle (16, 17).

For these reasons, it is crucial to improve the detection, diagnosis and understanding of bTB across affected species to enable development of more effective and comprehensive control strategies. Early and accurate diagnosis of subclinical infection can inform more efficient management of affected animals. Alternatively, if associations can be accurately established between *M. bovis* infection or bTB disease and detectable host responses, limited available resources can be focused toward removing animals or populations that pose transmission risks to preserve those with higher economic, conservation or genetic value. However, the immune responses that arise from interactions between animal hosts and *M. bovis* are typically species-specific and particularly in the case of wildlife species, less well-characterized. Subsequently, validated diagnostic tests based on specific host responses to *M. bovis* infection and bTB are also scarce in wildlife.

The diagnostic standard for *M. bovis* detection, still in use despite being developed over a century ago, is the TST. The TST measures a host cell-mediated immune (CMI) response to mycobacterial purified protein derivative (PPD) antigens, either *M. bovis*-derived (PPD<sub>b</sub>) alone or together with *M. avium* (PPD<sub>a</sub>) for the single intradermal comparative tuberculin test (SICCTT) (18, 19). In cattle, a meta-analysis of TST use in the UK and Ireland reported 100% specificity (Sp), in agreement with a Great Britain study displaying almost 100% Sp for standard and severe cut-off interpretations (20, 21). However, the sensitivity (Se) can range between 50 and 80%, with variations in Sp and Se between species and a lack of host-specific cut-off validation for all affected hosts (18, 21). A major confounding factor is the exposure to environmental mycobacteria in addition to vaccine strain antigens (for cattle in limited areas) that cause cross-reactions due to homology between antigenic peptides, demonstrated at gene and protein levels (19, 22, 23). In New Zealand, the TST displays reduced Se in deer exposed to environmental mycobacteria and is not recommended in herds with a high likelihood of *M. bovis* infection (14). When applied to fallow deer (*Dama dama*) in Texas (USA), the test had overall low Se and Sp, indicating minimal diagnostic value for this cervid species (14). There are also multiple cases of *M. bovis* crossing international borders in imported, infected deer due to negative TST results (14). In addition to variable test performance, the TST is subject to several limitations. The test is labor-intensive and logistically challenging in high income countries; in developing countries, this is exacerbated by restricted access to reagents and animals, veterinary capacity, and handling facilities (11, 24). An additional complication is management of cattle considered inconclusive reactors (IRs); in England and Wales, there were 3,755 IRs in 2015 alone (18). Animals in these herds may be infected, as suggested by the report that 21% of these herds had positive reactors when re-tested. In Ireland, between 11.8 and 21.4% of IRs slaughtered before a re-test were reported to be *M. bovis*-infected (18). However, movement of such herds is not typically restricted unless there is a recent history of TB, exacerbating *M. bovis* transmission risks when using the TST alone (18).

In attempting to address drawbacks associated with the TST in bovids, at least one ancillary test is recommended (25). One of the key focus areas of bTB research that has emerged is the discovery of new CMI biomarkers and consequently the development of CMI-based tests for the early detection of infection by pathogenic mycobacteria (26). Biomarker is a broad term defined as any indicator of pathogenic biological processes, either pathogen- or host-based (27, 28). The most common adjunct to the TST is the CMI biomarker-based interferon-gamma (IFN- $\gamma$ ) release assay (IGRA) (19, 29). However, despite improvements in Se for detecting *M. bovis*-infected animals, ancillary tests can introduce extra costs and logistical challenges. For example, IGRAs require that whole blood samples be processed within 8–24 h of collection, depending on the stimulation method, which is impractical if herds are located far from available laboratories (24). Moreover, IGRAs rely on a single measurement that is unable to discriminate *M. bovis* infection from bTB disease and further, may fail to diagnose early infection when blood is stimulated with more specific mycobacterial peptides instead of

PPDs (29, 30). To overcome this, a combination of biomarkers may be used to improve diagnostic Se. For example, progress has been made in enhancing the detection of bTB infection in cattle by combining IGRAs with the simultaneous measurement of antigen-specific interleukin-1 $\beta$  (IL-1 $\beta$ ) or IFN  $\gamma$ -induced protein 10 (IP-10) (29–31). A systematic review by Domingos et al. (10) of *M. bovis* diagnostic methods in wildlife species also suggested the application of at least two tests to aid the detection of infection and potentially different disease stages.

A primary goal for accurate *M. bovis* detection is the early identification of a maximal number of infected animals for more effective control measures. The investigation of candidate biomarkers for *M. bovis* infection and bTB is ongoing, as discussed below. However, if current biomarker research could be further advanced to differentiate infection from bTB disease, this would enable a focus on detecting stages in which the animal is potentially infectious, improving the elimination of major transmission risks or preventing infected individuals from transitioning to a diseased state. The primary *ante mortem* diagnostic tools in livestock and wildlife rely on the development of antigen-specific CMI responses to *M. bovis* (30, 32, 33). Therefore, this review will focus on current understanding and knowledge gaps regarding the host response to *M. bovis* infection and the use of host CMI biomarkers for the improved understanding and diagnosis of *M. bovis* infection and bTB disease.

## HOST RESPONSES TO MYCOBACTERIUM BOVIS

With the availability of bovid host and *M. bovis* genomes, the understanding of host responses to *M. bovis* has continued to develop (24). Immunity, in brief, comprises the innate and adaptive immune systems. The adaptive immune response has two distinct components, namely humoral and cell-mediated immunity, of which the latter is vital for host protection against *M. bovis* infection. All the major T lymphocyte subsets have demonstrated involvement in the anti-mycobacterial immune response in cattle (34). In *M. bovis*-infected cattle, CD4<sup>+</sup> T cells produce IFN- $\gamma$  for activation of macrophage anti-mycobacterial functions whereas CD8<sup>+</sup> T cells are involved in the lysis of infected cells (34). The development of a T helper type 1 (Th1)-based CMI response, resulting in production of cytokines and chemokines such as tumor necrosis factor- $\alpha$  (TNF- $\alpha$ ), IL-12, IL-6, and IFN- $\gamma$  by dendritic cells and macrophages, is considered essential for the control of mycobacterial infection (35). Cytokine production is activated by pathogen antigen presentation to immune cells, and disease progresses when these pathways are disrupted (36). Cytokines play a critical role in determining the characteristic immune responses to infection; the balance between Th1 and T helper type 2 (Th2) functions is often studied from the perspective of their cytokine profiles, each of which fluctuate throughout disease progression (35). Cytokine function can vary from pro-inflammatory, which promotes activation of cells to kill mycobacteria, to anti-inflammatory, which reduces the pro-inflammatory response to control and prevent tissue

damage by necrosis (37). In the primary stages of mycobacterial infections, Th1-dominant cytokine responses develop (36). The Th1 immune response is critical for defense against intracellular pathogens, most notably through the production of IFN- $\gamma$  (34). However, a shift from Th1- to Th2-based responses is typically observed as disease develops, with a shift in CMI responses along with increasing humoral (B cell) responses (38). The Th2 response is associated with the production of cytokines including IL-4, IL-5, and IL-10 with studies suggesting that the Th1/Th2 balance is critical for determining bTB disease progression and outcomes (39). Therefore, any changes in immune responses during the course of infection are likely to affect the diagnostic performance of immunological assays.

Although early detection of *M. bovis* infection is primarily dependent upon the measurement of CMI responses in many species, humoral responses have also been used to diagnose bTB (35, 40–42). In certain species, for example elephants (*Loxodonta africana* and *Elephas maximus*) and suids, anti-mycobacterial antibodies can be detected during early infection (43–46). In species such as cattle and lions (*Panthera leo*), on the other hand, antibody detection usually occurs only after bTB disease progresses and the immune responses shift toward a Th2 profile (41, 47). However, the application of serological tests requires insight into the humoral immune profile of specific species to determine the differences in immunodominant antigen recognition and response kinetics (48, 49). Due to a paradigm that early immune responses are cell-mediated, this has been the primary focus of bTB research in animals to date although further studies on comparative immunobiological responses in different species are warranted.

In cattle and some other species, a CMI-dominated early and specific response to *M. bovis* infection is observed with proliferation of antigen-specific T lymphocytes, secretion of the regulatory cytokine IL-2, and release of pro-inflammatory cytokines including IFN- $\gamma$ . These responses have been reported, for example, in two studies by Corner et al. (50) and Gormley and Corner (51) that investigated CMI responses to *M. bovis* in experimentally infected badgers, one of the few relatively well-studied non-bovid species. The earliest CMI immune responses were observed 3 weeks post infection (WPI) in the animals infected with the highest *M. bovis* dose; these animals also demonstrated the most consistent CMI responses of peripheral blood mononuclear cells (PBMCs) to *M. bovis* PPD (PPD<sub>b</sub>) stimulation. The overall CMI responses were also positively associated with pathological changes, i.e., the presence of gross lesions, detected *post mortem*. On the other hand, the antibody responses in badgers were only sporadically detected.

Functional genomics and proteomics have enabled a better understanding of CMI responses to *M. bovis* infection (52). Studies typically focus on the *in vitro* assessment of gene expression profiles in different cells or tissues, isolated after infection with *M. bovis* or related strains, and *ex vivo* analyses aimed at identifying cytokine gene expression signatures for the detection of *M. bovis*-infected animals. Wedlock et al. (53) compared gene expression in primary bovine alveolar macrophages (AMs) infected with a virulent *M. bovis* strain and an attenuated version. Although both strains grew at



comparable rates, the results suggested a 45% difference in gene expression between the two infection groups. Of the 10 most differentially expressed genes, with the virulent strain inducing higher levels of expression, seven of these were chemokines with *IL-8* and monocyte chemoattractant protein (MCP)-1 (*CCL2*) having the greatest expression. The conclusion was that AMs infected with virulent *M. bovis* displayed a more dominant pro-inflammatory gene expression profile than those infected with the attenuated strain. Another study using a similar method observed lower expression of chemokines from AMs of *M. bovis*-infected cattle than *M. tuberculosis*-infected cells, highlighting a possible mechanism employed by *M. bovis* to circumvent activation of the host's chemotactic response, thereby evading killing (54).

Although the host immune responses during *M. bovis* infection and disease remain less understood than for *M. tuberculosis*, recent studies have begun to shed more light on this complex pathogen-host interplay. However, susceptibility to infection, routes of infection and disease progression can vary significantly between the wide range of host species that are affected. Hence, it would be expected that immune responses and therefore, specific diagnostic biomarkers may also differ, impacting advances in host biomarker discovery and application (36).

## HOST DIAGNOSTIC BIOMARKERS OF PATHOGENIC MYCOBACTERIAL INFECTION

A suitable diagnostic biomarker or multiple marker biosignature, for infection or disease, is a host- (or pathogen-) specific molecule/protein that is associated with the underlying pathological process (28, 55). Identification of biomarker-based assays that can enable more accessible, affordable, and efficient diagnosis has been a high priority for TB and bTB diagnostic research in recent years (28, 56). Considering the World Health Organization's target product profiles, that define the performance and operational characteristics of suitable tests, it is expected that non-DNA markers are more likely to meet practical and cost targets (28, 57). Non-DNA methods can be performed without advanced instrumentation, utilize more easily accessible samples such as blood and serum, and are generally more affordable than DNA-based tests (27, 28). Hence, the focus of current bTB diagnostic research is host biomarkers with an emphasis on cytokine/chemokine (chemotactic cytokine) proteins and antibodies, in addition to the detection of cytokine RNA expression (5, 24, 58).

Critical barriers to progress regarding biomarker discovery include the lack of standardization in specimen collection methods and a reliance on convenient or opportunistic samples, in addition to inadequate handling and storage of samples which can drastically alter detectable biomarker levels (51, 59). Another common limitation is suboptimal statistical power due to low sample numbers, hence, associations between biomarkers and potential disease states are challenging to investigate and prove (59). A biomarker should address a definitive question related to a particular state, or the prognosis, of pathogenic mycobacterial

infection in individuals or populations (55). However, the stages of TB that have been elucidated from human research are complex and include infection, incipient or subclinical or active disease, and latency; moreover, these states are not regarded as fixed but instead constitute a dynamic spectrum that may be affected by multiple factors, many of which remain poorly understood (55, 60).

For *M. bovis* infections in animals, insight regarding the mycobacterial disease spectrum is even more limited (36, 51, 60). In general, *M. bovis* infection in animals is often not detectable until disease is advanced. In addition, clinical signs are often non-specific such as weight loss, decreased milk production (in dairy cattle), and occasionally coughing or other respiratory signs (11, 61). Chronic disease can progress to mortality over the course of months to years. The hallmark lesion of bTB in cattle is the granuloma that can be found in the lung, lymph nodes and potentially other organs (62). Granuloma stages have been well-described in cattle and are based on morphological characteristics, i.e., degree of necrosis and mineralization, and presence of a connective tissue capsule (63). However, *M. bovis* disease development and pathological lesions can vary widely between species, with cavitary pulmonary lesions instead of granulomas in goats and gastrointestinal infection observed in predators, for example lions (64–66).

To date, the only method of determining an animal's true infection status is comprehensive *post mortem* examination and a battery of mycobacteriological, immunological, histopathologic, and molecular tests (19). Accurate *ante mortem*, in-field reference tests for infection and/or active bTB disease are lacking (56). Current understanding of the pathogenesis of *M. bovis* infection is also confounded by the multitude of susceptible animal hosts and the complexity of the host-pathogen interactions (36, 51). Although naturally-infected animals are useful in the investigation of differences between infection and disease, experimental models illuminate disease progression kinetics and immune responses initiated from a fixed point in time with a set dose, generating the insight necessary for diagnostic test development (67, 68). A major limitation for *M. bovis* and bTB diagnostic research is the lack of clarity regarding case definitions for infection vs. active disease and, whether latent infections exist (51, 60, 69, 70). Considering the various limitations outlined above, the fitness for purpose criteria [as defined by the World Organization of Animal Health (OIE)] are critical for the validation and application of diagnostic bTB biomarkers in animals and should be applied on an individual species basis.

The *ante mortem* diagnosis of bTB in animals primarily relies on the detection of host CMI responses, most commonly with the use of protein and gene expression assays (5). Although the most widely used ancillary test, IGRA, in addition to the TST, can produce false negative results as the CMI responses required may diminish in advanced disease stages (anergy), while the humoral response increases (35, 69). Furthermore, IGRAs demonstrate limited Se in early infection stages and in general, bTB diagnostic assays are unable to distinguish infection from disease (13, 21, 25, 58, 71). On the other hand, a recent study by Bernitz et al. (72) observed that levels of IFN- $\gamma$  and IP-10 in incubated

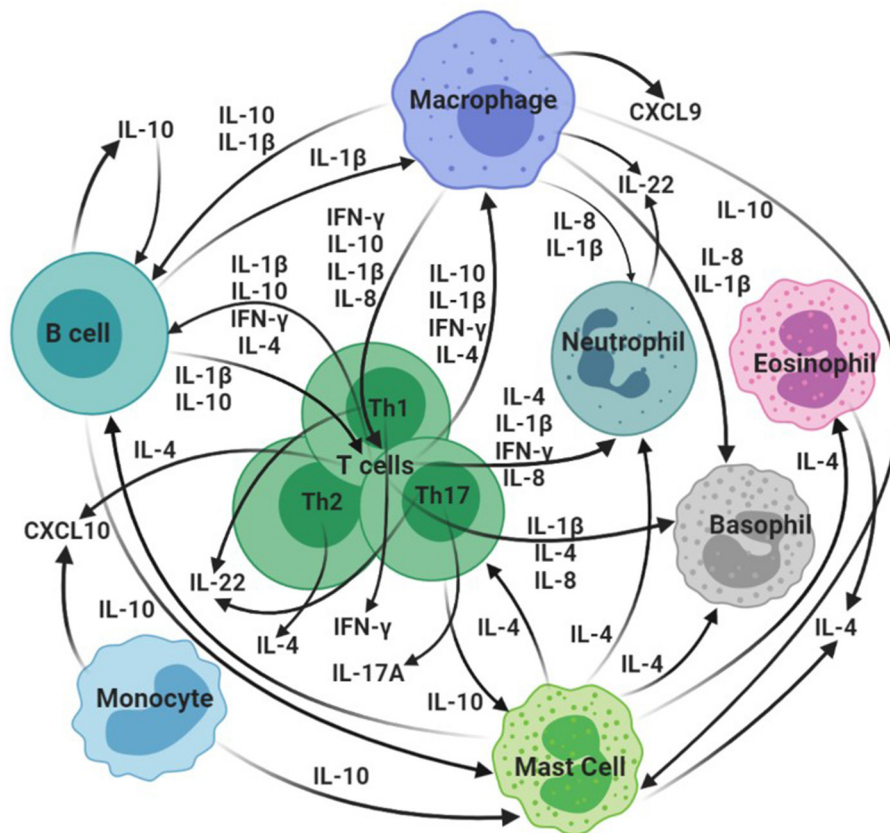


**FIGURE 1 |** Overview of hypothesized interactions of selected cytokines/chemokines identified as bTB biomarkers in domestic and wild animal species. CXCL10: IP-10. Created in BioRender.com.

unstimulated whole blood were elevated in infected buffaloes with observable pathological changes consistent with bTB in comparison to uninfected controls. Furthermore, increased IFN- $\gamma$  significantly correlated with increasing severity of pathological changes in the infected buffaloes, consistent with observations of associations between antigen-stimulated IFN- $\gamma$  and bTB pathology in cattle and badgers, demonstrating the potential for these cytokines to be used as indicators of bTB disease (72–74).

A limitation of cytokine/chemokine protein assays can be the inability to detect high levels of the biomarker target due to, for example, binding saturation limits; therefore, mRNA responses and their detection may provide a more robust alternative (5). There are several studies that investigate cytokine/chemokine RNA expression to achieve diagnostic test objectives. However, another purpose of biomarkers is to improve the fundamental understanding of disease pathogenesis, which is often the focus of bTB biomarker RNA expression research, for example studies that characterize the immunological profile of *M. bovis*-infected cattle (experimental or natural) by measuring cytokine/chemokine mRNA expression at various time points during infection and/or disease (35, 39, 53, 55, 75–77). Immune response changes during bTB disease progression, particularly in terms of anti- and pro-inflammatory cytokine/chemokine

profiles, can signify disease outcomes and hence play a role in the diagnosis and control of infection (35). The CMI response is the dominant immunological response to *M. bovis* (in most studied species), responsible for the killing and elimination mechanisms in addition to formation of characteristic granulomas against this intracellular pathogen (69). The following section will further describe some of the CMI biomarkers of infection and bTB disease in animals.

## CYTOKINE/CHEMOKINE BIOMARKERS OF MYCOBACTERIUM BOVIS INFECTION

Several promising cytokine/chemokine biomarkers of *M. bovis* infection and disease in domestic and wildlife species have been revealed in recent years, in addition to the widely recognized host biomarker IFN- $\gamma$ . These include, although are not limited to, IP-10, IL-1 $\beta$ , IL-4, IL-8, IL-17A, CXCL9, IL-10, and IL-22 (37, 40, 78–84). Both protein and gene expression assays have been used to assess biomarker levels in different species and have facilitated identification of additional targets for diagnostic development (5). This section will describe select current and

**TABLE 1** | Cell-mediated immune cytokines that have demonstrated potential as bovine TB biomarkers that distinguish *M. bovis*-infected from uninfected domestic and/or wild animal species.

Cytokine	Species	Reference(s)
IL-4*	Cattle, white-tailed deer	(37, 75, 76, 78)
IL-8*	Cattle	(39, 79, 84)
IL-17A*	Cattle	(80, 81, 85–89)
IL-22*	Cattle	(5, 25, 80, 88, 90–93)
IL-10*	Cattle, goat	(35, 37, 94–97)
IFN- $\gamma$ *	Multiple (see <b>Table 2</b> )	(72, 74)
IP-10*	Warthog, African buffalo, cattle	(29, 30, 72, 98, 99)
IL-1 $\beta$	Cattle	(5, 31, 82, 91)
CXCL9	Cattle, lion, spotted hyena, cheetah, warthog	(5, 25, 77, 92, 100–103)

IL, interleukin; IFN- $\gamma$ , interferon-gamma; IP, IFN- $\gamma$ -induced protein; \*have also shown potential to distinguish between different bTB states i.e., early infection, active disease.

candidate CMI biomarkers of *M. bovis* infection in domestic and wild animal species, as summarized in **Figure 1** and **Table 1**.

## IFN- $\gamma$

The cytokine IFN- $\gamma$  is a vital mediator of macrophage activation, amplifying macrophage cytokine release in response to *M. bovis* and playing a critical role in host protection and pathogen control (74, 104). The utility of various cytokine release assays based on IFN- $\gamma$  (IGRAs) has been demonstrated in cattle, leading to the acceptance of IGRAs as an adjunct to the TST in European legislation, and some countries outside of the European Union (61, 105). The first bTB *in vitro* IGRA was developed in the 1980's in Australia and is now used globally (106). Studies on *M. bovis* experimentally- and naturally-infected cattle have demonstrated the ability of IGRAs to detect a positive CMI response from as early as 2 weeks post-infection and often earlier than detection by the SICTT (34, 78, 107, 108). The most used IGRA platform in worldwide bTB control programmes is the Bovigam<sup>®</sup> which uses PPD<sub>b</sub> and PPD<sub>a</sub> stimulatory antigens (71). The Bovigam<sup>®</sup> IGRA is also effectively applied to *M. bovis* detection in goats and another PPD-based IGRA has been used in pigs (109, 110).

Currently, the primary ancillary method for *M. bovis* detection in African buffaloes is the IGRA, based on either PPD stimulation or the QuantiFERON<sup>®</sup> TB Gold (QFT) system that stimulates whole blood with *M. bovis*/*M. tuberculosis*-specific antigens early secretory antigenic target 6 (ESAT-6) and culture filtrate protein 10 (CFP-10) (32, 111). Thereafter, species-compatible IFN- $\gamma$  enzyme-linked immunosorbent assays (ELISAs) are used to detect the biomarker. Validated IFN- $\gamma$  ELISAs for buffaloes include the Bovigam<sup>®</sup> assay and Mabtech in-house, Cattletype<sup>®</sup>, and commercial Mabtech bovine IFN- $\gamma$  ELISAs (33, 111, 112). There are several other wildlife species for which IGRAs to detect *M. bovis* infection have been developed, as summarized in **Table 2**.

Using ESAT-6/CFP-10 (EC)-stimulated whole blood (QFT platform), IFN- $\gamma$  ELISAs have been modified for use in white rhinoceros (*Ceratotherium simum*) and wild dog (*Lycaon pictus*)

**TABLE 2** | Summary of interferon-gamma (IFN- $\gamma$ ) release assays (IGRAs) employed in domestic and wild animal species for *M. bovis* detection and bTB diagnosis.

Species	Reference(s)	Detection method	Stimulatory antigen(s)
Buffalo ( <i>Syncerus caffer</i> )	(32) (33) (111)	Bovigam <sup>®</sup> IGRA QFT/Mabtech ELISA QFT/Cattletype <sup>®</sup> ELISA	PPD EC EC
White rhino ( <i>Ceratotherium simum</i> )	(113)	QFT/Mabtech ELISA	EC
Wild dog ( <i>Lycaon pictus</i> )	(114)	QFT/R&D Quantikine ELISA	EC
Badger ( <i>Meles meles</i> )	(115)	IGRA (in-house)	PPD/EC
Alpaca ( <i>Vicugna pacos</i> )	(116)	Mabtech ELISA	PPD/EC
Red deer ( <i>Cervus elaphus</i> )	(117)	IGRA (in-house)	PPD/EC/Rv
White-tailed deer ( <i>Odocoileus virginianus</i> )	(118)	Cervigam <sup>TM</sup> ELISA	PPD
Reindeer ( <i>Rangifer tarandus</i> )			
Sambar deer ( <i>Cervus unicolor</i> )			
Cattle ( <i>Bos taurus</i> )	(21) (Meta-analysis)	Various	PPD/EC
Goat ( <i>Capra hircus</i> )	(110)	Bovigam <sup>®</sup> IGRA	PPD
Pig	(109)	IGRA (in-house)	PPD

PPD, purified protein derivative (bovine/avian); EC, ESAT-6/CFP-10; Rv, Rv3615c/Rv3020; QFT, QuantiFERON<sup>®</sup>-TB Gold stimulation platform.

(113, 114). Using both PPD and EC stimulatory antigens, IGRAs have also been used in badgers, with good Se and Sp, alpacas (*Vicugna pacos*), and red deer (*Cervus elaphus*) for which Rv3615c and Rv3020 antigens were also used (115–117). The Cervigam<sup>TM</sup> IFN- $\gamma$  ELISA (developed for red deer), used with plasma from PPD-stimulated whole blood, has also displayed promise for bTB diagnosis in white-tailed deer in addition to reindeer (*Rangifer tarandus*) and sambar deer (*Cervus unicolor*) (118).

Although IFN- $\gamma$  has proved invaluable for several species as a biomarker of *M. bovis* infection, in other species, including lions and warthogs (*Phacochoerus africanus*), it does not appear to be as useful (83, 98). It has also been observed that depending on the infection phase, IGRAs (and the SICTT) may fail to detect *M. bovis*-infected animals, which could be due to either very early infection (when a response detectable by the IGRA is still forming) or a depressed (anergic) immune state occurring in the later stages of bTB (119, 120). In addition, there may be individual or species differences in immune responses, resulting in failure of IGRAs to detect infection. For example, suids and New World camelids have robust humoral responses to mycobacterial infection and although detection of IFN- $\gamma$  has

been reported, these assays are not commonly used as diagnostic tests in these species (46, 100, 109, 116, 121). Moreover, IGRA results can be confounded by co-infections with environmental strains, vaccination (in some domestic species) and, although contended, possible interference by previous testing including the SICTT (13, 69). The host immune response to mycobacteria is naturally linked to disease progression yet bTB generally presents with extended and advanced, poorly described disease stages, posing an additional challenge for the extension of IFN- $\gamma$ -based diagnostics to distinguish infection from active disease (120, 122). However, correlations between IFN- $\gamma$  and *M. bovis* pathology have been preliminarily detected in badgers and buffaloes (72, 74). Moreover, investigating the associations between cytokine responses at both a gene and protein level, alongside host-specific pathological changes, can provide more insight on the diagnostic potential of IFN- $\gamma$  and additional biomarkers (5, 63, 75, 94, 123, 124).

## IP-10

The IFN- $\gamma$ -induced chemokine IP-10, expressed by lymphocytes and monocytes, is produced at high levels in humans, cattle and African buffaloes, up to 100-fold more than IFN- $\gamma$ , following infection with tuberculous mycobacteria (99, 125, 126). It has a role in delayed type hypersensitivity reactions and antigen-induced levels of IP-10 have shown promise for early detection of *M. bovis* infection in animals that may be negative on other tests (such as IGRAs) (30, 98, 125, 126).

Considering the potential for IP-10 to be a more sensitive marker than IFN- $\gamma$ , there are still relatively few studies in bTB-affected species. Using a Kingfisher Biotech (St Paul, MN, United States) bovine IP-10 ELISA and QFT whole blood stimulation, a significantly higher antigen-specific IP-10 response was able to distinguish *M. bovis*-infected from culture negative warthogs (98). The same has been shown in African buffaloes using the same platform, and IP-10 has demonstrated high test Se in this species (30, 40). Furthermore, higher levels of IP-10 in incubated samples without antigen stimulation have been correlated to the detection of *M. bovis* pathology in infected buffalo populations (72). Using the same assay as for buffaloes, Parsons et al. (99) showed a strong correlation between IP-10 and IFN- $\gamma$  release, and the robustness of IP-10 as a biomarker of *M. bovis* infection in cattle. Waters et al. (127) also observed antigen-specific IP-10 mRNA responses in PBMCs from cattle, starting at 29 days after *M. bovis* challenge, that were highly correlated to IFN- $\gamma$  mRNA levels; and Palmer et al. (5) confirmed the potential of IP-10, with mRNA isolation and protein release from whole blood, for bTB diagnosis in cattle. However, similar to what Parsons et al. (99) reported, high levels of IP-10 in unstimulated plasma from both infected and uninfected cattle were observed for some individuals. The parallel measurement of IP-10 with IFN- $\gamma$  has also demonstrated the potential to augment detection of *M. bovis*-infected cattle and buffaloes, highlighting the benefit of host biomarker signatures for enhanced bTB diagnosis (29, 30).

## IL-1 $\beta$

IL-1 $\beta$  is one of the multiple cytokines secreted, primarily by innate immune cells such as monocytes and macrophages, with IFN- $\gamma$ , to orchestrate an immune response toward mycobacterial infection and is viewed as one of the major pro-inflammatory cytokines (82, 128). Limited biomarker studies beyond cattle include the detection of IL-1 $\beta$  mRNA and protein in heat-inactivated *M. bovis*-immunized red deer compared to controls and, in a separate study of red deer, an observed association with disease progression after challenge with an *M. bovis* field strain (95, 129). Jones et al. (31) found IL-1 $\beta$  cytokine levels to be much higher in *M. bovis*-infected compared to uninfected cattle, using whole blood stimulated with either PPDs or EC. Elnaggar et al. (82) found similar results when stimulating blood with EC antigens, with significant differences observed between the infected group, and both non-tuberculous mycobacteria-exposed and uninfected control cattle. Palmer et al. (5) investigated IL-1 $\beta$  expression in whole blood stimulated with EC and Rv3615c, showing significantly higher levels in the *M. bovis*-challenged cattle, compared to uninfected controls, at 5-, 8-, and 12-weeks post infection (WPI). Rusk et al. (91) demonstrated significant upregulation of IL-1 $\beta$  by *M. bovis*-specific T cells, isolated from stimulated PBMCs, by transcriptomics analysis and T cell/macrophage co-cultures using experimentally infected calves. Finally, the study by Jones et al. (31) applied IFN- $\gamma$  and IL-1 $\beta$  assays in parallel to observe a 5% increase in Se without any loss of Sp, using the EC antigens, when compared to measuring IFN- $\gamma$  alone; this reiterates the utility of biomarker signatures for more efficient diagnosis. Although not used in the context of mycobacterial infection, IL-1 $\beta$  and IL-8 sequences have been reported for the Asian elephant (*Elephas maximus*) and may provide a foundation for investigating antigen-specific immune responses using gene expression assays (130).

## IL-4

A characteristic indicator of the Th2 immune response to mycobacteria, IL-4 plays an anti-inflammatory role such as controlling tissue damage by down-regulating pro-inflammatory responses (37). Rhodes et al. (78) investigated IL-4 cytokine expression in PBMC culture supernatants, after stimulation with PPDs or EC, using experimentally and naturally *M. bovis*-infected cattle. The overall IL-4 response, in comparison to IFN- $\gamma$ , was delayed with activity peaking at 6–8 WPI. Challenge with a low dose of *M. bovis* caused a reduced IFN- $\gamma$  response although a specific IL-4 response remained evident. In naturally infected cattle, increased IL-4 differentiated these animals from uninfected controls with Se equivalent to that of IFN- $\gamma$  (78). These findings are similar to a study by Blanco et al. (39) in which IL-4 expression in PBMCs was elevated in five of nine naturally infected cattle, compared to controls.

Two studies by Thacker et al. (75, 76) on experimentally infected white-tailed deer and cattle, respectively, also found that increased IL-4 gene expression distinguished *M. bovis*-infected from uninfected animals when investigating PBMCs stimulated with PPDs or EC. The highest IL-4 levels in deer were at 12, 16, or 24 WPI; for cattle, the peak was earlier (at 4 WPI) with a decline thereafter, similar to the Rhodes et al. (78) study. In



the deer, *M. bovis* infection resulted in consistently more IL-4 production in animals with less pathological changes compared to the high pathology group. In cattle, however, IL-4 expression was higher in the high pathology group overall, regardless of stimulus and the low pathology group was indistinguishable from the uninfected group. In contrast, Widdison et al. (37) assessed infected cattle 16 WPI, when the acute infection phase was more controlled and chronic disease was starting to develop. In this study, a significant reduction in IL-4 with an increase in the IFN- $\gamma$ /IL-4 ratio was observed in *M. bovis*-challenged animals. Moreover, there was a significant negative correlation between IL-4 expression, and both lymph node scores and the number of mycobacteria isolated. This supports the hypothesis of a conversion from Th1- to Th2-dominated responses in the first 3 months post *M. bovis*-infection in cattle (76). These findings also suggest that species-specific patterns of cytokine responses need to be defined.

In summary, it appears that the observed delay of the IL-4 response relative to IFN- $\gamma$  corresponds to the anti-inflammatory role of IL-4 in *M. bovis* infection (37, 78). Two of the cattle infection studies demonstrated early peaks in IL-4 expression followed by rapid decreases, while IFN- $\gamma$  responses remained detectable when lesion development would be expected to begin (75, 78). This suggests that IL-4 may reduce IFN- $\gamma$ -induced pathology and does not compromise the protective response, although results have suggested that the switch from Th1 to Th2 responses may occur later than 3 months PI (76). Although not yet investigated outside bovines and cervids, the potential for IL-4 to distinguish infection states warrants further investigation.

## IL-8

The precise role of the chemokine IL-8 in TB has not been fully elucidated, although studies have demonstrated IL-8 binding to tubercle bacilli and interactions with the pathogen that appear to enhance mycobactericidal characteristics of macrophages and neutrophils (131). Increased IL-8 is also required for granuloma formation (84).

Widdison et al. (79) investigated RNA expression of IL-8 in lymph node tissue from *M. bovis*-challenged cattle. The infected cohort displayed lesions at necropsy, representing a well-established infection stage and the same cohort displayed significantly elevated IL-8 expression. Widdison et al. (79) also observed a positive correlation between IL-8 expression levels and lesion severity, together with the bacterial load, in the lymph nodes examined. In contrast, Blanco et al. (39) observed decreased IL-8 expression in naturally infected vs. healthy cattle. The lack of IL-8 upregulation, together with the observed Th1 cytokine profile in PPD<sub>b</sub> stimulated PBMCs, was indicative of active infection (39). In humans, low IL-8 mRNA expression, in combination with other markers, allows differentiation between active and latent TB (132).

A more recent study by Gao et al. (84) investigated naturally *M. bovis*-infected cattle, further characterized by a nested PCR, on *M. bovis* bacteria shed into nasal exudates, that could identify animals that posed higher transmission risks (i.e., PCR-positive and at a more advanced bTB stage). An IL-8 assay was performed with PPD<sub>b</sub>- and EC-stimulated whole blood from

cohorts of infected/PCR-negative (bTB<sub>PCR-N</sub>), infected/PCR-positive (bTB<sub>PCR-P</sub>), and uninfected cattle. Both stimuli resulted in significantly increased IL-8 in both *M. bovis*-infected cohorts compared to the uninfected cattle. Interestingly, unstimulated IL-8 was significantly higher in the bTB<sub>PCR-N</sub> cohort than both the bTB<sub>PCR-P</sub> and uninfected cohort. The concentrations of PPD-stimulated IL-8 were also positively correlated with IFN- $\gamma$  and were higher than the levels of IFN- $\gamma$ , IL-17A, and IP-10. In addition, PPD-stimulated IL-8 production was able to better discriminate *M. bovis*-infected animals from uninfected animals than IP-10 and IL-17A and showed good agreement with the TST and IGRA with a relative Se and Sp of >90 and >98%, respectively (84). Although relatively less reported, results obtained from studies of IL-8 in cattle suggest an important role of this chemokine in *M. bovis* infections (84). However, further research to determine the potential of IL-8 as a bTB biomarker is still required.

## IL-17A

The pro-inflammatory cytokine IL-17A (IL-17), produced by Th17 lymphocytes, has been identified as a primary effector cytokine necessary for detection and clearing of tubercle bacilli (133). Studies of IL-17A in bTB have demonstrated its role in immunity against mycobacterial infection, in addition to participation in granuloma formation (85). Blanco et al. (86) studied *IL-17A* mRNA expression in PPD<sub>b</sub>-stimulated PBMCs from experimentally infected cattle and found that animals with macroscopic bTB lesions developed higher *IL-17A* expression compared to cattle without lesions, with statistical significance at 60- and 90-days PI (DPI). Aranday-Cortes et al. (80) also noted upregulation of *IL-17A* mRNA in lymph node lesions 13 WPI, in comparison to control lymph node tissue. This upregulation occurred at each granuloma stage investigated. Notably, as granulomas developed, expression decreased until there was significantly less *IL-17A* in more advanced compared to early-stage lesions.

In addition to increased *IL-17A* gene expression, increased protein production has also been observed in *M. bovis* infection. McGill et al. (87) observed significantly higher levels of PPD<sub>b</sub>/EC-stimulated IL-17A protein secreted by PBMCs from experimentally *M. bovis*-infected cattle between 3 and 6 WPI. Increased numbers of antigen-specific IL-17A-secreting cells have also been found in blood from infected animals, with CD4<sup>+</sup> T cells discovered to be the prominent source of IL-17A following stimulation. Similar findings in cattle were also reported by Steinbach et al. (88). Waters et al. (81) investigated IL-17A protein in whole blood and mRNA from PBMCs of experimentally infected cattle and observed a >9-fold upregulation post-infection, with correlations between gene expression and protein release, and between IL-17A and IFN- $\gamma$  production. Moreover, higher IL-17A concentrations at 2.5 WPI correlated with increased lesion severity and mycobacterial burdens in cattle. Using stimulated PBMCs, Xin et al. (89) also observed significantly higher PPD<sub>b</sub>-stimulated IL-17A mRNA and protein in naturally and experimentally infected cattle compared to uninfected controls. The marked IL-17A responses elicited by *M. bovis* in cattle, combined with correlations to bTB

pathology, point to the utility of IL-17A as a promising indicator of bTB disease progression.

## CXCL9

The chemokine CXCL9, also known as monokine induced by IFN- $\gamma$  (MIG), has been reported as a mediator of the bovine anti-mycobacterial response during bTB, with a proposed role in attracting activated T cells, and granuloma development or maintenance (76, 77). Aranday-Cortes et al. (92) investigated CXCL9 expression in lymph node granulomas of experimentally *M. bovis*-infected cattle. The early-stage granulomas showed significantly upregulated expression compared to the control tissue, followed by a significant decrease in CXCL9 in early to advanced granulomas as lesions progressed. In contrast, Palmer et al. (77) studied pulmonary granulomas at 150 DPI and observed overall high and significantly elevated CXCL9 expression compared to non-lesion lung tissue; however, the expression did not differ significantly between different granuloma stages. The differences in these two studies were attributed to tissue type, among other factors (77, 134). Klepp et al. (25) investigated CXCL9 expression in PBMCs from naturally *M. bovis*-infected cattle and significant differences were observed between infected and healthy animals. Similarly, Palmer et al. (5) also observed significantly elevated CXCL9 gene expression and protein levels in *M. bovis*-challenged cattle in response to EC/Rv3615c or PPD<sub>b</sub> antigens, with detectable CXCL9 responses by 2 WPI, which remained consistently and significantly higher than that of the control group.

In lions, EC-stimulated blood was used to assess CXCL9 expression, and significantly increased levels of CXCL9 enabled discrimination between *M. bovis*-infected, -exposed, and uninfected lion cohorts (83, 101). Also using EC (QFT) stimulated blood, Higgitt et al. (102) and Kerr et al. (103) were able to detect *M. bovis* immune sensitization by upregulation of CXCL9 in spotted hyenas (*Crocuta crocuta*) and cheetahs (*Acinonyx jubatus*), respectively. In addition, Roos et al. (100) was able to show that upregulation of CXCL9 could distinguish between *M. bovis*-infected and uninfected warthogs.

Overall, studies on CXCL9 have demonstrated high levels of expression in tuberculous lung and thoracic lymph nodes, in addition to stimulated whole blood, in cattle and other species infected with *M. bovis*. The CXCL9 responses display a robustness akin to that of the IP-10 biomarker, although without the confounding effect of spontaneous production such as that of IP-10 in unstimulated samples (5).

## IL-10

The Th2-associated cytokine IL-10 is a critical anti-inflammatory mediator of innate and adaptive responses to pathogenic mycobacteria (35). The function of IL-10 is to deactivate macrophages and decrease production of reactive nitrogen and oxygen species; hence, in its absence, a stronger Th1 immune response is incited, while high levels of IL-10 are associated with increased susceptibility to mycobacterial infection (77, 135).

There appears to be an inverse relationship between IL-10 and IFN- $\gamma$ . Welsh et al. (35) analyzed PBMC cytokine mRNA of experimentally infected cattle, and reported high IL-10 levels

prior to infection, which gradually declined following infection as higher IFN- $\gamma$  expression was detected. However, there was a sharp increase in IL-10 at 26 WPI, with levels higher than those pre-infection, in cattle that showed the greatest severity of disease. In addition, this was correlated with decreasing CMI and increasing humoral responses (35).

Similar patterns were seen in IL-10 expression in tissues. Widdison et al. (37) studied IL-10 expression in lymph node tissue, noting a significant decrease in IL-10 and an increase in the IFN- $\gamma$ /IL-10 ratio in infected compared to uninfected cattle. There was also a significant negative correlation between lesion scores and mycobacterial load in lymph nodes and IL-10 expression. These results are similar to those from Thacker et al. (76) who also compared IL-10 between a high and low pathology groups of *M. bovis*-infected cattle in which they discovered two-fold lower IL-10 expression in the high pathology cohort. However, these two studies were conducted at 16 and 18 WPI. Considering the role of IL-10 in limiting tissue destruction, hence smaller and less necrotic lesions displaying the highest IL-10 levels, these results were unsurprising and could explain the later peak (26 WPI) observed by Welsh et al. (35). In the Widdison et al. study, the combined observation of suppressed IL-4, IL-10, IL-6, and TNF in the infected group, together with maintenance of IL-12 and IFN- $\gamma$  levels, suggested that suppression was specific and not just a general consequence of infection and necrosis from a developing chronic response.

Interestingly, Blanco et al. (96) did not observe any downregulation of IL-10 in PBMCs from infected cattle with lesions, and the expression level was similar to that of infected animals without lesions. Similarly, Palmer et al. (77) observed no difference in IL-10 expression between granulomas and non-lesioned lung tissue, noting that the low levels observed were expected of active granulomas. However, when combined with IL-2 and IL-17 in a predictive biomarker combination, IL-10 enhanced the classification of infected/lesion-negative animals and was hence acknowledged as a potential identifier of disease progression in herds with no clinical signs of bTB (96). The ratio IFN- $\gamma$ /IL-10 has also been acknowledged as a potential indicator of *M. bovis* disease severity in red deer (95). However, most studies used a single time point to assess IL-10 expression, which may not reflect the dynamic levels of cytokines during granuloma formation. In support of this, Canal et al. (94) observed significantly higher IL-10 expression in more advanced (stage III and IV) granulomas of lymph nodes and lung, compared to stages I and II, in naturally *M. bovis* infected cattle. Finally, lung lesions and respiratory lymph nodes from goats, experimentally infected with *M. bovis*, revealed high levels of IL-10 and highlighted the important role of this cytokine in granuloma formation (97).

## IL-22

The cytokine IL-22 is part of the IL-10 family and is produced by natural killer, mast and T cells, predominantly cell types Th17 and Th22 (80). Together with IL-17A, IL-22 has emerged as a critical effector cytokine required for the detection and clearance of bacilli in TB studies, however, its role in bTB is less studied. It has been shown to induce protection and may inhibit mycobacterial growth inside macrophages (136).

Aranday-Cortes et al. (80) investigated IL-22 mRNA in a murine bTB model, followed by a study in PBMCs from infected cattle, and observed a 74-fold upregulation of IL-22 in the lungs of infected compared to naïve mice and highly significant upregulation in the PPD<sub>b</sub>-stimulated PBMCs of the infected cattle. The predominant source of IL-22 was CD4<sup>+</sup> T cells, similar to IFN- $\gamma$ . Ray Waters et al. (90) and Steinbach et al. (88) confirmed these observations both at the gene and protein level, respectively, with the latter using naturally *M. bovis*-infected cattle. Palmer et al. (5) also observed upregulated IL-22 expression in infected cattle, at 5, 8, 12, and 16 WPI, compared to uninfected controls.

Another study by Aranday-Cortes et al. (92) examined tuberculous granulomas from infected cattle. The study reported upregulation of IL-22 in bTB lymph node lesions with a clear trend of decreasing mRNA expression from granulomas in early to advanced stages, indicating the potential of IL-22 as a biomarker for bTB pathology. Rusk et al. (91) also noted a lack of IL-22 expression by T cells within late-stage granulomas from lung and mediastinal lymph nodes, confirmed by Palmer et al. (93) who observed very low expression levels of IL-22 in lymph nodes with advanced granulomatous lesions, i.e., samples collected at  $\pm 21$  WPI, with no differences in expression between granulomatous and uninfected lymph nodes. Klepp et al. (25) studied IL-22 expression in PBMCs from naturally infected cattle and in addition to observing upregulation of IL-22 in the infected group, also found that IL-22 could significantly differentiate *M. bovis* infected cattle with either negative TST or IGRA results from uninfected animals. Hence, IL-22 may be useful as an ancillary biomarker for bTB detection where the results from the TST and IGRA fail to detect infected animals.

## DISCUSSION

This review describes host CMI biomarkers with diagnostic potential for the detection of *M. bovis* infection and bTB, with a focus on more recent research and knowledge gaps, especially as these pertain to wildlife species. The CMI response is a vital component of host adaptive immunity to *M. bovis* (34, 35). Cattle and badger studies have demonstrated the involvement of the major T lymphocyte types and production of CMI-based cytokines and chemokines during *M. bovis* immune response development, accompanied by a shift from the predominant pro-inflammatory, Th1-biased response to more anti-inflammatory, Th2 functions as infection develops (36, 37, 51, 94). With a focus on the observation and measurement of CMI responses, detected through changes in gene expression, protein release or both, promising diagnostic biomarker targets and their associated limitations for multi-species application have emerged.

The choice of CMI-based methods for diagnostic purposes is in part motivated by the early and specific response that is elicited in most *M. bovis* host species studied to date (51). The delayed type hypersensitivity reaction measured *in vivo* by the TST is mimicked in stimulated blood cultures and can therefore result in a higher Se and Sp, due to the controlled *in vitro* conditions and parameters, for *M. bovis* detection (43, 58). Additionally, the

specific cytokines and chemokines, produced during the adaptive immune response, that are detected by these assays is a feature applicable to most (if not all) mammalian species, thus allowing for translational use across species. Further advantages of *in vitro* CMI assays include even earlier detection times of an immune response than the TST (as early as 1-week post infection), only a single immobilization or handling event to collect blood samples, and more potential for the standardization of tests and reagents without in-field variation and operator bias (69). Moreover, the cost differences between *in vivo* (TST) and *in vitro* CMI assays may be over-estimated and CMI tools could prove more cost-efficient than assumed, with further cost reductions anticipated by increased use allowing the scale-up of production, and the automation of assays (such as ELISA kits) that lower laboratory costs (13).

The most used cytokine biomarker for TB diagnostic assays is IFN- $\gamma$ , a critical Th1 cytokine produced upon lymphocyte activation in defense against *M. bovis* (43). This cytokine is also vital for the formation and function of granulomas, a hallmark of the response to *M. bovis* in host species (94, 120). Compared with other cytokine assays to date, IGRAs are robust and comparatively easy to standardize, and the development of new IGRAs for multiple non-bovine species has been suggested for bTB screening and control (13, 120). The increasingly widespread use of IGRAs (such as Bovigam®) in cattle, due to US- and EU-approval as a TST adjunct for parallel testing in bTB eradication programs to increase Se, may also explain interest in its use for wildlife species. Although IGRAs have been successfully applied to several domestic and wildlife species, including but not limited to cattle, goats, cervids, buffalo, white rhinoceros, and wild dogs, there have been limitations encountered when using them in other *M. bovis* host species (43, 111, 113, 114, 137). Aside from technical challenges related to the lack of available diagnostic tests and reagents for most wildlife, this may also be due to species heterogeneity in predominant immune response pathways to *M. bovis* (45, 51). Although *M. bovis* was first strongly associated with cattle, this pathogen has adapted and evolved to infect a broad range of animal host species, which may present with shared or unique characteristics in their immune responses (4, 9, 120). Although less studied, there may be differences in the IFN protein structure or amount produced between species, resulting in decreased expression and thus detection of this cytokine as observed in lions and warthogs (83, 98). Another difference between species is disease susceptibility together with infection pressure in the specific environment, hence, some animals could be exposed to high pathogen doses leading to rapid disease progression, or lower levels resulting in sub-clinical infection (137). The disease state and dose-dependent immune response may also influence the patterns of cytokines detected, as observed in experimentally infected badgers that showed consistent CMI responses with a high dose of *M. bovis* yet those with subclinical presentation had weak CMI responses, although with no effects on the humoral response (51). This could explain the more efficient use of alternative biomarkers or methods observed in species such as lions and warthogs, in which IFN- $\gamma$  detection appeared less optimal (45, 47, 83, 98). However, biomarker signatures associated with a subclinical bTB



state in animals have not yet been investigated, in contrast to human studies (138). A final factor to consider is the influence of *M. bovis* strains on host immune responses. Although it is acknowledged that the virulence of pathogenic mycobacteria is linked to genetic and phenotypic characteristics, this has only been confirmed for *M. tuberculosis*, aided by in-depth research using animal models (120, 139). Hosts of *M. bovis* are typically outbred species, thus, discerning the influence of *M. bovis* lineage from host heterogeneity is challenging. However, virulence variations between strains have been reported that suggest potential correlations between strain genetic differences and bTB development (139, 140).

In addition to a dominant early response, changes in IFN- $\gamma$  responses have been correlated to pathological changes, although an IGRA to distinguish between *M. bovis* infection and bTB disease has not yet been developed (84, 89). Considering the correlations observed between *IFNG* expression and granulomatous lesion development, the quantitative measurement of IFN- $\gamma$  in different cohorts of defined bTB states from early infection to active disease could enable the development of an IFN- $\gamma$  cytokine assay to differentiate *M. bovis*-infected from diseased animals. However, species specific validation would be critical due to observed differences in *IFNG* expression profiles during bTB progression, as observed between fallow deer and cattle (93, 94, 123). In light of the potential drawbacks to IFN- $\gamma$  detection, including sample handling that necessitates a short period between blood collection and processing and variable test performance parameters depending on species and disease stage, alternative cytokines, and chemokines to IFN- $\gamma$  have emerged as additional tools for *M. bovis* infection and bTB diagnosis.

Pro-inflammatory cytokines are released early after *M. bovis* infection and are thus expected to be promising candidates for biomarkers of infection due to the predominant Th1 response observed in several host species. In addition to IFN- $\gamma$ , two major pro-inflammatory cytokines are IL-1 $\beta$  and IL-6, although not much more than a role in general mycobacterial infection is known for the latter. The former, IL-1 $\beta$ , has demonstrated high Se for *M. bovis* detection in cattle, particularly when used in parallel with an IGRA (5, 31). Although not explicitly pro-inflammatory, two biomarkers (IP-10 and IL-8) have been detected at higher concentrations than IFN- $\gamma$  and have shown possible correlation with bTB progression in cattle and African buffaloes (5, 72, 84). Considering their robust response early after *M. bovis* infection, these biomarkers could be well-suited for detecting *M. bovis* infection in less studied species. Another cytokine that demonstrates robust levels from an early infection stage is CXCL9, responsible for CD4<sup>+</sup> lymphocyte recruitment (5, 100, 101).

There are limitations associated with CMI-based diagnostics that include reduced Se due to anergy (reduced detectable Th1-biased CMI responses as bTB progresses), and interference from co-infection and vaccination (120). However, the application of a parallel testing scheme, whereby at least two different tests able to detect slightly different sub-populations of infected animals (i.e., animals at different stages of infection) are used together, has shown promise in combatting these drawbacks, particularly

in *M. bovis*-endemic settings (69, 111). The demonstration of two dominant pro-inflammatory cytokines, IFN- $\gamma$  and IL-1 $\beta$ , that increased Se without compromising Sp when diagnosing *M. bovis* infection in cattle, indicates that even slight differences in cytokine pathways and functions can provide a testing scheme to improve detection of the maximum number of infected animals. Moreover, for species in which IFN- $\gamma$  detection is problematic, the detection of additional or alternative pro-inflammatory cytokines could aid the early detection of *M. bovis*. Therefore, considering the robust levels of IL-8 and its good agreement with both the TST and IGRAs, this marker could also prove a promising option for enhancing *M. bovis* detection. Another example of parallel application is the measurement of IP-10 with IFN- $\gamma$  that has enhanced Se in buffaloes and cattle, with high IP-10 production having a particular advantage in very early stages of infection (29, 30). Moreover, Klepp et al. (25) demonstrated the utility of IL-22 for the diagnosis of *M. bovis* infections that both the TST and IGRA failed to detect, not unexpected from a cytokine marker that stems from a separate and recently described T cell lineage, Th17.

Infection with *M. bovis* typically results in an early Th1 bias that tends to decline as the Th2 response increases, with shifts from Th1 to Th2 responses showing correlations to increased pathology (94). Hence, whether the objective is optimum detection of all infected animals, the detection of highly infectious individuals (i.e., animals that are shedding *M. bovis* bacilli) or the distinction between infection and active disease, it is expected that a diagnostic algorithm would benefit from using a combination of pro- and anti-inflammatory biomarkers. Moreover, the immunological response to *M. bovis*, in terms of bTB disease progression, is a dynamic process and non-linear (77). Thus, different biomarker signatures could be used to identify bTB progression, as suggested by Blanco et al. (96), Kelley et al. (56), and Palmer et al. (5). One example, shown by immunohistochemical analysis of granulomatous lesions of lymph nodes and lung in cattle, is the combination of pro-inflammatory IFN- $\gamma$  and IL-1 $\beta$  with IL-10 (94). The two pro-inflammatory cytokines demonstrated contrasting yet equally significant associations with granuloma development and lesioned vs. non-lesioned tissue, highlighting the diversity of individual cytokine functions. The study also observed a lack of IL-10 expression in advanced granulomas that correlates with previous findings of progressively decreasing IL-10 in cattle with severe pathology (76, 94). The anti-inflammatory cytokines IL-4 and IL-10, which typically present with inverse correlations to IFN- $\gamma$  over the course of infection, have shown good potential in distinguishing disease states; thus, their inclusion is suggested for biomarker signatures that cover both early and late stages of infection and bTB, with the potential to enhance diagnostic Se or Sp particularly for enhanced detection of infected animals (37, 75, 78, 94, 95). A panel of biomarkers could also provide a promising method for wildlife species in particular, due to the measurement of varied immune responses from a single sample that would provide greater confidence in the animals' disease state without the need for repeat testing, a significant challenge for most wildlife testing. Alternative potential biomarkers of bTB disease progression include IL-17A, also of the Th17 subset, and



CXCL9 due to the observed increase as infection progresses with additional correlations to lesion severity (25, 81). This highlights the utility of adding biomarkers from different T cell subsets in a bTB testing scheme and warrants their investigation in wild animal species, especially considering the infeasibility and lack of standardization of the TST outside of common domestic species.

Due to the recognized role of wildlife in the maintenance of *M. bovis*, research on the development of assays for wild species (partially or fully validated) is increasing. A significant challenge in the development of CMI biomarkers for *M. bovis* in wildlife is the difficulty in obtaining sufficient reference samples to investigate and validate diagnostic assays. The lack of validated *ante mortem* tests makes diagnostic tests even more challenging to perform under field conditions, particularly in endemic settings (19, 56). Furthermore, the procurement of gold standard reference cohorts remains a trade-off between obtaining reliable samples and the loss of valuable animals, particularly for negative cohorts, that are required to obtain data from *post mortem* examination and mycobacterial culture (43). There are statistical tools that provide alternatives to the use of reference standards, such as latent-class or Bayesian approaches; however, statistical methods require large sample sizes, among other limitations (19, 21, 71). In acknowledgment of these challenges, recent policy (in the form of additional chapters for the OIE Terrestrial Manual) was adopted between 2014 and 2016, including statistical approaches to validation, that extends to the validation standards for diagnostic tests to wildlife (Chapter 2.2.7., OIE Terrestrial Manual 2018). Two validation pathways are provided that allow provisional recognition of a test if the complete validation process is hindered. This agrees with the chapter's emphasis on fit-for-purpose assays, particularly as diagnostic testing objectives may differ between domestic animal and wildlife species. The chapter also recognizes the difficulties in obtaining wildlife reference standards (particularly negative cohorts), suggesting latent-class models for performance estimates in lieu of a perfect (gold standard) reference (141). On the other hand, the imperfections of the gold standard requirement for mycobacterial culture have been acknowledged more recently; hence, alternative definitions for reference cohorts that improve test performance parameters may also be applicable (13, 51, 69).

The successful use of IGRAs and other cytokine assays in wildlife depends on the availability (and costs) of suitable tests or reagents. However, commercial CMI biomarker detection platforms are being developed and optimized using common domestic species with unknown cross reactivity to wildlife species. Therefore, researchers may need to develop novel species-specific reagents and assays, although these would have a very limited market. However, if cross reactivity can be determined using commercial reagents, this has the advantage of ready access by other researchers without having to exchange reagents. Indirect ELISAs with cross-reactive reagents have facilitated their use in related species, such as the application of bovine ELISAs to African buffaloes (32, 111) or equine ELISAs in white rhinoceros (113). However, another viable alternative is cytokine gene expression assays that can be adapted or developed for use in closely related species and even extended

to non-related species if the sequences are conserved, which has been demonstrated for cytokine sequences in wildlife species (26, 142). Gene expression assays have been used in less common species such as warthogs, hyenas, and lions (83, 98, 102). The development of cytokine and chemokine multiplex assays that detect several targets simultaneously in a single sample (of small volume), with options for customization, has also aided the development of biomarker signatures (13, 143). Recently, the MILLIPLEX® bovine cytokine/chemokine platform demonstrated detection of several novel protein markers in buffaloes, with the aim to enhance *M. bovis* detection and potentially differentiate bTB disease states with the use of multiple diagnostic markers in this species (112). Transcriptome analysis has also been conducted using *in vitro* murine bTB models and PBMCs from cattle to identify more comprehensive gene panels involved in responses to *M. bovis*, although correlations between signatures and a potential incipient vs. advanced bTB state remain an avenue for future research (80, 144). Considering the multiple challenges faced when validating a single new CMI-based diagnostic assay, including the limited funding and research on candidate biomarkers in wildlife, the lack of progress regarding multiple marker signatures is not surprising. Moreover, the costs and feasibility of performing these assays for a range of species should be considered when prioritizing the development of biosignatures for wildlife bTB diagnosis.

The success of management and control strategies for bTB is only as effective as the diagnostic assays it relies upon. The use of CMI cytokine and chemokine biomarkers has already improved insight on the comparative immunology of *M. bovis*-infected hosts, with experimental and natural infection studies conducted in cattle, badgers and cervids, among other species. Moreover, understanding the contribution and role of dominant profiles, such as the Th1/Th2 responses, to the development of pathology aids the identification and development of diagnostic biomarkers and biomarker panels. However, despite progress in understanding *M. bovis*-induced immune responses, the research and diagnostic biomarkers described here are still primarily restricted to cattle. In comparison to domestic species, limited resources are allocated to studies of bTB in wildlife, resulting in a paucity of information on *M. bovis* infection and disease development in other naturally infected hosts (43, 51). Hence, more species-specific research is required, together with the development of standardized, multi-species tests and reagents, and investigation of candidate biomarkers in alternative samples types, i.e., serum, due to the practical, in-field and diagnostic potential of circulating responses. CMI-based assays may also be further improved with the addition of enhanced, immunodominant antigens for stimulation (in addition to ESAT-6 and CFP-10) to increase test Se and Sp. Additionally, advances in techniques from multiplex biomarker detection platforms to powerful statistical approaches that estimate population characteristics when true disease status is unknown, or when logistical challenges prevent acquisition of gold standard reference cohorts, will further enable the validation of enhanced immunological tools in both domestic animals and wildlife.

## AUTHOR CONTRIBUTIONS

KS, MM, and WG conceived the idea for the review. MM and RW provided funding. KS, MM, LK, WG, and RW contributed to the drafting and editing of the manuscript. All authors reviewed the manuscript.

## REFERENCES

- Michel AL. Improving specific disease outcomes through a One Health approach-tuberculosis. *Rev Sci Tech.* (2014) 33:583–92. doi: 10.20506/rst.33.2.2310
- Romha G, Gebu G, Asefa A, Mamo G. Epidemiology of *Mycobacterium bovis* and *Mycobacterium tuberculosis* in animals: transmission dynamics and control challenges of zoonotic TB in Ethiopia. *Prev Vet Med.* (2018) 158:1–17. doi: 10.1016/j.prevetmed.2018.06.012
- OIE Bulletin. Panorama. *Controlling Bovine Tuberculosis: A One Health Challenge.* (2019). doi: 10.20506/bull.2019.1.2909
- Gagneux S. Ecology and evolution of *Mycobacterium tuberculosis*. *Nat Rev Microbiol.* (2018) 16:202–13. doi: 10.1038/nrmicro.2018.8
- Palmer MV, Thacker TC, Rabideau MM, Jones GJ, Kanipe C, Vordermeier HM, et al. Biomarkers of cell-mediated immunity to bovine tuberculosis. *Vet Immunol Immunopathol.* (2020) 220:109988. doi: 10.1016/j.vetimm.2019.109988
- Graham J, Smith GC, Delahay RJ, Bailey T, McDonald RA, Hodgson D. Multi-state modelling reveals sex-dependent transmission, progression and severity of tuberculosis in wild badgers. *Epidemiol Infect.* (2013) 141:1429–36. doi: 10.1017/S0950268812003019
- Hlokwe TM, van Helden P, Michel AL. Evidence of increasing intra and inter-species transmission of *Mycobacterium bovis* in South Africa: are we losing the battle? *Prev Vet Med.* (2014) 115:10–7. doi: 10.1016/j.prevetmed.2014.03.011
- Tsao K, Robbe-Austerman S, Miller RS, Portacci K, Grear DA, Webb C. Sources of bovine tuberculosis in the United States. *Infect Genet Evol.* (2014) 28:137–43. doi: 10.1016/j.meegid.2014.09.025
- Brites D, Loiseau C, Menardo F, Borrell S, Boniotti MB, Warren R, et al. A new phylogenetic framework for the animal-adapted *Mycobacterium tuberculosis* complex. *Front Microbiol.* (2018) 9:2820. doi: 10.3389/fmicb.2018.02820
- Domingos SCB, Carioca Júnior HR, Lilenbaum W, Santa Rosa MT, Pereira CD, Medeiros LS. A systematic review on the distribution of *Mycobacterium bovis* infection among wildlife in the Americas. *Trop Anim Health Prod.* (2019) 51:1801–5. doi: 10.1007/s11250-019-01954-7
- Michel AL, Müller B, van Helden PD. *Mycobacterium bovis* at the animal-human interface: a problem, or not? *Vet Microbiol.* (2010) 140:371–81. doi: 10.1016/j.vetmic.2009.08.029
- Sichewo PR, Vander Kelen C, Thys S, Michel AL. Risk practices for bovine tuberculosis transmission to cattle and livestock farming communities living at wildlife-livestock-human interface in northern KwaZulu Natal, South Africa. *PLoS Negl Trop Dis.* (2020) 14:e0007618. doi: 10.1371/journal.pntd.0007618
- Schiller I, Oesch B, Vordermeier HM, Palmer MV, Harris BN, Orloski KA, et al. Bovine tuberculosis: a review of current and emerging diagnostic techniques in view of their relevance for disease control and eradication. *Transbound Emerg Dis.* (2010) 57:205–20. doi: 10.1111/j.1865-1682.2010.01148.x
- Mackintosh CG, De Lisle GW, Collins DM, Griffin JFT. Mycobacterial diseases of deer. *N Z Vet J.* (2004) 52:163–74. doi: 10.1080/00480169.2004.36424
- Thomas J, Infantes-Lorenzo JA, Moreno I, Romero B, Garrido JM, Juste R, et al. A new test to detect antibodies against *Mycobacterium tuberculosis* complex in red deer serum. *Vet J.* (2019) 244:98–103. doi: 10.1016/j.tvjl.2018.12.021
- Ford AK, Niedringhaus KD, Anderson AN, LaCour JM, Nemeth NM. Disseminated *Mycobacterium kansasii* infection in a white-tailed deer and implications for public and livestock health. *J Vet Diagnostic Investig.* (2019) 32:147–51. doi: 10.1177/1040638719895475
- Salvador LCM, O'Brien DJ, Cosgrove MK, Stuber TP, Schooley A, Crispell J, et al. Disease management at the wildlife-livestock interface: using whole-genome sequencing to study the role of elk in *Mycobacterium bovis* transmission in Michigan, USA. *Mol Ecol.* (2019) 28:2192–205. doi: 10.1111/mec.15061
- Brunton LA, Prosser A, Pfeiffer DU, Downs SH. Exploring the fate of cattle herds with inconclusive reactors to the tuberculin skin test. *Front Vet Sci.* (2018) 5:228. doi: 10.3389/fvets.2018.00228
- Srinivasan S, Jones G, Veerasami M, Steinbach S, Holder T, Zewude A, et al. A defined antigen skin test for the diagnosis of bovine tuberculosis. *Sci Adv.* (2019) 5:eaax4899. doi: 10.1126/sciadv.aax4899
- Goodchild AV, Downs SH, Upton P, Wood JLN, De La Rua-Domenech R. Specificity of the comparative skin test for bovine tuberculosis in Great Britain. *Vet Rec.* (2015) 177:258. doi: 10.1136/vr.102961
- Núñez-García J, Downs SH, Parry JE, Abernethy DA, Broughan JM, Cameron AR, et al. Meta-analyses of the sensitivity and specificity of ante-mortem and post-mortem diagnostic tests for bovine tuberculosis in the UK and Ireland. *Prev Vet Med.* (2018) 153:94–107. doi: 10.1016/j.prevetmed.2017.02.017
- Arend SM, Van Meijgaarden KE, De Boer K, Cerdá De Palou E, Van Soelingen D, Ottenhoff THM, et al. Tuberculin skin testing and *in vitro* T cell responses to ESAT-6 and culture filtrate protein 10 after infection with *Mycobacterium marinum* or *M. kansasii* *J Infect.* (2002) 186:1797–807. doi: 10.1086/345760
- Vordermeier HM, Brown J, Cockle PJ, Franken WPJ, Arend SM, Ottenhoff THM, et al. Assessment of cross-reactivity between *Mycobacterium bovis* and *M. kansasii* ESAT-6 and CFP-10 at the T-cell epitope level. *Clin Vaccine Immunol.* (2007) 14:1203–9. doi: 10.1128/01.00116-07
- Lamont EA, Janagama HK, Ribeiro-Lima J, Vulchanova L, Seth M, Yang M, et al. Circulating *Mycobacterium bovis* peptides and host response proteins as biomarkers for unambiguous detection of subclinical infection. *J Clin Microbiol.* (2014) 52:536–43. doi: 10.1128/JCM.02433-13
- Klepp LI, Eirin ME, Garbaccio S, Soria M, Bigi F, Blanco FC. Identification of bovine tuberculosis biomarkers to detect tuberculin skin test and IFN- $\gamma$  release assay false negative cattle. *Res Vet Sci.* (2019) 122:7–14. doi: 10.1016/j.rvsc.2018.10.016
- Goosen WJ, Parsons SDC, Miller MA, van Helden PD, Warren RM, Cooper D. The evaluation of candidate biomarkers of cell-mediated immunity for the diagnosis of *Mycobacterium bovis* infection in African buffaloes (*Syncerus caffer*). *Vet Immunol Immunopathol.* (2014) 162:198–202. doi: 10.1016/j.vetimm.2014.10.008
- Walzl G, McNerney R, du Plessis N, Bates M, McHugh TD, Chegou NN, et al. Tuberculosis: advances and challenges in development of new diagnostics and biomarkers. *Lancet Infect Dis.* (2018) 18:e199–210. doi: 10.1016/S1473-3099(18)30111-7
- MacLean E, Broger T, Yerliyak S, Fernandez-Carballo BL, Pai M, Denking CM. A systematic review of biomarkers to detect active tuberculosis. *Nat Microbiol.* (2019) 4:748–58. doi: 10.1038/s41564-019-0380-2
- Coad M, Doyle M, Steinbach S, Gormley E, Vordermeier M, Jones G. Simultaneous measurement of antigen-induced CXCL10 and IFN- $\gamma$  enhances test sensitivity for bovine TB detection in cattle. *Vet Microbiol.* (2019) 230:1–6. doi: 10.1016/j.vetmic.2019.01.007
- Bernitz N, Kerr TJ, Goosen WJ, Clarke C, Higgitt R, Roos EO, et al. Parallel measurement of IFN- $\gamma$  and IP-10 in QuantiFERON®-TB Gold (QFT) plasma improves the detection of *Mycobacterium bovis*

- infection in African buffaloes (*Syncerus caffer*). *Prev Vet Med.* (2019) 169:104700. doi: 10.1016/j.prevetmed.2019.104700
31. Jones GJ, Pirson C, Hewinson RG, Vordermeier HM. Simultaneous measurement of antigen-stimulated interleukin-1 $\beta$  and gamma interferon production enhances test sensitivity for the detection of *Mycobacterium bovis* infection in cattle. *Clin Vaccine Immunol.* (2010) 17:1946–51. doi: 10.1128/CVI.00377-10
  32. Michel AL, Cooper D, Jooste J, de Klerk LM, Jolles A. Approaches towards optimising the gamma interferon assay for diagnosing *Mycobacterium bovis* infection in African buffalo (*Syncerus caffer*). *Prev Vet Med.* (2011) 98:142–51. doi: 10.1016/j.prevetmed.2010.10.016
  33. Parsons SDC, Cooper D, McCall AJ, McCall WA, Streicher EM, le Maitre NC, et al. Modification of the QuantiFERON-TB Gold (In-Tube) assay for the diagnosis of *Mycobacterium bovis* infection in African buffaloes (*Syncerus caffer*). *Vet Immunol Immunopathol.* (2011) 142:113–8. doi: 10.1016/j.vetimm.2011.04.006
  34. Pollock JM, Welsh MD, McNair J. Immune responses in bovine tuberculosis: towards new strategies for the diagnosis and control of disease. *Vet Immunol Immunopath.* (2005) 108:37–43. doi: 10.1016/j.vetimm.2005.08.012
  35. Welsh MD, Cunningham RT, Corbett DM, Girvin RM, McNair J, Skuce RA, et al. Influence of pathological progression on the balance between cellular and humoral immune responses in bovine tuberculosis. *Immunology.* (2005) 114:101–11. doi: 10.1111/j.1365-2567.2004.02003.x
  36. Palmer MV, Waters WR. Advances in bovine tuberculosis diagnosis and pathogenesis: what policy makers need to know. *Vet Microbiol.* (2006) 112:181–90. doi: 10.1016/j.vetmic.2005.11.028
  37. Widdison S, Schreuder LJ, Villarreal-Ramos B, Howard CJ, Watson M, Coffey TJ. Cytokine expression profiles of bovine lymph nodes: effects of *Mycobacterium bovis* infection and Bacille Calmette-Guérin vaccination. *Clin Exp Immunol.* (2006) 144:281–9. doi: 10.1111/j.1365-2249.2006.03053.x
  38. Dlugovitzky D, Bay ML, Rateni L, Fiorenza G, Vietti L, Farroni MA, et al. Influence of disease severity on nitrite and cytokine production by peripheral blood mononuclear cells (PBMC) from patients with pulmonary tuberculosis (TB). *Clin Exp Immunol.* (2000) 122:343–9. doi: 10.1046/j.1365-2249.2000.01394.x
  39. Blanco FC, Schierloh P, Bianco MV, Caimi K, Meikle V, Alito AE, et al. Study of the immunological profile towards *Mycobacterium bovis* antigens in naturally infected cattle. *Microbiol Immunol.* (2009) 53:460–7. doi: 10.1111/j.1348-0421.2009.00141.x
  40. Goosen WJ, Cooper D, Miller MA, van Helden PD, Parsons SDC. IP-10 is a sensitive biomarker of antigen recognition in whole-blood stimulation assays used for the diagnosis of *Mycobacterium bovis* infection in African buffaloes (*Syncerus caffer*). *Clin Vaccine Immunol.* (2015) 22:974–8. doi: 10.1128/CVI.00324-15
  41. Lyashchenko KP, Grandison A, Keskinen K, Sikar-Gang A, Lambotte P, Esfandiari J, et al. Identification of novel antigens recognized by serum antibodies in bovine tuberculosis. *Clin Vaccine Immunol.* (2017) 24:e00259–17. doi: 10.1128/CVI.00259-17
  42. Lyashchenko KP, Gortazar C, Miller MA, Waters WR. Spectrum of antibody profiles in tuberculous elephants, cervids, and cattle. *Vet Microbiol.* (2018) 214:89–92. doi: 10.1016/j.vetmic.2017.12.013
  43. Maas M, Michel AL, Rutten VPM G. Facts and dilemmas in diagnosis of tuberculosis in wildlife. *Comp Immunol Microbiol Infect Dis.* (2013) 36:269–85. doi: 10.1016/j.cimid.2012.10.010
  44. Miller MA, Gortazar C, Roos EO, Rialde MA, Johnathan-Lee A, Sridhara AA, et al. Serological reactivity to MPB83 and CFP10/ESAT-6 antigens in three suid hosts of *Mycobacterium bovis* infection. *Vet Microbiol.* (2019) 234:285–8. doi: 10.1016/j.vetmic.2019.07.018
  45. Roos EO, Olea-Popelka F, Buss P, de Klerk-Lorist LM, Cooper D, van Helden PD, et al. Seroprevalence of *Mycobacterium bovis* infection in warthogs (*Phacochoerus africanus*) in bovine tuberculosis-endemic regions of South Africa. *Transbound Emerg Dis.* (2018) 65:1182–9. doi: 10.1111/tbed.12856
  46. Sridhara AA, Johnathan-Lee A, Elahi R, Rialde MA, Gortazar C, Waters WR, et al. Strong antibody responses to *Mycobacterium bovis* infection in domestic pigs and potential for reliable serodiagnostics. *Vet Immunol Immunopathol.* (2021) 231:110161. doi: 10.1016/j.vetimm.2020.110161
  47. Miller M, Joubert J, Mathebula N, De Klerk-Lorist LM, Lyashchenko KP, Bengis R, et al. Detection of antibodies to tuberculosis antigens in free-ranging lions (*Panthera leo*) infected with *Mycobacterium bovis* in Kruger National Park, South Africa. *J Zoo Wildl Med.* (2012) 43:317–23. doi: 10.1638/2011-0171.1
  48. Lesellier S, Corner L, Costello E, Sleeman P, Lyashchenko K, Greenwald R, et al. Antigen specific immunological responses of badgers (*Meles meles*) experimentally infected with *Mycobacterium bovis*. *Vet Immunol Immunopathol.* (2008) 122:35–45. doi: 10.1016/j.vetimm.2007.11.005
  49. Lyashchenko KP, Sridhara AA, Johnathan-Lee A, Sikar-Gang A, Lambotte P, Esfandiari J, et al. Differential antigen recognition by serum antibodies from three bovid hosts of *Mycobacterium bovis* infection. *Comp Immunol Microbiol Infect Dis.* (2020) 69:101424. doi: 10.1016/j.cimid.2020.101424
  50. Corner LAL, Costello E, Lesellier S, O'Meara D, Sleeman DP, Gormley E. Experimental tuberculosis in the European badger (*Meles meles*) after endobronchial inoculation of *Mycobacterium bovis*: I. Pathology and bacteriology. *Res Vet Sci.* (2007) 83:53–62. doi: 10.1016/j.rvsc.2006.10.016
  51. Gormley E, Corner LAL. Pathogenesis of *Mycobacterium bovis* infection: the badger model as a paradigm for understanding tuberculosis in animals. *Front Vet Sci.* (2018) 4:247. doi: 10.3389/fvets.2017.00247
  52. Waters WR, Palmer MV, Thacker TC, Davis WC, Sreevatsan S, Coussens P, et al. Tuberculosis immunity: opportunities from studies with cattle. *J Immunol Res.* (2011) 2011:768542. doi: 10.1155/2011/768542
  53. Wedlock DN, Kawakami RP, Koach J, Buddle BM, Collins DM. Differences of gene expression in bovine alveolar macrophages infected with virulent and attenuated isogenic strains of *Mycobacterium bovis*. *Int Immunopharmacol.* (2006) 6:957–61. doi: 10.1016/j.intimp.2006.01.003
  54. Widdison S, Watson M, Piercy J, Howard C, Coffey TJ. Granulocyte chemotactic properties of *M. tuberculosis* versus *M. bovis*-infected bovine alveolar macrophages. *Mol Immunol.* (2008) 45:740–9. doi: 10.1016/j.molimm.2007.06.357
  55. Wallis RS, Pai M, Menzies D, Doherty TM, Walzl G, Perkins MD, et al. Biomarkers and diagnostics for tuberculosis: progress, needs, and translation into practice. *Lancet.* (2010) 375:1920–37. doi: 10.1016/S0140-6736(10)60359-5
  56. Kelley HV, Waibel SM, Sidiki S, Tomatis-Souverbille C, Scordo JM, Hunt WG, et al. Accuracy of two point-of-care tests for rapid diagnosis of bovine tuberculosis at animal level using non-invasive specimens. *Sci Rep.* (2020) 10:1–10. doi: 10.1038/s41598-020-62314-2
  57. Yerlikaya S, Broger T, MacLean E, Pai M, Denkiner CM. A tuberculosis biomarker database: the key to novel TB diagnostics. *Int J Infect Dis.* (2017) 56:253–7. doi: 10.1016/j.ijid.2017.01.025
  58. Chambers MA. Review of the diagnosis of tuberculosis in non-bovid wildlife species using immunological methods - an update of published work since 2009. *Transbound Emerg Dis.* (2013) 60:14–27. doi: 10.1111/tbed.12094
  59. Poste G. Bring on the biomarkers. *Nature.* (2011) 469:156–7. doi: 10.1038/469156a
  60. García JS, y, Bigi MM, Klepp LI, Blanco FC, Bigi F. Does *Mycobacterium bovis* persist in cattle in a non-replicative latent state as *Mycobacterium tuberculosis* in human beings? *Vet Microbiol.* (2020) 247:108758. doi: 10.1016/j.vetmic.2020.108758
  61. Good M, Bakker D, Duignan A, Collins DM. The history of *in vivo* tuberculin testing in bovines: tuberculosis, a “One Health” issue. *Front Vet Sci.* (2018) 5:59. doi: 10.3389/fvets.2018.00059
  62. Palmer MV, Waters WR, Thacker TC. Lesion development and immunohistochemical changes in granulomas from cattle experimentally infected with *Mycobacterium bovis*. *Vet Pathol.* (2007) 44:863–74. doi: 10.1354/vp.44-6-863
  63. Carrisoza-Urbina J, Morales-Salinas E, Bedolla-Alva MA, Hernández-Pando R, Gutiérrez-Pabello JA. Atypical granuloma formation in *Mycobacterium bovis*-infected calves. *PLoS ONE.* (2019) 14:e0218547. doi: 10.1371/journal.pone.0218547
  64. Domingo M, Vidal E, Marco A. Pathology of bovine tuberculosis. *Res Vet Sci.* (2014) 97:20–9. doi: 10.1016/j.rvsc.2014.03.017
  65. Palmer MV, Thacker TC, Waters WR, Gortazar C, Corner LAL. *Mycobacterium bovis*: a model pathogen at the interface of livestock, wildlife, and humans. *Vet Med Internatl.* (2012) 2012:236205. doi: 10.1155/2012/236205
  66. Viljoen IM, van Helden P, Millar RP. *Mycobacterium bovis* infection in the lion (*Panthera leo*): current knowledge,



- conundrums and research challenges. *Vet Microbiol.* (2015) 177:252–60. doi: 10.1016/j.vetmic.2015.03.028
67. Lesellier S, Corner L, Costello E, Sleeman P, Lyashchenko KP, Greenwald R, et al. Immunological responses following experimental endobronchial infection of badgers (*Meles meles*) with different doses of *Mycobacterium bovis*. *Vet Immunol Immunopathol.* (2009) 127:174–80. doi: 10.1016/j.vetimm.2008.09.012
  68. Chambers MA, Aldwell F, Williams GA, Palmer S, Gowtage S, Ashford R, et al. The effect of oral vaccination with *Mycobacterium bovis* BCG on the development of tuberculosis in captive European badgers (*Meles meles*). *Front Cell Infect Microbiol.* (2017) 7:6. doi: 10.3389/fcimb.2017.00006
  69. de la Rua-Domenech R, Goodchild AT, Vordermeier HM, Hewinson RG, Christiansen KH, Clifton-Hadley RS. Ante mortem diagnosis of tuberculosis in cattle: a review of the tuberculin tests,  $\gamma$ -interferon assay and other ancillary diagnostic techniques. *Res Vet Sci.* (2006) 81:190–210. doi: 10.1016/j.rvsc.2005.11.005
  70. Álvarez AH, Estrada-Chávez C, Flores-Valdez MA. Molecular findings and approaches spotlighting *Mycobacterium bovis* persistence in cattle. *Vet Res.* (2009) 40:22–36. doi: 10.1051/vetres/2009005
  71. Bezos J, Casal C, Romero B, Schroeder B, Hardegger R, Raebler AJ, et al. Current ante-mortem techniques for diagnosis of bovine tuberculosis. *Res Vet Sci.* (2014) 97:S44–52. doi: 10.1016/j.rvsc.2014.04.002
  72. Bernitz N, Kerr TJ, Goosen WJ, Higgitt RL, de Waal C, Clarke C, et al. Impact of *Mycobacterium bovis*-induced pathology on interpretation of QuantiFERON®-TB Gold assay results in African buffaloes (*Syncerus caffer*). *Vet Immunol Immunopathol.* (2019) 217:109923. doi: 10.1016/j.vetimm.2019.109923
  73. Vordermeier HM, Whelan A, Cockle PJ, Farrant L, Palmer N, Hewinson RG. Use of synthetic peptides derived from the antigens ESAT-6 and CFP-10 for differential diagnosis of bovine tuberculosis in cattle. *Clin Diagn Lab Immunol.* (2001) 8:571–8. doi: 10.1128/CDLI.8.3.571-578.2001
  74. Tomlinson AJ, Chambers MA, McDonald RA, Delahay RJ. Association of quantitative interferon- $\gamma$  responses with the progression of naturally acquired *Mycobacterium bovis* infection in wild European badgers (*Meles meles*). *Immunology.* (2015) 144:263–70. doi: 10.1111/imm.12369
  75. Thacker TC, Palmer MV, Waters WR. Correlation of cytokine gene expression with pathology in white-tailed deer (*Odocoileus virginianus*) infected with *Mycobacterium bovis*. *Clin Vaccine Immunol.* (2006) 13:640–7. doi: 10.1128/CVI.00024-06
  76. Thacker TC, Palmer MV, Waters WR. Associations between cytokine gene expression and pathology in *Mycobacterium bovis* infected cattle. *Vet Immunol Immunopathol.* (2007) 119:204–13. doi: 10.1016/j.vetimm.2007.05.009
  77. Palmer MV, Thacker TC, Waters WR. Analysis of cytokine gene expression using a novel chromogenic *in-situ* hybridization method in pulmonary granulomas of cattle infected experimentally by aerosolized *Mycobacterium bovis*. *J Comp Pathol.* (2015) 153:150–9. doi: 10.1016/j.jcpa.2015.06.004
  78. Rhodes SG, Buddle BM, Hewinson RG, Vordermeier HM. Bovine tuberculosis: immune responses in the peripheral blood and at the site of active disease. *Immunology.* (2000) 99:195–202. doi: 10.1046/j.1365-2567.2000.00944.x
  79. Widdison S, Watson M, Coffey TJ. Correlation between lymph node pathology and chemokine expression during bovine tuberculosis. *Tuberculosis.* (2009) 89:417–22. doi: 10.1016/j.tube.2009.09.003
  80. Aranday-Cortes E, Hogarth PJ, Kaveh DA, Whelan AO, Villarreal-Ramos B, Lalvani A, et al. Transcriptional profiling of disease-induced host responses in bovine tuberculosis and the identification of potential diagnostic biomarkers. *PLoS ONE.* (2012) 7:e30626. doi: 10.1371/journal.pone.0030626
  81. Waters WR, Maggioli MF, Palmer MV, Thacker TC, McGill JL, Vordermeier HM, et al. Interleukin-17A as a biomarker for bovine tuberculosis. *Clin Vaccine Immunol.* (2016) 23:168–80. doi: 10.1128/CVI.00637-15
  82. Elnaggar MM, Abdellrazek GS, Elsisy A, Mahmoud AH, Shyoub A, Sester M, et al. Evaluation of antigen specific interleukin-1 $\beta$  as a biomarker to detect cattle infected with *Mycobacterium bovis*. *Tuberculosis.* (2017) 105:53–9. doi: 10.1016/j.tube.2017.04.009
  83. Olivier TT, Viljoen IM, Hofmeyr J, Hausler GA, Goosen WJ, Tordiffe ASW, et al. Development of a gene expression assay for the diagnosis of *Mycobacterium bovis* infection in African lions (*Panthera leo*). *Transbound Emerg Dis.* (2017) 64:774–81. doi: 10.1111/tbed.12436
  84. Gao X, Guo X, Li M, Jia H, Lin W, Fang L, et al. Interleukin 8 and pentaxin (C-reactive protein) as potential new biomarkers of bovine tuberculosis. *J Clin Microbiol.* (2019) 57:e00274–19. doi: 10.1128/JCM.00274-19
  85. Vordermeier HM, Villarreal-Ramos B, Cockle PJ, McAulay M, Rhodes SG, Thacker T, et al. Viral booster vaccines improve *Mycobacterium bovis* BCG-induced protection against bovine tuberculosis. *Infect Immun.* (2009) 77:3364–73. doi: 10.1128/IAI.00287-09
  86. Blanco FC, Bianco MV, Meikle V, Garbaccio S, Vagnoni L, Forrellad M, et al. Increased IL-17 expression is associated with pathology in a bovine model of tuberculosis. *Tuberculosis.* (2011) 91:57–63. doi: 10.1016/j.tube.2010.11.007
  87. McGill JL, Sacco RE, Baldwin CL, Telfer JC, Palmer MV, Ray Waters W. Specific recognition of mycobacterial protein and peptide antigens by  $\gamma\delta$  T cell subsets following infection with virulent *Mycobacterium bovis*. *J Immunol.* (2014) 192:2756–69. doi: 10.4049/jimmunol.1302567
  88. Steinbach S, Vordermeier HM, Jones J. GCD4+ and  $\psi$ T Cells are the main producers of IL-22 and IL-17A in lymphocytes from *Mycobacterium bovis*-infected cattle. *Sci Rep.* (2016) 6:29990. doi: 10.1038/srep29990
  89. Xin T, Gao X, Yang H, Li P, Liang Q, Hou S, et al. Limitations of using IL-17A and IFN- $\gamma$ -induced protein 10 to detect bovine tuberculosis. *Front Vet Sci.* (2018) 5:28. doi: 10.3389/fvets.2018.00028
  90. Ray Waters W, Palmer MV. *Mycobacterium bovis* infection of cattle white-tailed deer: translational research of relevance to human tuberculosis. *ILAR J.* (2015) 56:26–43. doi: 10.1093/ilar/ilv001
  91. Rusk RA, Palmer MV, Waters WR, McGill JL. Measuring bovine  $\gamma\delta$  T cell function at the site of *Mycobacterium bovis* infection. *Vet Immunol Immunopathol.* (2017) 193–4:38–49. doi: 10.1016/j.vetimm.2017.10.004
  92. Aranday-Cortes E, Bull NC, Villarreal-Ramos B, Gough J, Hicks D, Ortiz-Peláez Á, et al. Upregulation of IL-17A, CXCL9 and CXCL10 in early-stage granulomas induced by *Mycobacterium bovis* in cattle. *Transbound Emerg Dis.* (2013) 60:525–37. doi: 10.1111/j.1865-1682.2012.01370.x
  93. Palmer MV, Thacker TC, Waters WR. Differential cytokine gene expression in granulomas from lungs and lymph nodes of cattle experimentally infected with aerosolized *Mycobacterium bovis*. *PLoS ONE.* (2016) 11:e0167471. doi: 10.1371/journal.pone.0167471
  94. Canal AM, Pezzone N, Cataldi A, Zumarraga M, Larzabal M, Garbaccio S, et al. Immunohistochemical detection of pro-inflammatory and anti-inflammatory cytokines in granulomas in cattle with natural *Mycobacterium bovis* infection. *Res Vet Sci.* (2017) 110:34–9. doi: 10.1016/j.rvsc.2016.10.006
  95. Thomas J, Risalde MÁ, Serrano M, Sevilla I, Geijo M, Ortiz JA, et al. The response of red deer to oral administration of heat-inactivated *Mycobacterium bovis* and challenge with a field strain. *Vet Microbiol.* (2017) 208:195–202. doi: 10.1016/j.vetmic.2017.08.007
  96. Blanco FC, Bigi F, Soria MA. Identification of potential biomarkers of disease progression in bovine tuberculosis. *Vet Immunol Immunopathol.* (2014) 160:177–83. doi: 10.1016/j.vetimm.2014.04.008
  97. Gonzalez-Juarrero M, Bosco-Lauth A, Podell B, Soffler C, Brooks E, Izzo A, et al. Experimental aerosol *Mycobacterium bovis* model of infection in goats. *Tuberculosis.* (2013) 93:558–64. doi: 10.1016/j.tube.2013.05.006
  98. Roos EO, Olea-Popelka F, Buss P, de Klerk-Lorist LM, Cooper D, Warren RM, et al. IP-10: a potential biomarker for detection of *Mycobacterium bovis* infection in warthogs (*Phacochoerus africanus*). *Vet Immunol Immunopathol.* (2018) 201:43–8. doi: 10.1016/j.vetimm.2018.05.007
  99. Parsons SDC, McGill K, Doyle MB, Goosen WJ, Van Helden PD, Gormley E. Antigen-specific IP-10 release is a sensitive biomarker of *Mycobacterium bovis* infection in cattle. *PLoS ONE.* (2016) 11:e0155440. doi: 10.1371/journal.pone.0155440
  100. Roos EO, Scott LA, Ndou S, Olea-Popelka F, Buss PE, de Klerk-Lorist LM, et al. Cytokine gene expression assay as a diagnostic tool for detection of *Mycobacterium bovis* infection in warthogs (*Phacochoerus africanus*). *Sci Rep.* (2019) 9:16525. doi: 10.1038/s41598-019-53045-0
  101. Sylvester TT, Martin LE, Buss P, Loxton AG, Hausler GA, Rossouw L, et al. Prevalence and risk factors for *Mycobacterium bovis* infection in African lions (*Panthera leo*) in the Kruger National Park. *J Wildl Dis.* (2017) 53:372–6. doi: 10.7589/2016-07-159
  102. Higgitt RL, Buss PE, van Helden PD, Miller MA, Parsons SDC. Development of gene expression assays measuring immune



- responses in the spotted hyena (*Crocuta crocuta*). *Afr Zool.* (2017) 52:99–104. doi: 10.1080/15627020.2017.1309300
103. Kerr TJ, Gumbo R, Goosen WJ, Rogers P, Last RD, Miller MA. Novel techniques for detection of *Mycobacterium bovis* infection in a cheetah. *Emerg Infect Dis.* (2020) 26:630. doi: 10.3201/eid2603.191542
  104. Denis M, Buddle BM. Iron modulates the replication of virulent *Mycobacterium bovis* in resting and activated bovine and possum macrophages. *Vet Immunol Immunopathol.* (2005) 107:189–99. doi: 10.1016/j.vetimm.2005.04.010
  105. Palmer MV. Emerging understanding of tuberculosis and the granuloma by comparative analysis in humans, cattle, zebrafish, nonhuman primates. *Vet Pathol.* (2018) 55:8–10. doi: 10.1177/0300985817712795
  106. Clegg TA, Doyle M, Ryan E, More SJ, Gormley E. Characteristics of *Mycobacterium bovis* infected herds tested with the interferon-gamma assay. *Prev Vet Med.* (2019) 168:52–9. doi: 10.1016/j.prevetmed.2019.04.004
  107. Buddle BM, Keen D, Thomson A, Jowett G, McCarthy AR, Heslop J, et al. Protection of cattle from bovine tuberculosis by vaccination with BCG by the respiratory or subcutaneous route, but not by vaccination with killed *Mycobacterium vaccae*. *Res Vet Sci.* (1995) 59:10–6. doi: 10.1016/0034-5288(95)90023-3
  108. Waters WR, Whelan AO, Lyashchenko KP, Greenwald R, Palmer MV, Harris BN, et al. Immune responses in cattle inoculated with *Mycobacterium bovis*, *Mycobacterium tuberculosis*, or *Mycobacterium kansasii*. *Clin Vaccine Immunol.* (2010) 17:247–52. doi: 10.1128/CI.00442-09
  109. Pesciaroli M, Russo M, Mazzone P, Aronica V, Fiasconaro M, Boniotti MB, et al. Evaluation of the interferon-gamma (IFN- $\gamma$ ) assay to diagnose *Mycobacterium bovis* infection in pigs. *Vet Immunol Immunopathol.* (2012) 148:369–72. doi: 10.1016/j.vetimm.2012.06.020
  110. Bezos J, Casal C, Díez-Delgado I, Romero B, Liandris E, Álvarez J, et al. Goats challenged with different members of the *Mycobacterium tuberculosis* complex display different clinical pictures. *Vet Immunol Immunopathol.* (2015) 167:185–9. doi: 10.1016/j.vetimm.2015.07.009
  111. Bernitz N, Clarke C, Roos EO, Goosen WJ, Cooper D, van Helden PD, et al. Detection of *Mycobacterium bovis* infection in African buffaloes (*Syncerus caffer*) using QuantiFERON®-TB Gold (QFT) tubes and the Qiagen cattle type® IFN-gamma ELISA. *Vet Immunol Immunopathol.* (2018) 196:48–52. doi: 10.1016/j.vetimm.2017.12.010
  112. Smith K, Kleynhans L, Snyders C, Bernitz N, Cooper D, van Helden P, et al. Use of the MILLIPLEX® bovine cytokine/chemokine multiplex assay to identify *Mycobacterium bovis*-infection biomarkers in African buffaloes (*Syncerus caffer*). *Vet Immunol Immunopathol.* (2021) 231:110152. doi: 10.1016/j.vetimm.2020.110152
  113. Chileshe J, Roos EO, Goosen WJ, Buss P, Hausler G, Rossouw L, et al. An interferon-gamma release assay for the diagnosis of the *Mycobacterium bovis* infection in white rhinoceros (*Ceratotherium simum*). *Vet Immunol Immunopathol.* (2019) 217:109931. doi: 10.1016/j.vetimm.2019.109931
  114. Higgitt RL, van Schalkwyk OL, de Klerk-Lorist LM, Buss PE, Caldwell P, Rossouw L, et al. An interferon gamma release assay for the detection of immune sensitization to *Mycobacterium bovis* in African wild dogs (*Lycan pictus*). *J Wildl Dis.* (2018) 55:529–36. doi: 10.7589/2018-03-089
  115. Dalley D, Davé D, Lesellier S, Palmer S, Crawshaw T, Hewinson RG, et al. Development and evaluation of a gamma-interferon assay for tuberculosis in badgers (*Meles meles*). *Tuberculosis.* (2008) 88:235–43. doi: 10.1016/j.tube.2007.11.001
  116. Rhodes S, Holder T, Clifford D, Dexter I, Brewer J, Smith N, et al. Evaluation of gamma interferon and antibody tuberculosis tests in alpacas. *Clin Vaccine Immunol.* (2012) 19:1677–83. doi: 10.1128/CI.00405-12
  117. Rialde MÁ, Thomas J, Sevilla I, Serrano M, Ortiz JA, Garrido J, et al. Development and evaluation of an interferon gamma assay for the diagnosis of tuberculosis in red deer experimentally infected with *Mycobacterium bovis*. *BMC Vet Res.* (2017) 13:341. doi: 10.1186/s12917-017-1262-6
  118. Palmer MV, Waters WR, Whipple DL, Slaughter RE, Jones SL. Evaluation of an *in vitro* blood-based assay to detect production of interferon-gamma by *Mycobacterium bovis*-infected white-tailed deer (*Odocoileus virginianus*). *J Vet Diagn Invest.* (2004) 16:17–21. doi: 10.1177/104063870401600104
  119. Rodriguez-Campos S, Smith NH, Boniotti MB, Aranaz A. Overview and phylogeny of *Mycobacterium tuberculosis* complex organisms: implications for diagnostics and legislation of bovine tuberculosis. *Res Vet Sci.* (2014) 97:S5–19. doi: 10.1016/j.rvsc.2014.02.009
  120. Pereira AC, Reis AC, Ramos B, Cunha MV. Animal tuberculosis: impact of disease heterogeneity in transmission, diagnosis and control. *Transbound Emerg Dis.* (2020) 67:1828–46. doi: 10.1111/tbed.13539
  121. Krajewska-Wedzina M, Didkowska A, Sridhara AA, Elahi R, Johnathan-Lee A, Radulski K, et al. Transboundary tuberculosis: importation of alpacas infected with *Mycobacterium bovis* from the United Kingdom to Poland and potential for serodiagnostic assays in detecting tuberculin skin test false-negative animals. *Trans Emerg Dis.* (2020) 2020:1–9. doi: 10.1111/tbed.13471
  122. O'Hare A, Orton RJ, Bessell PR, Kao RR. Estimating epidemiological parameters for bovine tuberculosis in British cattle using a Bayesian partial-likelihood approach. *Proc R Soc B Biol Sci.* (2014) 281:20140248. doi: 10.1098/rspb.2014.0248
  123. García-Jiménez WL, Fernández-Llario P, Gómez L, Benítez-Medina JM, García-Sánchez A, Martínez R, et al. Histological and immunohistochemical characterisation of *Mycobacterium bovis* induced granulomas in naturally infected Fallow deer (*Dama dama*). *Vet Immunol Immunopathol.* (2012) 149:66–75. doi: 10.1016/j.vetimm.2012.06.010
  124. Silva Miranda M, Breiman A, Allain S, Deknuydt F, Altare F. The tuberculous granuloma: an unsuccessful host defence mechanism providing a safety shelter for the bacteria? *Clin Dev Immunol.* (2012) 2012:139127. doi: 10.1155/2012/139127
  125. Whittaker E, Gordon A, Kampmann B. Is IP-10 a better biomarker for active and latent tuberculosis in children than IFN- $\gamma$ ? *PLoS ONE.* (2008) 3:e3901. doi: 10.1371/journal.pone.0003901
  126. Qiu X, Tang Y, Yue Y, Zeng Y, Li W, Qu Y, et al. Accuracy of interferon- $\gamma$ -induced protein 10 for diagnosing latent tuberculosis infection: a systematic review and meta-analysis. *Clin Microbiol Infect.* (2019) 25:667–72. doi: 10.1016/j.cmi.2018.12.006
  127. Waters WR, Thacker TC, Nonnecke BJ, Palmer MV, Schiller I, Oesch B, et al. Evaluation of gamma interferon (IFN- $\gamma$ )-induced protein 10 responses for detection of cattle infected with *Mycobacterium bovis*: comparisons to IFN- $\gamma$  responses. *Clin Vaccine Immunol.* (2012) 19:346–51. doi: 10.1128/CI.05657-11
  128. Schenk M, Fabri M, Krutzik SR, Lee DJ, Vu DM, Sieling PA, et al. Interleukin-1 $\beta$  triggers the differentiation of macrophages with enhanced capacity to present mycobacterial antigen to T cells. *Immunology.* (2014) 141:174–80. doi: 10.1111/imm.12167
  129. López V, González-Barrio D, Lima-Barbero JF, Ortiz JA, Domínguez L, Juste R, et al. Oral administration of heat-inactivated *Mycobacterium bovis* reduces the response of farmed red deer to avian and bovine tuberculin. *Vet Immunol Immunopathol.* (2016) 172:21–5. doi: 10.1016/j.vetimm.2016.03.003
  130. Swami SK, Vijay A, Nagarajan G, Kaur R, Srivastava M. Molecular characterization of pro-inflammatory cytokines interleukin-1 $\beta$  and interleukin-8 in Asian elephant (*Elephas maximus*). *An Biotech.* (2016) 27:66–76. doi: 10.1080/10495398.2015.1088449
  131. Krupa A, Fol M, Dziadek BR, Kepka E, Wojciechowska D, Brzostek A, et al. Binding of CXCL8/IL-8 to *Mycobacterium tuberculosis* modulates the innate immune response. *Mediators Inflamm.* (2015) 2015:124762. doi: 10.1155/2015/124762
  132. Wu B, Huang C, Kato-Maeda M, Hopewell PC, Daley CL, Krensky AM, et al. Messenger RNA expression of IL-8, FOXP3, and IL-12 $\beta$  differentiates latent tuberculosis infection from disease. *J Immunol.* (2007) 178:3688–94. doi: 10.4049/jimmunol.178.6.3688
  133. Okamoto Yoshida Y, Umemura M, Yahagi A, O'Brien RL, Ikuta K, Kishihara K, et al. Essential role of IL-17A in the formation of a mycobacterial infection-induced granuloma in the lung. *J Immunol.* (2010) 184:4414–22. doi: 10.4049/jimmunol.0903332
  134. Shu D, Heiser A, Neil Wedlock D, Luo D, de Lisle GW, Buddle BM. Comparison of gene expression of immune mediators in lung and pulmonary lymph node granulomas from cattle experimentally infected with *Mycobacterium bovis*. *Vet Immunol Immunopathol.* (2014) 160:81–9. doi: 10.1016/j.vetimm.2014.03.017
  135. Jacobs M, Fick L, Allie N, Brown N, Ryffel B. Enhanced immune response in *Mycobacterium bovis* Bacille Calmette Guérin (BCG)-infected IL-10-deficient mice. *Clin Chem Lab Med.* (2005) 40:893–902. doi: 10.1515/CCLM.2002.158

136. Mehta PK, Dharra R, Thakur Z. Cattle as experimental model to study immunopathogenesis of tuberculosis. *Mycobact Dis.* (2017) 07:1000248. doi: 10.4172/2161-1068.1000248
137. Broughan JM, Crawshaw TR, Downs SH, Brewer J, Clifton-Hadley RS. *Mycobacterium bovis* infections in domesticated non-bovine mammalian species. Part 2: a review of diagnostic methods. *Vet J.* (2013) 198:346–51. doi: 10.1016/j.tvjl.2013.09.007
138. Chegou NN, Heyckendorf J, Walzl G, Lange C, Ruhwald M. Beyond the IFN- $\gamma$  horizon: biomarkers for immunodiagnosis of infection with *Mycobacterium tuberculosis*. *Eur Respir J.* (2014) 43:1472–86. doi: 10.1183/09031936.00151413
139. Zimpel CK, Patan,é J, Guedes A, de Souza RF, Silva-Pereira TT, Camargo N, et al. Global distribution and evolution of *Mycobacterium bovis* lineages. *Front Microbiol.* (2020) 11:843. doi: 10.3389/fmicb.2020.00843
140. de la Fuente J, Díez-Delgado I, Contreras M, Vicente J, Cabezas-Cruz A, Tobes R, et al. Comparative genomics of field isolates of *Mycobacterium bovis* and *M. caprae* provides evidence for possible correlates with bacterial viability and virulence. *PLoS Negl Trop Dis.* (2015) 9:e0004232. doi: 10.1371/journal.pntd.0004232
141. OIE (World Organisation of Animal Health). *Manual of Diagnostic Tests and Vaccines for Terrestrial Animals (Terrestrial Manual)*. 8th ed (2018). Available online at: <https://www.oie.int/standard-setting/terrestrial-manual/access-online/>
142. Landolfi JA, Mikota SK, Chosy J, Lyashchenko KP, Giri K, Gairhe K, et al. Comparison of systemic cytokine levels in *Mycobacterium* spp. seropositive and seronegative Asian elephants (*Elephas maximus*). *J Zoo Wildlife Med.* (2010) 41:445–55. doi: 10.1638/2009-0163.1
143. Coad M, Clefford D, Rhodes SG, Glyn Hewinson R, Martin Vordermeier H, Whelan AO. Repeat tuberculin skin testing leads to desensitisation in naturally infected tuberculous cattle which is associated with elevated interleukin-10 and decreased interleukin-1 beta responses. *Vet Res.* (2010) 41:14–24. doi: 10.1051/vetres/2009062
144. Churbanov A, Milligan B. Accurate diagnostics for bovine tuberculosis based on high-throughput sequencing. *PLoS ONE.* (2012) 7:e50147. doi: 10.1371/journal.pone.0050147

**Conflict of Interest:** The authors declare that the research was conducted in the absence of any commercial or financial relationships that could be construed as a potential conflict of interest.

Copyright © 2021 Smith, Kleynhans, Warren, Goosen and Miller. This is an open-access article distributed under the terms of the Creative Commons Attribution License (CC BY). The use, distribution or reproduction in other forums is permitted, provided the original author(s) and the copyright owner(s) are credited and that the original publication in this journal is cited, in accordance with accepted academic practice. No use, distribution or reproduction is permitted which does not comply with these terms.



# Local Pulmonary Immunological Biomarkers in Tuberculosis

Hazel Morrison\* and Helen McShane

The Jenner Institute, University of Oxford, Oxford, United Kingdom

## OPEN ACCESS

### Edited by:

Adam Penn-Nicholson,  
Foundation for Innovative New  
Diagnostics, Switzerland

### Reviewed by:

Warwick Britton,  
The University of Sydney, Australia  
Björn Corleis,  
Friedrich-Loeffler-Institute, Germany

### \*Correspondence:

Hazel Morrison  
hazel.morrison@ndm.ox.ac.uk

### Specialty section:

This article was submitted to  
Microbial Immunology,  
a section of the journal  
Frontiers in Immunology

**Received:** 12 December 2020

**Accepted:** 10 February 2021

**Published:** 05 March 2021

### Citation:

Morrison H and McShane H (2021)  
Local Pulmonary Immunological  
Biomarkers in Tuberculosis.  
Front. Immunol. 12:640916.  
doi: 10.3389/fimmu.2021.640916

Regardless of the eventual site of disease, the point of entry for *Mycobacterium tuberculosis* (*M.tb*) is via the respiratory tract and tuberculosis (TB) remains primarily a disease of the lungs. Immunological biomarkers detected from the respiratory compartment may be of particular interest in understanding the complex immune response to *M.tb* infection and may more accurately reflect disease activity than those seen in peripheral samples. Studies in humans and a variety of animal models have shown that biomarkers detected in response to mycobacterial challenge are highly localized, with signals seen in respiratory samples that are absent from the peripheral blood. Increased understanding of the role of pulmonary specific biomarkers may prove particularly valuable in the field of TB vaccines. Here, development of vaccine candidates is hampered by the lack of defined correlates of protection (COPs). Assessing vaccine immunogenicity in humans has primarily focussed on detecting these potential markers of protection in peripheral blood. However, further understanding of the importance of local pulmonary immune responses suggests alternative approaches may be necessary. For example, non-circulating tissue resident memory T cells ( $T_{RM}$ ) play a key role in host mycobacterial defenses and detecting their associated biomarkers can only be achieved by interrogating respiratory samples such as bronchoalveolar lavage fluid or tissue biopsies. Here, we review what is known about pulmonary specific immunological biomarkers and discuss potential applications and further research needs.

**Keywords:** tuberculosis, biomarkers, pulmonary, mucosal, vaccines

## INTRODUCTION

Tuberculosis (TB) remains one of the top ten causes of death worldwide. Around a quarter of the world's population are estimated to be infected with *Mycobacterium tuberculosis* (*M.tb*) (1). The World Health Organization's (WHO) End TB Strategy has set the goals of reducing TB incidence by 90% and TB deaths by 95% globally by 2035. If there is any chance of meeting these ambitious targets, new tools to combat this devastating disease will be needed. These include an urgent need for improved diagnostic tests, shorter treatment regimens and more effective vaccines (2).

The range of clinical phenotypes following *M.tb* exposure spans complete elimination of the pathogen through immunologically contained latent infection to active TB disease (3). This spectrum is governed by complex and incompletely understood interactions between the pathogen and host innate and adaptive immune responses. Innate immune mechanisms within the lung mucosa may be responsible for early clearance of *M.tb* bacilli prior to T-cell sensitization in exposed individuals who appear to be resistant to *M.tb* infection (4). Of those who do have presumed latent *M.tb* infection (LTBI), 5–10% of immunocompetent individuals go on to develop TB disease in their lifetime (5), with the remaining majority achieving immunological equipoise.

Incomplete knowledge of the desired immune responses needed to prevent either active disease or initial infection is one of the key barriers to effective vaccine development (6). It is well-characterized that a T-helper 1 (Th1) cell-mediated adaptive immune response is required, but insufficient, for protection (7, 8). Likewise, whilst antigen-specific interferon gamma (IFN- $\gamma$ ) plays a key role, the level of vaccine-induced IFN- $\gamma$  in the blood does not correlate with protection (9, 10). Understanding the host immune responses that are needed to confer adequate protection against *M.tb* would dramatically help in the development and prioritization of vaccines that induce these putative responses.

An immunological biomarker is a measurable characteristic of the immune system that can be assessed as an indicator of normal immune function, disease process, or response to a therapeutic intervention (11). Biomarkers of disease can be used in diagnosis and disease monitoring. Vaccines aim to induce an immunological response to prevent infection or reduce disease severity, termed protection. Biomarkers that are believed to correspond with this effect are termed immune correlates of protection (COP) (12) and form the main focus of biomarkers discussed in this review.

The majority of TB studies looking at biomarkers of protection, both from disease and from infection, have focussed on the peripheral blood compartment in humans and blood and lymphoid organs in animal models. Regardless of the site of active disease, the predominant route via which *M.tb* bacilli enter the body is via aerosol droplets that are deposited onto alveolar surfaces of the lungs (4). Systemic immunity does not necessarily reflect pulmonary immune responses in the bronchoalveolar spaces at this site of entry for *M.tb* in humans. Cells of both the innate (such as alveolar macrophages) and adaptive (such as tissue resident memory cells) components of the pulmonary immune system play an increasingly recognized role that may be interrogated in the search for markers of protection.

## INNATE IMMUNITY WITHIN THE LUNG

### Trained Immunity

Trained immunity refers to immunological memory within the innate immune system, leading to an augmented response to subsequent, often heterologous insults (13). Innate immune memory is induced in animals after vaccination with BCG (14, 15) although the precise mechanisms via which this occurs are still being studied. Studies of TB contacts show that despite high levels of exposure, up to 30–50% of individuals do not become infected with *M.tb*, as evidenced by non-reactive tuberculin skin tests and negative IFN- $\gamma$  release assay (IGRA) testing (16). BCG vaccination correlates with this state of immune protection, suggesting that BCG-potentiated innate immunity may contribute to early *M.tb* clearance (17).

Given this, it is unclear why, in mice, BCG does not protect against *M.tb* in the first 14 days post-challenge (18). The kinetics and role of the innate immune response need further study. Controlled human infection models with serial mucosal and systemic sampling allow us to define the kinetics of innate and adaptive immunity and may help us understand this further.

## Alveolar Macrophages

In CD4/CD8 T-cell knock out mice, subcutaneous BCG vaccination induces lasting protective immunity within 7 days, prior to any adaptive immune mechanisms (18). Cells from the lungs of vaccinated mice show a higher proportion of tissue resident macrophages (CD11b<sup>+</sup>F4/80<sup>+</sup>) compared to circulating monocytes. Following an infection, or in this case immunization, monocytes may differentiate into interstitial lung macrophages, which then self-perpetuate within the pulmonary compartment. This may represent a mechanism via which BCG induces innate immune memory within the lung (18).

Respiratory viral infection has been found to induce immune memory in lung resident mouse alveolar macrophages (AMs), which go on to produce accelerated levels of detectable neutrophil chemokines, such as CXCL1 and CXCL2 upon restimulation. These trained AMs protect against secondary bacterial infection, with a memory response that is not reliant on circulating monocytes (19).

In a recent model using T-cell depleted mice, mucosal, but not intramuscular, vaccination with an adenoviral-vectored vaccine expressing the *M.tb* antigen 85A resulted in upregulation of activation markers, such as MHC II, on alveolar and pulmonary interstitial macrophages. This corresponded with reduced *M.tb* burden after challenge and suggests that activated airway macrophages may play an important role in early *M.tb* control (20). Debate is ongoing about the precise role AM play in *M.tb* control. AMs do not readily express pro-inflammatory genes until 10 days after host *M.tb* infection, which may allow early mycobacterial replication (21). AM-depleted mice show defective granuloma formation, but increased recruitment of other phagocytic and cytotoxic cells to the lungs, with corresponding improved *M.tb* clearance (22).

AM have been shown to leave the alveolar space and transport *M.tb* to the lung interstitium in an IL-1 dependent manner, proliferating within the lung to form aggregates (23). Whether this represents the initiation of effective immunological control or the first step in *M.tb* dissemination is not clear. Systemic BCG immunization in mice has been shown to hasten this egress of *M.tb*-infected AM from the alveoli into the lung interstitium, increase attraction of monocyte-derived macrophages to the site of infection and promote the early transfer of *M.tb* from AM to other phagocytic cells (24). In humans, infant AM are less able to control *M.tb* replication *in vitro* than adult AM, which may partly explain their susceptibility to more severe, disseminated forms of TB disease. Infant AM were found to express lower levels of chemotactic cytokines including chemokine (C-X-C motif) ligand 9 (CXCL9), suggesting that failure of AM to recruit additional mononuclear cells to the site of infection may result in failure of initial *M.tb* control (25).

## Innate Lymphoid Cells

Innate lymphoid cells (ILCs) mediate protective immunity in a variety of tissues, including the lungs. Activated ILCs proliferate in the lungs of mice following mucosal BCG vaccination and lead to increased levels of IFN- $\gamma$  production (26).

Group 3 ILCs (ILC3s) have similar functionality to Th-17 cells, including production of IL-17 and IL-22. In a human



lung tissue explant model, ILC3s upregulate IL-22 and GM-CSF following *ex vivo* *M.tb* infection (27) and IL-22 producing ILCs have been shown to enhance phagolysosomal fusion leading to mycobacterial growth inhibition (28). Inhibition of phagolysosomal fusion is one of the key immune mechanisms whereby *M.tb* evades host immunity.

ILC3s proliferate in the lungs of *M.tb* infected mice, leading to early alveolar macrophage accumulation. ILC knockout mice showed loss of early AM-mediated *M.tb* control, which could be rescued by adoptive cell transfer (ACT) of lung ILCs from *M.tb*-infected control mice (29). ACT of ILC3s also prolonged the survival of diabetic *M.tb*-infected mice, with increased IL-22 production resulting in reduced lung epithelial damage (30). Loss of ILCs, in particular ILC3, leads to a decrease in AM recruitment within the lung and subsequent higher mycobacterial burden during *M.tb* infection (29).

Distinct populations of CD103-expressing ILC2 and ILC3s and CXCR5-expressing ILC3s have been identified in human *M.tb*-infected lung tissue (29). CXCR5 signaling is essential in the formation of inducible bronchus associated lymphoid tissue (iBALT). iBALT is seen surrounding granuloma formation in non-human primate (NHP) and humans with LTBI, but not TB disease (31). iBALT proliferation in the lungs of mice lacking lymph nodes and spleen may be sufficient to control *M.tb* infection (32).

These studies suggest that ILC3s in particular may have a protective role in early *M.tb* control, via CXCR5-dependant iBALT formation and the production of IL-22 and IL-17. Mouse models of intranasal BCG vaccination have shown a correlation between protection and levels of IL-17 producing cells within the lungs following *M.tb* challenge (33).

## Mucosal-Associated Invariant and $\gamma\delta$ T Cells

Mucosal-associated invariant T (MAIT) cells preferentially reside in mucosal tissues, including the pulmonary mucosa. They express pattern recognition receptors, conferring innate immune function, and secrete IFN- $\gamma$  following stimulation. In humans and NHPs, MAIT cells are enriched in the lungs and BAL fluid following *M.tb* infection and NHP MAITs express activation markers such as CD69 following both *M.tb* challenge and intradermal (ID) BCG vaccination (34, 35). In rhesus macaques, intravenous (IV) BCG vaccination induces pulmonary MAIT expansion, which corresponds with subsequent protection against *M.tb* challenge (36). Following *M.bovis* infection, MAIT cell deficient mice show higher bacterial colony forming units (CFUs) at early time points compared to wild-type mice (37), highlighting a potential role for MAITs in early mycobacterial clearance.

$\gamma\delta$  T-cells are defined by heterodimeric T-cell receptors (TCRs) composed of  $\gamma$  and  $\delta$  chains and are enriched in epithelial and mucosal tissues, including lung alveoli. The majority are activated in an MHC-independent manner and produce cytotoxic granules and canonical pro-inflammatory cytokines, including IFN- $\gamma$ , TNF- $\alpha$ , and IL-17. Their activation results in

killing of *M.tb* infected macrophages (38). Following bacterial infection, lung  $\gamma\delta$  T-cells in mice exhibit increased expression of activation markers such as CD69 and CD25, and proliferate by local expansion rather than recruitment from the periphery (39). In NHPs, expansion of lung  $\gamma\delta$  T-cells by selective vaccination reduces disease pathology and dissemination following *M.tb* challenge (40).

## ADAPTIVE PULMONARY IMMUNITY

### Lung Tissue Resident Memory Cells

Tissue resident memory cells ( $T_{RM}$ ) represent a distinct subset of lymphocytes. They share functional similarities with central and effector memory T-cells, but remain situated within localized tissue compartments and do not recirculate into the blood stream. They have been demonstrated at sites including the skin, intestines, urogenital tract, and lung mucosa (41–44). This positioning at key anatomical barrier sites means that  $T_{RM}$  can respond rapidly to potential infective stimuli and lung  $T_{RM}$  may signify the first line of adaptive cellular defense against specific respiratory pathogens, including *M.tb*.

Due to the highly vascular nature of the lungs, distinguishing genuine  $T_{RM}$ , truly resident in the lung mucosa, from blood lymphocytes that egress from the vasculature following a stimulus such as infection, is difficult. Mouse models, using techniques such as parabiosis and *in vivo* intravascular staining, have confirmed that true lung  $T_{RM}$  cells are identifiable and do not re-enter the peripheral circulation, in comparison to lymphoid memory T cells.

Many of the techniques employed in animal models to delineate  $T_{RM}$  from pulmonary vascular lymphocytes are not feasible in humans but have been crucial in confirming that biomarkers seen in humans correspond to  $T_{RM}$  specific markers identified in animals. Upregulation of CD69 is a key marker of  $T_{RM}$  activation at a variety of sites including the lung and results in inhibition of sphingosine 1-phosphate-mediated lymphocyte migration (45). Additionally, CD8<sup>+</sup>  $T_{RM}$  cells express the  $\alpha E\beta 7$  integrin heterodimer, identified by CD103 marker staining (46). Other significant markers of lung  $T_{RM}$  in both human and animal models include PD-1, CD44, CXCR3, and integrins including CD49a, CD11a, and VLA-4 (45), with KLRG-1 and CD62L downregulated (47). CD4<sup>+</sup>  $T_{RM}$  form a heterogeneous group, with some displaying an effector profile ( $T_{bet}^{+}$ ) and others appearing more regulatory ( $Foxp3^{hi}$  IL-10<sup>hi</sup>). In contrast, pulmonary CD8<sup>+</sup>  $T_{RM}$  cells appear more homogenous, expressing predominantly Th1 cytokines (48).

The key importance of these cells in animal models of respiratory infection has been shown in several studies. In murine adoptive transfer studies, CXCR3<sup>hi</sup>CD4<sup>+</sup> T-cells preferentially localize to the lung parenchyma and are better at controlling *M.tb* infection than their CX3CR1<sup>hi</sup>KLRG1<sup>hi</sup> equivalents which remain within the vasculature (47). Intranasal immunization of mice with a recombinant influenza A vaccine expressing the PR8.p25 Ag85B epitope led to the development CD4<sup>+</sup>  $T_{RM}$  throughout the lung parenchyma. Persistence of these cells following FTY720-induced intravascular lymphopaenia indicates true tissue-resident memory status, without reliance

on circulating cells, and was sufficient for protection against subsequent *M.tb* challenge (49).

Route of vaccination may alter the magnitude and character of the adaptive pulmonary immune response, but it is unclear if this will necessarily lead to improved overall protective efficacy. For example, airway mucosal boosting following parental priming with the subunit vaccine candidate H56:CAF01 results in a significant increase in pulmonary  $T_{RM}$  and early local T-cell responses, without conferring any additional protection against *M.tb* challenge (50). Intramuscular vaccination of mice with the adjuvanted subunit TB vaccine candidate ID-93 results in a systemic, TH1-dominated immune response. In contrast, following ID-93 intranasal immunization, a predominantly IL-17A-producing, TH-17 response is seen; with an increase in antigen specific  $CD4^+$   $T_{RM}$  in the lung and BAL fluid. Despite these differences, the level of protection conferred was equal across the different delivery methods (51). In a recent study, protection conferred by intra-tracheal administration of the fusion protein TB vaccine candidate, CysVac2, was associated with the induction of higher levels of antigen-specific  $CD4^+$  lung  $T_{RM}$ , expressing IL-17, and ROR $\gamma$ T (52).

While intradermal BCG vaccination is able to generate antigen-specific pulmonary  $T_{RM}$  in mice, mucosal BCG vaccination produces increased numbers of both  $CD4^+$  and  $CD8^+$   $T_{RM}$  and this corresponds with subsequent enhanced protection against *M.tb* challenge (48, 53). Mucosal transfer of sorted airway resident T-cells, in particular  $CD8^+$   $T_{RM}$ , from mucosally BCG-vaccinated mice provided increased protection against *M.tb* challenge in recipient mice (48). Non-human primates immunized with intravenous BCG were found to have significantly higher levels of  $CD69^+$  (with a subset of  $CD103^+$ ) lung parenchymal  $CD4^+$  T-cells than intradermal or aerosol immunized animals and this was associated with sterilizing immunity against *M.tb* challenge (36).

These findings suggest that vaccination routes and strategies which induce pulmonary  $CD4^+$  and  $CD8^+$   $T_{RM}$  may result in superior levels of protection. This may be one reason why levels of peripheral circulating antigen-specific T-cells do not adequately correlate with protection. Biomarkers of  $T_{RM}$  may be useful as correlates of vaccine induced protection, but would require a significant change in sampling methods to assess vaccine efficacy.

## Lung Mucosal Antibodies IgA

The role of the humoral immune system in TB control is uncertain. In humans, *M.tb* infection induces *M.tb*-specific IgA, as well as IgG, antibodies in BAL fluid, but their precise role and level of interaction with *M.tb* at the mucosal level remains unknown (54, 55).

Secretory Immunoglobulin A (sIgA) is the predominant isotype in mucosal secretions and may contribute to protection. Intranasal administration of purified human sIgA to mice leads to increased *M.tb* clearance and improved disease control (56). Knockout mice lacking the polymeric IgR receptor necessary for IgA transport to the respiratory mucosa are more susceptible to *M.tb* infection than wild-type mice (57). In a BCG challenge

model, IgA deficient mice are more susceptible to infection than wild-type (58).

## LINKING THE INNATE AND ADAPTIVE IMMUNE SYSTEM

A functional mycobacterial growth inhibition assay (MGIA), which measures the sum of the parts of the innate and adaptive immune response, may be a useful tool to facilitate vaccine development. Such a tool could also allow the interrogation of potential COP by depletion studies using serum, peripheral blood mononuclear cells (PBMCs) or other specific cell types. To date such an assay has been optimized for use in whole blood and PBMC (59, 60). Using mucosal samples in such an assay may further identify lung specific protective mechanisms in future.

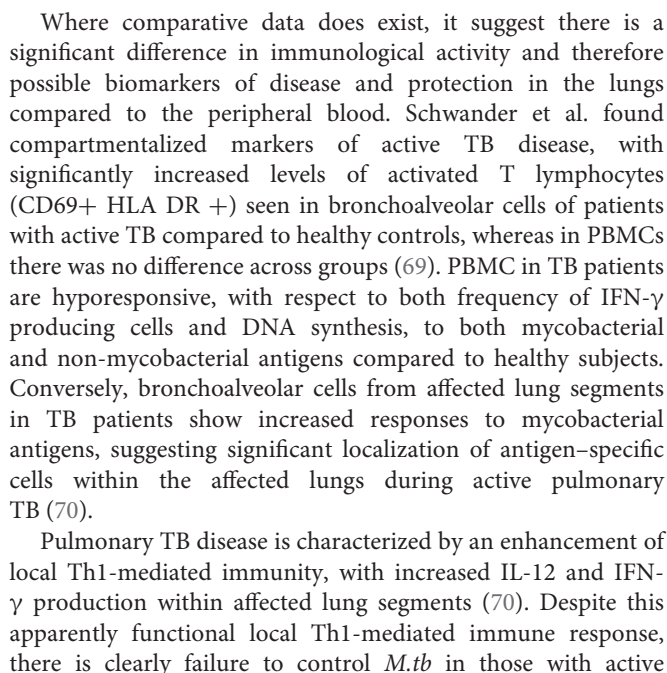
## INTERROGATING PULMONARY MUCOSAL IMMUNITY

Animal and human studies that focus on sampling the lung mucosal compartment will improve our understanding of lung mucosal immunity to *M.tb*. Parallel animal and human studies would allow more detailed interrogation of these processes. Delivery of vaccine candidates via aerosol routes has been shown to induce specific mucosal immune components that can be compared across species, with BAL samples from macaques and humans following aerosol MVA85A showing increased levels of antigen-specific cellular immune responses compared to peripheral blood (61–63). Further detailed mechanistic interrogation of lung-specific immunity is possible in the more tractable murine model (64, 65).

## Specific Challenges of Human Studies

The study of human lung immunity gives the opportunity to interrogate the interaction between the host and *M.tb* bacilli at the site of natural infection. However, significant barriers exist. Obtaining high quality respiratory samples for immunological analysis generally requires invasive sampling (see **Figure 1**). The scarcity of these resources in areas with the highest burdens of TB disease, coupled with the costs and ethical considerations of invasive sampling, may explain the relative lack of immunological studies focussing on the human pulmonary microenvironment (4).

How best to sample the human pulmonary compartment remains the subject of debate. Sputum (induced or spontaneous) is often too contaminated, for example with upper airway epithelial cells and microbes, to provide detailed immunological analysis of the lower respiratory tract. Bronchoalveolar lavage (BAL) can be used to obtain bronchoalveolar cells (66). Studies comparing BAL cells to lung tissue biopsies in healthy controls and TB patients suggest that BAL cells are a reasonable representation of lung cellular composition (67). However, this assumption may not hold true for HIV infected individuals, where significant depletion of lung interstitial  $CD4^+$  T cells may occur despite relatively normal  $CD4^+$  T cells levels in bronchoalveolar cells (68).



disease. Suppressive cytokines, including IL-4, TGF- $\beta$  and IL-10, are increased in bronchoalveolar cell samples of active TB compared with healthy controls (71) and may represent distinct local immunosuppressive mechanisms that interfere with Th1-mediated effectors in the bronchoalveolar environment. One difficulty in studying the respiratory mucosal immune response to *M.tb* infection in humans is the inability to define precisely the time of infection. Due to the varying clinical course and potential for latency, active disease may only be diagnosed months or years after the point of infection. In other diseases, such as influenza, malaria and typhoid, controlled human infection models (CHIMs) have been used to interrogate the immune response and can also be used to evaluate vaccine efficacy. Treatment for active TB disease requires a lengthy combination of potentially toxic medications, and proof of definitive cure may not be possible. For these reasons, a CHIM with *M.tb* would not be ethical. However, use of alternative mycobacterial models to mimic *M.tb* infection are being explored. For example, BCG may be used as a surrogate, as it does not cause active disease in immunocompetent humans but is a live replicating mycobacteria that stimulates an immune response. Interrogation of the

pulmonary mucosal immune response following a defined time point infection with BCG may lead to greater understanding of key immunological mechanisms, in particular in the early stages of infection.

Bronchoscopic instillation of BCG into lung segments of healthy, HIV-negative participants in South Africa with a range of TB phenotypes was shown to be safe and resulted in changes to differentially expressed genes and proteomics in the BAL fluid which were not detectable in the blood, suggesting a highly localized response (72). Studies in our group are ongoing to define the human innate and adaptive immune response to a defined time point challenge with aerosol BCG, and specifically comparing the peripheral and pulmonary compartment (Clinical trials.gov/NCT03912207). Parallel ongoing studies in non-human primates will add value to this work.

## DISCUSSION

Growing evidence shows that immunological responses are compartmentalized and biomarkers present in the peripheral blood may be poorly representative of important, local effects within the lungs. Innate, trained and adaptive components of the pulmonary immune system are likely to play an interconnected role in protection, with distinct features of lung mucosal immunity such as alveolar macrophages, BALT and T<sub>RM</sub> all warranting further investigation. The characterization of these immunological responses at the natural site of *M.tb* infection is of paramount importance, both in to increase our understanding of pathogenesis and more specifically to aid rational vaccine development.

Pre-clinical animal models play a key role in defining the pulmonary immune response to both *M.tb* and systemic and mucosally-delivered TB vaccines. Carefully designed small studies in humans can complement and add to these pre-clinical studies. Interrogating the initial stages of *M.tb* immunity in human lungs, for example in healthy household contacts, would have the potential to distinguish biomarkers of protective

immunity (COP) at the site of initial host contact with *M.tb*. Logistical and ethical difficulties in obtaining invasive human pulmonary sample in these circumstances mean that more novel investigative strategies may be needed.

Vaccine development in TB faces a paradox—a vaccine-induced COP can only be validated in large field trials of an effective vaccine. However, selection of which candidate vaccines to take forward for such costly trials requires some level of discrimination. As evidenced by the compartmentalized nature of immunological biomarkers in both human and animal models, peripheral blood biomarkers, whilst easier to obtain, may not be the best choice of read-out for rational vaccine selection.

CHIMs in healthy volunteers, either with BCG or potentially in future with rationally attenuated *M.tb* strains, may prove an alternative strategy to delineate human immunological response to a defined time point infection (73). Davids et al. human lung challenge model showed that responses to *in-vitro* and *in-vivo* PPD and BCG stimulation were significantly different, raising the prospect that the study of vaccine-induced immune biomarkers of protection may need to focus more on lung mycobacterial challenges and sampling, rather than peripheral blood (72). Given the considerable technical obstacles this approach faces, it could prove more likely that if pulmonary correlates of protection (or disease) are identified, systemic surrogate markers may be identifiable that can then be more easily appraised in future studies.

## AUTHOR CONTRIBUTIONS

HMo wrote the first draft of the manuscript. HMo and HMc contributed to manuscript revision and read and approved the submitted version.

## FUNDING

HMc is a Wellcome Trust Investigator (WT 206331/Z/17/Z). The views expressed are those of the author(s) and not necessarily those of the Wellcome Trust.

## REFERENCES

- Houben RM, Dodd PJ. The global burden of latent tuberculosis infection: a re-estimation using mathematical modelling. *PLoS Med.* (2016) 13:e1002152. doi: 10.1371/journal.pmed.1002152
- WHO. *Implementing the End TB Strategy: The Essentials*. Geneva: World Health Organisation; 2016.
- Basaraba RJ, Hunter RL. Pathology of tuberculosis: how the pathology of human tuberculosis informs and directs animal models. *Microbiol Spectr.* (2017) 5. doi: 10.1128/microbiolspec.TB2-0029-2016
- Schwander S, Dheda K. Human lung immunity against *Mycobacterium tuberculosis*: insights into pathogenesis and protection. *Am J Respir Crit Care Med.* (2011) 183:696–707. doi: 10.1164/rccm.201006-0963PP
- Comstock GW, Livesay VT, Woolpert SF. The prognosis of a positive tuberculin reaction in childhood and adolescence. *Am J Epidemiol.* (1974) 99:131–8. doi: 10.1093/oxfordjournals.aje.a121593
- Wilkie MEM, McShane H. TB vaccine development: where are we and why is it so difficult? *Thorax.* (2015) 70:299–301. doi: 10.1136/thoraxjnl-2014-205202
- Mogues T, Goodrich ME, Ryan L, LaCourse R, North RJ. The relative importance of T cell subsets in immunity and immunopathology of airborne *Mycobacterium tuberculosis* infection in mice. *J Exp Med.* (2001) 193:271–80. doi: 10.1084/jem.193.3.271
- Lyadova IV, Panteleev AV. Th1 and Th17 cells in tuberculosis: protection, pathology, and biomarkers. *Mediator Inflamm.* (2015) 2015:854507. doi: 10.1155/2015/854507
- Leal IS, Smedegård B, Andersen P, Appelberg R. Failure to induce enhanced protection against tuberculosis by increasing T-cell-dependent interferon-gamma generation. *Immunology.* (2001) 104:157–61. doi: 10.1046/j.1365-2567.2001.01305.x
- Mittrücker HW, Steinhoff U, Köhler A, Krause M, Lazar D, Mex P, et al. Poor correlation between BCG vaccination-induced T cell responses and protection against tuberculosis. *Proc Natl Acad Sci USA.* (2007) 104:12434–9. doi: 10.1073/pnas.0703510104
- Biomarkers and surrogate endpoints: preferred definitions and conceptual framework. *Clin Pharmacol Ther.* (2001) 69:89–95. doi: 10.1067/mcp.2001.113989



12. Plotkin SA. Correlates of protection induced by vaccination. *Clin Vaccine Immunol.* (2010) 17:1055–65. doi: 10.1128/CVI.00131-10
13. Netea MG, van der Meer JW. Trained Immunity: an Ancient Way of Remembering. *Cell Host Microbe.* (2017) 21:297–300. doi: 10.1016/j.chom.2017.02.003
14. Sakuma T, Suenaga T, Yoshida I, Azuma M. Mechanisms of enhanced resistance of *Mycobacterium bovis* BCG-treated mice to ectromelia virus infection. *Infect Immun.* (1983) 42:567–73. doi: 10.1128/IAI.42.2.567-573.1983
15. van 't Wout JW, Poell R, van Furth R. The role of BCG/PPD-activated macrophages in resistance against systemic candidiasis in mice. *Scand J Immunol.* (1992) 36:713–9. doi: 10.1111/j.1365-3083.1992.tb03132.x
16. Morrison J, Pai M, Hopewell PC. Tuberculosis and latent tuberculosis infection in close contacts of people with pulmonary tuberculosis in low-income and middle-income countries: a systematic review and meta-analysis. *Lancet Infect Dis.* (2008) 8:359–68. doi: 10.1016/S1473-3099(08)70071-9
17. Verrall AJ, Alisjahbana B, Apriani L, Novianty N, Nurani AC, van Laarhoven A, et al. Early clearance of *Mycobacterium tuberculosis*: the INFECT case contact cohort study in Indonesia. *J Infect Dis.* (2020) 221:1351–60. doi: 10.1093/infdis/jiz168
18. Bickett TE, McLean J, Creissen E, Izzo L, Hagan C, Izzo AJ, et al. Characterizing the BCG induced macrophage and neutrophil mechanisms for defense against *Mycobacterium tuberculosis*. *Front Immunol.* (2020) 11:1202. doi: 10.3389/fimmu.2020.01202
19. Yao Y, Jeyanthan M, Haddadi S, Barra NG, Vaseghi-Shanjani M, Damjanovic D, et al. Induction of autonomous memory alveolar macrophages requires T cell help and is critical to trained immunity. *Cell.* (2018) 175:1634–50.e17. doi: 10.1016/j.cell.2018.09.042
20. D'Agostino MR, Lai R, Afkhami S, Khera A, Yao Y, Vaseghi-Shanjani M, et al. Airway macrophages mediate mucosal vaccine-induced trained innate immunity against *Mycobacterium tuberculosis* in early stages of infection. *J Immunol.* (2020) 205:2750–62. doi: 10.4049/jimmunol.2000532
21. Rothchild AC, Olson GS, Nemeth J, Amon LM, Mai D, Gold ES, et al. Alveolar macrophages generate a noncanonical NRF2-driven transcriptional response to *Mycobacterium tuberculosis* in vivo. *Sci Immunol.* (2019) 4:eaaw6693. doi: 10.1126/sciimmunol.aaw6693
22. Leemans JC, Juffermans NP, Florquin S, van Rooijen N, Vervordeldonk MJ, Verbon A, et al. Depletion of alveolar macrophages exerts protective effects in pulmonary tuberculosis in mice. *J Immunol.* (2001) 166:4604. doi: 10.4049/jimmunol.166.7.4604
23. Cohen SB, Gern BH, Delahaye JL, Adams KN, Plumlee CR, Winkler JK, et al. Alveolar macrophages provide an early *Mycobacterium tuberculosis* niche and initiate dissemination. *Cell Host Microbe.* (2018) 24:439–46.e4. doi: 10.1016/j.chom.2018.08.001
24. Delahaye JL, Gern BH, Cohen SB, Plumlee CR, Shafiani S, Gerner MY, et al. Cutting edge: bacillus calmette-guérin-induced T cells shape *Mycobacterium tuberculosis* infection before reducing the bacterial burden. *J Immunol.* (2019) 203:807. doi: 10.4049/jimmunol.1900108
25. Goenka A, Prise IE, Connolly E, Fernandez-Soto P, Morgan D, Cavet JS, et al. Infant alveolar macrophages are unable to effectively contain *Mycobacterium tuberculosis*. *Front Immunol.* (2020) 11:486. doi: 10.3389/fimmu.2020.00486
26. Steigler P, Daniels NJ, McCulloch TR, Ryder BM, Sandford SK, Kirman JR. BCG vaccination drives accumulation and effector function of innate lymphoid cells in murine lungs. *Immunol Cell Biol.* (2018) 96:379–89. doi: 10.1111/imcb.12007
27. Maertzdorf J, Tönnies M, Lozza L, Schommer-Leitner S, Mollenkopf H, Bauer TT, et al. *Mycobacterium tuberculosis* Invasion of the human lung: first contact. *Front Immunol.* (2018) 9:1346. doi: 10.3389/fimmu.2018.01346
28. Dhiman R, Indramohan M, Barnes PF, Nayak RC, Paidipally P, Rao LV, et al. IL-22 produced by human NK cells inhibits growth of *Mycobacterium tuberculosis* by enhancing phagolysosomal fusion. *J Immunol.* (2009) 183:6639–45. doi: 10.4049/jimmunol.0902587
29. Ardain A, Domingo-Gonzalez R, Das S, Kazer SW, Howard NC, Singh A, et al. Group 3 innate lymphoid cells mediate early protective immunity against tuberculosis. *Nature.* (2019) 570:528–32. doi: 10.1038/s41586-019-1276-2
30. Tripathi D, Radhakrishnan RK, Sivangala Thandi R, Paidipally P, Devalraju KP, Neela VSK, et al. IL-22 produced by type 3 innate lymphoid cells (ILC3s) reduces the mortality of type 2 diabetes mellitus (T2DM) mice infected with *Mycobacterium tuberculosis*. *PLoS Pathog.* (2019) 15:e1008140. doi: 10.1371/journal.ppat.1008140
31. Stylianou E, Paul MJ, Reljic R, McShane H. Mucosal delivery of tuberculosis vaccines: a review of current approaches and challenges. *Exp Rev Vaccines.* (2019) 18:1271–84. doi: 10.1080/14760584.2019.1692657
32. Kashino SS, Vallerskog T, Martens G, Trout J, Keyser A, Taylor J, et al. Initiation of acquired immunity in the lungs of mice lacking lymph nodes after infection with aerosolized *Mycobacterium tuberculosis*. *Am J Pathol.* (2010) 176:198–204. doi: 10.2353/ajpath.2010.090446
33. Uranga S, Marinova D, Martin C, Aguilo N. Protective efficacy and pulmonary immune response following subcutaneous and intranasal BCG administration in mice. *J Vis Exp.* (2016) 19115. doi: 10.3791/54440
34. Gold MC, Napier RJ, Lewinsohn DM. MR1-restricted mucosal associated invariant T (MAIT) cells in the immune response to *Mycobacterium tuberculosis*. *Immunol Rev.* (2015) 264:154–66. doi: 10.1111/imr.12271
35. Greene JM, Dash P, Roy S, McMurtrey C, Awad W, Reed JS, et al. MR1-restricted mucosal-associated invariant T (MAIT) cells respond to mycobacterial vaccination and infection in nonhuman primates. *Mucosal Immunol.* (2017) 10:802–13. doi: 10.1038/mi.2016.91
36. Darrah PA, Zeppa JJ, Maiello P, Hackney JA, Wadsworth MH, 2nd, Hughes TK, et al. Prevention of tuberculosis in macaques after intravenous BCG immunization. *Nature.* (2020) 577:95–102. doi: 10.1038/s41586-019-1817-8
37. Chua WJ, Truscott SM, Eickhoff CS, Blazevic A, Hoft DF, Hansen TH. Polyclonal mucosa-associated invariant T cells have unique innate functions in bacterial infection. *Infect Immun.* (2012) 80:3256–67. doi: 10.1128/IAI.00279-12
38. Meraviglia S, El Daker S, Dieli F, Martini F, Martino A.  $\gamma\delta$  T cells cross-link innate and adaptive immunity in *Mycobacterium tuberculosis* infection. *Clin Dev Immunol.* (2011) 2011:587315. doi: 10.1155/2011/587315
39. Kirby AC, Newton DJ, Carding SR, Kaye PM. Evidence for the involvement of lung-specific gammadelta T cell subsets in local responses to *Streptococcus pneumoniae* infection. *Eur J Immunol.* (2007) 37:3404–13. doi: 10.1002/eji.200737216
40. Shen L, Frencher J, Huang D, Wang W, Yang E, Chen CY, et al. Immunization of V $\gamma$ 2V $\delta$ 2 T cells programs sustained effector memory responses that control tuberculosis in nonhuman primates. *Proc Natl Acad Sci USA.* (2019) 116:6371–8. doi: 10.1073/pnas.1811380116
41. Masopust D, Choo D, Vezys V, Wherry EJ, Duraiswamy J, Akondy R, et al. Dynamic T cell migration program provides resident memory within intestinal epithelium. *J Exp Med.* (2010) 207:553–64. doi: 10.1084/jem.20090858
42. Teijaro JR, Turner D, Pham Q, Wherry EJ, Lefrançois L, Farber DL. Cutting edge: tissue-retentive lung memory CD4<sup>+</sup>T cells mediate optimal protection to respiratory virus infection. *J Immunol.* (2011) 187:5510–4. doi: 10.4049/jimmunol.1102243
43. Mackay LK, Rahimpour A, Ma JZ, Collins N, Stock AT, Hafon ML, et al. The developmental pathway for CD103(+)CD8<sup>+</sup> tissue-resident memory T cells of skin. *Nat Immunol.* (2013) 14:1294–301. doi: 10.1038/ni.2744
44. Mackay LK, Stock AT, Ma JZ, Jones CM, Kent SJ, Mueller SN, et al. Long-lived epithelial immunity by tissue-resident memory T (TRM) cells in the absence of persisting local antigen presentation. *Proc Natl Acad Sci USA.* (2012) 109:7037–42. doi: 10.1073/pnas.1202288109
45. Kumar BV, Ma W, Miron M, Granot T, Guyer RS, Carpenter DJ, et al. Human tissue-resident memory T cells are defined by core transcriptional and functional signatures in lymphoid and mucosal sites. *Cell Rep.* (2017) 20:2921–34. doi: 10.1016/j.celrep.2017.08.078
46. Wu T, Hu Y, Lee YT, Bouchard KR, Benecet A, Khanna K, et al. Lung-resident memory CD8<sup>+</sup>T cells (TRM) are indispensable for optimal cross-protection against pulmonary virus infection. *J Leukoc Biol.* (2014) 95:215–24. doi: 10.1189/jlb.0313180
47. Sakai S, Kauffman KD, Schenkel JM, McBerry CC, Mayer-Barber KD, Masopust D, et al. Cutting edge: control of *Mycobacterium tuberculosis* infection by a subset of lung parenchyma-homing CD4<sup>+</sup>T cells. *J Immunol.* (2014) 192:2965–9. doi: 10.4049/jimmunol.1400019

48. Perdomo C, Zedler U, Kühl AA, Lozza L, Saikali P, Sander LE, et al. Mucosal BCG vaccination induces protective lung-resident memory T cell populations against tuberculosis. *mBio*. (2016) 7:e01686–16. doi: 10.1128/mBio.01686-16
49. Flórido M, Muflihah H, Lin LCW, Xia Y, Sierro F, Palendira M, et al. Pulmonary immunization with a recombinant influenza A virus vaccine induces lung-resident CD4(+) memory T cells that are associated with protection against tuberculosis. *Mucosal Immunol*. (2018) 11:1743–52. doi: 10.1038/s41385-018-0065-9
50. Woodworth JS, Christensen D, Cassidy JP, Agger EM, Mortensen R, Andersen P. Mucosal boosting of H56:CAF01 immunization promotes lung-localized T cells and an accelerated pulmonary response to *Mycobacterium tuberculosis* infection without enhancing vaccine protection. *Mucosal Immunol*. (2019) 12:816–26. doi: 10.1038/s41385-019-0145-5
51. Orr MT, Beebe EA, Hudson TE, Argilla D, Huang PW, Reese VA, et al. Mucosal delivery switches the response to an adjuvanted tuberculosis vaccine from systemic TH1 to tissue-resident TH17 responses without impacting the protective efficacy. *Vaccine*. (2015) 33:6570–8. doi: 10.1016/j.vaccine.2015.10.115
52. Counoupas C, Ferrell KC, Ashhurst A, Bhattacharyya ND, Nagalingam G, Stewart EL, et al. Mucosal delivery of a multistage subunit vaccine promotes development of lung-resident memory T cells and affords interleukin-17-dependent protection against pulmonary tuberculosis. *NPJ Vaccines*. (2020) 5:105. doi: 10.1038/s41541-020-00255-7
53. Bull NC, Stylianou E, Kaveh DA, Pinpathomrat N, Pasricha J, Harrington-Kandt R, et al. Enhanced protection conferred by mucosal BCG vaccination associates with presence of antigen-specific lung tissue-resident PD-1(+) KLRG1(-) CD4(+) T cells. *Mucosal Immunol*. (2019) 12:555–64. doi: 10.1038/s41385-018-0109-1
54. Demkow U, Białas-Chromiec B, Filewska M, Sobiecka M, Kuś J, Szturmowicz M, et al. Humoral immune response against mycobacterial antigens in bronchoalveolar fluid from tuberculosis patients. *J Physiol Pharmacol*. (2005) 56(Suppl 4):79–84.
55. Raja A, Baughman RP, Daniel TM. The detection by immunoassay of antibody to mycobacterial antigens and mycobacterial antigens in bronchoalveolar lavage fluid from patients with tuberculosis and control subjects. *Chest*. (1988) 94:133–7. doi: 10.1378/chest.94.1.133
56. Alvarez N, Otero O, Camacho F, Borrero R, Tirado Y, Puig A, et al. Passive administration of purified secretory IgA from human colostrum induces protection against *Mycobacterium tuberculosis* in a murine model of progressive pulmonary infection. *BMC Immunol*. (2013) 14(Suppl 1):S3. doi: 10.1186/1471-2172-14-S1-S3
57. Tjärnlund A, Rodríguez A, Cardona PJ, Guirado E, Ivanyi J, Singh M, et al. Polymeric IgR knockout mice are more susceptible to mycobacterial infections in the respiratory tract than wild-type mice. *Int Immunol*. (2006) 18:807–16. doi: 10.1093/intimm/dx1017
58. Rodríguez A, Tjärnlund A, Ivanji J, Singh M, García I, Williams A, et al. Role of IgA in the defense against respiratory infections IgA deficient mice exhibited increased susceptibility to intranasal infection with *Mycobacterium bovis* BCG. *Vaccine*. (2005) 23:2565–72. doi: 10.1016/j.vaccine.2004.11.032
59. Fletcher HA, Tanner R, Wallis RS, Meyer J, Manjaly ZR, Harris S, et al. Inhibition of mycobacterial growth *in vitro* following primary but not secondary vaccination with *Mycobacterium bovis* BCG. *Clin Vaccine Immunol*. (2013) 20:1683–9. doi: 10.1128/CI.00427-13
60. Tanner R, O'Shea MK, White AD, Müller J, Harrington-Kandt R, Matsumiya M, et al. The influence of haemoglobin and iron on *in vitro* mycobacterial growth inhibition assays. *Sci Rep*. (2017) 7:43478. doi: 10.1038/srep43478
61. Satti I, Meyer J, Harris SA, Manjaly Thomas ZR, Griffiths K, Antrobus RD, et al. Safety and immunogenicity of a candidate tuberculosis vaccine MVA85A delivered by aerosol in BCG-vaccinated healthy adults: a phase 1, double-blind, randomised controlled trial. *Lancet Infect Dis*. (2014) 14:939–46. doi: 10.1016/S1473-3099(14)70845-X
62. White AD, Sibley L, Dennis MJ, Gooch K, Betts G, Edwards N, et al. Evaluation of the safety and immunogenicity of a candidate tuberculosis vaccine, MVA85A, delivered by aerosol to the lungs of macaques. *Clin Vaccine Immunol*. (2013) 20:663–72. doi: 10.1128/CI.00690-12
63. Manjaly Thomas ZR, Satti I, Marshall JL, Harris SA, Lopez Ramon R, Hamidi A, et al. Alternate aerosol and systemic immunisation with a recombinant viral vector for tuberculosis, MVA85A: a phase I randomised controlled trial. *PLoS Med*. (2019) 16:e1002790. doi: 10.1371/journal.pmed.1002790
64. Stylianou E, Harrington-Kandt R, Beglov J, Bull N, Pinpathomrat N, Swarbrick GM, et al. Identification and evaluation of novel protective antigens for the development of a candidate tuberculosis subunit vaccine. *Infect Immun*. (2018) 86:1–16. doi: 10.1128/IAI.00014-18
65. Kaveh DA, Garcia-Pelayo MC, Bull NC, Sanchez-Cordon PJ, Spiropoulos J, Hogarth PJ. Airway delivery of both a BCG prime and adenoviral boost drives CD4 and CD8 T cells into the lung tissue parenchyma. *Sci Rep*. (2020) 10:18703. doi: 10.1038/s41598-020-75734-x
66. Helmers RA, Dayton CS, Floerchinger C, Hunninghake GW. Bronchoalveolar lavage in interstitial lung disease: effect of volume of fluid infused. *J Appl Physiol*. (1989) 67:1443–6. doi: 10.1152/jappl.1989.67.4.1443
67. Law KF, Jagirdar J, Weiden MD, Bodkin M, Rom WN. Tuberculosis in HIV-positive patients: cellular response and immune activation in the lung. *Am J Respir Crit Care Med*. (1996) 153(4 Pt 1):1377–84. doi: 10.1164/ajrcrm.153.4.8616569
68. Corleis B, Bucsan AN, Deruaz M, Vrbanc VD, Lisanti-Park AC, Gates SJ, et al. HIV-1 and SIV infection are associated with early loss of lung interstitial CD4+ T cells and dissemination of pulmonary tuberculosis. *Cell Rep*. (2019) 26:1409–18.e5. doi: 10.1016/j.celrep.2019.01.021
69. Schwander SK, Sada E, Torres M, Escobedo D, Sierra JG, Alt S, et al. T Lymphocytic and immature macrophage alveolitis in active pulmonary tuberculosis. *J Infect Dis*. (1996) 173:1267–72. doi: 10.1093/infdis/173.5.1267
70. Schwander SK, Torres M, Sada E, Carranza C, Ramos E, Tary-Lehmann M, et al. Enhanced responses to *Mycobacterium tuberculosis* antigens by human alveolar lymphocytes during active pulmonary tuberculosis. *J Infect Dis*. (1998) 178:1434–45. doi: 10.1086/314454
71. Herrera MT, Torres M, Nevells D, Perez-Redondo CN, Ellner JJ, Sada E, et al. Compartmentalized bronchoalveolar IFN-gamma and IL-12 response in human pulmonary tuberculosis. *Tuberculosis*. (2009) 89:38–47. doi: 10.1016/j.tube.2008.08.002
72. Davids M, Pooran A, Hermann C, Mottay L, Thompson F, Cardenas J, et al. A Human lung challenge model to evaluate the safety and immunogenicity of PPD and live bacillus Calmette-Guérin. *Am J Respir Crit Care Med*. (2020) 201:1277–91. doi: 10.1164/rccm.201908-1580OC
73. McShane H. Controlled human infection models: is it really feasible to give people tuberculosis? *Am J Respir Crit Care Med*. (2020) 201:1180–1. doi: 10.1164/rccm.201912-2408ED

**Conflict of Interest:** The authors declare that the research was conducted in the absence of any commercial or financial relationships that could be construed as a potential conflict of interest.

Copyright © 2021 Morrison and McShane. This is an open-access article distributed under the terms of the Creative Commons Attribution License (CC BY). The use, distribution or reproduction in other forums is permitted, provided the original author(s) and the copyright owner(s) are credited and that the original publication in this journal is cited, in accordance with accepted academic practice. No use, distribution or reproduction is permitted which does not comply with these terms.



# Male Sex Bias in Immune Biomarkers for Tuberculosis

Graham H. Bothamley<sup>1,2,3\*</sup>

<sup>1</sup> TB Team, Department of Respiratory Medicine, Homerton University Hospital, London, United Kingdom, <sup>2</sup> Faculty of Infectious and Tropical Diseases, London School of Hygiene and Tropical Medicine, London, United Kingdom, <sup>3</sup> Blizard Institute, Barts and The London School of Medicine and Dentistry, Queen Mary University of London, London, United Kingdom

## OPEN ACCESS

### Edited by:

Adam Penn-Nicholson,  
Foundation for Innovative New  
Diagnostics, Switzerland

### Reviewed by:

Sara Suliman,  
Brigham and Women's Hospital and  
Harvard Medical School,  
United States

Katie Louise Flanagan,  
RMIT University, Australia

### \*Correspondence:

Graham H. Bothamley  
g.bothamley@nhs.net

### Specialty section:

This article was submitted to  
Microbial Immunology,  
a section of the journal  
Frontiers in Immunology

**Received:** 12 December 2020

**Accepted:** 22 February 2021

**Published:** 16 March 2021

### Citation:

Bothamley GH (2021) Male Sex Bias in  
Immune Biomarkers for Tuberculosis.  
Front. Immunol. 12:640903.  
doi: 10.3389/fimmu.2021.640903

Males have a bias toward developing sputum smear-positive pulmonary tuberculosis, whereas other forms of the disease have an equal sex ratio. Immune responses are known to be affected by estrogen and testosterone. Biomarkers may therefore be affected by these hormones, especially between 16 and 45 years of age when the differences are most marked. Using large data sets, we examined whether the male bias was significant in terms of diagnosis or predictive ability for the development of disease in those exposed to tuberculosis. Despite the large numbers, the need to specify homogeneous population groups for analysis affected the statistical power to discount a useful biomarker. In general, males showed higher interferon-gamma responses to TB antigens ESAT-6 and CFP-10, whilst females had stronger tuberculin responses in those with sputum smear- and culture-positive tuberculosis, but smaller responses in those who were screened for tuberculosis and who did not develop disease. Importantly, in contacts of sputum smear-positive pulmonary tuberculosis, more males who did not develop tuberculosis had tuberculin skin tests in the range between 10 and 14 mm, suggesting that sex-specific cut-offs might be better than general cut-off values for determining who should receive preventive treatment. Immunocytochemistry of the tuberculin responses correlated with cell numbers only in females. Total and anti-lipoarabinomannan IgM antibody levels were lower in males, whereas total and anti-BCG IgE antibody levels were higher. Evaluation of biomarkers should take account of the spectrum of tuberculosis and male sex bias for sputum smear-positive pulmonary tuberculosis. These findings improve our understanding of how immune responses contribute to the pathogenesis of infectious tuberculosis as well as suggesting clinical applications of the differences between the sexes.

**Keywords:** sex-bias, tuberculosis, biomarkers, interferon-gamma release assay, delayed-type hypersensitivity, diagnosis, prognosis

## INTRODUCTION

Biomarkers are “intended as substitutes for a clinical endpoint... to predict clinical benefit (or harm) based on ... scientific evidence” (1). In tuberculosis, mycobacterial culture and identification of the species is the gold standard for diagnosis. The detection of DNA (e.g., Xpert MTB/RIF) or proteins (e.g., MPT64) found only in *Mycobacterium tuberculosis* (Mtb) can be seen as part of this process. One step removed is to use the immune system to amplify the signal, by measuring immune responses from T cells (e.g., interferon-gamma release assays, IGRAs) or B cells (antibody

to epitopes or antigens restricted to Mtb). The next step removed is to measure T cell or antibody responses to antigens that contain both specific and cross-reactive antigens (tuberculin purified protein derivative—PPD, Antigen60 or sonicated extracts of Mtb). A further step back may measure total antibody levels or inflammatory markers. Such proteomic measures may be involved in the causal outcome (clinical disease requiring treatment), to distinguish those forms of tuberculosis (TB) which require treatment compared to those that do not. Proteomic measures parallel clinical judgment from chest radiographs and symptoms, all of which may recommend further medical specific investigations for TB. However, at this distance from the causative organism, such markers may also represent tissue damage or be merely bystanders.

The term “subclinical disease” is variously used to identify those who have TB disease but either have no symptoms or who were only identified by active case finding. Clinicians would also use this term for those who present with negative bacteriology and a normal chest X-ray, who later develop active disease, e.g., those detected in contact tracing who then over the period of observation (usually 60–90 days after their first visit) develop disease that can be diagnosed microbiologically. This form of disease is common in those with HIV infection, where treatment with antiretroviral therapy (ART) reveals active TB. Separate to this category are those close contacts of an infectious case of TB who show immunological evidence of exposure to Mtb (loosely term latent tuberculosis infection—LTBI) and are offered preventive treatment or radiological follow-up over a year. “Incipient” tuberculosis, where there is “metabolic activity to indicate ongoing or impending progression of infection” (2), would include those with LTBI and raised inflammatory markers, including cytokines, or a signature transcriptome or metabolome. The term “diagnostic utility” includes identifying new cases of active TB for full treatment, those with recent contact and those screened for TB who are most likely to develop active for preventive treatment (better termed “prognostic utility”), and those where a combination of immunological, transcriptomic and proteomic tests suggests “incipient” TB for a clinical decision as to the mode of treatment.

The hypothesis was that immune responses known to be affected by estrogen and testosterone might affect the level and diagnostic utility of a biomarker especially in sputum smear- and culture-positive tuberculosis (S+PTB), where the male to female sex-ratio is of the order of 2:1 (3–8, and annual reports thereafter). In this analysis, the influence of sex-specific effects on T cell and antibody responses will be explored using data from publications whose purpose was to establish the role of these biomarkers in predicting or establishing a diagnosis of active TB.

## METHODS

### Data Sources

IGRA data were from the UK PREDICT TB study (9,870 records, a cohort study with follow-up of 2.5–7.6 years) (3), NIHR 4147 Blood Tests in Tuberculosis III (945 records, a cohort study with follow-up of at least 8 years) (4), Epitope-Specific Antibody Levels in Tuberculosis (747 records, a cohort

study with follow-up of at least two years) (5–8) and an in-depth study of Indonesians affected by tuberculosis and leprosy (349 records, a cross-sectional study) (9–11). These publications provide details on the methods of measurement of the T cell assays, immunocytochemistry and antibody levels and the ethical approvals of each study.

### Patient Selection

Children under 16 years of age were excluded from the data analysis. Where possible, females were selected as aged 16–45 years to exclude post-menopausal women without high estrogen levels. The reduction of testosterone with age is less abrupt and therefore analyses are specified as to whether the same cut-off as for females were used or whether the adult male population > 16 years was used. Pregnancy was an exclusion factor for the UK PREDICT TB study (3) and for analysis of other data.

Active tuberculosis was limited to those with sputum smear- and culture-positive pulmonary tuberculosis (S+PTB), as this form of tuberculosis is responsible for the difference in incidence between the sexes. However, one analysis looks at a combined population of smear-positive and smear-negative culture-positive pulmonary tuberculosis patients. The aim was to avoid any bias toward males, which often occurs due to the ease of sputum smear examination.

### Definition of Recent and Pre-Existing TB Exposure

Recent infection was defined as having a household contact of sputum-smear-positive pulmonary tuberculosis, with a positive IGRA, without HIV co-infection or previous tuberculosis. For more distant exposure, migrants from countries with an incidence of tuberculosis > 100 per 100,000, not born in the UK, without HIV co-infection, recent contact with or previous TB were selected.

### IGRAs

In assessing the QuantiFERON Gold-in-Tube (QFT) data, negative controls were assessed if  $\leq 8$  IU/mL (10 IU/mL = 12.04 ng/mL), as per the manufacturer's standard operating procedure. Similarly, only mitogen positive controls were evaluated if  $> 0.5$  IU/mL; all values in the 1000s were eliminated as being probably due to a transcribing error. Indeterminate results were not included in the denominators and did not contribute to the analysis. Cut-offs were determined by the manufacturer's cut-off (0.35 IU/mL for QFT) and the upper limit of the dilution curve for measuring IFN $\gamma$  ( $\geq 10$  IU/mL). The corresponding values for the TB-SPOT.TB test were defined according to the manufacturer's standard operating procedure as a negative control with  $\leq 10$  spots, an adequate positive (with mitogen) control as  $\geq 20$  spots and a positive test as  $\geq 8$  spots above the negative control; strong reactors were defined as those tests with  $> 100$  spots. Borderline tests were used only in assessing the prognostic utility, but were usually excluded together with indeterminate tests from the denominators.



## Tuberculin Responses

Tuberculin responses were grouped by mm of induration as in the ATS guidelines (12). The majority of responses were to tuberculin-PPD RT23. New tuberculin was prepared as a sonicated extract of Mtb, thereby including non-secreted proteins, lipid and polysaccharide antigens compared to tuberculin-PPD (13), and was used in the Indonesian study data and in examining the immunocytochemistry of the response to Mtb antigens (11). Where the areas of induration were used, these were calculated by multiplying the measurements in two axes (without dividing by  $\pi/2$ , if indurations were considered perfect ellipses). The “cut-offs” for immunocytochemistry were determined in relation to the delayed hypersensitivity responses from patients and controls, being the point at which the CD4+, CD8+, and CD14+ cell numbers began to rise; these corresponded to between 8 and 9 mm of induration to new tuberculin.

## Antibody Titers

Total IgM, IgG, and IgA were measured by laser nephelometry (11) and IgE levels by radioimmunoassay (10); cut-off titers were determined from normal reference ranges. Anti-BCG IgE levels were measured by radioallergoabsorbent test after competition with purified BCG antigen (10). IgM, IgG, and IgA levels to purified antigens were measured by ELISA (6) and epitope-specific antibody levels measured by a competition assay using monoclonal antibodies to the species-restricted epitopes (5, 7–9); cut-off titers were determined as the mean + 2SD of control samples. As data were normalized by log. transformation, zero values were noted separately under “diagnostic utility” in the tables.

## Statistical Analysis

Statistical analysis was performed using 2020 GraphPad Software. Student's t-test was employed for normalized data and the chi-squared test for diagnostic utility. Where the standard deviation was large, suggesting that the data had not been sufficiently

normalized by log. transformation, the Mann-Whitney *U*-test was used and *P*-values then relate to the latter test. Pearson's rank correlation was used to compared log. transformed values of PPD and new tuberculin, Spearman's rank correlation to compare antibody titers.

For diagnostic utility, a table of the number required for a power analysis relating to differences in sensitivity has been supplied (Table 1). *P*-values are given only where  $P < 0.1$  (comparable to a false detection rate of  $< 10\%$ ). The cut-offs were defined for each test as the manufacturer's chosen endpoints, the normal ranges or from the mean + 2SD for new tests. For the diagnosis of sputum smear- and culture-positive pulmonary tuberculosis, the discrimination of active from LTBI by IGRAs and tuberculin has not been calculated, noting the poor specificities from many past studies. The prognostic utility for predicting the development of TB was compared between males and females for sensitivity and specificity of the specified criterion. Receiver-Operator Characteristic (ROC) analysis was conducted using the web-based calculator of John Hopkins University, Baltimore (<http://www.jrocf.it.org>); differences between AUCs were assessed for significance using the online calculator [http://vassarstats.net/roc\\_comp.html](http://vassarstats.net/roc_comp.html).

## RESULTS

### Developing the Hypotheses

We conducted a systematic review of sex-related immune responses, using the comprehensive MeSH terms “estrogen,” “testosterone,” “sex,” “immune response,” without time limit. Titles and abstracts underwent a first screen; relevant articles were selected for a second screen, which included full text review. Most hormone-induced sex-specific immune responses have been studied in animal models and in relation to non-infectious diseases, such as autoimmunity (rheumatoid arthritis, lupus, extrinsic allergic encephalitis/multiple

**TABLE 1** | Sample sizes to detect differences according to sensitivity at  $P < 0.05$  and power of 80%.

	Sensitivity of test in females							80%	90%
	10%	20%	30%	40%	50%	60%	70%		
Difference <sup>a</sup>									
+5%									
Male	1004	1623	2053	2295	2348	2213	1890	1378	676
Female	502	812	1026	1148	1174	1106	945	689	338
+10%									
Male	287	431	529	579	582	538	447	308	NA
Female	144	216	264	290	291	269	224	154	
+15%									
Male	142	202	240	258	255	231	186	119	NA
Female	71	101	120	129	128	116	93	60	
+20%									
Male	87	118	137	145	141	124	96	NA	NA
Female	44	59	68	72	70	60	48		

<sup>a</sup> Assumes enrolment at usual male to female ratio in S+PTB of 2:1. + = males > females.

Where male sensitivity < females, same numbers apply but using sensitivity of test in females = (100–given sensitivity) in table.

**TABLE 2 |** Hypotheses derived from literature review of hormone-induced sex-specific immune responses.

Immune response	Diagnostic measure	Predictions <sup>a</sup>
<b>T cell</b>		
Spontaneous IFN $\gamma$ production	Negative control IGRA	F > M (14)
Mitogen IFN $\gamma$ production	Positive control IGRA	F > M (15, 16)
Antigen-specific IFN $\gamma$ production	IGRA test result	F > M (16)
Delayed hypersensitivity		
Tuberculin response	48 h induration to tuberculins	F > M
	Blood flow velocity	F > M
	Central necrosis/slow blood flow	Uncertain
Histopathology		
	CD4+ T cells	F > M (17, 18)
	CD8+ T cells	M > F (19, 20)
	Macrophages (CD14+)	M > F
<b>Antibody</b>		
Total	Globulin (g/L)	F > M (21, 22)
	IgM	F > M (22)
	IgG	No difference
	IgA	No difference
	IgE	M = F (23) or M > F (24)
Anti-mycobacterial antibody	IgEsp	M > F (25)
IgG antibody to purified antigens <sup>b</sup> (21)	38 kDa	F > M (26)
	32 kDa/Antigen 85B	Or M > F (27)
	30 kDa/Antigen 85A	
	Hsp16/16 kDa/	M > F (28)
	Hsp65	
	19 kDa	M > F (28–31)
	Lipoarabinomannan (LAM)	M > F (28–31)
Epitope-specific antibody	Competition assay with mAbs	
	Protein antigens	F > M (26)
	Anti-LAM antibodies	M > F (28)

<sup>a</sup> Hormone-induced sex-specific immune responses have been studied in models not closely related to tuberculosis.

<sup>b</sup> More antigens and higher antibody levels are found in patients with S+PTB, especially if there are lung cavities, both features of male disease.

sclerosis), estrogen receptor- $\alpha^+$  breast cancer or infections, such as lymphocytic choriomeningitis virus. The predictions listed in **Table 2** are therefore somewhat removed from the topic of human TB. The testing of these hypotheses in sputum smear- and culture-positive pulmonary tuberculosis may indicate whether further exploration of particular immune responses, in order to understand the male predominance of smear-positive pulmonary tuberculosis, is merited.

One of the difficulties in evaluating data from patients with TB is that selection of patients with different forms of the disease will affect the conclusions, depending on how many have S+PTB, where the male bias will then affect the data (32, 33). This can be especially problematic when comparing LTBI with active disease, where those with LTBI will have an equal sex ratio and active disease has a male predominance, e. g. NK cells are less in number in females than males and therefore associations with active TB may be sex-specific (34, 35).

## T Cell Responses

### Smear- and Culture-Positive Pulmonary Tuberculosis (S+PTB)

In general, IGRAs are not recommended for patients with symptoms and investigations suggesting pulmonary tuberculosis—a sputum smear is usually obtained! For this reason, there are few data and certainly numbers are insufficient to gain enough power to avoid a type II error of attributing a non-significant value as excluding the hypothesis of a difference between the sexes, even for a 20% difference (see **Table 1**).

Similarly, tuberculin testing would not normally be performed in those with sputum smear-positive pulmonary tuberculosis (S+PTB), except as part of a formal study, such as that in Indonesia comparing PPD-RT23 with new tuberculin [**Supplementary Figure 1**, (11)]. With both tuberculins, the diameters of induration were slightly higher in females, but only with new tuberculin did the differences approach statistical significance (**Table 3**:  $t = 1.8$ ,  $P = 0.07$ ). Females showed a greater

**TABLE 3 |** Sex and T cell responses in sputum smear- and culture-positive pulmonary tuberculosis (and sputum smear-positive OR negative but culture-positive pulmonary tuberculosis only where indicated).

Test	Females		Males		P-value	“Diagnostic” utility n (%)			
	n	Values	n	Values		Criterion	Females	Males	P-value
IGRA-QFT <sup>a</sup>									
TB antigen (positives only; log ± SD)	16		37			0-0.34 IU/mL	1 (6.3)	3 (8.1)	NS
	16	0.62 ± 0.549	34	0.54 ± 0.49	NS	≥ 0.35 IU/mL	15 (93.8)	34 (91.9)	NS
						≥ 10 IU/ml	6 (37.5)	9 (26.5)	NS
Culture-positive PTB: TB antigen (positives only; log ± SD)	32		62			0-0.34 IU/mL	5 (15.6)	6 (9.7)	NS
	27	0.55 ± 0.55	56	0.60 ± 0.57	NS	≥ 0.35 IU/mL	27 (84.4)	56 (90.3)	NS
						≥ 10 IU/ml	10 (31.3)	16 (25.8)	NS
Delayed hypersensitivity									
PPD-RT23 (mm induration ± SD)	57	17.4 ± 5.9	64	16.6 ± 4.9	NS	≥ 15	50 (87.7)	54 (84.4)	NS
						≥ 10	54 (94.7)	59 (92.2)	NS
						0	1 (1.8)	1 (1.6)	NS
New tuberculin (mm induration ± SD)	96	13.9 ± 3.6	115	12.9 ± 3.9	0.07	≥ 15	46 (47.9)	42 (36.5)	NS
						≥ 10	87 (90.6)	100 (87.0)	NS
						0	2 (2.1)	4 (3.5)	NS
Blood Flow velocity (V ± SD)	46	6.70 ± 2.30	55	5.81 ± 1.90	0.037				
Central slowing	46	NA	55	NA		Present	12 (26.1)	7 (12.7)	0.09
Immunocytochemistry (new tuberculin)									
CD4+ cells (log ± SD)	36	2.64 ± 0.23	45	2.62 ± 0.18	NS	2.82	10 (27.8)	9 (20.0)	0.09
CD8+ cells (log ± SD)	37	2.09 ± 0.39	46	2.00 ± 0.39	NS	2.22	17 (46.0)	13 (28.9)	0.11
CD14+ macrophages (log ± SD)	36	2.78 ± 0.18	45	2.73 ± 0.16	NS	3.02	2 (5.6)	0 (0)	NA

<sup>a</sup>Includes only those aged 16-45 year (for UK PREDICT TB study diagnosis of culture-positive pulmonary tuberculosis within 2 months of first screening).

blood flow velocity ( $t = 2.12$ ,  $P = 0.037$ ). Statistical significance had been observed, but only in HLA-DR15-negative subjects in the Indonesian study (tuberculin, females median 16.75 (range 4 to 22) vs. males 15 (11 to 20), Mann-Whitney  $U$ -test,  $P = 0.016$ ; blood flow velocity, females  $7.3 \pm 2.3$  vs. males  $5.7 \pm 1.8$ ,  $t = 2.12$ ,  $df = 31$ ,  $P = 0.04$ ) (36). The immunocytochemistry data showed a correlation between induration and CD4+, CD8+, and CD14+ cell numbers in females but not in males (Figure 1).

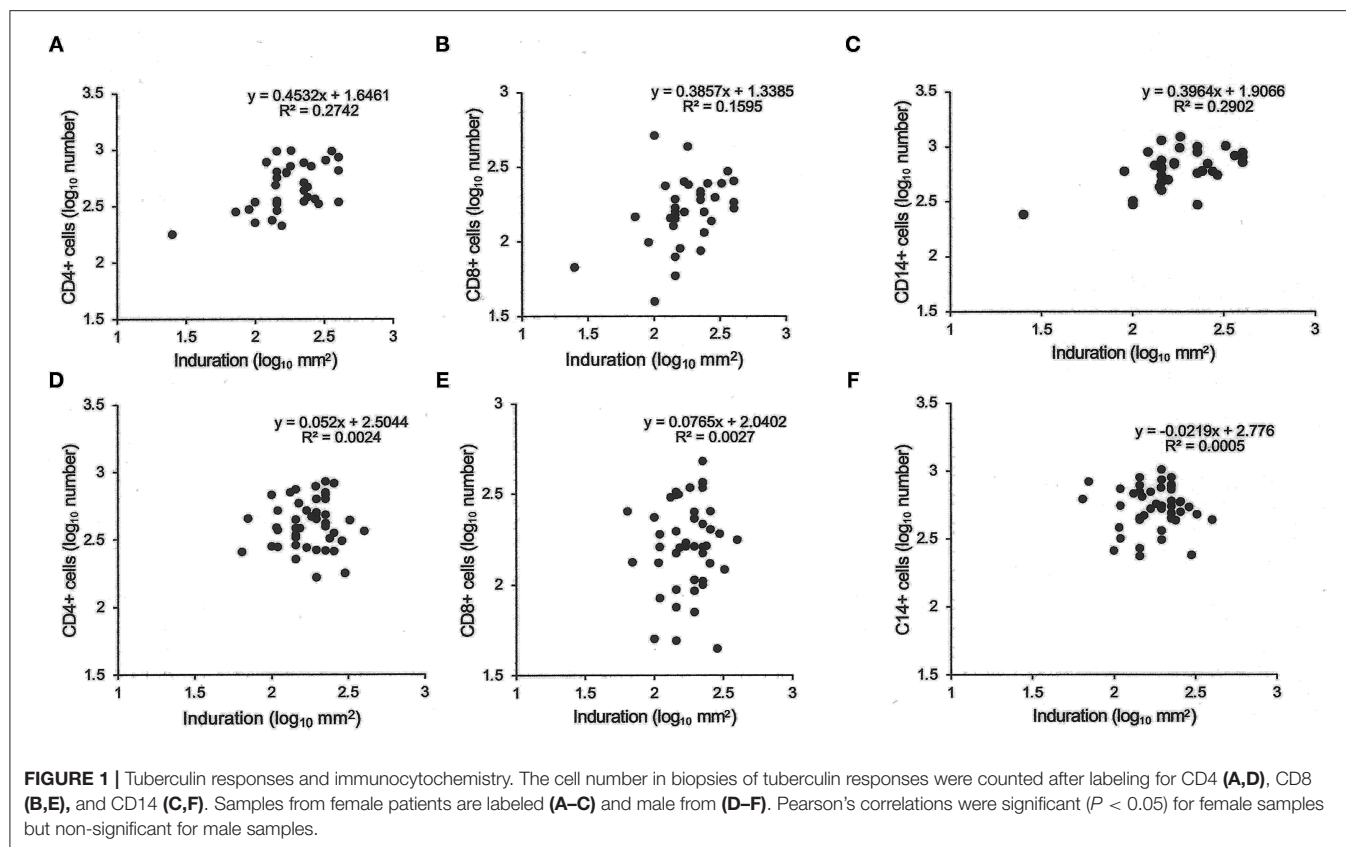
### Exposure to Tuberculosis

There were few differences between males and females in their QFT results (Table 4). In migrants who did not develop tuberculosis, males showed greater spontaneous IFN $\gamma$  production ( $t = 3.2$ ,  $P = 0.0013$ ; Table 4). Using a cut-off of  $\geq 0.35$  IU/mL, more males than females also had higher values ( $\chi^2 = 11.3$ ,  $P = 0.008$ ). However, if they went on to develop tuberculosis later, no difference was detected. IFN $\gamma$  values in response to mitogen were also greater in males than females. Males had a greater response to the RD1 antigens if they had a positive test and did not develop TB, whereas levels were lower, although not significantly so, in males compared to females who developed TB later. With the T-SPOT.TB test, the differences in titers were not significant, except for spontaneous IFN $\gamma$  production in migrants who had a negative result, where again males had higher values (Table 4). Fewer male contacts of infectious tuberculosis showed a complete lack of response to tuberculin and more males had positive responses as defined by the different cut-off indurations (Table 5). Males were also more

likely to have to have a tuberculin response  $\geq 5$  mm and less likely to be anergic (Table 5), even though males were less likely to have received BCG vaccination ( $\chi^2 = 10.5$ ,  $P = 0.001$ ). There was no effect of IGRA status on these differences between males and females.

### Antibody Levels

Total globulin levels did not differ between males and females aged 16–45 years. Total IgM was lower and IgE higher in males with sputum smear- and culture-positive tuberculosis. IgE anti-BCG antibody levels were measured using a radioallergoabsorbent assay (RAST), measuring the inhibition of binding of specific  $^{125}$ I-labeled anti-IgE by a standard preparation of sonicated BCG-Glaxo with five dilutions tested against a standard serum to establish a standard curve (10), and showed no significant difference in titers, although titers greater than  $10^3$  kU/L were more frequent in males than females (Table 6). There were limited data on IgM to purified antigens, but titers to lipoarabinomannan (LAM) were lower in males than females ( $t = 2.17$ ,  $P = 0.048$ ). Although IgG antibody levels to purified antigens, both proteins and LAM, and epitope-specific antibody levels to Mtb-restricted epitopes of these antigens (which do not distinguish class of antibody) showed a 1000-fold variation among individuals, no significant differences were found between the sexes. In an attempt to investigate the difference between males and females in their response to LAM, IgM, and IgG titers were ranked and compared to the ranked antibody titers to the ML34 epitope (all antibody classes assayed).



The ranked IgM titers compared to ranked ML34 minus ranked IgG correlated well in females but showed no relationship in males (females,  $\rho = 0.74$ ,  $P = 0.01$ , males  $\rho = 0.06$ ,  $P = 0.96$ ; **Figure 2**).

## Diagnostic and Prognostic Utility

There was no difference between males and females aged 16–45 years in the value of the tests examined in supporting the diagnosis of tuberculosis. However, male migrants were more likely to have a T-SPOT.TB test that recommended preventive treatment but, despite the lack of preventive treatment as specified in the protocol of the UK PREDICT TB study, were less likely to develop active disease (**Figure 3A**). In the UK PREDICT TB series, a cut-off of  $>15$  spots in females would not affect the number of TB cases identified but would prevent 32 from receiving unnecessary preventive treatment. For males, increasing the cut-off to 20 would have doubled the number of missed cases of TB from 6 to 12 at a benefit of reducing unnecessary preventive treatment in 99 migrants.

For contacts of sputum smear-positive pulmonary TB who did not develop TB, males were more likely to have indurations between 10 and 14 mm than females ( $\chi^2 = 4.8$ ,  $P = 0.03$ ; **Figure 3B**). For male contacts of S+PTB, raising the cut-off for preventive treatment to  $\geq 15$  mm would prevent 38 unnecessary treatments of LTBI, without affecting appropriate preventive treatment for those who went on to develop TB. Lowering the cut-off in females to  $< 10$  mm, would add 19

preventive treatments for those who didn't develop TB but identify a further case of TB [1/9 (11%) total TB cases] for whom preventive treatment would have been valuable. In male migrants, raising the cut-off to  $\geq 15$  mm would prevent unnecessary chemoprophylaxis for 142, but miss one case of TB [1/20 (5%)]. For females, lowering the cut-off to  $< 10$  mm would add 110 unnecessary treatments, but identify one [1/9 (11%) total cases of TB] for whom preventive treatment would be valuable.

## DISCUSSION

### Key Findings

Significant differences in levels of a biomarker may not translate into significant differences in diagnostic or prognostic utility and *vice versa*. This was especially important when assessing zero values or non-responders, when log. transformation is required to normalize a population result of responders (see **Table 4**). Secondly, despite having studies with almost 10,000 participants, the requirement to test hypotheses in homogeneous populations led to numbers that were only occasionally sufficient to have enough power to draw a statistical conclusion. This was especially important in addressing questions such as the predictive power of a biomarker to establish which of the infected population might develop active TB.

In terms of immune responses, the predictions that females would exhibit a more robust T cell and antibody response to infection (28) were only partially sustained. In order to



**TABLE 4 |** Sex and IGRAs after exposure to tuberculosis.

Test	Female 16-44 years		Males 16-44 years		P-value	“Diagnostic” utility <i>n</i> (%)			
	<i>n</i>	Values	<i>n</i>	Values		Criterion	Females	Males	P-value
IGRA-QFT <sup>a</sup>									
Contacts S+PTB (number)	297		161						
TB antigen (positive tests only—no TB; log ± SD)	51	0.48 ± 0.48	49	0.49 ± 0.49	NS	≥0.35	25 (16.1) <sup>b</sup>	33 (22.9) <sup>b</sup>	NS
TB antigen (positive tests only—TB; median, range)	5	2.72 (0, 9.2)	5	4.01 (1.74, 10)	NS	IU/mL	5 (71.4)	5 (83.3)	NS
Migrants									
Spontaneous IFN $\gamma$ (negative tests only; log ± SD)	953	−0.85 ± 0.33	1051	−0.80 ± 0.36	<0.0013		95 (10.0)	145 (13.8)	0.008
Spontaneous IFN $\gamma$ (positive tests only; log ± SD)	236	−0.74 ± 0.41	288	−0.66 ± 0.45	0.03	≥ 0.35/mL	44 (18.7)	63 (21.9)	NS
Mitogen IFN $\gamma$ (negative tests only; log ± SD)	823	1.14 ± 0.33	941	1.21 ± 0.30	<0.0001		652 (79.2)	822 (87.4)	<0.0001
Mitogen IFN $\gamma$ (positive tests only; log ± SD)	194	1.12 ± 0.33	244	1.19 ± 0.21	0.005	>10 IU/mL	130 (67.0)	185 (75.8)	0.042
TB antigen (positive tests only—no TB; log ± SD)	231	0.24 ± 0.47	287	0.39 ± 0.49	0.005		231 (20.2) <sup>b</sup>	287 (21.9) <sup>b</sup>	NS
TB antigen (TB developed: median, range)	10	2.88 (0, 8.76)	21	0.41 (0, 10)	NS	≥0.35 IU/mL	7 (70.0)	11 (52.4)	NS
T-SPOT.TB <sup>c</sup>									
Contacts S+PTB (number)	164		144			Positives	20 (13.0)	35 (24.8)	0.01
TB antigen [positive tests, no TB; median (range)]	20	28.5 (8, 320)	35	26 (8,195)	NS	TB later and	0	0	0
TB antigen [TB, positive tests: median (range)]	7	15 (0, 162)	5	75 (2, 164)	NS	positive	3 (42.9)	4 (80.0)	NS
Migrants									
Spontaneous IFN $\gamma$ (negative tests; median, range)	973	0 (0, 8)	968	0 (0, 8)	0.02	Positives	0	0	NA
Spontaneous IFN $\gamma$ (positive tests; median, range)	174	0 (0, 7)	268	0 (0, 8)	NS	Positives	0	0	NA
Mitogen IFN $\gamma$ (negative tests; median, range)	695	50 (20, 255)	760	50 (20, 265)	NS	≥ 100 spots	145 (20.9)	146 (19.2)	NS
Mitogen IFN $\gamma$ (positive tests; median, range)	116	50 (22, 231)	199	50 (24, 233)	NS	≥ 100 spots	17 (14.7)	22 (11.1)	NS
TB antigen (positive tests, no TB; median, range)	169	31 (8, 250)	263	32 (8, 398)	NS	Positives	169 (14.8)	263 (21.3)	0.00004
TB antigen (TB developed; median, range)	8	56 (16, 358)	14	25 (9, 193)	NS	TB later and positive	8 (80.0)	14 (70.0)	NS

<sup>a</sup> Contacts of S+PTB showed no difference in negative and positive controls, nor TB antigen values.

<sup>b</sup> QFT denominators UK PREDICT TB study only: for contacts of S+PTB were 164 (females) and 144 (males) and for migrants TB antigen QFT were 1,144 (female) and 1,311 (male).

<sup>c</sup> T-SPOT denominators UK PREDICT TB study only, excluding borderline and indeterminate results: for contacts of S+PTB were 154 (female) and 141 (male) and for migrants, spontaneous interferon- $\gamma$  was higher in males ( $\chi^2 = 5.4$  for those with visible spots compared to those with no spots,  $P = 0.02$ ) TB antigen data were 1,153 (females) and 1,254 (males).

**TABLE 5 |** Delayed hypersensitivity responses to tuberculin (PPD) during screening for tuberculosis.

Test	Females, 16-45 years		Males, 16-45 years		P-value	“Diagnostic” utility: n (%)			
	n	Induration (log mean ± SD)	n	Induration (log mean ± SD)		Criterion	Female	Male	P-value
Contacts S+PTB									
No TB	207		210			≥ 15	86 (41.5)	89 (42.4)	NS
	126	1.18 ± 0.22	147	1.18 ± 0.23	NS	≥ 10	105 (50.7)	127 (60.5)	0.045
						≥ 5	123 (59.4)	142 (67.6)	0.082
						0	81 (39.1)	63 (30.0)	0.05
TB developed later	8		6			≥ 15	4 (50.0)	4 (66.7)	NS
	7	1.17 ± 0.25	6	1.26 ± 0.19	NS	≥ 10	5 (62.5)	5 (83.3)	NS
						≥ 5	7 (87.5)	6 (100)	NS
						0	1 (12.5)	0 (0)	NS
Migrants									
No TB	1102		1183			≥ 15	157 (14.3)	177 (15.0)	NS
	514	0.92 ± 0.31	602	0.97 ± 0.27	NS	≥ 10	267 (24.2)	319 (27.0)	NS
						≥ 5	422 (38.3)	535 (45.2)	0.0008
						0	588 (53.4)	581 (49.1)	0.04
TB developed later	9		20			≥ 15	5 (55.6)	11 (55.5)	NS
	8	1.21 ± 0.13	15	1.18 ± 0.18	NS	≥ 10	7 (77.8)	13 (65.5)	NS
						≥ 5	8 (88.9)	15 (75.0)	NS
						0	1 (11.1)	5 (25.0)	NS
Treated TB	9		9			≥ 15	2 (22.2)	2 (22.2)	NS
	6	1.05 ± 0.26	8	1.01 ± 0.24	NS	≥ 10	5 (55.6)	6 (66.7)	NS
						≥ 5	6 (66.7)	7 (77.8)	NS
						0	3 (33.3)	1 (11.1)	NS

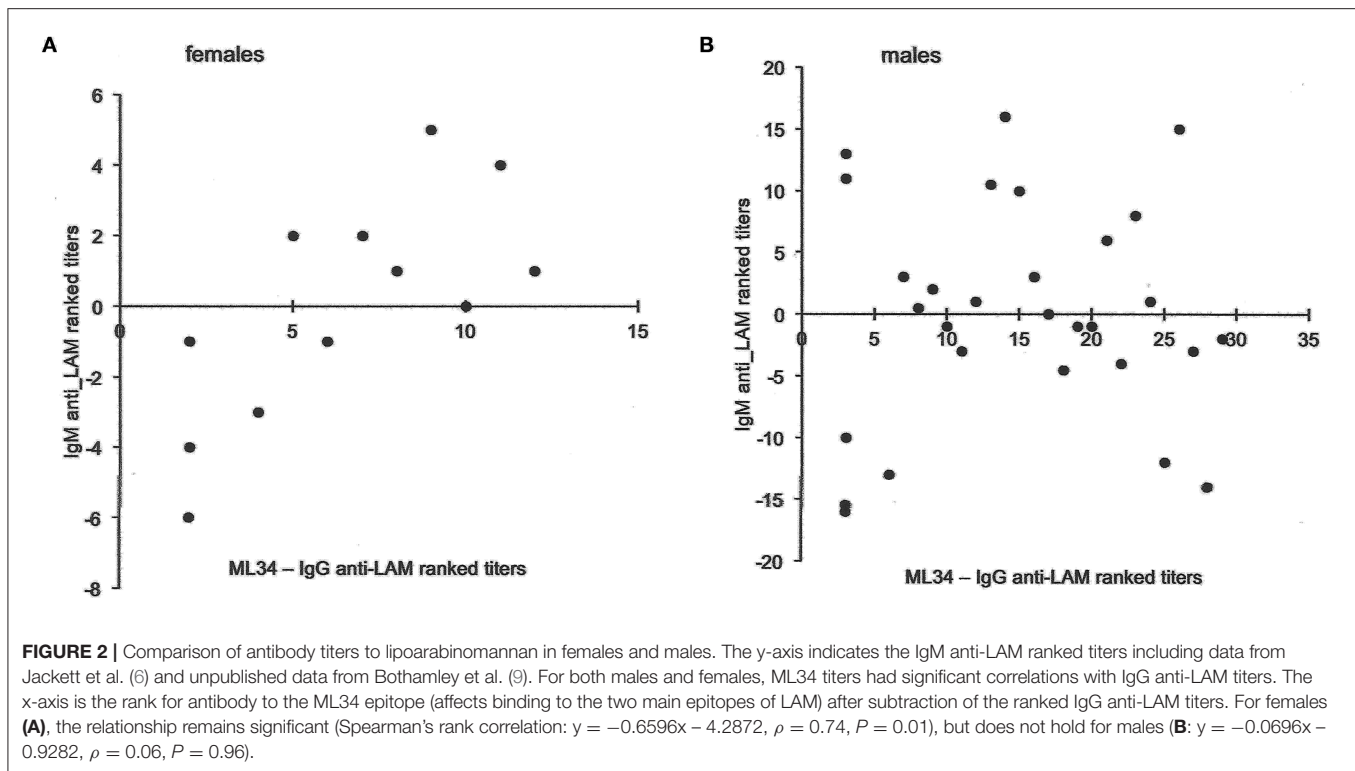
**TABLE 6 |** Sex differences in antibody levels in S+PTB.

Test	Female		Male		P-value	Criterion	Diagnostic utility: n (%)		
	n	Mean ± SD	n	Mean ± SD			F	M	P-value
Total globulin <sup>a</sup>									
Globulin (g/L)	76	42.0 ± 7.09	167	43.6 ± 7.04	NS	> 32 g/L	71 (93.4)	120 (95.2)	NS
Immunoglobulin class									
IgM (g/L: mean ± SD)	49	2.30 ± 0.69	61	1.80 ± 0.74	0.0004	> 2.5 g/L	15 (30.6)	8 (13.1)	0.025
IgG (g/L: mean ± SD)	49	25.20 ± 7.80	61	24.10 ± 8.90	NS	> 16 g/L	45 (91.8)	55 (90.2)	NS
IgA (g/L: mean ± SD)	49	5.36 ± 2.34	61	5.08 ± 1.92	NS	> 3g/L	40 (81.6)	55 (90.2)	NS
IgE (log IU/ml: mean ± SD)	48	2.82 ± 0.59	61	3.07 ± 0.64	0.038	> 320 U/L	33 (68.8)	50 (82.0)	NS
IgE anti-BCG antibody RAST (log. mean ± SD)	49	3.27 ± 0.95	61	3.52 ± 0.71	NS	>3	25 (51.0)	47 (77.0)	0.004
IgM to lipoarabinomannan <sup>a</sup>	11		15			0	6 (54.5)	4 (26.7)	NS
	5	2.28 ± 0.39	11	1.62 ± 0.62	0.048	>1.68	5 (45.5)	4 (26.7)	NS <sup>b</sup>

<sup>a</sup> Only ages 16-45 years.<sup>b</sup>  $\chi^2 = 5.7$ ,  $P = 0.017$  for those with any measurable titers.

avoid the effect of males having a higher incidence of TB, a greater TB burden and more lung inflammation, only males and females with sputum smear- and culture-positive pulmonary TB (S+PTB) or with culture-positive TB irrespective of smear status within the spectrum of active disease were each compared (Table 3). In S+PTB, the tuberculin responses of males showed lower blood flow velocities and there was a tendency to smaller areas of induration compared to females. In S+PTB, immunocytochemistry showed that females, but not males, gave a

positive correlation between induration and cell type. In contrast, looking at HIV-negative migrants not born in the UK without known contact with TB who did not develop active TB, males screened for tuberculosis showed fewer anergic responses and more tuberculin responses between 5 and 10 mm induration whilst females had more responses between 10 and 15 mm induration without developing TB. Males had higher IFN $\gamma$  levels both spontaneously and after mitogen stimulation (QFT only) and to TB antigens (T-SPOT.TB only) compared to females.



Males with S+PTB had higher globulin levels, but lower IgM antibody and higher IgE and anti-BCG IgE. No differences in antibody levels to species-restricted epitopes or their purified antigens were found, except for IgM to lipoarabinomannan, compared to females.

## Limitations

We have not included children on the grounds that the circulating hormonal differences between the sexes would be absent. We have not included data from those with HIV co-infection, on the grounds that the immune responses might differ due to their immune status rather than any sex-specific effect. The choice of 16–45 years was an estimation in the absence of data regarding female participants' menopause. The upper limit of > 100 spots in the T-SPOT.TB assay was only available for a selection of the population, as one laboratory in the UK PREDICT TB study did not measure the high control if samples had a count of > 20 spots.

A positive sputum smear usually short circuits the diagnostic process and IGRAs may therefore have indicated those with atypical features or from whom a sputum sample was difficult to obtain, but the sex ratio of tests did not differ from that of disease and there was a determined attempt to obtain immunological markers in all studies.

The selection of two homogenous populations screened for TB (household contacts of S+PTB without HIV co-infection or previous tuberculosis and migrants not born in the UK without HIV co-infection or previous tuberculosis

and with no recent TB contact) for analysis showed that even in aggregated large studies, the power to detect a significant difference and exclude a type II error may still be low.

## Sex-Related Differences in Tuberculosis Incidence and Infection Rate

One of the drivers of this analysis was the fact that sputum smear- and culture-positive tuberculosis (S+PTB) is found in males more than females (37). Some have ascribed the difference to an excess of social risk factors for developing TB (38). Others have estimated social contact to suggest that males have a greater chance of being infected with TB (39). However, these analyses do not account for the form of tuberculosis. The UK national surveys of tuberculosis (40–45) indicated that only in S+PTB is there a male predominance, but no sex predominance was noted for extra-pulmonary and smear-negative pulmonary TB. These surveys have the advantage that access to healthcare is free and possible gender bias in its uptake in fact shows a female preference. A comparison between active and passive case-finding in India showed the same male predominance in those with S+PTB, again suggesting that this is a real biological difference rather than being related to healthcare access (46). Our data show that although more male migrants were identified than females, the rate of positive QFTs did not differ, although for the T-SPOT.TB there were more positive tests. The rate of progression to active disease in the UK PREDICT TB data (3) did not differ between the

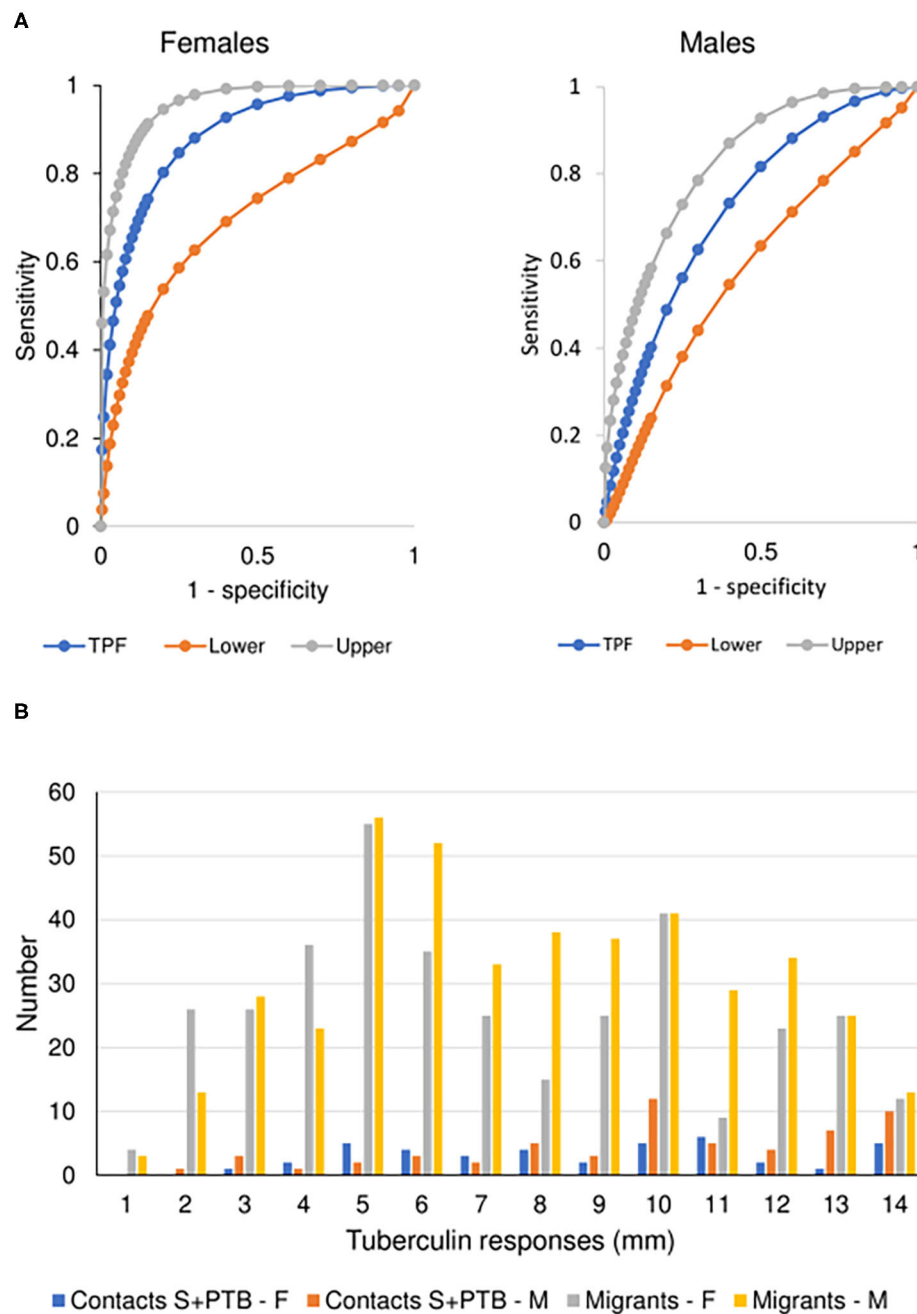


**FIGURE 3 |** Prognostic utility of immunological tests for tuberculosis. **(A)** Comparison of ROC curves for T-SPOT.TB tests in migrant females and males. TPF = true positive fraction (sensitivity). The upper and lower 95% confidence intervals are given, showing overlap between the sexes. AUC females = 0.884 [10 TB cases, 1,165 no TB; AUC males = 0.727 (20 TB cases, 1,285 no TB);  $z = 1.65$ ,  $P$  (one-tailed) = 0.49]. See **Table 4**. **(B)** Sex-specific differences in borderline (1–14 mm) tuberculin skin tests in subjects who did not develop tuberculosis. The majority of responses were 0 mm (contacts, female  $n = 81$ , male = 63; migrants, female = 588, male = 581) or  $\geq 15$  mm (contacts, female  $n = 86$ , male = 89; migrants, female = 157, male = 177). Females predominate in smaller responses ( $< 5$  mm) and males in larger responses (10–14 mm). See **Table 5**.

sexes for positives with either IGRA (**Tables 4, 5**). However, one could argue that the numbers developing TB were too low to be confident of identifying any differences between the sexes.

## Cell-Mediated Immunity

The literature had suggested that females would have greater cell-mediated immunity (47). That this generalization is not universal is exemplified by the differences between the sexes



in terms of vaccine responses, where females in general exhibit better responses but there are some vaccines, such as pneumococcal polysaccharide, where males appear to have higher antibody levels and benefit more in terms of prevention of disease (21, 48). Female neonates benefited more from BCG-enhanced trained immunity in Guinea-Bissau for protection against other respiratory infections (49) and, in adults, BCG has been used to reduce autoimmunity pathology (50). With BCG vaccination, males showed a stronger cytokine response to re-vaccination but reduced systemic inflammation (51). Our data show that males with active tuberculosis had fewer IFN $\gamma$  responses > 10 IU/ml if they had sputum smear- and culture-positive pulmonary tuberculosis, but including both smear-negative and smear-positive patients into a group of culture-positive pulmonary tuberculosis resulted in a non-significant difference.

The T-SPOT.TB test has been evaluated in healthcare workers and shown a higher percentage of positive results in males (4.26%) than females (3.12%), but the age structure and homogeneity of the populations combined could not be assessed (52). Male migrants to the United States showed higher QFT and tuberculin responses than females (53). In our studies, male migrants with a positive IGRA who did not develop TB produced more background IFN $\gamma$ , more IFN $\gamma$  in response to mitogens and higher IFN $\gamma$  levels to the ESAT-6 and CFP-10 antigens. This suggests that males with distant sensitization to RD1 antigens who are protected against developing TB show a good IFN $\gamma$  response. The differences between the two IGRAs requires explanation. The QFT does not account for cell number as the substrate for the test is whole blood. The speculation is that males have more peripheral blood mononuclear cells/mL blood capable of secreting IFN $\gamma$  than females. Where the number of PBMCs is standardized, as in the T-SPOT.TB test, this difference is no longer apparent. On the other hand, where the number of PBMCs is standardized, either there are more antigen-specific cells that can secrete IFN $\gamma$  in males, or the stimulated cells produce more IFN $\gamma$ /cell in males than females.

Early findings showed that DTH responses could be suppressed in female mice and in male mice with reduced testosterone by diethylstilbestrol, a synthetic estrogen (54). Estrogen also downregulates macrophage migration inhibitory factor (MIF) (55), a pivotal cytokine in the tuberculin response (56). Testosterone increases monocyte chemoattractant protein-1 but had no effect on MIF in a randomized treatment trial of testosterone vs. strength training in men over 62 years (57). Tuberculin responses did not differ significantly between males and females, except in migrants who did not develop TB and had larger responses. The immunocytochemistry data did not show the predicted increase in macrophages in males. In S+PTB, females but no males showed a correlation between the area of induration and cell phenotypes. Detailed phenotyping of DTH responses, especially of M1 and M2 subtypes of macrophages (58–60) and gene expression with spatial information (61), could give an indication as to this unexpected difference between males and females with S+PTB in their tuberculin responses and perhaps give

an insight as to why the sex ratio in S+PTB is skewed toward males.

## Humoral Responses

Hypergammaglobulinemia is a feature of TB (62). In chronic infections, low levels of IgM antibody may indicate malnutrition as much as a defect in natural antibody-producing plasma cells (63) and rare genetic defects linked to the X-chromosome where the CD40L resides and to autosomal defects (64, 65). Usually, males have an increased expression of toll-like receptor (TLR)-2 and 4 (28). The expectation would then be that antigens such as LAM would give rise to T-independent antibody more readily in males than females and class-switching might be more effective (66). IgM antibody to LAM was lower in males but IgG antibody did not differ between the sexes in those with S+PTB. IgM may also be found in immune complexes (67, 68), which appear to have a role in pathogenesis (69). Such immune complexes to LAM and other antigens in sputum smear- and culture-positive pulmonary tuberculosis might reduce circulating serum IgM antibody levels.

Anti-BCG IgG, but not IgM, levels were found to be high in patients with pulmonary tuberculosis (70). Total IgE antibody has been found to be high in TB patients, to show a negative correlation with tuberculin responses and to resolve with successful treatment (71). In our data, IgE anti-BCG levels were found to be higher in males with sputum smear- and culture-positive tuberculosis. This might indicate a greater Th2 response in males compared to females in this form of TB. Early studies had shown that protection against tuberculosis could be transferred by cells but not by serum (72). Furthermore, as the bacterial load increased tuberculin responses were increasingly anergic and antibody levels increased (73). The resistance of many Mtb antigens to degradation by professional phagocytes and the importance of non-replicating tubercle bacilli promotes a Th2 response (74). The Th2 response can be seen as part of a greater “type 2” response encompassing a range of cells in addition to T cells, many different cytokines, different macrophage and NK cell sub-types and having a basis in metabolic changes related to the degree of inflammation (75). The fact that in the same part of the tuberculosis disease spectrum differences remain between males and females, suggests that the events leading to less IgM and more IgE-specific responses occur during early immune activation. Such a traction of the immune response after tuberculosis infection toward one which is ineffective might be responsible for male preponderance of sputum smear- and culture-positive pulmonary tuberculosis. Migrants who did not develop TB showed higher IFN $\gamma$  responses than females, suggesting that the problem of a Th2 immune response occurs after the disease has elicited an immune response and that a better Th1 response in the initial stages of infection in males is required to prevent progression to active disease.

## Diagnostic Utility

Although there were significant differences in levels of IFN $\gamma$  between males and females, these did not affect the numbers

that would have been given preventive treatment for TB. The data were insufficient to recommend any change in the definition of a positive T-SPOT.TB test as a prognostic agent to identify those likely to develop TB. However, the tuberculin responses did differ such that a cut-off induration of 10mm might be desirable for females compared to a cut-off induration of 15mm in those aged between 16 and 45 years.

## AREAS FOR FUTURE STUDY

The first is general, regarding the use of biomarkers. Many studies use a broad-brush classifying TB as a single entity for comparison with LTBI, for instance. The differences between S+PTB and smear-negative culture-positive TB or extra-pulmonary TB in terms of antibody titers and specificities has been reported before (6, 76, 77) and is noted in terms of QFT responses between sputum smear- and culture-positive pulmonary tuberculosis and sputum smear-positive or negative culture-positive pulmonary tuberculosis (Table 3). Furthermore, the inclusion of mixtures of TB patients with variable proportions of patients with S+PTB, a part of the TB spectrum that has a male predominance, may confuse sex-related differences in biomarkers with that for TB itself. Re-analysis of these data sets by site of TB disease and by sex may provide useful insights as to the validity of proposed biomarkers and the pathogenesis of infectious forms of TB.

Our data suggests that males, rather than females, appear to be better able to produce IFN $\gamma$ , and stronger delayed-type hypersensitivity (DTH) except in S+PTB. Whether this unexpected reversal of expected Th1 responses is an effect of BCG vaccination should be examined in studies specifically designed to address this hypothesis.

The role of natural antibodies and B cell subsets (78) in tuberculosis infection outcomes is of interest, especially in relation to anti-LAM IgM and IgG antibodies (79, 80).

Before considering a sex-specific cut-off value for tuberculin testing or the T-SPOT.TB test, a much larger number of patients who develop TB is needed in order to determine whether the benefits would outweigh the risks of a delayed diagnosis of TB.

## CONCLUSIONS

This analysis suggests that the differences in immune responses between the sexes do not affect diagnostic utility. However, in deciding who should have preventive treatment for TB, males screened as contacts of sputum smear-positive tuberculosis and migrants screened for LTBI should perhaps have a higher cut-off for the tuberculin skin test. Immunologically, the difference between migrants with evidence of exposure to tuberculosis compared to the population with sputum smear- and culture-positive pulmonary tuberculosis suggests that the male predominance in the latter might be due to immune dysregulation, with poorer IFN $\gamma$  responses in those who go on to develop active disease. The lack of association between induration and CD4+, CD8+, and

CD14+ cell numbers in the tuberculin DTH response in males with S+PTB requires further definition. The lower levels of IgM antibody and IgM anti-LAM antibody require further exploration to define whether this is an association or causative in the poorer T cell responses in males with S+PTB.

## DATA AVAILABILITY STATEMENT

The original contributions presented in the study are included in the article/**supplementary material**, further inquiries can be directed to the corresponding author/s.

## ETHICS STATEMENT

The studies involving human participants were reviewed and approved by the UK PREDICT TB procedures and protocol were approved by the Brent NHS Research Ethics Committee (10/H7017/14). Blood Tests in Tuberculosis III was approved by the East London and City Health Authority Research Ethics Committee (P/03/285). The Indonesian study obtained ethical approval from the ethics committees of Airlangga University, Surabaya and Dundee Medical School. Epitope-Specific Antibody Levels in Tuberculosis was approved by the Brompton Hospitals Ethics Committee (London Chest Hospital, 1985). The patients/participants provided their written informed consent to participate in this study.

## AUTHOR CONTRIBUTIONS

The author conceived the study, performed the systematic review, the statistical analysis and drafted the manuscript.

## FUNDING

Funding for the UK PREDICT TB study was from the National Institute for Health Research Health Technology Assessment Programme 08-68-01. Blood Tests in Tuberculosis III was funded by US NIH R01 A1053531 and the UK NHS Research and Development Culyer allocation. The Indonesian Study was funded by the MRC Tuberculosis and Related Infections Unit, the Wellcome Trust and the KNCV. Epitope-Specific Antibody Levels in Tuberculosis was funded by the MRC Tuberculosis and Related Infections Unit.

## ACKNOWLEDGMENTS

The author acknowledges the study participants and their communities, and all staff related to the original trials. The author acknowledges the work of previous collaborators in the original publications, with special thanks to Professor Juraj Ivanyi formerly Director of the MRC Tuberculosis and Related Infections Unit, Professor John Grange of the Brompton Hospital, Professor John Swanson Beck from the Dundee

Medical School, Dr. Robin Rudd and Jean Hibbs at the London Chest Hospital, Professor Tony Catanzaro for obtaining funding from the National Institutes of Health USA, Professor Ibrahim Abubakar and Dr. Rishi Gupta for providing data from the UK PREDICT TB study.

## REFERENCES

1. Institute of Medicine. *Evaluation of Biomarkers and Surrogate Endpoints in Chronic Disease*. (2010). Available online at: <http://www.iom.edu/Reports/2010/Evaluation-of-Biomarkers-and-Surrogate-Endpoints-in-Chronic-Disease.aspx>
2. Drain PK, Bajema KL, Dowdy D, Dheda K, Naidoo K, Schumacher SG, et al. Incipient and subclinical tuberculosis: a clinical review of early stages and progression of infection. *Clin Microbiol Rev*. (2018) 31:e00021–18. doi: 10.1128/CMR.00021-18
3. Abubakar A, Drobniewski F, Southern J, Sitch A, Jackson C, Lipman M, et al. Prognostic value of interferon gamma release assays and tuberculin skin test in predicting the development of active tuberculosis: the UK PREDICT TB cohort study. *Lancet Infect Dis*. (2018) 18:1077–87. doi: 10.1016/S1473-3009(18)30355-4
4. Boyd AE, Ashcroft A, Lipman M, Bothamley G. Limited value of T-SPOT.TB test in diagnosing active tuberculosis: a prospective Bayesian analysis. *J Infection*. (2011) 63:456–61. doi: 10.1016/j.inf.2011.04.003
5. Bothamley G, Udani P, Rudd R, Festenstein F, Ivanyi J. Humoral response to defined epitopes of tubercle bacilli in adult pulmonary and child tuberculosis. *Eur J Clin Microbiol Infect Dis*. (1988) 7:639–45. doi: 10.1007/BF01964242
6. Jackett PS, Bothamley GH, Batra HV, Mistry A, Young DB, Ivanyi J. Specificity of antibodies to immunodominant mycobacterial antigens in tuberculosis. *J Clin Microbiol*. (1988) 26:2313–8. doi: 10.1128/JCM.26.11.2313-2313.1988
7. Bothamley GH, Rudd R, Festenstein F, Ivanyi J. Clinical value of the measurement of *Mycobacterium tuberculosis*-specific antibody in pulmonary tuberculosis. *Thorax*. (1992) 47:270–5. doi: 10.1136/thx.47.4.270
8. Bothamley GH. Epitope-specific antibody levels demonstrate recognition of new epitopes and changes in titer but not affinity during treatment of tuberculosis. *Clin Lab Diag Immunol*. (2004) 11:942–51. doi: 10.1128/CDLI.11.5.942-951.2004
9. Bothamley GH, Beck JS, Schreuder GMT, D'Amaro J, de Vries RRP, Kardjito T, et al. Association of tuberculosis and *M. tuberculosis*-specific antibody levels with HLA. *J Infect Dis*. (1989) 159:549–55. doi: 10.1093/infdis/159.3.549
10. Yong AJ, Grange JM, Tee RD, Beck JS, Bothamley GH, Kemeny DM, et al. Total and anti-mycobacterial IgE levels in serum from patients with tuberculosis and leprosy. *Tubercle*. (1989) 70:273–9. doi: 10.1016/0041-3879(89)90021-4
11. Bothamley GH, Gibbs JH, Beck JS, Schreuder GMT, de Vries RRP, Grange JM, et al. Delayed hypersensitivity and HLA in smear-positive pulmonary tuberculosis. *Int Arch Allergy Immunol*. (1995) 106:38–45. doi: 10.1159/000236888
12. Lewinsohn DM, Leonard MK, LoBue PA, Cohn DL, Daley CL, Desmond E, et al. Official American Thoracic Society/Infectious Diseases Society of America/Centers for Disease Control and Prevention clinical practice guidelines: diagnosis of tuberculosis in adults and children. *Clin Infect Dis*. (2017) 64:e1. doi: 10.1093/cid/ciw694
13. Stanford JL, Lema E. The use of a sonicate preparation of *Mycobacterium tuberculosis* (New Tuberculin) in the assessment of BCG vaccination. *Tubercle*. (1983) 64:278–82. doi: 10.1016/0041-3879(83)90024-7
14. Gubbels Bupp MR, Jorgensen TM. Androgen-induced immunosuppression. *Front Immunol*. (2018) 9:794. doi: 10.3389/fimmu.2018.00794
15. Zhang MA, Rego D, Moshkova M, Kebir H, Chruscinski A, Nguyen H, et al. Peroxisome proliferator-activated receptor (PPAR) $\alpha$  and  $\gamma$  regulate IFN $\gamma$  and IL-17A production by human T cells in a sex-specific way. *Proc Natl Acad Sci USA*. (2012) 109:9505–10. doi: 10.1073/pnas.1118458109
16. Maret A, Coudert JD, Garidou L, Foucras G, Gourdy P, Krust A, et al. Estradiol enhances primary antigen-specific CD4 T cell responses and Th1 development *in vivo*. Essential role of estrogen receptor  $\alpha$  expression in hematopoietic cells. *Eur J Immunol*. (2003) 33:512–21. doi: 10.1002/immu.200310027
17. Bongen E, Lucian H, Khatri A, Fragiadakis GK, Bjornson ZB, Nolan GP, et al. Sex differences in the blood transcriptome identify robust changes in immune cell proportions with aging and influenza infection. *Cell Rep*. (2019) 29:1961–73. doi: 10.1016/j.celrep.2019.10.019
18. Mo R, Chen J, Grolleau-Julius A, Murphy HS, Richardson BC, Yung RL. Estrogen regulates CCR gene expression and function in T lymphocytes. *J Immunol*. (2005) 174:6023–9. doi: 10.4049/jimmunol.174.10.6023
19. Bouman A, Schipper M, Heinman MJ, Faas MM. Gender difference in the non-specific and specific immune response in humans. *Am J Reprod Immunol*. (2004) 52:19–26. doi: 10.1111/j.1600-0897.2004.00177.x
20. Marquez EJ, Chung C-H, Marches R, Rossi EJ, Nehar-Belaid D, Eroglu A, et al. Sexual-dimorphism in human immune system aging. *Nat Comm*. (2020) 11:751. doi: 10.1038/s41467-020-14396-9
21. Zimmermann P, Curtis N. Factors that influence the immune response to vaccination. *Clin Microbiol Rev*. (2019) 32:e00084–18. doi: 10.1128/CMR.00084-18
22. Butterworth M, McClellan B, Alansmith M. Influence of sex in immunoglobulin levels. *Nature*. (1967) 214:1224–5. doi: 10.1038/2141224a0
23. Mathur S, Mathur RS, Goust JM, Williamson HO, Fudenberg HH. Cyclic variations in white cell subpopulations in the human menstrual cycle: correlations with progesterone and estradiol. *Clin Exp Immunol*. (1977) 30:403–7.
24. Pauwels P, van der Straeten M. Total serum IgE levels in normal and patients with chronic non-specific lung diseases. *Allergy*. (1978) 33:254–60. doi: 10.1111/j.1398-9995.1978.tb01545.x
25. Kornitzky Y, Topilsky M, Fireman E, Kivity S. Specific IgE antibodies to aeroallergens and food among Israelis. *Ann Allergy Asthma Immunol*. (1999) 83:149–52. doi: 10.1016/S1081-1206(10)62627-0
26. Klein SL, Flanagan KL. Sex differences in immune responses. *Nat Rev Immunol*. (2016) 16:626–38. doi: 10.1038/nri.2016.90
27. Kunnath-Velayudhan S, Salamon H, Wang H-Y, Davidow AL, Molina DM, Huynh VT, et al. Dynamic antibody responses to the *Mycobacterium tuberculosis* proteome. *Proc Nat Acad Sci USA*. (2010) 107:14703–8. doi: 10.1073/pnas.1009080107
28. Taneja V. Sex hormones determine immune response. *Front Immunol*. (2018) 9:1931. doi: 10.3389/fimmu.2018.01931
29. Yang YH, Ngo D, Jones M, Simpson E, Fritzemeier KH, Morand EF. Endogenous estrogen regulation of inflammatory arthritis and cytokine expression in male mice, predominantly via estrogen receptor  $\alpha$ . *Arthritis Rheum*. (2010) 62:1017–25. doi: 10.1002/art.27330
30. Lee BR, Jeong SK, Ahn BC, Lee B-J, Shin SJ, Yum JS, et al. Combination of TLR1/2 and TLR3 ligands enhances CD4<sup>+</sup> T cell longevity and antibody responses by modulating type I IFN production. *Sci Rep*. (2016) 6:32526. doi: 10.1038/srep32526
31. Chin ST, Ignatius J, Suraiya S, Tye GJ, Sarmiento ME, Acosta A, et al. Comparative study of IgA VH3 gene usage in healthy TST- and TST+ populations exposed to tuberculosis: deep sequencing analysis. *Immunology*. (2015) 144:302–11. doi: 10.1111/imm.12372
32. Chavez K, Ravindran, Dehnad A, Khan IH. Gender biased immune-biomarkers in active tuberculosis and correlation of their profiles to efficacy of therapy. *Tuberculosis*. (2016) 99:17–24. doi: 10.1016/j.tube.2016.03.009
33. Jacobs AJ, Mongkolsapaya J, Sreanont GR, McShane H, Wilkerson RJ. Antibodies and tuberculosis. *Tuberculosis*. (2016) 101:102–13. doi: 10.1016/j.tube.2016.08.001
34. Lee BW, Yap HK, Chew FT, Quah TC, Prabhakaran K, Chan GS, et al. Age- and sex-related changes in lymphocyte populations of healthy

## SUPPLEMENTARY MATERIAL

The Supplementary Material for this article can be found online at: <https://www.frontiersin.org/articles/10.3389/fimmu.2021.640903/full#supplementary-material>



- Asian subjects: from birth to adulthood. *Cytometry*. (1996) 26:8–15. doi: 10.1002/(SICI)1097-0320(19960315)26:1<8::AID-CYTO2>3.0.CO;2-E
35. Chowdhury RR, Vallania F, Yang Q, Lopez Angel CJ, Darboe F, Penn-Nicholson A, et al. A multi-cohort study of the immune factors associated with *M. tuberculosis* infection outcomes. *Nature*. (2018) 560:644–8. doi: 10.1038/s41586-018-0439-x
  36. Bothamley GH, Grange J, Beck J. Gender differences in immune response to tuberculosis. *Am J Respir Med Crit Care*. (2001) 163: A660.
  37. Horton KC, MacPherson P, Houben RMGJ, White RG, Corbett EL. Sex differences in tuberculosis burden and notifications in low- and middle-income countries: a systematic review and meta-analysis. *PLoS Med*. (2016) 13:e1002119. doi: 10.1371/journal.pmed.1002119
  38. Marçôa R, Ribeiro AI, Zão I, Duarte R. Tuberculosis and gender – factors influencing the risk of tuberculosis among men and women by age group. *Pulmonology*. (2018) 24:199–202. doi: 10.1016/j.pulmoe.2018.03.004
  39. Horton KC, Hoey AL, Béraud G, Corbett EL, White RG. Systematic review and meta-analysis of sex differences in social contact patterns and implications for tuberculosis control and transmission. *Emerg Infect Dis*. (2020) 26:910–9. doi: 10.3201/eid2605.190574
  40. MRC Tuberculosis and Chest Diseases Unit. National survey of tuberculosis notifications in England and Wales 1978–9. *BMJ*. (1980) 281:895–8. doi: 10.1136/bmj.281.6245.895
  41. MRC Tuberculosis and Chest Diseases Unit. National survey of notifications of tuberculosis in England and Wales in 1983. *BMJ*. (1985) 291:658–61. doi: 10.1136/bmj.291.6496.658
  42. MRC Tuberculosis and Chest Diseases Unit. National survey of tuberculosis notifications in England and Wales in 1983: characteristics of disease. *Tubercle*. (1987) 68:19–32. doi: 10.1016/0041-3879(87)90023-7
  43. MRC Cardiothoracic Epidemiology Group. National survey of notifications of tuberculosis in England and Wales in 1988. *Thorax*. (1992) 47:770–5. doi: 10.1136/thx.47.10.770
  44. Kumar D, Watson JM, Charlett A, Nicholas S, Derbyshire JH. Tuberculosis in England and Wales in 1993: results of a national survey. Public Health Laboratory Service/British Thoracic Society/Department of Health Collaborative Group. *Thorax*. (1997) 52:1060–7. doi: 10.1136/thx.52.12.1060
  45. Rose AM, Watson JM, Graham C, Nunn AJ, Drobniewski F, Ormerod LP, et al. Public Health Laboratory Service/British Thoracic Society/Department of Health Collaborative Group. Tuberculosis at the end of the 20<sup>th</sup> century in England and Wales: results of a national survey in 1998. *Thorax*. (2001) 56:173–9. doi: 10.1136/thorax.56.3.173
  46. Shewade HD, Gupta V, Satyanarana S, Pandey P, Bajpal UN, Tripathy JP et al. Patient characteristics, health seeking and delays among new sputum smear positive TB patients identified through active case finding when compared to passive case finding in India. *PLoS ONE*. (2019) 14:e0213345. doi: 10.1371/journal.pone.0213345
  47. Oertelt-Prigione S. The influence of sex and gender on the immune response. *Autoimmunity Rev*. (2012) 11:A479–A485. doi: 10.1016/j.autrev.2011.11.022
  48. Cook IF. Sexual dimorphism of humoral immunity with human vaccines. *Vaccine*. (2008) 26:3551–5. doi: 10.1016/j.vaccine.2008.04.054
  49. Stensballe LG, Nante E, Jensen IP, Kofoed PE, Pulson A, Jensen H, et al. Acute lower respiratory tract infections and respiratory syncytial virus in infants in Guinea-Bissau: a beneficial effect of BCG vaccination for girls community based case-control study. *Vaccine*. (2005) 23:1251–7. doi: 10.1016/j.vaccine.2004.09.006
  50. Angelidou A, Diray-Arce J, Conti MG, Smolen KK, van Haren SD, Dowling DJ, et al. BCG as a case study for precision vaccine development: lessons from vaccine heterogeneity, trained immunity and immune ontogeny. *Front Microbiol*. (2020) 11:332. doi: 10.3389/fmicb.2020.00332
  51. Koeken VA, de Bree LCJ, Mourits VP, Moorlag SJ, Walk J, Cirovic B, et al. BCG vaccination in humans inhibits systemic inflammation in a sex-dependent manner. *J Clin Invest*. (2020) 130:5591–602. doi: 10.1172/JCI133935
  52. King TC, Upfal M, Gottlieb A, Adamo, Bernacki E, Kadlecck CP, et al. T-SPOT.TB interferon- $\gamma$  release assay performance in healthcare worker screening at nineteen U.S. hospitals. *Am J Respir Crit Care Med*. (2015) 192:367–73. doi: 10.1164/rccm.201501-0199OC
  53. Mahan CS, Johnson DE, Curley C, van der Kuyp F. Concordance of positive tuberculin skin test and an interferon gamma release assay in bacilli-Calmette-Guérin vaccinated persons. *Int J Tuberc Lung Dis*. (2011) 15:174–8.
  54. Kato K, Chen Y, Nakane A, Minagawa T, Fujieda K, Kimura T, et al. Suppression of delayed-type hypersensitivity in mice pretreated with diethylstilbesterol: involvement of sex hormones in immunomodulation. *J Leukoc Biol*. (1988) 43:530–8. doi: 10.1002/jlb.43.6.530
  55. Ashcroft GS, Mills SJ, Lei K, Gibbons L, Jeong M-J, Taniguchi M, et al. Estrogen modulates cutaneous wound healing by downregulating macrophage migration inhibitory factor. *J Clin Invest*. (2003) 111:1309–18. doi: 10.1172/JCI200316288
  56. Bernhagen J, Bacher M, Calandra T, Metz CN, Doty SB, Donnelly, et al. An essential role for macrophage migration inhibitory factor in the tuberculin delayed-type hypersensitivity reaction. *J Exp Med*. (1996) 183:277–82. doi: 10.1084/jem.183.1.277
  57. Glintborg D, Christensen LL, Kvorning T, Larsen R, Brixen K, Hougaard DM, et al. Strength training and testosterone treatment have opposing effects on migration inhibitor factor levels in ageing men. *Mediators Inflamm*. (2013) 2013:539156. doi: 10.1155/2013/539156
  58. Ma Q. Polarization of immune cells in the pathologic response to inhaled particles. *Front Immunol*. (2020) 11:1060. doi: 10.3389/fimmu.2020.01060
  59. Kumar R, Singh P, Kolloli A, Shi L, Bushkin Y, Tyagi S, et al. Immunometabolism of phagocytes during *Mycobacterium tuberculosis* infection. *Front Mol Biosci*. (2019) 6:105. doi: 10.3389/fmolb.2019.00105
  60. Chávez-Galán L, Ollerios ML, Vesin D, Garcia I. Much more than M1 and M2 macrophages, there are also CD169+ and TCR+ macrophages. *Front Immunol*. (2015) 6:263. doi: 10.3389/fimmu.2015.00263
  61. Rodrigues SG, Stickels RR, Goeva A, Martin CA, Murray E, Vanderburg CR, et al. Slide-seq: a scalable technology for measuring genome-wide expression at high spatial resolution. *Science*. (2019) 363:1463–7. doi: 10.1126/science.aaw1219
  62. Schaffner F, Turner GC, Eshbaugh DE, Buckingham WB, Popper H. Hypergammaglobulinemia in pulmonary tuberculosis. *AMA Arch Intern Med*. (1953) 92:490–3. doi: 10.1001/archinte.1953.002400220038008
  63. Lobo PI. Role of natural IgM autoantibodies (IgM-NAA) and IgM anti-leukocyte antibodies (IgM-ALA) in regulating inflammation. *Curr Top Microbiol Immunol*. (2017) 408:89–117. doi: 10.1007/82\_2017\_37
  64. Bhushan A, Covey LR. CD40:CD40L interactions in X-linked and non-X-linked hyper-IgM syndromes. *Immunol Res*. (2001) 24:311–24. doi: 10.1385/IR:24:3:311
  65. Heinold A, Hanebeck B, Daniel V, Heyder J, Tran TH, Döhler B, et al. Pitfalls of “hyper”-IgM syndrome: a new CD40 ligand mutation in the presence of low IgM levels. A case report and a critical review of the literature. *Infection*. (2010) 38:491–6. doi: 10.1007/s15010-010-0061-9
  66. Pone EJ, Xu Z, White CA, Zan H, Casali P. B cell TLRs and induction of immunoglobulin class-switch DNA recombination. *Front Biosci (Landmark Ed)*. (2012) 17:2594–615. doi: 10.2741/4073
  67. Samuel AM, Ashtekar MD, Ganatra RD. Significance of circulating immune complexes in pulmonary tuberculosis. *Clin Exp Immunol*. (1984) 58:317–24.
  68. Ashtekar MD, Samuel AD. Circulating immune complexes in pulmonary tuberculosis. *J Clin Lab Immunol*. (1985) 18:91–5.
  69. Ridley MJ, Marianayagam Y, Spector WG. Experimental granulomas induced by mycobacterial immune complexes in rats. *J Pathol*. (1982) 136:59–72. doi: 10.1002/path.1711360106
  70. Aoki A, Hagiwara E, Shirai A, Ishigatsubo Y, Kenji Tokubo T, Yokata S, et al. Their titers and recognized molecules of IgG class anti-BCG antibody in sera from patients with tuberculosis. *Nihon Kyobu Shikkan Gakkai Zasshi*. (1991) 28:729–35.
  71. Adams JFA, Schölvinck EH, Gie RP, Potter PC, Beyers N, Beyers AD. Decline in total serum IgE after treatment for tuberculosis. *Lancet*. (1999) 353:2030–32. doi: 10.1016/s0140-6736(98)-8510-9
  72. Mackanness GB. The immunology of anti-tuberculosis immunity. *Am Rev Respir Dis*. (1968) 97:337–44. doi: 10.1164/arrd.1968.97.3.337
  73. Daniel TM, Oxtoby MJ, Pinto EM, Moreno ES. The immune spectrum in patients with pulmonary tuberculosis. *Am Rev Respir Dis*. (1981) 123:556–9. doi: 10.1164/arrd.1981.123.5.556
  74. von Moltke J, Pepper M. Sentinels of the Type 2 immune response. *Trends Immunol*. (2018) 39:99–111. doi: 10.1016/j.it.2017.10.004
  75. Bothamley G. What next? Basic Research, new treatments a patient-centred approach. In: Migliori GB, Bothamley G, Duarte R, Rendon



- A, editors. *Tuberculosis*. Lausanne: ERS Monogram. (2018). p. 414–29. doi: 10.1183/2312508X.10026118
76. Bothamley G, Batra J, Ramesh V, Chandramuki A, Ivanyi J. Serodiagnostic value of the 19 kilodalton antigen of *Mycobacterium tuberculosis* in Indian patients. *Eur J Clin Microbiol Infect Dis*. (1992) 11:912–5. doi: 10.1007/BF01962372
  77. Chandramuki A, Bothamley GH, Brennan PJ, Ivanyi J. Levels of antibody to defined antigens of *Mycobacterium tuberculosis* in tuberculous meningitis. *J Clin Microbiol*. (1989) 27:821–5. doi: 10.1128/JCM.27.5.821-825.1989
  78. Sebina I, Biraro IA, Dockrell HM, Elliott AM, Cose S. Circulating B-lymphocytes as potential biomarkers of tuberculosis infection activity. *PLoS ONE*. (2014) 9:e106796. doi: 10.1371/journal.pone.0106796
  79. Costello AM, Kumar A, Narayan V, Akbar MS, Ahmed S, Abou-Zeid C, et al. Does antibody to mycobacterial antigens, including lipoarabinomannan, limit dissemination in childhood tuberculosis? *Trans R Soc Trop Med Hyg*. (1992) 86:686–92. doi: 10.1016/0035-9203(92)90192-f
  80. Correia-Neves M, Sundling C, Cooper A, Källén G. Lipoarabinomannan in active and passive protection against tuberculosis. *Front Immunol*. (2019) 10:1968. doi: 10.3389/fimmu.2019.01968

**Conflict of Interest:** The author declares that the research was conducted in the absence of any commercial or financial relationships that could be construed as a potential conflict of interest.

Copyright © 2021 Bothamley. This is an open-access article distributed under the terms of the Creative Commons Attribution License (CC BY). The use, distribution or reproduction in other forums is permitted, provided the original author(s) and the copyright owner(s) are credited and that the original publication in this journal is cited, in accordance with accepted academic practice. No use, distribution or reproduction is permitted which does not comply with these terms.



# Validation of Differentially Expressed Immune Biomarkers in Latent and Active Tuberculosis by Real-Time PCR

Prem Perumal<sup>1</sup>, Mohamed Bilal Abdullatif<sup>1</sup>, Harriet N. Garland<sup>1</sup>, Isobella Honeyborne<sup>2</sup>, Marc Lipman<sup>3</sup>, Timothy D. McHugh<sup>2</sup>, Jo Southern<sup>4</sup>, Ronan Breen<sup>5</sup>, George Santis<sup>5</sup>, Kalaarasan Ellappan<sup>6</sup>, Saka Vinod Kumar<sup>6</sup>, Harish Belgode<sup>6</sup>, Ibrahim Abubakar<sup>4</sup>, Sanjeev Sinha<sup>7</sup>, Seshadri S. Vasani<sup>1,8</sup>, Noyal Joseph<sup>6</sup> and Karen E. Kempell<sup>1\*</sup>

## OPEN ACCESS

### Edited by:

Adam Penn-Nicholson,  
Foundation for Innovative New  
Diagnostics, Switzerland

### Reviewed by:

Andre G. Loxton,  
South African Medical Research  
Council, South Africa  
Hazel Marguerite Dockrell,  
University of London, United Kingdom

### \*Correspondence:

Karen E. Kempell  
Karen.Kempell@phe.gov.uk

### Specialty section:

This article was submitted to  
Microbial Immunology,  
a section of the journal  
Frontiers in Immunology

**Received:** 30 September 2020

**Accepted:** 23 December 2020

**Published:** 16 March 2021

### Citation:

Perumal P, Abdullatif MB, Garland HN, Honeyborne I, Lipman M, McHugh TD, Southern J, Breen R, Santis G, Ellappan K, Kumar SV, Belgode H, Abubakar I, Sinha S, Vasani SS, Joseph N and Kempell KE (2021) Validation of Differentially Expressed Immune Biomarkers in Latent and Active Tuberculosis by Real-Time PCR. *Front. Immunol.* 11:612564. doi: 10.3389/fimmu.2020.612564

<sup>1</sup> Public Health England, Porton Down, Salisbury, Wiltshire, United Kingdom, <sup>2</sup> Centre for Clinical Microbiology, University College London, Royal Free Campus, London, United Kingdom, <sup>3</sup> UCL Respiratory, University College London, Royal Free Campus, London, United Kingdom, <sup>4</sup> Institute for Global Health, University College London, London, United Kingdom, <sup>5</sup> Guy's and St Thomas' NHS Foundation Trust, London, United Kingdom, <sup>6</sup> Jawaharlal Institute of Postgraduate Medical Education and Research, Dhanvantri Nagar, Gorimedu, Puducherry, India, <sup>7</sup> Department of Medicine, All India Institute of Medical Sciences, Ansari Nagar, New Delhi, India, <sup>8</sup> Department of Health Sciences, University of York, York, United Kingdom

Tuberculosis (TB) remains a major global threat and diagnosis of active TB (ATB) both extra-pulmonary (EPTB), pulmonary (PTB) and latent TB (LTBI) infection remains challenging, particularly in high-burden countries which still rely heavily on conventional methods. Although molecular diagnostic methods are available, e.g., Cepheid GeneXpert, they are not universally available in all high TB burden countries. There is intense focus on immune biomarkers for use in TB diagnosis, which could provide alternative low-cost, rapid diagnostic solutions. In our previous gene expression studies, we identified peripheral blood leukocyte (PBL) mRNA biomarkers in a non-human primate TB aerosol-challenge model. Here, we describe a study to further validate select mRNA biomarkers from this prior study in new cohorts of patients and controls, as a prerequisite for further development. Whole blood mRNA was purified from ATB patients recruited in the UK and India, LTBI and two groups of controls from the UK (i) a low TB incidence region (CNTRLA) and (ii) individuals variably-domiciled in the UK and Asia ((CNTRLB), the latter TB high incidence regions). Seventy-two mRNA biomarker gene targets were analyzed by qPCR using the Roche Lightcycler 480 qPCR platform and data analyzed using GeneSpring™ 14.9 bioinformatics software. Differential expression of fifty-three biomarkers was confirmed between MTB infected, LTBI groups and controls, seventeen of which were significant using analysis of variance (ANOVA): CALCOCO2, CD52, GBP1, GBP2, GBP5, HLA-B, IFIT3, IFITM3, IRF1, LOC400759 (GBP1P1), NCF1C, PF4V1, SAMD9L, S100A11, TAF10, TAPBP, and TRIM25. These were analyzed using receiver operating characteristic (ROC) curve analysis. Single biomarkers and biomarker combinations were further assessed using simple arithmetic algorithms. Minimal combination biomarker panels were delineated for primary diagnosis of ATB (both PTB

and EPTB), LTBI and identifying LTBI individuals at high risk of progression which showed good performance characteristics. These were assessed for suitability for progression against the standards for new TB diagnostic tests delineated in the published World Health Organization (WHO) technology product profiles (TPPs).

**Keywords:** tuberculosis, biomarker, qPCR, validation, diagnosis, immune

## INTRODUCTION

*Mycobacterium tuberculosis* (MTB), the causative agent of tuberculosis (TB) is the leading cause of infectious disease worldwide (1, 2), accounting for the deaths of approximately 1.3 million people each year (3). The United Kingdom (UK) has seen an increase in TB since the late 1980s, with rates higher than the rest of Europe (4), and there are currently around 6000 new cases each year (5). In 2016, 73.6% of confirmed TB cases in the UK were foreign-born, with India and Pakistan the most frequent countries of origin (6, 7). For India in the same period the estimated incidence of TB was approximately 2.8 million people per year, accounting for about a quarter of the world's TB cases (8–10) and resulting in considerable mortality (11). Optimal patient care requires early detection, intervention with antibiotic therapy and judicious ongoing management of infectious individuals (8, 12–14). If untreated, each person with pulmonary ATB will infect others at a high rate, on average between 5 and 15 close contacts every year (15).

It is estimated that one quarter of the world's population are latently infected with MTB (LTBI); approximately 2.3 billion individuals (2). This is an enormous reservoir of people at risk of both spreading TB and developing future disease (16–22). A key priority in TB diagnosis is to predict which of those individuals with LTBI [i.e., with a positive purified protein derivative (PPD) or interferon  $\gamma$  release assay (IGRA)] are in fact still harboring TB bacilli after exposure and are likely to progress to active disease, compared to those who have been exposed and mounted a successful immune response, but cleared the bacilli and are not likely progress to active disease (7, 9, 19, 23–25). Although diagnosis of ATB has been the keystone of the public health response to TB in many countries, including the UK, decreasing the infection reservoir through detection and preventative therapy of LTBI is also essential in achieving disease reduction targets (21, 22, 26–31). There is currently no gold standard method for diagnosing LTBI (32, 33). Identification of individuals with LTBI or incipient ATB (iATB), who are at risk of progression to active disease, but are still relatively asymptomatic is a priority to prevent progression to active disease and to limit disease spread to uninfected individuals (9, 34–36). The LTBI group comprises a heterogeneous group of individuals displaying an immune reaction to PPD mycobacterial antigens (37–39). This represents a spectrum of individuals from those who have completely cleared TB bacilli after exposure or infection, to individuals who are harboring actively replicating, live bacteria in the relative absence of clinical symptoms (incipient active TB (iATB)). These latter individuals are potential reservoirs of infection (40–42) and can spread

disease. This is a major problem for control of disease dissemination and LTBI is a key source of infection in high income countries. People with LTBI will often go undiagnosed (14, 40) and are at high risk of progression to active disease. It is predicted that approximately 5% to 10% of individuals with LTBI will progress to ATB during their lifetime (7, 23, 31). The risk of progression from latent to active TB is particularly high among children under the age of 5 years and among people with compromised immunity (1).

As treatment entails risks and costs (43), preventive treatment of LTBI infection should be selectively targeted to the population groups at highest risk for progression to ATB disease, who would benefit most from treatment (9, 34, 44). If caught early enough treatment can be implemented which is less rigorous and results in less severe disease/long term organ damage and fewer relapses (16, 22, 40). Isoniazid monotherapy for 6 months is the primary recommended treatment for LTBI in both adults and children in countries with high and low TB incidence, in contrast to the more intensive combined treatment/DOTS for ATB (13). Non-compliance with anti-mycobacterial therapies contribute to difficulties in disease eradication (25, 45, 46). The treatment for TB is lengthy and patient compliance to long-term drug treatment is varied, with patients often stopping therapy when their symptoms cease (1, 47–50). Failure to complete the treatment regimen promotes the development of multi drug resistance (25, 51–54) and contributes to ongoing barriers for disease eradication (14, 55–57).

The current WHO guidelines for diagnosis and management of TB are outlined as part of their End-TB strategy (2, 58), the primary pillar being diagnosis, as stated in the report “Early diagnosis of TB including universal drug-susceptibility testing, and systematic screening of contacts and high-risk groups”. The report further states that “TB is the 10th leading cause of death worldwide, and since 2007 it has been the leading cause of death from a single infectious agent, ranking above HIV/AIDS. Most of these deaths could be prevented with early diagnosis and appropriate treatment”. The current WHO-endorsed platform for diagnosis of sputum positive TB is the Cepheid GeneXpert, although comprehensive diagnosis still relies on a combination of this with other traditional methods, e.g., chest X-ray and mycobacterial culture from sputum (12). GeneXpert has been widely implemented in many countries globally and has had a positive impact on TB diagnosis and patient management (59–64). However, some high-burden countries like India have reported operational issues with the platform and associated hardware and consumables costs (65, 66) and it not universally available in all high burden countries (34, 67). Its use in India is being recommended for diagnosis of pediatric TB (64, 65).

Opportunities for other diagnostic tests to bridge gaps in the current testing portfolio are still evident but will require investment (34, 67, 68). Many TB patients, particularly with EPTB and also LTBI/iATB do not have MTB positive sputum, are consequently harder to diagnose and can further contribute to TB under-diagnosis (12, 21, 33, 69, 70).

Despite considerable investment in research and development for new diagnostics and therapeutics, TB control and eradication has proved challenging (34, 71). Development of rapid, simple and cost-effective diagnostic tests for ATB, particularly EPTB and LTBI are imperative for TB control (72–80). A simple, rapid and cost-effective alternative, which could perhaps be run on a variety of already embedded laboratory platforms and which could diagnose all sub-types of disease is an attractive proposition. Indirect, non-pathogen directed assays employing host immune biomarkers have become the focus of much interest in bridging gaps in the diagnostic portfolio (77, 79–81). These may play an important role in improving primary diagnosis for EPTB (82–88) and LTBI (82, 89–92), assisting clinicians in informing anti-TB treatments and to determine/monitor the response to treatment (14, 83, 87, 91, 93–101). According to Scriba and co-workers a biomarker-based test would reduce incidence by 20% and could reduce over-diagnosis and treatment using methods like IGRA (102), which are poor predictors of disease progression, with pooled positive predictive values of less than 3%.

Numerous studies and reviews have been published evaluating the current status of biomarkers with potential for active, latent and incipient TB diagnosis, many derived from work profiling the host peripheral blood, immune cell transcriptional response (85, 86, 102–106) (82, 90, 93, 94, 96, 101, 107–113). In one of the initial studies Berry and co-workers identified a complex 393 gene panel which could identify individuals with active TB compared with controls and a 86 gene signature which discriminated active TB from other inflammatory and infectious diseases (107). The same group then went on to identify panels which could distinguish pulmonary TB, pulmonary sarcoidosis, pneumonia and lung cancer (114). This field of research has subsequently become a focus of intense interest and these and a number of other groups have identified various discriminatory signatures for the various forms and stages of TB; ATB, EPTB, LTBI and incipient TB and also for exposure in household contacts, risk of progression to active disease and response to therapy (82, 96, 108–113, 115–136). Some of these have subsequently been reviewed or further validated in comparative cohort studies by other workers in the field (88–90, 110, 126, 136–139). Of the previously published blood transcriptional biomarker panels for active pulmonary tuberculosis reviewed recently by Turner et al. (137), four panels achieved the highest diagnostic accuracy and two met the minimum but not optimum WHO target product profiles (TPP) requirements for a triage test (74, 140); Sweeney et al. [Sweeney3 (120)], Roe et al. [Roe3 and BATF2 (119, 121)] (78) and Kaforou et al. [Kaforou25 (132)]. In a similar study by Gupta et al. (89), eight panels showed promise for discrimination of incipient TB with receiver operating characteristic curves

ranging from 0.70 to 0.77. These predominantly reflected genes from interferon and tumor necrosis factor-inducible gene expression modules. There is still a need to define biomarker panels which will fulfill the WHO TPP optimal requirements for a triage test and for a confirmatory test.

We have previously shown differential expression of PBL gene mRNAs in response to MTB infection in a *Macaca fascicularis* model of TB (141). These non-human primate models are considered to most closely reflect the disease seen in humans (142, 143) and are widely used, particularly for vaccine development (144–146). Microarray hybridization analyses of macaque peripheral blood mRNAs to human whole genome arrays revealed many temporally expressed, gene expression changes, in response to MTB challenge. A selection of significant, differentially regulated immune mRNA biomarkers was identified, which were shared with previously published human data sets (Patent WO2015170108A1). Here we investigate 72 of the most highly-significant biomarkers by quantitative, real-time PCR (qPCR) in two new cohorts of TB patients and controls from the UK and India. This study was conducted to validate previous findings from the NHP model and confirm biomarker suitability for ongoing diagnostic test development for both ATB (both EPTB and PTB) and LTBI. We discuss the performance of these biomarkers, both singly and in combination with reference to WHO target product profiles and their suitability for inclusion in low complexity qPCR assays. We also present initial observations on the utility of some biomarkers/biomarker configurations to identify LTBI individuals at high risk of progression to ATB and which may differentiate different sub-types of TB, i.e., pulmonary (PTB) and extra-pulmonary (EPTB).

## MATERIALS AND METHODS

### Study Participants and Sample Collection

All participants recruited to the study were aged  $\geq 18$  years old. Patients with PTB and EPTB were recruited at two of India's medical institutes of national importance (1) The All India Institute of Medical Sciences (AIIMS), New Delhi and (2) The Jawaharlal Institute of Postgraduate Medical Education & Research (JIPMER), Puducherry, located in regions of high TB incidence [designated groups IPTB ( $n = 47$ ) and IEPTB ( $n = 42$ )]. Patients with PTB were also recruited at Guy's and St Thomas' and Royal Free London NHS Foundation Trusts, London UK (low TB incidence site; designated group UKPTB ( $n = 63$ )). Individuals with suspected LTBI ( $n = 103$ ) and matched negative controls [CNTRLB ( $n = 102$ )] were recruited from individuals variably-domiciled in the UK and Asia, resident in the greater London area as part of the UK PREDICT TB study, i.e. (4, 42), by Public Health England Centre for Infections, 61 Colindale Avenue London and University College, London UK. This was a prospective cohort study, recruiting participants from 54 centers in London, Birmingham, and Leicester, at high risk for latent tuberculosis infection (i.e., recent contact with someone with active tuberculosis [contacts] or a migrant who had arrived



in the UK in the past 5 years from-or who frequently travelled to a country with a high burden of tuberculosis [migrants]]. Exclusion criteria included prevalent cases of tuberculosis. Individuals with suspected LTBI were identified using the standard Mantoux tuberculin skin test ((TST) i.e., skin-test positive) and/or positivity for one or more of the interferon  $\gamma$  release assay tests (IGRA)—QuantiFERON® TB Gold In-Tube ((QFG) QIAGEN GmbH, Hilden, Germany) and T-SPOT®.TB ((TSPOT) Oxford Immunotec Ltd, Oxford, UK). CNTRLB were identified as negative using these test combinations. All patient sample details are given in **Supplementary Table S1** (inside file: **Supplementary Table 1.1**), the number of samples obtained per study site given in **Supplementary Table S1** (inside file: **Supplementary Table 1.2**). Several individuals from the LTBI group were found to have progressed to active disease during study follow up [see **Supplementary Table S1** (inside file: **Supplementary Table 1.3**)]. LTBI were analyzed either as a combined group (LTBI,  $n = 103$ ) or stratified into non-progressors to active TB (LTBI\_NPR,  $n = 95$ ) or progressors to active TB (LTBI\_PR,  $n = 8$ ) for all ongoing analyses. Other negative controls (CNTRLA,  $n = 20$ ) were recruited at PHE, Porton Down, Salisbury, UK (Study Number 12/WA/0303).

All patients recruited to the study at partner sites in India were recruited under an approval from the JIPMER Institute Ethics committee (Human studies), AIIMS Institute Ethics committee and PHE, UK (India Study Number JIP/IEC/2015/11/522, UK Study Number PHE0186). The experiments were carried out in accordance with the approved guidelines of the collaborating institutions. Whole blood samples were collected by venipuncture at a single time point in PAXgene™ (PreAnalytiX, SWZ) or Tempus™ Blood RNA tubes (Applied Biosystems, UK) and stored at  $-80^{\circ}\text{C}$  until further processing.

## Total RNA Extraction and cDNA Synthesis

Total RNA was extracted from the blood samples of study participants using either the PAXgene Blood RNA or Tempus Spin RNA extraction kits, in accordance with the manufacturer's instructions. The PAXgene Blood RNA kit (QIAGEN) was used to extract total RNA from all UK group samples and the Tempus Spin RNA Isolation Kit (Applied Bio systems) was used to extract total RNA from all Indian group samples. Although two different RNA extraction methods were used, there are no conflicting reports as to the likely impact of these on the accuracy of downstream qPCR gene target determination (118–123). Differences are reported as relating mainly to miRNAs and not mRNAs (as quantified in this study). To minimize experimental technical variation between samples, mRNA targets were normalized to the average of three internal house-keeping control genes prior to data export and downstream analysis, to minimize any potential sources of technical variation. The concentration and purity of mRNAs were then assessed using a Nanodrop ND-1000 spectrophotometer (Thermo Scientific, EUA). mRNA integrity was further assessed using the Agilent 2100 Bioanalyzer (Agilent Technologies). Purified RNA was immediately processed for complementary DNA (cDNA) conversion using Transcriptor First Strand cDNA synthesis Kit (Roche) as per the instructions provided by the manufacturer.

The cDNA was then immediately analyzed using qPCR or stored at  $-20^{\circ}\text{C}$  until use.

## Roche Real-Time Ready qPCR Assays

Seventy-two test genes of significance were selected for qPCR validation from our previous studies (141). Details and function of all target genes are given in **Supplementary Table S1** (inside file: **Supplementary Table 1.4**). A summary of the overlap with select previously published gene panels is given in **Supplementary Table S2** (inside files: **Supplementary Tables 2.1 to 2.8**) (genes overlapping with those analyzed in this study highlighted in red text). Glucose-6-phosphate dehydrogenase (G6PD), phosphoglycerate kinase 1 (PGK1) and ribosomal protein L13a (RPL13A) were selected for inclusion as controls from available default control gene options in the Roche Real-Time ready (RTR) assay design center, which showed consistent, invariant expression across control and test groups in the previously published NHP data set.

Expression levels of all human test and control genes were determined using pre-designed or bespoke RTR assays, designed using the RTR assay design configurator (configuration numbers 10059401, 100059386 and 10059377) and arrayed in 384 well format. All qPCR assays were performed in duplicate on the Roche LightCycler 480 (LC480) using TaqMan PCR Probe Master Mix (Roche) and according to the manufacturer's instructions, using the following cycling conditions (i) preheat for 1 cycle at  $95^{\circ}\text{C}$  for 10 minutes (ii) amplification for 45 cycles:  $95^{\circ}\text{C}$  for 10 s,  $60^{\circ}\text{C}$  for 30 s,  $72^{\circ}\text{C}$  for 1 s (ii) cooling to  $40^{\circ}\text{C}$  for 10 s. Data were normalized to the average of the three control genes prior to export using the LC480 software. Normalized data ( $\Delta\text{Ct}$  values) were then exported in .txt file format prior to further analysis.

## Data Analysis and Visualization of qPCR Outputs Using GeneSpring 14.9™

Normalized data exported from the Roche LC480 were imported into Microsoft Excel. The mean of two duplicate data points was calculated using the Average (X) function. Averaged data was then imported into GeneSpring 14.9™ (GX14.9) for further statistical and differential gene expression analyses, using baseline transformation to the median of all samples (without further normalization). All data were then assessed for quality and filtered by error, where the % coefficient of variance (%CV) was  $>200$  (maximizing the number of entities exhibiting expression differences across all samples and removing those with poor or no signals). Statistically significant features were identified using either one-way analysis of variance (ANOVA) analysis using Benjamini-Hochberg false discovery rate (BH FDR, at a corrected p-value cutoff  $p < 0.05$ ) across all groups, or t-tests for comparisons between individual groups (also using BH FDR and a cutoff  $p < 0.05$ ). All further analyses and graphical depiction of data outputs were conducted using other functions in GX14.9 using default settings, e.g., scatter plot, regression and unbiased hierarchical cluster analyses (either Euclidean (EUC) or Pearson's centered (PC) distance metrics using Ward's linkage rule and the cluster entities setting). Other data analyses were

conducted using various functions in “R”, Microsoft Excel or Sigmaplot 12.0 (Systat Software Inc.).

## Receiver Operating Characteristic/Area Under the Curve and Performance Analysis

Receiver Operating Characteristic/area under the curve (ROC/AUC) analyses were performed using normalized, exported mean LC480 qPCR  $\Delta$ Ct values. ROC curves were plotted using “R”  $\times$  64 3.4.0 Software using the ROCR package or the ROC analysis tool of Sigmaplot 12.0. The accuracy and performance of each candidate single biomarker was measured by calculating area under the curve (AUC) values. Cutoff values were predicted by measuring the optimal accuracy of the curve, from which the sensitivity and specificity of each biomarker/biomarker panel test were determined. Optimal cutoffs were selected to obtain best sensitivity and specificity and to compare biomarker performance. Combined panels of biomarkers were also assessed to determine whether these could show improved discrimination between control and infected TB groups over single biomarkers. Simple algorithms consisting of biomarkers combined additively were assessed by ROC analysis and the diagnostic performance further assessed using sensitivity, specificity, cutoff values, likelihood ratios and positive (PPV) and negative (NPV) predictive value calculations. Select biomarker panel configurations were also evaluated to WHO TPP requirements for triage minimum and optimum and confirmatory test minimum requirements using the Sigmaplot 12.0 ROCR/ROC analysis functions. Outputs were depicted graphically using either Sigmaplot 12.0 or GraphPad 8.0.

## Receiver Operating Characteristic/Area Under the Curve and Performance Analysis for Optimal Biomarker Panels on Previously Published Data Sets

Previously published data sets from Singhanian et al. [GSE107991, GSE107992, GSE107993, GSE107994 (109)], Leong et al. [GSE101705 (110)], Turner et al. [E-MTAB-8290 (137)], and Zak et al. [GSE79362 (111)] studies were downloaded and normalized numeric expression values for the relevant panel gene entities extracted. These were analyzed for ROC/AUC and overall performance to WHO TPP requirements for select, significant composite gene biomarker panels from this study as described above (section 2.5).

## RESULTS

### Quality Assessment of Normalized Data Signals and Cluster Analysis

Normalized, exported mean Roche Lightcycler qPCR  $\Delta$ Ct values were imported into GX14.9 and assessed for signal quality. Fifty-three of seventy-two gene entities remained after filtering by error (%CV >200). Samples were assigned to their specific control and disease groups, i.e., (i) low TB incidence region UK control (CNTRLA) (ii) low TB incidence region UK control from the PREDICT TB study (CNTRLB) (iii) low TB incidence

region UK LTBI from the PREDICT TB study (LTBI), variously stratified according to progression (LTBI\_PR) or non-progression (LTBI\_NPR) to ATB (iv) low TB incidence region UK TB (UKPTB) (v) high TB incidence region India extra-pulmonary TB (IEPTB) (vi) high TB incidence region India pulmonary TB (IPTB).

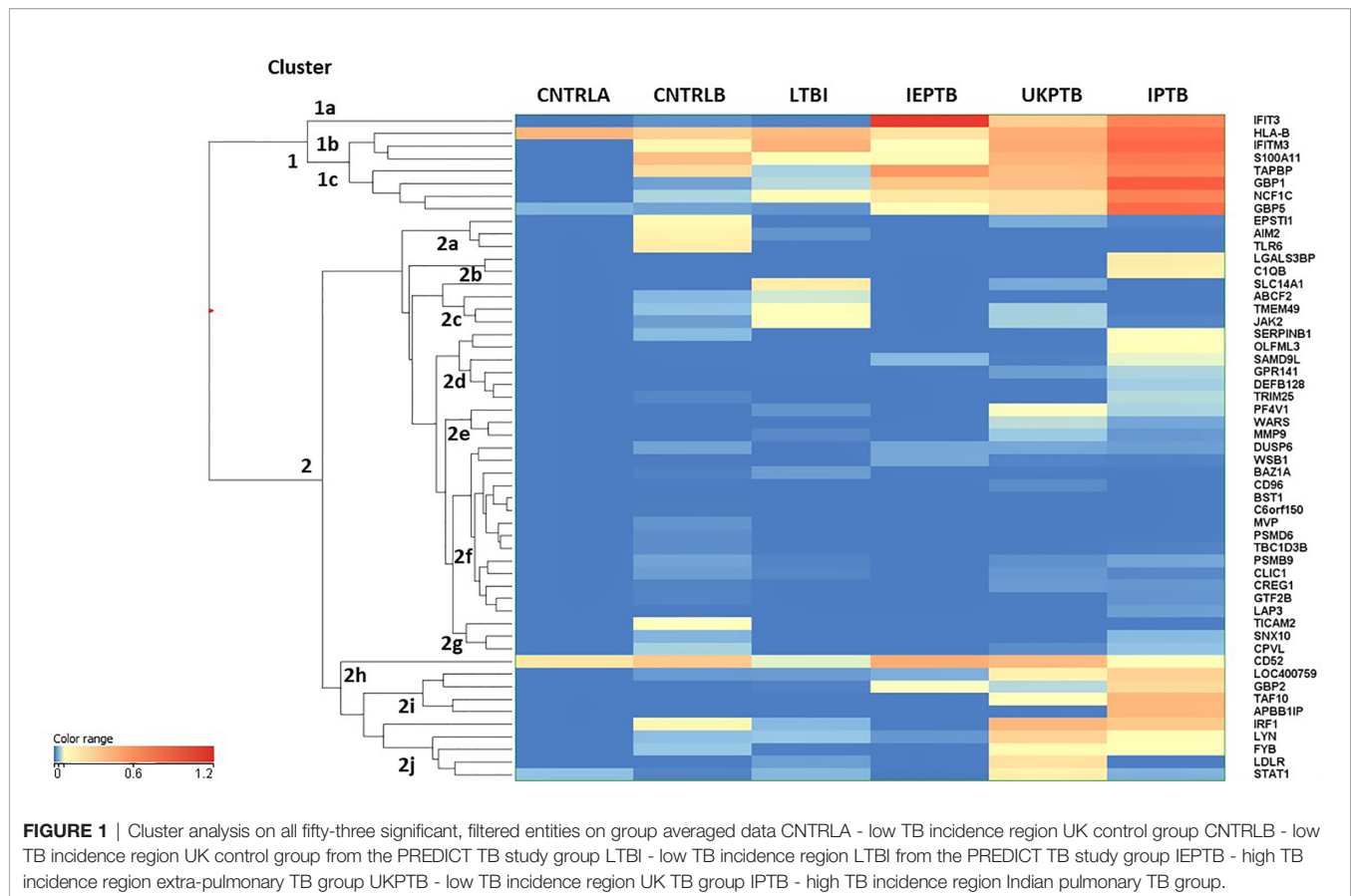
An unbiased EUC cluster analysis was then performed on filtered data, the results are given in **Figure 1**. Two clear main clusters of entity expression could be seen using this analysis; clusters 1 and 2, with associated sub-clusters. Overall, there was an observed pattern of increasing differential regulation of biomarkers in the TB disease groups compared with the control groups, from LTBI through IEPTB, UKPTB and IPTB. The composition of biomarkers varied slightly in the comparisons between groups, although there was also some overlap of entity expression between groups. Gene entities in cluster 1 appeared to delineate groups associated with generalized presumed exposure and/or infection with MTB. Cluster 2 and associated sub-cluster gene entities exhibited variable expression between exposed or infected groups, clusters 2i and 2j featured entities which associated more strongly with ATB. CD52 (cluster 2h) appears more generically differentially expressed across the groups, but slightly down-regulated in LTBI.

Cluster 1 includes only eight entities, some of which are interferon regulated, e.g., IFIT3 and GBP1, others include entities associated with MHC class I antigen processing, e.g., HLA-B and TAPBP and associated with neutrophil and/or other innate immune cell activity, e.g., IFITM3, S100A11 and NCF1C; (i) in cluster 1a, IFIT3 is only associated with the ATB disease groups (ii) cluster 1b the entities associate mainly with the high incidence control (CNTRLB) and ATB groups, although HLA-B also appears expressed in the low incidence (CNTRLA) group and (iii) cluster 1c, the entities associate with the LTBI, IEPTB, UKPTB and IPTB groups (**Figure 1**).

Cluster 2 featured immune-related entities which were differentially regulated between sub-groups, (i) cluster 2a with the CNTRLB group, (ii) clusters 2b, 2d, and 2j with the IPTB group, (iii) cluster 2c with the UKPTB group, (iv) cluster 2e predominantly with the UKPTB group, (v) cluster 2f weakly with the CNTRLB, UKPTB and IPTB groups and (vi) cluster 2g with the CNTRLB and more weakly with the IPTB group, (vii) cluster 2h associated across all groups but more weakly with the LTBI and IPTB groups, (viii) cluster 2i with the IEPTB, UKPTB and IPTB groups and (ix) cluster 2j with the CNTRLB, LTBI, UKPTB and IPTB groups (i.e., all test groups except the IEPTB group). Thus, good differential expression of gene entities was observed between the low TB incidence controls (CNTRLA) and the other groups, i.e., those with ATB from low TB (UKPTB) and high TB incidence regions (IEPTB and IPTB).

### Analysis of Normalized qPCR Data Using Analysis of Variance

To determine the best performing biomarkers for onward progression from those displaying a positive signal post-filtration, Analysis of Variance (ANOVA) was performed



across all groups using BH FDR (corrected  $p$  value  $< 0.05$ ) and using the Student–Newman–Keuls differences in means (SNK), post-hoc test. Seventeen of the fifty-three gene entities from the %CV filtered data set were found to be statistically significant and differentially regulated across the groups using this analysis; including CD52, GBP1, GBP2, GBP5, HLA-B, IFIT3, IFITM3, IRF1, LOC400759 (GBP1P1), NCF1C, PF4V1, S100A11, SAMD9L, STAT1, TAF10, TAPBP, and TRIM25 (17-plex signature). The number of entities that were discriminatory between groups from the ANOVA SNK analysis are summarized in **Supplementary Table S1** (inside file: **Supplementary Table 1.5**) and **Supplementary Information S1, Figure 1.1**.

### Cluster and Scatterplot Analysis of Significant Differentially Regulated Entities

To further investigate group-specific changes in the seventeen, statistically significant differentially regulated biomarkers, PC unbiased cluster analysis was performed across the control, stratified LTBI (LTBI\_NPR and LTBI\_PR) and other ATB disease groups (**Supplementary Information S2, Figure 2.1** and ANOVA  $p$ - and fold change values in **Supplementary Table S3** (inside files: **Table 3.1** with pairwise,  $p$  values from the SNK post hoc test table given in **Table 3.2**). individual line plots (average expression  $\pm$  standard error) for each of these entities

are given in **Supplementary Information S1, Figures 1.2 to 1.18**.

Two distinct clusters were observed, each of which could be divided into four sub-clusters, which further delineate differential expression of the key biomarkers between the control and TB-exposed or infected groups. In addition, clear differences in expression could be seen between the LTBI progressors and non-progressors for a number of these gene biomarkers (boxed in red).

The 17-plex signature was further analyzed in greater detail using scatter plot analysis (**Figure 2**), for the LTBI\_NPR and LTBI\_PR groups. Seven of these biomarkers showed clear differential expression between the two groups (**Supplementary Information S2, Figure 2.1**, with fold change differences given in **Supplementary Table S3** (inside file: **Table 3.3**). IFITM3, S100A11, GBP1, GBP5, STAT1 and LOC400759 (GBP1P1), were upregulated in the LTBI-PR group and HLA-B, TAPBP, NCF1C, PF4V1, CD52 and IRF1 were downregulated. Regression analysis using the 17-plex signature gave a best fit line  $R^2$  value of 0.735 (**Figure 2A**), however using the six upregulated biomarkers plus HLA-B (7-plex signature) alone, the  $R^2$  value increased to 0.828 (**Figure 2B**). Addition of any other differentially markers to the panel did not provide any further improvement to the  $R^2$  value. These showed therefore good potential for identifying “high risk” pre-progressor LTBI patients at an early stage of disease for preventative interventions.

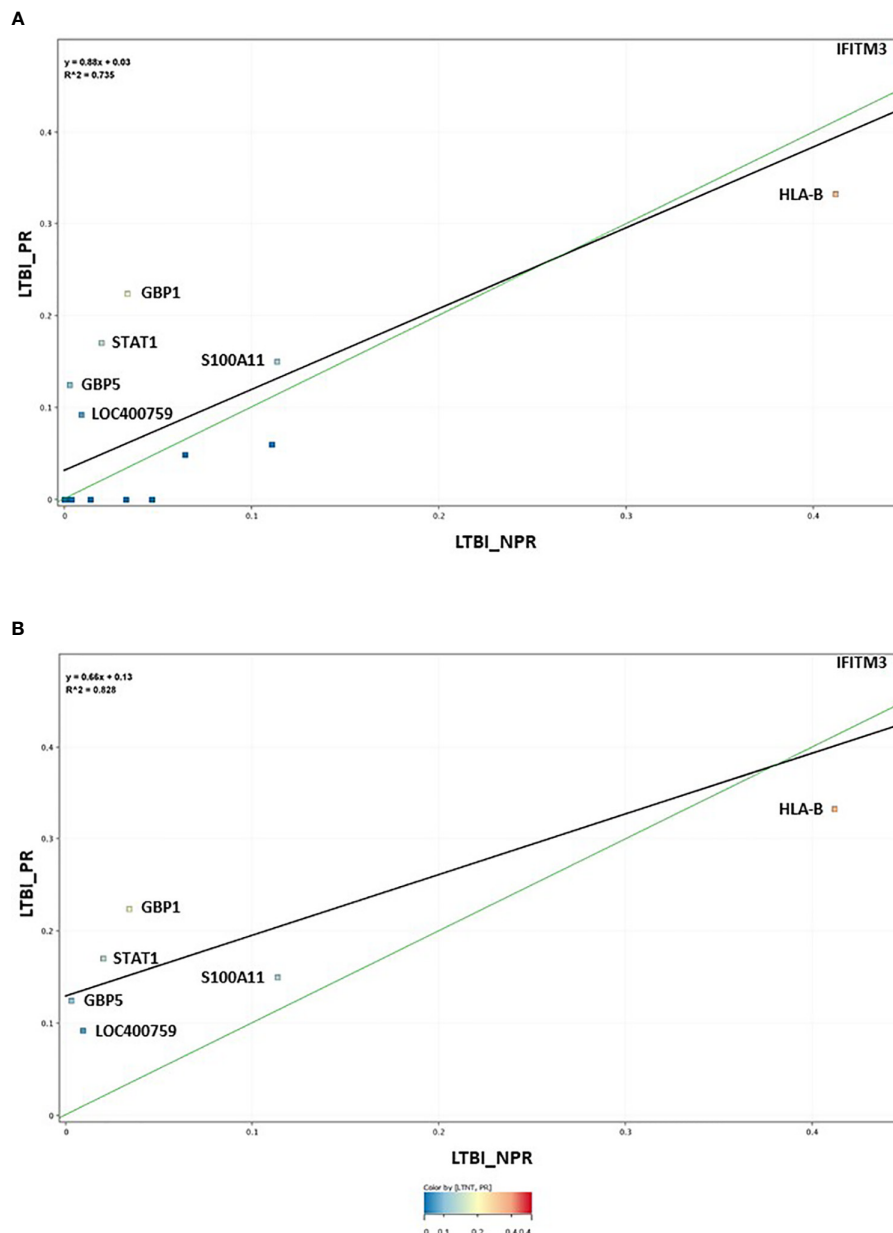


**FIGURE 2 | (A)** Scatter graph depiction of the seventeen statistically significant entities in LTBI non-progressor and LTBI progressor groups, with associated linear regression ( $R^2$ ) significance analysis **(B)** Scatter graph depiction of the seven preferred, differentially expressed entities in LTBI non-progressor and LTBI progressor groups, with associated linear regression ( $R^2$ ) significance analysis.

## Analysis of Control and LTBI Groups Using 7plex Cumulative Average Expression

Inherent variability in biomarker expression was observed between individuals within all the groups (depicted in heatmap format in **Supplementary Information 4, Figure 4.1**) and particularly control group CNTRLB. Some individuals within this group have high positivity for select key biomarkers. Using the normalized numeric  $\Delta C_t$  values for the 7-plex signature, we assessed whether these markers could provide a means for stratifying individuals in the control, LTBI\_NPR and LTBI\_PR

groups into high, medium and low risk categories, using a simple arithmetic cumulative index (**Supplementary Table S3** (inside file: **Table 3.4**). ROC curve analyses were not conducted due to an imbalance in the number of individuals in the control and LTBI\_NPR groups, relative to the LTBI\_PR group ( $n = 8$ ) **Supplementary Table S3** (inside files: **Table 3.1** with pairwise, group t-test p values given in **Table 3.2**). Individuals in these groups were ranked according to their cumulative average expression values (CAE) for the 7-plex signature, then cutoff points set at (i) equal to and greater than the mean ( $> \bar{X}$ )



(ii) equal to and greater than the mean plus one standard deviation ( $\bar{X} + \text{SD}$ ) or (ii) equal to and greater than the mean plus two standard deviations ( $\bar{X} + 2\text{SD}$ ). Three LTBI\_NPR, two LTBI\_PR, four CNTRLB (including patients 1053, 2439 and 1864 highlighted in **Supplementary Information 4, Figure 4.1**) had cumulative values over  $\bar{X} + 2\text{SD}$ . No CNTRLA individuals had cumulative values over  $\bar{X} + 2\text{SD}$ . Ten LTBI\_NPR, one LTBI\_PR, ten CNTRLB and no CNTRLA individuals had cumulative values between  $\bar{X} + 2\text{SD}$  and  $\bar{X} + \text{SD}$ . Twenty-nine LTBI\_NPR, 1 LTBI\_PR, 16 CNTRLB and 6 CNTRLA individuals had cumulative values greater than  $\bar{X}$ , but less than  $\bar{X} + \text{SD}$ . These results would suggest that both the CNTRLB and LTBI groups are heterogeneous. The CNTRLB group may be a mixture of true negative, exposed uninfected and LTBI infected and the LTBI group a mixture of exposed (currently) uninfected and exposed (currently) infected. Those in the upper ranges for the CAE in both groups are potentially at higher risk of progression to ATB. However, further work needs to be done to assess the performance of this 7-plex panel for stratification purposes, with a greater number of patients and controls to follow up.

These results suggest that the TST and IGRA tests used to define these groups may have incorrectly assigned some individuals in the CNTRLB and LTBI groups. There were near equivalent numbers in each stratified category and the groups look similar in ranked distribution. This information further suggests use of individual or low-complexity gene biomarker panels will be unlikely to be sufficient for stratification of LTBI and high-risk control groups, due to inherent variabilities in expression between individuals, which may lead to omissions in identifying “true” infected individuals. A more complex multi-biomarker approach will be required to give requisite test sensitivity.

## Determination of Single Biomarker Receiver Operating Characteristic Profiles

Pairwise comparisons for all seventeen significant differentially-expressed single biomarkers were conducted across all infected and control groups [**Supplementary Table S3** (inside files: **Table 3.5, 3.5A** for controls vs ATB, **3.5B** for controls vs LTBI and **Table 3.5C** for controls&LTBI vs ATB)], ranked according to specificity). The accuracy of single biomarker discriminatory performance across the main active TB disease groups is summarized in **Supplementary Table S1** (inside file: **Supplementary Table 1.6**) and between the LTBI\_PR and LTBI\_NPR groups in **Supplementary Table S1** (inside file: **Supplementary Table 1.7**). Many of these single biomarkers gave AUC values above 0.9, the cutoff considered to be an indicator of very high accuracy (up-regulated in the test group, highlighted in bold black text and dark grey fill). Others gave AUC values above 0.8, considered to be an indicator of high accuracy (highlighted in normal text and medium gray fill). Many others gave AUC values above 0.7, the cutoff considered to be an indicator of moderate accuracy (highlighted in normal text and light grey fill). Some gene biomarkers gave AUC curve values below a cutoff of 0.3 indicating an inverse relationship of the markers between the control and test groups ((i.e., down-

regulated in the test group) highlighted in white italic text and very dark grey fill). From these analyses, many of the significant gene biomarkers were observed to show good performance between disease and control groups. The best performing across all groups were GBP1, GBP2, IFIT3 and SAMD9L (up-regulated) and TAF10 (down-regulated). Several others with more moderate or group-specific performance were also considered viable candidates for ongoing diagnostic algorithm development. IFITM3 showed the best performance in delineating the LTBI group from both groups of controls and IRF1, TAPBP, and TRIM25 may highlight subtle differences in expression between the two LTBI groups.

Performance/accuracy and discrimination between control and disease groups were assessed for likelihood ratios (LR) and positive/negative predictive values (PPV/NPV), using defined qPCR thresholds. Cutoff values which discriminated all ATB from controls were selected at a fixed sensitivity of 80% for PPV and NPV calculations. The accuracy and discriminatory performance between control and disease groups was very good for many biomarkers. Using predicted cutoff values at 80% sensitivity, the LR+ values approached 10 and LR- were correspondingly low. GBP1 attained a specificity of 91.8% at 80% sensitivity and good PPV/NPV (92.42% and 78.87% respectively) when discriminating all ATB from all controls, IFIT3 also showed good performance with a specificity of 90.98% at 80% sensitivity (PPV/NPV; 90.98% and 78.57% respectively). These results suggest both biomarkers would be very good diagnostic candidates for ATB.

GBP1 and IFIT3 showed less impressive performances for LTBI. GBP1 attained a specificity of 61.68% at 80% sensitivity and PPV/NPV (72.53% and 68.84% respectively) and IFIT3 37.38% specificity at 80% sensitivity (PPV/NPV; 69.69% and 57.14% respectively). The best performing marker for discrimination of LTBI from all controls was IFITM3, with a specificity of 64.49% at 80% sensitivity and PPV/NPV (74.19% and 72.06% respectively). These results emphasize again the difficulties in discriminating LTBI from controls, compared with the superior performance of select biomarkers for the ATB group and suggest that the use of individual gene biomarkers would be unlikely to be sufficient for primary disease diagnosis, due to somewhat lower NPV values. This may lead to omissions in identifying infected individuals, due to the likelihood of false negatives and to some lesser extent false positives with individual biomarkers. It was decided therefore to investigate a multi-biomarker panel approach for on-going diagnostic development.

## Determination of Biomarker Panel Receiver Operating Characteristic Profiles and Determination of Diagnostic Algorithms for Diagnostic Test Development

To improve the overall sensitivity and performance, various combinations of gene biomarkers were trialed to determine the optimal configuration to distinguish the various TB disease groups (LTBI (both LTBI\_NPR and LTBI\_PR), IEPTB, UKPTB, and IPTB) from the control groups (CNTRLA and

CNTRLB), with a view to identifying diagnostic panels. qPCR values were combined or subtracted additively according to empirically designed algorithms, then tested using pairwise ROC curve analyses. Illustrations of the best performing combinations are given in full in **Supplementary Table S3** (inside files: **Table 3.6**, **3.6A** for controls vs ATB, **3.6B** for controls vs LTBI and **Table 3.6C** for controls&LTBI vs ATB). These are summarized in **Table 1** across the main active TB disease groups and **Table 2** across the LTBI\_PR and LTBI\_NPR groups respectively.

The gene combinations which gave most consistent high accuracy discrimination between all control and ATB groups were GBP1+IFIT3 (ROC/AUC = 0.945, **Figure 3A** and depicted in scatterplot format in **Figure 4A**). Inclusion of SAMD9L (GBP1+IFIT3+SAMD9L) reduced the AUC value slightly (ROC/AUC = 0.944, **Figure 3B** and **Figure 4B**), but increased the specificity and PPV and NPV values, suggesting combining these three biomarkers may give the best overall test performance. This latter 3-plex gene combination also worked reasonably well for discrimination of Control&LTBI vs ATB groups (**Supplementary Table S3** (inside file: **Table 3.6C**)). The distribution of individuals above the defined cutoffs for each of

these two combinations seen in **Figures 4A, B** show the high accuracy discrimination across all three ATB groups, compared with the CNTRLA group. The UKPTB group shows a greater range of positive and negative results above and below the cutoff value (−0.46) and may be more heterogeneous. At this cutoff only three IPTB patients and one IEPTB appear as false negatives. More moderate accuracy discrimination was observed between the LTBI and both control groups at the same cutoff (AUC = 0.79). Similar results were shown for GBP1+IFIT3+SAMD9L (**Figure 4B**). As discussed above the combination of GBP1+IFITM3 improved the ability to discriminate LTBI from combined controls but not from ATB (**Figures 3C** and **4C**).

Other combination panels of gene biomarkers were trialed to determine the optimal configurations distinguishing LTBI (LTBI\_NPR and LTBI\_PR) from control groups (see **Table 2** and **Supplementary Table S3** (inside file: **Table 3.6B**)). GBP1 + IFITM3 showed high accuracy for discrimination of the LTBI groups from the CNTRLA group (AUC = 0.96) and more moderately when including the CNTRLB group (AUC = 0.809), (**Figures 3C** and **4C**). GBP1+IFIT3 showed best performance for discriminating LTBI from ATB (**Table 2**) with an AUC of 0.865. Small differences were detected between non-

**TABLE 1 |** Summary of AUC ROC values for control and ATB group pairwise comparisons using simple, composite arithmetic algorithms.

Group/Algorithm	Biomarker ROC Curve Value				
	GBP1+GBP2 +IFIT3+SAMD9L +TAPBP	GBP1+ GBP2+IFIT3 +SAMD9L	GBP1+ IFIT3 +SAMD9L	GBP1+GBP2 +IFIT3	GBP1 +IFIT3
CNTRLA vs IEPTB	0.969	0.981	0.981	0.985	0.981
CNTRLA vs UKPTB	0.945	0.952	0.937	0.962	0.956
CNTRLA vs IPTB	0.977	0.970	0.977	0.982	0.980
CNTRLB vs IEPTB	0.911	0.951	0.958	0.951	0.957
CNTRLB vs UKPTB	0.870	0.906	0.915	0.907	0.916
CNTRLB vs IPTB	0.938	0.949	0.959	0.947	0.956
CNTRLA vs All ACTIVE TB	0.962	0.968	0.961	0.982	0.970
CNTRLB vs All ACTIVE TB	0.902	0.932	0.940	0.931	0.940
CNTRLA&CNTRLB vs All ACTIVE TB	0.911	0.938	0.944	0.939	0.945

**TABLE 2 |** Summary of AUC ROC values for control, latent and combined ATB group pairwise comparisons using simple, composite arithmetic algorithms.

Group/Algorithm	ROC/AUC Values for Group Pairwise Comparisons using Composite Biomarker Panel Gene Algorithms			
	GBP1+ IFITM3	GBP1 + IFIT3	GBP1+ IFIT3 + IFITM3	GBP1+IFITM3+ S100A11
CNTRLA vs LTBI-NPR	0.960	0.853	0.966	0.987
CNTRLA vs LTBI-PR	0.981	0.806	0.975	0.987
CNTRLA vs LTBI	0.961	0.849	0.967	0.994
CNTRLB vs LTBI-NPR	0.777	0.7815	0.776	0.590
CNTRLB vs LTBI-PR	0.799	0.734	0.793	0.592
CNTRLB vs LTBI	0.779	0.778	0.777	0.590
CNTRLA&CNTRLB vs LTBI	0.809	0.790	0.808	0.655
CNTRLA&CNTRLB vs LTBI-NPR	0.807	0.793	0.807	0.655
CNTRLA&CNTRLB vs LTBI-PR	0.829	0.746	0.823	0.658
LTBI-NPR vs IPTB	0.792	0.909	0.814	0.830
LTBI -PR vs IPTB	0.753	0.838	0.79	0.795
LTBI VS ALL ACTIVE TB	0.629	0.865	0.685	0.711

progressor and progressor groups. Additionally, the combination of GBP1 + IFIT3 + IFITM3 achieved an ROC/AUC = 0.808, showing this combination could also be used for discrimination of LTBI and ATB. The ability to discriminate ATB from controls with or without LTBI was shown for all three panel combinations (shown in boxplot format in **Figures 5A–C**).

Diagnostic accuracy was further assessed using fixed sensitivities and/or specificities for the WHO TPPs (74, 140) for triage or confirmatory tests (given in **Supplementary Table S3** (inside file: **Table 3.7**) — TB triage test; minimum  $\geq 90\%$  sensitivity and 70% specificity, TB optimal test;  $\geq 95\%$  sensitivity and 80% specificity, TB confirmatory test;  $\geq 98\%$  specificity and 65% sensitivity), with a side by side comparison of the panels' performance given in **Supplementary Table S3** (inside file: **Table 3.8**). The combination of GBP1+IFIT3 met the minimum and optimal triage and the confirmatory test requirements for all pairwise comparisons using CNTRLA alone, but not with CNTRLB alone or when CNTRLB was combined with CNTRLA, with the exception of the EPTB group. GBP1+IFIT3+SAMD9L met the minimum and optimal triage and the confirmatory test requirements for all pairwise comparisons using CNTRLA alone, except the UKPTB group. However, it showed good performance for the CNTRLB and CNTRLA&B combinations vs all ATB for the confirmatory test performance.

## Determination of Biomarker Panel Receiver Operating Characteristic Profiles and Performance of the Optimal Biomarker Panels on Previously Published Data Sets

The performance of the panels on previously published data sets was then conducted [**Supplementary Table S4**, (inside **Table: 4.1**)]. Overall the performance of the panels was good, with high ROC/AUC values, however the results were variable. Most of the panels met either the minimal triage or confirmatory test requirements, except for the GSE107993 (Singhania\_Leicester LTBI non-progressor study set), GSE79362 and E-MTAB-8290 data sets, where there was no minimal requirement positivity observed. Several of the preferred biomarker combinations met the minimum triage requirements for many of the study sets, including GSE107994 (Singhania\_Leicester LTBI progressor study set). GBP1+GBP2+IFIT3+SAMD9L also met the confirmatory test minimum for controls vs ATB. The 7plex signature met the minimum and optimum triage and confirmatory test requirements for controls vs ATB and LTBI vs ATB and the minimum requirements for controls vs LTBI progressors. The GSE107992 data set showed good performance for most of the panels, except the optimal triage requirement for GBP1 + IFIT3, GBP1 + IFIT3+ SAMD9L and GBP1 + GBP2 + IFIT3 + SAMD9L +TAPBP.

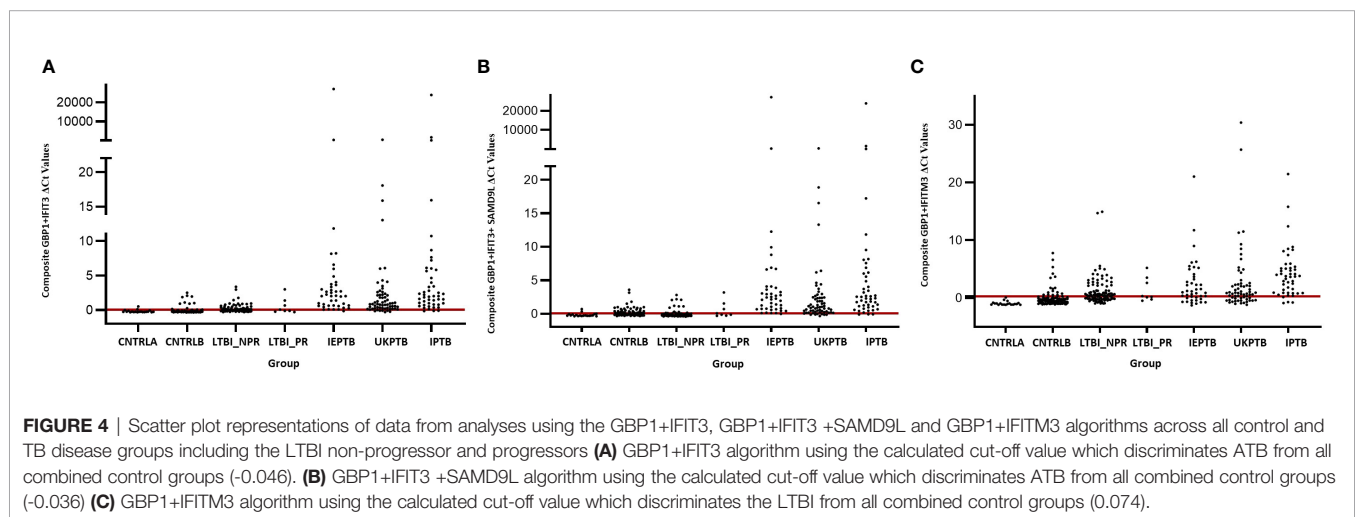
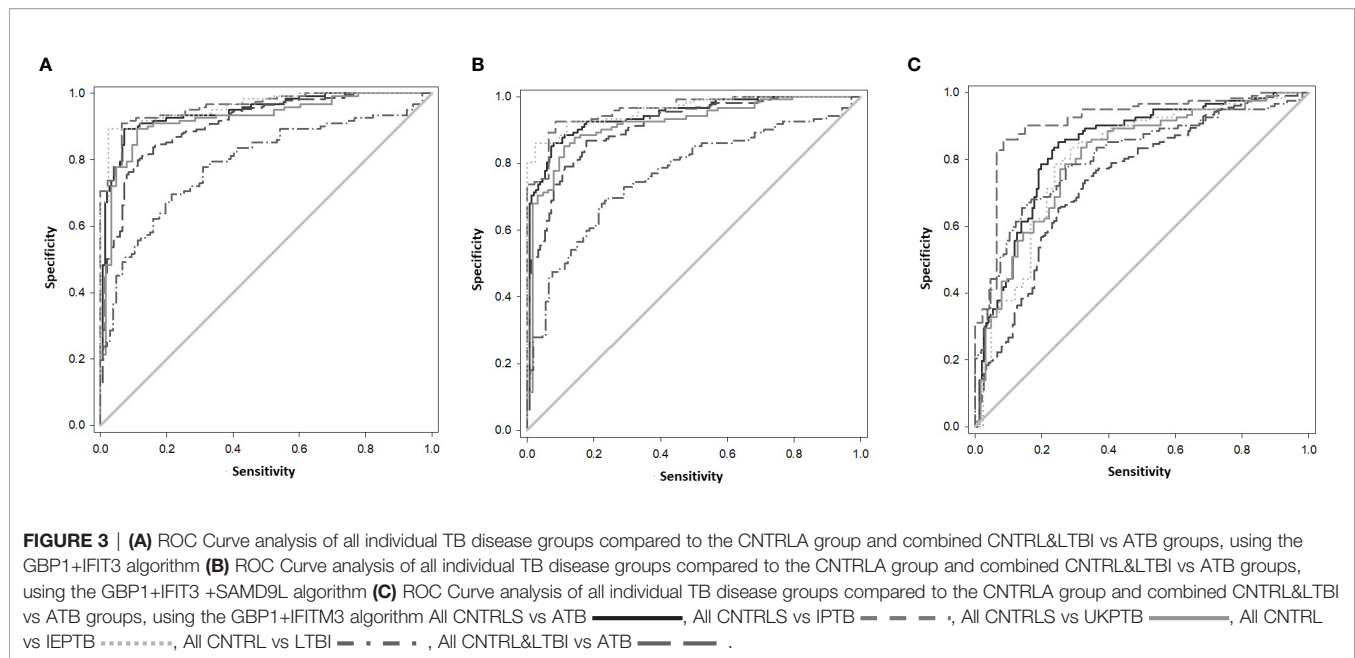
## DISCUSSION

Here we describe Roche LightCycler 480 qPCR validation of differentially-regulated whole blood PBL mRNA gene

biomarkers, previously identified in an NHP model of pulmonary TB (141), in 2 cohorts of patients with active TB (ATB) and a cohort of patients with latent TB (LTBI), compared with two groups of controls (CNTRLA and CNTRLB). Determination of candidate biomarker expression was conducted across ATB patient groups with pulmonary TB (UKPTB and IPTB), extra-pulmonary TB (IEPTB) and latent TB (LTBI\_NPR and NPR\_PR). Fifty-three of seventy-two biomarkers showed differential gene expression signals between disease groups and controls after quality filtration (%CV >200), on this platform. Seventeen highly significant markers were identified from this filtered data set using ANOVA; CALCOCO2, CD52, GBP1, GBP2, GBP5, HLA-B, IFIT3, IFITM3, IRF1, LOC400759 (GBP1P1), NCF1C, PF4V1, SAMD9L, S100A11, TAF10, TAPBP, and TRIM25 were further analyzed. The results showed a predominance of interferon-regulated gene entities, i.e., IRF1, STAT1, IFIT3, IFITM3, GBP1, LOC400759 (GBP1P1), GBP2, GBP5, and TRIM25 along with other entities associated with immune function. Using unbiased cluster analysis, the significant markers showed differential expression profiles across the control and study groups and increasing patterns of expression in active disease groups. Involvement of interferons and dysregulation of interferon-regulated genes in TB has been documented extensively elsewhere (101, 105, 107, 147–151), and our study further confirms these observations. Some inferences as to the underlying biology of biased expression across the groups could be made (a fuller description of gene biological function and group specific expression is given in **Supplementary Table S1** (inside file: **Supplementary Table 1.4** and **Supplementary Information S4**). Gene expression patterns may suggest some phased expression of interferon-regulated genes associated with different stages of disease.

ROC analyses revealed the single best performing biomarkers for discriminating both ATB and LTBI groups. Individual best performing biomarkers were then assessed for performance in combination using simple algorithms with the aim of developing minimal, multiplex biomarker panels for diagnosis. Various combinations were trialed empirically, with smaller two and three multiplexes giving good performance characteristics. The panels have shown good sensitivity, specificity and PPV/NPV. Combinations of GBP1, IFIT3, IFITM3 and SAMD9L using simple arithmetic algorithms looked promising for diagnosis of most ATB presentations. They may also be useful for diagnosis of LTBI and identification of individuals at high risk of progression.

The key diagnostic panel for all types of ATB was determined to be GBP1 and IFIT3, which gave the best performance both individually and in combination (combined AUC = 0.95). The combination of GBP1+IFIT3 could also discriminate LTBI samples from controls with a fairly good degree of accuracy (combined AUC = 0.79), but with reduced resolution compared with the preferred combination of GBP1 + IFITM3 (combined AUC = 0.809). The combination of GBP1 and IFIT3 met both the minimum and optimum TTP profile criteria for both the triage and confirmatory test when single and combined ATB groups were compared with the CNTRLA group. When the CNTRLB group was used as comparator this combination met

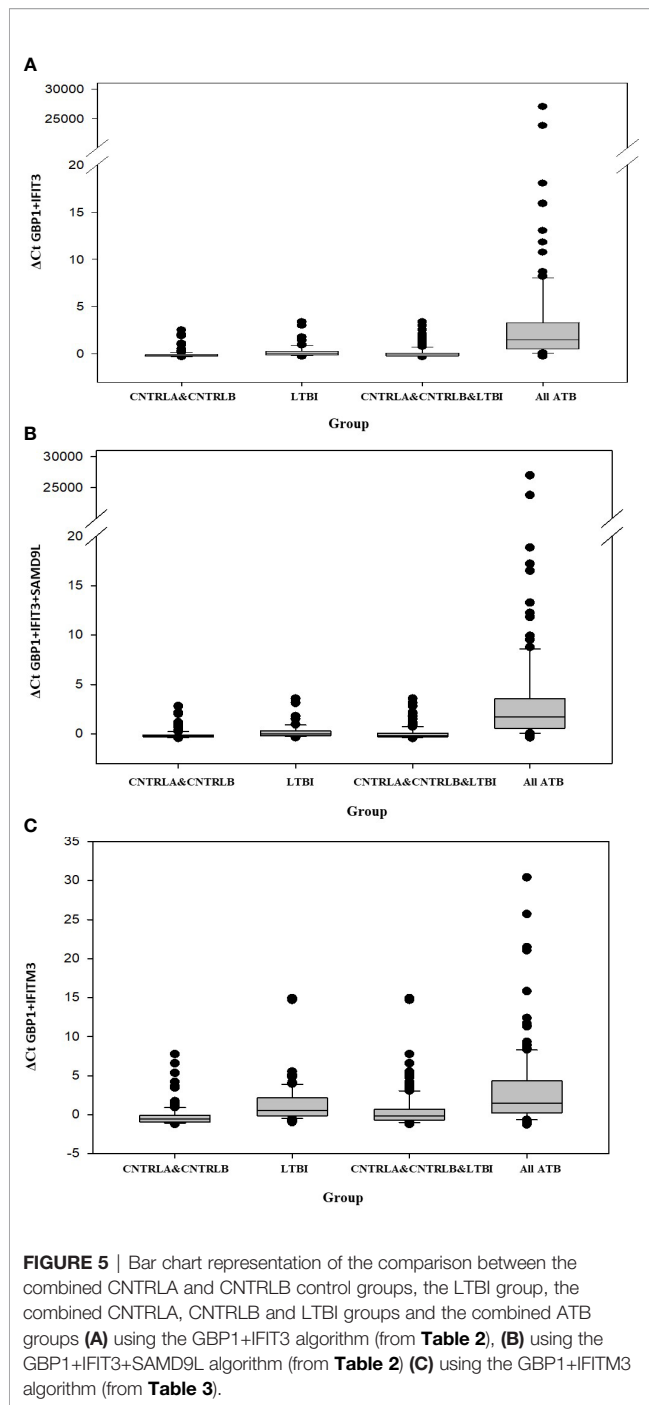


the minimum triage test criteria only for the UKPTB, IPTB and IEPTB groups and the combined ATB group. It met the minimum criteria for the confirmatory test for the IEPTB and IPTB, but not the UKPTB or combined ATB groups. When the CNTRLA and CNTRLB groups were combined and the ATB groups then compared, this combination met the minimum triage criteria for all single ATB groups and the combined ATB group, but the optimal criteria for the triage test for the IEPTB group and the minimum confirmatory test for the IEPTB and IPTB groups only. When the CNTRLA, CNTRLB and LTBI groups were combined and compared with the single and combined ATB groups, this biomarker combination met the minimum criteria for the triage test only. These results demonstrated the potential for this minimum biomarker set to be used as both a triage and confirmatory test; however, its

performance is influenced by the comparator group used. The results show clear differences between the control groups, again suggesting the CNTRLB group is a biased comparator, due to the likely presence of TB positive individuals. If these tests were used in an unbiased fashion, a proportion of the samples in the CNTRLB and LTBI groups would flag up as positive above the assigned threshold test cutoffs and be identified for potential follow up. This biomarker combination was not useful for discrimination of any combination of control or LTBI groups.

Inclusion of SAMD9L (GBP1+IFIT3 +SAMD9L) achieved a reduced AUC value of 0.94 but improved sensitivity and positive and negative predictive values (PPV & NPV), suggesting that this combination could give overall best performance (i.e., reducing the number of false negatives). This combination met many of the minimum and optimum TTP profile criteria for both the





triage and confirmatory test, similarly to GBP1 and IFIT3, but its performance did not compare as favorably for the confirmatory test, except for all ATB groups vs CNTRLB singly as comparator and in combination with CNTRLA. Similar results were also observed with the other combinations, some of which show improved performance for discriminating between LTBI and ATB for the minimum triage requirement. It can be seen that the various biomarker combinations give slightly different results

and any resulting developed test could potentially be tailored according to intended end use, particularly for discrimination between LTBI and ATB.

GBP1+ IFITM3 met the minimum and optimal performance criteria for the LTBI\_NPR and combined LTBI groups for the triage test in comparison with CNTRLA, but the minimum criteria for the LTBI\_PR group only. It met the confirmatory test criteria for the LTBI\_PR group, but not for the LTBI\_NPR and combined LTBI groups. These results are likely to be influenced by differences between LTBI and the two different control groups, due to heterogeneity in the CNTRLB group, which may contain mis-assigned LTBI or preclinically infected individuals, as discussed previously. The GBP1+ IFITM3 panel distinguishes LTBI from unambiguously uninfected negative control groups, with good sensitivity and thus be useful as a rule out test. It may also pick up previously unidentified LTBI classified negative using the Mantoux or IGRA tests. However, more complex multiplex assays may be required for high confidence detection of LTBI and asymptomatic pre-progressor TB patients at a relatively early, latent stage of disease, due to high inherent variability between individuals in the control and LTBI groups and also a relatively low level of biomarker gene expression in these individuals compared with those in the ATB groups. Various combinations of GBP1, IFITM3, GBP5, HLA-B, LOC400759, S100A11 and STAT1 may be useful for LTBI primary diagnosis and stratification, however this requires further study.

There have been a significant number of comparative studies investigating various biomarkers/biomarker panels for MTB diagnosis (88–91, 97, 110, 137, 138, 152–155). Some of the biomarkers validated in this study have been identified by other workers in the field previously as highly useful key components of other TB-diagnostic panels, e.g., GBP1, GBP2, LOC400759 (GBP1P1), GBP5, STAT1, IFIT3 & IFITM3 (110, 114, 115), adding confidence to our own observations. The overall view that this is a valid approach and a productive pipeline for new diagnostic test development, as evidenced in published market evaluation reports (60, 75–77, 79, 81, 85, 87, 155–157). However, to date few have been postulated to fulfill the WHO minimum requirements for progression (89, 110, 137). GBP1 and IFITM3 have been previously reported as components of a four-gene signature from Maertzdorf et al. for discrimination of TB infected from healthy individuals (123). This panel was included as part of prior signature evaluation studies by Leong et al (110, 138). They showed that both complex and relatively simple biomarker combinations, could be useful diagnostically and that some of the smaller panels evaluated previously exhibit good performance characteristics. These would be more amenable to simple, cost-effective assay development. Turner and co-workers also evaluated a number of previously published biomarker signatures to benchmark their diagnostic accuracy against the WHO TPPs for a tuberculosis triage test and found none which met the optimum criteria and two which met the minimum criteria, Roe3 and Sweeney3. These did not meet the minimum requirement for a confirmatory test (89, 137). Our study may offer biomarker panels which fulfill the WHO

minimum criteria and triage optimum and confirmatory minimum requirements, dependent on the control group(s) used for comparison.

Zak et al. reported GBP1 in a signature for disease risk (111), where GBP1, STAT1, and TAP1 were considered to be protective and associated with a good clinical outcome. Sweeney et al. reported a three-gene signature GBP5+DUSP3+KLF2 that can correctly identify ATB from healthy controls and LTBI at high risk of progression (120). In comparison to these panels, our GBP1+ IFIT3 and GBP1+IFIT3 +SAMD9L panels gave similar results for discrimination of ATB from controls (AUC - 0.95 and 0.94), and for discrimination of ATB from LTBI non-progressors (AUC - 0.91). Additionally, our GBP1+ IFITM3 panel could identify LTBI from both combined control groups with an AUC of 0.81. When just the CNTRLA control group only was used, the AUC increased to 0.96. The performance of our GBP1+ IFIT3 and GBP1+IFIT3 +SAMD9L panels for ATB also compare favorably with the Indian-lasso-24 signature published by Leong [(110) AUC 0.984] and the RISK6 signature published recently by Penn-Nicholson et al. (AUC 0.936). Our panels exhibited slightly reduced ROC curve values than the lasso-24 on the same data set, however they are smaller and more amenable to multiplex assay development.

One observation from the Leong study is the small number of ATB outlier patient samples which fall outside of the experimental error and appear as false negatives in the scatter plots. There appears to be a subgroup of patients which segregate with the control samples. This is consistent with our own observations in our study where a proportion of patients in the ATB groups test negative for most of the biomarkers assayed. It would be interesting to determine whether these represent a subgroup of patients displaying a different clinical profile to the others or symptom status as proposed previously by Blankley and co-workers (112), e.g., disease severity, defective immune response/developed anergy. This is worth further investigation and could perhaps be characterized using other analytical means, e.g. flow cytometry.

In summary, we have validated a number of TB-associated whole blood PBL immune gene markers in new cohorts of patients and controls using qPCR, of which seventeen were significant. Their utility in primary determination of ATB (both pulmonary and extra-pulmonary manifestations) and LTBI has been assessed using ROC curve analysis and evaluated against the WHO TPP requirements for a triage and confirmatory test. ATB disease could be detected with a high degree of accuracy and sensitivity, including EPTB with LTBI detected at a somewhat reduced level. We have shown that minimally small configurations of biomarkers show comparable performance in relation to other studies. They exhibit the requisite TPP requirements for further evaluation and development on our data set, however variable performance was observed with other previously published data sets. This may be due in part to technical variation with the variety of assay platforms used, the contribution of which may be underestimated in contemporary comparison studies. Our biomarker panels could be easily formulated into a simple

multiplex qPCR assay format and used in diagnosis/screening surveillance for all TB presentations, however further validation is required. The assays in this study were conducted on the Roche lightCycler 480, but these could be adapted easily to run on any qPCR platform as part of a low cost, rapid testing/screening program. Further work is underway to develop these panels as clinically useful, utilitarian diagnostic tests.

## STUDY LIMITATIONS

A key limitation of the study is the choice of control groups. The study includes controls, latent TB and TB patients recruited in the UK, but only TB patients in India. The preferred control group for the Indian group samples would be region-matched disease-free individuals and those with other respiratory conditions/infections. The number of LTBI individuals progressing to active disease is also relatively small and this limits the power of the statistical analysis, as they could not be analyzed as a separate group with the analytical methods used. In addition, the Indian blood samples were banked in Tempus tubes while those in the UK were banked into PAXgene tubes, which may have had an impact on the consistency of RNA extraction and recovery. Limited demographic information was available on the patients included in the study. Future studies would be planned to address these issues and further empower the analyses.

## DATA AVAILABILITY STATEMENT

The raw data supporting the conclusions of this article will be made available by the authors, without undue reservation.

## ETHICS STATEMENT

The studies involving human participants were reviewed and approved by JIPMER Institute Ethics committee, AIIMS Institute Ethics committee, the NHS Health Research Authority Research Ethics (NRES) Committee for London - Camden & Islington and PHE. The patients/participants provided their written informed consent to participate in this study.

## AUTHOR CONTRIBUTIONS

PP, MA, and KE conducted the experimental work. IH, ML, TM, JS, RB, GS, SK, IA, SS, and NJ provided control and patient samples and clinical and scientific expertise to the project. PP, NJ, SV, and KK designed the study protocol and managed the study. PP, MA, HG, and KK conducted the data analysis, and HG, IH, ML, TM, KE, NJ, and KK wrote and edited the paper. All authors contributed to the article and approved the submitted version.

## FUNDING

This study was funded by the UK Department of Health and Social Care Grant in Aid and the Public Health England Pipeline fund. The views expressed in this publication are those of the authors and not necessarily those of PHE or the DH.

## ACKNOWLEDGMENTS

We acknowledge Mark Sutton for assistance with proof-reading the manuscript.

## SUPPLEMENTARY MATERIAL

The Supplementary Material for this article can be found online at: <https://www.frontiersin.org/articles/10.3389/fimmu.2020.612564/full#supplementary-material>

**Supplementary Table S1 | Table 1.1.** Details of Patient and Control Samples **Table 1.2** Summary of numbers of patients per group and affiliations **Table 1.2.** Summary of patients or controls recruited per collaborating site used in the study **Table 1.3.** Number of participants per PREDICT TB LTBI and CNTRLB study groups study groups classified by TST IGRA status and progression to active TB **Table 1.4** Gene entities validated in study using Roche Real-time Ready qPCR assays with assay configuration identifiers and ascribed biological function **Table 1.5** Summary of the differentially expressed gene entities between the control, latent and active TB disease groups in the study from ANOVA SNK analysis **Table 1.6** ROC/AUC values from pairwise comparisons for single biomarkers between control, latent and active TB disease groups **Table 1.7** ROC/AUC values from pairwise comparisons for single biomarkers between control and latent TB progressor and non-progressor groups.

**Supplementary Table S2 |** Summary of genes from previously published studies overlapping with those analyzed in this study (highlighted in red text) and performance to WHO TPP requirements based on source or reviewed sensitivity and specificity values.

**Supplementary Table S3 | Table 3.1.** p values of entities differentially regulated between groups from ANOVA performed across all groups using BH FDR (corrected p value < 0.05) and the SNK *post hoc* test, plus direction of regulation. **Table 3.2.** Detailed comparison of entities differentially regulated between groups from the SNK *post hoc* test table, comparison and p values for significant entities only. **Table 3.3.** Fold change comparison for all 17 statistically significant biomarkers between the LTBI-NPR and LTBI-PR groups. **Table 3.4.** Individuals in the CNTRLA, CNTRLB, LTBI-NPR, and LTBI-PR groups ranked according to their cumulative average expression values for the 7plex signature, using cutoff points set at equal to and greater than the mean ( $\bar{X}$ ) and  $1(\bar{X} + SD)$  or  $2(\bar{X} + 2SD)$  standard deviations above the mean; Greater than  $\bar{X} + 2SD$  ■, between  $\bar{X} + SD$  and  $(\bar{X} + 2SD)$  ■, between  $(\bar{X})$  and  $(\bar{X} + SD)$  ■ **Table 3.5.** ROC/AUC results, plus sensitivity, specificity, likelihood ratios and positive and negative predictive values for single significant biomarkers across all ATB and LTBI groups compared with controls

**Table 3.6.** ROC/AUC results, plus sensitivity, specificity, likelihood ratios and positive and negative predictive values for key combinations of significant biomarkers across all ATB and LTBI groups compared with controls **Table 3.7.** Diagnostic accuracy of biomarker panels assessed using fixed sensitivities and/or specificities defined by the WHO technology product profiles for triage or confirmatory tests **Table 3.8.** Comparison of performance of biomarker panels (A–F) with regard to control and patient groups and the WHO technology product profiles for the minimum and optimal triage and confirmatory tests.

**Supplementary Table S4 |** Performance of optimal biomarker panels on other previously published data sets.

**Supplementary information S1 | Figure 1.1** Distribution of the number of entities differentially regulated between groups from ANOVA, performed across all groups using BH FDR (corrected p value < 0.05) and using the SNK *post hoc* test. **Figure 1.2.** Line graph of CD52 normalized intensity values across all TB disease and control groups. **Figure 1.3.** Line graph of GBP1 normalized intensity values across all TB disease and control groups. **Figure 1.4.** Line graph of GBP2 normalized intensity values across all TB disease and control groups. **Figure 1.5.** Line graph of GBP5 normalized intensity values across all TB disease and control groups. **Figure 1.6.** Line graph of HLA-B normalized intensity values across all TB disease and control groups. **Figure 1.7.** Line graph of IFIT3 normalized intensity values across all TB disease and control groups. **Figure 1.8.** Line graph of IFITM3 normalized intensity values across all TB disease and control groups. **Figure 1.9.** Line graph of IRF1 normalized intensity values across all TB disease and control groups. **Figure 1.10.** Line graph of LOC400759 normalized intensity values across all TB disease and control groups. **Figure 1.11.** Line graph of NCF1C normalized intensity values across all TB disease and control groups. **Figure 1.12.** Line graph of PF4V1 normalized intensity values across all TB disease and control groups. **Figure 1.13.** Line graph of S100A11 normalized intensity values across all TB disease and control groups. **Figure 1.14.** Line graph of SAMD9L normalized intensity values across all TB disease and control groups. **Figure 1.15.** Line graph of STAT1 normalized intensity values across all TB disease and control groups. **Figure 1.16.** Line graph of TAF10 normalized intensity values across all TB disease and control groups. **Figure 1.17.** Line graph of TAPBP normalized intensity values across all TB disease and control groups. **Figure 1.18.** Line graph of TRIM25 normalized intensity values across all TB disease and control groups.

**Supplementary Information S2 | Figure 2.1.** Cluster analysis on group averaged data for all statistically significant entities from ANOVA (p < 0.05) (A) low TB incidence region UK control group (CNTRLA) (B) low TB incidence region UK control from the PREDICT TB study group (CNTRLB) (C) low TB incidence region UK Latent TB from the PREDICT TB study group (LTBI) (D) high TB incidence region extra-pulmonary TB group (IEPTB) (E) low TB incidence region UK pulmonary TB group (UKPTB) (F) high TB incidence region pulmonary TB group (IPTB). Entities which show expression differences between the LTBI\_NPR and LTBI\_PR groups are boxed in red, with the boxed region showing the highest expression compared to that in the relative other group.

**Supplementary Information S3 | Figure 3.1** Heatmap of the 17-plex entities showing individual expression profiles across the disease and control groups. The top three ranked patient samples 2439, 1053 and 1864 from the cumulative scoring analysis using the 7-plex signature are highlighted with red arrows.

**Supplementary Information S4 |** Description of the group association and biological function of the 17 statistically significant biomarkers from **Supplementary Information S4.**

## REFERENCES

- Bloom BR, Atun R, Cohen T, Dye C, Fraser H, Gomez GB, et al. Tuberculosis. In: H KK, S Bertozzi, B BR and P Jha, editors. *Major Infectious Diseases*. Washington (DC) (2017). doi: 10.1596/978-1-4648-0524-0\_ch11
- World Health Organisation. 2020 *Global Tuberculosis Report*. The World Health Organisation (2020). Available at: [https://www.who.int/tb/publications/global\\_report/en/](https://www.who.int/tb/publications/global_report/en/).
- Holmes KK, Bertozzi S, Bloom BR, Jha P, Gelband H, DeMaria LM, et al. Major Infectious Diseases: Key Messages from Disease Control Priorities. In: KK Holmes, S Bertozzi, BR Bloom and P Jha, editors. *Major Infectious Diseases, 3rd ed.* Washington (DC) (2017). doi: 10.1596/978-1-4648-0524-0\_ch1
- Abubakar I, Lalvani A, Southern J, Sitch A, Jackson C, Onyima O, et al. Two interferon gamma release assays for predicting active tuberculosis: the UK PREDICT TB prognostic test study. *Health Technol Assess* (2018) 22 (56):1–96. doi: 10.3310/hta22560

5. Hayward S, Harding RM, McShane H, Tanner R. Factors influencing the higher incidence of tuberculosis among migrants and ethnic minorities in the UK. *F1000Res* (2018) 7:461. doi: 10.12688/f1000research.14476.2
6. Abarca Tomas B, Pell C, Bueno Cavanillas A, Guillen Solvas J, Pool R, Roura M. Tuberculosis in migrant populations. A systematic review of the qualitative literature. *PLoS One* (2013) 8(12):e82440. doi: 10.1371/journal.pone.0082440
7. Crawshaw AF, Pareek M, Were J, Schillinger S, Gorbacheva O, Wickramage KP, et al. Infectious disease testing of UK-bound refugees: a population-based, cross-sectional study. *BMC Med* (2018) 16(1):143. doi: 10.1186/s12916-018-1125-4
8. Jilani TN, Avula A, Zafar Gondal A, Siddiqui AH. *Active Tuberculosis*. Treasure Island (FL: StatPearls (2020).
9. Sharma N, Basu S, Chopra KK. Achieving TB elimination in India: The role of latent TB management. *Indian J Tuberc* (2019) 66(1):30–3. doi: 10.1016/j.ijtb.2018.10.006
10. Pattnaik S. Analysis of tuberculosis case report in Hyderabad district of Telangana state. *J Family Med Prim Care* (2018) 7(3):561–4. doi: 10.4103/jfmpc.jfmpc\_110\_18
11. Mathur N, Chatla C, Syed S, Patel Y, Pattnaik S, Mathai D, et al. Prospective 1-year follow-up study of all cured, new sputum smear positive tuberculosis patients under the Revised National Tuberculosis Control Program in Hyderabad, Telangana State, India. *Lung India* (2019) 36(6):519–24. doi: 10.4103/lungindia.lungindia\_143\_19
12. Long B, Liang SY, Koyfman A, Gottlieb M. Tuberculosis: a focused review for the emergency medicine clinician. *Am J Emerg Med* (2019) 38(5):1014–22. doi: 10.1016/j.ajem.2019.12.040
13. Jelinska A, Zajac M, Dadej A, Tomczak S, Geszke-Moritz M, Muszalska-Kolos I. Tuberculosis - Present Medication and Therapeutic Prospects. *Curr Med Chem* (2020) 27(4):630–56. doi: 10.2174/0929867325666181120100025
14. Tiberi S, du Plessis N, Walzl G, Vjecha MJ, Rao M, Ntouni F, et al. Tuberculosis: progress and advances in development of new drugs, treatment regimens, and host-directed therapies. *Lancet Infect Dis* (2018) 18(7):e183–e98. doi: 10.1016/S1473-3099(18)30110-5
15. World Health Organisation. *Tuberculosis*. The World Health Organization (2020). Available at: <https://www.who.int/news-room/fact-sheets/detail/tuberculosis>.
16. Harries AD, Kumar AMV, Satyanarayana S, Takarinda KC, Timire C, Dlodlo RA. Treatment for latent tuberculosis infection in low- and middle-income countries: progress and challenges with implementation and scale-up. *Expert Rev Respir Med* (2020) 14(2):195–208. doi: 10.1080/17476348.2020.1694907
17. Chaw L, Chien LC, Wong J, Takahashi K, Koh D, Lin RT. Global trends and gaps in research related to latent tuberculosis infection. *BMC Public Health* (2020) 20(1):352. doi: 10.1186/s12889-020-8419-0
18. Knight GM, McQuaid CF, Dodd PJ, Houben R. Global burden of latent multidrug-resistant tuberculosis: trends and estimates based on mathematical modelling. *Lancet Infect Dis* (2019) 19(8):903–12. doi: 10.1016/S1473-3099(19)30307-X
19. Houben R, Esmail H, Emery JC, Joslyn LR, McQuaid CF, Menzies NA, et al. Spotting the old foe-revisiting the case definition for TB. *Lancet Respir Med* (2019) 7(3):199–201. doi: 10.1016/S2213-2600(19)30038-4
20. Houben RM, Dodd PJ. The Global Burden of Latent Tuberculosis Infection: A Re-estimation Using Mathematical Modelling. *PLoS Med* (2016) 13(10):e1002152. doi: 10.1371/journal.pmed.1002152
21. Jagger A, Reiter-Karam S, Hamada Y, Getahun H. National policies on the management of latent tuberculosis infection: review of 98 countries. *Bull World Health Organ* (2018) 96(3):173–84F. doi: 10.2471/BLT.17.199414
22. Getahun H, Matteelli A, Abubakar I, Aziz MA, Baddeley A, Barreira D, et al. Management of latent Mycobacterium tuberculosis infection: WHO guidelines for low tuberculosis burden countries. *Eur Respir J* (2015) 46(6):1563–76. doi: 10.1183/13993003.20154606.E60
23. Zenner D, Loutet MG, Harris R, Wilson S, Ormerod LP. Evaluating 17 years of latent tuberculosis infection screening in north-west England: a retrospective cohort study of reactivation. *Eur Respir J* (2017) 50(1):1602505. doi: 10.1183/13993003.02505-2016
24. Zenner D, Hafezi H, Potter J, Capone S, Matteelli A. Effectiveness and cost-effectiveness of screening migrants for active tuberculosis and latent tuberculous infection. *Int J Tuberc Lung Dis* (2017) 21(9):965–76. doi: 10.5588/ijtld.16.0935
25. Gupta RK, Lipman M, Story A, Hayward A, de Vries G, van Hest R, et al. Active case finding and treatment adherence in risk groups in the tuberculosis pre-elimination era. *Int J Tuberc Lung Dis* (2018) 22(5):479–87. doi: 10.5588/ijtld.17.0767
26. Assefa Y, Woldeyohannes S, Gelaw YA, Hamada Y, Getahun H. Screening tools to exclude active pulmonary TB in high TB burden countries: systematic review and meta-analysis. *Int J Tuberc Lung Dis* (2019) 23(6):728–34. doi: 10.5588/ijtld.18.0547
27. Uplekar M, Weil D, Lonnroth K, Jaramillo E, Lienhardt C, Dias HM, et al. WHO's new end TB strategy. *Lancet* (2015) 385(9979):1799–801. doi: 10.1016/S0140-6736(15)60570-0
28. Uplekar M, Raviglione M. WHO's End TB Strategy: From stopping to ending the global TB epidemic. *Indian J Tuberc* (2015) 62(4):196–9. doi: 10.1016/j.ijtb.2015.11.001
29. Uplekar M. Implementing the End TB Strategy: Well begun will be half done. *Indian J Tuberc* (2015) 62(2):61–3. doi: 10.1016/j.ijtb.2015.03.001
30. Zenner D, Stagg HR, Harris RJ, Abubakar I. Treatment of latent tuberculosis infection. *Ann Intern Med* (2015) 162(5):394–5. doi: 10.7326/L15-5058-3
31. Zenner D, Beer N, Harris RJ, Lipman MC, Stagg HR, van der Werf MJ. Treatment of Latent Tuberculosis Infection: An Updated Network Meta-analysis. *Ann Intern Med* (2017) 167(4):248–55. doi: 10.7326/M17-0609
32. Ling DI, Pai M, Schiller I, Dendukuri N. A Bayesian framework for estimating the incremental value of a diagnostic test in the absence of a gold standard. *BMC Med Res Methodol* (2014) 14:67. doi: 10.1186/1471-2288-14-67
33. Norbis L, Miotto P, Alagna R, Cirillo DM. Tuberculosis: lights and shadows in the current diagnostic landscape. *New Microbiol* (2013) 36(2):111–20.
34. Reid MJA, Arinaminpathy N, Bloom A, Bloom BR, Boehme C, Chaisson R, et al. Building a tuberculosis-free world: The Lancet Commission on tuberculosis. *Lancet* (2019) 393(10178):1331–84. doi: 10.1016/S0140-6736(19)30024-8
35. Ahmad S. Pathogenesis, immunology, and diagnosis of latent Mycobacterium tuberculosis infection. *Clin Dev Immunol* (2011) 2011:814943. doi: 10.1155/2011/814943
36. Segal-Maurer S. Tuberculosis in Enclosed Populations. *Microbiol Spectr* (2017) 5(2):TNM17-0041-2017. doi: 10.1128/microbiolspec.TNM17-0041-2017
37. Esmail H, Barry CE, Young DB, Wilkinson RJ. The ongoing challenge of latent tuberculosis. *Philos Trans R Soc Lond B Biol Sci* (2014) 369(1645):20130437. doi: 10.1098/rstb.2013.0437
38. Robertson BD, Altmann D, Barry C, Bishai B, Cole S, Dick T, et al. Detection and treatment of subclinical tuberculosis. *Tuberculosis (Edinb)* (2012) 92(6):447–52. doi: 10.1016/j.tube.2012.06.004
39. Barry CE, Boshoff HI, Dartois V, Dick T, Ehrt S, Flynn J, et al. The spectrum of latent tuberculosis: rethinking the biology and intervention strategies. *Nat Rev Microbiol* (2009) 7(12):845–55. doi: 10.1038/nrmicro2236
40. Chee CBE, Reves R, Zhang Y, Belknap R. Latent tuberculosis infection: Opportunities and challenges. *Respirology* (2018) 23(10):893–900. doi: 10.1111/resp.13346
41. Lin PL, Flynn JL. Understanding latent tuberculosis: a moving target. *J Immunol* (2010) 185(1):15–22. doi: 10.4049/jimmunol.0903856
42. Abubakar I, Drobniewski F, Southern J, Sitch AJ, Jackson C, Lipman M, et al. Prognostic value of interferon-gamma release assays and tuberculin skin test in predicting the development of active tuberculosis (UK PREDICT TB): a prospective cohort study. *Lancet Infect Dis* (2018) 18(10):1077–87. doi: 10.1016/S1473-3099(18)30355-4
43. Fox GJ, Dobler CC, Marais BJ, Denholm JT. Preventive therapy for latent tuberculosis infection-the promise and the challenges. *Int J Infect Dis* (2017) 56:68–76. doi: 10.1016/j.ijid.2016.11.006
44. Sharma SK, Mohanan S, Sharma A. Relevance of latent TB infection in areas of high TB prevalence. *Chest* (2012) 142(3):761–73. doi: 10.1378/chest.12-0142
45. Huddart S, MacLean E, Pai M. Location, location, location: tuberculosis services in highest burden countries. *Lancet Glob Health* (2016) 4(12):e907–e8. doi: 10.1016/S2214-109X(16)30248-0
46. Bacelo AC, do Brasil PE, Cople-Rodrigues CD, Ingebourg G, Paiva E, Ramalho A, et al. Dietary counseling adherence during tuberculosis



- treatment: A longitudinal study. *Clin Nutr ESPEN*. (2017) 17:44–53. doi: 10.1016/j.clnesp.2016.11.001
47. Kendall EA, Sahu S, Pai M, Fox GJ, Varaine F, Cox H, et al. What will it take to eliminate drug-resistant tuberculosis? *Int J Tuberc Lung Dis* (2019) 23 (5):535–46. doi: 10.5588/ijtld.18.0217
  48. Wurie FB, Cooper V, Horne R, Hayward AC. Determinants of non-adherence to treatment for tuberculosis in high-income and middle-income settings: a systematic review protocol. *BMJ Open* (2018) 8(1): e019287. doi: 10.1136/bmjopen-2017-019287
  49. Subbaraman R, de Mondesert L, Musiimenta A, Pai M, Mayer KH, Thomas BE, et al. Digital adherence technologies for the management of tuberculosis therapy: mapping the landscape and research priorities. *BMJ Glob Health* (2018) 3(5):e001018. doi: 10.1136/bmjgh-2018-001018
  50. Sabate E. *Adherence to Long Term Therapies: Evidence for Action*. WHO Library (2003). Available at: [https://www.who.int/chp/knowledge/publications/adherence\\_introduction.pdf?ua=1](https://www.who.int/chp/knowledge/publications/adherence_introduction.pdf?ua=1).
  51. Ahsan MJ, Garg SK, Vashistha B, Sharma P. Tuberculosis vaccines: hopes and hurdles. *Infect Disord Drug Targets* (2013) 13(5):318–21. doi: 10.2174/1871526513666131201125513
  52. Ormerod LP. Multidrug-resistant tuberculosis (MDR-TB): epidemiology, prevention and treatment. *Br Med Bull* (2005) 73-74:17–24. doi: 10.1093/bmb/ldh047
  53. Pozniak AL, Miller RF, Lipman MC, Freedman AR, Ormerod LP, Johnson MA, et al. BHIVA treatment guidelines for tuberculosis (TB)/HIV infection 2005. *HIV Med* (2005) 6 Suppl 2:62–83. doi: 10.1111/j.1468-1293.2005.00293.x
  54. Palomino JC, Martin A. Tuberculosis clinical trial update and the current anti-tuberculosis drug portfolio. *Curr Med Chem* (2013) 20(30):3785–96. doi: 10.2174/09298673113209990166
  55. Ahuja SD, Ashkin D, Avendano M, Banerjee R, Bauer M, Bayona JN, et al. Multidrug resistant pulmonary tuberculosis treatment regimens and patient outcomes: an individual patient data meta-analysis of 9,153 patients. *PLoS Med* (2012) 9(8):e1001300. doi: 10.1371/journal.pmed.1001300
  56. Tiberi S, Munoz-Torrico M, Duarte R, Dalcolmo M, D'Ambrosio L, Migliori GB. New drugs and perspectives for new anti-tuberculosis regimens. *Pulmonology* (2018) 24(2):86–98. doi: 10.1016/j.rppnen.2017.10.009
  57. Fox GJ, Mitnick CD, Benedetti A, Chan ED, Becerra M, Chiang CY, et al. Surgery as an Adjunctive Treatment for Multidrug-Resistant Tuberculosis: An Individual Patient Data Metaanalysis. *Clin Infect Dis* (2016) 62(7):887–95. doi: 10.1093/cid/ciw002
  58. World Health Organisation. *The End TB Strategy*. The World Health Organization (2020). Available at: <https://www.who.int/tb/strategy/en/>.
  59. Sohn H, Kasaie P, Kendall E, Gomez GB, Vassall A, Pai M, et al. Informing decision-making for universal access to quality tuberculosis diagnosis in India: an economic-epidemiological model. *BMC Med* (2019) 17(1):155. doi: 10.1186/s12916-019-1384-8
  60. Pai M, Schito M. Tuberculosis diagnostics in 2015: landscape, priorities, needs, and prospects. *J Infect Dis* (2015) 211 Suppl 2:S21–8. doi: 10.1093/infdis/jiu803
  61. Schumacher SG, Wells WA, Nicol MP, Steingart KR, Theron G, Dorman SE, et al. Guidance for Studies Evaluating the Accuracy of Sputum-Based Tests to Diagnose Tuberculosis. *J Infect Dis* (2019) 220(Supplement\_3):S99–107. doi: 10.1093/infdis/jiz258
  62. Schumacher SG, Thangakunam B, Denkinger CM, Oliver AA, Shakti KB, Qin ZZ, et al. Impact of point-of-care implementation of Xpert(R) MTB/RIF: product vs. process innovation. *Int J Tuberc Lung Dis* (2015) 19 (9):1084–90. doi: 10.5588/ijtld.15.0120
  63. Zar HJ, Workman LJ, Prins M, Bateman LJ, Mbhele SP, Whitman CB, et al. Tuberculosis Diagnosis in Children Using Xpert Ultra on Different Respiratory Specimens. *Am J Respir Crit Care Med* (2019) 200(12):1531–8. doi: 10.1164/rccm.201904-0772OC
  64. Sarin S, Huddart S, Raizada N, Parija D, Kalra A, Rao R, et al. Cost and operational impact of promoting upfront GeneXpert MTB/RIF test referrals for presumptive pediatric tuberculosis patients in India. *PLoS One* (2019) 14 (4):e0214675. doi: 10.1371/journal.pone.0214675
  65. TBfacts.org. *Genexpert*. The World Health Organization (2020). Available at: <https://tbfacts.org/genexpert/>.
  66. Nathavitharana RR, Yoon C, Macpherson P, Dowdy DW, Cattamanchi A, Somoskovi A, et al. Guidance for Studies Evaluating the Accuracy of Tuberculosis Triage Tests. *J Infect Dis* (2019) 220(Supplement\_3):S116–S25. doi: 10.1093/infdis/jiz243
  67. Cazabon D, Pande T, Kik S, Van Gemert W, Sohn H, Denkinger C, et al. Market penetration of Xpert MTB/RIF in high tuberculosis burden countries: A trend analysis from 2014 - 2016. *Gates Open Res* (2018) 2:35. doi: 10.12688/gatesopenres.12842.2
  68. Cazabon D, Alsdurf H, Satyanarayana S, Nathavitharana R, Subbaraman R, Daftary A, et al. Quality of tuberculosis care in high burden countries: the urgent need to address gaps in the care cascade. *Int J Infect Dis* (2017) 56:111–6. doi: 10.1016/j.ijid.2016.10.016
  69. Ramirez-Lapausa M, Menendez-Saldana A, Noguerado-Asensio A. [Extrapulmonary tuberculosis]. *Rev Esp Sanid Penit* (2015) 17(1):3–11. doi: 10.4321/S1575-06202015000100002
  70. Das P, Ahuja A, Gupta SD. Incidence, etiopathogenesis and pathological aspects of genitourinary tuberculosis in India: A journey revisited. *Indian J Urol* (2008) 24(3):356–61. doi: 10.4103/0970-1591.42618
  71. Agins BD, Ikeda DJ, Reid MJA, Goosby E, Pai M, Cattamanchi A. Improving the cascade of global tuberculosis care: moving from the “what” to the “how” of quality improvement. *Lancet Infect Dis* (2019) 19(12):E437–43. doi: 10.1016/S1473-3099(19)30420-7
  72. Hatherill M, Chaisson RE, Denkinger CM. Addressing critical needs in the fight to end tuberculosis with innovative tools and strategies. *PLoS Med* (2019) 16(4):e1002795. doi: 10.1371/journal.pmed.1002795
  73. Drain PK, Gardiner J, Hannah H, Broger T, Dheda K, Fielding K, et al. Guidance for Studies Evaluating the Accuracy of Biomarker-Based Nonsputum Tests to Diagnose Tuberculosis. *J Infect Dis* (2019) 220 (Supplement\_3):S108–S15. doi: 10.1093/infdis/jiz356
  74. Denkinger CM, Schumacher SG, Gilpin C, Korobitsyn A, Wells WA, Pai M, et al. Guidance for the Evaluation of Tuberculosis Diagnostics That Meet the World Health Organization (WHO) Target Product Profiles: An Introduction to WHO Process and Study Design Principles. *J Infect Dis* (2019) 220(Supplement\_3):S91–S8. doi: 10.1093/infdis/jiz097
  75. Zhao YL, Pang Y, Xia H, Du X, Chin D, Huan ST, et al. Market assessment of tuberculosis diagnostics in China in 2012. *Int J Tuberc Lung Dis* (2016) 20 (3):295–303. doi: 10.5588/ijtld.15.0156
  76. Maheshwari P, Chauhan K, Kadam R, Pujani A, Kaur M, Chitalia M, et al. Market assessment of tuberculosis diagnostics in India in 2013. *Int J Tuberc Lung Dis* (2016) 20(3):304–13. doi: 10.5588/ijtld.15.0571
  77. Kik SV, Denkinger CM, Casenghi M, Vadrnais C, Pai M. Tuberculosis diagnostics: which target product profiles should be prioritised? *Eur Respir J* (2014) 44(2):537–40. doi: 10.1183/09031936.00027714
  78. Kik SV, Denkinger CM, Chedore P, Pai M. Replacing smear microscopy for the diagnosis of tuberculosis: what is the market potential? *Eur Respir J* (2014) 43(6):1793–6. doi: 10.1183/09031936.00217313
  79. Kik SV, Denkinger CM, Jefferson C, Ginnard J, Pai M. Potential market for novel tuberculosis diagnostics: worth the investment? *J Infect Dis* (2015) 211 Suppl 2:S58–66. doi: 10.1093/infdis/jiu817
  80. Cobelens F, Kik S, Esmail H, Cirillo DM, Lienhardt C, Matteelli A. From latent to patent: rethinking prediction of tuberculosis. *Lancet Respir Med* (2017) 5(4):243–4. doi: 10.1016/S2213-2600(16)30419-2
  81. Denkinger CM, Kik SV, Cirillo DM, Casenghi M, Shinnick T, Weyer K, et al. Defining the needs for next generation assays for tuberculosis. *J Infect Dis* (2015) 211 Suppl 2:S29–38. doi: 10.1093/infdis/jiu821
  82. Penn-Nicholson A, Hraha T, Thompson EG, Sterling D, Mbandi SK, Wall KM, et al. Discovery and validation of a prognostic proteomic signature for tuberculosis progression: A prospective cohort study. *PLoS Med* (2019) 16 (4):e1002781. doi: 10.1371/journal.pmed.1002781
  83. Manngo PM, Gutschmidt A, Snyders CI, Mutavhatsindi H, Manyelo CM, Makhoba NS, et al. Prospective evaluation of host biomarkers other than interferon gamma in QuantiFERON Plus supernatants as candidates for the diagnosis of tuberculosis in symptomatic individuals. *J Infect* (2019) 79 (3):228–35. doi: 10.1016/j.jinf.2019.07.007
  84. Keshavjee S, Amanullah F, Cattamanchi A, Chaisson R, Dobos KM, Fox GJ, et al. Moving toward Tuberculosis Elimination. Critical Issues for Research in Diagnostics and Therapeutics for Tuberculosis Infection. *Am J Respir Crit Care Med* (2019) 199(5):564–71. doi: 10.1164/rccm.201806-1053PP
  85. Walz G, McNeerney R, du Plessis N, Bates M, McHugh TD, Chegou NN, et al. Tuberculosis: advances and challenges in development of new

- diagnostics and biomarkers. *Lancet Infect Dis* (2018) 18(7):e199–210. doi: 10.1016/S1473-3099(18)30111-7
86. Walzl G, Haks MC, Joosten SA, Kleynhans L, Ronacher K, Ottenhoff TH. Clinical immunology and a multiplex biomarkers of human tuberculosis. *Cold Spring Harb Perspect Med* (2014) 5(4):a018515. doi: 10.1101/cshperspect.a018515
  87. Wallis RS, Pai M, Menzies D, Doherty TM, Walzl G, Perkins MD, et al. Biomarkers and diagnostics for tuberculosis: progress, needs, and translation into practice. *Lancet* (2010) 375(9729):1920–37. doi: 10.1016/S0140-6736(10)60359-5
  88. MacLean E, Broger T, Yerlikaya S, Fernandez-Carballo BL, Pai M, Denking CM. A systematic review of biomarkers to detect active tuberculosis. *Nat Microbiol* (2019) 4(5):748–58. doi: 10.1038/s41564-019-0380-2
  89. Gupta RK, Turner CT, Venturini C, Esmail H, Rangaka MX, Copas A, et al. Concise whole blood transcriptional signatures for incipient tuberculosis: a systematic review and patient-level pooled meta-analysis. *Lancet Respir Med* (2020) 8(4):395–406. doi: 10.1016/S2213-2600(19)30282-6
  90. Warsinske H, Vashisht R, Khatri P. Host-response-based gene signatures for tuberculosis diagnosis: A systematic comparison of 16 signatures. *PLoS Med* (2019) 16(4):e1002786. doi: 10.1371/journal.pmed.1002786
  91. Warsinske HC, Rao AM, Moreira FMF, Santos PCP, Liu AB, Scott M, et al. Assessment of Validity of a Blood-Based 3-Genes Signature Score for Progression and Diagnosis of Tuberculosis, Disease Severity, and Treatment Response. *JAMA Netw Open* (2018) 1(6):e183779. doi: 10.1001/jamanetworkopen.2018.3779
  92. Mulenga H, Bunyasi EW, Mbandi SK, Mendelsohn SC, Kagina B, Penn-Nicholson A, et al. Performance of host blood transcriptomic signatures for diagnosing and predicting progression to tuberculosis disease in HIV-negative adults and adolescents: a systematic review protocol. *BMJ Open* (2019) 9(5):e026612. doi: 10.1136/bmjopen-2018-026612
  93. Wallis RS, Jakubiec W, Kumar V, Bedarida G, Silvia A, Paige D, et al. Biomarker-assisted dose selection for safety and efficacy in early development of PNU-100480 for tuberculosis. *Antimicrob Agents Chemother* (2011) 55(2):567–74. doi: 10.1128/AAC.01179-10
  94. Sumner T, Scriba TJ, Penn-Nicholson A, Hatherill M, White RG. Potential population level impact on tuberculosis incidence of using an mRNA expression signature correlate-of-risk test to target tuberculosis preventive therapy. *Sci Rep* (2019) 9(1):11126. doi: 10.1038/s41598-019-47645-z
  95. Ronacher K, Chegou NN, Kleynhans L, Djoba Siawaya JF, du Plessis N, Loxton AG, et al. Distinct serum biosignatures are associated with different tuberculosis treatment outcomes. *Tuberculosis (Edinb)* (2019) 118:101859. doi: 10.1016/j.tube.2019.101859
  96. Darboe F, Mbandi SK, Naidoo K, Yende-Zuma N, Lewis L, Thompson EG, et al. Detection of Tuberculosis Recurrence, Diagnosis and Treatment Response by a Blood Transcriptomic Risk Signature in HIV-Infected Persons on Antiretroviral Therapy. *Front Microbiol* (2019) 10:1441. doi: 10.3389/fmicb.2019.01441
  97. Singhania A, Wilkinson RJ, Rodrigue M, Haldar P, O'Garra A. The value of transcriptomics in advancing knowledge of the immune response and diagnosis in tuberculosis. *Nat Immunol* (2018) 19(11):1159–68. doi: 10.1038/s41590-018-0225-9
  98. Thompson EG, Du Y, Malherbe ST, Shankar S, Braun J, Valvo J, et al. Host blood RNA signatures predict the outcome of tuberculosis treatment. *Tuberculosis (Edinb)* (2017) 107:48–58. doi: 10.1016/j.tube.2017.08.004
  99. Jacobs R, Tshela E, Malherbe S, Kriel M, Loxton AG, Stanley K, et al. Host biomarkers detected in saliva show promise as markers for the diagnosis of pulmonary tuberculosis disease and monitoring of the response to tuberculosis treatment. *Cytokine* (2016) 81:50–6. doi: 10.1016/j.cyt.2016.02.004
  100. Jacobs R, Malherbe S, Loxton AG, Stanley K, van der Spuy G, Walzl G, et al. Identification of novel host biomarkers in plasma as candidates for the immunodiagnosis of tuberculosis disease and monitoring of tuberculosis treatment response. *Oncotarget* (2016) 7(36):57581–92. doi: 10.18632/oncotarget.11420
  101. Cliff JM, Kaufmann SH, McShane H, van Helden P, O'Garra A. The human immune response to tuberculosis and its treatment: a view from the blood. *Immunol Rev* (2015) 264(1):88–102. doi: 10.1111/imr.12269
  102. Scriba TJ, Mendelsohn SC. Headway made towards biosignatures for incipient tuberculosis. *Lancet Respir Med* (2020) 8(4):328–30. doi: 10.1016/S2213-2600(19)30355-8
  103. Mendelsohn SC, Mbandi SK, Hatherill M, Scriba TJ. Blood transcriptional signatures for tuberculosis testing. *Lancet Respir Med* (2020) 8(4):330–1. doi: 10.1016/S2213-2600(20)30045-X
  104. Blankley S, Berry MP, Graham CM, Bloom CI, Lipman M, O'Garra A. The application of transcriptional blood signatures to enhance our understanding of the host response to infection: the example of tuberculosis. *Philos Trans R Soc Lond B Biol Sci* (2014) 369(1645):20130427. doi: 10.1098/rstb.2013.0427
  105. O'Garra A, Redford PS, McNab FW, Bloom CI, Wilkinson RJ, Berry MP. The immune response in tuberculosis. *Annu Rev Immunol* (2013) 31:475–527. doi: 10.1146/annurev-immunol-032712-095939
  106. Berry MP, Blankley S, Graham CM, Bloom CI, O'Garra A. Systems approaches to studying the immune response in tuberculosis. *Curr Opin Immunol* (2013) 25(5):579–87. doi: 10.1016/j.coi.2013.08.003
  107. Berry MP, Graham CM, McNab FW, Xu Z, Bloch SA, Oni T, et al. An interferon-inducible neutrophil-driven blood transcriptional signature in human tuberculosis. *Nature* (2010) 466(7309):973–7. doi: 10.1038/nature09247
  108. Rajan JV, Semitala FC, Mehta T, Seielstad M, Montalvo L, Andama A, et al. A Novel, 5-Transcript, Whole-blood Gene-expression Signature for Tuberculosis Screening Among People Living With Human Immunodeficiency Virus. *Clin Infect Dis* (2019) 69(1):77–83. doi: 10.1093/cid/ciy835
  109. Singhania A, Verma R, Graham CM, Lee J, Tran T, Richardson M, et al. A modular transcriptional signature identifies phenotypic heterogeneity of human tuberculosis infection. *Nat Commun* (2018) 9(1):2308. doi: 10.1038/s41467-018-04579-w
  110. Leong S, Zhao Y, Joseph NM, Hochberg NS, Sarkar S, Pleskunas J, et al. Existing blood transcriptional classifiers accurately discriminate active tuberculosis from latent infection in individuals from south India. *Tuberculosis (Edinb)* (2018) 109:41–51. doi: 10.1016/j.tube.2018.01.002
  111. Zak DE, Penn-Nicholson A, Scriba TJ, Thompson E, Suliman S, Amon LM, et al. A blood RNA signature for tuberculosis disease risk: a prospective cohort study. *Lancet* (2016) 387(10035):2312–22. doi: 10.1016/S0140-6736(15)01316-1
  112. Blankley S, Graham CM, Turner J, Berry MP, Bloom CI, Xu Z, et al. The Transcriptional Signature of Active Tuberculosis Reflects Symptom Status in Extra-Pulmonary and Pulmonary Tuberculosis. *PLoS One* (2016) 11(10):e0162220. doi: 10.1371/journal.pone.0162220
  113. Blankley S, Graham CM, Levin J, Turner J, Berry MP, Bloom CI, et al. A 380-gene meta-signature of active tuberculosis compared with healthy controls. *Eur Respir J* (2016) 47(6):1873–6. doi: 10.1183/13993003.02121-2015
  114. Bloom CI, Graham CM, Berry MP, Rozakeas F, Redford PS, Wang Y, et al. Transcriptional blood signatures distinguish pulmonary tuberculosis, pulmonary sarcoidosis, pneumonias and lung cancers. *PLoS One* (2013) 8(8):e70630. doi: 10.1371/journal.pone.0070630
  115. Penn-Nicholson A, Mbandi SK, Thompson E, Mendelsohn SC, Suliman S, Chegou NN, et al. RISK6, a 6-gene transcriptomic signature of TB disease risk, diagnosis and treatment response. *Sci Rep* (2020) 10(1):8629. doi: 10.1038/s41598-020-65043-8
  116. Kwan PKW, Periaswamy B, De Sessions PF, Lin W, Molton JS, Naftalin CM, et al. A blood RNA transcript signature for TB exposure in household contacts. *BMC Infect Dis* (2020) 20(1):403. doi: 10.1186/s12879-020-05116-1
  117. Jacobsen M, Repsilber D, Gutschmidt A, Neher A, Feldmann K, Mollenkopf HJ, et al. Candidate biomarkers for discrimination between infection and disease caused by *Mycobacterium tuberculosis*. *J Mol Med (Berl)* (2007) 85(6):613–21. doi: 10.1007/s00109-007-0157-6
  118. Laux da Costa L, Delcroix M, Dalla Costa ER, Prestes IV, Milano M, Francis SS, et al. A real-time PCR signature to discriminate between tuberculosis and other pulmonary diseases. *Tuberculosis (Edinb)* (2015) 95(4):421–5. doi: 10.1016/j.tube.2015.04.008
  119. Roe JK, Thomas N, Gil E, Best K, Tsaliki E, Morris-Jones S, et al. Blood transcriptomic diagnosis of pulmonary and extrapulmonary tuberculosis. *JCI Insight* (2016) 1(16):e87238. doi: 10.1172/jci.insight.87238

120. Sweeney TE, Braviak L, Tato CM, Khatri P. Genome-wide expression for diagnosis of pulmonary tuberculosis: a multicohort analysis. *Lancet Respir Med* (2016) 4(3):213–24. doi: 10.1016/S2213-2600(16)00048-5
121. Roe J, Venturini C, Gupta RK, Gurry C, Chain BM, Sun Y, et al. Blood Transcriptomic Stratification of Short-term Risk in Contacts of Tuberculosis. *Clin Infect Dis* (2020) 70(5):731–7. doi: 10.1093/cid/ciz252
122. Maertzdorf J, Repsilber D, Parida SK, Stanley K, Roberts T, Black G, et al. Human gene expression profiles of susceptibility and resistance in tuberculosis. *Genes Immun* (2011) 12(1):15–22. doi: 10.1038/gene.2010.51
123. Maertzdorf J, McEwen G, Weiner J, Tian S, Lader E, Schriek U, et al. Concise gene signature for point-of-care classification of tuberculosis. *EMBO Mol Med* (2016) 8(2):86–95. doi: 10.15252/emmm.201505790
124. Qian Z, Lv J, Kelly GT, Wang H, Zhang X, Gu W, et al. Expression of nuclear factor, erythroid 2-like 2-mediated genes differentiates tuberculosis. *Tuberculosis (Edinb)* (2016) 99:56–62. doi: 10.1016/j.tube.2016.04.008
125. Gjoen JE, Jenun S, Sivakumaran D, Mukherjee A, Macaden R, Kabra SK, et al. Novel transcriptional signatures for sputum-independent diagnostics of tuberculosis in children. *Sci Rep* (2017) 7(1):5839. doi: 10.1038/s41598-017-05057-x
126. Gliddon HD, Kaforou M, Alikian M, Habgood-Coote D, Zhou C, Oni T, et al. Identification of reduced host transcriptomic signatures for tuberculosis and digital PCR-based validation and quantification. *bioRxiv* (2019) 583674. doi: 10.1101/583674
127. Sambarey A, Devaprasad A, Mohan A, Ahmed A, Nayak S, Swaminathan S, et al. Unbiased Identification of Blood-based Biomarkers for Pulmonary Tuberculosis by Modeling and Mining Molecular Interaction Networks. *EBioMedicine* (2017) 15:112–26. doi: 10.1016/j.ebiom.2016.12.009
128. Sambarey A, Devaprasad A, Baloni P, Mishra M, Mohan A, Tyagi P, et al. Meta-analysis of host response networks identifies a common core in tuberculosis. *NPJ Syst Biol Appl* (2017) 3:4. doi: 10.1038/s41540-017-0005-4
129. Verhagen LM, Zomer A, Maes M, Villalba JA, Del Nogal B, Eleveld M, et al. A predictive signature gene set for discriminating active from latent tuberculosis in Warao Amerindian children. *BMC Genomics* (2013) 14:74. doi: 10.1186/1471-2164-14-74
130. de Araujo LS, Vaas LA, Ribeiro-Alves M, Geffers R, Mello FC, de Almeida AS, et al. Transcriptomic Biomarkers for Tuberculosis: Evaluation of DOCK9, EPHA4, and NPC2 mRNA Expression in Peripheral Blood. *Front Microbiol* (2016) 7:1586. doi: 10.3389/fmicb.2016.01586
131. Duffy D, Nemes E, Llibre A, Rouilly V, Musvosvi M, Smith N, et al. Immune profiling enables stratification of patients with active TB disease or M. tuberculosis infection. *Clin Infect Dis* (2020) ciae1562. doi: 10.1093/cid/ciae1562
132. Kaforou M, Wright VJ, Oni T, French N, Anderson ST, Bangani N, et al. Detection of tuberculosis in HIV-infected and -uninfected African adults using whole blood RNA expression signatures: a case-control study. *PLoS Med* (2013) 10(10):e1001538. doi: 10.1371/journal.pmed.1001538
133. Anderson ST, Kaforou M, Brent AJ, Wright VJ, Banwell CM, Chagaluka G, et al. Diagnosis of childhood tuberculosis and host RNA expression in Africa. *N Engl J Med* (2014) 370(18):1712–23. doi: 10.1056/NEJMoa1303657
134. Suliman S, Thompson E, Sutherland J, Weiner Rd J, Ota MOC, Shankar S, et al. Four-gene Pan-African Blood Signature Predicts Progression to Tuberculosis. *Am J Respir Crit Care Med* (2018) 197(9):1198–208. doi: 10.1164/rccm.201711-2340OC
135. Sutherland JS, Loxton AG, Haks MC, Kassa D, Ambrose L, Lee JS, et al. Differential gene expression of activating Fcγ receptor classifies active tuberculosis regardless of human immunodeficiency virus status or ethnicity. *Clin Microbiol Infect* (2014) 20(4):O230–8. doi: 10.1111/1469-0691.12383
136. Estevez O, Anibarro L, Garet E, Pallares A, Barcia L, Calvino L, et al. An RNA-seq Based Machine Learning Approach Identifies Latent Tuberculosis Patients With an Active Tuberculosis Profile. *Front Immunol* (2020) 11:1470. doi: 10.3389/fimmu.2020.01470
137. Turner CT, Gupta RK, Tsaliki E, Roe JK, Mondal P, Nyawo GR, et al. Blood transcriptional biomarkers for active pulmonary tuberculosis in a high-burden setting: a prospective, observational, diagnostic accuracy study. *Lancet Respir Med* (2020) 8(4):407–19. doi: 10.1016/S2213-2600(19)30469-2
138. Leong S, Zhao Y, Ribeiro-Rodrigues R, Jones-López EC, Acuña-Villaorduña C, Rodrigues PM, et al. Cross-validation of existing signatures and derivation of a novel 29-gene transcriptomic signature predictive of progression to TB in a Brazilian cohort of household contacts of pulmonary TB. *Tuberculosis (Edinb)* (2020) 120:101898. doi: 10.1016/j.tube.2020.101898
139. Walter ND, Miller MA, Vasquez J, Weiner M, Chapman A, Engle M, et al. Blood Transcriptional Biomarkers for Active Tuberculosis among Patients in the United States: a Case-Control Study with Systematic Cross-Classification Evaluation. *J Clin Microbiol* (2016) 54(2):274–82. doi: 10.1128/JCM.01990-15
140. World Health Organisation. *High-priority target product profiles for new tuberculosis diagnostics: report of a consensus meeting*. (2014). Available at: [https://apps.who.int/iris/bitstream/handle/10665/135617/WHO\\_HTM\\_TB\\_2014.18\\_eng.pdf;jsessionid=66D7C7B71A2F6506FF0DFDFF9F671CC8?sequence=1](https://apps.who.int/iris/bitstream/handle/10665/135617/WHO_HTM_TB_2014.18_eng.pdf;jsessionid=66D7C7B71A2F6506FF0DFDFF9F671CC8?sequence=1).
141. Javed S, Marsay L, Wareham A, Lewandowski KS, Williams A, Dennis MJ, et al. Temporal Expression of Peripheral Blood Leukocyte Biomarkers in a Macaca fascicularis Infection Model of Tuberculosis; Comparison with Human Datasets and Analysis with Parametric/Non-parametric Tools for Improved Diagnostic Biomarker Identification. *PLoS One* (2016) 11(5):e0154320. doi: 10.1371/journal.pone.0154320
142. Foreman TW, Mehra S, Lackner AA, Kaushal D. Translational Research in the Nonhuman Primate Model of Tuberculosis. *ILAR J* (2017) 58(2):151–9. doi: 10.1093/ilar/ilx015
143. Pena JC, Ho WZ. Non-Human Primate Models of Tuberculosis. *Microbiol Spectr* (2016) 4(4):TBTB2-0007-2016. doi: 10.1128/microbiolspec.TBTB2-0007-2016
144. Darrah PA, Zeppa JJ, Maiello P, Hackney JA, Wadsworth MH2nd, Hughes TK, et al. Prevention of tuberculosis in macaques after intravenous BCG immunization. *Nature* (2020) 577(7788):95–102. doi: 10.1038/s41586-019-1817-8
145. Dijkman K, Sombroek CC, Vervenne RAW, Hofman SO, Boot C, Remarque EJ, et al. Prevention of tuberculosis infection and disease by local BCG in repeatedly exposed rhesus macaques. *Nat Med* (2019) 25(2):255–62. doi: 10.1038/s41591-018-0319-9
146. Harris SA, White A, Stockdale L, Tanner R, Sibley L, Sarfas C, et al. Development of a non-human primate BCG infection model for the evaluation of candidate tuberculosis vaccines. *Tuberculosis (Edinb)* (2018) 108:99–105. doi: 10.1016/j.tube.2017.11.006
147. Singhania A, Graham CM, Gabryšová L, Moreira-Teixeira L, Stavropoulos E, Pitt JM, et al. Transcriptional profiling unveils type I and II interferon networks in blood and tissues across diseases. *Nat Commun* (2019) 10(1):2887. doi: 10.1038/s41467-019-10601-6
148. Moreira-Teixeira L, Mayer-Barber K, Sher A, O'Garra A. Type I interferons in tuberculosis: Foe and occasionally friend. *J Exp Med* (2018) 215(5):1273–85. doi: 10.1084/jem.20180325
149. Michalska A, Blaszczyk K, Wesoly J, Bluysen HAR. A Positive Feedback Amplifier Circuit That Regulates Interferon (IFN)-Stimulated Gene Expression and Controls Type I and Type II IFN Responses. *Front Immunol* (2018) 9:1135. doi: 10.3389/fimmu.2018.01135
150. Donovan ML, Schultz TE, Duke TJ, Blumenthal A. Type I Interferons in the Pathogenesis of Tuberculosis: Molecular Drivers and Immunological Consequences. *Front Immunol* (2017) 8:1633. doi: 10.3389/fimmu.2017.01633
151. McNab F, Mayer-Barber K, Sher A, Wack A, O'Garra A. Type I interferons in infectious disease. *Nat Rev Immunol* (2015) 15(2):87–103. doi: 10.1038/nri3787
152. Togun TO, MacLean E, Kampmann B, Pai M. Biomarkers for diagnosis of childhood tuberculosis: A systematic review. *PLoS One* (2018) 13(9):e0204029. doi: 10.1371/journal.pone.0204029
153. Togun T, Pai M. The uncertain science of predicting tuberculosis. *Lancet Respir Med* (2017) 5(4):239–40. doi: 10.1016/S2213-2600(17)30059-0
154. Yerlikaya S, Broger T, MacLean E, Pai M, Denking CM. A tuberculosis biomarker database: the key to novel TB diagnostics. *Int J Infect Dis* (2017) 56:253–7. doi: 10.1016/j.ijid.2017.01.025
155. Fiore-Gartland A, Carpp LN, Naidoo K, Thompson E, Zak DE, Self S, et al. Considerations for biomarker-targeted intervention strategies for tuberculosis disease prevention. *Tuberculosis (Edinb)* (2018) 109:61–8. doi: 10.1016/j.tube.2017.11.009
156. Pai M, Nicol MP, Boehme CC. Tuberculosis Diagnostics: State of the Art and Future Directions. *Microbiol Spectr* (2016) 4(5):TBTB2-0019-2016. doi: 10.1128/microbiolspec.TBTB2-0019-2016

157. UNITAID. *TUBERCULOSIS: Diagnostics Technology Landscape, 5th Edition*. Unitaid (2017) Available at: <https://unitaid.org/assets/2017-Unitaid-TB-Diagnostics-Technology-Landscape.pdf>.

**Conflict of Interest:** The authors declare that the research was conducted in the absence of any commercial or financial relationships that could be construed as a potential conflict of interest.

Copyright © 2021 Perumal, Abdullatif, Garland, Honeyborne, Lipman, McHugh, Southern, Breen, Santis, Ellappan, Kumar, Belgode, Abubakar, Sinha, Vasan, Joseph and Kempell. This is an open-access article distributed under the terms of the Creative Commons Attribution License (CC BY). The use, distribution or reproduction in other forums is permitted, provided the original author(s) and the copyright owner(s) are credited and that the original publication in this journal is cited, in accordance with accepted academic practice. No use, distribution or reproduction is permitted which does not comply with these terms.





# Functional and Activation Profiles of Mucosal-Associated Invariant T Cells in Patients With Tuberculosis and HIV in a High Endemic Setting

Avuyonke Balfour<sup>1,2</sup>, Charlotte Schutz<sup>1,2</sup>, Rene Goliath<sup>2</sup>, Katalin A. Wilkinson<sup>2,3</sup>, Sumaya Sayed<sup>2</sup>, Bianca Sossen<sup>1,2</sup>, Jean-Paul Kanyik<sup>2</sup>, Amy Ward<sup>2</sup>, Rhandzu Ndzhukule<sup>2</sup>, Anele Gela<sup>4</sup>, David M. Lewinsohn<sup>5</sup>, Deborah A. Lewinsohn<sup>6</sup>, Graeme Meintjes<sup>1,2</sup> and Muki Shey<sup>1,2\*</sup>

<sup>1</sup> Department of Medicine, Faculty of Health Sciences, University of Cape Town, Cape Town, South Africa, <sup>2</sup> Wellcome Centre for Infectious Diseases Research in Africa (CIDRI-Africa), Faculty of Health Sciences, Institute of Infectious Disease and Molecular Medicine (IDM), University of Cape Town, Cape Town, South Africa, <sup>3</sup> The Francis Crick Institute, London, United Kingdom, <sup>4</sup> South African Tuberculosis Vaccine Initiative, Faculty of Health Sciences, Institute of Infectious Disease and Molecular Medicine (IDM), University of Cape Town, Cape Town, South Africa, <sup>5</sup> Division of Pulmonary and Critical Care Medicine, Department of Medicine, Oregon Health and Science University, Portland, OR, United States, <sup>6</sup> Division of Infectious Diseases, Department of Paediatrics, Oregon Health and Science University, Portland, OR, United States

## OPEN ACCESS

### Edited by:

Novel N. Chegou,  
Stellenbosch University, South Africa

### Reviewed by:

Seung-Jung Kee,  
Chonnam National University Hospital,  
South Korea  
Jennifer Ann Juno,  
The University of Melbourne, Australia

### \*Correspondence:

Muki Shey  
Muki.shey@uct.ac.za

### Specialty section:

This article was submitted to  
Microbial Immunology,  
a section of the journal  
Frontiers in Immunology

**Received:** 31 December 2020

**Accepted:** 24 February 2021

**Published:** 22 March 2021

### Citation:

Balfour A, Schutz C, Goliath R, Wilkinson KA, Sayed S, Sossen B, Kanyik J-P, Ward A, Ndzhukule R, Gela A, Lewinsohn DM, Lewinsohn DA, Meintjes G and Shey M (2021) Functional and Activation Profiles of Mucosal-Associated Invariant T Cells in Patients With Tuberculosis and HIV in a High Endemic Setting. *Front. Immunol.* 12:648216. doi: 10.3389/fimmu.2021.648216

**Background:** MAIT cells are non-classically restricted T lymphocytes that recognize and rapidly respond to microbial metabolites or cytokines and have the capacity to kill bacteria-infected cells. Circulating MAIT cell numbers generally decrease in patients with active TB and HIV infection, but findings regarding functional changes differ.

**Methods:** We conducted a cross-sectional study on the effect of HIV, TB, and HIV-associated TB (HIV-TB) on MAIT cell frequencies, activation and functional profile in a high TB endemic setting in South Africa. Blood was collected from (i) healthy controls (HC,  $n = 26$ ), 24 of whom had LTBI, (ii) individuals with active TB (aTB,  $n = 36$ ), (iii) individuals with HIV infection (HIV,  $n = 50$ ), 37 of whom had LTBI, and (iv) individuals with HIV-associated TB (HIV-TB,  $n = 26$ ). All TB participants were newly diagnosed and sampled before treatment, additional samples were also collected from 18 participants in the aTB group after 10 weeks of TB treatment. Peripheral blood mononuclear cells (PBMC) stimulated with BCG-expressing GFP (BCG-GFP) and heat-killed (HK) *Mycobacterium tuberculosis* (*M.tb*) were analyzed using flow cytometry. MAIT cells were defined as CD3<sup>+</sup> CD161<sup>+</sup> Vα7.2<sup>+</sup> T cells.

**Results:** Circulating MAIT cell frequencies were depleted in individuals with HIV infection ( $p = 0.009$ ). MAIT cells showed reduced CD107a expression in aTB ( $p = 0.006$ ), and reduced IFN $\gamma$  expression in aTB ( $p < 0.001$ ) and in HIV-TB ( $p < 0.001$ ) in response to BCG-GFP stimulation. This functional impairment was coupled with a significant increase in activation (defined by HLA-DR expression) in resting MAIT cells from HIV ( $p < 0.001$ ), aTB ( $p = 0.019$ ), and HIV-TB ( $p = 0.005$ ) patients, and higher HLA-DR expression in MAIT cells expressing IFN $\gamma$  in aTB ( $p = 0.009$ ) and HIV-TB ( $p = 0.002$ ) after stimulation with BCG-GFP and HK-*M.tb*. After 10 weeks of TB treatment, there was reversion in the observed functional impairment in total MAIT cells, with increases in CD107a ( $p = 0.020$ ) and IFN $\gamma$  ( $p = 0.010$ ) expression.

**Conclusions:** Frequencies and functional profile of MAIT cells in response to mycobacterial stimulation are significantly decreased in HIV infected persons, active TB and HIV-associated TB, with a concomitant increase in MAIT cell activation. These alterations may reduce the capacity of MAIT cells to play a protective role in the immune response to these two pathogens.

**Keywords:** MAIT cell, MAIT activation, human immunodeficiency virus, tuberculosis, MAIT cell function

## INTRODUCTION

Tuberculosis (TB) is one of the deadliest infectious diseases globally, with an estimated 10 million new cases and 1.4 million deaths in the year 2019 (1). South Africa has a high TB burden and accounts for about 3.6% of the global cases, with 360,000 cases of TB, and 58,000 deaths due to TB annually (1). One of the main drivers behind this high TB incidence is the Human Immunodeficiency Virus (HIV). South Africa had an estimated 7.5 million people living with HIV and reported about 200,000 new HIV infections in 2019 (2, 3). Of the total TB cases in 2019 in South Africa, 58% were from HIV infected people, these individuals had a disproportionally larger mortality rate of 62 (per 100,000 population) compared to HIV-negative individuals who had a mortality rate of 38 (1).

HIV and TB are both associated with impairment of the immune system (4, 5). HIV infection results in the depletion and functional impairment of CD4T cells that are crucial to the containment of *Mycobacterium tuberculosis* (6, 7). TB results in lymphopaenia and more rapid progression of untreated HIV infection and HIV-induced depletion of CD4T cells due to immune activation (5, 7). T cell immunity is therefore central in the pathogenesis of both infections.

Mucosal-associated invariant T (MAIT) cells have been shown to play a critical role in antibacterial immunity (8, 9). MAIT cells are an evolutionarily conserved, non-conventional, and innate-like subset of T cells that express a semi-invariant T cell receptor, TRAV1-2 (V $\alpha$ 7.2). This semi-invariant T cell receptor enables MAIT cells to recognize MHC-related protein 1 (MR1)-bound microbial vitamin metabolites, principally those derived from riboflavin pathways that are present in microbes but not in humans (10). MAIT cells can be identified through the expression of a variety of other markers such as IL-12R, IL-18R (11), the C-type lectin receptor, CD161, and CD26 (12). More recently, MR1 tetramers have been used to identify MAIT cells (13, 14). MAIT cells can be sub-divided into 3 different subsets; the predominant CD8+ subset, the CD4-, CD8- (double negative, DN) subset, and the CD4+ subset which has the lowest frequency (15).

Numerous studies have demonstrated that MAIT cells are responsive to bacteria-infected antigen presenting cells (APCs) (8, 9, 16). Chua et al. (8) demonstrated that MAIT cells have the capacity to inhibit intracellular bacterial growth in BCG-infected macrophages. Following antigen recognition, MAIT cells are activated and can rapidly produce a variety of cytokines such as IFN $\gamma$  and TNF- $\alpha$  (16, 17). In addition, MAIT cells also have the capacity to produce cytotoxic and cytolytic molecules such as granzyme B and perforin (18), thereby having capacity to kill

infected cells (9). *In vivo*, the absence of MR1 (and therefore MAIT cells) results in failure to control infection as mice lacking MR1 have been shown to have higher bacterial burden in their spleen and lungs compared to wild-type mice (8, 19, 20).

Studies that investigated the effect of HIV and TB disease on MAIT cells have shown decreased cell frequencies in both TB disease (21, 22) and chronic HIV infection (23–25). In TB disease, MAIT cells have also been shown to be functionally impaired with significantly lower expression of IFN $\gamma$ , TNF- $\alpha$ , IL-17, and granzyme B (18). In HIV however, findings on MAIT cell functions have been inconsistent. Leeansyah et al. (23) showed reduced frequencies of MAIT cells expressing IFN $\gamma$ , TNF- $\alpha$ , and IL-17 in people with HIV-1 infection, while Fernandez observed no significant differences in frequencies of MAIT cells expressing IFN $\gamma$  and TNF- $\alpha$  (25).

The impact of anti-retroviral treatment (ART) on MAIT cells has been investigated in several studies. Leeansyah et al. (23) and Wong et al. (22), found that the frequencies of MAIT cells were not fully restored by long-term ART and that there was only partial restoration of the capacity of MAIT cells to express IFN $\gamma$ , TNF- $\alpha$ , and IL-17 (23). Concentrations of these cytokines were higher in individuals on ART, but still lower than healthy uninfected controls (23). There are no published studies reporting the effect of TB treatment on MAIT cell frequencies and functions.

We evaluated the effect of HIV, TB, and HIV-associated TB on the frequencies and function of MAIT cells, including in different MAIT cell subsets. We also investigated the effect of the first 10 weeks of TB treatment on MAIT cell frequencies and function.

## METHODS AND MATERIALS

### Study Participants

Blood was collected from 138 participants recruited at Ubuntu HIV-TB Clinic, Khayelitsha, Cape Town, South Africa. Of these, 26 were HIV negative TB negative healthy controls (HC), 92% of whom had latent TB infection (LTBI), 50 were HIV positive TB negative and 70% had LTBI (HIV), 36 were HIV negative TB positive (aTB), and 26 had HIV-associated TB (HIV-TB). All study participants were screened for TB symptoms and had chest radiographs conducted. HC and HIV group participants were asymptomatic and had normal Chest X-rays. Active TB was confirmed or excluded by sputum culture and GeneXpert. We assessed healthy controls and HIV group participants for TB exposure using QuantiFERON-TB Gold Plus assay. Participants were considered to have latent infection if the IFN $\gamma$  concentrations were  $\geq 0.35$  IU/ml, and

without latent infection if IFN $\gamma$  concentrations were <0.35 IU/ml. Participants included into the 2 TB groups (aTB and HIV-TB) were recruited into the study before the start of TB treatment (or maximum of 3 doses). The study exclusion criteria included: declining HIV testing, pregnancy, having received more than three doses of TB treatment, presence of symptomatic anemia, and asthma or chronic obstructive pulmonary diseases. A subset of 18 individuals in the active TB group was chosen for repeat blood sample collection after 6–10 weeks (first 10 weeks) of TB treatment. Written informed consent was obtained from all study participants. Ethical approval for this study was obtained from the Faculty of Health Sciences Human Research Ethics Committee of the University of Cape Town (HREC Ref: 011/2017).

## Sample Processing

Blood samples were collected into Heparinized blood collection tubes. Peripheral blood mononuclear cells (PBMC) were isolated from blood *via* density gradient centrifugation with the Ficoll-Paque method and cryopreserved in fetal calf serum (FCS) containing 10% dimethyl sulfoxide (DMSO). These were then frozen at  $-80^{\circ}\text{C}$  overnight and transferred to liquid nitrogen for long-term storage.

## Cell Stimulations

Cryopreserved PBMC were thawed and rested in R10 media (10% FBS, 1% Penicillin/Streptomycin, 1% HEPES buffer, and 50 mM 2- $\beta$ -mercaptoethanol) at  $37^{\circ}\text{C}$  and 5%  $\text{CO}_2$  for 6 h prior to conducting stimulation assays. Following resting, cells were counted, and 1 million PBMC were stimulated with heat killed-*M.tb* (HK-*M.tb*) ( $5 \times 10^5$  CFU/ml), live *Mycobacterium bovis* BCG ( $1 \times 10^6$  and  $5 \times 10^6$  CFU/million cells, using BCG multiplicity of infection (MOI) = 1 (BCG 1) and BCG MOI = 5 (BCG 5), respectively) and PHA (4  $\mu\text{g/ml}$ ). For the background/unstimulated control, R10 media was used. Samples were incubated at  $37^{\circ}\text{C}$  and 5%  $\text{CO}_2$  for 18 h, following which, 100  $\mu\text{l}$  supernatant was collected, transferred into Sarstedt tubes and stored at  $-80^{\circ}\text{C}$ . Cells were then restimulated with respective antigen cocktails with the addition of anti-CD107a antibody and Monensin + Brefeldin and incubated for an additional 6 h at  $37^{\circ}\text{C}$  at 5%  $\text{CO}_2$ .

## Flow Cytometry

The following antibodies were used: CD161-BV605 (HP-3G10, BioLegend), CD11c-BV650 (clone B-ly6, BD Biosciences), CD107a-BV711 (clone H4A3, BioLegend), CD4-BV786 (clone SK3, BD Biosciences), V $\alpha$ 7.2-AF-647 (clone 3C10, BioLegend), HLA-DR-AF-700 (clone L243, BioLegend), CD8-APC-H7 (clone SK1, BD Biosciences), IFN $\gamma$ -V450 (clone B27, BD Biosciences), CD40-PerCp-Cy5.5 (clone 53C, BioLegend), CD3-ECD (clone UCHT1, Beckman Coulter), and PD1-BV711 (Clone EH12.2H7, BioLegend). Aqua fluorescent dye (Invitrogen) was used as a viability dye.

Following stimulation, cells were stained for viability with the aqua fluorescent dye and incubated for 10 min at room temperature. After viability staining, surface staining was performed with CD161, V $\alpha$ 7.2, CD4, and CD40. Cells were

then fixed and permeabilized with Cytotfix/Cytoperm buffer (BD Biosciences) followed by intracellular staining with CD3, CD8, CD14, CD11c, HLA-DR, and IFN $\gamma$ . The stained samples were acquired on a BD LSR Fortessa FACSDiva Software. A total of 500,000 events were collected and results analyzed using FlowJo (version 9.9.6, FlowJo LLC). We defined MAIT cells as CD3 $^{+}$ CD161 $^{+}$ V $\alpha$ 7.2 $^{+}$  T cells, after excluding doublets and dead cells.

## MR1 Tetramer Staining

For more precise identification of MAIT cells, and to validate the findings that we observed using antibodies, we used MR1 tetramers to investigate MAIT cell frequencies. For this, an MR1 tetramer conjugated to Allophycocyanin (APC), and loaded with 5-(2-oxopropylideneamino)-6-D-ribitylaminouracil (5-OP-RU), which is a known potent MAIT cell activating ligand, was used (Obtained from NIH Tetramer Core Facility, Emory University, Atlanta, GA, United States). PBMC were thawed and rested for 2 h, counted, and stained for viability. Cells were then stained with 50  $\mu\text{l}$  of 5-OP-RU-loaded MR1 tetramer (diluted 1:100) at  $37^{\circ}\text{C}$  for 30 min. As a control, cells were stained with 6-formyl pterin (PF) loaded MR1 tetramer (diluted 1:100). Cells were washed and stained extracellularly with CD161, CD3, CD4, CD8, PD1, and CD14. Following staining, cells were washed and fixed in 1% paraformaldehyde and acquired using a BD LSR flow cytometer.

## Statistical Analysis

Data visualization and statistical analyses were performed using GraphPad Prism (V.8.4.2, GraphPad Software). For statistical comparisons between the groups, the non-parametric Kruskal-Wallis test was used with a Dunn's test to correct for multiple comparisons. Wilcoxon signed rank tests were used for paired samples. IBM SPSS (version 27.0.1.0) was used for analysis of covariance (ANCOVA) to adjust for sex differences and Bonferroni tests for multiple comparisons. A *p*-value <0.05 was considered statistically significant. Spearman correlation analyses were used to analyze relationships between variables.

We used t-Stochastic Neighbor Embedding (t-SNE) in order to visualize the cell subset distribution and functional distribution of MAIT cells. Flow cytometry files for individual participants belonging to the same group were concatenated into one file for each group, the individual group files were then downsampled to obtain an equal number of events across the four groups, these files were then further concatenated into a single file for t-SNE. The following markers were used for T cell frequencies and MAIT cell functions; CD4, CD8, CD107a, HLA-DR, and IFN $\gamma$ . For MAIT cell subset frequencies, CD4, CD8, HLA-DR, CD107a, and IFN $\gamma$  were used.

## RESULTS

### Participant Characteristics

A total of 138 study participants were enrolled into the study, with patient characteristics summarized in **Table 1**. There were higher proportions of female participants in our HC (73.1%) and HIV group (76%) and a disproportionately large proportion of

**TABLE 1** | Participant demographics and clinical characteristics.

	Healthy controls (HC)	HIV only (HIV)	Active TB (aTB)	HIV-associated TB	p-value
n	26	50	36	26	
Females	19 (73.1 %)	38 (76.0%)	7 (19.4%)	14 (53.4%)	Chi-squared <0.001
Age, years	34 (26–40)	37 (31–43)	35 (24–43)	39 (31–44)	Kruskal-Wallis <0.112
CD4, cells/ $\mu$ l	ND	484 (333–541)	ND	222 (107–323)	Mann-Whitney <0.001
HIV VL, log10 copies/ml	ND	4.3 (3–5)	ND	4.7 (3.4–5)	Mann-Whitney 0.352
On ART:	NA	33 (66%)	NA	17 (65%)	
Yes		14 (28%)		7 (27%)	
No		3 (6%)		2 (8%)	
Unknown					
*QFT+	24 (92%)	34 (70%)	ND	ND	
QFT–	2 (8%)	14 (30%)	ND	ND	

\*No QFT results for 2 participants.

Categorical variables presented as count and percentage, n (%).

Continuous variables presented as median with IQR: median [IQR].

NA, Not applicable; ND, Not Done; QFT, QuantiFERON; IQR, Interquartile range.

males in the aTB group (80.6%). TB negative healthy controls were tested for TB exposure, 92% had positive QFT results suggesting latent TB infection (LTBI) and of the 48 HIV positive TB negative group participants that were tested for QFT, 70% were positive (Table 1).

## Frequencies of MAIT Cells Are Reduced in HIV Infection and During Active TB

We first sought to understand how HIV, TB and HIV-associated TB affect the frequencies of MAIT cells in blood. MAIT cells, defined as CD3<sup>+</sup>CD161<sup>+</sup>V $\alpha$ 7.2<sup>+</sup> T cells, were identified using the gating strategy summarized in Figure 1A.

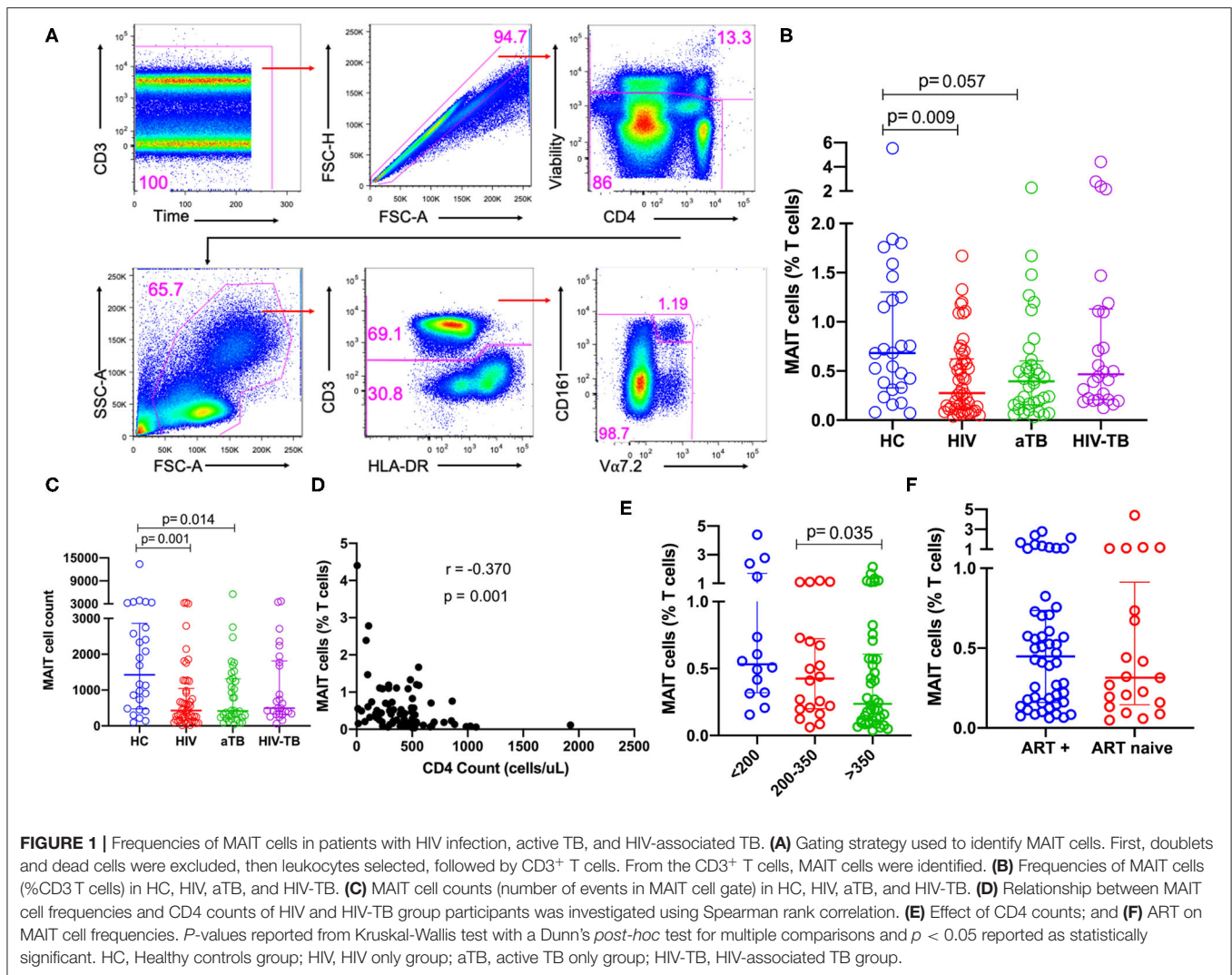
There were lower frequencies of MAIT cells in the HIV group ( $p = 0.009$ ) compared to HC and a trend toward lower frequencies in the aTB group ( $p = 0.057$ ) (Figure 1B). No significant differences were observed between the frequencies of MAIT cells in people with HIV-associated TB and healthy controls (Figure 1B). Looking at the numbers of MAIT cells (numbers of events in MAIT cell gate) showed a similar trend to MAIT cell frequencies, we observed lower numbers of MAIT cells in HIV ( $p = 0.001$ ) and aTB ( $p = 0.014$ ) compared to HC (Figure 1C). There was no significant difference in the number of MAIT cells between HIV-TB group and HC (Figure 1C). Supplementary Figure 1A shows that CD4 T cells are reduced from 39.7% in HC to 28.9% in the HIV group, and to 21.0% in the HIV-TB group. At the same time, CD8 T cells expanded from 33.2% in HC to 50.7% in the HIV group and 57.7% in the HIV-TB group.

We wanted to confirm whether our phenotypic analysis correlated with the now available MR1 tetramer, so we assessed MAIT cell frequencies using MR1-5-OP-RU in a subset of 10 HC, 10 HIV, 10 aTB, and 5 HIV-TB participants.

Supplementary Figure 1B shows representative flow plots of MAIT cells identified with MR1-5-OP-RU tetramers. We found significantly lower MAIT cells in the aTB group compared to HC ( $p = 0.025$ ) (Supplementary Figure 1C) while there were no significant differences between other groups. We found a strong positive correlation between the V $\alpha$ 7.2 antibody-identified MAIT cells and the MR1-5-OP-RU identified MAIT cells ( $r = 0.7009$ ,  $p < 0.0001$ ), (Supplementary Figure 1D). Supplementary Figure 1E shows the representative flow plots of MAIT cells identified with V $\alpha$ 7.2 antibody (top) and MR1-5-OP-RU tetramer (bottom). From these, we did not observe any significant differences between MAIT cells identified with V $\alpha$ 7.2 antibody and MAIT cells identified with MR1-5-OP-RU tetramer (Supplementary Figure 1F).

In the pooled HIV and HIV-TB groups, we assessed the effect of CD4 count, HIV VL and current ART status on MAIT cells. A significant but weak negative correlation was found between MAIT cell frequencies and CD4 counts ( $p = 0.001$ ,  $r = -0.370$ ) (Figure 1D), but frequencies were not correlated with HIV VL. We found that participants with CD4 counts above 350 cells/ $\mu$ l had significantly lower MAIT cell frequencies than participants with CD4 counts below 200 cells/ $\mu$ l ( $p = 0.035$ ) (Figure 1E). We did not see any significant difference in MAIT cell frequencies between people on ART and those not on ART (Figure 1F), and found no difference in MAIT cell frequencies in people with HIV VL loads below 1,000 copies/ml and those with HIV VL above 1,000 copies/ml (data not shown). We evaluated dead cells to understand whether MAIT cells were preferentially dying and investigated CD161 downregulation by gating on the CD161<sup>+</sup>V $\alpha$ 7.2<sup>+</sup> T cell population. We did not observe any significant differences in CD161 downregulation and cell death (data not shown).





## Evaluation of MAIT Cell Subsets in HIV Infection, Active TB, and HIV-Associated TB

In order to evaluate any changes that occurred in frequencies at subset level, CD161<sup>+</sup> Vα7.2<sup>+</sup> MAIT cells were separated by CD4 and CD8 to obtain the three different MAIT cell subsets: CD4<sup>+</sup>CD8<sup>-</sup> MAIT cells, CD8<sup>+</sup>CD4<sup>-</sup> MAIT cells, and CD4<sup>-</sup>CD8<sup>-</sup> MAIT cells, referred to as CD4, CD8 and DN MAIT cells, respectively (Figure 2A).

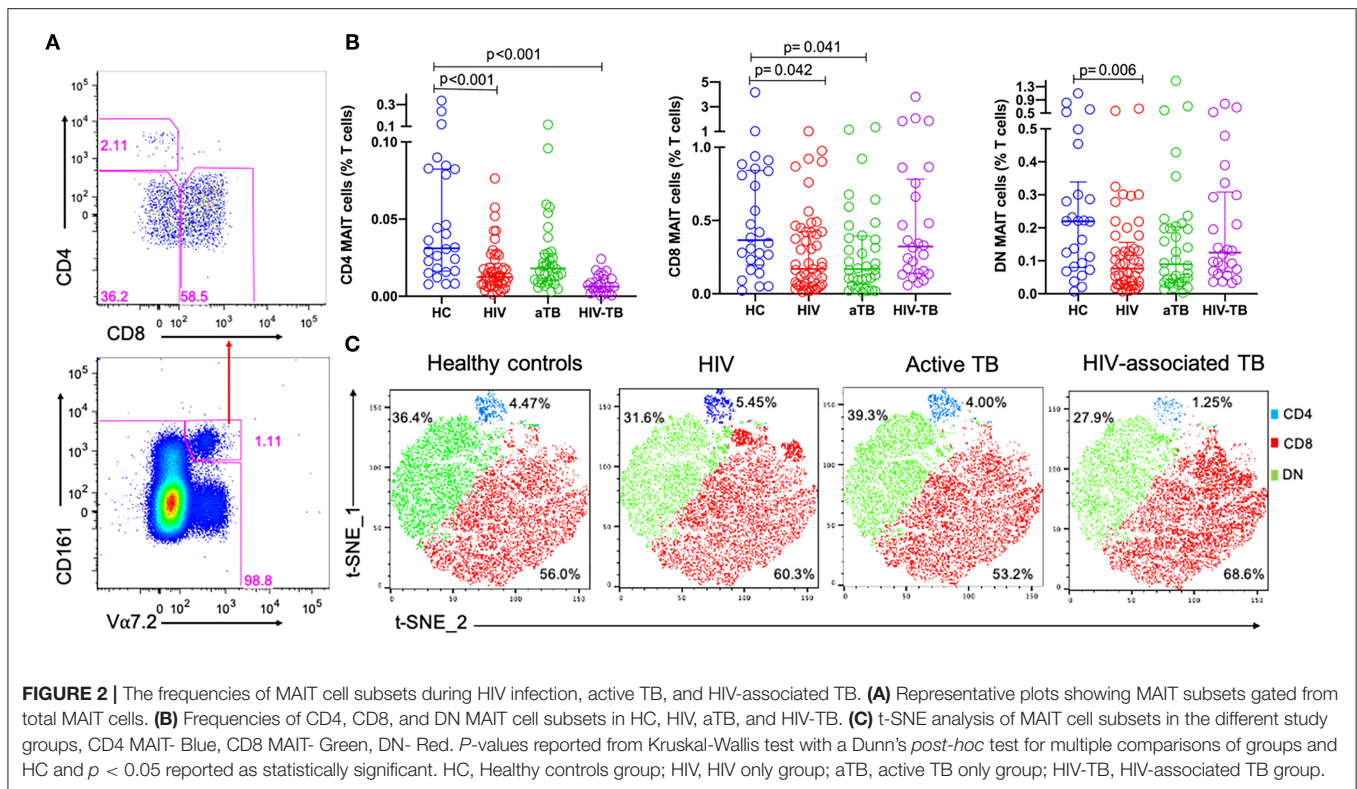
Figure 2B shows the frequencies of MAIT cell subsets as a proportion of total T cells. Frequencies of CD4 MAIT cells were lower in the groups with HIV (*p* < 0.001), and HIV-TB (*p* < 0.001) compared to CD4 MAIT cells in HC. CD8 MAIT cell frequencies were significantly lower in HIV (*p* = 0.042) and active TB groups (*p* = 0.041) compared to HC. DN MAIT cell frequencies were significantly lower in HIV group (*p* = 0.006) compared to HC (Figure 2B). From the t-SNE plots, it was clear that the CD8 (red) and DN (green) MAIT subsets make up significant proportions of MAIT cells compared to CD4 MAIT cells (blue). There were no large differences observed in the distributions of the different MAIT cell subsets except in

the HIV-TB group where CD4 MAIT cells were substantially depleted (1.25%) compared to HC (4.47%) (Figure 2C).

Due to the disproportionate number of males and females in our HC compared to other groups, especially the active TB group, we adjusted for the effect of sex using ANCOVA and corrected for multiple comparisons using a Bonferroni test. Similar trends were observed in which frequencies of MAIT cells were significantly lower in HIV group compared to HC (*p* = 0.024). Frequencies of CD4 MAIT subsets were significantly lower in all groups compared to HC (HIV, *p* < 0.001; aTB, *p* = 0.016; HIV-TB, *p* < 0.001). There were no significant differences in the frequencies of CD8 MAIT subsets. Lastly, frequencies of DN MAIT subsets were lower in HIV only group compared to HC (*p* = 0.039). *P*-values before and after correction for sex differences are presented in Supplementary Table 1.

## MAIT Cells Are Functionally Impaired in Active TB and HIV-Associated TB

In order to assess MAIT cell functions, we evaluated the expression of CD107a (marker of degranulation), and IFNγ as functional markers of mycobacterial stimulation. Figure 3A



shows the representative flow plots from the HC group for unstimulated cells and cells stimulated with BCG 1, HK-*M.tb*, and PHA.

In response to BCG 1 stimulation, no significant differences were observed in the frequencies of MAIT cells expressing CD107a between the HIV group and HC. Frequencies of MAIT cells expressing CD107a were significantly lower in the active TB group compared to HC ( $p = 0.006$ , **Figure 3B**). Frequencies of MAIT cells expressing IFN $\gamma$  were lower in active TB group ( $p < 0.001$ ) and HIV-associated TB ( $p < 0.001$ ) compared to HC **Figure 3B**. **Supplementary Table 2** shows the *p*-values and adjusted *p*-values for group comparisons of these MAIT frequencies and functions before and after correcting for multiple comparisons.

In response to HK-*M.tb* stimulation, we did not see any significant differences in the frequencies of MAIT cells expressing CD107a, although there were significantly lower frequencies of MAIT cells expressing IFN $\gamma$  in people with HIV-TB compared to HC ( $p = 0.044$ ) (**Figure 3C**). Upon stimulation with HK-*M.tb*, there were very low frequencies of MAIT cells expressing intracellular CD107a compared to BCG stimulation, as seen in **Figures 3A,B**.

We conducted t-SNE analyses on MAIT cells stimulated with BCG 1 (**Figure 3D**). In the t-SNE plots, a great proportion of MAIT cells were not responsive to BCG stimulation (cluster 1). The frequencies of MAIT cells expressing IFN $\gamma$  were represented as green, MAIT cells expressing CD107a were blue and those expressing HLA-DR as cyan. The frequencies of MAIT cells expressing IFN $\gamma$  were similar between HC and HIV group but were significantly lower in aTB compared to HC (6 vs. 19%). This depletion was coupled with the expansion in non-responsive

MAIT cells in cluster 1. Finally, MAIT cells expressing IFN $\gamma$  made up all of cluster 3, but a proportion of MAIT cells expressing CD107a also expressed IFN $\gamma$  and these were found mainly in cluster 2.

Assessing the effect of HIV-related parameters on MAIT cell function, there was a positive, albeit weak correlation between frequencies of MAIT cells expressing IFN $\gamma$  and the CD4 counts of participants with HIV (HIV and HIV-TB) ( $p < 0.001$ ,  $r = 0.395$ ) (**Figure 3E**). There were no significant differences in MAIT cells expressing CD107a, and IFN $\gamma$  between people on ART and those not on ART (**Figure 3F**). Participants with CD4 counts above 350 cells/ $\mu$ l had higher frequencies of MAIT cells expressing CD107a than participants with CD4 counts below 200 cells/ $\mu$ l ( $p = 0.045$ ) (**Figure 3G**). Similarly, there were higher frequencies of MAIT cells expressing IFN $\gamma$  in participants with CD4 counts above 350 cells/ $\mu$ l than those with CD4 counts below 200 cells/ $\mu$ l ( $p = 0.021$ ), and CD4 counts between 200 and 350 cells/ $\mu$ l ( $p = 0.043$ ) (**Figure 3G**).

We also assessed the response to stimulation with live BCG using higher MOI (BCG 5). We found no significant differences in the frequencies of MAIT cells expressing CD107a in the HIV and HIV-TB group. There were lower frequencies of MAIT cells expressing CD107a in the aTB group ( $p = 0.015$ ) compared to HC (**Table 2**). There were significantly lower frequencies of MAIT cells expressing IFN $\gamma$  in the aTB ( $p = 0.006$ ) and HIV-TB ( $p = 0.018$ ) compared to HC (**Table 2**). *P*-values for groups comparisons before and after correcting for multiple comparisons are shown in **Supplementary Table 3**.

Next, we looked at the functions of MAIT cell subsets in response to BCG 1 stimulation. For CD107a expression

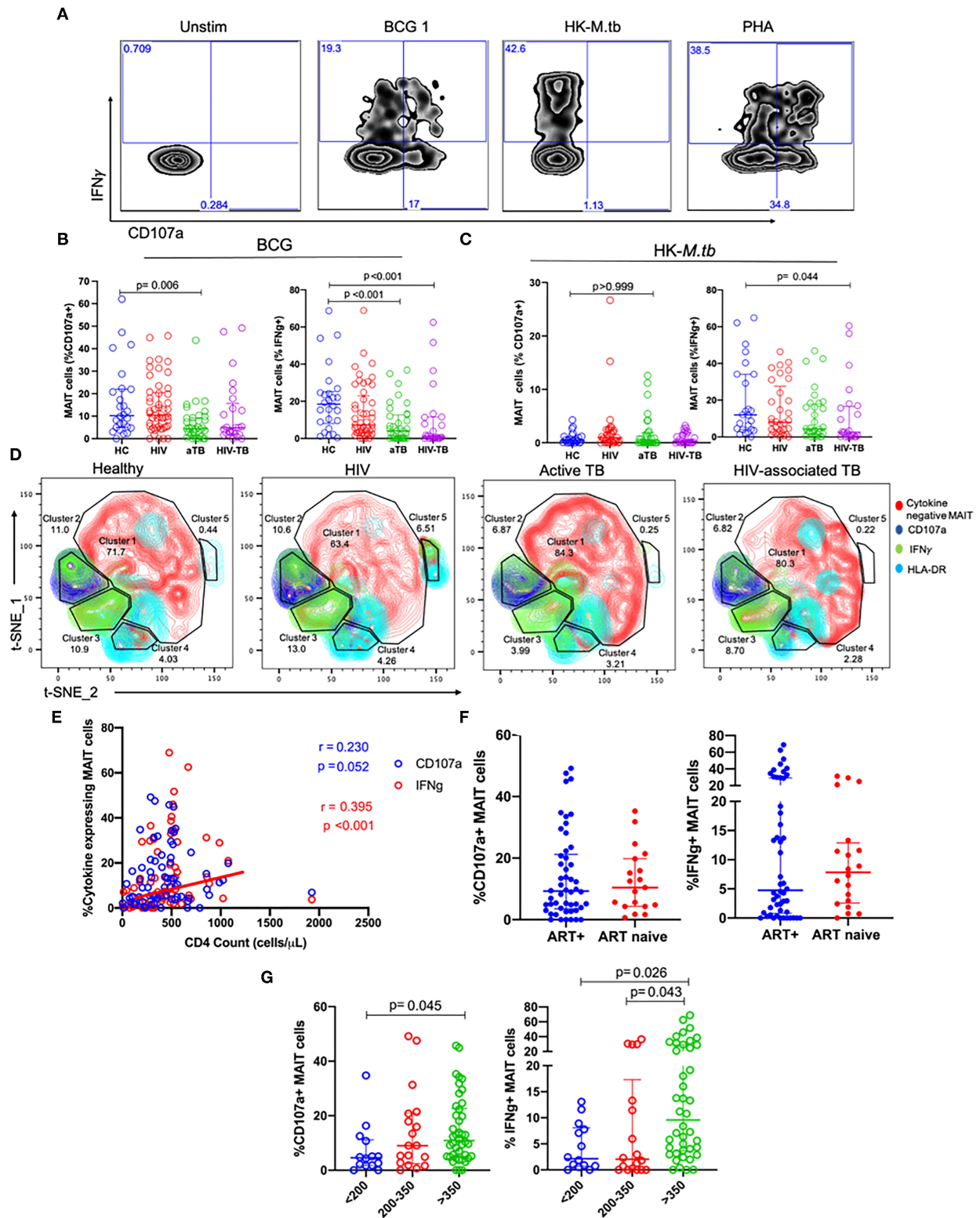


**FIGURE 3 |** MAIT cell responses after BCG and HK-*M.tb* stimulation. **(A)** Representative plots showing IFN $\gamma$  and CD107a expression after stimulation with BCG 1, heat-killed *M.tb* (HK-*M.tb*), and phytohemagglutinin (PHA). **(B,C)** Expression of CD107a and IFN $\gamma$  after BCG stimulation and HK-*M.tb* stimulation, respectively. **(D)** Contour plots for t-SNE analysis of MAIT cell functions between the different groups. red-cytokine-MAIT cells; dark-blue-CD107a+ MAIT cells; green-IFN $\gamma$ + MAIT cells. (Continued)



**FIGURE 3** | cells; light blue-HLA-DR+ MAIT cells. **(E)** CD4 counts of HIV and HIV-TB group participants and frequencies of MAIT cells expressing CD107a and IFN $\gamma$ , assessed using Spearman correlation. **(F)** Effect of ART on MAIT cells expressing CD107a and IFN $\gamma$ . **(G)** Effect of CD4 counts on MAIT cells expressing CD107a and IFN $\gamma$ . P-values reported from Kruskal-Wallis test with a Dunn's *post-hoc* test for multiple comparisons and  $p < 0.05$  reported as statistically significant. HC, Healthy controls group; HIV, HIV only group; aTB, active TB only group; HIV-TB, HIV-associated TB group.

**TABLE 2** | Median and interquartile range (IQR) of frequencies of cytokine-expressing MAIT cells in response to stimulation with higher MOI BCG (BCG 5).

Cytokine	HC	HIV		aTB		HIV-TB	
	Median (IQR)	Median (IQR)	p-value	Median (IQR)	p-value	Median (IQR)	p-value
CD107a	31.73 (19.59–58.17)	35.80 (20.65–47.29)	>0.999	20.41 (10.29–32.38)	0.015	30.80 (13.96–44.30)	0.694
HLA-DR	1.98 (1.00–5.00)	1.44 (0.01–4.55)	>0.999	0.71 (0.00–2.28)	0.105	1.62 (0.33–3.96)	>0.999
IFN $\gamma$	7.81 (2.54–17.52)	3.32 (0.62–9.72)	0.173	1.33 (0.03–5.08)	0.006	0.91 (0.03–7.87)	0.018

Ns, Not significant; HC, Healthy controls; HIV, HIV group; aTB, active TB group; HIV-TB, HIV-associated TB group.

by MAIT cell subsets, there were no significant differences in the CD4 MAIT cell subset. There was lower expression of CD107a in the CD8 MAIT cell subset in aTB group ( $p = 0.003$ ) and HIV-TB group ( $p = 0.026$ ) compared to HC (**Supplementary Figure 2A**). Frequencies of DN MAIT cells expressing CD107a were significantly lower in the active TB group ( $p = 0.013$ ) and HIV-TB group ( $p = 0.017$ ) compared to HC (**Supplementary Figure 2A**).

There were lower frequencies of CD4 MAIT cells expressing IFN $\gamma$  in HIV ( $p = 0.004$ ), aTB ( $p = 0.003$ ), and HIV-TB ( $p = 0.010$ ) compared to HC (**Supplementary Figure 2B**). For CD8 MAIT cell subsets expressing IFN $\gamma$ , frequencies were lower in aTB ( $p < 0.001$ ), and HIV-TB ( $p < 0.001$ ) compared to HC (**Supplementary Figure 2B**). Frequencies of DN MAIT subsets expressing IFN $\gamma$  were significantly reduced in aTB ( $p = 0.001$ ) and HIV-TB ( $p < 0.001$ ) compared to HC (**Supplementary Figure 2B**). For the HIV group, frequencies of CD8, and DN MAIT cells that expressed IFN $\gamma$  were similar to healthy controls.

After adjusting for sex differences, frequencies of MAIT cells expressing CD107a were lower in aTB group compared to HC ( $p = 0.046$ ) and were not statistically significant in HIV and HIV-TB group. Frequencies of MAIT cells expressing IFN $\gamma$  were lower in aTB ( $p = 0.024$ ), but only a trend in HIV-TB group ( $p = 0.072$ ) compared to HC (**Supplementary Table 1**). There were lower frequencies of CD8 MAIT subsets expressing IFN $\gamma$  in the aTB group ( $p = 0.016$ ) and HIV-TB ( $p = 0.045$ ) compared to HC (**Supplementary Table 1**).

We also assessed the effects of the 24-h stimulation on the frequencies of MAIT cells. Representative flow plots in **Supplementary Figure 3A** show MAIT cell frequencies after 24-h. incubation in the unstimulated cells (top) and MAIT cell frequencies after 24-h. stimulation with BCG 1 (bottom). In each group, there were no significant differences in the frequencies of MAIT cells between unstimulated cells and cells stimulated with BCG 1 (**Supplementary Figure 3B**).

## MAIT Cells Are Significantly Activated in HIV Infection, Active TB, and in HIV-Associated TB

We next investigated the effect of the different conditions on the activation status of MAIT cells. HLA-DR expression was used as a marker of T cell activation. There were no significant differences in frequencies of MAIT cells expressing HLA-DR between the groups (**Supplementary Figure 4**). HLA-DR median fluorescence intensity (MFI) on resting MAIT cells, was significantly higher in the HIV ( $p < 0.001$ ), active TB ( $p = 0.019$ ), and HIV-TB ( $p = 0.005$ ) compared to HC (**Figure 4A**).

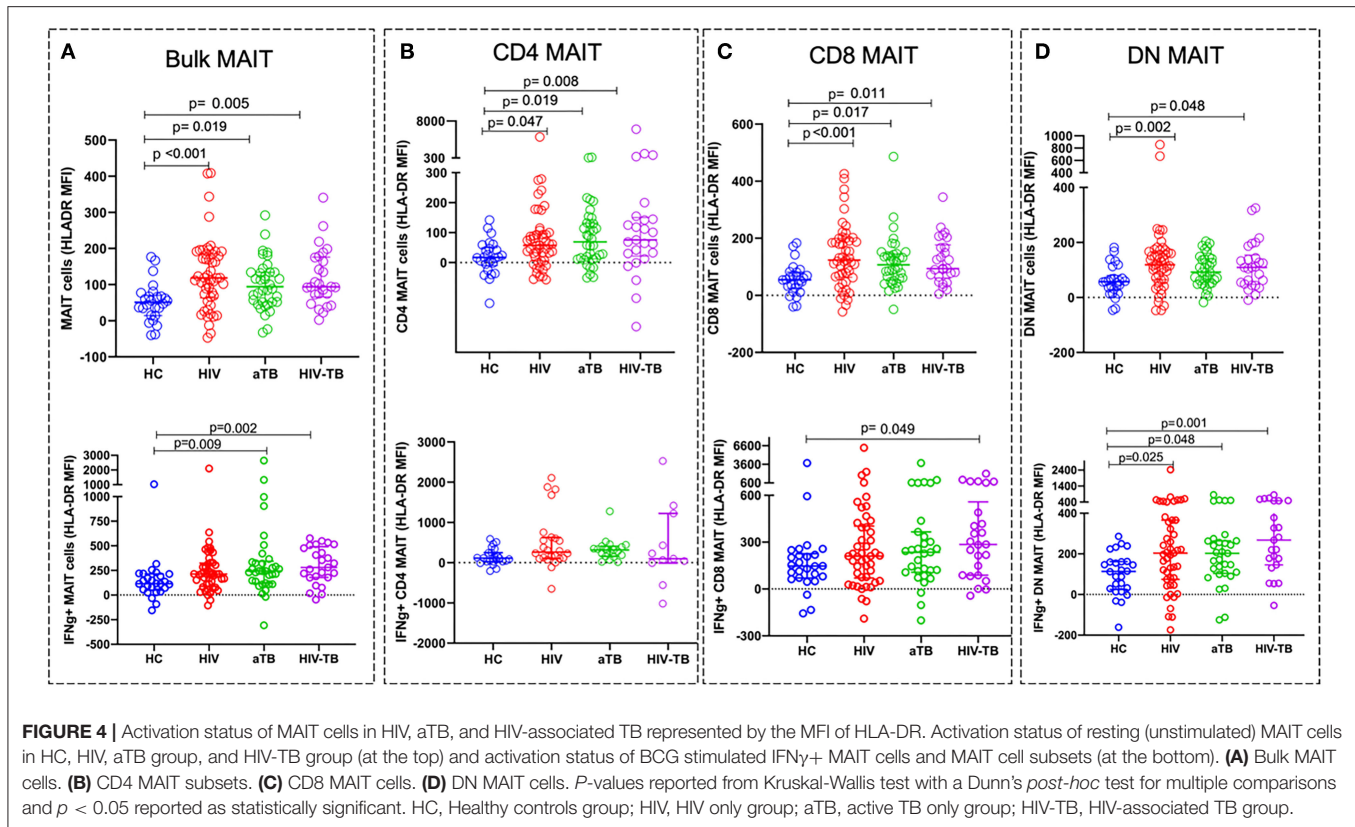
We also assessed specific MAIT cell activation status by analyzing the HLA-DR expression on MAIT cells expressing IFN $\gamma$  following stimulation with BCG 1. We observed higher activation status in IFN $\gamma$ <sup>+</sup> MAIT cells from active TB group ( $p = 0.009$ ) and HIV-TB group ( $p = 0.002$ ) compared to HC (**Figure 4A**).

For MAIT cell subset activation in unstimulated cells, we found that the MFI of HLA-DR on CD4 MAIT subsets was significantly higher in the HIV ( $p = 0.047$ ), aTB ( $p = 0.019$ ), and HIV-TB ( $p = 0.008$ ) compared to HC (**Figure 4B**). CD8 subsets activation was also elevated in HIV ( $p < 0.001$ ), aTB ( $p = 0.017$ ), and HIV-TB ( $p = 0.011$ ) compared to HC (**Figure 4C**). DN MAIT subset were found to be highly activated in HIV ( $p = 0.002$ ), and HIV-TB ( $p = 0.048$ ) (**Figure 4D**).

In response to BCG 1 stimulation, we observed that IFN $\gamma$ <sup>+</sup> CD8 MAIT cell subsets from HIV-TB had an elevated HLA-DR MFI ( $p = 0.049$ ) compared to HC (**Figure 4C**). IFN $\gamma$ <sup>+</sup> DN MAIT subsets from HIV, aTB, and HIV-TB all had higher HLA-DR MFI than healthy controls ( $p = 0.025$  in HIV,  $p = 0.048$  in aTB,  $p = 0.001$  in HIV-TB) (**Figure 4D**).

We assessed PD1 expression in a subset of HC ( $n = 10$ ), HIV ( $n = 10$ ), aTB ( $n = 10$ ), and HIV-TB ( $n = 5$ ) participants: the frequencies of MAIT cells expressing PD1 were significantly higher in the aTB group ( $p = 0.020$ ) (**Supplementary Figure 5**) compared to HC. There were no differences in MAIT cell subset





except for the DN where PD1 expression was lower in HIV-TB ( $p = 0.008$ ) compared to HC.

After adjusting for sex differences, HLA-DR MFI on bulk MAIT cells were higher in HIV group ( $p < 0.001$ ) and HIV-TB group ( $p = 0.030$ ). There were no significant differences in HLA-DR MFI in CD4 MAIT cells. There were higher HLA-DR MFI in CD8 MAIT cells and DN MAIT cells from HIV group (CD8 MAIT subset,  $p = 0.002$ ; DN MAIT subset,  $p = 0.015$ ) compared to HC (Supplementary Table 1).

## MAIT Cell Functions but Not Frequencies Are Restored After 10 Weeks of TB Treatment

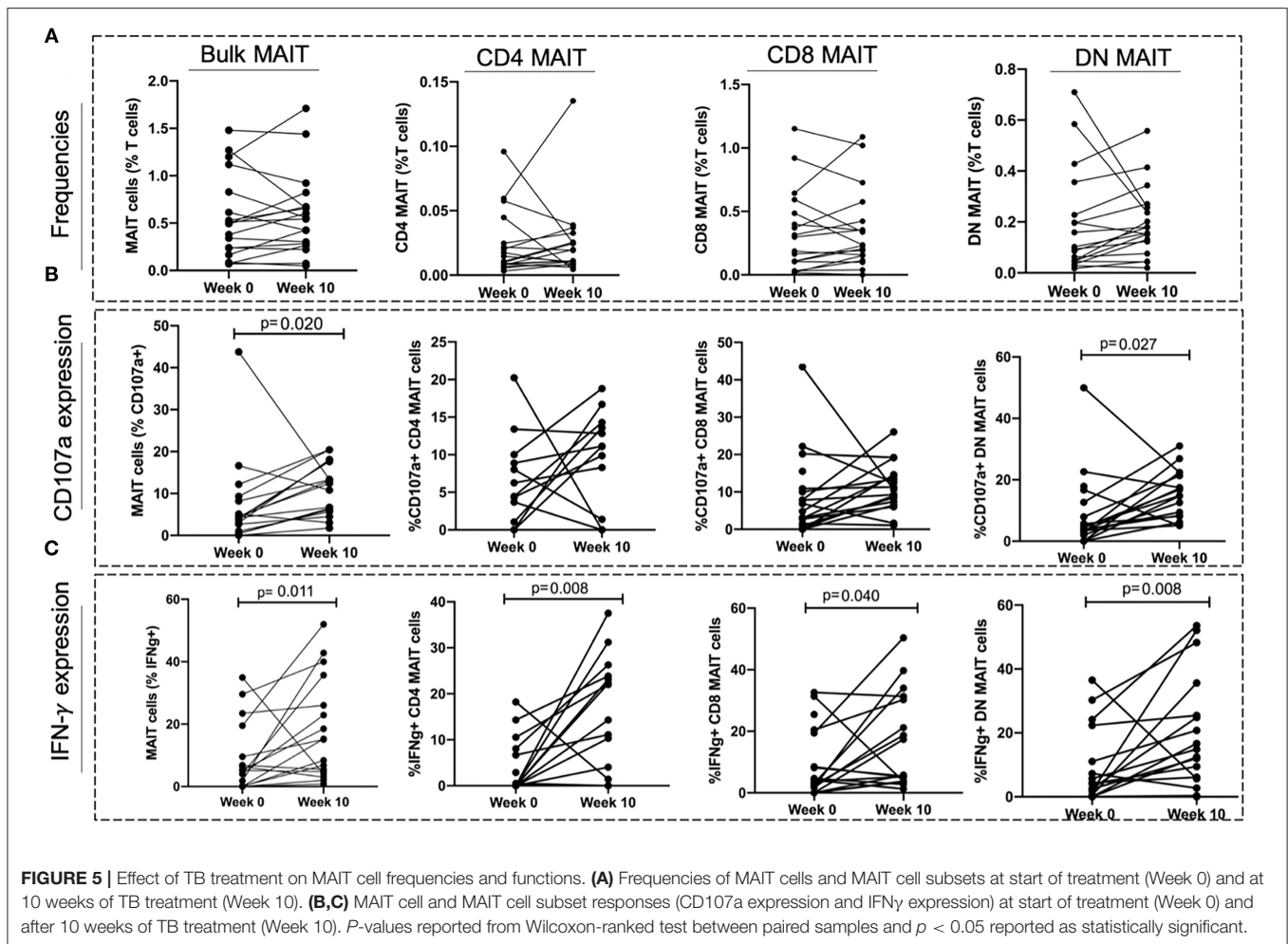
To investigate whether TB treatment induced any changes in MAIT cell frequencies and functions, a subset of 18 individuals from the aTB group were sampled after 6–10 (median of 8) weeks of TB treatment. No significant differences were observed in the MAIT cell frequencies between baseline (week 0) and week 10 of TB treatment (Figure 5A). There was an increase in the frequencies of MAIT cells expressing CD107a ( $p = 0.020$ ), and IFN $\gamma$  ( $p = 0.011$ ) after 10 weeks of TB treatment (Figures 5B,C).

We found no changes in CD4 and CD8 MAIT cells expressing CD107a after TB treatment (Figure 5B). The frequencies of DN MAIT cells expressing CD107a were higher after 10 weeks of TB treatment ( $p = 0.027$ ) (Figure 5B). Frequencies of all MAIT cell subsets expressing IFN $\gamma$  were higher after 10 weeks treatment (IFN $\gamma$ + CD4 MAIT;  $p = 0.008$ , IFN $\gamma$ + CD8 MAIT;  $p = 0.040$ , IFN $\gamma$ + DN MAIT;  $p = 0.008$ ) (Figure 5C).

## DISCUSSION

We investigated both the frequencies and function of MAIT cells in healthy adults, adults with HIV, active TB, and HIV-associated TB in a high endemic TB setting in South Africa. MAIT cell frequencies were depleted in people with HIV infection, and with active TB. Although MAIT cells in HIV infected, active TB, and HIV-associated TB patients had an elevated activation status, their functions were retained in response to BCG stimulation in HIV infected patients. In patients with active TB, MAIT cells were functionally impaired with lower expression of IFN $\gamma$  and increased activation. There were also increased frequencies of MAIT cells expressing PD1 in active TB. We observed that MAIT cell frequencies did not recover after 10 weeks of TB treatment, but their functional capacity (measured by CD107a and IFN $\gamma$  expression) did increase.

The depletion of blood MAIT cell frequencies in people with HIV and active TB has been described previously, and our findings are consistent with these previous studies (21–23), with the exception of the study by Suliman et al. (26). Suliman et al. (26) defined MAIT cells as CD3+ 5-OP-RU MR1 tetramer+, and showed that in a cohort of TB patients in South Africa and Peru that there was no significant difference in MAIT cell frequencies between TB patients and healthy controls, both with and without latent TB infection. We observed a non-significant decrease in MAIT cell frequencies in people with active TB when MAIT cells were defined using antibodies, but this decrease was significant when MAIT cells were more precisely defined using tetramers. It is thought that depletion of MAIT cells in blood during infection may be due to their recruitment to the sites of



infection (23, 27, 28). Leeansyah and colleagues reported that although MAIT cells were lost in the blood in HIV-1 infection, their frequencies were preserved in the rectal mucosa, suggesting that they are either preserved in these sites or that they migrate to mucosal sites as a response to infection and to maintain mucosal integrity (23, 25). More recently, it has been shown that there were increased MAIT cell frequencies in gut mucosa of people in the early stages of HIV infection compared to healthy controls suggesting early recruitment to mucosal tissues (29).

In TB disease, evidence also suggests that MAIT cells might be recruited to sites of infection and have been shown to be lost in blood of people with active TB but enriched in the lungs, with a capacity to secrete IFN $\gamma$  in response to co-culture with *M.tb*-infected lung epithelial cells (9). More recently, Wong et al. (28) showed that although individuals with active TB had fewer circulating TRAV1-2<sup>+</sup> CD8<sup>+</sup> T cells, they had 3 times more TRAV1-2<sup>+</sup> CD8<sup>+</sup> T cells in the bronchoalveolar lavage fluid (BAL) compared to matched healthy controls, suggesting recruitment to the lungs.

Interestingly, whereas we found lower frequencies in HIV infection and active TB, we did not see any significant differences in HIV-associated TB. Since participants with HIV-associated TB had lower CD4 counts and higher HIV viral loads, this observation could be explained by the severe depletion of

non-MAIT T cells in the CD3 compartment which leads to the relative enrichment of the MAIT compartment. Saeidi et al. (30) did not observe any significant differences in the frequencies of MAIT cells between people that had HIV-associated TB who were on ART and healthy controls. They showed that a group of HIV-associated TB patients who were not on ART had lower frequencies than healthy controls. This suggests that ART may have partially restored MAIT cell frequencies in HIV-associated TB. It is worth noting though, that the study defined MAIT cells as CD161<sup>++</sup> CD8<sup>+</sup> T cells whereas we defined them as CD161<sup>+</sup>V $\alpha$ 7.2<sup>+</sup> T cells. Another difference between the studies is the sample size; each of their groups had 10 individuals, fewer than in our study.

Similar to previous studies (22, 23), we did not see any differences in MAIT cell frequencies in individuals on ART and those not on ART, and we also did not see any correlations between MAIT cell frequencies and HIV VL. The observed inverse correlation of MAIT cell frequencies with CD4 counts seems largely driven by individuals with HIV-TB since MAIT cells in this group were inversely correlated with CD4 counts but this was not evident in the HIV only group.

The results from MR1-tetramer defined MAIT cells showed significantly lower frequencies of MAIT cells in active TB than healthy controls but not in HIV group compared to

healthy controls. This was different from the results from V $\alpha$ 7.2 identified MAIT cells which showed lower MAIT cells in HIV. It is not clear if this observation is due to the lower sample size. It could suggest that antibody staining may be technically insufficient for detecting all MAIT cells, especially if these markers are regulated differentially under different disease states. Gherardin et al. have suggested that this could lead to some MAIT cells being missed due to expression of alternate T cell receptors and low expression of CD161 (14, 31, 32). Some cells can be misclassified as MAIT cells and it has been demonstrated that some CD161<sup>+</sup>V $\alpha$ 7.2<sup>+</sup> MAIT cells were unable to bind to MR1-loaded tetramers (14, 33), and Swarbrick et al. (14) suggested that these cells share similar transcriptional profiles with MR1-restricted T cells but need further functional characterization.

We investigated MAIT cell functions by assessing the expression of CD107a and IFN $\gamma$  in response to BCG and HK-*M.tb*. In response to BCG, we observed no significant differences in the frequencies of MAIT cells expressing IFN $\gamma$  and CD107a between the HIV group and healthy controls. This was in contrast to previous studies that showed that HIV positive individuals had fewer MAIT cells expressing IFN $\gamma$ , CD107a, and granzyme B compared to healthy controls (23, 34). One fundamental difference between our study and these previous studies is that they both assessed MAIT cell responses to fixed *Escherichia coli* stimulation whereas we assessed functions using live BCG. Our findings were similar to those studies that did not report any significant differences in the MAIT cell functions between healthy controls and HIV positive individuals (25, 29). However, both of those studies investigated MAIT cell responses to MAIT cell ligand 5-OP-RU, IL-12, and IL-18 stimulation, and in early HIV infection where these functions may be maintained. Stimulation with HK-*M.tb* yielded very low expression of CD107a on MAIT cells and this is likely due to the denaturing of MAIT cell activating ligand due to heat-killing which may have led to an inability to activate MAIT cells in an MR1-dependent manner. However, there were increased IFN $\gamma$  responses which indicate that HK-*M.tb* may have still been able to activate MAIT cells through MR1-independent mechanisms. Interestingly, we only saw reduced frequencies of MAIT cells expressing IFN $\gamma$  in HIV-TB and not in aTB, suggesting that *M.tb* specific responses were still maintained in HIV and aTB group but not in HIV-TB. Although the specific MAIT cell ligands in both BCG and HK-*M.tb* have not been described, the observed MAIT cell responses to BCG in our study may be through both the MR1-dependent and MR1-independent mechanisms.

In TB participants, we saw that there were lower frequencies of MAIT cells expressing CD107a and IFN $\gamma$ . These results were consistent with those previously reported (9, 21). Interestingly, Wong et al. (28) recently showed that TRAV1-2<sup>+</sup> CD8 T cells (MAIT cells) in bronchoalveolar lavage (BAL) fluid had greater functional responses (TNF- $\alpha$  expression) to *Mycobacterium smegmatis*-infected APCs than peripheral blood MAIT cells in patients with untreated active TB. This suggests that there is functional impairment of MAIT cells during TB disease, but this impairment may not be in all compartments. This observed dysfunction has also been described in other T cell subsets and has been attributed to T cell exhaustion which is driven

by persistent antigen exposure and microbial translocation in HIV-associated TB (35).

It is possible that this diminished functional capacity is due to inhibition resulting from increased expression of inhibitory receptors such as PD1 and TIM-3 (34–36). We investigated whether PD1 expression could be a contributing factor as previously described (21, 30, 37). We found that resting MAIT cells in our disease groups were significantly more activated than healthy controls, and that in TB disease (active TB and HIV-associated TB) MAIT cells expressing IFN $\gamma$  following mycobacterial stimulation, were more activated than healthy controls. This suggests that there was already immune activation *in vivo*. We also observed that there were more MAIT cells expressing PD1 in active TB, which could indicate that there is immune inhibition *via* PD1 expression as a regulatory mechanism in chronic activation, which can lead to cell death (38, 39). Jiang et al. (21) have demonstrated that this impairment in MAIT cell function can be rescued by anti-PD1 therapy.

T cell functional impairment has also been associated with mycobacterial load as Day et al. (40) demonstrated that T cell functionality worsened with higher mycobacterial load and recovers after 6 months of TB treatment. We have also observed that the functional capacity in MAIT cells improves after 6–10 weeks of TB treatment, suggesting that we are seeing an improvement in MAIT cell functions as bacterial load decreases. Similar to bulk MAIT cells, MAIT cell subset frequencies were not restored after the first 10 weeks of TB treatment, but their functions were restored.

Our findings suggest that HIV positive participants with higher CD4 counts had more functional MAIT cells than those with lower CD4 counts, and the HIV VL and ART status did not seem to impact MAIT cell functions, which is in contrast to Leansyah et al. (23) who have reported increased frequencies of MAIT cells expressing IFN $\gamma$  in people on combination ART (cART). However, in their cohort, the analyses were conducted on paired samples from people before and after cART.

It is important to note that our healthy controls (and participants with HIV only) were predominantly latently infected with TB, thus our comparisons would most likely be representative of latent TB infection vs. active TB. One of the limitations of our study is that we did not collect any BAL samples and samples from other sites of infection and thus can only postulate that the observed reductions are due to recruitment to lungs and other sites of infection. Our HC and HIV groups had larger proportions of females than males, and our aTB group predominantly consisted of males, we adjusted for sex differences using ANCOVA and we found that sex did not significantly change our observed results. Another limitation of our study was the relatively small sample size in the different participant groups. A strength of our study was that the participant groups were well-characterized in terms of TB diagnosis and HIV and ART status. To our knowledge, this is the first study to investigate MAIT cell frequencies and functions in TB, HIV, and HIV-associated TB in South Africa.

In conclusion, we found that MAIT cells are reduced in blood of people with HIV and active TB but MAIT cell functions are maintained in HIV and impaired in active TB



and HIV-associated TB with significant activation in HIV, active TB, and HIV-associated TB. We have shown that MAIT cell frequencies were not restored after 10 weeks of TB treatment, but functional capacity did improve. These findings and those from previous studies suggest that MAIT cells play a role in TB pathogenesis, the precise nature of which remains to be defined. The alterations in MAIT cell frequencies and functions we observed may reduce the capacity of MAIT cells to play a protective role in the immune response to these two pathogens.

## DATA AVAILABILITY STATEMENT

The raw data supporting the conclusions of this article will be made available by the authors, without undue reservation.

## ETHICS STATEMENT

The studies involving human participants were reviewed and approved by University of Cape Town Faculty of Health Sciences Human Research Ethics Committee, HREC REF 011/2017. The patients/participants provided their written informed consent to participate in this study.

## AUTHOR CONTRIBUTIONS

MS conceived and supervised all aspects of the study. AB performed all experiments and analyses. GM co-conceived the study and provided intellectual inputs. KW, DML, and DAL provided intellectual input on study design, experimental set-up, and analyses. CS, RG, BS, SS, J-PK, AW, and RN provided clinical guidance and recruited study participants. AG provided intellectual and technical input on data analyses. All authors read and approved the final version of the manuscript.

## FUNDING

AB was supported by the National Research Foundation of South Africa (NRF: SFH180524334472 and SFH160718179350), Wellcome Centre for Infectious Disease Research in Africa (CIDRI-Africa) Ph.D. Fellowship, and Fogarty HIV-Associated Tuberculosis Training Programme (HATTP) Fellowship (D43 TW010559). MS was supported by the Wellcome Trust (Grant no: 211360/Z/18/Z) and the National Research Foundation of South Africa (NRF: UID127558). GM was supported by the Wellcome Trust (098316, 214321/Z/18/Z, and 203135/Z/16/Z), and the South African Research Chairs Initiative of the Department of Science and Technology and National Research Foundation (NRF) of South Africa (Grant no. 64787). The

fundors had no role in the study design, data collection, data analysis, data interpretation, or writing of this report. The opinions, findings and conclusions expressed in this manuscript reflect those of the authors alone.

## SUPPLEMENTARY MATERIAL

The Supplementary Material for this article can be found online at: <https://www.frontiersin.org/articles/10.3389/fimmu.2021.648216/full#supplementary-material>

**Supplementary Figure 1 |** Frequencies of MAIT cells using MR-1 tetramer. **(A)** Representative flow plots showing CD4 and CD8 T cells in the different study groups. **(B)** Representative flow plots showing MAIT cells identified with (i) 5-OP-RU MR1 tetramer and (ii) 6-FP MR1 loaded control tetramer. **(C)** Frequencies of MAIT cells in healthy controls, HIV group, aTB group, and HIV-associated TB group. **(D)** Correlation between antibody defined and MR1-OPRU tetramer defined MAIT cells. **(E)** Flow plots comparing frequencies of Vα7.2 antibody stained MAIT cells (top) and MR1 5-OP-RU stained MAIT cells (bottom). **(F)** Comparisons of MAIT cell frequencies in MAIT cell identified with Vα7.2 antibody and MAIT cells identified with MR1 5-OP-RU tetramer.

**Supplementary Figure 2 |** CD4, CD8, and DN MAIT cell subset responses to BCG 1 stimulation. **(A)** Expression of CD107a and **(B)** IFN $\gamma$  in the different MAIT cell subsets in response to BCG 1 stimulation. *P*-values reported from Kruskal-Wallis test with a Dunn's *post-hoc* test for multiple comparisons and *p* < 0.05 reported as statistically significant. HC, Healthy controls group; HIV, HIV only group; aTB, active TB only group; HIV-TB, HIV-associated TB group.

**Supplementary Figure 3 |** The effect of 24 h stimulation of the frequencies of MAIT cells. **(A)** Representative flow plots showing MAIT cell frequencies in unstimulated cells (top) and BCG stimulated cells (bottom). **(B)** Frequencies of MAIT cells in each group before and after BCG stimulation. *P*-value represents *p*-value from Wilcoxon rank test between paired samples.

**Supplementary Figure 4 |** Frequencies of MAIT cells expressing HLA-DR, a marker of T cell activation. **(A)** Representative flow plot showing frequencies of HLA-DR MAIT cells. **(B)** Summary plots showing the frequencies of MAIT cells expressing HLA-DR. **(C)** Summary plots of HLA-DR expression in the CD4, CD8, and DN MAIT cell subsets.

**Supplementary Figure 5 |** Expression of PD1 by resting MAIT cells and MAIT cell subsets during HIV, active TB, and HIV-associated TB. **(A)** Representative flow plots showing PD1 expression on MAIT cells. **(B)** PD1 expression on MAIT cells. **(C)** %PD1 expression on CD4 MAIT subset. **(D)** %PD1 expression on CD8 MAIT cell subset. **(E)** %PD1 expression on DN MAIT subset. *P*-values reported from Kruskal-Wallis test with a Dunn's *post-hoc* test for multiple comparisons and *p* < 0.05 reported as statistically significant. HC, Healthy controls group; HIV, HIV only group; aTB, active TB only group; HIV-TB, HIV-associated TB group.

**Supplementary Table 1 |** Significance levels for group comparisons for bulk MAIT cell and MAIT cell subset frequencies, functions, and activation before and after adjusting for the effect of gender using Analysis of Covariance (ANCOVA) and Bonferroni correction for multiple comparisons.

**Supplementary Table 2 |** *p*-values for group comparisons before and after adjusting for multiple comparisons using Dunn's test.

**Supplementary Table 3 |** *p*-values of group comparisons for BCG 5 stimulated MAIT cells, before and after adjusting for multiple comparisons using Dunn's test.

## REFERENCES

- World Health Organization. *Global Tuberculosis Report 2020*. Geneva: WHO (2020). vol. 66; p. 37–9.
- UNAIDS. Joint United Nations Programme on HIV/AIDS. *UNAIDS Data 2020*. Geneva: UNAIDS (2020). p. 436. Available online at: [https://www.unaids.org/sites/default/files/media\\_asset/2020\\_aids-data-book\\_en.pdf](https://www.unaids.org/sites/default/files/media_asset/2020_aids-data-book_en.pdf).
- Woldeesenbet SA, Kufa T, Barron P, Ayalew K, Cheyip M, Chirombo BC, et al. Assessment of readiness to transition from antenatal HIV surveillance surveys to PMTCT programme data-based HIV surveillance in South Africa: the 2017 antenatal sentinel HIV survey. *Int J Infect Dis.* (2020) 91:50–6. doi: 10.1016/j.ijid.2019.11.005
- Walker NF, Opondo C, Meintjes G, Jhilmee N, Friedland JS, Elkington PT, et al. Invariant natural killer t-cell dynamics in human immunodeficiency virus-associated tuberculosis. *Clin Infect Dis.* (2020) 70:1865–74. doi: 10.1093/cid/ciz501
- Diedrich CR, Flynn JAL. HIV-1/Mycobacterium tuberculosis coinfection immunology: how does HIV-1 exacerbate tuberculosis? *Infect Immun.* (2011) 79:1407–17. doi: 10.1128/IAI.01126-10



6. Riou C, Jhilmee N, Rangaka MX, Wilkinson RJ, Wilkinson KA. Tuberculosis antigen-specific T-cell responses during the first 6 months of antiretroviral treatment. *J Infect Dis.* (2020) 221:162–7. doi: 10.1093/infdis/jiz417
7. Walker NF, Meintjes G, Wilkinson RJ. HIV-1 and the immune response to TB Naomi. *Futur Virol.* (2013) 8:57–80. doi: 10.2217/fvl.12.123
8. Chua WJ, Truscott SM, Eickhoff CS, Blazevic A, Hoft DF, Hansen TH. Polyclonal mucosa-associated invariant T cells have unique innate functions in bacterial infection. *Infect Immun.* (2012) 80:3256–67. doi: 10.1128/IAI.00279-12
9. Gold MC, Cerri S, Smyk-Pearson S, Cansler ME, Vogt TM, Delepine J, et al. Human mucosal associated invariant T cells detect bacterially infected cells. *PLoS Biol.* (2010) 8:1–14. doi: 10.1371/journal.pbio.1000407
10. Kjer-Nielsen L, Patel O, Corbett AJ, Le Nours J, Meehan B, Liu L, et al. MR1 presents microbial vitamin B metabolites to MAIT cells. *Nature.* (2012) 491:717–23. doi: 10.1038/nature11605
11. Howson LJ, Salio M, Cerundolo V. MR1-restricted mucosal-associated invariant T cells and their activation during infectious diseases. *Front Immunol.* (2015) 6:303. doi: 10.3389/fimmu.2015.00303
12. Sharma PK, Wong EB, Napier RJ, Bishai WR, Ndung'u T, Kasprowitz VO, et al. High expression of CD26 accurately identifies human bacteria-reactive MR1-restricted MAIT cells. *Immunology.* (2015) 145:443–53. doi: 10.1111/imm.12461
13. Corbett AJ, Eckle SBG, Birkinshaw RW, Liu L, Patel O, Mahony J, et al. T-cell activation by transitory neo-antigens derived from distinct microbial pathways. *Nature.* (2014) 509:361–5. doi: 10.1038/nature13160
14. Swarbrick GM, Gela A, Cansler ME, Null MD, Duncan RB, Nemes E, et al. Postnatal expansion, maturation, and functionality of MR1T cells in humans. *Front Immunol.* (2020) 11:1–14. doi: 10.3389/fimmu.2020.556695
15. Dias J, Boulouis C, Gorin JB, Van Den Biggelaar RHGA, Lal KG, Gibbs A, et al. The CD4–CD8– MAIT cell subpopulation is a functionally distinct subset developmentally related to the main CD8+ MAIT cell pool. *Proc Natl Acad Sci U S A.* (2018) 115:E11513–22. doi: 10.1073/pnas.1812273115
16. Le Bourhis L, Dusseaux M, Bohineust A, Bessoles S, Martin E, Premel V, et al. MAIT cells detect and efficiently lyse bacterially-infected epithelial cells. *PLoS Pathog.* (2013) 9:e1003681. doi: 10.1371/journal.ppat.1003681
17. Dusseaux M, Martin E, Serriari N, Pégillet I, Premel V, Louis D, et al. Human MAIT cells are xenobiotic-resistant, tissue-targeted, CD161 hi IL-17-secreting T cells. *Blood.* (2011) 117:1250–9. doi: 10.1182/blood-2010-08-303339
18. Jiang J, Yang B, An H, Wang X, Liu Y, Cao Z, et al. Mucosal-associated invariant T cells from patients with tuberculosis exhibit impaired immune response. *J Infect.* (2016) 72:338–52. doi: 10.1016/j.jinf.2015.11.010
19. Le Bourhis L, Martin E, Pégillet I, Guihot A, Froux N, Coré M, et al. Antimicrobial activity of mucosal-associated invariant T cells. *Nat Immunol.* (2010) 11:701–8. doi: 10.1038/ni.1890
20. Smith DJ, Hill GR, Bell SC, Reid DW. Reduced mucosal associated invariant T-cells are associated with increased disease severity and *Pseudomonas aeruginosa* infection in cystic fibrosis. *PLoS ONE.* (2014) 9:e109891. doi: 10.1371/journal.pone.0109891
21. Jiang J, Wang X, An H, Yang B, Cao Z, Liu Y, et al. Mucosal-associated invariant T-cell function is modulated by programmed death-1 signaling in patients with active tuberculosis. *Am J Respir Crit Care Med.* (2014) 190:329–39. doi: 10.1164/rccm.201401-0106OC
22. Wong EB, Akilimali NA, Govender P, Sullivan ZA, Cosgrove C, Pillay M, et al. Low levels of peripheral CD161++CD8+ Mucosal Associated Invariant T (MAIT) cells are found in HIV and HIV/TB co-infection. *PLoS ONE.* (2013) 8:1–9. doi: 10.1371/journal.pone.0083474
23. Leeansyah E, Ganesh A, Quigley MF, Sönnberg A, Andersson J, Hunt PW, et al. Activation, exhaustion, and persistent decline of the antimicrobial MR1-restricted MAIT-cell population in chronic HIV-1 infection. *Blood.* (2013) 121:1124–35. doi: 10.1182/blood-2012-07-445429
24. Kurioka A, Ussher JE, Cosgrove C, Clough C, Fergusson JR, Smith K, et al. MAIT cells are licensed through granzyme exchange to kill bacterially sensitized targets. *Mucosal Immunol.* (2015) 8:429–40. doi: 10.1038/mi.2014.81
25. Fernandez CS, Amarasena T, Kelleher AD, Rossjohn J, McCluskey J, Godfrey DI, et al. MAIT cells are depleted early but retain functional cytokine expression in HIV infection. *Immunol Cell Biol.* (2015) 93:177–88. doi: 10.1038/icb.2014.91
26. Suliman S, Gela A, Mendelsohn SC, Iwany SK, Tamara KL, Mabwe S, et al. Peripheral blood mucosal-associated invariant T cells in tuberculosis patients and healthy mycobacterium tuberculosis-exposed controls. *J Infect Dis.* (2020) 222:995–1007. doi: 10.1093/infdis/jiaa173
27. Cosgrove C, Ussher JE, Rauch A, Gärtner K, Kurioka A, Hühn MH, et al. Early and non-reversible decrease of CD161++/MAIT cells in HIV infection. *Blood.* (2013) 121:951–61. doi: 10.1182/blood-2012-06-436436
28. Wong EB, Gold MC, Meermeier EW, Xulu BZ, Khuzwayo S, Sullivan ZA, et al. TRAV1-2+ CD8+ T-cells including oligoclonal expansions of MAIT cells are enriched in the airways in human tuberculosis. *Commun Biol.* (2019) 2:203. doi: 10.1038/s42003-019-0442-2
29. Lal KG, Kim D, Costanzo MC, Creegan M, Leeansyah E, Dias J, et al. Dynamic MAIT cell response with progressively enhanced innateness during acute HIV-1 infection. *Nat Commun.* (2020) 11:1–13. doi: 10.1038/s41467-019-13975-9
30. Saeidi A, Tien Tien VL, Al-Batran R, Al-Darraj HA, Tan HY, Yong YK, et al. Attrition of TCR V $\alpha$ 7.2+ CD161++ MAIT cells in HIV-tuberculosis co-infection is associated with elevated levels of PD-1 expression. *PLoS ONE.* (2015) 10:1–14. doi: 10.1371/journal.pone.0124659
31. Awad W, Meermeier EW, Sandoval-Romero ML, Le Nours J, Worley AH, Null MD, et al. Atypical TRAV1-2- T cell receptor recognition of the antigen-presenting molecule MR1. *J Biol Chem.* (2020) 295:14445–57. doi: 10.1074/jbc.RA120.015292
32. Meermeier EW, Laugel BF, Sewell AK, Corbett AJ, Rossjohn J, McCluskey J, et al. Human TRAV1-2-negative MR1-restricted T cells detect *S. pyogenes* and alternatives to MAIT riboflavin-based antigens. *Nat Commun.* (2016) 7:12506. doi: 10.1038/ncomms12506
33. Gherardin NA, Souter MNT, Koay HF, Mangas KM, Seemann T, Stinear TP, et al. Human blood MAIT cell subsets defined using MR1 tetramers. *Immunol Cell Biol.* (2018) 96:507–25. doi: 10.1111/imcb.12021
34. Tang X, Zhang S, Peng Q, Ling L, Shi H, Liu Y, et al. Sustained IFN- $\gamma$  stimulation impairs MAIT cell responses to bacteria by inducing IL-10 during chronic HIV-1 infection. *Sci Adv.* (2020) 6:1–13. doi: 10.1126/sciadv.aaz0374
35. Liu X, Li F, Niu H, Ma L, Chen J, Zhang Y, et al. IL-2 restores T-Cell dysfunction induced by persistent mycobacterium tuberculosis antigen stimulation. *Front Immunol.* (2019) 10:1–12. doi: 10.3389/fimmu.2019.02350
36. Amelio P, Portevin D, Hella J, Reither K, Kamwela L, Lweno O, et al. HIV infection functionally impairs *Mycobacterium tuberculosis*-specific CD4 and CD8 T-cell responses. *J Virol.* (2018) 93:e01728. doi: 10.1128/JVI.01728-18
37. Jiang J, Cao Z, Qu J, Liu H, Han H, Cheng X. PD-1-expressing MAIT cells from patients with tuberculosis exhibit elevated production of CXCL13. *Scand J Immunol.* (2020) 91:e12858. doi: 10.1111/sji.12858
38. Chiba A, Tamura N, Yoshikiyo K, Murayama G, Kitagaichi M, Yamaji K, et al. Activation status of mucosal-associated invariant T cells reflects disease activity and pathology of systemic lupus erythematosus. *Arthritis Res Ther.* (2017) 19:58. doi: 10.1186/s13075-017-1257-5
39. Groux H, Torpier G, Monté D, Mouton Y, Capron A, Ameisen JC. Activation-induced death by apoptosis in CD4+ T cells from human immunodeficiency virus-infected asymptomatic individuals. *J Exp Med.* (1992) 175:331–40. doi: 10.1084/jem.175.2.331
40. Day CL, Abrahams DA, Lerumo L, Janse van Rensburg E, Stone L, O'rie T, et al. Functional capacity of *Mycobacterium tuberculosis*-specific T cell responses in humans is associated with mycobacterial load. *J Immunol.* (2011) 187:2222–32. doi: 10.4049/jimmunol.1101122

**Conflict of Interest:** The authors declare that the research was conducted in the absence of any commercial or financial relationships that could be construed as a potential conflict of interest.

Copyright © 2021 Balfour, Schutz, Goliath, Wilkinson, Sayed, Sossen, Kanyik, Ward, Ndzhukule, Gela, Lewinsohn, Lewinsohn, Meintjes and Shey. This is an open-access article distributed under the terms of the Creative Commons Attribution License (CC BY). The use, distribution or reproduction in other forums is permitted, provided the original author(s) and the copyright owner(s) are credited and that the original publication in this journal is cited, in accordance with accepted academic practice. No use, distribution or reproduction is permitted which does not comply with these terms.



# Plasma Biomarkers of Risk of Tuberculosis Recurrence in HIV Co-Infected Patients From South Africa

Kimesha Pillay<sup>1</sup>, Lara Lewis<sup>1</sup>, Santhuri Rambaran<sup>1</sup>, Nonhlanhla Yende-Zuma<sup>1,2</sup>, Dersere Archary<sup>1,3</sup>, Santhanalakshmi Gengiah<sup>1</sup>, Dhineshree Govender<sup>1</sup>, Razia Hassan-Moosa<sup>1,2</sup>, Natasha Samsunder<sup>1</sup>, Salim S. Abdool Karim<sup>1,2,4</sup>, Lyle R. McKinnon<sup>1,5,6</sup>, Nesri Padayatchi<sup>1,2</sup>, Kogieleum Naidoo<sup>1,2</sup> and Aida Sivo<sup>1,3\*</sup>

<sup>1</sup> Centre for the AIDS Programme of Research in South Africa (CAPRISA), Durban, South Africa, <sup>2</sup> MRC-CAPRISA HIV-TB Pathogenesis and Treatment Research Unit, Doris Duke Medical Research Institute, University of KwaZulu-Natal, Durban, South Africa, <sup>3</sup> Department of Medical Microbiology, University of KwaZulu-Natal, Durban, South Africa, <sup>4</sup> Department of Epidemiology, Columbia University, New York City, NY, United States, <sup>5</sup> Department of Medical Microbiology and Infectious Diseases, University of Manitoba, Winnipeg, MB, Canada, <sup>6</sup> Department of Medical Microbiology, University of Nairobi, Nairobi, Kenya

## OPEN ACCESS

### Edited by:

Christof Geldmacher,  
University of Munich, Germany

### Reviewed by:

Björn Corleis,  
Friedrich-Loeffler-Institute, Germany  
Kondwani C. Jambo,  
Liverpool School of Tropical Medicine,  
United Kingdom

### \*Correspondence:

Aida Sivo  
aida.sivo@caprisa.org

### Specialty section:

This article was submitted to  
Microbial Immunology,  
a section of the journal  
Frontiers in Immunology

**Received:** 19 November 2020

**Accepted:** 08 March 2021

**Published:** 25 March 2021

### Citation:

Pillay K, Lewis L, Rambaran S, Yende-Zuma N, Archary D, Gengiah S, Govender D, Hassan-Moosa R, Samsunder N, Abdool Karim SS, McKinnon LR, Padayatchi N, Naidoo K and Sivo A (2021) Plasma Biomarkers of Risk of Tuberculosis Recurrence in HIV Co-Infected Patients From South Africa. *Front. Immunol.* 12:631094. doi: 10.3389/fimmu.2021.631094

There is an urgent need to identify immunological markers of tuberculosis (TB) risk in HIV co-infected individuals. Previously we have shown that TB recurrence in HIV co-infected individuals on ART was associated with markers of systemic inflammation (IL-6, IL1 $\beta$  and IL-1R $\alpha$ ). Here we examined the effect of additional acute inflammation and microbial translocation marker expression on risk of TB recurrence. Stored plasma samples were drawn from the TB Recurrence upon Treatment with HAART (TRuTH) study, in which individuals with previously treated pulmonary TB were screened for recurrence quarterly for up to 4 years. Recurrent TB cases ( $n = 37$ ) were matched to controls ( $n = 102$ ) by original trial study arm assignment and ART start date. Additional subsets of HIV infected ( $n = 41$ ) and HIV uninfected ( $n = 37$ ) individuals from Improving Recurrence Success (IMPRESS) study were sampled at active TB and post successful treatment completion. Plasma concentrations of soluble adhesion molecules (sMAdCAM, sICAM and sVCAM), lipopolysaccharide binding protein (LBP) and transforming growth factor-beta (TGF- $\beta$ 1, TGF- $\beta$ 2, TGF- $\beta$ 3) were measured by multiplex immunoassays and ELISA. Cytokine data was square root transformed in order to reduce variability. Multivariable analysis adjusted for a number of potential confounders measured at sample time-point: age, BMI, CD4 count, viral load (VL) and measured at baseline: presence or absence of lung cavities, previous history of TB, and WHO disease stage (4 vs 3). The following analytes were associated with increased risk of TB recurrence in the multivariable model: sICAM (aOR 1.06, 95% CI: 1.02-1.12,  $p = 0.009$ ), LBP (aOR 8.78, 95% CI: 1.23-62.66,  $p = 0.030$ ) and TGF- $\beta$ 3 (aOR 1.44, 95% CI 1.01-2.05,  $p = 0.044$ ). Additionally, we observed a positive correlation between LBP and sICAM ( $r = 0.347$ ,  $p < 0.0001$ ), and LBP and IL-6, identified to be one of the strongest predictors of TB risk in our previous study ( $r = 0.623$ ,  $p = 0.03$ ). These data show that increased risk of TB recurrence in HIV infected individuals on ART is likely associated with HIV mediated translocation of microbial products and the resulting chronic immune activation.

**Keywords:** inflammation, HIV, microbial translocation, antiretroviral (ARV) therapy, tuberculosis - pulmonary

## INTRODUCTION

Despite being a preventable and treatable disease, tuberculosis (TB) is currently one of the top ten causes of mortality globally and ranks above human immunodeficiency virus/acquired immunodeficiency syndrome (HIV/AIDS) as the primary cause of mortality from an infectious agent (1). Africa accounted for 25% of new TB cases in 2019, partly driven by the overlapping HIV epidemic. The risk of developing active TB disease in people living with HIV (PLHIV) is 18 (2–8) times higher compared to HIV uninfected individuals (1). There is a dire need to improve our ability to predict those most at risk for TB disease progression and poor TB treatment response especially among HIV infected patients to enable early implementation of mitigating clinical and public health measures.

The lack of reliable biomarkers of TB risk and treatment response has hindered TB management and drug development. Well defined correlates of TB risk and protection could facilitate rapid screening of new prevention methods and could improve diagnosis of active disease thereby slowing down transmission (9). TB biomarkers are needed partly because of inability to detect the bacterium or its products in easily accessible patient samples. The current diagnosis of active disease and monitoring of response to TB treatment relies on sputum samples, whose volume and quality vary during the course of the disease. Blood-based biomarkers would be advantageous for several reasons, mainly due to relative ease of sample collection, reduced transmission risk, and the ability to measure multiple biomarkers at the same time therefore improving the predictive power of the test (10).

Susceptibility to both HIV and TB infections as well as the course and outcome of the disease are affected by the inflammation induced changes in cytokine/chemokine expression (10–15). Inflammatory responses to both HIV and TB act similarly, whereby the initial response is needed to prevent and contain the infection. However, if left uncontrolled, this inflammatory response can lead to immune mediated pathology (16, 17). HIV mediated translocation of microbial products and the resulting chronic immune activation are known to increase the risk of opportunistic infections, including TB (14). On the other side, both latent and active TB have been shown to exacerbate immune activation in individuals co-infected with HIV (18) potentially contributing to faster HIV disease progression.

Utilizing specimens from the TB Recurrence upon Treatment with HAART (TRuTH) study we have previously identified several inflammatory markers of risk of TB recurrence (IL-6, IL-1 $\beta$  and IL-1R $\alpha$ ) and protection (IFN- $\beta$ ) in HIV co-infected individuals on antiretroviral therapy (ART) (11). Macaque models of TB/simian immunodeficiency virus (SIV) coinfection have demonstrated that SIV-mediated chronic immune activation was the likely driver of reactivation of latent TB infection (14). As the chronic inflammation during HIV/SIV infection is driven by HIV/SIV-mediated gastrointestinal damage and leakage of microbial products we wanted to assess the effect of lipopolysaccharide binding protein (LBP), as a surrogate marker of systemic LPS exposure (19, 20), on risk of TB recurrence in TB-HIV co-infected patients. We additionally expanded our initial observations and examined three adhesion

molecules: soluble intracellular adhesion molecule (sICAM), soluble vascular cell adhesion molecule (sVCAM) and soluble mucosal addressin cell adhesion molecule (sMAdCAM) for their roles in inflammation and cell recruitment to the mucosal tissues (21); and three isoforms of the transforming growth factor – beta family (TGF- $\beta$ 1, 2 and 3) for their roles in inflammation, immunoregulation and mucosal barrier repair (2, 3). The effect of the measured analytes on the risk of TB recurrence was done using specimens from the TB Recurrence upon Treatment with HAART (TRuTH) study, in which HIV infected individuals with previously treated pulmonary TB were screened for recurrence quarterly for up to 4 years. Additional cohort (Improving Recurrence Success, IMPRESS) was used to assess the effect of active TB and successful TB treatment completion on the expression of the measured analytes in both HIV infected and uninfected individuals.

## METHODS

### Study Participants

Informed written consent for study enrolment and sample storage for future analysis was obtained from all study participants. The University of KwaZulu-Natal's Biomedical Research Ethics Committee (BE659/17) approved this study. We analyzed stored plasma specimens from two Centre for the AIDS Programme of Research in South Africa (CAPRISA) study cohorts: the 005 TRuTH and CAPRISA 011 IMPRESS. All study participants were recruited and treated at the urban CAPRISA eThekweni Research Clinic in KwaZulu-Natal, South Africa.

The CAPRISA 005 TRuTH observational cohort study investigated the rate of TB recurrence in ART treated adults following completion of treatment for pulmonary TB (Clinical trial NCT 01539005). These participants were previously enrolled in the CAPRISA 003 SAPIt trial (4), which investigated timing of antiretroviral (ART) initiation during pulmonary TB treatment. Participants that entered TRuTH had a confirmatory negative status for TB upon completion of TB treatment. While retained on ART, participants were screened four times a year for a maximum of 4 years for TB recurrence. We conducted a nested case-control study using TRuTH stored samples, where cases, defined by TB recurrence that had an available pre-recurrence sample, were matched on ART start date in 1:3 ratio to controls, defined as those participants with no TB recurrence during follow-up. Cases were sampled at a minimum of 3 and maximum of 9 months prior to TB recurrence, and controls sampled at comparable time points to minimize the difference in sample cryopreservation length between groups. A subset of cases was followed longitudinally at additional time points: Recurrence/TB (2-month window before or after TB recurrence) and cure/post TB (capturing a 2 month-window before and 3 month- window after recurrent TB treatment completion date).

The CAPRISA 011 IMPRESS open-label randomized controlled study (Clinical trials NCT 02114684), compared TB treatment outcomes among previously treated TB patients receiving an



interventional Moxifloxacin containing TB regimen compared to standard of care for treatment of smear positive pulmonary TB (5). This study enrolled men and women who were HIV infected and uninfected, >18 years of age, with a documented previous history of TB and current sputum smear positive *Mycobacterium tuberculosis* (*M.tb*) infection. Patients were stratified by HIV status and randomized into the intervention and control arm. To analyze the effect of TB treatment completion on the expression of measured analytes (MAdCAM, ICAM, VCAM, LBP, TGF- $\beta$ 1, TGF- $\beta$ 2 and TGF- $\beta$ 3), a subset of HIV infected and HIV uninfected men and women were sampled at two time-points: active TB disease and post successful TB treatment completion (Cure). No matching was performed.

## Sample Collection and Processing

Acid citrate dextrose (ACD) tubes were used to collect peripheral blood. The blood was centrifuged for 10 minutes at 1600rpm, the plasma was retrieved and cryopreserved for future analysis at -80°C.

## Soluble Analyte Measurement

Plasma levels of sICAM and sVCAM were simultaneously quantified using the Milliplex MAP Human Sepsis kit (Millipore Corporation, St. Charles, MO). Plasma levels of TGF- $\beta$ 1, TGF- $\beta$ 2 and TGF- $\beta$ 3 were quantified using the Transforming Growth factor-beta kit (Bio-Rad, Laboratories Inc., Hercules, CA). All multiplex assays were analyzed on the Bio-Plex™ 200 system. Soluble LBP (sLBP) plasma levels were quantified using the Human Lipopolysaccharide Binding Protein ELISA (R&D Systems Inc., Minneapolis, MN). Soluble MAdCAM-1 (sMAdCAM-1) levels were quantified using the Hycult Biotech HK337 Human sMAdCAM-1 ELISA kit (Hycult, USA). ELISAs were analyzed using the VersaMax™ ELISA Microplate Reader with SoftMax® Pro Software. All assays were performed as per the manufacturer's instructions. Briefly, following sample dilutions were used: sMAdCAM-1 (1:10), TGF- $\beta$ 1/2/3 (1:16), sLBP (undiluted), sICAM/sVCAM (1:40). All samples measured for sMAdCAM, sICAM, sVCAM and LBP produced a value within the range of the standard curve (100% detectability). Samples measured for TGF- $\beta$ 1, TGF- $\beta$ 2 and TGF- $\beta$ 3 had high levels of detectability, where TGF- $\beta$ 1 was 97.92% and TGF- $\beta$ 2 and TGF- $\beta$ 3 were 89.06% detectable. The samples with values below the range of the standard curve were assigned the value half of the limit of detection (LOD/2). LODs for the measured analytes were as follows: sMAdCAM-1 (0.41 ng/ml), TGF- $\beta$ 1 (3.9 pg/ml), TGF- $\beta$ 2 (1.9 pg/ml), TGF- $\beta$ 3 (0.5 pg/ml), sLBP (1.5 ng/ml), sICAM (17.7 pg/ml), sVCAM (10.7 pg/ml).

## Statistical Analysis

All specimens were analyzed blinded to the clinical status, with longitudinal samples analyzed on the same plate. GraphPad Prism version 8.3.1 (GraphPad software, La Jolla, CA), SPSS version 24 and SAS version 9.4 were used to perform statistical analysis.

For comparison of baseline characteristics of TRuTH samples between cases and controls, the Wilcoxon signed rank and the McNemar tests were used. Cytokine data was square root transformed in order to reduce the variability, a phenomenon

that is known to affect most cytokine measurements. To determine if measured plasma analytes had an effect on the TB recurrence, we conducted a univariable and multivariable conditional logistic regression. Multivariable analysis adjusted for a number of potential confounders measured at sample time-point: age, body mass index (BMI), CD4 count, viral load (VL) and measured at baseline: presence or absence of lung cavities, previous history of TB, and World Health Organization (WHO) disease stage (4 vs 3). Longitudinal samples were compared using paired t-test or Wilcoxon signed rank test. Correlations between analytes were determined using Spearman correlation. The Benjamini-Hochberg method was applied to control for the false discovery rate (FDR), Q:5%.

Baseline and follow-up characteristics in IMPRESS were summarized using percentages and frequencies for categorical variables and median and interquartile range (IQR) values for continuous variables. Changes in measured analytes between active TB and TB cure were analyzed using a paired t-test for normally distributed variables and using a Wilcoxon signed rank test for variables that were not normally distributed. Individuals that failed treatment or for which TB recurrence was observed (n=3) were excluded from the analysis.

## RESULTS

### Study Participants Characteristics and Demographics

**TRuTH cohort:** The final analysis included 139 participants, of which 37 (19 males and 18 females) were cases and 102 (45 males and 57 females) were controls. The median age was 32 years [interquartile range (IQR) 28-35] for cases and 34 years (IQR 28-40) for controls ( $p=0.025$ ). The median CD4 count was 479.0 cell/mm<sup>3</sup> (IQR 339.0-834.0) and 458.5 cells/mm<sup>3</sup> (IQR 360.0 – 631.0,  $p=0.762$ ), for cases and controls, respectively. Despite ART, some participants had detectable viral loads (VLs): the mean (standard deviation) VL for cases was 1.61 (0.7) log copies/ml and 1.5 (0.6) log copies/ml for controls ( $p=0.319$ ). A detailed list of the TRuTH cohort characteristics can be found in **Supplementary Table 1**.

**IMPRESS study:** In total, 41 HIV infected and 33 HIV uninfected participants had samples available at both time points. Further 3 HIV infected individuals were excluded from analysis because they failed treatment. Out of the 38 HIV infected participants 16 were females and 22 males and out of the 33 HIV uninfected participants 2 were females and 31 males. The median age at enrolment was 35 (IQR 32-43) years for HIV infected and 33 (IQR 25-49) years for HIV uninfected participants. A detailed list of the IMPRESS cohort characteristics can be found in **Supplementary Table 2**.

### Measured Analytes as Predictors of TB Recurrence in TRuTH

To determine if measured plasma analytes had an effect on the rate of TB recurrence, we conducted a univariable and multivariable conditional logistic regression. In the univariable analysis, two



analytes were associated with increased odds of TB recurrence: sICAM [Odds Ratio (OR) 1.05, 95% Confidence Interval (CI) 1.01 – 1.08,  $p = 0.005$ ] and LBP (OR 3.28, 95% CI 1.02 – 10.59,  $p = 0.047$ ) (Table 1, Figure 1). These associations remained significant in the multivariable model: sICAM (aOR 1.06, 95% CI 1.02 – 1.12,  $p = 0.009$ ) and LBP (aOR 8.78, 95% CI 1.23 – 62.66,  $p = 0.030$ ). We also observed a significant correlation between sICAM and LBP expression ( $r = 0.347$ ,  $p < 0.001$ , Supplementary Table 3). In addition to LBP and sICAM, TGF- $\beta$ 3 (aOR 1.44, 95% CI 1.01 – 2.05,  $p = 0.044$ ) was significantly associated with increased risk of TB recurrence in the multivariable model (Table 1).

Previously, we measured the plasma expression of 23 plasma cytokines/chemokines to look at their impact on the risk of TB recurrence (11) in the TRuTH cohort. Here we examined if there

was a correlation between the expression of 23 measured cytokines/chemokines and sMAdCAM, sICAM, sVCAM, LBP, TGF- $\beta$ 1, TGF- $\beta$ 2 and TGF- $\beta$ 3 in 21 overlapping plasma samples. We observed significant positive correlations between LBP and IL-6 ( $r = 0.623$ ,  $p = 0.003$ ); sVCAM and IL-27 ( $r = 0.438$ ,  $p = 0.047$ ); TGF- $\beta$ 1 and sCD14 ( $r = 0.513$ ,  $p = 0.017$ ); and TGF- $\beta$ 2 with: IL-7 ( $r = 0.481$ ,  $p = 0.027$ ), IL-6 ( $r = 0.438$ ,  $p = 0.047$ ), and sCD14 ( $r = 0.456$ ,  $p = 0.038$ ) (Supplementary Table 4).

## Effect of TB Treatment Completion on Plasma Expression of Measured Analytes

A small subset of cases was followed longitudinally to observe the changes in plasma expression of measured analytes (sMAdCAM, sICAM, sVCAM, LBP, TGF- $\beta$ 1, TGF- $\beta$ 2 and TGF- $\beta$ 3) in response to TB treatment completion in the TRuTH cohort ( $n = 14$ ). No significant differences were observed in measured analyte expression between active TB and post TB treatment/ Cure time-point (Supplementary Table 5).

Next we examined the changes in plasma expression of measured analytes (LBP, sMAdCAM, sICAM, sVCAM, TGF- $\beta$ 1, TGF- $\beta$ 2 and TGF- $\beta$ 3) from active TB to post TB/cure in HIV infected ( $n = 38$ ) and HIV uninfected ( $n = 33$ ) participants from the IMPRESS study. We observed no significant differences in the expression of sMAdCAM, sICAM, sVCAM, TGF- $\beta$ 1, TGF- $\beta$ 2 and TGF- $\beta$ 3 between active TB and post TB cure in HIV infected and HIV uninfected participants (Table 2). A trend towards increased LBP levels following TB treatment was observed in HIV infected participants [Mean difference (MD) -2.03 (95% CI 4.17-0.12),  $p = 0.064$ ]. Conversely, HIV uninfected participants demonstrated the opposite trend, showing lower LBP levels at TB cure [MD 2.08 (95% CI -0.20-4.36),  $p = 0.073$ ] (Figure 2, Table 2).

**TABLE 1 |** Univariable and multivariable analysis of TRuTH plasma analytes (sMAdCAM, sICAM, sVCAM, LBP, TGF- $\beta$ 1, TGF- $\beta$ 2 and TGF- $\beta$ 3) as biomarkers of TB recurrence.

Cytokine	Univariable		Multivariable <sup>1</sup>	
	OR (95% CI)	p-value	aOR (95% CI)	p-value
sMAdCAM	0.99 (0.39 – 2.52)	0.984	0.94 (0.26 – 3.33)	0.922
sICAM	1.05 (1.01 – 1.08)	<b>0.005*</b>	1.06 (1.02 – 1.12)	<b>0.009</b>
sVCAM	1.02 (0.99 – 1.04)	0.142	1.02 (0.99 – 1.05)	0.222
LBP	3.28 (1.02 – 10.59)	<b>0.047</b>	8.78 (1.23 – 62.66)	<b>0.030</b>
TGF- $\beta$ 1	1.05 (0.97 – 1.12)	0.222	1.05 (0.98 – 1.14)	0.179
TGF- $\beta$ 2	1.09 (0.93 – 1.29)	0.274	1.15 (0.93 – 1.43)	0.194
TGF- $\beta$ 3	1.21 (0.95 – 1.55)	0.120	1.44 (1.01 – 2.05)	<b>0.044</b>

<sup>1</sup>Multivariable analysis adjusted for WHO stage of the disease, BMI, lung cavities, age, CD4 count, VL, gender and previous history of TB. \*Statistically significant association after FDR adjustment using 0.05 threshold.

Bold values:  $p$ -value < 0.05.

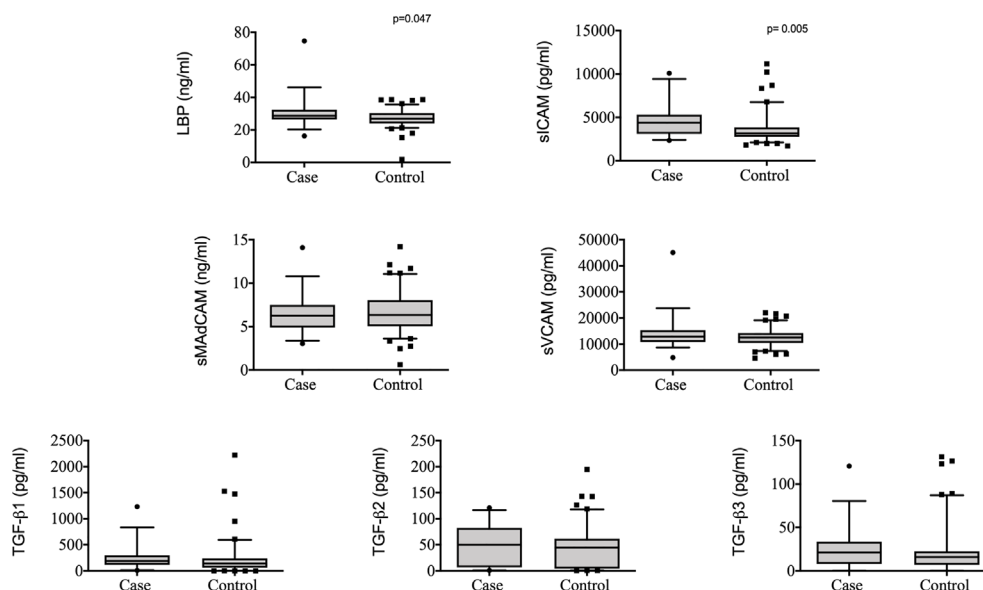


**FIGURE 1 |** Plasma levels of LBP, sMAdCAM, sICAM, sVCAM, TGF- $\beta$ 1, TGF- $\beta$ 2 and TGF- $\beta$ 3 in controls ( $n = 103$ ) and cases ( $n = 37$ ) from TRuTH. Analytes were plotted using Box and Whiskers (5–95%). P-values indicated in the figures are the result of univariable conditional logistic regression (please refer to Table 1 for full analysis).

**TABLE 2 |** Changes in measured analytes in response to TB treatment in HIV infected (n = 38) and HIV uninfected (n = 33) IMPRESS study participants.

Variable	HIV Infected (n = 38) Active TB – Post TB/Cure		HIV Uninfected (n = 33) Active TB – Post TB/Cure	
	Mean Difference (95% CI)	p - value	Mean Difference (95% CI)	p - value
sMAdCAM	0.355 (-0.264 to 0.974)	0.252 <sup>a</sup>	-0.264 (-0.75 to 0.221)	0.276 <sup>a</sup>
sICAM	-905.385 (-1926.394 to 115.624)	0.193 <sup>b</sup>	206.615 (-788.215 to 1201.446)	0.279 <sup>b</sup>
sVCAM	-1200.169 (-3392.082 to 991.743)	0.633 <sup>b</sup>	-485.88 (-2158.311 to 1186.552)	0.787 <sup>b</sup>
LBP	-2.026 (-4.173 to 0.122)	0.064 <sup>a</sup>	2.081 (-0.202 to 4.364)	0.073 <sup>a</sup>
TGF-β1	-539.684 (-1190.915 to 131.547)	0.135 <sup>b</sup>	246.483 (-466.95 to 959.917)	0.347 <sup>b</sup>
TGF-β2	-18.832 (-51.919 to 14.255)	0.395 <sup>b</sup>	7.006 (-21.552 to 35.564)	0.339 <sup>b</sup>
TGF-β3	-10.189 (-23.778 to 3.399)	0.160 <sup>b</sup>	2.42 (-9.019 to 13.858)	0.252 <sup>b</sup>

<sup>a</sup>p - value is represented from the paired t-test.

<sup>b</sup>p - value is represented from the Wilcoxon signed rank test.

Additionally we examined the differences in expression levels of measured analytes between HIV uninfected and HIV infected participants at both active TB and TB cure timepoints. Expression of LBP, sVCAM and TGF-β2 were significantly elevated in HIV infected participants at both active TB and TB cure ( $p < 0.02$ , **Figure 2**). Expression of sICAM ( $p = 0.019$ ) and TGF-β3 ( $p = 0.002$ ) were significantly elevated in HIV infected participants only at TB cure timepoint, likely due to TB – induced inflammatory changes at active TB (18). No significant differences were observed for sMADCAM and TGF-β1.

## DISCUSSION

HIV-TB co-epidemic is one of the major health challenges affecting sub-Saharan Africa. Considering the geographical overlap of the HIV and TB epidemics and the 18 fold higher risk of TB in HIV co-infected (1), there is an urgent need to identify TB prognostic markers in HIV co-infected individuals, in order to improve patient management and fast-track the development of novel therapeutics. Here we identified increased levels of LBP and sICAM as biomarkers of risk of TB recurrence in HIV co-infected patients.

In the univariable and multivariable logistic models, the risk of TB recurrence was significantly associated with increase in plasma expression of sICAM and LBP, known to play a role in inflammation and translocation of microbial products, respectively (6, 19, 21). ICAM, present on endothelial cells, is involved in the firm arrest and transmigration of leukocytes from blood vessels to tissues, and is an important early marker of immune activation and response (7, 8, 22). Soluble, circulating forms of ICAM have been involved in a range of proinflammatory responses, and increase in sICAM levels have been linked with a range of human diseases including atherosclerosis and heart failure (21, 22). Previous studies have shown that the concentration of sICAM is elevated in patients with active TB disease (23, 24) and serum concentration of sICAM has been linked to bacterial burden (23, 25, 26) and disease severity (10). The observed increase in sICAM prior to TB disease likely reflects increased systemic inflammation as a result of increased bacterial replication from new infection or reactivation of latent disease.

In serum, LBP is present as a soluble acute-phase protein which binds to LPS and stimulates an immune response by

presenting the LPS to cell surface pattern recognition receptors (PRRs) such as CD14 and toll like receptor 4 (TLR4) (20, 24). Increased concentrations of LBP have been observed in patients with sepsis and in healthy individuals injected with LPS (27, 28) as well as bronchoalveolar lavage fluids of healthy individuals and patients with lung injury (29). LBP was shown to be elevated in individuals with active TB and declined during treatment, suggesting that it may play an important role in the host reaction to TB (24). Increased levels of plasma LBP were associated with an increased risk of TB recurrence in this study. Since the TRUTH cohort only includes HIV co-infected individuals, increased LBP levels likely reflect both the HIV induced translocation of microbial products (30) as well as increase in TB bacterial burden. We also observed a strong positive correlation between LBP and sICAM as well as LBP and IL-6 identified to be one of the main pro-inflammatory cytokines associated with TB recurrence in our previous study (11). Interestingly, LPS was shown to be a strong inducer of both IL-6 and ICAM-1 (31, 32) suggesting that HIV-associated loss in gastrointestinal integrity and the resulting systemic inflammation could be fuelling the increased risk of TB recurrence in HIV co-infected individuals. HIV mediated gastrointestinal damage and the resulting translocation of microbial products (33) are known to cause immune activation and dysregulation of the host responses and as a result can lead to opportunistic infections including TB. This is supportive of a recent study in macaques co-infected with *M.tb* and SIV suggesting that SIV-driven chronic immune activation and dysregulation of T cell homeostasis associate with reactivation of latent TB (LTBI) (14). Furthermore changes in integrity of the gastrointestinal tract and resulting immune activation have been linked to lung inflammation, with 50% of adults who suffer with inflammatory bowel disease (IBD) and 33% of individuals who suffer with inflammatory bowel syndrome (IBS) having pulmonary involvement (34–36). This likely indicates that there is an inflammatory cross talk between different mucosal sites and that inflammation and dysbiosis in the gut can translate to inflammatory changes in the lungs (37).

After adjusting for covariates, the risk of TB recurrence was associated with increased concentrations of TGF-β3. TGF-β belongs to a superfamily of immunoregulatory cytokines which include three isoforms: TGF-β1, TGF-β2, and TGF-β3 (3). TGF-β controls the initiation and resolution of inflammation *via* regulation of

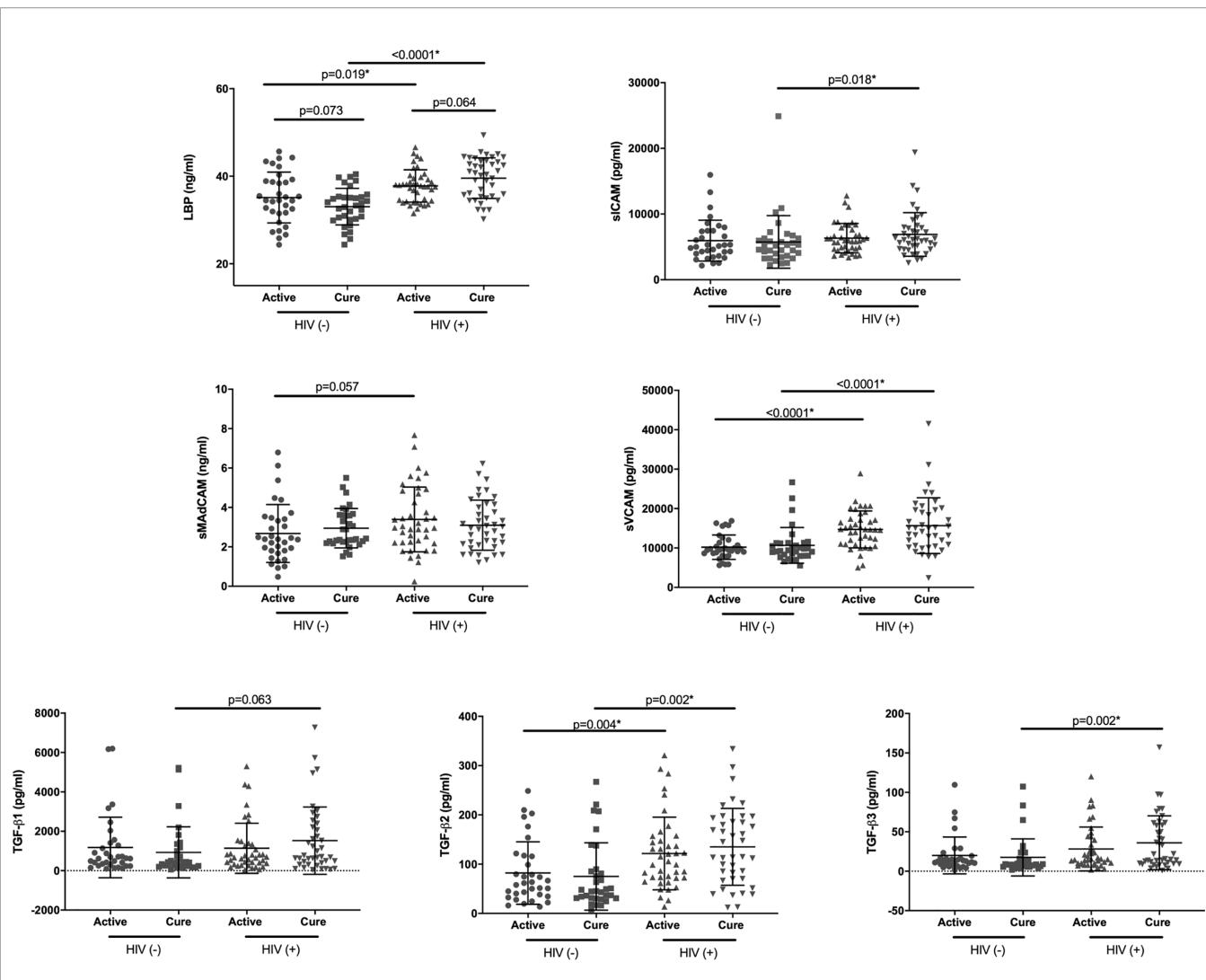


**FIGURE 2 |** Plasma levels of LBP, sAdCAM, sICAM, sVCAM, TGF- $\beta$ 1, TGF- $\beta$ 2 and TGF- $\beta$ 3 in HIV uninfected [HIV(-)] and HIV infected [HIV(+)] IMPRESS participants at active TB (active) and post-TB treatment (cure) timepoints. Based on the result of the normality test either parametric: paired t-test (Active vs Cure) and t-test (HIV+ vs HIV-), or non-parametric: Wilcoxon signed rank (Active vs Cure) and Mann-Whitney (HIV+ vs HIV-) tests were used for the analysis. \*Statistically significant association after FDR adjustment using 0.05 threshold.

chemotaxis, activation and survival of immune cells (38). Excess TGF- $\beta$  was shown to suppress T cell responses to *M.tb* antigens (39) and increased TGF- $\beta$  activity is a feature of active pulmonary TB (40). Increase in TGF- $\beta$ 3 prior to TB recurrence likely reflects the increase in systemic inflammation. Additionally, TGF- $\beta$ 1 and TGF- $\beta$ 2 expression was positively correlated with sCD14 expression, a known marker of active TB (11, 18, 41, 42). While there is a general lack of isoform-specific data on TGF- $\beta$ , isoform-specific knockout mice studies have shown non-redundant phenotypes. Specifically TGF- $\beta$ 3 knockout mice were shown to die perinatally due to developmental defects of the lung and defective palatogenesis (43).

We observed no significant changes in measured analytes between active TB disease and post TB treatment/cure timepoints in a small subset of patients from TRuTH cohort. Likewise when we examined the changes in the expression of LBP,

sAdCAM, sICAM, sVCAM, TGF- $\beta$ 1, TGF- $\beta$ 2 and TGF- $\beta$ 3 from active TB disease to TB treatment completion in HIV infected and HIV uninfected individuals from IMPRESS, no significant differences were observed. Although not statistically significant, there was a trend towards decreased concentrations of plasma LBP in HIV uninfected individuals following TB treatment, likely due to a decrease in TB bacterial burden which is consistent with previous studies in predominantly HIV uninfected individuals (24). A trend towards increased concentrations of plasma LBP was observed in HIV infected individuals following TB treatment, likely reflecting a decrease in the gastrointestinal integrity caused by progressing HIV infection (33, 44). When we examined the differences in the relevant analytes between HIV infected and HIV uninfected individuals at active TB and post-successful TB treatment, we

observed that LBP was significantly elevated in HIV infected individuals irrespective of the TB status, indicating that the HIV infection and resulting increase in systemic LPS exposure are the predominant drivers of increased LBP levels in co-infected patients. Plasma ICAM and TGF- $\beta$ 3 levels were only significantly elevated in HIV infected individuals post TB treatment completion, highlighting the effect of active TB in driving the increased expression of these markers (23, 25, 26).

Our study has several limitations. The observed associations are statistically modest and need to be confirmed in an independent human cohort to fully evaluate the predicative value of the identified biomarkers. The identified biomarkers of TB recurrence are only relevant in the context of TB-HIV co-infection. The analysis of the IMPRESS cohort is limited by an unequal gender distribution (specifically the predominance of men in the HIV-uninfected sample), a small sample size and resulting inability to stratify for potential confounders. Additional studies are needed to fully understand the relationship between treatment completion and disease severity, and the expression of the measured analytes.

In conclusion, we identified increased expression of plasma LBP and sICAM as biomarkers of TB recurrence in individuals who were receiving ART treatment in the TRUTH cohort. Our results support the notion of HIV associated chronic immune activation as the driving force in TB reactivation/reinfection in HIV infected individuals. Mitigating chronic immune activation through utilization of immune based interventions might not only lead to improved HIV outcome, but could significantly reduce the rates of TB recurrence and have a profound impact on reducing TB disease burden in HIV endemic settings. Further studies are needed to decipher the mechanism of how HIV mediated chronic immune activation increases the risk of TB reactivation in HIV co-infected individuals.

## DATA AVAILABILITY STATEMENT

The datasets generated for this study are available on request to the corresponding author.

## ETHICS STATEMENT

The studies involving human participants were reviewed and approved by the University of KwaZulu-Natal's Biomedical Research Ethics Committee (BE659/17). The patients/participants provided their written informed consent to participate in this study.

## AUTHOR CONTRIBUTIONS

Designed the study: AS and KN. Performed the experiments: KP and AS. Analyzed the data: KP, AS, SR, LL, NY-Z, and DA. Wrote the first

draft of the paper: KP and AS. Collected specimens and clinical data: SG, DG, and RH-M. Supervised clinical and/or experimental aspects of the study: AS, LM, DA, KN, NP, SA, and NS. All authors contributed to the article and approved the submitted version.

## FUNDING

The TRUTH study was supported by the Howard Hughes Medical Institute, Grant Number 55007065, as well as the Centers for Disease Control and Prevention (CDC) Cooperative Agreement Number UY2G/PS001350-02. Its contents are solely the responsibility of the authors and do not necessarily represent the official views of either the Howard Hughes Medical Institute or the Centers for Disease Control and Prevention (CDC). The research infrastructure to conduct this trial, including the data management, laboratory and pharmacy cores were established through the US National Institutes for Health's Comprehensive International Program of Research on AIDS grant (CIPRA, grant # AI51794). AS is supported by European & Developing Countries Clinical Trials partnership (EDCTP) Career Development Fellowship (TMA2016CDF-1582). KP and SR was supported by the National Research Foundation (Grant numbers: 96354 and 108038 respectively). DA was supported the NRF Research Career Advancement Fellowship (grant # RCA13101656388) and a senior fellowship through the European and Developing Countries Clinical Trials Partnership (EDCTP) (grant # TMA2017SF-1960) funds. Any opinion, funding, and conclusion or recommendations expressed in this material is that of the author and the NRF does not accept liability in this regard. Patient care was supported by the KwaZulu-Natal Department of Health and the U.S. President's Emergency Plan for AIDS Relief (PEPFAR). Research reported in this publication was supported by the Strategic Health Innovation Partnership (SHIP) Unit of the South African Medical Research Council, a grantee of the Bill & Melinda Gates Foundation, and the South African Medical Research Council. The funding sources listed here did not have any role in the analysis or preparation of the data in this manuscript, nor was any payment received by these or other funding sources for this manuscript.

## ACKNOWLEDGMENTS

Authors would like to thank all the research participants and the staff of the CAPRISA eThekweni clinic in KwaZulu-Natal, South Africa for their dedication to these studies.

## SUPPLEMENTARY MATERIAL

The Supplementary Material for this article can be found online at: <https://www.frontiersin.org/articles/10.3389/fimmu.2021.631094/full#supplementary-material>



# REFERENCES

- World Health Organization. *Global tuberculosis report*. Geneva, Switzerland: World Health Organization (2020).
- Travis MA, Sheppard D. TGF- $\beta$  activation and function in immunity. *Annu Rev Immunol* (2014) 32:51–82. doi: 10.1146/annurev-immunol-032713-120257
- Morikawa M, Derynck R, Miyazono K. TGF- $\beta$  and the TGF- $\beta$  Family: Context-Dependent Roles in Cell and Tissue Physiology. *Cold Spring Harbor Perspect Biol* (2016) 8:a021873. doi: 10.1101/cshperspect.a021873
- Abdool Karim SS, Naidoo K, Grobler A, Padayatchi N, Baxter C, Gray AL, et al. Integration of antiretroviral therapy with tuberculosis treatment. *N Engl J Med* (2011) 365:1492–501. doi: 10.1056/NEJMoa1014181
- Perumal R, Padayatchi N, Yende-Zuma N, Naidoo A, Govender D, Naidoo K. A moxifloxacin-based regimen for the treatment of recurrent drug-sensitive pulmonary tuberculosis: An open-label randomised controlled trial. *Clin Infect Dis* (2019) 70(1):90–8. doi: 10.1093/cid/ciz152
- Gutsmann T, Müller M, Carroll SF, MacKenzie RC, Wiese A, Seydel U. Dual role of lipopolysaccharide (LPS)-binding protein in neutralization of LPS and enhancement of LPS-induced activation of mononuclear cells. *Infection Immun* (2001) 69:6942–50. doi: 10.1128/IAI.69.11.6942-6950.2001
- Springer TA. Adhesion receptors of the immune system. *Nature* (1990) 346:425–34. doi: 10.1038/346425a0
- Seth R, Raymond FD, Makgoba MW. Circulating ICAM-1 isoforms: diagnostic prospects for inflammatory and immune disorders. *Lancet* (1991) 338:83–4. doi: 10.1016/0140-6736(91)90077-3
- Walzl G, Ronacher K, Hanekom W, Scriba TJ, Zumla A. Immunological biomarkers of tuberculosis. *Nat Rev Immunol* (2011) 11:343–54. doi: 10.1038/nri2960
- Sigal GB, Segal MR, Mathew A, Jarlsberg L, Wang M, Barbero S, et al. Biomarkers of Tuberculosis Severity and Treatment Effect: A Directed Screen of 70 Host Markers in a Randomized Clinical Trial. *EBIOM* (2017) 25:112–21. doi: 10.1016/j.jebiom.2017.10.018
- Sivro A, McKinnon LR, Yende-Zuma N, Gengiah S, Samsunder N, Abdool Karim SS, et al. Plasma Cytokine Predictors of Tuberculosis Recurrence in Antiretroviral-Treated Human Immunodeficiency Virus-infected Individuals from Durban, South Africa. *Clin Infect Dis* (2017) 65:819–26. doi: 10.1093/cid/cix357
- McKinnon LR, Liebenberg LJ, Yende-Zuma N, Archary D, Ngcapu S, Sivro A, et al. Genital inflammation undermines the effectiveness of tenofovir gel in preventing HIV acquisition in women. *Nat Med* (2018) 24:491–6. doi: 10.1038/nm.4506
- Masson L, Passmore J-AS, Liebenberg LJ, Werner L, Baxter C, Arnold KB, et al. Genital inflammation and the risk of HIV acquisition in women. *Clin Infect Dis* (2015) 61:260–9. doi: 10.1093/cid/civ298
- Buçan AN, Chatterjee A, Singh DK, Foreman TW, Lee T-H, Threeton B, et al. Mechanisms of reactivation of latent tuberculosis infection due to SIV coinfection. *J Clin Invest* (2019) 129:5254–60. doi: 10.1172/JCI125810
- Boulware DR, Hullsiek KH, Puronen CE, Rupert A, Baker JV, French MA, et al. Higher levels of CRP, D-dimer, IL-6, and hyaluronic acid before initiation of antiretroviral therapy (ART) are associated with increased risk of AIDS or death. *J Infect Dis* (2011) 203:1637–46. doi: 10.1093/infdis/jir134
- Sivro A, Su R-C, Plummer FA, Ball TB. Interferon responses in HIV infection: from protection to disease. *AIDS Rev* (2014) 16:43–51.
- Sousa J, Cá B, Maceiras AR, Simões-Costa L, Fonseca KL, Fernandes AI, et al. Mycobacterium tuberculosis associated with severe tuberculosis evades cytosolic surveillance systems and modulates IL-1 $\beta$  production. *Nat Commun* (2020) 11:1949. doi: 10.1038/s41467-020-15832-6
- Sullivan ZA, Wong EB, Ndung'u T, Kaspruwicz VO, Bishai WR. Latent and Active Tuberculosis Infection Increase Immune Activation in Individuals Co-Infected with HIV. *EBIOM* (2015) 2:334–40. doi: 10.1016/j.jebiom.2015.03.005
- Schumann RR. Function of lipopolysaccharide (LPS)-binding protein (LBP) and CD14, the receptor for LPS/LBP complexes: a short review. *Res Immunol* (1992) 143:11–5. doi: 10.1016/0923-2494(92)80074-u
- Schumann RR, Leong SR, Flagg GW, Gray PW, Wright SD, Mathison JC, et al. Structure and function of lipopolysaccharide binding protein. *Science* (1990) 249:1429–31. doi: 10.1126/science.2402637
- Gearing AJ, Newman W. Circulating adhesion molecules in disease. *Immunol Today* (1993) 14:506–12. doi: 10.1016/0167-5699(93)90267-O
- Lawson C, Wolf S. ICAM-1 signaling in endothelial cells. *Pharmacol Rep* (2009) 61:22–32. doi: 10.1016/S1734-1140(09)70004-0
- López Ramirez GM, Rom WN, Ciotoli C, Talbot A, Martiniuk F, Cronstein B, et al. Mycobacterium tuberculosis alters expression of adhesion molecules on monocytic cells. *Infection Immun* (1994) 62:2515–20. doi: 10.1128/IAI.62.6.2515-2520.1994
- Juffermans NP, Verbon A, van Deventer SJ, Buurman WA, van Deutekom H, Speelman P, et al. Serum concentrations of lipopolysaccharide activity-modulating proteins during tuberculosis. *J Infect Dis* (1998) 178:1839–42. doi: 10.1086/314492
- Demir T, Yalcinoz C, Keskinel I, Demiröz F, Yildirim N. sICAM-1 as a serum marker in the diagnosis and follow-up of treatment of pulmonary tuberculosis. *Int J Tuberculosis Lung Dis* (2002) 6:155–9.
- Mukae H, Ashitani J-I, Tokojima M, Ihi T, Kohno S, Matsukura S. Elevated levels of circulating adhesion molecules in patients with active pulmonary tuberculosis. *Respirology* (2003) 8:326–31. doi: 10.1046/j.1440-1843.2003.00471.x
- Froon AH, Dentener MA, Greve JW, Ramsay G, Buurman WA. Lipopolysaccharide toxicity-regulating proteins in bacteremia. *J Infect Dis* (1995) 171:1250–7. doi: 10.1093/infdis/171.5.1250
- van der Poll T, Coyle SM, Levi M, Jansen PM, Dentener M, Barbosa K, et al. Effect of a recombinant dimeric tumor necrosis factor receptor on inflammatory responses to intravenous endotoxin in normal humans. *Blood* (1997) 89:3727–34. doi: 10.1182/blood.V89.10.3727
- Martin TR, Mathison JC, Tobias PS, Letúrcq DJ, Moriarty AM, Maunder RJ, et al. Lipopolysaccharide binding protein enhances the responsiveness of alveolar macrophages to bacterial lipopolysaccharide. Implications for cytokine production in normal and injured lungs. *J Clin Invest* (1992) 90:2209–19. doi: 10.1172/JCI116106
- Sandler NG, Douek DC. Microbial translocation in HIV infection: causes, consequences and treatment opportunities. *Nat Rev Microbiol* (2012) 10:655–66. doi: 10.1038/nrmicro2848
- Sawa Y, Ueki T, Hata M, Iwasawa K, Tsuruga E, Kojima H, et al. LPS-induced IL-6, IL-8, VCAM-1, and ICAM-1 expression in human lymphatic endothelium. *J Histochem Cytochem* (2008) 56:97–109. doi: 10.1369/jhc.7A7299.2007
- Fukuda K, Kumagai N, Yamamoto K, Fujitsu Y, Chikamoto N, Nishida T. Potentiation of lipopolysaccharide-induced chemokine and adhesion molecule expression in corneal fibroblasts by soluble CD14 or LPS-binding protein. *Invest Ophthalmol Vis Sci* (2005) 46:3095–101. doi: 10.1167/iovs.04-1365
- Brenchley JM, Price DA, Schacker TW, Asher TE, Silvestri G, Rao S, et al. Microbial translocation is a cause of systemic immune activation in chronic HIV infection. *Nat Med* (2006) 12:1365–71. doi: 10.1038/nm1511
- Yazar A, Atis S, Konca K, Pata C, Akbay E, Calikoglu M, et al. Respiratory symptoms and pulmonary functional changes in patients with irritable bowel syndrome. *Am J Gastroenterol* (2001) 96:1511–6. doi: 10.1111/j.1572-0241.2001.03748.x
- Budden KF, Gellatly SL, Wood DLA, Cooper MA, Morrison M, Hugenholtz P, et al. Emerging pathogenic links between microbiota and the gut–lung axis. *Nat Rev Microbiol* (2017) 15:55–63. doi: 10.1038/nrmicro.2016.142
- Keely S, Talley NJ, Hansbro PM. Pulmonary-intestinal cross-talk in mucosal inflammatory disease. *Mucosal Immunol* (2011) 5:7–18. doi: 10.1038/mi.2011.55
- Budden KF, Gellatly SL, Wood DLA, Cooper MA, Morrison M, Hugenholtz P, et al. Emerging pathogenic links between microbiota and the gut–lung axis. *Nat Rev Microbiol* (2017) 15:55–63. doi: 10.1038/nrmicro.2016.142
- Li MO, Wan YY, Sanjabi S, Robertson A-KL, Flavell RA. Transforming growth factor-beta regulation of immune responses. *Annu Rev Immunol* (2006) 24:99–146. doi: 10.1146/annurev.immunol.24.021605.090737
- Hirsch CS, Ellner JJ, Blinkhorn R, Toossi Z. In vitro restoration of T cell responses in tuberculosis and augmentation of monocyte effector function against Mycobacterium tuberculosis by natural inhibitors of transforming growth factor beta. *Proc Natl Acad Sci USA* (1997) 94:3926–31. doi: 10.1073/pnas.94.8.3926
- Aung H, Toossi Z, McKenna SM, Gogate P, Sierra J, Sada E, et al. Expression of transforming growth factor-beta but not tumor necrosis factor-alpha, interferon-gamma, and interleukin-4 in granulomatous lung lesions in tuberculosis. *Tuber Lung Dis* (2000) 80:61–7. doi: 10.1054/tuld.2000.0235

41. Lawn SD, Labeta MO, Arias M, Acheampong JW, Griffin GE. Elevated serum concentrations of soluble CD14 in HIV- and HIV+ patients with tuberculosis in Africa: prolonged elevation during anti-tuberculosis treatment. *Clin Exp Immunol* (2000) 120:483–7. doi: 10.1046/j.1365-2249.2000.01246.x
42. Liu Y, Ndumego OC, Chen T, Kim RS, Jenny-Avital ER, Ndung'u T, et al. Soluble CD14 as a Diagnostic Biomarker for Smear-Negative HIV-Associated Tuberculosis. *Pathogens* (2018) 7:26. doi: 10.3390/pathogens7010026
43. Kaartinen V, Voncken JW, Shuler C, Warburton D, Bu D, Heisterkamp N, et al. and cleft palate in mice lacking TGF-beta 3 indicates defects of epithelial-mesenchymal interaction. *Nat Genet* (1995) Dec11(4):415–21. doi: 10.1038/ng1295-415
44. Brenchley JM, Douek DC. HIV infection and the gastrointestinal immune system. *Mucosal Immunol* (2007) 1:23–30. doi: 10.1038/mi.2007.1

**Conflict of Interest:** The authors declare that the research was conducted in the absence of any commercial or financial relationships that could be construed as a potential conflict of interest.

Copyright © 2021 Pillay, Lewis, Rambaran, Yende-Zuma, Archary, Gengiah, Govender, Hassan-Moosa, Samsunder, Abdool Karim, McKinnon, Padayatchi, Naidoo and Sivo. This is an open-access article distributed under the terms of the Creative Commons Attribution License (CC BY). The use, distribution or reproduction in other forums is permitted, provided the original author(s) and the copyright owner(s) are credited and that the original publication in this journal is cited, in accordance with accepted academic practice. No use, distribution or reproduction is permitted which does not comply with these terms.



# Effect of Inflammatory Cytokines/Chemokines on Pulmonary Tuberculosis Culture Conversion and Disease Severity in HIV-Infected and -Uninfected Individuals From South Africa

## OPEN ACCESS

### Edited by:

Hazel Marguerite Dockrell,  
University of London, United Kingdom

### Reviewed by:

Maeva Dupont,  
University of Oxford, United Kingdom  
Jun-Jun Yeh,  
Ditmanson Medical Foundation  
Chia-Yi Christian Hospital, Taiwan  
Delia Goletti,  
Istituto Nazionale per le Malattie  
Infettive Lazzaro Spallanzani  
(IRCCS), Italy

### \*Correspondence:

Aida Sivo  
aida.sivo@caprisa.org

### Specialty section:

This article was submitted to  
Microbial Immunology,  
a section of the journal  
Frontiers in Immunology

**Received:** 13 December 2020

**Accepted:** 19 March 2021

**Published:** 01 April 2021

### Citation:

Rambaran S, Naidoo K, Lewis L,  
Hassan-Moosa R, Govender D,  
Samsunder N, Scriba TJ,  
Padayatchi N and Sivo A (2021) Effect  
of Inflammatory Cytokines/  
Chemokines on Pulmonary  
Tuberculosis Culture Conversion and  
Disease Severity in HIV-Infected  
and -Uninfected Individuals  
From South Africa.  
Front. Immunol. 12:641065.  
doi: 10.3389/fimmu.2021.641065

**Santhuri Rambaran<sup>1</sup>, Kogieleum Naidoo<sup>1,2</sup>, Lara Lewis<sup>1</sup>, Razia Hassan-Moosa<sup>1,2</sup>,  
Dhineshree Govender<sup>1</sup>, Natasha Samsunder<sup>1</sup>, Thomas J. Scriba<sup>3</sup>, Nesri Padayatchi<sup>1,2</sup>  
and Aida Sivo<sup>1,4\*</sup>**

<sup>1</sup> Centre for the AIDS Programme of Research in South Africa (CAPRISA), Durban, South Africa, <sup>2</sup> MRC-CAPRISA HIV-TB Pathogenesis and Treatment Research Unit, Doris Duke Medical Research Institute, University of KwaZulu-Natal, Durban, South Africa, <sup>3</sup> Department of Pathology, South African Tuberculosis Vaccine Initiative (SATVI), Institute of Infectious Disease and Molecular Medicine and Division of Immunology, University of Cape Town, Cape Town, South Africa, <sup>4</sup> Department of Medical Microbiology, University of KwaZulu-Natal, Durban, South Africa

Novel tuberculosis (TB) prevention and control strategies are urgently required. Utilising specimens from the Improving Retreatment Success (NCT02114684) trial we assessed the associations between inflammatory markers, measured during active TB, with treatment response and disease severity in HIV-infected and uninfected individuals. Multiplex immunoassays and ELISA were used to measure plasma expression of 24 cytokines/chemokines. Cytokines were log transformed to adjust for skewness. We conducted a nested, un-matched, case (n= 31) - control (n=101) study with cases defined as those participants who failed to sputum culture convert within 8-weeks of TB treatment initiation. Additionally, we examined the association between the measured cytokines and time to culture conversion and presence of lung cavitation using cox proportional hazards and logistic regression models, respectively. Multivariable analyses adjusted for a wide range of baseline clinical and demographic variables. IP-10 expression during active TB was associated with increased odds of sputum culture conversion by 8-weeks overall (aOR 4.255, 95% CI 1.025 – 17.544, p=0.046) and among HIV-infected individuals (OR 10.204, 95% CI 1.247 – 83.333, p=0.030). Increased MCP-3 (aHR 1.723, 95% CI 1.040 – 2.855, p=0.035) and IL-6 (aHR 1.409, 95% CI 1.045 – 1.899, p=0.024) expression was associated with a shorter time to culture conversion in the total cohort. Higher plasma expression of IL-6 (aHR 1.783, 95% CI 1.128 – 2.820, p=0.013), IL-1RA (aHR 2.595, 95% CI 1.136 – 5.926, p=0.024), IP-10 (aHR 2.068, 95% CI 1.034 – 4.137, p=0.040) and IL-1 $\alpha$  (aHR 2.008, 95% CI 1.053 – 3.831, p=0.035) were significantly associated with shorter time to culture conversion among HIV-infected individuals. Increased IL-6 and IL-1RA expression was significantly associated with the presence of

lung cavitation during active TB in the total cohort (OR 2.543, 95% CI 1.254 – 5.160,  $p=0.010$ ), (OR 4.639, 95% CI 1.203 – 21.031,  $p=0.047$ ) and in HIV-infected individuals (OR 2.644, 95% CI 1.062 – 6.585,  $p=0.037$ ), (OR 7.795, 95% CI 1.177 – 51.611,  $p=0.033$ ) respectively. Our results indicate that inflammatory cytokines/chemokines play an important role in TB disease outcome. Importantly, the observed associations were stronger in multivariable models highlighting the impact of behavioural and clinical variables on the expression of immune markers as well as their potential effects on TB outcome.

**Keywords:** inflammation, biomarker, lung cavitation, HIV, Tuberculosis

## INTRODUCTION

Tuberculosis is the leading cause of death from a single infectious agent with an estimated 10 million new infections reported in 2019 (1). Globally, among HIV-uninfected individuals, an estimated 1.2 million TB deaths occurred, and an additional 208,000 deaths were recorded among HIV-infected individuals in 2019. Africa accounted for 25% of the TB cases in 2019 and South Africa (SA) is one of eight countries accounting for two thirds of the global burden of TB. SA has the largest HIV epidemic in the world with 7.5 million people living with HIV, 200,000 new HIV infections and 72,000 deaths from AIDS-related illnesses in 2019 (UNAIDS Data, 2020). HIV-infected individuals are 15–22 times more likely to develop TB than HIV-uninfected individuals and TB is a leading cause of HIV-related deaths (WHO, 2019). Furthermore, despite suppressive ART, people living with HIV/AIDS (PLWHA) remain at heightened risk of recurrent TB during their lifetime.

Despite use of TB therapy for many decades, clinical decision making and monitoring of TB treatment response is universally dependent on microbiologic assessment of sputum culture conversion at 2 months post TB-treatment start, despite available data showing low predictive value of two-month sputum tests for predicting treatment failure and relapse (2). Moving away from sputum to more sensitive blood-based biomarkers is imperative for efficient monitoring of treatment efficacy, and early detection of treatment failure.

Measurement of plasma biomarkers could represent a cost-effective, real-time method to determine and understand an individual's immune status and its effect on TB risk and the subsequent response to TB therapy. A number of studies have examined the effect of soluble plasma cytokine/chemokine responses on TB severity and response to treatment and several cytokines/chemokines such as TNF $\alpha$ , IFN $\gamma$ , IL-1 $\beta$ , and IP-10 have been linked with disease outcome, presentation or severity (3–6). We have previously identified several inflammatory cytokines (including IL-1 $\beta$ , IL-6 and IL-1RA) associated with risk of TB recurrence in ART treated HIV co-infected cohort (7). Further characterisation of soluble biomarkers, especially in the context of TB/HIV co-infection, will provide valuable insight into the immunological pathways affected and provide new tools for TB screening and monitoring of treatment outcome.

Since HIV is known to cause dysregulation of the TB immune response (8, 9), here we aimed to determine if candidate plasma immune markers detected in individuals with recurrent, active TB disease, were associated with early and late culture conversion and disease severity in TB and TB-HIV co-infected individuals.

## MATERIALS AND METHODS

### Ethics Statement

Study participants were part of the CAPRISA 011 Improving Retreatment Success trial (IMPRESS, Clinicaltrials.gov, NCT02114684), approved by Medicines Control Council of South Africa (MCC Ref:20130510). Written informed consent was obtained from all study participants prior to enrolment. University of KwaZulu-Natal (UKZN) Biomedical Research Ethics Committee (BREC) reviewed and approved the study protocol (BFC029/13). The nested study protocol was reviewed and approved by UKZN BREC (BREC/00000014/2019).

### Study Participants

Study was performed on stored plasma specimens from CAPRISA 011 study participants that were recruited and treated at an urban clinic (CAPRISA eThekweni Research Clinic) adjoining the largest government outpatient TB facility, the Prince Cyril Zulu Communicable Disease Centre (PCZCDC) in KwaZulu-Natal (KZN), South Africa (SA) (10). All enrolled participants were adults  $\geq 18$  years, with a previous history of TB and the current diagnosis of rifampicin susceptible sputum smear-positive *Mycobacterium tuberculosis* (MTB) by GeneXpert MTB/RIF<sup>®</sup> technology. Smear microscopy grading was done using a standardized grading scale: smear 1+ (10 to 99 AFB in 100 fields), smear 2+ (1 to 10 AFB per field in at least 50 fields) and smear 3+ ( $>10$  AFB per field in at least 20 fields) (11). Both HIV-infected and uninfected participants were included in the study. Patients received 8 weeks of intensive phase TB treatment with 2 weekly clinical follow-up visits, and 16-weeks of continuous phase TB treatment with monthly clinical follow-up. We conducted a nested, un-matched case-control study. Cases were defined as those participants who failed to culture convert within 8-weeks of treatment initiation, where culture conversion was defined as the first of two negative sputum cultures at two consecutive visits without an intervening



culture positive result. Based on the definition and sample availability, 31 cases and 111 controls were selected for the study.

## Sample Processing

Peripheral blood was collected in acid citrate dextrose (ACD) tubes. Plasma was separated by centrifugation (1600rpm for 10') and cryopreserved at  $-80^{\circ}\text{C}$  until use.

## Cytokine/Chemokine Measurement

Cryopreserved plasma samples were thawed and mixed by vortexing before assays were performed. Cytokine/Chemokine levels were measured using the Millipore Milliplex<sup>®</sup> assays (Map Human Cytokine/Chemokine Panel I and IV) and analysed on a BioPlex-200 system (Bio-Rad). The Human Cytokine/Chemokine Panel I included the following cytokines and chemokines: pro-inflammatory [IL-1 $\alpha$ , IL-1 $\beta$ , IL-6, IL-12(p40), IL-12(p70), TNF $\alpha$ , IFN $\alpha$ 2], chemokines (IL-8, IP-10, MCP-1, MCP-3, MIP1 $\alpha$ , MIP1 $\beta$ ), adaptive (IFN $\gamma$ , IL-4, IL-15, IL-17 $\alpha$ ), anti-inflammatory (IL-10, IL-1RA), and growth factors (VEGF).

The Human Cytokine/Chemokine Panel IV included the following cytokines: IFN $\beta$  and IL-28B/IFN $\lambda$ 3. Soluble CD14 (sCD14) levels were measured using the Human CD14 Quantikine<sup>®</sup> ELISA Kit and human Lipopolysaccharide-Binding Protein (LBP) plasma levels were measured using the LBP kit (R&D Systems Inc, USA). All assays were performed following manufacturer's instructions. Samples with values outside the range of the standard curve were assigned the value half the limit of detection in pg/mL, LOD/2.

## Statistical Analyses

Fisher's Exact, Chi-Square and Mann-Whitney U tests were used to compare baseline characteristics between cases and controls. All biomarkers with more than 60% of samples above the limit of detection were analysed as continuous variables and log-transformed to adjust for skewness [IFN $\gamma$ , IL-1 $\beta$ , IL-1RA, IL-6, IL-8, IL-10, IL-12(p70), IL-17 $\alpha$ , IP-10, MCP-1, MIP-1 $\alpha$ , MIP-1 $\beta$ , TNF $\alpha$ , and VEGF-A]; those with more than 40% of samples below detectability were analysed as binary variables [IFN $\alpha$ 2, IL-1 $\alpha$ , IL-4, IL-12(p40), IL-15, MCP-3, IFN $\beta$  and IFN $\lambda$ /IL-28]. Logistic regression was used to measure the strength of association between plasma cytokine/chemokine expression at baseline and 8-week culture conversion status and discriminatory ability of the model was quantified using the area under the receiver operating curve (AUC). A Cox proportional hazards model was used to determine the association between cytokine/chemokine expression at baseline and time to culture conversion (first of two consecutive negative TB culture results), measured in days. To determine the association of plasma cytokine expression at baseline with disease severity measured by lung cavitation presence, a logistic regression model was used with presence of lung cavitation at baseline as the predictor outcome and AUC was measured. Multivariable analyses adjusted for a wide range of baseline clinical and demographic variables including study arm, age, sex, HIV status, lung cavitation, alcohol use, smoking and BMI. In addition, when analysing HIV-infected individuals CD4 counts, and viral load were adjusted for. Study arm was excluded in the multivariable lung cavitation analysis as this was not relevant for the studied timepoint. To

determine the association between the systemic levels of cytokines/chemokines and bacterial burden at baseline, a one-way ANOVA with Tukey's multiple comparisons test was done on normally distributed cytokines and non-parametric Kruskal Wallis test with Dunn's multiple comparisons test was done on not normally distributed cytokines. Statistical analyses were performed using IBM SPSS Statistics version 25, SAS version 9.4 and graphs were made using GraphPad Prism (V8.1.2).

## RESULTS

### Participant Characteristics

A total of 31 cases and 101 control samples were included in the final analysis. Ten controls were excluded from the original analysis as they did not meet the control definition (7 were not TB culture positive at baseline; 1 patient died before the 2<sup>nd</sup> TB culture negative result; and 2 had inconsistent TB culture results). There were no significant differences between cases and controls for the following characteristics: study arm, age, sex, HIV status, lung cavitation, CD4 count and viral load (**Table 1**). Body mass index (BMI) was significantly higher in controls [cases: 19.28 (IQR 17.96 – 19.98) vs controls: 20.42 (18.64 – 22.95), ( $p=0.031$ )]. There was a trend towards higher alcohol ( $p=0.067$ ) and cigarette use ( $p=0.051$ ) in cases.

### Effect of Plasma Cytokines/Chemokines Expression at Active TB on 8-Week TB Culture Conversion

We examined the association between plasma cytokine expression during active TB and early culture conversion (8 weeks). We observed no significant association between expression of measured cytokines/chemokines at active TB and TB culture conversion by 8 weeks in bivariable analysis adjusting for study arm (**Supplementary Table 1, Figure 1A**). Following multivariable analyses, adjusting for study arm, age, sex, BMI, HIV status, lung cavitation, alcohol use and smoking, we found that increased IP-10 expression was significantly associated with increased odds of early culture conversion [odds ratio (OR) 4.255, 95% CI 1.025 – 17.544,  $p=0.046$ ] (**Figure 1B, Supplementary Table 1**).

We next examined the association between cytokine expression at active TB and 8-week TB culture conversion among HIV-infected individuals while additionally adjusting for CD4 count, and viral load in a multivariable model (**Supplementary Table 2**). An increase in IP-10 expression during active TB was associated with increase in the odds of culture conversion by 8 weeks (OR 10.204, 95% CI 1.247 – 83.333,  $p=0.030$ ). The levels of IP-10 expression in all individuals and stratified by HIV status are shown in **Figure 1C**. While the sample size was too small to do a detailed analysis for the HIV-uninfected TB patients, IP-10 expression followed the same pattern across all subgroups irrespective of HIV status (**Figure 1C**). These results, in concordance with previously published data highlighting the importance of IP-10 in TB pathogenesis (12–17).

**TABLE 1 |** Demographic and clinical characteristics of study participants.

Variables	Cases n=31	Controls n=101	p-value
<b>Study Arm n (%)</b>			
HRZE -Control	18 (58)	45 (45)	.220
HRZM - Active	13 (42)	56 (55)	
<b>Age (y), median (IQR)</b>	34 (28 – 43)	36 (31 – 41)	.502
<b>Sex, n (%)</b>			
Male	25 (81)	70 (69)	.259
Female	6 (19)	31 (31)	
<b>Body mass index (kg/m<sup>2</sup>), median (IQR)</b>	19.28 (17.96 – 19.98)	20.42 (18.64 – 22.95)	<b>.031</b>
<b>HIV status n (%)</b>			
Negative	11 (35)	25 (25)	.256
Positive	20 (65)	76 (75)	
<b>CD4 cell count (cells/mm<sup>3</sup>), median (IQR)</b>	288 (214 – 410)	248 (127 – 413)	.311
<b>Viral load (copies/ml), median (IQR)</b>	3453 (20 – 18289)	5878 (20 – 111087)	.386
<b>ARV status* n (%)</b>			
Yes	10 (50)	31 (41)	.609
No	9 (45)	43 (57)	
<b>Lung Cavities n (%)</b>			
None	6 (19.3)	33 (32.7)	.317
One Lung	14 (45.2)	42 (41.6)	
Both Lungs	11 (35.5)	26 (25.7)	
<b>Days to first negative solid culture, median (IQR)<sup>#</sup></b>	84 (82 – 91)	42 (28 – 55)	<b>&lt;.0001</b>
<b>Alcohol Use in the past 3 months n (%)</b>			
Yes	13 (42)	24 (24)	.067
<b>Smoking in past 3months n (%)</b>			
Yes	15 (48)	29 (29)	.051
<b>Smear Grade n (%)</b>			
1+	6 (19.4)	21 (20.8)	.124
2+	2 (6.4)	22 (21.8)	
3+	23 (74.2)	58 (57.4)	

\*3 missing ARV status.

<sup>#</sup>Measures for all variables, except days to first negative culture are reported at baseline. Significant p-values (<0.05) are bolded.

## Effect of Plasma Cytokine/Chemokine Expression at Active TB on Overall Time to Culture Conversion

In order to further assess the impact of systemic inflammation during TB active disease on treatment response we used a Cox proportional hazards model to examine the association between cytokine expression during active TB and days to culture conversion (n=132). In the bivariable analysis, increased expression of IL-1RA (p=0.008) and MIP-1 $\beta$  (p=0.041) were significantly associated with shorter time to culture conversion (**Figure 2A**). In the multivariable analysis increased expression of MCP-3 [adjusted hazards ratio (aHR) 1.723, 95% CI 1.040 – 2.855, p=0.035] and of IL-6 (aHR 1.409, 95% CI 1.045 – 1.899,

p=0.024) during active TB were significantly associated with shorter time to culture conversion (**Figure 2B**, **Supplementary Figure 1** and **Supplementary Table 3**).

A sub-analysis of HIV-infected individuals was performed adjusting for the effects of viral load and CD4 count (**Supplementary Table 4**). In the bivariable and multivariable models, higher IL-1RA (aHR 2.595, 95% CI 1.136 – 5.926, p=0.024) and IL-1 $\alpha$  (aHR 2.008, 95% CI 1.053 – 3.831, p=0.035) expression were significantly associated with shorter time to culture conversion. IL-6 (aHR 1.783, 95% CI 1.128 – 2.820, p=0.013) and IP-10 (aHR 2.068, 95% CI 1.034 – 4.137, p=0.040) were significantly associated with shorter time to culture conversion in the multivariable model. Observed increase in inflammatory markers during active TB likely contribute to enhanced cellular responses and faster bacterial clearance.

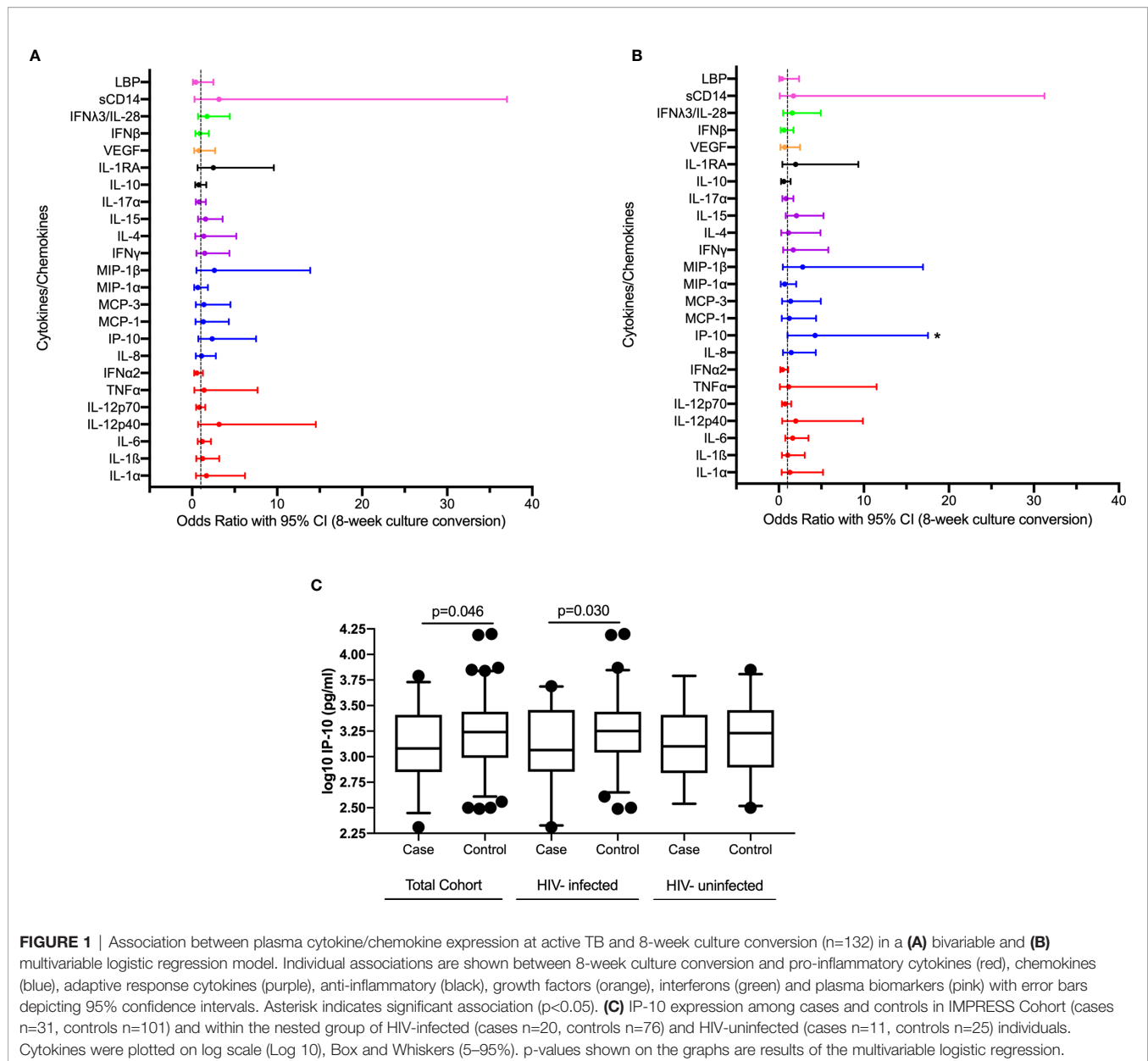
## Effect of Plasma Cytokines/Chemokines Expression at Active TB on Disease Severity

To determine the association between systemic levels of cytokines/chemokines and disease severity measured by the presence of lung cavitation, we compared circulating levels of cytokines/chemokines in all individuals with cavitory and non-cavitory disease using logistic regression. In the bivariable analysis, increased expression of IL-6 (p=0.04) was significantly associated with cavitory disease. IL-6 (OR 2.543, 95% CI 1.254 – 5.160, p=0.010) and IL-1RA (OR 4.639, 95% CI 1.203 – 21.031, p=0.047) positively associated with the odds of lung cavitation in the multivariable model (**Figures 3A, B**, **Supplementary Table 5**).

We performed a sub-analysis of the HIV-infected individuals and adjusted for viral load and CD4 count (**Supplementary Table 6**). Increased expression of IL-6 (OR 2.644, 95% CI 1.062 – 6.585, p=0.037) and IL-1RA (OR 7.795, 95% CI 1.177 – 51.611, p=0.033) were associated with increased odds of cavitation. IL-6 and IL-1RA expression among total cohort and stratified by HIV status in those with and without cavitory disease show similar patterns irrespective of HIV status (**Figure 3C**). These results highlight the dual nature of the host immune response with similar responses being associated with bacterial clearance as well as disease severity and tissue damage.

## Association Between Plasma Cytokine/Chemokine Expression and Bacterial Burden at Active TB

To determine the association between systemic levels of cytokines/chemokines and bacterial burden at active disease, we examined the differences in plasma cytokine/chemokine levels in patients with different smear grades (classified as 1+, 2+ and 3+). We observed no clear dose response with any of the measured cytokines/chemokines and smear grade (**Figure 4**). There was a trend towards higher IP-10 expression in Smear 2+, compared to the Smear 1+ group and trend for higher MIP-1 $\alpha$  in Smear 3+ compared to Smear 1+ group (**Figure 4A**). In HIV-infected patients IP-10 levels were higher in Smear 2+ when compared to Smear 1+ group (**Figure 4B**). In the HIV-uninfected group,

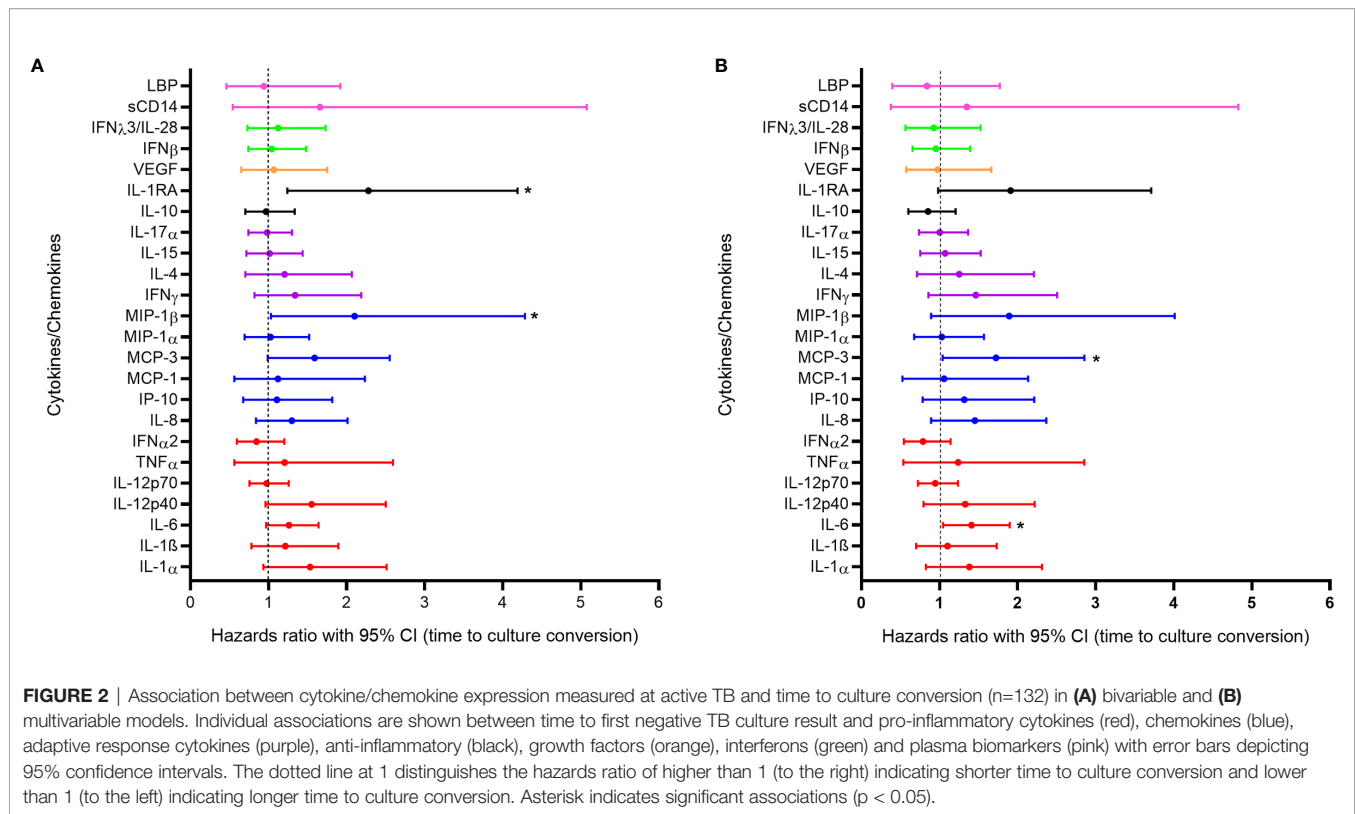


IL-10, IFN $\gamma$  and IL-1RA levels tended to be higher in Smear 3+ compared to Smear 2+ group (Figure 4C). Our data indicated that measured systemic plasma cytokines/chemokines are not reliable indicators of the bacterial load as measured by the smear grades.

## DISCUSSION

Identification and characterisation of host biomarkers of TB disease severity and treatment response are important tools in progress towards TB elimination and control (18). Here we characterised the role of several plasma cytokines/chemokines, measured during active TB, on early and delayed culture conversion and disease severity in HIV-infected and -uninfected individuals.

Increased IP-10 levels during active TB were associated with early bacterial clearance after 2 months of intensive TB therapy in the total cohort as well as HIV-infected subgroup after adjusting for covariates. IP-10 (also known as CXCL10) is a chemokine that induces chemotaxis, apoptosis, cell growth inhibition and angiostasis (19). A number of published studies have highlighted the role of IP-10 in TB pathogenesis and the potential of using IP-10 as a biomarker of treatment response in TB patients (12–17). Additionally, IP-10 was shown to contribute to the inhibition of mycobacterial replication in the *ex vivo* model of human whole blood assay (20). Due to its stability and high expression, IP-10 has demonstrated potential to be developed into a simple point-of-care (POC) test (21–23). Our data supports these observations and highlights the role of



IP-10 in TB clearance among HIV-infected and -uninfected patients with recurrent TB.

After adjusting for covariates, IL-6 and MCP-3 were significantly associated with shorter time to culture conversion in the total cohort. Chemokines, such as MCP-3 play an important role in host response to MTB, with MTB-exposed macrophages showing highly increased MCP-3 expression (24). Furthermore, a strain of BCG that secretes high levels of functional MCP-3 displayed improved immunogenicity and enhanced antigen-specific T cell responses (25). Similar to IP-10, increased MCP-3 levels during active TB likely contribute to enhanced cellular responses and faster bacterial clearance. In addition to its previously identified role as a biomarker of active pulmonary TB (26–28), we found that increased IL-6 expression at active disease is significantly associated with faster bacterial clearance. IL-6, a pleiotropic proinflammatory cytokine, plays an important role in generation of T and B cell responses. Importantly, IL-6 is known to play an important role in protective host immune responses to TB (29, 30) and is essential for generating Th1 cellular responses considered central for MTB control (31). In addition to IL-6 and IP-10, IL-1RA and IL-1 $\alpha$  demonstrated an association with shorter time to culture conversion in HIV-infected individuals. IL-1 $\alpha$  is an important immunoregulatory cytokine that depending on the magnitude of stress or damage caused by the infection can initiate an inflammatory response or reparative fibrosis (32). IL-1RA is a member of IL-1 family that binds to the IL-1 receptor but does not induce a response (33); its expression is upregulated

by inflammatory cytokines including IL-1 $\alpha$  and IL-6 as an anti-inflammatory control mechanism (34, 35). IL-1 and IL-1R were shown to be critical for host resistance to MTB (36, 37), while IL-1RA was shown to be a marker of TB disease activity (38, 39). While some of the markers seem to be affected by HIV infection, IL-6 levels are correlated with overall shorter time to culture conversion in both patient groups. Overall, our data shows that the magnitude and nature of inflammatory cytokine expression during active TB disease can be indicative of more efficient cellular response and host's ability to clear the infection.

Pulmonary cavitation, a hallmark of pulmonary TB, is associated with high bacterial burden and subsequent increase in inflammatory response. Additionally, the host immune response is thought to drive the development of TB cavities (40). Our results indicate that increased plasma IL-6 and IL-1RA levels are associated with cavitory disease in both HIV-infected and uninfected TB patients. Elevated concentrations of both IL-6 (41) and IL-1RA in bronchoalveolar lavage (BAL) fluid were previously found to be associated with tissue necrosis and resulting cavity formation in patients with active pulmonary TB (42). Associations of IL-6 and IL-1RA with bacterial clearance and disease severity (measured by lung cavitation) highlight the dual nature of the host immune response to infections; while immune activation is required for successful pathogen clearance and initiation of protective cellular responses it can also contribute to immune mediated lung pathology and worsened disease outcome.

We observed no clear dose response between, measured plasma cytokines/chemokines and bacterial burden as



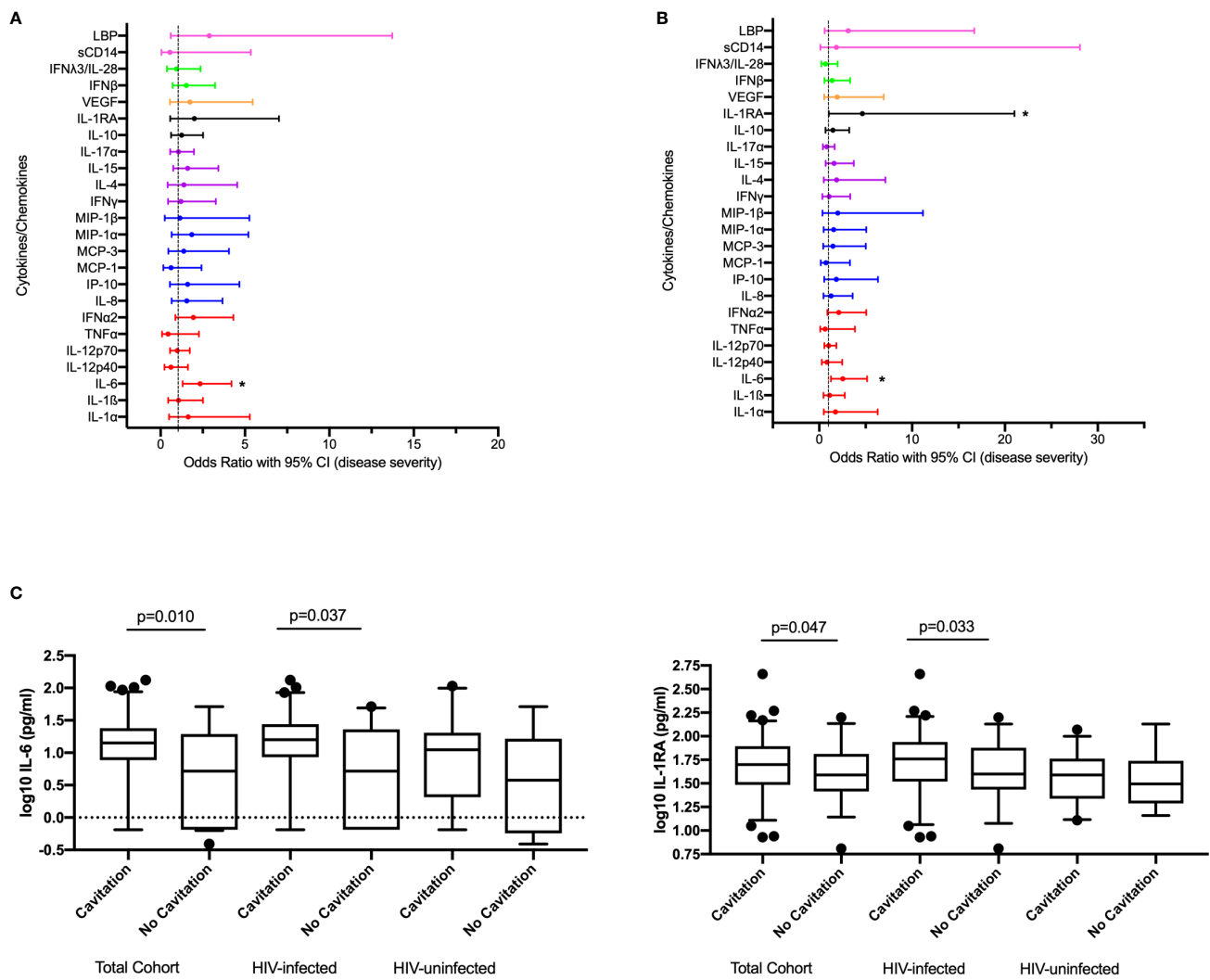


**FIGURE 3** | Association between cytokine/chemokine expression measured at active TB and disease severity measured by lung cavitation ( $n=132$ ) in both (A) univariable and (B) multivariable model. Individual associations are shown between 8-week culture conversion and pro-inflammatory cytokines (red), chemokines (blue), adaptive response cytokines (purple), anti-inflammatory (black), growth factors (orange), interferons (green) and plasma biomarkers (pink) with error bars depicting 95% confidence intervals. The dotted line at 1 is the interpretation of odds ratio. Asterisk in (A, B) indicates significant associations ( $p < 0.05$ ). (C) IL-6 and IL-1RA plasma levels associated with cavitory versus non-cavitory disease in total cohort (Cavitation  $n=93$ , no cavitation  $n=39$ ), HIV-infected participants (Cavitation  $n=63$ , no cavitation  $n=33$ ) and HIV-uninfected individuals (Cavitation  $n=30$ , no cavitation  $n=6$ ). Cytokines were plotted on log scale (Log 10), Box and Whiskers (5–95%). p-values shown on the graph (C) are the results of the multivariable logistic regression.

measured by smear grades. Sputum acid fast bacilli provides an indication of bacillary load and is most often used to monitor TB patients in resource limited settings; however, this method does not distinguish live and dead organisms, has low sensitivity and the specificity predicting treatment failure or relapse is modest (2, 43, 44).

Our study has several limitations, including a relatively small sample size and a clinically complex cohort of patients requiring correction for a wide range of covariates. Future studies should examine cellular phenotypes in order to link the observed inflammatory responses with protective cellular responses to MTB. Our study was focused on drug susceptible TB and

future research should also assess immune biomarkers in drug-resistant TB as host immune responses are known to vary between different MTB isolates (45–49). Our study additionally demonstrates that the identified inflammatory markers of disease have low predicative power when considered on their own, with AUC values ranging from 0.56 – 0.65 (Supplementary Figure 2). The associations we observed were stronger in the multivariable models highlighting the important effect of other behavioural and clinical variables on the expression of immune markers and their potential confounding effects on TB outcome (50–55).

In summary, our study confirms the importance of inflammatory markers, including IP-10 and IL-6, in TB disease

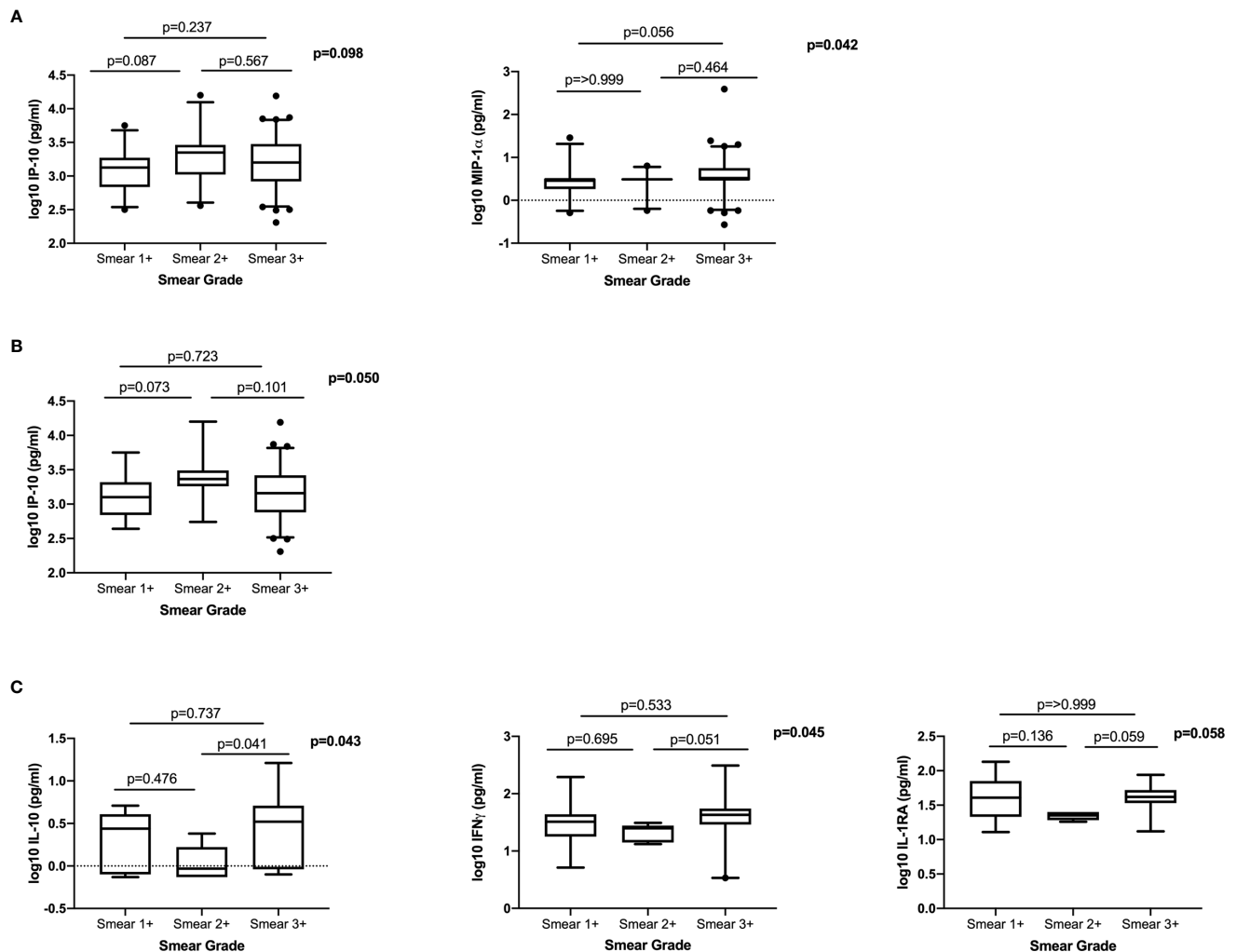


**FIGURE 4 |** The relationship between plasma cytokines/chemokines and bacterial burden measured by smear grades: **(A)** Total cohort; (Smear 1+ n= 27, Smear 2+ n=24, Smear 3+ n=81), **(B)** HIV-infected (Smear 1+ n=16, Smear 2+ n=18, Smear 3+ n=62) and **(C)** HIV-uninfected (Smear 1+ n=11, Smear 2+ n=6, Smear 3+ n=19). Only cytokines that were significantly different or trending towards significance are shown. Based on distribution IP-10 was analysed using a one-way ANOVA with Tukey's multiple comparisons test and MIP-1α, IFNγ, IL-10 and IL-1RA were analysed using non-parametric Kruskal Wallis test with Dunn's multiple comparisons test. Cytokines were plotted on log scale (Log 10), Box and Whiskers (5–95%).

pathogenesis. Further studies are needed to confirm the utility of identified inflammatory markers in TB management. The development and progression of TB disease are influenced by combined effects of various immune as well as behavioural and clinical variables that will have to be considered when utilising immune biomarkers as predictors of risk or protection.

## DATA AVAILABILITY STATEMENT

The original contributions presented in the study are included in the article/**Supplementary Material**. Further inquiries can be directed to the corresponding author.

## ETHICS STATEMENT

The studies involving human participants were reviewed and approved by Biomedical Research Ethics Committee, University of KwaZulu-Natal. The patients/participants provided their written informed consent to participate in this study.

## AUTHOR CONTRIBUTIONS

AS, KN, and SR conceptualized and designed the study. SR and AS performed the experiments. SR, AS, LL, and KN analyzed the data. SN, AS, and KN wrote the manuscript. AS, KN, NS, RH-M, DG, TS, and NP supervised clinical and/or experimental aspects

of the study. All authors contributed to the article and approved the submitted version.

## FUNDING

Research reported in this publication was supported by the Strategic Health Innovation Partnerships (SHIP) Unit of the South African Medical Research Council with funds received from the South African Department of Science and Technology and by the European and Developing Countries Clinical Trials Partnership (EDCTP) (TA.2011.40200.044). SR was supported by the National Research Foundation (Grant Number: 108038). Any opinion, finding, and conclusion or recommendations expressed in this material is that of the author and the NRF does not accept liability in this regard. AS is supported by

EDCTP Career Development Fellowship (TMA2016CDF-1582) and NP is supported by EDCTP Senior Fellowship (TMA2018SF-2467).

## ACKNOWLEDGMENTS

The authors would like to thank all of research participants and the staff at CAPRISA for their dedication to these studies.

## SUPPLEMENTARY MATERIAL

The Supplementary Material for this article can be found online at: <https://www.frontiersin.org/articles/10.3389/fimmu.2021.641065/full#supplementary-material>

## REFERENCES

1. WHO Publication. *Global Tuberculosis Report 2020* (2020). Available at: [https://www.who.int/tb/publications/global\\_report/en/](https://www.who.int/tb/publications/global_report/en/) (Accessed October 26, 2020).
2. Horne DJ, Royce SE, Gooze L, Narita M, Hopewell PC, Nahid P, et al. Sputum monitoring during tuberculosis treatment for predicting outcome: systematic review and meta-analysis. *Lancet Infect Dis* (2010) 10(6):387–94. doi: 10.1016/S1473-3099(10)70071-2
3. Jo EK, Park JK, Dockrell HM. Dynamics of cytokine generation in patients with active pulmonary tuberculosis. *Curr Opin Infect Dis* (2003) 16(3):205–10. doi: 10.1097/00001432-200306000-00004
4. Mihret A, Bekele Y, Bobosha K, Kidd M, Aseffa A, Howe R, et al. Plasma cytokines and chemokines differentiate between active disease and non-active tuberculosis infection. *J Infect* (2013) 66(4):357–65. doi: 10.1016/j.jinf.2012.11.005
5. Kumar NP, Moideen K, Banurekha VV, Nair D, Babu S. Plasma Proinflammatory Cytokines Are Markers of Disease Severity and Bacterial Burden in Pulmonary Tuberculosis. *Open Forum Infect Dis* (2019) 6(7):ofz257. doi: 10.1093/ofid/ofz257
6. Kumar NP, Moideen K, Nancy A, Viswanathan V, Shruthi BS, Sivakumar S, et al. Plasma chemokines are biomarkers of disease severity, higher bacterial burden and delayed sputum culture conversion in pulmonary tuberculosis. *Sci Rep* (2019) 9(1):18217. doi: 10.1038/s41598-019-54803-w
7. Sivro A, McKinnon LR, Yende-Zuma N, Gengiah S, Samsunder N, Abdool Karim SS, et al. Plasma Cytokine Predictors of Tuberculosis Recurrence in Antiretroviral-Treated Human Immunodeficiency Virus-infected Individuals from Durban, South Africa. *Clin Infect Dis* (2017) 65(5):819–26. doi: 10.1093/cid/cix357
8. Skogmar S, Schon T, Balcha TT, Sturegard E, Jansson M, Bjorkman P. Plasma Levels of Neopterin and C-Reactive Protein (CRP) in Tuberculosis (TB) with and without HIV Coinfection in Relation to CD4 Cell Count. *PLoS One* (2015) 10(12):e0144292. doi: 10.1371/journal.pone.0144292
9. Wyndham-Thomas C, Corbiere V, Selis E, Payen MC, Goffard JC, Van Vooren JP, et al. Immune Activation by Mycobacterium tuberculosis in HIV-Infected and -Uninfected Subjects. *J Acquir Immune Defic Syndr* (2017) 74(1):103–11. doi: 10.1097/QAI.0000000000001157
10. Perumal R, Padayatchi N, Yende-Zuma N, Naidoo A, Govender D, Naidoo K. A Moxifloxacin-based Regimen for the Treatment of Recurrent, Drug-sensitive Pulmonary Tuberculosis: An Open-label, Randomized, Controlled Trial. *Clin Infect Dis* (2020) 70(1):90–8. doi: 10.1093/cid/ciz152
11. Rieder HL, Van Deun A, Kam KM, Kim SJ, Chonde TM, Trébucq A, et al. *Table II.3. Grading scales for bright field (Ziehl-Neelsen) and fluorescence microscopy, Priorities for Tuberculosis Bacteriology Services in Low-income countries. 2nd. International Union Against Tuberculosis and Lung Disease* (2007).
12. Cannas A, Calvo L, Chiacchio T, Cuzzi G, Vanini V, Lauria FN, et al. IP-10 detection in urine is associated with lung diseases. *BMC Infect Dis* (2010) 10:333. doi: 10.1186/1471-2334-10-333
13. Azzurri A, Sow OY, Amedei A, Bah B, Diallo S, Peri G, et al. IFN-gamma-inducible protein 10 and pentraxin 3 plasma levels are tools for monitoring inflammation and disease activity in Mycobacterium tuberculosis infection. *Microbes Infect* (2005) 7(1):1–8. doi: 10.1016/j.micinf.2004.09.004
14. Su WL, Perng WC, Huang CH, Yang CY, Wu CP, Chen JH. Association of reduced tumor necrosis factor alpha, gamma interferon, and interleukin-1beta (IL-1beta) but increased IL-10 expression with improved chest radiography in patients with pulmonary tuberculosis. *Clin Vaccine Immunol* (2010) 17(2):223–31. doi: 10.1128/CVI.00381-09
15. Riou C, Perez Peixoto B, Roberts L, Ronacher K, Walzl G, Manca C, et al. Effect of standard tuberculosis treatment on plasma cytokine levels in patients with active pulmonary tuberculosis. *PLoS One* (2012) 7(5):e36886. doi: 10.1371/journal.pone.0036886
16. Petrone L, Bondet V, Vanini V, Cuzzi G, Palmieri F, Palucci I, et al. First description of agonist and antagonist IP-10 in urine of patients with active TB. *Int J Infect Dis* (2019) 78:15–21. doi: 10.1016/j.ijid.2018.09.001
17. Blauenfeldt T, Petrone L, Del Nonno F, Baiocchi A, Falasca L, Chiacchio T, et al. Interplay of DDP4 and IP-10 as a Potential Mechanism for Cell Recruitment to Tuberculosis Lesions. *Front Immunol* (2018) 9:1456. doi: 10.3389/fimmu.2018.01456
18. Walzl G, Ronacher K, Hanekom W, Scriba TJ, Zumla A. Immunological biomarkers of tuberculosis. *Nat Rev Immunol* (2011) 11(5):343–54. doi: 10.1038/nri2960
19. Liu M, Guo S, Hibbert JM, Jain V, Singh N, Wilson NO, et al. CXCL10/IP-10 in infectious diseases pathogenesis and potential therapeutic implications. *Cytokine Growth Factor Rev* (2011) 22(3):121–30. doi: 10.1016/j.cytogfr.2011.06.001
20. Palucci I, Battah B, Salustri A, De Maio F, Petrone L, Ciccocanti F, et al. IP-10 contributes to the inhibition of mycobacterial growth in an ex vivo whole blood assay. *Int J Med Microbiol* (2019) 309(5):299–306. doi: 10.1016/j.ijmm.2019.05.005
21. Sutherland JS, Mendy J, Gindeh A, Walzl G, Togun T, Owolabi O, et al. Use of lateral flow assays to determine IP-10 and CCL4 levels in pleural effusions and whole blood for TB diagnosis. *Tuberc (Edinb)* (2016) 96:31–6. doi: 10.1016/j.tube.2015.10.011
22. Hoel IM, Jorstad MD, Marijani M, Ruhwald M, Mustafa T, Dyrhol-Riise AM. IP-10 dried blood spots assay monitoring treatment efficacy in extrapulmonary tuberculosis in a low-resource setting. *Sci Rep* (2019) 9(1):3871. doi: 10.1038/s41598-019-40458-0
23. Tonby K, Ruhwald M, Kvale D, Dyrhol-Riise AM. IP-10 measured by Dry Plasma Spots as biomarker for therapy responses in Mycobacterium Tuberculosis infection. *Sci Rep* (2015) 5:9223. doi: 10.1038/srep09223
24. Vouret-Craviari V, Cenizales S, Poli G, Mantovani A. Expression of monocyte chemotactic protein-3 in human monocytes exposed to the

- mycobacterial cell wall component lipoarabinomannan. *Cytokine* (1997) 9 (12):992–8. doi: 10.1006/cyto.1997.0242
25. Ryan AA, Spratt JM, Britton WJ, Triccas JA. Secretion of functional monocyte chemotactic protein 3 by recombinant *Mycobacterium bovis* BCG attenuates vaccine virulence and maintains protective efficacy against *M. Tuberc Infect Infect Immun* (2007) 75(1):523–6. doi: 10.1128/IAI00897-06
  26. Anbarasu D, Raja CP, Raja A. Multiplex analysis of cytokines/chemokines as biomarkers that differentiate healthy contacts from tuberculosis patients in high endemic settings. *Cytokine* (2013) 61(3):747–54. doi: 10.1016/j.cyt.2012.12.031
  27. Phalane KG, Kriel M, Loxton AG, Menezes A, Stanley K, van der Spuy GD, et al. Differential expression of host biomarkers in saliva and serum samples from individuals with suspected pulmonary tuberculosis. *Mediators Inflammation* (2013) 2013:981984. doi: 10.1155/2013/981984
  28. Zambuzi FA, Cardoso-Silva PM, Espindola MS, Soares LS, Galvao-Lima LJ, Brauer VS, et al. Identification of promising plasma immune biomarkers to differentiate active pulmonary tuberculosis. *Cytokine* (2016) 88:99–107. doi: 10.1016/j.cyt.2016.08.030
  29. Martinez AN, Mehra S, Kaushal D. Role of interleukin 6 in innate immunity to *Mycobacterium tuberculosis* infection. *J Infect Dis* (2013) 207(8):1253–61. doi: 10.1093/infdis/jit037
  30. Ladel CH, Blum C, Dreher A, Reifenberg K, Kopf M, Kaufmann SH. Lethal tuberculosis in interleukin-6-deficient mutant mice. *Infect Immun* (1997) 65 (11):4843–9. doi: 10.1128/IAI.65.11.4843-4849.1997
  31. Leal IS, Smedegard B, Andersen P, Appelberg R. Interleukin-6 and interleukin-12 participate in induction of a type 1 protective T-cell response during vaccination with a tuberculosis subunit vaccine. *Infect Immun* (1999) 67(11):5747–54. doi: 10.1128/IAI.67.11.5747-5754.1999
  32. Di Paolo NC, Shayakhmetov DM. Interleukin 1 $\alpha$  and the inflammatory process. *Nat Immunol* (2016) 17(8):906–13. doi: 10.1038/ni.3503
  33. Arend WP, Malyak M, Guthridge CJ, Gabay C. Interleukin-1 receptor antagonist: role in biology. *Annu Rev Immunol* (1998) 16:27–55. doi: 10.1146/annurev.immunol.16.1.27
  34. Tilg H, Trehu E, Atkins MB, Dinarello CA, Mier JW. Interleukin-6 (IL-6) as an anti-inflammatory cytokine: induction of circulating IL-1 receptor antagonist and soluble tumor necrosis factor receptor p55. *Blood* (1994) 83 (1):113–8. doi: 10.1182/blood.V83.1.113.bloodjournal831113
  35. Bargetzi MJ, Lantz M, Smith CG, Torti FM, Olsson I, Eisenberg SP, et al. Interleukin-1 beta induces interleukin-1 receptor antagonist and tumor necrosis factor binding protein in humans. *Cancer Res* (1993) 53(17):4010–3.
  36. Mayer-Barber KD, Andrade BB, Barber DL, Hieny S, Feng CG, Caspar P, et al. Innate and adaptive interferons suppress IL-1 $\alpha$  and IL-1 $\beta$  production by distinct pulmonary myeloid subsets during *Mycobacterium tuberculosis* infection. *Immunity* (2011) 35(6):1023–34. doi: 10.1016/j.immuni.2011.12.002
  37. Guler R, Parihar SP, Spohn G, Johansen P, Brombacher F, Bachmann MF. Blocking IL-1 $\alpha$  but not IL-1 $\beta$  increases susceptibility to chronic *Mycobacterium tuberculosis* infection in mice. *Vaccine* (2011) 29(6):1339–46. doi: 10.1016/j.vaccine.2010.10.045
  38. Juffermans NP, Verbon A, van Deventer SJ, van Deutekom H, Speelman P, van der Poll T. Tumor necrosis factor and interleukin-1 inhibitors as markers of disease activity of tuberculosis. *Am J Respir Crit Care Med* (1998) 157(4 Pt 1):1328–31. doi: 10.1164/ajrccm.157.4.9709126
  39. Ji DX, Yamashiro LH, Chen KJ, Mukaida N, Kramnik I, Darwin KH, et al. Type I interferon-driven susceptibility to *Mycobacterium tuberculosis* is mediated by IL-1 $\alpha$ . *Nat Microbiol* (2019) 4(12):2128–35. doi: 10.1038/s41564-019-0578-3
  40. Ong CW, Elkington PT, Friedland JS. Tuberculosis, pulmonary cavitation, and matrix metalloproteinases. *Am J Respir Crit Care Med* (2014) 190(1):9–18. doi: 10.1164/rccm.201311-2106PP
  41. Casarini M, Ameglio F, Alemanno L, Zangrilli P, Mattia P, Paone G, et al. Cytokine levels correlate with a radiologic score in active pulmonary tuberculosis. *Am J Respir Crit Care Med* (1999) 159(1):143–8. doi: 10.1164/ajrccm.159.1.9803066
  42. Tsao TC, Hong J, Li LF, Hsieh MJ, Liao SK, Chang KS. Imbalances between tumor necrosis factor- $\alpha$  and its soluble receptor forms, and interleukin-1 $\beta$  and interleukin-1 receptor antagonist in BAL fluid of cavitary pulmonary tuberculosis. *Chest* (2000) 117(1):103–9. doi: 10.1378/chest.117.1.103
  43. Hamid Salim A, Aung KJ, Hossain MA, Van Deun A. Early and rapid microscopy-based diagnosis of true treatment failure and MDR-TB. *Int J Tuberc Lung Dis* (2006) 10(11):1248–54.
  44. Datta S, Sherman JM, Bravard MA, Valencia T, Gilman RH, Evans CA. Clinical evaluation of tuberculosis viability microscopy for assessing treatment response. *Clin Infect Dis* (2015) 60(8):1186–95. doi: 10.1093/cid/ciu1153
  45. Manca C, Tsenova L, Barry CE, Bergtold A, Freeman S, Haslett PA, et al. *Mycobacterium tuberculosis* CDC1551 induces a more vigorous host response in vivo and in vitro, but is not more virulent than other clinical isolates. *J Immunol* (1999) 162(11):6740–6.
  46. Tsenova L, Ellison E, Harbacheuski R, Moreira AL, Kurepina N, Reed MB, et al. Virulence of selected *Mycobacterium tuberculosis* clinical isolates in the rabbit model of meningitis is dependent on phenolic glycolipid produced by the bacilli. *J Infect Dis* (2005) 192(1):98–106. doi: 10.1086/430614
  47. Manca C, Tsenova L, Bergtold A, Freeman S, Tovey M, Musser JM, et al. Virulence of a *Mycobacterium tuberculosis* clinical isolate in mice is determined by failure to induce Th1 type immunity and is associated with induction of IFN- $\alpha$ / $\beta$ . *Proc Natl Acad Sci U.S.A.* (2001) 98(10):5752–7. doi: 10.1073/pnas.091096998
  48. Manca C, Tsenova L, Freeman S, Barczak AK, Tovey M, Murray PJ, et al. Hypervirulent *M. tuberculosis* W/Beijing strains upregulate type I IFNs and increase expression of negative regulators of the Jak-Stat pathway. *J Interferon Cytokine Res* (2005) 25(11):694–701. doi: 10.1089/jir.2005.25.694
  49. Geffner L, Yokobori N, Basile J, Schierloh P, Balboa L, Romero MM, et al. Patients with multidrug-resistant tuberculosis display impaired Th1 responses and enhanced regulatory T-cell levels in response to an outbreak of multidrug-resistant *Mycobacterium tuberculosis* M and Ra strains. *Infect Immun* (2009) 77(11):5025–34. doi: 10.1128/IAI.00224-09
  50. Stapleton RD, Dixon AE, Parsons PE, Ware LB, Suratt BTNetwork NARDS. The association between BMI and plasma cytokine levels in patients with acute lung injury. *Chest* (2010) 138(3):568–77. doi: 10.1378/chest.10-0014
  51. Wang T, He C. Pro-inflammatory cytokines: The link between obesity and osteoarthritis. *Cytokine Growth Factor Rev* (2018) 44:38–50. doi: 10.1016/j.cytogr.2018.10.002
  52. Crews FT, Bechara R, Brown LA, Guidot DM, Mandrekar P, Oak S, et al. Cytokines and alcohol. *Alcohol Clin Exp Res* (2006) 30(4):720–30. doi: 10.1111/j.1530-0277.2006.00084.x
  53. Chen H, Cowan MJ, Hasday JD, Vogel SN, Medvedev AE. Tobacco smoking inhibits expression of proinflammatory cytokines and activation of IL-1R-associated kinase, p38, and NF- $\kappa$ B in alveolar macrophages stimulated with TLR2 and TLR4 agonists. *J Immunol* (2007) 179(9):6097–106. doi: 10.4049/jimmunol.179.9.6097
  54. Klein SL, Flanagan KL. Sex differences in immune responses. *Nat Rev Immunol* (2016) 16(10):626–38. doi: 10.1038/nri.2016.90
  55. Yu T, Li J, Ma S. Adjusting confounders in ranking biomarkers: a model-based ROC approach. *Brief Bioinform* (2012) 13(5):513–23. doi: 10.1093/bib/bbs008

**Conflict of Interest:** The authors declare that the research was conducted in the absence of any commercial or financial relationships that could be construed as a potential conflict of interest.

The handling editor declared a past co-authorship with one of the authors TS.

Copyright © 2021 Rambaran, Naidoo, Lewis, Hassan-Moosa, Govender, Samsunder, Scriba, Padayatchi and Sivro. This is an open-access article distributed under the terms of the Creative Commons Attribution License (CC BY). The use, distribution or reproduction in other forums is permitted, provided the original author(s) and the copyright owner(s) are credited and that the original publication in this journal is cited, in accordance with accepted academic practice. No use, distribution or reproduction is permitted which does not comply with these terms.





# Lymphocyte Non-Specific Function Detection Facilitating the Stratification of *Mycobacterium tuberculosis* Infection

## OPEN ACCESS

Ying Luo<sup>1</sup>, Ying Xue<sup>2</sup>, Yimin Cai<sup>3</sup>, Qun Lin<sup>1</sup>, Guoxing Tang<sup>1</sup>, Huijuan Song<sup>1</sup>, Wei Liu<sup>1</sup>, Liyan Mao<sup>1</sup>, Xu Yuan<sup>1</sup>, Yu Zhou<sup>4</sup>, Weiyong Liu<sup>1\*</sup>, Shiji Wu<sup>1\*</sup>, Ziyong Sun<sup>1\*</sup> and Feng Wang<sup>1\*</sup>

### Edited by:

Christof Geldmacher,  
University of Munich, Germany

### Reviewed by:

Carmen Judith Serrano,  
Mexican Social Security Institute  
(IMSS), Mexico  
Virginie ROZOT,  
South African Tuberculosis Vaccine  
Initiative SATVI, South Africa  
Catherine Riou,  
University of Cape Town, South Africa

### \*Correspondence:

Weiyong Liu  
weiyongliu@gmail.com  
Shiji Wu  
wilson547@163.com  
Ziyong Sun  
zysun@tjh.tjmu.edu.cn  
Feng Wang  
fengwang@tjh.tjmu.edu.cn

### Specialty section:

This article was submitted to  
Microbial Immunology,  
a section of the journal  
Frontiers in Immunology

**Received:** 14 December 2020

**Accepted:** 23 March 2021

**Published:** 19 April 2021

### Citation:

Luo Y, Xue Y, Cai Y, Lin Q, Tang G, Song H, Liu W, Mao L, Yuan X, Zhou Y, Liu W, Wu S, Sun Z and Wang F (2021) Lymphocyte Non-Specific Function Detection Facilitating the Stratification of *Mycobacterium tuberculosis* Infection. *Front. Immunol.* 12:641378. doi: 10.3389/fimmu.2021.641378

<sup>1</sup> Department of Laboratory Medicine, Tongji Hospital, Tongji Medical College, Huazhong University of Science and Technology, Wuhan, China, <sup>2</sup> Department of Immunology, School of Basic Medicine, Tongji Medical College, Huazhong University of Science and Technology, Wuhan, China, <sup>3</sup> Department of Epidemiology and Biostatistics, Key Laboratory of Environmental Health of Ministry of Education, School of Public Health, Tongji Medical College, Huazhong University of Science and Technology, Wuhan, China, <sup>4</sup> Department of Laboratory Medicine, Zhejiang Provincial People's Hospital, People's Hospital of Hangzhou Medical College, Hangzhou, China

**Background:** Inadequate tuberculosis (TB) diagnostics, especially for discrimination between active TB (ATB) and latent TB infection (LTBI), are major hurdle in the reduction of the disease burden. The present study aims to investigate the role of lymphocyte non-specific function detection for TB diagnosis in clinical practice.

**Methods:** A total of 208 participants including 49 ATB patients, 64 LTBI individuals, and 95 healthy controls were recruited at Tongji hospital from January 2019 to October 2020. All subjects were tested with lymphocyte non-specific function detection and T-SPOT assay.

**Results:** Significantly positive correlation existed between lymphocyte non-specific function and phytohemagglutinin (PHA) spot number. CD4<sup>+</sup> T cell non-specific function showed the potential for differentiating patients with negative T-SPOT results from those with positive T-SPOT results with an area under the curve (AUC) of 0.732 (95% CI, 0.572–0.893). The non-specific function of CD4<sup>+</sup> T cells, CD8<sup>+</sup> T cells, and NK cells was found significantly lower in ATB patients than in LTBI individuals. The AUCs presented by CD4<sup>+</sup> T cell non-specific function, CD8<sup>+</sup> T cell non-specific function, and NK cell non-specific function for discriminating ATB patients from LTBI individuals were 0.845 (95% CI, 0.767–0.925), 0.770 (95% CI, 0.683–0.857), and 0.691 (95% CI, 0.593–0.789), respectively. Application of multivariable logistic regression resulted in the combination of CD4<sup>+</sup> T cell non-specific function, NK cell non-specific function, and culture filtrate protein-10 (CFP-10) spot number as the optimally diagnostic model for differentiating ATB from LTBI. The AUC of the model in distinguishing between ATB and LTBI was 0.939 (95% CI, 0.898–0.981). The sensitivity and specificity were 83.67% (95% CI, 70.96%–91.49%) and 90.63% (95% CI, 81.02%–95.63%) with the threshold as 0.57. Our established model

showed superior performance to TB-specific antigen (TBAg)/PHA ratio in stratifying TB infection status.

**Conclusions:** Lymphocyte non-specific function detection offers an attractive alternative to facilitate TB diagnosis. The three-index diagnostic model was proved to be a potent tool for the identification of different events involved in TB infection, which is helpful for the treatment and management of patients.

**Keywords:** tuberculosis, active tuberculosis, latent tuberculosis infection, diagnosis, model, lymphocyte non-specific function

## INTRODUCTION

Tuberculosis (TB) is a major public issue caused by *Mycobacterium tuberculosis* (MTB) infection, with around 10 million cases and 1.4 million deaths in 2019 reported by World Health Organization (1). It is estimated that one-quarter population were during latent TB infection (LTBI) and 5-10% of these individuals would progress to active TB (ATB) during their life (2, 3). The stratification of TB infection is required for proposed TB control strategies that focus on timely treatment to reduce risk for disease progression in order to diminish MTB transmission (4). However, the current challenge still includes the lack of effective approach for discrimination between ATB and other status including LTBI. Novel and accurate diagnostic tests to identify active cases are urgently needed.

The diagnosis of ATB could be achieved by visualization of acid-fast bacilli by microscopy, mycobacterial culture, or molecular tests including GeneXpert MTB/RIF. Nevertheless, each approach has additional limitations, such as the poor sensitivity of microscopy, time-consuming of culture, the high cost of molecular tests (5). Even in the era of the GeneXpert MTB/RIF Ultra, challenge remains due to unsatisfactory sensitivity for clinical requirement (6, 7), which highlights the fact that better diagnostics might have to be achieved based on host factors rather than pathogen detection. However, the current use of blood-based available immunological tests including T-SPOT.TB (T-SPOT) and QuantiFERON-TB Gold In-Tube (QFT-GIT) was limited by their poor ability to reliably stratify ATB from LTBI especially in TB endemic areas (8, 9). Recent advances have been developed in blood signatures including transcriptome (10), proteome (11), genome (12), metabolome (13), cytokines (14, 15), and markers on immune cells (16, 17) for identifying ATB, raising hopes for translation into available assays. However, due to the fact that the application of these emerging methods has not been verified with sufficient repetition and large sample size, the real diagnostic utility under actual clinical conditions remains unclear (18). Besides, some tests require complicated procedures or expensive equipment to carry out, which limits their potential use in many resource-poor settings (19). Therefore, successful application of these test faces many challenges in the pathway from discovery to final use.

Some studies have shown that poor immune status was one characteristic of ATB patients, suggesting that the evaluation of host immunity could be applied as a potential direction for TB diagnosis and monitoring (13, 20–22). Unfortunately, difficulties

existed in host immunity evaluation of ATB patients due to the limitations of current tests such as lymphocyte subset analysis and the measurement of serum protein (23). These available methods could not fully reflect the immune status of host. Our team have previously developed lymphocyte non-specific function detection—a novel approach for evaluating host immunity based on phorbol-12-myristate-13-acetate (PMA)/ionomycin stimulation. And we have confirmed the performance of this method for host immunity evaluation in a variety of diseases including infection and autoimmune diseases (24, 25). Thus, it is worth considering whether lymphocyte non-specific function detection could be applied to diagnose TB. On the other hand, TB-specific antigen (TBAg)/phytohemagglutinin (PHA) ratio has been proposed as a potential diagnostic candidate for ATB by Wang and his colleague in recent years (26, 27). This simple calculation made it possible for T-SPOT to distinguish between ATB and LTBI by dividing the spot number of TBAg well by that of PHA well (28). However, the spot number of PHA well might be inaccurate in case of high value (29). Although our previous study showed that reducing the number of cells added to the PHA well could improve the accuracy of the results, this improvement requires an additional operation and might not be suitable for clinical application (30). Besides, TBAg/PHA ratio was helpless in identifying ATB with negative T-SPOT results due to its computational limitations. Several studies have demonstrated that the combination of multiple indicators could promote ATB diagnosis (31, 32). Accordingly, we speculate that the use of the combination of lymphocyte non-specific function (non-specific marker) and T-SPOT (TB-specific marker) has the potential to improve rapid differential diagnosis between ATB and LTBI. Consequently, we investigated the potential value of lymphocyte non-specific function detection and its combination with T-SPOT for determining MTB infection status by enrolling subjects with ATB and LTBI. We demonstrated the advantages of utilizing lymphocyte non-specific function detection for the analysis of patients with MTB infection.

## METHODS

### Study Design

Adult participants aged 18 years or older were enrolled for performing T-SPOT assay and lymphocyte non-specific function detection at Tongji hospital from January 2019 to

October 2020. Patients with ATB, individuals with LTBI, and healthy controls (HC) were identified and recruited based on laboratory and clinical evaluation. ATB was diagnosed by positive GeneXpert MTB/RIF or mycobacterial culture on sputum or bronchoalveolar lavage fluid with symptoms compatible of ATB including prolonged cough, chest pain, weakness or fatigue, weight loss, fever, and night sweats. Participants receiving anti-TB medication in two months prior to the enrollment were excluded from the analysis. LTBI was defined by a positive T-SPOT test without symptomatic, microbiological, or radiological evidences of ATB and history of TB. HC was defined by a negative T-SPOT test, while without any symptoms or signs of diseases. The laboratory scientists who performed the immunological and microbiological assays were blinded to the clinical data including disease status of participants. This study was reviewed and approved by the committee of Tongji hospital, Tongji Medical College, Huazhong University of Science and Technology.

### Lymphocyte Non-Specific Function Assay

PMA/ionomycin-stimulated lymphocyte non-specific function assay was performed as described previously (24). The procedures are described in brief as following: (1) 100  $\mu$ l of heparinized venous blood was diluted with 400  $\mu$ l of IMDM medium; (2) the diluted sample was incubated in the presence of Leukocyte Activation Cocktail (Becton Dickinson GolgiPlug<sup>TM</sup>) for 4 h; (3) the cells were labeled with antibodies (anti-CD45, anti-CD3, anti-CD4, anti-CD8, and anti-CD56) (BD Biosciences); (4) the cell were fixed and permeabilized; (5) the cells were stained with intracellular anti-interferon-gamma (IFN- $\gamma$ ) antibody (BD Biosciences); and (6) the cells were analyzed with FACSCanto flow cytometer. The percentages of IFN- $\gamma$ <sup>+</sup> cells in different cell subsets were defined as the non-specific function of them (**Supplementary Figure 1**) (e.g., the percentage of IFN- $\gamma$ <sup>+</sup> cells in CD3<sup>+</sup>CD4<sup>+</sup>CD8<sup>-</sup> cells was regarded as the non-specific function of CD4<sup>+</sup> T cells; the percentage of IFN- $\gamma$ <sup>+</sup> cells in CD3<sup>+</sup>CD4<sup>-</sup>CD8<sup>+</sup> cells was regarded as the non-specific function of CD8<sup>+</sup> T cells; the percentage of IFN- $\gamma$ <sup>+</sup> cells in CD3<sup>-</sup>CD56<sup>+</sup> cells was regarded as the non-specific function of NK cells). Given that the background is very low in the assay (the proportion of IFN- $\gamma$ <sup>+</sup> cells under 0.1%), we did not subtract the background when reporting lymphocyte non-specific function.

### T-SPOT Assay

Heparin anticoagulated peripheral blood was collected and analyzed using T-SPOT assay (Oxford Immunotec, Oxford, UK) according to the manufacturer's instructions. Briefly, peripheral blood mononuclear cells (PBMCs) were separated by Ficoll-Hypaque gradient centrifugation. Then, the isolated PBMCs ( $2.5 \times 10^5$ ) were added to 96-well plates precoated with antibody against IFN- $\gamma$ . Four wells were used for each subject: medium well, early secreted antigenic target 6 (ESAT-6) well, culture filtrate protein 10 (CFP-10) well, and PHA well. Plates were incubated for 16–20 h at 37°C with 5% CO<sub>2</sub> and developed using an anti-IFN- $\gamma$  antibody conjugate and substrate to detect

the presence of secreted IFN- $\gamma$ . Spot-forming cells (SFC) were counted with an automated enzyme-linked immunospot (ELISPOT) reader (CTL Analyzers, Cleveland, OH, USA). The test result was positive if ESAT-6 and/or CFP-10 spot number minus negative control spot number  $\geq 6$ . The test result was negative if both ESAT-6 spot number minus negative control spot number and CFP-10 spot number minus negative control spot number  $\leq 5$ . Results were considered undetermined if the spot number in the PHA well were  $< 20$  or if spot number in the medium well were  $> 10$ . The ratio of ESAT-6 SFC to PHA SFC (ESAT-6/PHA ratio) and CFP-10 SFC to PHA SFC (CFP-10/PHA ratio) were calculated. The larger of the above two values was defined as the TBAG/PHA ratio of one participant.

### Statistical Analysis

Continuous variables were expressed as means  $\pm$  standards deviation (SD) or median (interquartile range). Categorical variables were expressed as number (%). Comparison was performed using Mann-Whitney *U* test for continuous variables and Chi-square test or Fisher's exact test for categorical variables. All statistical tests were two sided. Statistical significance was considered when  $P < 0.05$ . For the identification of a diagnostic model, all variables with statistical significance were taken as candidates for multivariable logistic regression analyses, and the regression equation (diagnostic model) was obtained. The regression coefficients of the model were regarded as the weights for the respective variables, and a score for each participant was calculated. The performance of various indicators was evaluated by the receiver operating characteristic (ROC) curve analysis. Area under the curve (AUC), sensitivity, specificity, positive predictive value (PPV), negative predictive value (NPV), positive likelihood ratio (PLR), negative likelihood ratio (NLR), and accuracy, together with their 95% confidence intervals (CI), were calculated. The AUCs were compared using the *z* statistic with the procedure of DeLong et al. (33). Data were analyzed using SPSS version 25.0 (SPSS, Inc., Chicago, IL, USA), MedCalc version 11.6 (MedCalc, Mariakerke, Belgium), GraphPad Prism version 8 (GraphPad Software, San Diego, CA, USA), and R 4.0.2 program (R Core Team).

## RESULTS

### Participants' Characteristics

A total of 208 participants including 49 ATB patients, 64 LTBI individuals, and 95 HC were consecutively enrolled to the analysis. All included participants were HIV-negative. No difference was observed between ATB and LTBI in respect to the distribution of age and sex (**Table 1**). Among 49 patients diagnosed as ATB, 10 subjects had negative T-SPOT results, while the remaining 39 had positive T-SPOT results. **Table 2** described the characteristics of ATB subjects with negative T-SPOT results and those with positive T-SPOT results. There was no evidence of difference in the distribution of genders and underlying diseases between the groups.

**TABLE 1 |** Demographic and clinical characteristics of included subjects.

Variables	ATB (n = 49)	LTBI (n = 64)	HC (n = 95)
Age, years	48 (29-60)	50 (40-61)	47 (33-57)
Sex, male, %	27 (55.1%)	41 (64.06%)	60 (63.16%)
TB history	11 (22.45%)	0 (0%)	0 (0%)
Underlying condition or illness			
Diabetes mellitus	7 (14.29%)	8 (12.5%)	0 (0%)
Solid tumor	5 (10.2%)	6 (9.38%)	0 (0%)
Hematological malignancy	1 (2.04%)	1 (1.56%)	0 (0%)
End-stage renal disease	4 (8.16%)	7 (10.94%)	0 (0%)
Liver cirrhosis	2 (4.08%)	3 (4.69%)	0 (0%)
Organ transplantation	2 (4.08%)	1 (1.56%)	0 (0%)
Immunosuppressive condition*	7 (14.29%)	4 (6.25%)	0 (0%)
Positive mycobacterial culture	40 (81.63%)	NA	NA
Positive GeneXpert MTB/RIF	36 (73.47%)	NA	NA

ATB, active tuberculosis; LTBI, latent tuberculosis infection; HC, healthy controls; TB, tuberculosis; NA, not applicable.

\*Patients who underwent organ transplantation, chemotherapy or took immunosuppressants within 3 months. Data were presented as medians (25th-75th percentiles) or numbers (percentages).

**TABLE 2 |** Demographic and clinical characteristics of ATB patients with negative and positive T-SPOT results.

Variables	ATB with negative T-SPOT result (n = 10)	ATB with positive T-SPOT result (n = 39)	P*
Age, years	52 (26-56)	48 (29-61)	0.673
Sex, male, %	5 (50%)	22 (56.41%)	0.716
TB history	3 (30%)	8 (20.51%)	0.521
Presence of BCG scar	4 (40%)	17 (43.59%)	0.838
Underlying condition or illness			
Diabetes mellitus	2 (20%)	5 (12.82%)	0.563
Solid tumor	1 (10%)	4 (10.26%)	0.981
Hematological malignancy	0 (0%)	1 (2.56%)	1
End-stage renal disease	1 (10%)	3 (7.69%)	1
Liver cirrhosis	0 (0%)	2 (5.13%)	1
Organ transplantation	1 (10%)	1 (2.56%)	0.37
Immunosuppressive condition†	2 (20%)	5 (12.82%)	0.563
Positive mycobacterial culture	8 (80%)	32 (82.05%)	0.881
Positive GeneXpert MTB/RIF	7 (70%)	29 (74.36%)	0.781

ATB, active tuberculosis; BCG, bacille Calmette-Guérin; TB, tuberculosis.

\*Comparisons were performed between these two groups using Mann-Whitney U test, chi-square test, or Fisher's exact test. †Patients who underwent organ transplantation, chemotherapy, or took immunosuppressants within 3 months. Data were presented as medians (25th-75th percentiles), or numbers (percentages).

## The Correlation Between PHA Spot Number and Lymphocyte Non-Specific Function

We examined the correlation between PHA spot number and lymphocyte non-specific function. It was observed that significantly positive correlation existed between PHA spot number and CD4<sup>+</sup> T cell non-specific function ( $r=0.410$ ,  $P<0.001$ ), CD8<sup>+</sup> T cell non-specific function ( $r=0.296$ ,  $P<0.001$ ), and NK cell non-specific function ( $r=0.326$ ,  $P<0.001$ ) (Figure 1A). Furthermore, we stratified PHA spot number and found the trend that lymphocyte non-specific function increased with the increasing PHA spot number (Figures 1B, C).

## Lymphocyte Non-Specific Function for Identifying ATB With False-Negative T-SPOT Result

We compared lymphocyte non-specific function between ATB with negative T-SPOT result and those with positive T-SPOT result. It was found that CD4<sup>+</sup> T cell non-specific function was significantly lower in patients with negative T-SPOT result than in those with positive T-SPOT results, while no significant difference presented in CD8<sup>+</sup> T cell non-specific function and NK cell non-specific function between these two groups (Figure 2A). When comparing with HC, the lymphocyte non-specific function of ATB was significantly lower regardless of T-SPOT results (Figure 2A). Besides, there was no significant difference between the two groups in PHA spot number (Figure 2B). Further ROC curve analysis showed that CD4<sup>+</sup> T cell non-specific function had an AUC of 0.732 (95% CI, 0.572-0.893) for discriminating negative T-SPOT results from positive T-SPOT results among ATB patients (Figure 2C).

## Lymphocyte Non-Specific Function for Distinguishing Between ATB and LTBI

We compared lymphocyte non-specific function between ATB patients and LTBI individuals. It was found that the non-specific function of CD4<sup>+</sup> T cells, CD8<sup>+</sup> T cells, and NK cells was significantly lower in patients diagnosed with ATB than those with LTBI (Figure 3A). While no significant difference was observed in lymphocyte non-specific function between LTBI and HC (Figure 3A). And then we performed ROC curve analysis. The results of the diagnostic accuracy of lymphocyte non-specific function in distinguishing ATB from LTBI were shown in Figure 3B. The AUCs presented by CD4<sup>+</sup> T cell non-specific function, CD8<sup>+</sup> T cell non-specific function, and NK cell non-specific function were 0.845 (95% CI, 0.767-0.925), 0.770 (95% CI, 0.683-0.857), 0.691 (95% CI, 0.593-0.789) respectively (Figure 3B, Table 3). Concretely, when 11.7% was used as the threshold, the sensitivity and specificity of CD4<sup>+</sup> T cell non-specific function for distinguishing ATB from LTBI was 61.22% (95% CI, 47.25%-73.57%) and 90.63% (95% CI, 81.02%-95.63%), respectively. The cutoff value of 41.6% for CD8<sup>+</sup> T cell non-specific function showed a sensitivity of 46.94% (95% CI, 33.70%-60.62%) and specificity of 90.63% (95% CI, 81.02%-95.63%). The sensitivity and specificity for NK cell non-specific function were 28.57% (95% CI, 17.85%-42.41%) and 90.63% (95% CI, 81.02%-95.63%) with the threshold as 61.7% (Table 3).

## Combination of Lymphocyte Non-Specific Function and T-SPOT for Differentiating ATB From LTBI

The comparison in T-SPOT between ATB and LTBI was performed. No difference was observed between ATB and LTBI in ESAT-6 spot number while CFP-10 spot number was significantly higher in ATB patients than that in LTBI individuals (Figure 4A). ROC curve analysis indicated limited performance for ESAT-6 spot number and CFP-10 spot number (Figure 4C). Given that the pattern of lymphocyte non-specific function was inverse to that observed by T-SPOT between ATB



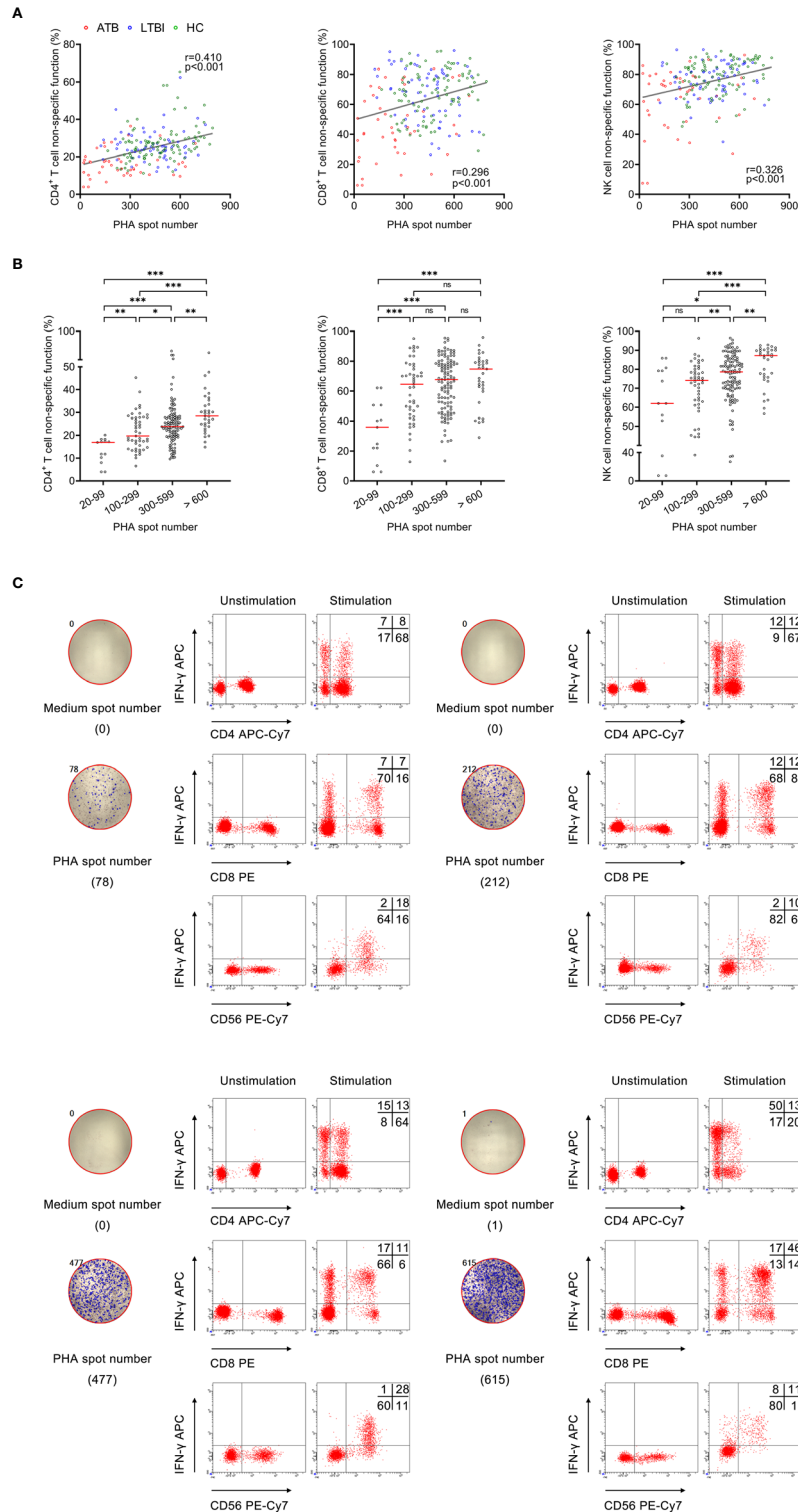


**FIGURE 1 |** The relationship between PHA spot number and lymphocyte non-specific function. **(A)** Correlation between PHA spot number and non-specific function of CD4<sup>+</sup> T cells, CD8<sup>+</sup> T cells, and NK cells in 208 participants. Each symbol represents an individual donor. **(B)** Scatter plots showing the results of CD4<sup>+</sup> T cell non-specific function, CD8<sup>+</sup> T cell non-specific function, and NK cell non-specific function under different PHA spot number. Horizontal lines indicate the median. \**P* < 0.05; \*\**P* < 0.01; \*\*\**P* < 0.001; ns, no significance (Mann-Whitney *U* test). **(C)** Flow plots showing the representative results of CD4<sup>+</sup> T cell non-specific function, CD8<sup>+</sup> T cell non-specific function, and NK cell non-specific function under different PHA spot number. PHA, phytohemagglutinin.

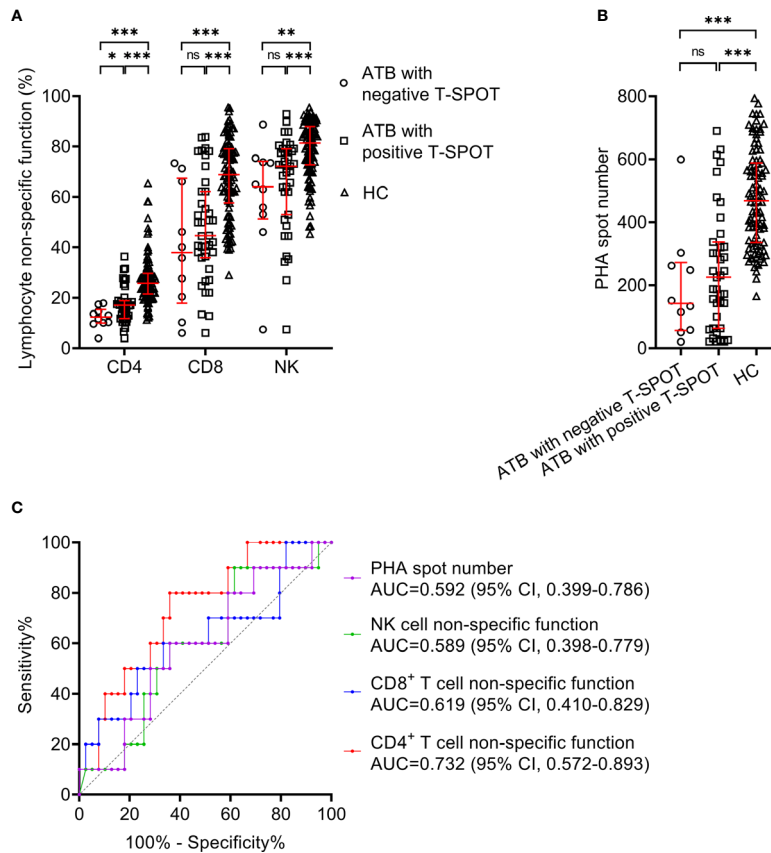


**FIGURE 2** | Lymphocyte non-specific function detection for identifying ATB patients with false-negative T-SPOT result. **(A)** Scatter plots showing the results of lymphocyte non-specific function in ATB with negative T-SPOT result ( $n=10$ ), ATB with positive T-SPOT result ( $n=39$ ) and HC ( $n=95$ ). Bars indicated the medians and interquartile ranges.  $^*P < 0.05$ ;  $^{**}P < 0.01$ ;  $^{***}P < 0.001$ ; ns, no significance (Mann-Whitney  $U$  test). **(B)** Scatter plots showing PHA spot number in ATB with negative T-SPOT result ( $n=10$ ), ATB with positive T-SPOT result ( $n=39$ ) and HC ( $n=95$ ). Bars indicated the medians and interquartile ranges.  $^{***}P < 0.001$ ; ns, no significance (Mann-Whitney  $U$  test). **(C)** ROC analysis showing the performance of CD4<sup>+</sup> T cell non-specific function, CD8<sup>+</sup> T cell non-specific function, NK cell non-specific function, and PHA spot number in distinguishing ATB patients with negative T-SPOT result from those with positive T-SPOT result. ATB, active tuberculosis; HC, healthy controls; PHA, phytohemagglutinin; ROC, receiver operating characteristic; AUC, area under the curve; CI, confidence interval.

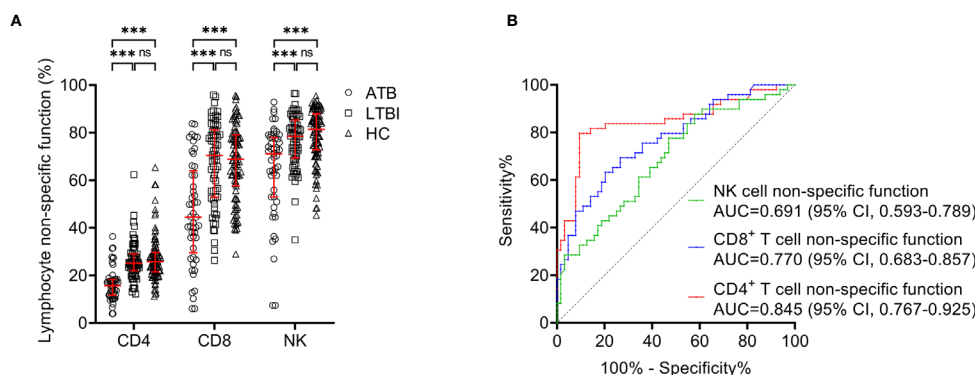


**FIGURE 3** | Lymphocyte non-specific function detection for distinguishing between ATB and LTBI. **(A)** Scatter plots showing the results of CD4<sup>+</sup> T cell non-specific function, CD8<sup>+</sup> T cell non-specific function, and NK cell non-specific function in ATB patients ( $n=49$ ), LTBI individuals ( $n=64$ ), and HC ( $n=95$ ). Bars indicated the medians and interquartile ranges.  $^{***}P < 0.001$ ; ns, no significance (Mann-Whitney  $U$  test). **(B)** ROC analysis showing the performance of CD4<sup>+</sup> T cell non-specific function, CD8<sup>+</sup> T cell non-specific function, and NK cell non-specific function in discriminating ATB patients from LTBI individuals. ATB, active tuberculosis; LTBI, latent tuberculosis infection; HC, healthy controls; ROC, receiver operating characteristic; AUC, area under the curve; CI, confidence interval.

TABLE 3 | The performance of various indicators for distinguishing between ATB and LTBI.

Variables	Cutoff value	AUC (95% CI)	Sensitivity (95% CI)	Specificity (95% CI)	PPV (95% CI)	NPV (95% CI)	PLR (95% CI)	NLR (95% CI)	Accuracy
CFP-10 spot number	34	0.649 (0.540-0.758)	36.73% (24.66%-50.73%)	90.63% (81.02%-95.63%)	75.00% (55.10%-88.00%)	65.17% (54.83%-74.25%)	3.92 (1.68-9.13)	0.70 (0.56-0.88)	67.26%
CD4 <sup>+</sup> T cell non-specific function (%)	17.3	0.845 (0.767-0.925)	61.22% (47.25%-73.57%)	90.63% (81.02%-95.63%)	83.33% (68.11%-92.13%)	75.32% (64.65%-83.60%)	6.53 (2.95-14.44)	0.43 (0.30-0.61)	77.88%
CD8 <sup>+</sup> T cell non-specific function (%)	41.6	0.770 (0.683-0.857)	46.94% (33.70%-60.62%)	90.63% (81.02%-95.63%)	79.31% (61.61%-90.16%)	69.05% (58.51%-77.92%)	5.01 (2.21-11.34)	0.59 (0.44-0.77)	71.68%
NK cell non-specific function (%)	61.7	0.691 (0.593-0.789)	28.57% (17.85%-42.41%)	90.63% (81.02%-95.63%)	70.00% (48.10%-85.45%)	62.37% (52.21%-71.54%)	3.05 (1.26-7.36)	0.79 (0.65-0.96)	63.72%
Diagnostic model	0.57	0.939 (0.898-0.981)	83.67% (70.96%-91.49%)	90.63% (81.02%-95.63%)	87.23% (74.83%-94.02%)	87.88% (77.86%-93.73%)	8.93 (4.13-19.31)	0.18 (0.10-0.34)	87.61%

ATB, active tuberculosis; LTBI, latent tuberculosis infection; CFP-10, culture filtrate protein 10; AUC, area under the curve; PPV, positive predictive value; NPV, negative predictive value; PLR, positive likelihood ratio; NLR, negative likelihood ratio; CI, confidence interval.

and LTBI, we predicted that the combination of these two assays would be leveraged for improving the stratification of patient groups. Consequently, we calculated the ratio of ESAT-6, CFP-10, or TBAG spot number to lymphocyte non-specific function. We found the ratios were obviously higher in ATB patients than LTBI individuals (Figure 4B). However, the discriminatory power measured by the AUC presented lower than 0.75 for all ratios (Figure 4D). Nonetheless, further cluster analysis using heatmap and the overlap between lymphocyte non-specific function and T-SPOT assay still showed that the combination of these two assays might improve the diagnostic value (Figures 4E, F). To establish the diagnostic model based on a combination of the two approaches for distinguishing ATB from LTBI, all variables with statistical significance were used for multivariable logistic regression analysis. The diagnostic model in distinguishing ATB from LTBI were built as follows:  $P = 1/[1 + e^{-(0.039 \times \text{CFP-10 spot number} - 0.363 \times \text{CD4}^+ \text{ T cell non-specific function} - 0.052 \times \text{NK cell non-specific function} + 9.679)}]$   $P$ , predictive value;  $e$ , natural logarithm. The three-marker diagnostic model distinguished patients with ATB disease from those with LTBI with an AUC of 0.939 (95% CI, 0.898-0.981) and demonstrated a sensitivity and specificity of 83.67% (95% CI, 70.96%-91.49%) and 90.63% (95% CI, 81.02%-95.63%) respectively while using 0.57 as the threshold (Table 3, Figures 4G, H). Z tests between the ROC curves showed a significant improvement for the model compared to either lymphocyte non-specific function ( $\text{CD4}^+$  T cell non-specific function,  $P=0.011$ ;  $\text{CD8}^+$  T cell non-specific function,  $P<0.001$ ; NK cell non-specific function,  $P<0.001$ ) or T-SPOT (ESAT-6 spot number,  $P<0.001$ ; CFP-10 spot number,  $P<0.001$ ).

### Comparison Between Diagnostic Model and TBAG/PHA Ratio for Discriminating ATB From LTBI

The value of TBAG/PHA ratio for distinguishing between ATB patients and LTBI individuals was also analyzed. ESAT-6/PHA ratio, CFP-10/PHA ratio, and TBAG/PHA ratio were found significantly higher in patients with ATB than individuals with LTBI (Figure 5A). Further ROC curve analysis showed that ESAT-6/PHA ratio, CFP-10/PHA ratio, and TBAG/PHA ratio had AUCs of 0.690 (95% CI, 0.583-0.799), 0.772 (95% CI, 0.676-0.869), and 0.749 (95% CI, 0.645-0.852) for discriminating ATB from LTBI, in comparison to 0.939 (95% CI, 0.898-0.981) for the diagnostic model (Table 4, Figure 5B). The AUC of diagnostic model was superior than those achieved for the individual ratios in T-SPOT (ESAT-6/PHA ratio,  $P<0.001$ ; CFP-10/PHA ratio,  $P=0.001$ ; TBAG/PHA ratio,  $P<0.001$ ). In addition, we evaluated the utility of these indicators for discriminating ATB from LTBI among subjects with positive T-SPOT results. The diagnostic model presented an AUC of 0.935 (95% CI, 0.890-0.981), which was comparable to that obtained based on all patients previously (Figures 5C, E). While the performance of ESAT-6/PHA ratio, CFP-10/PHA ratio, and TBAG/PHA ratio was obviously increased. The AUCs of ESAT-6/PHA ratio, CFP-10/PHA ratio, and TBAG/PHA ratio were 0.815 (95% CI, 0.727-0.903), 0.899 (95% CI, 0.837-0.961), and 0.889 (95% CI, 0.827-0.952), respectively (Figures 5D, E). However, our established

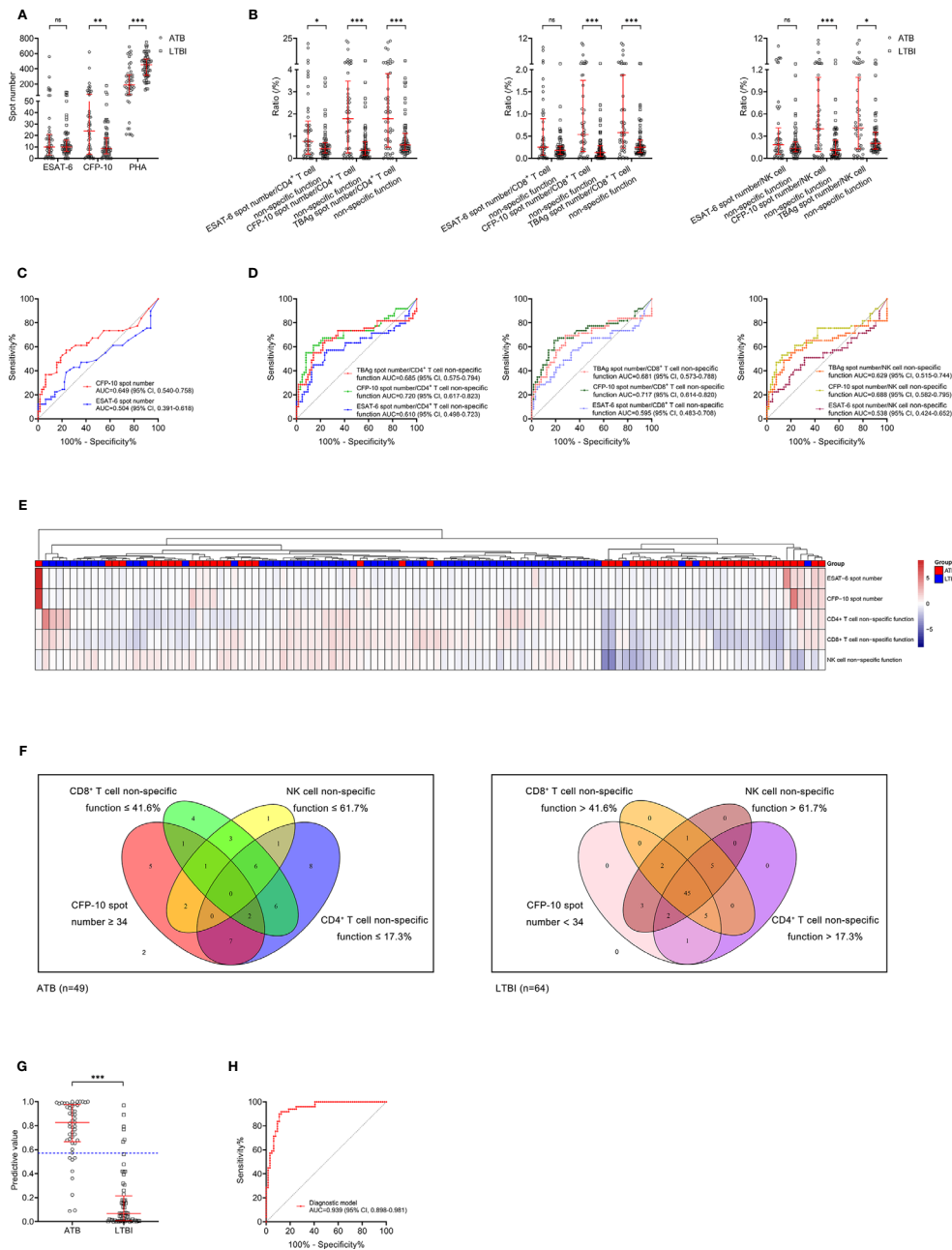


**FIGURE 4** | Combination of lymphocyte non-specific function and T-SPOT for differentiating ATB from LTBI. **(A)** Scatter plots showing the results of ESAT-6 spot number, CFP-10 spot number, and PHA spot number in ATB patients (n=49) and LTBI individuals (n=64). Bars indicated the medians and interquartile ranges. \*\* $P < 0.01$ ; \*\*\* $P < 0.001$ ; ns, no significance (Mann-Whitney  $U$  test). **(B)** Scatter plots showing the ratio of MTB-specific antigen spot number/lymphocyte non-specific function in ATB patients (n=49) and LTBI individuals (n=64). Bars indicated the medians and interquartile ranges. \* $P < 0.05$ ; \*\*\* $P < 0.001$ ; ns, no significance (Mann-Whitney  $U$  test). **(C)** ROC analysis showing the performance of ESAT-6 spot number and CFP-10 spot number in discriminating ATB patients from LTBI individuals. **(D)** ROC analysis showing the performance of MTB-specific antigen spot number/lymphocyte non-specific function in discriminating ATB patients from LTBI individuals. **(E)** Heatmap showing the cluster analysis of lymphocyte non-specific function and T-SPOT results in ATB patients (n=49) and LTBI individuals (n=64). Each rectangle indicates a result of a subject. **(F)** Venn diagrams showing the overlap of CD4<sup>+</sup> T cell non-specific function, CD8<sup>+</sup> T cell non-specific function, NK cell non-specific function, and CFP-10 spot number in ATB patients (n=49) and LTBI individuals (n=64). **(G)** Scatter plots showing the predictive value of diagnostic model in ATB patients (n=49) and LTBI individuals (n=64). Bars indicated the medians and interquartile ranges. \*\*\* $P < 0.001$  (Mann-Whitney  $U$  test). Blue dotted line indicates the cutoff value in distinguishing these two groups. **(H)** ROC analysis showing the performance of diagnostic model based on the combination of CD4<sup>+</sup> T cell non-specific function, NK cell non-specific function, and CFP-10 spot number in discriminating ATB patients from LTBI individuals. ESAT-6, early secreted antigenic target 6; CFP-10, culture filtrate protein 10; PHA, phytohemagglutinin; MTB, *Mycobacterium tuberculosis*; ATB, active tuberculosis; LTBI, latent tuberculosis infection; ROC, receiver operating characteristic; AUC, area under the curve; CI, confidence interval.



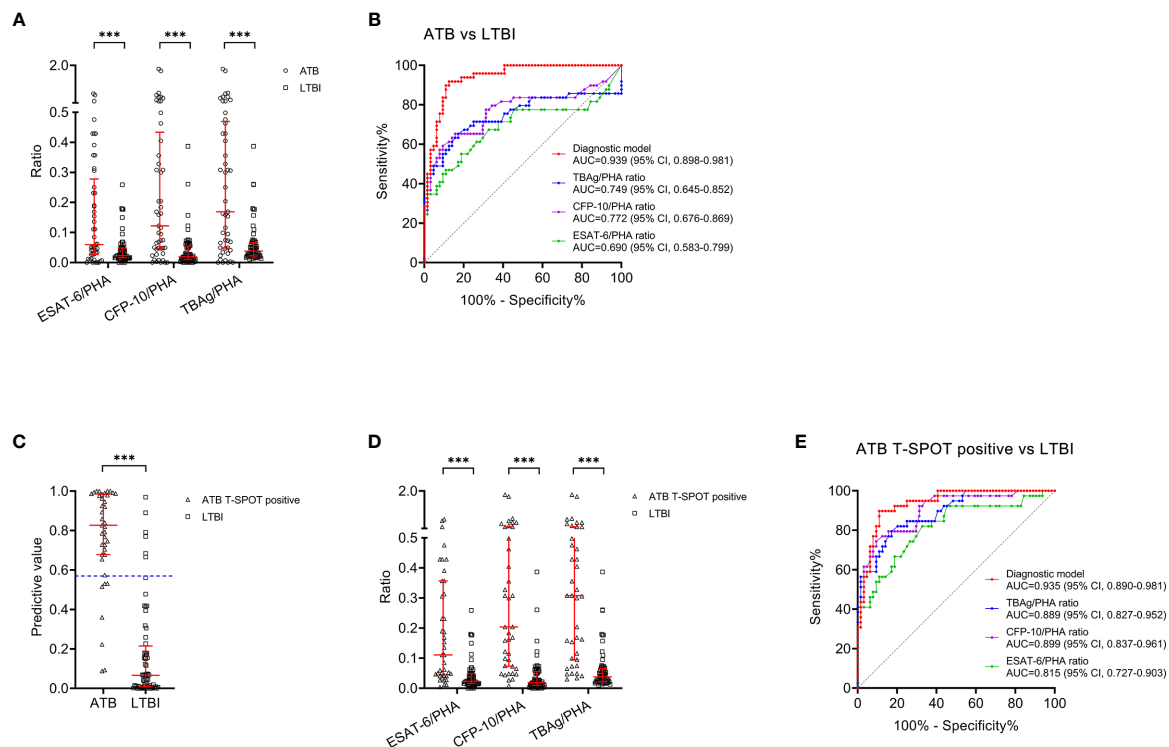


**FIGURE 5 |** Comparison between the diagnostic model and TBAG/PHA ratio for discriminating ATB from LTBI. **(A)** Scatter plots showing the values of ESAT-6/PHA ratio, CFP-10/PHA ratio, and TBAG/PHA ratio in ATB patients ( $n=49$ ) and LTBI individuals ( $n=64$ ). Bars indicated the medians and interquartile ranges.  $***P < 0.001$  (Mann-Whitney  $U$  test). **(B)** ROC analysis showing the performance of ESAT-6/PHA ratio, CFP-10/PHA ratio, TBAG/PHA ratio, and the diagnostic model in discriminating ATB patients from LTBI individuals. **(C)** Scatter plots showing the predictive value of diagnostic model in ATB patients with positive T-SPOT result ( $n=39$ ) and LTBI individuals ( $n=64$ ). Bars indicated the medians and interquartile ranges.  $***P < 0.001$  (Mann-Whitney  $U$  test). **(D)** Scatter plots showing the values of ESAT-6/PHA ratio, CFP-10/PHA ratio, and TBAG/PHA ratio in ATB patients with positive T-SPOT result ( $n=39$ ) and LTBI individuals ( $n=64$ ). Bars indicated the medians and interquartile ranges.  $***P < 0.001$  (Mann-Whitney  $U$  test). **(E)** ROC analysis showing the performance of ESAT-6/PHA ratio, CFP-10/PHA ratio, TBAG/PHA ratio, and the diagnostic model in discriminating ATB patients with positive T-SPOT result from LTBI individuals. ESAT-6, early secreted antigenic target 6; CFP-10, culture filtrate protein 10; PHA, phytohemagglutinin; TBAG, tuberculosis-specific antigen; ATB, active tuberculosis; LTBI, latent tuberculosis infection; ROC, receiver operating characteristic; AUC, area under the curve; CI, confidence interval.

diagnostic model still showed superior or comparable performance compared to the ratios (ESAT-6/PHA ratio,  $P=0.017$ ; CFP-10/PHA ratio,  $P=0.298$ ; TBAG/PHA ratio  $P=0.219$ ) (Table 5).

## DISCUSSION

The TB continues relentlessly, especially during the current global COVID-19 pandemic, killing more than other infection, while the progress being lagging behind other major infectious diseases (34–38). A fundamental issue with controlling the disease is the inadequacy of current available tests for stratification of status of MTB infection (39). Multiple disadvantages present including unsatisfactory sensitivity, high cost as well as reliance on complicated infrastructure. Novel approaches are needed to overcome the limitations of existing immunodiagnostic tests, including their inability for differentiating between ATB and LTBI.

There was rare study elucidating lymphocyte non-specific function detection for stratifying MTB infection. Our study benchmarked the value of lymphocyte non-specific function in the diagnosis of ATB for the first time. It was observed that  $CD4^+$  T cell non-specific function showed certain potential in identifying T-SPOT-negative ATB patients. Furthermore, we found that lymphocyte non-specific function detection including  $CD4^+$  T cell non-specific function,  $CD8^+$  T cell non-specific function, and NK cell non-specific function could be used to distinguish between ATB and LTBI. In view of the fact that the combination of multiple parameters may perform better than single parameter alone in many studies (20, 21, 40), we further successfully established a three-index diagnostic model that could discriminate ATB from LTBI with good utility based on the combination of lymphocyte non-specific function and T-SPOT assay. The diagnostic model based on the combination of  $CD4^+$  T cell non-specific function, NK cell non-specific function, and CFP-10 spot number established in the present study was 90.63% specific and identified 83.67% of ATB cases, indicating that it could be used as a rule-in ATB diagnostic test to allow

**TABLE 4** | The value of ESAT-6/PHA ratio, CFP-10/PHA ratio and TBAg/PHA ratio for discriminating ATB from LTBI.

Variables	Cutoff value	AUC (95% CI)	Sensitivity (95% CI)	Specificity (95% CI)	PPV (95% CI)	NPV (95% CI)	PLR (95% CI)	NLR (95% CI)	Accuracy
ESAT-6/PHA ratio	0.13	0.691 (0.583-0.799)	40.82% (28.21%-54.75%)	92.19% (82.98%-96.82%)	80.00% (60.87%-91.14%)	67.05% (66.69%-75.97%)	5.22 (2.11-12.94)	0.64 (0.50-0.82)	69.91%
IFP-10/PHA ratio	0.115	0.772 (0.676-0.869)	53.06% (39.39%-66.30%)	93.75% (85.00%-97.54%)	86.67% (70.32%-94.69%)	72.29% (61.84%-80.77%)	8.49 (3.17-22.73)	0.50 (0.37-0.68)	76.11%
lAg/PHA ratio	0.16	0.749 (0.645-0.852)	53.06% (39.38%-66.30%)	90.63% (81.02%-95.63%)	81.25% (64.69%-91.11%)	71.60% (60.98%-80.27%)	5.66 (2.53-12.67)	0.52 (0.38-0.70)	74.34%

ESAT-6, early secreted antigenic target 6; CFP-10, culture filtrate protein 10; ATB, active tuberculosis; LTBI, latent tuberculosis infection; AUC, area under the curve; PPV, positive predictive value; NPV, negative predictive value; PLR, positive likelihood ratio; NLR, negative likelihood ratio; CI, confidence interval.

rapid treatment initiation. Furthermore, we compared our established model with TBaG/PHA ratio-another TB diagnostic indicator reported in the previous studies and found that the diagnostic performance of our model was better than that of TBaG/PHA ratio.

Confirming previous reports, T-SPOT based on detection an immune response under TB-specific antigen stimulation could not stratify ATB and LTBI well (13, 41, 42). Only CFP-10 spot number showed certain potential for differential diagnosis of ATB and LTBI in the current study. We first analyzed the utility of the ratio of TB-specific antigen spot number to lymphocyte non-specific function in distinguishing ATB from LTBI, but unfortunately, no great effect was observed. However, we found the potential of the combination of lymphocyte non-specific function and T-SPOT in determining the status of TB infection through the analysis of Venn diagram and heatmap and we further successfully established a diagnostic model through multivariable logistic regression. TBAg/PHA ratio is a simple calculation based on T-SPOT assay itself. We compared its performance with the model we established in distinguishing ATB from LTBI and found that our model was significantly better than TBAg/PHA ratio. Notably, we observed that most of the previous studies targeted for the diagnostic performance of TBAg/PHA ratio were based on T-SPOT-positive subjects. Thus, the inclusion of T-SPOT-negative patients in our study would reduce the value of TBAg/PHA ratio. Therefore, we additionally compared the ability of two methods to differentiate ATB from LTBI in T-SPOT-positive patients. It was observed that the performance of the diagnostic model hardly changed while the performance of TBAg/PHA ratio was obviously increased. But the AUCs of CFP-10/PHA ratio and TBAg/PHA ratio were still lower than that of diagnostic model. These findings indicated the robustness and superiority of our established model.

An interesting question is why the combination of TBAg spot number and lymphocyte non-specific function is better than TBAg/PHA ratio in distinguishing ATB from LTBI. We think there are two reasons to explain this issue. First, lymphocyte non-specific function detection is better and more comprehensive than the number of PHA spots in reflecting host immunity. Although we found a significantly positive correlation between lymphocyte non-specific function and the number of PHA spots, the number of PHA spots signifies the broad-spectrum response of lymphocytes to PHA. In addition, the *r* values observed in the correlation between lymphocyte non-specific function and PHA spot number also reflected high variability among different patients. While lymphocyte non-specific function detection could reflect the ability of activation, chemotaxis, and cytotoxicity of lymphocytes (43). Second, lymphocyte non-specific function detection is more stable than the readout of PHA spot number. The counting of PHA spot number would have poor repeatability due to the experimental operation and inaccuracy in reading high values (29). On the contrary, our previous results showed that lymphocyte non-specific function detection was extremely stable (coefficients of variations within 5%) (24). Therefore, lymphocyte non-specific function is superior to PHA spot number, especially as a reproducible and widely accepted diagnostic indicator. Another question is why

**TABLE 5 |** The performance of various methods for differentiating ATB from LTBI in participants with positive T-SPOT results.

Variables	Cutoff value	AUC (95% CI)	Sensitivity (95% CI)	Specificity (95% CI)	PPV (95% CI)	NPV (95% CI)	PLR (95% CI)	NLR (95% CI)	Accuracy
ESAT-6/PHA ratio	0.13	0.815 (0.727-0.903)	48.72% (33.86%-63.80%)	92.19% (82.98%-96.62%)	79.17% (59.53%-90.76%)	74.68% (64.11%-82.97%)	6.24 (2.53-15.35)	0.56 (0.41-0.76)	75.73%
CFP-10/PHA ratio	0.115	0.899 (0.837-0.961)	66.67% (50.98%-79.37%)	93.75% (85.00%-97.54%)	86.67% (70.32%-94.69%)	82.19% (71.88%-89.29%)	10.67 (4.03-28.26)	0.36 (0.23-0.56)	83.50%
TBAG/PHA ratio	0.16	0.889 (0.827-0.952)	64.10% (48.42%-77.26%)	90.63% (81.02%-95.63%)	80.65% (63.72%-90.81%)	80.56% (69.97%-88.05%)	6.84 (3.08-15.17)	0.40 (0.26-0.61)	80.58%
Diagnostic model	0.57	0.936 (0.890-0.981)	82.05% (67.33%-91.02%)	90.63% (81.02%-95.63%)	84.21% (69.58%-92.56%)	89.23% (79.40%-94.69%)	8.75 (4.03-19.01)	0.20 (0.10-0.39)	87.38%

ATB, active tuberculosis; LTBI, latent tuberculosis infection; ESAT-6, early secreted antigenic target 6; CFP-10, culture filtrate protein 10; AUC, area under the curve; PPV, positive predictive value; NPV, negative predictive value; PLR, positive likelihood ratio; NLR, negative likelihood ratio; CI, confidence interval.

ESAT-6 spot number was not included to the diagnostic model. We think this may due to the significantly positive correlation between ESAT-6 spot number and CFP-10 spot number (**Supplementary Figure 2**). However, one kind of situation often occurs, that is, some patients only show ESAT-6 response. But our diagnostic model only included CFP-10 spot number. Therefore, we also established a model incorporating ESAT-6 spot number. We found the AUC produced by this model was similar to the former (**Supplementary Figure 3**).

Negative T-SPOT result in ATB was a common phenomenon (44, 45). Although some studies have explored the reasons for these negative results, this issue has not been fully explained. The occurrence of false-negative T-SPOT results in microbiologically confirmed ATB was generally considered to be partially caused by some host factors such as immunosuppression or malnutrition (44, 46). Nevertheless, due to the lack of uniform and reliable assessment methods for host immunity, most studies embodied this concept with the patient's underlying diseases, age, or the number of lymphocytes (45–47). In this study, we introduced lymphocyte non-specific function to this field for the first time and discovered the potential of lymphocyte non-specific function represented by CD4<sup>+</sup> T cell. It was undeniable that its value is limited with an AUC of only 0.72. But this may also indicate that the appearance of false-negative T-SPOT results is more likely to be caused by a variety of factors, such as the breadth of antigen coverage and defective cell response. Nonetheless, it might improve diagnostic accuracy when used in conjunction with other indicators. Further research targeted for multi-dimensional explanation need to be carried out.

Several limitations should be noticed in this study. First, given the relatively small sample size is an obvious caveat of our study, an independent cohort with larger population should be replicated in the future. Second, since both T-SPOT and flow cytometry were unusually used in TB-endemic setting with low income, the diagnostic model established in the present study might be not applicable in these areas. Nevertheless, our model could help validate other low-cost methods. Third, regarding that infection including HIV infection and COVID-19 might affect the IFN- $\gamma$  secretion of lymphocyte, further investigation targeted for the influence of underlying conditions such as co-infection on lymphocyte non-specific function detection are needed in the future. Fourth, due to the requirement for elaborate procedures, expensive equipment, and well-trained personnel, the applicability of the model might be limited in clinical practice. Finally, since we did not dynamically monitor lymphocyte non-specific function during anti-TB treatment in the present study, further well-designed studies should be conducted to clarify the benefit and efficacy from lymphocyte non-specific function based immune monitoring.

In summary, our findings demonstrated the ability to classify ATB patients and LTBI individuals by detecting lymphocyte non-specific function and the potential advantages of combining lymphocyte non-specific function detection and T-SPOT for improving classification in MTB infection. Importantly, the detection of lymphocyte non-specific function not only plays a complementary diagnostic role, but may also provide advantages if further developed as an approach for immune monitoring and

management in TB patients. Regarding that the numerous challenges still present in combating TB and critical need for better tools, our novel and adaptable lymphocyte non-specific function detection may support ongoing efforts in eliminating TB globally. The early diagnosis and guided initiation of anti-TB treatment brought by the present diagnostic model would help reduce transmission and mortality of the disease.

## DATA AVAILABILITY STATEMENT

The original contributions presented in the study are included in the article/**Supplementary Material**. Further inquiries can be directed to the corresponding authors.

## ETHICS STATEMENT

The studies involving human participants were reviewed and approved by the committee of Tongji hospital, Tongji Medical College, Huazhong University of Science and Technology. The patients/participants provided their written informed consent to participate in this study.

## AUTHOR CONTRIBUTIONS

YL, YX, WYL, SW, ZS, and FW designed and oversaw the study. QL and GT contributed to lymphocyte non-specific function assay. HS, WL, and LM conducted T-SPOT assay. XY and YZ coordinated data collection and management. YL and YC did the statistical analysis. YL wrote the first manuscript draft. All authors contributed to the article and approved the submitted version.

## REFERENCES

1. World Health Organization. *Global tuberculosis report 2020*. Geneva, Switzerland: World Health Organization (2020). Available at: <https://apps.who.int/iris/rest/bitstreams/1312164/retrieve>.
2. Houben RM, Dodd PJ. The Global Burden of Latent Tuberculosis Infection: A Re-estimation Using Mathematical Modelling. *PLoS Med* (2016) 13(10): e1002152. doi: 10.1371/journal.pmed.1002152
3. Cohen A, Mathiasen VD, Schön T, Wejse C. The global prevalence of latent tuberculosis: a systematic review and meta-analysis. *Eur Respir J* (2019) 54(3):1900655. doi: 10.1183/13993003.00655-2019
4. Keshavjee S, Amanullah F, Cattamanchi A, Chaisson R, Dobos KM, Fox GJ, et al. Moving Toward Tuberculosis Elimination: Critical Issues for Research in Diagnostics and Therapeutics for Tuberculosis Infection. *Am J Respir Crit Care Med* (2018) 199(5):564–71. doi: 10.1164/rccm.201806-1053PP
5. World Health Organization. *Implementing tuberculosis diagnostics: A policy framework*. Geneva, Switzerland: World Health Organization (2015). Available at: <https://apps.who.int/iris/rest/bitstreams/720125/retrieve>.
6. Horne DJ, Kohli M, Zifodya JS, Schiller I, Dendukuri N, Tollefson D, et al. Xpert MTB/RIF and Xpert MTB/RIF Ultra for pulmonary tuberculosis and

## FUNDING

This work was funded by the National Natural Science Foundation (grant number 81401639 and 81902132) and the National Mega Project on Major Infectious Disease Prevention of China (grant number 2017ZX10103005-007).

## ACKNOWLEDGMENTS

We thank the clinical immunology and microbiology laboratories of Tongji Hospital for technical assistance as well as the patients and their families.

## SUPPLEMENTARY MATERIAL

The Supplementary Material for this article can be found online at: <https://www.frontiersin.org/articles/10.3389/fimmu.2021.641378/full#supplementary-material>

**Supplementary Figure 1 |** The flow analysis template of lymphocyte non-specific function assay. Diluted whole blood was stimulated with Leukocyte Activation Cocktail for 4 h. Representative flow plots showing the gating strategies of IFN- $\gamma$ <sup>+</sup> cells in CD4<sup>+</sup>, CD8<sup>+</sup> T cells, and NK cells.

**Supplementary Figure 2 |** The correlation between ESAT-6 spot number and CFP-10 spot number. Scatter plot showing the correlation between ESAT-6 spot number and CFP-10 spot number. ESAT-6, early secreted antigenic target 6; CFP-10, culture filtrate protein 10.

**Supplementary Figure 3 |** The performance of the diagnostic model incorporating ESAT-6 spot number in distinguishing ATB patients from LTBI individuals. Scatter plots showing the predictive value of diagnostic model incorporating ESAT-6 spot number in ATB patients (n=49) and LTBI individuals (n=64). Bars indicated the medians and interquartile ranges. \*\*\*P<0.001 (Mann-Whitney U test). Blue dotted line indicates the cutoff value in distinguishing these two groups. ROC analysis showing the performance of diagnostic model incorporating ESAT-6 spot number in discriminating ATB patients from LTBI individuals.

7. rifampicin resistance in adults. *Cochrane Database Syst Rev* (2019) 6: CD009593. doi: 10.1002/14651858.CD009593.pub4
8. Esmail A, Tomasichio M, Meldau R, Makambwa E, Dheda K. Comparison of Xpert MTB/RIF (G4) and Xpert Ultra, including trace readouts, for the diagnosis of pulmonary tuberculosis in a TB and HIV endemic setting. *Int J Infect Dis* (2020) 95:246–52. doi: 10.1016/j.ijid.2020.03.025
9. Du F, Xie L, Zhang Y, Gao F, Zhang H, Chen W, et al. Prospective Comparison of QFT-GIT and T-SPOT.TB Assays for Diagnosis of Active Tuberculosis. *Sci Rep* (2018) 8(1):5882. doi: 10.1038/s41598-018-24285-3
10. Zhou G, Luo Q, Luo S, Teng Z, Ji Z, Yang J, et al. Interferon- $\gamma$  release assays or tuberculin skin test for detection and management of latent tuberculosis infection: a systematic review and meta-analysis. *Lancet Infect Dis* (2020) 20(12):1457–69. doi: 10.1016/S1473-3099(20)30276-0
11. Turner CT, Gupta RK, Tsaliki E, Roe JK, Mondal P, Nyawo GR, et al. Blood transcriptional biomarkers for active pulmonary tuberculosis in a high-burden setting: a prospective, observational, diagnostic accuracy study. *Lancet Respir Med* (2020) 8(4):407–19. doi: 10.1016/S2213-2600(19)30469-2
12. Garay-Baquero DJ, White CH, Walker NF, Tebruegge M, Schiff HF, Ugarte-Gil C, et al. Comprehensive plasma proteomic profiling reveals biomarkers for active tuberculosis. *JCI Insight* (2020) 5(18):e137427. doi: 10.1172/jci.insight.137427



12. Warsinske H, Vashisht R, Khatri P. Host-response-based gene signatures for tuberculosis diagnosis: A systematic comparison of 16 signatures. *PLoS Med* (2019) 16(4):e1002786. doi: 10.1371/journal.pmed.1002786
13. Dai Y, Shan W, Yang Q, Guo J, Zhai R, Tang X, et al. Biomarkers of iron metabolism facilitate clinical diagnosis in Mycobacterium tuberculosis infection. *Thorax* (2019) 74(12):1161–7. doi: 10.1136/thoraxjnl-2018-212557
14. Suzukawa M, Takeda K, Akashi S, Asari I, Kawashima M, Ohshima N, et al. Evaluation of cytokine levels using QuantiFERON-TB Gold Plus in patients with active tuberculosis. *J Infect* (2020) 80(5):547–53. doi: 10.1016/j.jinf.2020.02.007
15. Sudbury EL, Clifford V, Messina NL, Song R, Curtis N. Mycobacterium tuberculosis-specific cytokine biomarkers to differentiate active TB and LTBI: A systematic review. *J Infect* (2020) 81(6):873–81. doi: 10.1016/j.jinf.2020.09.032
16. Musvosvi M, Duffy D, Filander E, Africa H, Mabwe S, Jaxa L, et al. T-cell biomarkers for diagnosis of tuberculosis: candidate evaluation by a simple whole blood assay for clinical translation. *Eur Respir J* (2018) 51(3):1800153. doi: 10.1183/13993003.00153-2018
17. Adekambi T, Ibegbu CC, Cagle S, Kalokhe AS, Wang YF, Hu Y, et al. Biomarkers on patient T cells diagnose active tuberculosis and monitor treatment response. *J Clin Invest* (2015) 125(5):1827–38. doi: 10.1172/JCI77990
18. MacLean E, Broger T, Yerliya S, Fernandez-Carballo BL, Pai M, Denninger CM. A systematic review of biomarkers to detect active tuberculosis. *Nat Microbiol* (2019) 4(5):748–58. doi: 10.1038/s41564-019-0380-2
19. Lu LL, Das J, Grace PS, Fortune SM, Restrepo BI, Alter G. Antibody Fc Glycosylation Discriminates Between Latent and Active Tuberculosis. *J Infect Dis* (2020) 222(12):2093–102. doi: 10.1093/infdis/jiz643
20. Luo Y, Xue Y, Yuan X, Lin Q, Tang G, Mao L, et al. Combination of prealbumin and tuberculosis-specific antigen/phytohemagglutinin ratio for discriminating active tuberculosis from latent tuberculosis infection. *Int J Clin Pract* (2020) 75(4):e13831. doi: 10.1111/ijcp.13831
21. Luo Y, Xue Y, Lin Q, Tang G, Yuan X, Mao L, et al. A combination of iron metabolism indexes and tuberculosis-specific antigen/phytohemagglutinin ratio for distinguishing active tuberculosis from latent tuberculosis infection. *Int J Infect Dis* (2020) 97:190–6. doi: 10.1016/j.ijid.2020.05.109
22. Cegielski JP, McMurray DN. The relationship between malnutrition and tuberculosis: evidence from studies in humans and experimental animals. *Int J Tuberc Lung Dis* (2004) 8(3):286–98.
23. Folds JD, Schmitz JL. Clinical and laboratory assessment of immunity. *J Allergy Clin Immunol* (2003) 111(2):S702–S1124. doi: 10.1067/mai.2003.122
24. Luo Y, Xie Y, Zhang W, Lin Q, Tang G, Wu S, et al. Combination of lymphocyte number and function in evaluating host immunity. *Aging (Albany NY)* (2019) 11(24):12685–707. doi: 10.18632/aging.102595
25. Lin Q, Wang Y, Luo Y, Tang G, Li S, Zhang Y, et al. The Effect of Host Immunity on Predicting the Mortality of Carbapenem-Resistant Organism Infection. *Front Cell Infect Microbiol* (2020) 10:480. doi: 10.3389/fcimb.2020.00480
26. Wang F, Hou HY, Wu SJ, Zhu Q, Huang M, Yin B, et al. Using the TBAG/PHA ratio in the T-SPOT(R).TB assay to distinguish TB disease from LTBI in an endemic area. *Int J Tuberc Lung Dis* (2016) 20(4):487–93. doi: 10.5588/ijtld.15.0756
27. Bosco MJ, Hou H, Mao L, Wu X, Ramroop KD, Lu Y, et al. The performance of the TBAG/PHA ratio in the diagnosis of active TB disease in immunocompromised patients. *Int J Infect Dis* (2017) 59:55–60. doi: 10.1016/j.ijid.2017.03.025
28. Wang F, Yu J, Zhou Y, Luo Y, Wu S, Huang M, et al. The Use of TB-Specific Antigen/Phytohemagglutinin Ratio for Diagnosis and Treatment Monitoring of Extrapulmonary Tuberculosis. *Front Immunol* (2018) 9:1047. doi: 10.3389/fimmu.2018.01047
29. Wang F, Liu K, Peng J, Luo Y, Tang G, Lin Q, et al. Combination of Xpert MTB/RIF and TBAG/PHA Ratio for Prompt Diagnosis of Active Tuberculosis: A Two-Center Prospective Cohort Study. *Front Med (Lausanne)* (2020) 7:119. doi: 10.3389/fmed.2020.00119
30. Luo Y, Tang G, Lin Q, Mao L, Xue Y, Yuan X, et al. Combination of mean spot sizes of ESAT-6 spot-forming cells and modified tuberculosis-specific antigen/phytohemagglutinin ratio of T-SPOT.TB assay in distinguishing between active tuberculosis and latent tuberculosis infection. *J Infect* (2020) 81(1):81–9. doi: 10.1016/j.jinf.2020.04.038
31. Zhou Y, Du J, Hou HY, Lu YF, Yu J, Mao LY, et al. Application of ImmunoScore Model for the Differentiation between Active Tuberculosis and Latent Tuberculosis Infection as Well as Monitoring Anti-tuberculosis Therapy. *Front Cell Infect Microbiol* (2017) 7:457. doi: 10.3389/fcimb.2017.00457
32. Katakura S, Kobayashi N, Hashimoto H, Kamimaki C, Tanaka K, Kubo S, et al. Identification of a novel biomarker based on lymphocyte count, albumin level, and TBAG/PHA ratio for differentiation between active and latent tuberculosis infection in Japan. *Tuberculosis (Edinb)* (2020) 125:101992. doi: 10.1016/j.tube.2020.101992
33. DeLong ER, DeLong DM, Clarke-Pearson DL. Comparing the areas under two or more correlated receiver operating characteristic curves: a nonparametric approach. *Biometrics* (1988) 44(3):837–45. doi: 10.2307/2531595
34. McQuaid CF, McCreesh N, Read JM, Sumner T, Group CC-W, Houben R, et al. The potential impact of COVID-19-related disruption on tuberculosis burden. *Eur Respir J* (2020) 56(2):2001718. doi: 10.1183/13993003.01718-2020
35. Owolabi OA, Jallow AO, Jallow M, Sowe G, Jallow R, Genekah MD, et al. Delay in the diagnosis of pulmonary tuberculosis in The Gambia, West Africa: A cross-sectional study. *Int J Infect Dis* (2020) 101:102–6. doi: 10.1016/j.ijid.2020.09.029
36. Saunders MJ, Evans CA. COVID-19, tuberculosis and poverty: preventing a perfect storm. *Eur Respir J* (2020) 56(1):2001348. doi: 10.1183/13993003.01348-2020
37. Komiya K, Yamasue M, Takahashi O, Hiramatsu K, Kadota JJ, Kato S. The COVID-19 pandemic and the true incidence of Tuberculosis in Japan. *J Infect* (2020) 81(3):e24–e5. doi: 10.1016/j.jinf.2020.07.004
38. Lai CC, Yu WL. The COVID-19 pandemic and tuberculosis in Taiwan. *J Infect* (2020) 81(2):e159–e61. doi: 10.1016/j.jinf.2020.06.014
39. World Health Organization. *A Global Strategy for tuberculosis research and innovation*. Geneva, Switzerland: World Health Organization (2020). Available at: <https://apps.who.int/iris/rest/bitstreams/1312195/retrieve>.
40. Luo Y, Yan F, Xue Y, Mao L, Lin Q, Tang G, et al. Diagnostic utility of pleural fluid T-SPOT and interferon-gamma for tuberculous pleurisy: A two-center prospective cohort study in China. *Int J Infect Dis* (2020) 99:515–21. doi: 10.1016/j.ijid.2020.08.007
41. Goletti D, Carrara S, Butera O, Amicosante M, Ernst M, Sauzullo I, et al. Accuracy of immunodiagnostic tests for active tuberculosis using single and combined results: a multicenter TBNET-Study. *PLoS One* (2008) 3(10):e3417. doi: 10.1371/journal.pone.0003417
42. Kang WL, Wang GR, Wu MY, Yang KY, Er-Tai A, Wu SC, et al. Interferon-Gamma Release Assay is Not Appropriate for the Diagnosis of Active Tuberculosis in High-Burden Tuberculosis Settings: A Retrospective Multicenter Investigation. *Chin Med J (Engl)* (2018) 131(3):268–75. doi: 10.4103/0366-6999.223860
43. Hou H, Zhou Y, Yu J, Mao L, Bosco MJ, Wang J, et al. Establishment of the Reference Intervals of Lymphocyte Function in Healthy Adults Based on IFN-gamma Secretion Assay upon Phorbol-12-Myristate-13-Acetate/Ionomycin Stimulation. *Front Immunol* (2018) 9:172. doi: 10.3389/fimmu.2018.00172
44. Pan L, Jia H, Liu F, Sun H, Gao M, Du F, et al. Risk factors for false-negative T-SPOT.TB assay results in patients with pulmonary and extra-pulmonary TB. *J Infect* (2015) 70(4):367–80. doi: 10.1016/j.jinf.2014.12.018
45. Liao CH, Lai CC, Tan CK, Chou CH, Hsu HL, Tasi TH, et al. False-negative results by enzyme-linked immunospot assay for interferon-gamma among patients with culture-confirmed tuberculosis. *J Infect* (2009) 59(6):421–3. doi: 10.1016/j.jinf.2009.09.012
46. Nguyen DT, Teeter LD, Graves J, Graviss EA. Characteristics Associated with Negative Interferon-gamma Release Assay Results in Culture-Confirmed Tuberculosis Patients, Texas, USA, 2013–2015. *Emerg Infect Dis* (2018) 24(3):534–40. doi: 10.3201/eid2403.171633
47. Yang C, Zhang S, Yao L, Fan L. Evaluation of risk factors for false-negative results with an antigen-specific peripheral blood-based quantitative T

cell assay (T-SPOT((R)). TB) in the diagnosis of active tuberculosis: A large-scale retrospective study in China. *J Int Med Res* (2018) 46(5):1815–25. doi: 10.1177/0300060518757381

**Conflict of Interest:** The authors declare that the research was conducted in the absence of any commercial or financial relationships that could be construed as a potential conflict of interest.

Copyright © 2021 Luo, Xue, Cai, Lin, Tang, Song, Liu, Mao, Yuan, Zhou, Liu, Wu, Sun and Wang. This is an open-access article distributed under the terms of the Creative Commons Attribution License (CC BY). The use, distribution or reproduction in other forums is permitted, provided the original author(s) and the copyright owner(s) are credited and that the original publication in this journal is cited, in accordance with accepted academic practice. No use, distribution or reproduction is permitted which does not comply with these terms.



# Development of ESAT-6 Based Immunosensor for the Detection of *Mycobacterium tuberculosis*

Rishabh Anand Omar<sup>1</sup>, Nishith Verma<sup>2,3\*</sup> and Pankaj Kumar Arora<sup>1\*</sup>

<sup>1</sup> Department of Environmental Microbiology, Babasaheb Bhimrao Ambedkar University, Lucknow, India, <sup>2</sup> Centre for Environmental Science and Engineering, Indian Institute of Technology Kanpur, Kanpur, India, <sup>3</sup> Department of Chemical Engineering, Indian Institute of Technology Kanpur, Kanpur, India

## OPEN ACCESS

### Edited by:

Christof Geldmacher,  
University of Munich, Germany

### Reviewed by:

Antresh Kumar,  
Central University of South Bihar, India  
Yogendra Kumar Mishra,  
University of Southern Denmark,  
Denmark  
Kamlesh Shrivastava,  
Pandit Ravishankar Shukla University,  
India

### \*Correspondence:

Nishith Verma  
vermanishith@gmail.com  
Pankaj Kumar Arora  
arora484@gmail.com

### Specialty section:

This article was submitted to  
Microbial Immunology,  
a section of the journal  
Frontiers in Immunology

**Received:** 15 January 2021

**Accepted:** 04 May 2021

**Published:** 19 May 2021

### Citation:

Omar RA, Verma N and Arora PK  
(2021) Development of ESAT-6 Based  
Immunosensor for the Detection of  
*Mycobacterium tuberculosis*.  
Front. Immunol. 12:653853.  
doi: 10.3389/fimmu.2021.653853

Early secreted antigenic target of 6 kDa (ESAT-6) has recently been identified as a biomarker for the rapid diagnosis of tuberculosis. We propose a stable and reusable immunosensor for the early diagnosis of tuberculosis based on the detection and quantification of ESAT-6 via cyclic voltammetry (CV). The immunosensor was synthesized by polymerizing aniline dispersed with the reduced graphene oxide (rGO) and Ni nanoparticles, followed by surface modification of the electroconductive polyaniline (PANI) film with anti-ESAT-6 antibody. Physicochemical characterization of the prepared materials was performed by several analytical techniques, including FE-SEM, EDX, XRD, FT-IR, Raman, TGA, TPR, and BET surface area analysis. The antibody-modified Ni-rGO-PANI electrode exhibited an approximately linear response ( $R^2 = 0.988$ ) towards ESAT-6 during CV measurements over the potential range of -1 to +1 V. The lower detection limit for ESAT-6 was approximately  $1.0 \text{ ng mL}^{-1}$ . The novelty of this study includes the development of the reusable Ni-rGO-PANI-based electrochemical immunosensor for the early diagnosis of tuberculosis. Furthermore, this study successfully demonstrates that electro-conductive PANI may be used as a polymeric substrate for Ni nanoparticles and rGO.

**Keywords:** *Mycobacterium tuberculosis*, cyclic voltammetry, ESAT-6, immunosensor, reduced graphene oxide, polyaniline

## INTRODUCTION

Tuberculosis (TB) is an airborne disease that can be transmitted through coughing, sneezing, laughing, and even talking (1). It is one of the leading causes of death in the world. The causative agent of tuberculosis is the *Mycobacterium tuberculosis* (*Mtb*) bacterium. Therefore, an early detection of *Mtb* is critical to preventing the spread of infection and to eradicating the disease.

Many traditional biochemical methods, including acid-fast staining, culturing, and colony counting have been used to detect tuberculosis. However, these methods are time-consuming, often inaccurate, and provide only qualitative data. In recent years, various transduction techniques have been developed using fiber optics, surface plasmon resonance, piezoelectrics, and magnetoelastics. These techniques are rapid and accurate but too expensive to be used on a diagnostic level, especially in developing countries where the spread of *Mtb* is common (2–4).

In recent years, the development of electrochemical sensors to diagnose *Mtb* has drawn keen interest. Electrochemical sensors identify a biomarker using a suitable recognition element that is immobilized on a substrate. A change in the current response occurs when the recognition element interacts with biomarkers in the diagnostic fluid. In this context, poly L-lysine (5), antigen-specific antibodies (6–8), and DNA aptamers (9–12) have been successfully tested as the recognition elements. Although such sensors are accurate and fast, extraction of biomolecules (including DNA) from clinical samples is tedious and complex, requiring a sophisticated molecular laboratory to process samples collected from patients infected with tuberculosis. The preparation cost is also high, considering that DNA probes must be specifically grafted to the substrate (13–15).

Early secreted antigenic target of 6 kDa protein (ESAT-6) is the major virulence factor of *Mycobacterium*, which is secreted in the blood and sputum of infected persons. ESAT-6 is secreted only by the *Mycobacterium* pathogenic species. Thus, it is a potential biomarker for *Mtb*, whose detection can be rapid, specific, and accurate at all stages of the infection. It should be noted that the *Mtb*-infected sputum and blood also contain other proteins such as CPF-10 and antigen-85, but monoclonal antibodies are specific to their antigens, binding only through a specific epitope (16). A gold-plated screen-printed electrode (SPE) has been successfully immobilized with the anti ESAT-6 antibody as the recognition element for the *Mtb* biomarker at 7 ng mL<sup>-1</sup> (17). The electrochemical sensor showed a good linearity (0.992) over the measured concentration range. However, the sensor was not tested for stability and reusability. Moreover, SPE is expensive, making production of the sensors cost-prohibitive.

Recent studies have demonstrated that the metal-reduced graphene oxide (rGO) composite-based sensors are capable of detecting various biomolecules such as cholesterol, creatinine, and glucose (18–21). Graphene-based materials also have some unique physicochemical properties such as adsorption, chemical stability, and amenability to surface functionalization, which can facilitate detection of a wide range of biomolecules (22, 23). Inclusion of the metal nanoparticles (NPs) such as Au, Ag, Cu, Co, and Ni in the electrode material increases the sensitivity and speed of the sensor, attributed to an increased direct electron transfer (24–32). However, Au and Ag are expensive metals. While Cu and Co are inexpensive, they display cytotoxicity and have unstable (transient) oxidation states. Ni is an inexpensive, non-toxic, and stable metal used for sensing applications. Further, polyaniline (PANI) is frequently used as a conductive material for many electrical and electronic applications (20, 33). Therefore, a composite of Ni, rGO, and PANI is a potential candidate for the electrode, and is the focus of the present study.

Here, we describe a cyclic voltammetry (CV)-based immunosensor using a Ni-rGO-PANI electrode that targets the ESAT-6 virulence factor of *Mtb* using the anti-ESAT-6 antibody as the recognition element. The developed sensor is capable of detecting ESAT-6 both qualitatively and quantitatively. To the authors' knowledge, this is the first study that describes the Ni-rGO-PANI-based electrochemical immunosensor for the

detection of *Mtb* infection at an early stage. Furthermore, the electroconductive PANI is used as the polymeric substrate for the Ni and rGO NPs, also for the first time. The prepared sensor is tested at different ESAT-6 concentrations and its performance is compared to published data, wherever possible.

## MATERIAL AND METHODS

### Chemicals and Reagents

ESAT-6 (Pro-291) and Ag85B (Pro-589) proteins were purchased from Prospecc Protein Specialist (Germany). Anti-ESAT-6 monoclonal antibody (SC-57730) was purchased from Santa Cruz Biotechnology (Germany). Dithiobis (succinimidyl propionate) (DSP) was purchased from TCI chemicals (India). Graphite powder were purchased from S.D. Fine Chemical Ltd (India). 4-acetamidophenol (AP), glucose (Glu), uric acid (U), L-ascorbic acid (AA), creatinine (Cre), cholesterol (Chl), barbituric acid (BA), and L-glutamine (Glt) were purchased from Tata Chemicals, India. Bovine albumin serum (BSA), aniline monomer, ammonium persulfate ((NH<sub>4</sub>)<sub>2</sub>S<sub>2</sub>O<sub>8</sub>), disodium hydrogen phosphate (Na<sub>2</sub>HPO<sub>4</sub>), potassium dihydrogen phosphate (KH<sub>2</sub>PO<sub>4</sub>), nickel nitrate (Ni(NO<sub>3</sub>)), hydrogen peroxide (H<sub>2</sub>O<sub>2</sub>), sodium chloride (NaCl), potassium permanganate (KMnO<sub>4</sub>), potassium chloride (KCl), hydrochloric acid (HCl), nitric acid (HNO<sub>3</sub>), and sulfuric acid (H<sub>2</sub>SO<sub>4</sub>) were purchased from Merck (Germany). The healthy human blood samples were collected from a clinical diagnostic laboratory, where *Mycobacterium* infection was already checked by culture plate method. The samples were declared (certified) free from any disease including *Mycobacterium* infection by the diagnostic laboratory. Zero-grade hydrogen (H<sub>2</sub>) and nitrogen (N<sub>2</sub>) gases were purchased from Sigma Gases (India). All solutions were prepared in Type 1 ultrapure water using the Elix Mili Q system (USA).

### Synthesis of GO

The material was prepared from graphite powder by Hummers' method with some modifications (34, 35). Briefly, 1 g of graphite powder, 0.75 g of sodium nitrate, and 37.5 mL of concentrated H<sub>2</sub>SO<sub>4</sub> (98% w/w) were transferred to a 1 L conical flask. The flask was placed on an ice bath under stirred conditions using a magnetic stirrer. Approximately 4.5 g of KMnO<sub>4</sub> was added slowly to the mixture. The mixture turned dark green. The solution was stirred for 2 h and then removed from the ice bath, and left at ~30°C under stirring for five days. The solution became viscous and turned dark brown. Approximately 100 mL of H<sub>2</sub>SO<sub>4</sub> (5% w/w) was added to the solution. There was no change in color, indicating the formation of GO. The solution was stirred for another 2 h. Approximately 3 mL of 30% (w/w) H<sub>2</sub>O<sub>2</sub> was added to the solution. The solution turned golden yellow. Stirring continued for 1 h. The solution was centrifuged at 3842 g for 20 min and the suspension was washed five times each with distilled water and 1 M HCl, and finally with distilled water until pH of the suspension reached ~7. The suspension was transferred to Petri dishes and left for drying in air for 4 days.



## Preparation of the NiO-GO Mixture

Approximately 1 g of dried GO was added to a 50 mL volume of 0.4 M  $\text{NiNO}_3$  solution. The mixture was sonicated for 2 h to disperse GO in the salt solution. The solution was centrifuged at 3842 g for 20 min. The suspension was transferred to Petri dishes and left to dry in air for 4 days (36, 37). The prepared  $\text{NiNO}_3$ -GO mixture was calcined in a tubular furnace at 450°C for 4 h under  $\text{N}_2$  flow at 200 standard cubic cm per min (sccm) to convert  $\text{NiNO}_3$  to NiO. The NiO-GO mixture was subjected to the  $\text{H}_2$ -reduction (200 sccm) at 600°C for 2 h to convert NiO to Ni and GO to rGO. Reduction temperature was determined using temperature-programmed reduction (TPR) analysis.

## Preparation of PANI

Approximately 9 mL of aniline was added to 150 mL of distilled water in a round-bottom flask. The flask was placed on the ice bath. The temperature of the mixture was adjusted between 0 - 5°C. The solution was stirred continuously using a magnetic stirrer. Approximately 10 mL of 9 M HCl was added dropwise to the solution. Approximately 100 mL of  $(\text{NH}_4)_2\text{S}_2\text{O}_8$  (11% w/w) solution was added dropwise to the aniline solution. The solution turned dark green. The solution was stirred for another 2 h and then centrifuged at 3842 g for 10 min. The supernatant was discarded and the residual suspension of PANI was washed with distilled water until its pH reached ~7 (38).

## Synthesis of the Ni-rGO-PANI Electrode

The prepared Ni-rGO mixture (~4% w/w) was added to PANI. The mixture was sonicated for 2 h in distilled water to uniformly disperse Ni-rGO in PANI. The sonicated mixture was centrifuged at 3842 g for 15 min. The residual slurry suspension was cast as a ~2 mm-thick film on Petri dishes and left to dry in air for 5 days. The dried Ni-rGO-PANI metal-carbon-polymer composite film was cut into rectangular (10 mm x 5 mm) pieces to be used as the test electrodes. Samples of rGO-PANI (without Ni) and the PANI substrate (without Ni and rGO) were prepared for comparison.

## Preparation of PBS Buffer and Synthetic Clinical Samples

Approximately 8 g of NaCl, 0.2 g of KCl, 1.44 g of  $\text{Na}_2\text{HPO}_4$ , and 0.24 g of  $\text{KH}_2\text{PO}_4$  were transferred to 800 mL of Milli-Q water in a 1 L-conical flask. The solution pH was adjusted to 7.2 using 1 M HCl, and the final volume was maintained at 1 L. The solution was sterilized for 15 min in an autoclave at 121°C. Approximately 1 mL of the PBS was mixed in ESAT-6 protein to prepare the stock solution of  $1 \mu\text{g mL}^{-1}$ . Stock solutions of the interfering biomolecules (Ag85, AP, Glu, U, AA, Cre, Chl, BA, and Glt) were also prepared in the same PBS solution.

Blood samples (2 mL) were collected in EDTA tube containing anticoagulant enzymes and stored at 4°C for the clinical measurements. The as-received samples were centrifuged at 2400 rpm for 15 min to separate the erythrocytes (RBC and WBC) from blood plasma (supernatant fluid). Approximately 0.01 mL plasma solution was used to prepare the synthetic clinical samples at different concentrations of ESAT-6.

## Electrode Surface Modification

The prepared Ni-rGO-PANI electrodes were first washed with distilled water and dried in  $\text{N}_2$  flow. Dried electrodes were immersed in an acetone solution containing 1 mM of DSP for 1 h at ~30°C. DSP interacts with the Ni NPs through Ni-sulfide bond. At the other end, it interacts with the antibody *via* amide bond (17, 39, 40). The DSP-coated electrodes were washed with acetone and distilled water to remove excess DSP from the electrode surface. Washed electrodes (DSP-Ni-rGO-PANI) were immersed in PBS buffer (pH 7.2) containing 100 ng  $\text{mL}^{-1}$  of anti-ESAT-6 antibody. The entire electrode and antibody solution were incubated overnight at 4°C. The incubated electrode samples were washed using the PBS buffer to remove unbound antibodies. The washed samples (Ab-DSP-Ni-rGO-PANI) were soaked in BSA (1% w/w) solution at ~30°C for 1 h to block the free sites in DSP. The samples were washed with PBS to remove excess BSA. The prepared material (BSA-Ab-DSP-Ni-rGO-PANI) was used as the sensing electrode for ESAT-6. In the surface modification step described above, DSP served as the cross-linking agent for the anti-ESAT-6 antibody. DSP contains two amine-reactive N-hydroxyl succinimide (NHS) esters that react with primary amines on the antibody to make a stable amide bond with subsequent release of the NHS group. **Figure 1** describes the preparation- and surface modification steps for the sensing electrode schematically (17, 39, 40).

## Physicochemical Characterization

Ni loading in the electrode material was determined by leaching the metal from an approximately 0.1 g of the Ni-rGO sample in 10 mL of concentrated  $\text{HNO}_3$ . The mixture was heated at 80°C for 2 days until the solution became colorless. After cooling to ~30°C, the solution turned light green. Solution volume was maintained at 10 mL using 1% (w/w) nitric acid. Metal concentration in the leachate was measured using atomic absorption spectrometry (AAS) (Varian AA-420, USA) equipped with a deuterium background corrector and a hollow cathode lamp as the radiation source.

Specific surface area ( $S_{\text{BET}}$ ) of the prepared materials was determined using an Autosorb-1C instrument (Quantachrome, USA).  $\text{N}_2$  was used as an adsorbate probe molecule at 77 K over the  $P/P_0$  values ranging from 0.01 to 0.99. The reduction temperature of NiO-GO was determined from TPR analysis using the Quantachrome instrument.  $\text{H}_2$ -reduction was performed from 0 to 900°C. A ramp rate of 10°C per min was used for the reduction step. Surfaces of the materials were observed using high-resolution field emission scanning electron microscopy (FE-SEM) (JSM 7100F/JEOL, Netherlands) and the metal distributions were determined using energy-dispersive X-ray spectrometer (EDX) attached to the FE-SEM. Crystal lattices of the materials were determined using X-ray diffraction spectroscopy (XRD) (Pananalytical X'Pert Pro, UK). The samples were dried in vacuum and analysis was performed using Ni- $k_\alpha$  radiation ( $k = 1.54178 \text{ \AA}$ ) in the  $2\theta$  range 20–100° at a scan rate of 3° per min. Functional groups in the material surface were determined using Fourier-transform infrared spectroscopy (FT-IR) (Bruker Tensor 27, Germany). Spectra were recorded over the range 600–4000  $\text{cm}^{-1}$ .

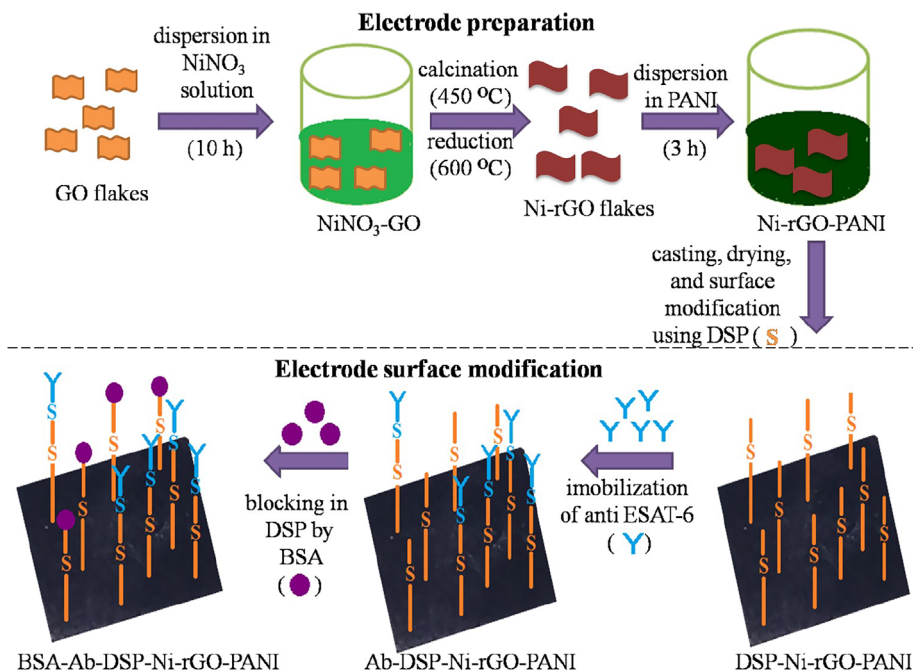


**FIGURE 1** | Electrode preparation and surface modification.

Graphitic content in the material was determined using Raman spectroscopy (Spex 1403, Singapore) with a He-Ne laser. The spectra were recorded using 532 nm excitation wavelength over the range 1000–3000  $\text{cm}^{-1}$ .

## Electrode Electrochemical Characterization

All electrochemical measurements were performed using the Autolab workstation (Metrohm, USA). In the three-electrode assembly, Ni-rGO-PANI was used as the working electrode, and Ag/AgCl and a Pt rod were used as the reference and counter electrodes, respectively. Analysis was performed in PBS solution at pH 7.2; this value was chosen because blood and sputum pH values for patients infected with TB are in the range (7.0–7.4) (41) and (6.8–7.5) (42), respectively. CV analysis was performed to determine electrode activity towards the antibody-antigen interactions from -1 to 1 V with a starting potential of 0 V at a scan rate of 10  $\text{mV s}^{-1}$ . EIS measurements were performed to determine impedance on the material surface. The measurements were taken over the frequency range  $10^{-4}$ – $10^2$  kHz under a set potential of 0 V, integration time of 0.125 s, and amplitude of 0.01 mV. All measurements were performed in triplicate; the data are reported as the mean of the measurements.

## RESULT AND DISCUSSION

### SEM and EDX Analysis

The SEM images of BSA-Ab-DSP-Ni-rGO-PANI at various stages of preparation are shown in **Figures 2A–F**. Flake-like

structure was observed in the GO sample (**Figure 2A**). Shiny dots in **Figure 2B** indicate that the Ni NPs are dispersed on the surface of the rGO flakes (indicated by arrow). The presence of Ni NPs on the surface of rGO was confirmed by the EDX analysis. The SEM image of PANI indicated an amorphous structure containing the randomly distributed micron-sized long particles (**Figure 2C**). A relatively more compact and dense structure was observed after the addition of Ni and rGO (**Figure 2D**), confirming the inclusion of rGO as well as Ni NPs. The supplementary file can be referred for the SEM images of the treated samples, viz., SEM images post-surface modification of Ni-rGO-PANI with DSP (**Supplementary Figure 1A**), antibody immobilization (**Supplementary Figure 1B**), and BSA (**Figure 2E** and **Supplementary Figure 1C**). Surface modification of Ni-rGO-PANI with DSP resulted in the coverage of the electrode surface with DSP layer, possibly blocking the pore-mouths, confirmed by the BET surface area analysis. **Figure 2F** and **Supplementary Figures 1D–F** show the EDX spectra of the fresh Ni-rGO-PANI sample and that of the sample after each surface modification step. The inset table shows elemental distributions, which confirms the presence of Ni (11.40% w/w) in Ni-rGO-PANI (before surface modification). The amount successively decreased to 6.4, 5.5 and 3.2% (w/w) after the surface modifications with DSP, Ab and BSA, respectively, confirming the coating of the surface modifying agents.

### Ni-Loading

The amount of Ni in Ni-rGO was quantitatively analyzed by the AAS analysis, and the metal loading was determined to be

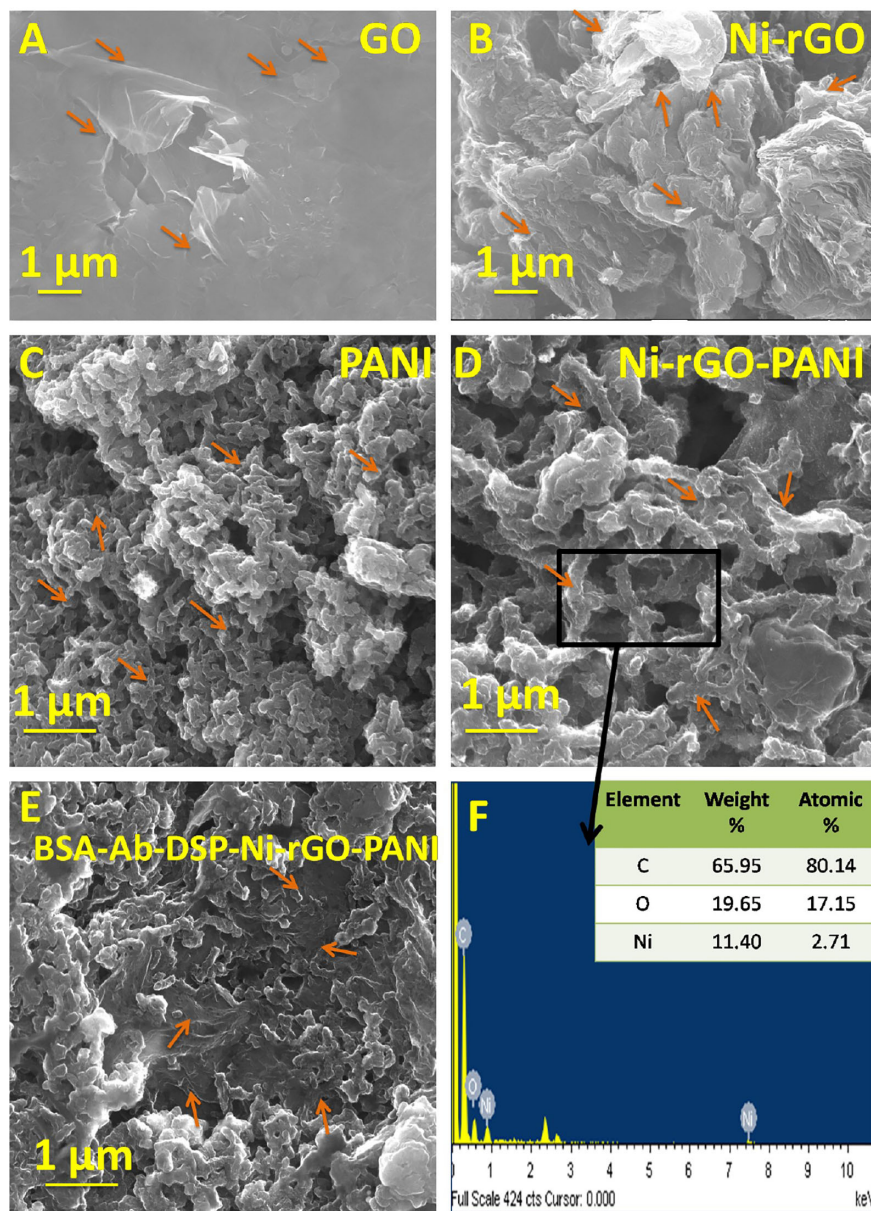


**FIGURE 2** | SEM images of (A) GO, (B) Ni-rGO, (C) PANI, (D) Ni-rGO-PANI, (E) BSA-Ab-DSP-Ni-rGO-PANI, and (F) EDX spectra of Ni-rGO-PANI. The arrows indicate the specific structures of the material.

approximately 59 mg/g. The data indicate a good amount of Ni-loading in the precursor material for the electrode. A relatively higher Ni-loading renders the resulting composite material to be a good electroconductive, which is beneficial for sensing application (28).

### TPR Analysis

**Figure 3A** shows the TPR spectra of GO and NiO-rGO. A sharp peak is observed at  $\sim 164^{\circ}\text{C}$  in GO, indicating the reduction of GO below  $200^{\circ}\text{C}$ . Only one peak was observed for NiO-rGO over the temperature range  $329 - 554^{\circ}\text{C}$ , indicating the reduction of

NiO to Ni. No peak was observed for GO, confirming the formation of rGO (reduction of GO to rGO) during calcinations. As mentioned earlier, the  $\text{H}_2$ -reduction was performed at  $600^{\circ}\text{C}$  to convert NiO to Ni in the NiO-rGO mixture.

### Raman Analysis

Raman spectra of the prepared materials (graphite powder, GO, Ni-rGO, Ni-rGO-PANI, and BSA-Ab-DSP-Ni-rGO-PANI) are shown in **Figure 3B**. Two bands, namely D and G, were detected in all materials; these are attributed to the D-band



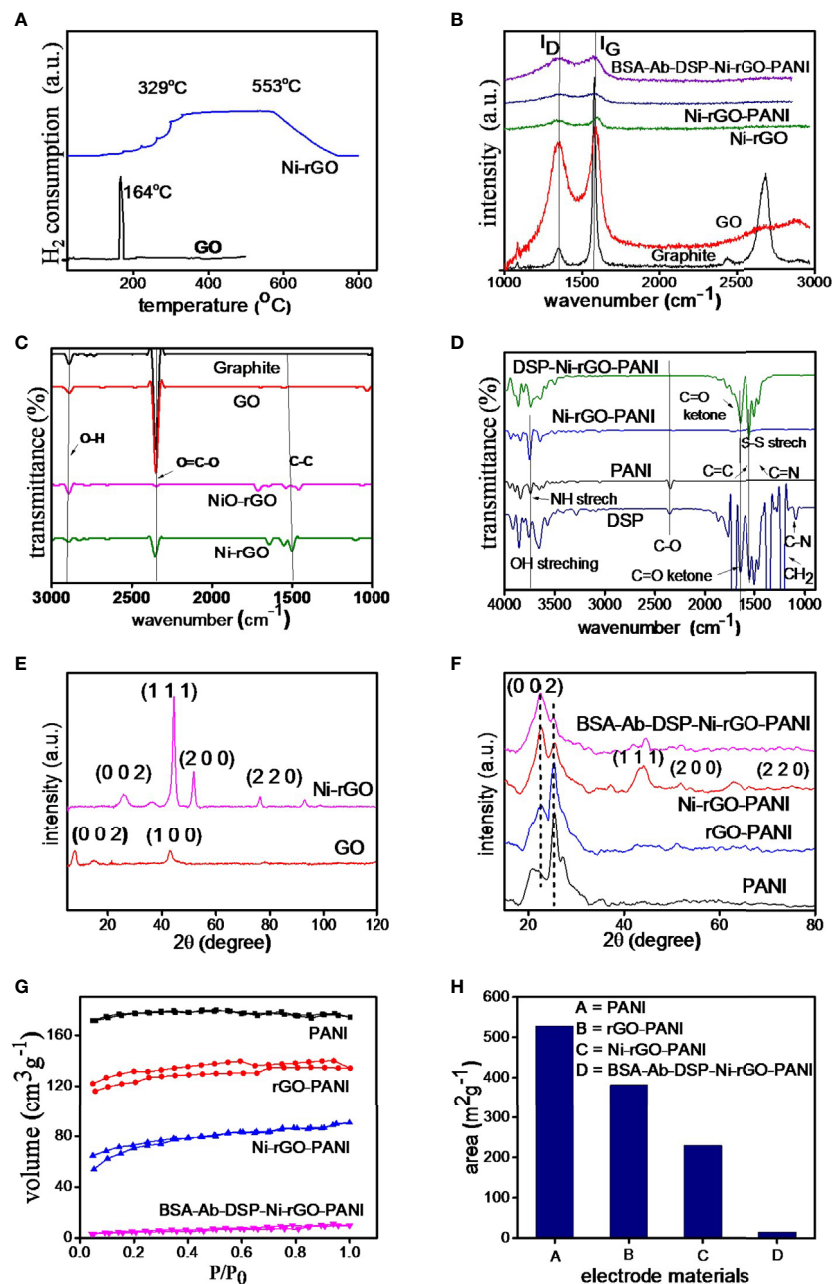


**FIGURE 3 |** (A) TPR of GO and NiO-GO, (B) RAMAN spectra of electrode materials, (C, D) FT-IR and (E, F) XRD spectra of the substrate and surface-modified materials, (G) BET isotherms and (H) surface area of the materials.

( $\sim 1343.27 \text{ cm}^{-1}$ ) signifying the disordered phase, and the G-band ( $\sim 1589.43 \text{ cm}^{-1}$ ) signifying the graphitic characteristics of the material. Graphite powder showed an additional 2D band, indicating the layered structure of the material. The  $I_D/I_G$  ratios were 0.10, 0.89, 0.98, 0.97, and 0.99 for graphite, GO, Ni-rGO, Ni-rGO-PANI, and BSA-Ab-DSP-Ni-rGO-PANI, respectively. An increase in the ratio is observed for Ni-rGO, indicating a decrease in the relative graphitic content of the

material. Further modification with PANI and antibody did not alter the graphitic characteristics of the material.

### FT-IR Analysis

**Figure 3C** shows the FT-IR spectra of graphitic powder, GO, NiO-rGO, and Ni-rGO. Common characteristic peaks observed at  $\sim 1200$ ,  $2300$ , and  $2800 \text{ cm}^{-1}$  in the materials are assigned to the aromatic ring C-C groups, carboxylic O=C-O, and O-H groups,



respectively. The intensity of the O=C-O peak decreased in the H<sub>2</sub>-reduced samples, indicating reduction of NiO and GO to Ni and rGO, respectively. **Figure 3D** shows the spectra of the DSP-modified materials. Three characteristic peaks were observed in PANI. Peaks at  $\sim 2200$ ,  $1750$ , and  $1600\text{ cm}^{-1}$  are attributed to the C-O, C $\equiv$ N, and C=C and groups, respectively. These peaks were observed in all three PANI-based materials. Five characteristic peaks were observed in DSP. Peaks at  $\sim 1750$ ,  $1650$ ,  $1500$ ,  $1250$  and  $1200\text{ cm}^{-1}$  are attributed to C=C, C=N, S-S, C=O ketone, and H-C-H stretching, respectively. These peaks were also observed in all DSP-coated materials, confirming the DSP coating on Ni-rGO-PANI.

## XRD Analysis

**Figure 3E** shows the XRD spectra of GO and Ni-rGO. The peak located at  $2\theta$  angle  $\sim 10^\circ$  in GO corresponds to the (0 0 1) crystallographic plane of C. However, the peak is absent in the rGO-containing materials, indicating conversion of GO to rGO during the H<sub>2</sub>-reduction step. The characteristic peaks observed at  $\sim 35$ ,  $43$ , and  $78^\circ$  in Ni-rGO correspond to the crystallographic (0 0 2), (1 1 1), and (2 2 0) planes of Ni, respectively. The peak at  $\sim 30^\circ$  in Ni-rGO-PANI is attributed to the presence of PANI and those at  $\sim 50$ ,  $55$ , and  $75^\circ$  are attributed to the (1 1 1), (2 0 0), and (2 2 0) planes of Ni, confirmed from JCPDS#70-0989 (**Figure 3F**).

## BET Analysis

**Figure 3G** shows N<sub>2</sub> adsorption-desorption isotherms of the prepared materials. The isotherms show the type-II characteristics as per the IUPAC classifications. BET areas were calculated from the isotherms. A relatively higher surface area was measured in the PANI film, indicating the porous characteristics of the material; this is consistent with SEM results that revealed pores in the material, discussed earlier (**Figure 3H**). BET surface area decreased as expected, with inclusion of rGO and Ni NPs in PANI, as the pores were partially blocked. It may be mentioned that the main objective of performing the BET analysis was to determine the surface area of the substrate (PANI). Coating (surface modification) of the electrode with DSP/Ab/BSA caused blocking of the pore mouths on the electrode surface. Thus, the BET area significantly decreased, corroborating the formation of a DSP/Ab/BSA layer on the Ni-rGO-PANI surface (**Supplementary Table 1**).

## CV and EIS Analysis

CV was performed on PANI, rGO-PANI, and Ni-rGO-PANI. Prior to the analysis, the scan rate was optimized using CV analysis at different rates  $10$ ,  $25$ ,  $50$ ,  $75$ ,  $100$ ,  $125$ , and  $150\text{ mV s}^{-1}$  (**Supplementary Figure 2A**). The current responses of the bare electrode (without surface modifications) in PBS showed a liner relationship with the square root of the scan rates (**Supplementary Figure 2B**), indicating the diffusion-controlled electron exchange mechanism at the surface of the electrode (43, 44).

The best electrode response (sharp and distinguished peak) was determined at  $10\text{ mVs}^{-1}$ . Hence, all analysis were performed at the scan rate of  $10\text{ mVs}^{-1}$ . PANI showed negligible peak

current during the CV measurements in PBS alone, as also reported in the literature (**Figure 4A**) (45, 46). However, rGO-PANI showed a reduction peak at the potential of approximately  $-0.1\text{ V}$  with a current response of  $0.62\text{ mA}$ , attributed to the electrocatalytic effects of rGO (47–49). The reduction potential slightly shifted in the range  $0.5 - 0.6\text{ V}$  in Ni-rGO-PANI. However, a relatively higher current response ( $0.82\text{ mA}$ ) was measured, attributed to the inclusion of the electrocatalytic Ni NPs in the material (50–52). EIS measurements were performed to determine the surface impedances of PANI, rGO-PANI, and Ni-rGO-PANI (**Figure 4B**). Data were fitted with Randles model circuit, as shown in the inset of the figure. **Supplementary Figure 2C** shows the magnified fitting-segment over the low impedance values for clarity. Solution resistances ( $R_s$ ) were approximately the same ( $\sim 1230\ \Omega$ ) for all materials. Charge-transfer resistance ( $R_{ct}$ ) was approximately  $11080\ \Omega$  at the PANI surface.  $R_{ct}$  decreased to  $\sim 10450$  and  $8804\ \Omega$  in rGO-PANI and Ni-rGO-PANI, respectively, which indicates low impedance on Ni-rGO-PANI; this is attributed to increased mobility of free electrons at the electrode surface because of the synergistic effects between rGO and Ni NPs (20, 45, 46, 53). Based on the data, PANI and rGO-PANI were removed from further consideration; in this study, only the Ni-rGO-PANI surface was modified with the antibody for *Mtb* sensing.

CV analysis of DSP-coated Ni-rGO-PANI displayed a similar reduction peak to that of Ni-rGO-PANI, however, at a diminished reduction potential ( $0.6\text{ V}$ ) and peak current ( $0.52\text{ mA}$ ) (**Figure 4C**). Further modifications of DSP-Ni-rGO-PANI by the antibody and BSA did not result in decrease of the reduction potential. The responses diminished in the surface-modified materials (**Figure 4C**), as the relative amounts of Ni in the surface-modified electrodes decreased, confirmed by the EDX analysis (**Supplementary Figure 1**). The role of the Ni NPs during sensing is, therefore, only to enhance the electroconductivity of the electrode. **Figure 4D** summarizes the peak currents measured for the materials.

## Sensor Calibration

The prepared BSA-Ab-DSP-Ni-rGO-PANI sensor was calibrated using seven different concentrations of the biomarker over the range  $1 - 100\text{ ng mL}^{-1}$ . Peak currents were measured over the range  $-0.5 - -0.6\text{ V}$  during CV analysis (**Figure 4E**). At  $0\text{ ng/mL}$ , the antibodies (bounded at the electrode surface) were free without adsorbing any protein molecules. Over the concentration range  $1 - 100\text{ ng mL}^{-1}$ , the antibodies interacted with the protein molecules *via* adsorption. The resistivity of the electrode increased, which caused decrease in the activity of electrode, requiring a relatively higher potential for the response. Therefore, the peak position slightly shifted to the more negative potentials. Currents decreased with increasing concentrations; this is attributed to an increased resistance of the electrode materials resulting from increased ESAT-6 bonding to the antibody (anti-ESAT-6) at high concentrations. When a protein molecule binds to an antibody, the insulating property of the electrode surface increases because of the non-conductive characteristics of the protein molecule. The insulation on the surface of the electrode blocks the movement of electrons,

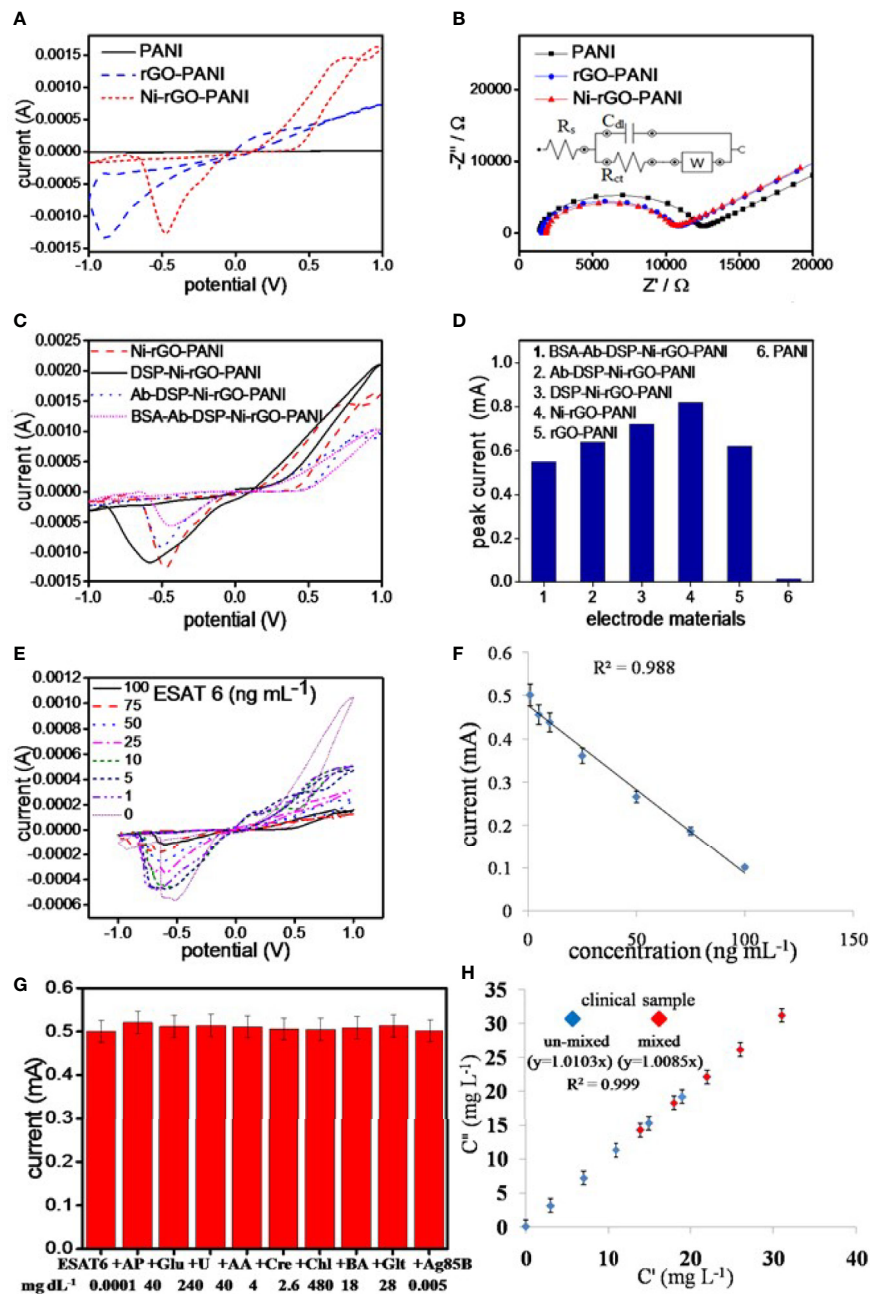


**FIGURE 4 |** (A) CV and (B) EIS analysis of the electrode materials, (C) CV analysis of the surface modified electrodes, (D) peak currents in the surface modified materials, (E) CV analysis of BSA-Ab-DSP-Ni-rGO-PANI at different ESAT-6 concentration, (F) calibration plot for the prepared TB sensor, (G) selectivity data measured at LOD, and (H) measurements in the synthetic clinical samples ( $C'$ ) vs. prepared ESAT-6 ( $C'$ ) in the clinical samples.

resulting in decrease of the peak currents during the CV analysis (17). Calibration data showed a good linearity ( $R^2 = 0.988$ ) over the measured ESAT-6 concentration range (Figure 4F). Current peaks were detected to a minimum concentration of  $1 \text{ ng mL}^{-1}$ . Peak currents corresponding to the measured concentrations, standard deviations (S.D.), and % relative standard deviations (RSD) are presented in **Supplementary Table 2**. The limit of

detection (LOD) and limit of quantification (LOQ) for ESAT-6 are  $1.042$  and  $3.065 \text{ ng mL}^{-1}$ , respectively, calculated using the following equations:

$$\text{LOD} = 3 \times \sigma_{\text{blank}}/S$$

$$\text{LOQ} = 10 \times \sigma/S.$$

where,  $\sigma_{\text{blank}}$ ,  $\sigma$ , and  $S$  are the standard deviation of the blank electrode, the standard deviation of the lowest concentration measured during the calibration, and the slope of calibration line, respectively.

## Selectivity and Interference Tests

The prepared sensor was tested for ESAT-6 along with another biomolecule present in human blood of healthy and infected people to confirm the selectivity of the sensor towards ESAT-6 protein molecule. Ag85B is also a TB biomarker, which is a secretory protein of *Mycobacterium tuberculosis*. Similarly, the biomolecules such as AP, Glu, U, AA, Cre, Chl, BA, and Glt are commonly present in blood and may interfere with the measurements. The concentrations of these molecules were used at the concentration levels two-times the respective upper permissible concentration in human blood (22, 54–56). The measurements were performed over the potential range optimized earlier. The ESAT-6 concentrations were taken at the lower and upper concentrations (1 and 100 ng mL<sup>-1</sup>, respectively) of the calibration curve. The CV measurements revealed no peaks other than that for ESAT-6 in the presence of the biomolecules (Supplementary Figure 2D). Also, the peak current value was approximately the same as before (without biomolecules) at LOD (Figure 4G) and at high concentration of the calibration plot (Supplementary Figure 2E). The data, therefore, clearly indicated the selectivity of the prepared sensor in this study towards ESAT-6 with negligible interference of the other biomolecules towards the detection of ESAT-6.

## Measurements in Blood Samples

The clinical blood samples were processed as described earlier in the Materials and Method section. The ESAT-6 protein was mixed at five different concentrations in blood plasma, and the concentration were measured using the CV analysis at the earlier optimized parameters. Supplementary Table 3 shows the SD values less than 0.2 and the RSD values less than 2%, clearly indicating the BSA-Ab-DSP-Ni-rGO-PANI electrode capable of measuring the ESAT-6 concentrations accurately in human blood. To validate the clinical measurements, five extra blood samples were prepared by mixing two clinical samples in the same volume (1:1). The new samples were termed as AC (A+C), AD (A+D), BD (B+D), CD (C+D) and CE (C+E). The CV measurements were taken and the data for peak currents are presented in Figure 4H. The SD and RSD values were determined to be < 1 and 2%, respectively. A calibration curve was plotted against the actual vs. prepared concentrations. The regressed lines were found to be approximately linear for the un-mixed and mixed samples. The data confirm that the BSA-Ab-DSP-Ni-rGO-PANI electrode was capable of detecting ESAT-6 in human blood efficiently and accurately.

## Measurement in Healthy (Recovered From Tuberculosis Infection) Blood Samples

ESAT-6 concentrations were measured in the blood samples of the patients recovered from the tuberculosis infection. As mentioned earlier, the samples were collected from the clinical

diagnostic laboratory. Blood cells were separated as per the previously described procedure. As shown in the CV spectra, the peak intensity was measured to be the same as that for 0 ng/ml concentration of the biomarker (ESAT-6) (Supplementary Figure 2F). It was inferred that ESAT-6 in healthy people was absent or below the detection limit of the sensor.

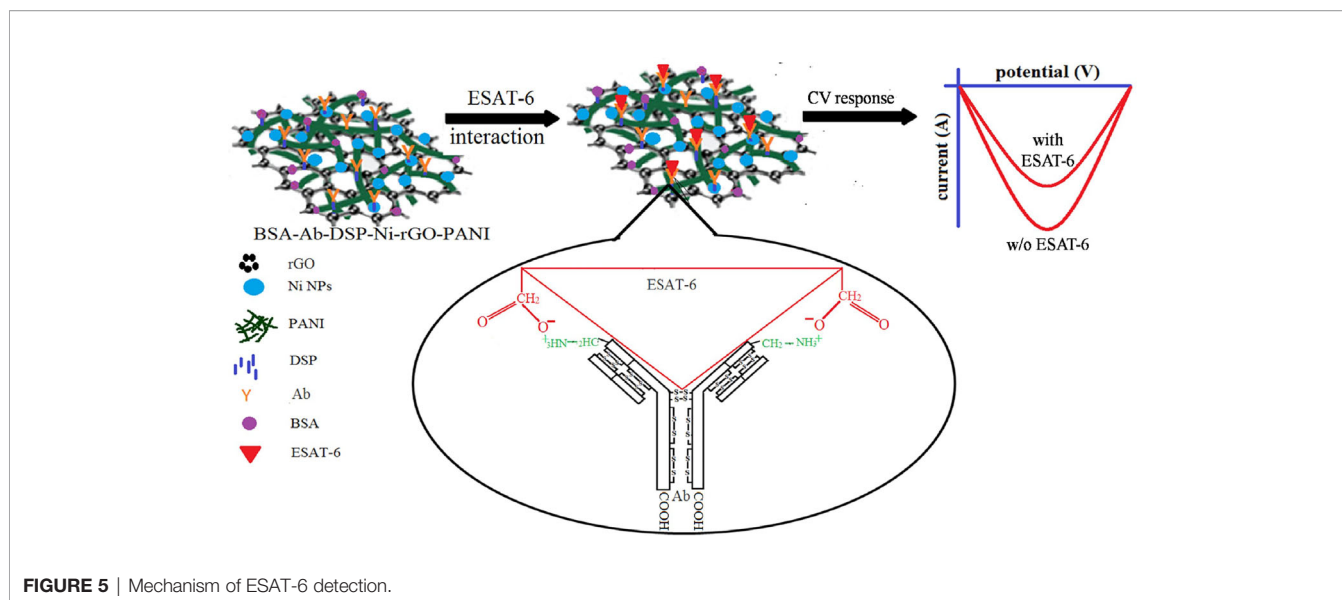
## Reuse of Spent Electrodes

Spent electrodes (BSA-Ab-DSP-Ni-rGO-PANI) were repeatedly washed with acetone and PBS, and dried in a N<sub>2</sub> atmosphere. Washed electrodes were subjected to another surface modification using the DSP cross-linker and ESAT-6 antibody. CV data were recorded at each step of the modification, as with the earlier electrodes. Sensor responses of the reused electrodes were approximately the same as those of the fresh electrodes (Supplementary Figure 2G). The washing, surface modification, and sensing steps were repeated more than ten times with the same electrode; CV data confirmed approximately the same response as before for the BSA-Ab-DSP-Ni-rGO-PANI electrode (Supplementary Figure 2H). Clearly, the Ni-rGO-PANI electrode (substrate/base) material can be used multiple times without decrease in its activity towards TB detection.

## Stability of the Electrode

BSA-Ab-DSP-Ni-rGO-PANI electrode samples were stored for 6 months in the refrigerator at 0°C under a sterile environment. CV analysis was performed on the preserved electrodes under the same conditions as described earlier to assess the stability of the material. Current peaks had approximately the same magnitudes as measured earlier for the fresh samples over the same potential range, indicating the material to be stable when stored in a sterilized environment (Supplementary Figure 2I). A plausible mechanism of the antigen–antibody interaction and ESAT-6 detection is schematically described in Figure 5. The ESAT-6 antigen binds with the antibody (anti ESAT-6) through ionic interaction between the O<sup>-</sup> of carboxylic group in the antigen and ammonium ion (NH<sub>3</sub><sup>+</sup>) of peptide chain in antibody via the electron transfer (57). During the sensing, the responses decreased with increasing concentrations of ESAT-6, as the antigen formed insulating layers, blocking the electron transfer (Figure 5) (17). Supplementary Figure 3 shows the digital photograph of the prepared electrode (Supplementary Figure 3A) and the sensing instrument (Supplementary Figure 3B) (58, 59).

We compared, wherever possible, the performances of the sensor prepared in this study with those of the electrochemical sensors discussed in the literature (Table 1) (5–7, 9, 12–14, 17, 54, 58). Using different biomarkers and their corresponding recognition elements, most of the *Mtb* sensors displayed a low detection limit and good linearity. In addition, reproducibility among these sensors is reported between 3 and 10 times. As mentioned earlier, only Diouani et al. (2016) have developed the anti-ESAT-6 recognition element-based electrochemical TB biosensor, however, using a relatively expensive SPE (17). On the other hand, the *Mtb* sensor developed in this study is based on the Ni-rGO-PANI electrode and uses the same recognition element (ESAT-6). The LOD of the sensor is 1.042 ng mL<sup>-1</sup>,



which is significantly lower than most of the previously developed sensors. Furthermore, the electrode material is stable and reusable, and the assay time is short.

## CONCLUSIONS

An electroconductive Ni-rGO-PANI electrode-based immunosensor was prepared to quantitatively detect ESAT-6, a biomarker for *Mtb*. Various physicochemical and electrochemical characterization techniques confirmed the effective step-wise surface modifications of the electrode with DSP, antibody, and BSA. CV analysis (potential range -1 to +1 V, starting potential 0 V, scan rate 10 mV s<sup>-1</sup>) demonstrated a decrease in peak current and distinct

peak-to-peak separation, indicating the successful immobilization of the antibody recognition element on the electrode surface. The electrode was able to detect ESAT-6 over the concentration range 1 - 100 ng mL<sup>-1</sup> with good linearity ( $R^2 = 0.988$ ). Analysis revealed that Ni-rGO-PANI is stable and that the sensor could be reused repeatedly after surface cleaning and modification; thus, both the material and preparation method are cost-effective. Future tests with the ESAT-6 immunosensor using serum and sputum from both TB-positive and -negative patients are required to implement this assay for a rapid and specific TB diagnosis. The BSA-AB-DSP-Ni-rGO-PANI-based immunosensor developed in this study will also be tested for the diagnosis of real samples of patients infected with tuberculosis infection, in collaboration with a medical college and/or medical research laboratories.

**TABLE 1** | Comparative performances of the TB electrochemical sensors.

Biomarker	Recognition element	Detection* technique	Detection limit	Stability	Reusability	Reproducibility	Linearity	Linearity range ( $\mu\text{g mL}^{-1}$ )	Assay time	Ref.
ESAT-6	Anti ESAT-6 (on Ni-rGO-PANI electrode)	CV	1.042 ng mL <sup>-1</sup>	> 6 months	> 10 times	>3 times	0.9814	0.001 - 0.01	~ 15 min	This study
ESAT-6	Anti ESAT-6 antibody (on gold-plated SPE)	SWV	7 ng mL <sup>-1</sup>	-	-	3 times	0.9920	0.01 - 50	-	17
Mycolic acid	Anti mycolic acid antibody	EIS	-	-	-	-	-	-	-	7
<i>Mtb</i>	Anti <i>Mtb</i> antibodies	CV	1 ng mL <sup>-1</sup>	-	-	3 times	0.999	0.05 - 0.5	-	6
<i>Mtb</i> DNA	DNA probe	DPV	1 CFU mL <sup>-1</sup>	-	-	-	-	-	90 min	9
Interferon $\gamma$	DNA aptamer	SWV	1 ng mL <sup>-1</sup>	-	-	10 times	0.9801	0.005-0.16	-	54
<i>Mtb</i> DNA	DNA Probe	DPV	10 $\mu\text{g mL}^{-1}$	-	-	-	0.8591	0.01 - 10	-	5
<i>Mtb</i> DNA	DNA Probe	CV	50 $\mu\text{g mL}^{-1}$	2-3 weeks	-	10 times	0.9870	-	-	58
E-DNA	DNA Probe	SWV	0.03 fM	-	-	4 times	-	-	-	14
<i>Mtb</i> DNA	DNA aptamer	EIS	100 CFU mL <sup>-1</sup>	-	-	3 times	0.9375	10 <sup>-5</sup> -0.01	2 h	12
<i>Mtb</i> DNA	DNA Probe	DVP	1.25 ng mL <sup>-1</sup>	-	-	-	-	-	-	13

\*SWV, square wave voltammetry; DPV, differential pulse voltammetry.



## DATA AVAILABILITY STATEMENT

The original contributions presented in the study are included in the article/**Supplementary Material**. Further inquiries can be directed to the corresponding authors.

## AUTHOR CONTRIBUTIONS

RO: Methodology, Data curation, Writing original draft. NV: Supervision, Investigation, Writing - review and editing. PA: Supervision, Writing - review and editing. All authors contributed to the article and approved the submitted version.

## REFERENCES

- Mi X, He F, Xiang M, Lian Y, Yi S. Novel Phage Amplified Multichannel Series Piezoelectric Quartz Crystal Sensor for Rapid and Sensitive Detection of *Mycobacterium Tuberculosis*. *Anal Chem* (2011) 84:939–46. doi: 10.1021/ac2020728
- Marais BJ, Pai M. New Approaches and Emerging Technologies in the Diagnosis of Childhood Tuberculosis. *Respir Rev* (2007) 8:124–33. doi: 10.1016/j.prv.2007.04.002
- Zhou L, He X, He D, Wang K, Qin D. Biosensing Technologies for *Mycobacterium Tuberculosis* Detection: Status and New Developments. *Clin Dev Immunol* (2011) 2011:1–8. doi: 10.1155/2011/193963
- Yemini M, Levi Y, Yagil E, Rishpon J. Specific Electrochemical Phage Sensing for *Bacillus Cereus* and *Mycobacterium Smegmatis*. *Bioelectrochemistry* (2007) 70:180–84. doi: 10.1016/j.bioelechem.2006.03.014
- Torres-Chavolla E, Alcolija EC. Nanoparticle Based Dna Biosensor for Tuberculosis Detection Using Thermophilic Helicase-Dependent Isothermal Amplification. *Biosens Bioelectron.* (2011) 26:4614–18. doi: 10.1016/j.bios.2011.04.055
- Diaz-González M, González-García MB, Costa-García A. Immunosensor for *Mycobacterium Tuberculosis* on Screen-Printed Carbon Electrodes. *Biosens Bioelectron.* (2005) 20:2035–43. doi: 10.1016/j.bios.2004.09.035
- Mathebula NS, Pillay J, Toschi G, Verschoor JA, Ozoemena KI. Recognition of Anti-Mycolic Acid Antibody at Self-Assembled Mycolic Acid Antigens on a Gold Electrode: A Potential Impedimetric Immunosensing Platform for Active Tuberculosis. *Chem Commun* (2009) 23:3345–47. doi: 10.1039/B905192A
- Nellaippan S, Kumar AS. Electrocatalytic Oxidation and Flow Injection Analysis of Isoniazid Drug Using a Gold Nanoparticles Decorated Carbon Nanofibers-Chitosan Modified Carbon Screen Printed Electrode in Neutral Ph. *J.Electroanal. Chem* (2017) 801:171–78. doi: 10.1016/j.jelechem.2017.07.049
- Lavana S, Das R, Dhiman A, Myneedu VP, Verma A, Singh N, et al. Aptamer-Based TB Antigen Tests for the Rapid Diagnosis of Pulmonary Tuberculosis: Potential Utility in Screening for Tuberculosis. *ACS Infect Dis* (2018) 4:1718–26. doi: 10.1021/acscinfecdis.8b00201
- Zaid MHM, Abdullah J, Yusof NA, Sulaiman Y, Wasoh H, Noh MFM, et al. Pna Biosensor Based on Reduced Graphene Oxide/Water Soluble Quantum Dots for the Detection of *Mycobacterium Tuberculosis*. *Sens. Actuators B Chem* (2017) 241:1024–34. doi: 10.1016/j.snb.2016.10.045
- Singh A, Choudhary M, Singh MP, Verma HN, Singh SP, Arora K. Dna Functionalized Direct Electro-Deposited Gold Nanoaggregates for Efficient Detection of *Salmonella Typhi*. *Bioelectrochemistry* (2015) 105:7–15. doi: 10.1016/j.bioelechem.2015.03.005
- Zhang X, Feng Y, Duan S, Su L, Zhang J, He F. *Mycobacterium Tuberculosis* Strain H37Rv Electrochemical Sensor Mediated by Aptamer and Aunps–DNA. *ACS Sens* (2019) 4:849–55. doi: 10.1021/acscsensors.8b01230
- Thiruppathiraja C, Kamatchiammal S, Adaikkappan P, Santhosh DJ, Alagar M. Specific Detection of *Mycobacterium Sp.* Genomic Dna Using Dual Labeled Gold Nanoparticle Based Electrochemical Biosensor. *Anal Biochem* (2011) 417:73–9. doi: 10.1016/j.ab.2011.05.034
- Miodek A, Mejri N, Gomgnimbou M, Sola C, Korri-Yousoufi H. E-Dna Sensor of *Mycobacterium Tuberculosis* Based on Electrochemical Assembly of

## ACKNOWLEDGMENTS

The authors acknowledge the Department of Science and Technology (DST) and Ministry of Science and Education, Delhi for providing financial support (DST/CNS/2017239) for this study.

## SUPPLEMENTARY MATERIAL

The Supplementary Material for this article can be found online at: <https://www.frontiersin.org/articles/10.3389/fimmu.2021.653853/full#supplementary-material>

- Nanomaterials (Mwcnts/Ppy/Pamam). *Anal Chem* (2015) 87:9257–64. doi: 10.1021/acs.analchem.5b01761
- Gharekhani H, Olad A, Hosseinzadeh F. Reduced Graphene Oxide Nanoribbon Immobilized Gold Nanoparticle Based Electrochemical DNA Biosensor for the Detection of *Mycobacterium Tuberculosis*. *J Mater Chem B* (2018) 6:5181–87. doi: 10.1039/C8TB01604F
- Schuh R, Kremmer E, Ego E, Wasiliu M, Thierfelder S. Determination of Monoclonal Antibody Specificity by Immunoabsorption and Western Blotting. *J Immunol Methods* (1992) 152:59–67. doi: 10.1016/0022-1759(92)90089-C
- Diouani MF, Ouerghi O, Refai A, Belgacem K, Tlili C, Laouini D, et al. Detection of ESAT-6 by a Label Free Miniature Immuno-Electrochemical Biosensor as a Diagnostic Tool for Tuberculosis. *Mater Sci Eng. C* (2017) 474:65–470. doi: 10.1016/j.msec.2016.12.051
- Pandey I, Bairagi PK, Verma N. Electrochemically Grown Polymethylene Blue Nanofilm on Copper-Carbon Nanofiber Nanocomposite: An Electrochemical Sensor for Creatinine. *Sens. Actuators B Chem* (2018) 277:562–70. doi: 10.1016/j.snb.2018.09.036
- Bairagi PK, Verma N. Electrochemically Deposited Dendritic Poly (Methyl Orange) Nanofilm on Metal-Carbon-Polymer Nanocomposite: A Novel non-Enzymatic Electrochemical Biosensor for Cholesterol. *J Electroanal. Chem* (2018) 814:134–43. doi: 10.1016/j.jelechem.2018.02.011
- Krishnan SK, Singh E, Singh P, Meyyappan M, Nalwa HS. A Review on Graphene-Based Nanocomposites for Electrochemical and Fluorescent Biosensors. *RSC Adv* (2019) 9:8778–81. doi: 10.1039/C8RA09577A
- Alwarappan S, Erdem A, Liu C, Li CZ. Probing the Electrochemical Properties of Graphene Nanosheets for Biosensing Applications. *J Phys Chem C*. (2009) 113:8853–57. doi: 10.1021/jp9010313
- Bairagi PK, Verma N. Electro-Polymerized Polyacrylamide Nano Film Grown on a Ni-reduced Graphene Oxide-Polymer Composite: A Highly Selective non-Enzymatic Electrochemical Recognition Element for Glucose. *Sens. Actuators B Chem* (2019) 289:216–25. doi: 10.1016/j.snb.2019.03.057
- Zhu X, Xu J, Duan X, Lu L, Zhang K, Yu Y, et al. Controlled Synthesis of Partially Reduced Graphene Oxide: Enhance Electrochemical Determination of Isoniazid With High Sensitivity and Stability. *J Electroanal. Chem* (2015) 757:183–91. doi: 10.1016/j.jelechem.2015.09.038
- Pei Y, Hu M, Tu F, Tang X, Huang W, Chen S, et al. Ultra-Rapid Fabrication of Highly Surface-Roughened Nanoporous Gold Film From AuSn Alloy With Improved Performance for Nonenzymatic Glucose Sensing. *Biosens. Bioelectron.* (2018) 117:758–65. doi: 10.1016/j.bios.2018.07.021
- Zhang P, Sun T, Rong S, Zeng D, Yu H, Zhang Z, et al. A Sensitive Amperometric AChE-biosensor for Organophosphate Pesticides Detection Based on Conjugated Polymer and Ag-rGO-NH<sub>2</sub> Nanocomposite. *Bioelectrochemistry* (2019) 127:163–70. doi: 10.1016/j.bioelechem.2019.02.003
- Lin S, Feng W, Miao X, Zhang X, Chen S, Chen Y, et al. A Flexible and Highly Sensitive Nonenzymatic Glucose Sensor Based on DVD-laser Scribed Graphene Substrate. *Biosens. Bioelectron.* (2018) 110:89–96. doi: 10.1016/j.bios.2018.03.019
- Ziołkowski R, Olejniczak AB, Górski Ł, Janusik J, Leśnikowski ZJ, Malinowska E. Electrochemical Detection of DNA Hybridization Using Metallocarborane

- Unit. *Bioelectrochemistry* (2012) 87:78–83. doi: 10.1016/j.bioelechem.2011.10.005
28. Nie H, Yao Z, Zhou X, Yang Z, Huang S. Nonenzymatic Electrochemical Detection of Glucose Using Well-Distributed Nickel Nanoparticles on Straight Multi-Walled Carbon Nanotubes. *Biosens. Bioelectron* (2011) 30:28–34. doi: 10.1016/j.bios.2011.08.022
  29. Sun A, Zheng J, Sheng Q. Highly Sensitive non-Enzymatic Glucose Sensor Based on Nickel and Multi-Walled Carbon Nanotubes Nanohybrid Films Fabricated by One-Step Co-Electrodeposition in Ionic Liquids. *Electrochim. Acta* (2012) 65:64–9. doi: 10.1016/j.electacta.2012.01.007
  30. Singh S, Bairagi PK, Verma N. Candle Soot-Derived Carbon Nanoparticles: An Inexpensive and Efficient Electrode for Microbial Fuel Cells. *Electrochim. Acta* (2018) 264:119–27. doi: 10.1016/j.electacta.2018.01.110
  31. Yu H, Jian X, Jin J, Wang F, Wang Y, Qi GC. Preparation of Hybrid Cobalt-Iron Hexacyanoferrate Nanoparticles Modified Multi-Walled Carbon Nanotubes Composite Electrode and its Application. *J Electroanal. Chem* (2013) 700:47–53. doi: 10.1016/j.jelechem.2013.03.015
  32. Absalan G, Akhond M, Soleimani M, Ershadifar H. Efficient Electrocatalytic Oxidation and Determination of Isoniazid on Carbon Ionic Liquid Electrode Modified With Electrodeposited Palladium Nanoparticles. *J Electroanal. Chem* (2016) 761:1–7. doi: 10.1016/j.jelechem.2015.11.041
  33. Kononenko NA, Loza NV, Shkirskaia SA, Falina IV, Khanukaeva DY. Influence of Conditions of Polyaniline Synthesis in Perfluorinated Membrane on Electrotransport Properties and Surface Morphology of Composites. *J Solid State Electrochem.* (2015) 19:2623–31. doi: 10.1007/s10008-015-2829-4
  34. Marcano DC, Kosynkin DV, Berlin JM, Sinitskii A, Sun Z, Slesarev A, et al. Improved Synthesis of Graphene Oxide. *ACS Nano*. (2010) 4:4806–14. doi: 10.1021/nn1006368
  35. Kumar A, Omar RA, Verma N. Efficient Electro-Oxidation of Diclofenac Persistent Organic Pollutant in Wastewater Using Carbon Film-Supported Cu-rGO Electrode. *Chemosphere* (2020) 248:126030. doi: 10.1016/j.chemosphere.2020.126030
  36. Lv W, Sun F, Tang DM, Fang HT, Liu C, Yang QH, et al. A Sandwich Structure of Graphene and Nickel Oxide With Excellent Supercapacitive Performance. *J Mater Chem* (2011) 21:9014–19. doi: 10.1039/C1JM10400D
  37. Zhao B, Song J, Liu P, Xu W, Fang T, Jiao Z, et al. Monolayer Graphene/Nio Nanosheets With Two-Dimension Structure for Supercapacitors. *J Mater Chem* (2011) 21:18792–98. doi: 10.1039/C1JM13016A
  38. Amano K, Ishikawa H, Kobayashi A, Satoh M, Hasegawa E. Thermal Stability of Chemically Synthesized Polyaniline. *Synth. Met.* (1994) 62:229–32. doi: 10.1016/0379-6779(94)90210-0
  39. Cabrita JF, Abrantes LM, Viana AS. N-Hydroxysuccinimide-Terminated Self-Assembled Monolayers on Gold for Biomolecules Immobilisation. *Electrochim. Acta* (2005) 50:2117–24. doi: 10.1016/j.electacta.2004.09.019
  40. Omar RA, Verma N, Arora PK. Sequential Desulfurization of Thiol Compounds Containing Liquid Fuels: Adsorption Over Ni-Doped Carbon Beads Followed by Biodegradation Using Environmentally Isolated *Bacillus Zhangzhouensis*. *Fuel* (2020) 277:118208. doi: 10.1016/j.fuel.2020.118208
  41. Kellum JA. Determinants of Blood Ph in Health and Disease. *Crit Care* (2000) 6:1–9. doi: 10.1186/cc644
  42. Masuda M, Sato T, Sakamaki K, Kudo M, Kaneko T, Ishigatsubo Y. The Effectiveness of Sputum Ph Analysis in the Prediction of Response to Therapy in Patients With Pulmonary Tuberculosis. *Peer J* (2015) 3:1448. doi: 10.7717/peerj.1448
  43. Zhong H, Yuan R, Chai Y, Li W, Zhong X, Zhang Y. In Situ Chemo-Synthesized Multi-Wall Carbon Nanotube-Conductive Polyaniline Nanocomposites: Characterization and Application for a Glucose Amperometric Biosensor. *Talanta* (2011) 85:104–11. doi: 10.1016/j.talanta.2011.03.040
  44. Bairagi PK, Goyal A, Verma N. Methyl Nicotinate Biomarker of Tuberculosis Voltammetrically Detected on Cobalt Nanoparticle-Dispersed Reduced Graphene Oxide-Based Carbon Film in Blood. *Sens. Actuators B Chem* (2019) 297:126754. doi: 10.1016/j.snb.2019.126754
  45. Kulandaivalu S, Zainal Z, Sulaiman Y. Influence of Monomer Concentration on the Morphologies and Electrochemical Properties of PEDOT, PANI, and PPy Prepared From Aqueous Solution. *Int J Polym. Sci* (2016) 2016:1–12. doi: 10.1155/2016/8518293
  46. Chen WC, Wen TC, Gopalan A. Negative Capacitance for Polyaniline: An Analysis Via Electrochemical Impedance Spectroscopy. *Synth. Met.* (2002) 128:179–89. doi: 10.1016/S0379-6779(01)00667-1
  47. Lashkenari MS, Ghasemi AK, Ghorbani M, Rezaei S. Fabrication of RGO/PANI-supported Pt/Cu Nanoparticles as Robust Electrocatalyst for Alkaline Methanol Electrooxidation. *J Mater Sci.: Mater Electron* (2021) 32:4833–45. doi: 10.1007/s10854-020-05222-5
  48. Chen N, Ren Y, Kong P, Tan L, Feng H, Luo Y. In Situ One-Pot Preparation of Reduced Graphene Oxide/Polyaniline Composite for High-Performance Electrochemical Capacitors. *Appl Surf. Sci* (2017) 392:71–9. doi: 10.1016/j.apsusc.2016.07.168
  49. Ng JC, Tan CY, Ong BH, Matsuda A, Basirun WJ, Tan WK, et al. Novel Palladium-Guanine-Reduced Graphene Oxide Nanocomposite as Efficient Electrocatalyst for Methanol Oxidation Reaction. *Mater Res Bull* (2019) 112:213–20. doi: 10.1016/j.materresbull.2018.12.029
  50. Darvishi S, Souissi M, Karimzadeh F, Kharaziha M, Sahara R, Ahadian S. Ni Nanoparticle-Decorated Reduced Graphene Oxide for non-Enzymatic Glucose Sensing: An Experimental and Modeling Study. *Electrochim. Acta* (2017) 240:388–98. doi: 10.1016/j.electacta.2017.04.086
  51. Ayoub H, Griveau S, Lair V, Brunswick P, Cassir M, Bedioui F. Electrochemical Characterization of Nickel Electrodes in Phosphate and Carbonate Electrolytes in View of Assessing a Medical Diagnostic Device for the Detection of Early Diabetes. *Electroanalysis* (2010) 22:2483–90. doi: 10.1002/elan.201000307
  52. Moharana M, Mallik A. Nickel Electrocrystallization in Different Electrolytes: An in-Process and Post Synthesis Analysis. *Electrochim Acta* (2013) 98:1–10. doi: 10.1016/j.electacta.2013.03.031
  53. Choi W, Shin HC, Kim JM, Choi JY, Yoon WS. Modeling and Applications of Electrochemical Impedance Spectroscopy (EIS) for Lithium-Ion Batteries. *J Electrochem. Sci Technol* (2020) 11:1–13. doi: 10.33961/jecst.2019.00528
  54. Liu Y, Tuleouva N, Ramanculov E, Revzin A. Aptamer-Based Electrochemical Biosensor for Interferon Gamma Detection. *Anal Chem* (2010) 82:8131–36. doi: 10.1021/ac101409t
  55. Wang H, Yuan X, Zeng G, Wu Y, Liu Y, Jiang Q, et al. Three Dimensional Graphene Based Materials: Synthesis and Applications From Energy Storage and Conversion to Electrochemical Sensor and Environmental Remediation. *Adv Colloid Interfac Sci* (2015) 221:41–59. doi: 10.1016/j.cis.2015.04.005
  56. Trzaskowski M, Napiórkowska A, Augustynowicz-Kopeć E, Ciach T. Detection of Tuberculosis in Patients With the Use of Portable Spr Device. *Sens. Actuators B Chem* (2018) 260:786–92. doi: 10.1016/j.snb.2017.12.183
  57. Van Oss CJ, Good RJ, Chaudhury MK. Nature of the Antigen-Antibody Interaction: Primary and Secondary Bonds: Optimal Conditions for Association and Dissociation. *J Chromatogr B* (1986) 376:111–19. doi: 10.1016/S0378-4347(00)80828-2
  58. Torati SR, Reddy V, Yoon SS, Kim C. Electrochemical Biosensor for *Mycobacterium Tuberculosis* DNA Detection Based on Gold Nanotubes Array Electrode Platform. *Biosens. Bioelectron* (2016) 78:483–88. doi: 10.1016/j.bios.2015.11.098
  59. Jayeoye TJ, Rujiralai T. Sensitive and Selective Colorimetric Probe for Fluoride Detection Based on the Interaction Between 3-Aminophenylboronic Acid and Dithiobis (Succinimidylpropionate) Modified Gold Nanoparticles. *New J Chem* (2020) 44:5711–19. doi: 10.1039/D0NJ00897D

**Conflict of Interest:** The authors declare that the research was conducted in the absence of any commercial or financial relationships that could be construed as a potential conflict of interest.

Copyright © 2021 Omar, Verma and Arora. This is an open-access article distributed under the terms of the Creative Commons Attribution License (CC BY). The use, distribution or reproduction in other forums is permitted, provided the original author(s) and the copyright owner(s) are credited and that the original publication in this journal is cited, in accordance with accepted academic practice. No use, distribution or reproduction is permitted which does not comply with these terms.



# The Frequency and Effect of Granulocytic Myeloid-Derived Suppressor Cells on Mycobacterial Survival in Patients With Tuberculosis: A Preliminary Report

Malika Davids<sup>1</sup>, Anil Pooran<sup>1</sup>, Liezel Smith<sup>1,2</sup>, Michele Tomasicchio<sup>1</sup> and Keertan Dheda<sup>1,3\*</sup>

<sup>1</sup> Centre for Lung Infection and Immunity, Division of Pulmonology, Department of Medicine and UCT Lung Institute & South African MRC/UCT Centre for the Study of Antimicrobial Resistance, University of Cape Town, Cape Town, South Africa, <sup>2</sup> DSI-NRF Centre of Excellence for Biomedical Tuberculosis Research; South African Medical Research Council Centre for Tuberculosis Research; Division of Molecular Biology and Human Genetics, Faculty of Medicine and Health Sciences, Stellenbosch University, Cape Town, South Africa, <sup>3</sup> Department of Immunology and Infection, Faculty of Infectious and Tropical Diseases, London School of Hygiene and Tropical Medicine, London, United Kingdom

## OPEN ACCESS

### Edited by:

Adam Penn-Nicholson,  
Foundation for Innovative New  
Diagnostics, Switzerland

### Reviewed by:

Carmen Judith Serrano,  
Mexican Social Security Institute  
(IMSS), Mexico  
Jayne S. Sutherland,  
Medical Research Council The  
Gambia Unit (MRC), Gambia

### \*Correspondence:

Keertan Dheda  
Keertan.dheda@uct.ac.za

### Specialty section:

This article was submitted to  
Microbial Immunology,  
a section of the journal  
Frontiers in Immunology

**Received:** 05 March 2021

**Accepted:** 05 May 2021

**Published:** 01 June 2021

### Citation:

Davids M, Pooran A, Smith L,  
Tomasicchio M and Dheda K (2021)  
The Frequency and Effect of  
Granulocytic Myeloid-Derived  
Suppressor Cells on Mycobacterial  
Survival in Patients With Tuberculosis:  
A Preliminary Report.  
Front. Immunol. 12:676679.  
doi: 10.3389/fimmu.2021.676679

**Introduction:** Protective host responses in those exposed to or infected with tuberculosis (TB) is thought to require a delicate balance between pro-inflammatory and regulatory immune responses. Myeloid-derived suppressor cells (MDSCs), regulatory cells that dampen T-cell function, have been described in cancer and other infectious diseases but there are limited data on their role in TB.

**Methods:** Peripheral blood was obtained from patients with active pulmonary TB and participants with presumed latent TB infection (LTBI) from Cape Town, South Africa. MDSC frequency was ascertained by flow cytometry. Purified MDSCs were used to assess (i) their suppressive effect on T-cell proliferation using a Ki67 flow cytometric assay and (ii) their effect on mycobacterial containment by co-culturing with H37Rv-infected monocyte-derived macrophages and autologous pre-primed effector T-cells with or without MDSCs. Mycobacterial containment was measured by plating colony forming units (CFU).

**Results:** MDSCs (CD15<sup>+</sup>HLA-DR<sup>+</sup>CD33<sup>+</sup>) had significantly higher median frequencies (IQR) in patients with active TB (n=10) versus LTBI (n= 10) [8.2% (6.8–10.7) versus 42.2% (27–56) respectively; p=0.001]. Compared to MDSC-depleted peripheral blood mononuclear and effector T cell populations, dilutions of purified MDSCs isolated from active TB patients suppressed T-cell proliferation by up to 72% (n=6; p=0.03) and significantly subverted effector T-cell-mediated containment of H37Rv in monocyte-derived macrophages (n=7; 0.6% versus 8.5%; p=0.02).

**Conclusion:** Collectively, these data suggest that circulating MDSCs are induced during active TB disease and can functionally suppress T-cell proliferation and subvert mycobacterial containment. These data may inform the design of vaccines and

immunotherapeutic interventions against TB but further studies are required to understand the mechanisms underpinning the effects of MDSCs.

**Keywords:** myeloid derived suppressor cells, MDSC, tuberculosis, immunology, biomarkers

## INTRODUCTION

Tuberculosis (TB) is the leading cause of death due to a single infectious agent (1). Although TB is largely a curable disease with a global treatment success rate of ~85%, almost 1.5 million people succumbed to the disease in 2019 (1). This is likely to worsen due the rapid emergence and global spread of drug resistant forms of the disease which threaten to derail advances in TB control (2). Eradication of TB is only likely to be achieved with an effective vaccine. Currently, the only licensed TB vaccine is an attenuated strain of *Mycobacterium bovis* (*M.b.v.*), BCG (3). BCG confers protection against severe forms of TB disease in children but offers limited protection (~30%) against adult forms of pulmonary disease (4). Data from recently trialled vaccine candidates have not offered much hope. For instance, MVA85A did not show any improvement compared to BCG despite compelling pre-clinical animal data (5), and the more recently trailed M72/AS01 performed much better but was still only associated with an efficacy of only ~50% (6). These studies and their outcomes highlight our incomplete understanding of the immune mechanisms underpinning protective immunity and bacterial persistence.

One of the central hallmarks of active TB disease is a failed T-cell effector immune response (7). However, there is still much that is not known about the specific immune mechanisms underpinning failed T-cell immunity (8). In active TB disease immunity associated with recovery is traditionally thought to be primarily driven by pro-inflammatory effector T-cells, and cytotoxic CD8 cells (8). However, the host immunity also involves several regulatory mechanisms for suppressing T-cell responses against *M. tb*-specific antigens, which may be leveraged by pathogens to their advantage. Such strategies may also underpin the extensive immunopathology associated with TB.

Myeloid-derived suppressor cells (MDSCs) is one type of regulatory cell that potently regulates cancer immunity at the site of pathology (9). MDSCs have a morphology similar to granulocytes and/or monocytes (10). In healthy individuals, immature myeloid cells are generated in the bone marrow and rapidly differentiate into mature macrophages, dendritic cells, or granulocytes (10). MDSCs can broadly be classified into three groups: 1) early-stage-MDSC (LIN<sup>1</sup>HLA-DR<sup>-low</sup>CD11b<sup>+</sup>CD33<sup>+</sup>), 2) polymorphonuclear-MDSC (HLA-DR<sup>-low</sup>CD14<sup>-</sup>CD15<sup>+</sup>CD33<sup>+/dim</sup>), and 3) monocytic-MDSC (HLA-DR<sup>-low</sup>CD14<sup>+</sup>CD15<sup>-</sup>CD33<sup>+</sup>) (10). This report specifically focuses on polymorphonuclear-MDSCs (PMN-MDSCs), also known as granulocytic-MDSCs.

Others have previously shown that regulatory pathways (11, 12), including MDSCs are upregulated in patients with active TB (13–17), their frequency in peripheral blood decreases with

successful treatment (14), and MDSCs are able to inhibit T-cell proliferation (13). However, data are limited to a handful of studies (less than 5), and there are hardly any data from humans or TB-endemic settings (13). Furthermore, there are no published data about the biological significance of these cells and the ability of MDSCs to directly restrict mycobacterial growth. Thus, their role during *M. tb* infection remains unclear. To address these knowledge gaps, we explored the levels of M-MDSCs in patients with active TB versus those who are latently infected, and whether they abrogated the ability of effector T-cells to contain mycobacterial growth.

## METHODS

### Participants and Ethical Approval

HIV-uninfected participants were recruited from various primary healthcare clinics around Cape Town between January 2017 and February 2019. Presumed LTBI participants were healthy asymptomatic individuals with no clinical or radiological evidence of previous or active TB disease and were both tuberculin skin test (TST; induration >10mm) and interferon-gamma release assay (QuantiFERON<sup>®</sup>-TB Gold) positive. TB patients were microbiologically confirmed by sputum smear microscopy, Xpert MTB/RIF, and/or MGIT sputum culture, and had <1 week of anti-TB therapy at the time of recruitment. Informed written consent was obtained from all patients and the study was approved by the UCT Research Ethics Committee. Participants were excluded from the study if they were HIV-infected, pregnant or younger than 18 years of age.

### Flow Cytometry

Peripheral blood was obtained from all study participants by venipuncture. 100μl whole blood were seeded in a 96-well tissue culture plate and either left unstimulated or stimulated with 12μg/ml purified protein derivative (PPD; Statens Serum Institute) overnight at 37°C with 5% CO<sub>2</sub>. The cells were subsequently stained using fluorescently labelled antibodies specific for cell surface markers [CD14, CD33, HLA-DR and CD15; (BD Biosciences, Ebiosciences, Biolegend)]. Thereafter, the cells were fixed in 4% paraformaldehyde and data acquired on an LSRII flow cytometer.

### Myeloid-Derived Suppressor Cells Isolation

MDSCs were isolated as previously described by Lechner et al. (18), with modifications. Briefly, whole blood was separated over a density gradient (Histopaque 1077, Sigma-Aldrich) into the



1) plasma, 2) mononuclear cell (PBMC) layer, and 3) erythrocyte/granulocyte layer. The layer containing erythrocytes and granulocytes were harvested and erythrocytes were lysed (BD cell lysis solution). The granulocytic cell fraction was incubated with CD15 MACSiBead particles for positive selection of CD15 cells. HLA-DR<sup>+</sup> cells were isolated from the CD15<sup>+</sup> cell fraction by immuno-magnetic separation (MACS beads, MACS LS-column, Miltenyi Biotec). The CD15<sup>+</sup>HLA-DR<sup>+</sup> cell fraction was incubated with CD33 microbeads for positive selection of CD15<sup>+</sup>HLA-DR<sup>+</sup>CD33<sup>+</sup> cells (Miltenyi Biotec). Purity of the MDSC population exceeded 95% as confirmed by flow cytometry.

## Ki67 Suppression Assay

The suppressive effect of MDSCs on T-cell proliferation was evaluated using a Ki67 flow cytometry proliferation assay, as previously described (11). Briefly, on day 0, PBMCs were co-cultured with purified MDSCs as follows: duplicate wells containing  $0.5 \times 10^6$  PBMCs were stimulated with PPD (12 μg/ml) to generate effector T-cells and co-cultured with MDSCs at ratios of 1:1, 2:1 and 4:1 (PBMCs: MDSCs) for 6 days at 37°C and 5% CO<sub>2</sub>. Additional experimental control wells were set up including (1) unstimulated PBMCs as a negative control; and (2) PBMCs stimulated with PPD (12 μg/ml) as a proliferation control. On day 6, the cells were harvested and stained for Ki67 expression as per manufacturer instructions (Biolegend, USA). Briefly, the cells were harvested and washed with cold 70% ethanol and, after centrifugation, stained for Ki67, CD3, CD33, CD15 and HLA-DR (Biolegend, USA). Data was acquired on an LSR-II flow cytometer and analysed using FACSDiva software. The percentage (%) proliferation was calculated as follows: [(% MDSC<sup>+</sup>Ki67<sup>+</sup> cells in experimental condition/% MDSC<sup>+</sup>Ki67<sup>+</sup> cells in proliferation control) X 100]. The percentage suppression was calculated as 100 – (% proliferation).

## Mycobacterial Containment Assay

A mycobacterial containment assay was used, as previously described (11), to determine the effect of MDSCs on the ability of PPD-driven effector T-cells to effectively contain *M. tb* within blood monocyte-derived macrophages (MDMs).  $1 \times 10^6$ /ml PBMCs were seeded into a tissue culture plate and were cultured undisturbed for 5 days to allow monocytes to adhere to the plastic and differentiate into macrophages. Thereafter, the plate was washed to remove non-adherent cells and the MDMs were infected with H37Rv at a multiplicity of infection (MOI) of 1:1. In parallel, purified MDSCs were co-cultured with PPD-stimulated PBMCs (12 μg/ml) at specific ratios [MSDC: T<sub>eff</sub> at 1:2 ( $5 \times 10^4$ : $10 \times 10^4$  cells); and 1:4 ( $2.5 \times 10^4$ : $10 \times 10^4$  cells)] and incubated for 6 days at 37°C and 5% CO<sub>2</sub>. The various effector T-cell/MDSC combinations were subsequently co-cultured with H37Rv-infected macrophages for 24 hours. Additional wells included a reference control containing H37Rv-infected MDMs only, a positive *M. tb* containment control containing H37Rv-infected MDMs co-cultured with effector T-cells (T<sub>eff</sub>). Intracellular *M.tb*, released by lysis of infected MDMs, was subsequently cultured on Middlebrook 7H10 agar and expressed as colony forming units per ml (CFU/ml). The percentage (%) mycobacterial containment was also reported

and was defined as the reduction in *M. tb* survival compared to the reference control (H37Rv infected MDM only).

## Statistical Analysis

The data were tested for normality using the Shapiro-Wilk test. The Mann Whitney t test was used to assess immunophenotyping differences between the participant's groups. The Wilcoxon ranked sum test was used to assess differences within participant groups. Statistical analyses were performed using GraphPad Prism version 6.0 (GraphPad software) and SPSS Statistics version 23 (SPSS Inc.).

## RESULTS

### Clinical Characteristics of Study Participants

A total of 33 HIV-uninfected participants were recruited and classified into 2 groups (**Table 1**): microbiologically-confirmed participants with pulmonary TB (TB; n=23), and presumed-latently infected participants (LTBI; n=10) as determined by a positive tuberculin skin test (TST-positive) and Quantiferon Gold in-tube test (both positive). All participant groups were matched for age, sex and gender (**Table 1**); univariate analysis showed that good matching was achieved. All participants had no previous history of TB.

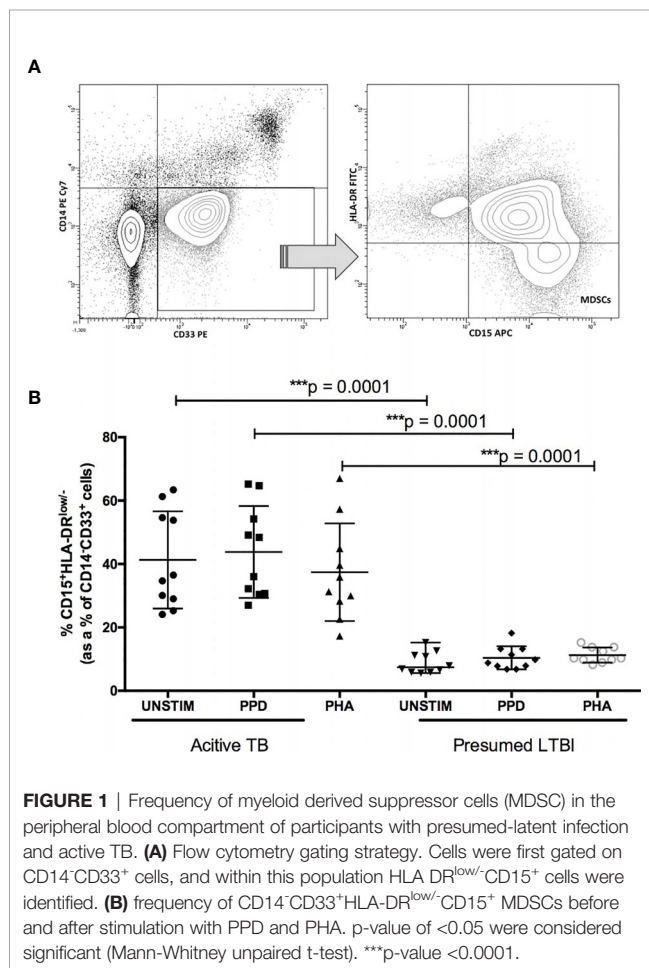
### Frequency of Myeloid-Derived Suppressor Cells in Peripheral Blood

In peripheral blood stimulated with PPD, we found a significant increase in the frequency of MDSCs (HLA-DR<sup>low</sup>CD14<sup>+</sup>CD15<sup>+</sup>CD33<sup>+</sup>) in patients with active TB (median = 42.2%; IQR: 28.1–56.3) compared to participants with LTBI (median = 8.2%; IQR: 7.6 – 10.2;  $p < 0.001$ ; **Figure 1**).

**TABLE 1 |** Demographics and clinical characteristics of participants with latent TB infection (LTBI) and drug-sensitive TB (DS-TB).

Characteristics	Presumed-LTBI	DS-TB	All participants	p-value
<b>Patient numbers (n)</b>	10	23	33	NA
<b>Age (years; <sup>a</sup>IQR)</b>	32 (28-49)	35 (26-48)	34 (26-49)	0.34
<b>Gender (%)</b>				
Male	5 (50)	12 (52)	17 (52)	0.89
Female	5 (50)	11 (48)	16 (48)	
<b>Ethnicity (%)</b>				
Black African	3 (30)	9 (39)	12 (36)	0.74
Mixed race	4 (40)	10 (44)	14 (42)	
European descent	3 (30)	4 (17)	7 (21)	
<b>Median duration of treatment</b>	NA	5 (4-12)	5 (4-12)	NA
<b>prior to blood donation (days; <sup>a</sup>IQR)</b>				
<b>Smear status</b>				
Smear 1+ positive (%)	NA	3 (13)	NA	NA
Smear 2+ positive (%)	NA	12 (52)	NA	
Smear 3+ positive (%)	NA	8 (35)	NA	

NA, not applicable.



## Ki67 Suppression Assay

The functional capability of the MDSC to suppress PPD-driven effector T-cell proliferative responses was evaluated using a Ki67 flow cytometry assay. MDSCs were isolated from the peripheral blood of patients with active TB disease (n=6). MDSC purity was confirmed to be greater than 95% (**Table 1**, online supplement). The proliferation control, which contained PPD-driven effector T-cells only, displayed limited T-cell suppression (median 10.95%; range: 6.75 – 19.25% T-cell suppression; **Figure 2B**). However, the addition of MDSCs to PPD-driven effector T-cells at ratios of 1:1, 2:1, and 4:1 (effector T cells: MDSCs) resulted in significant suppression of T-cells [median (range): 75% (72.62 – 95.9%), 69% (61.25 – 89.70%) and 65% (59.05 – 84%) T-cell suppression respectively; **Figure 2**].

## Mycobacterial Containment Assay

The mycobacterial containment assay was used to determine the effect of MDSC, isolated from the peripheral blood of patients with active TB (n= 7), on the ability of PPD-driven effector T-cells to effectively contain *M. tb* within autologous MDMs.

In terms of absolute CFUs, a significant decrease was observed in wells containing effector T-cells ( $T_{eff}$ ) co-cultured with H37Rv-infected MDMs ( $T_{eff}$ :  $4.3 \times 10^4$  CFU/ml) compared to wells only

containing H37Rv infected MDMs (MDM only;  $7.1 \times 10^4$  CFU/ml;  $p=0.0002$ ; **Figure 2C**). However, when MDSCs and effector T-cells were co-cultured with H37Rv-infected MDMs, there was an increase in CFU/ml compared to the  $T_{eff}$  well ( $p=0.02$ ; **Figure 2C**).

The same data, for greater clarity, were also differently expressed as % mycobacterial (*M.tb*) containment, defined as the % change in CFU/ml relative to the H37Rv-infected MDMs reference control. As such, the H37Rv-infected MDM control or reference represented 0% *M. tb* containment, or in other words, 100% *M.tb* survival. The addition of effector T-cells together with the H37Rv-infected MDMs, represented the “positive control”. In the positive control 30.6% *M.tb* containment was observed, however this level of containment was significantly reduced when MDSCs were introduced into the culture (2:1 = 9.2% and 4:1 = 8.5% *M.tb* containment;  $p=0.02$ ).

## DISCUSSION

We found that patients with active TB disease had significantly higher frequencies of circulating MDSCs. These cells suppressed the proliferative capabilities of PPD-specific effector T cells and attenuated mycobacterial containment *in vitro*.

The role of MDSCs in TB has been contentious. We have shown, for the first time in humans, that MDSCs can modulate T-cell activity, thus enhancing mycobacterial growth *in vitro*. Our results indicate that MDSCs can modulate an immune response that favours *M.tb* survival. The mechanism by which this occurs deserves further study. Previous murine studies that examined the direct effect of MDSCs on mycobacterial survival, showed that infected MDSCs were unable to directly kill mycobacteria (19), despite their ability to produce nitric oxide (20). Knaul et al. found that *M.tb*-infected MDSCs, similar to macrophages, can release pro-inflammatory (IL-1 and IL-6), but also anti-inflammatory cytokines (IL-10), thus providing a possible mechanism for our observations (21). However, further work is now required to study an array of possible mechanisms by which might potentially including Th2 cytokines, cell-to-cell contact, and other humoral mechanisms etc.

We found the levels of MDSC were significantly higher in patients with active TB compared to those with presumed-LTBI, and that MDSCs suppressed T-cell proliferation. Indeed, MDSCs were first described as suppressor cells recruited to tumor sites (10), where the increased levels of MDSCs significantly correlated with aggressive disease, poor patient prognosis and immune escape (18). More recently, MDSCs were shown to be upregulated during active TB disease in adults (13, 14) and in HIV-TB co-infected children (17), and in the same patients are able to suppress T cell proliferation (13, 14) and alter cytokine expression (13). However, although we confirm these observations, we have extended these findings to show that the anti-proliferative and immune-modulatory effects translate into sub-optimal mycobacterial containment.

There are several limitations to our findings. The immunophenotype of study participants was analysed in the peripheral blood compartment, and whether these effects occur at the site of

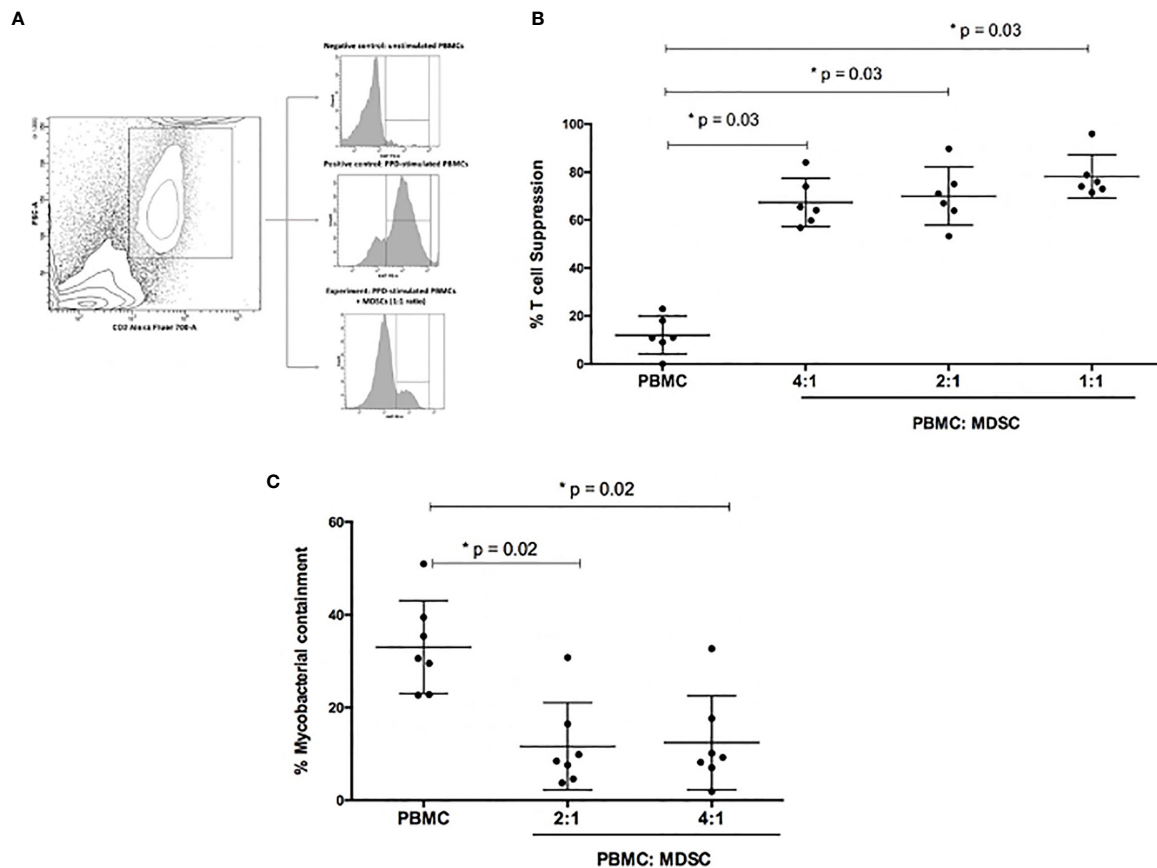


**FIGURE 2 |** Functional capabilities of myeloid derived suppressor cells (MDSC) was tested. **(A)** Illustrates the flow cytometry gating strategy. **(B)** Outlines suppression of PPD-driven T-cell proliferation by MDSCs at different ratios. Effector T-cells were co-cultured with MDSCs at a ratio of 4:1, 2:1 and 1:1, respectively. The percentage proliferation was measured using Ki67 flow cytometry staining. **(C)** Mycobacterial containment assays using peripheral blood cells from active TB patients to determine the effect of MDSCs from TB patients on mycobacterial survival. Briefly, monocyte-derived macrophages (MDMs) were infected with H37Rv and then co-cultured with PPD pre-primed effector T-cells with or without MDSCs for 24 hours. The impact of MDSCs on mycobacterial containment was assessed by plating surviving intracellular bacteria, and the magnitude of mycobacterial containment is expressed as % of the reference control (MDM only) for each experimental condition. \*p-value of <0.05 were considered significant (Wilcoxon matched pairs test).

disease remain unknown. However, harvesting cells from the lung is constrained by cost, ethical and infection control considerations. Second, our study sample size was limited, and we only recruited patients from one geographical setting. Nevertheless, we were able to demonstrate statistically significant differences between the groups, which together with the impact on proliferation, suggest that these are likely biologically meaningful observations. Third, we did not explore the immune mechanism by which MDSCs subverted the ability of T-cells to kill *M.tb*. However, this was limited by available funding but is likely to begin shortly.

Fourth, containment was used to define how MDSCs can modulate the function of effector T cells to control *M.tb*. As described in our previous publication (22), it is difficult to quantify anti-mycobacterial activity as our assay cannot distinguish between organisms that have been killed or those that have entered a non-replicating state. However, containment is a much more biologically meaningful outcome measure as compared to biomarker proxies, including cytokines or receptor

signaling pathways, that may indicate protection. Although the latter are commonly used in human studies, they may merely represent a bystander effect rather than having a causal link.

In conclusion, persons with active TB disease, compared to those with presumed-LTBI, demonstrate an altered immuno-phenotype characterized by a high frequency of MDSCs. MDSCs isolated from patients with active TB disease were highly suppressive and could attenuate mycobacterial containment *in vitro*. Collectively, these data suggest a contributing role for MDSCs in the immuno-pathogenesis of TB and MDSCs may be potential targets that could be exploited to design vaccines or host-directed therapies.

## AUTHOR'S NOTE

LS is currently based at Stellenbosch University, but all work outlined in this study was performed when she was based at the Centre for Lung Infection and Immunity at the University of Cape Town.

## DATA AVAILABILITY STATEMENT

The raw data supporting the conclusions of this article will be made available by the authors, without undue reservation.

## ETHICS STATEMENT

The studies involving human participants were reviewed and approved by University of Cape Town Research committee. Patients/participants provided their written informed consent to participate in this study.

## AUTHOR CONTRIBUTIONS

Study concept and design: MD, AP, and KD. Laboratory work: MD, AP, LS, and MT. Analysis and interpretation: MD, AP, LS, MT, and

KD. Drafting of manuscript: MD, AP, LS, MT, and KD. All authors contributed to the article and approved the submitted version.

## FUNDING

KD and the work presented here was supported by the South African MRC (RFA-EMU-02-2017) and the EDCTP (TMA-2015SF-1043 & TMA- 1051-TESAI).

## SUPPLEMENTARY MATERIAL

The Supplementary Material for this article can be found online at: <https://www.frontiersin.org/articles/10.3389/fimmu.2021.676679/full#supplementary-material>

## REFERENCES

- WHO. *WHO Global Tuberculosis Report* (2020). Available at: <https://apps.who.int/iris/bitstream/handle/10665/336069/9789240013131-eng.pdf> (Accessed February 15 2021).
- Kurz SG, Furin JJ, Bark CM. Drug-Resistant Tuberculosis: Challenges and Progress. *Infect Dis Clinics* (2016) 30(2):509–22. doi: 10.1016/j.idc.2016.02.010
- Colditz GA, Brewer TF, Berkey CS, Wilson ME, Burdick E, Fineberg HV, et al. Efficacy of BCG Vaccine in the Prevention of Tuberculosis: Meta-Analysis of the Published Literature. *Jama* (1994) 271(9):698–702. doi: 10.1001/jama.271.9.698
- Roy A, Eisenhut M, Harris R, Rodrigues L, Sridhar S, Habermann S, et al. Effect of BCG Vaccination Against Mycobacterium Tuberculosis Infection in Children: Systematic Review and Meta-Analysis. *BMJ* (2014) 349. doi: 10.1136/bmj.g4643
- Tameris MD, Hatherill M, Landry BS, Scriba TJ, Snowden MA, Lockhart S, et al. Safety and Efficacy of MVA85A, a New Tuberculosis Vaccine, in Infants Previously Vaccinated With BCG: A Randomised, Placebo-Controlled Phase 2b Trial. *Lancet* (2013) 381(9871):1021–8. doi: 10.1016/S0140-6736(13)60177-4
- Tait DR, Hatherill M, Van Der Meeren O, Ginsberg AM, Van Brakel E, Salaun B, et al. Final Analysis of a Trial of M72/AS01E Vaccine to Prevent Tuberculosis. *New Engl J Med* (2019) 381(25):2429–39. doi: 10.1056/NEJMoa1909953
- Behar SM, Carpenter SM, Booty MG, Barber DL, Jayaraman P. Orchestration of Pulmonary T Cell Immunity During Mycobacterium Tuberculosis Infection: Immunity Interruptus. *Semin Immunol* (2014) 26(6):559–77. doi: 10.1016/j.smim.2014.09.003
- Sia JK, Rengarajan J. Immunology of Mycobacterium Tuberculosis Infections. *Gram-Positive Pathog* (2019), 1056–86. doi: 10.1128/9781683670131.ch64
- Law AM, Valdes-Mora F, Gallego-Ortega D. Myeloid-Derived Suppressor Cells as a Therapeutic Target for Cancer. *Cells* (2020) 9(3):561. doi: 10.3390/cells9030561
- Youn JI, Gabrilovich DI. The Biology of Myeloid-Derived Suppressor Cells: The Blessing and the Curse of Morphological and Functional Heterogeneity. *Eur J Immunol* (2010) 40(11):2969–75. doi: 10.1002/eji.201040895
- Davids M, Pooran AS, Pietersen E, Wainwright HC, Binder A, Warren R, et al. Regulatory T Cells Subvert Mycobacterial Containment in Patients Failing Extensively Drug-Resistant Tuberculosis Treatment. *Am J Respir Crit Care Med* (2018) 198(1):104–16. doi: 10.1164/rccm.201707-1441OC
- Semple PL, Binder AB, Davids M, Maredza A, van Zyl-Smit RN, Dheda K. Regulatory T Cells Attenuate Mycobacterial Stasis in Alveolar and Blood-Derived Macrophages From Patients With Tuberculosis. *Am J Respir Crit Care Med* (2013) 187(11):1249–58. doi: 10.1164/rccm.201210-1934OC
- Du Plessis N, Loeberberg L, Kriel M, von Groote-Bidlingmaier F, Ribechini E, Loxton AG, et al. Increased Frequency of Myeloid-Derived Suppressor Cells During Active Tuberculosis and After Recent Mycobacterium Tuberculosis Infection Suppresses T-cell Function. *Am J Respir Crit Care Med* (2013) 188(6):724–32. doi: 10.1164/rccm.201302-0249OC
- El Daker S, Sacchi A, Tempestilli M, Carducci C, Goletti D, Vanini V, et al. Granulocytic Myeloid Derived Suppressor Cells Expansion During Active Pulmonary Tuberculosis is Associated With High Nitric Oxide Plasma Level. *PloS One* (2015) 10(4):e0123772. doi: 10.1371/journal.pone.0123772
- Kumar NP, Sridhar R, Banurekha VV, Jawahar MS, Nutman TB, Babu S. Role of Myeloid Derived Suppressor Cells in Tuberculosis Infection and Disease. *BMC Infect Dis* (2014) 14(3):1–. doi: 10.1186/1471-2334-14-S3-O18
- Yang B, Wang X, Jiang J, Zhai F, Cheng X. Identification of CD244-expressing Myeloid-Derived Suppressor Cells in Patients With Active Tuberculosis. *Immunol Lett* (2014) 158(1-2):66–72. doi: 10.1016/j.imlet.2013.12.003
- Du Plessis N, Jacobs R, Gutschmidt A, Fang Z, van Helden PD, Lutz MB, et al. Phenotypically Resembling Myeloid Derived Suppressor Cells are Increased in Children With HIV and Exposed/Infected With Mycobacterium Tuberculosis. *Eur J Immunol* (2017) 47(1):107–18. doi: 10.1002/eji.201646658
- Lechner MG, Megiel C, Russell SM, Bingham B, Arger N, Woo T, et al. Functional Characterization of Human Cd33+ and Cd11b+ Myeloid-Derived Suppressor Cell Subsets Induced From Peripheral Blood Mononuclear Cells Co-Cultured With a Diverse Set of Human Tumor Cell Lines. *J Trans Med* (2011) 9(1):1–20. doi: 10.1186/1479-5876-9-90
- Agrawal N, Streat I, Pei G, Weiner J, Kotze L, Bandermann S, et al. Human Monocytic Suppressive Cells Promote Replication of Mycobacterium Tuberculosis and Alter Stability of In Vitro Generated Granulomas. *Front Immunol* (2018) 9:2417. doi: 10.3389/fimmu.2018.02417
- Martino A, Badell E, Abadie V, Balloy V, Chignard M, Mistou M-Y, et al. Mycobacterium Bovis Bacillus Calmette-Guérin Vaccination Mobilizes Innate Myeloid-Derived Suppressor Cells Restraining In Vivo T Cell Priming Via IL-1R-dependent Nitric Oxide Production. *J Immunol* (2010) 184(4):2038–47. doi: 10.4049/jimmunol.0903348
- Knaul JK, Jörg S, Oberbeck-Mueller D, Heinemann E, Scheuermann L, Brinkmann V, et al. Lung-Residing Myeloid-Derived Suppressors Display Dual Functionality in Murine Pulmonary Tuberculosis. *Am J Respir Crit Care Med* (2014) 190(9):1053–66. doi: 10.1164/rccm.201405-0828OC
- Tomasichio M, Davids M, Pooran A, Theron G, Smith L, Semple L, et al. The Injectable Contraceptive Medroxyprogesterone Acetate Attenuates Mycobacterium Tuberculosis-Specific Host Immunity Through the



Glucocorticoid Receptor. *J Infect Dis* (2019) 219(8):1329–37. doi: 10.1093/infdis/jiy657

**Conflict of Interest:** The authors declare that the research was conducted in the absence of any commercial or financial relationships that could be construed as a potential conflict of interest.

Copyright © 2021 Davids, Pooran, Smith, Tomasicchio and Dheda. This is an open-access article distributed under the terms of the Creative Commons Attribution License (CC BY). The use, distribution or reproduction in other forums is permitted, provided the original author(s) and the copyright owner(s) are credited and that the original publication in this journal is cited, in accordance with accepted academic practice. No use, distribution or reproduction is permitted which does not comply with these terms.



# Tuberculosis Risk Stratification of Psoriatic Patients Before Anti-TNF- $\alpha$ Treatment

Farida Benhadou<sup>1</sup>, Violette Dirix<sup>2</sup>, Fanny Domont<sup>2</sup>, Fabienne Willaert<sup>1</sup>, Anne Van Praet<sup>2</sup>, Camille Locht<sup>3</sup>, Françoise Mascart<sup>2\*</sup> and Véronique Corbière<sup>2</sup>

<sup>1</sup> Dermatology Department, Hôpital Erasme, Université Libre de Bruxelles (U.L.B.), Brussels, Belgium, <sup>2</sup> Laboratory of Vaccinology and Mucosal Immunity, Université Libre de Bruxelles (U.L.B.), Brussels, Belgium, <sup>3</sup> Univ. Lille, CNRS, Inserm, CHU Lille, Institut Pasteur de Lille, U1019 – UMR 8204 – CIL - Center for Infection and Immunity of Lille, Lille, France

## OPEN ACCESS

### Edited by:

Hazel Marguerite Dockrell,  
University of London, United Kingdom

### Reviewed by:

Vignesh Ramachandran,  
University of Kuala Lumpur, Malaysia  
Graham H. Bothamley,  
Homerton University Hospital NHS  
Foundation Trust, United Kingdom

### \*Correspondence:

Françoise Mascart  
francoise.mascart@erasme.ulb.ac.be

### Specialty section:

This article was submitted to  
Microbial Immunology,  
a section of the journal  
Frontiers in Immunology

**Received:** 26 February 2021

**Accepted:** 17 May 2021

**Published:** 03 June 2021

### Citation:

Benhadou F, Dirix V, Domont F,  
Willaert F, Van Praet A, Locht C,  
Mascart F and Corbière V (2021)  
Tuberculosis Risk Stratification  
of Psoriatic Patients Before  
Anti-TNF- $\alpha$  Treatment.  
Front. Immunol. 12:672894.  
doi: 10.3389/fimmu.2021.672894

Psoriasis is a skin inflammatory condition for which significant progress has been made in its management by the use of targeted biological drugs. Detection of latent *M. tuberculosis* infection (LTBI) is mandatory before starting biotherapy that is associated with reactivation risk. Together with evaluation of TB risk factors and chest radiographs, tuberculin skin tests (TST) and/or blood interferon- $\gamma$ -release assays (IGRA), like the QuantiFERON (QFT), are usually performed to diagnose *M. tuberculosis* infection. Using this approach, 14/49 psoriatic patients prospectively included in this study were identified as LTBI (14 TST<sup>+</sup>, induration size  $\geq 10$ mm, 8 QFT<sup>+</sup>), and 7/14 received prophylactic anti-TB treatment, the other 7 reporting past-treatment. As the specificity and sensitivity of these tests were challenged, we evaluated the added value of an IGRA in response to a mycobacterial antigen associated with latency, the heparin-binding haemagglutinin (HBHA). All but one TST<sup>+</sup> patient had a positive HBHA-IGRA, indicating higher sensitivity than the QFT. The HBHA-IGRA was also positive for 12/35 TST<sup>-</sup>QFT<sup>-</sup> patients. Measurement for 15 psoriatic patients (12 with HBHA-IGRA<sup>+</sup>) of 8 chemokines in addition to IFN- $\gamma$  revealed a broad array of HBHA-induced chemokines for TST<sup>+</sup>QFT<sup>-</sup> and TST<sup>-</sup>QFT<sup>-</sup> patients, compared to a more restricted pattern for TST<sup>+</sup>QFT<sup>+</sup> patients. This allowed us to define subgroups within psoriatic patients characterized by different immune responses to *M. tuberculosis* antigens that may be associated to different risk levels of reactivation of the infection. This approach may help in prioritizing patients who should receive prophylactic anti-TB treatment before starting biotherapies in order to reduce their number.

**Keywords:** psoriasis, Tumor necrosis factor- $\alpha$  inhibitors, latent tuberculosis infection, tuberculin skin tests, interferon- $\gamma$ -release assays, QuantiFERON, heparin-binding haemagglutinin

## INTRODUCTION

Psoriasis is a frequent skin inflammatory condition with a worldwide prevalence of 3%, characterized by erythematous and scaly plaques that may affect any part of the body (1, 2). Psoriatic patients may develop comorbidities, such as psoriatic arthritis and cardiovascular diseases, leading to the concept of a systemic immune-mediated inflammatory disease (IMID) (3). Significant

progress has been made in the management of psoriasis by the use of targeted biological drugs, initially limited to tumor necrosis factor- $\alpha$  (TNF- $\alpha$ ) inhibitors (4). Patients receiving TNF- $\alpha$ -targeted therapies have an increased risk of reactivation of a latent *Mycobacterium tuberculosis* infection (LTBI), and although there are few and discrepant specific reports in psoriatic patients (5), the risk of active tuberculosis (aTB) is, according to a recent meta-analysis, doubled for patients treated with anti-TNF- $\alpha$  (6). The use of biological drugs to treat psoriasis was further extended to other therapeutic agents targeting the interleukin (IL)-23/IL-17 axis (7, 8), but their potential risk of reactivation of LTBI is not yet firmly established (9).

Classically, *M. tuberculosis* infection in humans is thought to present either as aTB or as LTBI defined by the presence of immunological responses to mycobacterial antigens in absence of clinical symptoms of disease (10, 11). LTBI subjects are thought to present a life-long risk of reactivation of the infection, with 5 to 15% of them developing aTB during their lifetime (11). Recent data however challenged this concept and indicated that LTBI comprises a range of infection outcomes associated with different bacterial persistence and host containment, from cleared infection to low-grade TB (10). It became evident that these last individuals are probably more at risk to reactivate the infection compared to other LTBI subjects.

In view of the higher risk of psoriatic patients to reactivate LTBI when receiving TNF- $\alpha$ -targeted therapies, detection of LTBI before initiating biotherapies is mandatory and essential to provide preventive anti-TB treatment (9, 12). This detection is nowadays based on the classical definition of LTBI, e.g. on the detection of memory T cell responses to mycobacterial antigens, revealing the presence of host sensitization to these antigens (11). The tuberculin skin test (TST) is the gold standard for this detection since decades, in spite of possible false-positive results in Bacillus Calmette-Guérin (BCG)-vaccinated subjects and in non-tuberculous mycobacteria (NTM)-infected patients (13), and despite possible lower sensitivity in patients suffering from IMiD with immune-suppressive treatment history (14). Therefore, TST has been replaced in several countries by interferon-gamma (IFN- $\gamma$ ) release assays (IGRAs). These blood tests measure the IFN- $\gamma$  secretion within whole blood or by peripheral blood mononuclear cells (PBMC), upon *in vitro* stimulation with peptides from the mycobacterial antigens early-secreted antigenic target-6 (ESAT-6), culture filtrate protein-10 (CFP-10), and sometimes TB7.7 (9). These IGRAs, commercially available as the QuantiFERON (QFT) (Qiagen, Hilden, Germany) or the T-SPOT.TB (Oxford Immunotec, Oxford, United Kingdom), are more specific for *M. tuberculosis* infection than TST, as the antigens used for *in vitro* stimulation are absent from BCG and most NTM. In addition, they both include positive and negative controls to identify possible false negatives. However, they were reported by several authors to have lower sensitivity than initially thought to detect immune responses to *M. tuberculosis* antigens (14), so that in Belgium, a low TB incidence country (<10 new cases/100.000 inhabitants/year) with a low BCG vaccination coverage, IGRAs are recommended only in case of doubtful TST results, or to increase

sensitivity in patients already receiving immunosuppressive drugs (www.fares.be).

Using either TST or IGRA to detect LTBI before the initiation of TNF- $\alpha$ -targeted agents is however not optimal as prophylactic anti-TB treatment in these selected patients did not provide them complete protection from developing aTB (15). Therefore, in addition to a careful evaluation of the patient's risk factors for LTBI and chest X-ray radiography to exclude aTB, a dual strategy performing both tests (TST and IGRA) is now largely recommended to reduce any possible risk of developing aTB. The positivity of any of these tests for the diagnosis of LTBI should be considered (16). Unfortunately, neither the TST, nor the IGRA allowed us to detect patients with the highest risk of reactivation as they cannot differentiate the newly recognized different stages within the spectrum of LTBI and are positive both in LTBI subjects and in patients with aTB (17).

Given the limitations of the TST and the commercial IGRAs to diagnose LTBI in patients with IMiD, and their inability to select among LTBI subjects those who have the highest risk to reactivate the infection, we evaluated in this study the added value of an IGRA based on the latency-associated antigen heparin-binding haemagglutinin (HBHA), reported to detect LTBI with high sensitivity and specificity (18), and we compared the results of the HBHA-IGRA to those of the TST and of the QFT.

## MATERIAL AND METHODS

### Study Population

Forty-nine adult patients suffering from psoriasis were prospectively recruited from the outpatient clinic of the Dermatology department at the "hôpital Erasme" as part of their evaluation before starting biotherapy (Ethics Committee 021/406, P2012/082). TB screening performed for all participants included TST (0.1 ml tuberculin PPD RT23 2 TU, SSI, Copenhagen, DK), chest X-ray, and QFT. TST were read after 72 hours and the results were assessed in the context of the patient's individual TB risk factors. In the absence of TB risk factors, TST<sup>+</sup>QFT<sup>-</sup> patients without chest X-Ray sign suggesting aTB, were considered as non-infected with *M. tuberculosis*. QFT<sup>+</sup> and/or TST<sup>+</sup> patients (induration size  $\geq 15$  mm) were considered as LTBI after exclusion of aTB. In the context of patients at risk to reactivate LTBI, patients with a TST positivity between 10 and 14 mm were also considered as being LTBI (www.fares.be). Four patients were treated with methotrexate at the time of inclusion. Ten others already received anti-TNF- $\alpha$  antibodies and were included in this study before changing their biotherapy. When they were initially evaluated for possible LTBI before their first anti-TNF- $\alpha$  treatment, 3/10 were considered LTBI and received at that time prophylactic anti-TB treatment.

### QuantiFERON-TB Gold

QFT (QuantiFERON-TB Gold In-tube) was performed according to the manufacturer instructions (www.qiagen.com). A positive QFT test was defined as  $\geq 0.35$  IU/ml IFN- $\gamma$  released

in response to the mycobacterial peptides, after subtraction of the concentration obtained for the unstimulated condition, with a result > 25% of the unstimulated condition.

### HBHA-IFN- $\gamma$ Release Assay (IGRA)

PBMC were isolated from fresh blood samples and *in vitro* stimulated during 24 hours at 37°C under 5% CO<sub>2</sub> with 2  $\mu$ g/ml HBHA, left unstimulated in culture medium (negative control) or were stimulated with 0.5  $\mu$ g/ml staphylococcal enterotoxin B (SEB, Sigma-Aldrich, Bornem, Belgium) (positive control). IL-7 was added in the culture medium at 1 ng/ml to increase the sensitivity of the 24 hrs assay (19). HBHA was purified from *Mycobacterium bovis* BCG culture supernatants by heparin-Sepharose chromatography (Sepharose CL-6B; Pharmacia LKB, Piscataway, NJ) (20). The bound material was eluted by a 0-500 mM NaCl gradient and was further passed through a reverse-phase high-pressure liquid chromatography (HPLC; Beckman Gold System), using a Nucleosil C18 column (TSK gel Super ODS; Interchim) equilibrated in 0.05% trifluoroacetic acid. Elution was performed by a linear 0-80% acetonitrile gradient and HBHA eluted at 60% acetonitrile (21). The HPLC chromatogram revealed a single peak and analysis by SDS-PAGE showed a single band after Coomassie-blue staining, indicating the absence of contamination of HBHA with other proteins.

Cell culture supernatants were frozen at -20°C until measurement of secreted cytokines/chemokines. IFN- $\gamma$  concentrations were measured by ELISA (19). IFN- $\gamma$  concentrations < 50 pg/ml in the non-stimulated condition and > 200 pg/ml in the positive controls were required for further analysis of the results. When detectable, IFN- $\gamma$  concentrations obtained under non-stimulated conditions were subtracted from those obtained in response to HBHA. A positive HBHA-IGRA was defined as IFN- $\gamma$  concentrations  $\geq$  50 pg/ml IFN- $\gamma$  as previously determined by ROC curve analysis comparing results obtained for LTBI subjects to those of non-infected controls (19).

### Multiple Cytokine/Chemokine Measurements

Based on our previous experience with *M. tuberculosis*-infected patients, 8 cytokines/chemokines were measured in addition to IFN- $\gamma$  in the 24 h culture supernatants of HBHA-stimulated PBMC from 12 HBHA-IGRA<sup>+</sup> psoriatic patients and from 3 HBHA-IGRA<sup>-</sup> patients taken as negative controls: granulocyte macrophage colony-stimulation factor (GM-CSF), IFN- $\gamma$ , IL-1 $\beta$ , IL-2, IL-6, IL-10, IL-17A, macrophage inflammatory protein (MIP-1 $\alpha$ ), and TNF- $\alpha$ . The cytokine/chemokine concentrations were measured by Milliplex human cytokine/chemokine kits (Merck, Belgium) according to the manufacturer's instructions with supernatants dilution factors specific for each analyte to obtain concentrations within the standard curves. Results were analyzed with a Bio-Plex<sup>®</sup> MAGPIX<sup>™</sup> Multiplex reader, Bio-Plex Manager<sup>™</sup> MP Software and Bio-Plex Manager 6.1 Software (BIO-RAD laboratories, Nazareth Eke, Belgium). When detectable, the analyte concentrations in the antigen-free conditions were

subtracted from those obtained with antigen stimulation. Concentrations below the detection limit were allocated an arbitrary value of 5 pg/ml, whilst results exceeding the assay's upper limit of detection were attributed the concentration corresponding to this limit. For each marker, the positivity limit was arbitrarily determined as being minimum 4 times the detection limit or maximum 2 times the median concentration obtained for non-infected patients when cytokines/chemokines were detectable. A grey zone of doubtful positivity defined as  $\pm$  20% of the cut-off value was established for each analyte. A scale representing the intensity of cytokine/chemokine concentrations was established for each analyte from negative values to doubtful, low and strong cytokine/chemokine concentrations.

### Statistical Analysis

Differences between several groups were assessed by the non-parametric Kruskal-Wallis test, followed by the non-parametric Dunn test. Differences between HBHA-induced IFN- $\gamma$  concentrations at two different time-points were evaluated by the paired Wilcoxon test. A value of  $p < 0.05$  (\*) was considered significant. All results were obtained with the Graphpad Prism Software version 4.0.

## RESULTS

### Prevalence of *M. tuberculosis* Infection in Psoriatic Patients According to Standard Criteria

In Belgium, a low-TB incidence country, forty-nine adult patients suffering from psoriasis were prospectively recruited from the outpatient clinic of the Dermatology department (hôpital Erasme), as part of their evaluation before starting biotherapy. The main demographic and clinical characteristics of these patients are reported in **Table 1**. Eleven patients had a positive TST  $\geq$  15 mm and, in the absence of clinical and/or radiological signs of aTB, were classified as LTBI. Three had a TST induration size between 10 and 14 mm, and in the context of a future biotherapy, they were considered as LTBI as recommended in Belgium, and 35 patients had a negative TST (**Figure 1**). TST results were probably not influenced by previous BCG vaccination recorded for 2/14 TST<sup>+</sup> and for 4/35 TST<sup>-</sup> patients (**Table 1**). To avoid possible false negative TST results in patients with abnormal cellular immune responses due to their pathology and/or their treatment, QFT was performed on all patients, as now largely recommended. The QFT was positive for 8/49 patients, all of them having a positive TST ( $\geq$  10 mm) (**Figure 1**). TST and QFT results were not correlated (**Figure 2A**), and the presence of LTBI risk factors was higher in the QFT<sup>+</sup> (6/8 = 75%) than in the QFT<sup>-</sup> (3/6 = 50%) LTBI patients (**Table 1**). Altogether, this resulted in a pre-selection of patients for prophylactic anti-TB treatment of 14/49 patients (28.6%).

Thirty-eight/49 included patients received anti-TNF- $\alpha$  (n=29) or anti-IL-23/12 (n=9) antibodies after inclusion in this study, and none of them developed aTB during a 2 year follow-up. An alternative therapeutic option was chosen for the other 11



**TABLE 1 |** Demographic and clinical characteristics of the study population.

	TST <sup>+</sup>			TST <sup>-</sup>	
	QFT <sup>+</sup> HBHA-IGRA <sup>+</sup> n=8	QFT <sup>-</sup> HBHA-IGRA <sup>+</sup> n=5	QFT <sup>-</sup> HBHA-IGRA <sup>-</sup> n=1	QFT <sup>-</sup> HBHA-IGRA <sup>+</sup> n=12	QFT <sup>-</sup> HBHA-IGRA <sup>-</sup> n=23
<b>Age (years), median (range)</b>	52 (34–82)	41 (34–51)	61	44 (35–54)	50 (25–67)
<b>Male, n (%)</b>	8 (100)	4 (80)	0 (0)	6 (50)	14 (61)
<b>PASI, median (range)</b>	10 (7–15)	12 (10–27)	11	12 (8–27)	12 (5–33)
<b>Ethnic origin, n (%)</b>					
Caucasian	6 (75)	4 (80)	/	10 (83)	18 (78)
African	2 (25)	1 (20)	/	2 (17)	5 (22)
Asian	/	/	1 (100)	/	/
<b>BCG vaccination, n (%)</b>					
No	7 (87)	2 (40)	1	11 (92)	19 (83)
Yes	1 (13)	1 (20)	/	/	4 (17)
Unknown	0	2 (40)	/	1 (8)	/
<b>Risk factors for LTBI/aTB, n (%)</b>					
High TB incidence country (Birth, Travel)	4 (50)	1 (20)	1 (100)	1 (8)	2 (9)
Contact or possible contact with TB patients (family/work)	2 (25)	/	/	1 (8)	3 (13)
Chest X-ray suggestive of previous TB	1* (12.5)	1 (20)	/	/	/
<b>TB History, n (%)</b>					
aTB	2 (25)	1 (20)	/	/	/
LTBI	4 (50)	2 (40)	/	/	/
<b>Ongoing psoriasis treatment, n (%)</b>					
Adalimumab	2 (25)	/	/	/	3 (13)
Etanercept	/	1 (20)	/	3 (25)	1 (4.3)
Methotrexate	1 (12.5)	/	1 (100)	/	2 (9)

TST, Tuberculin Skin Test; QFT, QuantiFERON TB Gold In tube; HBHA, Heparin-binding haemagglutinin; IGRA, Interferon gamma release assay; n, number; PASI, Psoriasis Area Severity Index; BCG, Bacille Calmette-Guérin; LTBI, Latent Tuberculosis Infection; aTB, active Tuberculosis; \*patient with 2 risk factors: he was born and travel in high TB incidence country and had chest X-ray suggestive of previous aTB.

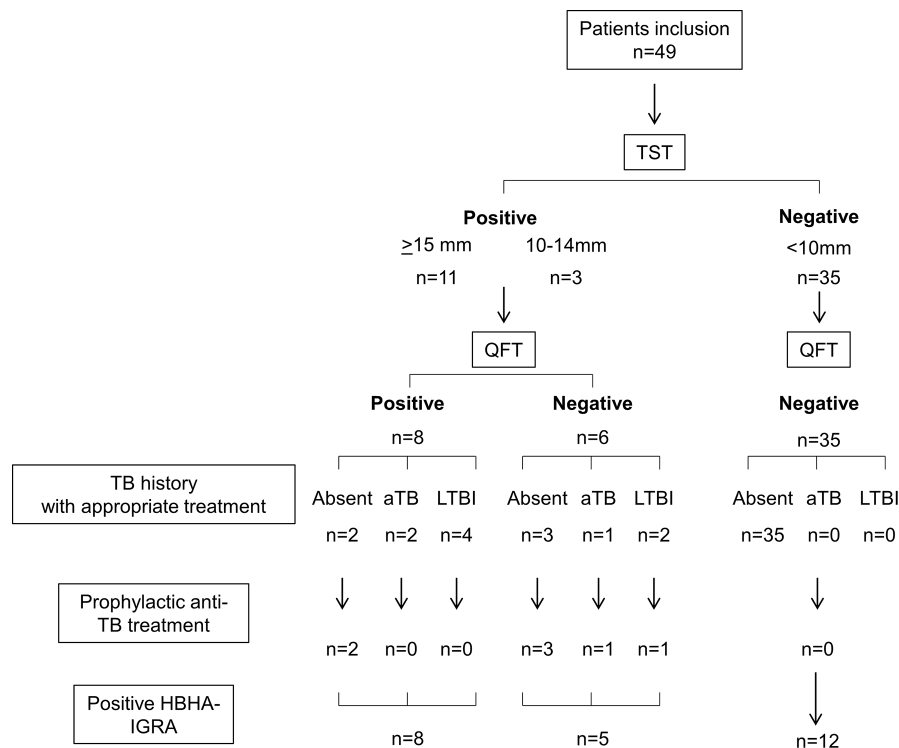


**FIGURE 1 |** Algorithm of the patients' classification. n, number of patients; TST, tuberculin skin test; QFT, QuantiFERON TB Gold In tube; TB, tuberculosis; HBHA-IGRA, Heparin-binding haemagglutinin-interferon-gamma release assay.

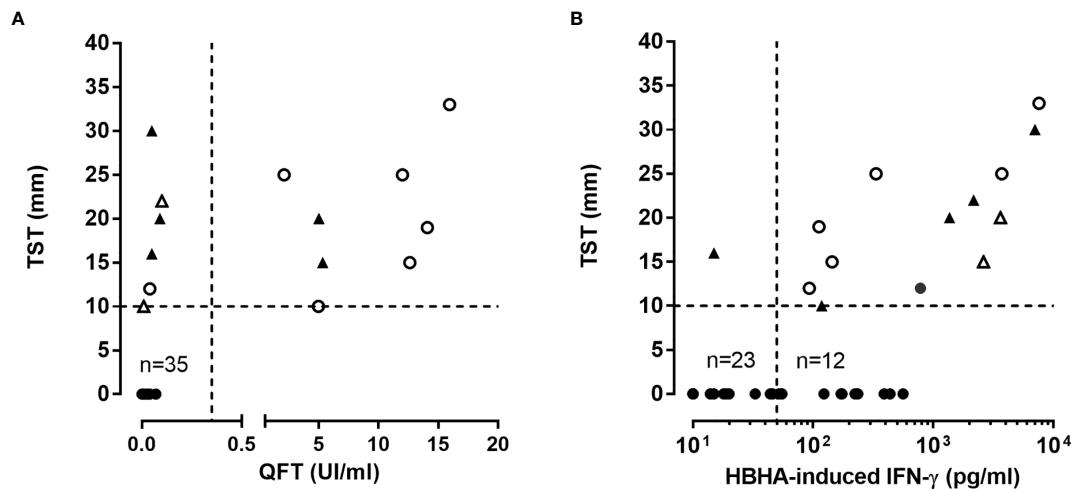


**FIGURE 2** | Correlation between immunoassays performed in psoriatic patients. **(A)** TST and QFT results were compared in all patients. Triangles represent patients who received anti-TB prophylaxis, open symbols represent patients with a past anti-TB treatment. **(B)** TST and HBHA-IGRA results were compared in all patients. Triangles represent patients who received anti-TB prophylaxis and open symbols (triangle or circle) represent QFT<sup>+</sup> patient. TST results are given as the size of induration in mm, QFT results are expressed in international unit (UI) of IFN- $\gamma$  per ml of blood, and HBHA-IGRA results are reported as concentration of IFN- $\gamma$  (pg/ml) released in 24 h culture supernatants of PBMC incubated with HBHA.

patients. Among the 14 patients pre-selected for an initial prophylactic anti-TB treatment, 7 did not receive it because they reported a past-treatment for LTBI ( $n=5$ , less than 5 years before their inclusion), or for aTB ( $n=2$  without radiological sequela) (Figures 1 and 2A with open symbols for patients with a past treatment).

### Added Value of the HBHA-IGRA

As the QFT was recently reported to be less sensitive to detect LTBI subjects than previously thought, even in a healthy population (14), and as the sensitivity of the HBHA-IGRA was reported to be higher than that of the QFT and to help to stratify LTBI subjects in different subgroups (18, 22), we evaluated the sensitivity of the HBHA-IGRA to detect *M. tuberculosis* infection in this cohort of psoriatic patients. Among the 14 TST<sup>+</sup> patients, 13 of them had a positive HBHA-IGRA result, indicating that the HBHA-IGRA were better correlated with the TST than the QFT (Figures 1 and 2B). The only TST<sup>+</sup> patient with a negative HBHA-IGRA was a patient with a TB risk factor (nurse) on immunosuppressive treatment (methotrexate), with a TST induration size of 16 mm in spite of a negative QFT (Figure 2B). Among the 13 TST<sup>+</sup> HBHA-IGRA<sup>+</sup> patients, only 8 had a positive QFT (represented by open symbols on Figure 2B). The results of the HBHA-IGRA were not considered for the decision to provide or to avoid prophylactic anti-TB treatment, as this test was still under investigation in these potentially immunocompromised patients (Figure 1).

The HBHA-IGRA was also positive for 12/35 patients that were negative for both TST and QFT (Figures 1 and 2B). The demographic and clinical characteristics of these patients were not different from those of the TST<sup>+</sup> patients (Table 1). A trend for lower HBHA-induced IFN- $\gamma$  concentrations in these patients compared to the TST<sup>+</sup> patients was observed, but the differences

were not significant (Figure 3). These results indicate that within the all cohort of psoriatic patients, 51% of them have developed an IFN- $\gamma$  response to the mycobacterial antigen HBHA.

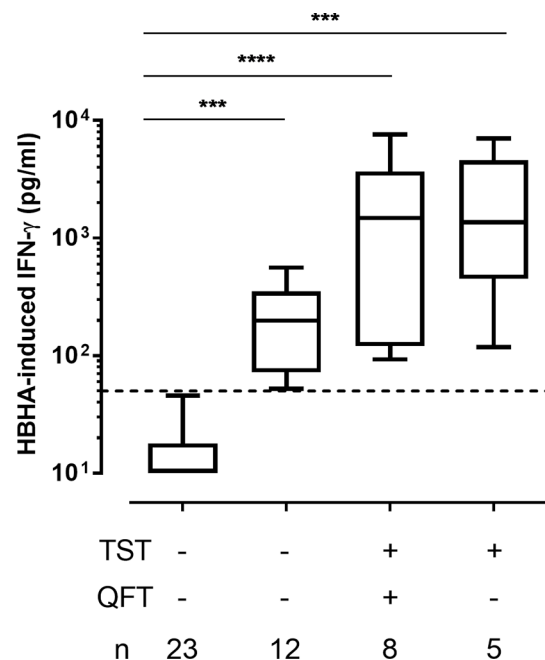


**FIGURE 3** | HBHA-induced- IFN- $\gamma$  concentrations. IFN- $\gamma$  concentrations were measured in 24 h culture supernatants of PBMC incubated with HBHA. Patients were subdivided into 4 groups according to their TST and QFT status. Boxplots represent medians and interquartile ranges (25th-75th), with whiskers (min-max). Dotted lines indicate the positivity cut-off for HBHA-IGRA. \*\*\* $p \leq 0.001$ ; \*\*\*\* $p \leq 0.0001$ .

## Serial HBHA-IGRA During Biotherapy

Twelve patients with a positive HBHA-IGRA were re-tested after one or two years of treatment with anti-TNF- $\alpha$  (n=7) or anti-IL-23 antibodies (n=5). Six of them were initially TST<sup>+</sup> (with 5 QFT<sup>+</sup> and 2/5 prophylactically treated for TB before starting the biotherapy), whereas the other 6 were TST<sup>-</sup>QFT<sup>-</sup>. They all were persistently positive in the HBHA-IGRA, and for 10/12 patients, the HBHA-induced IFN- $\gamma$  concentrations were even higher during biotherapy than before treatment (p=0.002) (**Figure 4**). One patient, initially TST<sup>-</sup>QFT<sup>-</sup>, had a very strong increase in the HBHA-induced IFN- $\gamma$  concentration between the two IGRAs (from 231 pg/ml to 39,919 pg/ml), and the QFT became positive at the second blood sampling (13.83 UI/ml) (open circle on **Figure 4**). This patient reported professional contact with a patient with aTB in the months preceding the second IGRA, so that following this contact, and after exclusion of aTB, he received prophylactic anti-TB treatment for LTBI.

## HBHA-Induced Chemokines

To further characterize the HBHA-induced immune responses in psoriatic patients, we analyzed a panel of selected cytokines/chemokines induced by HBHA in 12 HBHA-IGRA<sup>+</sup> patients, and compared the results to those obtained for 3 HBHA-IGRA<sup>-</sup> TST<sup>-</sup>QFT<sup>-</sup> patients included as controls. Among the HBHA-

IGRA<sup>+</sup> patients, 5 were TST<sup>+</sup>QFT<sup>+</sup>, 3 were TST<sup>+</sup>QFT<sup>-</sup>, and 4 were TST<sup>-</sup>QFT<sup>-</sup> (Supplementary **Figure 1**).

No HBHA-induced cytokine/chemokine was detected for the 3 psoriatic patients with an absence of identified immune response to *M. tuberculosis* (TST<sup>-</sup>QFT<sup>-</sup>HBHA-IGRA<sup>-</sup>) and hence considered as non-infected (**Figure 5**). In contrast, the 12 HBHA-IGRA<sup>+</sup> patients were characterized by various profiles of HBHA-induced cytokines/chemokines. A restricted profile of HBHA-induced cytokines characterized TST<sup>+</sup>QFT<sup>+</sup> psoriatic patients, compared to the TST<sup>+</sup>QFT<sup>-</sup> patients (**Figure 5**). Most TST<sup>+</sup>QFT<sup>+</sup>HBHA-IGRA<sup>+</sup> patients secreted IL-2, TNF- $\alpha$  and IL-10 in response to HBHA, in addition to IFN- $\gamma$ , whereas the proportion of these patients secreting GM-CSF, IL-17A, IL-1 $\beta$ , IL-6 and MIP-1 $\alpha$  in response to HBHA was very low (**Figure 5B**), with low concentrations of these chemokines when they were detected (**Figure 5A**). TST<sup>+</sup>QFT<sup>+</sup>HBHA-IGRA<sup>+</sup> patients also secreted IFN- $\gamma$ , IL-2 and TNF- $\alpha$  in response to HBHA, but they all additionally secreted GM-CSF, IL-6, MIP-1 $\alpha$ , and most of them also secreted IL-10 and IL-1 $\beta$ , and 1/3 secreted IL-17A. All these chemokines were secreted at high concentrations (**Figure 5A**). These HBHA-induced chemokine profiles were not a consequence of psoriasis but rather reflected the LTBI status of the patients, as they share similar profiles with LTBI subjects who did not suffer from psoriasis (V.C. unpublished). Finally, all HBHA-IGRA<sup>+</sup> patients in spite of negative TST and QFT secreted TNF- $\alpha$ , IL-10, IL-1 $\beta$  and IL-6 in addition to IFN- $\gamma$  in response to HBHA. Most of them secreted GM-CSF and MIP-1 $\alpha$ , and 1/4 secreted IL-17A, whereas only 50% of them secreted low concentrations of IL-2 (**Figure 5**). The profile of HBHA-induced cytokines/chemokines was thus similar in HBHA-IGRA<sup>+</sup> patients who were TST<sup>-</sup>QFT<sup>-</sup> and those who were TST<sup>+</sup>QFT<sup>+</sup>.

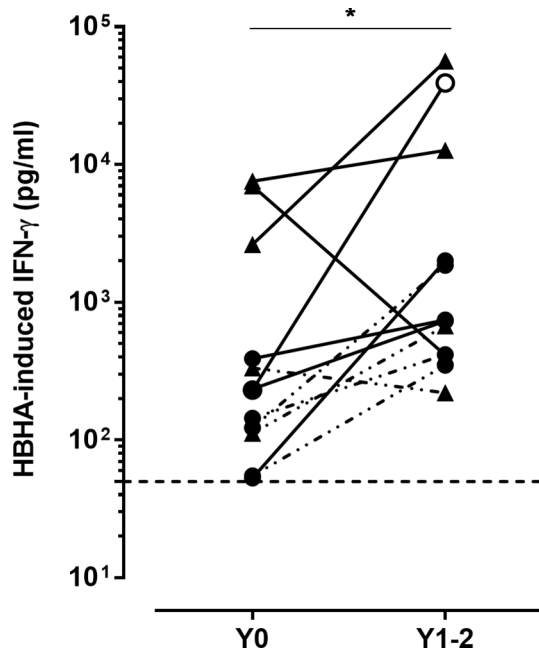


**FIGURE 4 |** Kinetics of the HBHA-induced IFN- $\gamma$  responses. HBHA-induced IFN- $\gamma$  concentrations were measured in 24 h culture supernatants of HBHA-stimulated PBMC, before starting biotherapy (Y0) and 1 to 2 years later (Y1-2) in 12 patients. Triangles represent TST<sup>+</sup> patients, and circles represent TST<sup>-</sup> patients. Open circle represents a patient in contact with a TB index case. The lines bridge results from the same patient. Filled lines indicated patients treated with anti-TNF- $\alpha$  antibodies, whereas dotted lines are for patients treated with anti-IL-23 antibodies. The horizontal dotted line indicates the positivity cut-off for HBHA-IGRA. \*p  $\leq$  0.05.

## DISCUSSION

Using the recommended strategy to detect LTBI among psoriatic patients eligible to receive biological treatment, i.e. combining TST and IGRA after evaluation of the patients' risk factors and chest X-ray results, we identified here 28.6% of LTBI psoriatic patients. This is a high proportion of LTBI patients for a low TB incidence country like Belgium where the prevalence of positive TST among healthy unexposed adolescents is 0.2% (V. Sizaire, FARES, personal communication). Among 54 adults with Crohn disease evaluated before anti-TNF- $\alpha$  treatment, we found only 3.7% of TST<sup>+</sup>QFT<sup>+</sup> patients (2/54), a prevalence which remains quite low (V. Corbière, personal communication), whereas the prevalence of positive TST among TB contacts reaches 30% in Belgium (V. Sizaire, FARES – personal communication). Even if 6/50 patients mentioned a contact or a possible contact with a TB patient, the results of this study indicate that the prevalence of LTBI among psoriatic patients is elevated, in agreement with some previous reports also applying TST and/or IGRA-based guidelines for LTBI screening of psoriatic patients before anti-TNF- $\alpha$  treatment (15, 23). Based on TST only, 50% of patients with psoriasis who were candidates for biological therapy were treated for LTBI in Greece (23), and up to 20% in Spain (24). In these two studies, the TST cut-off level was  $\geq$  5 mm, which could at least partially explain the high prevalence of possible LTBI. Based on T-SPOT.TB only, 20% of psoriatic patients screened before anti-TNF- $\alpha$  treatment were treated for

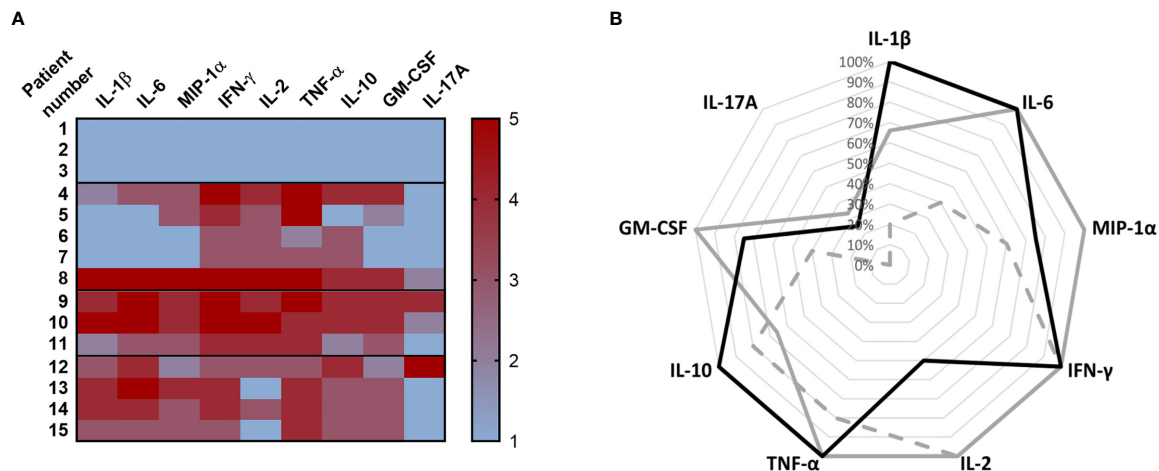


**FIGURE 5** | HBHA-induced cytokine/chemokine profiles. PBMC from 3 different groups of patients were *in vitro* stimulated with HBHA during 24 h and cytokines/chemokines were measured in the culture supernatants using a multiparameter based immunoassay. **(A)** Heat-map of the HBHA-induced cytokine/chemokine secretions. Three TST<sup>+</sup> patients (patient n°1 to 3) were included in parallel to 5 TST<sup>+</sup> QFT<sup>+</sup> patients (patient n°4 to 8), 3 TST<sup>+</sup> QFT<sup>+</sup> patients (patient n°9 to 11) and 4 TST<sup>+</sup> QFT<sup>+</sup> but HBHA<sup>+</sup> patients (patient n°12 to 15). A color scale representing the intensity of the cytokine/chemokine concentrations was established for each analyte from negative values (1, blue) to doubtful (2, pink), low and strong cytokine/chemokine concentrations (3 to 5, from light red to dark red). **(B)** Radar chart of the HBHA-induced cytokine/chemokine profiles indicating the percentages of patients within each group secreting IL-1 $\beta$ , IL-6, MIP-1 $\alpha$ , IFN- $\gamma$ , IL-2, TNF- $\alpha$ , IL-10, GM-CSF and IL-17A at concentrations higher than the upper limit of the grey zone around the defined cut-off value. TST<sup>+</sup>QFT<sup>+</sup>HBHA-IGRA<sup>+</sup> patients are represented by the dotted line (n=5), TST<sup>+</sup>QFT<sup>+</sup>HBHA-IGRA<sup>+</sup> patients are represented by the grey line (n=3), and TST<sup>+</sup>QFT<sup>+</sup>HBHA-IGRA<sup>+</sup> patients are represented by the black line (n=4).

LTBI in Switzerland (25). These authors recommended to base the diagnosis of LTBI on T-SPOT.TB only rather than on TST, as most of their patients were BCG vaccinated and as they reported strong association between the T-SPOT.TB results and the presence of risk factors for LTBI (25). High prevalence of LTBI among psoriatic patients as defined by a positive TST in the Greek and Belgian studies may be attributed to possible false positive TST results due to previous BCG vaccination or immune responses to NTM. The proportion of BCG vaccinated patients in our cohort was however low (12%) as systematic BCG vaccination is not recommended in Belgium, and the proportions of TST<sup>+</sup> ( $\geq 10$  mm) attributable to BCG is very low (1%) if tested  $\geq 10$  years after BCG vaccination (13). Concerning a possible interference of NTM on the positivity of the TST, it remains unlikely even if it cannot formally be excluded. As nicely analyzed by Farhat et al. (13) in an extensive review of the literature and meta-analysis estimating the false positive TST results between 10 and 14 mm due to NTM, it appears that this proportion ranged from 0.1% in Montreal or France to reach a maximum of 2.3% in India (13). False-positive TST results due to immune responses to NTM in our study are unlikely as only two QFT<sup>+</sup> patients had TST induration size  $< 15$  mm (between 10 and 14 mm): one of them reported active TB history during infancy, and the other was previously treated for LTBI. All the other patients considered as LTBI had a TST induration size  $\geq 15$  mm. Finally, we cannot formally excluded that false positive TST in psoriatic patients could occur as a result of the pro-inflammatory state of their skin (26). However, if we considered only the QFT results, the incidence of LTBI in our patients cohort reached 16% which remain higher than in the general population in Belgium. We therefore conclude that psoriatic patients evaluated for LTBI when eligible for a

biotherapy are characterized by a high incidence of LTBI. As previously suggested by Ramagopalan (27), this might be due to a predisposition of patients with a past TB to develop an IMID like psoriasis as 3 patients reported a past history of TB.

As LTBI is now recognized as being an heterogeneous group of individuals with different risk of reactivation of the infection, it is widely accepted that different subgroups should be identified based on different immune responses with the aim to identify those who are most likely to reactivate the infection (10, 11). In view of the high proportion of LTBI patients detected among psoriatic patients by classical tests, this is of utmost importance within these cohorts of patients to avoid unnecessary and potentially toxic preventive anti-TB treatment. By evaluating here in addition to the QFT, the IFN- $\gamma$  response to a latency-associated mycobacterial antigen, HBHA, and by analyzing also a panel of other chemokines induced by this antigen, we identified different subgroups of psoriatic patients based on their immune responses to mycobacterial antigens. The HBHA-IGRA was positive in all but one TST<sup>+</sup> patients, and may therefore eventually be proposed to replace the TST, which is difficult to perform in psoriatic patients with extensive skin lesions. Among the 13 TST<sup>+</sup>HBHA-IGRA<sup>+</sup> patients, only 8 of them had a positive QFT defining two different groups of patients with an immune response to mycobacterial antigens. The analysis of a large array of chemokines and cytokines induced by HBHA in these psoriatic patients further allowed us to substantiate the existence of two clearly distinct subgroups. Whereas TST<sup>+</sup>HBHA<sup>+</sup>QFT<sup>+</sup> patients secreted several chemokines (IL-1 $\beta$ , IL-6, MIP-1 $\alpha$ , GM-CSF), as well as IL-2, TNF- $\alpha$ , and for some of them, IL-17A, reported to play a role in protection against TB (28), TST<sup>+</sup>HBHA<sup>+</sup>QFT<sup>+</sup> patients had a more restricted profile of cytokines induced by HBHA. As HBHA was reported to be a



protective antigen against TB in mouse models of vaccination with HBHA followed by a challenge with *M. tuberculosis* (29, 30), and as in humans, HBHA-immune responses are more common in LTBI subjects and in treated aTB patients than in untreated patients with aTB (18, 21, 29), our results suggest that the broad array of HBHA-induced chemokines associated with a negative QFT may identify patients with a lower risk of reactivation of the *M. tuberculosis* infection. QFT<sup>+</sup> patients are in contrast probably those with a higher risk of reactivation as they also have increased frequencies of *M. tuberculosis* antigens induced regulatory T cells subsets (31), known to be preferentially elevated in patients with aTB (32). Combining the results of the HBHA-induced immune responses with those of the QFT may therefore help to stratify the LTBI psoriatic patients in different subgroups and to identify patients who should be prioritized to receive prophylactic anti-TB treatment before starting biotherapy, those with a positive QFT, and not those with an isolated positive HBHA-IGRA who are better protected by their immune responses against an eventual reactivation of *M. tuberculosis* infection. This proposed attitude would have result in the prophylactic treatment of only 2/49 patients (4%) in place of 7/49 (14%) in our cohort of psoriatic patients.

We further identified a third group of psoriatic patients with positive immune responses to mycobacterial antigens. A subgroup of patients had positive HBHA-IGRA in spite of negative TST and negative QFT. Similarly to results obtained in TST<sup>+</sup> patients, these HBHA-IGRA were persistently positive, often with higher responses after 1 or 2 years of biotherapy than before treatment. This suggests the existence in these patients of mycobacteria-specific memory immune responses and is consistent with a rise in intensity of IGRA responses reported previously during biotherapies (33). These HBHA-IGRA<sup>+</sup>TST<sup>-</sup> patients had less frequent LTBI risk factors than the TST<sup>+</sup>QFT<sup>+</sup> LTBI patients, and we cannot formally exclude a possible interference from immune responses to *M. avium* in these patients as HBHA is produced by this NTM as well (34). However HBHA proteins produced by different mycobacteria differ in their structure and activity (34), and the importance of the precise amino acid sequence and of the methylation pattern of HBHA for its recognition by T cells from LTBI subjects was demonstrated (35). Interestingly, the HBHA-induced chemokines and cytokines profiles were very similar in these HBHA-IGRA<sup>+</sup>TST<sup>-</sup> patients to those found for TST<sup>+</sup>QFT<sup>-</sup> HBHA-IGRA<sup>+</sup> patients. The induction by HBHA of IL-1 $\beta$  and IL-6 secretions in both TST<sup>+</sup>QFT<sup>-</sup> and TST<sup>-</sup>QFT<sup>-</sup> patients further suggests the possible presence in these patients of innate memory cells, as described in association with trained immunity induced by previous BCG vaccination (36, 37). These HBHA-induced immune responses do however not imply that all these psoriatic patients have an enhanced risk of TB reactivation. On the contrary, these HBHA-induced immune responses may contribute to a better protection of these patients against a reactivation or a new infection with *M. tuberculosis*. The development of LTBI (TST<sup>+</sup>QFT<sup>+</sup>) after exposure to a TB index case reported here in a psoriatic patient under anti-TNF- $\alpha$  treatment, having initially an immune response to HBHA with a negative TST, support this hypothesis and suggests that this patient was at least partially protected against the development of aTB disease.

We conclude that the incidence of LTBI in psoriatic patients is high, even in a low TB incidence country, and that sensitive immunological tests should be used to detect them. Combining different immunological tests may help to select patients who should be prioritized to receive prophylactic anti-TB treatment before starting biotherapies. Based on the indirect evidence of protective immune responses against aTB induced by HBHA in humans and on direct evidence in animal models, we propose that HBHA-IGRA<sup>+</sup>QFT<sup>-</sup> patients should not be prioritized to receive anti-TB prophylaxis before anti-TNF- $\alpha$  treatment, but that the persistence of their protective anti-HBHA immune response during treatment should be controlled. However, more information on the predictive value of HBHA-induced immune responses for the protection against aTB development in psoriatic patients are still needed.

## DATA AVAILABILITY STATEMENT

The raw data supporting the conclusions of this article will be made available by the authors, without undue reservation.

## ETHICS STATEMENT

The study involving human participants was reviewed and approved by the Comité d'éthique hospitalo-facultaire Erasme-ULB (021/406). The patients/participants provided their written informed consent to participate in this study.

## AUTHOR CONTRIBUTIONS

FB: conceptualization, investigation, resources, writing. VD: conceptualization, data curation, methodology. FD: investigation. FW: resources. AV: data curation, investigation. CL: resources, writing. FM: conceptualization, formal analysis, funding acquisition, supervision, visualization, writing. VC: conceptualization, data curation, formal analysis, investigation, methodology, project administration, validation, writing. All authors contributed to the article and approved the submitted version.

## ACKNOWLEDGMENTS

The authors thank J.P. Van Vooren for critically reading the manuscript and V. Sizaïre (FARES) for providing personal communication on the prevalence of latent and active TB in Belgium.

## SUPPLEMENTARY MATERIAL

The Supplementary Material for this article can be found online at: <https://www.frontiersin.org/articles/10.3389/fimmu.2021.672894/full#supplementary-material>

## REFERENCES

- Nestle FO, Kaplan DH, Barker J. Psoriasis. *N Engl J Med* (2009) 361(5):496–509. doi: 10.1056/NEJMra0804595
- Parisi R, Symmons DP, Griffiths CE, Ashcroft DM. Identification and Management of Associated Comorbidity (IMPACT) Project Team: Global Epidemiology of Psoriasis: A Systematic Review of Incidence and Prevalence. *J Invest. Dermatol* (2013) 133(2):377–85. doi: 10.1038/jid.2012.339
- Oliveira Mde F, Rocha Bde O, Duarte GV. Psoriasis: Classical and Emerging Comorbidities. *An Bras Dermatol* (2015) 90(1):9–20. doi: 10.1590/abd1806-4841.20153038
- Campa M, Ryan C, Menter A. An Overview of Developing TNF-alpha Targeted Therapy for the Treatment of Psoriasis. *Expert Opin Investig Drugs* (2015) 24(10):1343–54. doi: 10.1517/13543784.2015.1076793
- Petiscelli L, Ricceri F, Prignano F. Tuberculosis Reactivation Risk in Dermatology. *J Rheumatol* (2014) 91:65–70. doi: 10.3899/jrheum.140104
- Zhang Z, Fan W, Yang G, Xu Z, Wang J, Cheng Q, et al. Risk of Tuberculosis in Patients Treated With TNF-alpha Antagonists: A Systematic Review and Meta-Analysis of Randomised Controlled Trials. *BMJ Open* (2017) 7(3):e012567. doi: 10.1136/bmjopen-2016-012567
- Blauvelt A, Papp KA, Griffiths CE, Randazzo B, Wasfi Y, Shen YK, et al. Efficacy and Safety of Guselkumab, an anti-interleukin-23 Monoclonal Antibody, Compared With Adalimumab for the Continuous Treatment of Patients With Moderate to Severe Psoriasis: Results From the Phase III, Double-Blinded, Placebo- and Active Comparator-Controlled VOYAGE 1 Trial. *J Am Acad Dermatol* (2017) 76(3):405–17. doi: 10.1016/j.jaad.2016.11.041
- Blauvelt A, Gooderham M, Iversen L, Ball S, Zhang L, Agada NO, et al. Efficacy and Safety of Ixekizumab for the Treatment of Moderate-to-Severe Plaque Psoriasis: Results Through 108 Weeks of a Randomized, Controlled Phase 3 Clinical Trial (UNCOVER-3). *J Am Acad Dermatol* (2017) 77(5):855–62. doi: 10.1016/j.jaad.2017.06.153
- Pai M, Riley LW, Colford JM Jr. Interferon- $\gamma$  Assays in the Immunodiagnosis of Tuberculosis: A Systematic Review. *Lancet Infect Dis* (2004) 4(12):761–76. doi: 10.1016/S1473-3099(04)01206-X
- Cadena AM, Fortune SM, Flynn JL. Heterogeneity in Tuberculosis. *Nat Rev Immunol* (2017) 17(11):691–702. doi: 10.1038/nri.2017.69
- Gethahun H, Matteelli A, Abubakar I, Abdel Aziz M, Baddeley A, Barreira D, et al. Management of Latent Mycobacterium Tuberculosis Infection: WHO Guidelines for Low Tuberculosis Burden Countries. *Eur Respir J* (2015) 46:1563–76. doi: 10.1183/13993003.01245-2015
- Lin J, Ziring D, Desai S, Kim S, Wong M, Korin Y, et al. Tnfalpha Blockade in Human Diseases: An Overview of Efficacy and Safety. *Clin Immunol* (2008) 126(1):13–30. doi: 10.1016/j.clim.2007.08.012
- Farhat M, Greenaway C, Pai M, Menzies D. False-Positive Tuberculin Skin Tests: What is the Absolute Effect of BCG and non-Tuberculous Mycobacteria? *Int J Tuberc Lung Dis* (2006) 10(11):1192–204. PMID: 17131776
- Doan TN, Eisen DP, Rose MT, Slack A, Stearnes G, McBryde ES. Interferon-gamma Release Assay for the Diagnosis of Latent Tuberculosis Infection: A Latent-Class Analysis. *PloS One* (2017) 12(11):e0188631. doi: 10.1371/journal.pone.0188631
- Sichletidis L, Settas L, Spyrtos D, Chloros D, Patakas D. Tuberculosis in Patients Receiving anti-TNF Agents Despite Chemoprophylaxis. *Int J Tuberc Lung Dis* (2006) 10(10):1127–32. PMID: 17044206
- Kim HC, Jo KW, Jung YJ, Yoo B, Lee CK, Kim YG, et al. Diagnosis of Latent Tuberculosis Infection Before Initiation of Anti-Tumor Necrosis Factor Therapy Using Both Tuberculin Skin Test and QuantiFERON-TB Gold In Tube Assay. *Scand J Infect Dis* (2014) 46(11):763–9. doi: 10.3109/00365548.2014.938691
- Hoffmann H, Avsar K, Göres R, Mavi AC, Hofman-Thiel S. Equal Sensitivity of the New Generation QuantiFERON-TB Gold Plus in Direct Comparison With the Previous Test Version QuantiFERON-TB Gold IT. *Clin Microbiol Infect* (2016) 22:701–3. doi: 10.1016/j.cmi.2016.05.006
- Hougardy JM, Schepers K, Place S, Drowart A, Lechevin V, Verscheure V, et al. Heparin-Binding-Hemagglutinin-Induced IFN-gamma Release as a Diagnostic Tool for Latent Tuberculosis. *PloS One* (2007) 2(10):e926. doi: 10.1371/journal.pone.0000926
- Wyndham-Thomas C, Corbiere V, Dirix V, Smits K, Domont F, Libin M, et al. Key Role of Effector Memory CD4+ T Lymphocytes in a Short-Incubation Heparin-Binding Hemagglutinin Gamma Interferon Release Assay for the Detection of Latent Tuberculosis. *Clin Vaccine Immunol* (2014) 21(3):321–8. doi: 10.1128/CVI.00651-13
- Menozi FD, Rouse JH, Alavi M, Laude-Sharp M, Muller J, Bisschoff R, et al. Identification of a Heparin-Binding Hemagglutinin Present in Mycobacteria. *J Exp Med* (1996) 184:993–1001. doi: 10.1084/jem.184.3.993
- Masungi C, Temmerman S, Van Vooren JP, Drowart A, Pethe K, Menozi FD, et al. Differential T and B Cell Responses Against Mycobacterium Tuberculosis Heparin-Binding Hemagglutinin Adhesin in Infected Healthy Individuals and Patients With Tuberculosis. *J Inf Dis* (2002) 185:513–20. doi: 10.1086/338833
- Corbière V, Pottier G, Bonkain F, Schepers K, Verscheure V, Lecher S, et al. Risk Stratification of Latent Tuberculosis Defined by Combined Interferon Gamma Release Assays. *PloS One* (2012) 7(8):e43285. doi: 10.1371/journal.pone.0043285
- Bassukas ID, Kosmidou M, Gaitanis G, Tsiouri G, Tsianos E. Patients With Psoriasis are More Likely to be Treated for Latent Tuberculosis Infection Prior to Biologics Than Patients With Inflammatory Bowel Disease. *Acta Derm Venereol* (2011) 91(4):444–6. doi: 10.2340/00015555-1106
- Sanchez-Moya AI, Garcia-Doval I, Carretero G, Sanchez-Carazo J, Ferrandiz C, Herrera Ceballos E, et al. Latent Tuberculosis Infection and Active Tuberculosis in Patients With Psoriasis: A Study on the Incidence of Tuberculosis and the Prevalence of Latent Tuberculosis Disease in Patients With Moderate-Severe Psoriasis in Spain. BIOBADADERM Registry. *J Eur Acad Dermatol Venereol* (2013) 27(11):1366–74. doi: 10.1111/jdv.12011
- Lafitte E, Janssens JP, Roux-Lombard P, Thielen AM, Barde C, Marazza G, et al. Tuberculosis Screening in Patients With Psoriasis Before Antitumour Necrosis Factor Therapy: Comparison of an Interferon-Gamma Release Assay vs. Tuberculin Skin Test. *Br J Dermatol* (2009) 161(4):797–800. doi: 10.1111/j.1365-2133.2009.09331
- Bassukas ID, Gaitanis G, Constantopoulos SH. Diagnosis of Tuberculosis in Patients With Psoriasis: The Need for a Modified Approach. *Eur Respir J* (2011) 38(1):231–2. doi: 10.1183/09031936.00016611
- Ramagopalan SV, Goldacre R, Skingsley A, Conlon C, Goldacre MJ. Associations Between Selected Immune-Mediated Diseases and Tuberculosis: Record-Linkage Studies. *BMC Med* (2013) 11:97. doi: 10.1186/1741-7015-11-97
- Khader SA, Bell GK, Pearl JE, Fountain JJ, Rangel-Moreno J, Cilley GE, et al. IL-23 and IL-17 in the Establishment of Protective Pulmonary CD4+ T Cell Responses After Vaccination and During Mycobacterium Tuberculosis Challenge. *Nat Immunol* (2007) 8(4):369–77. doi: 10.1038/ni1449
- Temmerman S, Pethe K, Parra M, Alonso S, Rouanet C, Pickett T, et al. Methylation-Dependent T Cell Immunity to Mycobacterium Tuberculosis Heparin-Binding Hemagglutinin. *Nat Med* (2004) 10(9):935–41. doi: 10.1038/nm1090
- Parra M, Pickett T, Delogu G, Dheenadhyalan V, Debie AS, Locht C, et al. The Mycobacterial Heparin-Binding Hemagglutinin is a Protective Antigen in the Mouse Aerosol Challenge Model of Tuberculosis. *Infect Immun* (2004) 72(12):6799–805. doi: 10.1128/IAI.72.12.6799-6805.2004
- Serrano CJ, Castaneda-Delgado JE, Trujillo-Ochoa JL, Gonzalez-Amaro R, Garcia-Hernandez MH, Enciso-Moreno JA. Regulatory T-cell Subsets in Response to Specific Mycobacterium Tuberculosis Antigens In Vitro Distinguish Among Individuals With Different QFT and TST Reactivity. *Clin Immunol* (2015) 157(2):145–55. doi: 10.1016/j.clim.2015.02.008
- Hougardy JM, Place S, Hildebrand M, Drowart A, Debie AS, Locht C, et al. Regulatory T Cells Depress Immune Responses to Protective Antigens in Active Tuberculosis. *Am J Respir Crit Care Med* (2007) 176(4):409–16. doi: 10.1164/rccm.200701-084OC
- Sauzullo I, Mengoni F, Mascia C, Pavone P, Savelloni G, Massetti AP, et al. Diagnostic Performance in Active TB of QFT-Plus Assay and Co-Expression of CD25/CD134 in Response to New Antigens of Mycobacterium Tuberculosis. *Med Microbiol Immunol* (2019) 208(2):171–83. doi: 10.1007/s00430-018-00576-4
- Lefrancois LH, Bodier CC, Lecher S, Gilbert FB, Cochart T, Harichaux G, et al. Purification of Native HBHA From Mycobacterium Avium Subsp. Paratuberculosis. *BMC Res Notes* (2013) 6:55. doi: 10.1186/1756-0500-6-55

35. Corbière V, Segers J, Desmet R, Lecher S, Loyens M, Petit E, et al. Natural T Cell Epitope Containing Methyl Lysines on Mycobacterial Heparin-Binding Hemagglutinin. *J Immunol* (2020) 204:1715–23. doi: 10.4049/jimmunol.1901214
36. Arts RJW, Moorlag S, Novakovic B, Li Y, Wang SY, Oosting M, et al. Bcg Vaccination Protects Against Experimental Viral Infection in Humans Through the Induction of Cytokines Associated With Trained Immunity. *Cell Host Microbe* (2018) 23(1):89–100.e5. doi: 10.1016/j.chom.2017.12.010
37. Moorlag S, Roring RJ, Joosten LAB, Netea MG. The Role of the Interleukin-1 Family in Trained Immunity. *Immunol Rev* (2018) 281(1):28–39. doi: 10.1111/imr.12617

**Conflict of Interest:** The authors declare that the research was conducted in the absence of any commercial or financial relationships that could be construed as a potential conflict of interest.

Copyright © 2021 Benhadou, Dirix, Domont, Willaert, Van Praet, Locht, Mascart and Corbière. This is an open-access article distributed under the terms of the Creative Commons Attribution License (CC BY). The use, distribution or reproduction in other forums is permitted, provided the original author(s) and the copyright owner(s) are credited and that the original publication in this journal is cited, in accordance with accepted academic practice. No use, distribution or reproduction is permitted which does not comply with these terms.



# Integrative Multi-Omics Reveals Serum Markers of Tuberculosis in Advanced HIV

Sonya Krishnan<sup>1\*†</sup>, Artur T. L. Queiroz<sup>2,3†</sup>, Amita Gupta<sup>1,4,5†</sup>, Nikhil Gupte<sup>1,4</sup>, Gregory P. Bisson<sup>6</sup>, Johnstone Kumwenda<sup>7</sup>, Kogieleum Naidoo<sup>8,9</sup>, Lerato Mohapi<sup>10</sup>, Vidya Mave<sup>4</sup>, Rosie Mngqibisa<sup>11</sup>, Javier R. Lama<sup>12</sup>, Mina C. Hosseinipour<sup>13,14</sup>, Bruno B. Andrade<sup>2,3,15,16†</sup> and Petros C. Karakousis<sup>1,5\*†</sup> on behalf of the ACTG A5274 REMEMBER NWCS 414 Study Team

## OPEN ACCESS

### Edited by:

Novel N. Chegou,  
Stellenbosch University, South Africa

### Reviewed by:

Amit Singh,  
All India Institute of Medical Sciences,  
India  
Willy Ssengooba,  
Makerere University, Uganda  
Myrsini Kaforou,  
Imperial College London,  
United Kingdom

### \*Correspondence:

Sonya Krishnan  
skrish25@jhmi.edu  
Petros C. Karakousis  
petros@jhmi.edu

<sup>†</sup>These authors have contributed  
equally to this work

### Specialty section:

This article was submitted to  
Microbial Immunology,  
a section of the journal  
Frontiers in Immunology

**Received:** 06 March 2021

**Accepted:** 13 May 2021

**Published:** 08 June 2021

### Citation:

Krishnan S, Queiroz ATL, Gupta A, Gupte N, Bisson GP, Kumwenda J, Naidoo K, Mohapi L, Mave V, Mngqibisa R, Lama JR, Hosseinipour MC, Andrade BB and Karakousis PC (2021) Integrative Multi-Omics Reveals Serum Markers of Tuberculosis in Advanced HIV. *Front. Immunol.* 12:676980. doi: 10.3389/fimmu.2021.676980

<sup>1</sup> Center for Clinical Global Health Education and Center for Tuberculosis Research, Division of Infectious Diseases, Department of Medicine, Johns Hopkins University School of Medicine, Baltimore, MD, United States, <sup>2</sup> Instituto Gonçalo Moniz, Fundação Oswaldo Cruz, Salvador, Brazil, <sup>3</sup> Multinational Organization Network Sponsoring Translational and Epidemiological Research (MONSTER) Initiative, Salvador, Brazil, <sup>4</sup> Byramjee Jeejeebhoy Government Medical College-Johns Hopkins University Clinical Research Site, Pune, India, <sup>5</sup> Department of International Health, Johns Hopkins Bloomberg School of Public Health, Baltimore, MD, United States, <sup>6</sup> Department of Medicine, Division of Infectious Diseases, Perelman School of Medicine at the University of Pennsylvania, Philadelphia, PA, United States, <sup>7</sup> College of Medicine-Johns Hopkins Project, Blantyre, Malawi, <sup>8</sup> Centre for the AIDS Programme of Research in South Africa, Nelson R Mandela School of Medicine, College of Health Sciences, University of KwaZulu-Natal, Durban, South Africa, <sup>9</sup> South African Medical Research Council-CAPRISA HIV-TB Pathogenesis and Treatment Research Unit, Doris Duke Medical Research Institute, University of KwaZulu-Natal, Durban, South Africa, <sup>10</sup> Soweto ACTG CRS, Perinatal HIV Research Unit, University of the Witwatersrand, Johannesburg, South Africa, <sup>11</sup> Durban International Clinical Research Site, Enhancing Care Foundation, Durban, South Africa, <sup>12</sup> Asociación Civil Impacta Salud y Educación, Lima, Peru, <sup>13</sup> University of North Carolina Project-Malawi, Lilongwe, Malawi, <sup>14</sup> Division of Infectious Diseases, Department of Medicine, University of North Carolina at Chapel Hill School of Medicine, Chapel Hill, NC, United States, <sup>15</sup> Curso de Medicina, Faculdade de Tecnologia e Ciências (FTC), Salvador, Brazil, <sup>16</sup> Curso de Medicina, Escola Bahiana de Medicina e Saúde Pública (EBMSP), Salvador, Brazil

Tuberculosis (TB) accounts for disproportionate morbidity and mortality among persons living with HIV (PLWH). Conventional methods of TB diagnosis, including smear microscopy and Xpert MTB/RIF, have lower sensitivity in PLWH. Novel high-throughput approaches, such as miRNAomics and metabolomics, may advance our ability to recognize subclinical and difficult-to-diagnose TB, especially in very advanced HIV. We conducted a case-control study leveraging REMEMBER, a multi-country, open-label randomized controlled trial comparing 4-drug empiric standard TB treatment with isoniazid preventive therapy in PLWH initiating antiretroviral therapy (ART) with CD4 cell counts <50 cells/ $\mu$ L. Twenty-three cases of incident TB were site-matched with 32 controls to identify microRNAs (miRNAs), metabolites, and cytokines/chemokines, associated with the development of newly diagnosed TB in PLWH. Differentially expressed miRNA analysis revealed 11 altered miRNAs with a fold change higher than 1.4 or lower than -1.4 in cases relative to controls ( $p < 0.05$ ). Our analysis revealed no differentially abundant metabolites between cases and controls. We found higher TNF $\alpha$  and IP-10/CXCL10 in cases ( $p = 0.011$ ,  $p = 0.0005$ ), and higher MDC/CCL22 in controls ( $p = 0.0072$ ). A decision-tree algorithm identified gamma-glutamylthreonine and hsa-miR-215-5p as the optimal variables to classify incident TB cases (AUC 0.965; 95% CI 0.925-



1.000). hsa-miR-215-5p, which targets genes in the TGF- $\beta$  signaling pathway, was downregulated in cases. Gamma-glutamylthreonine, a breakdown product of protein catabolism, was less abundant in cases. To our knowledge, this is one of the first uses of a multi-omics approach to identify incident TB in severely immunosuppressed PLWH.

**Keywords:** tuberculosis, HIV, microRNA, metabolomics, biomarker, multi-omics

## INTRODUCTION

In resource-limited countries, human immunodeficiency virus (HIV) and tuberculosis (TB) account for a large burden of infectious disease and contribute significantly to morbidity and mortality. In 2019, there were an estimated 690,000 deaths from HIV/AIDS, with 33% of deaths attributed to HIV-associated TB (1). HIV increases the risk of reactivation of latent TB 20-fold, with escalating risk as CD4<sup>+</sup> T cells decline (2). HIV and TB co-infection subsequently becomes a lethal combination, with each infection accelerating the progression of the other, as both lead to deterioration of immunologic function.

There is an urgent need to identify persons living with HIV (PLWH) at risk of developing TB, as these individuals could benefit from enhanced monitoring and clinical assessment. Conventional methods of TB diagnosis have limitations in PLWH, as sputum smear microscopy is negative in 24–61% cases of pulmonary TB and HIV co-infection (3). The rapid molecular assay Xpert MTB/RIF offers enhanced diagnostic capabilities but, for smear-negative cases, has an estimated sensitivity of only 55% in PLWH, compared to 67% in HIV-negative individuals (4, 5). Furthermore, the use of sputum-based diagnostic assays does not adequately address extrapulmonary TB, a more common disease in PLWH (6, 7). Thus, novel rapid molecular assays using other readily available biospecimens are urgently needed to improve the diagnosis of both pulmonary and extrapulmonary TB in HIV-infected individuals.

Increasingly, there has been a shift to using host-based assays for TB diagnosis. *Mycobacterium tuberculosis* infection profoundly alters host metabolism and whole-body energy consumption, and metabolites have been profiled in plasma and serum using <sup>1</sup>H nuclear magnetic resonance (NMR) spectroscopy and liquid chromatography with tandem mass spectrometry (LC-MS/MS) (8–14). In addition to metabolites, host microRNAs (miRNAs) have been studied as circulating biomarkers for various diseases, including TB (15, 16). miRNAs are stable, small, noncoding RNAs involved in the regulation of gene expression, apoptosis, cell cycle control, and development (17), and their dysregulation has been implicated in the pathogenesis of numerous cancers and autoimmune diseases (18–20), as well as TB and other infectious diseases (21–26).

Previous studies have focused on identifying circulating host metabolite or miRNA profiles for TB diagnosis, however there are limited data on the changes of these analytes in the serum of patients with TB and HIV co-infection. Furthermore, HIV infection alone leads to changes in host serum metabolites and miRNAs (27–33), thus the profile of altered metabolites and

miRNAs in TB and HIV co-infection may differ compared to either TB infection or HIV infection. In this study we used a multi-omics approach to identify metabolites, miRNA, and cytokines/chemokines associated with the development of newly diagnosed TB in PLWH, leveraging clinical data and biospecimens from the AIDS Clinical Trials Group Study 5274 “Reducing Early Mortality and Morbidity by Empiric TB Treatment” (REMEMBER) (34). We hypothesize that TB induces changes in the metabolism and inflammatory state of the HIV-infected host which can be detected in the serum and can be used for the diagnosis of pulmonary and extrapulmonary TB. The novel use of a multi-omics approach in HIV/TB co-infection could further identify contributory pathways in the development of TB and could highlight future potential therapeutic targets to aid in the prevention of TB morbidity and mortality.

## MATERIALS AND METHODS

### Study Design

We conducted a case-control study from participants enrolled in REMEMBER, an international, multi-site, open-label randomized control trial comparing empiric 4-drug TB therapy with isoniazid preventive therapy in PLWH (34). This study assessed TB and mortality in adults with HIV and CD4<sup>+</sup> T cell counts <50 cells/ $\mu$ L within 48 weeks of initiating antiretroviral therapy (ART).

### Study Population

REMEMBER trial participants were recruited from 18 outpatient research clinics in 10 countries (Malawi, South Africa, Haiti, Kenya, Zambia, India, Brazil, Zimbabwe, Peru, and Uganda) (34). A total of 850 participants were enrolled from October 31, 2011, to June 9, 2014. All participants were HIV-infected, ART-naïve individuals, aged 13 years or older, with a CD4<sup>+</sup> T cell count <50 cells/ $\mu$ L, and had no evidence of active TB. Participants were randomized to receive empiric 4-drug TB therapy or isoniazid preventive therapy and were all initiated on ART. At baseline, participants were screened for TB prior to enrolling, with all 18 sites using symptoms screening, microscopy for identification of acid-fast bacilli in sputum, sputum culture, chest radiography, and only 5 sites using Xpert MTB/RIF assay. Individuals were excluded if they had confirmed or suspected TB, had received TB therapy within 96 weeks prior to study entry, had received isoniazid preventive therapy 48 weeks prior to study entry, or had a household contact diagnosed with multidrug-resistant TB. Other inclusion

criteria included liver transaminase (AST or ALT) levels  $\leq 2.5$  times the upper limit of normal, a creatinine clearance of at least 30 mL/min, and a Karnofsky score of at least 30.

For our case-control study, we randomly selected 23 cases who developed incident TB, defined as a TB diagnosis within 48 weeks of randomization. Cases were selected from 57 TB events in the parent trial, based on sample availability. The specimen used for biomarker analysis was selected from the scheduled study visit closest to the time of TB diagnosis. Participants originated from 5 clinical sites in South Africa, India, and Peru. Incident TB cases were either microbiologically confirmed or were adjudicated by an external clinical TB endpoint review committee. For each case, up to two study-time and site-matched controls were randomly selected by incidence density sampling, with a total of 32 controls selected. For controls, a stored biospecimen within  $\pm 4$  weeks of the time of the corresponding case TB diagnosis was used for biomarker analysis. Cases and controls were followed for 96 weeks after study entry.

## Sample Collection

Six mL of whole blood was collected in plain vacutainer and was transported to the processing lab at ambient temperature within 2 hours of collection. Blood was allowed to clot up to 30 minutes and was spun at 1000–1200  $\times$  g for 10 minutes. Serum aliquots were prepared and stored at  $-70^{\circ}\text{C}$ . Each site shipped serum on dry ice to the United States. Per participant, a total of one aliquot of 1 mL of serum was used to complete miRNA, metabolite, and cytokine analyses.

## miRNA Next Generation Sequencing (NGS)

RNA was isolated using the miRNeasy Serum/Plasma Advanced Kit (QIAGEN) according to the manufacturer's recommendation. In brief, library preparation was performed using the QIAseq miRNA Library Kit (QIAGEN). A total of 5  $\mu\text{L}$  RNA was converted into miRNA NGS libraries. Adapters containing unique molecular identifiers (UMIs) were ligated to the RNA. Then RNA was converted to cDNA with amplification of cDNA using PCR followed by sample purification. Library preparation quality control (QC) was performed using either Bioanalyzer 2100 (Agilent) or TapeStation 4200 (Agilent). The libraries were pooled in equimolar ratios and were quantified using qPCR. The library pool was then sequenced on a NextSeq500 sequencing instrument according to the manufacturer instructions. Raw data was de-multiplexed and FASTQ files for each sample were generated using the bcl2fastq software (Illumina, Inc.). FASTQ data were checked using the FastQC tool. Cutadapt (1.11) was used to extract information of adapter and UMI in raw reads, and output from Cutadapt was used to remove adapter sequences and to collapse reads by UMI with in-house script. Bowtie2 (2.2.2) was used for mapping the reads.

## miRNA Statistical Analysis

The count miRNA expression matrix was examined using the DESeq2 package from R 4.0.2 to identify differentially expressed miRNAs following the comparison of cases versus controls based

on the metadata (35). We defined miRNA as differentially expressed when statistical test values (False Discovery Rate adjusted p-value) were lower than 0.05 and the fold change/difference was higher than 1.4 or lower than  $-1.4$ . A total of 2555 miRNAs were used in the analysis. Candidate differentially expressed miRNAs were visualized in a volcano plot with EnhancedVolcano package from R (version 4.0.2). For the enrichment analysis, the targets from the differentially expressed miRNAs were retrieved from mirTarBase and scanned by the REACTOME database using compareCluster package from R (version 4.0.2) (36, 37). The expression values from miRNA were normalized with variance stabilizing transformation with *varianceStabilizingTransformation* function, without prior information of samples, and were used for downstream analysis with a decision-tree algorithm.

## Quantitative Metabolomics Analysis

Sample preparation was performed at Metabolon, Inc. (Durham, North Carolina) using the automated MicroLab STAR system from Hamilton Company with quality-control analyses performed as previously described (38, 39). Briefly, for quality control purposes, numerous recovery standards were added prior to the first step in the extraction process. Organic solvent was removed by briefly placing samples on a TurboVap<sup>®</sup> (Zymark). The sample extracts were stored overnight under nitrogen before preparation for analysis by ultrahigh performance liquid chromatography-tandem mass spectroscopy (UPLC-MS/MS). All methods utilized a Waters ACQUITY UPLC and a Thermo Scientific Q-Exactive high resolution/accurate mass spectrometer (MS) interfaced with a heated electrospray ionization (HESI-II) source and Orbitrap mass analyzer operated at 35,000 mass resolution. Sample extract was dried and reconstituted in solvents for optimization of analysis as previously described (40). MS analysis used dynamic exclusion to alternate between MS and data-dependent MS<sup>n</sup> scans, with scan range covering 70–1000 m/z. Metabolon's hardware and software were used to extract, peak-identify, and QC-process raw data, as previously described (40). Metabolon libraries of purified standards or recurrent unknown entities were used to identify compounds.

## Metabolite Statistical Analysis

Group comparison analysis was performed with the omu package in R (version 4.0.2) using a nonparametric test (41). The fold-change value for each compound was estimated with the omu\_summary function. A total of 621 metabolites were evaluated. Differentially abundant metabolites were defined when statistical test values (False Discovery Rate adjusted p-value) were lower than 0.05 and the fold change was higher than 1 or lower than  $-1$ .

## Quantification of Serum Cytokines and Chemokines

Serum samples were thawed from storage at  $-80^{\circ}\text{C}$  and were filtered using a Millipore human cytokine/chemokine magnetic bead method. Serum levels of epidermal growth factor (EGF), fibroblast growth factor (FGF-2), eotaxin/CCL11, transforming growth factor- $\alpha$  (TGF- $\alpha$ ), granulocyte colony-stimulating factor

(GCSF), FMS-like tyrosine kinase 3 ligand (Flt-3L), granulocyte-macrophage colony-stimulating factor (GM-CSF), fractalkine/CX3CL1, interferon- $\alpha$ 2 (IFN- $\alpha$ 2), interferon- $\gamma$  (IFN- $\gamma$ ), growth related oncogene (GRO), IL-10, monocyte chemoattractant protein-3 (MCP-3/CCL7), IL-12, macrophage-derived chemokine (MDC/CCL22), IL-13, IL-15, sCD40L, IL-17/CTLA8, IL1Ra, IL-1a, IL-9, IL-1b, IL-2, IL-3, IL-4, IL-5, IL-6, IL-7, IL-8/CXCL8, IP-10/CXCL10, monocyte chemoattractant protein-1 (MCP-1/CCL2), macrophage inflammatory protein 1- $\alpha$  (MIP-1 $\alpha$ /CCL3), macrophage inflammatory protein 1- $\alpha$  (MIP-1 $\alpha$ /CCL4), tumor necrosis factor- $\alpha$  (TNF $\alpha$ ), tumor necrosis factor- $\alpha$  (TNF- $\alpha$ /LTA), and vascular endothelial growth factor (VEGF) were measured using Luminex assays following vendor guidelines and a Luminex 100 apparatus (Luminex, Oosterhout, Netherlands), according to the manufacturer's instructions.

## Serum Marker Statistical Analysis

The Luminex data (concentrations in pg/ml) were compared across the groups using the Wilcoxon-Mann-Whitney U test, and the results were displayed in box plots.

## Combining “Omics” Data for Biomarker Identification

The variance stabilizing transformation miRNA expression values, the log-transformed metabolite data, and the pg/ml values from the serum markers were combined into one dataset and were used to perform a decision-tree approach for identification of a minimal variable set to best classify the groups. The analysis input included 2555 miRNAs, 621 metabolites, and 37 cytokines/chemokines. The best tree was indicated by output from the analysis using the Complexity Parameter, which maximizes the tree classification accuracy. The machine-learning-based decision-tree algorithm, with 1000 leave one out cross-validations, was applied to identify the minimal variable (miRNA/metabolite/serum cytokine or chemokine) set

which exhibited the highest classification power to describe the cases and controls with the rpart package (42). Principal Component Analysis was performed in R 4.0.2, using the function *prcomp*, in order to compare and visualize grouping in the source data (miRNAomics, metabolomics and cytokines/chemokines). The resulting variables were retrieved from the dataset and the classification was assessed by receiver operating characteristic (ROC) curve and the area under the curve (AUC) values. Subgroup analysis based on microbiological confirmation of TB status was not performed, as specified *a priori*, due to small sample size.

## Ethics Statement

Local ethics committees and the Institutional Review Boards at Johns Hopkins University and participating site institutions approved this study (IRB00123874). Written informed consent was provided by all participants (NCT01380080).

## RESULTS

### Study Population

Among the 23 cases of incident TB, 12 were diagnosed with pulmonary TB (PTB) and 11 were diagnosed with extrapulmonary TB (EPTB). Fourteen cases (61%) were microbiologically confirmed by smear, culture and/or Xpert MTB/RIF assay and the remaining met criteria for diagnosis of TB by an external clinical TB endpoint review committee. The characteristics of cases and controls are shown in **Table 1**. The median time to TB diagnosis in the cases was 4.6 weeks following initiation of ART and TB therapy (either 4-drug empiric therapy or isoniazid preventative therapy) (**Supplemental Figure 1**). The median time from TB diagnosis to specimen collection (occurring during a scheduled clinic visit) was 0.6 weeks. Thirty-one of 32 controls were not suspected of having TB and remained TB-free at up to 96 weeks of observation after study

**TABLE 1 |** Characteristics of cases and controls.

Study Characteristics		TB Case (n=23)	Control (n=32)	p-value
Sex (n,%)	Male	13 (56.5)	13 (40.6)	0.41
	Female	10 (43.5)	19 (59.4)	0.41
Age (median, IQR)		34 (31-41)	35 (30.5-41)	0.70
Baseline CD4 (median, IQR)		32 (26-44)	24.5 (14-37)	0.53
Baseline HIV Log Viral Load (median, IQR)		5.69 (5.24-6.22)	5.41 (5.02-5.68)	0.007
WHO Stage 3 or 4 (n,%)		7 (30.87)	7 (21.87)	0.72
TB Therapy Arm (n,%)	Empiric 4-drug	12 (52.17)	16 (50)	0.87
	IPT	11 (47.83)	16 (50)	0.87
Time to TB Diagnosis in Weeks (median, IQR)		4.6 (2-16.1)	—	
Type of TB (n,%)	PTB	12 (52.17)	—	
	EPTB	11 (47.83)	—	
BMI < 18.5 kg/m <sup>2</sup> (n,%)		6 (26.09)	5 (15.62)	0.67
Albumin (median, IQR)		3.55 (3.1-3.9)	3.8 (3.4-4.3)	0.015
Hemoglobin $\geq$ 8 $\mu$ g/dL (n, %)		21 (91.30)	32 (100)	0.09

IQR, Interquartile range; WHO, World Health Organization; TB, Tuberculosis; IPT, Isoniazid preventative therapy; PTB, Pulmonary TB; EPTB, Extrapulmonary TB; BMI, Body Mass Index (BMI).

entry. One control had suspected TB meningitis at week 1 but was ultimately diagnosed with cryptococcal meningitis based on the presence of cryptococcal antigen in the cerebrospinal fluid. Repeating analyses excluding this control did not alter the results.

### Profile of Differentially Expressed miRNAs

Our analysis of differentially expressed miRNAs in serum resulted in 11 altered miRNA with a log-fold change higher than 1.4 or lower than -1.4 in cases relative to controls ( $p < 0.05$ , **Figure 1A**). Ten miRNAs (hsa-miR-29b-3p, hsa-miR-30c-2-3p, hsa-miR-197-5p, hsa-miR-340-3p, hsa-miR-452-5p, hsa-miR-671-3p, hsa-miR-885-5p, hsa-miR-941, hsa-miR-3127-5p and hsa-miR-3605-5p) were upregulated and one (hsa-miR-215-5p) was downregulated (**Figure 1A**). We performed pathway enrichment analysis of target genes to investigate potential pathways predicted to be influenced by these differentially expressed miRNAs. Twenty-five pathways were found as probably influenced by the upregulated miRNAs and 4 as probably influenced by the downregulated miRNA (**Figure 1B**). Notable pathways targeted by upregulated miRNAs include cell cycle regulation (“PI3K-Akt signaling pathway” and “p53 signaling pathway”), endocrinological pathways, and pathways related to numerous cancers. The TGF- $\alpha$  signaling pathway was influenced by the downregulated miRNA (hsa-miR-215-5p).

### Comparison of Serum Metabolite Levels

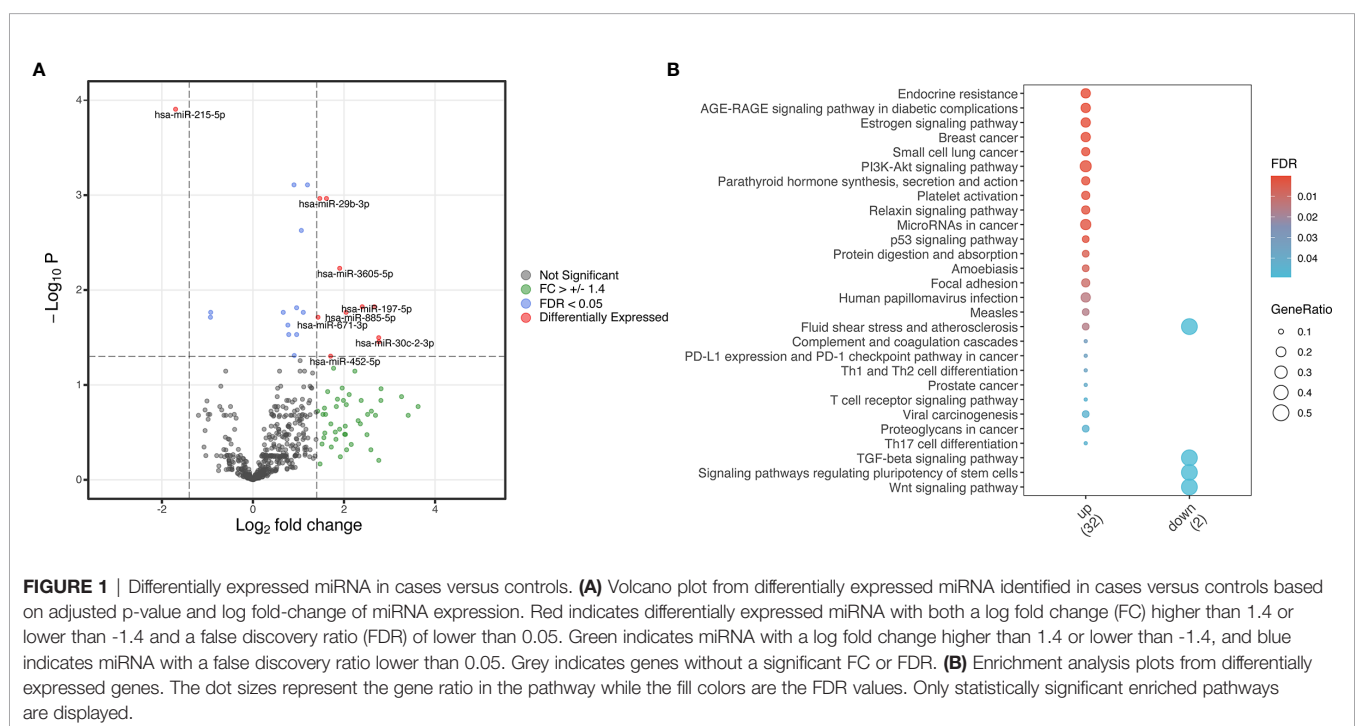
Our analysis revealed no differentially abundant metabolites between cases and controls. All differences in serum metabolite abundance were not significant after the False Discovery Ratio (FDR) correction (**Supplemental Figure 2**).

### Comparison of Serum Cytokines and Chemokines

Of the 37 cytokines/chemokines measured in serum, we observed 3 with statistically significant differences between cases and controls: TNF $\alpha$ , IP-10/CXCL10 and MDC/CCL22 (**Figure 2**). TNF $\alpha$  was higher in cases (44.2 pg/ml) versus controls (30.25 pg/ml) ( $p = 0.0072$ ) as was IP-10/CXCL10 (619.9 pg/ml in cases versus 378.65 pg/ml in controls;  $p = 0.0005$ ). MDC/CCL22 was higher in controls (978.7 pg/ml) compared to cases (686.2 pg/ml) ( $p = 0.011$ ).

### Combining Omics Data for Identifying a TB Biomarker Panel in HIV Patients

A decision-tree algorithm identified gamma-glutamylthreonine and hsa-miR-215-5p as the optimal variables to classify incident TB cases (**Figure 3A**). Despite the absence of differentially abundant metabolites in cases versus controls, the  $\log_2$  gamma-glutamylthreonine value was indicated as a classification variable in the decision tree along with variance stabilizing transformation values of hsa-miR-215-5p. Gamma-glutamylthreonine and hsa-miR-215p were less abundant in cases. This metabolite/miRNA pair was able to classify the samples with only 5 errors (**Figure 3B**). Of the 5 misclassifications, two were controls and three were cases. Among the cases, one was cultured-confirmed EBTB, one was non-microbiologically confirmed EPTB, and the last was non-microbiologically confirmed PTB. The metabolite/miRNA pair showed a strong ability to accurately discriminate TB cases from controls with a sensitivity of 0.81 (95% CI 0.66-0.94), a specificity of 0.78 (95% CI 0.61-0.96), and an AUC of 0.965 (95% CI 0.925-1.000) (**Figure 3C**). Integration of cytokine markers did not improve the AUC. Leave-one-out cross validation had an accuracy of 0.907 (95% CI 0.82-0.98), a no-information rate of





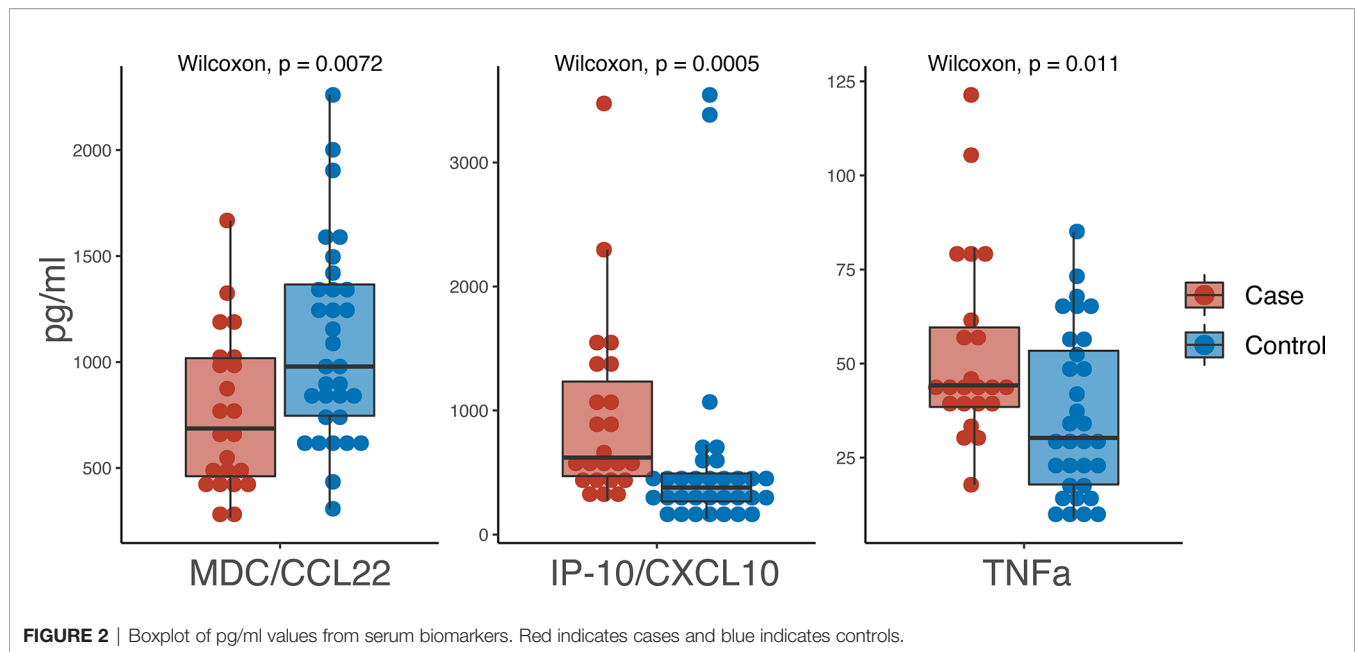


**FIGURE 2** | Boxplot of pg/ml values from serum biomarkers. Red indicates cases and blue indicates controls.

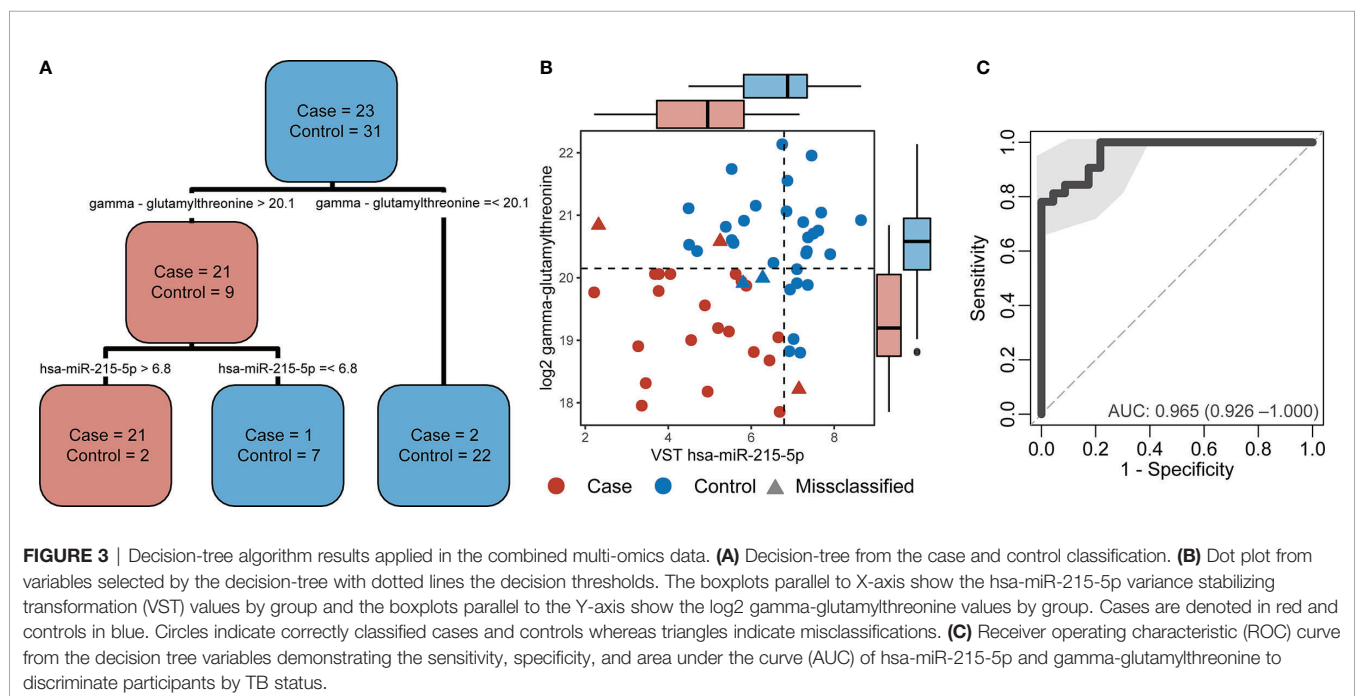


**FIGURE 3** | Decision-tree algorithm results applied in the combined multi-omics data. (A) Decision-tree from the case and control classification. (B) Dot plot from variables selected by the decision-tree with dotted lines the decision thresholds. The boxplots parallel to X-axis show the hsa-miR-215-5p variance stabilizing transformation (VST) values by group and the boxplots parallel to the Y-axis show the log<sub>2</sub> gamma-glutamylthreonine values by group. Cases are denoted in red and controls in blue. Circles indicate correctly classified cases and controls whereas triangles indicate misclassifications. (C) Receiver operating characteristic (ROC) curve from the decision tree variables demonstrating the sensitivity, specificity, and area under the curve (AUC) of hsa-miR-215-5p and gamma-glutamylthreonine to discriminate participants by TB status.

0.544, a sensitivity of 0.869, and a specificity of 0.967 with Principal Component Analysis shown in **Supplemental Figure 3**.

## DISCUSSION

In this study, we used three different modalities and integrated omics analysis comparing HIV-infected adults with and without incident TB to identify serum markers characteristic of incident TB. Our case-control study was comprised of

severely immunocompromised PLWH initiating ART from geographically diverse regions. Our cases of incident TB developed despite participants receiving either 4-drug empiric TB therapy or isoniazid preventive therapy at the time of ART initiation. We found that 11 miRNAs were differentially expressed in incident TB cases, as were three serum cytokines (TNFa, IP-10/CXCL10 and MDC/CCL22), with significant differences between cases and controls. We found no differentially abundant metabolites between cases and controls at the time of TB diagnosis. Finally, a decision-tree algorithm

approach using the multi-omics data revealed that two variables, gamma-glutamylthreonine and hsa-miR-215-5p, had the ability to accurately discriminate incident TB cases from controls with an AUC of 0.965. To our knowledge, this is one of the first uses of a multi-omics approach to identify incident TB in a severely immunosuppressed cohort of PLWH.

Our data contribute to a growing body of literature assessing the role of miRNAs in TB pathogenesis. Only one miRNA, hsa-miR-215-5p, was downregulated in incident TB cases versus controls. hsa-miR-215-5p, a widely studied miRNA found to be dysregulated in numerous cancers, targets genes in the cell cycle and signaling pathways, cell migration, cellular metabolism, and the TGF- $\beta$  signaling pathway (18). In a case-control study of HIV-negative TB-infected participants, Wang et al. found that miR-215 was significantly increased in patients with TB following two months of treatment, relative to untreated TB patients (25). Our enrichment analysis showed the TGF- $\alpha$  signaling pathway as likely influenced by the downregulated hsa-miR-215-5p, consistent with previous studies (43, 44). TGF- $\alpha$  has been implicated in TB pathogenesis, through suppression of IFN- $\gamma$  and with upregulated TGF- $\alpha$ 1 inhibiting cytotoxic T-cell function in granulomas, leading to promotion of mycobacterial growth (45, 46).

Some of the pathways targeted by our identified upregulated miRNAs have been linked to TB pathogenesis, including PI3K/AKT/mTORC1 and p53. In a study of individuals with culture-proven pulmonary tuberculosis, *Mycobacterium tuberculosis* (Mtb) was found *in vitro* to inhibit signaling through the PI3K/AKT/mTORC1 pathway, leading to increased MMP-1, thus contributing to a tissue destructive phenotype facilitating granuloma cavitation and TB transmission (47). In an *in vivo* murine model of TB, as well as in human peripheral mononuclear blood cells, pharmacologic inhibition of the AKT/mTOR pathway also led to blunted cellular responses to Mtb (48). Tumor suppressor p53, a regulator of DNA repair, cell cycle arrest, and apoptosis, has also been found to have antituberculosis activity. Mtb has been found to suppress apoptosis in alveolar epithelial cells *in vitro* and this was associated with increased replication of intracellular bacteria (49). Furthermore, macrophages deficient in p53 have higher intracellular survival of Mtb and lower rates of apoptosis compared to wild type macrophages (50). The 10 upregulated miRNAs in our study found to be more abundant in the serum of cases relative to controls have not been associated with TB in prior studies (23–26, 47). The latter studies, however, did not assess the abundance of circulating miRNAs in a severely immunocompromised PLWH cohort, which may account for some of the differences in our findings.

We found that TNF $\alpha$  and IP-10/CXCL10 were elevated in cases at the time of incident TB diagnosis, whereas MDC/CCL22 was elevated in controls. TNF $\alpha$  and IP-10/CXCL10 were recently identified as two biomarkers among a 4-biomarker signature predictive of incident versus prevalent TB in a less immunosuppressed cohort of PLWH (51). IP-10/CXCL10, a chemokine secreted in response to INF $\gamma$ , has been established as a biomarker of latent and active TB (52–54). IP-10/CXCL10 has also been identified as predictive of incident TB in two

additional studies of PLWH (55, 56). High baseline TNF $\alpha$  has recently been found to be associated with incident TB in an HIV-negative cohort (57).

The field of metabolomics has been applied to the study of TB and HIV co-infection, with a recent study finding that precursors of arachidonic acid and linoleic acid metabolism were altered in a TB-IRIS group compared to a non-IRIS group (13). While we did not find any differentially abundant metabolites in our study, gamma-glutamylthreonine, a breakdown product of protein catabolism (58), did have the ability to accurately discriminate incident TB cases from controls when combined with hsa-miR-215-5p (AUC 0.965). A multi-omics approach has been increasingly employed to investigate novel mechanisms of complex diseases, offering insight into genotype-phenotype relationships (59–61).

Our study has several limitations. There is some degree of heterogeneity between cases and controls, given the multi-site nature of the REMEMBER trial and the two treatment arms of empiric 4-drug anti-TB therapy versus isoniazid preventative therapy (34). Furthermore, our highly immunosuppressed cohort of PLWH (CD4<sup>+</sup> T cell counts <50 cells/ $\mu$ L) had other prevalent and incident co-infections in addition to TB, which likely contributed to further heterogeneity in our results. This could in part explain the lack of differences in serum metabolites between our two groups. Since our study was conducted in participants with advanced HIV, it is unclear if these findings would apply to an earlier stage of HIV.

Another limitation of the study pertains to the selection of controls. Given the case-control nature of the study design, one control was suspected of having TB meningitis but was ultimately diagnosed with antigen-confirmed cryptococcal meningitis. The controls remained TB-free for up to 96 weeks of observation from study entry. Although controls were screened for TB at baseline by symptoms, chest radiography, smear, and sputum culture, some controls received empiric 4-drug anti-TB therapy, which could have treated subclinical TB. However, the effect of such a misclassification would likely have minimized differences between the two groups. Nonetheless, future studies evaluating and validating these markers in participants who did not receive empiric TB therapy would be beneficial. Furthermore, based on sample availability, we had access to a relatively small sample size of cases and controls, limiting our power. We were unable to validate our findings due to limited existing databases containing cytokines, metabolites, and miRNAs studied in a similar cohort of highly immunocompromised PLWH who develop incident TB. Based on the nature of our case-control study design, we were able to evaluate markers at the time of incident TB diagnosis but were not able to extend this to a predictive model, as we did not evaluate serum markers at baseline.

Our findings could provide the basis for future blood-based studies of cytokines, metabolites, and miRNAs for validation and development of a TB diagnostic signature, however further validation is needed, particularly in geographically and ethnically diverse HIV seropositive populations with varying degrees of immune suppression. The WHO Target Product Profile for TB biomarker diagnostic tests recommends

development and testing against a gold standard of confirmed pulmonary TB, with a goal specificity of  $\geq 98\%$  and a sensitivity of  $\geq 65\%$  (62). While our model had a sensitivity of 0.81 (95% CI: 0.65–0.93) at a specificity of 98%, it was developed in both confirmed and adjudicated cases of PTB and EPTB. Future directions would include testing this miRNA/metabolite pair in a larger sample of PLWH with culture-confirmed pulmonary TB. In the future, integrated omics analysis could be used in longitudinal cohorts to determine if this miRNA/metabolite pair (or other profiles) is predictive of TB progression in a severely immunocompromised HIV cohort, a group that is at high risk of developing TB and experiencing subsequent mortality due to TB.

In summary, our data indicate that two variables, gamma-glutamylthreonine and hsa-miR-215-5p, had the ability to accurately discriminate incident TB cases from controls in a severely immunosuppressed PLWH cohort. These data provide insight into dysregulated disease pathways in individuals with advanced HIV who developed active TB disease, despite receipt of TB prophylaxis at the initiation of ART.

## DATA AVAILABILITY STATEMENT

The datasets presented in this study can be found in online repositories. The names of the repository/repositories and accession number(s) can be found below: <https://www.ncbi.nlm.nih.gov/geo/>, GSE166557.

## ETHICS STATEMENT

The studies involving human participants were reviewed and approved by Johns Hopkins Institutional Review Board. The patients/participants provided their written informed consent to participate in this study.

## AUTHOR CONTRIBUTIONS

AG and PK contributed to conception and design of the study. PK, AG, GB, JK, KN, LM, VM, RM, JL, and MH contributed to acquisition of data. AG, NG, AQ, and SK organized the database. AQ, BA, NG, and SK performed statistical analysis and interpreted data. SK wrote the first draft of the manuscript.

## REFERENCES

- World Health Organization. *Global Tuberculosis Report 2020*. Geneva: World Health Organization (2020). Available at: <http://library1.nida.ac.th/term-paper6/sd/2554/19755.pdf>.
- Pawłowski A, Jansson M, Sköld M, Rottenberg ME, Källénus G. Tuberculosis and HIV Co-Infection. *PLoS Pathog* (2012) 8:1–7. doi: 10.1371/journal.ppat.1002464
- Getahun H, Harrington M, O'Brien R, Nunn P. Diagnosis of Smear-Negative Pulmonary Tuberculosis in People With HIV Infection or AIDS in Resource-Constrained Settings: Informing Urgent Policy Changes. *Lancet* (2007) 369:2042–9. doi: 10.1016/S0140-6736(07)60284-0
- Theron G, Peter J, Van Zyl-Smit R, Mishra H, Streicher E, Murray S, et al. Evaluation of the Xpert MTB/RIF Assay for the Diagnosis of Pulmonary Tuberculosis in a High HIV Prevalence Setting. *Am J Respir Crit Care Med* (2011) 184:132–40. doi: 10.1164/rccm.201101-0056OC
- Horne D, Kohli M, Zifodya J, Schiller I, Dendukuri N, Tollefson D, et al. Xpert MTB/RIF and Xpert MTB/RIF Ultra for Pulmonary Tuberculosis and Rifampicin Resistance in Adults (Review). *Cochrane Database Syst Rev* (2019) 6:1–276. doi: 10.1002/14651858.CD009593.pub4. [www.cochranelibrary.com](http://www.cochranelibrary.com)

AQ, AG, BA, and PK wrote sections of the manuscript. All authors contributed to the article and approved the submitted version.

## FUNDING

Research reported in this publication was supported by the National Institute of Allergy and Infectious Diseases of the National Institutes of Health under award numbers UM1 AI068634, UM1 AI068636, and UM1 AI106701. The work was also supported by the Johns Hopkins Baltimore-Washington-India Clinical Trials Unit (BWI CTU) (NIH/NIAID UM1AI069465). This research was supported by grants from the AIDS Clinical Trials Group (ACTG) and CRDF Global to PK. This work was also supported by the Johns Hopkins University Center for AIDS Research (P30AI094189). SK was also supported by the National Institute of Health T32 AI007291-27. PCK was also supported by the NIH/NIAID grant K24AI143447.

## ACKNOWLEDGMENTS

This work was presented at the Conference on Retroviruses and Opportunistic Infections, March 6–10, 2021. The authors thank the participants and co-investigators of the A5274 REMEMBER. They acknowledge Evelyn Hogg and Rebecca LeBlanc for organization of contributing sites and sample shipment.

## SUPPLEMENTARY MATERIAL

The Supplementary Material for this article can be found online at: <https://www.frontiersin.org/articles/10.3389/fimmu.2021.676980/full#supplementary-material>

**Supplementary Figure 1** | Time to TB diagnosis from study enrollment in cases.

**Supplementary Figure 2** | Differentially abundant metabolites in cases versus controls. Analysis revealed no differentially abundant metabolites, as differences between cases and controls were not statistically significant after the False Discovery Ratio (FDR) correction.

**Supplementary Figure 3** | Principal component analysis of different input data. (A) miRNA expression data; (B) Metabolite data; (C) Cytokine/chemokine data.

6. Sama JN, Chida N, Polan RM, Nuzzo J, Page K, Shah M. High Proportion of Extrapulmonary Tuberculosis in a Low Prevalence Setting: A Retrospective Cohort Study. *Public Health* (2016) 138:101–7. doi: 10.1016/j.puhe.2016.03.033
7. Teixeira F, Raboni SM, Ribeiro C EL, França JC, Broska AC, Souza NL. Human Immunodeficiency Virus and Tuberculosis Coinfection in A Tertiary Hospital in Southern Brazil: Clinical Profile and Outcomes. *Microbiol Insights* (2018) 11:1–8. doi: 10.1177/1178636118813367
8. Macallan DC, McNurlan MA, Kurpad AV, de Souza G, Shetty PS, Calder AG, et al. Whole Body Protein Metabolism in Human Pulmonary Tuberculosis and Undernutrition: Evidence for Anabolic Block in Tuberculosis. *Clin Sci (Lond)* (1998) 94:321–31. doi: 10.1042/cs0940321
9. Zhou A, Ni J, Xu Z, Wang Y, Lu S, Sha W, et al. Application of 1H NMR Spectroscopy-Based Metabolomics to Sera of Tuberculosis Patients. *J Proteome Res* (2013) 12:4642–9. doi: 10.1021/pr4007359
10. Lau SKP, Lee KC, Curreen SOT, Chow WN, To KKW, Hung IFN, et al. Metabolomic Profiling of Plasma From Patients With Tuberculosis by Use of Untargeted Mass Spectrometry Reveals Novel Biomarkers for Diagnosis. *J Clin Microbiol* (2015) 53:3750–9. doi: 10.1128/JCM.01568-15
11. Vrieling F, Alisjahbana B, Sahiratmadja E, van Crevel R, Harms AC, Hankemeier T, et al. Plasma Metabolomics in Tuberculosis Patients With and Without Concurrent Type 2 Diabetes at Diagnosis and During Antibiotic Treatment. *Sci Rep* (2019) 9:1–12. doi: 10.1038/s41598-019-54983-5
12. Frediani JK, Jones DP, Tukvadze N, Uppal K, Sanikidze E, Kipiani M, et al. Plasma Metabolomics in Human Pulmonary Tuberculosis Disease: A Pilot Study. *PLoS One* (2014) 9:e108854. doi: 10.1371/journal.pone.0108854
13. Silva C, Graham B, Webb K, Ashton LV, Harton M, Luetkemeyer AF, et al. A Pilot Metabolomics Study of Tuberculosis Immune Reconstitution Inflammatory Syndrome. *Physiol Behav* (2017) 176:139–48. doi: 10.1016/j.jid.2019.04.015.A
14. Collins JM, Walker DI, Jones DP, Tukvadze N, Liu KH, Tran VT, et al. High-Resolution Plasma Metabolomics Analysis to Detect Mycobacterium Tuberculosis-associated Metabolites That Distinguish Active Pulmonary Tuberculosis in Humans. *PLoS One* (2018) 13:e0205398. doi: 10.1371/journal.pone.0205398
15. Xu Z, Zhou A, Ni J, Zhang Q, Wang Y, Lu J, et al. Differential Expression of miRNAs and Their Relation to Active Tuberculosis. *Tuberculosis* (2015) 95:395–403. doi: 10.1016/j.tube.2015.02.043
16. Chakrabarty S, Kumar A, Raviprasad K, Mallya S, Satyamoorthy K, Chawla K. Host and MTB Genome Encoded miRNA Markers for Diagnosis of Tuberculosis. *Tuberculosis* (2019) 116:37–43. doi: 10.1016/j.tube.2019.04.002
17. Gevert LFR, MacRae JJ. Regulation of microRNA Function in Animals. *Nat Rev Mol Cell Biol* (2019) 20:21–37. doi: 10.1038/s41580-018-0045-7
18. Vychytilova-Faltejskova P, Slaby O. MicroRNA-215: From Biology to Theranostic Applications. *Mol Aspects Med* (2019) 70:72–89. doi: 10.1016/j.mam.2019.03.002
19. Rupaimoole R, Slack FJ. MicroRNA Therapeutics: Towards a New Era for the Management of Cancer and Other Diseases. *Nat Rev Drug Discov* (2017) 16:203–21. doi: 10.1038/nrd.2016.246
20. Garo LP, Murugaiyan G. Contribution of MicroRNAs to Autoimmune Diseases. *Cell Mol Life Sci* (2016) 73:2041–51. doi: 10.1007/s00018-016-2167-4
21. Skalsky RL, Cullen BR. Viruses, microRNAs, and Host Interactions. *Annu Rev Microbiol* (2010) 64:123–41. doi: 10.1146/annurev.micro.112408.134243
22. Staedel C, Darfeuille F. MicroRNAs and Bacterial Infection. *Cell Microbiol* (2013) 15:1496–507. doi: 10.1111/cmi.12159
23. Sabir N, Hussain T, Shah SZA, Peramo A, Zhao D, Zhou X. miRNAs in Tuberculosis: New Avenues for Diagnosis and Host-Directed Therapy. *Front Microbiol* (2018) 9:602. doi: 10.3389/fmicb.2018.00602
24. Ruiz-Tagle C, Naves R, Balcells ME. Unraveling the Role of microRNAs in Mycobacterium Tuberculosis Infection and Disease: Advances and Pitfalls. *Infect Immun* (2020) 88:1–17. doi: 10.1128/IAI.00649-19
25. Wang C, Yang S, Liu CM, Jiang TT, Chen ZL, Tu HH, et al. Screening and Identification of Four Serum miRNAs as Novel Potential Biomarkers for Cured Pulmonary Tuberculosis. *Tuberculosis* (2018) 108:26–34. doi: 10.1016/j.tube.2017.08.010
26. Fu Y, Yi Z, Wu X, Li J, Xu F. Circulating microRNAs in Patients With Active Pulmonary Tuberculosis. *J Clin Microbiol* (2011) 49:4246–51. doi: 10.1128/JCM.05459-11
27. Scarpelini B, Zanoni M, Sucupira MCA, Truong HHM, Janini LMR, Segurado IDC, et al. Plasma Metabolomics Biosignature According to HIV Stage of Infection, Pace of Disease Progression, Viremia Level and Immunological Response to Treatment. *PLoS One* (2016) 11:e0161920. doi: 10.1371/journal.pone.0161920
28. Castellano P, Prevedel L, Valdebenito S, Eugenin EA. HIV Infection and Latency Induce a Unique Metabolic Signature in Human Macrophages. *Sci Rep* (2019) 9:3941. doi: 10.1038/s41598-019-39898-5
29. Peltenburg NC, Schoeman JC, Hou J, Mora F, Harms AC, Lowe SH, et al. Persistent Metabolic Changes in HIV-infected Patients During the First Year of Combination Antiretroviral Therapy. *Sci Rep* (2018) 8:16947. doi: 10.1038/s41598-018-35271-0
30. Narla V, Bhakta N, Freedman JE, Tanriverdi K, Maka K, Deeks SG, et al. Unique Circulating microRNA Profiles in HIV Infection. *J Acquir Immune Defic Syndr* (2018) 79:644–50. doi: 10.1097/QAI.0000000000001851
31. Modai S, Farberov L, Herzig E, Isakov O, Hizi A, Shomron N. HIV-1 Infection Increases microRNAs That Inhibit Dicer1, HRB and HIV-EP2, Thereby Reducing Viral Replication. *PLoS One* (2019) 14:e0211111. doi: 10.1371/journal.pone.0211111
32. Pilakka-Kanthikeel S, Saiyed ZM, Napuri J, Nair MPN. MicroRNA: Implications in HIV, a Brief Overview. *J Neurovirol* (2011) 17:416–23. doi: 10.1007/s13365-011-0046-1
33. Su B, Fu Y, Liu Y, Wu H, Ma P, Zeng W, et al. Potential Application of microRNA Profiling to the Diagnosis and Prognosis of HIV-1 Infection. *Front Microbiol* (2018) 9:3185. doi: 10.3389/fmicb.2018.03185
34. Hosseinipour MC, Bisson GP, Miyahara S, Sun X, Moses A, Riviere C, et al. Empirical Tuberculosis Therapy Versus Isoniazid in Adult Outpatients With Advanced HIV Initiating Antiretroviral Therapy (REMEMBER): A Multicountry Open-Label Randomised Controlled Trial. *Lancet* (2016) 387:1198–209. doi: 10.1016/S0140-6736(16)00546-8
35. Love MI, Huber W, Anders S. Moderated Estimation of Fold Change and Dispersion for RNA-seq Data With DESeq2. *Genome Biol* (2014) 15:1–21. doi: 10.1186/s13059-014-0550-8
36. Yu G, He QY. Reactomepa: An R/Bioconductor Package for Reactome Pathway Analysis and Visualization. *Mol Biosyst* (2016) 12:477–9. doi: 10.1039/c5mb00663e
37. Yu G, Wang LG, Han Y, He QY. ClusterProfiler: An R Package for Comparing Biological Themes Among Gene Clusters. *Omi A J Integr Biol* (2012) 16:284–7. doi: 10.1089/omi.2011.0118
38. Evans AM, DeHaven CD, Barrett T, Mitchell M, Milgram E. Integrated, Nontargeted Ultrahigh Performance Liquid Chromatography/ Electrospray Ionization Tandem Mass Spectrometry Platform for the Identification and Relative Quantification of the Small-Molecule Complement of Biological Systems. *Anal Chem* (2009) 81:6656–67. doi: 10.1021/ac901536h
39. Dutta NK, Klinkenberg LG, Vazquez MJ, Segura-Carro D, Colmenarejo G, Ramon F, et al. Inhibiting the Stringent Response Blocks Mycobacterium Tuberculosis Entry Into Quiescence and Reduces Persistence. *Sci Adv* (2019) 5:1–13. doi: 10.1126/sciadv.aav2104
40. Dutta NK, Tornheim JA, Fukutani KF, Paradkar M, Tiburcio RT, Kinikar A, et al. Integration of Metabolomics and Transcriptomics Reveals Novel Biomarkers in the Blood for Tuberculosis Diagnosis in Children. *Sci Rep* (2020) 10:1–11. doi: 10.1038/s41598-020-75513-8
41. Tiffany CR, Bäumler AJ. Omu, a Metabolomics Count Data Analysis Tool for Intuitive Figures and Convenient Metadata Collection. *Microbiol Resour Annu* (2019) 8:11–3. doi: 10.1128/mra.00129-19
42. Therneau T, Atkinson B, Ripley B, Ripley MB. *Rpart: Recursive Partitioning and Regression Trees. R Packag Version 4.1-10* (2015). Available at: <http://cran.ma.ic.ac.uk/web/packages/rpart/rpart.pdf%5Chttps://cran.r-project.org/web/packages/rpart/rpart.pdf>.
43. Mu J, Pang Q, Guo YH, Chen JG, Zeng W, Huang YJ, et al. Functional Implications of microRNA-215 in TGF-β1-Induced Phenotypic Transition of Mesangial Cells by Targeting CTNNB1P1. *PLoS One* (2013) 8:e58622. doi: 10.1371/journal.pone.0058622
44. Kato M, Arce L, Wang M, Putta S, Lanting L, Natarajan R. A microRNA Circuit Mediates Transforming Growth Factor-β1 Autoregulation in Renal Glomerular Mesangial Cells. *Kidney Int* (2011) 80:358–68. doi: 10.1038/ki.2011.43
45. Warsinske HC, Pienaar E, Linderman JJ, Mattila JT, Kirschner DE. Deletion of TGF-β1 Increases Bacterial Clearance by Cytotoxic T Cells in a Tuberculosis Granuloma Model. *Front Immunol* (2017) 8:1843. doi: 10.3389/fimmu.2017.01843



46. Hirsch CS, Hussaint R, Toossi Z, Dawood G, Shahid F, Ellner JJ. Tuberculosis: Suppression of Antigen-Driven Blastogenesis and Interferon  $\gamma$  Production. *Proc Natl Acad Sci U S A* (1996) 93:3193–8. doi: 10.1073/pnas.93.8.3193
47. Brace PT, Tezera LB, Bielecka MK, Mellows T, Garay D, Tian S, et al. Mycobacterium Tuberculosis Subverts Negative Regulatory Pathways in Human Macrophages to Drive Immunopathology. *PLoS Pathog* (2017) 13:1–25. doi: 10.1371/journal.ppat.1006367
48. Lachmandas E, Beigier-Bompadre M, Cheng SC, Kumar V, van Laarhoven A, Wang X, et al. Rewiring Cellular Metabolism Via the AKT/mTOR Pathway Contributes to Host Defence Against Mycobacterium Tuberculosis in Human and Murine Cells. *Eur J Immunol* (2016) 46:2574–86. doi: 10.1002/eji.201546259
49. Danelishvili L, McGarvey J, Li YJ, Bermudez LE. Mycobacterium Tuberculosis Infection Causes Different Levels of Apoptosis and Necrosis in Human Macrophages and Alveolar Epithelial Cells. *Cell Microbiol* (2003) 5:649–60. doi: 10.1046/j.1462-5822.2003.00312.x
50. Lim YJ, Lee J, Choi JA, Cho SN, Son SH, Kwon SJ, et al. M1 Macrophage dependent-p53 Regulates the Intracellular Survival of Mycobacteria. *Apoptosis* (2020) 25:42–55. doi: 10.1007/s10495-019-01578-0
51. Lesosky M, Rangaka MX, Pienaar C, Coussens AK, Goliath R, Mathee S, et al. Plasma Biomarkers to Detect Prevalent or Predict Progressive Tuberculosis Associated With Human Immunodeficiency Virus-1. *Clin Infect Dis* (2019) 69:295–305. doi: 10.1093/cid/ciy823
52. Qiu X, Xiong T, Su X, Qu Y, Ge L, Yue Y, et al. Accumulate Evidence for IP-10 in Diagnosing Pulmonary Tuberculosis. *BMC Infect Dis* (2019) 19:924. doi: 10.1186/s12879-019-4466-5
53. Tonby K, Ruhwald M, Kvale D, Dyrholm-Riise AM. IP-10 Measured by Dry Plasma Spots as Biomarker for Therapy Responses in Mycobacterium Tuberculosis Infection. *Sci Rep* (2015) 5:1–6. doi: 10.1038/srep09223
54. Petrone L, Vanini V, Chiacchio T, Petruccioli E, Cuzzi G, Schininà V, et al. Evaluation of IP-10 in Quantiferon-Plus as Biomarker for the Diagnosis of Latent Tuberculosis Infection. *Tuberculosis* (2018) 111:147–53. doi: 10.1016/j.tube.2018.06.005
55. Shivakoti R, Gupte N, Tripathy S, Poongulali S, Kanyama C, Berendes S, et al. Inflammation and Micronutrient Biomarkers Predict Clinical HIV Treatment Failure and Incident Active TB in HIV-Infected Adults: A Case-Control Study. *BMC Med* (2018) 16:161. doi: 10.1186/s12916-018-1150-3
56. Tenforde MW, Gupte N, Dowdy DW, Asmuth DM, Balagopal A, Pollard RB, et al. C-Reactive Protein (CRP), Interferon Gamma-Inducible Protein 10 (IP-10), and Lipopolysaccharide (LPS) are Associated With Risk of Tuberculosis After Initiation of Antiretroviral Therapy in Resource-Limited Settings. *PLoS One* (2015) 10:1–16. doi: 10.1371/journal.pone.0117424
57. Reichler MR, Hirsch C, Yuan Y, Khan A, Dorman SE, Schluger N, et al. Predictive Value of TNF- $\alpha$ , Ifn- $\gamma$ , and IL-10 for Tuberculosis Among Recently Exposed Contacts in the United States and Canada. *BMC Infect Dis* (2020) 20:1–14. doi: 10.1186/s12879-020-05185-2
58. Wishart DS, Feunang YD, Marcu A, Guo AC, Liang K, Vázquez-Fresno R, et al. Hmdb 4.0: The Human Metabolome Database for 2018. *Nucleic Acids Res* (2018) 46:D608–17. doi: 10.1093/nar/gkx1089
59. Hasin Y, Seldin M, Lusis A. Multi-Omics Approaches to Disease. *Genome Biol* (2017) 18:1–15. doi: 10.1186/s13059-017-1215-1
60. Leon-Mimila P, Wang J, Huertas-Vazquez A. Relevance of Multi-Omics Studies in Cardiovascular Diseases. *Front Cardiovasc Med* (2019) 6:91. doi: 10.3389/fcvm.2019.00091
61. Eddy S, Mariani LH, Kretzler M. Integrated Multi-Omics Approaches to Improve Classification of Chronic Kidney Disease. *Nat Rev Nephrol* (2020) 16:657–68. doi: 10.1038/s41581-020-0286-5
62. World Health Organization. *High-Priority Target Product Profiles for New Tuberculosis Diagnostics*. Geneva: World Health Organization (2014). Available at: [https://www.who.int/tb/publications/tpp\\_report/en/](https://www.who.int/tb/publications/tpp_report/en/).

**Disclaimer:** The content is solely the responsibility of the authors and does not necessarily represent the official views of the National Institutes of Health.

**Conflict of Interest:** The authors declare that the research was conducted in the absence of any commercial or financial relationships that could be construed as a potential conflict of interest.

The handling editor declared a past co-authorship with one of the authors NK.

Copyright © 2021 Krishnan, Queiroz, Gupta, Gupte, Bisson, Kumwenda, Naidoo, Mohapi, Mave, Mngqibisa, Lama, Hosseinipour, Andrade and Karakousis. This is an open-access article distributed under the terms of the Creative Commons Attribution License (CC BY). The use, distribution or reproduction in other forums is permitted, provided the original author(s) and the copyright owner(s) are credited and that the original publication in this journal is cited, in accordance with accepted academic practice. No use, distribution or reproduction is permitted which does not comply with these terms.



# A 2-Dose AERAS-402 Regimen Boosts CD8<sup>+</sup> Polyfunctionality in HIV-Negative, BCG-Vaccinated Recipients

Dhanasekaran Sivakumaran<sup>1,2</sup>, Gretta Blatner<sup>3,4\*†</sup>, Rasmus Bakken<sup>1,2</sup>, David Hokey<sup>4</sup>, Christian Ritz<sup>1,5</sup>, Synne Jenum<sup>6</sup> and Harleen M. S. Grewal<sup>1,2\*†</sup>

## OPEN ACCESS

### Edited by:

Novel N. Chegou,  
Stellenbosch University,  
South Africa

### Reviewed by:

Cecilia Lindestam Arlehamn,  
La Jolla Institute for Immunology (LJLI),  
United States  
Nicole Frahm,  
Bill & Melinda Gates  
Medical Research Institute,  
United States  
Douglas Bruce Lowrie,  
Fudan University, China

### \*Correspondence:

Harleen M. S. Grewal  
Harleen.Grewal@uib.no  
Gretta Blatner  
grettab922@gmail.com

<sup>†</sup>These authors have contributed  
equally in this work

### Specialty section:

This article was submitted to  
Microbial Immunology,  
a section of the journal  
Frontiers in Immunology

**Received:** 27 February 2021

**Accepted:** 18 May 2021

**Published:** 11 June 2021

### Citation:

Sivakumaran D, Blatner G,  
Bakken R, Hokey D, Ritz C,  
Jenum S and Grewal HMS (2021)  
A 2-Dose AERAS-402  
Regimen Boosts CD8<sup>+</sup>  
Polyfunctionality in HIV-Negative,  
BCG-Vaccinated Recipients.  
Front. Immunol. 12:673532.  
doi: 10.3389/fimmu.2021.673532

<sup>1</sup> Department of Clinical Science, Bergen Integrated Diagnostic Stewardship Cluster, Faculty of Medicine, University of Bergen, Bergen, Norway, <sup>2</sup> Department of Microbiology, Haukeland University Hospital, University of Bergen, Bergen, Norway, <sup>3</sup> Biomedical Advanced Research and Development Authority (BARDA), Department of Health and Human Services, Washington, DC, United States, <sup>4</sup> Aeras Global TB Vaccine Foundation, Rockville, MD, United States, <sup>5</sup> Department of Nutrition, Exercise and Sports, University of Copenhagen, Copenhagen, Denmark, <sup>6</sup> Department of Infectious Diseases, Oslo University Hospital, Oslo, Norway

Despite the widespread use of BCG, tuberculosis (TB) remains a global threat. Existing vaccine candidates in clinical trials are designed to replace or boost BCG which does not provide satisfying long-term protection. AERAS-402 is a replication-deficient Ad35 vaccine encoding a fusion protein of the *M. tuberculosis* (*Mtb*) antigens 85A, 85B, and TB10.4. The present phase I trial assessed the safety and immunogenicity of AERAS-402 in participants living in India – a highly TB-endemic area. Healthy male participants aged 18–45 years with a negative QuantiFERON-TB Gold in-tube test (QFT) were recruited. Enrolled participants (n=12) were randomized 2:1 to receive two intramuscular injections of either AERAS-402 (3 × 10<sup>10</sup> viral particles [vp]); (n=8) or placebo (n=4) on study days 0 and 28. Safety and immunogenicity parameters were evaluated for up to 182 days post the second injection. Immunogenicity was assessed by a flow cytometry-based intracellular cytokine staining (ICS) assay and transcriptional profiling. The latter was examined using dual-color-Reverse-Transcriptase-Multiplex-Ligation-dependent-Probe-Amplification (dc-RT MLPA) assay. AERAS-402 was well tolerated, and no vaccine-related serious adverse events were recorded. The vaccine-induced CD8<sup>+</sup> T-cell responses were dominated by cells co-expressing IFN-γ, TNF-α, and IL-2 (“polyfunctional” cells) and were more robust than CD4<sup>+</sup> T-cell responses. Five genes (*CXCL10*, *GNLY*, *IFI35*, *IL1B* and *PTPRCv2*) were differentially expressed between the AERAS-402-group and the placebo group, suggesting vaccine-induced responses. Further, compared to pre-vaccination, three genes (*CLEC7A*, *PTPRCv1* and *TAGAP*) were consistently up-regulated following two doses of vaccination in the AERAS-402-group. No safety concerns were observed for AERAS-402 in healthy Indian adult males. The vaccine-induced predominantly polyfunctional CD8<sup>+</sup> T cells in response to Ag85B, humoral immunity, and altered gene expression profiles in peripheral blood mononuclear cells (PBMCs) indicative of activation of various immunologically relevant biological pathways.

**Keywords:** TB vaccine, tuberculosis, T-cell responses, transcriptional profiling, AERAS-402, Phase 1 trial

## INTRODUCTION

Tuberculosis (TB) remains a major global health challenge. The only TB vaccine in common use, bacillus Calmette-Guérin (BCG), is estimated to reduce the risk of severe TB in children by about 70% (1), but does not prevent contagious TB sufficiently for epidemiological control. A more efficient vaccine would have a large positive impact on global health. Correlates of protection are important to accelerate clinical vaccine development, as they allow much smaller trials of shorter duration to select promising candidates. Currently, no approved correlates of protection exist, but these could be an immunological biomarker or a combination of biomarkers (signature) that are measured in validated assays. Although absolute determinants of protection against *M. tuberculosis* (*Mtb*) are not yet fully understood, T cell immunity is strongly believed to be crucial (2). Therefore, vaccine candidates that induce or boost T cell immunity may hold the key to success. Human *Mtb*-specific CD8<sup>+</sup> T cells are distinguished by both their preferential recognition of heavily infected cells and restriction by human leukocyte antigen-B (3, 4). Increasing evidence suggests that polyfunctional CD8<sup>+</sup> T cells, that possess capacities of cytokine production and cytotoxicity (5), have an essential role in the complex interplay resulting in *Mtb* containment and protective immunity. Most vaccine trials have assessed immunogenicity applying T cell stimulation assays with intracellular cytokine staining to characterize changes in vaccine induced CD4 and CD8 T cell populations. However, these assays likely provide limited information on other potentially important immune effects on peripheral blood mononuclear cells [PBMCs] (6).

AERAS-402 is a replication-deficient, adenovirus serotype 35 (Ad35) containing DNA that encodes a fusion protein of three major *Mtb* antigens (Ags) containing both CD4 and CD8 T cell epitopes: Ag85A, Ag85B, and TB10.4 (7–9). Antigen 85A is a 32-kDa protein member of the mycolyl transferase complex involved in cell wall synthesis. It contains several CD4<sup>+</sup> T cell epitopes and at least one CD8<sup>+</sup> T cell epitope. Used in a vaccine, Ag85A has protected against *Mtb* challenge in both mice and guinea pigs (10, 11) and is immunogenic in humans (12). Antigen 85B, also referred to as  $\alpha$ -antigen, is a 30-kDa mycolyl transferase protein (13, 14), secreted early during *Mtb* infection. It has been previously demonstrated to induce substantial protective immunity against aerosol challenge in the guinea pig TB test system (15). Ag85B is also a component of H4 and H56 subunit vaccines and proved immunogenic in clinical trials of these vaccines (16, 17). Antigen TB10.4 is one of the three members of the very similar ESAT-6 group of proteins found in *Mtb* culture supernatants and known to induce more robust polyfunctional T-cell responses in TB patients compared to *Mtb*-uninfected subjects with/without previous BCG-vaccination (18, 19). A fusion protein of TB10.4 and Ag85B induced a significant additive protective efficacy against aerosol challenge of tuberculosis 10 weeks after immunization of mice (20).

AERAS-402 vaccine phase I trials have previously been conducted in BCG-vaccinated healthy adults in the US (C-001-402, C-008-402 and C-009-402) (21) and South Africa (C-003-402) (22). In these studies, AERAS-402 had a safety profile

comparable to other vaccine candidates (21, 23, 24). A robust induction of CD8<sup>+</sup> T cell responses was observed that appeared to be dose-dependent in some subjects, while CD4<sup>+</sup> T cell responses were measurable but less prominent (22). Ag85A/B were more immunogenic than TB10.4 (21). Since this study was conducted in 2011, results have been presented in Phase 2 trials evaluating an MVA85A vaccine, a modified Ankara vaccine expressing Ag85A, in infants (C-020-485) (25). H4:IC31, a candidate subunit vaccine that consists of a recombinant fusion protein (H4) and IC31 adjuvant, signaling through toll-like receptor 9 (TLR9), containing mycobacterial antigens Ag85B and TB10.4 in adolescents (C-040-004) (26) neither study showed protection of these antigens against TB infection. Additionally, results from a phase 2 adaptive dose finding study of Aeras 402 (C-029-402) showed that while AERAS-402 had a good safety profile, the immune response was lower than that seen in adults (25).

The objective of the present study (C-004-402) was to evaluate the safety and immunogenicity of the AERAS-402 vaccine for the first time in an Indian population. We performed a phase 1, double-blind, placebo-controlled study. Immunogenicity was assessed by flow cytometry, serology, and a novel high-throughput inexpensive technique for targeted gene expression profiling: Dual-color-Reverse-Transcriptase-Multiplex-Ligation-dependent-Probe-Amplification (dc-RT MLPA).

## MATERIALS AND METHODS

### Study Approvals and Information on Consent

The study was reviewed and approved by the Government of India Directorate General of Health Services, Office of the Drugs Controller General (Biological Division), Ref no: LL/RA/825/2007 and the Independent Ethics Committee Consultants Bangalore. The phase 1 clinical trial (C-004-402) was registered at (<https://clinicaltrials.gov/>), and the identifier no: NCT01378312. Written informed consent was obtained from each participant prior to the conduct of any protocol-specific activity or study entry. The study was carried out following the ethical principles outlined in the Declaration of Helsinki and in accordance with the US Code of Federal Regulations for protection of human subjects (21 CFR 50), Institutional Review Boards (21 CFR 56), and the obligations of clinical investigators (21 CFR 312).

### Study Design, Enrolment, and Vaccination

The study was conducted at Lotus lab, Bangalore, India (12.9303° N, 77.6217° E) between February 2011 and October 2011. The major inclusion criteria were i) age 18 through 45 years on Study Day 0, ii) had BCG vaccination at least 5 years ago, iii) documented through medical history or presence of scar, iv) has Body Mass Index (BMI) between 19 and 30 (kg/m<sup>2</sup>), v) has ability to complete follow-up period of 182 days as required by the protocol, and vi) has completed written informed consent.

The major exclusion criteria were i) acute illness on the day of randomization, ii) oral temperature  $\geq 37.5^{\circ}\text{C}$  on the day of randomization, iii) used immunosuppressive medication/received immunoglobulin or blood products/received any standard vaccine within 42 days, iv) history or evidence (including chest X-ray) of active tuberculosis, tuberculin skin test evidence of *Mtb* infection, defined as 15 mm of induration or greater and laboratory test evidence of *Mtb* infection, v) abnormal laboratory parameters and use of intravenous drugs. Enrolled subjects were randomized 2:1 to receive two intramuscular injections of either AERAS-402 ( $3 \times 10^{10}$  viral particles [vp]) or placebo (normal saline solution) on study days 0 and 28 (**Figure 1**).

The sample size for this study was selected as adequate for an initial review of the developing safety profile of AERAS-402 in a BCG-vaccinated population at the selected dose level, rather than for statistical reasons. A sample size of eight subjects in the AERAS-402 treatment group permitted initial estimates of the incidence of adverse events; given eight subjects receiving AERAS-402, this study had an 80% or greater chance of detecting an adverse event with a rate of occurrence of 18% in the study population under consideration.

## Follow Up and Safety Evaluations

Subjects had vital signs (blood pressure, pulse, and oral temperature) measured just before receiving each vaccination with AERAS-402 or placebo and at 30 minutes and 60 minutes

post vaccination, and two days after vaccination. Blood was collected for routine clinical chemistry and hematology at screening and post vaccination. Vaccination was administered on days 0 and 28, and safety and immunogenicity were assessed on days 0, 7, 14, 28, 35, 42, 56 and 182.

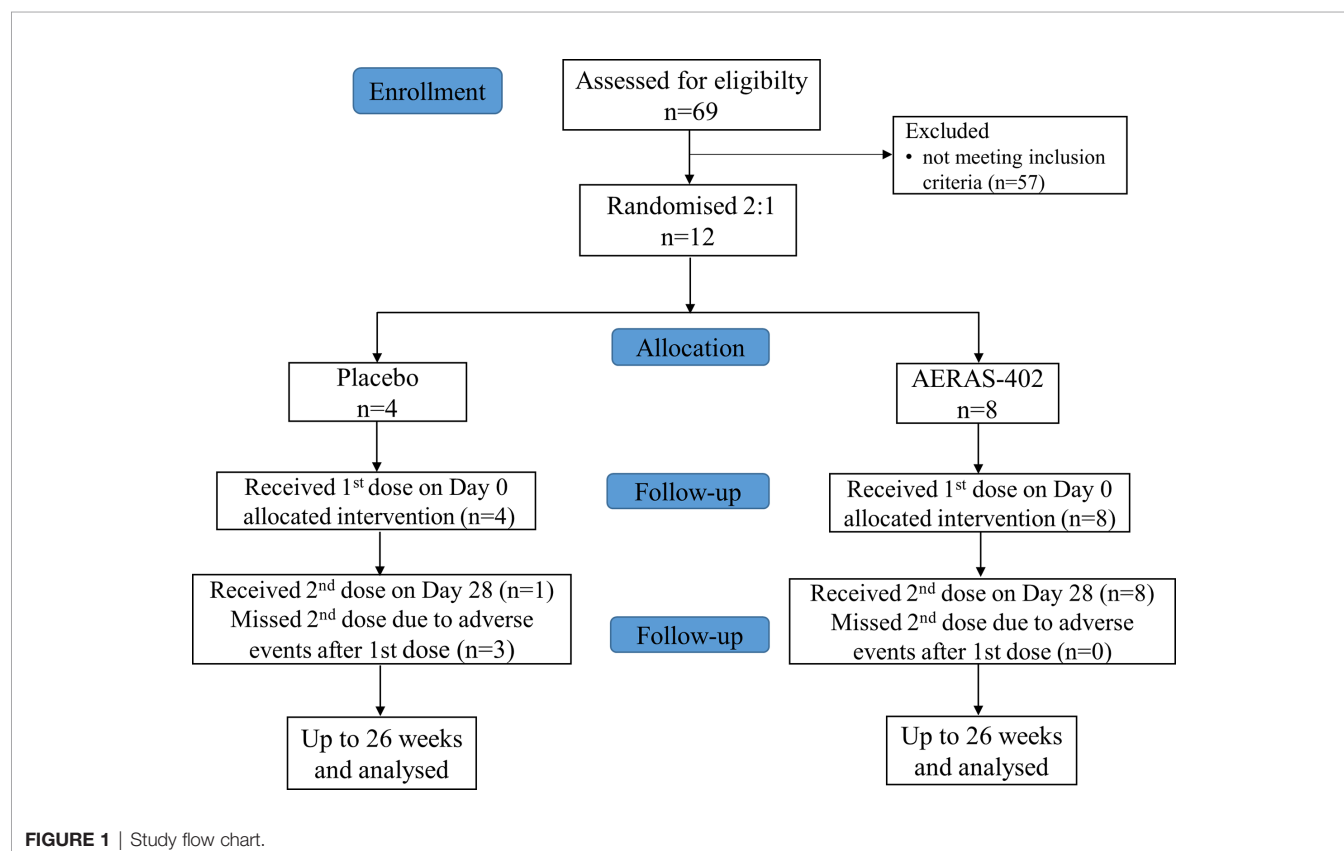
Adverse events (AEs) were collected for 28 days after each immunization and solicited AEs, including assessment for local injection site reactions (pain, redness and swelling at the site of injection; arthralgia; conjunctivitis; diarrhea; dysuria; fatigue; fever; headache; malaise; myalgia; sore throat; and upper respiratory tract infection) were recorded by subjects on diary cards for 14 days after each vaccination. Serious adverse events were collected from the time of first study vaccine dosing through study day 182. Adverse events were graded by severity and relationship to study vaccine using predefined criteria.

## Tuberculin Skin Test (TST) and QuantiFERON-TB Gold

TST (measured in millimeters at the transverse induration) and QFT- TB Gold tests were conducted at screening and at study day 182.

## Peripheral Blood Mononuclear Cell (PBMC) Intracellular Cytokine Staining (ICS) Assay and Flow Cytometry

PBMCs were sent from Bangalore to Aeras Rockville, MD, USA. The PBMC ICS assay was performed as previously described





(27). Briefly, PBMCs were thawed and rested overnight and then stimulated for 5–6 hours at 37°C with 0.4% Dimethyl Sulfoxide (DMSO; negative control), 0.5 µg/mL Staphylococcal enterotoxin B (SEB; positive control) or with peptide pools, one pool per antigen (1 µg/peptide/mL with pools for Ag85A, Ag85B and TB10.4), in the presence of Brefedin A and monensin (GolgiStop and GolgiPlug), both from BD Biosciences USA and used at 1 µL per well. Peptide pools were 15mers overlapping by 11 amino acids and spanning the sequences of the vaccine encoded antigens. Cells were then stained using viability dye (Live/Dead Aqua, Invitrogen, USA), anti-CD4-V450, and anti-CD8 PE-Cy5, then fixed and permeabilized for intracellular staining using anti-CD3 APC-Cy7, anti-IFN- $\gamma$  APC, anti-TNF- $\alpha$  FITC, and anti-IL-2 PE (all antibodies from BD Biosciences, USA). Data were acquired using a BD LSRII flow cytometer (BD Biosciences, USA) and analyzed using FlowJo software (TreeStar Inc., USA). Immunogenicity was determined by first gating on live, singlet CD3+ T cells and then gating CD4+ and CD8+ T cells and calculating the percentage of each population that was cytokine positive. DMSO subtraction was performed prior to plotting the results. The gating strategy for vaccinated and placebo recipients are provided as a **Supplementary Figure 1**.

### Anti-Mycobacterial Antibodies by ELISA

The serum samples were tested at 1:100 dilution to measure antigen-specific antibodies by ELISA. Briefly, the ELISA was performed as follows: recombinant *Mtb* antigen Ag85B purified in-house at Aeras was coated at 1.5 µg/ml onto 96-well ELISA plates. The immobilized antigen was incubated with 100 µL of serum samples at 1:100 dilution to capture antigen-specific antibodies. The captured antibodies were then probed by the addition of 100 µL of biotinylated anti-IgG antibodies at 1:500 dilution and detected by adding 100 µL of colorimetric substrate solution. The substrate color development was stopped using 50 µL of stop solution and the color intensity was read using a spectrophotometer and analyzed with SoftMax<sup>®</sup> Pro 5.4.1 data acquisition & analysis software.

### Adenovirus 35 Neutralization

Adenovirus 35 serum neutralization activity was assayed pre-vaccination with placebo or AERAS-402 at study day 0, and at study day 182. Briefly, neutralizing antibody titers against Adenovirus type 35 were determined using the validated neutralizing antibody assay at Crucell using a previously published method (28). Luminescence counts were recorded on a 1450 Micro Beta Trilux. Data were imported into MS Excel to calculate 90% inhibition titers.

### Sample Preparation and RNA Extraction

An aliquot of frozen PBMCs were shipped from Aeras Rockville, MD, USA to Bergen, Norway for the dcRT-MLPA assay. The PBMCs were thawed at 37°C water bath and ~2 million cells (avg: 4.45, min: 0.2, max: 15.73, SD: 3.19) were immediately transferred into 1.7ml sterile RNase-free tubes containing 1ml of RNeasy<sup>®</sup> RNA stabilization solution (ThermoFisher Scientific). Following incubation at room temperature for 1

hours, subsequently the samples were stored at -70°C for further analysis.

Total RNA was extracted from the PBMCs using the RNeasy Mini Kit (Qiagen, Hilden, Germany) with RNase free DNase on-column digestion (Qiagen, Hilden, Germany) according to the manufacturer's instructions. The total RNA concentration and purity (A260/280 nm ratio) were measured using a Nanodrop spectrophotometer (Thermoscientific, Wilmington, Delaware, U.S.A.).

### Dual-color Reverse Transcriptase-Multiplex Ligation-Dependent Probe Amplification (dcRT-MLPA)

We used a novel high-throughput technique, which requires only ~125 ng of total RNA for analyzing a predefined panel of genes of interest. RNA samples from 12 subjects: 4 received placebo, and 8 received AERAS-402 vaccine (PBMC samples from six time points, i.e., days 0, 7, 28, 35, 42, and 182) were used for dcRT-MLPA analysis. A modified one-step protocol of dcRT-MLPA was used as previously described (29). A total of 150 genes (including 4 housekeeping genes), distributed in two panels were assessed, based primarily on their posited or confirmed roles in TB immunology. The first gene set contains 58 genes that included type-1 interferon-inducible genes (30) known to be upregulated in adult TB and genes associated with predicted risk for TB in South African neonates (31); the innate and adaptive gene set contains 92 genes which known for involvement in general inflammation and myeloid cell activation, and genes involved in the adaptive immune system, comprising Th1/Th2-responses, regulatory T-cell markers and B-cell associated genes (32). DcRT-MLPA probes and primers (reverse transcription gene target-specific primers, right- and left-hand half MLPA probes, FAM labelled MLPA primers, HEX labelled MAPH primers) were obtained from the Department of Infectious Diseases, Leiden Medical University, Leiden, The Netherlands. The dcRT-MLPA reagents were purchased from MRC Holland, The Netherlands. Samples with a concentration <50 ng µL<sup>-1</sup> were concentrated at 45°C using a speed vacuum concentrator (Eppendorf AG, Hamburg, Germany). A positive control for each gene panel (using synthetic template oligonucleotides as hybridization templates) and a commercial Human Universal Reference RNA were included on each plate. The amplified PCR products were diluted 1:10 with nuclease-free water and added to a mixture of Hi-Di-Formamide with 400HD ROX size standard. The PCR products were denatured at 95°C for 5 minutes and then immediately cooled on ice. Subsequently, the PCR fragments were analyzed on a 3730-capillary sequencer in Gene scan mode (Life Technologies, Carlsbad, California, USA).

### DcRT-MLPA Data Processing

Data were analyzed using GeneMapper software version 5.0 (Life Technologies, Carlsbad, California, USA). The default peak detection settings were inspected and adjusted if necessary. The peak area (in arbitrary units) was normalized against GAPDH using Microsoft Excel spreadsheet software. The genes that had no or little expression (peak area < 200

arbitrary units) were assigned to a threshold value of 200 arbitrary units.

## Statistical Methods

Descriptive statistics were performed to summarize AERAS-402 adverse events and immunogenicity. Mann-Whitney test (placebo vs. vaccinated) and paired t-test (pre vaccination vs. post vaccination) analysis were performed where appropriate. No multiplicity adjustment of p-values was applied. Mean difference and corresponding standard errors were reported. IBM SPSS software version 24.0 (IBM, Bergen, Norway) was used. Dot plots were created using GraphPad Prism 8 (GraphPad software, San Diego, CA). WebGestalt (WEB-based GENE SeT AnaLysis Toolkit) (33) is one of the most widely used gene set enrichment analysis tools that help users extract biological insights from genes of interest. WebGestalt and the Functional Enrichment Analysis (FunRich) tool (34) was applied for the gene enrichment and network pathway analysis. The top results were ranked using the Benjamini–Hochberg method for controlling the false discovery rate. A p-value < 0.05 was considered significant.

## RESULTS

### Subject Demographics and Vaccination

Between Feb 2011 and April 2011, 69 subjects were screened and 12 recruited and randomized to the AERAS-402 group (n=8) or placebo (n=4). Demographic and other baseline characteristics were well balanced between the groups (Table 1). All 8 subjects in the AERAS-402 group and one subject in the placebo group received both study vaccinations; the remaining 3 subjects in the

placebo group did not receive the second vaccination due to adverse events. All 12 subjects completed the study follow up period of 182 days.

### AERAS-402 Safety

No serious adverse events were reported. All 8 subjects in the AERAS-402-group and 4 subjects in the placebo-group reported at least 1 AE after either the study day 0 or study day 28 vaccination, and the majority of AEs were mild-moderate (Table 2). One subject in the AERAS-402-group had severe AEs (transient injection site pain, myalgia, and fatigue after the study day 0 vaccination) considered related to the study vaccine, but all AEs resolved within 7 days. Two AEs were reported for more than 1 subject in both intervention groups: decreased hemoglobin (reported for all subjects in both treatment groups) and injection site pain (5 in the AERAS-402 group vs. 0 in the placebo group). Note that in this study, decrease of any magnitude in hemoglobin from baseline was recorded as an AE.

The 3 subjects, in the placebo group that did not receive their second vaccination due to the following abnormal laboratory values at Study Day 28:

- i. Grade 1 hematuria which was considered unlikely to be related to study vaccine.
- ii. Grade 3 CPK which was considered unlikely to be related to study vaccine.
- iii. Grade 1 decreased hemoglobin which was considered not related to study vaccine.

These abnormal laboratory values were reported as adverse events. Due to the exclusion criteria specifying that laboratory values were required to be within local laboratory normal ranges

TABLE 1 | Demographic and Baseline Characteristics.

Parameter	Placebo 2 Doses	AERAS-402 (3 x 10 <sup>10</sup> vp) 2 Doses	Total
	(n=4)	(n=8)	(n=12)
<b>Age (years)</b>			
n	4	8	12
Mean	28.3	27.4	27.7
<b>Age Group (years), n (%)</b>			
18-30	4 (100.0)	7 (87.5)	11 (91.7)
31-40	0 (0.0)	1 (12.5)	1 (8.3)
<b>Gender, n (%)</b>			
Male	4 (100.0)	8 (100.0)	12 (100.0)
<b>Race, n (%)</b>			
Indian	4 (100.0)	8 (100.0)	12 (100.0)
<b>Height (cm)</b>			
n	4	8	12
Mean	164.80	168.55	167.30
<b>Weight (kg)</b>			
n	4	8	12
Mean	62.28	69.50	67.09
<b>Body Mass Index (kg/m<sup>2</sup>)</b>			
n	4	8	12
Mean	22.97	24.47	23.97
<b>Documentation of BCG Vaccination, n (%)</b>			
Medical history	4 (100.0)	8 (100.0)	12 (100.0)
Presence of scar	4 (100.0)	8 (100.0)	12 (100.0)

**TABLE 2** | Number of subjects (%) with AEs for study day 0 or 28 post-vaccination.

Solicited/Unsolicited events	Placebo 2 Doses	AERAS-402 (3 x 10 <sup>10</sup> vp) 2 Doses
	(n=4) (%)	(n=8) (%)
Subjects with at least 1 adverse event	4 (100.0)	8 (100.0)
Investigations	4 (100.0)	8 (100.0)
Blood creatine phosphokinase increased	1 (25.0)	0 (0.0)
Blood creatinine increased	1 (25.0)	0 (0.0)
Hemoglobin decreased	4 (100.0)	8 (100.0)
Lymphocytes count increased	1 (25.0)	0 (0.0)
Neutrophils count decreased	0 (0.0)	1 (12.5)
Neutrophils count increased	0 (0.0)	1 (12.5)
White blood cells count increased	0 (0.0)	1 (12.5)
General disorders and administration site conditions	0 (0.0)	5 (62.5)
Gastrointestinal disorders	0 (0.0)	1 (12.5)
Musculoskeletal and connective tissue disorders	0 (0.0)	1 (12.5)
Respiratory, thoracic and mediastinal disorders	0 (0.0)	1 (12.5)
Renal and urinary disorders	1 (25.0)	0 (0.0)

in order to receive the Study Day 28 vaccination, all three subjects did not receive the second dose of study vaccine, but were followed to study completion, Study Day 182.

### AERAS-402 Administered at Two Doses Induces Polyfunctional CD8<sup>+</sup> T Cell Responses

Antigen-specific CD4<sup>+</sup> and CD8<sup>+</sup> expression of the cytokines IFN- $\gamma$ , TNF- $\alpha$ , and/or IL-2 alone or in combination to the individual AERAS-402 antigens, Ag85A, Ag85B, and TB10.4, are presented by the intervention group in **Figures 2A–F**. AERAS-402 induced responses to Ag85B constituted the most convincing differences between the AERAS-402-group and the placebo-group. AERAS-402 induced vaccine specific CD4<sup>+</sup> and CD8<sup>+</sup> T-cell response (mean response) peaked at day-35 and -42 of post vaccination of both doses. However, the magnitude of CD8<sup>+</sup> T cell responses was in general higher than CD4 T cell responses. Vaccine-induced responses peaked at study days 35 and 42 (7 and 14 days after the second dose of vaccination) and were in some cases, sustained through study day 182.

Frequencies of Ag85B-specific CD8 T cell >0.05% at day 35 and 42, were observed in 7/8 (87.5%) in the AERAS-402-group compared to 0/4 (0%) in the placebo-group (**Supplementary Figure 2**). Individual trajectories stratified for intervention group are demonstrated in **Figures 3A, B**. The most prominent CD8<sup>+</sup> T cell subsets (Boolean gating) to Ag85B at study day 35 were the polyfunctional IFN- $\gamma$ IL-2<sup>+</sup>TNF- $\alpha$ <sup>+</sup> and bifunctional IFN- $\gamma$ <sup>+</sup>TNF- $\alpha$ <sup>+</sup> subsets (**Figure 3C**).

### AERAS-402 Administered at Two Doses Boosts Specific Antibody Production

Ag85B antibodies were detected in the AERAS-402-group with peak responses at study days 42 and 56. Ag85B antibodies were not measurable in the placebo-group (**Supplementary Figure 3**).

### Anti-Adenovirus 35 Antibodies

Pre-existing antibodies towards adenovirus could affect vaccine efficacy. Therefore, Adenovirus 35 serum neutralizing activity was assessed pre-vaccination. A response >LLOQ for Adenovirus

35 serum neutralizing activity was detected in 2/8 in the AERAS-402-group and 3/4 in the placebo group (**Table 3**). At study day 182 of the six subjects in the AERAS-402 recipients with neutralizing activity  $\leq$  LLOQ at study day 0, two subjects had a shift in Adenovirus 35 neutralizing activity response to >LLOQ.

### Similar TST and QFT-G Responses Following Vaccination

For all 12 subjects, the TST induration and QFT were measured on screening day and study day 182. The TST mean induration decreased from screening to study day 182 in both groups (**Table 4**). None of the study participants had QFT conversion at day 182.

### AERAS-402 Induced Gene Expression in PBMCs

Gene expression levels for 7/46 genes in the type-1 interferon inducible gene set and 24/85 genes in the innate and adaptive gene set, were undetectable in all 63 samples. For the remaining genes with detectable levels, results of the comparison of gene expression between the AERAS-402-group and the placebo-group are shown in **Tables 5A, B**. Post-vaccination at day 7, day 35 and day 182, transcription of *IFIT5*, *PTPRCv2* and *IL1B* was upregulated (all  $p < 0.05$ ) in the AERAS-402-group compared to the placebo-group (**Figures 4A, B, E**). At day 42, the transcription of *CXCL10* was upregulated ( $p = 0.048$ ) and the transcription of *GNLY* down-regulated ( $p = 0.036$ ) in the AERAS-402-group compared to the placebo-group (**Figures 4C, D**).

We then assessed the change in gene expression profiles from baseline up to day 182 within each intervention group (**Tables 5A, B**). Among 132 unique genes, 33 genes were differentially expressed in the vaccination and placebo groups and were selected for functional categories and used for the enrichment analysis. WebGestalt identified the most significant gene sets and showed that the inflammasome and T cell receptor complexes were significantly ranked higher than other complexes. The Gene Ontology enrichment in the biological process is highlighted with colors based on FDR significance (**Figure 5A**). Each ontology consists of a set of gene ontology

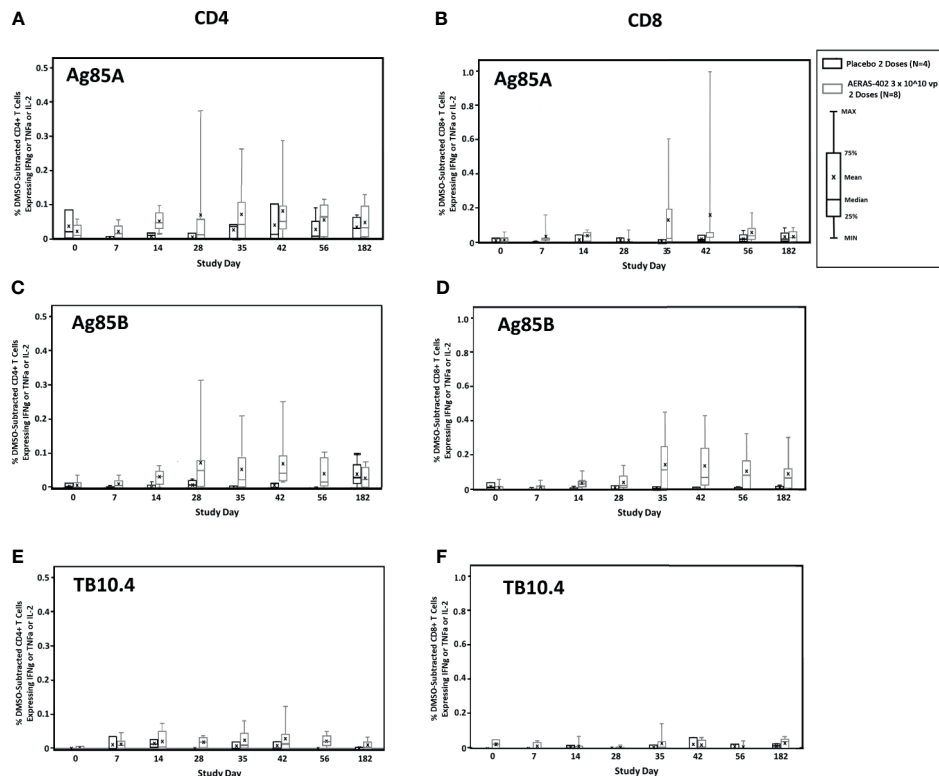


**FIGURE 2 |** T cell responses to vaccine-encoded antigens. PBMCs were thawed, rested overnight, and stimulated for 5-6 hours with DMSO (negative control), SEB (positive control), or peptide pools corresponding to the vaccine antigens Ag85A (A, B), Ag85B (C, D), or TB10.4 (E, F). Specimens were then stained for viability, phenotypic markers, and intracellular cytokine expression and evaluated by flow cytometry. Data were analyzed using FlowJo software to generate cytokine Boolean gates. Each gate was subjected to DMSO subtraction to remove background. Negative results following DMSO-subtraction were set to zero. The sum of these gates was then used to determine the total cytokine response for CD4+ (A, C, E) and CD8+ (B, D, F) T cells for the AERAS-402-vaccinated (grey bars) or placebo control (black bars) groups. Bars are plotted for each group and time point for the total response (any cytokine alone or in combination for IFN- $\gamma$  or IL-2 or TNF- $\alpha$ ). Bars represent the 25<sup>th</sup> to 75<sup>th</sup> percentile, with the cross bar representing the median response. The mean is indicated by an “x” and the error bars represent the minimum and maximum responses.

(GO) terms, which are organised in a hierarchy, or directed acyclic graph (DAG), as shown in **Figure 5B**. As expected by the fact that AERAS-402 was designed to induce T cell responses, signaling related to the T cell receptor are engaged. In addition, the FunRich arranged the differentially expressed genes into two functional categories, including biological processes and cellular components. The parameters for the interception of biological pathways are indicated in **Figure 5C**.

### Comparison of Gene Expression Profiles Between Pre and Post Vaccination

The gene expression profiling shows that compared to pre-vaccination, the innate immune genes (*CLEC7A* and *NLRP3*); T-cell associated genes (*PTPRCv1* and *TAGAP*) were consistently upregulated (all  $p \leq 0.05$ ) at 4- time points in the AERAS-402-group (**Table 5A**). Next, compared to pre-vaccination, on day-7 after the first and second dose of vaccination (i.e., day-7 and day-35, respectively), the innate immune genes (*CCL5*, *CXCL13*) and T-cell subset specific genes (*CD3E*, *PTPRCv2* [CD45RO]) were upregulated (all  $p < 0.05$ ). Similarly, on day-7 after the second dose of vaccination (i.e., day-35; **Table 5A**), the innate immune

response NLR and NOD-like specific genes (*NLRP1*, *NLRP3*, and *NOD1*) were upregulated (all  $p < 0.01$ ). Correspondingly, at day-35 and -42, following the second vaccination, three genes that are involved in innate immunity (*NLRP3*, *VEGF* and *ZNF331*;  $p < 0.05$ ) were up-regulated, whereas the T-cell associated *GZMA* was downregulated ( $p < 0.05$ ). The changes observed in gene expression profiles suggest broad vaccine-induced changes. Notably, none of these changes were observed in the placebo-group (**Table 5B**).

### DISCUSSION

In line with previous phase 1 trials of AERAS-402 in other populations (22), we report an acceptable safety profile for this vaccine candidate in healthy BCG vaccinated *Mtb*-uninfected adults. The vaccine also induced promising immunogenicity, with robust polyfunctional T-cell responses to Ag85B predominantly in CD8 subsets that peaks at day 35 and 42, corresponding to one week following the second vaccination. There were no serious adverse events that were related to the



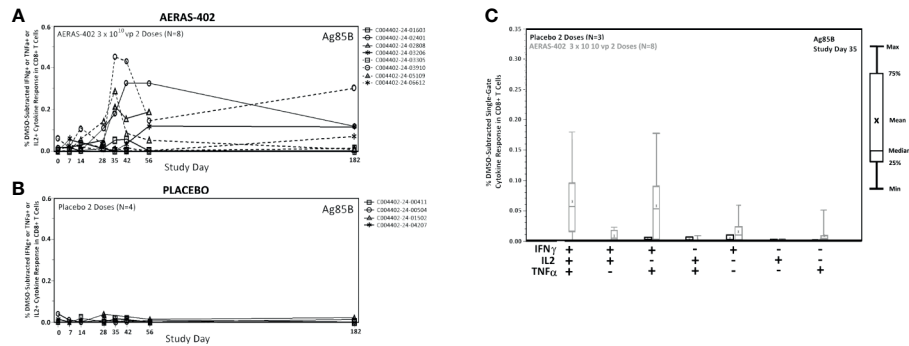


**FIGURE 3 |** CD8<sup>+</sup> cytokine responses to Ag85B. PBMCs were thawed, rested overnight, and stimulated for 5-6 hours with DMSO (negative control), SEB (positive control), or peptide pools corresponding to the vaccine antigens Ag85A, Ag85B, or TB10.4. Specimens were then stained for viability, phenotypic markers, and intracellular cytokine expression and evaluated by flow cytometry. Data was analyzed using Flow Jo software to generate cytokine Boolean gates. Each gate was subjected to DMSO subtraction to remove background. Negative results following background subtraction are set to zero. The sum of these gates was then used to determine the total cytokine response for vaccinated (**A**) and placebo control (**B**) groups or plotted by functionality to assess the polyfunctional response (**C**). Lines (**A, B**) are plotted for each individual subject. CD8<sup>+</sup> Single-Gate (Boolean; **C**) ICS responses for Ag85B at Study Day are shown for vaccinated (gray bars) and placebo (black bars) groups. Bars represent the 25<sup>th</sup> to 75<sup>th</sup> percentile, with the cross bar representing the median response. The Mean is indicated by an “x” and the error bars represent the minimum and maximum responses.

**TABLE 3 |** AERAS-402 anti-Ad35 Neutralizing Activity.

Parameter/Study Day (Time)	Placebo 2 Doses (n=4)	AERAS-402 (3 x 10 <sup>10</sup> vp) 2 Doses (n=8)
<b>Response &gt; LLOQ, n (%)</b>		
Study Day 0 (Pre-Vaccination)	3 (75.0)	2 (25.0)
Study Day 182	3 (75.0)	4 (50.0)
<b>Shift from Study Day 0 (Pre-Vaccination) to Study Day 182 (%)</b>		
> LLOQ to > LLOQ	3/4 (75.0)	2/8 (25.0)
> LLOQ to ≤ LLOQ	0/4 (0.0)	0/8 (0.0)
≤ LLOQ to ≤ LLOQ	1/4 (25.0)	4/8 (50.0)
≤ LLOQ to > LLOQ	0/4 (0.0)	2/8 (25.0)

**TABLE 4 |** Tuberculin Skin Test (TST) results.

Study Day (Time)/Parameter	Placebo2 Doses (n=4)	AERAS-402(3 x 10 <sup>10</sup> vp)2 Doses (n=8)
<b>Screening</b>		
n	4	8
Mean	7.3 ± 4.5	6.9 ± 3.0
0-10 mm, n (%)	3 (75.0)	7 (87.5)
11-15 mm, n (%)	1 (25.0)	1 (12.5)
<b>Study Day 182</b>		
n	4	8
Mean	5.3 ± 3.86	3.9 ± 0.83
0-10 mm, n (%)	3 (75.0)	8 (100.0)
11-15 mm, n (%)	1 (25.0)	0 (0.0)
<b>Shift from screening to study day 182, (%)</b>		
0-10 mm to 0-10 mm	3/4 (75.0)	7/8 (87.5)
11-15 mm to 0-10 mm	0/4 (0.0)	1/8 (12.5)
11-15 mm to 11-15 mm	1/4 (25.0)	0/8 (0.0)

vaccine, mild grade abnormal hematology was seen in AERAS-402 candidates.

CD4<sup>+</sup> T cells play a central role in TB protective immunity (35, 36). Consistent with the previous report (22), AERAS-402

induced a vaccine-specific CD4<sup>+</sup> T-cell response, which was dominated by the polyfunctional IFN- $\gamma$ <sup>+</sup>TNF- $\alpha$ <sup>+</sup>IL-2<sup>+</sup> subset to all antigens (**Figures 2, 3**). The results seen in this study are consistent with previous studies demonstrating that the vaccine-

**TABLE 5A** | Comparison of baseline measurements of each biomarkers that changed with post-vaccination of AERAS-402.

	Genes	day 0 and day 7 <sup>ψ</sup>			day 0 and day 28 <sup>ψ</sup>			day 0 and day 35 <sup>ψ</sup>			day 0 and day 42 <sup>ψ</sup>			day 0 and day 182 <sup>ψ</sup>		
		Mean difference	SE Mean	p-value	Mean difference	SE Mean	p-value	Mean difference	SE Mean	p-value	Mean difference	SE Mean	p-value	Mean difference	SE Mean	p-value
Type-1 IFN inducible	<b>CXCL10</b>	451.7	367.9	0.265	859.4	537.4	0.161	142.7	293.0	0.643	268.4	841.1	0.470	587.5	78.6	<b>0.001</b>
	<b>IFI35</b>	468.4	873.0	0.611	1671.3	1283.8	0.241	-617.0	1076.7	0.578	305.1	1077.2	0.789	2702.7	895.7	<b>0.030</b>
	<b>IFIT3</b>	683.6	469.5	0.196	576.0	357.1	0.158	919.4	1218.4	0.479	118.0	476.1	0.815	1424.2	431.0	<b>0.021</b>
Hanekom set	<b>TAP2</b>	232.1	304.9	0.475	513.7	200.4	<b>0.043</b>	250.0	248.1	0.353	-127.0	246.4	0.626	22.7	345.4	0.950
	<b>BMP6</b>	1838.4	1822.5	0.352	995.7	1243.5	0.454	345.4	1058.1	0.755	1412.2	1173.3	0.909	3552.0	1134.9	<b>0.026</b>
	<b>GUSB</b>	293.7	257.6	0.298	376.1	218.8	0.136	131.6	163.3	0.451	137.1	148.2	0.399	818.8	287.3	<b>0.036</b>
	<b>KIF1B</b>	491.9	260.8	0.108	324.7	225.0	0.199	268.4	140.6	0.105	122.3	191.1	0.552	457.7	154.3	<b>0.031</b>
	<b>LYN</b>	383.9	162.2	0.056	1336.7	383.2	<b>0.013</b>	655.3	291.2	0.065	711.2	336.4	0.088	1796.5	1036.8	0.144
	<b>VEGF</b>	-18.4	21.0	0.413	133.1	86.8	0.176	130.4	51.6	<b>0.045</b>	276.3	64.3	<b>0.008</b>	-29.8	39.5	0.484
	<b>CCL5</b>	6127.4	2222.7	<b>0.033</b>	2371.1	1947.8	0.269	3833.6	1562.6	<b>0.050</b>	-544.1	1364.4	0.710	3306.2	2832.9	0.296
Innate and adaptive	<b>CCR7</b>	715.3	349.6	0.087	450.3	216.6	0.083	1173.3	336.8	<b>0.013</b>	446.4	393.2	0.320	319.8	326.5	0.372
	<b>CD3E</b>	3363.9	1015.1	<b>0.016</b>	2700.3	885.1	<b>0.022</b>	2821.0	954.2	<b>0.025</b>	671.0	1066.1	0.564	1407.0	867.2	0.166
	<b>CD8A</b>	979.9	557.8	0.129	580.9	480.6	0.272	1470.4	515.5	<b>0.029</b>	37.6	586.2	0.952	497.2	781.8	0.553
	<b>CLEC7A</b>	1627.7	696.3	0.056	1932.7	800.4	<b>0.050</b>	1372.4	407.9	<b>0.015</b>	1213.6	409.3	<b>0.041</b>	1907.2	595.9	<b>0.024</b>
	<b>CXCL13</b>	581.1	185.3	<b>0.020</b>	313.6	163.8	0.104	312.0	88.6	<b>0.012</b>	290.0	229.4	0.275	373.8	169.6	0.079
	<b>GATA3</b>	179.9	65.5	<b>0.033</b>	122.1	41.4	<b>0.026</b>	83.3	55.6	0.185	68.8	78.2	0.429	45.7	63.0	0.501
	<b>GZMA</b>	-734.4	720.0	0.347	-2111.6	542.5	<b>0.008</b>	-1690.9	688.0	<b>0.049</b>	-2813.0	502.2	<b>0.005</b>	821.8	1800.9	0.667
	<b>NLRC4</b>	-128.1	154.4	0.438	-81.1	50.8	0.161	-358.4	110.7	<b>0.018</b>	389.0	452.4	0.438	417.0	321.4	0.251
	<b>NLRP1</b>	2473.6	1179.9	0.081	2599.7	692.8	<b>0.009</b>	2436.4	406.2	<b>0.001</b>	1425.4	940.8	0.240	1971.8	1466.9	0.237
	<b>NLRP3</b>	166.0	148.5	0.306	674.3	197.6	<b>0.014</b>	389.9	172.6	<b>0.001</b>	752.9	89.8	<b>0.001</b>	63.7	177.6	0.735
	<b>NOD1</b>	321.9	169.7	0.107	390.9	153.2	<b>0.043</b>	256.0	66.3	<b>0.008</b>	46.6	264.7	0.869	258.3	143.2	0.131
	<b>PTPRCv1</b>	3436.4	862.3	<b>0.007</b>	2378.7	833.5	<b>0.029</b>	2426.3	622.1	<b>0.008</b>	1613.6	914.0	0.152	2243.3	847.3	<b>0.046</b>
	<b>PTPRCv2</b>	927.0	359.7	<b>0.042</b>	709.6	371.1	0.104	791.6	170.3	<b>0.004</b>	-145.0	370.2	0.716	769.8	504.9	0.188
	<b>TAGAP</b>	2718.0	809.5	<b>0.015</b>	1475.1	467.7	<b>0.020</b>	2064.0	568.9	<b>0.011</b>	356.8	604.1	0.587	1906.0	713.8	<b>0.044</b>
	<b>TLR4</b>	-26.9	53.8	0.636	77.6	38.2	0.088	-77.3	68.3	0.301	131.2	148.0	0.428	340.0	124.1	<b>0.041</b>
	<b>TLR7</b>	-763.0	304.2	<b>0.046</b>	-223.0	327.8	0.522	-603.1	315.6	0.105	-257.4	682.3	0.725	290.7	193.3	0.193
	<b>ZNF331</b>	437.0	244.6	0.124	210.4	100.0	0.080	920.1	300.4	<b>0.022</b>	741.0	192.4	<b>0.018</b>	17.3	30.6	0.596

ψ - 7 subjects; ¥ - 6 subjects. SE, Standard error; p-value obtained based on paired t-test. The significant p-values are in bold.

**TABLE 5B** | Comparison of baseline measurements of each biomarkers that changed with post-vaccination of placebo.

	Genes	day 0 and day 7 <sup>ψ</sup>			day 0 and day 28 <sup>ψ</sup>			day 0 and day 35 <sup>ψ</sup>			day 0 and day 42 <sup>ψ</sup>			day 0 and day 182 <sup>ψ</sup>		
		Mean difference	SE Mean	p-value	Mean difference	SE Mean	p-value	Mean difference	SE Mean	p-value	Mean difference	SE Mean	p-value	Mean difference	SE Mean	p-value
Type-1 IFN inducible	<b>IFI6</b>	1660.33	562.55	0.098	1118.67	88.83	<b>0.006</b>	718.33	387.76	0.205	1650.67	870.80	0.198	1888.00	285.85	<b>0.022</b>
	<b>IFIT5</b>	53.33	242.18	0.846	381.33	64.06	<b>0.027</b>	107.00	69.35	0.263	104.67	115.51	0.461	483.67	235.96	0.177
	<b>IFI44</b>	464.33	601.68	0.521	896.66	255.9	0.073	187.67	44.82	<b>0.050</b>	113.06	115.47	0.432	770.00	341.56	0.153
	<b>IFI44L</b>	175.00	264.92	0.577	370.67	85.49	<b>0.049</b>	-22.00	156.04	0.901	189.33	109.41	0.226	250.33	255.65	0.431
	<b>OAS3</b>	-109.67	75.65	0.284	21.67	138.15	0.89	-211.33	43.23	<b>0.039</b>	59.33	152.09	0.734	-101.33	163.68	0.599
Innate immunity	<b>NOD2</b>	23.00	66.00	0.787	96.5	7.5	<b>0.049</b>	49.50	0.50	<b>0.006</b>	31.33	75.01	0.750	14.00	57.00	0.847

A3 subjects; SE, Standard error; p-value obtained based on paired t-test. The significant p-values are in bold.

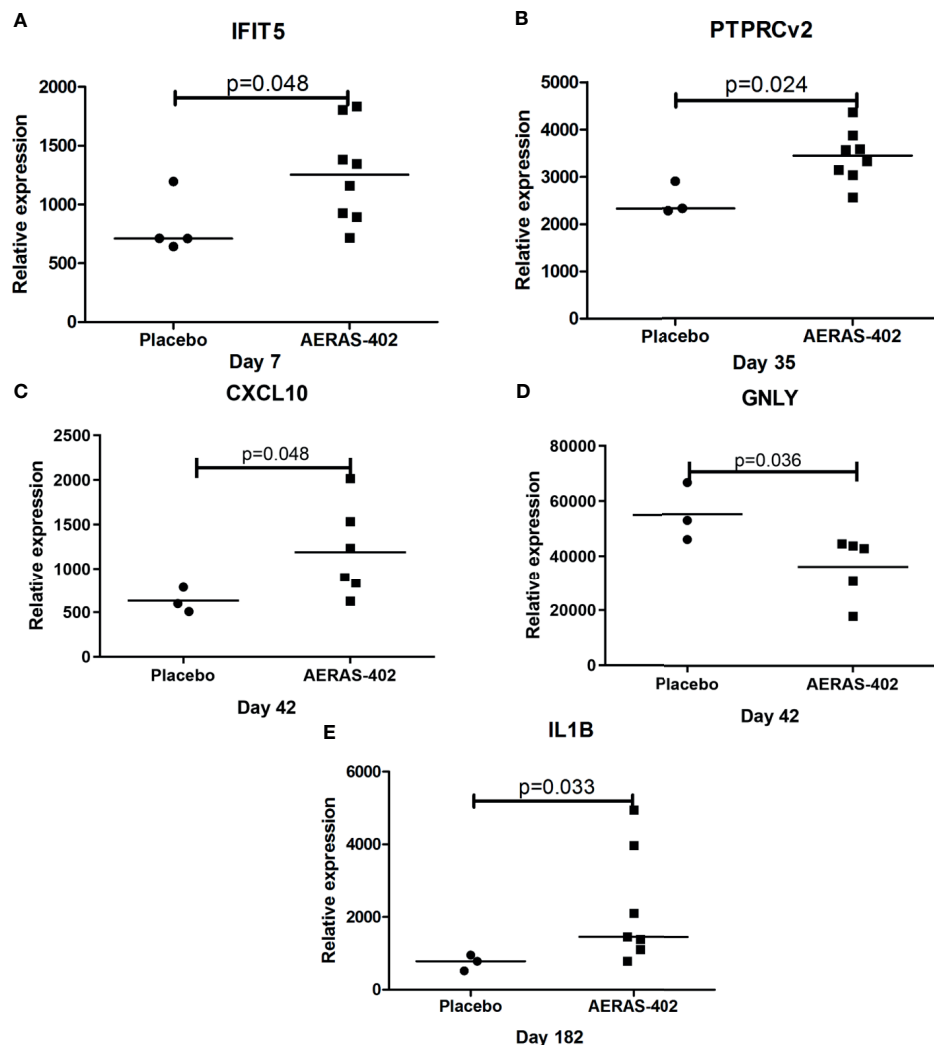
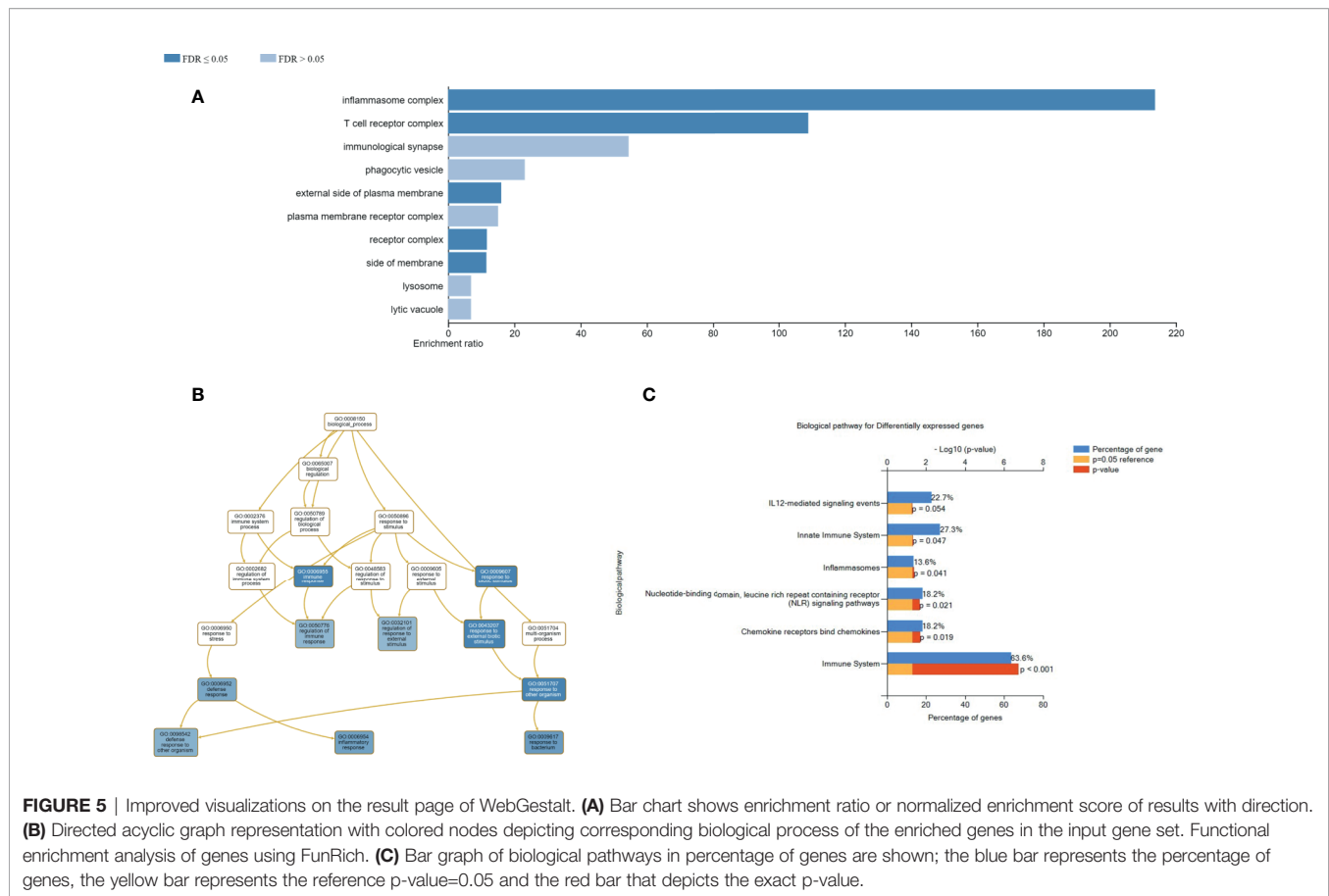


**FIGURE 4** | Mann-Whitney test was applied. Dot-plot graph depicting genes that were differentially expressed between the AERAS-402 and placebo recipients. Day 7 (A); day 35 (B); day 42 (C, D); day 182 (E).

induced a robust CD8<sup>+</sup> T-cell response against Ag85A, Ag85B and TB10.4 (Figure 2) (22). Nevertheless, to date, most new TB vaccines have been reported to induce reasonable CD4<sup>+</sup> T-cell responses, but relatively negligible CD8<sup>+</sup> T-cell responses, despite evidence from recent studies indicating that CD8<sup>+</sup> T cells mediate essential roles in protective immunity against TB (5, 37–39) including cytolytic functions to kill *Mtb*-infected cells via granule-mediated function (via perforin, granzymes, and granzysin) and Fas-Fas ligand interaction to induce apoptosis. In humans, CD8<sup>+</sup> T cells can produce granzysin, which can kill *Mtb* directly (40). Despite having the same or similar antigens, the immune response that is generated against the TB antigens can vary greatly based on the method of delivery. For example, protein/adjuvant combinations drive primarily CD4<sup>+</sup> T cell responses and antibody responses. However, vaccines that include adenoviral vectors are better suited for

stronger induction of the cellular arm of the adaptive immune system, including CD8<sup>+</sup> cytotoxic T cells.

We report that the present study is the first TB clinical vaccine phase I trial to assess vaccine induced PBMC transcriptomes. Compared to the placebo group, two genes (*IFIT5* and *PTPRCv2*) were upregulated in the 7-days following the 1<sup>st</sup> and 2<sup>nd</sup> dose of vaccination, respectively, while *CXCL10* and *GNLY* were differentially expressed between the intervention groups 14-days following the 2<sup>nd</sup> dose of vaccination. Interestingly, 6 months post-vaccination *IL1B* was upregulated in the AERAS 402 group. These genes are evocative of robust CD4<sup>+</sup> and CD8<sup>+</sup> T cell responses as observed in the T-cell stimulation assay, which likely includes activation of the type-1 interferon and cytotoxicity genes. Besides, we have identified three genes (*CLEC7A*, *PTPRCv1*, and *TAGAP*) that are consistently induced following two doses of AERAS-402: The C-type lectin



receptors are a class of signaling pattern recognition receptors, macrophages, neutrophils and dendritic cells express CLEC7A. The innate immunity component CLEC7A (Dectin-1) interacts with *Mtb*, leading to increased inflammatory cytokine production in macrophages (41, 42). The T-cell associated gene *PTPRCv1* (CD45RA) is expressed on naive T cells, as well as the effector cells in both CD4 and CD8. After antigen experience, central and effector memory T cells gain expression of *PTPRCv2* (CD45RO) and lose expression of CD45RA (43). The *TAGAP* encodes the T-cell activation Rho-GTPase-activating protein, and expression of *TAGAP* induced during T-cell activation (44). The function of *TAGAP* is currently unknown; however, a very recent study from del Rosario RC et al. (45), have reported that, in response to *Mtb* infection, an up-regulation of *TAGAP* involved in the enrichment of differential acetylation (DA) peaks in granulocytes. The nucleotide-binding domain, leucine-rich repeat-containing protein (NLR) family play key roles in innate immune defense, including protection against several major respiratory pathogens as well as in producing key Th1 and Th17 cell-promoting cytokines (46).

AERAS-402 incorporates Ad35, which has been shown to be prevalent in only 20% of individuals in sub-Saharan Africa (47) with neutralizing titers > 200 in less than 5% of individuals; this vector is able to induce potent immune responses against the encoded target

antigen. Anti-Ad35–neutralizing antibodies were present in 25% of participants in this trial before AERAS-402 vaccination, which is noticeably higher than reported elsewhere (22). AERAS-402 post-vaccination at day 182, anti-Ad35–neutralizing antibodies were detected in half of the participants in this study. In contrast, anti-Ad35–neutralizing antibodies were detected a higher proportion in the placebo than AERAS-402 recipients.

To our knowledge, we are the first to explore transcriptional profiling in a phase 1 TB clinical trial and propose that immune related transcriptional biomarkers correlate with AERAS-402 recipients and the altered gene expression profiles are indicative of activation of immunologically relevant biological pathways. No safety concerns were observed for AERAS-402 in healthy Indian adult males. The vaccine also induced promising immunogenicity, predominantly to the Ag85B antigen consisting of polyfunctional T cell responses most robust for CD8 subsets, humoral immunity and altered gene expression profiles in PBMCs indicative of a localized activation of different biological pathways. Further, pre-existing antibodies towards the viral vector may likely impact on vaccine efficacy. Nonetheless, research on vaccine biomarkers has so far received little attention as an independent scientific priority from most of the main research-funding agencies and policymakers. More efforts are necessary to highlight the importance of vaccine biomarkers on the global vaccine agenda.



## DATA AVAILABILITY STATEMENT

The raw data supporting the conclusions of this article will be made available by the authors, without undue reservation.

## ETHICS STATEMENT

The study was reviewed and approved by the Government of India Directorate General of Health Services, Office of the Drugs Controller General (Biological Division), Ref no: LL/RA/825/2007 and the Independent Ethics Committee Consultants Bangalore. The phase 1 clinical trial was registered at (<https://clinicaltrials.gov/>), and the identifier no: NCT01378312. Written informed consent was obtained from each participant prior to the conduct of any protocol-specific activity or study entry. The study was carried out following the ethical principles outlined in the Declaration of Helsinki and in accordance with the US Code of Federal Regulations for protection of human subjects (21 CFR 50), Institutional Review Boards (21 CFR 56), and the obligations of clinical investigators (21 CFR 312). The patients/participants provided their written informed consent to participate in this study.

## AUTHOR CONTRIBUTIONS

DH performed the ICS. GB prepared the first draft; DH wrote sections on ICS and RB wrote the sections on transcription profiling together with DS and SJ. DS conducted the RNA extraction, dcRT-MLPA experiments. DS and CR performed the data analysis and generated **Table 5** and **Figures 1, 4** and **5**, with contribution from SJ and HG. DS undertook revisions of manuscript with contribution from GB, DH, RB, CR, SJ, and HG. All authors contributed to the article and approved the submitted version.

## REFERENCES

- Colditz GA, Berkey CS, Mosteller F, Brewer TF, Wilson ME, Burdick E, et al. The Efficacy of Bacillus Calmette-Guerin Vaccination of Newborns and Infants in the Prevention of Tuberculosis: Meta-Analyses of the Published Literature. *Pediatrics* (1995) 96(1 Pt 1):29–35.
- Dalmia N, Ramsay AJ. Prime-Boost Approaches to Tuberculosis Vaccine Development. *Expert Rev Vaccines* (2012) 11(10):1221–33. doi: 10.1586/erv.12.94
- Lewinsohn DA, Heinzel AS, Gardner JM, Zhu L, Alderson MR, Lewinsohn DM. Mycobacterium Tuberculosis-Specific CD8+ T Cells Preferentially Recognize Heavily Infected Cells. *Am J Respir Crit Care Med* (2003) 168(11):1346–52. doi: 10.1164/rccm.200306-837OC
- Lewinsohn DA, Winata E, Swarbrick GM, Tanner KE, Cook MS, Null MD, et al. Immunodominant Tuberculosis CD8 Antigens Preferentially Restricted by HLA-B. *PloS Pathog* (2007) 3(9):1240–9. doi: 10.1371/journal.ppat.0030127
- Lin PL, Flynn JL. Cd8 T Cells and Mycobacterium Tuberculosis Infection. *Semin Immunopathol* (2015) 37(3):239–49. doi: 10.1007/s00281-015-0490-8
- Nyendak M, Swarbrick GM, Duncan A, Cansler M, Huff EW, Hokey D, et al. Adenovirally-Induced Polyfunctional T Cells Do Not Necessarily Recognize the Infected Target: Lessons From a Phase I Trial of the AERAS-402 Vaccine. *Sci Rep* (2016) 6:36355. doi: 10.1038/srep36355
- Havenga M, Vogels R, Zuidgeest D, Radosevic K, Mueller S, Sieuwerts M, et al. Novel Replication-Incompetent Adenoviral B-group Vectors: High Vector Stability and Yield in PER.C6 Cells. *J Gen Virol* (2006) 87(Pt 8):2135–43. doi: 10.1099/vir.0.81956-0
- Geluk A, van Meijgaarden KE, Franken KL, Drijfhout JW, D'Souza S, Necker A, et al. Identification of Major Epitopes of Mycobacterium Tuberculosis AG85B That are Recognized by HLA-A\*0201-restricted Cd8+ T Cells in HLA-transgenic Mice and Humans. *J Immunol* (2000) 165(11):6463–71. doi: 10.4049/jimmunol.165.11.6463
- Billeskov R, Vingsbo-Lundberg C, Andersen P, Dietrich J. Induction of CD8 T Cells Against a Novel Epitope in TB10.4: Correlation With Mycobacterial Virulence and the Presence of a Functional Region of Difference-1. *J Immunol* (2007) 179(6):3973–81. doi: 10.4049/jimmunol.179.6.3973
- McShane H, Behboudi S, Goonetilleke N, Brookes R, Hill AV. Protective Immunity Against Mycobacterium Tuberculosis Induced by Dendritic Cells Pulsed With Both CD8(+)- and CD4(+)-T-cell Epitopes From Antigen 85A. *Infect Immun* (2002) 70(3):1623–6. doi: 10.1128/IAI.70.3.1623-1626.2002
- Brooks JV, Frank AA, Keen MA, Bellisle JT, Orme IM. Boosting Vaccine for Tuberculosis. *Infect Immun* (2001) 69(4):2714–7. doi: 10.1128/IAI.69.4.2714-2717.2001
- McShane H, Pathan AA, Sander CR, Keating SM, Gilbert SC, Huygen K, et al. Recombinant Modified Vaccinia Virus Ankara Expressing Antigen 85A Boosts BCG-primed and Naturally Acquired Antimycobacterial Immunity in Humans. *Nat Med* (2004) 10(11):1240–4. doi: 10.1038/nm1128

## FUNDING

Research Council of Norway Global Health and Vaccination Research (GLOBVAC) projects: RCN 179342, 192534 and 248042, the University of Bergen (Norway); EDCTP2 programme supported by the European Union; the St. John's Research Institute, Bangalore, India. Aeras funded by the Bill and Melinda Gates Foundation, Seattle WA.

## ACKNOWLEDGMENTS

Barbara Shepherd and Bridget Colvin, for assistance with preparation of the manuscript. Aud Eliassen at the sequencing laboratory, Haukeland University Hospital, Bergen, Norway. Dr. Vanya Dhagat for serving as the Principal Investigator at Lotus Labs Pvt. Lmt. In Bangalore, India and the 15 volunteers for their participation in the study. We thank Prof. Tom Ottenhoff and Dr. Marielle C. Haks at the Dept. of Infectious Diseases, Leiden Medical University, Leiden, The Netherlands for providing the dcRT-MLPA probes and primers (Reverse transcription gene target specific primers, right hand and left-hand half MLPA probes, FAM labelled MLPA primers, HEX labelled MAPH primers). Prof. Mario Vaz and the late Dr. John Kenneth from the St. John's Research Institute, Bangalore for administrative aspects connected to the study as well, practical facilitation of sample storage.

## SUPPLEMENTARY MATERIAL

The Supplementary Material for this article can be found online at: <https://www.frontiersin.org/articles/10.3389/fimmu.2021.673532/full#supplementary-material>

13. Wiker HG, Harboe M. The Antigen 85 Complex: A Major Secretion Product of Mycobacterium Tuberculosis. *Microbiol Rev* (1992) 56(4):648–61. doi: 10.1128/MR.56.4.648-661.1992
14. Belisle JT, Vissa VD, Sievert T, Takayama K, Brennan PJ, Besra GS. Role of the Major Antigen of Mycobacterium Tuberculosis in Cell Wall Biogenesis. *Science* (1997) 276(5317):1420–2. doi: 10.1126/science.276.5317.1420
15. Horwitz MA, Harth G, Dillon BJ, Maslesa-Galic S. Recombinant Bacillus Calmette-Guerin (BCG) Vaccines Expressing the Mycobacterium Tuberculosis 30-kDa Major Secretory Protein Induce Greater Protective Immunity Against Tuberculosis Than Conventional BCG Vaccines in a Highly Susceptible Animal Model. *Proc Natl Acad Sci U S A* (2000) 97(25):13853–8. doi: 10.1073/pnas.250480397
16. Luabeya AK, Kagina BM, Tameris MD, Geldenhuys H, Hoff ST, Shi Z, et al. First-in-Human Trial of the Post-Exposure Tuberculosis Vaccine H56:IC31 in Mycobacterium Tuberculosis Infected and non-Infected Healthy Adults. *Vaccine* (2015) 33(33):4130–40. doi: 10.1016/j.vaccine.2015.06.051
17. Norrby M, Vesikari T, Lindqvist L, Maeurer M, Ahmed R, Mahdavi S, et al. Safety and Immunogenicity of the Novel H4:IC31 Tuberculosis Vaccine Candidate in BCG-Vaccinated Adults: Two Phase I Dose Escalation Trials. *Vaccine* (2017) 35(12):1652–61. doi: 10.1016/j.vaccine.2017.01.055
18. Skjot RL, Oettinger T, Rosenkrands I, Ravn P, Brock I, Jacobsen S, et al. Comparative Evaluation of Low-Molecular-Mass Proteins From Mycobacterium Tuberculosis Identifies Members of the ESAT-6 Family as Immunodominant T-cell Antigens. *Infect Immun* (2000) 68(1):214–20. doi: 10.1128/IAI.68.1.214-220.2000
19. Skjot RL, Brock I, Arend SM, Munk ME, Theisen M, Ottenhoff TH, et al. Epitope Mapping of the Immunodominant Antigen TB10.4 and the Two Homologous Proteins TB10.3 and TB12.9, Which Constitute a Subfamily of the Esat-6 Gene Family. *Infect Immun* (2002) 70(10):5446–53. doi: 10.1128/IAI.70.10.5446-5453.2002
20. Dietrich J, Aagaard C, Leah R, Olsen AW, Stryhn A, Doherty TM, et al. Exchanging ESAT6 With TB10.4 in an Ag85B Fusion Molecule-Based Tuberculosis Subunit Vaccine: Efficient Protection and ESAT6-based Sensitive Monitoring of Vaccine Efficacy. *J Immunol* (2005) 174(10):6332–9. doi: 10.4049/jimmunol.174.10.6332
21. Hoft DF, Blazevic A, Stanley J, Landry B, Sizemore D, Kpamegan E, et al. A Recombinant Adenovirus Expressing Immunodominant TB Antigens can Significantly Enhance BCG-Induced Human Immunity. *Vaccine* (2012) 30(12):2098–108. doi: 10.1016/j.vaccine.2012.01.048
22. Abel B, Tameris M, Mansoor N, Gelderbloem S, Hughes J, Abrahams D, et al. The Novel Tuberculosis Vaccine, AERAS-402, Induces Robust and Polyfunctional CD4+ and CD8+ T Cells in Adults. *Am J Respir Crit Care Med* (2010) 181(12):1407–17. doi: 10.1164/rccm.200910-1484OC
23. Meyer J, Harris SA, Satti I, Poulton ID, Poyntz HC, Tanner R, et al. Comparing the Safety and Immunogenicity of a Candidate TB Vaccine MVA85A Administered by Intramuscular and Intradermal Delivery. *Vaccine* (2013) 31(7):1026–33. doi: 10.1016/j.vaccine.2012.12.042
24. Satti I, Meyer J, Harris SA, Manjaly Thomas ZR, Griffiths K, Antrobus RD, et al. Safety and Immunogenicity of a Candidate Tuberculosis Vaccine MVA85A Delivered by Aerosol in BCG-Vaccinated Healthy Adults: A Phase 1, Double-Blind, Randomized Controlled Trial. *Lancet Infect Dis* (2014) 14(10):939–46. doi: 10.1016/S1473-3099(14)70845-X
25. Tameris MD, Hatherill M, Landry BS, Scriba TJ, Snowden MA, Lockhart S, et al. Safety and Efficacy of MVA85A, A New Tuberculosis Vaccine, in Infants Previously Vaccinated With BCG: A Randomized, Placebo-Controlled Phase 2b Trial. *Lancet* (2013) 381(9871):1021–8. doi: 10.1016/S0140-6736(13)60177-4
26. Nemes E, Geldenhuys H, Rozot V, Rutkowski KT, Ratangee F, Bilek N, et al. Prevention of M. Tuberculosis Infection With H4:IC31 Vaccine or BCG Revaccination. *N Engl J Med* (2018) 379(2):138–49. doi: 10.1056/NEJMoa1714021
27. Kagina BM, Mansoor N, Kpamegan EP, Penn-Nicholson A, Nemes E, Smit E, et al. Qualification of a Whole Blood Intracellular Cytokine Staining Assay to Measure Mycobacteria-Specific CD4 and CD8 T Cell Immunity by Flow Cytometry. *J Immunol Methods* (2015) 417:22–33. doi: 10.1016/j.jim.2014.12.003
28. Sprangers MC, Lakhai W, Koudstaal W, Verhoeven M, Koel BF, Vogels R, et al. Quantifying Adenovirus-Neutralizing Antibodies by Luciferase Transgene Detection: Addressing Preexisting Immunity to Vaccine and Gene Therapy Vectors. *J Clin Microbiol* (2003) 41(11):5046–52. doi: 10.1128/JCM.41.11.5046-5052.2003
29. Gjoen JE, Jenum S, Sivakumaran D, Mukherjee A, Macaden R, Kabra SK, et al. Novel Transcriptional Signatures for Sputum-Independent Diagnostics of Tuberculosis in Children. *Sci Rep* (2017) 7(1):5839. doi: 10.1038/s41598-017-05057-x
30. Berry MP, Graham CM, McNab FW, Xu Z, Bloch SA, Oni T, et al. An Interferon-Inducible Neutrophil-Driven Blood Transcriptional Signature in Human Tuberculosis. *Nature* (2010) 466(7309):973–7. doi: 10.1038/nature09247
31. Fletcher HA, Filali-Mouhim A, Nemes E, Hawkrig A, Keyser A, Njikan S, et al. Human Newborn Bacille Calmette-Guerin Vaccination and Risk of Tuberculosis Disease: A Case-Control Study. *BMC Med* (2016) 14:76. doi: 10.1186/s12916-016-0617-3
32. Joosten SA, Fletcher HA, Ottenhoff TH. A Helicopter Perspective on TB Biomarkers: Pathway and Process Based Analysis of Gene Expression Data Provides New Insight Into TB Pathogenesis. *PLoS One* (2013) 8(9):e73230. doi: 10.1371/journal.pone.0073230
33. Liao Y, Wang J, Jaehnig EJ, Shi Z, Zhang B. WebGestalt 2019: Gene Set Analysis Toolkit With Revamped UIs and Apis. *Nucleic Acids Res* (2019) 47(W1):W199–205. doi: 10.1093/nar/gkz401
34. Wang J. Functional Enrichment Analysis. In: W Dubitzky, O Wolkenhauer, K-H Cho, H Yokota, editors. *Encyclopedia of Systems Biology*. New York, NY: Springer New York (2013). p. 772–.
35. Lawn SD, Myer L, Edwards D, Bekker LG, Wood R. Short-Term and Long-Term Risk of Tuberculosis Associated With CD4 Cell Recovery During Antiretroviral Therapy in South Africa. *AIDS* (2009) 23(13):1717–25. doi: 10.1097/QAD.0b013e32832d3b6d
36. Green AM, Difazio R, Flynn JL. IFN-Gamma From CD4 T Cells is Essential for Host Survival and Enhances CD8 T Cell Function During Mycobacterium Tuberculosis Infection. *J Immunol* (2013) 190(1):270–7. doi: 10.4049/jimmunol.1200061
37. Woodworth JS, Behar SM. Mycobacterium Tuberculosis-Specific CD8+ T Cells and Their Role in Immunity. *Crit Rev Immunol* (2006) 26(4):317–52. doi: 10.1615/CritRevImmunol.v26.i4.30
38. Mittrucker HW, Steinhoff U, Kohler A, Krause M, Lazar D, Mex P, et al. Poor Correlation Between BCG Vaccination-Induced T Cell Responses and Protection Against Tuberculosis. *Proc Natl Acad Sci USA* (2007) 104(30):12434–9. doi: 10.1073/pnas.0703510104
39. Chen CY, Huang D, Wang RC, Shen L, Zeng G, Yao S, et al. A Critical Role for CD8 T Cells in a Nonhuman Primate Model of Tuberculosis. *PLoS Pathog* (2009) 5(4):e1000392. doi: 10.1371/journal.ppat.1000392
40. Stenger S, Hanson DA, Teitelbaum R, Dewan P, Niazi KR, Froelich CJ, et al. An Antimicrobial Activity of Cytolytic T Cells Mediated by Granulysin. *Science* (1998) 282(5386):121–5. doi: 10.1126/science.282.5386.121
41. Rothfuchs AG, Bafica A, Feng CG, Egen JG, Williams DL, Brown GD, et al. Dectin-1 Interaction With Mycobacterium Tuberculosis Leads to Enhanced IL-12p40 Production by Splenic Dendritic Cells. *J Immunol* (2007) 179(6):3463–71. doi: 10.4049/jimmunol.179.6.3463
42. Kang DD, Lin Y, Moreno JR, Randall TD, Khader SA. Profiling Early Lung Immune Responses in the Mouse Model of Tuberculosis. *PLoS One* (2011) 6(1):e16161. doi: 10.1371/journal.pone.0016161
43. Pathakumari B, Devasundaram S, Raja A. Altered Expression of Antigen-Specific Memory and Regulatory T-Cell Subsets Differentiate Latent and Active Tuberculosis. *Immunology* (2018) 153(3):325–36. doi: 10.1111/imm.12833
44. Mao M, Biery MC, Kobayashi SV, Ward T, Schimmack G, Burchard J, et al. T Lymphocyte Activation Gene Identification by Coregulated Expression on DNA Microarrays. *Genomics* (2004) 83(6):989–99. doi: 10.1016/j.ygeno.2003.12.019
45. del Rosario RCH, Poschmann J, Kumar P, Cheng C, Ong ST, Hajan HS, et al. Histone Acetylome-Wide Association Study of Tuberculosis. *bioRxiv* (2019) *BioRxiv* 644112 [Preprint]. doi: 10.1101/644112
46. Lavelle EC, McNaughton A, McNeela E. NLRP3 in Protective Immunity and Vaccination Against Respiratory Infection. *Expert Rev Vaccines* (2011) 10(3):255–7. doi: 10.1586/erv.11.12

47. Kostense S, Koudstaal W, Sprangers M, Weverling GJ, Penders G, Helmus N, et al. Adenovirus Types 5 and 35 Seroprevalence in AIDS Risk Groups Supports Type 35 as a Vaccine Vector. *AIDS* (2004) 18(8):1213–6. doi: 10.1097/00002030-200405210-00019

**Conflict of Interest:** The authors declare that the research was conducted in the absence of any commercial or financial relationships that could be construed as a potential conflict of interest.

Copyright © 2021 Sivakumaran, Blatner, Bakken, Hokey, Ritz, Jennum and Grewal. This is an open-access article distributed under the terms of the Creative Commons Attribution License (CC BY). The use, distribution or reproduction in other forums is permitted, provided the original author(s) and the copyright owner(s) are credited and that the original publication in this journal is cited, in accordance with accepted academic practice. No use, distribution or reproduction is permitted which does not comply with these terms.

## GLOSSARY

Ag85	Antigen 85
Ad	Adenovirus
AE	adverse event
BCG	Bacillus Calmette-Guérin
BD	Becton Dickinson
BMP	Bone Morphogenetic Protein
CD	Cluster of differentiation 4
CFR	Code of Federal Regulations
CCL	C-C Motif Chemokine Ligand
CXCL	C-X-C motif chemokine
CLEC	C-Type Lectin domain Containing
DCRT-	Dual color Reverse Transcriptase-Multiplex Ligation Dependent
MLPA	Probe Amplification
DMEM	Dulbecco's Modified Eagle Medium
DMSO	Dimethyl Sulfoxide
ELISA	Enzyme Linked Immunosorbent Assay
FunRich	Functional Enrichment Analysis
HIV	Human immunodeficiency virus
GAPDH	Glyceraldehyde-3-Phosphate Dehydrogenase
GNLY	Granulysin
GUSB	Glucuronidase Beta
GZMA	Granzyme A
IBM	International Business Machines
ICS	Intracellular Cytokine Staining

(Continued)

## Continued

<i>IFN-<math>\gamma</math></i>	Interferon gamma
<i>IFI</i>	Interferon Induced
<i>IFIT</i>	Interferon Induced protein with tetratricopeptide
<i>IL1B</i>	Interleukin 1 beta
<i>IL-2</i>	Interleukin 2
<i>KIF</i>	Kinesin Family Member
<i>LLOQ</i>	Lower limit of quantitation
<i>Mtb</i>	<i>M. tuberculosis</i>
<i>NLRP</i>	Nucleotide-binding oligomerization domain, Leucine rich Repeat and Pyrin domain containing
<i>NOD</i>	Nucleotide Binding Oligomerization Domain
<i>PBMC</i>	Peripheral blood mononuclear cells
<i>PCR</i>	Polymerase chain reaction
<i>PPD</i>	Purified protein derivative
<i>PTPRCv1</i>	Protein tyrosine phosphatase receptor type
<i>QFT</i>	QuantIFERON-TB Gold in-tube test
<i>RPMI</i>	Roswell Park Memorial Institute
<i>SAE</i>	Serious adverse events
<i>SE</i>	Standard Error
<i>SEB</i>	Staphylococcal enterotoxin B
<i>WebGestalt</i>	WEB-based GENE SeT AnaLysis Toolkit
<i>VEGF</i>	Vascular Endothelial Growth Factor
<i>TAGAP</i>	T Cell Activation Rho-GTPase Activating Protein
<i>TB</i>	Tuberculosis
<i>TLR</i>	Toll-like receptor
<i>TNF-<math>\alpha</math></i>	Tumor Necrosis Factor alpha
<i>TST</i>	Tuberculin Skin Test
<i>ZNF</i>	Zinc Finger Protein





# The Evaluation and Validation of Blood-Derived Novel Biomarkers for Precise and Rapid Diagnosis of Tuberculosis in Areas With High-TB Burden

Zhen Gong<sup>1†</sup>, Yinzong Gu<sup>1†</sup>, Kunlong Xiong<sup>2†</sup>, Jinxia Niu<sup>3</sup>, Ruijuan Zheng<sup>2</sup>, Bo Su<sup>2</sup>, Lin Fan<sup>2\*</sup> and Jianping Xie<sup>1\*</sup>

<sup>1</sup> State Key Laboratory Breeding Base of Eco-Environment and Bio-Resource of the Three Gorges Area, Key Laboratory of Eco-Environments in Three Gorges Reservoir Region, Ministry of Education, School of Life Sciences, Institute of Modern Biopharmaceuticals, Southwest University, Chongqing, China, <sup>2</sup> Shanghai Key Laboratory of Tuberculosis, Shanghai Clinic and Research Center of Tuberculosis, Shanghai Pulmonary Hospital, Tongji University School of Medicine, Shanghai, China, <sup>3</sup> College of Fisheries and Life Sciences, Shanghai Ocean University, Shanghai, China

## OPEN ACCESS

### Edited by:

Hazel Marguerite Dockrell,  
University of London, United Kingdom

### Reviewed by:

C. Gopi Mohan,  
Amrita Vishwa Vidyapeetham  
University, India  
Marco Pio La Manna,  
University of Palermo, Italy

### \*Correspondence:

Lin Fan  
fanlinsj@163.com  
Jianping Xie  
georgex@swu.edu.cn

<sup>†</sup> These authors have contributed  
equally to this work

### Specialty section:

This article was submitted to  
Microbial Immunology,  
a section of the journal  
Frontiers in Microbiology

**Received:** 14 March 2021

**Accepted:** 27 April 2021

**Published:** 14 June 2021

### Citation:

Gong Z, Gu Y, Xiong K, Niu J, Zheng R, Su B, Fan L and Xie J (2021) The Evaluation and Validation of Blood-Derived Novel Biomarkers for Precise and Rapid Diagnosis of Tuberculosis in Areas With High-TB Burden. *Front. Microbiol.* 12:650567. doi: 10.3389/fmicb.2021.650567

Tuberculosis (TB) remains a highly contagious public health threat. Precise and prompt diagnosis and monitoring of treatment responses are urgently needed for clinics. To pursue novel and satisfied host blood-derived biomarkers, we streamlined a bioinformatic pipeline by integrating differentially expressed genes, a gene co-expression network, and short time-series analysis to mine the published transcriptomes derived from whole blood of TB patients in the GEO database, followed by validating the diagnostic performance of biomarkers in both independent datasets and blood samples of Chinese patients using quantitative real-time PCR (qRT-PCR). We found that four genes, namely UBE2L6 (Ubiquitin/ISG15-conjugating enzyme E2 L6), BATF2 (Basic leucine zipper transcriptional factor ATF-like), SERPING1 (Plasma protease C1 inhibitor), and VAMP5 (Vesicle-associated membrane protein 5), had high diagnostic value for active TB. The transcription levels of these four gene combinations can reach up to 88% sensitivity and 78% specificity (average) for the diagnosis of active TB; the highest sensitivity can achieve 100% by parallel of BATF2 and VAMP5, and the highest specificity can reach 89.5% through a combination of SERPING1, UBE2L6, and VAMP5, which were significantly higher than 75.3% sensitivity and 69.1% specificity by T-SPOT.TB in the same patients. Quite unexpectedly, the gene set can assess the efficacy of anti-TB response and differentiate active TB from Latent TB infection. The data demonstrated these four biomarkers might have great potency and advantage over IGRAs in the diagnosis of TB.

**Keywords:** tuberculosis, blood biomarkers, BATF2, UBE2L6, VAMP5, SERPING1

**Abbreviations:** BATF2, Basic leucine zipper transcriptional factor ATF-like; GS, Gene significance; MTB, Mycobacterium tuberculosis; MM, Module membership; NIH GEO, National Institutes of Health Gene Expression Omnibus; POCT, Point-of-care tests; qRT-PCR, quantitative real-time PCR; TB, Tuberculosis; IGRAs, interferon  $\gamma$  release assays; STEM, Short Time-series Expression Miner; TST, Tuberculin skin testing.

## INTRODUCTION

Despite decades of vaccine immunization and anti-TB chemotherapy, tuberculosis (TB) caused by *Mycobacterium tuberculosis* (MTB) remains a devastating disease and an enormous burden to global public health, with around one fourth of the population at risk of being infected, about 10 million new TB incidences, and 1.2 million deaths worldwide in 2019 (WHO, 2019). Rapid and precise diagnosis of active TB largely represents an unmet clinical need (Pai and Schito, 2015). Traditional diagnosis has defects, such as the low sensitivity (12–15%) of acid-fast bacilli (AFB) and time-consuming nature of cultures (Akkaya and Kurtoglu, 2019). Molecular diagnostics such as Xpert MTB/RIF (Cepheid, Sunnyvale, CA, United States) can achieve a sensitivity of 34–66.7% for smear negative- Pulmonary TB (PTB) and extrapulmonary TB (Qureshi et al., 2019; Wu et al., 2019). Xpert MTB/RIF ultra can improve the sensitivity for TB but has decreased specificity compared with Xpert MTB/RIF (Wu et al., 2019; Jiang et al., 2020). Current etiological methods have limited sensitivity in smear-negative active TB, especially paucibacillary TB (Steingart et al., 2013). Therefore, etiological methods are not suitable for fast diagnosis of TB. Blood-derived biomarkers for precise and rapid diagnosis of TB are intensively studied to meet clinical needs.

The most applied blood-derived immunological method for diagnosis of TB was interferon- $\gamma$  release assays (IGRAs) and tuberculin skin testing (TST), however, they cannot distinguish active TB from latent TB infection (LTBI) or HIV positive patients (Rangaka et al., 2012). Mycobacteria-specific cytokines are intensively explored as a biomarker to distinguish latent TB infection from active TB (Marc et al., 2015). The diagnostics based on biomarkers derived from blood samples have recently been intensively explored (Denkinger et al., 2015), and also meet WHO's target product characteristics. The blood-based biomarkers' diagnostics have great advantages (Sweeney and Khatri, 2016; Walter et al., 2016) for quick samples collection and quantification, as well as point-of-care tests (POCT) (Wallis et al., 2010). However, based on existing research results, effective biomarkers based on whole blood are still lacking.

The host transcriptome response to MTB infection is a valuable source for this end, as exemplified by the abundant National Institutes of Health Gene Expression Omnibus (NIH GEO). To transform the transcriptome data into clinically actionable TB diagnostics, we curated nine transcriptome datasets based on the whole blood from NCBI that meet the statistical criteria for effective data analysis (Figure 1A). In combination with clinical sample analysis, we determined the specificity and sensitivity of the candidate in the diagnosis of active tuberculosis. The results showed that the effectiveness of the novel diagnostic biomarker was significantly better than T-SPOT.TB. In summary, in this study, a four-gene set (UBE2L6, BATF2, SERPING1, and VAMP5) was validated as a novel method for the diagnosis of active PTB, as well as a biomarker for monitoring anti-TB treatment efficacy.

## MATERIALS AND METHODS

### Microarray Data Information and Usage in Discovery/Validation Stage

Gene Expression Omnibus (GEO) datasets from published microarray-based studies of PTB versus LTBI or other diseases were collected for data mining. From the nine datasets (GSE19491, GSE40553, GSE56153, GSE42834, GSE39941, GSE37250, GSE103119, GSE94438, and GSE124548), 2804 samples were obtained (Table 1). After screening for the most relevant and comprehensive blood samples, 1654 samples were kept for further study. However, most samples are highly heterologous for processing methods, and cannot be directly used for analysis. GSE19491 has very comprehensive information with a large number of samples and was assayed by the same laboratory with uniform methods. Multiple individuals were included in this dataset, such as PTB, LTBI, HC, and other pulmonary diseases. Additionally, the change of transcriptome during treatment monitoring was also analyzed. Specifically, three subseries (GSE19439, GSE19442, and GSE19444) in GSE19491 containing the transcriptome data of TB, LTBI, and HC were used for gene differential expression and correlation analysis. Therefore, GSE19491 was used as the discovery dataset to find the differential expression by Limma, correlation by WGCNA, and time-course trend by STEM.

GSE40553 and GSE56153 contained the time-course transcriptome data of TB patients post treatment. GSE42834 contained patients with active TB or miscellaneous pulmonary diseases. GSE37250 and GSE39941 are samples from patients of TB and other diseases with or without HIV co-infection. GSE94438 samples are from household contact subjects (Suliman et al., 2018). Thence, we chose the six datasets for validation.

Another three datasets (GSE103119, GSE124548, and GSE42834) were used to validate the biomarker specificity. GSE103119 contained patients with pneumonia caused by bacteria or virus (except MTB) and healthy subjects, while GSE124548 samples are from cystic fibrosis patients, used to differentiate pulmonary diseases.

Datasets first underwent quantile normalization and were log2 transformed. We mapped the probes to gene symbols based on the probe data before Dec 5, 2018 from GEO.

### Identification of Biomarkers From Multiple Datasets

In order to discover the molecules most likely to be biomarkers of tuberculosis from the data set, we combined multiple data analysis methods: Differentially expressed genes (DEGs), Co-expression network analysis, and Time series analyses.

### Real-Time qPCR Validation of Differentially Expressed Genes by Prospective Clinical Study

Patients who met inclusive criteria were prospectively enrolled into this study from January 1, 2019 to July 31, 2019 in Shanghai Pulmonary Hospital. The study was approved by the

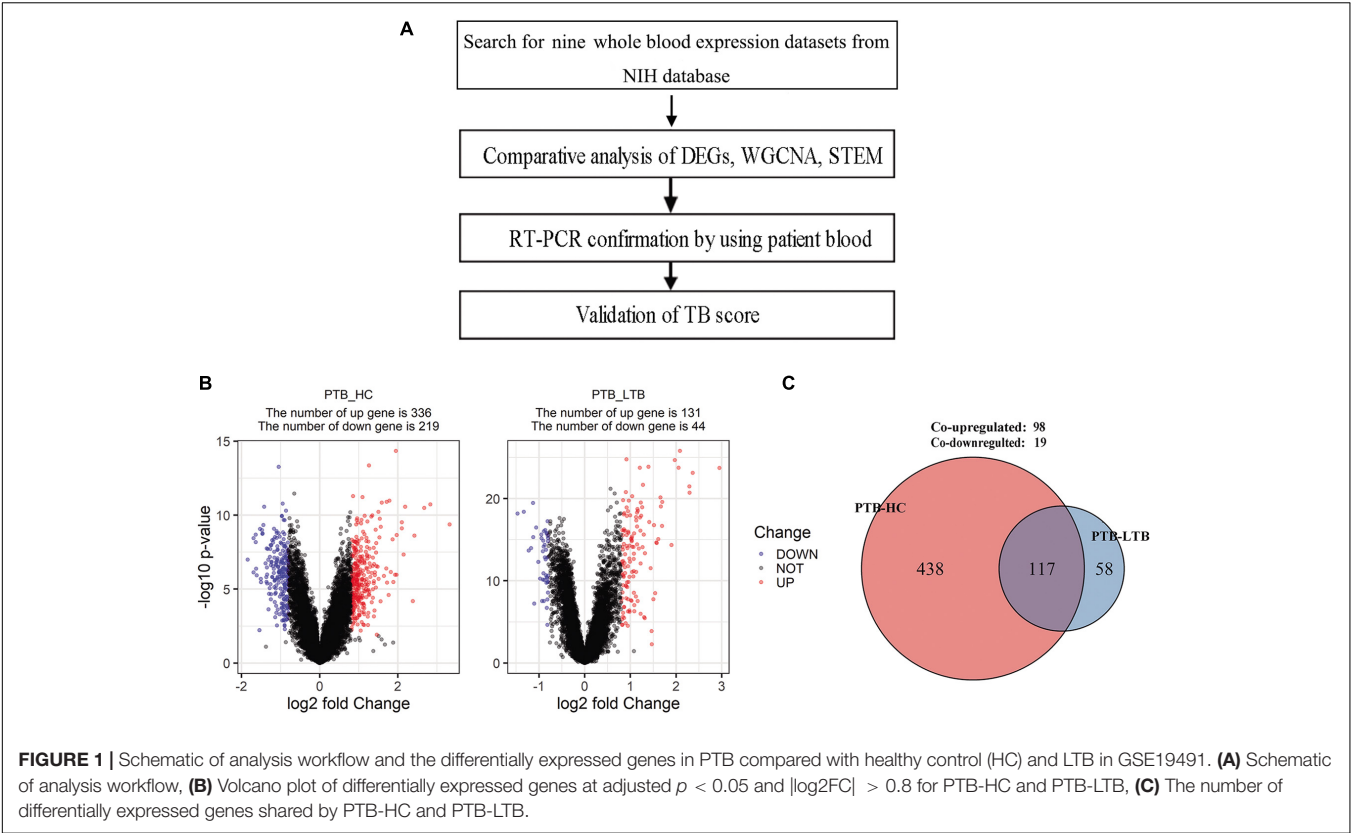


TABLE 1 | Geo information used in this study.

	Year	Reference	Platform	Participants Age	Race distribution	Participants classification	Treatment
GSE19491 (SubSeries: GSE19435, GSE19439, GSE19442, GSE19444)	2010	Berry	GPL6947	Adults	African European	PTB, LTB, and HC;	3 time-points: 0, 2, 12 months in GSE19435
GSE40553	2012	Bloom	GPL10558	Adults	European	PTB	5 time-points: 0, 0.5, 2, 6, 12 months
GSE56153	2014	Ottenhoff	GPL6883	Adults	Asian	PTB, HC	3 time-points: Active, Treatment, Recover
GSE42834	2013	Bloom	GPL10558	Adults	–	PTB, lung cancer, other pulmonary diseases	–
GSE39941	2014	Anderson	GPL10558	Children	African	PTB, other diseases (HIV +/-)	–
GSE37250	2013	Anderson	GPL10558	Adults	African	PTB, other diseases (HIV +/-)	–
GSE103119	2018	Wallihan	GPL10558	Children	–	HC, pneumonia caused by bacterial or viral infections	–
GSE94438	2018	Thompson	GPL11154	Adults	African	household contact	2 time-points: 6, 18 months
GSE124548	2019	Kopp	GPL20301	Adults	–	pulmonary disease caused by cystic fibrosis	–

Institutional Review Board of Shanghai Pulmonary Hospital, School of Medicine, Tongji University (approval number: K17-022) and the enrolled patients signed informed consent forms. Included patients donated 2 ml peripheral venous blood for RNA extraction.

The inclusion criteria are: patients diagnosed with pulmonary TB (PTB), lung cancer, or pneumonia; those who are serum HIV negative; and patients willing to be included in this study. Diagnostic standards were as followed: PTB was diagnosed by MTB MGIT 960 culture positive consistent with WHO guidelines

of diagnosis and treatment on pulmonary tuberculosis (19); lung cancer was confirmed by pathology examination; and pneumonia was diagnosed according to the national guideline.

The exclusion criteria are: patients with an uncertain diagnosis, HIV positive patients, those taking immunosuppressive agents, cases complicated by cancer or other complications or other pulmonary diseases, or patients reluctant to attend the study.

Quantitative real-time PCR (qRT-PCR) was used to validate the differential expression of the four shortlisted genes in blood samples from participants. 2.0 mL peripheral venous blood was taken directly into PAXgene blood RNA tubes (PreAnalytiX, Hombrechtikon, Switzerland) and stored at  $-20^{\circ}\text{C}$  for use. RNA was extracted from PAXgene tubes stored blood. Before analysis, all test samples and primers were assigned random numerical codes that masked the disease, control status, and the gene identity. The qRT-PCR-based validation and GEO data mining were done in a fully blind manner. The primers used are listed in **Table 2**. The gene expression levels were quantified relative to the transcription of  $\beta$ -actin by using an optimized comparative  $\text{Ct}$  ( $\Delta\Delta\text{Ct}$ ) value method.

## Validation of TB Score

By data mining and validating by clinical study, we defined the geometric mean of the four gene transcription levels as the TB score ( $\text{TBscore} = \sqrt[4]{\text{UBE2L6} \times \text{BATF2} \times \text{SERPING1} \times \text{VAMP5}}$ ) (Sweeney et al., 2016). This TB score was directly tested for diagnostic power by receiver operating characteristic (ROC) curves using the R package pROC. Violin plots showed the TB score for a dataset response to treatment at specific time points. Violin plot error bars showed the inter-quartile range (IQR) between non-normal distributions within subsets. Between-groups TB score comparisons were done with the Wilcoxon rank sum test. Significance levels were set at two-tailed  $p < 0.05$ . All computation and calculations were done in the R language (version 3.5.1).

## T-SPOT.TB Assay

T-SPOT.TB was performed in accordance with the manufacturer's instructions (Oxford Immunotec Ltd.). Blood samples were collected immediately prior to the tests in order to

avoid potential interferences, and patients who received blood transfusions or underwent positron emission tomography-computed tomography scans within 1 week of the test were recommended to undergo a second test 2 weeks later. Peripheral blood mononuclear cells (PBMCs) were separated from blood samples using Ficoll-Hypaque gradient centrifugation at  $400 \times g$  for 30 min at  $20^{\circ}\text{C}$ . PBMCs were seeded on precoated IFN- $\gamma$  ELISpot plates and incubated with media without an antigen (as a negative control), media containing peptide antigens derived from ESAT-6 (labeled panel A) or peptide antigens derived from CFP-10 (labeled panel B), or media containing phytohemagglutinin (as a positive control) in a 5%  $\text{CO}_2$  atmosphere at  $37^{\circ}\text{C}$  for 20 h. 29–31. After counting the number of spot-forming cells, results are reported with negative control results subtracted (i.e., measured sfu number minus sfu number of negative control), according to the recommendations of the manufacturer. The values for ESAT-6 (panel A) and CFP-10 (panel B) were also scored individually using the same procedure and the maximum of them was regarded as the final result of T-SPOT.TB. All T-SPOT.TB testing was performed before the patients were prescribed anti-TB medications.

## Statistical Analysis

Statistical and machine learning methods (R packages: limma, WGCNA, pROC, and STEM software) were employed to discover and validate the biomarker genes for TB diagnosis and treatment response based on the mRNA levels in blood samples. The analyses were carried out using scripts written in Rstudio. The differences in gene expression levels between TB patients' and healthy controls' blood samples were compared using the Wilcoxon test. Multiple comparisons were carried out in patients with lung cancer, pneumonia, and TB by Kruskal-Wallis. Significance levels were set at  $p < 0.05$ .

## RESULTS

### Four Candidate Biomarker Genes Were Found by Integrating the Results of DEGs, WGCNA, and STEM Analysis

The DEGs in the three subseries of GSE19491 were analyzed using the limma package following data preprocessing. A total of 555 DEGs were identified, including 336 up-regulated genes and 219 down-regulated genes in PTB compared to HC and 175 DEGs w including 131 up-regulated genes and 44 down-regulated genes in PTB compared to LTB (**Figure 1B**). Finally, 117 DEGs were found to be shared by both PTB-HC and PTB-LTB, containing 98 up-regulated genes and 19 down-regulated genes (**Figure 1C**).

4807 genes in 134 samples were analyzed by WGCNA to find the modules of highly correlated genes. By a power of 8, 14 modules were found (**Figure 2A**). Among all modules, the black module with 270 genes had the highest correlation coefficient ( $p = 5\text{e-}24$ ;  $r = 0.74$ ) with PTB (**Figure 2B**). An intra-modular analysis of GS and MM of the genes in the black module found that GS and MM were significantly correlated ( $p = 6.6\text{e-}70$ ;  $r = 0.83$ ), further supporting that the genes in the black module were highly correlated (**Figure 2D**). To investigate whether these

**TABLE 2** | Primers used in this study.

Genes	Primers
BATF2 (NM_138456.3)	F-CACCAGCAGCACGAGTCTC R-TGTGCGAGGCAACAGGAG
UBE2L6 (NM_004223.3)	F-CGCGCTGTGTGCGGG R-GCAGGGGCTCCCTGATATTC
VAMP5 (NM_006634.2)	F-ATGCGTAACAACCTCGGCAAG R-GGCCAGGTTCTGTGTAGTCTT
SERPING1 (NM_001032295.1)	F-GGGATGCTTTGGTAGATTCTCC R-GAGGATGCTCTCCAGGTTTGT
$\beta$ -actin	R-ACAGTTGGTCCATAGCCTGC F-TTCCTTCCTGGGCATGGAGTCC R-TGGCGTACAGGTCTTTGCGG



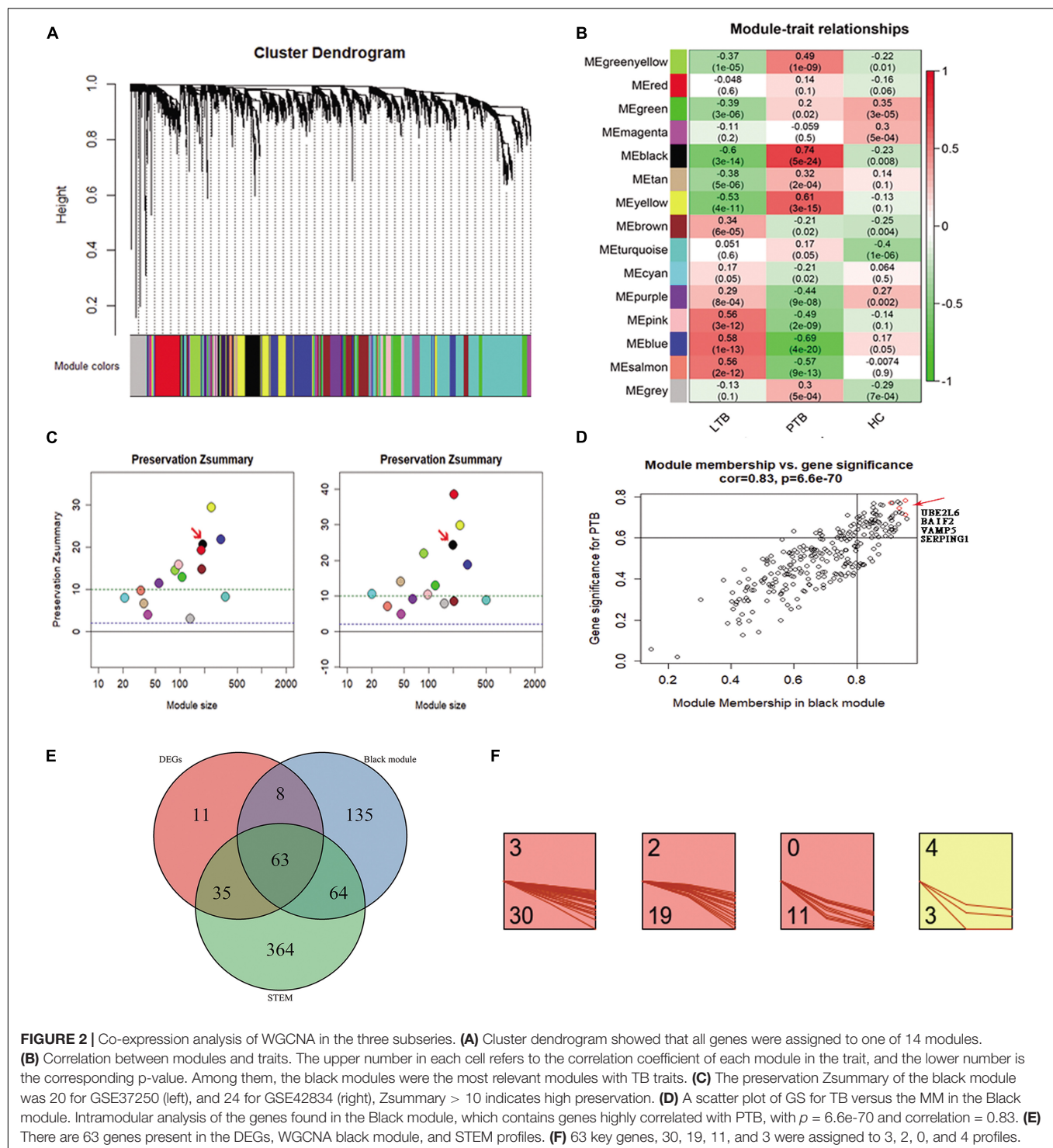


**FIGURE 2 |** Co-expression analysis of WGCNA in the three subseries. **(A)** Cluster dendrogram showed that all genes were assigned to one of 14 modules. **(B)** Correlation between modules and traits. The upper number in each cell refers to the correlation coefficient of each module in the trait, and the lower number is the corresponding p-value. Among them, the black modules were the most relevant modules with TB traits. **(C)** The preservation Zsummary of the black module was 20 for GSE37250 (left), and 24 for GSE42834 (right), Zsummary > 10 indicates high preservation. **(D)** A scatter plot of GS for TB versus the MM in the Black module. Intramodular analysis of the genes found in the Black module, which contains genes highly correlated with PTB, with  $p = 6.6e-70$  and correlation = 0.83. **(E)** There are 63 genes present in the DEGs, WGCNA black module, and STEM profiles. **(F)** 63 key genes, 30, 19, 11, and 3 were assigned to 3, 2, 0, and 4 profiles.

modules are conserved in our network, two independent datasets of GSE37250 and GSE42834 datasets were used to test the preservation of these modules. Zsummary > 10 indicates high preservation. Black modules in the GSE37250 and GSE42834 had Z-summary 20, 24, indicating they are well-preserved network in our study (Figure 2C).

To minimize the candidate genes for biomarkers, we conducted a comparative analysis and found 63 genes (Supplementary Table 1) present in the DEGs, WGCNA black module, and STEM profiles (Figure 2E). Of the 63 key genes, 30, 19, 11, and 3 were assigned to 3, 2, 0, and 4 profiles (Figure 2F). They were significantly enriched in immune

**TABLE 3** | Patient's information.

	TB	LC	Pulmonary inflammation	HP
Number of people	51	30	32	16
Gender (male, proportion)	78.4%	–	–	56.25%
Age (median, range, and years)	35 (20–83)	–	–	20–40
Date of inspection	1/2019 and 6/2019	7/2019	7/2019	7/2019

TB, Tuberculosis; LC, Lung cancer; HP, Healthy population.

response related terms in the GO, Reactome pathway, and Uniprot keywords enrichment analyses by STRING website (Szkarczyk et al., 2017). This result encouraged us to further explore the roles of the 63 genes in TB.

Too many genes might be counterproductive for rapid and precise biomarker diagnosis. We further shortlisted the 63 genes to four genes (SERPING1, BATF2, UBE2L6, and VAMP5), due to their highest GS and MM in the black module, reduced constantly in STEM profile 3, and differentially expressed in both the PTB versus LTB and PTB versus HC. Together, the transcriptional levels of the four genes correlated with TB and changed significantly during treatment. It implied that the four genes might play essential roles in the development of TB and could be candidates for new diagnostic biomarkers.

### Four Genes Showed Good Clinical Performance by Real-Time qPCR Validation in Peripheral Blood From Patients

To validate the clinical efficacy of the four genes, 150 participants were included; of them, 14 cases were excluded due to obscure diagnosis, and a total of 126 participants were finally enrolled into the study. They were classified into four groups: 51 cases with active PTB, 30 cases with pulmonary lung cancer (TUMOR), 30 cases with pneumonia (INFLA), and 15 cases as healthy donor (HC). Patient's clinical characteristics were shown in Table 3.

The transcription levels of the four genes were detected by qRT-PCR. The results showed that BATF2, SERPING1, UBE2L6, and VAMP5 were significantly increased in PTB compared with HC (Wilcoxon test,  $P < 0.05$ ).

We further plotted the ROC curve to evaluate diagnostic power (Figure 3). The results showed that the diagnostic power of a single gene was relatively lower than their combination and the ROC curve of each gene is different from these of TB score by genes combination (venkatraman method (Venkatraman, 2015),  $P < 0.05$ ). In the patient samples, the combination of three genes (BATF2-SERP1G1-VAMP5 and BATF2-SERP1G1-UBE2L6) or two genes (BATF2-SERP1G1 and SERP1G1-VAMP5) can improve the diagnostic performance, and there was no difference in the ROC curve in between those matches with the four-gene combination (Supplementary Image 1). The results from Chinese patients were different from those reported in the GEO data in which the combination of four genes showed better performance. The performance of four gene combinations in Chinese patients can reach up to 100% for sensitivity or specificity, the average sensitivity or specificity is  $AUC = 0.84$ ,

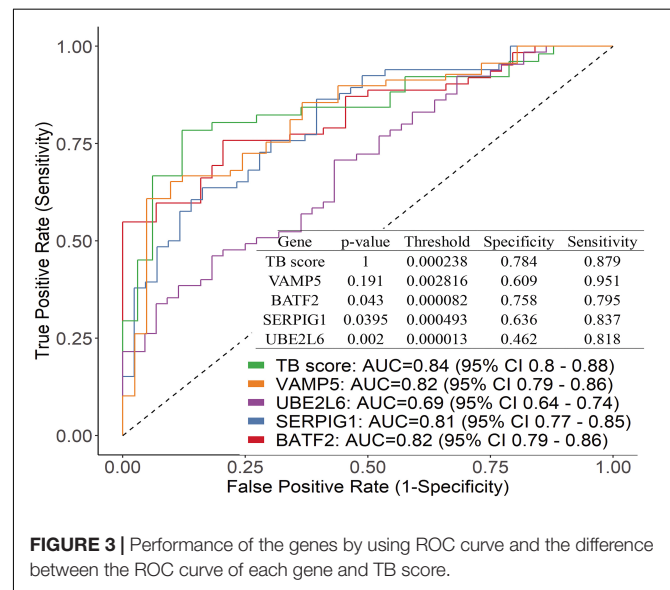


**FIGURE 3** | Performance of the genes by using ROC curve and the difference between the ROC curve of each gene and TB score.

sensitivity = 88%, and specificity = 78%, similar to that by pure GEO datasets analysis from a non-Chinese population, which has an  $AUC = 0.86$ , sensitivity = 86%, and specificity = 81%.

### The Diagnostic Efficacy of the Four Genes for Active TB Is Significantly Higher Than That of T-SPOT.TB Conducted Over the Same Patients

To compare the four candidate biomarkers and T.SPOT's performance for the diagnosis of active TB, all patients were tested by T-SPOT.TB. 75.3% sensitivity and 69.1% specificity were found, suggesting that the diagnostic accuracy of T-SPOT.TB for active tuberculosis is significantly lower than the four genes in areas with high TB burden.

### Four Genes Have Good Specificity for Active TB Diagnosis

In the clinic, other lung diseases often confound the accuracy of tuberculosis diagnosis to a large extent. The diagnostic specificity of candidate markers is crucial. In order to verify the specificity of the four genes, we examined TB score in independent gene expression datasets from clinical TB samples, comparing its efficacy among four types of comparisons by ROC curve (Figure 4): (1) PTB versus HC [ $AUC 1.00$  (95% CI 0.99–1.00)] and other pulmonary diseases : PTB versus

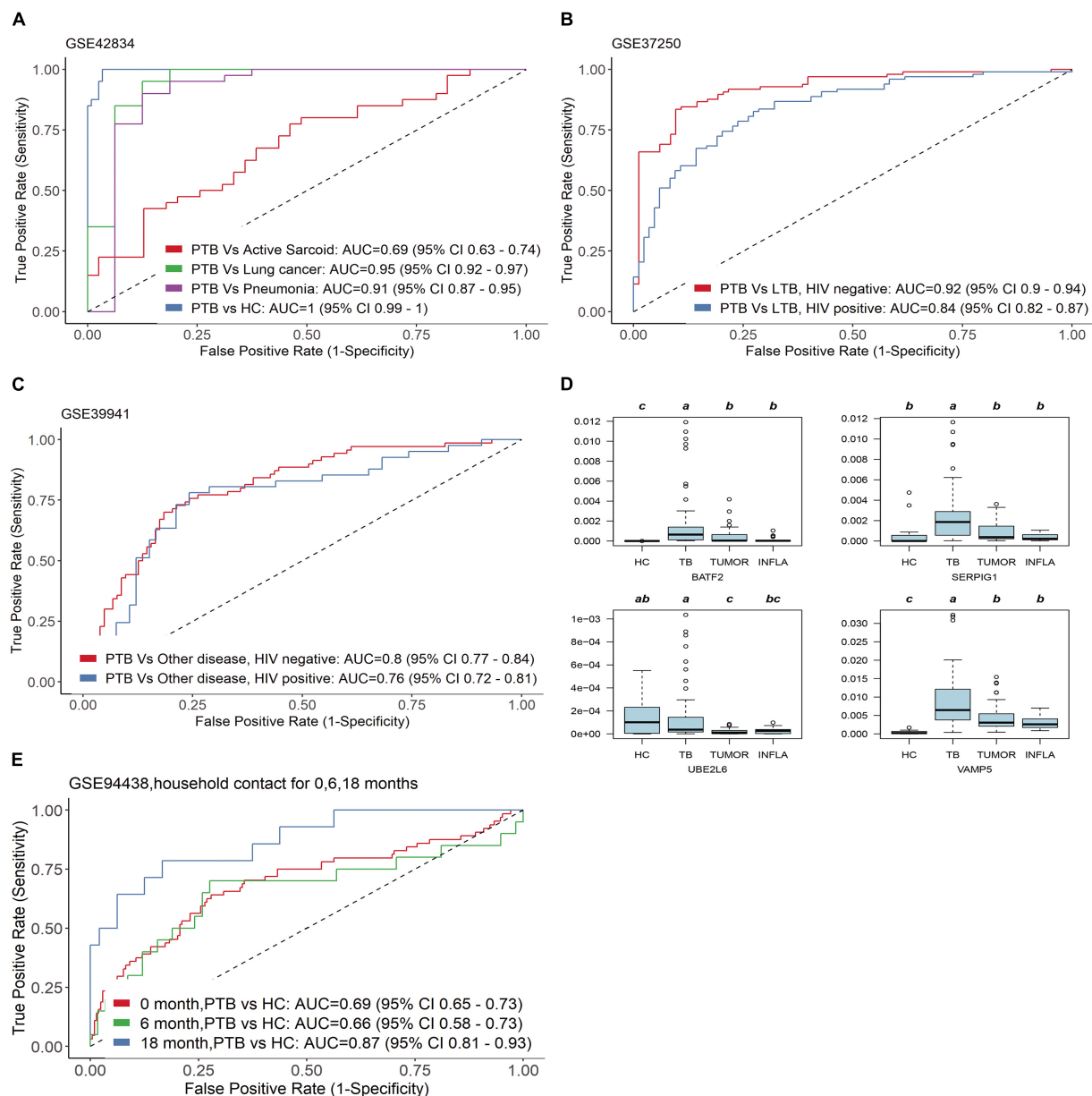


**FIGURE 4 |** Four genes have good specificity for active TB diagnosis. **(A,D)** PTB versus HC and other pulmonary diseases, **(B)** active TB versus LTBI with HIV and active TB versus LTBI without HIV, **(C)** active TB versus other diseases with HIV or without HIV in GSE39941. **(E)** The four genes can predict whether close contacts of tuberculosis patients will develop active TB.

sarcoidosis AUC 0.69 (95% CI 0.63–0.74); PTB versus Lung cancer AUC 0.95 (95% CI 0.92–0.97); PTB versus Pneumonia AUC 0.91 (95% CI 0.87–0.95) in GSE42834 (**Figure 4A**); (2) active TB versus LTBI with HIV (AUC 0.84 (95% CI 0.82–0.87)) and active TB versus LTBI without HIV [AUC 0.92 (95% CI 0.90–0.94)] in GSE37250 (**Figure 4B**); (3) active TB versus other diseases with HIV [AUC 0.76 (0.72–0.81)] or without HIV [AUC 0.80 (0.77–0.84)] in GSE39941 (**Figure 4C**); and (4) active TB patients response to treatment at specific time points (GSE40553 and GSE56153). The TB score did well across all conditions (mean AUC 0.86, sensitivity 86%,

and specificity 81%) except sarcoidosis, which might be due to the common disease-related signatures in TB and sarcoidosis (Maertzdorf et al., 2012).

We further examined the transcription level of the four genes in blood samples from patients with tumors (TUMOR) and pneumonia (INFLA). The results showed that the transcription of the four genes in PTB was significantly higher than that in HC, TUMOR, and INFLA (**Figure 4D**). The transcription of SERP1G were about 3–7 times in PTB compared with HC, TUMOR, and INFLA. Those in HC, TUMOR, and INFLA were almost identical, but they were about 3–7 times in PTB compared

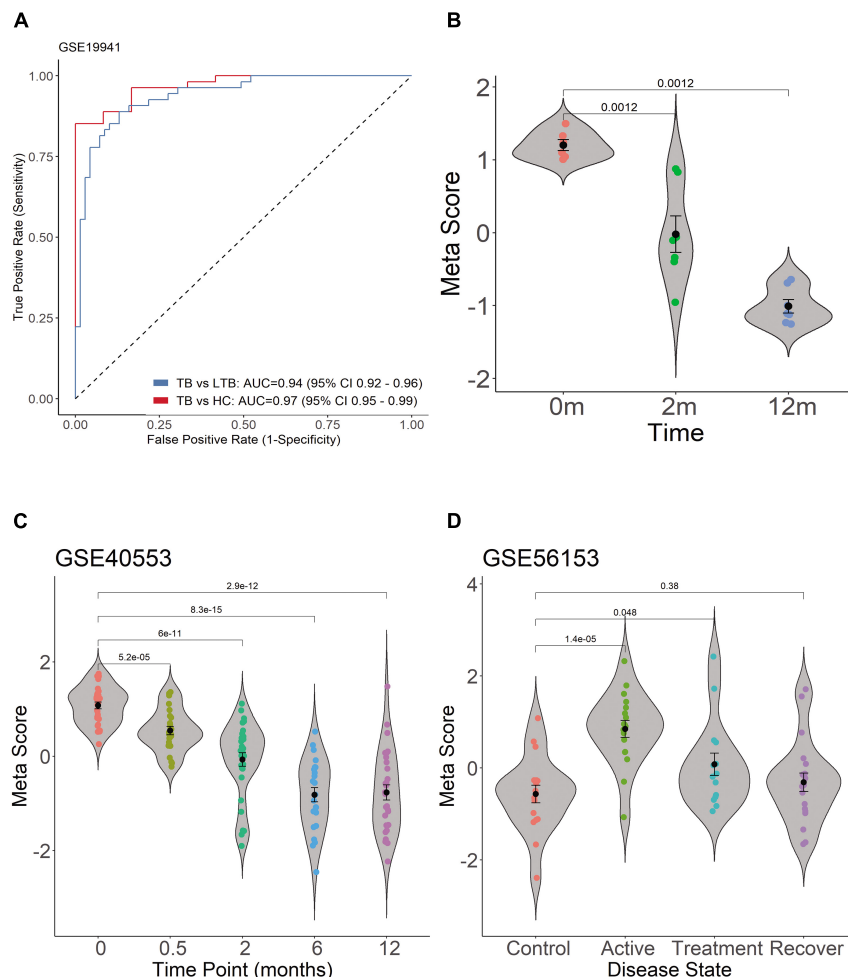


**FIGURE 5 |** Diagnostic performance of TB score by using ROC curve in GSE19941 and violin plots in GSE19941, GSE40553, and GSE56153. **(A)** Four genes can distinguish PTB and HC, and can differentiate active PTB from LTBI. **(B)** The scores of TB patients decreased significantly after effective treatment. **(C)** The TB score was significantly decreased after treatment for PTB. **(D)** The TB scores of patients return to normal after treatment between healthy control and recovery patients.

with HC, TUMOR, and INFLA. The transcription levels of BATF2, UBE2L6, and VAMP5 in TUMOR and INFLA were also similar and were slightly higher than those in HC. However, the transcription levels of the above three genes in PTB were about 3–8 times higher than those in TUMOR and 3–15 times higher than that in INFLA (**Supplementary Table 2**).

In addition, the four genes can also predict whether close contacts of tuberculosis patients will develop active TB. According to GSE94438, TB score can effectively identify those who developed TB 18 months after contact with active tuberculosis [AUC 0.87 (95% CI 0.81–0.93)] (**Figure 4E**).

### The Four Genes Can Also Be Biomarkers for Treatment Efficacy and Differential Diagnosis via Cross-Validation of TB Score in Independent Test Datasets

As expected, when we investigated TB score in the discovery datasets, we found the four-gene set can differentiate active TB

from HC with AUC 0.97 (95% CI 0.95–0.99) and differentiate active PTB from LTBI with AUC 0.94 (95% CI 0.92–0.96) (**Figure 5A**). The scores of TB patients decreased significantly after effective treatment (**Figure 5B**).

The transcription of the four genes decreased gradually with effective TB treatment in GSE40553 and GSE56153 databases (**Supplementary Image 2**). Therefore, we tested whether TB score of the four genes can be used to assess the treatment response in databases. For the active TB patients under lengthy treatment, the TB score was significantly decreased after treatment (**Figure 5C**). In GSE56153, the TB scores of patients returned to normal after treatment between healthy control and recovery (**Figure 5D**, Wilcoxon  $p > 0.05$ ). The results indicate that the four genes can be biomarkers to monitor treatment efficacy. In summary, the four gene's signatures are excellent specific TB diagnostic biomarkers in the pilot test. However, multiple center clinical studies with more cases should be conducted in the future.



## DISCUSSION AND CONCLUSION

Novel biomarkers for rapid and reliable TB diagnosis and treatment efficacy monitors are urgently needed to reduce or eliminate the global burden of TB. Here, we used both a prospective study and public datasets with more than 1,000 whole blood patient samples across a range of ages and countries to find diagnostic biomarker genes for the diagnosis of active TB. We found a four-gene set (UBE2L6, BATF2, SERPING1, and VAMP5), and cross-validated it in five additional independent whole blood datasets. The results showed that the four-gene set is robust for the diagnosis of active PTB with other pulmonary TB and HC, while the diagnostic performance is not affected by HIV status based on the datasets. In addition, the four-gene set can help to distinguish active TB from LTBI, which is usually accomplished by TST or IGRAs test. More importantly, we have confirmed that the accuracy of the novel detection method is significantly higher than that of the IGRAs test. The transcription levels of the four-gene decreased stepwise upon effective treatment and could also be biomarkers to monitor treatment efficacy. Whether they can be biomarkers for treatment failure or relapse remains to be determined. Our data indicated that the combination of the four gene set can reach sensitivity of 88 and 78% specificity for the PTB which were significantly higher than 75.3% of sensitivity and 69.1% of specificity by T-SPOT.TB in the same cohort population. The novel biomarkers can reach as high as 100% sensitivity by parallel of BATF2 and VAMP5 and 89.5% specificity by combination of SERPING1, UBE2L6, and VAMP5. The most effective three gene combination is BATF2-SERPING1-VAMP5 with 77% specificity and 91% sensitivity for the diagnosis of PTB. The most effective combination of two genes is SERPING1-VAMP5 (76% specificity and 86% sensitivity).

The host immune response is crucial for the outcome of active TB. However, the genes and pathways involved in host immune response to *M. tuberculosis* infection or persistence remain elusive. Based on Genecards annotation, the four genes are all involved in well-established immune response, but very few studies associated them with TB. The protein-protein interaction network of the four genes constructed *via* STRING-DB database showed that they are strongly associated with ubiquitination, immune cell differentiation, complement activation, and vesicle trafficking (**Supplementary Image 3**), which are important cellular responses during host interaction with *M. tuberculosis*. BATF2, also called SARI, is a member of the BATF subfamily of basic leucine zipper proteins regulated by interferon and an inhibitor of AP-1 in human cells (Haiqing et al., 2011), which controls the differentiation of lineage-specific cells in the immune system (Murphy et al., 2013), and Batf2/Irf1 induces inflammatory responses in mycobacterial infection (Sugata et al., 2015). Ubiquitin conjugating enzyme E2 L6 (UBE2L6) serves as an E2 enzyme for post-translational addition of an ubiquitin-like protein ISG15 which is vital for antiviral immunity (Skaug and Chen, 2010) and is involved in the type-I interferon response in active TB disease (Ottenhoff et al., 2012). Vesicle-associated membrane protein 5 (VAMP5) is a member of the SNARE protein family, which regulates the docking and fusion of intracellular membrane vesicles (Hong, 2005) and is involved in

the development or function of the respiratory system (Ikezawa et al., 2018). VAMP5 controls intracellular transport events, including endocytosis, exocytosis, and internal recycling (Tajika et al., 2014). SERPING1-encoded serpin peptidase Inhibitor (C1Inh), a member of a large family of serine proteases, can influence the complement C1q levels which can mark active disease in human tuberculosis (Cai et al., 2014; Horwitz et al., 2019). By single cell RNA-seq transcriptome of patients with tuberculosis, we found that four genes are highly expressed in white blood cells of patients with tuberculosis. In general, the levels of these four genes in CD14<sup>+</sup> or CD16<sup>+</sup> monocytes show the highest trend, among which VAMP5 is relatively higher. This is consistent with the role of monocytes in tuberculosis bacteria. VAMP5 is involved in vesicle transport and has the highest level in monocytes. In addition, the complement activation pathway may also be involved in the elimination of tuberculosis. The sequence-structure-function of the found protein is closely related to its predicted role in tuberculosis. The specific high expression of these genes in TB patients may suggest that they play an important role in the immune response against tuberculosis. Our ongoing study found that the inhibition of BATF2 can benefit the host, suggesting a promising drug target. In addition to the four genes, 63 other key genes we identified were intensively associated with immune response by functional enrichment analysis. Further exploring the immune roles of the 63 genes is worthwhile and might provide more biomarker candidates.

The datasets used in our study have been used by other teams to explore TB diagnostic biomarkers. There is surprisingly little overlap between our results and other reports. Kafrou and colleagues (Myrsini et al., 2013) identified a 44-transcript signature which can distinguish PTB from other diseases (including only one of our genes, SERPING1) and a 27-transcript signature which can distinguish TB from latent TB (including only one of our genes, VAMP5). Berry et al. (2010) found an 86-gene signature which is related to neutrophil-driven type I interferon (no overlap with our four genes) and can discriminate PTB from other inflammatory and infectious diseases. Bloom et al. (2013) identified 144-transcript signature which distinguished PTB from other lung diseases and controls (none of our four genes in it). Anderson et al. (2014) assessed transcript signatures in children and found a 51-transcript signature for distinguishing TB from other diseases (including only one of our genes, VAMP5) and 42-transcript signature for distinguishing TB from latent TB infection (none of our four genes were in it). Bloom et al. (2012) reported an active TB 664-transcript signature and a treatment-specific 320-transcript signature significantly diminished after 2 weeks of treatment. Zak et al. (2016) identified a 16 gene signature which can predict tuberculosis progression. The size of their gene panel is too large to be clinically affordable or actionable for rapid qRT-PCR-based assay. In contrast, our four genes can differentiate active TB from latent TB and other diseases. The four-gene set will reduce the cost in its clinical qRT-PCR-based diagnosis. Similarly, Costa et al. (2015) found a three-gene set (GZMA, GBP5, and FCGR1A), Sutherland and colleagues (Maertzdorf et al., 2016) found a four-gene set (GBP1, IFITM3, P2RY14, and

ID3), Ottenhoff et al. (2012) found a three-gene set (IL15RA, UBE2L6, and GBP4), Sweeney et al. (2016) found a three-gene set (GBP5, DUSP3, and KLF2), and Roe et al. (2019) found a three-gene set (BATF2, GBP5, and SCARF1) in blood samples that can distinguish TB. But our biomarker genes are different and validated in a Chinese population.

The discrepancy between our result and other reports might have resulted from the ethnicity or the bioinformatic pipelines. Our approach uniquely integrated three bioinformatics methods and validated the results by prospective study in a Chinese population. We explored transcript signatures *via* integrating differential expression genes, co-expression networks, and expression trends, which can interpret the expression data from multiple dimensions. This rigorous pipeline might underlie the good performance of the four genes. However, this pipeline might miss some candidate biomarkers. There might be additional biomarker genes which can be included for better performance in regions with low incidence rates of active tuberculosis.

Although there are some reports that clearly affirm that some of these genes can be used as a biomarker for TB diagnosis, the effectiveness of a single gene is flawed. The flexible application of the four genes set that we found is a fast and effective diagnostic method for active TB disease. Moreover, this four genes set can also be used as detection molecules for the treatment effect of TB, and are expected to play an important role in quickly distinguishing PTB from LTBI.

In summary, we demonstrated that the four-gene set (BATF2, UBE2L6, VAMP5, and SERPING1) is a robust blood-based diagnostic for active TB across seven datasets containing more than 1,200 clinical samples, the sensitivity or specificity of which can reach 100%, though the mean AUC = 0.86, sensitivity = 86%, and specificity = 81%. They span a variety of age, infection or exposure status, ethnicity (Sutherland et al., 2014) and genetic backgrounds, and diverse circulating lineages of *M. tuberculosis*. This was further validated in 126 human blood specimens from a Chinese population. The four-gene set can serve as biomarkers to improve clinical diagnosis and treatment response monitoring of TB.

## DATA AVAILABILITY STATEMENT

The datasets presented in this study can be found in online repositories. The names of the repository/repositories and accession number(s) can be found in the article/**Supplementary Material**.

## REFERENCES

- Akkaya, O., and Kurtoglu, M. G. (2019). Comparison of conventional and molecular methods used for diagnosis of mycobacterium tuberculosis in clinical samples. *Clin. Lab.* 65. doi: 10.7754/Clin.Lab.2019.190145
- Anderson, S. T., Myrsini, K., Brent, A. J., Wright, V. J., Banwell, C. M., George, C., et al. (2014). Diagnosis of childhood tuberculosis and host RNA expression in Africa. *N. Engl. J. Med.* 370, 1712–1723.
- Berry, M. P., Graham, C. M., McNab, F. W., Xu, Z., Bloch, S. A., Oni, T., et al. (2010). An interferon-inducible neutrophil-driven blood transcriptional

## ETHICS STATEMENT

The studies involving human participants were reviewed and approved by the study protocols were approved by the Institutional Review Board at the Hospital (K17-022). All participants provided written informed consent prior to participation in the study. The patients/participants provided their written informed consent to participate in this study.

## AUTHOR CONTRIBUTIONS

YG, XK, ZG, JN, and RZ performed the experiments. YG, LF, and JX analyzed the data. BS and LF diagnosed the patients and collected samples for all clinically related ethical approval. ZG, YG, LF, and JX designed the study and wrote the manuscript. All authors have read and approved the manuscript.

## FUNDING

This work was supported by the National Natural Science Foundation (grant numbers 82072246, 81871182, and 81371851), National Key R&D Plan (2016YFC0502304), and the National Megaprojects for Key Infectious Diseases (grant numbers 2008ZX10003-006, 2008ZX10003-001).

## SUPPLEMENTARY MATERIAL

The Supplementary Material for this article can be found online at: <https://www.frontiersin.org/articles/10.3389/fmicb.2021.650567/full#supplementary-material>

**Supplementary Table 1** | The 63 genes were found in the DEGs, WGCNA black module, and STEM profiles.

**Supplementary Table 2** | The transcription of the four genes in PTB, HC, TUMOR, and INFLA.

**Supplementary Image 1** | Different combinations of four genes showed different advantages in the diagnosis of active TB.

**Supplementary Image 2** | The transcription of the four genes decreased gradually with effective TB treatment in GSE40553, GSE56153 databases.

**Supplementary Image 3** | The protein-protein interaction network of the four genes constructed *via* STRING-DB database.

- signature in human tuberculosis. *Nature* 466, 973–977. doi: 10.1038/nature09247
- Bloom, C. I., Graham, C. M., Berry, M. P. R., Rozakeas, F., Redford, P. S., Wang, Y., et al. (2013). Transcriptional blood signatures distinguish pulmonary tuberculosis, pulmonary sarcoidosis, pneumonias and lung cancers. *PLoS One* 8:e70630. doi: 10.1371/journal.pone.0070630
- Bloom, C. I., Graham, C. M., Berry, M. P. R., Wilkinson, K. A., Tolu, O., Fotini, R., et al. (2012). Detectable changes in the blood transcriptome are present after two weeks of antituberculosis therapy. *PLoS One* 7:e46191. doi: 10.1371/journal.pone.0046191

- Cai, Y., Yang, Q., Tang, Y., Zhang, M., Liu, H., Zhang, G., et al. (2014). Increased complement C1q level marks active disease in human tuberculosis. *PLoS One* 9:e92340. doi: 10.1371/journal.pone.0092340
- Costa, L. L. D., Delcroix, M., Costa, E. R. D., Prestes, I. V., Milano, M., Francis, S. S., et al. (2015). A real-time PCR signature to discriminate between tuberculosis and other pulmonary diseases. *Tuberculosis* 95, 421–425. doi: 10.1016/j.tube.2015.04.008
- Denkinger, C. M., Kik, S. V., Cirillo, D. M., Casenghi, M., Shinnick, T., Weyer, K., et al. (2015). Defining the needs for next generation assays for tuberculosis. *J. Infect. Dis.* 211(Suppl. 2):S29.
- Haiqing, M., Xiaoting, L., Yibing, C., Ke, P., Jiancong, S., Hui, W., et al. (2011). Decreased expression of BATF2 is associated with a poor prognosis in hepatocellular carcinoma. *Int. J. Cancer* 128, 771–777. doi: 10.1002/ijc.25407
- Hong, W. (2005). SNAREs and traffic. *Biochim. Biophys. Acta* 1744, 120–144.
- Horwitz, J. K., Chun, N. H., and Heeger, P. S. (2019). Complement and transplantation: from new mechanisms to potential biomarkers and novel treatment strategies. *Clin. Lab. Med.* 39, 31–43. doi: 10.1016/j.cll.2018.10.004
- Ikezawa, M., Tajika, Y., Ueno, H., Murakami, T., Inoue, N., and Yorifuji, H. (2018). Loss of VAMP5 in mice results in duplication of the ureter and insufficient expansion of the lung. *Dev. Dyn.* 247, 754–762. doi: 10.1002/dvdy.24618
- Jiang, J., Yang, J., Shi, Y., Jin, Y., Tang, S., Zhang, N., et al. (2020). Head-to-head comparison of the diagnostic accuracy of Xpert MTB/RIF and Xpert MTB/RIF Ultra for tuberculosis: a meta-analysis. *Infect. Dis. (Lond.)* 52, 763–775. doi: 10.1080/23744235.2020.1788222
- Maertzdorf, J., McEwen, G., Weiner, J. III, Tian, S., Lader, E., Schriek, U., et al. (2016). Concise gene signature for point-of-care classification of tuberculosis. *EMBO Mol. Med.* 8, 86–95. doi: 10.15252/emmm.201505790
- Maertzdorf, J., Weiner, J., Mollenkopf, H.-J., Network, T., Bauer, T., Prasse, A., et al. (2012). Common patterns and disease-related signatures in tuberculosis and sarcoidosis. *Proc. Natl. Acad. Sci. U.S.A.* 109, 7853–7858. doi: 10.1073/pnas.1121072109
- Marc, T., Binita, D., Susan, D., Nicole, R., Benjamin, F., Kattia, C. B., et al. (2015). Mycobacteria-specific cytokine responses detect tuberculosis infection and distinguish latent from active tuberculosis. *Am. J. Respir. Crit. Care Med.* 192, 485–499. doi: 10.1164/rccm.201501-0059oc
- Murphy, T. L., Tussiwand, R., and Murphy, K. M. (2013). Specificity through cooperation: BATF-IRF interactions control immune-regulatory networks. *Nat. Rev. Immunol.* 13, 499–509. doi: 10.1038/nri3470
- Myrsini, K., Wright, V. J., Tolu, O., Neil, F., Anderson, S. T., Nonwakazi, B., et al. (2013). Detection of tuberculosis in HIV-infected and -uninfected African adults using whole blood RNA expression signatures: a case-control study. *PLoS Med.* 10:e1001538. doi: 10.1371/journal.pmed.1001538
- Ottenhoff, T. H., Dass, R. H., Yang, N., Zhang, M. M., Wong, H. E., Sahiratmadja, E., et al. (2012). Genome-wide expression profiling identifies type 1 interferon response pathways in active tuberculosis. *PLoS One* 7:e45839. doi: 10.1371/journal.pone.0045839
- Pai, M., and Schito, M. (2015). Tuberculosis diagnostics in 2015: landscape, priorities, needs, and prospects. *J. Infect. Dis.* 211, S21–S28.
- Qureshi, S., Sohaila, A., Hannan, S., Amir Sheikh, M. D., and Qamar, F. N. (2019). Comparison of Xpert MTB/RIF with AFB smear and AFB culture in suspected cases of paediatric tuberculosis in a tertiary care hospital, Karachi. *J. Pak. Med. Assoc.* 69, 1273–1278.
- Rangaka, M. X., Wilkinson, K. A., Glynn, J. R., Ling, D., Menzies, D., Mwansa-Kambafwile, J., et al. (2012). Predictive value of interferon- $\gamma$  release assays for incident active tuberculosis: a systematic review and meta-analysis. *Lancet Infect. Dis.* 12, 45–55. doi: 10.1016/s1473-3099(11)70210-9
- Roe, J., Venturini, C., Gupta, R., Gurry, C., and Noursadeghi, M. (2019). Blood transcriptomic stratification of short-term risk in contacts of tuberculosis. *Clin. Infect. Dis.* 70, 731–737.
- Skaug, B., and Chen, Z. J. (2010). Emerging role of ISG15 in antiviral immunity. *Cell* 143, 187–190. doi: 10.1016/j.cell.2010.09.033
- Steingart, K. R., Sohn, H., Schiller, I., Kloda, L. A., Boehme, C. C., Pai, M., et al. (2013). Xpert®; MTB/RIF assay for pulmonary tuberculosis and rifampicin resistance in adults. *Cochrane Database Syst. Rev.* 1:CD009593.
- Sugata, R., Reto, G., Parihar, S. P., Sebastian, S., Bogumil, K., Hajime, N., et al. (2015). Batf2/Irf1 induces inflammatory responses in classically activated macrophages, lipopolysaccharides, and mycobacterial infection. *J. Immunol.* 194, 6035–6044. doi: 10.4049/jimmunol.1402521
- Suliman, S., Thompson, E., Sutherland, J., Weiner, J. III, Ota, M. O. C., Shankar, S., et al. (2018). Four-gene pan-african blood signature predicts progression to tuberculosis. *Am. J. Respir. Crit. Med.* 197, 1198–1208. doi: 10.1164/rccm.201711-2340OC
- Sutherland, J. S., Loxton, A. G., Haks, M. C., Kassa, D., Ambrose, L., Lee, J. S., et al. (2014). Differential gene expression of activating Fc $\gamma$  receptor classifies active tuberculosis regardless of human immunodeficiency virus status or ethnicity. *Clin. Microbiol. Infect.* 20, O230–O238.
- Sweeney, T. E., Braviak, L., Tato, C. M., and Khatri, P. (2016). Genome-wide expression for diagnosis of pulmonary tuberculosis: a multicohort analysis. *Lancet Respir. Med.* 4, 213–224. doi: 10.1016/s2213-2600(16)00048-5
- Sweeney, T. E., and Khatri, P. (2016). Blood transcriptional signatures for tuberculosis diagnosis: a glass half-empty perspective—Authors' reply. *Lancet Respir. Med.* 4:e29. doi: 10.1016/S2213-2600(16)30039-X
- Szklarczyk, D., Morris, J. H., Cook, H., Kuhn, M., Wyder, S., Simonovic, M., et al. (2017). The STRING database in 2017: quality-controlled protein–protein association networks, made broadly accessible. *Nucleic Acids Res.* 45, D362–D368.
- Tajika, Y., Takahashi, M., Khairani, A. F., Ueno, H., Murakami, T., and Yorifuji, H. (2014). Vesicular transport system in myotubes: ultrastructural study and signposting with vesicle-associated membrane proteins. *Histochem. Cell Biol.* 141, 441–454. doi: 10.1007/s00418-013-1164-z
- Venkatraman, E. S. (2015). A permutation test to compare receiver operating characteristic curves. *Biometrics* 56, 1134–1138. doi: 10.1111/j.0006-341x.2000.01134.x
- Wallis, R. S., Pai, M., Menzies, D., Doherty, T. M., Walzl, G., Perkins, M. D., et al. (2010). Biomarkers and diagnostics for tuberculosis: progress, needs, and translation into practice. *Lancet* 375, 1920–1937. doi: 10.1016/s0140-6736(10)60359-5
- Walter, N. D., Reves, R., and Davis, J. L. (2016). Blood transcriptional signatures for tuberculosis diagnosis: a glass half-empty perspective. *Lancet Respir. Med.* 4:e28. doi: 10.1016/S2213-2600(16)30038-8
- WHO (2019). *Global Tuberculosis Report 2019*. Geneva: World Health Organisation.
- Wu, X., Tan, G., Gao, R., Yao, L., Bi, D., Guo, Y., et al. (2019). Assessment of the Xpert MTB/RIF Ultra assay on rapid diagnosis of extrapulmonary tuberculosis. *Int. J. Infect. Dis.* 81, 91–96. doi: 10.1016/j.ijid.2019.01.050
- Zak, D. E., Penn-Nicholson, A., Scriba, T. J., Thompson, E., Suliman, S., Amon, L. M., et al. (2016). A blood RNA signature for tuberculosis disease risk: a prospective cohort study. *Lancet* 387, 2312–2322. doi: 10.1016/s0140-6736(15)01316-1

**Conflict of Interest:** The authors declare that the research was conducted in the absence of any commercial or financial relationships that could be construed as a potential conflict of interest.

Copyright © 2021 Gong, Gu, Xiong, Niu, Zheng, Su, Fan and Xie. This is an open-access article distributed under the terms of the Creative Commons Attribution License (CC BY). The use, distribution or reproduction in other forums is permitted, provided the original author(s) and the copyright owner(s) are credited and that the original publication in this journal is cited, in accordance with accepted academic practice. No use, distribution or reproduction is permitted which does not comply with these terms.



# Monocyte and Macrophage miRNA: Potent Biomarker and Target for Host-Directed Therapy for Tuberculosis

Pavithra Sampath, Krisna Moorthi Periyasamy, Uma Devi Ranganathan and Ramalingam Bethunaickan\*

Department of Immunology, National Institute for Research in Tuberculosis, Chennai, India

## OPEN ACCESS

### Edited by:

Hazel Marguerite Dockrell,  
University of London, United Kingdom

### Reviewed by:

Roberta Olmo Pinheiro,  
Fundação Oswaldo Cruz (Fiocruz),  
Brazil

Carmen Judith Serrano,  
Mexican Social Security Institute  
(IMSS), Mexico

### \*Correspondence:

Ramalingam Bethunaickan  
bramalingam@gmail.com;  
ramalingam.b@nirt.res.in

### Specialty section:

This article was submitted to  
Microbial Immunology,  
a section of the journal  
Frontiers in Immunology

**Received:** 12 February 2021

**Accepted:** 11 May 2021

**Published:** 25 June 2021

### Citation:

Sampath P, Periyasamy KM, Ranganathan UD and Bethunaickan R (2021) Monocyte and Macrophage miRNA: Potent Biomarker and Target for Host-Directed Therapy for Tuberculosis. *Front. Immunol.* 12:667206. doi: 10.3389/fimmu.2021.667206

The end TB strategy reinforces the essentiality of readily accessible biomarkers for early tuberculosis diagnosis. Exploration of microRNA (miRNA) and pathway analysis opens an avenue for the discovery of possible therapeutic targets. miRNA is a small, non-coding oligonucleotide characterized by the mechanism of gene regulation, transcription, and immunomodulation. Studies on miRNA define their importance as an immune marker for active disease progression and as an immunomodulator for innate mechanisms, such as apoptosis and autophagy. Monocyte research is highly advancing toward TB pathogenesis and biomarker efficiency because of its innate and adaptive response connectivity. The combination of monocytes/macrophages and their relative miRNA expression furnish newer insight on the unresolved mechanism for Mycobacterium survival, exploitation of host defense, latent infection, and disease resistance. This review deals with miRNA from monocytes, their relative expression in different disease stages of TB, multiple gene regulating mechanisms in shaping immunity against tuberculosis, and their functionality as biomarker and host-mediated therapeutics. Future collaborative efforts involving multidisciplinary approach in various ethnic population with multiple factors (age, gender, mycobacterial strain, disease stage, other chronic lung infections, and inflammatory disease criteria) on these short miRNAs from body fluids and cells could predict the valuable miRNA biosignature network as a potent tool for biomarkers and host-directed therapy.

**Keywords:** monocyte and macrophage miRNAs, tuberculosis, differential expression, immune regulation, autophagy and biomarkers

## INTRODUCTION

Tuberculosis being the life-threatening disease caused by *Mycobacterium tuberculosis* (MTB) is intricate to understand their mycobacterial-mediated host immune subversion. The intracellular nature and delayed cell division of MTB added access to dodge the host microbicidal effect for its survival. The host's innate defense ability and the pathogen's strategy in evading the host's immunity determine the sequel of TB infection (1). MTB establishes infection through multiple modalities, such as i) circumvent phagolysosome fusion and phagocytosis destruction; ii) neutralize the acidic environment (2, 3); iii) blocks the formation of the apoptotic envelope (4); iv) inhibits the plasma membrane repair,



leading to the spread of infection through macrophage necrosis (5); v) suppresses activation of immune cells and antigen presentation; vi) limits the proinflammatory response by restricting proinflammatory cytokines; and vii) modulates the disease responsive genes and miRNAs through their targeted pathways. The disease becomes complex as the stages of infection are varied from latency to drug resistance because of the evolution of MTB strains. One third of the population exhibit latent infection, in which MTB remains dormant for a long period and becomes susceptible to the active disease under immune compromised condition. This latency is a menace to mankind as the diagnosis and its effective treatment toward breakdown of the disease in future need unbridled enthusiastic investigations. However, the management of the latent condition can be made possible with public awareness by improving the incidence of TB determinants, such as malnutrition, poverty, smoking, and diabetes, or through the development of new treatment or vaccines (6). The emergence of drug-resistant *Mycobacterium* due to poor treatment adherence (acquired resistance) and the transmission of drug-resistant strains (primary resistance) is another peril in TB research toward the end TB strategy (7). The multi-drug resistance and its treatment pose multiple challenges as it requires prolonged treatment duration, complex drugs (second-line fluoroquinolones) that may affect adherence along with lower treatment success rate (6). Other co-morbidities, like AIDS and diabetes, intensify TB disease pathogenesis.

Mononuclear cells (monocytes/macrophages) are professional phagocytic defenders against TB infection (8). The disputed behavior of monocytes as a defender against antimycobacterial activity exhibited by CD16<sup>neg</sup> subset and habitat for MTB promoted by CD16<sup>pos</sup> subset is well accepted for TB disease (9, 10). The disease-specific perturbation in the mononuclear cell subsets and their immune phenotypes contributed to underlying pathophysiology and as biomarkers for MTB infection. However, the unresolved mechanisms and the pathways affected can be studied through the molecular impression of these subsets from omics platforms in a quest for differentially expressed mRNAs and miRNAs. miRNAs are short, biologically conserved noncoding RNAs that participate in the regulation of inflammatory response, tumorigenesis, and other biological processes. Several studies focused on miRNAs revealed altered miRNA levels during infection and their impact in modulating immune functions within macrophages from TB patients (11–13). Thus, miRNA studies open up new avenues and fascinate the researchers for constructing miRNA-based vaccines, biomarkers, and host-directed therapies. This review is focused on monocyte/macrophage miRNAs, their differential expression, regulatory function, and biomarker utility in tuberculosis disease.

## miRNAs

Micro RNAs are discovered as biologically conserved, short noncoding RNAs (14–16) that constitute 18 to 25 nucleotides in length. This groundbreaking innovation by Ambros and Ruvkun prompted the researchers to investigate their functional behavior toward host immune regulation and disease pathogenesis,

which resulted in the exponential growth of published studies on miRNA reported by Almeida et al. (17).

miRNAs work as mRNA repressors inhibiting protein synthesis (18), translational activators (19), and molecular decoys for RNA-binding proteins (20), depending on the environment and cell type. The processing, maturation, expression, and action of miRNAs are regulated through multiple mechanisms: a) single-nucleotide polymorphism interfere with the processing and maturation of miRNAs that affect their expression profile (21); b) modulation of epigenetic mechanisms, such as histone acetylation and DNA methylation, influence the transcriptional rate of miRNAs (22); c) impairment in the mRNA-miRNA interactions by the competition of miRNAs with cellular factors and mRNAs with other competitive RNAs (pseudogenes, long non-coding RNAs, and circular RNAs) (23, 24); and d) occurrence of miRNA editing through nucleotide modification by adenosine or cytidine deaminases (21, 25). miRNA research and transcriptomic platform enabled the disease-mediated deregulation of miRNAs and their targeted pathways in multiple diseases, including cancer (26, 27), cardiovascular diseases (28, 29), autoimmune diseases (30, 31), and infectious diseases (32, 33).

## MONOCYTE AND MACROPHAGE miRNAs

The disease-oriented modification for any microbial infection is visualized primarily on monocytic cell lineage as being the first-line defenders of innate immunity. Immunological aspect-derived alterations in the subset composition of monocytes/macrophages decipher the role of a pathogen in the peripheral compartment. However, the stimulus for the alteration is better studied through their responsive mRNA and miRNAs. miRNA research for TB is advancing toward a proper understanding of disease mechanism for better prognosis and early prevention. The immune efficiency and other cellular processes of monocyte/macrophages are governed by various miRNAs in both healthy and disease states (34).

Many reports available for the miRNAs mediated monocytic biological functions, such as tissue homeostasis, signaling, cell differentiation, apoptosis, cell motility, cytokine production, inflammatory responses, resolution of inflammation, and other immune responses (35–40). A trio of miRNAs constituting miR-146a, miR-21, and miR-155 are the principal regulators of inflammatory pathways in myeloid cells (41). miR-511 was identified as the putative positive regulator of Toll-like receptor 4 during monocyte differentiation by Tserel et al. (42). miR-214, as suggested by Li et al., targets the phosphatase and tensin homolog in monocyte survival induction during advanced glycation (43). miR-20a, miR-106a, and miR-17 of miR-17/92 and miR-106a/363 clusters are involved in tuning the proinflammatory cytokine production, infiltration of macrophages, and phagocytosis through targeting the expression of signal-regulatory protein alpha (44). Upon Notch activation, miR-148a-3p promotes M1 polarization by hindering M2 activation (45). Myeloid cell differentiation to granulocytes or monocytes is governed by miR-223 with negative control on NLRP3 inflammasome activity (46).

The intense research on miRNA profiling of monocyte subsets delivered their unique profile and regulated functions. Dang et al. deciphered the role of miR-432 in apoptotic potential and miR-19a in cell motility. They also observed that miR-345 was involved in the inflammatory responses by targeting RelA. Besides, upregulated miR-34 in CD16+ monocytes are suggestive of their differentiation ability to dendritic cells by altering the expression of Wingless-Type MMTV Integration Site Family, Member 1 (WNT1), and Jagged 1 (JAG1) (34, 47). Richard et al. focused on the sequencing of miRNAs among monocyte subsets in humans and mice to identify their role in monocyte heterogeneity. From their work, they suggested three miRNAs—miR-21, miR-150, and miR-146a—as immune regulators that mediate resolution of inflammation in the myeloid cells (48). MicroRNA profiling of intermediate monocytes (CD14++ CD16+) yielded a unique miRNA profile, and their connected pathways are involved in gene regulation, TLR, and cytokine-mediated signaling, phagocytosis, antigen processing, and presentation, as well as lipid and triglyceride metabolism (49).

## MicroRNA AS A PROMINENT IMMUNE REGULATOR OF MACROPHAGE MECHANISMS DURING TB

miRNAs regulate about 60% of mammalian genes through its effective binding to 3' UTR on mRNA and leads to translational repression and mRNA degradation (50, 51). Most of the cellular

functions in humans are governed by single or multiple miRNAs. The emergence of miRNA research uncovered the possibility of pathogen (specially their cell wall components) induced alteration of miRNA levels (52). The altered miRNA profile could enhance the disease progression by modulation of the innate and adaptive responses through the hindrance of cell differentiation (53). The distinctive role of miRNA in the maintenance of immune homeostasis and activation of immune defense is largely studied (54). Upon MTB infection, several miRNAs modulate the host mechanism, either favoring the host or the pathogen. In most cases, the underlying causes for host immune evasion by the Mycobacterium are associated with miRNAs. The host signaling pathways, cytokine production, and killing machinery are adversely affected by miRNAs as represented in **Figure 1**.

## miRNAs IN SIGNALING PATHWAYS AND CYTOKINE PRODUCTION

The prime innate defense recognition starts with the Toll-like receptors (TLRs) upon induction with pathogen-associated molecular patterns (PAMPs). However, this initial priming is affected by multiple miRNAs during MTB infection. TLR/MyD88 activation and cytokine response are inhibited by miR-30a in MTB-infected THP-1 cells (55). TLR3 signaling is attenuated by miR-27a through targeting TICAM1 and c-Abl-BMP signaling (56). Survival of Mycobacterium is favored through the upregulation of miR-26a

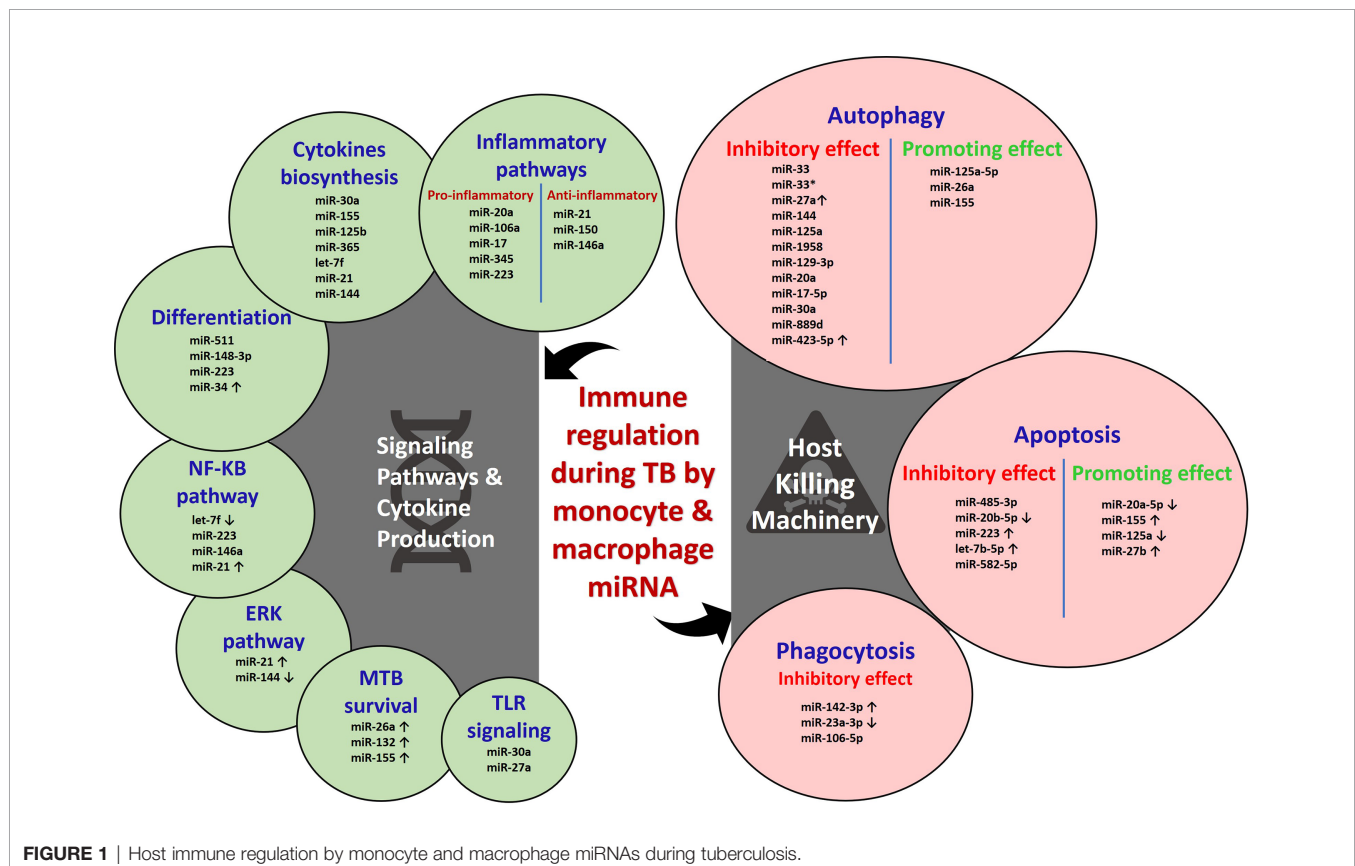


**FIGURE 1** | Host immune regulation by monocyte and macrophage miRNAs during tuberculosis.

and miR-132 induced by live and attenuated MTB that negatively controls p300 mRNA in human monocyte-derived macrophages (human MDMs). miR-132 and miR-26a dampen the host responsiveness toward IFN- $\gamma$  genes, phagocytosis process, and decreases the HLA-DR and FC $\gamma$ RI levels (57). Inhibition of NF- $\kappa$ B pathway with the hindered downstream secretion of cytokines, chemokines, and NOS is achieved through the increased expression of A20 (TNFAIP3) by downregulated let-7f induction mediated by ESAT-6 in both *in vitro* and *in vivo* conditions (58). miR-223 and miR-146a also negatively control the NF- $\kappa$ B pathway in MTB-infected macrophages and suppress the proinflammatory response and the clearance of pathogen (59–62). Infection with BCG induces elevation of miR-21 *via* NF- $\kappa$ B and ERK pathways that target IL-12p35 mRNA through which it inhibits IL-12 production and T-cell priming function by APCs (63).

The activity of miR-155 is focused on various cell types, such as macrophages, dendritic cells, and T cells. ESAT-6 induces miR-155 in a time- and dose-dependent manner, which downregulates SHIP1, leading to an ultimate increase of the AKT phosphorylation and, thus, exerts pro-survival of MTB on macrophages. Host IL-6 production and Cox-2 activity are limited by upregulated miR-155, as the Cox-2 is essential to prevent necrosis by generating PGE<sub>2</sub> and restricting lipoxin A<sub>4</sub> (LXA<sub>4</sub>) (1, 64). The mycobacterial component, such as Lipo Mannan from virulent MTB and *M. smeg*, induces a differential response in human MDMs. TB-LM induces higher miR-125b expression that targets the TNF mRNA and inhibits TNF biosynthesis through inhibition of TLR-2-mediated miR-155 expression, whereas *M. smeg* LM induces miR-155 expression and downregulates miR-125b and SHIP1, thereby increasing-PI3K/Akt signaling and TNF production followed by an enhanced proinflammatory response (50). The interpretation of the role of miR-155 in pro-inflammatory responses is quite contradictory as suggested by infection studies with virulent MTB and *M. smeg* LM (1, 50). This strongly reinforces the synchronized regulatory effect of miR-155 along with a host of miRNAs and, thus, cannot be studied alone (1). An inverse correlation was seen with miR-144 and TPL2 protein levels as the downregulation of miR-144 in MTB-infected human MDMs targets TPL2 mRNA, and their enhancement leads to activation of ERK1/2 phosphorylation and downstream IL-1 $\beta$ , IL-6, and TNF  $\alpha$  production (65). Pro-inflammatory cytokine response is suppressed through upregulated miR-32-5p targeting Follistatin-like protein (FSTL1) (66). Downregulation of miR-365 is inversely correlated with IL-6 levels in active TB patients (67).

## miRNAs IN HOST KILLING MACHINERY

The human host has an enormous killing machinery, like phagocytosis, apoptosis, and autophagy, and so on, for the invading pathogen. The intracellular MTB, however, exploits the host defense through various strategies. The recent transcriptomic approach sheds light on miRNA-based modulatory responses by Mycobacterium. The phagocytic function of macrophages is attenuated in the different stages by the Mycobacterium-induced miRNAs. The bacterial encounter and imbibe are affected through N-wasp by miR-142-3p. N-wasp is an actin-binding protein essential for actin dynamics in the

phagocytosis process that was negatively regulated by upregulated miR-142-3p in J774A.1 cell line and primary human macrophages during MTB infection (68). Mononuclear cell function and phagocytosis are inhibited in active TB patients, where miR-23a-3p is downregulated. miR-23a-3p targets IRF1/SP1 through TLR4/TNF- $\alpha$ /TGF- $\beta$ 1/IL-10 signaling (69). The principal lysosomal enzyme of phagocytosis process for MTB clearance is cathepsin proteases. miR-106-5p targets the 3' UTR cathepsin and suppresses the lysosomal activity in MTB-infected macrophages (70).

The downstream killing machinery of phagocytosed pathogen actively occurred through apoptosis of infected macrophages. Macrophages infected with Beijing strain demonstrate its virulence by escaping from host apoptosis and macrophage lysis through miR-485-3p (71). Upon infection with MTB, RAW264.7 macrophages establish attenuated apoptosis through the reduction of miR-20b-5p and elevation of its target Mcl-1 (72). Increased miR-223 expression in macrophages of active TB patients negatively suppresses forkhead box O3 (FOXO3) to inhibit apoptosis (62). The secreted protein MPT64 inhibits apoptosis of RAW264.7 macrophages *via* NF- $\kappa$ B/miR-21/Bcl-2 pathway (73). Inhibition of apoptosis through the downregulation of Fas protein is demonstrated in THP-1 macrophages mediated by upregulated let-7b-5p (74). The decrease in the apoptotic monocytes of active TB patients and decreased apoptosis in THP-1 cells are mediated through the downregulation of FOXO-1 by miR-582-5p (75). Some of the miRNAs positively promote apoptosis for enhanced mycobacterial clearance. For example, reduction of miR-20a-5p is observed in THP-1 macrophages and CD14+ monocytes of active TB patients. Reduced miR-20a-5p inversely increases Bim expression through its target JNK2, which could promote apoptosis (76). Infection of macrophages with *M. bovis* BCG results in elevated miR-155 expression, which could induce apoptosis through PKA signaling by inhibiting PKI- $\alpha$  (77). Sp110-mediated suppression of miR-125a in RAW264.7 macrophages enhances the expression of Bmf, which could induce apoptosis (78). Upregulated miR-27b enhances p53 signaling, thus favoring apoptosis and bacterial killing by downregulating Bag2 (79).

Autophagy is a highly regulated eukaryotic cellular pathway in which intracellular pathogens are trapped in autophagosomes and degraded in lysosomes. Induction of xenophagy (a selective form of autophagy against microbes) in monocyte-derived macrophages is one of the innate immune mechanisms to intracellular pathogens, such as MTB (80). However, MTB is a successful intracellular pathogen and can escape from host responses by expression of some of the miRNAs and affects autophagy machinery (81). Certain miRNAs control both mycobacterial survival and autophagy pathways by targeting their proteins within macrophages through its altered expression (82, 83). miRNA-33 and miRNA-33\* inhibit the fusion of lysosome with bacterial endosome by targeting ATG5, ATG12, LC3B, and LAMP proteins and lipid metabolism by targeting transcription factors FOXO3 and TFEB (84). The occurrence of active TB is suggested because of the suppression of autophagosome-lysosome fusion in macrophages by miR-423-5p



through post-transcriptional regulation of VPS33A (85). Active TB patients and MTB-infected mice abundantly express miR-27a, which blocks the  $\text{Ca}^{2+}$  signaling through ER-located  $\text{Ca}^{2+}$  transporter protein CACN2D. Blockade of  $\text{Ca}^{2+}$  signaling inhibits the formation of autophagosome (86). The autophagy protein, DRAM2, promotes PtdInt3K, which initiates the nucleation of autophagosome formation. In human and murine monocytes or macrophages, MIR144/hsa-miR-144 and miR-125a help in mycobacterial survival by forming a complex with the 3' UTR of DRAM2 mRNA (87, 88).

TB infection triggered the expression of a new type of miRNA, i.e., miR-1958, which silences the ATG5 in RAW264.7 cells (89). miR-129-3p favors MTB survival by inhibiting ATG4B (90). miR-20a promotes BCG survival by affecting the expression of both ATG7 and ATG16L1 (91). miR-17-5p blocks autophagy by blocking ULK1 in BCG-infected RAW264.7 cells (92). Chen et al. showed that miR-30a inhibits the autophagy pathway and negative correlation between Beclin and miR-30a (93). miR-889d affects the tumor necrosis factor-like weak inducer of apoptosis (TWEAK), which maintains the granuloma formation and promotes the maturation of AMPK (94). miR-125a-5p overexpression was observed in *M. avium*-infected THP1-derived macrophages and targets STAT-3, which activates the autophagy (95). At the same time, miR-26a targets the KLF4, by which it inhibits MTB survival, and miR-17/PKC $\delta$ /STAT3 pathways also attenuate MTB by activating autophagy (96).

According to Wang et al., miR-155 targets Rheb (autophagy blocker) and promotes autophagy (97). PCED1BAS1 is down-regulated in TB patients, which directly binds with miR-155, and subsequently inhibits the activity of miR-155 (98). miR-155 expression helps in the survival of MTB by regulating ATG3 protein in dendritic cells (99). Yang et al. found that the expression of miR-155 was diminished in patients with spinal tuberculosis-induced intervertebral disc destruction and affects its target MMP-11 expression (100).

## miRNAs AS BIOMARKERS

TB biomarker research is ongoing for decades as the disease still causes higher mortality due to multiple factors, such as host immune evasion by MTB, latency condition, drug resistance, and lack of prognostic and protective biomarkers. Many researchers have identified TB-specific-modulated cytokines and genes as biomarkers. However, those are not prominently emerging out since most of them are identified in smaller sample groups that lack sensitivity, differentiation ability, and reproducibility. The potent, robust, minimally invasive, rapid, universally acceptable biomarker is yet to be identified. Immune regulatory miRNAs emerge as a new class of disease-specific diagnostic markers (101, 102). The differential expression of miRNAs in disease phenomenon manifests their biomarker potential. To date, multiple studies are focused on miRNA sequencing from different samples involving PBMCs, serum/plasma, sputum, urine, and exosomes. The candidate biomarkers identified from circulation and PBMCs for discriminating TB from healthy are miR-144\* (103), miR155\* and miR155 (104); miR-93\*, miR-

3125, and miR-29a (105); miR-889, miR-576-3p, and miR-361-5p (106); miR-3179, miR-19b\*, and miR-147 (11); miR-146a (107); and miR-625-3p (108). A review by Pederson et al. gives a complete biomarker profile on circulating miRNAs (109). However, our focus is on the monocyte/macrophage-based markers since most miRNAs are involved in evading their immune defense. This will help to understand the underlying pathogenesis and for identifying TB-specific biomarkers. The differential expression of miRNAs from MTB infection studies on macrophages and the monocyte-derived macrophages are depicted in **Table 1** and **Figure 2**.

Although many studies are available on the macrophage infection-derived miRNAs, the actual *in vivo* scenario of a patient is minimal. The limitations of these biomarker candidates are variable between the studies, and each was performed on identifying the miRNA targets for understanding the disease pathology. In the future, the biomarker efficiency of these candidates should be largely examined as multi-centric studies with diverse ethnicities.

## miRNAs IN HOST-DIRECTED THERAPY (HDT)

Host-directed therapy is one of the emerging strategies to improve the host immunity and eliminate pathogens in which vitamins, repurposed drugs, cytokines, miRNAs, and monoclonal antibodies are used as an adjunct with chemotherapy. It helps to control challenges of TB treatments, such as drug resistance, the toxicity of chemotherapy, and immune reconstitute inflammatory syndrome, and so on (116). Induction of autophagy is one of the host-mediated therapy for tuberculosis (117) and is induced by mTOR kinase inhibitors and certain immunomodulators, such as rapamycin and vitamin D<sub>3</sub>, respectively (118, 119). The PubMed search on miRNAs in HDT for tuberculosis yielded no results. However, many HDT strategies using miRNAs have been proposed by Sabir et al. (96). They suggested direct administration of miRNAs or the use of siRNAs to modulate the host responses. The downregulated anti-mycobacterial miRNAs can be induced by synthetic oligos, and the overexpressed pro-mycobacterial miRNAs can be repressed using anti-miRNA complementary to mature miRNA (120–122). This approach will benefit the host in achieving the proper signaling and their downstream pro-inflammatory responses. Synthetic delivery of miRNAs to macrophages is possible with nanoparticles or liposomes (123, 124). Novel HDT approaches on miRNA-mediated induction of host killing machinery (phagocytosis, apoptosis, and autophagy) could be a beneficial therapy to evade the pathogen strategies and for efficient pathogen clearance.

## FUTURE PERSPECTIVES

The research of miRNA-mediated regulation of TB is enormous; however, the pro diagnosis and effective therapy for TB are



**TABLE 1 |** Monocyte/macrophage-based miRNAs as biomarker candidates for TB.

Cells	Differentially Expressed miRNAs	Analysis Platform	Reference
<b>Human</b>			
MDMs infected with MTB or BCG	miR-155, miR-146a, miR-145, miR-222, miR-27a, and miR-27b	Taqman low-density array	(110)
MDMs from TB patients, LTB, and Healthy individuals	TB vs HC: Upregulated (hsa-miR-16, hsa-miR-137, hsa-miR-140-3p, hsa-miR-193a-3p, hsa-miR-501-5p, and hsa-miR-598) Downregulated (hsa-miR-95) LTB vs TB: Upregulated (hsa-miR-101 and hsa-miR-150) Unique expression in LTB (miR-146b-3p and hsa-miR-296-5p)	Taqman microarray quantitative PCR	(71)
MDM infected with TB LM	miR-125-b	qPCR	(50)
MDM infected with <i>M. smeg</i> LM	miR-155		
MDM infected with MTB H37Rv	Upregulated (miR-155, miR-21, miR-146a, miR-29a, miR-26a, let-7b, miR-34, miR-132 & miR-138) Downregulated (miR-660, miR-144, miR-301b, miR-128, miR-423-3p, miR-410, miR-27a, miR-93, miR-107, miR-345, miR-221, miR-25, miR-23b, miR-361-5p, miR-130b & miR-340)	Nanostring nCounter miRNA assay	(65)
MDM infected with MTB	Upregulated (miR-132, miR-146-5p, miR-30e, let-7i, miR-490-3p, miR-29c, miR-26a, miR-21, let-7b & miR-29a) Downregulated (miR-25, miR-23b, miR-331-3p, miR-423-3p, miR-548f, miR-340, miR-24, miR-107, miR-93, miR-324-5p, miR-188-5p, miR-130b, miR-410, miR-361-5p, miR-197, miR-27a, miR-128, miR-345, miR-379, miR-133a & miR-221. Upregulated-miR-582-5p	Nanostring nCounter miRNA assay	(57)
Primary monocytes and MDMs from active TB patients and controls	Upregulated-miR-582-5p	qPCR	(75)
Primary macrophages from TB patients vs controls	Upregulated miR-223	qPCR	(62)
Macrophages from TB patients and controls	Downregulated miR-365	qPCR	(67)
MDM infected with MTB	Upregulated miR-106b-5p	qPCR	(70)
<b>Mouse</b>			
BMDMs infected with MTB	6 upregulated (miR-21, miR-21*, miR-146a, miR-146 b, miR210, and miR-155), 1 downregulated (miR-223)	Microarray and qPCR	(111)
BMDMs infected with Mtb	4 upregulated (miR-24, miR-142, miR-155, and miR-212) and 3 downregulated (miR-19a, miR-202, and miR-376a)	Gene expression microarray	(112)
BMDMs infected with BCG	miR-21	Taqman quantitative real-time PCR	(63)
BMDMs infected with MTB	Upregulated miR-27b	qPCR	(79)
BMDMs infected with MTB	3 upregulated (miR-155, miR-146a & miR-21)	Taqman low-density arrays	(1)
Mouse peritoneal macrophages & BMDMs	Upregulated miR-146a	qPCR	(60)
<b>Cell Line</b>			
U937 macrophages	149 DE (miR-424-5p, miR-493-5p, miR-27 b-3p, miR-296-5p, miR-377-5p, miR-3680-5p)	Microarray	(113)
THP-1 cells infected with Beijing/W or non-Beijing/W strains	13 downregulated (let-7e, let-7f, miR-10a, miR-21, miR-26a, miR-99a, miR-140-3p, miR-150, miR-181a, miR-320, miR-339-5p, miR-425, and miR-582-5p)	Taqman microarray quantitative PCR	(71)
THP-1 cells infected with virulent or avirulent Mtb strains	9 DE (miR-30a, miR-30e, miR-155, miR-1275, miR-3665, miR-3178, miR-4484, miR-4668-5p, and miR-4497)	Microarray	(114)
THP-1 cells infected with MTB HN878	12 upregulated (miR-33b*, miR-146a, miR-155, miR-132, miR-146b-5p, miR-720, miR-30e, miR-661, miR-140-3p, miR-3651, miR-328, and miR-378)		(115)
THP-1 cells and U937 cells	Upregulated miR-32-5p	qPCR	(66)
THP-1 cells	Upregulated miR-30a	qPCR	(55)
RAW264.7 cells and infected with MTB	3 upregulated (miR-155, miR-146a, and miR-21)	Taqman low-density arrays	(1)
RAW264.7 cells infected with MTB	Upregulated miR-27b	qPCR	(79)
RAW264.7 cells infected with MTB	Downregulated let-7f	SYBR Green-based miRNA profiling array	(58)
RAW264.7 cells	Downregulated miR-20b-5p	Semi quantitative PCR	(72)

lacking widely. As miRNAs are regulators and modulators of the immune response, the avenue for potential biomarkers and therapeutic possibilities are much promising. Some of the key factors to be considered for future research on miRNA are as follows:

1. Various circulating miRNAs are available from many studies as biomarkers but research on identifying cell-oriented miRNAs, particularly monocytes and macrophages will help better to understand the evasion of initial defense.

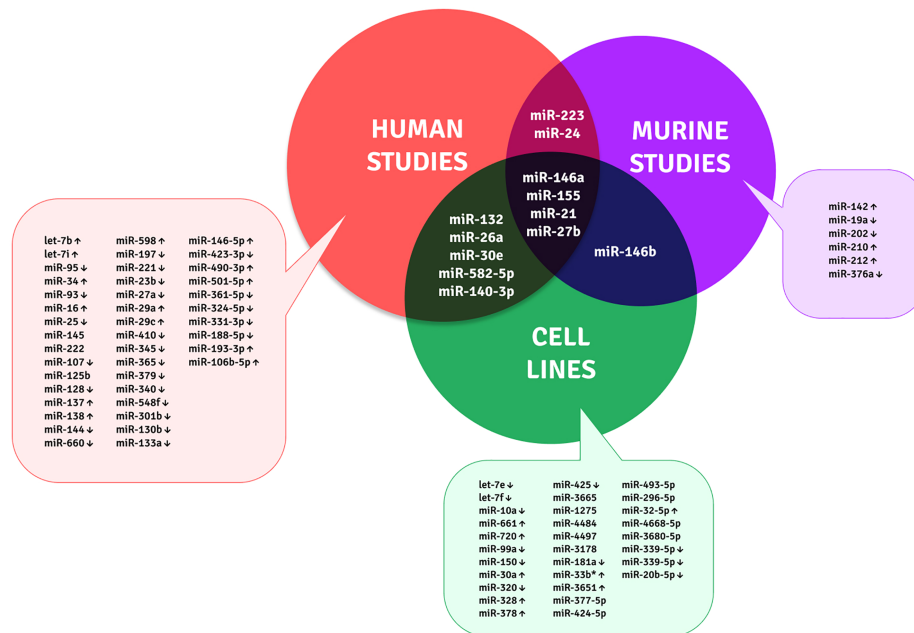


**FIGURE 2 |** Unique and shared miRNA biomarker candidates for TB within monocytes and macrophages across human, murine, and cell line studies.

- Research on identified miRNAs to investigate their diagnostic efficacy and therapeutic value is highly needed. This will help address whether this differential expression is really specific for TB or overlaps with a disease of similar pathology.
- The mycobacterial strain-specific miRNA expression is another concern since there is diversity in TB strains, and the distribution is different in different geographical locations.
- Deep single-cell sequencing approach may enable the complete miRNA profile for better understanding their biosignatures.
- Patient samples from all disease stages of TB at diagnosis and during treatment may give the disease-based profile during the entire course of infection for understanding their pathophysiology.
- Novel HDT approaches using nanoparticle and siRNAs for direct modulation of these expression signatures to induce the host-mediated defense responses against *Mycobacterium* will open up a better therapy adjunct with minimal chemotherapy.
- More animal studies with miRNA/long non-coding RNA intervention for TB therapeutics should be carried out and explored.

Future collaborative efforts involving multidisciplinary approach in various ethnic population with multiple factors (age, gender, mycobacterial strain, disease stage, other chronic lung infections, and inflammatory disease criteria) on these short miRNAs from body fluids and cells could predict the valuable miRNA biosignature network for biomarker discovery and host-directed therapy.

## AUTHOR CONTRIBUTIONS

PS and KP contributed to the literature collection, writing, drafting, and revision of the manuscript. PS, UR, and RB participated in the conception of the idea, design, drafting, revision, and approval of the manuscript. All authors contributed to the article and approved the submitted version.

## FUNDING

PS has been supported by the DST-INSPIRE fellowship. KP has been supported by the ICMR Fellowship. RB has been supported by the DBT Ramalingaswami Fellowship, Ministry of Science and Technology, Government of India.

## REFERENCES

- Kumar R, Halder P, Sahu SK, Kumar M, Kumari M, Jana K, et al. Identification of a Novel Role of ESAT-6-Dependent miR-155 Induction During Infection of Macrophages With *Mycobacterium Tuberculosis*. *Cell Microbiol* (2012) 14(10):1620–31. doi: 10.1111/j.1462-5822.2012.01827.x
- Flannagan RS, Cosío G, Grinstein S. Antimicrobial Mechanisms of Phagocytes and Bacterial Evasion Strategies. *Nat Rev Microbiol* (2009) 7:355–66. doi: 10.1038/nrmicro2128
- Meena LS, Rajni. Survival Mechanisms of Pathogenic *Mycobacterium Tuberculosis* H37Rv. *FEBS J* (2010) 277:2416–27. doi: 10.1111/j.1742-4658.2010.07666.x

4. Gan H, Lee J, Ren F, Chen M, Kornfeld H, Remold HG. *Mycobacterium Tuberculosis* Blocks Crosslinking of Annexin-1 and Apoptotic Envelope Formation on Infected Macrophages to Maintain Virulence. *Nat Immunol* (2008) 9:1189–97. doi: 10.1038/ni.1654PMID:18794848
5. Divangahi M, Chen M, Gan H, Desjardins D, Hickman TT, Lee DM, et al. *Mycobacterium Tuberculosis* Evades Macrophage Defenses by Inhibiting Plasma Membrane Repair. *Nat Immunol* (2009) 10:899–906. doi: 10.1038/ni.1758
6. Global Tuberculosis Report. Geneva: World Health Organization (2020).
7. Shah N, Wright A, Bai GH. Worldwide Emergence of Extensively Drug-Resistant Tuberculosis (XDR TB): Global Survey of Second-Line Drug Resistance Among *Mycobacterium Tuberculosis* Isolates. *Emerg Infect Dis* (2007) 13:380–7. doi: 10.3201/eid1303.061400
8. Sampath P, Moideen K, Ranganathan UD, Bethunaickan R. Monocyte Subsets: Phenotypes and Function in Tuberculosis Infection. *Front Immunol* (2018) 9:1726. doi: 10.3389/fimmu.2018.01726
9. Philips JA, Ernst JD. Tuberculosis Pathogenesis and Immunity. *Annu Rev Pathol* (2012) 7:353–84. doi: 10.1161/annurev-pathol-011811-132458
10. Balboa L, Barrios-Payan J, González-Domínguez E, Lastrucci C, Lugo-Villarino G, Mata-Espinoza D, et al. Diverging Biological Roles Among Human Monocyte Subsets in the Context of Tuberculosis Infection. *Clin Sci (Lond)* (2015) 129(4):319–30. doi: 10.1042/CS20150021
11. Yi Z, Fu Y, Ji R, Li R, Guan Z. Altered microRNA Signatures in Sputum of Patients With Active Pulmonary Tuberculosis. *PLoS One* (2012) 7(8):e43184. doi: 10.1371/journal.pone.0043184
12. Zhou L, Guo L, Tang J, Zhang A, Liu X, Xu G. miR-144 Regulates BCG- and Rapamycin-Induced Autophagy by Targeting Atg4a in RAW264.7 Cells. *Chin J Cell Mol Immunol* (2015) 31(2):163–7.
13. Kleinstaub K, Heesch K, Schattling S, Kohns M, Sander Julch C, Walz G, et al. Decreased Expression of miR-21, miR-26a, miR-29a, and miR-142-3p in CD4 (+) T Cells and Peripheral Blood From Tuberculosis Patients. *PLoS One* (2013) 8(4):e61609. doi: 10.1371/journal.pone.0061609
14. Lee RC, Feinbaum RL, Ambros V. The C. Elegans Heterochronic Gene lin-4 Encodes Small RNAs With Antisense Complementarity to lin-14. *Cell* (1993) 75:843–54. doi: 10.1016/0092-8674(93)90529-Y
15. Wightman B, Ha I, Ruvkun G. Post Transcriptional Regulation of the Heterochronic Gene lin-14 by lin-4 Mediates Temporal Pattern Formation in C. Elegans. *Cell* (1993) 75:855–62. doi: 10.1016/0092-8674(93)90530-4
16. O'Brien J, Hayder H, Zayed Y, Peng C. Overview of MicroRNA Biogenesis, Mechanisms of Actions, and Circulation. *Front Endocrinol* (2018) 9:402. doi: 10.3389/fendo.2018.00402
17. Almeida MI, Reis RM, Calin GA. MicroRNA History: Discovery, Recent Applications, and Next Frontiers. *Mutat Res* (2011) 717(1–2):1–8. doi: 10.1016/j.mrfmmm.2011.03.009
18. Guo H, Ingolia NT, Weissman JS, Bartel DP. Mammalian microRNAs Predominantly Act to Decrease Target mRNA Levels. *Nature* (2010) 466(7308):835–40. doi: 10.1038/nature09267
19. Vasudevan S, Tong Y, Steitz JA. Switching From Repression to Activation: microRNAs can Up-Regulate Translation. *Science* (2007) 318(5858):1931–4. doi: 10.1126/science.1149460
20. Eiring AM, Harb JG, Neviani P, Garton C, Oaks JJ, Spizzo R, et al. miR-328 Functions as an RNA Decoy to Modulate hnRNP E2 Regulation of mRNA Translation in Leukemic Blasts. *Cell* (2010) 140(5):652–65. doi: 10.1016/j.cell.2010.01.007
21. Correia de Sousa M, Gjorgjieva M, Dolicka D, Sobolewski C, Foti M. Deciphering Mirnas' Action Through miRNAs Editing. *Int J Mol Sci* (2019) 20(24):6249. doi: 10.3390/ijms20246249
22. Chuang JC, Jones PA. Epigenetics and microRNAs. *Pediatr Res* (2007) 61(5 Pt 2):24R–9R. doi: 10.1203/pdr.0b013e3180457684
23. Sobolewski C, Calo N, Portius D, Foti M. MicroRNAs in Fatty Liver Disease. *Semin Liver Dis* (2015) Feb35(1):12–25. doi: 10.1055/s-0034-1397345
24. Gjorgjieva M, Sobolewski C, Dolicka D, Correia de Sousa M, Foti M. miRNAs and NAFLD: From Pathophysiology to Therapy. *Gut* (2019) Nov68(11):2065–79. doi: 10.1136/gutjnl-2018-318146
25. Blanc V, Davidson NO. APOBEC-1-Mediated RNA Editing. *Wiley Interdiscip Rev Syst Biol Med* (2010) 2(5):594–602. doi: 10.1002/wsbm.82
26. Li C, Feng Y, Coukos G, Zhang L. Therapeutic microRNA Strategies in Human Cancer. *AAPS J* (2009) 11(4):747–57. doi: 10.1208/s12248-009-9145-9
27. Calin GA, Sevignani C, Dumitru CD, Hyslop T, Noch E, Yendamuri S, et al. Human microRNA Genes Are Frequently Located at Fragile Sites and Genomic Regions Involved in Cancers. *Proc Natl Acad Sci USA* (2004) 101(9):2999–3004. doi: 10.1073/pnas.0307323101
28. van Rooij E, Sutherland LB, Liu N, Williams AH, McAnally J, Gerard RD, et al. A Signature Pattern of Stress-Responsive microRNAs That Can Evoke Cardiac Hypertrophy and Heart Failure. *Proc Natl Acad Sci USA* (2006) 103(48):18255–60. doi: 10.1073/pnas.0608791103
29. Edwards JK, Pasqualini R, Arap W, Calin GA. MicroRNAs and Ultraconserved Genes as Diagnostic Markers and Therapeutic Targets in Cancer and Cardiovascular Diseases. *J Cardiovasc Transl Res* (2010) 3(3):271–9. doi: 10.1007/s12265-010-9179-5
30. Stanczyk J, Pedrioli DM, Brentano F, Sanchez-Pernaute O, Kolling C, Gay RE, et al. Altered Expression of MicroRNA in Synovial Fibroblasts and Synovial Tissue in Rheumatoid Arthritis. *Arthritis Rheumatol* (2008) 58(4):1001–9. doi: 10.1002/art.23386
31. Dai Y, Huang YS, Tang M, Lv TY, Hu CX, Tan YH, et al. Microarray Analysis of microRNA Expression in Peripheral Blood Cells of Systemic Lupus Erythematosus Patients. *Lupus* (2007) 16(12):939–46. doi: 10.1177/0961203307084158
32. Acuña SM, Floeter-Winter LM, Muxel SM. MicroRNAs: Biological Regulators in Pathogen-Host Interactions. *Cells* (2020) 9(1):113. doi: 10.3390/cells9010113
33. Yang T, Ge B. miRNAs in Immune Responses to *Mycobacterium Tuberculosis* Infection. *Cancer Lett* (2018) 431:22–30. doi: 10.1016/j.canlet.2018.05.028
34. Dang TM, Wong WC, Ong SM, Li P, Lum J, Chen J, et al. MicroRNA Expression Profiling of Human Blood Monocyte Subsets Highlights Functional Differences. *Immunology* (2015) 145(3):404–16. doi: 10.1111/imm.12456
35. Self-Fordham JB, Naqvi AR, Uttamani JR, Kulkarni V, Nares S. MicroRNA, Dynamic Regulators of Macrophage Polarization and Plasticity. *Front Immunol* (2017) 8:1062. doi: 10.3389/fimmu.2017.01062
36. O'Connell RM, Rao DS, Baltimore D. microRNA Regulation of Inflammatory Responses. *Annu Rev Immunol* (2012) 30:295–312. doi: 10.1146/annurev-immunol-020711-075013
37. Nahid MA, Pauley KM, Satoh M, Chan EKL. miR-146a Is Critical for Endotoxin-Induced Tolerance: Implication in Innate Immunity. *J Biol Chem* (2009) 284:34590–9. doi: 10.1074/jbc.M109.056317
38. Bazzoni F, Rossato M, Fabbri M, Gaudiosi D, Mirolo M, Mori L, et al. Induction and Regulatory Function of miR-9 in Human Monocytes and Neutrophils Exposed to Proinflammatory Signals. *Proc Natl Acad Sci USA* (2009) 106:5282–7. doi: 10.1073/pnas.0810909106
39. Bala S, Tilahun Y, Taha O, Alao H, Kodys K, Catalano D, et al. Increased microRNA-155 Expression in the Serum and Peripheral Monocytes in Chronic HCV Infection. *J Transl Med* (2012) 10:151. doi: 10.1186/1479-5876-10-151
40. Huang HC, Yu HR, Huang LT, Huang HC, Chen RF, Lin IC, et al. miRNA-125b Regulates TNF- $\alpha$  Production in CD14+ Neonatal Monocytes Via Post-Transcriptional Regulation. *J Leukoc Biol* (2012) 92:171–82. doi: 10.1189/jlb.1211593
41. Quinn SR, O'Neill LA. A Trio of microRNAs That Control Toll-Like Receptor Signaling. *Int Immunol* (2011) 23:421–5. doi: 10.1093/intimm/dxr034
42. Tserel L, Runnel T, Kisand K, Pihlap M, Bakhoff L, Kolde R, et al. MicroRNA Expression Profiles of Human Blood Monocyte-Derived Dendritic Cells and Macrophages Reveal miR-511 as Putative Positive Regulator of Toll-Like Receptor 4. *J Biol Chem* (2011) 286:26487–95. doi: 10.1074/jbc.M110.213561
43. Li L-M, Hou DX, Guo YL, Yang JW, Liu Y, Zhang CY, et al. Role of microRNA-214-Targeting Phosphatase and Tensin Homolog in Advanced Glycation End Product-Induced Apoptosis Delay in Monocytes. *J Immunol* (2011) 186:2552–60. doi: 10.4049/jimmunol.1001633
44. Zhu D, Pan C, Li L, Bian Z, Lv Z, Shi L, et al. MicroRNA-17/20a/106a Modulate Macrophage Inflammatory Responses Through Targeting Signal-Regulatory Protein  $\alpha$ . *J Allergy Clin Immunol* (2013) 132:426–36.e8. doi: 10.1016/j.jaci.2013.02.005
45. Huang F, Zhao JL, Wang L, Gao CC, Liang SQ, An DJ, et al. miR-148a-3p Mediates Notch Signaling to Promote the Differentiation and M1 Activation

- of Macrophages. *Front Immunol* (2017) 8:1327. doi: 10.3389/fimmu.2017.01327
46. Haneklaus M, Gerlic M, O'Neill LA, Masters SL. miR-223: Infection, Inflammation and Cancer. *J Intern Med* (2013) 274:215–26. doi: 10.1111/joim.12099
  47. Hashimi ST, Fulcher JA, Chang MH, Gov L, Wang S, Lee B, et al. MicroRNA Profiling Identifies miR-34a and miR-21 and Their Target Genes JAG1 and WNT1 in the Coordinate Regulation of Dendritic Cell Differentiation. *Blood* (2009) 114:404–14. doi: 10.1182/blood-2008-09-179150
  48. Duroux-Richard I, Robin M, Peillex C, Apparailly F. MicroRNAs: Fine Tuners of Monocyte Heterogeneity. *Front Immunol* (2019) 10:2145. doi: 10.3389/fimmu.2019.02145
  49. Zawada AM, Zhang L, Emrich IE, Rogacev KS, Krezdorn N, Rotter B, et al. MicroRNA Profiling of Human Intermediate Monocytes. *Immunobiology* (2017) 222(3):587–96. doi: 10.1016/j.imbio.2016.11.006
  50. Rajaram MV, Ni B, Morris JD, Brooks MN, Carlson TK, Bakthavachalu B, et al. Mycobacterium Tuberculosis Lipomannan Blocks TNF Biosynthesis by Regulating Macrophage MAPK-Activated Protein Kinase 2 (MK2) and microRNA miR-125b. *Proc Natl Acad Sci USA* (2011) 108(42):17408–13. doi: 10.1073/pnas.1112660108
  51. Taganov KD, Boldin MP, Chang KJ, Baltimore D. NF- $\kappa$ B-Dependent Induction of microRNA miR-146, an Inhibitor Targeted to Signaling Proteins of Innate Immune Responses. *Proc Natl Acad Sci USA* (2006) 103:12481–6. doi: 10.1073/pnas.0605298103
  52. Moschos SA, Williams AE, Perry MM, Birrell MA, Belvisi MG, Lindsay MA. Expression Profiling *In Vivo* Demonstrates Rapid Changes in Lung microRNA Levels Following Lipopolysaccharide-Induced Inflammation But Not in the Anti-Inflammatory Action of Glucocorticoids. *BMC Genomics* (2007) 240:1–12. doi: 10.1186/1471-2164-8-240
  53. Baltimore D, Boldin MP, O'Connell RM, Rao DS, Taganov KD. MicroRNAs: New Regulators of Immune Cell Development and Function. *Nat Immunol* (2008) 9:839–45. doi: 10.1038/nri.209PMID:18645592
  54. O'Connell RM, Rao DS, Chaudhuri AA, Baltimore D. Physiological and Pathological Roles for Micro-RNAs in the Immune System. *Nat Rev Immunol* (2010) 10(2):111–22. doi: 10.1038/nri2708
  55. Wu Y, Sun Q, Dai L. Immune Regulation of miR-30 on the Mycobacterium Tu- Berculosis-Induced TLR/MyD88 Signaling Pathway in THP-1 Cells. *Exp Ther Med* (2017) 14:3299–303. doi: 10.3892/etm.2017.4872
  56. Mahadik K, Prakhkar P, Rajmani RS, Singh A, Balaji KN. c-Abl-TWIST1 Epi-Genetically Dysregulate Inflammatory Responses During Mycobacterial Infection by Co-Regulating Bone Morphogenesis Protein and miR27a. *Front Immunol* (2018) 9:85. doi: 10.3389/fimmu.2018.00085
  57. Ni B, Rajaram MV, Lafuse WP, Landes MB, Schlesinger LS. Mycobacterium Tuberculosis Decreases Human Macrophage IFN- $\gamma$  Responsiveness Through miR-132 and miR-26a. *J Immunol* (2014) 193(9):4537–47. doi: 10.4049/jimmunol.1400124
  58. Kumar M, Sahu SK, Kumar R, Subuddhi A, Maji RK, Jana K, et al. MicroRNA Let-7 Modulates the Immune Response to Mycobacterium Tuberculosis Infection Via Control of A20, an Inhibitor of the NF- $\kappa$ B Pathway. *Cell Host Microbe* (2015) 17(3):345–56. doi: 10.1016/j.chom.2015.01.007
  59. Saba R, Sorensen DL, Booth SA. MicroRNA-146a: A Dominant, Negative Regulator of the Innate Immune Response, *Front. Immunol* (2014) 5:578. doi: 10.3389/fimmu.2014.00578
  60. Li S, Yue Y, Xu W, Xiong S. MicroRNA-146a Represses Mycobacteria-Induced Inflammatory Response and Facilitates Bacterial Replication Via Targeting IRAK-1 and TRAF-6. *PLoS One* (2013) 8:e81438. doi: 10.1371/journal.pone.0081438
  61. Liu, Wang R, Jiang J, Yang B, Cao Z, Cheng X. miR-223 Is Upregulated in Monocytes From Patients With Tuberculosis and Regulates Function of Monocyte-Derived Macrophages. *Mol Immunol* (2015) 67:475–81. doi: 10.1016/j.molimm.2015.08.006
  62. Xi X, Zhang C, Han W, Zhao H, Zhang H, Jiao J. MicroRNA-223 Is Upregulated in Active Tuberculosis Patients and Inhibits Apoptosis of Macrophages by Targeting FOXO3. *Genet. Test Mol Biomarkers* (2015) 19:650–6. doi: 10.1089/gtmb.2015.0090
  63. Wu Z, Lu H, Sheng J, Li L. Inductive microRNA-21 Impairs Anti-Mycobacterial Responses by Targeting IL-12 and Bcl-2. *FEBS Lett* (2012) 586(16):2459–67. doi: 10.1016/j.febslet.2012.06.004
  64. Chen M, Divangahi M, Gan H, Shin DSJ, Hong S, Lee DM, et al. Lipid Mediators in Innate Immunity Against Tuberculosis: Opposing Roles of PGE2 and LXA4 in the Induction of Macrophage Death. *J Exp Med* (2008) 205:2791–2801. doi: 10.1084/jem.20080767
  65. Liu HY. Down-Regulation of miR-144 After Mycobacterium Tuberculosis Infection Promotes Inflammatory Factor Secretion From Macrophages Through the Tpl2/ERK Pathway. *Cell Mol Biol (Noisy-le-grand)* (2016) 62(2):87–93.
  66. Zhang ZM, Zhang AR, Xu M, Lou J, Qiu WQ. TLR-4/miRNA-32-5p/FSTL1 Signaling Regulates Mycobacterial Survival and Inflammatory Responses in Mycobacterium Tuberculosis-Infected Macrophages. *Exp Cell Res* (2017) 352:313–21. doi: 10.1016/j.yexcr.2017.02.025
  67. Song Q, Li H, Shao H, Li C, Lu X. MicroRNA-365 in Macrophages Regulates Mycobacterium Tuberculosis-Induced Active Pulmonary Tuberculosis Via Interleukin-6. *Int J Clin Exp Med* (2015) 8:15458–65.
  68. Bettencourt P, Marion S, Pires D, Santos LF, Lastrucci C, Carmo N, et al. Actin-Binding Protein Regulation by microRNAs as a Novel Microbial Strategy to Modulate Phagocytosis by Host Cells: The Case of N-Wasp and miR-142-3p. *Front Cell Infect Microbiol* (2013) 3:19. doi: 10.3389/fcimb.2013.00019
  69. Chen YC, Lee CP, Hsiao CC, Hsu PY, Wang TY, Wu CC, et al. MicroRNA-23a-3p Down-Regulation in Active Pulmonary Tuberculosis Patients With High Bacterial Burden Inhibits Mononuclear Cell Function and Phagocytosis Through TLR4/TNF- $\alpha$ /TGF- $\beta$ 1/IL-10 Signaling Via Targeting IRF1/SP1. *Int J Mol Sci* (2020) 21(22):8587. doi: 10.3390/ijms21228587
  70. Pires D, Bernard EM, Pombo JP, Carmo N, Fialho C, Gutierrez MG, et al. Mycobacterium Tuberculosis Modulates miR-106b-5p to Control Cathepsin S Expression Resulting in Higher Pathogen Survival and Poor T-Cell Activation. *Front Immunol* (2017) 8:1819. doi: 10.3389/fimmu.2017.01819
  71. Zheng L, Leung E, Lee N, Lui G, To KF, Chan RC, et al. Differential MicroRNA Expression in Human Macrophages With Mycobacterium Tuberculosis Infection of Beijing/W and Non-Beijing/W Strain Types. *PLoS One* (2015) 10(6):e0126018. doi: 10.1371/journal.pone.0126018
  72. Zhang D, Yi Z, Fu Y. Downregulation of miR-20b-5p Facilitates Mycobacterium Tuberculosis Survival in RAW 264.7 Macrophages Via Attenuating the Cell Apoptosis by Mcl-1 Upregulation. *J Cell Biochem* (2019) 120(4):5889–96. doi: 10.1002/jcb.27874
  73. Wang Q, Liu S, Tang Y, Liu Q, Yao Y. MPT64 Protein From Mycobacterium Tuberculosis Inhibits Apoptosis of Macrophages Through NF- $\kappa$ B-miRNA21-Bcl-2 Pathway. *PLoS One* (2014) 9(7):e100949. doi: 10.1371/journal.pone.0100949
  74. Tripathi A, Srivastava V, Singh BN. hsa-let-7b-5p Facilitates Mycobacterium Tuberculosis Survival in THP-1 Human Macrophages by Fas Downregulation. *FEMS Microbiol Lett* (2018) 365(7). doi: 10.1093/femsle/fny040
  75. Liu Y, Jiang J, Wang X, Zhai F, Cheng X. miR-582-5p Is Upregulated in Patients With Active Tuberculosis and Inhibits Apoptosis of Monocytes by Targeting FOXO1. *PLoS One* (2013) 8(10):e78381. doi: 10.1371/journal.pone.0078381
  76. Zhang G, Liu X, Wang W, Cai Y, Li S, Chen Q, et al. Down-Regulation of miR-20a-5p Triggers Cell Apoptosis to Facilitate Mycobacterial Clearance Through Targeting JNK2 in Human Macrophages. *Cell Cycle* (2016) 15(18):2527–38. doi: 10.1080/15384101.2016.1215386
  77. Ghorpade DS, Leyland R, Kurowska-Stolarska M, Patil SA, Balaji KN. MicroRNA-155 Is Required for Mycobacterium Bovis BCG-Mediated Apoptosis of Macrophages. *Mol Cell Biol* (2012) 32(12):2239–53. doi: 10.1128/MCB.06597-11
  78. Wu Y, Guo Z, Yao K, Miao Y, Liang S, Liu F, et al. The Transcriptional Foundations of Sp110-Mediated Macrophage (RAW264.7) Resistance to Mycobacterium Tuberculosis H37Ra. *Sci Rep* (2016) 6:22041. doi: 10.1038/srep22041
  79. Liang S, Song Z, Wu Y, Gao Y, Gao M, Liu F, et al. MicroRNA-27b Modulates Inflammatory Response and Apoptosis During *Mycobacterium tuberculosis*



- Infection. *Infect J Immunol* (2018) 200(10):3506–18. doi: 10.4049/jimmunol.1701448
80. Siqueira MDS, Ribeiro RDM, Travassos LH. Autophagy and Its Interaction With Intracellular Bacterial Pathogens. *Front Immunol* (2018) 9:935. doi: 10.3389/fimmu.2018.00935
  81. Abdalla AE, Duan X, Deng W, Zeng J, Xie J. MicroRNAs Play Big Roles in Modulating Macrophages Response Toward Mycobacteria Infection. *Infect Genet Evol* (2016) 45:378–82. doi: 10.1016/j.meegid.2016.09.023
  82. Kim JK, Kim TS, Basu J, Jo EK. MicroRNA in Innate Immunity and Autophagy During Mycobacterial Infection. *Cell Microbiol* (2017) 19(1): e12687. doi: 10.1111/cmi.12687
  83. Zhao Y, Wang Z, Zhang W, Zhang L. MicroRNAs Play an Essential Role in Autophagy Regulation in Various Disease Phenotypes. *BioFactors* (2019) 45(6):844–56. doi: 10.1002/biof.1555
  84. Ouimet M, Koster S, Sakowski E, Ramkhalawon B, Van Solingen C, Oldebeken S, et al. Mycobacterium Tuberculosis Induces the miR-33 Locus to Reprogram Autophagy and Host Lipid Metabolism. *Nat Immunol* (2016) 17(6):677–86. doi: 10.1038/ni.3434
  85. Tu H, Yang S, Jiang T, Wei L, Shi L, Liu C, et al. Elevated Pulmonary Tuberculosis Biomarker miR-423-5p Plays Critical Role in the Occurrence of Active TB by Inhibiting Autophagosome-Lysosome Fusion. *Emerg Microbes Infect* (2019) 8(1):448–60. doi: 10.1080/22221751.2019.1590129
  86. Liu F, Chen J, Wang P, Li H, Zhou Y, Liu H, et al. MicroRNA-27a Controls the Intracellular Survival of Mycobacterium Tuberculosis by Regulating Calcium-Associated Autophagy. *Nat Commun* (2018) 9(1):1–14. doi: 10.1038/s41467-018-06836-4
  87. Kim JK, Yuk JM, Kim SY, Kim TS, Jin HS, Yang CS, et al. MicroRNA-125a Inhibits Autophagy Activation and Antimicrobial Responses During Mycobacterial Infection. *J Immunol* (2015) 194(11):5355–65. doi: 10.4049/jimmunol.1402557
  88. Kim JK, Lee HM, Park KS, Shin DM, Kim TS, Kim YS, et al. MIR144\* Inhibits Antimicrobial Responses Against Mycobacterium Tuberculosis in Human Monocytes and Macrophages by Targeting the Autophagy Protein DRAM2. *Autophagy* (2017) 13(2):423–41. doi: 10.1080/15548627.2016.1241922
  89. Ding S, Qu Y, Yang S, Zhao YE, Xu G. Novel miR-1958 Promotes Mycobacterium Tuberculosis Survival in RAW264. 7 Cells by Inhibiting Autophagy Via Atg5. *J Microbiol Biotechnol* (2019) 29(6):989–98. doi: 10.4014/jmb.1811.11062
  90. Qu Y, Ding S, Ma Z, Jiang D, Xu X, Zhang Y, et al. MiR-129-3p Favors Intracellular BCG Survival in RAW264. 7 Cells by Inhibiting Autophagy Via Atg4b. *Cell Immunol* (2019) 337:22–32. doi: 10.1016/j.cellimm.2019.01.004
  91. Guo L, Zhao J, Qu Y, Yin R, Gao Q, Ding S, et al. microRNA-20a Inhibits Autophagic Process by Targeting ATG7 and ATG16L1 and Favors Mycobacterial Survival in Macrophage Cells. *Front Cell Infect Microbiol* (2016) 6:134. doi: 10.3389/fcimb.2016.00134
  92. Duan X, Zhang T, Ding S, Wei J, Su C, Liu H, et al. microRNA-17-5p Modulates Bacille Calmette-Guerin Growth in RAW264. 7 Cells by Targeting ULK1. *PloS One* (2015) 10(9):e0138011. doi: 10.1371/journal.pone.0138011
  93. Chen Z, Wang T, Liu Z, Zhang G, Wang J, Feng S, et al. Inhibition of Autophagy by MiR-30A Induced by Mycobacteria Tuberculosis as a Possible Mechanism of Immune Escape in Human Macrophages. *Jpn J Infect Dis* (2015) 68(5):420–4. doi: 10.7883/yoken.JJID.2014.466
  94. Chen DY, Chen YM, Lin CF, Lo CM, Liu HJ, Liao TL. MicroRNA-889 Inhibits Autophagy to Maintain Mycobacterial Survival in Patients With Latent Tuberculosis Infection by Targeting TWEAK. *Mbio* (2020) 11(1): e03045–19. doi: 10.1128/mBio.03045-19
  95. Wang Y, Chen C, Xu XD, Li H, Cheng MH, Liu J, et al. Levels of miR-125a-5p Are Altered in Mycobacterium Avium-Infected Macrophages and Associate With the Triggering of an Autophagic Response. *Microbes Infect* (2020) 22(1):31–9. doi: 10.1016/j.micinf.2019.07.002
  96. Sabir N, Hussain T, Shah SZA, Peramo A, Zhao D, Zhou X. miRNAs in Tuberculosis: New Avenues for Diagnosis and Host-Directed Therapy. *Front Microbiol* (2018) 9:602. doi: 10.3389/fmicb.2018.00602
  97. Wang J, Yang K, Zhou L, Wu Y, Zhu M, Lai X, et al. MicroRNA-155 Promotes Autophagy to Eliminate Intracellular Mycobacteria by Targeting Rheb. *PloS Pathog* (2013) 9(10):e1003697. doi: 10.1371/journal.ppat.1003697
  98. Li M, Cui J, Niu W, Huang J, Feng T, Sun B, et al. Long non-Coding PCED1B-AS1 Regulates Macrophage Apoptosis and Autophagy by Sponging miR-155 in Active Tuberculosis. *Biochem Biophys Res Commun* (2019) 509(3):803–9. doi: 10.1016/j.bbrc.2019.01.005
  99. Etna MP, Sinigaglia A, Grassi A, Giacomini E, Romagnoli A, Pardini M, et al. Mycobacterium Tuberculosis-Induced miR-155 Subverts Autophagy by Targeting ATG3 in Human Dendritic Cells. *PloS Pathog* (2018) 14(1): e1006790. doi: 10.1371/journal.ppat.1003697
  100. Yang C, Shi Z, Hu J, Wei R, Yue G, Zhou D. miRNA-155 Expression and Role in Pathogenesis in Spinal Tuberculosis-Induced Intervertebral Disc Destruction. *Exp Ther Med* (2019) 17(4):3239–46. doi: 10.3892/etm.2019.7313
  101. Rodriguez A, Vigorito E, Clare S, Warren MV, Couttet P, Soond DR, et al. Requirement of bic/microRNA-155 for Normal Immune Function. *Science* (2007) 316:608–11. doi: 10.1126/science.1139253
  102. Jackson AL, Levin AA. Developing microRNA Therapeutics: Approaching the Unique Complexities. *Nucleic Acid Ther* (2012) 22:213–25. doi: 10.1089/nat.2012.0356PMID:22913594
  103. Liu Y, Wang X, Jiang J, Cao Z, Yang B, Cheng X. Modulation of T Cell Cytokine Production by miR-144\* With Elevated Expression in Patients With Pulmonary Tuberculosis. *Mol Immunol* (2011) 48:1084–90. doi: 10.1016/j.molimm.2011.02.001
  104. Wu J, Lu C, Diao N, Zhang S, Wang S, Wang F, et al. Analysis of microRNA Expression Profiling Identifies miR-155 and miR-155\* as Potential Diagnostic Markers for Active Tuberculosis: A Preliminary Study. *Hum Immunol* (2012) 73(1):31–7. doi: 10.1016/j.humimm.2011.10.003
  105. Fu Y, Yi Z, Wu X, Li J, Xu F. Circulating microRNAs in Patients With Active Pulmonary Tuberculosis. *J Clin Microbiol* (2011) 49:4246–51. doi: 10.1128/JCM.05459-11
  106. Qi Y, Cui L, Ge Y, Shi Z, Zhao K, Guo X, et al. Altered Serum microRNAs as Biomarkers for the Early Diagnosis of Pulmonary Tuberculosis Infection. *BMC Infect Dis* (2012) 12:384. doi: 10.1186/1471-2334-12384
  107. Spinelli SV, Diaz A, D'Attilio L, Marchesini MM, Bogue C, Bay ML, et al. Altered microRNA Expression Levels in Mononuclear Cells of Patients With Pulmonary and Pleural Tuberculosis and Their Relation With Components of the Immune Response. *Mol Immunol* (2013) 53:265–9. doi: 10.1016/j.molimm.2012.08.008
  108. Wang J, Zhu X, Xiong X, Ge P, Liu H, Ren N, et al. Identification of Potential Urine Proteins and microRNA Biomarkers for the Diagnosis of Pulmonary Tuberculosis Patients. *Emerg Microbes Infect* (2018) 7(1):63. doi: 10.1038/s41426-018-0066-5
  109. Pedersen JL, Bokil NJ, Saunders BM. Developing New TB Biomarkers, Are miRNA the Answer? *Tuberculosis (Edinb)* (2019) 118:101860. doi: 10.1016/j.tube.2019.101860
  110. Furci L, Schena E, Miotto P, Cirillo DM. Alteration of Human Macrophages microRNA Expression Profile Upon Infection With Mycobacterium Tuberculosis. *Int J Mycobacteriol* (2013) 2(3):128–34. doi: 10.1016/j.ijmyco.2013.04.006
  111. Iwai H, Funatogawa K, Matsumura K, Kato-Miyazawa M, Kirikae F, Kiga K, et al. MicroRNA-155 Knockout Mice Are Susceptible to Mycobacterium Tuberculosis Infection. *Tuberculosis (Edinb)* (2015) 95(3):246–50. doi: 10.1016/j.tube.2015.03.006
  112. Rothchild AC, Sissons JR, Shafiani S, Plaisier C, Min D, Mai D, et al. MiR-155-Regulated Molecular Network Orchestrates Cell Fate in the Innate and Adaptive Immune Response to Mycobacterium Tuberculosis. *Proc Natl Acad Sci USA* (2016) 113(41):E6172–81. doi: 10.1073/pnas.1608255113
  113. Meng QL, Liu F, Yang XY, Liu XM, Zhang X, Zhang C, et al. Identification of Latent Tuberculosis Infection-Related microRNAs in Human U937 Macrophages Expressing Mycobacterium Tuberculosis Hsp16.3. *BMC Microbiol* (2014) 14:37. doi: 10.1186/1471-2180-14-37
  114. Das K, Saikolappan S, Dhandayuthapani S. Differential Expression of miRNAs by Macrophages Infected With Virulent and Avirulent Mycobacterium Tuberculosis. *Tuberculosis* (2013) 93(Suppl):S47–50. doi: 10.1016/S1472-9792(13)70010-6
  115. Walter ND, Bemis L, Edwards M, Ovrrtsky A, Ramamoorthy P, Bai X, et al. Differential Expression of MicroRNA in Mycobacterium Tuberculosis-Infected Human Macrophages. *Am J Respir Crit Care Med* (2012) 185:A1011. doi: 10.1164/ajrcm-conference.2012.185.1\_MeetingAbstracts.A1011

116. Palucci I, Delogu G. Host Directed Therapies for Tuberculosis: Futures Strategies for an Ancient Disease. *Chemotherapy* (2018) 63(3):172–80. doi: 10.1159/000490478
117. Paik S, Kim JK, Chung C, Jo EK. Autophagy: A New Strategy for Host-Directed Therapy of Tuberculosis. *Virulence* (2019) 10(1):448–59. doi: 10.1080/21505594.2018.1536598
118. Bento CF, Empadinhas N, Mendes V. Autophagy in the Fight Against Tuberculosis. *DNA Cell Biol* (2015) 34(4):228–42. doi: 10.1089/dna.2014.2745
119. Periyasamy KM, Ranganathan UD, Tripathy SP, Bethunaickan R. Vitamin D–A Host Directed Autophagy Mediated Therapy for Tuberculosis. *Mol Immunol* (2020) 127:238–44. doi: 10.1016/j.molimm.2020.08.007
120. Meister G, Landthaler M, Dorsett Y, Tuschl T. Sequence-Specific Inhibition of microRNA- and siRNA-Induced RNA Silencing. *RNA* (2004) 10:544–50. doi: 10.1261/rna.5235104
121. Grimm D, Streetz KL, Jopling CL, Storm TA, Pandey K, Davis CR, et al. Fatality in Mice Due to Oversaturation of Cellular microRNA/Short Hairpin RNA Pathways. *Nature* (2006) 7092:537–41. doi: 10.1038/nature04791
122. Baumann V, Winkler J. MiRNA-based Therapies: Strategies and Delivery Platforms for Oligonucleotide and Non-Oligonucleotide Agents. *Future Med Chem* (2014) 17:1967–84. doi: 10.4155/fmc.14.116
123. Duan W, Yang T, Zhou SF, Wang ZL, Zhou ZW, He ZX. Novel Targeting of PEGylated Liposomes for Codelivery of TGF-Beta1 siRNA and Four Antitubercular Drugs to Human Macrophages for the Treatment of Mycobacterial Infection: A Quantitative Proteomic Study. *Drug Des Dev Ther* (2015) 9:4441–70. doi: 10.2147/DDDT.S79369
124. Moore LB, Sawyer AJ, Saucier-Sawyer J, Saltzman WM, Kyriakides TR. Nanoparticle Delivery of miR-223 to Attenuate Macrophage Fusion. *Biomaterials* (2016) 89:127–35. doi: 10.1016/j.biomaterials.2016.02.036

**Conflict of Interest:** The authors declare that the research was conducted in the absence of any commercial or financial relationships that could be construed as a potential conflict of interest.

Copyright © 2021 Sampath, Periyasamy, Ranganathan and Bethunaickan. This is an open-access article distributed under the terms of the Creative Commons Attribution License (CC BY). The use, distribution or reproduction in other forums is permitted, provided the original author(s) and the copyright owner(s) are credited and that the original publication in this journal is cited, in accordance with accepted academic practice. No use, distribution or reproduction is permitted which does not comply with these terms.



# Lymphocyte-Related Immunological Indicators for Stratifying *Mycobacterium tuberculosis* Infection

## OPEN ACCESS

### Edited by:

Hazel Marguerite Dockrell,  
London School of Hygiene and  
Tropical Medicine, United Kingdom

### Reviewed by:

Marc Jacobsen,  
Heinrich Heine University of  
Düsseldorf, Germany  
Jiezuan Yang,  
Zhejiang University, China

### \*Correspondence:

Zhongju Chen  
hailong1228@163.com  
Yaowu Zhu  
yaowu\_zhu@163.com  
Weiyong Liu  
weiyongliu@gmail.com  
Shiji Wu  
wilson547@163.com  
Feng Wang  
fengwang@tjh.tjmu.edu.cn  
Ziyong Sun  
zysun@tjh.tjmu.edu.cn  
Ying Luo  
13349917282@163.com

### Specialty section:

This article was submitted to  
Microbial Immunology,  
a section of the journal  
Frontiers in Immunology

**Received:** 26 January 2021

**Accepted:** 10 June 2021

**Published:** 30 June 2021

### Citation:

Luo Y, Xue Y, Tang G, Cai Y, Yuan X,  
Lin Q, Song H, Liu W, Mao L, Zhou Y,  
Chen Z, Zhu Y, Liu W, Wu S, Wang F  
and Sun Z (2021) Lymphocyte-  
Related Immunological Indicators  
for Stratifying *Mycobacterium*  
*tuberculosis* Infection.  
Front. Immunol. 12:658843.  
doi: 10.3389/fimmu.2021.658843

Ying Luo<sup>1\*</sup>, Ying Xue<sup>2</sup>, Guoxing Tang<sup>1</sup>, Yimin Cai<sup>3</sup>, Xu Yuan<sup>1</sup>, Qun Lin<sup>1</sup>, Huijuan Song<sup>1</sup>,  
Wei Liu<sup>1</sup>, Liyan Mao<sup>1</sup>, Yu Zhou<sup>4</sup>, Zhongju Chen<sup>1\*</sup>, Yaowu Zhu<sup>1\*</sup>, Weiyong Liu<sup>1\*</sup>,  
Shiji Wu<sup>1\*</sup>, Feng Wang<sup>1\*</sup> and Ziyong Sun<sup>1\*</sup>

<sup>1</sup> Department of Laboratory Medicine, Tongji Hospital, Tongji Medical College, Huazhong University of Science and Technology, Wuhan, China, <sup>2</sup> Department of Immunology, School of Basic Medicine, Tongji Medical College, Huazhong University of Science and Technology, Wuhan, China, <sup>3</sup> Department of Epidemiology and Biostatistics, Key Laboratory of Environmental Health of Ministry of Education, School of Public Health, Tongji Medical College, Huazhong University of Science and Technology, Wuhan, China, <sup>4</sup> Department of Laboratory Medicine, Zhejiang Provincial People's Hospital, People's Hospital of Hangzhou Medical College, Hangzhou, China

**Background:** Easily accessible tools that reliably stratify *Mycobacterium tuberculosis* (MTB) infection are needed to facilitate the improvement of clinical management. The current study attempts to reveal lymphocyte-related immune characteristics of active tuberculosis (ATB) patients and establish immunodiagnostic model for discriminating ATB from latent tuberculosis infection (LTBI) and healthy controls (HC).

**Methods:** A total of 171 subjects consisted of 54 ATB, 57 LTBI, and 60 HC were consecutively recruited at Tongji hospital from January 2019 to January 2021. All participants were tested for lymphocyte subsets, phenotype, and function. Other examination including T-SPOT and microbiological detection for MTB were performed simultaneously.

**Results:** Compared with LTBI and HC, ATB patients exhibited significantly lower number and function of lymphocytes including CD4<sup>+</sup> T cells, CD8<sup>+</sup> T cells and NK cells, and significantly higher T cell activation represented by HLA-DR and proportion of immunosuppressive cells represented by Treg. An immunodiagnostic model based on the combination of NK cell number, HLA-DR<sup>+</sup>CD3<sup>+</sup> T cells, Treg, CD4<sup>+</sup> T cell function, and NK cell function was built using logistic regression. Based on receiver operating characteristic curve analysis, the area under the curve (AUC) of the diagnostic model was 0.920 (95% CI, 0.867-0.973) in distinguishing ATB from LTBI, while the cut-off value of 0.676 produced a sensitivity of 81.48% (95% CI, 69.16%-89.62%) and specificity of 91.23% (95% CI, 81.06%-96.20%). Meanwhile, AUC analysis between ATB and HC according to the diagnostic model was 0.911 (95% CI, 0.855-0.967), with a sensitivity of 81.48% (95% CI, 69.16%-89.62%) and a specificity of 90.00% (95% CI, 79.85%-95.34%).

**Conclusions:** Our study demonstrated that the immunodiagnostic model established by the combination of lymphocyte-related indicators could facilitate the status differentiation of MTB infection.

**Keywords:** lymphocyte, immunological biomarkers, immunodiagnostic model, active tuberculosis, latent tuberculosis infection, differential diagnosis

## INTRODUCTION

Tuberculosis (TB) remains a major global health issue as a leading infectious disease caused by *Mycobacterium tuberculosis* (MTB) infection (1). It was reported that there were around 10 million cases and 1.5 million deaths in 2019 (2). Most subjects suffered with MTB infection stay clinically asymptomatic which is called latent TB infection (LTBI). A relatively small proportion of these individuals would develop to active TB (ATB) during their life (3, 4). TB control strategies largely focus on identification and treatment of people with ATB. Accurate and early diagnosis could minimize therapy period and maximize quality of life. Therefore, developing novel biomarkers for TB diagnostics with satisfactory value has become a priority for TB control.

To date, ATB diagnosis mainly relies on either insensitive (acid fast bacilli smears) or time consuming (mycobacterial culture) methods (5). The clinical use of these approaches often leads to defer initiation of therapy. Molecular methods such as GeneXpert MTB/RIF and GeneXpert MTB/RIF Ultra have begun to overcome some of these barriers (6–8). However, such tests cannot show sufficient advantages due to their suboptimal sensitivity that cannot meet clinical needs (9). Besides, they are unable to differentiate live from dead mycobacteria, and remain prohibitively expensive to operate. Interferon gamma release assays, including QuantiFERON-TB Gold In-Tube based on enzyme-linked immunosorbent assay and T-SPOT based on enzyme-linked immune-spot assay, were available used to detect MTB infection (10–12). Nevertheless, both of these two methods could not distinguish between ATB and LTBI, while were also not recommended for ATB diagnosis especially in area with high TB burden (13).

Meanwhile, several studies described the utility of T cell receptor beta variable from peripheral blood for diagnosing MTB infection (14, 15). However, the current validation is limited and further exploration is needed. Multiple limitations registered by conventional tests of etiology hurdles to the timely diagnosis of disease and contribute to promote clinical progression as well as continued transmission. Recent advances in genomics (16, 17), transcriptomics (18–20), proteomics (21–23), and metabolomics (24–26) have effectively facilitated the diagnosis of TB. But these emerging methods often require prohibitively complex equipment and operations, which hinder their promotion of clinical applications. Meanwhile, most investigations in this area are preliminary. The results regarding clinical diagnostic value of these approaches were usually obtained in small sample populations or regions with limited incidence, and have not been verified by multiple centers and large sample sizes.

Besides, previous work has reported the low number of lymphocytes in TB patients (27). In addition, several studies have identified the specific characteristics of the immunophenotype in TB patients (28, 29). Furthermore, our team has previously introduced a novel method-lymphocyte function assay for evaluating lymphocyte function (30, 31). The test could reflect the activation, chemotaxis, and cytotoxicity of lymphocytes through the percentage of IFN- $\gamma$  released under PMA/ionomycin stimulation (32). We have verified its diagnostic and prognostic value among a variety of disease models including lymphoma (33), kidney transplantation (31), and carbapenem-resistant organism infection (34). Up to now, there are few investigations of lymphocyte function assay in the area of TB diagnosis. Therefore, it is necessary to conduct a more comprehensive assessment of TB patients by combining the number, phenotype, and function of lymphocytes. The present study aims to clarify lymphocyte-related immune signatures of individuals under different status of MTB infection and investigate the diagnostic role of these indicators for the distinction between ATB, LTBI, and healthy controls (HC).

## METHODS

### Study Design

The present study was performed at Tongji Hospital from January 2019 to January 2021. Adult participants with age equal or more than 18 years were consecutively enrolled to the study. ATB was diagnosed by the identification of MTB in sputum or bronchoalveolar lavage fluid based on mycobacterial culture or GeneXpert MTB/RIF with symptoms compatible of ATB including prolonged cough, chest pain, weakness or fatigue, weight loss, fever, and night sweats. LTBI was defined by positive T-SPOT result without symptomatic, microbiological, or radiological evidences of ATB as well as the history of TB (**Supplementary Figure 1**). Individuals with negative T-SPOT results and without any evidence of suspected ATB or other diseases were categorized as HC. Subjects with HIV infection or receiving anti-TB treatment for more than 2 weeks were excluded from the study. Besides, patients with other infectious diseases, tumors, and autoimmune diseases were excluded from this study. Lymphocyte-related immune profile including lymphocyte subsets, lymphocyte phenotype, and lymphocyte function was analyzed among ATB, LTBI, as well as HC. This study was approved by the ethics committee of Tongji Hospital, Tongji Medical College, Huazhong University of Science and Technology.



## Lymphocyte Subsets

Heparinized peripheral blood was collected for performing lymphocyte subset analysis. The percentages and numbers of CD4<sup>+</sup> T cells, CD8<sup>+</sup> T cells, NK cells, and B cells were determined by using TruCOUNT tubes and BD Multitest 6-color TBNK Reagent Kit (BD Biosciences, San Jose, CA, USA) according to the manufacturer's instructions. A volume of 50  $\mu$ l peripheral blood was labeled with 6-color TBNK antibody cocktail for 20 min in room temperature. After adding 450  $\mu$ l of FACS Lysing Solution, samples were analyzed with FACSCanto flow cytometer. Cells with positive CD45 expression and with low side scatter were gated as lymphocytes. TruCOUNT beads were gated based on side scatter and fluorescence intensity. CD3<sup>+</sup> cells in lymphocyte gate were defined as total T cells. CD3<sup>+</sup>CD4<sup>+</sup>CD8<sup>-</sup> and CD3<sup>+</sup>CD4<sup>-</sup>CD8<sup>+</sup> cells were respectively defined as CD4<sup>+</sup> T cells and CD8<sup>+</sup> T cells. CD16<sup>+</sup>CD56<sup>+</sup> cells and CD19<sup>+</sup> cells in CD3<sup>-</sup> cells were respectively defined as NK cells and B cells. The gating strategies for lymphocyte subsets analysis was shown in **Figure 1A**.

## Lymphocyte Function

Lymphocyte function assay was performed under PMA/ionomycin-stimulation as introduced previously (31). The operation was described as the following: (1) 100  $\mu$ l of whole peripheral blood was diluted with 400  $\mu$ l of IMDM medium (Gibco, Grand Island, NY, USA, cat 31980-030, plus 25mM HEPES and 3.024g/L Sodium Bicarbonate); (2) the diluted whole peripheral blood was incubated in the presence of Leukocyte Activation Cocktail (Becton Dickinson GolgiPlug<sup>TM</sup>) for 4 h; (3) the cells were labeled with antibodies including anti-CD45, anti-CD3, anti-CD4, anti-CD8, and anti-CD56 for 20 minutes at room temperature; (4) the cell were fixed and permeabilized;

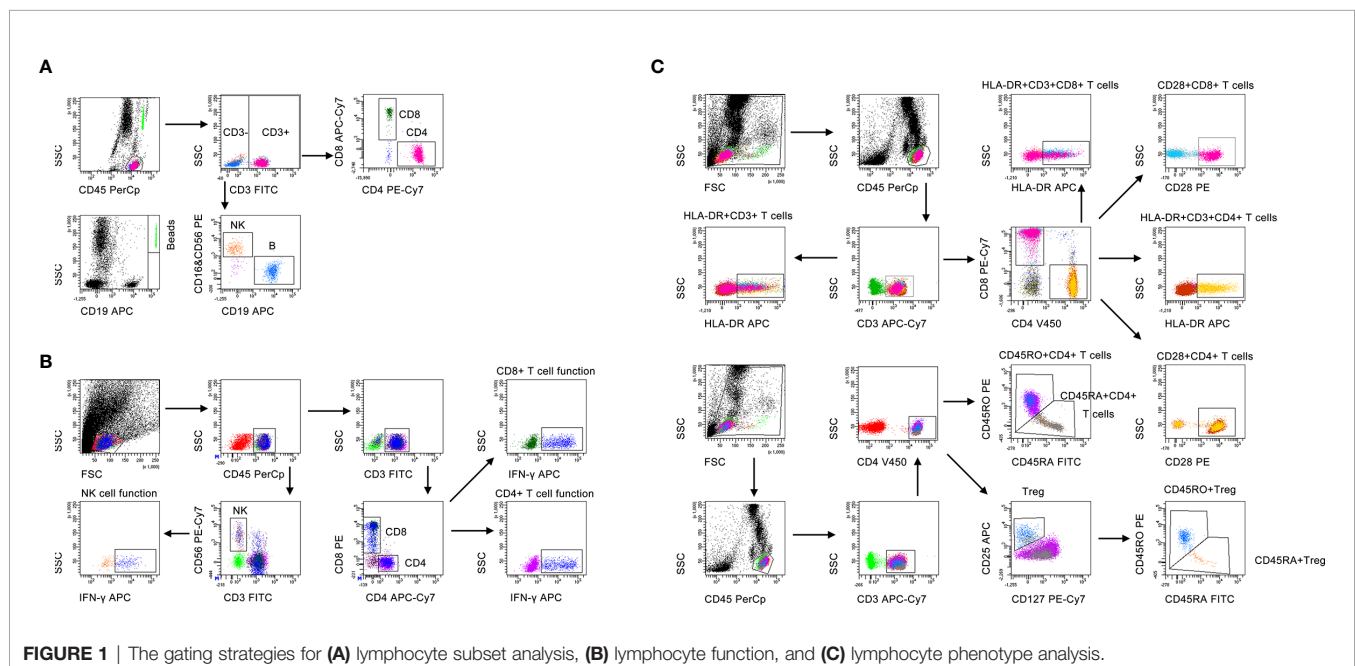
(5) the cells were stained with intracellular anti-IFN- $\gamma$  antibody; and (6) the cells were analyzed with FACSCanto flow cytometer. The percentages of IFN- $\gamma$ <sup>+</sup> cells in various cell subsets were defined as the function of them. Specially, the percentage of IFN- $\gamma$ <sup>+</sup> cells in CD3<sup>+</sup>CD4<sup>+</sup>CD8<sup>-</sup> cells was regarded as CD4<sup>+</sup> T cell function; the percentage of IFN- $\gamma$ <sup>+</sup> cells in CD3<sup>+</sup>CD4<sup>-</sup>CD8<sup>+</sup> cells was regarded as CD8<sup>+</sup> T cell function; the percentage of IFN- $\gamma$ <sup>+</sup> cells in CD3<sup>-</sup>CD56<sup>+</sup> cells was regarded as NK cell function. The gating strategies for lymphocyte function assay was shown in **Figure 1B**.

## Lymphocyte Phenotype

Heparinized peripheral blood was collected for performing lymphocyte phenotype analysis. The following monoclonal antibodies were added to 100  $\mu$ l of whole blood: anti-CD45, anti-CD3, anti-CD4, anti-CD8, anti-CD25, anti-CD127, anti-CD28, anti-HLA-DR, anti-CD45RA, and anti-CD45RO (BD Biosciences, San Jose, CA, USA). Isotype controls with irrelevant specificities were included as negative controls. Cell suspensions were incubated for 20 min at room temperature. The cells were washed and resuspended in 200  $\mu$ l of phosphate buffer saline after lysing red blood cells. Then, the cells were analyzed with FACSCanto flow cytometer. The gating strategies for lymphocyte phenotype analysis was shown in **Figure 1C**.

## Statistical Analysis

Continuous variables were presented as mean  $\pm$  standard deviation (SD) or median (interquartile range, IQR). The comparison between continuous variables was performed using T-test if the continuous value is normal distribution and homogeneity of variance or Mann-Whitney *U* test if not. Categorical variables were presented as numbers (percentages)



and compared using Chi-square test or Fisher's exact test. A two-tailed  $p$ -value less than 0.05 was considered statistically significant. For the establishment of immunodiagnostic model, indicators with statistical difference were selected and taken as candidates in multivariable logistic regression. Then, the regression equation (diagnostic model) was obtained. The regression coefficients of the model were regarded as the weights for the respective variables, and a score for each participant was calculated. Receiver operating characteristic (ROC) curve was plotted to evaluate the diagnostic performance of various indicators. Area under the curve (AUC), sensitivity, specificity, positive predictive value (PPV), negative predictive value (NPV), positive likelihood ratio (PLR), negative likelihood ratio (NLR), and accuracy as well as the corresponding 95% confidence interval (CI) were calculated. Z statistic was used for the comparison between AUCs with the procedure of Delong et al. (35). Data were analyzed using IBM SPSS 25.0 (SPSS Inc. Chicago, IL, USA), GraphPad Prism 8.0 (GraphPad Software, Inc. La Jolla, USA), MedCalc version 11.6 (MedCalc, Mariakerke, Belgium), and R 4.0.2 program (R Core Team).

## RESULTS

### Participant Characteristics

A total of 171 subjects including 54 ATB, 57 LTBI, and 60 HC were consecutively enrolled from January 2019 to January 2021 at Tongji Hospital. The demographic and clinical manifestation of all participants were summarized in **Table 1**. There was no significant difference in scale of age and gender between these three groups. The median age was around 51 years. Males were predominant in all groups.

### Lymphocyte Subsets in ATB, LTBI, and HC

We performed lymphocyte subset analysis among ATB patients, LTBI individuals, and HC. It was observed that compared with LTBI individuals, ATB patients showed significantly lower T cell number, B cell number, CD4<sup>+</sup> T cell number, CD8<sup>+</sup> T cell number, NK cell percentage, NK cell number, total percentage

of T cells, B cells and NK cells (T+B+NK cell percentage), total number of T cells, B cells and NK cells (T+B+NK cell number), and higher T cell percentage, CD8<sup>+</sup> T cell percentage (**Figure 2**). There was no significant difference in B cell percentage, CD4<sup>+</sup> T cell percentage, and CD4/CD8 ratio between these two groups.

For the comparison between ATB group and HC group. T cell percentage and CD8<sup>+</sup> T cell percentage were significantly higher, whereas T cell number, B cell number, CD4<sup>+</sup> T cell number, CD8<sup>+</sup> T cell number, NK cell percentage, NK cell number, T+B+NK cell percentage, and T+B+NK cell number were significantly lower in ATB patients than those in HC. No significant difference in B cell percentage, CD4<sup>+</sup> T cell percentage, and CD4/CD8 ratio was found between ATB and HC (**Figure 2**). No significant differences in all indicators among lymphocyte subset analysis were observed in between LTBI and HC (**Figure 2**).

### Lymphocyte Phenotype in ATB, LTBI, and HC

We characterized lymphocyte phenotype in ATB, LTBI, and HC. Most of the phenotypes did not significantly differ between ATB and non-ATB. Statistical differences were only found in HLA-DR expression on T cells and the proportion of Treg. Specifically, the proportions of HLA-DR<sup>+</sup>CD3<sup>+</sup> T cells and Treg in ATB patients were significantly higher than those in LTBI individuals or HC (**Figure 3**). The proportions of CD28<sup>+</sup>CD4<sup>+</sup> T cells, CD28<sup>+</sup>CD8<sup>+</sup> T cells, HLA-DR<sup>+</sup>CD3<sup>+</sup>CD4<sup>+</sup> T cells, HLA-DR<sup>+</sup>CD3<sup>+</sup>CD8<sup>+</sup> T cells, CD45RA<sup>+</sup>CD4<sup>+</sup> T cells, CD45RO<sup>+</sup>CD4<sup>+</sup> T cells, and CD45RO<sup>+</sup> Treg of participants with ATB did not differ significantly from LTBI or HC (**Figure 3**). No statistical difference was observed in all indexes among lymphocyte phenotype analysis between LTBI and HC (**Figure 3**).

### Lymphocyte Function in ATB, LTBI, and HC

Lymphocyte function was investigated in ATB, LTBI, and HC. It was found that the function of CD4<sup>+</sup> T cells, CD8<sup>+</sup> T cells, and NK cells was significantly lower in ATB patients than in LTBI individuals or HC, while no significant difference presented in

**TABLE 1** | Demographic and clinical characteristics of included subjects.

Variables	ATB (n = 54)	LTBI (n = 57)	HC (n = 60)
Age, years	51 (33-62)	51 (35-66)	52 (35-68)
Sex, male, %	31 (57.41%)	28 (49.12%)	34 (56.67%)
TB history	12 (22.22%)	0 (0%)	0 (0%)
Underlying condition or illness			
Diabetes mellitus	3 (5.56%)	3 (5.26%)	0 (0%)
End-stage renal disease	2 (3.7%)	2 (3.51%)	0 (0%)
Liver cirrhosis	2 (3.7%)	1 (1.75%)	0 (0%)
Positive mycobacterial culture	45 (83.33%)	N/A	N/A
Positive GeneXpert MTB/RIF	39 (72.22%)	N/A	N/A

ATB, active tuberculosis; LTBI, latent tuberculosis infection; HC, healthy controls; TB, tuberculosis; N/A, not applicable. Data were presented as medians (25th-75th percentiles) or numbers (percentages).

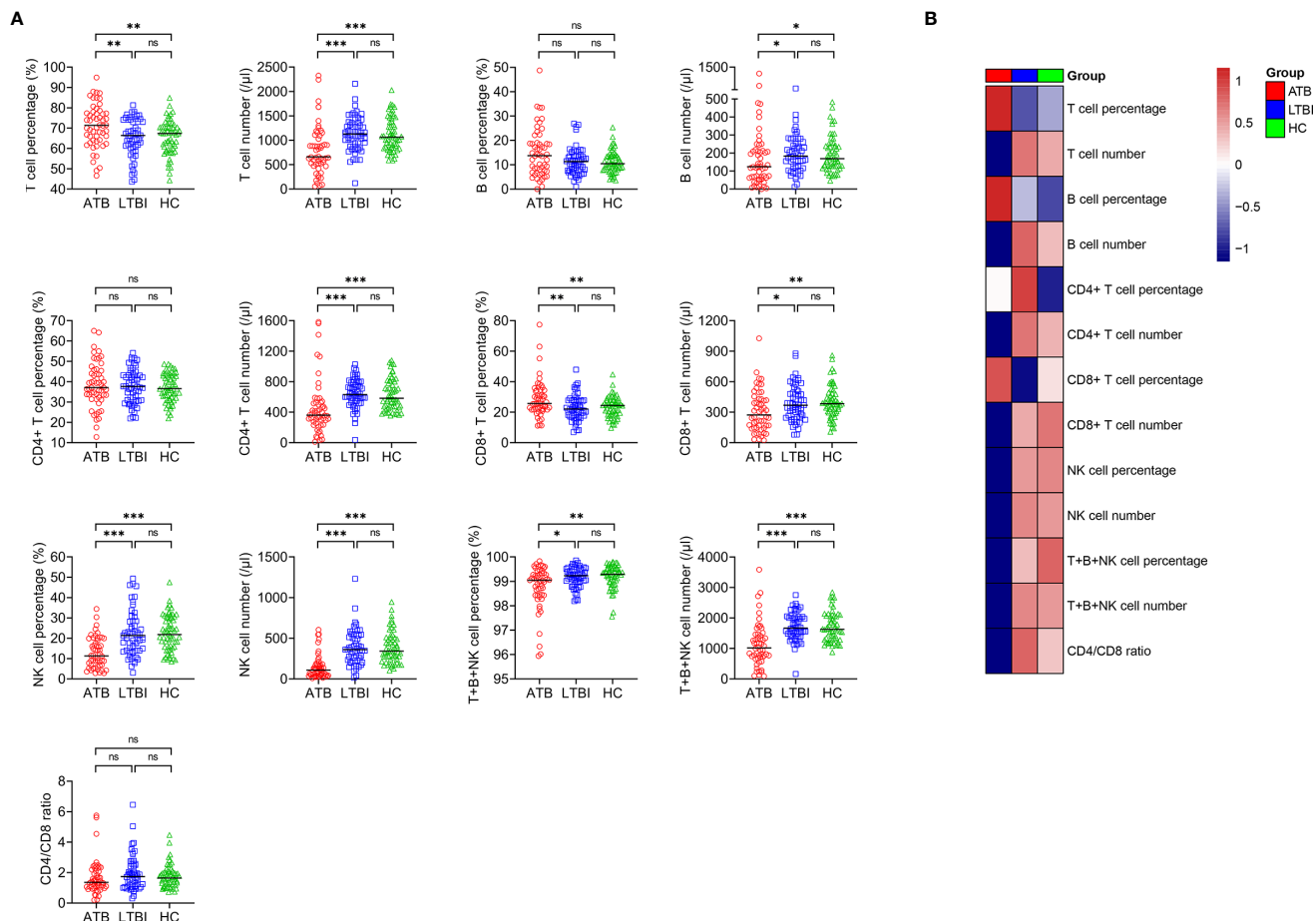


**FIGURE 2** | The results of lymphocyte subsets in ATB, LTBI, and HC. **(A)** Scatter plots showing the results of lymphocyte subsets in ATB ( $n = 54$ ), LTBI ( $n = 57$ ), and HC ( $n = 60$ ). Horizontal lines indicate the median.  $^*P < 0.05$ ,  $^{**}P < 0.01$ ,  $^{***}P < 0.001$ , ns, no significance (Mann-Whitney  $U$  test). **(B)** Heatmap showing the results of lymphocyte subsets in ATB group, LTBI group, and HC group. Each rectangle indicates the median result of a group. ATB, active tuberculosis; LTBI, latent tuberculosis infection; HC, healthy controls.

CD4<sup>+</sup> T cell function, CD8<sup>+</sup> T cell function, and NK cell function between LTBI and HC group (Figure 4).

## Establishing Immunodiagnostic Model for Stratifying the Status of MTB Infection

In order to investigate the possibility of combining different immune indicators to distinguish the status of MTB infection, we performed heatmap analysis and discovered the potential of combination of these indexes to distinguish ATB from non-ATB (Supplementary Figure 2). We next analyzed the cross set of indicators with significant differences in three groups. The overlap of 9 indicators with significant difference indicated the possible conjunct use for stratification (Figure 5).

To establish the diagnostic model based on a combination for differentiating ATB from LTBI, all variables with statistical significance were used for multivariable logistic regression

analysis. The diagnostic model was established as the follows:  $P = 1/[1 + e^{(-0.005 \times \text{NK cell number} + 0.102 \times \text{HLA-DR} + \text{CD3}^+ \text{ T cells} + 0.53 \times \text{Treg} - 0.147 \times \text{CD4}^+ \text{ T cell function} - 0.049 \times \text{NK cell function} + 3.95)}]$   $P$ , predictive value;  $e$ , natural logarithm. Venn diagram showed the overlap of these five parameters in ATB, LTBI, and HC groups and confirmed the appropriate combination of them (Figure 6). The AUC presented by the diagnostic model was 0.920 (95% CI, 0.867-0.973) (Table 2 and Figures 7A, B). The cutoff value of 0.676 for diagnostic model showed a sensitivity of 81.48% (95% CI, 69.16%-89.62%) and specificity of 91.23% (95% CI, 81.06%-96.20%) in distinguishing between ATB and LTBI (Table 2). We also applied the model to discriminate ATB from HC. It was observed that the sensitivity and specificity for the model were 81.48% (95% CI, 69.16%-89.62%) and 90.00% (95% CI, 79.85%-95.34%) with the threshold as 0.676 (Table 3 and Figures 7C, D). Meanwhile, the comparison between AUCs showed that the performance of the diagnostic model was superior to the individual immune indicator (Tables 2, 3 and Figure 8).

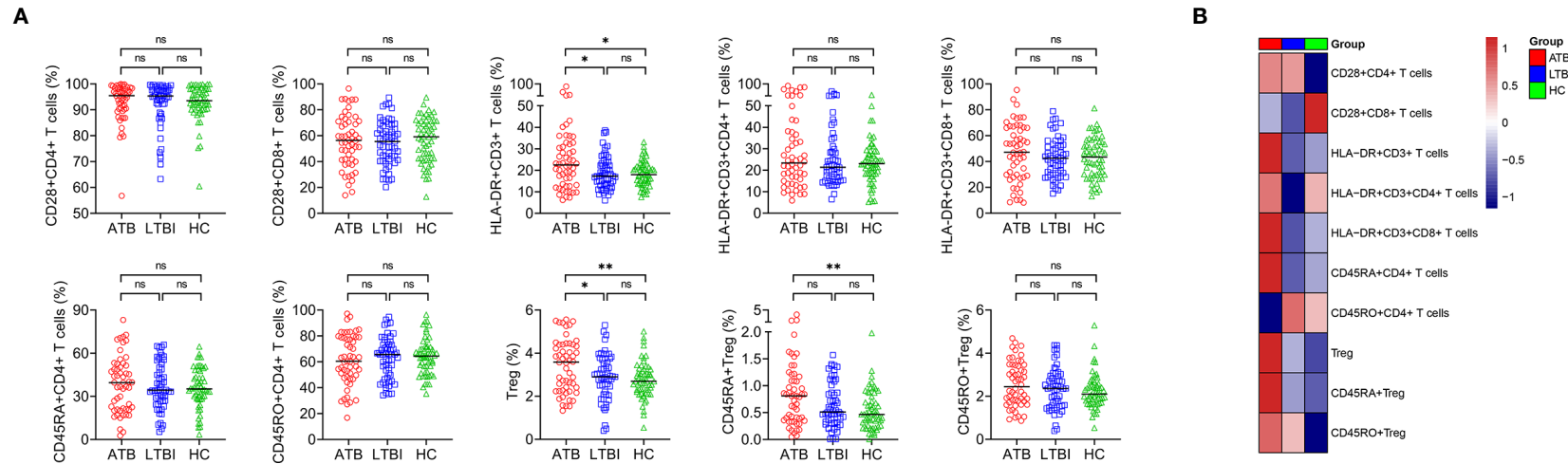


**FIGURE 3 |** The results of lymphocyte phenotype in ATB, LTBI, and HC. **(A)** Scatter plots showing the results of lymphocyte phenotype in ATB (n = 54), LTBI (n = 57), and HC (n = 60). Horizontal lines indicate the median. \* $P < 0.05$ , \*\* $P < 0.01$ , ns, no significance (Mann-Whitney  $U$  test). **(B)** Heatmap showing the results of lymphocyte phenotype in ATB group, LTBI group, and HC group. Each rectangle indicates the median result of a group. ATB, active tuberculosis; LTBI, latent tuberculosis infection; HC, healthy controls.

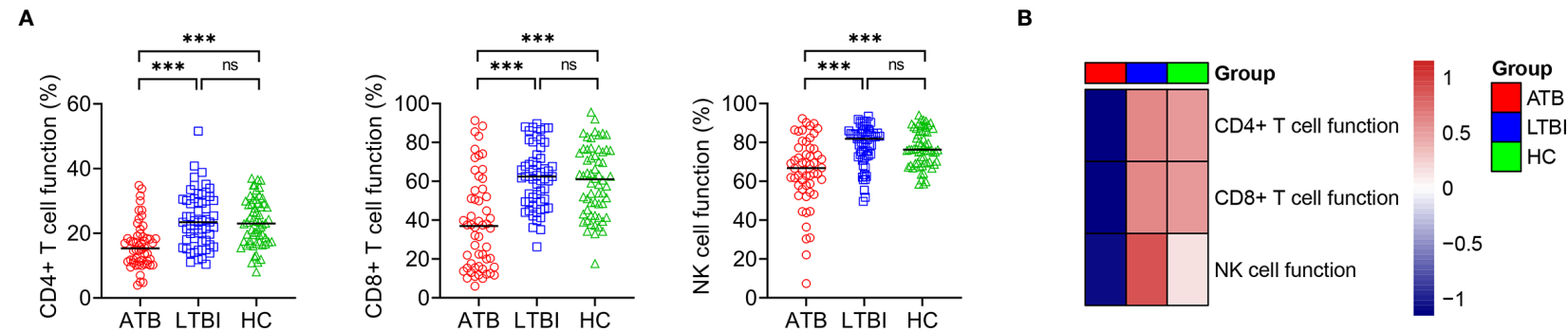
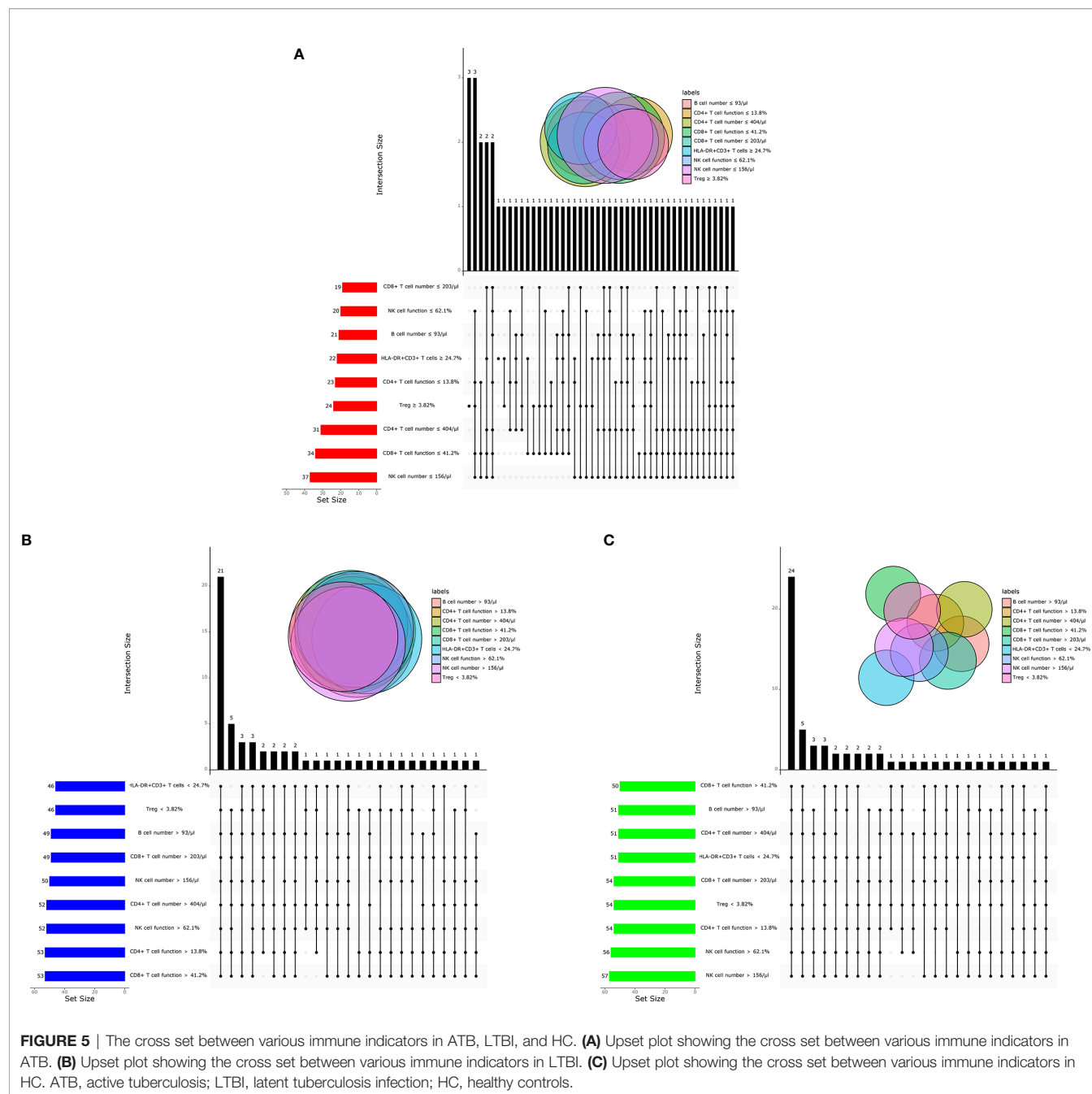


**FIGURE 4 |** The results of lymphocyte function in ATB, LTBI, and HC. **(A)** Scatter plots showing the results of lymphocyte function in ATB (n = 54), LTBI (n = 57), and HC (n = 60). Horizontal lines indicate the median. \*\*\* $P < 0.001$ , ns, no significance (Mann-Whitney  $U$  test). **(B)** Heatmap showing the results of lymphocyte function in ATB group, LTBI group, and HC group. Each rectangle indicates the median result of a group. ATB, active tuberculosis; LTBI, latent tuberculosis infection; HC, healthy controls.





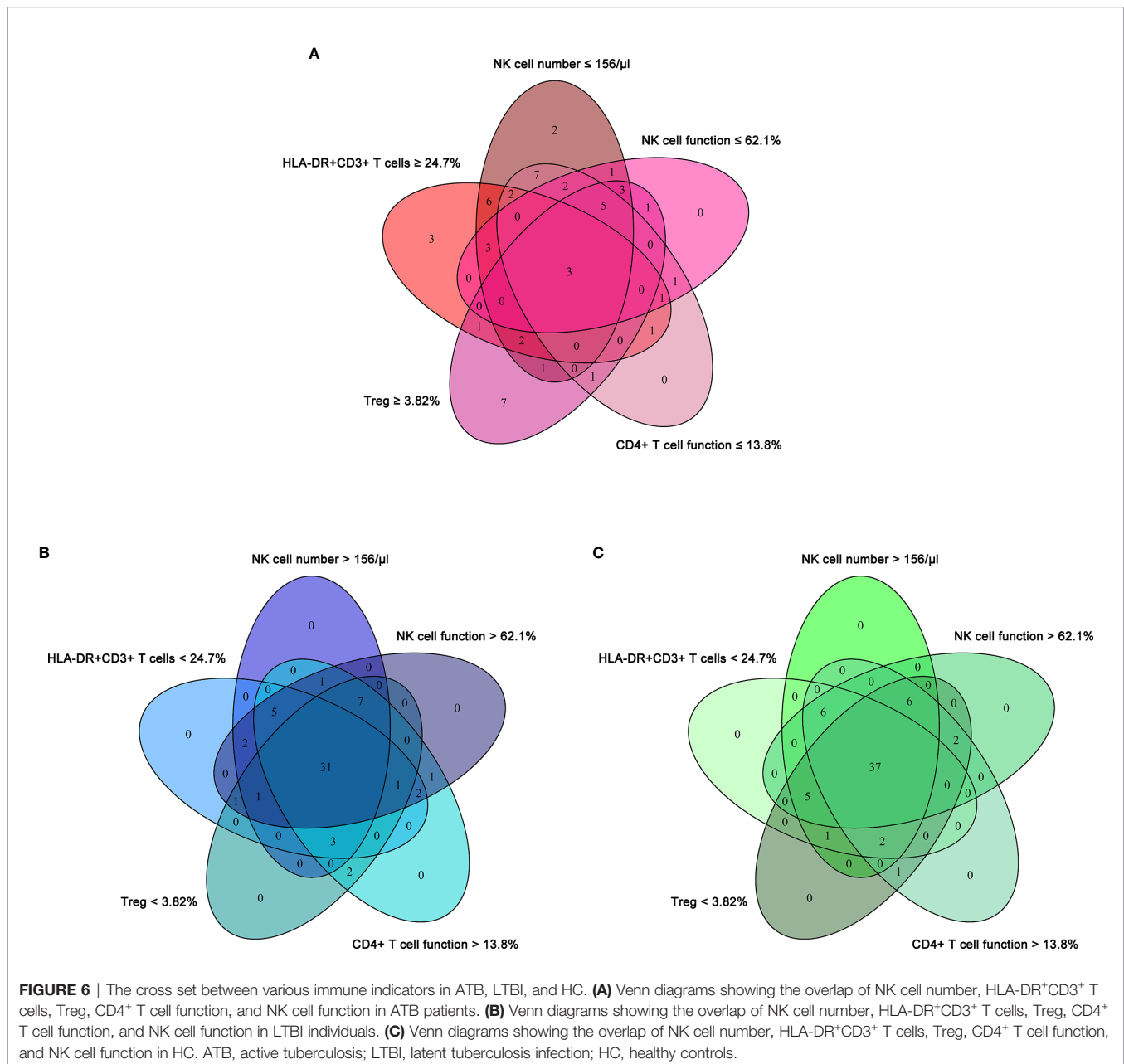
## The Relationship Between Immune Indicators in ATB Patients

We conducted correlation analysis of different immune indicators in ATB patients (**Figure 9A**). It was observed that the proportion of HLA-DR<sup>+</sup>CD3<sup>+</sup>CD4<sup>+</sup> T cells was significantly negative, whereas the proportion of Treg was significantly positive, with the number of CD4<sup>+</sup> T cells. There was a significantly positive correlation between the function of CD4<sup>+</sup> T cells and the expression of HLA-DR on these cells. The same

phenomenon was also presented in CD8<sup>+</sup> T cells. Meanwhile, statistically positive correlation existed between CD4<sup>+</sup> T cell function and CD8<sup>+</sup> T cell function (**Figure 9B**).

## DISCUSSION

Control of the TB pandemic remains hindered (36–38). Major challenges for TB control include the lack of specific drugs and



biomarkers for stratifying MTB infection, and the emergence of drug resistance (39–46). Current gold standard diagnostics that rely on bacteriological assays are slow and challenging to implement, as well as incompatible with the healthcare settings in which TB is frequently seen (47, 48). On the other hand, although many efforts including various omics have been made to overcome the issue, these methods have not been effectively verified, making it difficult to transform into clinical practice. Hence, the stratification of MTB infection still needs to be addressed with urgency.

Immune biomarkers based on flow cytometer have recently begun to emerge as clinically useful diagnostic and prognostic

markers of infectious disease (49–51). Growing evidence has demonstrated that TB may elicit specific patterns of immune response (52–54). Nonetheless, there was rare study targeted for comprehensive evaluation for host immunity towards MTB infection. Most previous studies focused on the number of lymphocyte or its subsets in ATB. A few studies explored the immunophenotype of ATB patients, while few studies evaluated lymphocyte function of subjects with MTB infection. Thus, these previous studies have not fully clarified the host immune landscape among subjects with MTB infection on account of methodological limitations. Our study simultaneously determined the immune characteristics of lymphocyte at

**TABLE 2 |** The performance of different methods for distinguishing between ATB and LTBI.

Methods	Cutoff value	AUC (95% CI)	Sensitivity (95% CI)	Specificity (95% CI)	PPV (95% CI)	NPV (95% CI)	PLR (95% CI)	NLR (95% CI)	Accuracy
CD4 <sup>+</sup> T cell number ( $\mu$ l)	404	0.788 <sup>†</sup> (0.694-0.882)	57.41% (44.16%-69.67%)	91.23% (81.06%-96.20%)	86.11% (71.34%-93.92%)	69.33% (58.17%-78.61%)	6.54 (2.75-15.59)	0.47 (0.34-0.64)	74.77%
CD8 <sup>+</sup> T cell number ( $\mu$ l)	203	0.633 <sup>‡</sup> (0.528-0.737)	35.19% (23.82%-48.52%)	85.96% (74.68%-92.71%)	70.37% (51.52%-84.15%)	58.33% (47.65%-68.29%)	2.51 (1.2-5.24)	0.75 (0.6-0.94)	61.26%
NK cell number ( $\mu$ l)	156	0.852 <sup>*</sup> (0.778-0.927)	68.52% (55.26%-79.32%)	87.72% (76.75%-93.92%)	84.09% (70.63%-92.07%)	74.63% (63.07%-83.51%)	5.58 (2.72-11.43)	0.36 (0.24-0.54)	78.38%
B cell number ( $\mu$ l)	93	0.629 <sup>‡</sup> (0.523-0.736)	38.89% (27.04%-52.21%)	85.96% (74.68%-92.71%)	72.41% (54.28%-85.30%)	59.76% (48.94%-69.70%)	2.77 (1.34-5.72)	0.71 (0.56-0.9)	63.06%
HLA-DR <sup>+</sup> CD3 <sup>+</sup> T cells (%)	24.7	0.611 <sup>‡</sup> (0.504-0.719)	40.74% (28.68%-54.03%)	80.70% (68.66%-88.87%)	66.67% (49.61%-80.25%)	58.97% (47.89%-69.22%)	2.11 (1.13-3.93)	0.73 (0.57-0.95)	61.26%
Treg (%)	3.82	0.613 <sup>‡</sup> (0.506-0.720)	44.44% (32.00%-57.62%)	80.70% (68.66%-88.87%)	68.57% (52.02%-81.45%)	60.53% (49.29%-70.75%)	2.3 (1.25-4.23)	0.69 (0.53-0.9)	63.06%
CD4 <sup>+</sup> T cell function (%)	13.8	0.766 <sup>‡</sup> (0.678-0.854)	42.59% (30.33%-55.84%)	92.98% (83.30%-97.24%)	85.19% (67.52%-94.09%)	63.10% (52.42%-72.63%)	6.07 (2.25-16.41)	0.62 (0.49-0.79)	68.47%
CD8 <sup>+</sup> T cell function (%)	41.2	0.782 <sup>†</sup> (0.692-0.873)	62.96% (49.63%-74.58%)	92.98% (83.30%-97.24%)	89.47% (75.87%-95.83%)	72.60% (61.44%-81.51%)	8.97 (3.41-23.59)	0.4 (0.28-0.57)	78.38%
NK cell function (%)	62.1	0.744 <sup>‡</sup> (0.650-0.838)	37.04% (25.42%-50.37%)	91.23% (81.06%-96.20%)	80.00% (60.87%-91.14%)	60.47% (49.90%-70.14%)	4.22 (1.71-10.45)	0.69 (0.55-0.86)	64.86%
Diagnostic model	0.676	0.920 (0.867-0.973)	81.48% (69.16%-89.62%)	91.23% (81.06%-96.20%)	89.80% (78.24%-95.56%)	83.87% (72.79%-91.00%)	9.29 (3.98-21.66)	0.2 (0.12-0.36)	86.49%

\*Compared with diagnostic model using z statistic,  $P < 0.05$ ; †compared with diagnostic model using z statistic,  $P < 0.01$ ; ‡compared with diagnostic model using z statistic,  $P < 0.001$ ; ATB, active tuberculosis; LTBI, latent tuberculosis infection; AUC, area under the curve; PPV, positive predictive value; NPV, negative predictive value; PLR, positive likelihood ratio; NLR, negative likelihood ratio; CI, confidence interval.

different stages of MTB infection from number, phenotype, and function for the first time. We confirmed the low levels of lymphocyte number and function, hyperactivation and high proportion of Treg in patients with ATB. These data indicate that ATB patients are in a state of hyperinflammatory but with low immune potential. TB is generally considered to be a disease with malnutrition. Some previous studies have reported the low level of serum iron (55) and prealbumin (56) in ATB patients. Thus, the low level of lymphocyte number and function found in our research echoed these phenomena. Furthermore, we discovered the potential of the combination of three types of immune indicators to differentiate the status of MTB infection through Venn diagram analysis, and successfully established an immunodiagnostic model using logistic regression. The model based on the combination of NK cell number, HLA-DR<sup>+</sup>CD3<sup>+</sup> T cells, Treg, CD4<sup>+</sup> T cell function, and NK cell function could efficaciously distinguish ATB from LTBI and HC.

Some publications have shown that the phenotype including HLA-DR, CD38, and Ki-67 on TB-specific cells was helpful for TB diagnosis (28, 57). However, this type of method requires additional specific stimulation for more than 12 hours. Besides, in order to obtain enough IFN- $\gamma$ <sup>+</sup> or TNF- $\alpha$ <sup>+</sup> cells for subgroup analysis, a large volume of peripheral blood is usually needed (57). The complexity of these operations makes it difficult into clinical transformation. In addition, owing to the existence of ATB patients with negative T-SPOT results and MTB infected individuals with low-value-T-SPOT results (58–61), the effectiveness of this method will be greatly reduced due to not getting enough TB-specific cells for analysis. On the other hand, some literature reported that cytokines including IL-2, IFN- $\gamma$ , and TNF- $\alpha$  have the potential to diagnose TB (62–65). However,

the value of most unstimulated cytokines was limited, the more advantageous diagnostic utility often also requires TB-specific stimulation. Moreover, the large heterogeneity between different studies also hinders the possibility of its translation into clinical practice (66). The detection of lymphocyte-related indicators that we performed in the present study requires only a small volume of peripheral blood plus short-term non-specific stimulation, while eliminating cumbersome extraction of peripheral blood mononuclear cells. Therefore, our established diagnostic model has more advantages in applying to clinical practice.

Regarding the indicators observed in this study, the immune profiles did not differ significantly between LTBI and HC groups. On the one hand, these data indicates that the host immunity of individuals with LTBI may temporarily successfully resist MTB. As a result, the body shows no immune barriers or defects as a whole. On the other hand, it may be that the immune indicators observed in our research are not specific and comprehensive, they cannot reflect the subtle difference of immune characteristics between the two groups. Various immune cell population including monocytes, dendritic cells, neutrophils need to be further analyzed in a broader spectrum. Meanwhile, detailed classification such as helper T cell and follicular helper T cell should be also conducted. These directions are also applicable to the expansion of immune observation in ATB group.

Several limitations should be noticed in the current study. First, the sample size in this study is relatively small, and stratified analysis targeted for different underlying diseases such as HIV infection has not been carried out. Validation by larger population in areas with different disease burdens would

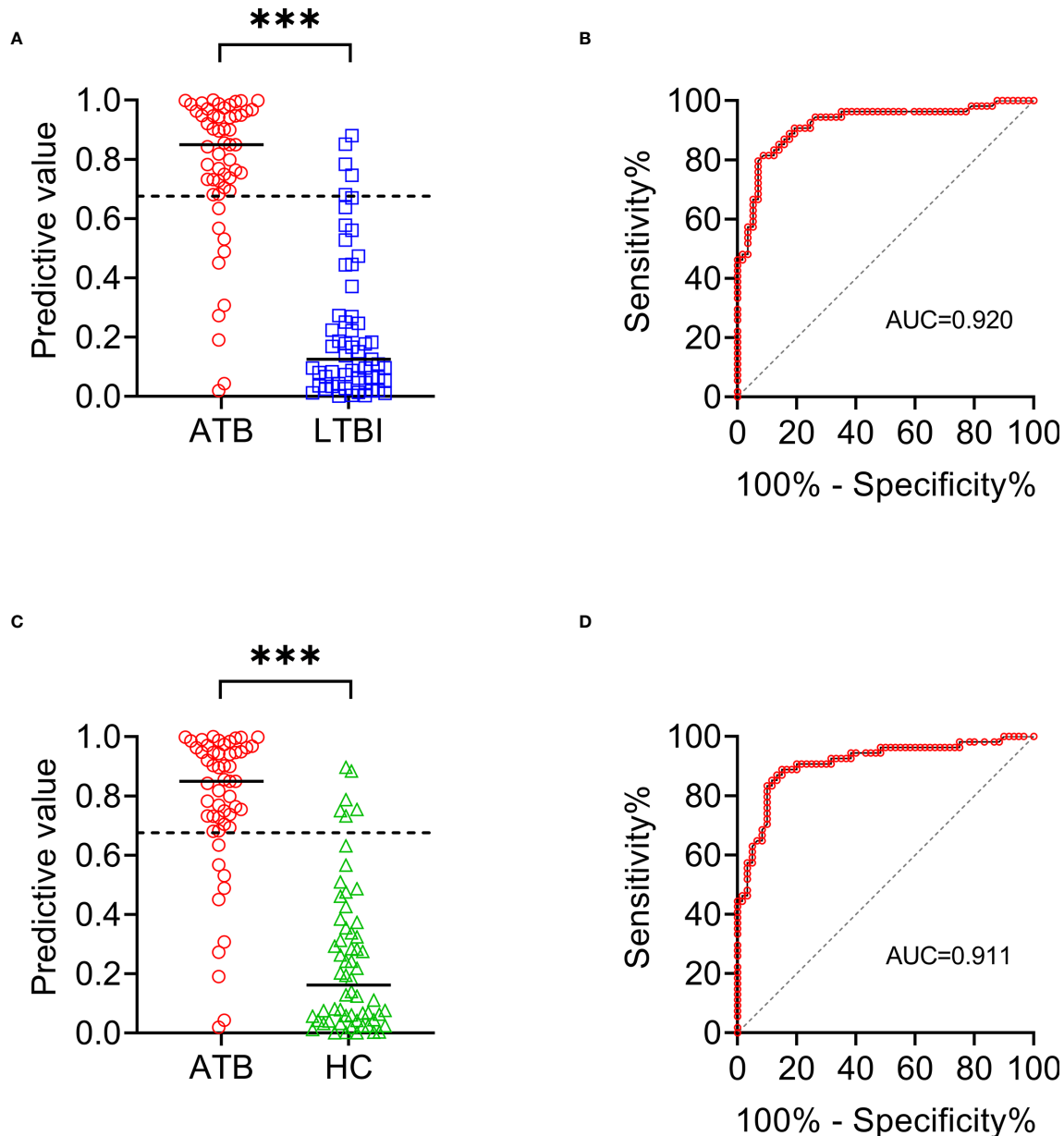


**FIGURE 7 |** The performance of established diagnostic model for distinguishing ATB from LTBI and HC. **(A)** Scatter plots showing the predictive value of diagnostic model in ATB patients ( $n = 54$ ) and LTBI individuals ( $n = 57$ ). Horizontal lines indicate the median. \*\*\* $P < 0.001$  (Mann-Whitney  $U$  test). Dotted line indicates the cutoff value in distinguishing these two groups. **(B)** ROC analysis showing the performance of diagnostic model in discriminating ATB patients from LTBI individuals. **(C)** Scatter plots showing the predictive value of diagnostic model in ATB patients ( $n = 54$ ) and HC ( $n = 60$ ). Horizontal lines indicate the median. \*\*\* $P < 0.001$  (Mann-Whitney  $U$  test). Dotted line indicates the cutoff value in distinguishing these two groups. **(D)** ROC analysis showing the performance of diagnostic model in discriminating ATB patients from HC. ATB, active tuberculosis; LTBI, latent tuberculosis infection; HC, healthy controls; ROC, receiver operating characteristic.

be further needed. Second, lymphocyte immune indicators analyzed in this study are not comprehensive enough, and multi-dimensional analysis using polychromatic flow cytometry is also very necessary. Third, given that time course comparisons under treatment, MTB-specific assays, and identified immune cell markers such as CD38 and CD27

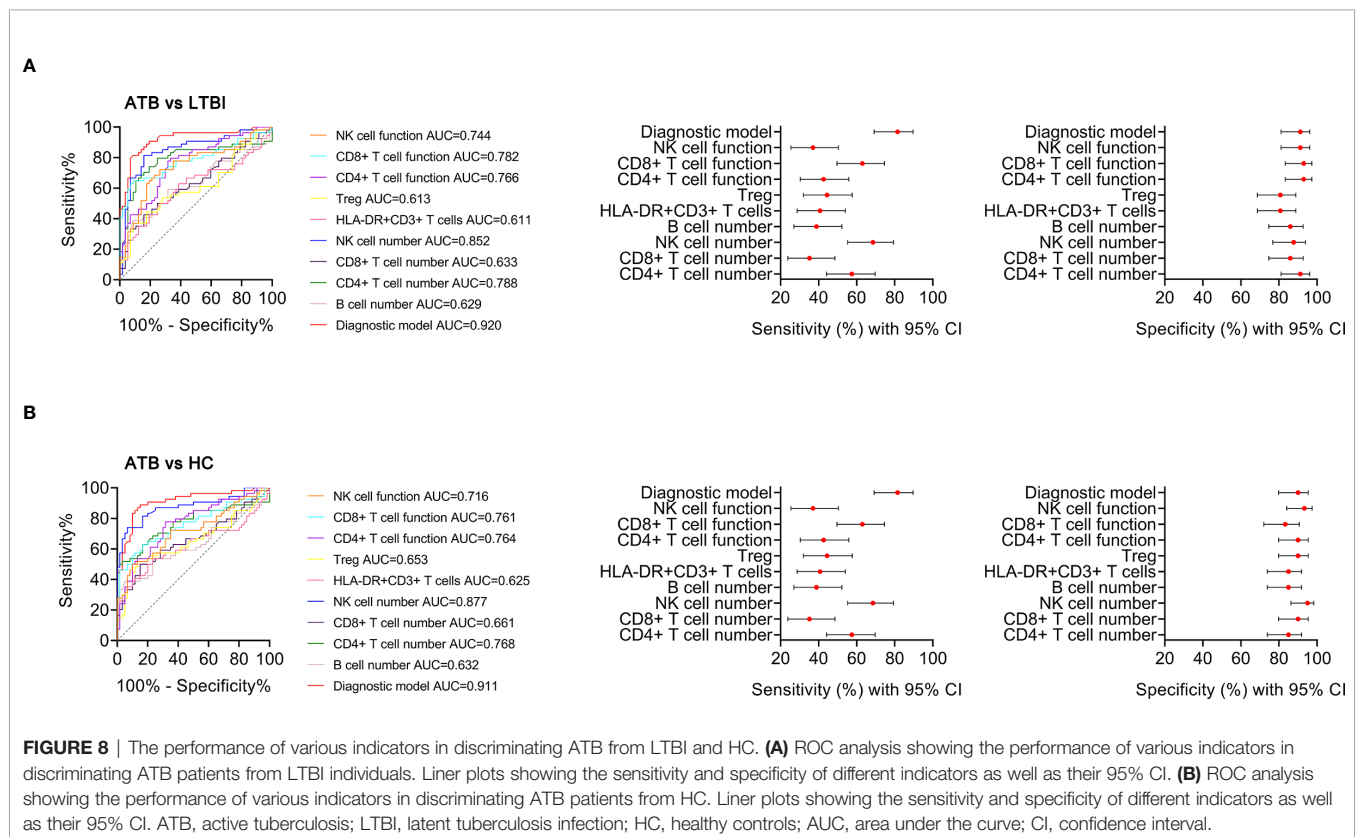
were missing in the present study (67, 68), further investigation targeting monitoring or conjunction of different methods are needed. Fourth, since the underlying diseases might affect the levels of these lymphocyte-related immune indicators, individuals with other infectious diseases, tumors, and autoimmune diseases were excluded from this study.



**TABLE 3** | The performance of different methods for distinguishing between ATB and HC.

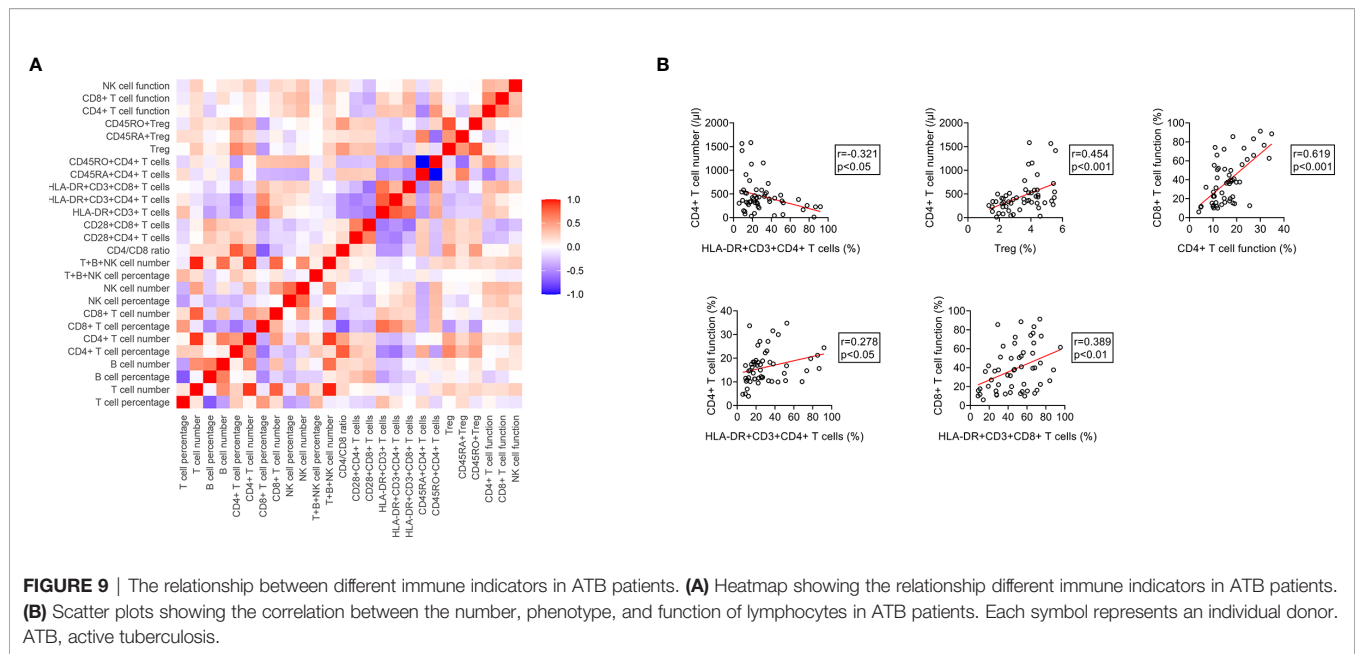
Methods	Cutoff value	AUC (95% CI)	Sensitivity (95% CI)	Specificity (95% CI)	PPV (95% CI)	NPV (95% CI)	PLR (95% CI)	NLR (95% CI)	Accuracy
CD4 <sup>+</sup> T cell number ( $\mu$ l)	404	0.768 <sup>†</sup> (0.675-0.862)	57.41% (44.16%-69.67%)	85.00% (73.89%-91.90%)	77.50% (62.50%-87.69%)	68.92% (57.66%-78.31%)	3.83 (2.01-7.29)	0.5 (0.36-0.7)	71.93%
CD8 <sup>+</sup> T cell number ( $\mu$ l)	203	0.661 <sup>†</sup> (0.558-0.764)	35.19% (23.82%-48.52%)	90.00% (79.85%-95.34%)	76.00% (56.57%-88.51%)	60.67% (50.29%-70.18%)	3.52 (1.52-8.16)	0.72 (0.58-0.89)	64.04%
NK cell number ( $\mu$ l)	156	0.877 (0.809-0.945)	68.52% (55.26%-79.32%)	95.00% (86.30%-98.29%)	92.50% (80.14%-97.42%)	77.03% (66.25%-85.13%)	13.7 (4.48-41.9)	0.33 (0.22-0.49)	82.46%
B cell number ( $\mu$ l)	93	0.632 <sup>‡</sup> (0.525-0.738)	38.89% (27.04%-52.21%)	85.00% (73.89%-91.90%)	70.00% (52.12%-83.34%)	60.71% (50.02%-70.47%)	2.59 (1.3-5.16)	0.72 (0.57-0.91)	63.16%
HLA-DR <sup>+</sup> CD3 <sup>+</sup> T cells (%)	24.7	0.625 <sup>‡</sup> (0.517-0.733)	40.74% (28.68%-54.03%)	85.00% (73.89%-91.90%)	70.97% (53.41%-83.91%)	61.45% (50.69%-71.19%)	2.72 (1.37-5.38)	0.7 (0.55-0.89)	64.04%
Treg (%)	3.82	0.653 <sup>‡</sup> (0.548-0.758)	44.44% (32.00%-57.62%)	90.00% (79.85%-95.34%)	80.00% (62.70%-90.50%)	64.29% (53.62%-73.70%)	4.44 (1.97-10.05)	0.62 (0.48-0.8)	68.42%
CD4 <sup>+</sup> T cell function (%)	13.8	0.764 <sup>†</sup> (0.676-0.852)	42.59% (30.33%-55.84%)	90.00% (79.85%-95.34%)	79.31% (61.61%-90.16%)	63.53% (52.92%-72.97%)	4.26 (1.88-9.67)	0.64 (0.5-0.81)	67.54%
CD8 <sup>+</sup> T cell function (%)	41.2	0.761 <sup>†</sup> (0.669-0.852)	62.96% (49.63%-74.58%)	83.33% (71.97%-90.69%)	77.27% (63.01%-87.16%)	71.43% (59.95%-80.68%)	3.78 (2.07-6.89)	0.44 (0.31-0.64)	73.68%
NK cell function (%)	62.1	0.716 <sup>†</sup> (0.620-0.813)	37.04% (25.42%-50.37%)	93.33% (84.08%-97.38%)	83.33% (64.15%-93.32%)	62.22% (51.90%-71.54%)	5.56 (2.03-15.23)	0.67 (0.54-0.84)	66.67%
Diagnostic model	0.676	0.911 (0.855-0.967)	81.48% (69.16%-89.62%)	90.00% (79.85%-95.34%)	88.00% (76.20%-94.38%)	84.38% (73.57%-91.29%)	8.15 (3.77-17.59)	0.21 (0.12-0.36)	85.96%

<sup>†</sup>Compared with diagnostic model using z statistic,  $P < 0.01$ ; <sup>‡</sup>compared with diagnostic model using z statistic,  $P < 0.001$ ; ATB, active tuberculosis; HC, healthy controls; AUC, area under the curve; PPV, positive predictive value; NPV, negative predictive value; PLR, positive likelihood ratio; NLR, negative likelihood ratio; CI, confidence interval.



More exploration targeting the effect of these underlying diseases on our established model should be conducted in the future. Eventually, the present study only focuses on the characteristics of lymphocytes among MTB infection. Other immune cells

including B cells and dendritic cells are also proved involved in the pathogenesis of TB (69–72). Therefore, different types of immune cells should be also included for a more comprehensive analysis.



In conclusion, our findings suggests that the diagnostic model based on the combination of lymphocyte-related indicators may be an adjunctive but useful method in the diagnosis of TB.

## DATA AVAILABILITY STATEMENT

The original contributions presented in the study are included in the article/**Supplementary Material**. Further inquiries can be directed to the corresponding authors.

## ETHICS STATEMENT

The studies involving human participants were reviewed and approved by the ethics committee of Tongji Hospital, Tongji Medical College, Huazhong University of Science and Technology. The patients/participants provided their written informed consent to participate in this study.

## AUTHOR CONTRIBUTIONS

YL and YX designed and oversaw the study; QL and GT contributed to lymphocyte function assay; HS and WL contributed to lymphocyte subset analysis; LM conducted lymphocyte phenotype analysis; XY, YuZ, ZC, YaZ, WYL, SW, FW, and ZS coordinated data collection and management. YL and YC did the statistical analysis. YL wrote the manuscript. All authors contributed to the article and approved the submitted version.

## FUNDING

This work was funded by Graduate Innovation Fund of Huazhong University of Science and Technology (grant number 2021yjsCXY088), National Mega Project on Major Infectious Disease Prevention of China (grant number 2017ZX10103005-007), and the National Natural Science Foundation (grant number 81401639 and 81902132).

## ACKNOWLEDGMENTS

We thank the Department of Laboratory Medicine of Tongji Hospital for technical assistance as well as the patients and their families.

## SUPPLEMENTARY MATERIAL

The Supplementary Material for this article can be found online at: <https://www.frontiersin.org/articles/10.3389/fimmu.2021.658843/full#supplementary-material>

**Supplementary Figure 1 |** Representative pictures showing the negative and positive results of T-SPOT assay. The number in the upper left corner of each graph indicates the number of spot-forming cells in each well. ESAT-6, early secreted antigenic target 6; CFP-10, culture filtrate protein 10; PHA, phytohemagglutinin.

**Supplementary Figure 2 |** The cluster analysis of immune indicators in ATB, LTBI, and HC. **(A)** Heatmap showing the cluster analysis of lymphocyte subsets, phenotype, and function in ATB patients ( $n = 54$ ) and LTBI individuals ( $n = 57$ ). Each rectangle indicates a result of a subject. **(B)** Heatmap showing the cluster analysis of lymphocyte subsets, phenotype, and function in ATB patients ( $n = 54$ ) and HC ( $n = 60$ ). Each rectangle indicates a result of a subject. ATB, active tuberculosis; LTBI, latent tuberculosis infection; HC, healthy controls.

## REFERENCES

- Furin J, Cox H, Pai M. Tuberculosis. *Lancet* (2019) 393(10181):1642–56. doi: 10.1016/S0140-6736(19)30308-3
- World Health Organization. *Global Tuberculosis Report 2020* Vol. 14. Switzerland: Geneva (2020). Available at: <https://apps.who.int/iris/rest/bitstreams/1312164/retrieve>.
- Xin H, Zhang H, Yang S, Liu J, Lu W, Bai L, et al. 5-Year Follow-Up of Active Tuberculosis Development From Latent Infection in Rural China. *Clin Infect Dis* (2020) 70(5):947–50. doi: 10.1093/cid/ciz581
- Cohen A, Mathiasen VD, Schön T, Wejse C. The Global Prevalence of Latent Tuberculosis: A Systematic Review and Meta-Analysis. *Eur Respir J* (2019) 54(3):1900655. doi: 10.1183/13993003.00655-2019
- World Health Organization. *Implementing Tuberculosis Diagnostics: A Policy Framework*. Switzerland: Geneva (2015). Available at: <https://apps.who.int/iris/rest/bitstreams/720125/retrieve>.
- Wang G, Wang S, Jiang G, Yang X, Huang M, Huo F, et al. Xpert MTB/RIF Ultra Improved the Diagnosis of Paucibacillary Tuberculosis: A Prospective Cohort Study. *J Infect* (2019) 78(4):311–6. doi: 10.1016/j.jinf.2019.02.010
- Liu XH, Xia L, Song B, Wang H, Qian XQ, Wei JH, et al. Stool-Based Xpert MTB/RIF Ultra Assay as a Tool for Detecting Pulmonary Tuberculosis in Children With Abnormal Chest Imaging: A Prospective Cohort Study. *J Infect* (2021) 82(1):84–9. doi: 10.1016/j.jinf.2020.10.036
- Zhang M, Xue M, He JQ. Diagnostic Accuracy of the New Xpert MTB/RIF Ultra for Tuberculosis Disease: A Preliminary Systematic Review and Meta-Analysis. *Int J Infect Dis* (2020) 90:35–45. doi: 10.1016/j.ijid.2019.09.016
- Cresswell FV, Tugume L, Bahr NC, Kwizera R, Bangdiwala AS, Musubire AK, et al. Xpert MTB/RIF Ultra for the Diagnosis of HIV-Associated Tuberculous Meningitis: A Prospective Validation Study. *Lancet Infect Dis* (2020) 20(3):308–17. doi: 10.1016/S1473-3099(19)30550-X
- Sester M, Sotgiu G, Lange C, Giehl C, Girardi E, Migliori GB, et al. Interferon-Gamma Release Assays for the Diagnosis of Active Tuberculosis: A Systematic Review and Meta-Analysis. *Eur Respir J* (2011) 37(1):100–11. doi: 10.1183/09031936.00114810
- Zhou G, Luo Q, Luo S, Teng Z, Ji Z, Yang J, et al. Interferon- $\gamma$  Release Assays or Tuberculin Skin Test for Detection and Management of Latent Tuberculosis Infection: A Systematic Review and Meta-Analysis. *Lancet Infect Dis* (2020) 20(12):1457–69. doi: 10.1016/S1473-3099(20)30276-0
- Zhang H, Xin H, Wang D, Pan S, Liu Z, Cao X, et al. Serial Testing of Mycobacterium Tuberculosis Infection in Chinese Village Doctors by QuantiFERON-TB Gold Plus, QuantiFERON-TB Gold in-Tube and T-SPOT.TB. *J Infect* (2019) 78(4):305–10. doi: 10.1016/j.jinf.2019.01.008
- World Health Organization. (2010). Strategic and Technical Advisory Group for Tuberculosis (STAG-TB), in: *Report of the 10th meeting*, Geneva, Switzerland: World Health Organization, 27–29 Sept. 2010, Rep Tenth Meet.
- Yang J, He J, Huang H, Ji Z, Wei L, Ye P, et al. Molecular Characterization of T Cell Receptor Beta Variable in the Peripheral Blood T Cell Repertoire in Subjects With Active Tuberculosis or Latent Tuberculosis Infection. *BMC Infect Dis* (2013) 13:423. doi: 10.1186/1471-2334-13-423
- Yang J, Xu K, Zheng J, Wei L, Fan J, Li L. Limited T Cell Receptor Beta Variable Repertoire Responses to ESAT-6 and CFP-10 in Subjects Infected With Mycobacterium Tuberculosis. *Tuberculosis (Edinb)* (2013) 93(5):529–37. doi: 10.1016/j.tube.2013.05.007
- Suliman S, Thompson E, Sutherland J, Weiner Rd J, Ota MOC, Shankar S, et al. Four-Gene Pan-African Blood Signature Predicts Progression to Tuberculosis. *Am J Respir Crit Care Med* (2018) 197(9):1198–208. doi: 10.1164/rccm.201711-2340OC
- Warsinske H, Vashisht R, Khatri P. Host-Response-Based Gene Signatures for Tuberculosis Diagnosis: A Systematic Comparison of 16 Signatures. *PLoS Med* (2019) 16(4):e1002786. doi: 10.1371/journal.pmed.1002786
- Ho J, Bokil NJ, Nguyen PTB, Nguyen TA, Liu MY, Hare N, et al. A Transcriptional Blood Signature Distinguishes Early Tuberculosis Disease From Latent Tuberculosis Infection and Uninfected Individuals in a Vietnamese Cohort. *J Infect* (2020) 81(1):72–80. doi: 10.1016/j.jinf.2020.03.066
- Turner CT, Gupta RK, Tsaliqi E, Roe JK, Mondal P, Nyawo GR, et al. Blood Transcriptional Biomarkers for Active Pulmonary Tuberculosis in a High-Burden Setting: A Prospective, Observational, Diagnostic Accuracy Study. *Lancet Respir Med* (2020) 8(4):407–19. doi: 10.1016/S2213-2600(19)30469-2
- Singhania A, Wilkinson RJ, Rodrigue M, Haldar P and O'Garra A. The Value of Transcriptomics in Advancing Knowledge of the Immune Response and Diagnosis in Tuberculosis. *Nat Immunol* (2018) 19(11):1159–68. doi: 10.1038/s41590-018-0225-9
- Garay-Baquero DJ, White CH, Walker NF, Tebruegge M, Schiff HF, Ugarte-Gil C, et al. Comprehensive Plasma Proteomic Profiling Reveals Biomarkers for Active Tuberculosis. *JCI Insight* (2020) 5(18):e137427. doi: 10.1172/jci.insight.137427
- Yang Q, Chen Q, Zhang M, Cai Y, Yang F, Zhang J, et al. Identification of Eight-Protein Biosignature for Diagnosis of Tuberculosis. *Thorax* (2020) 75(7):576–83. doi: 10.1136/thoraxjnl-2018-213021
- Togun T, Hoggart CJ, Agbla SC, Gomez MP, Egere U, Sillah AK, et al. A Three-Marker Protein Biosignature Distinguishes Tuberculosis From Other Respiratory Diseases in Gambian Children. *EBioMedicine* (2020) 58:102909. doi: 10.1016/j.ebiom.2020.102909
- Albors-Vaquer A, Rizvi A, Matzapetakis M, Lamosa P, Coelho AV, Patel AB, et al. Active and Prospective Latent Tuberculosis Are Associated With Different Metabolomic Profiles: Clinical Potential for the Identification of Rapid and Non-Invasive Biomarkers. *Emerg Microbes Infect* (2020) 9(1):1131–9. doi: 10.1080/22221751.2020.1760734
- Weiner J 3rd, Maertzdorf J, Sutherland JS, Duffy FJ, Thompson E, Suliman S, et al. Metabolite Changes in Blood Predict the Onset of Tuberculosis. *Nat Commun* (2018) 9(1):5208. doi: 10.1038/s41467-018-07635-7
- du Preez I, Luyes L, Loots DT. The Application of Metabolomics Toward Pulmonary Tuberculosis Research. *Tuberculosis (Edinb)* (2019) 115:126–39. doi: 10.1016/j.tube.2019.03.003
- Iliaz S, Iliaz R, Ortakoylu G, Bahadır A, Bağcı BA, Caglar E. Value of Neutrophil/Lymphocyte Ratio in the Differential Diagnosis of Sarcoidosis and Tuberculosis. *Ann Thorac Med* (2014) 9(4):232–5. doi: 10.4103/1817-1737.140135
- Adekambi T, Ibegbu CC, Cagle S, Kalokhe AS, Wang YF, Hu Y, et al. Biomarkers on Patient T Cells Diagnose Active Tuberculosis and Monitor Treatment Response. *J Clin Invest* (2015) 125(5):1827–38. doi: 10.1172/JCI77990
- Musvosvi M, Duffy D, Filander E, Africa H, Mabwe S, Jaxa L, et al. T-Cell Biomarkers for Diagnosis of Tuberculosis: Candidate Evaluation by a Simple Whole Blood Assay for Clinical Translation. *Eur Respir J* (2018) 51(3):1800153. doi: 10.1183/13993003.00153-2018
- Tang G, Yuan X, Luo Y, Lin Q, Chen Z, Xing X, et al. Establishing Immune Scoring Model Based on Combination of the Number, Function, and Phenotype of Lymphocytes. *Aging (Albany NY)* (2020) 12(10):9328–43. doi: 10.18632/aging.103208
- Luo Y, Xie Y, Zhang W, Lin Q, Tang G, Wu S, et al. Combination of Lymphocyte Number and Function in Evaluating Host Immunity. *Aging (Albany NY)* (2019) 11(24):12685–707. doi: 10.18632/aging.102595
- Hou H, Zhou Y, Yu J, Mao L, Bosco MJ, Wang J, et al. Establishment of the Reference Intervals of Lymphocyte Function in Healthy Adults Based on IFN-gamma Secretion Assay Upon Phorbol-12-Myristate-13-Acetate/Ionomycin Stimulation. *Front Immunol* (2018) 9:172. doi: 10.3389/fimmu.2018.00172
- Hou H, Luo Y, Wang F, Yu J, Li D, Sun Z. Evaluation of Lymphocyte Function by IFN-gamma Secretion Capability Assay in the Diagnosis of Lymphoma-Associated Hemophagocytic Syndrome. *Hum Immunol* (2019) 80(12):1006–11. doi: 10.1016/j.humimm.2019.09.003
- Lin Q, Wang Y, Luo Y, Tang G, Li S, Zhang Y, et al. The Effect of Host Immunity on Predicting the Mortality of Carbapenem-Resistant Organism Infection. *Front Cell Infect Microbiol* (2020) 10:480. doi: 10.3389/fcimb.2020.00480
- DeLong ER, DeLong DM, Clarke-Pearson DL. Comparing the Areas Under Two or More Correlated Receiver Operating Characteristic Curves: A Nonparametric Approach. *Biometrics* (1988) 44(3):837–45. doi: 10.2307/2531595
- Keshavjee S, Amanullah F, Cattamanchi A, Chaisson R, Dobos KM, Fox GJ, et al. Moving Toward Tuberculosis Elimination: Critical Issues for Research in Diagnostics and Therapeutics for Tuberculosis Infection. *Am J Respir Crit Care Med* (2019) 199(5):564–71. doi: 10.1164/rccm.201806-1053PP
- Komiyama K, Yamasue M, Takahashi O, Hiramatsu K, Kadota JI, Kato S. The COVID-19 Pandemic and the True Incidence of Tuberculosis in Japan. *J Infect* (2020) 81(3):e24–5. doi: 10.1016/j.jinf.2020.07.004
- Lai CC, Yu WL. The COVID-19 Pandemic and Tuberculosis in Taiwan. *J Infect* (2020) 81(2):e159–61. doi: 10.1016/j.jinf.2020.06.014

39. World Health Organization. *A Global Strategy for Tuberculosis Research and Innovation* Vol. 19. Switzerland: Geneva (2020). Available at: <https://apps.who.int/iris/rest/bitstreams/1312195/retrieve>.
40. World Health Organization. *Framework for the Evaluation of New Tests for Tuberculosis Infection* (2020). Available at: <https://apps.who.int/iris/rest/bitstreams/1288536/retrieve>.
41. Arnold A, Cooke GS, Kon OM, Dedicoat M, Lipman M, Loyse A, et al. Drug Resistant TB: UK Multicentre Study (DRUMS): Treatment, Management and Outcomes in London and West Midlands 2008–2014. *J Infect* (2017) 74(3):260–71. doi: 10.1016/j.jinf.2016.12.005
42. Pradipta IS, Forsman LD, Bruchfeld J, Hak E, Alffenaar JW. Risk Factors of Multidrug-Resistant Tuberculosis: A Global Systematic Review and Meta-Analysis. *J Infect* (2018) 77(6):469–78. doi: 10.1016/j.jinf.2018.10.004
43. Xu C, Pang Y, Li R, Ruan Y, Wang L, Chen M, et al. Clinical Outcome of Multidrug-Resistant Tuberculosis Patients Receiving Standardized Second-Line Treatment Regimen in China. *J Infect* (2018) 76(4):348–53. doi: 10.1016/j.jinf.2017.12.017
44. Outhred AC, Britton PN, Marais BJ. Drug-Resistant Tuberculosis – Primary Transmission and Management. *J Infect* (2017) 74:S128–35. doi: 10.1016/S0163-4453(17)30203-7
45. Lange C, Chesov D, Heyckendorf J, Leung CC, Udawadia Z, Dheda K. Drug-Resistant Tuberculosis: An Update on Disease Burden, Diagnosis and Treatment. *Respirology* (2018) 23(7):656–73. doi: 10.1111/resp.13304
46. Zumla A, Chakaya J, Centis R, D'Ambrosio L, Mwaba P, Bates M, et al. Tuberculosis Treatment and Management—An Update on Treatment Regimens, Trials, New Drugs, and Adjunct Therapies. *Lancet Respir Med* (2015) 3(3):220–34. doi: 10.1016/S2213-2600(15)00063-6
47. Hatherill M, Chaisson RE, Denkiner CM. Addressing Critical Needs in the Fight to End Tuberculosis With Innovative Tools and Strategies. *PLoS Med* (2019) 16(4):e1002795. doi: 10.1371/journal.pmed.1002795
48. Churchyard GJ, Swindells S. Controlling Latent TB Tuberculosis Infection in High-Burden Countries: A Neglected Strategy to End TB. *PLoS Med* (2019) 16(4):e1002787. doi: 10.1371/journal.pmed.1002787
49. Genel F, Atlihan F, Ozsu E, Ozbek E. Monocyte HLA-DR Expression as Predictor of Poor Outcome in Neonates With Late Onset Neonatal Sepsis. *J Infect* (2010) 60(3):224–8. doi: 10.1016/j.jinf.2009.12.004
50. Liu Z, Long W, Tu M, Chen S, Huang Y, Wang S, et al. Lymphocyte Subset (CD4+, CD8+) Counts Reflect the Severity of Infection and Predict the Clinical Outcomes in Patients With COVID-19. *J Infect* (2020) 81(2):318–56. doi: 10.1016/j.jinf.2020.03.054
51. Luo Y, Mao L, Yuan X, Xue Y, Lin Q, Tang G, et al. Prediction Model Based on the Combination of Cytokines and Lymphocyte Subsets for Prognosis of SARS-CoV-2 Infection. *J Clin Immunol* (2020) 40(7):960–9. doi: 10.1007/s10875-020-00821-7
52. Lancioni C, Swarbrick GM, Park B, Nyendak M, Nsereko M, Mayanja-Kizza H, et al. Recognition of CD8(+) T Cell Epitopes to Identify Adults With Pulmonary Tuberculosis. *Eur Respir J* (2019) 53(5):1802053. doi: 10.1183/13993003.02053-2018
53. Bussi C, Gutierrez MG. Mycobacterium Tuberculosis Infection of Host Cells in Space and Time. *FEMS Microbiol Rev* (2019) 43(4):341–61. doi: 10.1093/femsre/fuz006
54. Halliday A, Whitworth H, Kottoor SH, Niazi U, Menzies S, Kunst H, et al. Stratification of Latent Mycobacterium Tuberculosis Infection by Cellular Immune Profiling. *J Infect Dis* (2017) 215(9):1480–7. doi: 10.1093/infdis/jix107
55. Luo Y, Xue Y, Lin Q, Tang G, Yuan X, Mao L, et al. A Combination of Iron Metabolism Indexes and Tuberculosis-Specific Antigen/Phytohemagglutinin Ratio for Distinguishing Active Tuberculosis From Latent Tuberculosis Infection. *Int J Infect Dis* (2020) 97:190–6. doi: 10.1016/j.ijid.2020.05.109
56. Luo Y, Xue Y, Yuan X, Lin Q, Tang G, Mao L, et al. Combination of Prealbumin and Tuberculosis-Specific Antigen/Phytohemagglutinin Ratio for Discriminating Active Tuberculosis From Latent Tuberculosis Infection. *Int J Clin Pract* (2020) 75(4):e13831. doi: 10.1111/ijcp.13831
57. Silveira-Mattos PS, Barreto-Duarte B, Vasconcelos B, Fukutani KF, Vinhaes CL, Oliveira-de-Souza D, et al. Differential Expression of Activation Markers by Mycobacterium Tuberculosis-Specific CD4+ T-Cell Distinguishes Extrapulmonary From Pulmonary Tuberculosis and Latent Infection. *Clin Infect Dis* (2020) 71(8):1905–11. doi: 10.1093/cid/ciz1070
58. Liao CH, Lai CC, Tan CK, Chou CH, Hsu HL, Tasi TH, et al. False-Negative Results by Enzyme-Linked Immunosorbent Assay for Interferon-Gamma Among Patients With Culture-Confirmed Tuberculosis. *J Infect* (2009) 59(6):421–3. doi: 10.1016/j.jinf.2009.09.012
59. Pan L, Jia H, Liu F, Sun H, Gao M, Du F, et al. Risk Factors for False-Negative T-SPOT.TB Assay Results in Patients With Pulmonary and Extra-Pulmonary TB. *J Infect* (2015) 70(4):367–80. doi: 10.1016/j.jinf.2014.12.018
60. Nguyen DT, Teeter LD, Graves J, Graviss EA. Characteristics Associated With Negative Interferon-Gamma Release Assay Results in Culture-Confirmed Tuberculosis Patients, Texas, USA, 2013–2015. *Emerg Infect Dis* (2018) 24(3):534–40. doi: 10.3201/eid2403.171633
61. Luo Y, Tang G, Lin Q, Mao L, Xue Y, Yuan X, et al. Combination of Mean Spot Sizes of ESAT-6 Spot-Forming Cells and Modified Tuberculosis-Specific Antigen/Phytohemagglutinin Ratio of T-SPOT.TB Assay in Distinguishing Between Active Tuberculosis and Latent Tuberculosis Infection. *J Infect* (2020) 81(1):81–9. doi: 10.1016/j.jinf.2020.04.038
62. Won EJ, Choi JH, Cho YN, Jin HM, Kee HJ, Park YW, et al. Biomarkers for Discrimination Between Latent Tuberculosis Infection and Active Tuberculosis Disease. *J Infect* (2017) 74(3):281–93. doi: 10.1016/j.jinf.2016.11.010
63. Suzukawa M, Takeda K, Akashi S, Asari I, Kawashima M, Ohshima N, et al. Evaluation of Cytokine Levels Using QuantiFERON-TB Gold Plus in Patients With Active Tuberculosis. *J Infect* (2020) 80(5):547–53. doi: 10.1016/j.jinf.2020.02.007
64. Adankwah E, Nausch N, Minadzi D, Abass MK, Franken K, Ottenhoff THM, et al. Interleukin-6 and Mycobacterium Tuberculosis Dormancy Antigens Improve Diagnosis of Tuberculosis. *J Infect* (2020) 82(2):245–52. doi: 10.1016/j.jinf.2020.11.032
65. Wang F, Hou H, Xu L, Jane M, Peng J, Lu Y, et al. Mycobacterium Tuberculosis-Specific TNF-alpha Is a Potential Biomarker for the Rapid Diagnosis of Active Tuberculosis Disease in Chinese Population. *PLoS One* (2013) 8(11):e79431. doi: 10.1371/journal.pone.0079431
66. Sudbury EL, Clifford V, Messina NL, Song R, Curtis N. Mycobacterium Tuberculosis-Specific Cytokine Biomarkers to Differentiate Active TB and LTBI: A Systematic Review. *J Infect* (2020) 81(6):873–81. doi: 10.1016/j.jinf.2020.09.032
67. Acharya MP, Pradeep SP, Murthy VS, Chikkannaiah P, Kambar V, Narayanashetty S, et al. CD38 +CD27 -TNF-Alpha + on Mtb-specific CD4 + T Is a Robust Biomarker for Tuberculosis Diagnosis. *Clin Infect Dis* (2021). doi: 10.1093/cid/ciab144
68. Rodrigues DS, Medeiros EA, Weckx LY, Bonnez W, Salomao R, Kallas EG. Immunophenotypic Characterization of Peripheral T Lymphocytes in Mycobacterium Tuberculosis Infection and Disease. *Clin Exp Immunol* (2002) 128(1):149–54. doi: 10.1046/j.1365-2249.2002.01809.x
69. Liu Y, Wang R, Jiang J, Cao Z, Zhai F, Sun W, et al. A Subset of CD1c(+) Dendritic Cells Is Increased in Patients With Tuberculosis and Promotes Th17cell Polarization. *Tuberculosis (Edinb)* (2018) 113:189–99. doi: 10.1016/j.tube.2018.10.007
70. Simmons JD, Stein CM, Seshadri C, Campo M, Alter G, Fortune S, et al. Immunological Mechanisms of Human Resistance to Persistent Mycobacterium Tuberculosis Infection. *Nat Rev Immunol* (2018) 18(9):575–89. doi: 10.1038/s41577-018-0025-3
71. Kozakiewicz L, Chen Y, Xu J, Wang Y, Dunussi-Joannopoulos K, Ou Q, et al. B Cells Regulate Neutrophilia During Mycobacterium Tuberculosis Infection and BCG Vaccination by Modulating the Interleukin-17 Response. *PLoS Pathog* (2013) 9(7):e1003472. doi: 10.1371/journal.ppat.1003472
72. Achkar JM, Chan J, Casadevall A. B Cells and Antibodies in the Defense Against Mycobacterium Tuberculosis Infection. *Immunol Rev* (2015) 264(1):167–81. doi: 10.1111/imr.12276

**Conflict of Interest:** The authors declare that the research was conducted in the absence of any commercial or financial relationships that could be construed as a potential conflict of interest.

Copyright © 2021 Luo, Xue, Tang, Cai, Yuan, Lin, Song, Liu, Mao, Zhou, Chen, Zhu, Liu, Wu, Wang and Sun. This is an open-access article distributed under the terms of the Creative Commons Attribution License (CC BY). The use, distribution or reproduction in other forums is permitted, provided the original author(s) and the copyright owner(s) are credited and that the original publication in this journal is cited, in accordance with accepted academic practice. No use, distribution or reproduction is permitted which does not comply with these terms.





# Pre-Treatment Neutrophil Count as a Predictor of Antituberculosis Therapy Outcomes: A Multicenter Prospective Cohort Study

## OPEN ACCESS

### Edited by:

Christof Geldmacher,  
University of Munich, Germany

### Reviewed by:

David M. Lowe,  
University College London,  
United Kingdom  
Edward Charles Jones-Lopez,  
University of Southern California,  
United States

### \*Correspondence:

Afrânio L. Kritski  
kritski@gmail.com

<sup>†</sup>These authors have contributed  
equally to this work

### Specialty section:

This article was submitted to  
Microbial Immunology,  
a section of the journal  
Frontiers in Immunology

**Received:** 31 January 2021

**Accepted:** 01 June 2021

**Published:** 02 July 2021

### Citation:

Carvalho ACC, Amorim G,  
Melo MGM, Silveira AKA,  
Vargas PHL, Moreira ASR,  
Rocha MS, Souza AB, Arriaga MB,  
Araújo-Pereira M, Figueiredo MC,  
Durovni B, Lapa-e-Silva JR,  
Cavalcante S, Rolla VC, Sterling TR,  
Cordeiro-Santos M, Andrade BB,  
Silva EC, Kritski AL and the RePORT  
Brazil consortium (2021)  
Pre-Treatment Neutrophil Count  
as a Predictor of Antituberculosis  
Therapy Outcomes: A Multicenter  
Prospective Cohort Study.  
Front. Immunol. 12:661934.  
doi: 10.3389/fimmu.2021.661934

Anna Cristina C. Carvalho<sup>1,2†</sup>, Gustavo Amorim<sup>3†</sup>, Mayla G. M. Melo<sup>2,4†</sup>,  
Ana Karla A. Silveira<sup>2,4</sup>, Pedro H. L. Vargas<sup>2,4</sup>, Adriana S. R. Moreira<sup>2</sup>,  
Michael S. Rocha<sup>5,6</sup>, Alexandra B. Souza<sup>7</sup>, María B. Arriaga<sup>5,8,9</sup>,  
Mariana Araújo-Pereira<sup>5,8,9</sup>, Marina C. Figueiredo<sup>10</sup>, Betina Durovni<sup>11</sup>,  
José R. Lapa-e-Silva<sup>2</sup>, Solange Cavalcante<sup>11</sup>, Valeria C. Rolla<sup>12</sup>, Timothy R. Sterling<sup>10†</sup>,  
Marcelo Cordeiro-Santos<sup>7†</sup>, Bruno B. Andrade<sup>5,8,9,10,13,14†</sup>, Elisângela C. Silva<sup>2,4,15†</sup>,  
Afrânio L. Kritski<sup>2,4†</sup> and the RePORT Brazil consortium

<sup>1</sup> Laboratório de Inovações em Terapias, Ensino e Bioprodutos (LITEB), Instituto Oswaldo Cruz, Fundação Oswaldo Cruz, Rio de Janeiro, Brazil, <sup>2</sup> Programa Acadêmico de Tuberculose da Faculdade de Medicina, Universidade Federal do Rio de Janeiro, Rio de Janeiro, Brazil, <sup>3</sup> Department of Biostatistics, Vanderbilt University Medical Center, Nashville, TN, United States, <sup>4</sup> Laboratório de Micobacteriologia Molecular, Faculdade de Medicina e Complexo Hospitalar Hospital Universitário Clementino Fraga Filho—Instituto de Doenças do Tórax da Universidade Federal do Rio de Janeiro, Rio de Janeiro, Brazil, <sup>5</sup> Multinational Organization Network Sponsoring Translational and Epidemiological Research (MONSTER) Initiative, Salvador, Brazil, <sup>6</sup> Instituto Brasileiro para Investigação da Tuberculose, Fundação José Silveira, Salvador, Brazil, <sup>7</sup> Gerência de Micobacteriologia, Fundação de Medicina Tropical Doutor Heitor Vieira Dourado, Manaus, Brazil, <sup>8</sup> Laboratório de Inflamação e Biomarcadores, Instituto Gonçalo Moniz, Fundação Oswaldo Cruz, Salvador, Brazil, <sup>9</sup> Faculdade de Medicina, Universidade Federal da Bahia, Salvador, Brazil, <sup>10</sup> Division of Infectious Diseases, Department of Medicine, Vanderbilt University School of Medicine, Nashville, TN, United States, <sup>11</sup> Secretaria Municipal de Saúde do Rio de Janeiro, Rio de Janeiro, Brazil, <sup>12</sup> Instituto Nacional de Infectologia Evandro Chagas, Fundação Oswaldo Cruz, Rio de Janeiro, Brazil, <sup>13</sup> Curso de Medicina, Escola Bahiana de Medicina e Saúde Pública, Salvador, Brazil, <sup>14</sup> Curso de Medicina, Universidade Salvador (UNIFACS), Salvador, Brazil, <sup>15</sup> Laboratório Reconhecer Biologia, Centro de Biociência e Biotecnologia, Universidade Estadual do Norte Fluminense Darcy Ribeiro, Rio de Janeiro, Brazil

**Background:** Neutrophils have been associated with lung tissue damage in many diseases, including tuberculosis (TB). Whether neutrophil count can serve as a predictor of adverse treatment outcomes is unknown.

**Methods:** We prospectively assessed 936 patients (172 HIV-seropositive) with culture-confirmed pulmonary TB, enrolled in a multicenter prospective cohort study from different regions in Brazil, from June 2015 to June 2019, and were followed up to two years. TB patients had a baseline visit before treatment (month 0) and visits at month 2 and 6 (or at the end of TB treatment). Smear microscopy, and culture for *Mycobacterium tuberculosis* (MTB) were performed at TB diagnosis and during follow-up. Complete blood counts were measured at baseline. Treatment outcome was defined as either unfavorable (death, treatment failure or TB recurrence) or favorable (cure or treatment completion). We performed multivariable logistic regression, with propensity score regression adjustment, to estimate the association between neutrophil count with MTB culture result at month 2 and unfavorable treatment outcome. We used a propensity score adjustment instead of a fully adjusted regression model due to the relatively low number of outcomes.

**Results:** Among 682 patients who had MTB culture results at month 2, 40 (5.9%) had a positive result. After regression with propensity score adjustment, no significant association between baseline neutrophil count ( $10^3/\text{mm}^3$ ) and positive MTB culture at month 2 was found among either HIV-seronegative (OR = 1.06, 95% CI = [0.95;1.19] or HIV-seropositive patients (OR = 0.77, 95% CI = [0.51; 1.20]). Of 691 TB patients followed up for at least 18 months and up to 24 months, 635 (91.9%) were either cured or completed treatment, and 56 (8.1%) had an unfavorable treatment outcome. A multivariable regression with propensity score adjustment found an association between higher neutrophil count ( $10^3/\text{mm}^3$ ) at baseline and unfavorable outcome among HIV-seronegative patients [OR= 1.17 (95% CI= [1.06;1.30]). In addition, adjusted Cox regression found that higher baseline neutrophil count ( $10^3/\text{mm}^3$ ) was associated with unfavorable treatment outcomes overall and among HIV-seronegative patients (HR= 1.16 (95% CI = [1.05;1.27]).

**Conclusion:** Increased neutrophil count prior to anti-TB treatment initiation was associated with unfavorable treatment outcomes, particularly among HIV-seronegative patients. Further prospective studies evaluating neutrophil count in response to drug treatment and association with TB treatment outcomes are warranted.

**Keywords:** tuberculosis, neutrophils, treatment outcome, biomarker, neutrophil count

## INTRODUCTION

Neutrophils have been implicated in TB pathogenesis (1, 2). Several studies in animal models as well as in humans have revealed a prominent role of neutrophils in tissue damage during active TB, leading to more severe clinical presentations (3). There are increasing evidence that the neutrophil number and degree of neutrophil activation directly correlate with the degree of lung destruction seen in pulmonary TB (4). More recently, Ndlovu et al. described that high peripheral neutrophil count and low CD15 expression directly correlated with more severe lung damage on chest x-ray (5).

Neutrophils are also relevant for TB diagnosis, as several transcriptomic signatures indicate enriched pathways involving this cell type that can be used to distinguish active from latent TB infection (6).

Although several studies have evaluated the association between blood neutrophils and unfavorable TB treatment outcome (4, 7–14), there are limited data from well-powered prospective studies. A key advantage of neutrophils as a biomarker is that they can be measured in clinical laboratories in resource-limited settings.

To evaluate the relationship between blood neutrophil count and poor TB treatment outcome (i.e., treatment failure, mortality or relapse), we analyzed patients with positive *Mycobacterium tuberculosis* (MTB) culture of respiratory samples enrolled in the Regional Prospective Observational Research on Tuberculosis (RePORT) - Brazil cohort (15).

## METHODS

### Study Design

We performed a multicenter prospective observational cohort study of individuals with culture-confirmed pulmonary TB. All

study participants were enrolled in Regional Prospective Observational Research on Tuberculosis (RePORT)-Brazil (15), between June 2015 and June 2019, and were followed for up to two years. RePORT-Brazil includes two prospective cohorts: patients with pulmonary TB, and their close contacts. Objectives include the identification of clinical, radiological and laboratory variables associated with TB treatment outcome, and predictive of TB disease among contacts. Study sites were located in Rio de Janeiro State, Southeastern region (Centro Municipal de Saúde de Duque de Caxias - site A; Instituto Nacional de Infectologia Evandro Chagas - site D; Clínica da Família Rinaldo Delamare-site E); in the cities of Manaus, Northern region (site B), and Salvador, Northeastern region (site C).

These sites represent Brazilian cities with the highest TB burden (16). Site B and site D are HIV reference centers. In this study, we enrolled participants who had microbiologically confirmed TB, were over 18 years of age and provided written informed consent. Those who received anti-TB drugs (including fluoroquinolones) for more than 7 days in the 30 days prior to TB diagnosis were excluded. A trained nursing team conducted patient interviews and collected sociodemographic and clinical data. Participants underwent the following tests: chest radiograph, HIV testing, CD4 and viral load (if HIV-seropositive), complete blood count, glycated hemoglobin (HbA1c), sputum smear microscopy, Xpert-MTB-RIF (if available), mycobacterial culture (Lowenstein-Jensen medium or BD BACTEC MGIT) and drug susceptibility testing (proportion method or BD BACTEC GIT). The study participants had a baseline visit (M0) and follow-up visits at month 2 (M2) and month 6 (M6 or at the end of TB treatment), when clinical status was reassessed, and new smear/culture tests

were performed. Only drug susceptible TB patients followed up at least 2 months were included in the microbiological analysis; participants received standard 6-month treatment for TB, consisting of isoniazid, rifampicin, pyrazinamide, and ethambutol for 2 months followed by isoniazid and rifampicin for at least 4 months, following Brazilian National guidelines for TB control (16).

## Study Definitions and Procedures

Complete blood counts were performed only at baseline. Anemia was defined as hemoglobin levels <12 g/dL for females and <13.5 g/dL for males. Diabetes mellitus (DM) was diagnosed according to the baseline HbA1c, following the American Diabetes Association (ADA) guidelines (17). Patients with HbA1c  $\geq$  5.7% were classified as having dysglycemia and, among those, they were classified as having DM if HbA1c  $\geq$  6.5%, prediabetes (pre-DM) if HbA1c was between 5.7% and 6.4%. Patients with HbA1c lower than 5.7% were considered normoglycemic. Data on other variables such as age, sex, HIV serology, race/skin color (self-reported), body mass index (BMI), BCG scar, education level, income status, tobacco smoking status, alcohol consumption (according to CAGE questionnaire), illicit drug use, cavitation on chest radiograph and study site were obtained from all participants. Information about the symptoms of TB was also obtained at the baseline and at M2 and M6 visits. Neutrophil count at baseline as well as sputum smear and MTB culture results at month 2 were recorded. Treatment outcome was defined as either unfavorable (death from any cause, treatment failure or TB recurrence) or favorable (cure or treatment completion) following the World Health Organization (WHO) guidelines (18). Patients lost to follow-up were not included in the analysis of neutrophil count and TB treatment outcome.

## Data Analysis

Quantitative variables were presented as medians and interquartile ranges (IQR) and qualitative variables as percentages. The effect of baseline characteristics on the outcome of interest were computed *via* univariable logistic regression. P-values were computed *via* Wald tests.

Logistic regression analysis was also used to estimate associations between neutrophil count at baseline with smear microscopy, culture conversion at month 2 and TB treatment outcome, adjusting for HIV serology (and an interaction term). This was denoted as unadjusted logistic regression, since it did not take into account potential confounders. Data on the following clinical factors were collected: COPD; renal disease; hypertension; chemotherapy or radiotherapy; immunosuppressor drug (corticosteroid) and were included in the propensity score model.

Because the number of outcomes was relatively low, we were unable to fit a fully adjusted regression model including all covariates of interest. Instead, we fit a logistic regression model using propensity score adjustment (19). Propensity score adjustment, which may be seen as a variable reduction technique, is a two-step procedure: 1) in the first step, the propensity score is estimated by regressing the exposure variable on a set of covariates and 2) in the second step, the outcome of interest is regressed on the exposure while

controlling for the estimated propensity score, obtained in step 1. By this way any extra confounder is included in the outcome model *via* the estimated propensity score.

For our setting, the propensity score was fit *via* an ordinal regression, by regressing the exposure variable on a set of pre-specified covariates. We followed simulation results from (20), which showed better performance (i.e., smaller errors) when a fine stratification (20 strata) of the exposure was used and modelled *via* robust approaches, such as ordinal regression, that required no assumptions about underlying distributions. This propensity score model is constructed in the step 1 outlined above. It used the following covariates for adjustment: sex, age, race, smoking status, alcohol consumption, education level, income status, HIV serology status, cavitation on chest radiograph, DOT use (for TB treatment outcome only), study site, and (log-transformed) platelets, lymphocytes, glycated hemoglobin and hemoglobin values. All variables were selected *a priori*, based on data from the literature and clinical plausibility. Restricted cubic splines with 3 knots equally spaced were used to relax the linearity assumption, and an interaction between age and sex was also added to the propensity score model.

This two-step procedure allowed us to fit a larger set of covariates in the first step (to estimate the propensity score) and a smaller model in step 2 (21). Our main model regressed the outcome of interest on neutrophil count at baseline, HIV status, and on the estimated propensity score. We also added an interaction term of neutrophil count and HIV status. This was denoted as an adjusted model, since it took into account several potential confounders in the estimated propensity score. We did not stratify the exposure in this second and final step; neutrophil count was in its natural, continuous scale. To allow for non-linearity, the estimated propensity score was in the logit scale.

Finally, results were expressed in terms of point estimates and 95% confidence intervals; odds ratios were calculated, for interpretation purposes, for every 1,000 change of neutrophil count. Missing values were imputed 20 times *via* Markov Carlo Chained Equations (22) and final estimates were obtained *via* Rubin's rule (23). All analyses were performed using the statistical software R (24).

## Ethical Approval

The protocol, consent form, and study documents were approved by the institutional review boards at the study sites. Participation was voluntary, and written informed consent was obtained from all participants.

## RESULTS

### Study Population

Sample size for all analysis are displayed in **Figure S1**. Population demographics and laboratory values are depicted in **Table 1**. A total of 936 patients were included in the analysis, of whom 172 (18.4%) were HIV-seropositive. The overall median age at enrollment was of 35 years (IQR = 25.0; 49.0) and most

**TABLE 1 |** Sociodemographic characteristics and laboratory values for the study population.

	[ALL] N=936
<b>Sociodemographic characteristics</b>	
Age at enrollment:	35.0 [25.0;49.0]
Race/skin color: Non-black	692 (74.0%)
Sex: Male	619 (66.1%)
Smoking: Yes	213 (22.8%)
Smoking (years)	15.0 [5.0;25.0]
Alcohol: Yes	424 (45.3%)
HIV: Positive	172 (18.4%)
BCG scar: Yes	809 (86.5%)
Alcohol (years)	13.0 [6.00;27.0]
X-ray cavitation: Yes	465 (50.0%)
Literate: Yes	889 (95.1%)
Education (years):	9.00 [6.00;12.0]
Income: more than minimum wage	299 (32.6%)
HIV treatment <sup>a</sup> : Yes	127 (73.8%)
CD4 (cells/mm <sup>3</sup> )	135 [63.5;298]
Study site:	
A	179 (19.1%)
B	267 (28.5%)
C	240 (25.6%)
D	124 (13.2%)
E	126 (13.5%)
<b>Laboratory values</b>	
Leukocytes (10 <sup>3</sup> /mm <sup>3</sup> )	8.49 [6.53;10.7]
Neutrophils (10 <sup>3</sup> /mm <sup>3</sup> )	6.05 [4.39;7.97]
Lymphocytes (10 <sup>2</sup> /mm <sup>3</sup> )	15.5 [11.8;19.5]
Hemoglobin (g/dL)	12.1 [10.7;13.4]
Anemia: Yes	534 (57.5%)
Platelet (10 <sup>4</sup> /mm <sup>3</sup> )	38.5 [30.9;47.9]
Glycosylated Hemoglobin (%) (n= 927)	5.80 [5.40;6.40]
Glycosylated Hemoglobin (%):	
<5.7	416 (44.9%)
5.7-6.5	297 (32.0%)
≥6.5	214 (23.1%)

Values are represented as frequency (%) or median with interquartile range (IQR). Smoking: current smoker (Yes/No); Alcohol: current (Yes/No); HIV (Positive/Negative); Literate: literacy (Yes/No); Income: monthly salary; CD4: CD4 count at baseline; Study site: sites covered by RePORT. Anemia: hemoglobin levels <12 g/dL for female and <13.5 g/dL for male; <sup>a</sup>ART frequency was calculated among the persons living with HIV; Study sites: A – Caxias Health Center/Rio de Janeiro, B- Tropical Medicine Foundation/Manaus; C: Jose Silveira Foundation/Salvador; D: Evandro Chagas Institute-Rio de Janeiro; E: Rocinha – Municipality of Rio de Janeiro.

were non-black (74.0%), male (66.1%), had anemia (57.5%), and a BCG scar (86.5%); 45.3% were alcohol users, and 23.1% had DM. Compared to HIV-seronegative patients, as depicted in **Tables S1** and **S2**, HIV-seropositive participants were more likely to be non-black (OR = 2.22; 95% CI = 1.44; 3.54), male (OR = 1.94; 95% CI = 1.33;2.89), more likely to be treated in HIV reference centers, sites (B and D) (OR= 22.7; 95% CI = 11.0;55.4 and OR= 7.33; 95% CI = 3.25;19.0, respectively) and to have anemia (OR = 2.57; 95% CI= 1.78;3.78). On the other hand, HIV-seropositive individuals with TB were less likely to be tobacco smokers (OR= 0.61; 95% CI = 0.39;0.93); alcohol users (OR= 0.52; 95% CI = 0.36;0.74); BCG vaccinated (OR = 0.48; 95% CI = 0.32;0.74); have lung cavitory lesions on chest X-ray (OR = 0.20; 95% CI = 0.13;0.29), have high lymphocytes count (OR = 0.91; 95% CI= 0.88;0.94) and high glycosylated hemoglobin (OR= 0.79; 95% CI= 0.70;0.89).

The median neutrophil count at baseline was 6,050 cells/μL (IQR = 4,390;7,970). HIV-seropositive patients had lower neutrophil count, 5,050 cells/μL (IQR = 3,590;7,250) compared to HIV-seronegative, 6,120 cells/μL (IQR = 4,630;8,090). This difference was statistically significant at the 5% level (OR=0.92; 95% CI = 0.86;0.97).

## Association Between Neutrophils and TB Bacillary Load in Sputum at Baseline

**Tables S3** and **S4** show univariable comparisons for association between sociodemographic and laboratory values with smear positivity at study baseline, respectively. Current tobacco smokers, alcohol users, and those with lung cavitation had higher odds of being smear positive at M0 (OR= 1.62; 95% CI= 1.07, 2.52; OR=1.52; 95% CI=1.09-2.13; and OR = 3.10; 95% CI = 2.18, 4.45, respectively). Leukocytes (OR = 1.11 [1.05;1.17]), neutrophil (OR=1.11 [1.04;1.18]), and platelet (OR=1.02 [1.01;1.03]) counts were also associated with positive smear results. HIV-seropositive patients were less likely to be smear positive at baseline (OR = 0.34, 95% CI = 0.23;0.49).

Unadjusted and adjusted logistic regression models were used to estimate the association between neutrophil count at baseline with the odds of being smear positive at baseline. Results suggested highly different neutrophil counts between seropositive and seronegative patients (p-value < 0.001). The adjusted regression showed a strong association between neutrophil count and smear result at baseline among HIV-seronegative patients: OR = 1.16, 95% CI = 1.07, 1.26. This association was not seen among HIV-seropositive patients: OR = 0.99, 95% CI = 0.82, 1.20, as depicted in **Table 2** and **Figure S2**.

## Factors Associated With No Sputum Smear Conversion During TB Treatment

A total of 713 patients had sputum smear result at M2, from which 126 (17.7%) were still smear positive. Univariable logistic regressions are presented in **Tables S5** and **S6**, for sociodemographic and laboratory values, respectively. Increased age (OR = 1.03, 95% CI = 1.01;1.04), years of smoking (OR=1.04 95% CI= 1.01;1.07); alcohol use (OR= 1.03, 95% CI= 1.01;1.05); anemia (OR=1.67, 95% CI =1.11;2.53), and DM (OR=1.81, 95% CI =1.10;2.96) had higher chance of having smear positive sputum at M2. HIV-seropositive patients were also on average more likely to be smear positive at M2 (OR = 1.74, 95% CI = 1.11;2.68). Univariable analysis showed that neutrophil count was not statistically associated with higher odds of being sputum smear positive at month 2, as suggested by the boxplots in **Figure S3** (OR = 1.00, 95% CI = 0.94; 1.07) and depicted in **Table S6**.

Neutrophil count, however, differed significantly by HIV status (p-value < 0.01). Smear positive sputum at M2 was associated with higher neutrophil count among HIV-seronegative patients in both unadjusted and adjusted (by the propensity score) analysis (OR = 1.08, 95% CI = 1.01;1.16 and OR = 1.08, 95% CI = 1.00;1.17, respectively). Interestingly, among HIV-seropositive patients, the unadjusted analysis suggested an association between higher neutrophil count and lower odds of a smear positive sputum at M2 (OR = 0.78, 95%



CI = 0.65; 0.94). The adjusted analysis showed that for every increase in the neutrophil count by 1,000 units, the odds of being sputum smear positive at month 2 decreased on average by ~22% (OR = 0.78, 95% CI = 0.62;0.99). Results for both unadjusted and adjusted regression with propensity score adjustment are displayed in **Table 2**.

It is important to note that the relationship between neutrophil and smear positive at month 2 may not be linear, in the sense that high and low neutrophil counts would lead to poor prognosis (especially among HIV-seronegative patients). To explore this further, we re-fitted the model, using restricted cubic splines, with 3 knots equally spaced, to relax the linearity assumption. **Figure S4** provides two plots of the log odds of having a positive smear result at month 2 by neutrophil count, for both HIV-seropositive and HIV-seronegative patients. The figure shows that, for HIV-seropositive patients, higher neutrophil count is associated with better prognosis (smaller odds of being smear positive at month 2). This increment, however, may not be linear; there is large uncertainty when neutrophil count increase (wider 95% confidence interval - grey area). Among HIV-seronegative patients, we see the opposite trend: higher neutrophil count lead to worse prognosis. The trend, again, may not be linear, as data become less frequent for higher values, increasing uncertainty (again, wider 95% confidence intervals as neutrophil count increases).

In summary, both plots support our results: HIV-seropositive patients with higher neutrophil count seem less likely to be smear positive at month 2, while HIV-seronegative patients with higher neutrophil count seem more likely to be smear positive at month 2. Although the relationship may not be linear (more data are needed to address this issue), it seems unlikely that low neutrophil count lead to poor prognosis among HIV-seronegative patients.

## Characteristics Associated With No Sputum Culture Conversion During TB Treatment

A total of 886 patients had a visit reported at M2. Of these, 176 did not provide a respiratory sample, 631 had negative culture results for MTB, 28 patients had contaminated culture and 51 had positive results, from which 40 were found to be positive for MTB and 11 for nontuberculous mycobacterial (NTM). A total of 682 TB patients with reported positive or negative culture

results were included in the analysis, of which 40 (7 HIV-seropositive) were positive for MTB at M2. The 11 NTM cultures were not included as positive.

Univariable logistic regressions are presented in **Tables S7** and **S8**, for demographic and laboratory values, respectively, stratified by MTB status. The following variables were associated with positive MTB culture at M2: older age (OR= 1.05; 95% CI= 1.05; 1.07) and years of smoking (OR=1.04; 95% CI= 1.01; 1.07). HIV serology status was not associated with culture result at M2 (OR = 0.83, 95% CI = 0.33;1.83, for HIV-seropositive as reference level).

Unadjusted and propensity score adjusted logistic regressions did not show evidence of association between neutrophil count and culture conversion at M2, as indicated by the boxplots in **Figure S5** (e.g., OR=1.06, 95% CI= 0.95;1.19 and OR=0.77, 95% CI= 0.51;1.20, for seronegative and seropositive patients, respectively, in the adjusted analysis). Results for both unadjusted and adjusted regressions are displayed in **Table 2**.

## Blood Neutrophil Count as a Predictor of Unfavorable Anti-TB Treatment Outcomes

A total of 691 TB patients, followed-up for at least 18 months and maximum of 24 months, were used for analysis. Among them, 635 (91.9%) were either cured or completed treatment without bacteriologic confirmation of cure, while 56 (8.1%) developed an unfavorable treatment outcome: 22 died (4 related to TB, 13 not caused by TB and 5 with reasons that are not clearly related to TB), 25 had treatment failure and 9 TB recurrence.

Their baseline sociodemographic and laboratory values are displayed in **Tables 3** and **4**, stratified by TB treatment outcome. The following variables were associated with an unfavorable TB outcome: HIV infection (OR= 3.82, 95% CI= 2.11;6.80), treated at a HIV reference center (site B) (OR= 3.82, 95% CI= 1.64;10.6), anemia (OR= 1.78, 95% CI= 1.00;3.30), DM (OR= 3.30, 95% CI= 1.65;6.83), pre-DM (OR=2.11, 95% CI=1.04;4.39). Patients with higher neutrophil count were also more likely to have unsuccessful treatment in a univariable analysis (OR= 1.10, 95% CI= 1.02; 1.19); i.e., increasing neutrophil count by 1,000 units, the odds of developing an unfavorable TB treatment increased, on average, by 10%, as suggested by **Figure 1**.

Neutrophil count was again statistically different between patients in opposite HIV serology groups (p-value < 0.01).

**TABLE 2 |** Association between neutrophil count at baseline and the outcome of interest.

Outcome variable	Strata (size)	Unadjusted analysis	Adjusted analysis <sup>†</sup>
Positive Smear result at baseline	HIV-seronegative (756)	1.16 [1.07;1.25]	1.16 [1.07; 1.26]
	HIV-seropositive (171)	0.99 [0.91;1.08]	0.99 [0.82; 1.20]
Positive Smear result at month 2	HIV-seronegative (564)	1.08 [1.01; 1.16]	1.08 [1.00; 1.17]
	HIV-seropositive (145)	0.78 [0.65; 0.94]	0.78 [0.62; 0.99]
Positive MTB culture at month 2	HIV-seronegative (540)	1.08 [0.98; 1.20]	1.06 [0.95; 1.19]
	HIV-seropositive (131)	0.78 [0.53; 1.15]	0.77 [0.51; 1.20]
Unfavorable TB treatment outcome	HIV-seronegative (577)	1.19 [1.08; 1.32]	1.17 [1.06; 1.30]
	HIV-seropositive (144)	0.99 [0.87; 1.13]	0.98 [0.77; 1.24]

Both analysis control for HIV serology and its interaction with baseline neutrophil. <sup>†</sup> Model adjusting for the propensity score, which was regressed on the following covariates: sex, age, race, smoking status, alcohol consumption, education level, income status, cavitation on chest radiograph, study site, HIV status, DOT (for unfavorable TB treatment outcome) and (log-transformed) platelets, lymphocytes, glycated hemoglobin and hemoglobin values; results expressed in odds ratios (OR) with 95% confidence intervals.

**TABLE 3 |** Sociodemographic characteristics, stratified by TB treatment outcome.

	Favorable treatment outcome N=635	Unfavorable treatment outcome N=56	P-value
Age at enrollment:	37.0 [26.0;49.0]	36.5 [25.0;49.5]	0.964
Race/skin color: Non-black	471 (74.3%)	42 (75.0%)	0.925
Sex: Male	404 (63.6%)	37 (66.1%)	0.725
HIV: Yes	92 (14.5%)	22 (39.3%)	<0.001
HIV treatment: Yes	72 (88.9%)	15 (93.8%)	0.631
CD4 (cells/mm <sup>3</sup> )	150 [63.5;358]	112 [62.8;161]	0.059
Smoking: Yes	131 (20.6%)	11 (19.6%)	0.884
Smoking (years)	16.0 [6.00;26.0]	11.0 [5.25;20.0]	0.173
Alcohol: Yes	281 (44.3%)	21 (37.5%)	0.334
BCG scar: Yes	549 (86.6%)	48 (85.7%)	0.827
Alcohol (years)	14.0 [7.00;28.0]	13.0 [5.50;23.0]	0.681
X-ray cavitation: Yes	328 (54.5%)	25 (48.1%)	0.378
Literate: Yes	32 (5.04%)	2 (3.57%)	0.687
Education (years):	10.0 [6.00;12.0]	9.00 [5.00;12.0]	0.265
Income: more than minimum wage	223 (35.9%)	18 (32.1%)	0.583
DOT: Yes	408 (64.7%)	34 (60.7%)	0.554
Study site:			
A	125 (19.7%)	6 (10.7%)	Ref.
B	154 (24.3%)	29 (51.8%)	0.001
C	163 (25.7%)	13 (23.2%)	0.327
D	85 (13.4%)	6 (10.7%)	0.528
E	108 (17.0%)	2 (3.57%)	0.261

Values are represented as frequency (%) or median with interquartile range (IQR). 95% confidence intervals are displayed. P-values computed via Wald tests. Smoking: current smoker (Yes/No); Alcohol: current (Yes/No) Literate: literacy (Yes/No); Income: monthly salary. CD4: CD4 count at baseline. Study site: sites covered by RePORT. Favorable outcome: cured or treatment completion; Unfavorable outcome: death, treatment failure, recurrence. OR, odds ratio; DOT, direct observed treatment. Study sites: A – Caxias Health Center/Rio de Janeiro, B – Tropical Medicine Foundation/Manaus; C: Jose Silveira Foundation/Salvador; D: Evandro Chagas Institute-Rio de Janeiro; E: Rocinha – Municipality of Rio de Janeiro.

**TABLE 4 |** Laboratory values, stratified by TB treatment outcome.

	Favorable treatment outcome N=635	Unfavorable treatment outcome N=56	P-value
Neutrophils (10 <sup>3</sup> /mm <sup>3</sup> )	5.98 [4.36;7.64]	7.24 [4.41;9.89]	0.014
Glycosylated Hemoglobin (%)	5.80 [5.40;6.30]	6.15 [5.75;6.73]	0.448
Platelet (10 <sup>4</sup> /mm <sup>3</sup> )	38.7 [31.1;47.2]	39.6 [32.0;50.6]	0.176
Lymphocytes (10 <sup>2</sup> /mm <sup>3</sup> )	15.7 [12.1;19.5]	14.4 [9.77;21.1]	0.870
Leukocytes (10 <sup>3</sup> /mm <sup>3</sup> )	8.48 [6.49;10.4]	10.1 [6.45;13.2]	0.051
Hemoglobin (g/dL)	12.2 [11.1;13.4]	10.7 [9.50;12.6]	<0.001
Anemia: Yes	355 (56.2%)	39 (69.6%)	0.050
Glycosylated Hemoglobin (%):			
<5.7	294 (46.6%)	14 (25.0%)	Ref.
5.7-6.5	198 (31.4%)	20 (35.7%)	0.038
≥6.5	139 (22.0%)	22 (39.3%)	0.001

Values are represented as frequency (%) or median with interquartile range (IQR). 95% confidence intervals are displayed. P-values computed via Wald tests. Favorable outcome: cured or treatment completion; Unfavorable outcome: death, treatment failure, recurrence. Anemia: hemoglobin levels <12 g/dL for female and <13.5 g/dL for male. OR, odds ratio.

Unadjusted regression analysis demonstrated a strong association between higher neutrophil count and unfavorable treatment outcomes (OR= 1.19, 95% CI= 1.08; 1.32), which was again detected in the logistic regression with propensity score adjustment (OR= 1.17, 95% CI= 1.06; 1.30). Among HIV-seropositive patients, however, which accounted for 61 subjects (22 with unfavorable outcome), no association between neutrophil count at M0 and unfavorable treatment outcome was observed in the unadjusted nor in the adjusted analysis (OR = 0.99, 95% CI = 0.87; 1.13 and OR = 0.98, 95% CI = 0.77; 1.24, respectively). Results for both unadjusted and adjusted regressions are displayed in **Table 2**.

As the unfavorable outcome group contained a very heterogenous group, we re-ran the analysis above for 4 additional settings: 1) discarding deaths that were not related to TB; 2) restricting the follow-up time to 9 months (so all 9 patients with TB recurrence were not included as an unfavorable TB treatment outcome); 3) re-analyzing unfavorable TB treatment outcome, under a mixed-effect perspective, with study site as a random effect in the main outcome regression model; and 4) re-analyzing unfavorable TB treatment outcome, adjusting for leukocytes. In this last analysis, (log-transformed) leukocytes were included in the propensity score model. Results for all of these analyses were similar to those provided above,

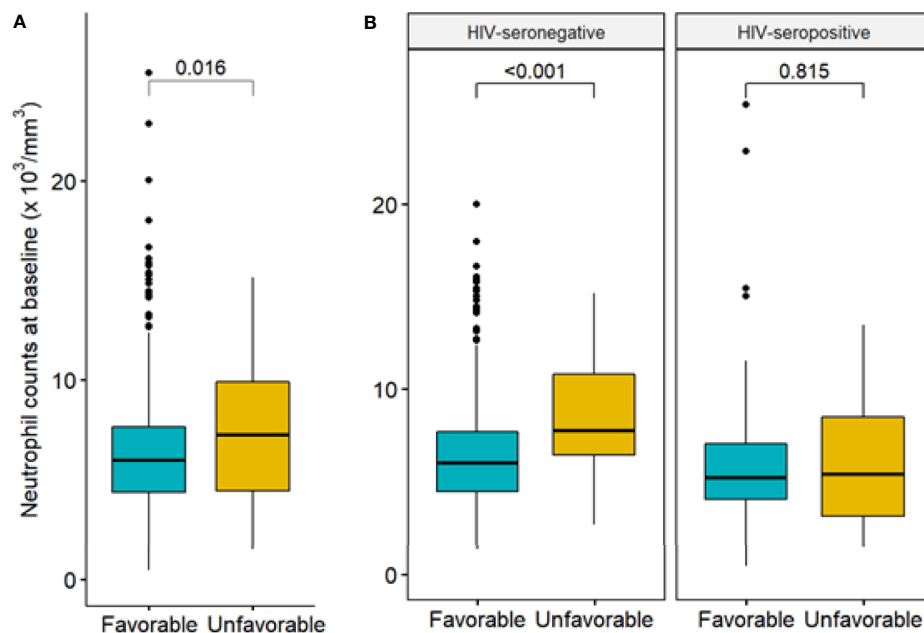


**FIGURE 1** | Neutrophil count at baseline by treatment outcome. **(A)** Comparison of neutrophil count at baseline by treatment outcome (favorable/unfavorable, among N=691 patients); **(B)** comparisons of neutrophil count by treatment outcome, stratified by HIV status (577 seronegative patients, with 34 unfavorable outcome, and 114 seropositive patients, with 22 unfavorable outcome). Favorable treatment: cure or treatment completion. Unfavorable treatment: death, failure, recurrence. P-value computed via Wald test.

with a statistically significant association between baseline neutrophil count with unfavorable treatment outcome among HIV-seronegative patients. These additional results are presented in **Table S9**.

**Figure 2** shows the Kaplan-Meier survival curve for time to unfavorable treatment outcome, by neutrophil count at baseline. The results indicated that higher neutrophil count at baseline was associated with higher chances of unfavorable treatment outcome. A Cox regression model with propensity score adjustment showed that neutrophil count differs substantially across HIV serology groups (p-value < 0.01). While the hazard of further developing an unfavorable treatment outcome was not significantly associated with neutrophil among HIV-seropositive patients, it was strongly associated with higher neutrophil count among HIV-seronegative patients. For every 1,000 units increase in neutrophil count at baseline, the hazard of further developing an unfavorable treatment outcome increased, on average, by 16% (HR= 1.16, 95% CI= 1.05; 1.27).

## DISCUSSION

Neutrophils have received prominence in the pathogenicity of TB, although few prospective well-powered studies have analyzed the role of blood neutrophil count in predicting treatment outcome of pulmonary TB patients.

The present study, performed in a well-characterized cohort of culture-confirmed pulmonary TB patients, found that pre-

treatment neutrophil count may serve as a reliable predictor of unfavorable TB treatment outcomes.

The association of neutrophil count with positive smear and cavity on chest radiograph was similar to those described by other groups (2, 5, 6). The association between higher neutrophil count and parenchymal findings in the chest radiogram was described by Kerkoff et al. (7) in HIV-seropositive and by de Mello et al. (2) in HIV-seronegative patients. Only in the study of Nodvlu et al. (5), who used radiological scores to analyze the extent of lung injury, the association between neutrophil count and chest radiographic findings was observed in both HIV-seropositive and negative patients.

In 2003, in addition to the presence of cavitation on chest radiograph, WHO guidelines recommended the sputum-smear examination at the end of the second month of treatment in patients with recently diagnosed pulmonary TB, and, if positive, the intensive phase of TB treatment should be extended (25). In recent years, it has been emphasized that culture conversion during treatment for TB has only a limited role in decision-making for advancing regimens into phase III trials or in predicting the outcome of treatment for individual patients (26, 27).

In our study, in univariable analysis, positive smear in month 2 was more frequent among older people, in patients infected with HIV, with anemia and DM. Neutrophil count was a statistically significant predictor at 5% level of positive smear in M2 only in TB/HIV-seronegative patients. Those results were also described by other authors (28–31).

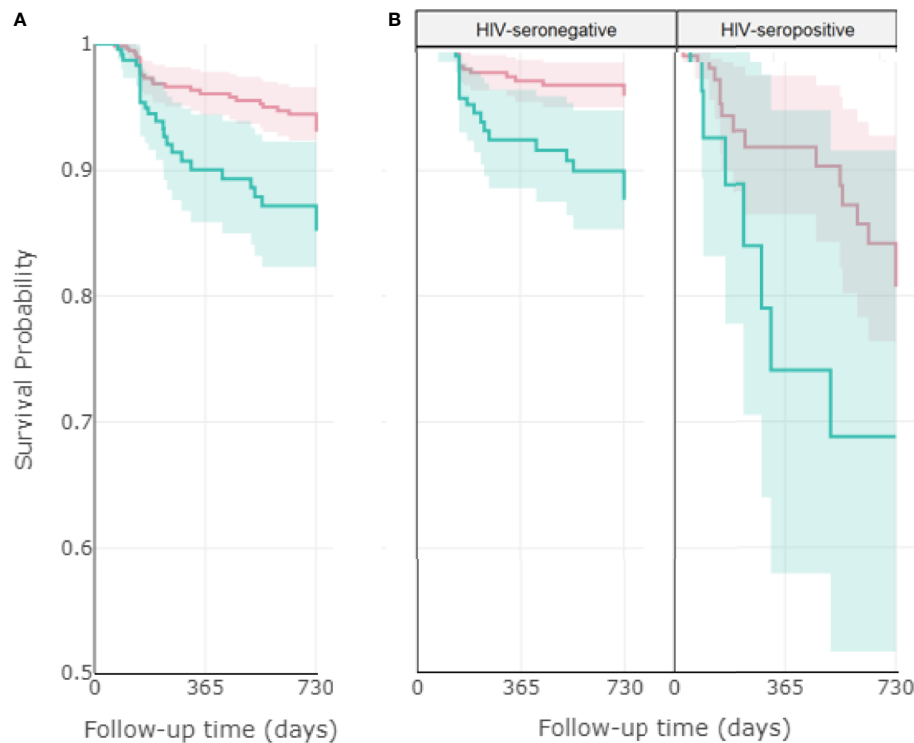


**FIGURE 2** | Association between neutrophil count at baseline with time until unfavorable treatment outcome. Kaplan-Meier curves comparing the impact of higher ( $>7500/\text{mm}^3$ ) and lower ( $<7500/\text{mm}^3$ ) neutrophil count at baseline on the probability of facing a favorable outcome, considering **(A)** the total population (919 patients), **(B)** stratified by HIV status (749 seronegative and 170 seropositive patients). The red line corresponds to low neutrophil count and the blue line corresponds to high neutrophil count, with their respective 95% confidence intervals. Favorable treatment: cure or treatment completion. Unfavorable treatment: death, failure, recurrence. Log rank p-values: 0.002 **(A)**,  $<0.001$  **(B, left)**, 0.1 **(B, right)**.

In addition, in the univariable analysis we identified the following variables associated with positive smear or culture results at M2: older age, smoking and alcohol use. Those results were also described in other series (28, 32, 33). Caetano Mota et al. (28), in a retrospective cohort of 136 adult patients with pulmonary TB confirmed by positive culture for MTB on sputum, found that older age was independently associated with delayed smear conversion. Nijenbandring de Boer et al. (32) evaluated 89 active pulmonary TB patients with positive sputum culture. After adjustment for cavities on the chest radiograph and alcohol use, they found that current tobacco smoking compared to current non-smoking remained significantly associated with culture non-conversion at 60 days of treatment anti-TB. Volkmann T et al. (33), using data reported to the National Tuberculosis Surveillance System in USA on 207,307 adult TB cases, confirmed that excess alcohol use was associated with lower rates of sputum culture conversion.

In our study, there was no significant association between neutrophil count at the beginning of TB treatment and positive culture at month 2, irrespective of HIV status. De Melo et al. (2) and Brambhat et al. (12) described similar results in TB/HIV-seronegative patients. Nodvlu et al. (5) reported an association between positive culture in month 2 and the level of CD15 expression, but not with neutrophil count at the time of TB

diagnosis, in both TB/HIV-seropositive and TB/HIV-seronegative patients.

In our large cohort of patients with pulmonary TB from high-burden cities in Brazil, the association of neutrophilia with unfavorable TB treatment outcome was confirmed in TB/HIV-seronegative patients, but not in TB/HIV-seropositive ones. Similar findings were described by other authors (5, 8, 13, 14). Barnes et al. (13), in USA, evaluating 191 consecutive HIV-seronegative adults with pulmonary TB found an association between neutrophil count and death. In the study of Lowe et al. (8), analyzing 855 TB patients with neutrophil count at baseline, neutrophilia was an independent risk for case fatality. Han et al. (14) carried out a retrospective study with 96 TB patients in South Korea. They found that high neutrophil/lymphocyte rate was also an independent predictor of in-hospital mortality.

On the other hand, HIV infection frequently reduces the neutrophil count (34). In addition, there is an impaired ability to phagocytize TB bacilli observed in TB/HIV-seropositive patients, but the phagocytosis capacity is restored after the use of antiretroviral therapy (35). In our cohort, median neutrophil count was lower in TB-HIV co-infected patients than in HIV-seronegative ones. Interestingly, we observed an inverse association between neutrophil count and smear-positivity in the sputum at M2 among HIV-seropositive patients, i.e., increasing neutrophil count



was associated with a lower chance of smear-positivity. This finding may indicate the importance of neutrophilic activity in the response to MTB infection. However, above a certain threshold, not yet determined, this exacerbated neutrophilic response cause tissue damage and may compromise TB outcome.

In the analysis of the association between neutrophilia and unfavorable TB treatment outcomes, abandonment and/or loss of follow-up were not included, as they could be confounding variables (35). As described in systematic meta-analysis/reviews (36–38) and more recently by Demitto et al. (30), we observed an association between unfavorable outcome and HIV infection, diabetes mellitus and anemia. The association between high neutrophil count, anemia and diabetes mellitus with unfavorable treatment outcome may result from a decrease in the ability of neutrophils to kill mycobacteria followed by a nonspecific inflammatory cascade, characterized by the production of cytokines and/or exacerbated necrotic cell death (2, 30, 31). Such events produce the accumulation of neutrophils due to persistence of systemic inflammation; similar results were described recently with Covid-19 (39). In addition, recent transcriptomic data obtained in whole blood from TB patients confirmed the signatures of neutrophils correlated with the radiographic extent of TB disease that decreased during the first 2 months of TB treatment (5). Together with other simple diagnostic tests, neutrophil monitoring could be valuable as a rule-out test and for identifying patients at baseline with a higher chance of unfavorable treatment outcome.

## Limitations

Collinearity, if there were any, was not an issue while estimating the propensity score. This is because the objective at this stage is to predict the propensity score, not inference.

We did not analyze other non-specific biomarkers of inflammatory response associated with severe pulmonary TB, such as C-reactive protein, albumin and globulin (2, 8, 40, 41). These proteins, produced by the liver, act as homeostasis breakers and thus, could potentially be used as biomarkers, in addition to the blood neutrophil count. Anemia and HbA1c could be additional variables that could be assessed in future studies. Furthermore, we used only biomarkers obtained from blood analysis, and therefore, it was not possible to analyze specific biomarkers associated with an immune response in the lung. In addition, the extent of lung involvement was not evaluated (42).

## Conclusion

In our cohort, high blood neutrophil count at baseline was associated with unfavorable TB treatment outcome in HIV-seronegative TB patients, but not in HIV-seropositive patients. We found no association between baseline neutrophil count and positive MTB culture at month 2. The knowledge of the association between high neutrophil count and unfavorable treatment outcome can potentially help the clinician guide care to improve outcomes in these high-risk patients. Our results reinforce the need to carry out further prospective studies to analyze the impact of host directed therapy, such as anti-inflammatory drugs, in patients with abnormal levels of simple biomarkers, such as neutrophil count.

## DATA AVAILABILITY STATEMENT

The raw data supporting the conclusions of this article will be made available by the authors upon request.

## ETHICS STATEMENT

The protocol, consent form, and study documents were approved by the institutional review boards at the study sites. Participation was voluntary, and written informed consent was obtained from all participants. The patients/participants provided their written informed consent to participate in this study.

## AUTHOR CONTRIBUTIONS

Conceptualization: AK, ES, MM. Data curation: GA, AK, ES, AC, MF, and MA-P. Investigation: AM, MR, AS, MA, MA-P, and ES. Formal analysis: MA, BD, JL, SC, VR, ES, TS, MC-S, BA, and AK. Funding acquisition: TS, BA, and AK. Methodology: AKS, PV, BD, JL, SC, VR, ES, TS, MC-S, BA, and AK. Project administration: MF, TS, BA, and AK. Resources: TS, BA, and AK. Software: GA. Supervision: AK and ES. Writing—original draft: AC, GA, ES, MM, TS, MC-S, BA, and AK. Writing—review and editing: all authors. All authors have read and agreed to the submitted version of the manuscript.

## FUNDING

Departamento de Ciência e Tecnologia, Ministério da Saúde, Brazil and the National Institutes of Allergy and Infectious Diseases, USA. The work of AK, BA, ES, GA, AC, MF, JL, SC, VR, BD, TS, and MC-S was supported by grants from NIH (U01AI069923, R01AI120790). BA, AK, and JL are senior scientists from the Conselho Nacional de Desenvolvimento Científico e Tecnológico (CNPq). MM received a scholarship from CNPq. MA received a scholarship from Fundação de Amparo à Pesquisa do Estado da Bahia (FAPESB). MA-P received a research fellowship from the Coordenação de Aperfeiçoamento de Pessoal de Nível Superior (CAPES, finance code: 001). The funders had no role in study design, data collection and analysis, decision to publish, or preparation of the manuscript.

## ACKNOWLEDGMENTS

The authors thank the study participants.

## SUPPLEMENTARY MATERIAL

The Supplementary Material for this article can be found online at: <https://www.frontiersin.org/articles/10.3389/fimmu.2021.661934/full#supplementary-material>

## REFERENCES

- Lyadova IV. Neutrophils in Tuberculosis: Heterogeneity Shapes the Way? *Mediators Inflamm* (2017) 2017. doi: 10.1155/2017/8619307
- de Melo MGM, Mesquita EDD, Oliveira MM, da Silva-Monteiro C, Silveira AKA, Malaquias TS, et al. Rede-TB Study Group. Imbalance of NET and Alpha-1-Antitrypsin in Tuberculosis Patients Is Related With Hyper Inflammation and Severe Lung Tissue Damage. *Front Immunol* (2019) 9:31471. doi: 10.3389/fimmu.2018.031471
- Robinson RT, Orme IM, Cooper AM. The Onset of Adaptive Immunity in the Mouse Model of Tuberculosis and the Factors That Compromise Its Expression. *Immunol Rev* (2015) 264(1):46–59. doi: 10.1111/imr.12259
- Muefong CN, Sutherland JS. Neutrophils in Tuberculosis-Associated Inflammation and Lung Pathology. *Front Immunol* (2020) 11:962. doi: 10.3389/fimmu.2020.00962
- Nodvlu LN, Peetluk L, Moodley S, Nhamoyebonde S, Ngoepe AT, Mazibuko M, et al. Increased Neutrophil Count and Decreased Neutrophil CD15 Expression Correlate With TB Disease Severity and Treatment Response Irrespective of HIV Co-Infection. *Front Immunol* (2020) 11:1872. doi: 10.3389/fimmu.2020.01872
- Bloom CI, Graham CM, Berry MP, Rozakeas F, Redford PS, Wang Y, et al. Transcriptional Blood Signatures Distinguish Pulmonary Tuberculosis, Pulmonary Sarcoidosis, Pneumonias and Lung Cancers. *PLoS One* (2013) 8:8. doi: 10.1371/annotation/7d9ec449-ae0-48fe-8111-0c110850c0c1
- Kerkhoff AD, Wood R, Lowe DM, Vogt M, Lawn SD. Blood Neutrophil Count in HIV-Infected Patients With Pulmonary Tuberculosis: Association With Sputum Mycobacterial Load. *PLoS One* (2013) 8(7):e67956. doi: 10.1371/journal.pone.0067956
- Lowe DM, Bandara AK, Packe GE, Barker RD, Wilkinson RJ, Griffiths CJ, et al. Neutrophilia Independently Predicts Death in Tuberculosis. *Eur Respir J* (2013) 42(6):1752–7. doi: 10.1183/09031936.00140913
- Abakay O, Abakay A, Sen HS, Tanrikulu AC. The Relationship Between Inflammatory Marker Levels and Pulmonary Tuberculosis Severity. *Inflammation* (2015) 38:691–6. doi: 10.1007/s10753-014-9978-y
- Nolan A, Condos R, Huie ML, Dawson R, Dheda K, Bateman E, et al. Elevated IP-10 and IL-6 From Bronchoalveolar Lavage Cells Are Biomarkers of Non-Cavitary Tuberculosis. *Int J Tuberc Lung Dis* (2013) 17(7):922–7. doi: 10.5588/ijtld.12.0610
- Leem AY, Song JH, Lee EH, Lee H, Sim B, Kim SY, et al. Changes in Cytokine Responses to TB Antigens ESAT-6, CFP-10 and TB 7.7 and Inflammatory Markers in Peripheral Blood During Therapy. *Sci Rep* (2018) 8:4–11. doi: 10.1038/s41598-018-19523-7
- Brahmbhatt S, Black GF, Carroll NM, Beyers N, Salker F, Kidd M, et al. Immune Markers Measured Before Treatment Predict Outcome of Intensive Phase Tuberculosis Therapy. *Clin Exp Immunol* (2006) 146:243–52. doi: 10.1111/j.1365-2249.2006.03211.x
- Barnes PF, Leedom JM, Chan LS, Wong SF, Shah J, Vachon LA, et al. Predictors of Short-Term Prognosis in Patients With Pulmonary Tuberculosis. *J Infect Dis* (1988) 158(2):366–71. doi: 10.1093/infdis/158.2.366
- Han Y, Kim SJ, Lee SH, Sim YS, Ryu YJ, Chang JH, et al. High Blood Neutrophil-Lymphocyte Ratio Associated With Poor Outcomes in Miliary Tuberculosis. *J Thorac Dis* (2018) 10(1):339–46. doi: 10.21037/jtd.2017.12.65
- Arriaga MB, Amorim G, Queiroz ATL, Rodrigues MMS, Araujo-Pereira M, Nogueira BMF, et al. Novel Stepwise Approach to Assess Representativeness of a Large Multicenter Observational Cohort of Tuberculosis Patients: The Example of RePORT Brazil. *Int J Infect Dis* (2020) 14:103:110–8. doi: 10.1016/j.ijid.2020.11.140
- Ministério da Saúde. *Manual De Recomendações Para O Controle Da Tuberculose No Brasil, 2ª Edição*. Brasília: Ministério da Saúde (2019).
- American Diabetes Association: Standards of Medical Care in Diabetes—2017. *Clin Diabetes* (2017) 35(1):5–26. doi: 10.2337/cd16-0067
- World Health Organization. *Definitions and Reporting Framework for Tuberculosis-2013 Revision* (2013). Available at: <https://www.who.int/tb/publications/definitions/en/>.
- Rosenbaum PR, Rubin DB. The Central Role of the Propensity Score in Observational Studies for Causal Effects. *Biometrika* (1983) 70(1):41–55. doi: 10.1093/biomet/70.1.41
- Naimi AI, Moodie EE, Auger N, Kaufman JS. Constructing Inverse Probability Weights for Continuous Exposures: A Comparison of Methods. *Epidemiology* (2014) 25(2):292–9. doi: 10.1097/EDE.0000000000000053
- D'Agostino RB Jr. Propensity Score Methods for Bias Reduction in the Comparison of a Treatment to a Non-Randomized Control Group. *Stat Med* (1998) 17(19):2265–81. doi: 10.1002/(sici)1097-0258(19981015)17:19<2265::aid-sim918>3.0.co;2-b
- van Buuren S, Groothuis-Oudshoorn K. Mice: Multivariate Imputation by Chained Equations in R. *J Stat Software* (2011) 45(3):1–67. doi: 10.18637/jss.v045.i03
- Little RJ, Rubin DB. *Statistical Analysis With Missing Data*. New York: John Wiley & Sons (2002).
- R Core Team. *R: A Language and Environment for Statistical Computing*. Vienna, Austria: R Foundation for Statistical Computing (2019).
- World Health Organization (WHO). *Treatment of Tuberculosis: Guidelines for National Programmes* (2003). Available at: [http://apps.who.int/iris/bitstream/handle/10665/67890/WHO\\_CDS\\_TB\\_2003.313\\_eng.pdf?sequence=1](http://apps.who.int/iris/bitstream/handle/10665/67890/WHO_CDS_TB_2003.313_eng.pdf?sequence=1).
- Horne DJ, Royce SE, Gooze L, Narita M, Hopewell PC, Nahid P, et al. Sputum Monitoring During Tuberculosis Treatment for Predicting Outcome: Systematic Review and Meta-Analysis. *Lancet Infect Dis* (2010) 10(6):387–94. doi: 10.1016/S1473-3099(10)70071-2
- Phillips PP, Mendel CM, Burger DA, Crook AM, Nunn AJ, Dawson R, et al. Limited Role of Culture Conversion for Decision-Making in Individual Patient Care and for Advancing Novel Regimens to Confirmatory Clinical Trials. *BMC Med* (2016) 14:19. doi: 10.1186/s12916-016-0565-y
- Caetano Mota P, Carvalho A, Valente I, Braga R, Duarte R. Predictors of Delayed Sputum Smear and Culture Conversion Among a Portuguese Population With Pulmonary Tuberculosis. *Rev Port Pneumol* (2012) 18(2):72–9. doi: 10.1016/j.rppneu.2011.12.005
- Ma Y, Huang ML, Li T, Du J, Shu W, Xie SH, et al. Role of Diabetes Mellitus on Treatment Effects in Drug-Susceptible Initial Pulmonary Tuberculosis Patients in China. *BioMed Environ Sci* (2017) 30(9):671–5. doi: 10.3967/bes2017.089
- Demitto FO, Araújo-Pereira M, Schmaltz CA, Sant'Anna FM, Arriaga MB, Andrade BB, et al. Impact of Persistent Anemia on Systemic Inflammation and Tuberculosis Outcomes in Persons Living With HIV. *Front Immunol* (2020) 24:11:588405. doi: 10.3389/fimmu.2020.588405
- Gil-Santana L, Cruz LAB, Arriaga MB, Miranda PFC, Fukutani KF, Silveira-Mattos PS, et al. Tuberculosis-Associated Anemia Is Linked to a Distinct Inflammatory Profile That Persists After Initiation of Antitubercular Therapy. *Sci Rep* (2019) 9(1):1381. doi: 10.1038/s41598-018-37860-5
- Nijenbandring de Boer R, Baptista de Oliveira Souza Filho J, Cobelens F, et al. Delayed Culture Conversion Due to Cigarette Smoking in Active Pulmonary Tuberculosis Patients. *Tuberculosis* (2014) 94(1):87–91. doi: 10.1016/j.tube.2013.10.005
- Volkman T, Moonan PK, Miramontes R, Oeltmann JE. Tuberculosis and Excess Alcohol Use in the United States, 1997–2012. *Int J Tuberc Lung Dis* (2015) 19:111–9. doi: 10.5588/ijtld.14.0516
- Sloand E. Hematologic Complications of HIV Infection. *AIDS Rev* (2005) 7:187–96.
- Lowe DM, Bangani N, Goliath R, Kampmann B, Wilkinson KA, Wilkinson RJ, et al. Effect of Antiretroviral Therapy on HIV-Mediated Impairment of the Neutrophil Antimicrobial Response. *Ann Am Thorac Soc* (2015) 12(11):1627–37. doi: 10.1513/AnnalsATS.201507-463OC
- Ragan EJ, Kleinman MB, Sweigart B, Gnatenko N, Parry CD, Horsburgh CR, et al. The Impact of Alcohol Use on Tuberculosis Treatment Outcomes: A Systematic Review and Meta-Analysis. *Int J Tuberc Lung Dis* (2020) 24(1):73–82. doi: 10.5588/ijtld.19.0080
- Huangfu P, Ugarte-Gil C, Golub J, Pearson F, Critchley J. The Effects of Diabetes on Tuberculosis Treatment Outcomes: An Updated Systematic Review and Meta-Analysis. *Int J Tuberc Lung Dis* (2019) 23(7):783–96. doi: 10.5588/ijtld.18.0433
- Chaves Torres NM, Quijano Rodríguez JJ, Porras Andrade PS, Arriaga MB, Netto EM. Factors Predictive of the Success of Tuberculosis Treatment: A Systematic Review With Meta-Analysis. *PLoS One* (2019) 14(12):e0226507. doi: 10.1371/journal.pone.0226507
- Thierry AR, Roch B. Neutrophil Extracellular Traps and By-Products Play a Key Role in COVID-19: Pathogenesis, Risk Factors, and Therapy. *J Clin Med* (2020) 9(9):E2942. doi: 10.3390/jcm9092942
- Sigal GB, Segal MR, Mathew A, Jarlsberg L, Wang M, Barbero S, et al. Biomarkers of Tuberculosis Severity and Treatment Effect: A Directed Screen of 70 Host Markers in a Randomized Clinical Trial. *EBioMedicine* (2017) 25:112–21. doi: 10.1016/j.ebiom.2017.10.018
- Singanayagam A, Manalan K, Connell DW, Chalmers JD, Sridhar S, Ritchie AI, et al. Evaluation of Serum Inflammatory Biomarkers as Predictors of

- Treatment Outcome in Pulmonary Tuberculosis. *Int J Tuberc Lung Dis* (2016) 12:1653–60. doi: 10.5588/ijtld.16.0159
42. Sood A, Mittal BR, Modi M, Chhabra R, Verma R, Rana N, et al. 18F-FDG PET/CT in Tuberculosis: Can Interim PET/CT Predict the Clinical Outcome of the Patients? *Clin Nucl Med* (2020) 45(4):276–82. doi: 10.1097/RLU.0000000000002968

**Conflict of Interest:** The authors declare that the research was conducted in the absence of any commercial or financial relationships that could be construed as a potential conflict of interest.

Copyright © 2021 Carvalho, Amorim, Melo, Silveira, Vargas, Moreira, Rocha, Souza, Arriaga, Araújo-Pereira, Figueiredo, Durovni, Lapa-e-Silva, Cavalcante, Rolla, Sterling, Cordeiro-Santos, Andrade, Silva, Kritski and the RePORT Brazil consortium. This is an open-access article distributed under the terms of the Creative Commons Attribution License (CC BY). The use, distribution or reproduction in other forums is permitted, provided the original author(s) and the copyright owner(s) are credited and that the original publication in this journal is cited, in accordance with accepted academic practice. No use, distribution or reproduction is permitted which does not comply with these terms.



# Antibody Subclass and Glycosylation Shift Following Effective TB Treatment

Patricia S. Grace<sup>1,2†</sup>, Sepideh Dolatshahi<sup>3†</sup>, Lenette L. Lu<sup>4</sup>, Adam Cain<sup>1</sup>, Fabrizio Palmieri<sup>5</sup>, Linda Petrone<sup>6</sup>, Sarah M. Fortune<sup>2</sup>, Tom H. M. Ottenhoff<sup>7</sup>, Douglas A. Lauffenburger<sup>8</sup>, Delia Goletti<sup>6</sup>, Simone A. Joosten<sup>7</sup> and Galit Alter<sup>1\*</sup>

<sup>1</sup> Ragon Institute of Massachusetts General Hospital, Massachusetts Institute of Technology, and Harvard University, Cambridge, MA, United States, <sup>2</sup> Department of Immunology and Infectious Disease, Harvard School of Public Health, Boston, MA, United States, <sup>3</sup> Department of Biomedical Engineering, University of Virginia, Charlottesville, VA, United States, <sup>4</sup> Department of Internal Medicine, University of Texas Southwestern Medical Center, Dallas, TX, United States, <sup>5</sup> Clinical Department, National Institute for Infectious Diseases (INMI), IRCCS L. Spallanzani, Rome, Italy, <sup>6</sup> Department of Epidemiology and Preclinical Research, National Institute for Infectious Diseases IRCCS (INMI) L. Spallanzani, Rome, Italy, <sup>7</sup> Department of Infectious Disease, Leiden University Medical Center, Leiden, Netherlands, <sup>8</sup> Department of Biological Engineering, Massachusetts Institute of Technology, Cambridge, MA, United States

## OPEN ACCESS

### Edited by:

Hazel Marguerite Dockrell,  
University of London

### Reviewed by:

Irena Trbojević-Akmačić,  
Genos Glycoscience Research  
Laboratory, Croatia  
Arshad Khan,  
University of Texas Health Science  
Center at Houston, United States

### \*Correspondence:

Galit Alter  
galter@partners.org

<sup>†</sup>These authors share first authorship

### Specialty section:

This article was submitted to  
Microbial Immunology,  
a section of the journal  
Frontiers in Immunology

Received: 12 March 2021

Accepted: 07 June 2021

Published: 05 July 2021

### Citation:

Grace PS, Dolatshahi S, Lu LL, Cain A, Palmieri F, Petrone L, Fortune SM, Ottenhoff THM, Lauffenburger DA, Goletti D, Joosten SA and Alter G (2021) Antibody Subclass and Glycosylation Shift Following Effective TB Treatment. *Front. Immunol.* 12:679973. doi: 10.3389/fimmu.2021.679973

With an estimated 25% of the global population infected with *Mycobacterium tuberculosis* (*Mtb*), tuberculosis (TB) remains a leading cause of death by infectious diseases. Humoral immunity following TB treatment is largely uncharacterized, and antibody profiling could provide insights into disease resolution. Here we focused on the distinctive TB-specific serum antibody features in active TB disease (ATB) and compared them with latent TB infection (LTBI) or treated ATB (txATB). As expected, di-galactosylated glycan structures (lacking sialic acid) found on IgG-Fc differentiated LTBI from ATB, but also discriminated txATB from ATB. Moreover, TB-specific IgG4 emerged as a novel antibody feature that correlated with active disease, elevated in ATB, but significantly diminished after therapy. These findings highlight 2 novel TB-specific antibody changes that track with the resolution of TB and may provide key insights to guide TB therapy.

**Keywords:** antibodies, tuberculosis, IgG4, Fc-glycosylation, TB therapy

## INTRODUCTION

Tuberculosis (TB) continues to be one of the leading causes of death by infectious disease globally, and while the development of new protective vaccines continues to be a critically important goal for the fight against TB disease (1, 2), detecting active TB (ATB), the TB state with the greatest likelihood of spreading *Mtb*, for immediate treatment could profoundly prevent TB spread (3–5). Current immune-based diagnostics, including the tuberculin-skin-test (TST) or the interferon-gamma release assay (IGRA), can detect individuals with TB but cannot distinguish individuals with ATB from latent TB infection (LTBI), which accounts for ~95% of world cases, therefore limiting the ability to identify disease that requires immediate treatment (6, 7). Furthermore, current immune diagnostics cannot distinguish those who have successfully completed therapy from those with ATB and actively replicating *Mtb*.



Given the heterogeneous manifestation of disease in individuals exposed to *Mtb*, it is not surprising that immune responses to *Mtb* are also heterogeneous. And in humans, features of the immune response such as numbers of circulating NK cells (8), neutrophils (9), B cells (9, 10) and T cells (9) have been observed to differ in TB-diseased individuals depending on their disease severity and clearance of replicating *Mtb* following treatment. Phenotypic differences in the T cell response to TB have also been shown to associate with disease severity, with higher frequencies of proliferating and TH1-cytokine producing CD4 T cells observed in ATB compared to LTBI (11–14); these T cells diminish from circulation following therapy (15, 16). In addition, inflammatory signatures that include type I interferon, captured through whole-blood RNA sequencing, demonstrate a strong association with ATB disease, which also diminishes with treatment (9, 17).

Antibody-based measures are attractive alternatives to cellular measures of disease activity; these disease-specific immune responses are easily and directly captured from serum in an antigen specific manner. Measuring antibodies in sera is also technically simple and relatively rapid when compared to the cumbersome and variable measures of cellular immune responses. Importantly, a single antibody molecule measures both antigen-specificity within the variable domain (Fab) and inflammatory state of the disease within the constant domain (Fc) (18). Alterations in disease-specific IgG properties including antigen specific titers (19, 20), isotype switching (21), and glycosylation (22–26) provide insights into disease relapse or severity across diseases ranging from cancer (27, 28), autoimmunity (29, 30), and infections (20, 31). While changes in disease-specific titers do not always reflect changes in disease activity (32–35), alterations in disease-specific Fc-properties provide critical qualitative insights into disease activity. Given that changes in IgG Fc-profiles also track with altered Fc-effector function, unique humoral markers of disease activity may also provide additional insights into the mechanism(s) of enhanced disease control and even elimination. Along these lines, recent studies of TB-specific antibodies highlight the disease discriminatory activity of IgG Fc-glycosylation features (36, 37) that may point to unexpected mechanisms of anti-microbial control (36, 38–42).

Recent data indicate that B cells change not only in number but also phenotype and function during TB disease and after treatment (10). While decreased TB-specific IgG titers have been noted in several studies following TB treatment (43, 44), it remains unclear whether antibody Fc-profiles also shift with treatment. Humoral profile shifts could provide insights into long-term immunity after successful *Mtb* clearance and point to markers of TB treatment success. Thus, in this study we aimed to determine how the humoral immune response to *Mtb* differed among the TB states: LTBI, ATB, and txATB. We profiled the TB-specific humoral immune responses in the serum of individuals previously profiled for B cell phenotype and function (10) using a systems serology approach (45). These measures included total serum antibody titers, antigen-specific antibody titers, and antibody-mediated functional responses in

human cells. And in light of our recent study of IgG glycans in LTBI/ATB discriminatory model performance, which found IgG-Fc glycans discriminated better compared to whole IgG and Fab-glycans (37); we focused on IgG-Fc glycans in the humoral profiling of this cohort. We observed significant differences in IgG-Fc glycosylation across individuals with LTBI and ATB disease, consistent with earlier observations in IgG from independent cohorts of LTBI and ATB individuals (37). Additionally, we found enrichment of TB-specific IgG4 among ATB individuals. Strikingly, these same antibody features distinguished ATB from txATB, suggesting that IgG4, in addition to IgG-Fc glycosylation, may also be a marker of ongoing inflammation and the ATB disease activity.

## METHODS

### Study Subjects

Sample collection was approved by the ethical committee of INMI, approval number 72/2015; informed written consent was obtained before collection. ATB was confirmed *via Mtb* sputum culture and patients were enrolled within 7 days of starting the TB treatment (isoniazid, rifampicin, ethambutol and pyrazinamide for 2 months, followed by isoniazid, rifampicin for 4 additional months (46). TxATB subjects were patients who completed a 6-month course treatment for culture-positive pulmonary TB and were culture-negative at 2 and 6 months of therapy. LTBI subjects were mainly contacts recently exposed (within the previous 6 months) to smear-positive ATB patients with positive QuantiFERON TB Gold In tube (QFT-IT) (Quiagen, Germany) but without symptoms or radiological signs of ATB. Healthy donors were QFT-IT- and HIV<sup>-</sup> individuals not undergoing immunosuppressive drug treatments. Serum samples were collected in heparin tubes. An additional 10 healthy HIV<sup>-</sup> donors from the Greater Boston, Massachusetts area were recruited by Ragon Institute of MGH, MIT, and Harvard for serum assay controls. Blood samples were collected in ACD tubes from different donors in the Boston-area, for the isolation of Neutrophils for ADNP assays. NK cells used for assessing antibody function were derived from buffy coats of healthy HIV<sup>-</sup> donors collected by the MGH Blood Donation Bank. All study participants for additional healthy negatives and primary cell isolation gave written, informed consent, approved by the institutional review boards at Massachusetts General Brigham Hospital.

### Total Immunoglobulin Quantification

Total quantities of IgG1, IgG2, IgG3, IgG4, IgM, and IgA were determined in serum samples diluted 1:15,000 and used the MILLIPLEX<sup>®</sup> MAP Human Isotyping Magnetic Bead Panel (Sigma-Millipore HGAMMAG-301K) to quantify total immunoglobulins.

### Antigens for Antibody Profiling

*Mtb* antigen used to profile antibody responses included: PPD (Staten Serum Institute), recombinant (rec.) Ag85A and Ag85B

combined in a 1:1 ratio (BEI Resources: NR-14871 and NR-4870), rec. ESAT6 and CFP10 combined in a 1:1 ratio (BEI Resources: NR-14868 and NR-49425), rec. GroES (BEI Resources: NR-14861), rec. glcB (provided by T. Ottenhoff), rec. HspX (BEI Resources; NR-49428). Non-TB infectious antigens included Influenza-HA antigen represented by a mixture of 7 recombinant HA antigens: H1N1-A/Brisbane/59/2007, B/Florida/4/2006, B/Malaysia/2506/2004, H1N1-A/Solomon Island/3/2006, H3N2-A/Wisconsin/67/X-161/2005, H3N2-A/Brisbane/10/2007 and H1N1-A/New Caledonia/20/99 (Immune Technology); tetanus toxin (Mass Biologics Lp1099p); and rec. pp65 for CMV (Abcam, 43041).

## Custom Luminex Assay for Ag-specific Titer Determination

Multiple unique Luminex MagPlex carboxylated bead regions (Luminex) were coupled with the above-mentioned antigens to determine the antigen-specific titers present in the cohort serum samples. Serum samples were diluted 1:30, 1:100, 1:300, and 1:1000, and 1:3000 to generate an area under the curve (AUC) measurement using the detection reagents total IgG, IgG1, IgG2, IgG3, IgG4, IgM, IgA1, and IgA2 (Southern Biotech).

## Antibody Dependent Cellular Phagocytosis (ADCP)

Biotinylated PPD was used to coat 1mm Neutravidin labeled yellow-green, fluorescent beads. Immune complexes were formed by combining PPD-beads, and combined with serum samples diluted 1:30, 1:100, 1:300, 1:1000 in PBS and incubated at 37°C for 2hrs. Complexes were washed,  $2 \times 10^4$  THP1 cells were added per well of 96-well plates and incubated for 1hr at 37°C. Samples were then washed and fixed for analysis of bead uptake on an iQue Screener. Phagocytic scores were calculated as previously described (36) across sample dilution series and were used to calculate AUC.

## Antibody Dependent Neutrophil Phagocytosis (ADNP)

Neutrophils were isolated from healthy donor blood collected in ACD tubes as previously described (36). Complexes were formed and incubated with isolated neutrophils as described for the ADCP above. After incubation, samples were stained with CD66b and fixed with 4%PFA. Bead phagocytosis was measured as described above, and the enrichment of neutrophils was confirmed with CD66b staining (BioLegend 305112). Phagocytic scores were determined as in ADCP across a serum dilution series ranging from 1:30 to 1:1000 and used to calculate Phagocytic Score AUC.

## Antibody Dependent NK Cells Activation

ELISA plates were coated with 50mL of 2µg/mL PPD overnight at 4°C. Coated plates were blocked with 5% BSA for 1hr at RT and washed 3x with PBS before 50µL of diluted serum (1:30, 1:100, 1:300, 1:1000) was added to each well. Serum dilutions were incubated 2hrs at 37°C on antigen-coated plated and washed prior to adding  $5 \times 10^4$  NK cells per well, isolated from healthy HIV<sup>-</sup> donor buffy coats by RosetteSep (Stem Cell 15065). CD107a-BV605

(BioLegend 328634), 5µg/mL brefeldin A (BioLegend 420601), and 0.7µL/mL GolgiStop (BD 554724) were also added to each well and incubated for 5hrs at 37°C. Following this incubation, NK cells were surface-stained with CD16-BV785 (BioLegend 302046), CD56-PE-Cy7 (BD 335791), and CD3-APC-Cy7 (BioLegend 300426). An intracellular stain was then performed using Perm/Fix Solution (BD 554714) with IFNγ-PE (BioLegend 506507) and anti-MIP1β-BV421 (BD 562900). Samples were fixed with 4% and NK cell activation was analyzed on the iQue Screener. AUC frequencies of NK cells bearing CD107a, expressing IFNγ and MIP1β across, were derived from the signal across the dilution series tested in the donor cells.

## Glycan Analysis of IgG-Fc

IgG was isolated from serum samples by incubating 10µL of serum diluted 1:20 in PBS with 25µL protein G beads (Millipore, Catalog #LSKMAGG10); the serum and beads were mixed at 4°C for 16hrs. Excess serum protein was washed, and IgG-bound beads resuspended in digestion buffer containing 1uL IdeZ (NEB Catalog #P0770S) and IgG was digested at 37°C for 2hr to remove Fab. IgG-Fc still bound to magnetic protein G beads were pelleted and washed on a magnet to separate Fc from Fab. Glycans from IgG-Fc were cleaved, enriched, and labeled with APTS according to manufacturer specifications in the Glycan Assure Kit (ThermoFisher A28676). To immune-precipitate and analyze antigen-specific IgG-Fc glycosylation, streptavidin-coated magnetic beads (NEB Cat# S1420S) were coated with biotinylated-PPD, as described above for ADCP. Antigen-coated beads were incubated with 300µL of serum at 4°C for 16hrs. Excess protein was washed off the beads with PBS and Fc of the antigen-bound IgG was cleaved with IdeZ as described above. Supernatants were taken from this IdeZ reaction for glycan cleavage and staining according to the Glycan Assure protocol. Samples were run with a LIZ 600 DNA ladder in Hi-Di formamide (Thermo Fisher 4408399) on an ABI 3130XL1 DNA sequencer. Data were analyzed using ThermoFisher Glycan Assure Analysis software; peaks were assigned based on migration of standards of known glycans and peak area was calculated. The measured peak areas per sample were totaled to report a relative frequency of each glycan structure identified.

## Data Visualization and Analysis

Univariate data visualization and statistical analysis were performed using GraphPad Prism (Version 8.3.1). For multivariate analysis, MATLAB computing environment (version 2018b, Mathworks, Natick, MA) was used, supported by the Statistics and Optimization toolboxes, as well as the third party PLS toolbox (Eigenvector Research, Inc, Manson, WA). Spearman network visualizations were performed using Cytoscape (version 3.6.0).

## Identification of TB Signatures With LASSO and OPLSDA

Computational analysis was used to build classification models that identify key features that most effectively resolved pairs of the LTBI, ATB and txATB states. These classification models were built using previously described methods (25, 45) combining (i)

Least Absolute Shrinkage and Selection Operator (LASSO) method (47), for feature selection, and (ii) classification using the LASSO-selected features. For LASSO selection, a previously described nested cross validation framework was used to validate the robustness of the classification model (48). Orthogonalized Partial Least Square Discriminant Analysis (OPLSDA) (49, 50) was used to visualize LASSO-selected variables and assess their predictive ability for classifying TB states (**Figures 2, 3, 4A, B**). These input variables were centered and scaled to a standard deviation of 1. PLSDA models consisting of two LVs were constructed and then orthogonalized to condense the Y-block variance (group separations) into the first Latent Variable (LV1). LV1 captures the variance in features that are in the direction of the pairwise separation of the groups, while LV2 describes the variation orthogonal to this predictive component. To assess each model, 5-fold cross validation (CV) was performed on the data (100 random 5-fold cross validation). To assess model significance, permutation test was performed on the cross validated models by randomly shuffling the labels. The OPLSDA models performed significantly better than random with CV Wilcoxon p values of lower than  $2E-3$  across pairwise group comparisons. Variable Importance in Projection (VIP) scores were calculated (51) to rank the importance of each variable in the projection of the PLS model. To emphasize the direction of the contribution of each variable, negative and positive signs were added to VIP scores to indicate negative and positive Loadings of each variable on LV1.

### Construction of the Correlation Network of the LASSO-Selected Features

Spearman correlation of the LASSO-selected Fc features to all original 78 TB-specific antibody features were calculated. Each node is a feature and the thickness of the edges between nodes is proportional to their correlation coefficients. The p-value depicting the significance of these correlations were corrected for multiple comparisons (Benjamini-Hochberg q-value  $< 0.05$ , testing the hypothesis of zero correlation). Only correlations with corrected p-values  $< 0.05$  were included.

### Three-Way PLSDA Model

The LASSO-selected features from the three pair-wise group comparisons were pooled (total of 8 features) and a PLSDA model was developed to separate the three groups of LTBI, ATB

and txATB. This model was not orthogonalized to better capture and visualize the pairwise group differences. The two-dimensional loadings on LV1 and LV2 were overlaid on the scores plot.

## RESULTS

### LTBI and ATB Plasma Have Distinct Profiles of Fc-Glycosylation and TB-Specific IgG Subclass

We previously described the biophysical and functional features of purified IgG found in LTBI and ATB from cohorts of individuals from South Africa and US/Mexico (36, 37). However, whether these differences persist, or differ following successful antibiotic treatment remains unclear. Thus, here we aimed to define the impact of therapy on shaping the TB-specific humoral immune in a cohort of LTBI (n=21), ATB (n=20), and txATB (n=23) from Italy, with an additional group of healthy control individuals (n=17) from Italy and the USA (**Table 1**). Similar levels of circulating, non-antigen-specific IgM, total IgG and the subclasses IgG1, IgG2, Ig3, and IgG4 were observed in the serum of healthy, LTBI, ATB, and txATB individuals (**Supplemental Figure 1A**). In contrast, total IgA titers were significantly elevated in ATB compared to LTBI and txATB (**Supplemental Figure 1A**), consistent with previous observations in TB (52, 53). Additional differences in antigen-specific isotype (**Supplemental Figures 1B–E**), subclass (**Supplemental Figure 2**), total IgG-Fc glycosylation (**Supplemental Figure 3**), and Fc-mediated functional antibody responses in monocytes, neutrophils, and NK cells (**Supplemental Figure 4**) were noted across groups. The differences observed across this collection of measures suggested distinct humoral profiles existed not only in LTBI and ATB, but also txATB.

Given the univariate differences across this cohort, we sought to identify the humoral features of our dataset, which could best discriminate subsets of TB diseased individuals by applying a conservative multivariate analytic method to define a minimal set of distinguishing humoral features. We first aimed to determine whether LTBI and ATB were fully resolvable using antibody features as had been previously observed (36), and further, whether a minimal set of antibody-features could be identified, which resembled previous antibody profile differences. A least absolute shrinkage and selection operator (LASSO) (47)

**TABLE 1** | Cohort Demographics.

	LTBI	ATB	txATB	Controls
Individuals:	21	20	23	17
Age, (median +IQR):	31 (21-77)	35 (23-67)	37 (17-70)	31(23-57)
Gender, Females:	15 (71%)	2 (10%)	15 (65%)	10 (59%)
BCG Vaccinated:	9 (41%)	19 (95%)	15 (65%)	5 (29%)
Mos. post treatment (median IQR):			8 (1-72)	
Origin, n (%):				
West Europe:	12 (57%)	1 (5%)	10 (43%)	14 (82%)
East Europe:	5 (24%)	15 (75%)	7 (30%)	2 (12%)
Asia:		1 (5%)	1 (4%)	
Africa:	2 (10%)	2 (10%)	3 (13%)	
South America:	2 (10%)	1 (5%)	2 (9%)	1 (6%)

was first applied to reduce the number of features in our highly correlated dataset (Data Sheet 1), to avoid overfitting, and define a minimal set of these features that could discriminate the LTBI and ATB disease states. Using PLS-DA for visualization, clear separation was observed between the LTBI and ATB antibody profiles (**Figure 1A**). Moreover, as few as 4 of the 78-total Fc-features selected by LASSO could resolve LTBI and ATB individuals, providing 91% cross-validation (CV) accuracy (**Figure 1B**); these included totaled di-galactosylated (G2); the di-galactosylated, fucosylated, and bisected (G2FB) structure; PPD-specific IgG4 levels; and singly-galactosylated, sialylated, fucosylated (G1S1F) structures.

Univariate plots of the LASSO-selected features revealed statistically significant differences in all 4 features when comparing LTBI and ATB groups (**Figures 1C–F**). Specifically, the levels of totaled G2 (**Figure 1C**) and the G2FB structure (**Figure 1E**) on total IgG-Fc were enriched in LTBI. While PPD-specific IgG4 levels and the G1S1F structure were enriched in ATB IgG-Fc (**Figures 1D, F**). The differential IgG-Fc

galactosylation seen across LTBI and ATB of this cohort is consistent with our previous observations in cohorts of LTBI and ATB samples from South Africa and the US/Mexico (36). However, the subclass enrichment of IgG4 antibodies in ATB represents a novel observation in TB disease. The coincidence of IgG4 and G1S1F on total IgG-Fc glycans of ATB is reminiscent of previous studies of subclass specific Fc-glycosylation, which found an enrichment in IgG4 of healthy individuals (54) and an elevation of G1S1F on IgG4 in patients with IgG4-related disease (55).

Given that the LASSO/PLS-DA model selects features that solely account for the greatest variance across the antibody profiles being compared, additional distinctive antibody features that are correlated with the LASSO-selected features are not highlighted in this analysis. To explore the additional humoral features of our dataset that distinguished LTBI and ATB, we next generated a Spearman correlation network of the LASSO-selected features to highlight the relationship of this minimal set of features with the remaining 74 features

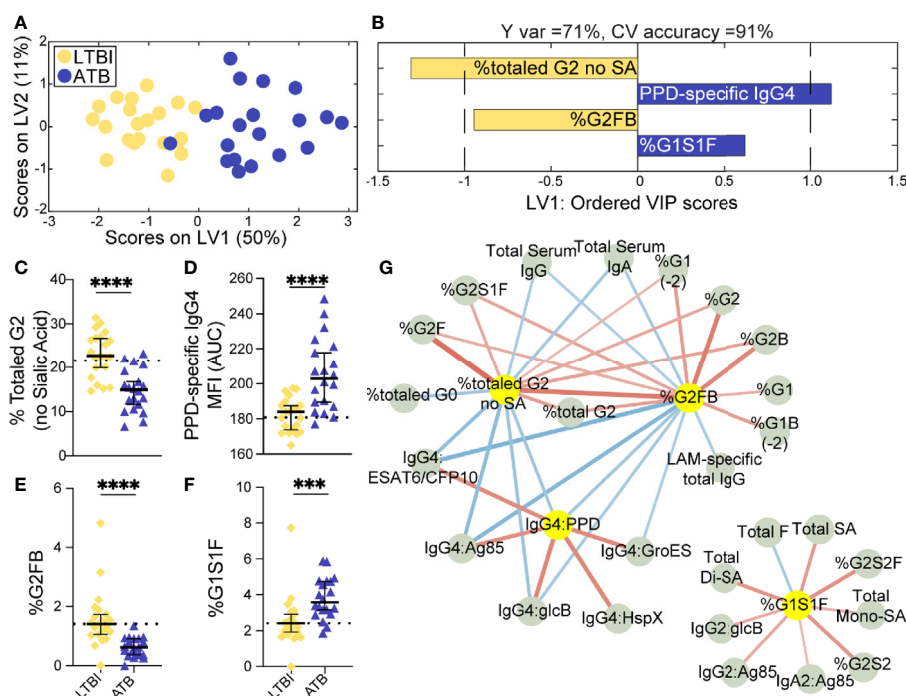


**FIGURE 1 |** Fc-glycosylation and TB-specific IgG subclass distinguish LTBI and ATB individuals. An orthogonalized PLS-DA (OPLS-DA) model was created based on four LASSO-identified antibody features that discriminate LTBI from ATB (**A, B**). Latent variable 1 (LV1) explains 71% of Y variance in the direction of LTBI and ATB separation. 5-fold cross validation (CV) was performed, resulting in 91% CV accuracy. The model significantly outperformed models based on shuffled group labels (permutation testing, Wilcoxon  $p=2E-5$ ) (**A**) PLS-DA scores plot depicts model separation of LTBI ( $n = 21$ , yellow dots) and ATB ( $n = 20$ , blue dots). LV1 and LV2 account for 50% and 11% of the variability of the input features. (**B**) Variable Importance in Projection (VIP) scores plot of top features providing the greatest resolution of LTBI and ATB in rank-order. Directions of the bars signify loadings on LV1 and colors represent the disease groups in which measures were enriched. Pairwise comparison of LTBI ( $n = 21$ , yellow diamonds) and ATB ( $n = 20$ , blue triangles) individuals (**C**) The frequencies of totaled G2 structures without sialic acid on IgG-Fc of LTBI and ATB individuals. (**D**) AUC of PPD-specific IgG4 titers. (**E**) percentage of G2FB glycan on IgG (**F**) percentage of G1S1F glycan on IgG. Univariate plots (**C–F**) show median and interquartile range of each LASSO-selected measure; statistically significant differences between LTBI and ATB groups calculated using Mann-Whitney test: \*\*\* $p < 0.0005$  and \*\*\*\* $p < 0.0001$ . The dotted lines represent median of healthy controls individuals tested. (**G**) Correlation analysis depicts other features that are positively (red lines) or negatively (blue lines) correlated with these four key features selected with LASSO (highlighted in yellow). The color intensity and width of the edges between nodes are proportional to the significance of correlation coefficients after correcting for multiple comparisons (Benjamini-Hochberg  $q$ -value  $< 0.05$ , testing the hypothesis of zero correlation). Only correlations with corrected  $p$ -values  $< 0.05$  were included.



measured (**Figure 1G**). Two networks emerged from this analysis: a large network linking the two LTBI enriched features (G2 and G2FB) linked *via* negative correlations to the ATB enriched IgG4 signature (**Figure 1G**, right), and a smaller second network consisting of features correlated with the ATB-associated G1S1F feature (**Figure 1G**, left). Importantly, IgG4 titers against multiple TB antigens, including intracellular TB proteins HspX and GroES, were co-correlated, pointing to a shift to IgG4 responses in ATB. Additionally, di-galactosylated features enriched in LTBI were linked to several galactosylated structures, reinforcing an overall elevated galactosylation profile in LTBI. Finally, total serum IgG and IgA levels, found to be elevated in ATB (**Supplemental Figure 1A**), were inversely correlated to the glycan features elevated in LTBI profile. These networks link qualitative/quantitative changes in the humoral profiles between LTBI and ATB states with the LASSO-selected features and highlight the unique enrichment of *Mtb*-specific IgG4 responses. Furthermore, depletion of IgG4 resulted in increased antibody effector function in neutrophils and NK cells (**Supplemental Figure 5**), pointing to IgG4 as a mechanistic player in dampening antibody function, as previously shown in HIV (56) and cancer (57). In summary, we find a critical recapitulation of glycan features of latency in an Italian cohort, highlighting the universal presence of this biomarker of ATB, that includes IgG4 levels, perhaps previously overlooked due to the purification methods used in our original study. These data reinforce a set of qualitative antibody Fc-features that discriminate LTBI from ATB.

## Treatment of ATB Correlates With Reduced TB-Specific IgG4 Titers and Inflammatory Glycan Signatures

Treatment of ATB and the resolution of replicating *Mtb* has been linked to the resolution of inflammatory cytokines (9), shift in T cell phenotypes (15) and NK cell abundance (8) in the blood. Along these lines, previous cellular profiling of this cohort of individuals indicated that B cells were less proliferative and produced fewer antibodies in ATB, while B cells functioned normally following treatment (10). Given these previously observed differences following TB treatment, we next aimed to determine whether a minimal set of humoral features could distinguish txATB from ATB and mirror the recovered B cell responses found in txATB individuals.

LASSO was applied to select minimal features that distinguished ATB and txATB, and PLSDA visualization of the selected features provided nearly perfect distinction between the disease states, with 92% cross-validation accuracy (**Figure 2A**). The LASSO-identified features included: total IgG-G2, -G2FB, -G1S1F glycans, and PPD-specific IgG4 (**Figure 2B**). These antibody features point to the resolution of inflammatory Fc-glycosylation with treatment, with elevated G2 (**Figure 2C**) and G2FB (**Figure 2D**) structures on txATB IgG-Fc compared to ATB. In contrast, the frequency of IgG-G1S1F structures was significantly higher in ATB compared to txATB (**Figure 2E**). Finally, PPD-specific IgG4 titers were lower in txATB compared to ATB (**Figure 2F**), with txATB levels of PPD-specific IgG4

equivalent to those found in healthy controls (**Supplemental Figure 2D**). Collectively, these data suggest that inflammatory glycans and PPD-specific IgG4 titers, markers of ATB, are diminished in txATB.

Again, to further probe the dataset for additional shifts in the humoral response related to the LASSO-selected features, we generated a Spearman correlation network between the LASSO-selected features and the remaining features. A single correlated network emerged (**Figure 2G**), including a dense cluster of glycans and TB-specific IgG4 features that all diminished in the setting of treatment. In addition to the network of IgG4 titers that inversely correlated with glycan structures enriched in txATB, IgG2 and IgG3 titers specific for Ag85A/B and HspX features arose in the network and inversely correlated to G2 features. These relationships suggest that in addition to IgG4 titers, individuals with ATB utilize additional IgG subclasses, during persistent infection and exposure to *Mtb* antigens, that likely resolve following treatment. Finally, IgM-specific responses to PPD and ESAT6/CFP10 emerged in this analysis and were linked to G2 levels on IgG-Fc in the txATB group. As the first class of antibody produced in primary antigen exposure (58), the elevation of TB-specific IgM titers in txATB point to a development of novel naïve humoral responses following resolution of replicating *Mtb* (**Supplemental Figure 1B**). Together, these data highlight a significant shift in antibody isotypes following treatment, with an overall reduction of inflammatory IgG-Fc glycans and concomitant contraction of the ATB-specific IgG4 immunity across TB-specific antigens.

## Higher TB-Specific Titers Distinguish txATB From LTBI

The overlapping features that distinguished both LTBI/ATB and ATB/txATB raised the question of whether humoral immunity in txATB and LTBI were largely similar or if humoral immunity could also distinguish these two states. Using LASSO/PLSDA on the humoral profiles, LTBI and txATB could be resolved with 81% cross-validation accuracy (**Figure 3A**). The LASSO selected features were largely enriched in the txATB compared to the LTBI individuals (**Figure 3B**); these included Ag85A/B-specific IgG and IgM titers as well as HspX-specific IgG1 titers (**Figures 3C, E, F**). And while the LASSO-selected TB titers did not reach univariate significance, the amount of antibody-mediated phagocytosis (ADCP) was significantly increased in txATB compared to LTBI (**Figure 3D**). These LASSO-selected features indicate higher antibody levels and function amongst txATB individuals. Moreover, network analysis underscored the prevalence of higher IgG1 titers against multiple TB-specificities in txATB individuals and pointed to the persistence of TB-specific antibodies in this recently treated population (**Figure 3G**). The elevated ADCP activity in txATB was linked to elevated neutrophil phagocytosis (ADNP), highlighting persistent antibody-mediated phagocytic activity following antibiotic treatment. Thus, txATB was distinguishable from LTBI in our multivariate analysis by higher antibody titers and enhanced opsonophagocytic function at the conclusion of treatment.

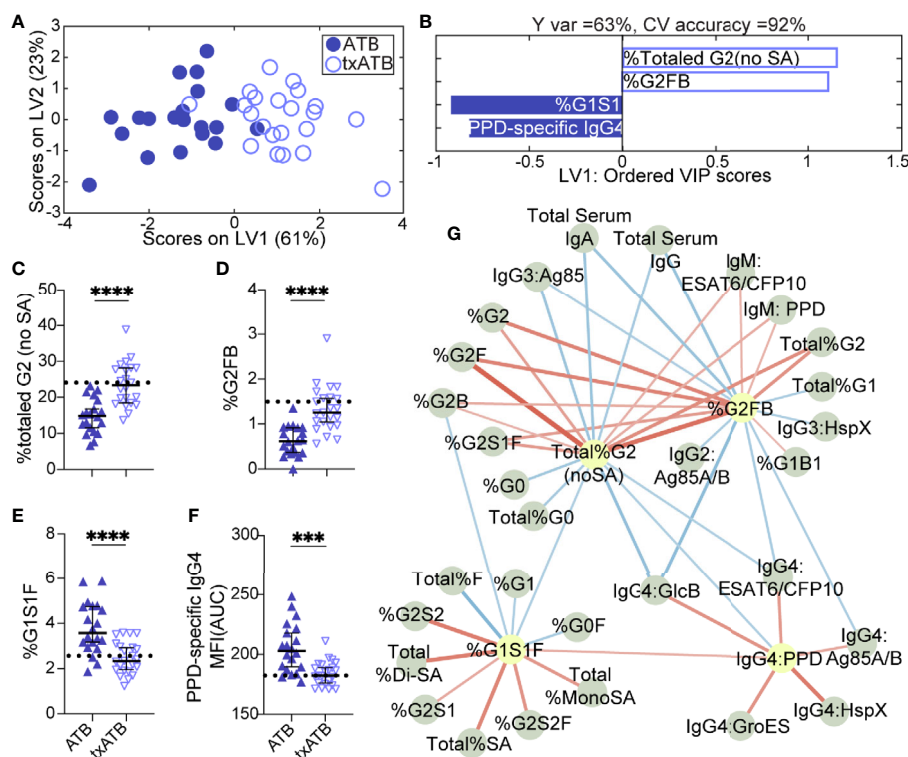


**FIGURE 2 |** Fc-glycosylation and TB-specific IgG subclass distinguish ATB and txATB individuals. An OPLSDA model was constructed using LASSO-identified antibody features as input and txATB and ATB group separation as output (A, B). LV1 explains 63% of the Y variance in the direction of the txATB and ATB. 5-fold cross validation resulted in 92% CV accuracy. The model performed significantly better than models based on shuffled group labels in permutation testing (Wilcoxon  $p=1E-5$ ). (A) OPLSDA scores plot depicts model separation of ATB ( $n = 20$ , blue dots) and txATB ( $n = 23$ , periwinkle open dots). LV1 and LV2 account for 61% and 23% of the variability in the input features. (B) VIP scores plot of top features providing the greatest resolution of ATB and txATB in rank-order. Directions of the bars signify loadings on LV1 and colors represent the disease groups in which measures were enriched. Pairwise comparison of ATB ( $n = 20$ , blue triangles) and txATB ( $n = 23$ , periwinkle open triangles) individuals (C) The frequencies of totaled G2 structures without sialic acid on IgG-Fc of ATB and txATB individuals. (D) percentage of G2FB glycan on IgG (E) percentage of G1S1F glycan on IgG. (F) AUC of PPD-specific IgG4 titers. Univariate plots (C–F) show median and interquartile range of LASSO-selected features and statistically significant differences between ATB and txATB groups calculated using Mann-Whitney test: \*\*\* $p < 0.0005$ , and \*\*\*\* $p < 0.0001$ . The dotted lines represent median of healthy controls (G) Correlation analysis depicts other features that are positively (red lines) or negatively (blue lines) correlated with these four key features selected with LASSO (highlighted in yellow). The color intensity and width of the edges between nodes are proportional to the significance of correlation coefficients after correcting for multiple comparisons (Benjamini-Hochberg q-value < 0.05, testing the hypothesis of zero correlation). Only correlations with corrected p-values < 0.05 were included.

## Antibody Titer and Glycosylation Distinguish txATB From ATB and LTBI

Given the ability of our pairwise models to distinguish TB states, we next aimed to resolve all three TB states simultaneously using the features previously selected by LASSO. Strikingly, this model discriminated between all three states with 80% classification accuracy (Figure 4A). ATB was most distinct from LTBI using these features and showed some overlap with txATB. However, interdigitation was observed across LTBI and txATB individuals, pointing to an overlap of humoral profiles in these disease states. LASSO-selected features were superimposed on the PLSDA plot, in the quadrant in which it was enriched (Figure 4A). PPD-specific IgG4 and IgG-Fc glycan, G1S1F, were uniquely enriched amongst the cluster of ATB individuals within the PLSDA. A markedly higher level of Ag85-specific IgG was also associated with the ATB cluster. Conversely, enhanced levels of PPD-

specific phagocytosis, elevated HspX-IgG, and Ag85-IgM were observed among txATB. Finally, enhanced di-galactosylation was observed on IgG-Fc from LTBI highlighting the importance of titers, function, and glycosylation, many of which were significantly elevated in LTBI and txATB compared to ATB at a univariate level (Figures 4B–I).

## DISCUSSION

With our growing appreciation of antibodies in TB immunity (36–39, 59, 60), changes in antibody isotype, subclass, and glycosylation are all emerging as biomarkers specific of disease activity. While many studies have described distinctive antibody features across LTBI and ATB disease, less is known about the changes in humoral immunity following treatment. Using

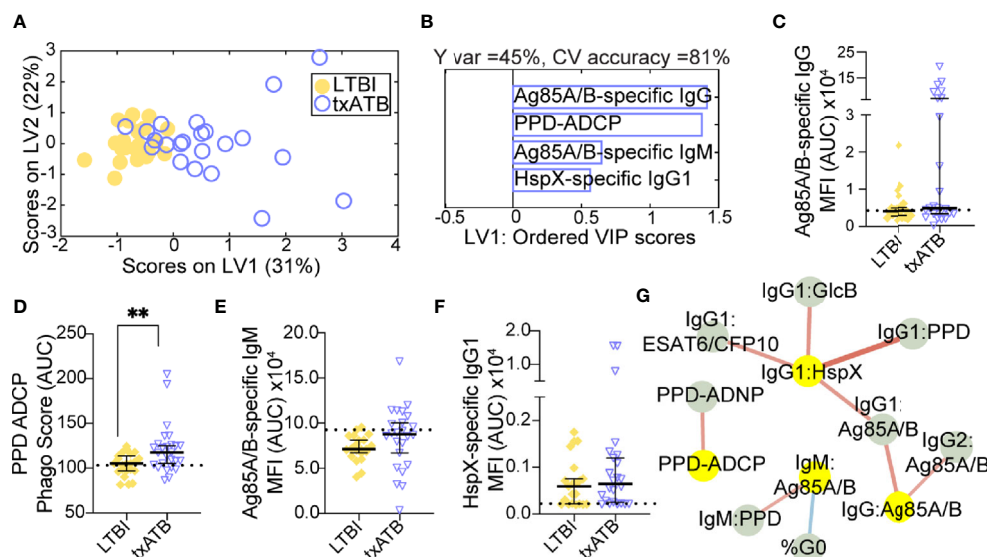


**FIGURE 3 |** TB-specific IgG titers distinguish LTBI and txATB individuals. An OPLS-DA models was constructed using the LASSO-selected features to discriminate LTBI and txATB (A, B). The variance in the direction of separation of LTBI and txATB was condensed on LV1 (Y variance = 45%). 5-fold cross validation was performed, resulting in 81% CV accuracy. Permutation testing was performed, which showed that this model performed significantly better than models based on shuffled group labels (Wilcoxon  $p=0.002$ ). (A) OPLS-DA scores plot depicts separation of LTBI ( $n=21$ , yellow dots) and txATB ( $n=23$ , periwinkle open dots). LV1 and LV2 account for 31% and 22% of the variability in the input features. (B) VIP scores plot of top features providing the greatest resolution of LTBI and txATB in rank-order. Directions of the bars signify loadings on LV1 and colors represent the disease groups in which measures were enriched Pairwise comparison of LTBI ( $n=21$ , yellow dots and diamonds) and txATB ( $n=23$ , periwinkle dots and triangles) individuals. (C) AUC Ag85A/B-specific total IgG titers. (D) PPD-specific ADCP Phago Score (E) AUC Ag85A/B-specific IgM titers (F) AUC HspX-specific IgG1 titers. Univariate plots (C–F) shows median and interquartile range of LASSO-selected features and statistically significant differences of the LASSO-selected features between LTBI and txATB groups calculated using Mann-Whitney test: \*\* $p < 0.01$ . The dotted lines represent median of healthy controls (G) Correlation analysis depicts other features that are positively (red lines) or negatively (blue lines) correlated with these four key features selected with LASSO (highlighted in yellow). Edges between nodes are weighted using significant correlation coefficients after correcting for multiple comparisons (Benjamini-Hochberg  $q$ -value  $< 0.05$ , testing the hypothesis of zero correlation). Only correlations with corrected  $p$ -values  $< 0.05$  were included.

systems serology, we observed significant differences in TB-specific antibody profiles across LTBI, ATB, and txATB, which highlight antibody changes that correlate with the burden of infection. As previously observed (36, 37), we found that LTBI and ATB are marked by distinct IgG-Fc glycosylation patterns, with an enrichment of glycans associated with inflammation in ATB. These observations are in line with an accumulation of inflammatory-glycans observed in antibodies of diseases including HIV (25) and autoimmune disorders (61–63). Importantly, we describe for the first time in txATB individuals an enrichment of G2 structures on IgG-Fc after the successful completion of treatment, pointing to IgG Fc-glycosylation as a marker of reduced replicating *Mtb*. A similar shift in IgG-Fc digalactosylation has been reported in a longitudinal study of IgG-Fc glycans in patients infected with hepatitis B; as treatment progresses and detectable viral DNA decreases, IgG-Fc digalactosylation increases (26). Additionally, we measured PPD-specific IgG-Fc glycans in the serum of a subset of TB diseased individuals from this cohort and found that levels of digalactosylated structures were also lower in ATB compared to LTBI and txATB (Supplemental Figures 6C, I). Unlike total IgG-Fc glycan measures, PPD-specific IgG-Fc was enriched for agalactosylated structures in ATB (Supplemental

Figure 6G), a glycan structure found to be enriched on IgG in other inflammatory diseases (25). Thus, inflammatory Fc-glycans mark disease activity and track with the presence of replicating *Mtb* in ATB individuals.

Beyond antibody glycan changes, humoral comparisons within this cohort pointed to TB-specific IgG4 as a novel humoral marker of TB disease activity. While consistently low in titer, previous studies noted elevated LAM-specific (64) and PPD-specific IgG4 titers (65) in HIV- and HIV+ individuals with ATB, respectively. IgG4 emerges through class-switch late in disease due to its distance on the human IgG locus, and with low Fc-receptor and complement affinity is selected under high antigen-burden when antibody titers are high. In diseases with prolonged antigen exposure and inflammation including parasitic infections (66, 67), chronic *Staphylococcus aureus* (*S. aureus*) infection (68), chronic infectious aortitis (69), melanoma (57), and even following repeated high-antigen dose immunization (56, 70, 71) elevated IgG4 levels have been described. And in the wake of resolving antigen burden, a longitudinal analysis of patients chronically infected with *Brugia malayi*, demonstrated a rapid loss of IgG4 titers, and a preservation of IgG1 responses following treatment (67). Similarly, we observed no change in TB-specific IgG1 titers and a loss of TB-specific IgG4 titers in txATB, pointing

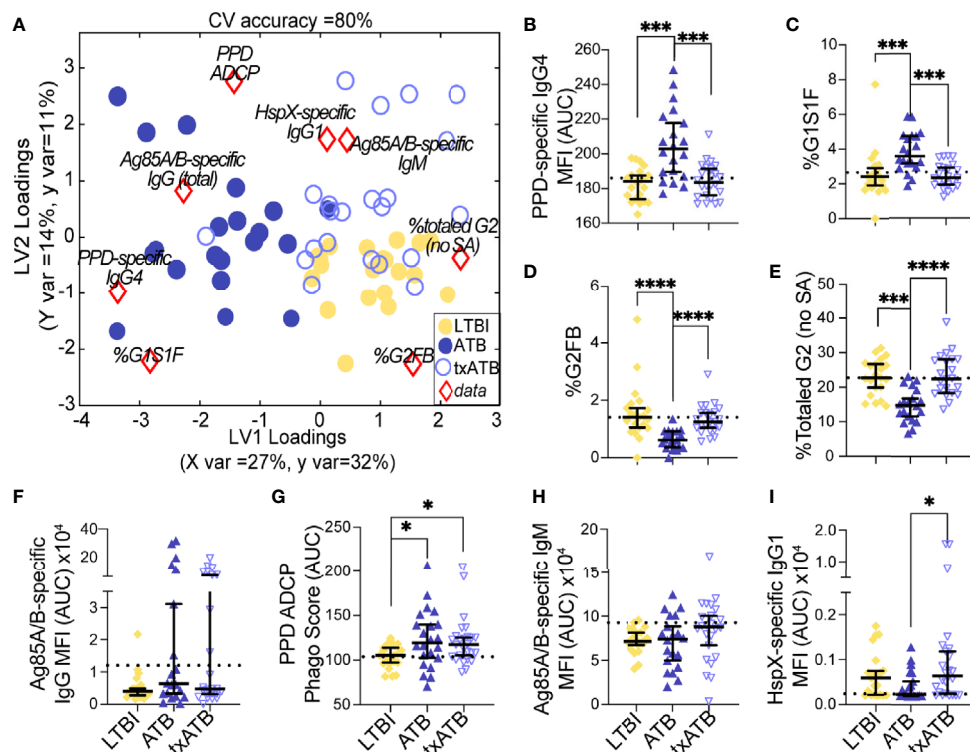


**FIGURE 4** | Fc-glycans, TB-specific titers, and isotypes distinguish individuals on the TB spectrum. Three-way comparison of LTBI ( $n = 21$ , yellow dots and diamonds), ATB ( $n = 20$ , blue dots and triangles), and txATB ( $n = 23$ , periwinkle dots and triangles) individuals. **(A)** Using the features described in **Figures 2–4**, a three-way PLSDA analysis summarizes the comparison of LTBI, ATB, and txATB. The depicted biplot overlays the scores plots of individuals color-coded based on their TB status on the two-dimensional loading plots of the 8 input features (red diamonds). LV1 accounts for 27% of variance in X and 32% of variance in Y, whereas LV2 explains 14% X variance and 11% Y variance. To assess the model performance, 5-fold cross validation was performed resulting in 80% CV accuracy. Permutation testing results showed that this model outperformed 90% of models based on shuffled group labels (Wilcoxon  $p = 0.1$ ). **(B)** AUC of PPD-specific IgG4 titers. **(C)** frequency of G1S1F glycan on IgG **(D)** frequency of G2FB glycan on IgG **(E)** The frequencies of totaled G2 structures without sialic acid on IgG-Fc. **(F)** AUC Ag85A/B-specific total IgG titers. **(G)** PPD-specific ADCP Phago Score. **(H)** AUC Ag85A/B-specific IgM titers **(I)** AUC HspX-specific IgG1 titers. Univariate plots **(B–I)** show median and interquartile range of the measured values and statistically significant differences between LTBI, ATB, and txATB groups were calculated using Kruskal-Wallis test with Dunn's multiple comparison test correction: \* $p < 0.05$ , \*\*\* $p < 0.0005$ , and \*\*\*\* $p < 0.0001$ .

to a similar trajectory of IgG4 as TB antigen is eliminated with therapy. And analogous to IgG2 and IgG3 titer declines observed following *Brugia malayi* treatment (67), although not statistically significant, we noted trends of decreased IgG2 and IgG3 titers in txATB compared to ATB in our co-correlate network analysis (**Figure 2G** and **Supplemental Figures 2B, C**). These data suggest that elimination of the antigen results in a shift of antibody subclass selection, with a more dramatic loss of IgG4 antibodies, suggesting that across TB disease, IgG4 may mark a more transient population of antibody-secreting cells that require high-antigenic stimulation to persist, making TB-specific IgG4 an attractive disease-specific marker of treatment success.

The balance of subclass, isotype, and glycosylation within an antibody immune complex can have significant functional consequences for Fc-mediated immune responses. IgG4 may arise to compensate for the pro-inflammatory activity of agalactosylated glycans that accumulate in active inflammatory diseases. In chronic parasitic infections, IgG4 levels are elevated in individuals with asymptomatic parasitic worm infection

compared to symptomatic patients, and this IgG4 has been linked to immune-suppressed states (72) and blocking of antibody-mediated hypersensitive responses in basophils (66). IgG4 tend to exhibit enhanced antigen-affinity (73, 74); thus, IgG4 may outcompete binding of functional TB-specific antibodies in immune complexes, thereby diminishing antibody effector activity. And a study focusing on IgG4 biology, using monoclonal antibodies, found that IgG4 antibody could block phagocytic functions of antibodies (57). Moreover, a study comparing Yanomami people and Brazilians of European descent with ATB, found an association of TST anergy and elevated TB-specific IgG4 in the Yanomami people with ATB (75), leading the authors to speculate that the Yanomami developed immune responses to *Mtb* infection that is poorly protective against TB disease. Thus, the presence of IgG4 titers may not only be indicative of high antigen-burden in ATB but might dampen the antibody-mediated functions in TB.

Our findings point to a unique antibody profile in txATB that differs from ATB and LTBI. Both inflammation-associated



glycosylation and IgG4 titers found in ATB are diminished upon completion of treatment, providing an attractive set of humoral features to explore more broadly in longitudinal studies tracking treatment success. It should be noted that our co-correlate network analysis in the pairwise comparisons of LTBI/ATB (**Figure 1G**), ATB/txATB (**Figure 2G**), and LTBI/txATB (**Figure 3G**) also highlighted both IgA and IgM related features that highly correlated with the features selected by LASSO/PLSDA models with additional discriminatory potential for the TB disease states studied here. We found significantly elevated total IgA, enriched in ATB, inversely correlated with digalactosylated IgG-Fc levels found in LTBI and txATB, suggesting expanded IgA titers also mark ATB state. Consistent with total IgA expansion in ATB, IgA2 titers specific for Ag85A/B were positively correlated were G1S1F on IgG-Fc (**Figure 1G**). While extensive antigens were not used to characterize the IgA response in this cohort, this observation is consistent with several findings of elevated TB-antigen specific IgA titers in untreated TB (52, 53, 76). Interestingly, PPD-IgM and HspX-IgG1 titers were significantly higher in txATB compared to ATB of this cohort (**Supplemental Figures 1 and 2**) and is consistent with a previous observation of expanded TB-specific antibody titers developing following TB treatment, which tracked with the control of replicating *Mtb* (77). Further studies will be important to identify *Mtb* antigen specificities that expand during therapy, which could be used to track treatment responses.

## DATA AVAILABILITY STATEMENT

The raw data supporting the conclusions of this article will be made available by the authors, without undue reservation.

## ETHICS STATEMENT

The studies involving human participants were reviewed and approved by INMI Ethical Committee Approval Number 72/

2015. The patients/participants provided their written informed consent to participate in this study.

## AUTHOR CONTRIBUTIONS

GA and PG conceived and designed the experiments. PG, AC, and LL performed the experiments. Data was analyzed by PG and SD. Multivariate analysis and modeling were performed by SD. Clinical cohort was established and collected by DG, FP, and LP. The manuscript was written by PG, SD, and GA with contributions from SJ, TO, DG, SF, and DL. All authors contributed to the article and approved the submitted version.

## FUNDING

This work was supported by the Ragon Institute (to GA), the SAMANA Kay MGH Research Scholar Program (to GA), NIH T32 AI007061 (to PG), and Italian Ministry of Health Ricerca corrente, Linea 4 (to DG).

## ACKNOWLEDGMENTS

We would like to acknowledge the patients, without whom this study would not have been possible. We are also grateful to the nurses and physicians who helped with clinical aspects necessary to perform this study (National Institute for Infectious Diseases, Rome, Italy). Special thanks to Valentina Vanini for the exceptional technical support and to Gilda Cuzzi for contributing to the clinical enrolment and patients' data base maintenance.

## SUPPLEMENTARY MATERIAL

The Supplementary Material for this article can be found online at: <https://www.frontiersin.org/articles/10.3389/fimmu.2021.679973/full#supplementary-material>

## REFERENCES

- Ottenhoff THM, Kaufmann SHE. Vaccines Against Tuberculosis: Where Are We and Where do We Need to Go? *PloS Pathog* (2012) 8(5):e1002607–e1002607. doi: 10.1371/journal.ppat.1002607
- Abu-Raddad LJ, Sabatelli L, Achterberg JT, Sugimoto JD, Longini JIM, Dye C, et al. Epidemiological Benefits of More-Effective Tuberculosis Vaccines, Drugs, and Diagnostic. *Proc Natl Acad Sci - PNAS* (2009) 106(33):13980–5. doi: 10.1073/pnas.0901720106
- Lönnroth K, Corbett E, Golub J, Godfrey-Faussett P, Uplekar M, Weil D, et al. Systematic Screening for Active Tuberculosis: Rationale, Definitions and Key Considerations [State of the Art Series. Active Case Finding/Screening. Number 1 in the Series]. *Int J Tuberculosis Lung Dis* (2013) 17(3):289–98. doi: 10.5588/ijtld.12.0797
- Marks GB, Nguyen NV, Nguyen PTB, Nguyen T-A, Nguyen HB, Tran KH, et al. Community-Wide Screening for Tuberculosis in a High-Prevalence Setting. *N Engl J Med* (2019) 381(14):1347–57. doi: 10.1056/NEJMoa1902129
- Lönnroth K, Migliori GB, Abubakar I, D'Ambrosio L, de Vries G, Diel R, et al. Towards Tuberculosis Elimination: An Action Framework for Low-Incidence Countries. *Eur Respir J* (2015) 45(4):928–52. doi: 10.1183/09031936.00214014
- Pai M, Denlinger CM, Kik SV, Rangaka MX, Zwerling A, Oxlade O, et al. Gamma Interferon Release Assays for Detection of Mycobacterium Tuberculosis Infection. *Clin Microbiol Rev* (2014) 27(1):3–20. doi: 10.1128/CMR.00034-13
- Meier T, Eulenbruch HP, Wrighton-Smith P, Enders G, Regnath T. Sensitivity of a New Commercial Enzyme-Linked Immunospot Assay (T SPOT-TB) for Diagnosis of Tuberculosis in Clinical Practice. *Eur J Clin Microbiol Infect Dis* (2005) 24(8):529–36. doi: 10.1007/s10096-005-1377-8
- Chowdhury RR, Vallania F, Yang Q, Angel CJL, Darboe F, Penn-Nicholson A, et al. A Multi-Cohort Study of the Immune Factors Associated With M. Tuberculosis Infection Outcomes. *Nature* (2018) 560(7720):644–8. doi: 10.1038/s41586-018-0439-x
- Berry MPR, Graham CM, McNab FW, Xu Z, Bloch SAA, Oni T, et al. An Interferon-Inducible Neutrophil-Driven Blood Transcriptional Signature in

- Human Tuberculosis. *Nature* (2010) 466(7309):973–7. doi: 10.1038/nature09247
10. Joosten SA, van Meijgaarden KE, del Nonno F, Baiocchi A, Petrone L, Vanini V, et al. Patients With Tuberculosis Have a Dysfunctional Circulating B-Cell Compartment, Which Normalizes Following Successful Treatment. *PLoS Pathog* (2016) 12(6):e1005687–1005624. doi: 10.1371/journal.ppat.1005687
  11. Janssens J-P, Roux-Lombard P, Perneger T, Metzger M, Vivien R, Rochat T. Quantitative Scoring of an Interferon-Gamma Assay for Differentiating Active From Latent Tuberculosis. *Eur Respir J* (2007) 30(4):722–8. doi: 10.1183/09031936.00028507
  12. Pollock KM, Whitworth HS, Montamat-Sicotte DJ, Grass L, Cooke GS, Kapembwa MS, et al. T-Cell Immunophenotyping Distinguishes Active From Latent Tuberculosis. *J Infect Dis* (2013) 208(6):952–68. doi: 10.1093/infdis/jit265
  13. Harari A, Rozot V, Enders FB, Perreau M, Stalder JM, Nicod LP, et al. Dominant TNF- $\alpha$  Mycobacterium Tuberculosis-Specific CD4+ T Cell Responses Discriminate Between Latent Infection and Active Disease. *Nat Med* (2011) 17(3):372–6. doi: 10.1038/nm.2299
  14. Goletti D, Lee M-R, Wang J-Y, Walter N, Ottenhoff THM. Update on Tuberculosis Biomarkers: From Correlates of Risk, to Correlates of Active Disease and of Cure From Disease. *Respirology* (2018) 23(5):455–66. doi: 10.1111/resp.13272
  15. Adekambi T, Ibegbu CC, Cagle S, Kalokhe AS, Wang YF, Hu Y, et al. Biomarkers on Patient T Cells Diagnose Active Tuberculosis and Monitor Treatment Response. *J Clin Invest* (2015) 125(5):1827–38. doi: 10.1172/JCI77990
  16. Goletti D, Lindestam Arlehamn CS, Scriba TJ, Anthony R, Cirillo DM, Alonzi T, et al. Can We Predict Tuberculosis Cure? What Tools Are Available? *Eur Respir J* (2018) 52(5):1801089–1801060. doi: 10.1183/13993003.01089-2018
  17. Cliff JM, Kaufmann SHE, McShane H, van Helden P, O'Garra A. The Human Immune Response to Tuberculosis and Its Treatment: A View From the Blood. *Immunol Rev* (2015) 264(1):88–102. doi: 10.1111/imr.12269
  18. Bournazos S, Wang TT, Dahan R, Maamary J, Ravetch JV. Signaling by Antibodies: Recent Progress. *Annu Rev Immunol* (2017) 35(1):285–311. doi: 10.1146/annurev-immunol-051116-052433
  19. Dryla A, Prustomersky S, Gelbmann D, Hanner M, Bettinger E, Kocsis B, et al. Comparison of Antibody Repertoires Against Staphylococcus Aureus in Healthy Individuals and in Acutely Infected Patient. *Clin Vaccine Immunol* (2005) 12(3):387–98. doi: 10.1128/CDLI.12.3.387-398.2005
  20. Stentzel S, Sundaramoorthy N, Michalik S, Nordengrün M, Schulz S, Kolata J, et al. Specific Serum IgG at Diagnosis of Staphylococcus Aureus Bloodstream Invasion Is Correlated With Disease Progression. *J Proteomics* (2015) 128(C):1–7. doi: 10.1016/j.jprot.2015.06.018
  21. Varshney AK, Wang X, Aguilar JL, Scharff MD, Fries BC. Isotype Switching Increases Efficacy of Antibody Protection Against Staphylococcal Enterotoxin B-Induced Lethal Shock and Staphylococcus Aureus Sepsis in Mice. *mBio* (2014) 5(3):615–9. doi: 10.1128/mBio.01007-14
  22. Arnold JN, Wormald MR, Sim RB, Rudd PM, Dwek RA. The Impact of Glycosylation on the Biological Function and Structure of Human Immunoglobulins. *Annu Rev Immunol* (2007) 25(1):21–50. doi: 10.1146/annurev.immunol.25.022106.141702
  23. de Jong SE, Selman MHJ, Adegnik AA, Amoah AS, van Riet E, Kruize YCM, et al. IgG1 Fc N-Glycan Galactosylation as a Biomarker for Immune Activation. *Sci Rep* (2016) 6(1):28207–28207. doi: 10.1038/srep28207
  24. Lin C-W, Tsai M-H, Li S-T, Tsai T-I, Chu K-C, Liu Y-C, et al. A Common Glycan Structure on Immunoglobulin G for Enhancement of Effector Functions. *Proc Natl Acad Sci - PNAS* (2015) 112(34):10611–6. doi: 10.1073/pnas.1513456112
  25. Ackerman ME, Crispin M, Yu X, Baruah K, Boesch AW, Harvey DJ, et al. Natural Variation in Fc Glycosylation of HIV-Specific Antibodies Impacts Antiviral Activity. *J Clin Invest* (2013) 123(5):2183–92. doi: 10.1172/JCI65708
  26. Ho C-H, Chien R-N, Cheng P-N, Liu J-H, Liu C-K, Su C-S, et al. Aberrant Serum Immunoglobulin G Glycosylation in Chronic Hepatitis B Is Associated With Histological Liver Damage and Reversible by Antiviral Therapy. *J Infect Dis* (2014) 211(1):115–24. doi: 10.1093/infdis/jiu388
  27. Theodoratou E, Thaci K, Agakov F, Timofeeva MN, Štambuk J, Pučić-Baković M, et al. Glycosylation of Plasma IgG in Colorectal Cancer Prognosis. *Sci Rep* (2016) 6(1):28098. doi: 10.1038/srep28098
  28. Ren S, Zhang Z, Xu C, Guo L, Lu R, Sun Y, et al. Distribution of IgG Galactosylation as a Promising Biomarker for Cancer Screening in Multiple Cancer Types. *Cell Res* (2016) 26(8):963–6. doi: 10.1038/cr.2016.83
  29. Di Sabatino A, Biagi F, Lenzi M, Frulloni L, Lenti MV, Giuffrida P, et al. Clinical Usefulness of Serum Antibodies as Biomarkers of Gastrointestinal and Liver Diseases. *Digestive liver Dis* (2017) 49(9):947–56. doi: 10.1016/j.dld.2017.06.010
  30. Rombouts Y, Ewing E, van de Stadt LA, Selman MHJ, Trouw LA, Deelder AM, et al. Anti-Citrullinated Protein Antibodies Acquire a Pro-Inflammatory Fc Glycosylation Phenotype Prior to the Onset of Rheumatoid Arthritis. *Ann Rheum Dis* (2015) 74(1):234–41. doi: 10.1136/annrheumdis-2013-203565
  31. Lee S-J, Liang L, Juarez S, Nanton MR, Gondwe EN, Msefula CL, et al. Identification of a Common Immune Signature in Murine and Human Systemic Salmonellosis. *Proc Natl Acad Sci* (2012) 109(13):4998–5003. doi: 10.1073/pnas.1111413109
  32. Demkow U, Filewska M, Michalowska-Mitczuk D, Kus J, Jagodzinski J, Zielonka T, et al. Heterogeneity of Antibody Response to Mycobacterial Antigens in Different Clinical Manifestations of Pulmonary Tuberculosis. *J Physiol Pharmacol an Off J Polish Physiol Soc* (2007) 58 Suppl 5(Pt 1):117–27.
  33. Wang S, Wu J, Chen J, Gao Y, Zhang S, Zhou Z, et al. Evaluation of Mycobacterium Tuberculosis-Specific Antibody Responses for the Discrimination of Active and Latent Tuberculosis Infection. *Int J Infect Dis* (2018) 70:1–9. doi: 10.1016/j.ijid.2018.01.007
  34. Lyashchenko K, Colangeli R, Houde M, Al Jahdali H, Menzies D, Gennaro ML. Heterogeneous Antibody Responses in Tuberculosis. *Infect Immun* (1998) 66(8):3936–40. doi: 10.1128/IAI.66.8.3936-3940.1998
  35. Alter G, Ottenhoff THM, Joosten SA. Antibody Glycosylation in Inflammation, Disease and Vaccination. *Semin Immunol* (2018) 39:102–10. doi: 10.1016/j.smim.2018.05.003
  36. Lu LL, Chung AW, Rosebrock TR, Ghebremichael M, Yu WH, Grace PS, et al. A Functional Role for Antibodies in Tuberculosis. *Cell* (2016) 167(2):1–26. doi: 10.1016/j.cell.2016.08.072
  37. Lu LL, Das J, Grace PS, Fortune SM, Restrepo BI, Alter G. Antibody Fc Glycosylation Discriminates Between Latent and Active Tuberculosis. *J Infect Dis* (2020) 64:111–0. doi: 10.1093/infdis/jiz643
  38. Li H, Wang X-x, Wang B, Fu L, Liu G, Lu Y, et al. Latently and Uninfected Healthcare Workers Exposed to TB Make Protective Antibodies Against Mycobacterium Tuberculosis. *Proc Natl Acad Sci USA* (2017) 114(19):5023–8. doi: 10.1073/pnas.1611776114
  39. Chen T, Blanc C, Liu Y, Ishida E, Singer S, Xu J, et al. Capsular Glycan Recognition Provides Antibody-Mediated Immunity Against Tuberculosis. *J Clin Invest* (2020) 2015(6):1609. doi: 10.1172/JCI128459
  40. Zimmermann N, Thormann V, Hu B, Köhler AB, Imai Matsushima A, Locht C, et al. Human Isotype-Dependent Inhibitory Antibody Responses Against Mycobacterium Tuberculosis. *EMBO Mol Med* (2016) 8(11):1325–39. doi: 10.15252/emmm.201606330
  41. de Valliere S, Abate G, Blazevic A, Heuertz RM, Hoft DF. Enhancement of Innate and Cell-Mediated Immunity by Antimycobacterial Antibodies. *Infect Immun* (2005) 73(10):6711–20. doi: 10.1128/IAI.73.10.6711-6720.2005
  42. Roy E, Stavropoulos E, Brennan J, Coade S, Grigorieva E, Walker B, et al. Therapeutic Efficacy of High-Dose Intravenous Immunoglobulin in Mycobacterium Tuberculosis Infection in Mice. *Infect Immun* (2005) 73(9):6101–9. doi: 10.1128/IAI.73.9.6101-6109.2005
  43. Mattos AMM, Chaves AS, Franken KLMC, Figueiredo BBM, Ferreira AP, Ottenhoff THM, et al. Detection of IgG1 Antibodies Against Mycobacterium Tuberculosis DosR and Rpf Antigens in Tuberculosis Patients Before and After Chemotherapy. *Tuberculosis (Edinburgh Scotland)* (2016) 96(C):65–70. doi: 10.1016/j.tube.2015.11.001
  44. Arias-Bouda LMP, Kuijper S, van der Werf A, Nguyen LN, Jansen HM, Kolk AHJ. Changes in Avidity and Level of Immunoglobulin G Antibodies to Mycobacterium Tuberculosis in Sera of Patients Undergoing Treatment for Pulmonary Tuberculosis. *Clin Diagn Lab Immunol* (2003) 10(4):702–9. doi: 10.1128/cdli.10.4.702-709.2003
  45. Chung AW, Kumar MP, Arnold KB, Yu WH, Schoen MK, Dunphy LJ, et al. Dissecting Polyclonal Vaccine-Induced Humoral Immunity Against HIV Using Systems Serology. *Cell (Cambridge)* (2015) 163(4):988–98. doi: 10.1016/j.cell.2015.10.027
  46. Gilpin C, Korobitsyn A, Migliori GB, Raviglione MC, Weyer K. The World Health Organization Standards for Tuberculosis Care and Management. *Eur Respir J* (2018) 51(3):1800098. doi: 10.1183/13993003.00098-2018

47. Tibshirani R. The Lasso Method for Variable Selection in the Cox Model. *Stat Med* (1997) 16(4):385–95. doi: 10.1002/(SICI)1097-0258(19970228)16:4<385::AID-SIM380>3.0.CO;2-3
48. Ackerman ME, Das J, Pittala S, Broge T, Linde C, Suscovich TJ, et al. Route of Immunization Defines Multiple Mechanisms of Vaccine-Mediated Protection Against SIV. *Nat Med* (2018) 24(10):1590–8. doi: 10.1038/s41591-018-0161-0
49. Arnold KB, Burgener A, Birse K, Romas L, Dunphy LJ, Shahabi K, et al. Increased Levels of Inflammatory Cytokines in the Female Reproductive Tract Are Associated With Altered Expression of Proteases, Mucosal Barrier Proteins, and an Influx of HIV-Susceptible Target Cells. *Mucosal Immunol* (2016) 9(1):194–205. doi: 10.1038/mi.2015.51
50. Lau KS, Juchheim AM, Cavaliere KR, Philips SR, Lauffenburger DA, Haigis KM. *In Vivo* Systems Analysis Identifies Spatial and Temporal Aspects of the Modulation of TNF- $\alpha$ -Induced Apoptosis and Proliferation by MAPK. *Sci Signaling* (2011) 4(165):ra16–6. doi: 10.1126/scisignal.2001338
51. Chong I-G, Jun C-H. Performance of Some Variable Selection Methods When Multicollinearity Is Present. *Chemom Intell Lab Syst* (2005) 78(1):103–12. doi: 10.1016/j.chemolab.2004.12.011
52. Alifano M, Sofia M, Mormile M, Micco A, Mormile AF, Del Pezzo M, et al. IgA Immune Response Against the Mycobacterial Antigen A60 in Patients With Active Pulmonary Tuberculosis. *Respiration Int Rev Thorac Dis* (1996) 63(5):292–7. doi: 10.1159/000196563
53. Abebe F, Belay M, Legesse M, Franken KLMC, Ottenhoff THM. IgA and IgG Against Mycobacterium Tuberculosis Rv2031 Discriminate Between Pulmonary Tuberculosis Patients, Mycobacterium Tuberculosis-Infected and non-Infected Individuals. *PloS One* (2018) 13(1):e0190989–0190919. doi: 10.1371/journal.pone.0190989
54. Chandler KB, Mehta N, Leon DR, Suscovich TJ, Alter G, Costello CE. Multi-Isotype Glycoproteomic Characterization of Serum Antibody Heavy Chains Reveals Isotype- and Subclass-Specific N-Glycosylation Profiles. *Mol Cell Proteomics* (2019) 18(4):686–703. doi: 10.1074/mcp.RA118.001185
55. Konno N, Sugimoto M, Takagi T, Furuya M, Asano T, Sato S, et al. Changes in N-Glycans of IgG4 and Its Relationship With the Existence of Hypocomplementemia and Individual Organ Involvement in Patients With IgG4-Related Disease. *PloS One* (2018) 13(4):e0196163. doi: 10.1371/journal.pone.0196163
56. Chung AW, Ghebremichael M, Robinson H, Brown E, Choi I, Lane S, et al. Polyfunctional Fc-Effector Profiles Mediated by IgG Subclass Selection Distinguish RV144 and VAX003 Vaccines. *Sci Trans Med* (2014) 6(228):228ra238–228ra238. doi: 10.1126/scitranslmed.3007736
57. Karagiannis P, Gilbert AE, Josephs DH, Ali N, Dodev T, Saul L, et al. IgG4 Subclass Antibodies Impair Antitumor Immunity in Melanoma. *J Clin Invest* (2013) 123(4):1457–74. doi: 10.1172/JCI65579
58. Boes M. Role of Natural and Immune IgM Antibodies in Immune Responses. *Mol Immunol* (2000) 37(18):1141–9. doi: 10.1016/S0161-5890(01)00025-6
59. Lu LL, Smith MT, Yu KKQ, Luedemann C, Suscovich TJ, Grace PS, et al. IFN- $\gamma$ -Independent Immune Markers of Mycobacterium Tuberculosis Exposure. *Nat Med* (2019) 25(6):997–87. doi: 10.1038/s41591-019-0441-3
60. Chen T, Blanc C, Eder AZ, Prados-Rosales R, Souza ACO, Kim RS, et al. Association of Human Antibodies to Arabinomannan With Enhanced Mycobacterial Opsonophagocytosis and Intracellular Growth Reduction. *J Infect Dis* (2016) 214(2):300–10. doi: 10.1093/infdis/jiw141
61. Kemna MJ, Plomp R, van Paassen P, Koeleman CAM, Jansen BC, Damoiseaux JGMC, et al. Galactosylation and Sialylation Levels of IgG Predict Relapse in Patients With PR3-ANCA Associated Vasculitis. *EBioMedicine* (2017) 17(C):108–18. doi: 10.1016/j.ebiom.2017.01.033
62. Bondt A, Selman MHJ, Deelder AM, Hazes JMW, Willemsen SP, Wuhler M, et al. Association Between Galactosylation of Immunoglobulin G and Improvement of Rheumatoid Arthritis During Pregnancy Is Independent of Sialylation. *J Proteome Res* (2013) 12(10):4522–31. doi: 10.1021/pr400589m
63. Wuhler M, Selman MHJ, McDonnell LA, Kumpfel T, Derfuss T, Khademi M, et al. Pro-Inflammatory Pattern of IgG1 Fc Glycosylation in Multiple Sclerosis Cerebrospinal Fluid. *J Neuroinflamm* (2015) 12(236):235–5. doi: 10.1186/s12974-015-0450-1
64. Yu X, Prados-Rosales R, Jenny-Avital ER, Sosa K, Casadevall A, Achkar JM. Comparative Evaluation of Profiles of Antibodies to Mycobacterial Capsular Polysaccharides in Tuberculosis Patients and Controls Stratified by HIV Status. *Clin Vaccine Immunol* (2012) 19(2):198–208. doi: 10.1128/CDLI.11.5.942-951.2004
65. van Woudenberg E, Irvine EB, Davies L, de Kock M, Hanekom WA, Day CL, et al. HIV Is Associated With Modified Humoral Immune Responses in the Setting of HIV/TB Coinfection. *mSphere* (2020) 5(3):603–19. doi: 10.1128/mSphere.00104-20
66. Hussain R, Poindexter RW, Ottesen EA. Control of Allergic Reactivity in Human Filariasis. Predominant Localization of Blocking Antibody to the IgG4 Subclass. *J Immunol (Baltimore Md 1950)* (1992) 148(9):2731–7.
67. Atmadja AK, Atkinson R, Sartono E, Partono F, Yazdanbakhsh M, Maizels RM. Differential Decline in Filaria-Specific IgG1, IgG4, and IgE Antibodies in Brugia Malayi-Infected Patients After Diethylcarbamazine Chemotherapy. *J Infect Dis* (1995) 172(6):1567–72. doi: 10.1093/infdis/172.6.1567
68. Swierstra J, Debets S, de Vogel C, Lemmens-den Toom N, Verkaik N, Ramdani-Bougues N, et al. IgG4 Subclass-Specific Responses to Staphylococcus Aureus Antigens Shed New Light on Host-Pathogen Interaction. *Infect Immun* (2015) 83(2):492–501. doi: 10.1128/IAI.02286-14
69. Siddiquee Z, Smith RN, Stone JR. An Elevated IgG4 Response in Chronic Infectious Aortitis Is Associated With Aortic Atherosclerosis. *Modern Pathol* (2015) 28(11):1428–34. doi: 10.1038/modpathol.2015.105
70. Aalberse RC, van der Gaag R, van Leeuwen J. Serologic Aspects of IgG4 Antibodies. I. Prolonged Immunization Results in an IgG4-Restricted Response. *J Immunol (Baltimore Md 1950)* (1983) 130(2):722–6.
71. Francis JN, James LK, Paraskevopoulos G, Wong C, Calderon MA, Durham SR, et al. Grass Pollen Immunotherapy: IL-10 Induction and Suppression of Late Responses Precedes IgG4 Inhibitory Antibody Activity. *J Allergy Clin Immunol* (2008) 121(5):1120–1125.e1122. doi: 10.1016/j.jaci.2008.01.072
72. Prodjinotho UF, Hoerauf A, Adjomey T. IgG4 Antibodies From Patients With Asymptomatic Bancroftian Filariasis Inhibit the Binding of IgG1 and IgG2 to C1q in a Fc-Fc-Dependent Mechanism. *Parasitol Res* (2019) 118(10):2957–68. doi: 10.1007/s00436-019-06451-2
73. Jackson KJL. Human Immunoglobulin Classes and Subclasses Show Variability in VDJ Gene Mutation Levelshuman Immunoglobulin Classes and Subclasses Show Variability in VDJ Gene Mutation Levels. *Immunol Cell Biol* (2014) 92(8):729–33. doi: 10.1038/icb.2014.44
74. Crescioli S, Correa I, Karagiannis P, Davies AM, Sutton BJ, Nestle FO, et al. IgG4 Characteristics and Functions in Cancer Immunity. *Curr Allergy Asthma Rep* (2016) 16(1):1–11. doi: 10.1007/s11882-015-0580-7
75. Sousa AO, Salem JI, Lee FK, Verçosa MC, Cruaud P, Bloom BR, et al. An Epidemic of Tuberculosis With a High Rate of Tuberculin Anergy Among a Population Previously Unexposed to Tuberculosis, the Yanomami Indians of the Brazilian Amazo. *Proc Natl Acad Sci USA* (1997) 94(24):13227–32. doi: 10.1073/pnas.94.24.13227
76. Awoniyi DO, Baumann R, Chegou NN, Kriel B, Jacobs R, Kidd M, et al. Detection of a Combination of Serum IgG and IgA Antibodies Against Selected Mycobacterial Targets Provides Promising Diagnostic Signatures for Active TB. *Oncotarget* (2017) 8(23):37525–37. doi: 10.18632/oncotarget.16401
77. Bothamley GH. Epitope-Specific Antibody Levels Demonstrate Recognition of New Epitopes and Changes in Titer But Not Affinity During Treatment of Tuberculosis. *Clin Diagn Lab Immunol* (2004) 11(5):942–51. doi: 10.1128/CDLI.11.5.942-951.2004

**Conflict of Interest:** GA is a co-founder of SeromYx Systems Inc. GA's interests were reviewed and are managed by Massachusetts General Hospital and Partners HealthCare in accordance with their conflict of interest policies.

The remaining authors declare that the research was conducted in the absence of any commercial or financial relationships that could be construed as a potential conflict of interest.

The handling Editor has declared past collaborations with the authors TO and SJ within the last two years.

Copyright © 2021 Grace, Dolatshahi, Lu, Cain, Palmieri, Petrone, Fortune, Ottenhoff, Lauffenburger, Goletti, Joosten and Alter. This is an open-access article distributed under the terms of the Creative Commons Attribution License (CC BY). The use, distribution or reproduction in other forums is permitted, provided the original author(s) and the copyright owner(s) are credited and that the original publication in this journal is cited, in accordance with accepted academic practice. No use, distribution or reproduction is permitted which does not comply with these terms.

# Advantages of publishing in Frontiers



## OPEN ACCESS

Articles are free to read  
for greatest visibility  
and readership



## FAST PUBLICATION

Around 90 days  
from submission  
to decision



## HIGH QUALITY PEER-REVIEW

Rigorous, collaborative,  
and constructive  
peer-review



## TRANSPARENT PEER-REVIEW

Editors and reviewers  
acknowledged by name  
on published articles

## Frontiers

Avenue du Tribunal-Fédéral 34  
1005 Lausanne | Switzerland

**Visit us:** [www.frontiersin.org](http://www.frontiersin.org)

**Contact us:** [frontiersin.org/about/contact](http://frontiersin.org/about/contact)



## REPRODUCIBILITY OF RESEARCH

Support open data  
and methods to enhance  
research reproducibility



## DIGITAL PUBLISHING

Articles designed  
for optimal readership  
across devices



## FOLLOW US

@frontiersin



## IMPACT METRICS

Advanced article metrics  
track visibility across  
digital media



## EXTENSIVE PROMOTION

Marketing  
and promotion  
of impactful research



## LOOP RESEARCH NETWORK

Our network  
increases your  
article's readership